February 2003 Volume 204 • Number 1

THE BIOLOGICAL BULLETIN

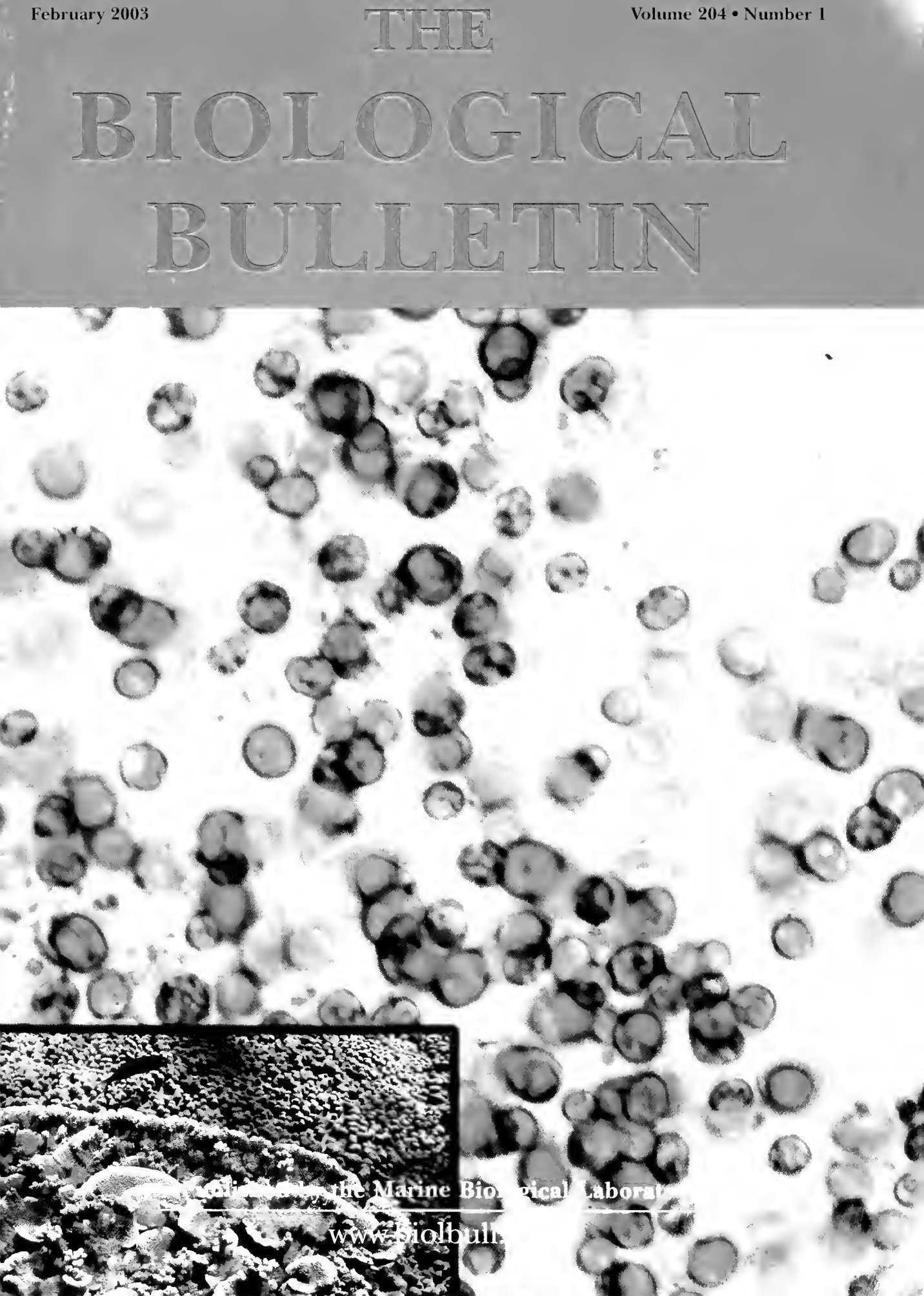

Published by the Marine Biological Laboratory

www.biolbull.org

INVERTED MICROSCOPES

DRAWN FROM EXPERIENCE.

ONLY NIKON COULD REINVENT INVERTED MICROSCOPY WITH THE NEW ECLIPSE TE2000 SERIES.

When they were launched, Nikon's Eclipse TE microscopes set new standards in optical performance, continuing a tradition of over twenty years of excellence in inverted microscopy.

Now, Nikon proudly introduces the next generation of Eclipse research inverted microscopes. The Eclipse TE2000 series incorporates past successes into a new design with innovations that are exactly what today's varied research techniques require.

Here are just some of the special features built into this extraordinary microscope:

- Multi-port design permitting addition of optional illumination sources and other attachments without modifying the microscope.
- Unique "Noise Terminator" thoroughly eliminates stray light for greater S/N ratio in fluorescence imaging.
- Super-nanoprecision Z-access control and increased stability for superior 3D imaging.
- Modular motorized components for automated control.
- Exclusive CFI60™ infinity optical system for excellent resolution with high numerical apertures and longer working distances.

The Eclipse TE2000 is available in three models, each configured to meet your research needs. Draw on Nikon's experience.
For more information, call 1-800-52-NIKON, ext. 392
or visit www.nikonuso.com
In Canada, call 1-866-99-NIKON

Visit MicroscopyU at
www.nikonuso.com to learn more
about inverted microscopy.

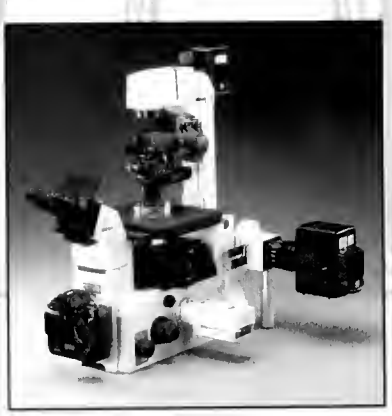

CFI60
ECLIPSE

Nikon

WHEN IT COMES TO SPEED AND HANDLING,

ABOUT THE ONLY THING NOT MOTORIZED IS YOU.

ROCKET SCIENCE.™

800 446 5967 olympusamerica.com/microscopes

Cover

Dinoflagellates are a diverse and ecologically important group of unicellular protists. Some of them are free-living, photosynthetic or heterotrophic constituents of the plankton; others are symbiotic. Dinoflagellates in the genus *Symbiodinium*, commonly called zooxanthellae, are intra- or intercellular symbionts of diverse marine invertebrates, including foraminiferans, sponges, cnidarians, and molluscs.

The image on the cover shows a throng of *Symbiodinium kawagutii* cells that were isolated from their symbiotic host, the Hawaiian stony coral *Montipora capitata* (= *M. verrucosa*)[1]; the coral appears in the inset. In 1987, on the basis of cytological evidence, R. J. Blank[2] speculated that the vegetative cells of *M. verrucosa* are haploid; but this finding was never corroborated. The question of ploidy is important, for it is central to our understanding of genome evolution and population genetics.

Now, for the first time, the methods of molecular genetics have been applied to the problem of haploidy in dinoflagellates. In this issue of *The Biological Bulletin* (p. 10), Scott R. Santos and Mary Alice Coffroth report that vegetative cells of *Symbiodinium* clade B symbiotic with gorgonians (sea fans and sea whips), and cultured cells from a range of hosts and locations, are haploid. Moreover, since *Symbiodinium* is monophyletic, *S. kawagutii* and other members of the genus must also be haploid.

The *Symbiodinium* cells on the cover are about 10 μm in diameter; they were photographed by Scott R. Santos (State University of New York at Buffalo). The photograph of *Montipora capitata* was taken by Frank Stanton (University of Hawaii) at a depth of about 1.5 meters; the coral is about 1 m in diameter. Materials and information for the cover and legend were provided by Fenny Cox (University of Hawaii). The cover was designed by Beth Liles, Marine Biological Laboratory, Woods Hole, Massachusetts.

[1] **Maragos, J. E. 1995.** Revised checklist of extant shallow-water stony coral species from Hawaii (Cnidaria: Anthozoa: Scleractinia). *Bishop Museum Occasional Papers* **42:** 54–55.

[2] **Blank, R. J. 1987.** Cell architecture of the dinoflagellate *Symbiodinium* sp. inhabiting the Hawaiian stony coral *Montipora verrucosa*. *Mar. Biol.* **94:** 143–155.

THE
BIOLOGICAL BULLETIN
FEBRUARY 2003

Published by
Marine Biological Laboratory
Woods Hole, Massachusetts

http://www.biolbull.org

CONTENTS

VOLUME 204, NO. 1: FEBRUARY 2003

SYMBIOSIS AND PARASITOLOGY

CELL BIOLOGY

NEUROBIOLOGY AND BEHAVIOR

DEVELOPMENT AND REPRODUCTION

PHYSIOLOGY AND BIOMECHANICS

ECOLOGY AND EVOLUTION

RESEARCH NOTE

THE BIOLOGICAL BULLETIN

THE BIOLOGICAL BULLETIN is published six times a year by the Marine Biological Laboratory, 7 MBL Street, Woods Hole, Massachusetts 02543.

Subscriptions and similar matter should be addressed to Subscription Administrator, THE BIOLOGICAL BULLETIN, Marine Biological Laboratory, 7 MBL Street, Woods Hole, Massachusetts 02543. Subscription includes both print and online journals. Subscription per year (six issues, two volumes): $280 for libraries; $105 for individuals. Subscription per volume (three issues): $140 for libraries; $52.50 for individuals. Back and single issues (subject to availability): $50 for libraries; $20 for individuals.

Communications relative to manuscripts should be sent to Michael J. Greenberg, Editor-in-Chief, or Pamela Clapp Hinkle, Managing Editor, at the Marine Biological Laboratory, 7 MBL Street, Woods Hole, Massachusetts 02543. Telephone: (508) 289-7149. FAX: 508-289-7922. E-mail: pclapp@mbl.edu.

http://www.biolbull.org

THE BIOLOGICAL BULLETIN is indexed in bibliographic services including *Index Medicus* and MEDLINE, *Chemical Abstracts, Current Contents, Elsevier BIOBASE/Current Awareness in Biological Sciences,* and *Geo Abstracts.*

Printed on acid free paper,
effective with Volume 180, Issue 1, 1991.

POSTMASTER: Send address changes to THE BIOLOGICAL BULLETIN, Marine Biological Laboratory, 7 MBL Street, Woods Hole, MA 02543.

Periodicals postage paid at Woods Hole, MA, and additional mailing offices.
ISSN 0006-3185

INSTRUCTIONS TO AUTHORS

The Biological Bulletin accepts outstanding original research reports of general interest to biologists throughout the world. Papers are usually of intermediate length (10–40 manuscript pages). A limited number of solicited review papers may be accepted after formal review. A paper will usually appear within four months after its acceptance.

Very short, especially topical papers (less than 9 manuscript pages including tables, figures, and bibliography) will be published in a separate section entitled "Research Notes." A Research Note in *The Biological Bulletin* follows the format of similar notes in *Nature.* It should open with a summary paragraph of 150 to 200 words comprising the introduction and the conclusions. The rest of the text should continue on without subheadings, and there should be no more than 30 references. References should be referred to in the text by number, and listed in the Literature Cited section in the order that they appear in the text. Unlike references in *Nature,* references in the Research Notes section should conform in punctuation and arrangement to the style of recent issues of *The Biological Bulletin.* Materials and Methods should be incorporated into appropriate figure legends. See the article by Lohmann *et al.* (October 1990, Vol. **179:** 214–218) for sample style. A Research Note will usually appear within two months after its acceptance.

The Editorial Board requests that regular manuscripts conform to the requirements set below; those manuscripts that do not conform will be returned to authors for correction before review.

1. ***Manuscripts.*** Manuscripts, including figures, should be submitted in quadruplicate, with the originals clearly marked. (Xerox copies of photographs are not acceptable for review purposes.) If possible, please include an electronic copy of the text of the manuscript. Label the disk with the name of the first author and the name and version of the wordprocessing software used to create the file. If the file was not created in some version of Microsoft Word, save the text in rich text format (rtf). The submission letter accompanying the manuscript should include a telephone number, a FAX number, and (if possible) an E-mail address for the corresponding author. The original manuscript must be typed in no smaller than 12 pitch or 10 point, using double spacing (*including* figure legends, footnotes, bibliography, etc.) on one side of 16- or 20-lb. bond paper, 8 by 11 inches. Please, no right justification. Manuscripts should be proofread carefully and errors corrected legibly in black ink. Pages should be numbered consecutively. Margins on all sides should be at least 1 inch (2.5 cm). Manuscripts should conform to the *Council of Biology Editors Style Manual,* 5th Edition (Council of Biology Editors, 1983) and to American spelling. Unusual abbreviations should be kept to a minimum and should be spelled out on first reference as well as defined in a footnote on the title page. Manuscripts should be divided into the following components: Title page, Abstract (of no more than 200 words), Introduction, Materials and Methods, Results, Discussion, Acknowledgments, Literature Cited, Tables, and Figure Legends. In addition, authors should supply a list of words and phrases under which the article should be indexed.

2. ***Title page.*** The title page consists of a condensed title or running head of no more than 35 letters and spaces, the manuscript title, authors' names and appropriate addresses, and footnotes listing present addresses, acknowledgments or contribution numbers, and explanation of unusual abbreviations.

3. ***Figures.*** The dimensions of the printed page, 7 by 9 inches, should be kept in mind in preparing figures for publication. We recommend that figures be about 1 times the linear dimensions of the final printing desired, and that the ratio of the largest to the smallest letter or number and of the thickest to the thinnest line not exceed 1:1.5. Explanatory matter generally should be included in legends, although axes should always be identified on the illustration itself. Figures should be prepared for reproduction as either line cuts or halftones. Figures to be reproduced as line cuts should be unmounted glossy photographic reproductions or drawn in black ink on white paper, good-quality tracing cloth or plastic, or blue-lined coordinate paper. Those to be reproduced as halftones should be mounted on board, with both designating numbers or letters and scale bars affixed directly to the figures. All figures should be numbered in consecutive order, with no distinction between text and plate figures and cited, in order, in the text. The author's name and an arrow indicating orientation should appear on the reverse side of all figures.

Digital art: The Biological Bulletin will accept figures submitted in electronic form; however, digital art must conform to the following guidelines. Authors who create digital images are wholly responsible for the quality of their material, including color and halftone accuracy.

Format. Acceptable graphic formats are TIFF and EPS. Color submissions must be in EPS format, saved in CMKY mode.

Software. Preferred software is Adobe Illustrator or Adobe Photoshop for the Mac and Adobe Photoshop for Windows. Specific instructions for artwork created with various software programs are available on the Web at the Digital Art Information Site maintained by Cadmus Professional Communications at http://cpc.cadmus.com/da/

Resolution. The minimum requirements for resolution are 1200 DPI for line art and 300 for halftones.

Size. All digital artwork must be submitted at its actual printed size so that no scaling is necessary.

Multipanel figures. Figures consisting of individual parts (*e.g.*, panels A, B, C) must be assembled into final format and submitted as one file.

Hard copy. Files must be accompanied by hard copy for use in case the electronic version is unusable.

Disk identification. Disks must be clearly labeled with the following information: author name and manuscript number; format (PC or Macintosh); name and version of software used.

Color: The Biological Bulletin will publish color figures and plates, but must bill authors for the actual additional cost of printing in color. The process is expensive, so authors with more than one color image should—consistent with editorial concerns, especially citation of figures in order—combine them into a single plate to reduce the expense. On request, when supplied with a copy of a color illustration, the editorial staff will provide a pre-publication estimate of the printing cost.

4. ***Tables, footnotes, figure legends, etc.*** Authors should follow the style in a recent issue of *The Biological Bulletin* in preparing table headings, figure legends, and the like. Because of the high cost of setting tabular material in type, authors are asked to limit such material as much as possible. Tables, with their headings and footnotes, should be typed on separate sheets, numbered with consecutive Arabic numerals, and placed after the Literature Cited. Figure legends should contain enough information to make the figure intelligible separate from the text. Legends should be typed double spaced, with consecutive Arabic numbers, on a separate sheet at the end of the paper. Footnotes should be limited to authors' current addresses, acknowledgments or contribution numbers, and explanation of unusual abbreviations. All such footnotes should appear on the title page. Footnotes are not normally permitted in the body of the text.

5. ***Literature cited.*** In the text, literature should be cited by the Harvard system, with papers by more than two authors cited as Jones *et al.*, 1980. Personal communications and material in preparation or in press should be cited in the text only, with author's initials and institutions, unless the material has been formally accepted and a volume number can be supplied. The list of references following the text should be headed Literature Cited, and must be typed double spaced on separate pages, conforming in punctuation and arrangement to the style of recent issues of *The Biological Bulletin*. Citations should include complete titles and inclusive pagination. Journal abbreviations should normally follow those of the U. S. A. Standards Institute (USASI), as adopted by BIOLOGICAL ABSTRACTS and CHEMICAL ABSTRACTS, with the minor differences set out below. The most generally useful list of biological journal titles is that published each year by BIOLOGICAL ABSTRACTS (BIOSIS List of Serials; the most recent issue). Foreign authors, and others who are accustomed to using THE WORLD LIST OF SCIENTIFIC PERIODICALS, may find a booklet published by the Biological Council of the U.K. (obtainable from the Institute of Biology, 41 Queen's Gate, London, S.W.7, England, U.K.) useful, since it sets out the WORLD LIST abbreviations for most biological journals with notes of the USASI abbreviations where these differ. CHEMICAL ABSTRACTS publishes quarterly supplements of additional abbreviations. The following points of reference style for THE BIOLOGICAL BULLETIN differ from USASI (or modified WORLD LIST) usage:

A. Journal abbreviations, and book titles, all underlined (for *italics*)

B. All components of abbreviations with initial capitals (not as European usage in WORLD LIST *e.g., J. Cell. Comp. Physiol.* NOT *J. cell. comp. Physiol.*)

C. *All* abbreviated components must be followed by a period, whole word components *must not* (*i.e., J. Cancer Res.*)

D. Space between all components (*e.g., J. Cell. Comp. Physiol.*, not *J.Cell.Comp.Physiol.*)

E. Unusual words in journal titles should be spelled out in full, rather than employing new abbreviations invented by the author. For example, use *Rit Vísindafjélags Íslendinga* without abbreviation.

F. All single word journal titles in full (*e.g., Veliger, Ecology, Brain*).

G. The order of abbreviated components should be the same as the word order of the complete title (*i.e., Proc.* and *Trans.* placed where they appear, not transposed as in some BIOLOGICAL ABSTRACTS listings).

H. A few well-known international journals in their preferred forms rather than WORLD LIST or USASI usage (*e.g., Nature, Science, Evolution* NOT *Nature, Lond., Science, N.Y.; Evolution, Lancaster, Pa.*)

6. ***Reprints, page proofs, and charges.*** Authors may purchase reprints in lots of 100. Forms for placing reprint orders are sent with page proofs. Reprints normally will be delivered about 2 to 3 months after the issue date. Authors will receive page proofs of articles shortly before publication. They will be charged the current cost of printers' time for corrections to these (other than corrections of printers' or editors' errors). Other than these charges for authors' alterations, *The Biological Bulletin* does not have page charges.

Reference: *Biol. Bull.* **204:** 1–9. (February 2003)

Iron-Dependent Hydrogenases of *Entamoeba histolytica* and *Giardia lamblia:* Activity of the Recombinant Entamoebic Enzyme and Evidence for Lateral Gene Transfer

JULIE E. J. NIXON[1], JESSICA FIELD[1], ANDREW G. McARTHUR[2], MITCHELL L. SOGIN[2], NIGEL YARLETT[3], BRENDAN J. LOFTUS[4], AND JOHN SAMUELSON[1,*]

[1] *Department of Immunology and Infectious Diseases, Harvard School of Public Health, 665 Huntington Ave., Boston, Massachusetts;* [2] *Josephine Bay Paul Center for Comparative Molecular Biology and Evolution, Marine Biological Laboratory, Woods Hole, Massachusetts;* [3] *Department of Biochemistry, Pace University, New York, New York; and* [4] *The Institute for Genomic Research, Rockville, Maryland*

Abstract. *Entamoeba histolytica* and *Spironucleus barkhanus* have genes that encode short iron-dependent hydrogenases (Fe-hydrogenases), even though these protists lack hydrogenosomes. To understand better the biochemistry of the protist Fe-hydrogenases, we prepared a recombinant *E. histolytica* short Fe-hydrogenase and measured its activity *in vitro*. A *Giardia lamblia* gene encoding a short Fe-hydrogenase was identified from shotgun genomic sequences, and RT-PCR showed that cultured entamoebas and giardias transcribe short Fe-hydrogenase mRNAs. A second *E. histolytica* gene, which encoded a long Fe-hydrogenase, was identified from shotgun genomic sequences. Phylogenetic analyses suggested that the short Fe-hydrogenase genes of entamoeba and diplomonads share a common ancestor, while the long Fe-hydrogenase gene of entamoeba appears to have been laterally transferred from a bacterium. These results are discussed in the context of competing ideas for the origins of genes encoding fermentation enzymes of these protists.

Introduction

One of the great recent discoveries in the cell biology of protists is that the hydrogenosome of *Trichomonas vaginalis*, cause of vaginitis, is a modified mitochondrion, in which the enzymes of oxidative phosphorylation have been replaced by fermentation enzymes that produce hydrogen gas (Müller, 1993, 1998; Bui *et al.*, 1996; Horner *et al.*, 1996; Andersson and Kurland, 1999; Rotte *et al.*, 2000). Proof of this idea includes the presence of mitochondrion-like chaperones and a mitochondrion-like ATP/ADP transporter within the hydrogenosome, as well as organelle-targeting sequences at the N-termini of hydrogenosomal proteins that are encoded in the nucleus (Johnson *et al.*, 1990; Hrdy and Müller, 1995a, b; Bui *et al.*, 1996; Bui and Johnson, 1996; Horner *et al.*, 1996; Bradley *et al.*, 1997; Dyall *et al.*, 2000).

The common origin of hydrogenosomes and mitochondria is included in a new biochemical explanation for the origin of mitochondria, called the hydrogen hypothesis (Martin and Müller, 1998). The hydrogen hypothesis, a revision of the widely accepted endosymbiont hypothesis (Gray *et al.*, 1999), suggests that the α-proteobacterium, which became the mitochondrion, was a facultative anaerobe that was selected for its ability to produce hydrogen in a methanogenic archaeal host. Consistent with this idea, multiple hydrogenosomal fermentation enzymes—including ferredoxin, succinyl-CoA synthetase, and malic enzyme—resemble their counterparts in mitochondria (Johnson *et al.*, 1990; Hrdy and Müller, 1995b). One alternative hypothesis suggests that the mitochondrial endosymbiont was selected for its ability to consume oxygen and thus protect the proto-eukaryote from oxidative damage (Andersson and Kurland, 1999). Another alternative hy-

Received 20 June 2002; accepted 6 December 2002.

* To whom correspondence should be addressed. Current address: Department of Molecular and Cell Biology, Boston University Goldman School of Dental Medicine, 715 Albany St., Boston, MA 02118. E-mail: jsamuels@bu.edu

pothesis suggests that the endosymbiosis was based upon cycling of sulfur (Searcy, 1992).

An iron-dependent hydrogenase (Fe-hydrogenase), which gives the hydrogenosome its name, transfers electrons from reduced ferredoxin to two protons to make hydrogen gas (Lindmark and Müller, 1973; Müller, 1993; Payne *et al.*, 1993; Bui and Johnson, 1996; Horner *et al.*, 2000). Fe-hydrogenase activity, which is detected using hydrogen gas and methyl viologen as a reporter, has been shown in extracts of eukaryotes with hydrogenosomes or plastids (Payne *et al.*, 1993; Wunschiers *et al.*, 2001). Fe-hydrogenases, which are also present in strictly anaerobic bacteria, are designated as long or short depending upon the number of N-half ferredoxin-like domains that are adjacent to a conserved C-half hydrogenase domain (Cammark, 1992). The structures of a short Fe-hydrogenase of *Desulfovibrio desulfuricans* and a long Fe-hydrogenase of *Clostridium pasteurianum* have been solved, and each revealed two ferredoxin-like [4Fe-4S] iron-sulfur centers and a hydrogenase active-site composed of a [4Fe-4S] center bridged to a [2Fe] cluster (Peters *et al.*, 1998; Nicolet *et al.*, 1999).

The reduced ferredoxin is produced within the hydrogenosome by pyruvate:ferredoxin oxidoreductase (PFOR), which decarboxylates pyruvate to acetyl-CoA and CO_2 (Lindmark and Müller, 1973; Müller, 1993; Payne *et al.*, 1993; Hrdy and Müller, 1995a; Horner *et al.*, 1999). It has been difficult to determine the phylogeny of the genes that encode Fe-hydrogenase and PFOR, because these iron-sulfur proteins are absent from mitochondria, α-proteobacteria, and most other eubacteria. The *pfor* genes of *T. vaginalis*, *Entamoeba histolytica* (cause of amoebic dysentery), and *Giardia lamblia* (a cause of diarrhea) appear to share a common ancestry, although no bacterial donor has been identified, and a gene encoding a second keto-acid oxidoreductase of *G. lamblia* appears to have a distinct ancestry (Reeves, 1984; Hrdy and Müller, 1995a; Rosenthal *et al.*, 1997; Brown *et al.*, 1998; Müller, 1998; Horner *et al.*, 1999; Huston and Petri, 2001). The *fe-hydrogenase* genes of *T. vaginalis*, *E. histolytica*, and *Spironucleus barkhanus* (a diplomonad similar to *G. lamblia*), each of which encodes a short Fe-hydrogenase, also appear to share a common ancestry, although no bacterial donor was identified (Horner *et al.*, 2000; van Hoek *et al.*, 2000). In contrast, the long *fe-hydrogenase* gene of the microaerophilic ciliate *Nyctotherus ovalis* appears to have a distinct ancestry.

The Fe-hydrogenase results are surprising for three reasons (Horner *et al.*, 2000). First, the fermentation enzymes of *E. histolytica* and *G. lamblia* are present in the cytosol rather than in an organelle (Reeves, 1984; Müller, 1993; Brown *et al.*, 1998; Mai *et al.*, 1999; Ghosh *et al.*, 2000). Entamoebas have a mitochondrion-derived organelle called the crypton or mitosome, while the giardial gene encoding a 60-kDa chaperonin appears to be endosymbiont-derived, but no organelle has been identified (Clark and Roger, 1995; Roger *et al.*, 1998; Mai *et al.*, 1999; Tovar *et al.*, 1999; Ghosh *et al.*, 2000). Second, entamoebas and diplomonads have long been thought not to produce hydrogen gas in culture, although a recent report suggests giardias may produce hydrogen under anaerobic conditions (Lindmark and Müller, 1973; Reeves, 1984; Brown *et al.*, 1998; Müller, 1998; Lloyd and Harris, 2002). Third, short *fe-hydrogenase* genes of *E. histolytica* and *S. barkhanus* appear to share a common ancestor, even though these two protists are not closely related to each other in phylogenies drawn with rRNA or protein sequences (Sogin and Silberman, 1998; Horner *et al.*, 2000; Bapteste *et al.*, 2002). The latter result suggested the possibility of lateral transfer of *fe-hydrogenase* genes between these protists. Recent phylogenetic studies suggest that numerous genes encoding fermentation enzymes and other proteins of *E. histolytica*, *G. lamblia*, and *T. vaginalis* may have been laterally transferred from prokaryotes (Rosenthal *et al.*, 1997; Doolittle, 1998, 1999; de Koning *et al.*, 2000; Field *et al.*, 2000; Nixon *et al.*, 2002).

With the goal of understanding better the biochemistry and evolution of Fe-hydrogenases of entamoebas and diplomonads, we performed the following studies. (1) The *E. histolytica* short Fe-hydrogenase 1 was expressed as a glutathione-S-transferase (GST) fusion-protein in *E. coli*, and its activity was measured *in vitro*. (2) The *G. lamblia fe-hydrogenase* gene was identified from shotgun genomic sequences, and mRNAs encoding short Fe-hydrogenases were detected in cultured giardias and entamoebas. (3) An *E. histolytica* gene encoding a long Fe-hydrogenase 2 was identified from genomic sequences and compared with other long Fe-hydrogenases. (4) Phylogenetic analyses were repeated with the addition of Fe-hydrogenases of *G. lamblia*, *E. histolytica*, the green alga *Chlamydomonas reinhardtii*, and the eubacterium *Megasphaera elsdenii*.

Materials and Methods

Cloning of the G. lamblia fe-hydrogenase *and* E. histolytica *genes and identification of mRNAs encoding Fe-hydrogenase from cultured entamoebas and giardias.* An *E. histolytica* EST (GenBank AB002772), which encodes the N-terminus of a putative short Fe-hydrogenase 1, was identified from GenBank using BLASTP and an amebic 2[4Fe-4S] ferredoxin sequence (Altschul *et al.*, 1997; Nixon *et al.*, 2002). The 3′ end of the *E. histolytica fe-hydrogenase 1* gene was isolated using 3′ RACE (FirstChoice RLM-RACE kit, Ambion Inc., Austin, Texas), and the entire entamoebic *fe-hydrogenase 1* gene was cloned, sequenced on both strands, and deposited in GenBank under accession number AAG09783. A second *Entamoeba fe-hydrogenase* gene, which encodes a long Fe-hydrogenase, was identified from assemblies of *E. histolytica* genome sequences at The Institute for Genomic Research. The *E. histolytica fe-hydroge-*

nase 2 gene was deposited in GenBank under accession number AY172963.

A shotgun clone from the *G. lamblia* genome sequencing project, which contained the 5′ end of a putative *fe-hydrogenase* gene, was used to identify the entire *fe-hydrogenase* gene from a *G. lamblia* genomic DNA library made in Lambda Zap (McArthur *et al.*, 2000). The *G. lamblia fe-hydrogenase* gene was sequenced on both strands and deposited in GenBank under accession number AAK28337. The N-termini of predicted entamoebic and giardial Fe-hydrogenases were examined with MITOP to determine whether organelle-targeting sequences might be present (Claros and Vincens, 1996).

Total RNA was prepared by lysing cultured entamoebas and giardias in a guanidinium isothiocyanate solution and by centrifuging the lysate through a cesium chloride gradient (Chomczynski and Sacchi, 1987). Reverse-transcriptase and polymerase chain reaction (RT-PCR) were performed with these RNAs and with primers specific for the *E. histolytica* and *G. lamblia* genes encoding short Fe-hydrogenase, malic enzyme, alcohol dehydrogenase E (ADHE), and ferredoxin 1 (entamoebas only) (Rosenthal *et al.*, 1997; Nixon *et al.*, 2002). For negative controls, PCR was performed without RT, and RT-PCR products were identified on agarose gels.

Expression of a recombinant short E. histolytica *Fe-hydrogenase and measurement of its activity.* A recombinant glutathione-S-transferase (GST) fusion-protein containing a short Fe-hydrogenase at its C-terminus was made by cloning the *E. histolytica* Fe-hydrogenase 1 coding region into the pGEX-6T vector (Smith and Johnson, 1988). The GST-Fe-hydrogenase 1 construct was transfected into *Escherichia coli* strain BL21, which was grown anaerobically and induced with isopropyl β-D-thiogalactopyranoside (IPTG). Bacteria were lysed by freezing and thawing, and the hydrogenase activities of the supernatant and of purified GST-Fe-hydrogenase 1 were determined. As a negative control, the activity of bacterial lysate expressing a GST-chitinase fusion protein was measured. In a septum-sealed cuvette, Fe-hydrogenase 1 activity was examined by incubation with 10 m*M* methyl viologen in 50 m*M* Tris-HCl (pH 8.0) and 5 m*M* dithioreitol, which had been bubbled with hydrogen for 15 min (Payne *et al.*, 1993). Reduction of methyl viologen was monitored at 600 nm. A negative control was bubbled with nitrogen instead of hydrogen.

We also measured Fe-hydrogenase activity from lysates of cultures of non-transformed *T. vaginalis* and from *E. histolytica* that had been transformed with a plasmid containing the entamoebic *fe-hydrogenase 1* gene under an *actin* gene promoter (Ghosh *et al.*, 2000). This construct was previously used to demonstrate the cytosolic location of the entamoebic Fe-hydrogenase 1.

Phylogenetic analyses. Amino acid sequences homologous to the *G. lamblia* and *E. histolytica* Fe-hydrogenases, which were identified in the nonredundant and unfinished microbial databases of GenBank using BLASTP and TBLASTN, respectively, were aligned using CLUSTALW (Thompson *et al.*, 1994; Altschul *et al.*, 1997). The alignment was adjusted manually using the SEQLAB program (Genetics Computer Group, Madison, Wisconsin). Regions that could not be unambiguously aligned were excluded, leaving 351 aligned amino acid positions for use in phylogenetic analyses. Phylogenetic analyses were performed using distance and parsimony methods by the computer programs TREE-PUZZLE (Strimmer and von Haeseler, 1996) and PHYLIP (Felsenstein, 1989). Pairwise distances were computed using TREE-PUZZLE under the Dayhoff model (Dayhoff *et al.*, 1978), with the inclusion of observed amino acid frequencies, estimated proportion of invariant sites, and estimation of among-site variation for the remaining sites according to a gamma distribution (four discrete categories). The optimal tree was inferred using the Fitch-Margoliash algorithm (Fitch and Margoliash, 1967), using the Fitch program, with global rearrangements and 100 random-addition replicates. Bootstrap values were obtained, using the 100 resampled datasets, under the same model using the PUZZLEBOOT program (available at http://www.tree-puzzle.de). The optimal tree under parsimony and related bootstrap values were determined using PHYLIP's PROTPARS program for parsimony.

Results and Discussion

A recombinant short Fe-hydrogenase 1 of E. histolytica *is active.* The amino-terminus of the *E. histolytica* Fe-hydrogenase 1 did not contain an organelle-targeting sequence (Claros and Vincens, 1996; Horner *et al.*, 2000). Indeed, an epitope-tagged Fe-hydrogenase 1 is present within the cytosol of transfected *E. histolytica* (Ghosh *et al.*, 2000). The activity of the entamoebic Fe-hydrogenase 1 was measured in lysates of *E. coli*, which were expressing a GST-entamoebic Fe-hydrogenase 1 fusion-enzyme (Table 1) (Smith and Johnson, 1988). The activity of the recombinant entamoebic Fe-hydrogenase 1 was present when hydrogen was bubbled into the medium but absent when nitrogen (negative control) was bubbled into the medium (Payne *et al.*, 1993). There was no Fe-hydrogenase activity in control *E. coli*, which were overexpressing a GST-chitinase fusion-protein. Recombinant entamoebic Fe-hydrogenase 1, which was purified on glutathione-agarose beads, had a decreased specific activity (data not shown). This was likely caused by exposure to oxygen during the purification procedure that probably inactivated the Fe-hydrogenase 1 iron-sulfur centers (Cammark, 1992; Payne *et al.*, 1993; Horner *et al.*, 2000). The specific activity of the GST-Fe-hydrogenase 1 fusion enzyme was about 10 times that of the native entamoebic Fe-hydrogenase 1 overexpressed in transfected *E. histolytica* (Table 1). Interestingly, the specific activity of

Table 1

Activities of Entamoeba histolytica *and* Trichomonas vaginalis *Fe-hydrogenases*

Sample	Hydrogenase activity (nmol/min/mg of protein)[a]
Bacteria transformed with *E. histolytica* Fe-hydrogenase	36 (2)
Transfected *E. histolytica* with Fe-hydrogenase	3.5 ± 0.7 (3)
Trichomonas vaginalis	167 ± 32 (9)
T. vaginalis + 0.47 mg *E. histolytica* lysate[b]	114 (2)

[a] Averages +/− standard deviations, where possible. Number of determinations in parentheses.

[b] Calculated K_i = 0.56 mg (amount of *E. histolytica* lysate in mg of protein to cause 50% reduction of *T. vaginalis* hydrogenase activity).

the *T. vaginalis* Fe-hydrogenase was greater than that of the recombinant entamoebic GST-entamoebic Fe-hydrogenase and was inhibited by a lysate of non-transfected entamoebas (Table 1). This may explain why it was difficult to detect Fe-hydrogenase activity in lysates of nontransfected entamoebas, even though Fe-hydrogenase 1 mRNAs were identified from them by RT-PCR (next section).

Cultured entamoebas and giardias express mRNAs encoding short Fe-hydrogenases. We isolated an *fe-hydrogenase* gene of *G. lamblia*, because we have frequently compared the fermentation enzymes of this diplomonad with those of *E. histolytica* (Rosenthal *et al.*, 1997; Field *et al.*, 2000; Nixon *et al.*, 2002). A search of the contigs predicted from the *G. lamblia* shogun sequences suggested that this gene, which predicts a short Fe-hydrogenase, is the only hydrogenase gene present within the giardial genome. Like the entamoebic Fe-hydrogenase 1, the predicted giardial Fe-hydrogenase lacked an N-terminal organelle-targeting sequence and had two ferredoxin-like iron-sulfur centers and a hydrogenase iron-sulfur center like those present in the short Fe-hydrogenases of *T. vaginalis*, *Desulfovibrio* sp., and *Clostridia* sp. (Cammark, 1992; Thompson *et al.*, 1994; Bui and Johnson, 1996; Horner *et al.*, 1996; Nicolet *et al.*, 1999). RT-PCR showed that cultured entamoebas and giardias contain mRNAs, which encode short Fe-hydrogenases (Fig. 1A, B). Negative controls without RT showed that the RT-PCR was not amplifying DNA from the extracts of cultured entamoebas and giardias. Because the giardial contigs predicted only one Fe-hydrogenase, which is expressed, it is likely that the hydrogenase activity recently detected in cultures of giardias derives from this enzyme (Lloyd and Harris, 2002). In contrast, entamoebas appear to have a second long hydrogenase (see next section), so if entamoebic hydrogenase activity is present, it might derive from one or more enzymes. These results suggest the possibility that entamoebas and giardias use protons as electron acceptors

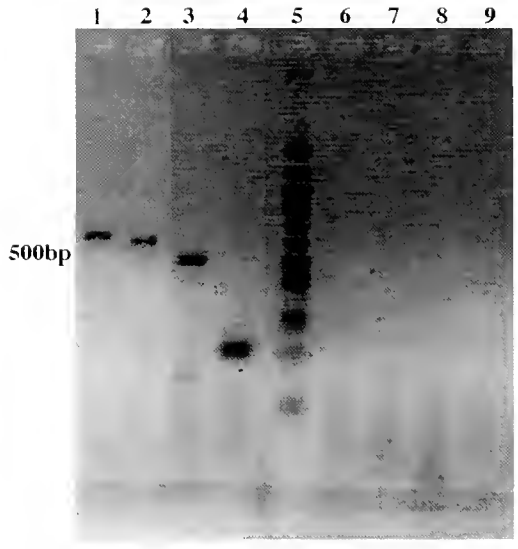

A

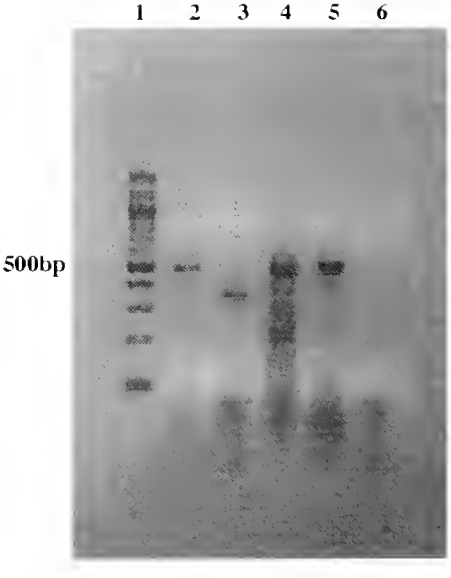

B

Figure 1. Agarose gels of ethidium-stained RT-PCR products from entamoebic and giardial mRNAs. Images are reversed for clarity of reproduction. (A) RT-PCR of amoebic mRNAs encoding malic enzyme (lane 1), Fe-hydrogenase (lane 2), alcohol dehydrogenase E (lane 3), and ferredoxin (lane 4). Size markers are shown in lane 5. Lanes 6–9 are the negative controls for malic enzyme, hydrogenase, ADHE, and ferredoxin, respectively. (B) RT-PCR of giardial mRNAs encoding ADHE (lane 3), Fe-hydrogenase (lane 4), and malic enzyme (lane 5). A negative control (no RT) for Fe-hydrogenase is shown in lane 6. A positive control for Fe-hydrogenase, using *Giardia lamblia* WB strain DNA, is shown in lane 2. Size markers are shown in lane 1.

```
Eh2  MSTQLTPLRNKIISEVVKCFKSGRFIEDIDKLPTILTDGDGWKPTSKFVHSREQEEGIYR
Td           IKREILVRIAKLQFEGKLQEGVHYIPREMVPRN.STPI.RCCIFHDR..EIMR
Bf           VRHKLLAKLVNLWKENKLTNEIDRLPIELSPRR.SRPLGRCCIHKER..AVYK

Eh2  EKVLSVLGF.VDGEYDDITPLHVYAQKALERT.SLHEPVFGISQKGCNKCHFNGYFVTQA
Td   HRVIARLGCSLENYDEEKT.LAQFAKEALERE.KPTWPMLTVLDEACNACVKSKYMITNA
Bf   YKLFPLLGFDMTDETDELTSLSEYARQALERKNKQKENILCVIDEACSSCVQVNYEVTNL
                                                      *  *

Eh2  CEGCTSRPCSVNCPKKCISFGEDGRAVINQNNCIKCGRCYKFCPYGAIISKSVPCVKACP
Td   CQACVARPCMMNCPKTAIAIS.GGRARIDEEKCINCGICLKNCPYHAVIKIPVPCEEACP
Bf   CRGCVARSCYMNCPKDAIRFRKNGQAKIDHDACISCGKCHQSCPYHAIVFIPVPCEEACP
     *  *    *   *                        x  x  x   x           *   *

Eh2  CGAMLDSPEGVKTIDFEKCINCGGCMRACPFGAILPRSNLIDVLK.ILPTKKVVACPAPS
Td   VGAISKDENGKERIDYHKCIFCGNCMRECPFGAMMDKGQIVDVIKHLMSGKKVSALYAPA
Bf   VKAISKDENGIEHIDESKCIYCGKCLNACPFGAIFEISQAFDVLEGIRSGEKMIAIPAPS
                         x  x  x   x

Eh2  IAAHFGKYDLALVSGGLIQVGFTSVEDVSYGADLCALNEAKEFEERIVKNKKDFMTTSCC
Td   VAAQF.KAVPGQLESALKKAGFNKVWEVAIGADITADREASEFEERMEHGHI.LMTTSCC
Bf   ILGQF.NTSIEAVYGALRQMGFADVVEVAQGAMDTVSHEAAELKEKLEEGQP.FMTTSCC
                                                          o

Eh2  PAYINAINKHMPELKENVSHTPTPMHFATQAVKDRDQETVTVFIGPCNAKRWETLQDSTT
Td   PAYVRAVKKHVPALVPCISDTRSPMHYTAELAKKEDPDCVTVFIGPCLAKRREGLEDEFV
Bf   PSYIELVNKHIPGMKPYVSSTGSPMYYAARIAKERHPDAKIVFIGPCVAKRKEARRDECV
                                                    o

Eh2  DYCLTFDEIFGLFEGSGIDLSKVQPYTFVDKAHKEGKIFAVSGGVASAVASLLPKEVPDG
Td   DYVLSIEELGALLTAKEIDISKEEALPGKITPTSSGRGFAASGGVAEAVRVRL.KKPEN.
Bf   DYILTFEEMASIFEGLDIQLEQTQPFSVLYTSVREAHGFAQAGGVMGAIKAYLGEEAKK.

Eh2  VIKPTIIDGFSQENFKRLKNFKKNI.........TGNLVEVMVCEGGCAYGPGCPGLNTP
Td   .LRPVLINGLNKEGMKQLASYGKIQSGELPHDSSTPNLVEVMSCEGGCIGGP
BF   .FSAIQVSDLNKKNIGLLRAAAKTG.......KAQGQFIEVMACEGGCISGP
                                                    o   o

Eh2  ATSAKIKIAVDKMEAHPEGRWVGLPNSQIKPIKVEN 504
```

Figure 2. Alignment of the predicted *Entamoeba histolytica* long Fe-hydrogenase 2 (Eh2) with predicted long Fe-hydrogenases of *Treponema denticola* (Td) and *Bacteroides fragilis* (Bf). Conserved Cys residues, which are shaded, include those that coordinate putative [4Fe-4S] iron-sulfur centers (marked with x's) and those that coordinate putative hydrogenase iron-sulfur centers (marked with o's). Other conserved Cys residues, which may be involved in coordinating iron-sulfur centers, are marked with asterisks. Amino acids at the beginning and end of the conserved Fe-hydrogenase domain are underlined.

when the organisms are growing under strictly anaerobic conditions in the bowel lumen (Brown *et al.*, 1998; Huston and Petri, 2001; Lloyd and Harris, 2002).

E. histolytica *has a* hydrogenase 2 *gene encoding a long Fe-hydrogenase.* The assemblies of the shotgun sequences of the *E. histolytica* genome predicted a long Fe-hydrogenase 2 (Fig. 2) in addition to the short Fe-hydrogenase 1. The entamoebic Fe-hydrogenase 2 was 504 amino acids long and had an N-terminal sequence, which included positively charged Lys and Arg that are often present at the N-termini of organellar proteins (Claros and Vincens, 1996). In addition, the N-terminus of Fe-hydrogenase 2 contained Ser and Leu residues, which are present at the N-termini of crypton and hydrogenosomal proteins (Bui *et al.*, 1996; Mai *et al.*, 1999). However, in the absence of experimental evidence, we cannot be sure that the entamoebic long Fe-hydrogenase is targeted to the crypton.

The entamoebic Fe-hydrogenase 2 was much more similar (>38% amino acid identities) to predicted long Fe-hydrogenases of *Bacteroides fragilis* and *Treponema denticola* than to short Fe-hydrogenases of entamoebas, giardias, trichomonads, and other anaerobic bacteria (<28% amino acid identities; Fig. 2). The entamoebic Fe-hydrogenase 2 and the predicted long Fe-hydrogenases of *B. fragilis*

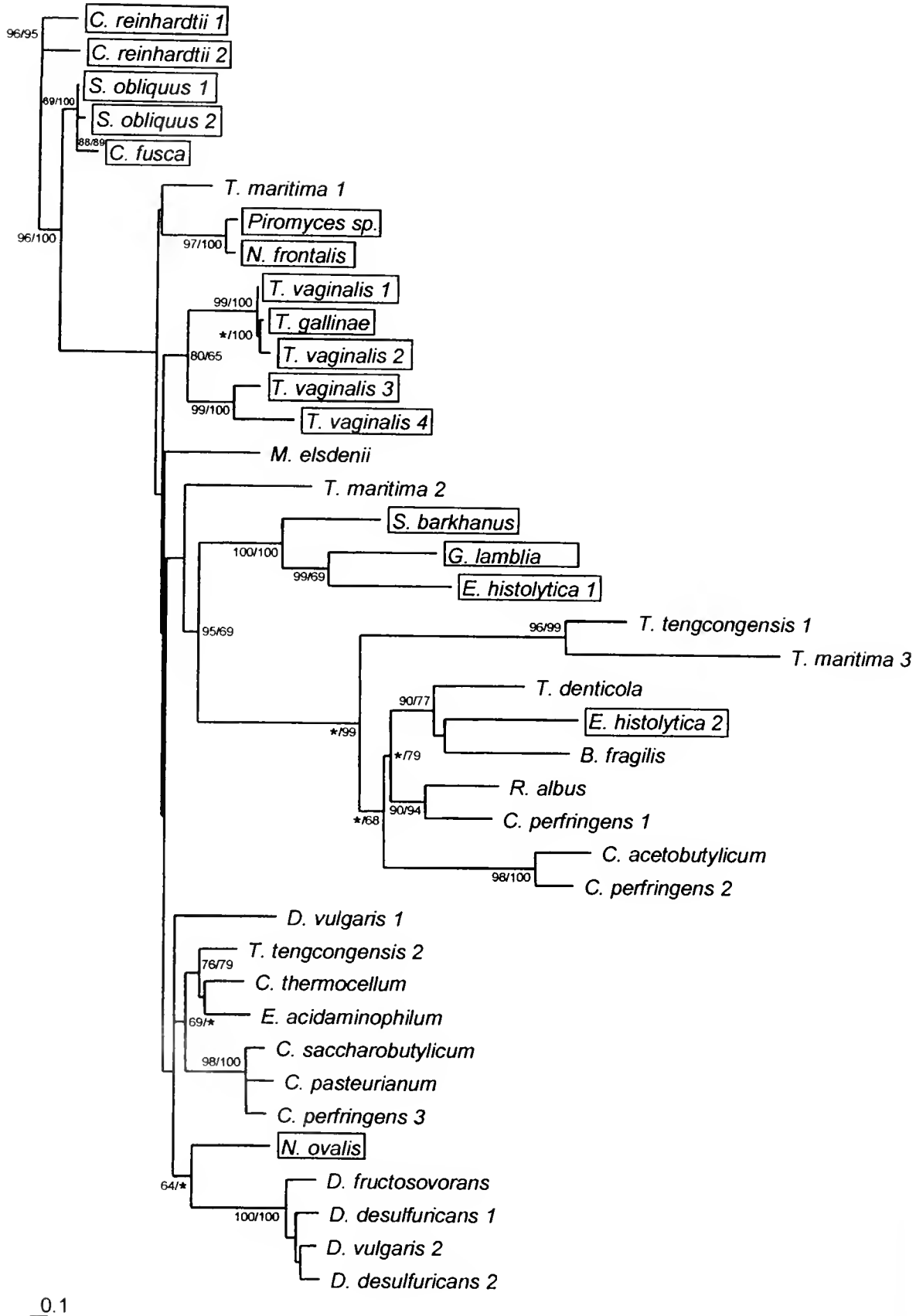
C. reinhardtii 1
C. reinhardtii 2
S. obliquus 1
S. obliquus 2
C. fusca
T. maritima 1
Piromyces sp.
N. frontalis
T. vaginalis 1
T. gallinae
T. vaginalis 2
T. vaginalis 3
T. vaginalis 4
M. elsdenii
T. maritima 2
S. barkhanus
G. lamblia
E. histolytica 1
T. tengcongensis 1
T. maritima 3
T. denticola
E. histolytica 2
B. fragilis
R. albus
C. perfringens 1
C. acetobutylicum
C. perfringens 2
D. vulgaris 1
T. tengcongensis 2
C. thermocellum
E. acidaminophilum
C. saccharobutylicum
C. pasteurianum
C. perfringens 3
N. ovalis
D. fructosovorans
D. desulfuricans 1
D. vulgaris 2
D. desulfuricans 2
96/95
69/100
88/89
96/100
97/100
99/100
*/100
80/65
99/100
100/100
99/69
95/69
96/99
90/77
*/99
*/79
90/94
*/68
98/100
76/79
69/*
98/100
64/*
100/100
0.1

and *T. denticola* each contained Cys residues that likely coordinate two ferredoxin-like [4Fe-4S] iron-sulfur centers (marked with x's in Fig. 2) and hydrogenase iron-sulfur centers (marked with o's), which have previously been identified in structures of short and long Fe-hydrogenases (Peters *et al.*, 1998; Nicolet *et al.*, 1999). In addition, the predicted entamoebic Fe-hydrogenase 2 had eight other N-terminal Cys residues, which aligned with those of the bacteroides and treponema long Fe-hydrogenases (marked with asterisks). Although these Cys residues probably coordinate other iron-sulfur centers, they remain unidentified, because they do not align with the N-terminal iron-sulfur centers of the long Fe-hydrogenase of *C. pasteurianum*, which has been crystallized (Peters *et al.*, 1998).

The entamoebic and giardial short fe-hydrogenase 1 *genes appear to share a common ancestry, while the entamoebic long* fe-hydrogenase 2 *gene appears to have been laterally transferred from a prokaryote.* Phylogenetic trees of Fe-hydrogenases from eubacteria and eukaryotes are star-shaped and contain few basal nodes that are strongly supported (Fig. 3). This result suggests that the Fe-hydrogenases are widely divergent and that little phylogenetic signal remains. For example, Fe-hydrogenases of closely related eukaryotes—either trichomonads, green algae (*Chlamydomonas reinhardtii*, *Scenedesmus obliquus*, and *Chlorella fusca*), or chytrid fungi (*Piromyces* sp. and *Neocallimastix frontalis*)—each grouped together, but Fe-hydrogenases of unrelated eukaryotes did not group together. In particular, our analysis does not support recent conclusions that hydrogenases of trichomonads are monophyletic with those of chytrid fungi (Voncken *et al.*, 2002) or with those of *E. histolytica* and *S. barkhanus* (Horner *et al.*, 2000).

The short *fe-hydrogenase* genes of *G. lamblia*, *S. barkhanus*, and *E. histolytica* appear to share a most recent common ancestry, although a particular bacterial donor was not identified. Remarkably, the short Fe-hydrogenase of *G. lamblia* was more similar to that of *E. histolytica* than to that of *S. barkhanus*. Because *G. lamblia* and *S. barkhanus* are diplomonads, which share a recent common ancestor in phylogenetic trees of rRNA and proteins (Sogin and Silberman, 1998), a possible explanation of these results is that the *E. histolytica fe-hydrogenase* gene was laterally transferred from a diplomonad (Rosenthal *et al.*, 1997; Doolittle, 1998, 1999; Müller, 1998; de Koning *et al.*, 2000; Field *et al.*, 2000; Nixon *et al.*, 2002). This lateral gene transfer would not have occurred recently, because the Fe-hydrogenases of entamoebas and giardias showed only a 40% amino acid identity with each other, and each *fe-hydrogenase* gene has the codon usage of its host. Alternatively, the diplomonad-*E. histolytica* sub-clade could be incorrectly rooted by the long branch connecting it to the remainder of the tree.

The common ancestry of genes encoding the *E. histolytica* long Fe-hydrogenase 2 and those of *B. fragilis* and *T. denticola* is strongly supported. This appears then to be an example of lateral gene transfer, as *Entamoeba* is not a close relative of either of these eubacteria (Rosenthal *et al.*, 1997; Doolittle, 1998, 1999; Müller, 1998; de Koning *et al.*, 2000; Field *et al.*, 2000; Nixon *et al.*, 2002). There was weak support for the pairing of Fe-hydrogenases of the ciliate *N. ovalis* and *Desulfovibrio* sp., as has been previously noted (Horner *et al.*, 2000; Voncken *et al.*, 2002). This suggests that the ciliate hydrogenase was derived by lateral gene transfer, but does not prove it.

Conclusions

This is the first time that an Fe-hydrogenase from a protist has been expressed as a GST-fusion protein in bacteria. This is also the first time that an *fe-hydrogenase* gene (encoding the long hydrogenase of entamoebas) has been inferred to have been laterally transferred from a bacterium, although numerous genes encoding fermentation enzymes (*e.g.*, alcohol dehydrogenases, malic enzyme, and acetyl-CoA syn-

Figure 3. Phylogenetic relationships of Fe-hydrogenases, inferred using a distance matrix generated by the Dayhoff+1+Γ model and the Fitch-Margoliash algorithm. Bootstrap values obtained using PUZZLEBOOT and PROTPARS, respectively, are shown at the relevant nodes. Bootstrap values below 50% are marked with an asterisk if the other bootstrap value is >50%. If both bootstrap values are below 50%, neither is marked. The scale bar indicates estimated sequence divergence per unit branch length. Sequences from eukaryotes, which are boxed, were from *Chlamydomonas reinhardtii* 1 and 2 [accession # 16945126 and 18026272]; *Chlorella fusca* [21732235]; *Entamoeba histolytica* 1 and 2 [9963974 and AY172963]; *Giardia lamblia* [13506793]; *Neocallimastix frontalis* [19547863]; *Nyctotherus ovalis* [4034791]; *Piromyces sp.* [19548180]; *Scenedesmus obliquus* 1 and 2 [12581498 and 13311187]; *Spironucleus barkhanus* [11127703]; *Trichomonas gallinae* [19548182]; *Trichomonas vaginalis* 1, 2, 3, and 4 [19547859, 11127701, 1171117, and 1345094]. Eubacterial sequences were from *Bacteroides fragilis* [unfinished microbial database]; *Clostridium acetobutylicum* [15896476]; *Clostridium pasteurianum* [557064]; *Clostridium perfringens* 1, 2, and 3 [18311557, 18309258, and 18311328]; *Clostridium saccharobutylicum* [488597]; *Clostridium thermocellum* [4927278]; *Desulfovibrio fructosovorans* [1914864]; *Desulfovibrio desulfuricans* 1 and 2 [4930044 and 13022069]; *Desulfovibrio vulgaris* 1 and 2 [97381 and 66319, respectively]; *Eubacterium acidominophilum* [14250935]; *Megasphaera elsdenii* [6650985]; *Ruminococcus albus* [unfinished microbial database]; *Thermoanaerobacter tengcongensis* 1 and 2 [20807184 and 20515894]; *Thermotoga maritima* 1, 2, and 3 [15644177, 7433127, and 4981985]; and *Treponema denticola* [unfinished microbial database].

thases) appear to have been laterally transferred from prokaryotes to amoebas and giardias (Rosenthal *et al.*, 1997; Field *et al.*, 2000; Nixon *et al.*, 2002). Although the evidence is weak, this may also be the first time that a gene (encoding the short hydrogenase of entamoebas) has been inferred to have been laterally transferred from another protist. Because the hypothesized lateral gene transfer would probably have occurred after the acquisition of the *fe-hydrogenase* gene by the diplomonad lineage, this particular result does not disprove the hydrogen hypothesis (Martin and Müller, 1998). However, the failure to demonstrate that the eukaryotic Fe-hydrogenases share a common ancestry, or to identify an α-proteobacterial donor for these eukaryotic *fe-hydrogenase* genes (Horner *et al.*, 2000), dampens our enthusiasm for the hydrogen hypothesis. These results suggest that the mitochondrial endosymbiont was selected for a property other than hydrogen production (*e.g.*, its ability to consume oxygen) (Andersson and Kurland, 1999) and that the presence of Fe-hydrogenases and other fermentation enzymes of microaerophilic eukaryotes may reflect a secondary adaptation to their anaerobic environment (Rosenthal *et al.*, 1997; Doolittle, 1998, 1999; de Koning *et al.*, 2000; Field *et al.*, 2000; Lloyd and Harris, 2002; Nixon *et al.*, 2002).

Acknowledgments

This work was supported by NIH grants (AI33492 to J.S., AI43273 to M.L.S., and AI46516 to B.J.L.).

Literature Cited

Altschul, S. F., T. L. Madden, A. A. Schaffer, J. Zhang, Z. Zhang, W. Miller, and D. J. Lipman. 1997. Gapped BLAST and PSI-BLAST: a new generation of protein database search programs. *Nucleic Acids Res.* **25:** 3389–3402.

Andersson, S. G., and C. G. Kurland. 1999. Origins of mitochondria and hydrogenosomes. *Curr. Opin. Microbiol.* **2:** 535–541.

Bapteste, E., H. Brinkmann, J. A. Lee, D. V. Moore, C. W. Sensen, P. Gordon, L. Durufle, T. Gaasterland, P. Lopez, M. Müller, and H. Philippe. 2002. The analysis of 100 genes supports the grouping of three highly divergent amoebae: *Dictyostelium, Entamoeba,* and *Mastigamoeba. Proc. Natl. Acad. Sci. USA* **99:** 1414–1419.

Bradley, P. J., C. J. Lahti, E. Plumper, and P. J. Johnson. 1997. Targeting and translocation of proteins into the hydrogenosome of the protist *Trichomonas:* similarities with mitochondrial protein import. *EMBO J.* **16:** 3484–3493.

Brown, D. M., J. A. Upcroft, M. R. Edwards, and P. Upcroft. 1998. Anaerobic bacterial metabolism in the ancient eukaryote *Giardia duodenalis. Int. J. Parasitol.* **28:** 149–164.

Bui, E. T., and P. J. Johnson. 1996. Identification and characterization of [Fe]-hydrogenases in the hydrogenosome of *Trichomonas vaginalis. Mol. Biochem. Parasitol.* **76:** 305–310.

Bui, E. T., P. J. Bradley, and P. J. Johnson. 1996. A common evolutionary origin for mitochondria and hydrogenosomes. *Proc. Natl. Acad. Sci. USA* **93:** 9651–9656.

Cammark, R. 1992. Iron-sulfur clusters in enzymes: themes and variations. *Adv. Inorg. Chem.* **38:** 281–322.

Choczynski, P., and N. Sacchi. 1987. Single-step method of RNA isolation by acid guanidinium-thiocyanate-phenol-chloroform extraction. *Anal. Biochem.* **162:** 156–159.

Clark, C. G., and A. J. Roger. 1995. Direct evidence for secondary loss of mitochondria in *Entamoeba histolytica. Proc. Natl. Acad. Sci. USA* **92:** 6518–6521.

Claros, M. G., and P. Vincens. 1996. Computational method to predict mitochondrially imported proteins and their targeting sequences. *Eur. J. Biochem.* **241:** 779–786.

Dayhoff, M. O., R. M. Schwartz, and B. C. Orcutt. 1978. Pp. 345–352 in *Atlas of Protein Sequence and Structure,* Vol. 5, suppl. 3. National Biomedical Research Foundation, Silver Spring, MD.

de Koning, A. P., F. S. Brinkman, S. J. Jones, and P. J. Keeling. 2000. Lateral gene transfer and metabolic adaptation in the human parasite *Trichomonas vaginalis. Mol. Biol. Evol.* **17:** 1769–1773.

Doolittle, W. F. 1998. You are what you eat: a gene transfer ratchet could account for bacterial genes in eukaryotic nuclear genomes. *Trends Genet.* **14:** 307–311.

Doolittle, W. F. 1999. Phylogenetic classification and the universal tree. *Science* **284:** 2124–2129.

Dyall, S. D., C. M. Koehler, M. G. Delgadillo-Correa, P. J. Bradley, E. Plumper, D. Leuenberger, C. W. Turck, and P. J. Johnson. 2000. Presence of a member of the mitochondrial carrier family in hydrogenosomes: conservation of membrane-targeting pathways between hydrogenosomes and mitochondria. *Mol. Cell. Biol.* **20:** 2488–2497.

Felsenstein, J. 1989. PHYLIP-phylogeny inference package (version 3.2). *Cladistics* **5:** 164–166.

Field, J., B. Rosenthal, and J. Samuelson. 2000. Early lateral transfer of genes encoding malic enzyme, acetyl-CoA synthetase and alcohol dehydrogenases from anaerobic prokaryotes to *Entamoeba histolytica. Mol. Microbiol.* **38:** 446–455.

Fitch, W. M., and E. Margoliash. 1967. Construction of phylogenetic trees. *Science* **155:** 279–284.

Ghosh, S., J. Field, R. Rogers, M. Hickman, and J. Samuelson. 2000. The *Entamoeba histolytica* mitochondrion-derived organelle (crypton) contains double-stranded DNA and appears to be bound by a double membrane. *Infect. Immun.* **68:** 4319–4322.

Gray, M. W., G. Burger, and B. F. Lang. 1999. Mitochondrial evolution. *Science* **283:** 1476–1481.

Horner, D. S., R. P. Hirt, S. Kilvington, D. Lloyd, and T. M. Embley. 1996. Molecular data suggest an early acquisition of the mitochondrion endosymbiont. *Proc. R. Soc. Lond. B. Biol. Sci.* **263:** 1053–1059.

Horner, D. S., R. P. Hirt, and T. M. Embley. 1999. A single eubacterial origin of eukaryotic pyruvate: ferredoxin oxidoreductase genes: implications for the evolution of anaerobic eukaryotes. *Mol. Biol. Evol.* **16:** 1280–1291.

Horner, D. S., P. G. Foster, and T. M. Embley. 2000. Iron hydrogenases and the evolution of anaerobic eukaryotes. *Mol. Biol. Evol.* **17:** 1695–1709.

Hrdy, I., and M. Müller. 1995a. Primary structure and eubacterial relationships of the pyruvate:ferredoxin oxidoreductase of the amitochondriate eukaryote *Trichomonas vaginalis. J. Mol. Evol.* **41:** 388–396.

Hrdy, I., and M. Müller. 1995b. Primary structure of the hydrogenosomal malic enzyme of *Trichomonas vaginalis* and its relationship to homologous enzymes. *J. Eukaryot. Microbiol.* **42:** 593–603.

Huston, C. D., and W. A. Petri. 2001. Emerging and reemerging intestinal protozoa. *Curr. Opin. Gastroenterol.* **17:** 17–23.

Johnson, P. J., C. E. d'Oliveira, T. E. Gorrell, and M. Müller. 1990. Molecular analysis of the hydrogenosomal ferrédoxin of the anaerobic protist *Trichomonas vaginalis. Proc. Natl. Acad. Sci. USA* **87:** 6097–6101.

Lindmark, D. G., and M. Müller. 1973. Hydrogenosome, a cytoplasmic organelle of the anaerobic flagellate *Trichomonas foetus,* and its role in pyruvate metabolism. *J. Biol. Chem.* **248:** 7724–7728.

Lloyd, D., and J. C. Harris. 2002. *Giardia:* highly evolved parasite or early branching eukaryote? *Trends Microbiol.* **10:** 122–127.

Mai, Z., S. Ghosh, M. Frisardi, B. Rosenthal, R. Rogers, and J. Samuelson. 1999. Hsp60 is targeted to a cryptic mitochondrion-derived organelle (crypton) in the microaerophilic protozoan parasite *Entamoeba histolytica*. *Mol. Cell. Biol.* **19:** 2198–2205.

Martin, W., and M. Müller. 1998. The hydrogen hypothesis for the first eukaryote. *Nature* **392:** 37–41.

McArthur, A. G., H. G. Morrison, J. E. Nixon, N. Q. Passamaneck, U. Kim, G. Hinkle, M. K. Crocker, M. E. Holder, R. Farr, C. I. Reich, G. E. Olsen, S. B. Aley, R. D. Adam, F. D. Gillin, and M. L. Sogin. 2000. The *Giardia* genome project database. *FEMS Microbiol. Lett.* **189:** 271–273.

Müller, M. 1993. The hydrogenosome. *J. Gen. Microbiol.* **139:** 2879–2889.

Müller, M. 1998. Enzymes and compartmentation of core energy metabolism of anaerobic protist—a special case in eukaryotic evolution. Pp. 109–127 in *Evolutionary Relationships among Protozoa*, G. H. Coombs, K. Vickerman, M. A. Sleigh, and A. Warren, eds. Kluwer Academic, London.

Nicolet, Y., C. Piras, P. Legrand, C. E. Hatchikian, and J. C. Fontecilla-Camps. 1999. *Desulfovibrio desulfuricans* iron hydrogenase: the structure shows unusual coordination to an active site Fe binuclear center. *Struct. Fold. Des.* **7:** 13–23.

Nixon, J. E. J., A. Wang, J. Field, H. G. Morrison, A. G. McArthur, M. L. Sogin, B. Loftus, and J. Samuelson. 2002. Evidence for lateral transfer of genes encoding ferredoxins, nitroreductases, NADH oxidase and alcohol dehydrogenase 3 from anaerobic prokaryotes to *Giardia lamblia* and *Entamoeba histolytica*. *Euk. Cell* **1:** 181–190.

Payne, M. J., A. Chapman, and R. Cammack. 1993. Evidence for an [Fe]-type hydrogenase in the parasitic protozoan *Trichomonas vaginalis*. *FEBS Lett.* **317:** 101–104.

Peters, J. W., W. N. Lanzilotta, B. J. Lemon, and L. C. Seefeldt. 1998. X-ray crystal structure of the Fe-only hydrogenase (CpI) from *Clostridium pasteurianum* to 1.8 angstrom resolution. *Science* **282:** 1853–1858.

Reeves, R. E. 1984. Metabolism of *Entamoeba histolytica* Scandinn, 1903. *Adv. Parasitol.* **23:** 105–142.

Roger, A. J., S. G. Svard, J. Tovar, C. G. Clark, M. W. Smith, F. D. Gillin, and M. L. Sogin. 1998. A mitochondrial-like chaperonin 60 gene in *Giardia lamblia:* evidence that diplomonads once harbored an endosymbiont related to the progenitor of mitochondria. *Proc. Natl. Acad. Sci. USA* **95:** 229–234.

Rosenthal, B., Z. Mai, D. Caplivski, S. Ghosh, H. de la Vega, T. Graf, and J. Samuelson. 1997. Evidence for the bacterial origin of genes encoding fermentation enzymes of the amitochondriate protozoan parasite *Entamoeba histolytica*. *J. Bacteriol.* **179:** 3736–3745.

Rotte, C., K. Henze, M. Müller, and W. Martin. 2000. Origins of hydrogenosomes and mitochondria. *Curr. Opin. Microbiol.* **3:** 481–486.

Searcy, D. G. 1992. Origins of mitochondria and chloroplasts from sulfur based symbiosis. Pp. 47–78 in *The Origin and Evolution of the Cell*, H. Hartman and K. Matsuna, eds. World Scientific, London.

Smith, D. B., and K. S. Johnson. 1988. Single-step purification of polypeptides expressed in *Escherichia coli* as fusions with glutathione S-transferase. *Gene* **67:** 31–40.

Sogin, M. L., and J. D. Silberman. 1998. Evolution of the protists and protistan parasites from the perspective of molecular systematics. *Int. J. Parasitol.* **28:** 11–20.

Strimmer, K., and A. von Haeseler. 1996. Quartet puzzling: a quarter maximum likelihood method for reconstructing tree topologies. *Mol. Biol. Evol.* **13:** 964–969.

Thompson, J. D., D. G. Higgins, and T. J. Gibson. 1994. CLUSTAL W: improving the sensitivity of progressive multiple sequence alignment through sequence weighting, position-specific gap penalties and weight matrix choice. *Nucl. Acids Res.* **22:** 4673–4680.

Tovar, J., A. Fischer, and C. G. Clark. 1999. The mitosome, a novel organelle related to mitochondria in the amitochondrial parasite *Entamoeba histolytica*. *Mol. Microbiol.* **32:** 1013–1021.

van Hoek, A. H., A. S. Akhmanova, M. A. Huynen, and J. H. Hackstein. 2000. A mitochondrial ancestry of the hydrogenosomes of *Nyctotherus ovalis*. *Mol. Biol. Evol.* **17:** 202–206.

Voncken, F. G., B. Boxma, A. H. van Hoek, A. S. Akhmanova, G. D. Vogels, M. Huynen, M. Veenhuis, and J. H. Hackstein. 2002. A hydrogenosomal [Fe]-hydrogenase from the anaerobic chytrid *Neocallimastix sp. L2*. *Gene* **284:** 103–112.

Wunschiers, R., K. Stangier, H. Senger, and R. Schulz. 2001. Molecular evidence for a Fe-hydrogenase in the green alga *Scenedesmus obliquus*. *Curr. Microbiol.* **42:** 353–360.

Reference: *Biol. Bull.* **204:** 10–20. (February 2003)

Molecular Genetic Evidence that Dinoflagellates Belonging to the Genus *Symbiodinium* Freudenthal Are Haploid

SCOTT R. SANTOS* AND MARY ALICE COFFROTH‡

Department of Biological Science, State University of New York at Buffalo, Buffalo, New York 14260-1300

Abstract. Microscopic and cytological evidence suggest that many dinoflagellates possess a haploid nuclear phase. However, the ploidy of a number of dinoflagellates remains unknown, and molecular genetic support for haploidy in this group has been lacking. To elucidate the ploidy of symbiotic dinoflagellates belonging to the genus *Symbiodinium*, we used five polymorphic microsatellites to examine populations harbored by the Caribbean gorgonians *Plexaura kuna* and *Pseudopterogorgia elisabethae;* we also studied a series of *Symbiodinium* cultures. In 690 out of 728 *Symbiodinium* samples *in hospite* (95% of the cases) and in all 45 *Symbiodinium* cultures, only a single allele was recovered per locus. Statistical testing of the *Symbiodinium* populations harbored by *P. elisabethae* revealed that the observed genotype frequencies deviate significantly from those expected under Hardy-Weinberg equilibrium. Taken together, our results confirm that, in the vegetative life stage, members of *Symbiodinium*, both cultured and *in hospite*, are haploid. Furthermore, based on the phylogenetics of the dinoflagellates, haploidy in vegetative cells appears to be an ancestral trait that extends to all 2000 extant species of these important unicellular protists.

Introduction

The ploidy of an organism can significantly affect genome evolution. For example, diploids carry twice as much DNA as haploids and may be expected to accumulate new beneficial mutations at a higher rate (Paquin and Adams, 1983). The genome of diploids may also evolve rapidly because they carry more than a single copy of an allele. These "extra" alleles, over time, may evolve new functions while "old" alleles continue to perform their original functions (Lewis and Wolpert, 1979). Haploids, on the other hand, tend to have deleterious mutations purged more rapidly from the population since they are not masked (Hughes and Otto, 1999). Furthermore, knowledge of ploidy is essential to the interpretation and understanding of population genetic data. Given the importance of ploidy to genome evolution and population genetics, it is surprising that questions pertaining to it remain for a number of organisms.

Dinoflagellates are a diverse and ecologically important group of unicellular protists. For example, some species are major photosynthetic or heterotrophic components of the plankton, and others are considered to be the causative agents of fish kills. Microscopic and cytological evidence from the species examined to date suggests that dinoflagellates (with the exception of *Noctiluca* spp.) possess a vegetative haploid nuclear phase (Pfiester and Anderson, 1987; Coats, 2002). However, ploidy has not been explicitly determined for a number of dinoflagellates, including the important genus *Symbiodinium* Freudenthal (Taylor, 1974). Members of *Symbiodinium*, commonly referred to as zooxanthellae, are intra- or intercellular symbionts of marine invertebrates, including foraminiferans, sponges, cnidarians, and molluscs (Glynn, 1996). Blank (1987) reconstructed the nucleus of *Symbiodinium kawagutii* and found that the chromosomes of this dinoflagellate could not be paired either by size, appearance, or distribution. This cytological result led to the speculation that the vegetative (coccoid) cells of *Symbiodinium* may be haploid (Blank, 1987). To date, the molecular genetic data necessary to establish the ploidy of these symbiotic dinoflagellates, or

Received 18 July 2002; accepted 28 November 2002.

* Present Address: Department of Biochemistry and Molecular Biophysics, University of Arizona, Tucson, Arizona 85721.

‡ To whom correspondence should be addressed. E-mail: coffroth@buffalo.edu

any dinoflagellate, are lacking. We resolve this lingering question by using microsatellites to elucidate the ploidy of *Symbiodinium*.

Microsatellites are simple, tandemly repeated DNA sequences (reviewed in Chambers and MacAvoy, 2000) that are distributed abundantly in the genomes of virtually all organisms (Bennett, 2000). These single-locus, multiallelic, codominant segments of DNA are highly versatile and accessible markers for population genetic studies. However, microsatellites have also been successfully applied as tools in determining an organism's ploidy. For example, recovery of two alleles from a single locus in a single individual or isolate demonstrates a diploid nuclear phase. On the other hand, if a single allele is recovered from each of multiple loci, and the result is replicated over multiple individuals or isolates, the data suggest a haploid nuclear phase. This rationale has been applied to numerous organisms, including a parasitic protozoan, *Trypanosoma cruzi* (Oliveira *et al.*, 1998); two parasitic fungi, *Magnaporthe grisea* (Brondani *et al.*, 2000) and *Aspergillus fumigatus* (Bart-Delabesse *et al.*, 1998); a diatom, *Ditylum brightwellii* (Rynearson and Armbrust, 2000); a bryophyte, *Polytrichum formosum* (van der Velde *et al.*, 2001); and a false spider mite, *Brevipalpus phoenicis* (Weeks *et al.*, 2001). In this investigation, we apply the same strategy to members of the genus *Symbiodinium*. Populations of *Symbiodinium* harbored by the gorgonians *Plexaura kuna* and *Pseudopterogorgia elisabethae*, as well as a series of *Symbiodinium* cultures, were screened with five polymorphic microsatellites. The results confirm that members of *Symbiodinium* are haploid in the vegetative life stage.

Materials and Methods

Biological materials and nucleic acid isolation

Samples of *Plexaura kuna* were collected from colonies at depths of 1–7 m at 10 sites in the San Blas Islands, Republic of Panama (n = 142); two sites in the Florida Keys (n = 12); and three sites in the Bahamas (n = 6). For *Pseudopterogorgia elisabethae*, samples were collected from 575 colonies at depths of 10–27 m at 12 sites in the Bahamas (n = 43–50 per site). The 12 *P. elisabethae* sites were Sweetings Cay, Gorda Rock, Little San Salvador, Cat Island, Rum Cay, Hog Cay, and two sites each at Abacos, Eleuthera, and San Salvador Islands. Immediately after collection, samples were preserved in either 95% ethanol or salt-saturated DMSO (Seutin *et al.*, 1991) or were frozen in a liquid nitrogen vapor shipper. Total nucleic acids were extracted and quantified from branch pieces (about 2 cm) of *P. kuna* according to the methods of Coffroth *et al.* (1992). Nucleic acids were extracted from branch pieces (about 3 cm) of *P. elisabethae* by first grinding the tissue in STE buffer (0.05 *M* Tris-HCl (pH = 8.0), 0.1 *M* EDTA, 0.1 *M* NaCl, 0.2% SDS) followed by a modified extraction protocol using the Prep-A-Gene DNA Extraction Kit (Bio-Rad Laboratories, Hercules, CA) (Shearer and Coffroth, unpubl.). These extraction methods extracted nucleic acids from both the gorgonian hosts and from their *Symbiodinium* populations *in hospite*.

Symbiodinium cultures, isolated from a range of invertebrate hosts and geographic locations (Table 1), were maintained as described in Santos *et al.* (2001). Total nucleic acids were extracted and quantified from fresh algal cultures (approximately 5×10^3 cells) as described above for the *P. kuna* samples. After extraction, all nucleic acid samples were stored at −20 °C.

Phylogenetic identification of Symbiodinium *populations and cultures*

The phylogenetic identity of the *Symbiodinium* populations harbored by *P. kuna* and *P. elisabethae*, as well as the *Symbiodinium* cultures, was determined by length heteroplasmy in domain V of chloroplast large subunit (cp23S) rDNA as described in Santos *et al.* (2003). This technique rapidly genotypes *Symbiodinium* isolates and places them into a phylogenetic framework based on cp23S-rDNA (Santos *et al.*, 2003).

Construction of Symbiodinium *microsatellite libraries*

Nucleic acids used in the construction of the microsatellite libraries for *P. kuna* and *P. elisabethae Symbiodinium* populations were obtained by different procedures. *Symbiodinium* was isolated from samples of *P. kuna* collected from around the Caribbean and purified of host tissue (described in Santos *et al.*, 2001) before the nucleic acids were extracted and quantified as described above for *P. kuna* samples. On the other hand, nucleic acids for the *Symbiodinium* microsatellite library from *P. elisabethae* were extracted from colonies collected at Sweetings Cay (n = 2) and San Salvador (n = 4) as described above. These preparations contained nucleic acids from both *P. elisabethae* and their *Symbiodinium* populations *in hospite*, with no effort being made to enrich for *Symbiodinium* nucleic acids. After extraction, nucleic acids were pooled according to host source and used to construct the microsatellite libraries. The libraries were constructed and screened for microsatellites with dinucleotide repeats as described in Ciofi and Bruford (1998).

Screening of microsatellite loci polymerase chain reaction primers

To ensure that the microsatellite loci were not part of the host gorgonian genome, PCR amplifications were carried out on nucleic acids extracted from planulae of *P. kuna* and *P. elisabethae*, which are asymbiotic upon release from the maternal colony (Kinzie, 1974; Coffroth *et al.*, 2001; see

Table 1

Information about the Symbiodinium *cultures that amplified with at least one of the two microsatellites primer sets designed for the* Symbiodinium *populations of* Pseudopterogorgia elisabethae

Host organism	Culture name	Collection location
Aiptasia pallida	FLAp#2	Florida Keys
A. pallida	FLAp#2 10AB	Florida Keys
A. pallida	FLAp#3 10AB	Florida Keys
A. pallida	FLAp#4 10AB	Florida Keys
Aiptasia pulchella	OkAp#1	Okinawa, Japan
A. pulchella	OkAp#9	Okinawa, Japan
A. pulchella	OkAp#10	Okinawa, Japan
Briareum asbestinum (polyp)[a]	#498[b]	Florida Keys
B. asbestinum (polyp)[a]	#579[b]	Florida Keys
B. asbestinum (polyp)[a]	#595[b]	Florida Keys
B. asbestinum (polyp)[a]	#1135[b]	Florida Keys
B. asbestinum (polyp)[a]	#1140[b]	Florida Keys
B. asbestinum (polyp)[a]	#1246[b]	Florida Keys
B. asbestinum (polyp)[a]	#1319[b]	Florida Keys
B. asbestinum (polyp)[a]	#1385[b]	Florida Keys
B. asbestinum (polyp)[a]	#1394[b]	Florida Keys
B. asbestinum (polyp)[a]	#1509[b]	Florida Keys
B. asbestinum (polyp)[a]	#1510[b]	Florida Keys
B. asbestinum (polyp)[a]	#1669[b]	Florida Keys
B. asbestinum (polyp)[a]	#1735[b]	Florida Keys
B. asbestinum (polyp)[a]	#1902[b]	Florida Keys
B. asbestinum (polyp)[a]	#2053[b]	Florida Keys
B. asbestinum (polyp)[a]	#2080[b]	Florida Keys
Plexaura kuna	Pk13	Florida Keys
P. kuna	Pk14	Florida Keys
P. kuna (polyp)[a]	Pk205	San Blas Islands, Panama
P. kuna (polyp)[a]	Pk206[b]	San Blas Islands, Panama
P. kuna (polyp)[a]	Pk208[b]	San Blas Islands, Panama
P. kuna (polyp)[a]	Pk215	San Blas Islands, Panama
P. kuna (polyp)[a]	Pk216	San Blas Islands, Panama
P. kuna (polyp)[a]	Pk225[b]	San Blas Islands, Panama
P. kuna (polyp)[a]	Pk226[b]	San Blas Islands, Panama
P. kuna	Pk801	Florida Keys
P. kuna	Pk807	Florida Keys
P. kuna (polyp)[a]	Pk702[b]	San Blas Islands, Panama
P. kuna (polyp)[a]	Pk703[b]	San Blas Islands, Panama
P. kuna (polyp)[a]	Pk704[b]	San Blas Islands, Panama
P. kuna (polyp)[a]	Pk705[b]	San Blas Islands, Panama
P. kuna (polyp)[a]	Pk706[b]	San Blas Islands, Panama
P. kuna (polyp)[a]	Pk707[b]	San Blas Islands, Panama
Pocillopora damicornis	Pd	Hawaii
Porites evermanni	Pe	Hawaii
Pseudopterogorgia elisabethae	SSPe	Bahamas
Unknown anemone	Cane	Hawaii
Zoanthus pacificus	Zp	Hawaii

[a] A polyp is defined as a newly settled and metamorphosed planula.
[b] Cultures that were started from a single dinoflagellate cell.

below). Nucleic acids were extracted from the planulae as described above for samples of *P. kuna*. To test for the presence of template nucleic acids (*i.e.*, cnidarian host DNA), PCR amplifications were conducted using the universal n18S-rDNA primer set ss5 and ss3 (Rowan and Powers, 1991). The asymbiotic nature of the planulae was then confirmed by the absence of a PCR product when the zooxanthella-biased n18S-rDNA primers ss5 and ss3z were used (Rowan and Powers, 1991). Both sets of reactions were carried out under the conditions described by Rowan and Powers (1991). Details of the five *Symbiodinium* microsatellite loci, including the sequences of the PCR primers and GenBank accession numbers, are given in Table 2.

Microsatellite amplifications and allele detection for Symbiodinium *populations*

PCR reactions for each *Symbiodinium* microsatellite locus were performed in 10-μl volumes containing 10 m*M* Tris-HCl (pH 8.3), 50 m*M* KCl, 0.001% gelatin, 200 μM dNTPs, 1 U *Taq* polymerase, approximately 10 ng of template DNA, and $MgCl_2$ and primers at concentrations detailed in Table 2. Thermocycling conditions were as follows: initial denaturing step of 94°C for 2–3 min, 35–39 cycles of 94°C for 30–45 s, annealing temperature of X° (see Table 2) for 30–45 s, 72°C for 30 s, and a final extension of 72°C for 3–5 min.

Most *Symbiodinium* microsatellite alleles from *P. kuna* were separated in 2% 0.5X Tris-borate (TBE) agarose gels and visualized by ethidium bromide staining. In addition, some *Symbiodinium* microsatellite alleles from *P. kuna* were amplified in the presence of ^{33}P-ATP (Sambrook *et al.*, 1989), separated in 6% polyacrylamide / 0.5X TBE gels under denaturing (7 *M* urea) conditions, and visualized by exposure to X-ray film. The sizes of *Symbiodinium* microsatellite alleles from *P. kuna* were determined either with a 100-bp DNA ladder (MBI Fermentas, Hanover, MD) for 2% agarose gels, or for polyacrylamide gels, with a ^{33}P-ATP puC19 plasmid sequencing reaction serving as a nucleotide size-ladder.

For *P. elisabethae*, *Symbiodinium* microsatellite alleles were labeled by incorporation of a 5′-IRD800 M13 Forward primer (see Table 2), and were separated in 25-cm-long, 0.25-mm-thick, 6.5% Long Ranger (FMC Bioproducts, Rockland, ME)/0.5X TBE gels under denaturing (7 *M* urea) conditions. Gel electrophoresis was performed at 1500 V, 40 W, 40 mA, 50 °C, and the default scan speed, with LI-COR's NEN Global IR2 DNA sequencer system (LI-COR Biotechnology Division, Lincoln, NE). The sizes of *Symbiodinium* microsatellite alleles from *P. elisabethae* were determined with the fragment analysis program Gene ImagIR v3.55 (Scanalytics Inc, Fairfax, VA) using DNA ladders (ladder 97–147 bp or 172–272 bp, rungs at 25-bp increments, ladders loaded every fifth lane) as size references.

In addition, *Symbiodinium* microsatellite-loci primer-sets for each host species were tested on the *Symbiodinium* populations of the other host species. For the host species

Table 2

Characterization and PCR amplification conditions of the five Symbiodinium *clade B microsatellite loci; size refers to the predicted PCR product size with original sequenced clone as template*

Microsatellite locus name	Motif type	Sequence of microsatellite motif	PCR primer sequences	Size (bp)
CA1′.7[a,b]	GT, interrupted pure	$(GT)_3GAT(GT)_4GC(GT)_{13}GAT(GT)_2$	CA1′.7UP: 5′-GCAGTGTGTTACCTTAAAGTGCGG-3′ CA1′.7DN: 5′-GTTTAGTTGAGCAACTTCCGAG-3′	345
GA2.8[a,b]	CA, interrupted pure	$(CA)_7CG(CA)_{21}$	GA2.8UP: 5′-TCGACTCTTGGCGCAAAATG-3′ GA2.8DN: 5′-GGGATGAAACACTGGGATAATCCAG-3′	174
GA4.84[a,b]	CA, interrupted complex	$(CAGA)_2(CA)_5CGAA(CA)_6(CG)_2CAGA(CA)_{13}CG(CA)_5(GA(CA)_2)_5GACG(CA)_5$	GA4.84UP: 5′-GATCAAACTCTTGTGATGAC-3′ GA4.84DN: 5′-GTCAGATTGTCATCAAAGACTGC-3′	175
CA4.86[c,d]	CA, interrupted complex	$(CACC)CA(CACC)_2(CA)_9$	CA4.86R: 5′-GCCTTCAATGCAATCACCTT-3′ CA4.86L[f]: 5′-GGAATTGGCCATCCCTCTAT-3′	193
CA6.38[c,e]	CA, interrupted pure	$(CA)_9CG(CA)_4$	CA6.38R: 5′-CAAAGAATATTCGGGGGTCA-3′ CA6.38L[f]: 5′-AGTTGATACGCCGGATGTGT-3′	112

[a] Microsatellite loci isolated from *Plexaura kuna Symbiodinium* populations *in hospite;* sequences deposited in GenBank under accession numbers AF549186-AF549188.

[b] 1.5 m*M* $MgCl_2$, 3 pmol of each primer, 60 °C annealing temperature.

[c] Microsatellite loci isolated from *Pseudopterogorgia elisabethae Symbiodinium* populations *in hospite;* sequences deposited in GenBank under accession numbers AF474165 and AF474169.

[d] 2.5 m*M* $MgCl_2$, 0.2 pmol CA4.86R, 0.18 pmol CA4.86LM13, 0.02 pmol 5′-IRD800 M13 Forward primer, 50 °C annealing temperature.

[e] 1.5 m*M* $MgCl_2$, 3 pmol CA6.38R, 2 pmol CA6.38LM13, 0.2 pmol 5′-IRD800 M13 Forward primer, 56 °C annealing temperature.

[f] Primers with M13 Forward sequence (5′-CACGACGTTGTAAAACGAC-3′) added for visualization on LI-COR's NEN® Global IR2 DNA Sequencer System (LI-COR Biotechnology Division, Lincoln, NE). See text for details.

comparisons, PCR reaction conditions and detection of *Symbiodinium* microsatellite alleles were as previously described.

A total of 45 *Symbiodinium* cultures were also screened with the five *Symbiodinium* microsatellite loci primer sets using the methods described above.

Statistical testing of microsatellite data

Exact probabilities (analogous to Fisher's exact test for 2×2 contingency tables) for the observed genotype frequencies and for those expected under Hardy-Weinberg equilibrium were used to determine whether populations of *Symbiodinium* harbored by *P. elisabethae* in the Bahamas deviate from Hardy-Weinberg equilibrium. Significance values were calculated with the computer program BIOSYS-2 (Swofford and Selander, 1981; modified by William C. Black, Department of Microbiology, Colorado State University; available at: ftp://lamar.colostate.edu/pub/web4/).

Results

Phylogenetic identification of Symbiodinium *populations and cultures*

The numerically dominant *Symbiodinium* in association with *Plexaura kuna* and *Pseudopterogorgia elisabethae* belong to *Symbiodinium* clade B (*sensu* Rowan and Powers, 1991), and more specifically, to *Symbiodinium* B184 (*sensu* Santos *et al.*, 2003). The *Symbiodinium* cultures also belong to clade B, with representatives from *Symbiodinium* B184, B211, and B223 (*sensu* Santos *et al.*, 2003; Table 3).

Genomic location of the microsatellite loci

Nucleic acids extracted from planulae of *P. kuna* and *P. elisabethae* failed to produce an amplicon with the zooxanthella-biased n18S-rDNA PCR primers ss5 and ss3z. On the other hand, an amplicon of approximately 1800 bp was generated from the same templates using the universal n18S-rDNA PCR primers ss5 and ss3 (data not shown). These results confirmed that the planulae were asymbiotic. Nucleic acids extracted from planulae and then used as templates for the microsatellite loci primer sets failed to produce PCR amplicons, whereas nucleic acids from adult tissue that contained *Symbiodinium* or nucleic acids isolated from *Symbiodinium* cultures produced PCR amplicons (see below) of the correct size (given in Table 2). Taken together, the data demonstrate that the microsatellite loci are located within the genome of *Symbiodinium*, and not that of the gorgonian hosts.

Table 3

Microsatellite and chloroplast genotypes for the Symbiodinium *cultures; a microsatellite genotype is defined as a unique combination of microsatellite allele sizes at loci CA4.86 and CA6.38*

Symbiodinium microsatellite allele size (bp)		*Symbiodinium* chloroplast large subunit rDNA (cp23S-rDNA) genotype[a]	Culture name	Host organism
Locus CA4.86	Locus CA6.38			
179	100	B184	Cane	Unknown anemone
		B184	OkAp#1	*Aiptasia pulchella*
		B184	OkAp#10	*A. pulchella*
		B184	OkAp#9	*A. pulchella*
		B184	Pd	*Pocillopora damicornis*
		B184	Pe	*Porites evermanni*
		B184	Zp	*Zoanthus pacificus*
179	102	B184	FLAp#2	*Aiptasia pallida*
		B184	FLAp#2 10AB	*A. pallida*
		B184	FLAp#3 10AB	*A. pallida*
		B184	FLAp#4 10AB	*A. pallida*
183	100	B184	Pk205	*Plexaura kuna* (polyp)[c]
		B184	Pk208[b]	*P. kuna* (polyp)[c]
		B184	Pk215	*P. kuna* (polyp)[c]
		B184	Pk216	*P. kuna* (polyp)[c]
		B184	Pk226[b]	*P. kuna* (polyp)[c]
187	"null"	B223	#498[b]	*Briareum asbestinum* (polyp)[c]
		B223	#579[b]	*B. asbestinum* (polyp)[c]
		B223	#1385[b]	*B. asbestinum* (polyp)[c]
191	104	B184	#595[b]	*B. asbestinum* (polyp)[c]
		B184	#1246[b]	*B. asbestinum* (polyp)[c]
		B184	#1394[b]	*B. asbestinum* (polyp)[c]
191	106	B184	#1135[b]	*B. asbestinum* (polyp)[c]
		B184	#1140[b]	*B. asbestinum* (polyp)[c]
		B184	#1319[b]	*B. asbestinum* (polyp)[c]
		B184	#1509[b]	*B. asbestinum* (polyp)[c]
		B184	#1510[b]	*B. asbestinum* (polyp)[c]
		B184	#1669[b]	*B. asbestinum* (polyp)[c]
		B184	#1735[b]	*B. asbestinum* (polyp)[c]
		B184	#1902[b]	*B. asbestinum* (polyp)[c]
		B184	#2053[b]	*B. asbestinum* (polyp)[c]
		B184	#2080[b]	*B. asbestinum* (polyp)[c]
		B184	Pk225[b]	*P. kuna* (polyp)[c]
		B184	Pk706[b]	*P. kuna* (polyp)[c]
		B184	Pk707[b]	*P. kuna* (polyp)[c]
193	98	B211	Pk702[b]	*P. kuna* (polyp)[c]
		B211	Pk703[b]	*P. kuna* (polyp)[c]
193	100	B184	Pk13	*P. kuna*
		B184	Pk14	*P. kuna*
		B184	Pk801	*P. kuna*
		B184	Pk807	*P. kuna*
193	104	B184	Pk206[b]	*P. kuna* (polyp)[c]
		B184	Pk704[b]	*P. kuna* (polyp)[c]
		B184	Pk705[b]	*P. kuna* (polyp)[c]
193	112	B184	SSPe	*Pseudopterogorgia elisabethae*

[a] *Sensu* Santos *et al.* (2003).

[b] Cultures that were started from a single dinoflagellate cell

[c] A polyp is defined as a newly settled and metamorphosed planula.

Microsatellites of Symbiodinium *within a host species*

For the *Symbiodinium* populations of *P. kuna*, four unique alleles were identified at locus CA1′.7, three at GA2.8, and three at GA4.84. The sizes of the alleles at each locus were CA1′.7 (approximately 360, 380, 400, 420 bp), GA2.8 (approximately 180, 190, 200 bp), and GA4.84 (approximately 280, 300, 310 bp). In 147 cases, only a single

allele per locus could be detected from a *P. kuna* colony, but the *Symbiodinium* populations from 13 colonies produced two distinct alleles at one or more loci. Thus, 8.1% of the *Symbiodinium* populations sampled from *P. kuna* individuals produced more than a single allele at any microsatellite locus.

When the *Symbiodinium* populations of *P. elisabethae* were screened at loci CA4.86 and CA6.38, 8 and 10 unique alleles, respectively, were identified from 568 of the 575 colonies that were examined (nucleic acids from seven colonies failed to amplify at either locus and were excluded from further analysis). Allele sizes for loci CA4.86 and CA6.38 ranged between 185–207 bp and 96–122 bp, respectively (Fig. 1). In most of these cases, only a single allele per locus could be detected from the *Symbiodinium* population of a *P. elisabethae* colony (Fig. 2). In 25 cases (4.4%), the *Symbiodinium* population from a *P. elisabethae* colony possessed two distinct alleles at one or more loci (example in Fig. 2). This pattern is similar to that observed for *Symbiodinium* microsatellites isolated and amplified from *P. kuna*.

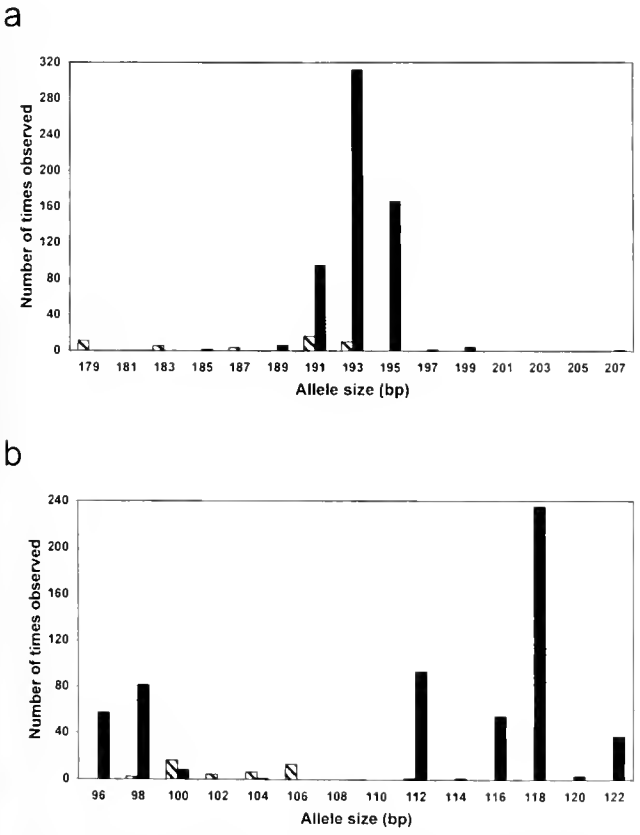

Figure 1. Size distribution of alleles at two microsatellite loci: (a) CA4.86 and (b) CA6.38. Solid bars, *Symbiodinium* populations of *Pseudopterogorgia elisabethae* (*in hospite*); diagonal strip bars, *Symbiodinium* cultures. Values for *P. elisabethae* are derived from all samples, include those that possessed two distinct alleles or a null allele at one or more loci.

Symbiodinium *microsatellites between host species*

Amplifications using the *Symbiodinium* microsatellite loci primer sets for one host species produced mixed results when applied to the *Symbiodinium* populations of the other host species. In many cases, the primers failed to produce an amplicon. However, when PCR amplification did occur, only a single allele was detected per locus (see fig. 4 of Santos *et al.*, 2001, for examples).

Microsatellites from Symbiodinium *cultures*

The *Symbiodinium* microsatellite loci CA1.7, GA2.8, and GA4.84 were not detected in any of the *Symbiodinium* cultures. However, the 45 cultures did amplify with at least one of the two *Symbiodinium* microsatellites primer sets isolated from *P. elisabethae* (Table 2). At loci CA4.86 and CA6.38, 5 and 6 alleles, respectively, were identified (Table 3, Fig. 1). Allele sizes for loci CA4.86 and CA6.38 ranged between 179–193 bp and 98–112 bp, respectively (Fig. 1). In each case, however, only a single allele was detected per locus.

Test for deviations from Hardy-Weinberg equilibrium

The observed genotype frequencies of the *Symbiodinium* populations inhabiting *Pseudopterogorgia elisabethae* from most of the 12 sites in the Bahamas were significantly different from those expected under Hardy-Weinberg equilibrium (Table 4). An excess of "homozygote" (genotypes with a single allele per locus) genotypes was present in the populations compared to the expected number based on allelic frequencies. In four cases, a single monomorphic allele was recovered from the population (Table 4).

Discussion

Microsatellite loci isolated from members of *Symbiodinium* clade B were amplified by PCR to assess ploidy in these symbiotic dinoflagellates. From most *Symbiodinium* populations harbored by *Plexaura kuna* and *Pseudopterogorgia elisabethae* (690 out of 728 samples; 95% of the cases), only a single allele was recovered per locus, and all 45 *Symbiodinium* cultures possessed a single allele per locus. Furthermore, an excess of "homozygous," or single allele per locus, genotypes in the *Symbiodinium* populations of *P. elisabethae* violated Hardy-Weinberg equilibrium. Nonconformity to the prediction of Hardy-Weinberg equilibrium indicates that one or more of its assumptions are not met in the population. The assumptions include (1) the organism is diploid; (2) reproduction is sexual; (3) the population is infinitely large; (4) mating occurs randomly; (5) generations are nonoverlapping; and (6) the population is free of genetic drift, migration, mutation, and natural selection (reviewed in Hartl and Clark, 1989). The *Symbiodinium* populations of *P. elisabethae* may violate many of

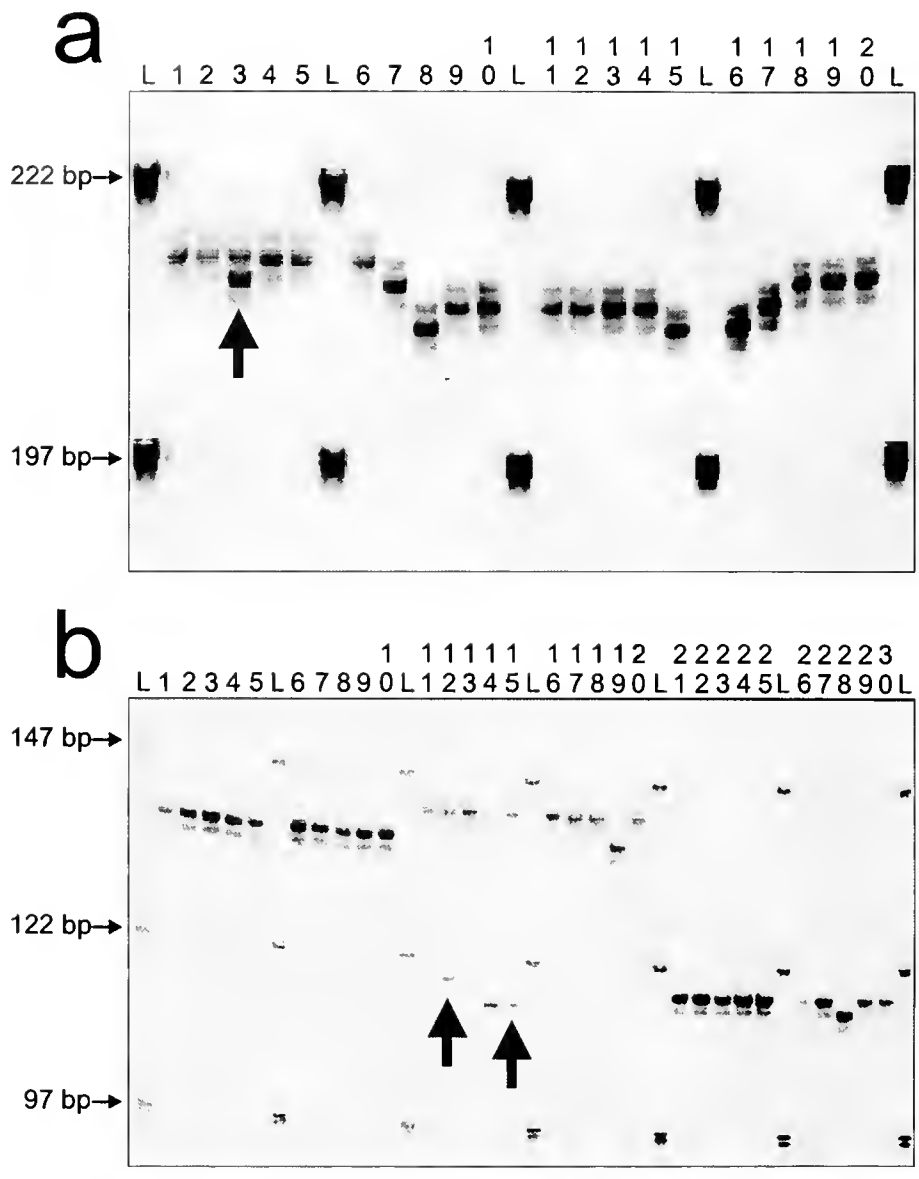

Figure 2. *Symbiodinium* populations from *Pseudopterogorgia elisabethae:* Polyacrylamide gel electrophoresis analysis of microsatellite alleles from two loci: (a) CA4.86 and (b) CA6.38. Number above lane represents individual samples of *P. elisabethae.* L represents DNA ladder lanes. Vertical arrows denote samples in which more than a single allele was amplified per locus.

these assumptions, but the predominance of "homozygous" genotypes in the *Symbiodinium* populations harbored by *P. kuna,* and in all *Symbiodinium* cultures, strongly suggests that at least the first assumption is being violated. If *Symbiodinium* were diploid in the vegetative life stage, more "heterozygous" genotypes should have been sampled. A possible explanation for the lack of heterozygous genotypes is that the *Symbiodinium* microsatellite loci are located in an organellar (*i.e.,* mitochondrial or chloroplast) genome. If so, a similar pattern of a single allele per locus would be observed. Although a microsatellite locus has been described from the chloroplast genome of a free-living dinoflagellate, *Heterocapsa triquetra* (Zhang *et al.,* 1999), it is highly unlikely that all five *Symbiodinium* microsatellite loci were isolated from the organellar genomes. Taken together, our results demonstrate that members of *Symbiodinium* clade B, both cultured and *in hospite,* possess a haploid nuclear phase. Moreover, since the genus is monophyletic (see, for example, Rowan and Powers, 1992; LaJeunesse, 2001; Santos *et al.,* 2002), our findings corroborate Blank's (1987) speculation that haploidy exists in *S. kawagutii* and extend it to all members of *Symbiodinium.*

If the vegetative life stage of *Symbiodinium* is haploid, why was more than a single allele sometimes recovered per

Table 4

Significant deviation of observed genotype frequencies from those expected under Hardy-Weinberg equilibrium for Symbiodinium *populations inhabiting* Pseudopterogorgia elisabethae *in the Bahamas*

Name/location of *Pseudopterogorgia elisabethae* populations (sample size)	*P* values	
	Locus CA4.86	Locus CA6.38
Sweetings Cay (44)	<0.001	<0.001
Gorda Rock (47)	<0.001	<0.001
Abacos Shallow (50)	<0.001	<0.001
Abacos Deep (48)	<0.001	<0.001
South Hampton Reef (47)	0.011	0.032
Little San Salvador (48)	<0.001	<0.001
East End Point of Eleuthera (44)	<0.001	<0.001
Cat Island (45)	<0.001	MA
San Salvador, Riding Rock (43)	MA	MA
San Salvador, Pillar Reef (50)	<0.001	MA
Rum Cay (46)	<0.001	<0.001
Hog Cay (46)	<0.001	<0.001

Values were calculated using exact probabilities (analogous to Fisher's exact test for 2 × 2 contingency tables) using the computer program BIOSYS-2 (Swofford and Selander, 1981; modified by William C. Black, Department of Microbiology, Colorado State University; available at: ftp://lamar.colostate.edu/pub/wcb4/). Samples that possessed a "null," or absent, allele at a locus were excluded from the analysis. MA designates a monomorphic allele recovered from the population.

locus *in hospite?* Among the samples of *P. kuna* and *P. elisabethae*, about 8.1% and 4.4%, respectively, gave this result. In these cases, the recovery of more than a single allele at a microsatellite locus suggests that the colonies harbored at least two genotypes of symbiotic algae. It has been demonstrated, using a combination of culturing and molecular techniques, that *P. kuna* and *P. elisabethae* can harbor more than a single genotype of *Symbiodinium* simultaneously (Goulet and Coffroth, 1997, 2003; Coffroth *et al.*, 2001; Santos *et al.*, 2001). Our data support this conclusion while suggesting that it is uncommon for colonies of these gorgonians to harbor more than one *Symbiodinium* genotype, at least at detectable concentrations. For these uncommon colonies, it remains to be determined whether the additional genotypes represent relicts of the initial symbiont uptake by the newly settled asymbiotic planulae or reflect populations that are secondarily acquired and contribute to the host in other ways.

Phylogenetic support for haploidy in Symbiodinium *and other dinoflagellates*

Our conclusion that *Symbiodinium* is haploid is consistent with data from most of the other dinoflagellates. The life cycle of nearly all dinoflagellates examined to date is dominated by asexual reproduction of haploid vegetative cells (Pfiester and Anderson, 1987). This observation, coupled with the monophyly of dinoflagellates (Saldarriaga *et al.*, 2001), suggests that all members of the dinoflagellates should possess a vegetative haploid nuclear phase. Interestingly, the vegetative cells of the red-tide dinoflagellate genus *Noctiluca* are thought to be diploid (Zingmark, 1970; Pfiester and Anderson, 1987). In *Noctiluca*, the first divisions of the gamete mother-cell nucleus are believed to be meiotic (Zingmark, 1970), which would imply diploidy in these dinoflagellates. Recently, the conclusion of diploidy in *Noctiluca* has been challenged (Schnepf and Drebes, 1993), but no definitive data have been presented to establish the ploidy of these dinoflagellates. We hypothesize, based on our knowledge of other dinoflagellates, that *Noctiluca* spp. possess a vegetative haploid nuclear phase. Analyses of microsatellite loci, such as we have done here for *Symbiodinium*, would be one way to test this hypothesis and settle the question of ploidy in *Noctiluca*.

A haploid nuclear phase in the dinoflagellates is consistent with that of their closest relatives. The Apicomplexa, obligate intracellular parasites of many vertebrate and invertebrate hosts, are thought to have evolved from, or shared a common ancestor with, the dinoflagellates (Wolters, 1991; Cavalier-Smith, 1993) about 395-929 Mya (Escalante and Ayala, 1995). The apicomplexan *Plasmodium falciparum*, one of the causative agents of human malaria, is haploid in its human host and only briefly diploid in its mosquito vector (Campbell, 1993; Conway *et al.*, 1999). Other apicomplexans, such as *Cryptosporidium parvum* and *Toxoplasma gondii*, also possess a haploid nuclear phase (Costa *et al.*, 1997; Feng *et al.*, 2002). Given the close evolutionary relationship between the two groups, the ancestral state in the progenitor of the apicomplexans and dinoflagellates was probably haploidy.

Evidence for fine-scale specificity in associations between host and Symbiodinium

Surprisingly, primer sets designed for amplification of the *Symbiodinium* microsatellite loci in one host species produced mixed results when applied to the *Symbiodinium* populations of the other host species or to *Symbiodinium* cultures. For example, primers designed for the symbiont populations of *P. kuna* were not very successful in amplifying the *Symbiodinium* populations of *P. elisabethae* colonies or algal cultures derived from a variety of hosts (Santos *et al.*, 2001; unpubl. data). Typically, the utility of a microsatellite system (*i.e.*, microsatellite primer sets) decreases as the phylogenetic distance between the samples being screened increases (Schlotterer, 1998). In these experiments, however, most (768 out of 773; 99.4%) of the samples belonged to a single lineage, *Symbiodinium* B184. Therefore, the microsatellite primer sets should have worked on all members of the group. This failure to amplify alleles from closely related, but non-focal, *Symbiodinium*

samples is probably due to mutational changes in the flanking regions of the microsatellite array. Mutations in these regions can lead to primer-template mismatch and thus to inhibition of the PCR reaction. In support of this hypothesis, we have sequenced alleles from loci CA4.86 and CA6.38 and found mutations, such as nucleotide substitutions and insertion-deletions (indels), in the microsatellite flanking regions from members of *Symbiodinium* B184, B211, and B223 (the evolution of *Symbiodinium* microsatellites will be discussed in a subsequent paper).

Although microsatellite alleles were not always recovered in the host species comparisons, an important conclusion can be drawn from these data. The specificity exhibited by the different microsatellite primer sets to the population of *Symbiodinium* from which they were designed and the consistent presence of "null," or absent, alleles in the other host species suggest that the two *Symbiodinium* B184 populations are genetically distinct from each another and specific to a given host species. The genetic differences are probably spread across the *Symbiodinium* genome, but at the minimum they are confined to mutations in the flanking regions of the microsatellite loci. Unfortunately, internal transcribed spacer (ITS) sequences—one of the most useful genetic markers for identifying *Symbiodinium* types (LaJeunesse, 2001)—are identical, or nearly so, in the two populations (Santos *et al.*, 2001); thus other genetic markers are needed to elucidate the relationship between them. Nevertheless, *P. kuna* and *P. elisabethae* appear to associate preferentially with genetically distinct *Symbiodinium* B184 populations, which provides evidence for fine-scale host-*Symbiodinium* specificity in these gorgonian species.

Microsatellites and Symbiodinium *diversity*

Consistent with other studies (Schoenberg and Trench, 1980; Colley, 1984; Goulet and Coffroth, 1997, 2003; Baillie *et al.*, 1998, 2000; Belda-Baillie *et al.*, 1999), our microsatellite data suggest an enormous amount of genotypic diversity within *Symbiodinium*, as illustrated by the following example. At loci CA4.86 and CA6.38, a total of 10 and 12 unique alleles, respectively, were recovered from samples belonging to *Symbiodinium* B184. Pairing alleles from each locus, under the assumption that there are no restrictions against particular combinations of alleles, generates 120 unique genotypes of *Symbiodinium* B184. However, we feel that this is a conservative estimate for several reasons. First, a minimal number of microsatellite loci are being employed. Data from other polymorphic microsatellite loci would distinguish more genotypes within *Symbiodinium* B184. Second, some alleles for CA4.86 and CA6.38 are missing from the data set because they have not yet been sampled (Fig. 1). The inclusion of any of these alleles would generate up to 210 unique genotypes of *Symbiodinium* B184. Third, the *Symbiodinium* B184 populations of hosts such as *P. kuna* possess "null" alleles at these loci, suggesting an additional level of diversity within the group (see above). Last it is extremely unlikely that this high level of genotypic diversity is confined to *Symbiodinium* B184. Thus, microsatellites will doubtlessly uncover high levels of genotypic diversity in most, if not all, of the 16 *Symbiodinium* lineages recognized in cp23S-rDNA phylogenies (Santos *et al.*, 2002, 2003).

Evidence for recombination in Symbiodinium

The finding that vegetative cells of *Symbiodinium* possess a haploid nuclear phase does not preclude recombination within the life cycle of these symbiotic dinoflagellates. For example, other haploid organisms maintain some form of recombination during their life cycle, including the green alga *Chlamydomonas* and members of the Acrasiomycota (cellular slime molds), the Bryophyta (mosses), the Pterophyta (ferns), the Apicomplexa, and the Dinophyceae (dinoflagellates) (Pfiester and Anderson, 1987; Campbell, 1993). In fact, the high allelic variability observed for allozymes (Schoenberg and Trench, 1980; Baillie *et al.*, 1998; Belda-Baillie *et al.*, 1999), random-amplified-polymorphic DNA (RAPDs) (Belda-Baillie *et al.*, 1999; Baillie *et al.*, 2000), and DNA fingerprints (Goulet and Coffroth, 1997, 2003) suggests extensive recombination in *Symbiodinium* (Baillie *et al.*, 2000; reviewed in LaJeunesse, 2001). This evidence for recombination, taken together with our finding of haploidy, lends strong support to *Symbiodinium* life cycle (a), as proposed by Fitt and Trench (1983). However, questions pertaining to recombination in these enigmatic dinoflagellates, such as the factors that induce it and whether it occurs inside or outside a host, remain to be answered.

Acknowledgments

We thank D. Brancato and J. Weaver for maintaining the *Symbiodinium* cultures, C. Gutierrez-Rodriguez for access to *P. elisabethae* samples and primers, Dr. H. R. Lasker (State University of New York at Buffalo) for help in collecting *P. kuna* and *P. elisabethae*, and Dr. R. A. Kinzie III (University of Hawaii; Hawaii Institute for Marine Biology) for access to *Symbiodinium* cultures. We are also grateful to the Kuna Nation and the Republic of Panama, the Bahamas Department of Fisheries, and the Florida Keys National Marine Sanctuary for permission to collect and export samples from Panama, the Bahamas, and Florida, respectively. The technical and logistical support of the staff and scientists of the Smithsonian Tropical Research Institute, the Don Gerace Research Center, the Keys Marine Lab, and the National Undersea Research Center in Key Largo is greatly appreciated. We also thank H.R. Lasker and two anonymous reviewers for comments that improved the manuscript. This research was supported by a National

Science Foundation (NSF) Minority Graduate Fellowship (SRS), NSF grants OCE-95-30057 and OCE-99-07319 (MAC), and a Caribbean Marine Research Center/NURC grant and New York State Sea Grant (MAC and H.R. Lasker).

Literature Cited

Baillie, B. K., V. A. Monje, V. Silvestre, M. Sison, and C. A. Belda-Baillie. 1998. Allozyme electrophoresis as a tool for distinguishing different zooxanthellae symbiotic with giant clams. *Proc. R. Soc. Lond. B* **256:** 1949–1956.

Baillie, B. K., C. A. Belda-Baillie, V. Silvestre, M. Sison, A. V. Gomez, E. D. Gomez, and V. Monje. 2000. Genetic variation in *Symbiodinium* isolates from giant clams based on random-amplified-polymorphic DNA (RAPD) patterns. *Mar. Biol.* **136:** 829–836.

Bart-Delabesse, E., J. F. Humbert, E. Delabesse, and S. Bretagne. 1998. Microsatellite markers for typing *Aspergillus fumigatus* isolates. *J. Clin. Microbiol.* **36:** 2413–2418.

Belda-Baillie, C. A., M. Sison, V. Silvestre, K. Villamor, V. Monje, E. D. Gomez, and B. K. Baillie. 1999. Evidence for changing symbiotic algae in juvenile tridacnids. *J. Exp. Mar. Biol. Ecol.* **241:** 207–221.

Bennett, P. 2000. Microsatellites. *J. Clin. Pathol. Mol. Pathol.* **53:** 177–183.

Blank, R. J. 1987. Cell architecture of the dinoflagellate *Symbiodinium* sp. inhabiting the Hawaiian stony coral *Montipora verrucosa*. *Mar. Biol.* **94:** 143–155.

Brondani, C., R. P. V. Brondani, L. R. Garrido, and M. E. Ferreira. 2000. Development of microsatellite markers for the genetic analysis of *Magnaporthe grisea*. *Genet. Mol. Biol.* **23:** 753–762.

Campbell, N. A. 1993. *Biology*. 3rd ed. Benjamin/Cummings Publishing, San Francisco, CA.

Cavalier-Smith, T. 1993. Kingdom Protozoa and its 18 phyla. *Microbiol. Rev.* **57:** 953–994.

Chambers, G. K., and E. S. MacAvoy. 2000. Microsatellites: consensus and controversy. *Comp. Biochem. Physiol.* **126:** 455–476.

Ciofi, C., and M. W. Bruford. 1998. Isolation and characterization of microsatellite loci in the Komodo dragon *Varanus komodoensis*. *Mol. Ecol.* **7:** 133–135.

Coats, D. W. 2002. Dinoflagellate life-cycle complexities. *J. Phycol.* **38:** 417–419.

Coffroth, M. A., H. R. Lasker, M. E. Diamond, J. A. Bruenn, and E. Bermingham. 1992. DNA fingerprinting of a gorgonian coral: a method for detecting clonal structure in a vegetative species. *Mar. Biol.* **114:** 317–325.

Coffroth, M. A., S. R. Santos, and T. L. Goulet. 2001. Early ontogenetic expression of specificity in a cnidarian-algal symbiosis. *Mar. Ecol. Prog. Ser.* **222:** 85–96.

Colley, N. J. 1984. The cell biology of dinoflagellate symbiosis in a coelenterate. Ph.D. dissertation. University of California, Santa Barbara, 174 pp.

Conway, D. J., C. Roper, A. M. J. Oduola, D. E. Arnot, P. G. Kremsner, M. P. Grobusch, C. F. Curtis, and B. M. Greenwood. 1999. High recombination rate in natural populations of *Plasmodium falciparum*. *Proc. Natl. Acad. Sci. USA* **96:** 4506–4511.

Costa, J. M., M. L. Darde, B. Assouline, M. Vidaud, and S. Bretagne. 1997. Microsatellite in the beta-tubulin gene of *Toxoplasma gondii* as a new genetic marker for use in direct screening of amniotic fluids. *J. Clin. Microbiol.* **35:** 2542–2545.

Escalante, A. A., and F. J. Ayala. 1995. Evolutionary origin of *Plasmodium* and other Apicomplexa based on rDNA genes. *Proc. Natl. Acad. Sci. USA* **92:** 5793–5797.

Feng, X., S. M. Rich, S. Tzipori, and G. Widmer. 2002. Experimental evidence for genetic recombination in the opportunistic pathogen *Cryptosporidium parvum*. *Mol. Biochem. Parasitol.* **119:** 55–62.

Fitt, W. K., and R. K. Trench. 1983. The relation of diel patterns of cell division to diel patterns of motility in the symbiotic dinoflagellate *Symbiodinium microadriaticum* Freudenthal in culture. *New Phytol.* **94:** 421–432.

Glynn, P. W. 1996. Coral reef bleaching: facts, hypotheses and implications. *Global Change Biol.* **2:** 495–509.

Goulet, T. L., and M. A. Coffroth. 1997. A within colony comparison of zooxanthellae genotypes in the Caribbean gorgonian *Plexaura kuna*. *Proc. 8th Int. Coral Reef Symp.* **2:** 1331–1334.

Goulet, T. L., and M. A. Coffroth. 2003. Genetic composition of zooxanthellae between and within colonies of the octocoral *Plexaura kuna*, based on small subunit rDNA and multilocus DNA fingerprinting. *Mar. Biol.* DOI 10.1007/s00227-002-0936-0.

Hartl, D. L., and A. G. Clark. 1989. Principles of population genetics. 2nd ed. Sinauer Associates, Sunderland, MA.

Hughes, J. S., and S. P. Otto. 1999. Ecology and the evolution of biphasic life cycles. *Am. Nat.* **154:** 306–320.

Kinzie, R. A. 1974. Experimental infection of aposymbiotic gorgonian polyps with zooxanthellae. *J. Exp. Mar. Biol. Ecol.* **15:** 335–345.

LaJeunesse, T. C. 2001. Investigating the biodiversity, ecology and phylogeny of endosymbiotic dinoflagellates in the genus *Symbiodinium* using the ITS region: in search of a "species" level marker. *J. Phycol.* **37:** 866–880.

Lewis, J., and L. Wolpert. 1979. Diploidy, evolution, and sex. *J. Theor. Biol.* **78:** 435–438.

Oliveira, R. P., N. E. Broude, A. M. Macedo, C. R. Cantor, C. L. Smith, and S. D. J. Pena. 1998. Probing the genetic population structure of *Trypanosoma cruzi* with polymorphic microsatellites. *Proc. Natl. Acad. Sci. USA* **95:** 3776–3780.

Paquin, C. E., and J. Adams. 1983. Frequency of fixation of adaptive mutations is higher in evolving diploid than haploid yeast populations. *Nature* **302:** 495–500.

Pfiester, L. A., and D. M. Anderson. 1987. Dinoflagellate reproduction. Pp. 611–648 in *The Biology of Dinoflagellates*, F.J.R. Taylor, ed. Blackwell Scientific Publications, London.

Rowan, R., and D. A. Powers. 1991. Molecular genetic identification of symbiotic dinoflagellates (zooxanthellae). *Mar. Ecol. Prog. Ser.* **71:** 65–73.

Rowan, R., and D. A. Powers. 1992. Ribosomal RNA sequences and the diversity of symbiotic dinoflagellates (zooxanthellae). *Proc. Natl. Acad. Sci. USA.* **89:** 3639–3643.

Rynearson, T. A., and E. V. Armbrust. 2000. DNA fingerprinting reveals extensive genetic diversity in a field population of the centric diatom *Ditylum brightwellii*. *Limnol. Oceanogr.* **45:** 1329–1340.

Saldarriaga, J. F., F.J.R. Taylor, P. J. Keeling, and T. Cavalier-Smith. 2001. Dinoflagellate nuclear SSU rRNA phylogeny suggests multiple plastid losses and replacements. *J. Mol. Evol.* **53:** 204–213.

Sambrook, J., E. F. Fritsch, and T. Maniatis. 1989. *Molecular Cloning: a Laboratory Manual*. Cold Spring Harbor Laboratory Press, Cold Spring Harbor, NY.

Santos, S. R., D. J. Taylor, and M. A. Coffroth. 2001. Genetic comparisons of freshly isolated vs. cultured symbiotic dinoflagellates: implications for extrapolating to the intact symbiosis. *J. Phycol.* **37:** 900–912.

Santos, S. R., D. J. Taylor, R. A. Kinzie III, M. Hidaka, K. Sakai, and M. A. Coffroth. 2002. Molecular phylogeny of symbiotic dinoflagellates inferred from partial chloroplast large subunit (23S)-rDNA sequences. *Mol. Phylogenet. Evol.* **23:** 97–111.

Santos, S. R., C. Gutierrez-Rodriguez, and M. A. Coffroth. 2003. Phylogenetic identification of symbiotic dinoflagellates via length het-

eroplasmy in domain V of chloroplast large subunit (cp23S)-rDNA sequences. *Mar. Biotechnol.* (In press).

Schlotterer, C. 1998. Microsatellites. Pp. 237–261 in *Molecular Genetic Analysis of Populations: A Practical Approach,* A. R. Hoelzel, ed. IRL Press, Oxford.

Schnepf, E., and G. Drebes. 1993. Anisogamy in the dinoflagellate *Noctiluca? Helgol. Meeresunters.* **47:** 265–273.

Schoenberg, D. A., and R. K. Trench. 1980. Genetic variation in *Symbiodinium (=Gymnodinium) microadriaticum* Freudenthal, and specificity in its symbiosis with marine invertebrates. I. Isozyme and soluble protein patterns of axenic cultures of *Symbiodinium microadriaticum. Proc. R. Soc. Lond.* **B 207:** 405–427.

Seutin, G., B. N. White, and P. T. Boag. 1991. Preservation of avian blood and tissue samples for DNA analyses. *Can. J. Zool.* **69:** 82–92.

Swofford, D. L., and R. B. Selander. 1981. BIOSYS-1: a FORTRAN program for the comprehensive analysis of electrophoretic data in population genetics and systematics. *J. Hered.* **72:** 281–283.

Taylor, D. L. 1974. Symbiotic marine algae: taxonomy and biological fitness. Pp. 245–262 in *Symbiosis in the Sea,* W. B. Vernberg, ed. University of South Carolina Press, Columbia, SC.

van der Verde, M., H. J. During, L. van de Zande, and R. Bijlsma. 2001. The reproductive biology of *Polytrichum formosum:* clonal structure and paternity revealed by microsatellites. *Mol. Ecol.* **10:** 2423–2434.

Weeks, A. R., F. Marec, and J.A.J. Breenwer. 2001. A mite species that consists entirely of haploid females. *Science* **292:** 2479–2482.

Wolters, J. 1991. The troublesome parasites: molecular and morphological evidence that Apicomplexa belong to the dinoflagellate-ciliate clade. *Biosystems* **25:** 75–83.

Zhang, Z., B. R. Green, and T. Cavalier-Smith. 1999. Single gene circles in dinoflagellate chloroplast genomes. *Nature* **400:** 155–159.

Zingmark, R. G. 1970. Sexual reproduction in the dinoflagellate *Noctiluca miliaris* Suriray. *J. Phycol.* **6:** 122–126.

Reference: *Biol. Bull.* **204:** 21–27. (February 2003)

Amebocyte Production Begins at Stage 18 During Embryogenesis in *Limulus polyphemus*, the American Horseshoe Crab

YVONNE COURSEY, NINA AHMAD, BARBARA M. McGEE, NANCY STEIMEL, AND MARY KIMBLE*

Department of Biology, University of South Florida, 4202 E. Fowler Ave., SCA 110, Tampa, Florida 33620-5150.

Abstract. *Limulus polyphemus*, the American horseshoe crab, has a single type of circulating blood cell, the granular amebocyte, which is the horseshoe crab's primary cellular defense against microbial infection. On exposure to gram-negative bacteria or their endotoxins, the amebocytes degranulate, releasing the clotting protein coagulogen and a number of proteases. The protease cascade converts the soluble coagulogen to insoluble coagulin, which forms fibrous clots that seal off the site of infection. The first description of this clotting reaction in the 1950s initiated development of *Limulus* amebocyte lysate and spurred an intensive study of the amebocytes. However, the site or sites and timing of amebocyte production have yet to be determined.

We report here that during embryonic development in *Limulus polyphemus*, amebocyte production begins at stage 18. The first amebocytes detected are found in developing hemocoel cavities, and the cells may derive from previously undifferentiated yolk nuclei.

Introduction

Granular amebocytes, the sole circulating blood cells in the hemolymph of *Limulus polyphemus*, have been studied for nearly 50 years. The amebocytes are the horseshoe crab's primary line of cellular defense against infection by the many gram-negative bacteria that share its marine habitat. Exposure to gram-negative bacteria or their endotoxins causes the amebocytes to degranulate through an exocytotic pathway (Bang, 1956; Dumont *et al.*, 1966; Armstrong and Rickles, 1982; Levin, 1985b; Ornberg, 1985). The granules contain a number of proteases and the primary clotting protein coagulogen. The proteases initiate a cascade that results in the conversion of the soluble coagulogen to insoluble coagulin. The coagulogen assembles into fibrous clots that seal off the site of infection, trapping the invading microorganisms (see Iwanaga, 2002, for review). Frederick Bang first described the clotting reaction in response to gram-negative bacteria in the 1950s, and subsequent studies by Bang, Levin, and colleagues (see Levin, 1985a, for review) led to the development of *Limulus* amebocyte lysate (LAL). LAL is widely used to test for the presence of endotoxins in intravenous fluids and drugs, vaccines, and solutions used in the decontamination of medical instruments. The molecular details of the protease cascade and the clotting reaction have been determined, and many of the genes involved have been cloned (Iwanaga, 2002).

Despite extensive study, the site of hemopoiesis has yet to be identified. Hilly and Gibson (1989) reported production of amebocytes in cultures of excised gill tissue; however, this has not been confirmed. Analysis of mRNA expression patterns in heart, muscle, coxal gland, brain, hepatopancreas, and midgut has ruled out these tissues as likely sites for amebocyte production (Miura *et al.*, 1995; Agarwala *et al.*, 1996). The consensus among those who study horseshoe crab blood is that the amebocytes are probably produced within the connective tissues, as has been suggested for other invertebrates that lack specific hematopoietic organs (Sawada and Tomonaga, 1996); however, this has yet to be demonstrated experimentally.

This paper addresses another major unanswered question about amebocyte production: when does it begin? Circulat-

Received 25 July 2002; accepted 1 November 2002.

* To whom correspondence should be addressed. E-mail: mkimble@chuma1.cas.usf.edu

ing blood cells can be seen in late-stage embryos and newly hatched first instar (trilobite) larvae (Bang, 1979). Liang *et al.* (1990) reported that blood cell production in *Tachypleus tridentatus* Leach (1819), the Japanese horseshoe crab, begins "at the stages of segmentation and appearance of limb buds." This appears to correspond to stages 13–15 in the staging scheme described by Sekiguchi (1973). Sekiguchi divided horseshoe crab embryogenesis into 21 stages, based on external morphological changes. Comparable morphological events occur in *T. tridentatus* and *L. polyphemus* embryos (Sekiguchi *et al.*, 1982, 1988). Assuming that similarity in external appearance also correlates with comparable internal development, we predicted that amebocyte production in *L. polyphemus* would also begin by embryonic stage 15. However, we show here that blood cell production in *L. polyphemus* does not begin until embryonic stage 18.

Materials and Methods

Embryo collection and processing for histological analysis

Fertilized horseshoe crab eggs were collected from beaches around Tampa Bay, Florida. The breeding season in Tampa Bay begins in late March and extends through mid-October. The eggs were collected by marking the location of mating pairs on the beach at high tide and then returning to the site 3 to 4 h later. The eggs were typically located 10–12 cm beneath the surface. In the laboratory, the eggs were separated from the bulk of the sand and maintained in plastic tubs in filtered seawater at 30 °C. Eggs were selected at timed intervals and stained with 0.02% neutral red to determine the stage of development as described by Sekiguchi *et al.* (1982).

Embryos (stages 12–21) and trilobite larvae were fixed overnight at 4 °C in a modified Bouin's fluid or in 3% formaldehyde in seawater, then dehydrated, infiltrated, and embedded in Unicryl as described previously (Kimble *et al.*, 2002). Sections of 4 to 5 μm were cut, using glass knives, and mounted on heated glass slides. Sections were stained with Giemsa, iron hematoxylin, or with an anti-coagulogen antibody, to identify amebocytes.

Antibody production

Polyclonal antibodies against coagulogen were raised in New Zealand White rabbits. Coagulogen was purified from amebocytes following the protocol of Miyata *et al.* (1984), as modified by P.B. Armstrong (University of California, Davis) and colleagues (pers. comm. to Y.C.). Blood samples were obtained from *L. polyphemus* adults. The amebocytes were allowed to settle overnight, and the supernatant (serum) was decanted. The cells were resuspended in 10% acetic acid and frozen. After thawing, the cell slurry was sonicated to release the coagulogen granules, and the granules were collected by centrifugation. The granule pellet was resuspended in ammonium bicarbonate and the pH adjusted to 7.0. Proteins were precipitated with 40% ammonium sulfate, resuspended in ammonium bicarbonate, dialyzed, and then run over a Sephadex G100 column. Fractions were collected and total protein concentration was checked by the BCA (bicinchoninic acid) assay. Fractions were analyzed by SDS-PAGE (sodium dodecyl sulfate-polyacrylamide gel electrophoresis). Column-purified proteins were mixed with adjuvant (complete for the first injection and incomplete for subsequent (boost) injections) and injected subcutaneously into rabbits. Boost injections were given at intervals of about 2 weeks. Following the third and subsequent boosts, blood samples were taken, and the serum was tested by protein blot analysis against column fraction 24 (fraction used for immunization), and against whole blood proteins from horseshoe crabs purchased from the Marine Biological Laboratory (Woods Hole, MA), or collected in Tampa Bay, for the presence of anti-coagulogen antibodies. Following the fourth boost (fifth injection), the rabbits were bled weekly for 4 months, after which they were euthanized and bled out. The serum was collected, aliquoted, and frozen at −80 °C.

Immunolocalization and microscopy

Sections were blocked using 5% normal goat serum in TBS (Tris buffered saline) for 1 h, and incubated with antiserum (1:10,000 final dilution), preimmune serum (1:5,000), or 5% goat serum, in TBS overnight at 30°C. Bound primary antibodies were detected by sequential incubation of the sections in a biotinylated anti-rabbit secondary antibody (1:30), ExtrAvidin alkaline phosphatase (1:30), and *Fast*® fast red TR/napthol AS-MX (Sigma). Cleavage of *Fast* fast red by alkaline phosphatase produces a bright red precipitate. Antibodies were diluted in TBS-tween, and the ExtrAvidin alkaline phosphatase was diluted in TBS. The *Fast* fast red TR/Napthol AS-MX was prepared according to manufacturer's instructions. Washes following the primary and secondary antibodies were in TBS-tween. Washes following the binding of the alkaline phosphatase were in TBS, with a final rinse in deionized water prior to addition of the *Fast* fast red. The color reaction was stopped after 5 min by rinsing with deionized water. Sections were post-stained with 0.5% methyl green. Coverslips were mounted with glycerol immediately before viewing. Sections were viewed and photographed on a Nikon inverted microscope.

Results

Blood cell production during embryogenesis

Blood cells in staged horseshoe crab embryos were initially identified using the histological stains Giemsa and

iron hematoxylin. Giemsa staining provides easy identification of different tissues, but the amebocyte granules stain only sporadically. Iron hematoxylin reproducibly stains the amebocyte granules, but the staining is similar in appearance to staining of the yolk. Despite these limitations, both staining techniques yielded the same result. Amebocytes were identified in stage 18 and older embryos (Fig. 1A–E), but not in earlier stage animals (not shown).

To confirm that the cells identified as amebocytes in the Giemsa and hematoxylin stained specimens are in fact amebocytes, embryos at the same stages of development were stained using an anti-coagulogen antiserum. On protein blots, the antiserum gives a strong, specific reaction to coagulogen when diluted 1:50,000 (arrowhead in Fig. 2B). In immunohistochemical studies, the antiserum specifically stains the coagulogen granules in amebocytes of trilobite larvae (Fig. 3A, B). In embryos, the antiserum specifically stains cytoplasmic granules in amebocytes beginning at stage 18 (Fig. 3C–E) of embryogenesis. No antibody staining was detected in earlier stage embryos (not shown).

In embryos at stages 18 and 19, the amebocytes were typically located in areas devoid of yolk and other ooplasmic components. These ooplasm-free regions appear to be precursors of the hemocoel cavities. They are typically located dorsal to the ventral plate of the embryo, between the epidermal cell layer and the layer of squamous mesodermal cells that overlays the central yolk mass (Fig. 1A, B). In some sections there also appears to be a second mesoderm layer directly beneath the epidermal cell layer. Thus the cavities may in fact be forming between two layers of mesodermal cells. In addition to the amebocytes, elements of connective tissue are frequently seen within these cavities (Fig. 1A). In embryos at later stages (late stage 20 and stage 21) and in trilobite larvae, most blood cells are found in the developing hemocoel cavities, associated with connective tissue, or within the heart. However, we have

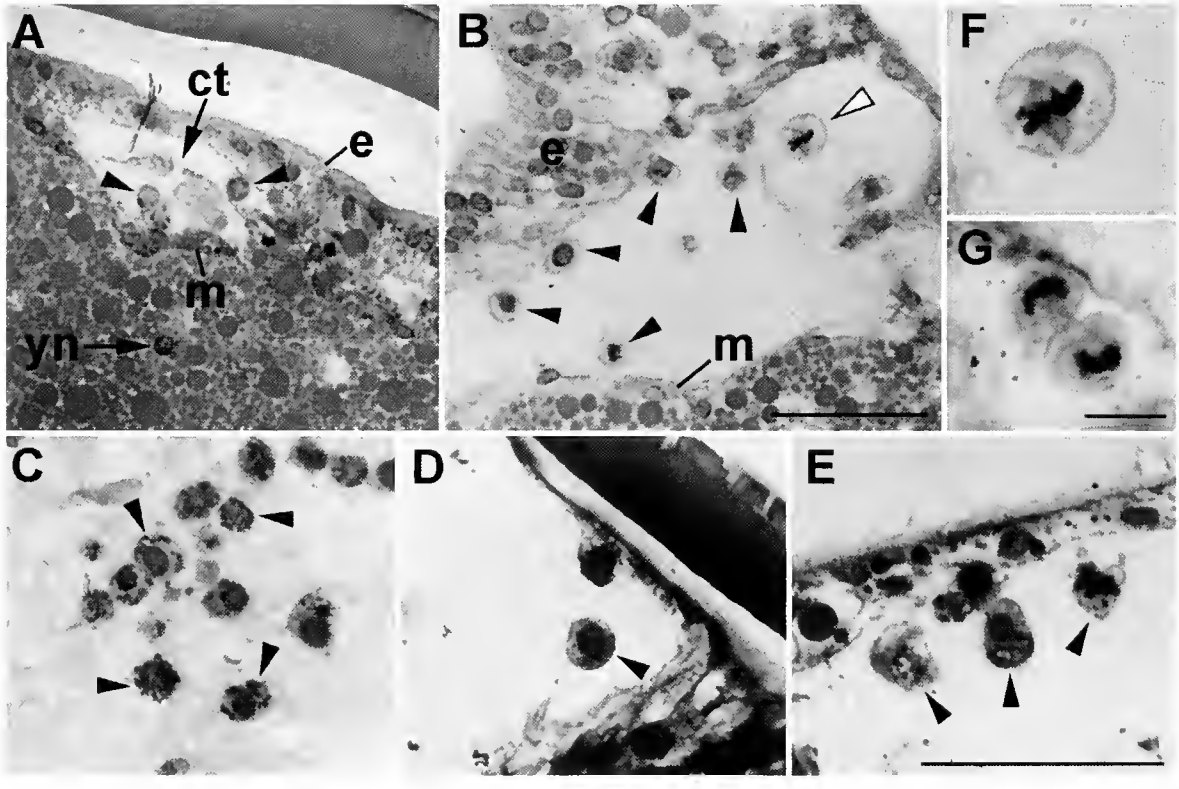

Figure 1. Amebocytes in embryos and larvae stained with Giemsa (A, B) or iron hematoxylin (C–E). (A, B) Sections from stage 18 embryos showing putative amebocytes (arrowheads) in developing hemocoel cavities. Open arrowhead in B indicates a cell that is in metaphase. (C) Section through the heart of a trilobite larva showing the granulated amebocytes (arrowheads). (D) Section from a stage 18 embryo showing two cells in a developing cavity. One has several darkly stained cytoplasmic granules (arrowhead). (E) Section from a stage 19 embryo showing several cells that contain cytoplasmic granules (arrowheads). (F) Higher magnification of the metaphase cell in panel B. (G) Sister cells in telophase from a different section of the same embryo as in B and F. ct, connective tissue; e, epidermal cell layer; m, mesodermal layer; yn, yolk nucleus. A and B are at the same magnification, bar in B = 50 μm. C–E are at the same magnification, bar in E = 50 μm. F and G are at the same magnification, bar in G = 10 μm.

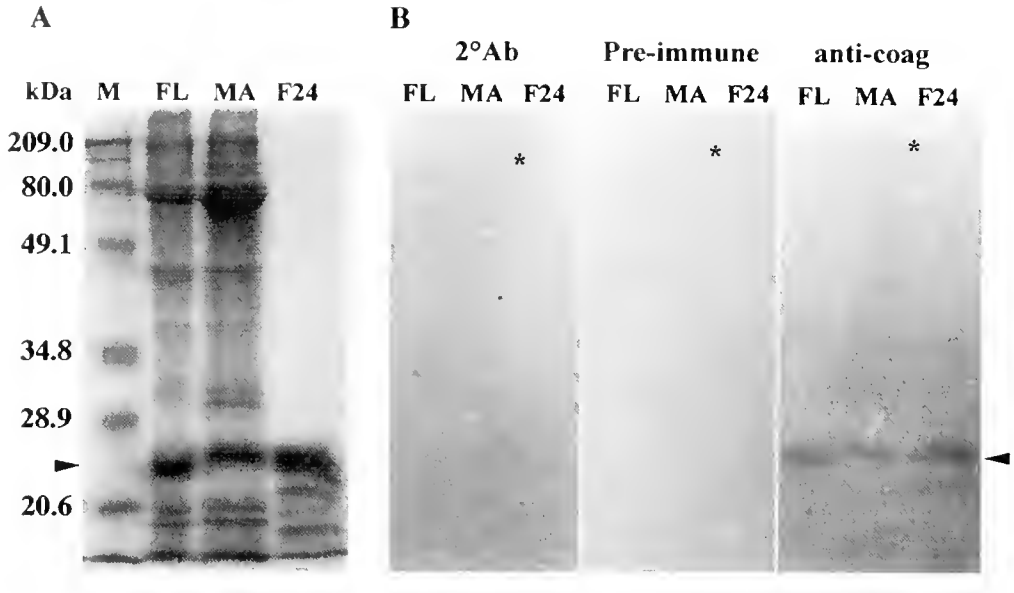

Figure 2. Protein gel and western blot analysis of total blood proteins from horseshoe crabs collected in Cape Cod (MA) and Tampa Bay (FL), and column fraction 24 (F24). (A) Coomassie-stained gel showing the three protein samples and molecular weight markers (kDa). The arrowhead to the left indicates the coagulogen protein band. (B) Blots from protein gels run in parallel with the gel shown in panel A. The blots were probed with the anti-coagulogen serum (anti-coag), pre-immune serum, or with secondary antibody (2°Ab) alone. The arrowhead at the right indicates the position of coagulogen. The asterisk indicates a high molecular mass band in the MA sample that binds the secondary antibody.

also observed blood cells in close association with isolated yolk masses (Fig. 3F, G).

Discussion

Amebocyte production begins at a later stage in Limulus polyphemus *than in* Tachypleus tridentatus

Using a combination of histological stains and an antibody that specifically recognizes the coagulogen protein in amebocytes and on protein blots, we have shown that amebocyte production in *L. polyphemus* begins at stage 18 of development. Amebocytes were identified in all subsequent embryonic stages (stages 19–21, days 7–14 post-fertilization) and in the trilobite larvae, but not in embryos prior to stage 18.

Stage 18 occurs during the 6th day post-fertilization and coincides with the first embryonic molt. At this stage the dorsal half of the embryo is still rounded and lacks distinguishing marks. The ventral side of the embryo is flattened, the prosomal appendages (chelicerae, pedipalps, and walking legs) have begun to lengthen, the stomodaeum is located slightly anterior to the chelicerae, and the lateral organs have begun to develop (Sekiguchi *et al.*, 1982). As mentioned previously, Liang *et al.* (1990) reported the identification of pro-amebocytes in transmission electron micrographs of stage 13–15 *T. tridentatus* embryos. The pro-amebocytes identified by these authors were first seen within the germ band (ventral plate), but in later stages were distributed diffusely in the connective tissue. Liang *et al.* (1990) suggested that the pro-amebocytes derived from the mesenchymal cell layer of the ventral plate. Despite careful examination of our sectioned embryos, we have not identified cells within the ventral plate that appear comparable to the proamebocytes described by Liang *et al.* (1990). However, the amebocytes that we observe in the hemocoel cavities of stage 18 embryos do correspond in appearance to their description of immature amebocytes. That is, the cells have relatively few coagulogen granules, and the granules, at least in some cells, appear to be smaller than granules in mature amebocytes (compare panel 3D with panels 3A and E–G). Additional studies will be necessary to determine if the apparent difference in granule size does in fact indicate cell maturity, or whether it reflects cell-to-cell variation. In addition, the developing hemocoel cavities, in which the immature amebocytes are observed, are typically located near, although not within, the ventral plate. For example, the cavity shown in Figure 1A was located between the ventral plate and the lateral organ. Thus the discrepancy in the location of the earliest amebocytes between the two species may be due to differences in how each group defines the ventral plate, rather than a significant difference in the actual location of the cells.

In agreement with Liang *et al.* (1990), we were not able to identify any obvious hematopoietic tissues in any of the

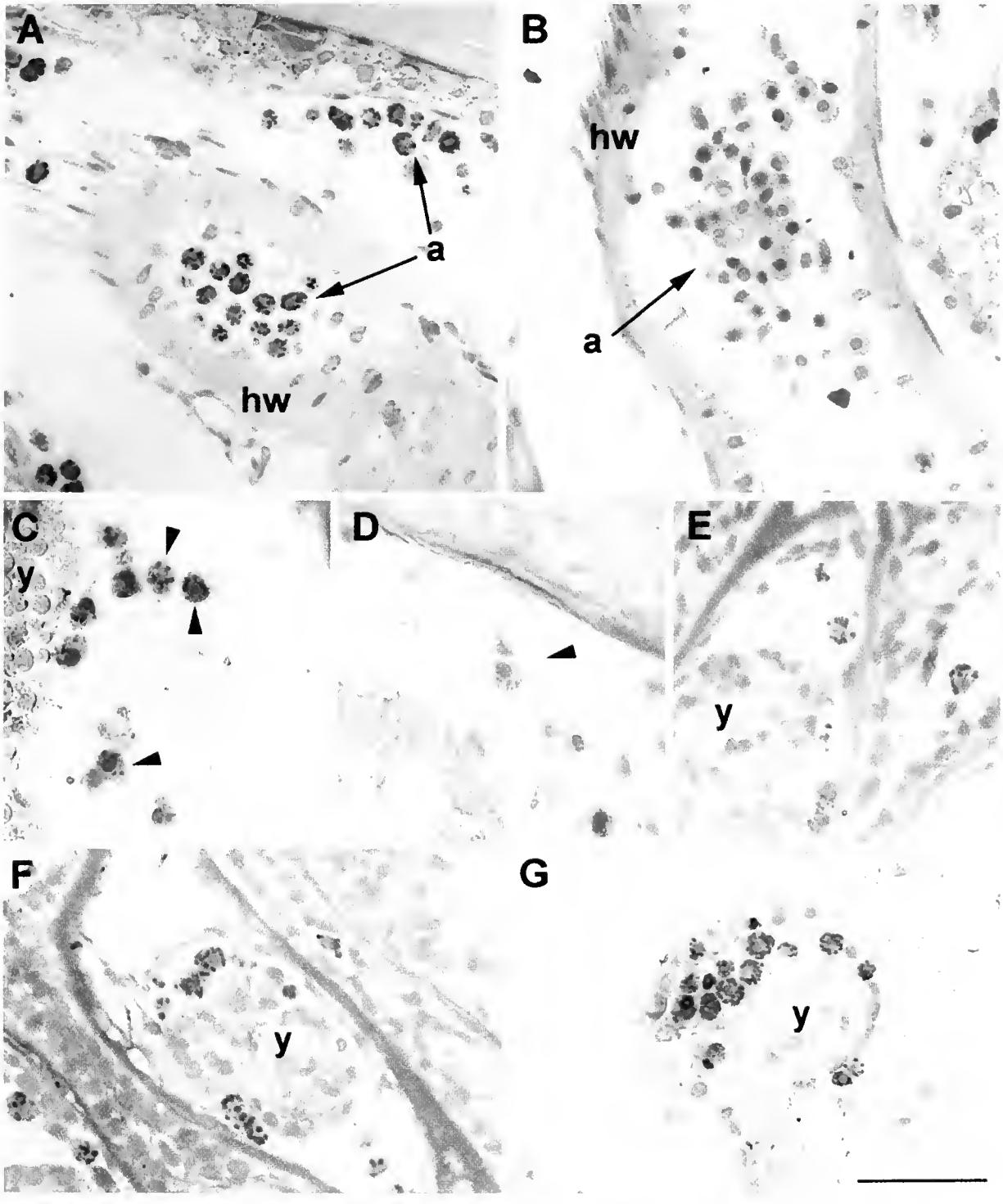

Figure 3. Amebocytes in embryos and larvae probed with the anti-coagulogen antibody and detected with *Fast* fast red. (A) Section through the heart and adjacent hemocoel regions of a trilobite larva stained with the anti-coagulogen antibody. (B) Section through the heart of a larva probed with secondary antibody only. (C, D) Amebocytes in developing hemocoel cavities of stage 18 embryos. (E) Amebocytes in a stage 20 embryo. (F, G) Amebocytes associated with distinct yolk masses in a late stage 20 embryo and a trilobite larva, respectively. a, amebocytes; hw, heart wall; y, yolk. All panels are at the same magnification, bar in G = 50 μm.

embryos or larvae examined. In stage 18 and 19 embryos, the amebocytes were always found in the developing hemocoel cavities and were usually in close association with elements of connective tissue. One possibility is that some of the cells of the developing connective tissue give rise to the first amebocytes in *L. polyphemus*. This would agree with the suggestion that the early amebocytes in *T. tridentatus* originate from mesenchymal cells (Liang *et al.*, 1990).

A second possibility is that the earliest amebocytes derive from yolk nuclei that cellularize and move out of the yolk mass into the developing hemocoel. Kishinouye (1893) suggested such an origin for amebocytes in embryos of *L. longispina* (*T. tridentatus* in current nomenclature [Sekiguchi, 1988]). Once the amebocytes have entered the cavities, they could associate with the connective tissue, forming foci in which cell division gives rise to additional amebocytes. Some dividing cells were seen within the cavities, in association with the connective tissue (Fig. 1B, F, G). These mitotic cells may represent pro-amebocytes that retain the ability to divide. It is generally accepted that mature amebocytes do not divide (Yeager and Tauber, 1935; Armstrong, 1985). As no dividing cells were observed in the embryos probed with the anti-coagulogen antibody or in those stained with iron hematoxylin, it remains to be determined whether the few mitotic cells that were observed in Giemsa-stained specimens represent pro-amebocytes.

Why amebocyte production begins at a later developmental stage in *L. polyphemus* than in *T. tridentatus* is not clear. One possibility is that the rate of development of internal structures and tissues relative to external morphological features is accelerated in *T. tridentatus* embryos compared to *L. polyphemus* embryos.

Analysis of sectioned material shows that stage 18 *L. polyphemus* embryos consist of relatively few cell types. In the ventral region and the growing appendages, the epidermal cells are typically columnar in shape, while the underlying mesodermal cells are flattened in appearance. Coelomic cavities have formed within some of the developing appendages, and within these we occasionally observe cells that have a fibroblast-like appearance. Also within the ventral plate are occasional cells having dark-staining cytoplasmic inclusions. These cells are most likely muscle precursors. In later stage embryos and larvae, cells with similarly stained inclusions are often seen adjacent to developing muscles. As one moves dorsally away from the ventral plate, there is a gradual transition in the epidermal cells from columnar through cuboidal to a flattened appearance. Similarly, the mesodermal cell layers in the dorsal region are very thin flat sheets that are often difficult to discern. By stage 18, the extension of the mesoderm over the central yolk mass appears to be complete or nearly so. The central region of the embryo is filled with yolk, within which are distributed numerous yolk nuclei. No evidence of internal organs is seen at this stage, although hemocoel cavities have begun to form. The cavities are located between the mesodermal cell layers, and within the cavities granular proamebocytes and elements of connective tissue are frequently observed. Also located in the dorsal regions of the embryo are cells that appear to be producing chitin-like material (based on the staining properties of the material). Finally, as mentioned before, the lateral organs, composed of distinct goblet-shaped cells, have begun to develop. Thus we are able to identify at most seven to eight distinct cell types in the stage 18 *L. polyphemus* embryos. How this compares with *T. tridentatus* embryos at the same stage of development remains to be determined.

Do the yolk nuclei represent a pool of multipotent cell precursors?

In contrast to many arthropods, horseshoe crabs retain significant numbers of yolk nuclei after cellular blastoderm formation (Kishinouye, 1893; Kingsley, 1892, 1893; Kimble *et al.*, 2002). The yolk nuclei persist throughout embryonic development. During the mid- to late stages of embryogenesis, some yolk nuclei probably function as vitellophages. After hatching, the residual yolk is incorporated into the developing midgut and digestive diverticulum, a network of blind-end caeca that extends throughout the prosoma. We have previously shown that some of the residual yolk nuclei cellularize to form the columnar epidermal lining of the digestive caeca, while others form a layer of flattened cells that surround the individual caeca (Kimble *et al.*, 2002).

In most arthropod species, the yolk nuclei or yolk cells function only as vitellophages, degenerating before the end of embryonic development (Anderson, 1973; Campos-Ortega and Hartenstein, 1997). In the terrestrial chelicerates, spiders and scorpions, most of the cleavage nuclei participate in blastoderm formation. Subsequently some cells repopulate the yolk mass, where they function as vitellophages. Eventually the vitellophages migrate to the surface of the yolk mass and form the endoderm epithelium (Anderson, 1973). Thus, a role for the yolk nuclei or vitellophages in formation of the gut endoderm appears to be common to most if not all chelicerates. However, participation in formation of the mesodermal components of the gut is apparently unique to the Xiphosura. If, as suggested here, some yolk nuclei cellularize and differentiate as amebocytes during late embryogenesis, it would suggest that retention of large numbers of yolk nuclei in horseshoe crab embryos provides the embryos with a pool of undetermined nuclei that can be utilized in a variety of distinct tissues during development.

Acknowledgments

We thank undergraduate students Evelyn Wurth, Carrie Ottoson, Nicole Tremblay, Kimberly Denton, Patrick Mella,

and Victoria Davis for assistance with sectioning and staining of the embryos. These studies were supported in part by grants to MK from the USF Research Council, and from NOAA, Office of Sea Grant, Department of Commerce, Grant # NA76RG-0120. The U.S. government is authorized to produce and distribute reprints for governmental purposes not withstanding any copyright that may appear hereon. YC was supported by grants/scholarships from Sigma Xi, Sigma Delta Epsilon Graduate Women in Science, Aylesworth/Old Salt, Sea Space, The American Association of University Women, and the Florida and Tampa Garden Clubs. NA was supported in part by the McNair Post-Baccalaureate Achievement Program.

Literature Cited

Agarwala, K. L., S. Kawabata, Y. Miura, Y. Kuroki, and S. Iwanaga. 1996. *Limulus* intracellular coagulation inhibitor type 3. Purification, characterization, cDNA cloning, and tissue localization. *J. Biol. Chem.* **271:** 23,768–23,774.

Anderson, D. T. 1973. *Embryology and Phylogeny in Annelids and Arthropods.* Pergamon Press, New York. 495 pp.

Armstrong, P. B. 1985. Adhesion and motility of the blood cells of *Limulus*. Pp. 77–124 in *Blood Cells of Marine Invertebrates: Experimental Systems in Cell Biology and Comparative Physiology*, W. D. Cohen, ed. Alan R. Liss, New York.

Armstrong, P. B., and F. R. Rickles. 1982. Endotoxin-induced degranulation of the *Limulus* amebocyte. *Exp. Cell Res.* **140:** 15–24.

Bang, F. B. 1956. A bacterial disease of *Limulus polyphemus*. *Bull. Johns Hopkins Hosp.* **98:** 325–351.

Bang, F. B. 1979. Ontogeny and phylogeny of response to gram-negative endotoxins among the marine invertebrates. Pp. 109–123 in *Biomedical Applications of the Horseshoe Crab (Limulidae)*, W. D. Cohen, ed. Alan R. Liss, New York.

Campos-Ortega, J. A., and V. Hartenstein. 1997. *The Embryonic Development of* Drosophila melanogaster, 2nd ed. Springer-Verlag, Berlin. 405 pp.

Dumont, J. N., E. Anderson, and G. Winner. 1966. Some cytologic characteristics of the hemocytes of *Limulus* during clotting. *J. Morphol.* **119:** 181–208.

Hilly, J. B., and D. G. Gibson. 1989. Culture of amebocytes on opened gill lamellae of the horseshoe crab, *Limulus polyphemus*. (abstract). *Am. Zool.* **29:** 112A.

Iwanaga, S. 2002. The molecular basis of innate immunity in the horseshoe crab. *Curr. Opin. Immunol.* **14:** 87–95.

Kimble, M., Y. Coursey, N. Ahmad, and G. W. Hinsch. 2002. Behavior of the yolk nuclei during embryogenesis, and development of the midgut diverticulum in the horseshoe crab, *Limulus polyphemus*. *Invertebr. Biol.* **121:** 365–377.

Kingsley, J. S. 1892. The embryology of *Limulus*. *J. Morphol.* **7:** 35–68.

Kingsley, J. S. 1893. The embryology of *Limulus*. Part II. *J. Morphol.* **8:** 195–268.

Kishinouye, K. 1893. On the development of *Limulus longispina*. *J. Coll. Sci. Imp. Univ. Japan* **5:** 53–100.

Levin, J. 1985a. The history of the development of the *Limulus* amebocyte lysate test. Pp. 3–28 in *Bacterial Endotoxins: Structure, Biomedical Significance, and Detection with the* Limulus *Amebocyte Lysate Test. Prog. Clin. Biol. Res.* 189.

Levin, J. 1985b. The role of amebocytes in the blood coagulation mechanism of the horseshoe crab *Limulus polyphemus*. Pp. 145–163 in *Blood Cells of Marine Invertebrates: Experimental Systems in Cell Biology and Comparative Physiology*, W. D. Cohen, ed. Alan R. Liss, New York.

Liang, P., T.-K. Cheng, Y.-Q. Wu, and W.-H. Wu. 1990. Ultrastructural observations on hemocytopoiesis in embryos of the horseshoe crab, *Tachypleus tridentatus*. *Proceedings of the XII International Congress of Electron Microscopy*, August 12–18, 1990, Seattle, WA. **3:** 506–507.

Miura, Y., S.-I. Kawabata, Y. Wakamiya, T. Nakamura, and S. Iwanaga. 1995. A *Limulus* intracellular coagulation inhibitor type 2. Purification, characterization, cDNA cloning, and tissue localization. *J. Biol. Chem.* **270:** 558–565.

Miyata, T., M. Hiranaga, M. Umezu, and S. Iwanaga. 1984. Amino acid sequence of the coagulogen from *Limulus polyphemus* hemocytes. *J. Biol. Chem.* **259:** 8924–8933.

Ornberg, R. L. 1985. Exocytosis in *Limulus* amebocytes. Pp. 127–142 in *Blood Cells of Marine Invertebrates: Experimental Systems in Cell Biology and Comparative Physiology*, W. D. Cohen, ed. Alan R. Liss, New York.

Sawada, T., and S. Tomonaga. 1996. The immunocytes of protostomes and deuterostomes as revealed by LM, EM and other methods. *Adv. Comp. Environ. Physiol.* **23:** 9–40.

Sekiguchi, K. 1973. A normal plate of the development of the Japanese horseshoe crab, *Tachypleus tridentatus*. *Sci. Rep. Tokyo Kyoiku Daigaku Sect.* **15:** 153–162.

Sekiguchi, K. 1988. History of the study. Pp. 1–9 in *Biology of Horseshoe Crabs*, K. Sekiguchi, ed. Science House, Tokyo.

Sekiguchi, K., Y. Yamamichi, and J. D. Costlow. 1982. Horseshoe crab developmental studies. I. Normal embryonic development of *Limulus polyphemus* compared with *Tachypleus tridentatus*. Pp. 53–73 in *Physiology and Biology of Horseshoe Crabs: Studies on Normal and Environmentally Stressed Animals*, J. Bonaventura, C. Bonaventura, and S. Tesh, eds. Alan R. Liss, New York.

Sekiguchi, K., Y. Yamamichi, H. Seshimo, and H. Sugita. 1988. Normal development. Pp. 133–181 in *Biology of Horseshoe Crabs*, K. Sekiguchi, ed. Science House, Tokyo.

Yeager, J. F., and O. E. Tauber. 1935. On the hemolymph cell counts of some marine invertebrates. *Biol. Bull.* **69:** 66–70.

Reference: *Biol. Bull.* **204:** 28–37. (February 2003)

High-Speed Video Analysis of the Escape Responses of the Copepod *Acartia tonsa* to Shadows

EDWARD J. BUSKEY[1,*] AND DANIEL K. HARTLINE[2]

[1] *Marine Science Institute, 750 Channel View Drive, Port Aransas, Texas 78373; and* [2] *Bekesy Laboratory of Neurobiology, Pacific Biomedical Research Center, University of Hawaii at Manoa, 1993 East-West Road, Honolulu, Hawaii 96822*

Abstract. The copepod *Acartia tonsa* exhibits a vigorous escape jump in response to rapid decreases in light intensity, such as those produced by the shadow of an object passing above it. In the laboratory, decreases in light intensity were produced using a fiber optic lamp and an electronic shutter to abruptly either nearly eliminate visible light or reduce light intensity to a constant proportion of its original intensity. The escape responses of *A. tonsa* to these rapid decreases in visible light were recorded on high-speed video using infrared illumination. The speed, acceleration, and direction of movement of the escape response were quantified from videotape by using automated motion analysis techniques. *A. tonsa* typically responds to decreases in light intensity with an escape jump comprising an initial reorientation followed by multiple power strokes of the swimming legs. These escape jumps can result in maximum speeds of over 800 mm s^{-1} and maximum accelerations of over 200 m s^{-2}. In *A. tonsa*, photically stimulated escape responses differ from hydrodynamically stimulated responses mainly in the longer latencies of photically stimulated responses and in the increased number of power strokes, even when the stimulus is near threshold; these factors result in longer escape jumps covering greater distances. The latency of responses of *A. tonsa* to this photic stimulus ranged from a minimum of about 30 ms to a maximum of more than 150 ms, compared to about 4 ms for hydrodynamically stimulated escape jumps. Average response latency decreased with increasing light intensity or increasing proportion of light eliminated. Little change was observed in the vigor of the escape response to rapid decreases in visible light over a wide range of adaptation intensities.

Received 7 June 2002; accepted 26 November 2002.

* To whom correspondence should be addressed. E-mail: buskey@utmsi.utexas.edu

Introduction

Planktonic copepods are an important link in marine food webs between microplankton and higher trophic levels. Copepods are well known for their vigorous escape responses (*e.g.*, Singarajah, 1969; Fields and Yen, 1997), which play an important role in predator avoidance (*e.g.*, Drenner *et al.*, 1978; Viitasalo *et al.*, 1998). These escape responses can be elicited by both hydrodynamic (Hartline *et al.*, 1999; Kiorboe *et al.*, 1999; Lenz and Hartline, 1999) and photic stimuli (Buskey *et al.*, 1986, 1987). Despite the scarcity of direct evidence that chemosensory stimuli, by themselves, can produce vigorous escape responses in calanoid copepods, there is evidence that such stimuli can cause copepods to exhibit changes in swimming activity (*e.g.*, Katona, 1973; Buskey, 1984). Predator-specific chemicals have also been shown to alter vertical migration behavior in freshwater zooplankton (*e.g.*, Tjossem, 1990; Ringelberg, 1991) and marine crab larvae (Forward and Rittschof, 2000), but similar effects are yet to be demonstrated in marine copepods (*e.g.*, Bollens *et al.*, 1994).

Light has long been known to have an important effect on the behavior of planktonic organisms, with much research emphasizing the effects of light on vertical migration (reviewed in Forward, 1988). Photophobic responses of copepods are thought to play a role in planktonic predator-prey interactions—both in terms of a predator-deterrent role of bioluminescence in dark-adapted copepods (Buskey and Swift, 1983, 1985) and in terms of a predator-avoidance role for copepods exposed to shadows in light-adapted copepods (Buskey *et al.*, 1986). Alterations in behavior of planktonic

organisms in response to decreases in light intensity have been demonstrated in neritic calanoid copepods (Buskey *et al.*, 1987) and crab larvae (Forward, 1977).

Recent studies have used strain gauges and high-speed video to provide the high temporal resolution necessary to describe, in detail, the kinetics of the escape responses of both tethered (Lenz and Hartline, 1999; Hartline *et al.*, 1999) and free-swimming (Buskey *et al.*, 2002) calanoid copepods to hydromechanical disturbances. These studies demonstrate that copepod response latencies (down to 2 ms) are among the fastest ever recorded. This rapidity is in part due to the myelination of the nerves of some calanoid copepods (Davis *et al.*, 1999), although extremely fast responses have also been found in *Acartia tonsa* (4 ms), which does not possess myelinated nerves (Buskey *et al.*, 2002). In this study, we use high-speed video recording and computerized motion analysis techniques to describe the kinetics of the escape responses of the calanoid copepod *A. tonsa* to photic stimuli, and we compare the results to those of previous studies that examined the escape behavior of this species in response to hydrodynamic stimuli.

Materials and Methods

During March and April 2001, live zooplankton were collected from the University of Texas Marine Science Institute pier located in the Aransas Ship Channel connecting the Gulf of Mexico with Aransas and Corpus Christi bays. A 0.5-m diameter, 153-μm-mesh plankton net was allowed to stream with the tidal current for 2–3 min. The contents of the cod end were diluted into a plastic bucket containing whole seawater and returned to the laboratory for sorting. The sample was examined under a dissecting microscope and adult male and female *Acartia tonsa* were removed using a wide-bore pipette. Twenty adults of a single sex were then placed in small, clear acrylic plastic aquaria (60 × 30 × 60 mm) containing filtered seawater. Each set of copepods was used in only one experiment. Before an experiment, the copepods to be used were allowed to adapt to a specific light intensity (100, 10, 1, 0.3 or 0.1 μmol photons m^{-2} s^{-1}) for at least 1 h at near-ambient temperatures (19 ± 1 °C for complete shadow experiments, 22 °C for partial shadow experiments).

Experiments were performed in a darkroom, and red-filtered flashlights were used for viewing equipment and taking notes, since *A. tonsa* has a very low visual sensitivity to red light (Stearns and Forward, 1984a). For experiments testing the response of *A. tonsa* to complete shadows (adaptation light intensity reduced by 100%), a Dolan Jenner model 3100 Fiber Lite illuminator was used as the light source for the stimulus. A single light guide was oriented vertically above the aquarium containing the copepods, producing a beam of about 2.5-cm diameter on a sheet of opal glass resting on top of the aquarium. Light intensity was adjusted to produce a nominal light intensity of 100 μmol photons m^{-2} s^{-1} as measured in air near the center of the aquarium; light intensity was measured using a LICOR LI-250 light meter with a LI-109A quantum sensor. The light was cut off using an electronic shutter for a period of 500 ms (Vincent Associates Uniblitz SD-10 shutter driver timer and model 255 shutter). Light intensities of 10, 1, 0.3, and 0.1 μmol photons m^{-2} s^{-1} were produced using a combination of neutral-density filters placed above the shutter at the tip of the light probe. The copepods were isolated from vibrational stimuli using a Newport bench-top vibration-isolating table.

In experiments where *A. tonsa* was subjected to partial reduction in light intensity, light was provided by a Dolan Jenner Model PL-180 quartz-halogen illuminator with dual branch light guides. The light beam from each branch of the light guide was directed from opposite sides at an angle of about 30° from vertical at the same area of opal glass directly over the small aquarium containing the copepods. One branch was fitted with the electronic Uniblitz shutter to cut off a fraction of the light striking the aquarium. The relative contribution of the light guides to total illumination of the chamber was modified using neutral-density filters. Only adult female copepods were used in studies of escape responses to partial reduction of light intensity.

In an experimental run, each group of copepods was allowed to further adapt to the new experimental setup for a minimum of 30 min after being moved. The position of copepods in the field of view was observed on the television monitor, and the shutter was actuated when at least 2 copepods could be observed. After each group of copepods was stimulated, the high-speed video would be played back at slow speed (1 frame s^{-1}) to record the number of copepods responding to the stimulus and the latency of the response. Each group of copepods was subjected to decreases in light intensity several times until a minimum of 20 copepods had been observed. These experiments were repeated with at least six different groups of copepods under each set of light-adaptation conditions.

Images of copepod escape responses were recorded at 1000 frames per second using a high-speed video camera (Kodak Motion Corder Analyzer Model SR-3000). The camera was equipped with a 50-mm f1.4 Nikon Nikkor lens, and viewed an area of about 25 × 30 mm. Additional lighting for recording copepod images during the absence or decrease of visible light during shadows was provided by a dark-field array of infrared-light-emitting diodes. The high-speed video camera recorded 2184 frames of video at 1000 frames per second. A signal from the electronic shutter was used to trigger the camera to capture half the video frames before and half after the decrease in light intensity. These frames were then played back at 30 frames per second and recorded on a Panasonic AG 6300 videocassette recorder.

These high-speed video records were then reviewed to

choose escape paths for computerized motion analysis. Analysis of the behavioral parameters associated with the complete escape response of *Acartia tonsa* was hindered by the vigor of the response. To have the image of the copepods large enough to be automatically tracked by our motion analysis system, the field of view was limited to about 25 × 30 mm, and some copepods swam out of the field of view during their escape response. We attempted to quantify behavioral parameters for 20 escape responses for each set of conditions. We chose escape responses in which the copepod's initial position could be observed, and whose trajectories covered a minimum of one-third of the screen (tracked for at least 1 cm). Because escape behaviors were recorded in two dimensions, only trajectories perpendicular to the recording camera were accurately recorded. To minimize errors through analysis of paths not perpendicular to the camera, the aspect ratios of copepod images were measured at the beginning, middle, and near the end of their escape jumps (Buskey *et al.*, 2002). Aspect ratios greater than 3 indicated that a copepod was nearly perpendicular to the line of view of the video camera. Escape responses with an aspect ratio less than 2.5 during part of their trajectory were not used for motion analysis. Since only 20 escape responses were quantified out of the more than 120 copepods observed, instances in which escape responses were recorded from the same copepod should be rare, if they occurred at all.

Swimming behavior of the copepods was quantified from videotapes using an Expertvision Cell-Trak video-computer motion-analysis system. High-speed video recorded at 1000 frames per second was transferred to videotape at 30 frames per second. These videotaped images of the copepods were digitized using the Motion Analysis VP-110 video-to-digital processor, and digitized outlines of the copepods were sent to a host computer at a rate of 30 frames per second. These digitized images were processed using Cell-Trak software to calculate the swimming speeds (mm s^{-1}), acceleration (m s^{-2}), and number of swimming leg thrusts per jump of the copepod's paths of travel. Jump latencies (time from stimulus to response) were determined by reviewing the videotapes frame-by-frame for a minimum of 200 ms. High-speed video analysis revealed an average delay of 6-ms between the signal sent to start the video sequence and the closing of the electronic shutter. Response latencies were corrected for this delay in stimulus onset. A copepod occasionally performed a single spontaneous jump during the 200-ms period after the decrease in light intensity. Spontaneous jumps consist of a single thrust of the swimming legs with lower peak speeds than escape jumps (Buskey *et al.*, 2002). These occurred both before and after the decrease in light intensity and were not counted as photic escape responses.

Results

Acartia tonsa responds to a rapid decrease in light intensity with a series of vigorous thrusts of the swimming legs. An example of a record of changes in swimming speed over time for the response of an adult female adapted to 100 μmol photons m^{-2} s^{-1} and subjected to a complete reduction in visible light is shown in Figure 1. In this example, the dashed vertical line represents the time at which light intensity decreased; the response was initiated 32 ms later as a series of 11 thrusts of the swimming legs. Although the action was not apparent in the swimming speed record, examination of high-speed video revealed a rapid reorientation of the body axis by about 40 degrees during the 2-ms period preceding the first escape thrust. Maximum speeds during these swimming thrusts ranged between 400 and 600 mm s^{-1}, with minimum speeds between thrusts decreasing to between 200 and 350 mm s^{-1}. The duration of each thrust of the swimming legs is about 8 ms (time from minimum speed at the beginning of one thrust to minimum speed at the beginning of the next thrust). The entire response lasted about 80 ms and displaced the copepod by about 31 mm. Examples of escape trajectories during photically stimulated escape jumps are shown in Figure 2A. These escape jumps, plotted from a common starting point, typically displace the copepod 10 to 15 mm from its original location. The range of responses observed, in terms of distance moved over time, ranges from 5 to 15 mm within the first 50 ms of the escape jump (Fig. 2B).

For complete reduction in light intensity, the proportion of copepods exhibiting an escape response varied with the light adaptation intensity. For adult male copepods, adapta-

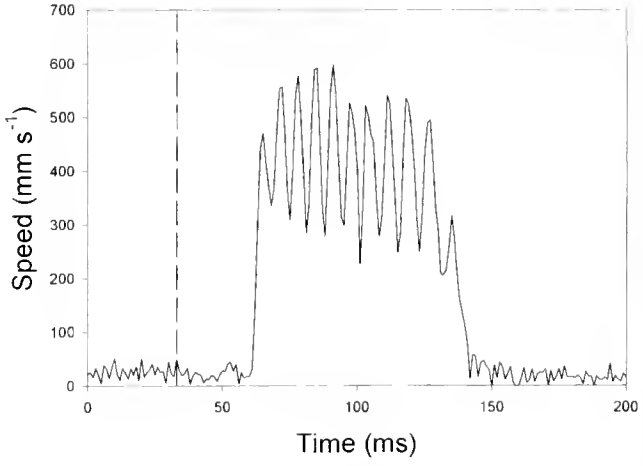

Figure 1. Example of a record of swimming speed over time for the photically stimulated escape response of an adult female specimen of *Acartia tonsa*. This copepod was adapted to a light intensity of 100 μmol photons m^{-2} s^{-1} and subjected to a 100% decrease in light intensity. The vertical dashed line represents the beginning of the decrease in light intensity.

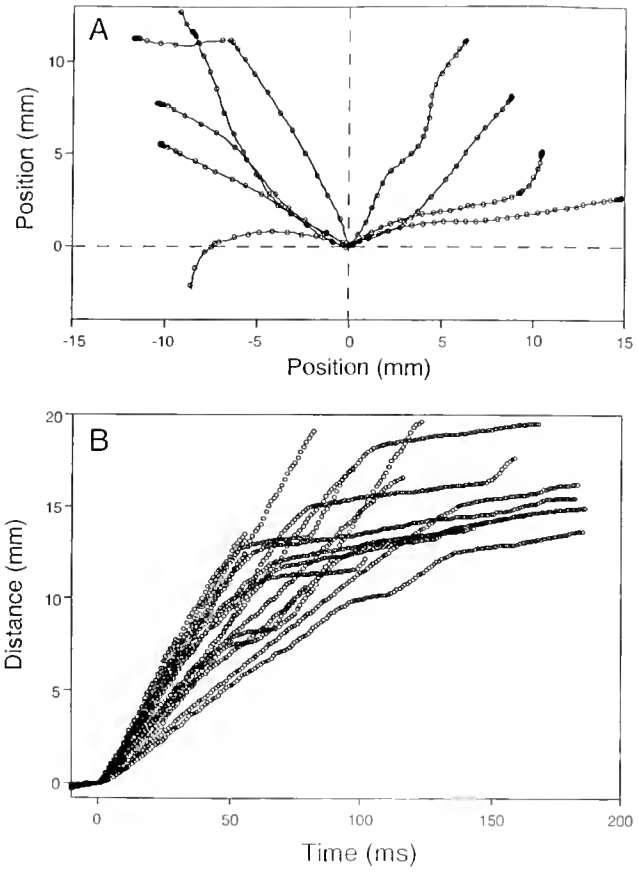

Figure 2. Displacement trajectories in the vertical plane plotted from a common starting point for escape responses to rapid decreases in light intensity of adult female specimens of *Acartia tonsa* (A). Distance from original position plotted against time (B).

tion intensities of 0.3 μmol photons m^{-2} s^{-1} and higher resulted in a response by about 80% of the copepods (Fig. 3A). For an adaptation intensity of 0.1 μmol photons m^{-2} s^{-1}, the response rate dropped rapidly to less than 10%. For adult females of *A. tonsa* the change in response rate with light adaptation intensity changed more gradually (Fig. 3B). At both 10 and 100 μmol photons m^{-2} s^{-1}, response rate was similar to that of males at the same intensity, about 80%. However, the response rate dropped to about 60% at 1.0 μmol photons m^{-2} s^{-1} and to less than 50% at 0.3 μmol photons m^{-2} s^{-1}. None of the females responded at an adaptation intensity of 0.1 μmol photons m^{-2} s^{-1}. Therefore, the threshold light intensity for stimulating escape responses with complete shadows is between 0.1 and 0.3 μmol photons m^{-2} s^{-1} for both adult males and females of *A. tonsa*.

For complete reduction in light intensity, the response latency between the initiation of the change in light intensity and the initiation of the first escape movement increases as the light adaptation intensity decreases (Fig. 3). For adult males, the mean response latencies progressively changed from 38 ms at 100 μmol photons m^{-2} s^{-1} to 90 ms at 0.1 μmol photons m^{-2} s^{-1}. A Kruskal-Wallis one-way ANOVA on ranks indicated a significant difference in response latencies at different adaptation intensities ($P < 0.001$). Dunn's method for pairwise comparisons revealed that all pairs of groups were significantly different from one another ($P < 0.05$). For adult females, the mean response latencies changed from 33 ms at 100 μmol photons m^{-2} s^{-1} to 96 ms at 0.3 μmol photons m^{-2} s^{-1}. A Kruskal-Wallis one-way ANOVA on ranks again indicated a significant difference in response latencies at different adaptation intensities ($P < 0.001$). Pairwise comparisons using Dunn's method indicated that latencies were significantly different from one another ($P < 0.05$) except for comparison of adaptation intensities of 0.3 and 1 μmol photons m^{-2} s^{-1}.

Although the response latencies changed for adult males of *A. tonsa* over the range of light adaptation intensities from 0.3 to 10 μmol photons m^{-2} s^{-1}, there was no evidence that the vigor of their escape behavior changed sig-

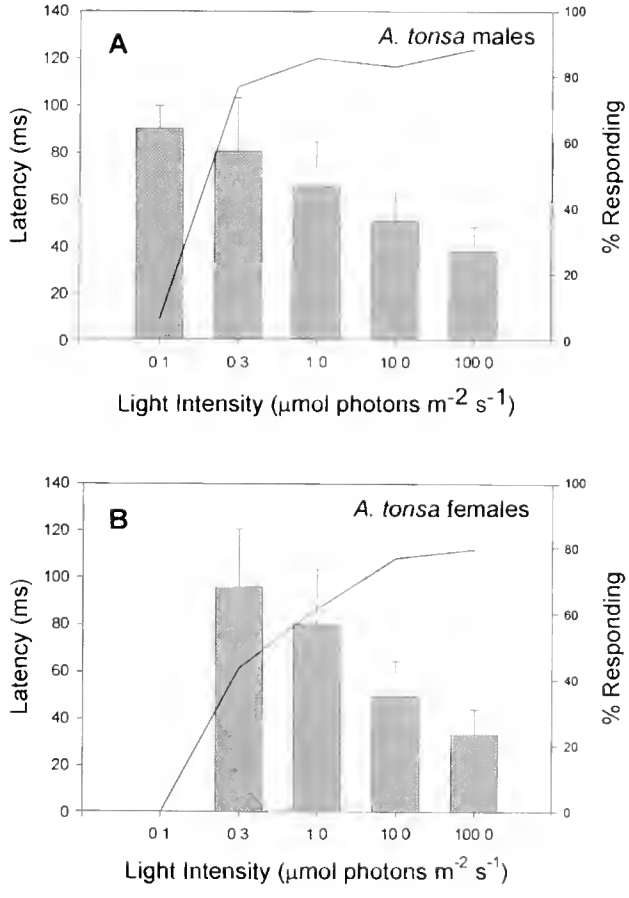

Figure 3. The percentage of copepods responding to complete shadows (solid line) for copepods adapted to a range in light intensities, and the mean latency between escape responses and initiation of the change in light intensity. Error bars represent 1 standard deviation. Responses of adult male (A) and adult female (B) specimens of *Acartia tonsa*.

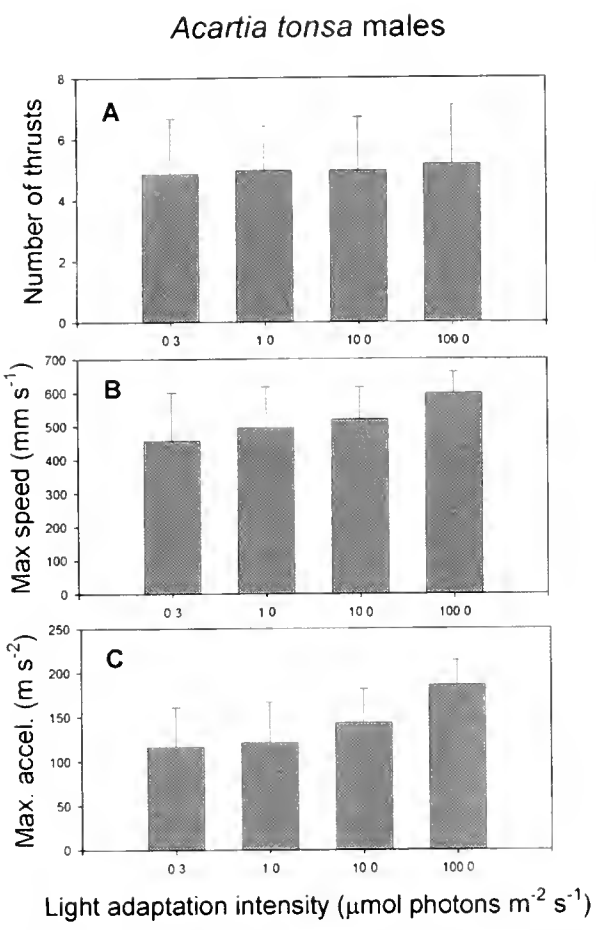

Figure 4. Characteristics of escape responses for male specimens of *Acartia tonsa* exposed to complete shadows, including average number of thrusts per escape response (A), maximum speed (mm s^{-1}) achieved during escape (B), and maximum acceleration (m s^{-2}) during escape (C). Copepods were adapted to light intensities of 0.3, 1, 10, or 100 μmol photons m^{-2} s^{-1}. Error bars represent 1 standard deviation.

nificantly until an adaptation intensity of 100 μmol photons m^{-2} s^{-1} was applied (Fig. 4). Although no significant change in the number of swimming leg thrusts in each escape response was observed, there was a significant change in average speed ($P < 0.001$, one-way ANOVA, data not shown), maximum speed ($P = 0.001$, Kruskal-Wallis one-way ANOVA on ranks), and maximum acceleration ($P < 0.001$, one-way ANOVA). Pairwise comparisons revealed that average speeds and maximum accelerations of adult males during escape responses were significantly different at an adaptation intensity of 100 μmol photons m^{-2} s^{-1} from those at each other intensity tested (Tukey test, $P < 0.05$). For maximum speed, adult male copepods adapted to 100 μmol photons m^{-2} s^{-1} were significantly different only from those at 1.0 and 0.3 μmol photons m^{-2} s^{-1} adaptation intensities (Dunn's method, $P < 0.05$).

Adult females of *A. tonsa* tested over a range of adaptation intensities from 0.3 to 100 μmol photons m^{-2} s^{-1} also showed some differences in escape behaviors at the highest adaptation intensity (Fig. 5). There was no significant difference in the number of thrusts of the swimming legs in each escape jump (one-way ANOVA, $P = 0.057$) or in average speed of escape responses over this range of adaptation intensities (one-way ANOVA, $P = 0.170$, data not shown). For maximum speed during escape, there was a significant difference between escape responses of copepods adapted to different light intensities (Kruskal-Wallis one-way ANOVA on ranks, $P = 0.04$). Dunn's method for pairwise comparison for all pairs revealed that only the maximum speeds for escape responses of copepods adapted to 0.3 and 100 μmol photons m^{-2} s^{-1} were significantly different ($P < 0.05$). For maximum acceleration achieved during escape responses, there was also a significant difference between copepods adapted to different light intensities (one-way ANOVA, $P < 0.001$). Pairwise comparison us-

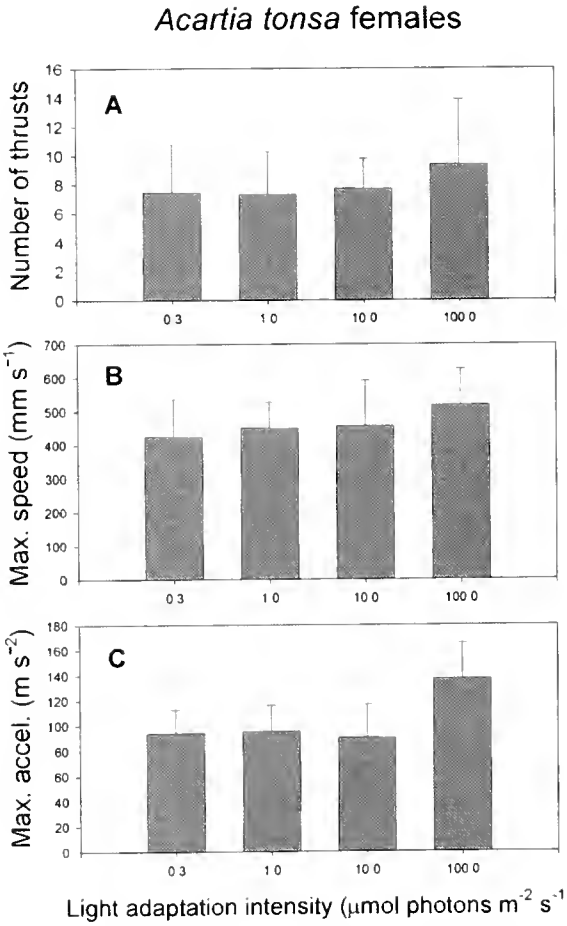

Figure 5. Characteristics of escape responses for female specimens of *Acartia tonsa* exposed to complete shadows, including average number of thrusts per escape response (A), maximum speed (mm s^{-1}) achieved during escape (B), and maximum acceleration (m s^{-2}) during escape (C). Copepods were adapted to light intensities of 0.3, 1, 10 or 100 μmol photons m^{-2} s^{-1}. Error bars represent 1 standard deviation.

Table 1

Summary of escape response parameters for adult females and males of Acartia tonsa *exposed to photic stimuli*

Parameter	Females	Males	*P*
Latency (ms)	68.2 (1.8; 29–159)	62.2 (1.3; 35–138)	<0.001*
Initial turn (deg)	41.3 (3.3; 5–103)	74.1 (4.6; 12–165)	<0.001*
Jump speed (mm s^{-1})	256 (10; 125–476)	293 (12; 83–383)	0.453
Maximum speed (mm s^{-1})	446 (15; 235–827)	494 (16; 214–727)	0.002*
Max. acceleration (m s^{-2})	93.3 (10.1; 54–156)	128 (6.0; 41–211)	<0.001*
Number of thrusts	7.5 (0.4; 3–15)	4.9 (0.2; 2–9)	<0.001*
Minimum speed between thrusts (mm s^{-1})	130 (2.2; 65–230)	147 (3.2; 65–256)	<0.001*
Thrust duration (ms)	8.8 (0.1; 4–13)	8.1 (0.1; 6–14)	<0.001*
Jump duration (ms)	74.6 (3.6; 33–136)	44.5 (1.8; 16–70)	<0.001*
Distance jumped (mm)	12.5 (0.6; 5.3–25.5)	8.6 (0.5; 3.4–15.1)	<0.001*

Data are pooled for jumps with adaptation intensities of 10, 1, and 0.3 μmol photons m^{-2} s^{-1}. Means are based on 54 escape jumps for females or 53 escape jumps for males. Standard error and range are given in parentheses. Probability (*P*) is based on the Mann-Whitney sum rank test. An asterisk * indicates a significant difference ($\alpha = 0.05$).

ing Tukey's test revealed that copepods adapted to 100 μmol photons m^{-2} s^{-1} had significantly different maximum accelerations from each of the other adaptation intensities ($P < 0.05$).

Since no significant differences were found between between escape response parameters for copepods adapted to 10, 1, or 0.3 μmol photons m^{-2} s^{-1}, results from these three intensities were pooled for comparisons between male and female escape response parameters. Females had significantly longer response latencies than males, but significantly smaller initial turns (Table 1). Although there were no significant differences in the average escape speed of males and females, males exhibited significantly higher maximum speeds and maximum accelerations than females. Females also performed significantly more thrusts per escape jump than did males; the time between thrusts was longer and the minimum speed between thrusts was slower for females compared to males (Table 1). Overall duration of the escape jump was significantly longer for females, and the distance jumped was significantly farther for females than for males.

There was also a difference in the dominant directionality of the escape responses between copepods adapted to low light intensities (1 μmol photons $m^{-2}s^{-1}$) and higher adaptation intensities (100 μmol photons $m^{-2}s^{-1}$). Analysis of the direction of travel of the copepods during their high-speed escape responses reveals that for copepods adapted to low light intensities, the dominant swimming direction in response to a complete shadow was upward (Fig. 6B), whereas copepods adapted to higher light intensities showed a larger proportion of lateral swimming during escape responses (Fig. 6A).

For copepods exposed to only partial reductions in light intensity, which should correspond to light change more similar to a natural shadow in nature, the proportion of copepods responding to these changes in light intensity

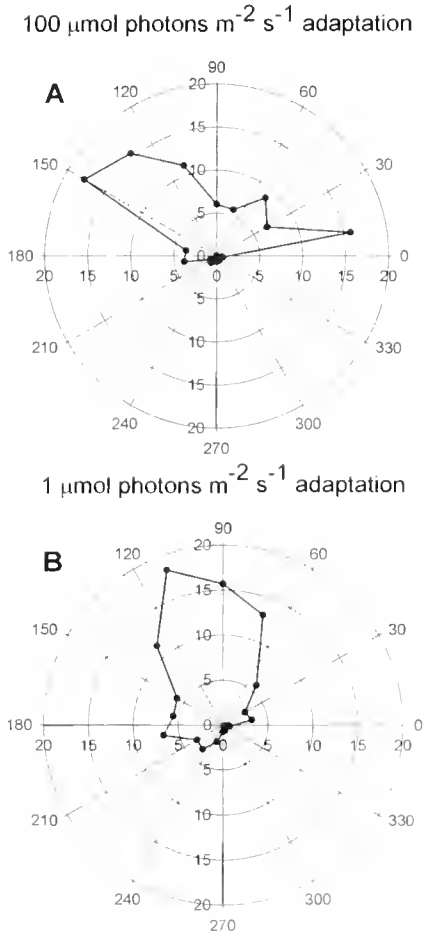

Figure 6. Polar plot of direction of travel in the vertical plane during escape responses of adult female specimens of *Acartia tonsa* adapted to 100 μmol photons m^{-2} s^{-1} light (A) or 1 μmol photons m^{-2} s^{-1} (B). Plots represent the percentage of time traveled in each direction during escape behaviors. The coordinate system is arbitrary, with 0 degrees representing motion to the right, 90 degrees representing motion upward, and so forth.

increased as the percent change in light intensity was increased (Fig. 7). For adult females adapted to a low light intensity (10 μmol photons $m^{-2}s^{-1}$), the proportion of copepods responding to light reductions dropped sharply from near 80% for a 100% reduction in light intensity to less than 10% for a 21% reduction in light intensity. For copepods adapted to higher light intensity (100 μmol photons $m^{-2}s^{-1}$), the proportion of copepods responding to reductions in light intensity declined more gradually from a response of 80% to a complete shadow to a response of less than 20% to a 21% shadow (Fig. 7). Response latencies did not change with percent light reduction in a systematic way. For adult females adapted to 10 μmol photons $m^{-2}s^{-1}$, there were significant differences in latency between copepods responding to 100%, 45%, and 28% reduction in light intensity (Kruskal-Wallis one-way ANOVA on ranks, $P = 0.001$). Too few copepods responded to a 21% reduction in light intensity to compare their latencies. Pairwise comparison to latencies at 100% reduction in light intensity showed that both groups differed significantly from this control group (Dunn's method, $P < 0.05$). For copepods adapted to 100 μmol photons $m^{-2}s^{-1}$, there were also significant differences in response latencies between groups (Kruskal-Wallis one-way ANOVA on ranks, $P < 0.001$), and latencies for 45% and 28% reductions in light intensity were significantly different from control latencies for complete shadows, but there was no difference for 21% reductions (Dunn's method).

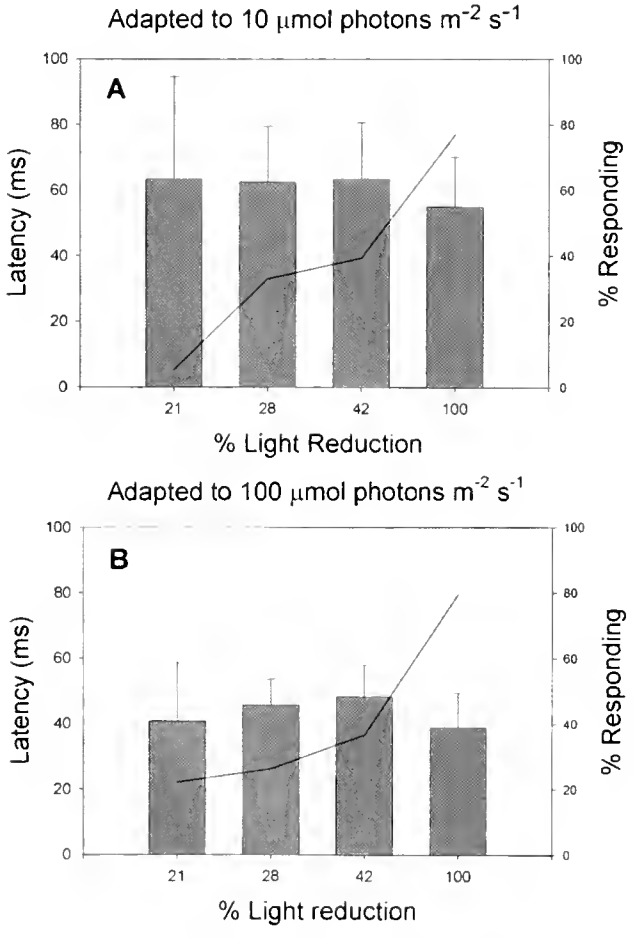

Figure 7. The percentage of adult female specimens of *Acartia tonsa* responding to shadows (solid line) with constant fractions of light reduction and the mean latency between escape responses and initiation of change in light intensity. Error bars represent 1 standard deviation. Copepods adapted to 10 μmol photons $m^{-2}s^{-1}$ (A), and copepods adapted to 100 μmol photons $m^{-2}s^{-1}$ (B).

Discussion

Calanoid copepods are consumed by a wide range of pelagic predators including other copepods, chaetognaths, jellyfish, fish, and whales. Their primary sensory system for direct detection of predators is often considered to be mechanoreception; copepods are extraordinarily sensitive to small hydromechanical disturbances (Kiørboe and Visser, 1999; Lenz and Hartline, 1999). Photoreception may also play a role in predator avoidance by copepods. Most calanoid copepods, including *Acartia tonsa*, possess only a simple naplius eye consisting of paired dorsal ocelli and a single ventral ocellus (Elofsson, 1966). These simple photoreceptors are not capable of image formation, but photoreception is thought to regulate the timing and extent of vertical migration in many copepod species (*e.g.*, Stearns and Forward, 1984b; reviewed in Forward, 1988) which indirectly helps copepods avoid attack by visual predators by remaining in low light environments during daylight hours.

Calanoid copepods may use photoreception to avoid direct attacks by predators through photophobic responses to rapid increases or decreases in light intensity (Buskey *et al.*, 1987). A commonly suggested function of the bioluminescence of dinoflagellates is as a deterrent against nocturnal predation (Tett and Kelly, 1973; Porter and Porter, 1979; Morin, 1983). Dark-adapted copepods exhibit strong escape responses to both natural and simulated dinoflagellate bioluminescence (Buskey *et al.*, 1983; Buskey and Swift, 1983, 1985). Dinoflagellate bioluminescence stimulated during the feeding of copepods may attract visual predators on the copepods through a "burglar alarm" effect (Burkenroad, 1943; Mensinger and Case, 1992; Abrahams and Townsend, 1993). Light-adapted copepods exhibit similar escape responses when exposed to rapid decreases in light intensity (Buskey *et al.*, 1986, 1987). These shadow responses might help copepods avoid "hydrocryptic" predators such as ctenophores and cnidarian medusae that produce only small hydrodynamic disturbances but cast shadows during the day as they descend in the water column.

To provide an effective defense against shadow-casting predators, it might seem that laterally oriented escape trajectories would be more effective than vertically oriented

responses, which might propel the copepod toward the predator. In this study, copepods adapted to low light intensities more often showed vertically oriented escape paths, while those adapted to higher light intensities more often moved laterally (Fig. 6). In a previous study of shadow responses of *Acartia tonsa* from Narragansett Bay, Rhode Island, copepods adapted to these lower intensities showed laterally directed escape responses (Buskey *et al.*, 1986). The reasons for the regional differences in behavioral responses of *A. tonsa* are uncertain. Coastal bays in Texas are generally shallower than Narragansett Bay and have weaker tidal currents (Hess and White, 1974; Armstrong, 1987). Members of this species are known to be strong vertical migrators (Stearns and Forward 1984b); in shallow subtropical bays they are closely associated with the bottom during the day (Stubblefield *et al.*, 1984; Buskey, 1993), rather than being suspended in the water column as they are in deeper environments with stronger currents. As a defense against shadow-generating benthic predators such as bottom-feeding fish, vertically directed escape responses might be effective adaptions for copepods closely associated with the bottom during the day.

Previous studies have used the same high-speed video analysis to examine hydrodynamically stimulated escape responses in *A. tonsa* (Buskey *et al.*, 2002). One of the salient differences we found between the photically and mechanically triggered escape behaviors in this species was the substantially larger minimum reaction time of the former (29 ms *vs.* 3 ms to first movement; Tables 1, 2). The shortest photically triggered behavioral responses we have found in the invertebrate literature is about 30 ms for the startle response (mesothoracic leg thrust) to sudden light decreases in *Drosophila melanogaster* (review: Wyman *et al.*, 1984). Larger animals are somewhat slower: 450 ms for the withdrawal reflex of leech (Laverack, 1969); 50 ms for the photic startle (flash) response of squid (Neumeister *et al.*, 2000); and 30 ms for the photophobic fast-start response to sudden darkening in small fish (Hartline, unpubl. data). In contrast, the reaction latencies to mechanical stimulation of several species is considerably shorter: 40 ms for leech (Laverack, 1969); 11 ms for response to air puff in slowly walking cockroach (Camhi and Nolen, 1981); and 5 ms for the Mauthner-mediated fast-start in adult zebra fish (Eaton *et al.*, 1977). Part of the reason for the difference between the two modalities is in the intrinsic speed of the sensory mechanism mediating the reaction. Mechanoreceptors in a wide variety of species employ direct mechanical links to transmit movement of the receptive surface (*e.g.*, a seta) directly to the ion channel in the membrane of the receptor cell, thus reducing delays to onset of receptor potentials to tens of microseconds (*e.g.*, Thurm, 1965; review: French, 1992). There is no need for time-consuming amplification beyond the initial molecular transduction event. Photic signals, on the other hand, involve an extensive biochemical cascade, including amplification of the original molecular event (photoisomerization of a rhodopsin-like compound) and diffusion of reactants to ionic channel sites in receptor membranes (review: Goldsmith, 1991). This takes time. Minimum latencies to onset of electrical changes are measured in milliseconds—10–20 ms in slow arthropod eyes, including most crustaceans; 3–6 ms in fast insect eyes (Bullock and Horridge, 1965); 7 ms in cuttlefish (Weeks and Duncan, 1974); 15–50 ms in cold-blooded vertebrates (Tomita, 1970, review and citations); 2 ms in monkey [at 38 °C], (Brown *et al.*, 1965). Thus the photic modality is an inherently slow one, and the faster mechanical one has some clear advantages for animal survival.

A second component of the physiology impacting re-

Table 2

Comparison of mean escape response parameters for adult males and adult females of Acartia tonsa *stimulated with photoic (PH) or hydrodynamic (HY) stimuli*

	Males			Females		
Parameter	PH	HY	*P*	PH	HY	*P*
Response latency (ms)	62.2	3.6	<0.001*	68.2	3.5	<0.001*
Initial turn (deg)	74.1	82.1	0.22	41.3	45.9	0.21
Jump speed (mm s^{-1})	293	213	0.09	256	188	<0.001*
Maximum speed (mm s^{-1})	494	432	0.001*	446	372	<0.001*
Max. acceleration (m s^{-2})	128	163	<0.001*	93	112	<0.001*
Number of thrusts	4.9	3.1	<0.001*	7.5	3.3	<0.001*
Minimum speed between thrusts (mm s^{-1})	147	166	0.272	130	133	0.889
Thrust duration (ms)	8.1	6.1	<0.001*	8.8	6.6	<0.001*
Jump duration (ms)	44.5	19.3	<0.001*	74.6	24.1	<0.001*
Distance jumped (mm)	8.6	4.2	<0.001*	12.5	4.6	<0.001*

Probability (*P*) based on the Mann-Whitney sum rank test. An asterisk * indicates a significant difference ($\alpha = 0.05$)
Data for responses to hydrodynamic stimuli are from Buskey *et al.* (2002).

sponse characteristics is the neural substrate for processing the sensory information and firing the motorneurons associated with effector muscle action. Although differences of 10–20 ms in the primary transduction processes could account for much of the observed difference in behavioral latencies in copepods, they are perhaps not enough to account for all. Both in *Drosophila* and several annelids, the system of giant fibers (axons) is involved in both photically and mechanically triggered reactions. The large diameter of these axons speeds the conduction of nerve impulses and is widely used throughout invertebrate groups in escape and startle reactions. Vertebrates utilize myelination of axons instead of large size to increase conduction speed. *Acartia* is known to possess giant mechanosensory fibers in its antennae (Yen *et al.*, 1992). It is not one of the myelinated species (Lenz *et al.*, 2000). It may be presumed to have similar giant fibers involved in escape reactions elsewhere in its nervous system, as do other copepods (Lowe, 1935; Park, 1966; Lenz *et al.*, 2000). However, the involvement of such elements is not yet certain in photic responses, and longer-latency pathways may be involved, as they are in the escape reactions of other organisms.

Several other aspects of photically triggered escape appeared different from those of the hydrodynamically triggered escape described by Buskey *et al.* (2002). Keeping in mind the intrinsic difficulties of inter-modality comparisons, we pooled the responses for copepods adapted to 0.3, 1, and 10 μmol photons $m^{-2}s^{-1}$ adaptation levels going to complete dark, which were not significantly different from one another in their escape parameters, to compare with the range of hydrodynamic stimulation of Buskey *et al.* (2002). In addition, adaptation temperature was slightly different for responses compared in the two studies (19 °C in this study *vs.* 22 °C in Buskey *et al.*, 2002), although there was no significant difference found in the response latencies of adult females of *A. tonsa* at 19 °C (Fig. 3) and 22 °C (Fig. 7) under the same light conditions. Maximum speeds in the photic responses were significantly higher for photically stimulated escape responses than for hydrodynamically stimulated responses in both male and female individuals of *A. tonsa* (Table 2). In contrast, maximum accelerations were significantly greater for hydrodynamically stimulated escape responses than for photically stimulated responses in both males and females. Photically stimulated reponses were also clearly more extensive than the hydrodynamically stimulated responses, with significantly more thrusts, longer jump duration, and greater distance jumped (Table 2). Interestingly, the duration of individual thrusts within an escape response was significantly greater for photically stimulated escapes for both males and females. The pattern that emerges from the various comparisons is that both the triggering of the escape (including the orientation component, and the excitation that keeps the neural circuits active) and the characteristics of the motor output are modality-specific. This calls into question the same central motor pattern generator being involved in both escape reactions. An increase in response vigor at the highest stimulus intensity was found in the present studies, but was not clearly apparent in our earlier work on mechanically evoked escape (Buskey *et al.*, 2002). However, other copepods do appear to adjust the vigor of response with the intensity of mechanical stimulus (Lenz and Hartline, 1999), so this feature, too, may be parallel between photic and mechanosensory systems. It would seem that the two sensory-motor systems have evolved semi-independently, each to protect the animal from a certain type of predatory threat. In doing so, they utilize common elements of motor pattern production and control; yet rather distinct circuitry that gives characteristics appropriate to each situation has been developed as well. When examined minutely, the escape circuitry of other organisms has often revealed a multiplicity of pathways at the motor as well as the sensory side (*e.g.*, Wine and Krasne, 1982; Eaton *et al.*, 2001). It remains to be seen whether such complications also occur in copepods.

Acknowledgments

This research was supported by the National Science Foundation through grant OCE 9910608. Cammie Hyatt and Becky Waggett assisted with sorting of copepods for experiments and with videotaping experiments. This is University of Texas Marine Science Institute Contribution Number 1246.

Literature Cited

Abrahams, M. V., and L. D. Townsend. 1993. Bioluminescence in dinoflagellates: a test of the burglar alarm hypothesis. *Ecology* **74:** 258–260.

Armstrong, N. E. 1987. The ecology of open-bay bottoms of Texas: a community profile. *U.S. Fish. Wildl. Serv. Biol. Rep.* **85:** 1–104.

Bollens, S. M., B. W. Frost, and J. R. Cordell. 1994. Chemical, mechanical and visual cues in the vertical migration behavior of the marine planktonic copepod *Acartia hudsonica*. *J. Plankton Res.* **16:** 555–564.

Brown, K. T., K. Watanabe, and M. Murakami. 1965. The early and late receptor potentials of monkey cones and rods. *Cold Spring Harbor Symp. Quant. Biol.* **30:** 457–482.

Bullock, T. H., and G. A. Horridge. 1965. *Structure and Function in the Nervous System of Invertebrates.* W.H. Freeman, San Francisco. 1719 pp. (Ch. 19).

Burkenroad, M. D. 1943. A possible function of bioluminescence. *J. Mar. Res.* **5:** 161–164.

Buskey, E. J. 1984. Swimming pattern as an indicator of the roles of copepod sensory systems in the recognition of food. *Mar. Biol.* **79:** 165–175.

Buskey, E. J. 1993. Annual pattern of micro- and mesozooplankton abundance and biomass in a subtropical estuary. *J. Plankton Res.* **15:** 907–924.

Buskey, E. J., and E. Swift. 1983. Behavioral responses of the coastal copepod *Acartia hudsonica* to simulated dinoflagellate bioluminescence. *J. Exp. Mar. Biol. Ecol.* **72:** 43–58.

Buskey, E. J., and E. Swift. 1985. Behavioral responses of oceanic zooplankton to simulated bioluminescence. *Biol. Bull.* **168:** 263–275.

Buskey, E. J., L. Mills, and E. Swift. 1983. The effects of dinoflagellate bioluminescence on the swimming behavior of a marine copepod. *Limnol. Oceanogr.* **28:** 575–579.

Buskey, E. J., C. G. Mann, and E. Swift. 1986. The shadow response of the estuarine copepod *Acartia tonsa*. *J. Exp. Mar. Biol. Ecol.* **103:** 65–75.

Buskey, E. J., C. G. Mann, and E. Swift. 1987. Photophobic responses of calanoid copepods: possible adaptive value. *J. Plankton Res.* **9:** 857–870.

Buskey, E. J., P. H. Lenz, and D. K. Hartline. 2002. Escape behavior of planktonic copepods to hydrodynamic disturbances: high speed video analysis. *Mar. Ecol. Prog. Ser.* **235:** 135–146.

Camhi, J. M., and T. G. Nolen. 1981. Properties of the escape system of cockroaches during walking. *J. Comp. Physiol.* **142:** 339–346.

Davis, A. D., T. M. Weatherby, D. K. Hartline, and P. H. Lenz. 1999. Myelin-like sheaths in copepod axons. *Nature* **398:** 571.

Drenner, R. W., J. R. Strickler, and W. J. O'Brien. 1978. Capture probability: the role of zooplankton escape in the selective feeding of planktivorous fish. *J. Fish. Res. Board Can.* **35:** 1370–1373.

Eaton, R. C., R. A. Bombardieri, and D. L. Meyer. 1977. The Mauthner-initiated startle response in teleost fish. *J. Exp. Biol.* **66:** 65–81.

Eaton, R. C., R.K.K. Lee, and M. B. Foreman. 2001. The Mauthner cell and other identified neurons of the brainstem escape network of fish. *Prog. Neurobiol.* **63:** 467–485.

Elofsson, R. 1966. The nauplius eye and frontal organs of the non-Malacostraca (Crustacea). *Sarsia* **25:** 1–128.

Fields, D. M., and J. Yen. 1997. The escape behavior of marine copepods in response to a quantifiable fluid mechanical disturbance. *J. Plankton Res.* **19:** 1289–1304.

Forward, R. B., Jr. 1977. Occurrence of a shadow response among brachyuran larvae. *Mar. Biol.* **39:** 331–341.

Forward, R. B., Jr. 1988. Diel vertical migration: zooplankton photobiology and behavior. *Oceanogr. Mar. Biol. Annu. Rev.* **26:** 361–393.

Forward, R. B., Jr., and D. Rittschof. 2000. Alteration of photoresponses involved in diel vertical migration of a crab larva by fish mucus and degradation products of mucopolysaccharides. *J. Exp. Mar. Biol. Ecol.* **245:** 277–292.

French, A. S. 1992. Mechanotransduction. *Annu. Rev. Physiol.* **54:** 135–152.

Goldsmith, T. H. 1991. Photoreception and vision. Pp. 171–245 in *Neural and Integrative Animal Physiology*, C.L. Prosser, ed. Wiley-Liss, New York.

Hartline, D. K., E. J. Buskey, and P. H. Lenz. 1999. Rapid jumps and bioluminescence elicited by controlled hydrodynamic stimuli in a mesopelagic copepod, *Pleuromamma xiphias*. *Biol. Bull.* **197:** 132–143.

Hess, K., and F. White. 1974. A numerical tidal model of Narragansett Bay. Sea Grant Marine Technical Rep. **20.** University of Rhode Island, Kingston, RI.

Katona, S. K. 1973. Evidence for sex pheromones in planktonic copepods. *Limnol. Oceanogr.* **18:** 574–583.

Kiørboe, T., and A. Visser. 1999. Predator and prey perception in copepods due to hydromechanical signals. *Mar. Ecol. Prog. Ser.* **179:** 81–95.

Kiørboe, T., E. Saiz, and A. Visser. 1999. Hydrodynamic signal perception in the copepod *Acartia tonsa*. *Mar. Ecol. Prog. Ser.* **179:** 97–111.

Laverack, M. S. 1969. Mechanoreceptors, photoreceptors, and rapid conduction pathways in the leech, *Hirudo medicinalis*. *J. Exp. Biol.* **50:** 129–140.

Lenz, P. H., and D. K. Hartline. 1999. Reaction times and force production during escape behavior of a calanoid copepod *Undinula vulgaris*. *Mar. Biol.* **133:** 249–258.

Lenz, P. H., D. K. Hartline, and A. D. Davis. 2000. The need for speed. I. Fast reactions and myelinated axons in copepods. *J. Comp. Physiol. A* **186:** 337–345.

Lowe, E. 1935. On the anatomy of a marine copepod, *Calanus finmarchicus* (Gunnerus). *Trans. R. Soc. Edinb.* **63:** 560–603.

Mensinger, A. F., and J. F. Case. 1992. Dinoflagellate luminescence increases susceptibility of zooplankton to teleost predation. *Mar. Biol.* **112:** 207–210.

Morin, J. G. 1983. Coastal bioluminescence: patterns and functions. *Bull. Mar. Sci.* **33:** 787–817.

Neumeister, H., B. Ripley, T. Preuss, and W. F. Gilly. 2000. Effects of temperature on escape jetting in the squid *Loligo opalescens*. *J. Exp. Biol.* **203:** 547–557.

Park, T. S. 1966. The biology of a calanoid copepod *Epilabidocera amphitrites* McMurrich. *Cellule* **66:** 129–251.

Porter, K. G., and J. W. Porter. 1979. Bioluminescence in marine plankton: a co-evolved antipredator system. *Am. Nat.* **114:** 458–461.

Ringelberg, J. 1991. Enhancement of the phototactic reaction in *Daphnia hyalina* by a chemical mediated by juvenile perch (*Perca fluviatilis*). *J. Plankton Res.* **13:** 17–25.

Singarajah, K. V. 1969. Escape reactions of zooplankton: avoidance of a pursuing siphon tube. *J. Exp. Mar. Biol. Ecol.* **3:** 171–178.

Stearns, D. E., and R. B. Forward, Jr. 1984a. Photosensitivity of the calanoid copepod *Acartia tonsa*. *Mar. Biol.* **82:** 85–89.

Stearns, D. E., and R. B. Forward, Jr. 1984b. Copepod photobehavior in a simulated natural light environment and its relation to nocturnal vertical migration. *Mar. Biol.* **82:** 91–100.

Stubblefield, C. L., C. M. Lascara, and M. Vecchione. 1984. Vertical distribution of zooplankton in a shallow turbid estuary. *Contr. Mar. Sci.* **27:** 93–104.

Tett, P. B., and M. G. Kelly. 1973. Marine bioluminescence. *Oceanogr. Mar. Biol. Annu. Rev.* **11:** 89–173.

Thurm, U. 1965. An insect receptor potential. *Cold Spring Harbor Symp. Quant. Biol.* **30:** 83–94.

Tjossem, S. F. 1990. Effect of fish chemical cues on vertical migration behavior of *Chaoborus*. *Limnol. Oceanogr.* **35:** 1456–1468.

Tomita, T. 1970. Electrical activity of vertebrate photoreceptors. *Quart. Rev. Biophy.* **3:** 179–222.

Viitasalo, M., T. Kiørboe, J. Flinkman, L. Pedersen, and W. W. Visser. 1998. Predation vulnerability of planktonic copepods: consequences of predator foraging strategies and prey sensory abilities. *Mar. Ecol. Prog. Ser.* **175:** 129–142.

Weeks, F. I., and G. Duncan. 1974. Photoreception by a cephalopod retina: response dynamics. *Exp. Eye Res.* **19:** 493–509.

Wine, J. J., and F. B. Krasne. 1982. The cellular organization of crayfish escape behavior. Pp. 241–292 in *The Biology of Crustacea* Vol. 4, *Neural Integration and Behavior*, D.C. Sandeman and H.L. Atwood, eds. Academic Press, New York.

Wyman, R. J., J. B. Thomas, L. Salkoff, and D. G. King. 1984. The *Drosophila* giant fiber system. Pp. 133–161 in *Neural Mechanisms of Startle Behavior*, R.C. Eaton, ed. Plenum, New York.

Yen, J., P. H. Lenz, D. V. Gassie, and D. K. Hartline. 1992. Mechanoreception in marine copepods: electrophysiological studies on the first antennae. *J. Plankton Res.* **14:** 495–512.

Reference: *Biol. Bull.* **204:** 38–49. (February 2003)

Behavioral Thermoregulation in *Hemigrapsus nudus*, the Amphibious Purple Shore Crab

I. J. McGAW

Department of Biological Sciences, University of Nevada Las Vegas, 4505 Maryland Parkway, Las Vegas, Nevada 89154-4004; and Bamfield Marine Sciences Centre, 100 Pachena Road, Bamfield, British Columbia V0R 1B0, Canada

Abstract. The thermoregulatory behavior of *Hemigrapsus nudus*, the amphibious purple shore crab, was examined in both aquatic and aerial environments. Crabs warmed and cooled more rapidly in water than in air. Acclimation in water of 16 °C (summer temperatures) raised the critical thermal maximum temperature (CTMax); acclimation in water of 10 °C (winter temperatures) lowered the critical thermal minimum temperature (CTMin). The changes occurred in both water and air. However, these survival regimes did not reflect the thermal preferences of the animals. In water, the thermal preference of crabs acclimated to 16 °C was 14.6 °C, and they avoided water warmer than 25.5 °C. These values were significantly lower than those of the crabs acclimated to 10 °C; these animals demonstrated temperature preferences for water that was 17 °C, and they avoided water that was warmer than 26.9 °C. This temperature preference was also exhibited in air, where 10 °C acclimated crabs exited from under rocks at a temperature that was 3.2 °C higher than that at which the 16 °C acclimated animals responded. This behavioral pattern was possibly due to a decreased thermal tolerance of 16 °C acclimated crabs, related with the molting process. *H. nudus* was better able to survive prolonged exposure to cold temperatures than to warm temperatures, and there was a trend towards lower exit temperatures with the lower acclimation (10 °C) temperature. Using a complex series of behaviors, the crabs were able to precisely control body temperature independent of the medium, by shuttling between air and water. The time spent in either air or water was influenced more strongly by the temperature than by the medium. In the field, this species may experience ranges in temperatures of up to 20 °C; however, it is able to utilize thermal microhabitats underneath rocks to maintain its body temperature within fairly narrow limits.

Received 10 May 2002; accepted 17 October 2002.
E-mail: imcgaw@ccmail.nevada.edu

Introduction

Intertidal organisms experience abrupt, frequently large, changes in temperature as a result of alternating episodes of exposure to air and water (Vernberg and Vernberg, 1972). These changes in temperature may pose an additional burden to amphibious organisms that are already challenged by the switch between ventilatory media (Greenaway *et al.*, 1996).

Hemigrapsus nudus, the purple shore crab, is a common species in the mid- to high-intertidal zone of rocky shores along the northeastern Pacific (Schmitt, 1921; Dehnel, 1960; Low, 1970; Daly, 1981). These crabs are involuntarily exposed as the tide recedes, but they are active in air (Burnett and McMahon, 1987). The species can tolerate temperatures up to 33.6 °C for short periods of time (Todd and Dehnel, 1960); however, exposure to suboptimal temperature regimes is associated with compensatory physiological responses in decapod crustaceans.

The aerobic metabolism of crustaceans, like that of most other aquatic organisms, is temperature dependent. Oxygen uptake increases in *Carcinus maenas*, the green shore crab, as the temperature of the water is raised (Taylor and Wheatly, 1979); likewise, oxygen consumption in *Homarus gammarus*, the European lobster, decreases (for a short time) as temperature is lowered (Whiteley *et al.*, 1995). Increases in temperature also influence oxygen delivery to the tissues by causing a reduction in the carrying capacity of the hemolymph for oxygen and the binding of oxygen to the hemocyanin (Taylor, 1981; Truchot, 1983).

Heart rate is directly related to temperature in a number

of crustacean species (deFur and Mangum, 1979; Taylor and Wheatly, 1979; DeWachter and McMahon, 1996; Stillman and Somero, 1996; Pirro *et al.*, 1999; Jury and Watson, 2000; Fredrich *et al.*, 2000). Heating increases heart rate and cardiac output but decreases stroke volume in *Cancer magister*, the Dungeness crab (DeWachter and McMahon, 1996). This is associated with an increase in hemolymph perfusion of the carapace, gonads, and musculature of the pereiopods (DeWachter and McMahon, 1996). Cooling causes a decrease in cardiac parameters: heart rate and cardiac output drop sharply in low temperature, and hemolymph flow is directed away from anterior structures to more ventral structures (Fredrich *et al.*, 2000).

Since exposure to high or low temperatures can be metabolically costly, the ability of crabs to sense temperature and orient to a "thermal niche" should be advantageous in minimizing physiological stress. In addition, many processes such as molting, growth, reproduction, and maturation of eggs are temperature dependent (Sastry, 1983a, b); therefore, selection of optimal temperatures should also maximize growth and reproductive potential (Hutchison and Maness, 1979). A number of crustacean species are known to exhibit behavioral thermoregulation. *Homarus americanus*, the American lobster, can thermoregulate precisely for up to 6 days, preferring temperatures in the 15–21 °C range (Reynolds and Casterlin, 1979a; Crossin *et al.*, 1998). Lobsters are able to detect water temperature differences of as little as 1 °C and exhibit directional taxis (Jury and Watson, 2000). *Carcinus maenas*, the green shore crab, avoids adverse temperatures, showing emersion responses at 28 °C in the laboratory (Taylor and Wheatly, 1979). *Procambarus clarkii*, the red swamp crayfish, has a broad temperature tolerance (Payette and McGaw, 2001) and prefers water with a mean temperature of 23–24 °C (Espina *et al.*, 1993; Ramirez *et al.*, 1994). An animal's thermal preference can be also be influenced by the acclimation temperature. Acclimation to warm temperatures results in a higher temperature preference in *Homarus americanus*, the American lobster (Crossin *et al.*, 1998), and in *Astacus astacus*, a crayfish (Kivivuori, 1994). Temperature acclimation has an opposite effect on the crayfish *Orconectes immunis*, with animals acclimated to warm water selecting cooler temperatures than those acclimated to cold water (Crawshaw, 1974).

Most of the articles on behavioral thermoregulation in decapod crustaceans have concentrated on fully aquatic species (see Crossin *et al.*, 1998). Much less information exists on amphibious species that are emersed in the intertidal zone twice daily (Thurman, 1998). *H. nudus* is exposed to a wide range of temperatures on both a tidal and diurnal basis (Todd and Dehnel, 1960; Greenaway *et al.*, 1996). Therefore, the aim of this study was to investigate the thermal ecology of this amphibious species and to assess the role of behavioral reactions, in both water and air, in minimizing the effects of thermal stress.

Materials and Methods

Adult male and female purple shore crabs, *Hemigrapsus nudus*, of 25–40-mm carapace width, were collected intertidally in Barkley Sound, British Columbia, during the months of May to August in 2000 and 2001. They were transferred to 40-liter aquaria at the Bamfield Marine Sciences Centre and maintained in aerated seawater at a salinity of 33 ppt ± 0.5 ppt on a natural light-dark cycle. The crabs were held at water temperatures of either 16 °C ± 0.5 °C or 10 °C ± 0.5 °C for at least 2 weeks. These temperatures approximated those measured in the field during summer and winter respectively (Gosselin and Chia, 1995). More extreme temperatures were not used because the animals tended to molt at higher temperatures and become lethargic at lower temperatures. The crabs were fed sea lettuce, *Ulva lactuca, ad libitum*. Approximately equal numbers of each sex were used, and individual crabs were not re-used in any experiment.

Rate of change of body temperature

Changes in the body temperature of *H. nudus* ($n = 10$) were studied in water and air. To measure blood temperature, a catheter-mounted (PE90) thermocouple (Physitemp IT18) was inserted through a small hole drilled in the first abdominal segment and guided to lie against the sternal artery. The crabs were returned to the holding tank and allowed to settle for 15 min. Animals ($n = 10$) were then transferred to water or air of 5 °C or 20 °C. The amount of time required for the body temperature to equilibrate with the surrounding medium was recorded at 30-s intervals using a BAT 12 digital thermometer (Physitemp Instruments).

Critical thermal maximum and minimum temperatures

The critical thermal maximum (CTMax) and critical thermal minimum (CTMin) temperatures of *H. nudus* were assessed in air and in water ($n = 30$). Crabs were acclimated to 10 °C or 16 °C and were studied separately, with the starting temperature being 10° or 16 °C, respectively. The temperature of the air was raised (or cooled) at 0.5 °C/min in an incubator (Percival Instruments [Boone, Iowa]; model 135LL), and the temperature was monitored at 1-min intervals with a Physitemp BAT12 digital thermometer. A volume of 5 liters of water was used, and the temperature was raised (or cooled) at 0.5 °C/min by way of a recirculating water bath (VWR Scientific Instruments). The water was aerated, and the temperature was monitored with the Physitemp thermometer. At random intervals, the crabs were turned on their backs until the first animal

reached its CTMax or CTMin; that is, until the animal could no longer right itself within 1 min (Cuculescu *et al.*, 1998). Thereafter, all remaining crabs were inverted together every minute and the CTMax or CTMin was recorded for each individual.

Temperature preference behavior

The temperature preference range of *H. nudus* was determined using an elongated (length, 300 cm) cylindrical (diameter, 12 cm) chamber that was orientated horizontally. Heating and cooling recirculating water baths at either end of the chamber maintained the temperature gradient between 7 °C and 30 °C. The placement of the heating and cooling water baths was alternated between each trial, to eliminate any bias for either end of the chamber. Airstones minimized any vertical thermal stratification in the gradient and ensured that the water did not become hypoxic. Shelters (broken glass beakers) were placed along the length of the chamber to reduce stress, *H. nudus* is highly thigmotactic and will remain active, attempting to escape, unless there is a place to shelter (McGaw, 2001). This atypical behavior could obscure thermoregulatory responses. Crabs—a maximum of five at any one time (8 repetitions; total n = 40)—were introduced into the gradient at random locations; using this number of *H. nudus* in experiments does not affect the thermotolerance of an individual (Todd and Dehnel, 1960). After 3 h, a temperature reading was taken at the position of each individual crab. Those crabs acclimated to either 10 °C or 16 °C were studied separately. In control experiments, the temperature was maintained at either a constant 10 °C or a constant 16 °C; crabs were then introduced randomly into the apparatus, and their position was recorded after 3 h.

Temperature avoidance

The following two experiments were designed to test the responses of the crabs after they had sensed a change in temperature. Behavioral responses consisted of migration from underneath a shelter as the temperature changed. Experiments were performed in both aquatic and aerial environments.

The first experiment (aquatic) was carried out in a modified two-choice chamber (Fig.1), which contained seawater (32 ppt), in one side, as well as pieces of broken glass beakers for shelter. The chamber was held in an incubator (Percival Instruments Model 135LL), which allowed independent control of air temperature. Five animals per trial (5 repetitions; n = 25) were placed in the seawater and allowed to settle for 30 min. Any animals that exited the water within this period were not used in the experiments. The starting temperature of experiments was either 10 °C or 16 °C for each group of acclimated crabs. The temperature of the seawater was raised at 0.5 °C/min using a recirculating water bath (VWR Scientific Instruments). The temperature at which the crabs made a voluntary migration into air was recorded; this behavior was defined as "emigration" (Taylor and Wheatly, 1979). The experiment was repeated with air temperatures of 5 °C, 20 °C, and 35 °C, each at 50%–70% relative humidity. Experiments were then carried out to assess the lower preference range. The water was cooled at 0.5 °C/min, and emigration temperature from the seawater was recorded at the three air temperatures. The water side of the chamber was alternated between trials to avoid any preference associated with either side of the chamber.

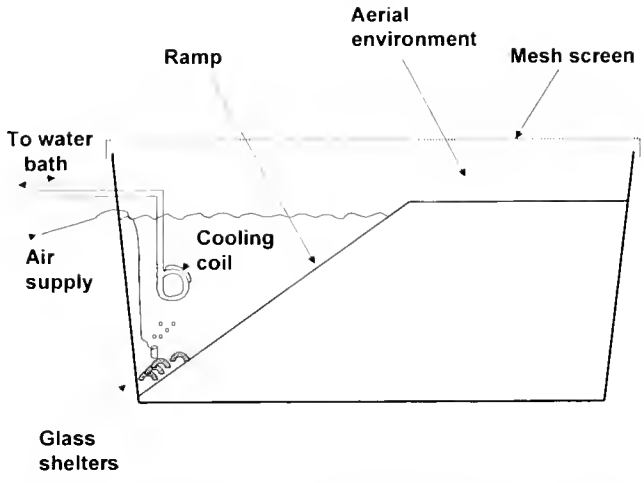

Figure 1. Modified two-choice chamber used to measure exit temperatures from water into air, shuttling behavior between air and water, and behavioral control of body temperature.

For the second experiment, temperature avoidance was tested in air using a chamber measuring 45 cm × 45 cm × 8 cm deep, with a gauze bottom to allow air to circulate. Flat tiles were placed in the chamber. Five animals were then introduced into the chamber and allowed to settle under the tiles. Any animals that migrated from under the tiles within 30 min were not used in the experiments. The chamber was held in an incubator (Percival Instruments), with the starting temperature for the two acclimated groups being either 10 °C or 16 °C. The air temperature was then raised by 0.5 °C/min, and the temperature (measured under the tiles) at which the crabs exited from under the tile shelters was recorded (n = 25). The experiment was repeated by lowering the temperature, by 0.5 °C/min, and observing the temperature at which the crabs exited from under the shelters. All recordings were made in constant dim red light.

Shuttling behavior

A time-lapse video recorder and camera (Panasonic AG-RT600AS VCR and Panasonic WV-BP120 camera) was used to monitor the shuttling behavior of individual crabs

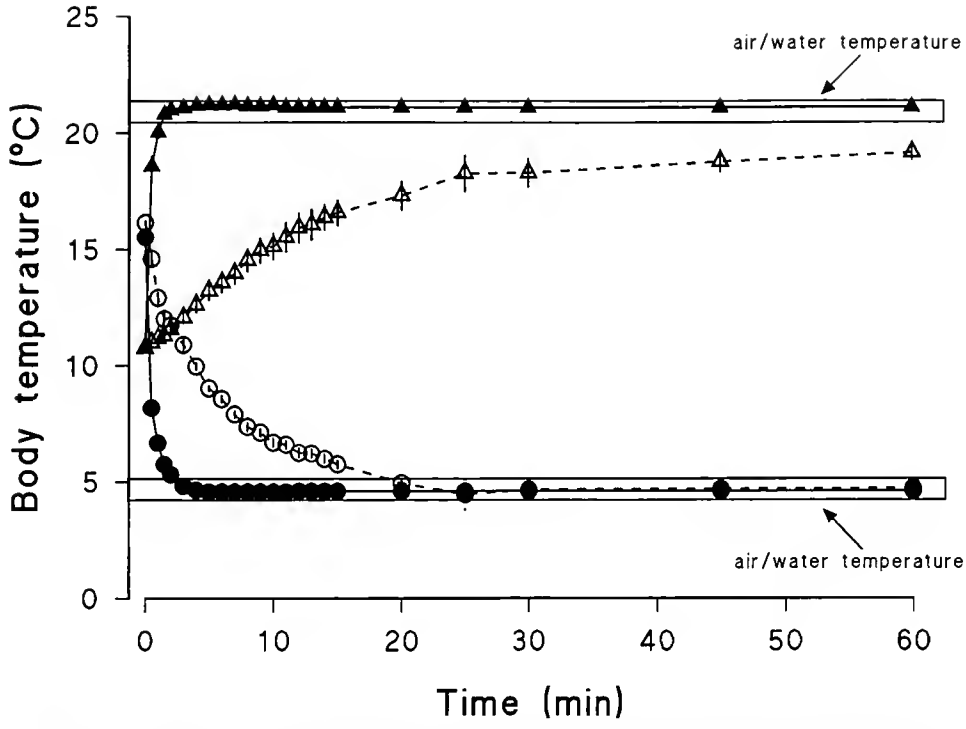

Figure 2. Changes in body temperature (mean ± SEM) of 10 *Hemigrapsus nudus*, after transfer from 10 °C water to 20 °C air (△), from 10 °C water to 20 °C water (▲), from 16 °C water to 5 °C air (○), and from 16 °C water to 5 °C water (●). In some cases error bars are smaller than the symbols.

between air and water at temperatures of 10 °C, 20 °C, and 30 °C. The choice chamber was set up in an incubator with glass shelters in both air and water. Four crabs (acclimated to 16 °C) were placed in the water (2 repetitions, total n = 8 for each treatment). The number of shuttles, duration of shuttles, and total time spent in air and water were recorded over a 24-h period in constant dim red light.

Behavioral control of body temperature

The body temperature of eight crabs (acclimated to 16 °C) was recorded with a thermocouple (Physitemp IT 18) introduced through the first abdominal segment. The thermocouple was connected to a BAT 12 digital thermometer (Physitemp Instruments); data were recorded on an ADInstruments Powerlab data acquisition package. The two-choice chamber was placed in an incubator (Percival, model 135LL), and a recirculating water bath allowed independent heating or cooling of the seawater. An animal was initially placed in the shallow water, and the change in its body temperature was followed for 12 h as it shuttled between air and water. A variety of water and air temperature combinations were offered, separated by differing increments.

Regulation of body temperature in the field

Regulation of body temperature was assessed in freshly collected crabs in the field. Crabs were fitted with thermocouples (Physitemp IT18) on a 2-m lead (n = 5). Each crab was released on a falling high tide and allowed to settle; body temperature was recorded at half-hour intervals until the following high tide, using a BAT12 digital thermometer (Physitemp Instruments). At the same time, air temperatures were recorded 5 cm above the rock surface, and seawater temperature was recorded at the low tide, using a Physitemp IT14 thermocouple calibrated against a mercury thermometer. Experiments were repeated on days when air temperatures were higher or lower than the ambient seawater temperature.

Results

Rate of change of body temperature

An increase or decrease in water temperature of about 10 °C resulted in a rapid change in body temperature (Fig. 2). Body temperature equilibrated with the surrounding water, within 2–3 min. In air, body temperature changed more slowly, and heat loss from the body was more rapid than heat gain. The body temperature took 25 min to equilibrate to a 10 °C drop in air temperature, but it failed to reach equilibrium with the surrounding air within the 60-min experimental period when the temperature was raised by 10 °C. Although body temperature reached 90% of the final temperature within 20 min, it increased slowly thereafter.

Table 1

Thermal preference of Hemigrapsus nudus *with increasing temperature*

Air temperature (°C)	Water temperature (°C) at emigration*	
	Crabs acclimated to 10 °C	Crabs acclimated to 16 °C
5	25.5 ± 0.81	25.3 ± 0.68
20	27.4 ± 0.61	24.7 ± 0.39
35	27.9 ± 0.66	25.7 ± 0.53

* Mean (±standard error of the mean) upper temperature at which crabs (n = 25) emigrated from water into air with a temperature of 5 °C, 20 °C, or 35 °C as the temperature of the water was raised.

Critical thermal maximum and minimum temperatures

In water, the CTMax of 31.1 °C ± a standard error of the mean (SEM) of 0.16 °C for crabs acclimated to 10 °C was significantly lower than the CTMax of 33.6 ± 0.11 °C for crabs acclimated to 16 °C (Student's t test = −2.32, P = 0.02). The difference between the two acclimation groups was greater in air. Crabs acclimated to 10 °C had a CTMax of 33.2 ± 0.34 °C, which was significantly lower than the CTMax of 35.3 ± 0.5 °C for 16 °C acclimated animals (t test = −3.45, P = 0.001). In addition, the CTMax values in water were significantly lower than those in air (ANOVA, F = 7.55, P = 0.007).

Acclimation to either 10 °C or 16 °C also affected the critical thermal minimum temperature. The CTMin in water of 3.5 ± 0.14 °C for crabs acclimated to 10 °C was significantly lower than the 4.82 ± 0.14 °C for 16 °C acclimated crabs (t test = −6.71, $P < 0.001$). A similar trend was observed in air, with CTMin values of 3.44 ± 0.15 °C and 3.99 ± 0.12 °C, for 10 °C and 16 °C acclimated crabs, respectively (t test = −2.89, P = 0.005). As with CTMax, there was a significant effect associated with the medium: the CTMin values in air were significantly lower than those in water (ANOVA, F = 10.41, P = 0.002).

Temperature preference

When 40 crabs (again, acclimated to either 10 °C or 16 °C) were placed randomly in a thermal gradient of 7 °C to 30 °C, there was considerable movement within the first 30 min. Temperature selection appeared to be complete after 3 h, with very little movement in the gradient thereafter. Although a small percentage of the crabs selected the extreme temperatures of 7 °C or 30 °C, most were distributed between 11 °C and 24 °C. The mean preference range of 17.01 °C ± 0.65 °C SEM for 10 °C acclimated crabs was significantly higher than the 14.60 °C ± 0.78 °C selected by 16 °C acclimated crabs (t test = 2.37, P = 0.02). Control experiments were carried out for the two acclimation temperatures, with no thermal gradient. Control crabs did not show a preference for any area of the gradient tank.

A similar effect of acclimation on temperature preference was observed in the temperature-avoidance experiments. When the temperature of the water was gradually increased, crabs exited from under the shelters and started to become active between 19–21 °C, but did not leave the water at this temperature. Although there were three different air temperatures that crabs could emigrate into, the air temperature had no significant effect on emigration temperatures from water (Table 1) (ANOVA, F = 2.47, P = 0.088). Since air temperature had no effect on behavior, data for the three air temperatures was pooled. There was a significant behavioral effect based on acclimation: crabs acclimated to 10 °C had a mean emigration temperature of 26.94 ± 0.24 °C; this was significantly higher than the mean emigration temperature of 25.25 ± 0.19 °C for crabs acclimated to 16 °C (ANOVA, F = 10.47, P = 0.002). All crabs had left the water when the temperature reached 34 °C.

Although all crabs left the water when the temperature was raised, this was not the case when the water temperature was lowered. Only 45% of the crabs acclimated to 10 °C and 30% of the crabs acclimated to 16 °C emigrated from the water. The rest of the crabs remained in the water even though the temperature was reduced below their CTMin, incapacitating them. Statistical results for the animals that exhibited emigration behavior are given in Table 2. Air temperature had no significant effect on the emigration temperature of the crabs (ANOVA, F = 0.14, P = 0.87). Although the mean emigration temperature of 4.95 ± 0.31 °C for 10 °C acclimated animals was lower than the 5.79 ± 0.42 °C for 16 °C acclimated crabs, this difference was statistically insignificant (ANOVA, F = 2.58, P = 0.113).

Therefore, in water, 10 °C acclimated crabs have a preference range between 4.95 °C and 26.94 °C, with a mean preference of 17.1 °C. The crabs acclimated to 16 °C have a mean temperature preference of 14.60 °C with a narrower preference range between 5.79 °C and 25.25 °C.

Acclimation to either 10 °C or 16 °C had a similar effect on temperature avoidance in air. When the temperature of

Table 2

Thermal preference of Hemigrapsus nudus *with decreasing temperature*

Air temperature (°C)	Water temperature (°C) at emigration*	
	Crabs acclimated to 10 °C	Crabs acclimated to 16 °C
5	4.72 ± 0.53	5.87 ± 0.51
20	5.23 ± 0.57	5.24 ± 0.61
35	4.91 ± 0.66	6.26 ± 0.89

* Mean (±standard error of the mean) temperature at which crabs (n = 25) emigrated from water into air with a temperature of 5 °C, 20 °C, or 35 °C as the temperature of the water was lowered.

Table 3

Shuttling behavior of Hemigrapsus nudus *from water into air when both media were maintained at 10 °C, 20 °C, or 30 °C*

	Parameter*		
Temperature (°C)	Number of shuttles	Duration of each shuttle (min)	Percent time spent in air/24 h
10	26.4 ± 5.1	8.6 ± 0.9	16.6 ± 11.3
20	18.0 ± 4.3	21.2 ± 8.1	24.5 ± 23.5
30	27.3 ± 6.2	28.5 ± 7.5	64.3 ± 16.5

* Values are the mean (±standard error of the mean) response for 8 crabs.

the air was gradually raised, the crabs exited from under tiles in an attempt to escape. The mean exit temperature for crabs acclimated to 10 °C was 27.39 ± 0.62 °C; this was significantly higher than the exit temperature of 24.17 ± 0.58 °C recorded for 16 °C acclimated crabs (t test = −3.8, $P < 0.001$). Consistent with lower emersion temperatures in water, not all crabs exited from under shelters as the air temperature was gradually reduced. Five of the 25 crabs acclimated to 10 °C remained under the shelters, while 10 of the crabs acclimated to 16 °C did not exit. Statistical analysis includes only the animals exhibiting this exit behavior. Although the mean exit temperature of 4.36 ± 0.47 °C recorded for 10 °C acclimated crabs was lower than the 5.85 ± 0.7 °C recorded for 16 °C acclimated animals, this difference was statistically insignificant (t test = −1.82, $P = 0.077$). Therefore, the temperature preference range in air for 10 °C acclimated crabs was 4.36 °C to 27.39 °C, which was broader than that for 16 °C acclimated animals (5.85 °C to 24.17 °C).

Shuttling behavior

The shuttling movement of 16 °C acclimated crabs between air and water was studied during a 24-h period to determine the number and duration of excursions into air (Table 3). There was no significant difference in the number of shuttles between air and water as a result of ambient temperature (ANOVA, $F = 0.96$, $P = 0.4$). There was a trend towards an increase in the average duration of each excursion into air as the temperature increased, but it was not statistically significant (ANOVA, $F = 3.01$, $P = 0.05$). When the percentage of time (per 24-h period) that each crab spent in air was considered, a significant pattern emerged (Table 3). As the temperature increased, the crabs spent a significantly greater total percentage of time in air (ANOVA, $F = 14.72$, $P < 0.001$). The percent of time that the crabs spent in air at 30 °C was significantly higher than time spent in 10 °C and 20 °C conditions, but there was no significant difference between 10 °C and 20 °C (Tukey test, $q = 1.18$, $P = 0.684$)

Behavioral control of body temperature

When offered a choice of 20 °C water with 8 °C air (trial 5), the crabs remained in the water most of the time; the mean body temperature of 20.3 °C ± 0.2 °C SD was not significantly different from the water temperature (Fig. 3). The body temperature in experimental trial 5 was significantly higher than in the other trials (Tukey test, $P < 0.05$). In experimental trial 4 (14 °C water and 24 °C air), the crabs also remained in the water; again, the mean body temperature of 14.2 ± 0.3 °C was not significantly different from that of the water (Fig 3). In all other trials, the crabs maintained the body temperature at levels between the temperature of the air and the water. In the shallow water of the chamber, periodically, a crab either raised or submerged itself to control its body temperature between mean values of 7.7 ± 0.9 °C and 14.6 ± 1.5 °C.

Examination of the body temperature of individual crabs shows the thermoregulatory responses in more detail (Fig. 4a–d). When the water was held at 4–5 °C and the air at 33–34 °C (Fig. 4a), the crab spent the first 2 h shuttling

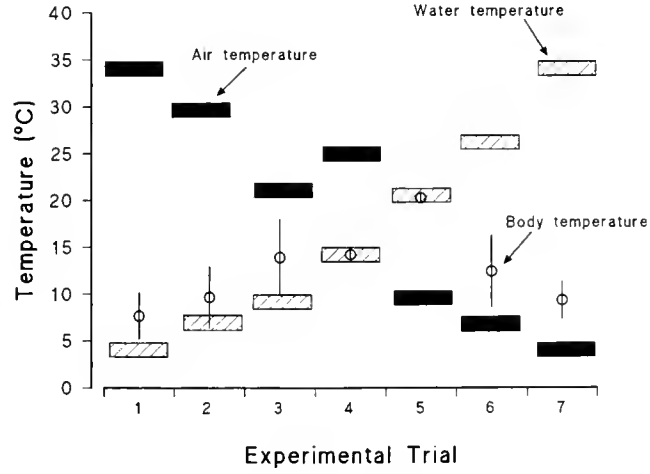

Figure 3. Mean body temperature (±SD) of *Hemigrapsus nudus* (n = 8) when offered a choice between air and water, maintained at different temperatures relative to one another. Hashed bars represent water temperature, and solid bars represent air temperatures.

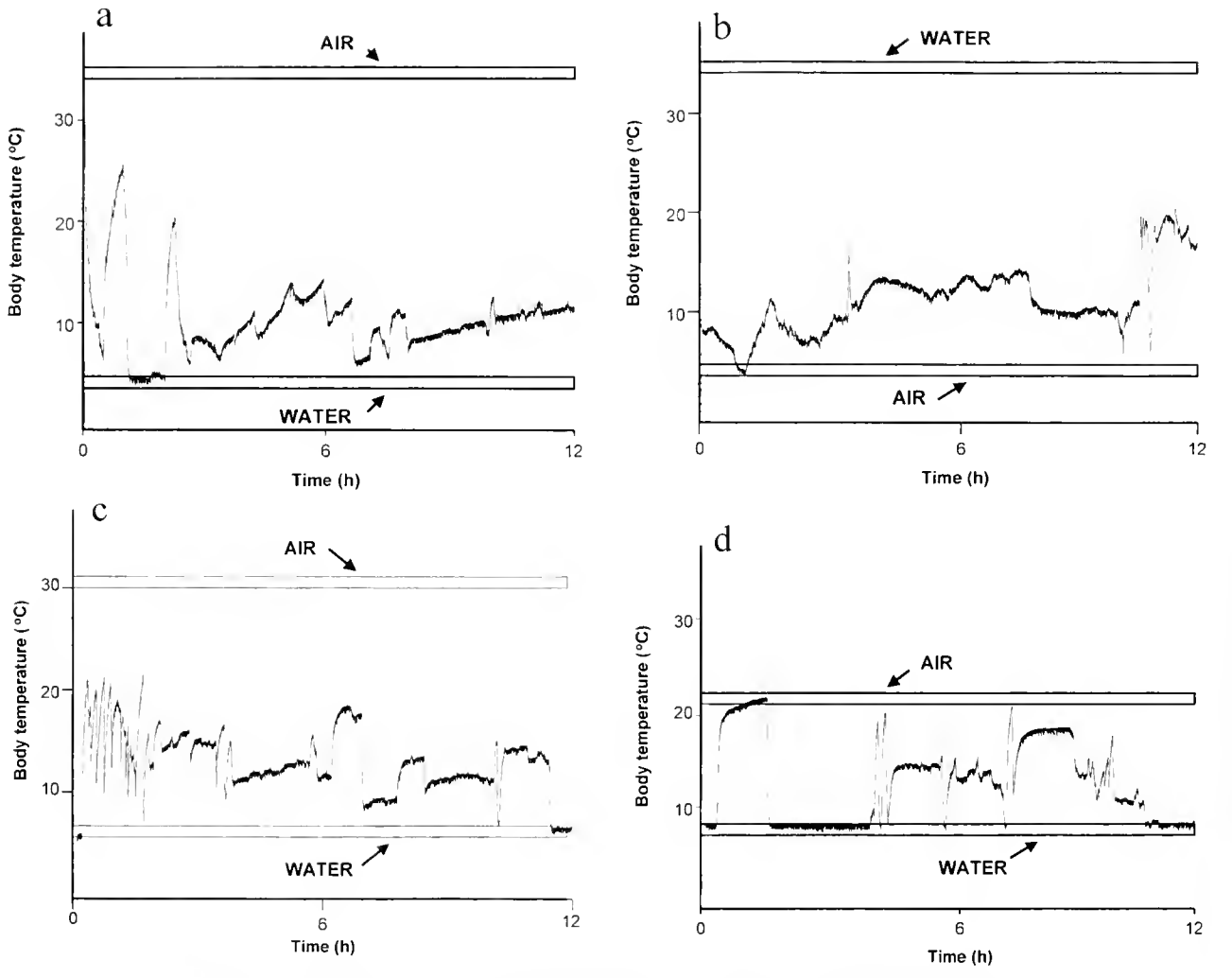

Figure 4. Representative examples of body temperatures of individual *Hemigrapsus nudus* in a two-choice chamber with the ability to shuttle between air and water of different temperatures. (a) Water of 4–5 °C and air of 33–34 °C. (b) Water of 33–34 °C and air of 4–5 °C. (c) Water of 6–7 °C and air of 30–31 °C. (d) Water of 8–9 °C and air of 20–21 °C.

between air and water, after which it raised or submerged itself in the water to maintain a body temperature of about 8–13 °C. When the temperatures of the air and water were reversed (4–5 °C air and 33–34 °C water), the crab (Fig 4b) was still able to maintain a body temperature between 8 and 13 °C for most of the 12-h experimental period. When the difference between air and water was decreased (8–9 °C water and 29–30 °C air), body temperature fluctuated somewhat during the first 2 h when the crab was active; thereafter, body temperature was maintained between 10 °C and 17 °C (Fig. 4c). When air and water temperatures (20–21 °C air and 8–9 °C water) approached limits within the animal's preference range (Table 1, 2), the crab tended to shuttle back and forth between air and water, spending extended periods of time in either medium, where body temperature equilibrated with the medium (Fig. 4d).

Body temperature in the field

Changes in body temperature of *H. nudus* were recorded in the field during an intertidal period (Fig. 5). Body temperature was monitored on a cold day (Fig 5a), when the air temperature dropped below that of the seawater. Although air temperatures fell from 18 °C to 10.7 °C, body temperatures decreased only slightly. The mean body temperature of the crabs ($n = 5$) dropped from 17.65 ± 0.28 °C SEM when initially emersed, down to 14.92 ± 0.44 °C at the end of the intertidal period. This was only a 16% drop in body temperature, compared to a drop of 41% in the temperature of the surrounding air. Body temperature increased rapidly when the crabs were re-immersed, reaching 16.5 ± 0.27 °C as it equilibrated with the seawater.

On a warm day (Fig. 5b) the air temperature quickly rose

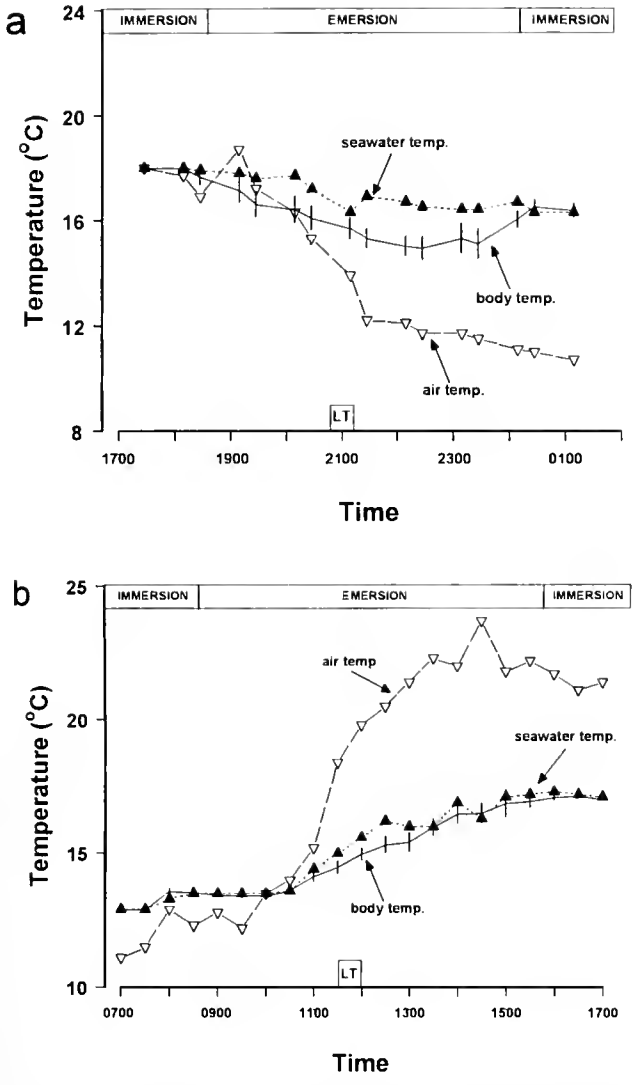

Figure 5. Changes in body temperature (mean ± SEM) of 5 specimens of *Hemigrapsus nudus* (solid line) in the intertidal zone. Crabs were released during a falling tide and monitored until the following high tide. Seawater temperatures (dotted line, solid symbols) and air temperatures (dashed line, open symbols) were also recorded during this time. Times of emersion and immersion of the crabs, as well as low tide (LT), are indicated on the graphs. Recordings were made on (a) 8 July 2001, when surrounding air temperatures were lower than ambient seawater temperatures and (b) 23 July 2001, when air temperature was higher than seawater temperature.

from 11 °C in the morning to 22–24 °C by early afternoon. Despite this 12 °C rise in air temperature, the body temperatures of the crabs did not change as rapidly, and reached only 16.86 ± 0.51 °C by the end of exposure period in air. The change in body temperature was similar to the observed increase in seawater temperature during the day (Fig. 5b). When the crabs were re-immersed, their body temperatures quickly equilibrated with the seawater.

Discussion

The observed rates of change in body temperature (Fig. 2) were similar to those reported previously for *Hemigrapsus nudus* (Greenaway *et al.*, 1996). In lobsters, heat loss in air is more rapid than heat gain (Whiteley *et al.*, 1995); this was also observed here for *H. nudus* (Fig. 2), probably due to the evaporative heat loss in air. During these experiments, several of the crabs regurgitated frothed fluids from the stomach, smeared this over the ventral carapace with the chelae, and raised their body above the substrate. This foaming behavior has been reported for a number of crab species (Lindeberg, 1980; Maitland, 1990) and can used to reduce body temperature (Jansen, 1970). However, there was no evidence to suggest that the *H. nudus* specimens were using this method to slow their rate of heating. The relative humidities of 60%–70% used during the experiments, which mimicked conditions measured in the field, could have reduced the effectiveness of (but not eliminated) evaporative cooling (Edney, 1961). Although foaming behavior was not observed in the field, it is possible that it could reduce heating rates on warm days with low relative humidity (Thurman, 1998). Fiddler crabs (*Uca* species) are able to maintain a body temperature below that of the surrounding air by changing posture, blanching, and evaporating water from the body surface (Wilkens and Fingerman, 1965; Smith and Miller, 1973; Thurman, 1998). In the present study, there was no difference in heating or cooling rates when comparing live and dead animals (not shown), suggesting that there is no active mechanism that allows *H. nudus* to control the rate of heat gain or loss from the body.

When *H. nudus* was acclimated to different temperatures, an increase in the upper survival limits occurred as a result of the higher acclimation temperature; this has been reported previously for *H. nudus* (Todd and Dehnel, 1960), as well as for other species of crustaceans (Mundahl and Benton, 1990; Lagerspetz and Bowler, 1993; Korhonen and Lagerspetz, 1996; Cuculescu *et al.*, 1998; Stillman and Somero, 2000). However, much less is known about the critical thermal minima. In the present study, acclimation to a lower temperature extended the CTMin. Acclimation to a wider range of temperatures has also been shown to extend the CTMin range in other crustaceans (Layne *et al.*, 1987; Stillman and Somero, 1996).

Survival limits in air as a function of temperature have not been investigated previously for *H. nudus*. Interestingly, both the CTMax and CTMin were greater in air than in water. The heating and cooling rate in the incubator (0.5 °C/min) was adequate to allow equalization of the body with the surrounding air (unpubl. data; Fig. 2). These results are somewhat surprising: an animal would already be physiologically challenged by the switch in ventilatory media (Greenaway *et al.*, 1996), because an increase in air temperature decreases the oxygen-carrying capacity of the

hemocyanin and results in thermal acidosis (Morris *et al.*, 1996b). The CTMax was determined close to the body of the crab rather than by using internal temperature probes, which tended to tangle around the legs when the crabs were turned over, affecting the ability of the animal to right itself. Even though relative humidities in the incubator were high (60%–80%), a degree of evaporative cooling could have kept the body temperature a degree or so cooler than the surrounding air (unpubl. data; Fig. 2). This would suggest that the upper lethal limits in air were probably similar to those measured in water. However, if evaporative cooling reduced the body temperature, then the CTMin in air would also be expected to occur at a higher temperature than in water. This did not happen in the present study.

The thermal preference behavior of crabs acclimated to 10 °C and 16 °C, ascertained in a thermal gradient and by temperature-aversion experiments (Table 1), did not reflect their temperature tolerances: in both cases, 10 °C acclimated crabs had a higher temperature preference than those acclimated to 16 °C. In the temperature-aversion experiments, the oxygen tension was maintained at constant levels, so the emigration from water was a direct consequence of temperature. Indeed, aquatic hypoxia is not an impetus for emersion in this species (Morris *et al.*, 1996c). The air temperature that the crabs could exit into did not affect the exit temperature from the water (Table 1). This was unexpected, since acute exposure to higher air temperature (>15 °C) is costly and is associated with thermal acidosis and compensatory increases in cardiac output to maintain adequate oxygen uptake (Morris *et al.*, 1996a, b). Acclimation to 10 °C or 16 °C also influenced aversion behavior in air. When the air temperature was raised, crabs acclimated to 10 °C exited from under stones at a higher temperature than did 16 °C acclimated crabs. The adaptive significance of this behavior is unclear, since 16 °C acclimated crabs are more tolerant of higher temperatures (CTMax values). Thus, the effect of acclimation on behavior is apparently the opposite of its effect on survival regimes. In other reports on thermoregulatory behavior, lobsters that are acclimated to warm water choose warmer temperatures than do cold-acclimated individuals, possibly to maintain an optimal thermal regime for metabolic activities (Crossin *et al.*, 1998). When *Astacus astacus*, a crayfish, is acclimated to cold or warm water, this also directly affects thermal preference (Kivivuori, 1994). Acclimation to either 15 °C or 25 °C has no effect on the emersion response of the shore crab *Carcinus maenas*, which exits into air when the water temperature reaches 28 °C (Taylor and Wheatly, 1979). Likewise, acclimation to differing temperatures has no effect on the temperature preference of *Procambarus clarkii*, the red swamp crayfish (Espina *et al.*, 1993). In contrast to these responses, when the crayfish *Orconectes immunis* is acclimated to cold water, it tends to choose higher temperatures than animals acclimated to warm water, yet no explanation is given for this paradox (Crawshaw, 1974).

Several factors can be eliminated as causes for the unexpected behavior observed in the present study. (1) The crabs were not responding to temperature increases of a particular magnitude, as occurs in lobsters (Cooke-Schreiber *et al.*, 2001). (2) The warming rate of the water (0.5 °C/min) was slow enough to allow the body temperature to equilibrate with the surrounding medium (Fig. 2). (3) Although the crabs were introduced into the apparatus in groups of five, this was unlikely to have a substantial effect on their behavior: they were roughly equal in size and there was ample shelter—both of these factors would reduce aggressive interactions between animals (Jacoby, 1981). (4) Although *Carcinus maenas* exhibits a behavioral hypothermia when exposed to hypoxic conditions (DeWachter *et al.*, 1997), this is probably not the case for *H. nudus* because oxygen levels were maintained during experiments and this species does not modify its behavior in response to hypoxia (Morris *et al.*, 1996c). (5) Finally, the acclimation period of 2 weeks should have been long enough for an increased temperature tolerance (Layne *et al.*, 1987; Cuculescu *et al.*, 1998). Indeed, rapid acclimation to thermal zones is an advantage for intertidal organisms: *H. nudus*, which acclimatizes within 48 h (Todd and Dehnel, 1960), is no exception.

When considering factors that could have influenced this overt behavior, it is worth noting that *H. nudus* could not be acclimated to temperatures greater than 16 °C without inducing widespread molting. Because the entire molting process can take several weeks (O'Halloran and O'Dor, 1988), it is possible that the 16 °C acclimated crabs were just starting to molt (D_1 or D_2 stage) without visible signs. Early stages of the molting process are associated with biochemical and physiological changes (see Chang, 1995) and make *H. nudus* less tolerant of high temperatures (Todd and Dehnel, 1960). The crabs acclimated to 10 °C would not undergo molting and could be expected to be more tolerant of the higher temperature regimes than the 16 °C acclimated crabs, which would avoid warmer temperatures. In addition, activity levels of cold-acclimated *Astacus astacus* decrease when these crayfish are warmed in water (Lehti-Koivunen and Kivivuori, 1994); if this were the case here for *H. nudus*, then cold-acclimated crabs would be less active and would not exhibit an escape response until a higher temperature.

Though all animals showed avoidance behavior when the temperature was increased, this was not the case when temperature was lowered. Only 30%–45% of the crabs emigrated from water and 20%–40% remained under shelters in the air. As expected, crabs acclimated to 10 °C appeared to emigrate at a lower temperature than those acclimated to 16 °C. However, since only animals that emigrated from the water or from under shelters were used in the analyses, this difference was not statistically signifi-

cant (Table 2). The reason that not all the animals exited when the temperature decreased becomes apparent when their long-term survival in extreme temperatures is considered. The crabs also did not recover after a few minutes of exposure at CTMax; they did, however, recover from cooling, even after several hours of exposure below CTMin. The same result is reported for *Astacus astacus* (Lehti-Koivunen and Kivivuori, 1994). Since *H. nudus* can survive exposure to low temperatures these crabs would not benefit from leaving the water or a protective shelter, where they would become vulnerable to predation.

The results of the shuttling experiments between air and water (Table 3) correspond to the behavioral patterns observed in the avoidance experiments. In cold water (10 °C), *H. nudus* individuals made fewer excursions into air; therefore the total time spent in air was also less (Table 3). At higher temperatures, the crabs were more active, making a greater number of excursions and spending a greater amount of time in air. In air, *H. nudus* is able to take up sufficient oxygen *via* an increased cardiac output (Morris *et al.*, 1996a, b). However, this is not without cost, especially at higher temperatures, where hemocyanin affinity and pH are affected to a greater degree, suggesting that oxygen delivery to the tissues declines when *H. nudus* breathes air at warm temperatures (Morris *et al.*, 1996a, b). Given these factors, the opposite behavior with respect to temperature may have been expected. However, as temperature increases in both air and water, so does oxygen uptake. The possible advantages of emigration from warm water into warm air could be a reduction in oxygen demand, as a consequence of evaporative cooling across the gills (Taylor and Wheatly, 1979). In addition, the CTMax values showed that the crabs tolerate higher temperatures in air than in water, which may explain why they spend more time in air at higher temperatures. In the present study, only two or three animals (tested at the 30 °C regime) spent longer than 5 h emersed (Table 3), whereas Greenaway *et al.* (1996) found that *H. nudus* can remain emersed for up to 8 h. These workers were using colder water temperatures (10–13 °C) than this animal is normally exposed to in summer (Gosselin and Chia, 1995). Thus, the crabs were probably moving into the warmer air (19–22 °C) due to a thermal preference rather than to the selection of a particular medium. To test this hypothesis, the behavior of *H. nudus* was investigated as crabs shuttled between air and water of differing temperatures, to determine if they were able to maintain the body temperature within a preferred range.

Although purple shore crabs are unlikely to encounter such extreme differences in air and water temperatures as shown in Figure 3, the results obtained suggest that they possess well-developed thermosensory mechanisms. The crabs tended to migrate to the air-water interface; although a slight microhabitat may have existed there, they exhibited a complex series of behaviors that suggested they were using the thermal properties of both media to control body temperature (Fig. 3). The crabs raised or submerged their bodies in the shallow water of the chamber, thus gaining the benefits of evaporative cooling from the gills (Taylor and Wheatly, 1979) without the imbalances in pH and hemocyanin affinity caused by longer emersion in adverse temperature regimes (Morris *et al.*, 1996a, b, c). Maintenance of an optimal body temperature, rather than selection of a particular medium, appeared to be most important factor. In support of this conclusion, when water temperatures of 4–5 °C and air temperatures of 33–34 °C were offered (Fig. 3, trial 1), the crabs were able to maintain a body temperature of about 8–12 °C, independent of the two media (Fig. 4a). When air and water temperatures were reversed (Fig. 3, trial 7), the body temperature was still maintained within similar limits (Fig. 4b).

It was also important to investigate the thermoregulatory behavior of *H. nudus* in the field, since this species displays different behaviors in its natural environment (McGaw, 2001). Greenaway *et al.* (1996) suggest that *H. nudus* may routinely experience 10 °C differences in body temperature in the field. Certainly, the porcelain crab *Petrolisthes cinctipes*, which occupies a similar niche, may be exposed to temperatures under rocks in excess of 20 °C (Stillman and Somero, 1996). And even though *H. nudus* voluntarily exits into air in the laboratory (Greenaway *et al.*, 1996; Burnett and McMahon, 1987), this was not observed in any of the experimental animals in the field. They remained under rocks or deep in crevices during the intertidal period. This behavior has adaptive significance in that it keeps crabs in close contact with cover, thus avoiding the threat of predation (Low, 1970; Daly, 1981; McGaw, 2001). Indeed, *H. nudus* prefers to shelter underneath larger boulders, which provide the added advantages of heating or cooling more slowly (Stillman and Somero, 1996). Thus, using subtle movements within this thermal microhabitat, the crabs were able to maintain their body temperature independent of the surrounding air (Fig. 5). Additionally, the prevailing weather conditions can have a profound effect on the microhabitat and behavior of animals (Stillman and Somero, 1996). I have observed crabs active at low tide on humid or dull days; clearly other factors, in combination with temperature, play a role in emersion behavior and deserve further investigation.

H. nudus is well adapted for an existence in the intertidal zone (Morris *et al.*, 1996a, b, c; Greenaway *et al.*, 1996). The present study demonstrates that this species is able to detect differences in its thermal environment and use the thermal properties of both water and air to control its body temperature within a fairly narrow range. This study extends the work on thermoregulatory behavior in aquatic crustaceans (Crawshaw, 1974; Reynolds and Casterlin, 1979a, b, c, d; Lewis and Roer, 1988; Mundahl and Benton, 1990; Espina *et al.*, 1993; Kivivuori, 1994; Lehti-Koivunen and

Kivivuori, 1994; Crossin *et al.*, 1998) by examining the responses of an amphibious species during exposure to temperature change in both aquatic and aerial environments.

Acknowledgments

I thank the Director and staff of the Bamfield Marine Sciences Centre for the use of facilities. I also thank Drs. Winsor Watson III (Univ. of New Hampshire) and Steven Jury (SUNY) for helpful discussion. This work was supported by a UNLV SITE and New Investigator Award.

Literature Cited

Burnett, L. E., and B. R. McMahon. 1987. Gas exchange, hemolymph acid-base status and the role of branchial water stores during air exposure in three littoral crab species. *Physiol. Zool.* **60:** 27–36.

Chang, E. S. 1995. Physiological and biochemical changes during the molt cycle in decapod crustaceans: an overview. *J. Exp. Mar. Biol. Ecol.* **193:** 1–14.

Cooke-Schreiber, S. M., S. H. Jury, and W. H. Watson III. 2001. Seasonal difference in behavioral thermoregulation in the lobster, *Homarus americanus*. *Am. Zool.* **40:** 978A.

Crawshaw, L. I. 1974. Temperature selection and activity in the crawfish *Orconectes immunis*. *J. Comp. Physiol.* **95:** 161–172.

Crossin, G. T., S. Abdulazziz Al-Ayoub, S. H. Jury, W. H. Howell, and W. H. Watson III. 1998. Behavioral thermoregulation in the American lobster *Homarus americanus*. *J. Exp. Biol.* **201:** 365–374.

Cuculescu, M., D. Hyde, and K. Bowler. 1998. Thermal tolerance of two species of marine crab, *Cancer pagurus* and *Carcinus maenas*. *J. Therm. Biol.* **23:** 107–110.

Daly, G. P. 1981. Competitive interactions among three crab species in the intertidal zone. *Ph.D. Thesis*. University of Oregon.

deFur, P. L., and C. P. Mangum. 1979. The effects of environmental variables on the heart rates of invertebrates. *Comp. Biochem. Physiol.* **62A:** 283–294.

Dehnel, P. A. 1960. Effect of temperature and salinity on the oxygen consumption of two intertidal crabs. *Biol. Bull.* **118:** 215–249.

DeWachter, B., and B. R. McMahon. 1996. Temperature effects on heart performance and regional hemolymph flow in the crab *Cancer magister*. *Comp. Biochem. Physiol.* **114(1):** 27–33.

DeWachter, B., F. J. Sartorius, and H. O. Portner. 1997. The anaerobic end product lactate has a behavioural and metabolic signalling function in the shore crab *Carcinus maenas*. *J. Exp. Biol.* **200:** 1015–1024.

Edney, E. B. 1961. The water and heat relationships of fiddler crabs (*Uca* spp.). *Trans. R. Soc. S. Afr.* **36:** 71–91.

Espina, S., F. D. Herrera, and L. F. Buckle. 1993. Preferred and avoided temperatures in the crawfish, *Procambarus clarkii*. *J. Therm. Biol.* **18:** 35–39.

Fredrich, M., B. DeWachter, F. J. Sartorius, and H. O. Portner. 2000. Cold tolerance and the regulation of cardiac performance and hemolymph distribution in *Maja squinado* (Crustacea: Decapoda). *Physiol. Biochem. Zool.* **73:** 406–415.

Gosselin, L. A., and F. S. Chia. 1995. Characterizing temperate rocky shores from the perspective of an early juvenile snail: the main threats to survival of newly hatched *Nucella emarginata*. *Mar. Biol.* **122:** 625–635.

Greenaway, P., S. Morris, B. R. McMahon, C. A. Farrelly, and K. L. Gallagher. 1996. Air breathing by the purple shore crab *Hemigrapsus nudus* (Dana). I. Morphology, behaviour and respiratory gas exchange. *Physiol. Zool.* **69:** 785–805.

Hutchison, V. H., and J. D. Maness. 1979. The role of behavior in temperature acclimation and tolerance in ectotherms. *Am. Zool.* **19:** 367–384.

Jacoby, C. A. 1981. Behavior of the purple shore crab *Hemigrapsus nudus* Dana, 1851. *J. Crustac. Biol.* **1:** 531–544.

Jansen, P. 1970. Eco-physiological studies on the "posing" behaviour of *Uca tangeri. Forma Functio* **2:** 58–100.

Jury, S. H., and W. H. Watson III. 2000. Thermosensitivity of the lobster, *Homarus americanus*, as determined by cardiac assay. *Biol. Bull.* **199:** 257–264.

Kivivuori, L. A. 1994. Temperature selection behaviour of cold and warm acclimated crayfish (*Astacus astacus*). *J. Therm. Biol.* **19:** 291–297.

Korhonen, I. A., and K. Y. H. Lagerspetz. 1996. Heat shock response and thermal acclimation in *Asellus aquaticus*. *J. Therm. Biol.* **21:** 49–56.

Lagerspetz, K. Y. H., and K. Bowler. 1993. Variation in heat tolerance of individual *Asellus aquaticus* during thermal acclimation. *J. Therm. Biol.* **18:** 137–143.

Layne, J. R., D. L. Claussen, and M. L. Manis. 1987. Effects of acclimation temperature, season and time of day on the critical thermal maxima and minima of the crayfish *Orconectes rusticus*. *J. Therm. Biol.* **12:** 183–187.

Lehti-Koivunen, S. M., and L. A. Kivivuori. 1994. Effect of temperature acclimation in the crayfish *Astacus astacus* (L.) on the locomotor activity during a cycle of temperature change. *J. Therm. Biol.* **19:** 299–304.

Lewis, D. H., and R. D. Roer. 1988. Thermal preference in distribution of blue crabs, *Callinectes sapidus*, in a power plant cooling pond. *J. Crustac. Biol.* **8:** 283–289.

Lindeberg, W. J. 1980. Behaviour of the Oregon mud crab *Hemigrapsus oregonensis* (Dana) (Brachyura: Grapsidae). *Crustaceana* **39:** 263–281.

Low, C. J. 1970. Factors affecting the distribution and abundance of two species of beach crab, *Hemigrapsus oregonensis* and *Hemigrapsus nudus*. *MSc Thesis*. University of British Columbia, BC, Canada.

Maitland, D. P. 1990. Carapace and branchial water circulation and water related behaviours in the semaphore crab *Heloecius cordiformis* (Decapoda: Brachyura: Ocypodidae). *Mar. Biol.* **105:** 275–286.

McGaw, I. J. 2001. Impacts of habitat complexity on physiology: Purple shore crabs tolerate osmotic stress for shelter. *Estuarine Coastal Shelf Sci.* **53:** 865–876.

Morris, S., P. Greenaway, and B. R. McMahon. 1996a. Air breathing by the purple shore crab *Hemigrapsus nudus* (Dana). II. Respiratory gas and acid-base status in response to emersion. *Physiol. Zool.* **69:** 806–838.

Morris, S., P. Greenaway, and B. R. McMahon. 1996b. Air breathing by the purple shore crab *Hemigrapsus nudus* (Dana). III. Haemocyanin function in respiratory gas transport. *Physiol. Zool.* **69:** 839–863.

Morris, S., P. Greenaway, and B. R. McMahon. 1996c. Air breathing by the purple shore crab *Hemigrapsus nudus* (Dana). IV. Aquatic hypoxia as an impetus for emersion? Oxygen uptake, respiratory gas transport, and acid-base state. *Physiol. Zool.* **69:** 864–886.

Mundahl, N. D., and M. J. Benton. 1990. Aspects of the thermal ecology of the rusty crayfish *Orconectes rusticus* (Girard). *Oecologia* **82:** 210–216.

O'Halloran, M. J., and R. K. O'Dor. 1988. Molt cycle of male snow crabs *Chionoecetes opilio* from observations of external features, setal changes and feeding behavior. *J. Crustac. Biol.* **8:** 164–176.

Payette, A. L., and I. J. McGaw. 2001. Can ovigerous crayfish (*Procambarus clarkii*) control their brooding environment through behavior? *Arizona-Nevada Acad. Sci.* **36:** 12A.

Pirro, M. D., S. Cannicci, and G. Santini. 1999. A multi-factorial experiment on heart rate variations in the intertidal crab *Pachygrapsus marmoratus*. *Mar. Biol.* **135:** 341–345.

Ramirez, L. F. B., F. D. Herrera, F. C. Sandoval, B. B. Sevilla, and M. H. Rodriguez. 1994. Deil thermoregulation of the crawfish *Procambarus clarkii* (Crustacea, Cambridae). *J. Therm. Biol.* **19:** 419–422.

Reynolds, W. H., and M. E. Casterlin. 1979a. Behavioral thermoregulation and activity in *Homarus americanus*. *Comp. Biochem. Physiol.* **64A:** 25–28.

Reynolds, W. H., and M. E. Casterlin. 1979b. Thermoregulatory behavior of the pink shrimp *Penaeus duorarum* Burkenroad. *Hydrobiologia* **67:** 179–182.

Reynolds, W. H., and M. E. Casterlin. 1979c. Behavioral thermoregulation in the grass shrimp *Palaemonetes vulgaris* (Say). *Rev. Can. Biol.* **38:** 45–46.

Reynolds, W. H., and M. E. Casterlin. 1979d. Behavioral thermoregulation in the spiny lobster *Panulirus argus*. *Hydrobiologia* **66:** 141–143.

Sastry, A. N. 1983a. Pelagic larval ecology and development. Pp. 213–282 in *The Biology of Crustacea,* Vol. 7: *Behavior and Ecology,* F. J. Vernberg and W. B. Vernberg, eds. Academic Press, New York.

Sastry, A. N. 1983b. Ecological aspects of reproduction. Pp. 179–270 in *The Biology of Crustacea,* Vol. 8: *Environmental Adaptations,* F. J. Vernberg and W. B. Vernberg, eds. Academic Press, New York.

Schmitt, W. L. 1921. The marine decapod Crustacea of California. *Univ. Calif. Publ. Zool.* **23:** 1–470.

Smith, W. K., and P. C. Miller. 1973. The thermal ecology of two South Florida fiddler crabs *Uca rapax* (Smith) and *Uca pugilator* (Bose). *Physiol. Zool.* **46:** 186–207.

Stillman, J. H., and G. N. Somero. 1996. Adaptation to temperature stress and aerial exposure in congeneric species of intertidal porcelain crabs (Genus: *Petrolisthes*): correlation of physiology, biochemistry and morphology with vertical distribution. *J. Exp. Biol.* **199:** 1845–1855.

Stillman, J. H., and G. N. Somero. 2000. A comparative analysis of the upper thermal tolerance limits of eastern Pacific porcelain crabs, Genus *Petrolisthes:* influences of latitude, vertical zonation, acclimation and phylogeny. *Physiol. Biochem. Zool.* **73:** 200–208.

Taylor, E. W. 1981. Some effects of temperature on respiration in decapodan crustaceans. *J. Therm. Biol.* **6:** 239–248.

Taylor, E. W., and M. G. Wheatly. 1979. The behaviour and respiratory physiology of the shore crab, *Carcinus maenas* (L.) at moderately high temperatures. *J. Comp. Physiol.* **130:** 309–316.

Thurman, C. L. 1998. Evaporative water loss, corporal temperature and the distribution of sympatric crabs (*Uca*) from South Texas. *Comp. Biochem. Physiol.* **119A:** 279–286.

Todd, M. E., and P. A. Dehnel. 1960. Effect of temperature and salinity on heat tolerance in two grapsoid crabs *Hemigrapsus nudus* and *Hemigrapsus oregonensis*. *Biol. Bull.* **118:** 150–172.

Truchot, J. P. 1983. Regulation of acid-base balance Pp. 431–457 in *The Biology of Crustacea,* Vol 5: *Internal Anatomy and Physiological Regulation,* L. H. Mantel, ed. Academic Press, New York.

Vernberg, W. B., and F. J. Vernberg. 1972. *Environmental Physiology of Marine Organisms.* Springer, New York.

Whiteley, N. M., A. H. Al-Wassia, and E. W. Taylor. 1995. The effects of sudden changes in temperature on aquatic and aerial respiration in the lobster *Homarus gammarus* (L.). *Mar. Freshw. Behav. Physiol.* **27(1):** 13–27.

Wilkens, J. L., and M. Fingerman. 1965. Heat tolerance and temperature relationships of the fiddler crab, *Uca pugilator,* with reference to body coloration. *Biol. Bull.* **128:** 133–141.

Reference: *Biol. Bull.* **204:** 50–56. (February 2003)

Synthesis of a High-Density Lipoprotein in the Developing Blue Crab (*Callinectes sapidus*)

ANNA WALKER[1], SEICHI ANDO[2], AND RICHARD F. LEE[3,*]

[1] *Department of Pathology, Mercer University School of Medicine, Macon, Georgia 31207;*
[2] *Lipoprotein Research Laboratory, Department of Fisheries Science, Kagoshima University, 4-50-20 Shimoarata, Kagoshima 890-0056, Japan; and* [3] *Skidaway Institute of Oceanography, Savannah, Georgia 31411*

Abstract. An important lipoprotein in the hemolymph of crustaceans is LpI. It transports lipid to peripheral tissues and also has a role in crustacean immune recognition. We employed a monoclonal antibody specific for the LpI peptide to demonstrate by ELISA, western blot and immunohistochemistry the appearance of LpI during development of *Callinectes sapidus*, the blue crab. LpI was first found in stage 5 embryos and appeared to be synthesized by lateral basophilic cuboidal cells that demonstrated cytoplasmic immunoreactivity for LpI at their interface with the yolk mass. The embryonic cuboidal cells bore a strong cytologic resemblance to the hepatopancreas cells of later stages (zoea, megalopae, adults), which were also immunoreactive for LpI.

Introduction

The hemolymph of male and female decapod crustaceans contains a high-density lipoprotein (LpI) with concentrations ranging from 1.1 to 2.0 mg/l (Lee and Puppione, 1988; Spaziani, 1988; Lee, 1991; Spaziani and Wang, 1991; Stratakis *et al.*, 1992; Tom *et al.*, 1993; Yepiz-Plascencia *et al.*, 1995; Ruiz-Verdugo *et al.*, 1997). It plays an important role in transporting lipids from the hepatopancreas to peripheral tissues such as muscle, and functions as a β-1,3-glucan-binding protein in crustacean immune recognition (Khayat *et al.*, 1994; Hall *et al.*, 1995; Kang and Spaziani, 1995).

Embryos of *Callinectes sapidus*, the blue crab, develop in egg sacs through a series of 10 stages (Table 1) over a period of 16–23 days. At stage 10, they emerge from the egg sacs as swimming zoea larvae; these metamorphose into megalopae, then into juvenile crab forms, and ultimately become adult crabs. Until they emerge from egg sacs, embryos are nutritionally dependent on lipids and lipovitellin stored within the eggs. Lipovitellin (LpII) is a high-density lipoprotein that differs from LpI in density, sediment coefficient, and peptide components (Lee and Puppione, 1988; Lee and Walker, 1995).

In adult blue crabs, LpI is composed of phospholipids (45%), cholesterol (2%), triacylglycerols (3%), and one peptide (49%, molecular mass 112 kD) (Lee and Puppione, 1988). Although LpI was reported in juvenile and adult blue crabs, it has not been previously reported in crab oocytes or embryos. We employed a monoclonal antibody specific for the LpI peptide to demonstrate—by ELISA, western blot, and immunohistochemistry—the appearance of LpI during blue crab development. In addition, we offer immunohistochemical evidence that the developing hepatopancreas is the site of LpI synthesis in embryonic and larval stage blue crabs, and remains so in the adult.

Materials and Methods

Collection of crabs, isolation of LpI, and purification of LpI peptide

Blue crabs were collected by trawling in the estuaries near Skidaway Island, Georgia (USA). Hemolymph was collected with a 5-ml disposable syringe from the base of the swimming leg and centrifuged in a low-speed centrifuge (3 °C) for 10 min at 2000 × *g* to remove clotted materials and cells. Hemolymph lipoproteins were separated from other hemolymph proteins by adjusting the density of the

Received 25 July 2002; accepted 8 November 2002.
* To whom correspondence should be addressed. E-mail: dick@skio.peachnet.edu

Table 1

Description of embryo stages of Callinectes sapidus

Stage	Description	Elapsed Time (hours at 27 °C)
1	Fertilization	0
2	Early cleavage; morula (random mass of yolk cells)	12
3	Late cleavage; blastula (mass of undifferentiated yolk cells)	36
4	Embryonic naupliar stage; transparent embryo above the yolk	85
5	Early appendage formation; embryo invading ventral portion of yolk	110
6	Embryonic eye; eye appears as scarlet crescent; elongating appendages	160
7	Presence of beating heart; pigmented appendages	180
8	Oval, pigmented eye; 50% of yolk utilized; clear appendages	210
9	Compound eye with dark pigmentation; only small amounts of yolk	230
10	Protozoeae stage ready for hatching into free-swimming zoea	280

hemolymph and then centrifuging it (Beckman L5-40 ultracentrifuge, 40.3 rotor). Salt solutions used to adjust the solutions densities were prepared according to the methods outlined by Lindgren (1975). Solution densities were verified by refractometry using an Abbe refractometer (Bausch and Lomb). Consistent with an earlier study (Lee and Puppione, 1988), lipoproteins with densities less than 1.063 g/ml were not detected in blue crab hemolymph. Thus, blue crab high-density lipoprotein (Lpl) was isolated by adjusting the density of hemolymph to 1.21 g/ml with solid potassium bromide, followed by 40 h of centrifugation at 117,000 × *g*. The floating layer of high-density lipoprotein was removed and dialyzed for 24 h at 4 °C against 0.22 *M* NaCl containing 1 m*M* EDTA and 2 m*M* sodium azide. After dialysis, lipoproteins were run on vertical slab gels (7% polyacrylamide, 0.1% sodium dodecyl sulfate (SDS), 0.8% mercaptoethanol), following the procedures of Laemmli (1970). The protein band (apoLpl) was visualized with 0.3 *M* copper chloride. The apoLpl was cut from the gel and eluted by electrodialysis (Electro-Eluter model 422, Bio-Rad). The eluted apoLpl was dialyzed against 0.22 *M* NaCl. SDS- polyacryamide electrophoresis of the purified peptide was carried out to verify its purity. Purified apoLpl was used as the antigen for the preparation of monoclonal antibodies.

Monoclonal antibody production

Four female BLB/c mice were immunized with 50 μl of apoLpl (0.1 mg/ml) mixed with Freud's complete adjuvant. The injections were repeated twice (4 weeks and 6 weeks after the original injection) with 25 μg of apoLpl in Freud's incomplete adjuvant. Three days after the last injection, the mice were sacrificed and spleens removed. The mouse spleen cells were fused with a mouse myeloma strain Sp2/0, using polyethylene glycol as the fusing agent, as described by Galfre and Milstein (1981). After fusing, cells were plated in hypoxanthine/aminopterin/thymidine selection medium in microplates on a feeder layer consisting of mouse peritoneal macrophages. The wells were screened by indirect ELISA (enzyme-linked immunosorbent assay) for antibodies to apoLpl. The positive hybridomas were cloned by limiting dilution. The hybridomas were grown on RPMI 1640 medium (Gibco) supplemented with 10% fetal calf serum and 0.01% streptomycin and penicillin.

Indirect ELISA assay for apoLpl

An indirect ELISA assay was used to test antibodies, using the procedures described by Lee and Walker (1995), and absorbance was measured at 410 nm with an ELISA microplate reader (model EL307C, Bio-Tek Instruments).

Indirect competitive ELISA for apoLpl

A criss-cross serial dilution analysis was carried out to determine the optimal concentrations of apoLpl and antibody (Hornbeck *et al.*, 1992). The procedures for the indirect competitive ELISA for apoLpl using the monoclonal antibody McAb 1 are described in Lee and Walker (1995). Absorbances of the standards or extracts (A) were divided by the absorbance of the antibody not pre-incubated with antigen (A_0). The A/A_0 values for standards were plotted against the Lpl concentration on a linear-log graph to construct a standard curve. Concentrations of Lpl in egg/embryos were calculated from a standard curve prepared on the day of the assay.

Collection, extraction, and Lpl determination in oocytes

Ovaries were dissected from adult female crabs that were 12-14 d post-molt. Oocytes were washed out of minced ovaries with filtered seawater, followed by passage through nylon filters of different sizes to obtain a clean oocyte preparation. Light microscopy was used to determine oocyte diameters. After homogenization, the protein in oocyte extracts was determined by the method of Bradford (1976). Lpl concentrations in oocyte extracts were determined by competitive ELISA.

Collection, extraction, and Lpl determination in different embryo stages

Embryo stages 1 thru 10 are within an egg sac, from which the free-swimming zoea stage emerges (Table 1). The color of the sponge is indicative of the embryo stage: the color changes from bright orange to yellow to reddish

brown, and finally from dark brown to black just before hatching. Females with eggs (sponging female) at different stages were collected by trawling in the estuaries of coastal Georgia. The embryos in the sponge were staged by examination under a dissecting microscope. Using forceps, pieces of sponge were removed from a sponge-carrying female and gently shaken into 100 ml of seawater in a beaker. Embryos in a 1-ml aliquot of the water were counted to estimate the total number in the beaker, then the remaining water was filtered and the embryos collected on the filter. A hand-held homogenizer was used to homogenize 1000 embryos in 2 ml of 0.1 *M* phosphate buffer (pH 7.5). The extracts were centrifuged at 5000 × *g* for 10 min. The amount of LpI in aliquots of the supernatants (0.4 ml; 200 embryos) was determined by indirect competitive ELISA.

Collection, extraction, and LpI assay of larval forms

Zoeae were collected, extracted and LpI assays were carried out as described above. Megalopae were collected in plankton net tows in coastal Georgia estuaries during the period (spring tide in June) when megalopae enter the estuaries from offshore. They also were processed as described above.

Immunoblot (western blot) of LpI

Proteins from embryo or larval extracts were transferred from sodium dodecyl sulfate slab gels to nitrocellulose according to the methods described in Milne *et al.* (1992). After electrophoretic transfer, the membranes were probed with the monoclonal antibody (2 μg/ml) for LpI (McAbI) for 1 h, followed by rabbit anti-mouse alkaline phosphatase conjugates for 1 h. Western blue (bromochlorodindoylyl phosphate/nitroblue tetrazolium) was the chromogen (Promega). Pre-stained protein standards were used as molecular mass markers.

Immunohistochemistry

Blue crab embryos, larvae, and portions of adult hepatopancreas and ovaries were fixed in 10% neutral buffered formalin containing 1% zinc sulfate and processed for light microscopy. Standard immunohistochemical techniques (Lee and Walker, 1995) were used to probe sections of these tissues for the presence of anti-LpI immunoreactivity.

Results

Monoclonal antibody to quantify ApoLpI

Five monoclonal antibodies to apoLpI were developed. All of these antibodies reacted positively to blue crab LpI in an enzyme-linked immunosorbent assay (ELISA). One of the antibodies to apoLpI (McAbI) showed the strongest reaction to LpI. This antibody was used in an indirect, competitive ELISA to quantify LpI in oocytes, embryos, and larval forms. LpI could be detected at concentrations as low as 10 ng/ml of buffer. Using this assay and immunoblots, we found that LpI was absent from developing oocytes, newly fertilized eggs, and stages 1 through 4 embryos (Fig. 1). LpI concentrations increased steadily from stage 5 (2.3 ng/embryo, 1150 ng/ml of extract) to zoea (22.6 ng/zoea). While the concentration of LpI was increasing, yolk appeared to be decreasing such that very little yolk remained in stage 9/10 embryos. Western blots using McAbI on extracts of stages 1 through 10 showed no bands for stages 1 through, 4 and then a single immunoreactive band of increasing density (data not shown).

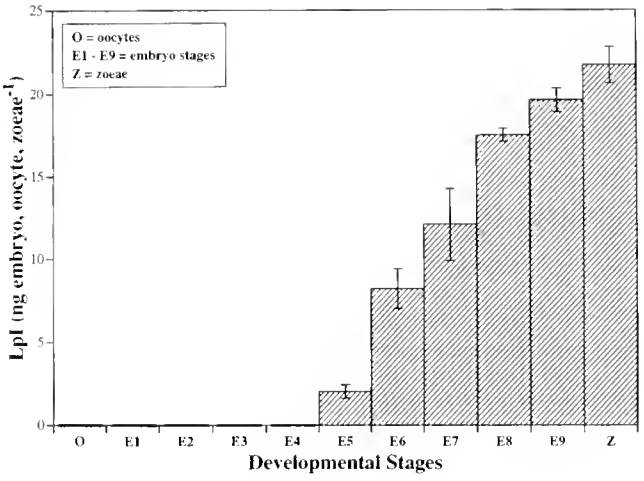

Figure 1. Amount of LpI in oocytes, different embryo stages (see Table 1 for description of each stage), and zoea. LpI determined by enzyme-linked immunosorbent assay (ELISA) as described in Materials and Methods. The values given are the mean ± standard deviation ($n = 3$) for 200 pooled individuals.

Immunohistochemistry using the anti-LpI antibody

Embryos. No immunoreactivity for LpI was observed in developing oocytes or in early embryo stages 1–4 (Fig. 2a). Beginning in stage 5, there were scattered immunoprecipitates within the yolk mass and at the interface with the embryonic cell mass. In addition to the morphologic changes of embryonic cell mass, individual cells dispersed throughout the yolk appeared at this time; these may represent vitellocytes. By stage 7 there were bilateral aggregates of cuboidal cells at the pole of the embryonic cell mass (Fig. 2b). The cuboidal cells had large nuclei with prominent nucleoli, moderate amounts of basophilic cytoplasm, and apical accumulations of anti-LpI immunoprecipitates. Tiny foci of anti-LpI immunoreactivity also seemed to be present in minute slit-like spaces on the non-yolk side of the cuboidal cells. By stage 10, the residual yolk was divided into bilateral masses, each encompassed by a circumference of cuboidal cells; these cells are

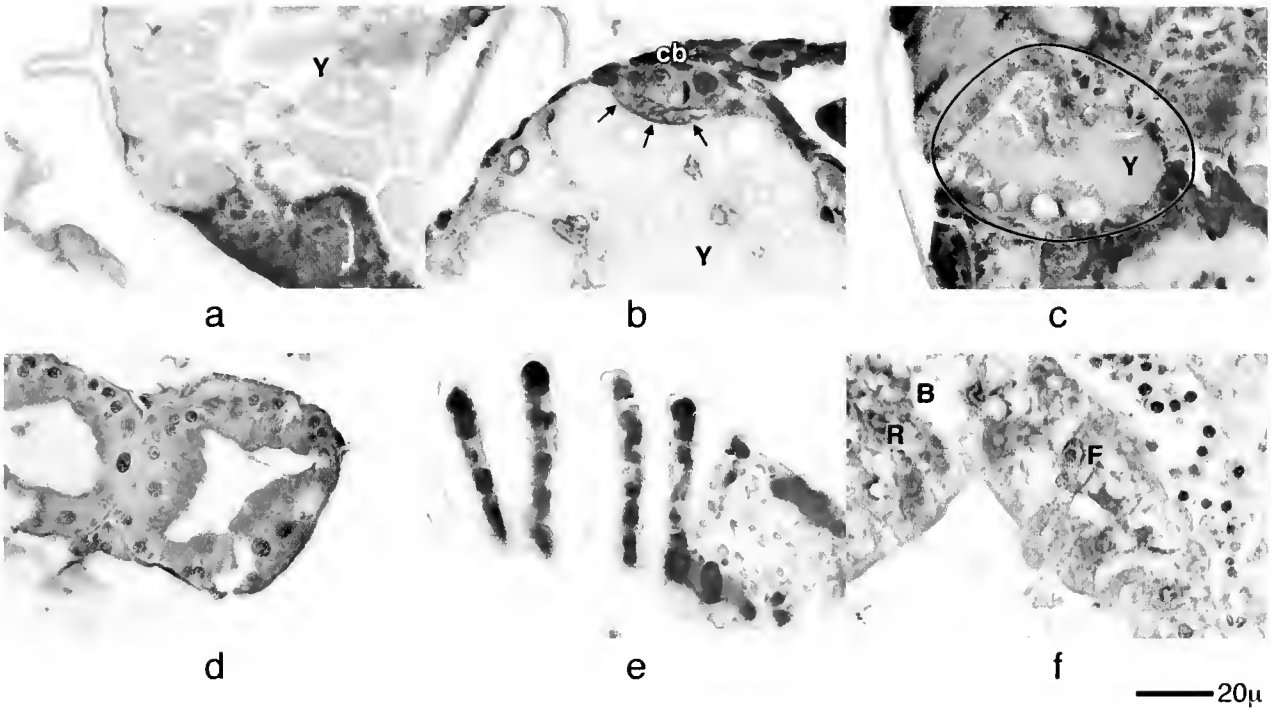

Figure 2. Immunohistochemical study using anti-Lpl Hematoxylin counterstain; original magnifications ×1000; bar = 20 μm). (a) Stage 4 embryo: Neither the embryonic cell mass nor the adjacent yolk (y) demonstrates immunoreactivity for Lpl. (b) Stage 7 embryo: Focal immunoprecipitates decorate the yolk (y) and are also localized at the interface of the lateral cuboidal cells (cb) with the yolk (arrows). (c) Stage 10 embryo (protozoea): The yolk (y) has been reduced to small bilateral masses surrounded by cuboidal cells. One such mass is delineated in this image. There are immunoprecipitates within the yolk and within the cytoplasm of the cuboidal cells. (d) Hepatopancreas of megalope: The hepatopancreas is composed of tubules of cuboidal and low columnar cells. Immunoprecipitates are concentrated at the apices. (e) Gill of megalope: The hemolymph within the vascular spaces is strongly immunoreactive for Lpl, while the background tissue elements are nonreactive. (f) Adult hepatopancreas: Immunoreactivity for Lpl is concentrated in the cytoplasm of the vacuolated (R and B) cells. In this preparation, the cytoplasm of the F cells is obscured by the more intense cytoplasmic reactivity of the R and B cells, but their nuclei (F) can still be seen.

assumed to be the anlagen of the hepatopancreas. Anti-Lpl immunoreactivity was present within the yolk residue and could also be seen in the cytoplasm of the cuboidal cells (Fig. 2c).

Larvae. The hepatopancreas of the megalopae consisted of a collection of tubular glands, less complex than the adult hepatopancreas. The glands were lined by a single layer of epithelium surrounded by a basement membrane. The lining cells were cuboidal to low columnar in shape and had basophilic cytoplasm. They resembled the anti-Lpl-reactive cuboidal cells observed in late embryo stages. The nuclei were centrally located in some cells and basally oriented in others. The nuclei of some cells had prominent nucleoli. Most cells had a cytoplasmic accumulation of granular anti-Lpl immunoprecipitate that appeared to be concentrated in the apical regions (Fig. 2d). Although occasional cells seemed to have some cytoplasmic vacuolization, they did not exhibit the definite morphologic features of cytologic specialization seen in adult hepatopancreatic cells. The hemolymph within the vascular spaces of the megalopae gills was intensely immunoreactive for Lpl, but the structural cells were nonreactive (Fig. 2e). Cellular constituents from other tissues—including muscle, eye, nerve, cuticular epithelial, and stomach—were not immunoreactive for Lpl.

Adults. The cytoplasm of lipid-rich R and vacuolated B cells in the hepatopancreas was intensely decorated with granular anti-Lpl immunoprecipitate. The non-vaculolated, basophilic F cells, in contrast, demonstrated little cytoplasmic immunoreactivity for Lpl (Fig. 2f). The F cells possessed prominent nuclei with large nucleoli, reminiscent of the nuclear features of the hepatopancreas cells of the megalopae.

Discussion

The immunohistochemical, ELISA, and western blot work support our conclusion that the lipoprotein Lpl is produced in embryonic tissues, appearing first in stage 5 embryos. In stage 5 embryos, basophilic cuboidal cells with

prominent nuclei are present at the lateral edges of the embryonic cell mass. We assume that these cuboidal cells are the site of Lpl synthesis, since they demonstrate cytoplasmic immunoreactivity for Lpl at their interface with yolk. Once synthesized, the Lpl apparently diffuses into the adjacent yolk mass. These cuboidal cells in the embryo bear a strong cytologic resemblance to the hepatopancreas cells, which have also been shown to synthesize Lpl. Lovett and Felder (1990) noted the presence of morphologically similar cuboidal cells in the larval hepatopancreas of the white shrimp, *Penaeus setiferus*.

It seems unlikely that Lpl is formed directly from lipovitellin (LplI), since the two lipoproteins are biochemically quite dissimilar. They differ in molecular mass, primary amino acid sequence, and three-dimensional structure (Lee and Puppione, 1988; Yepiz-Plascencia *et al.*, 1998). Moreover, Lpl does not react with antibodies to LplI (Tom *et al.*, 1993).

It has been shown in a number of arthropod groups that, during embryonic development, yolk proteins are degraded by proteases to amino acids and low-molecular-weight peptides (McGregor and Loughton, 1974; Garesse *et al.*, 1980; Ezquieta and Vallejo, 1985; Perona and Vallejo, 1985; Purcell *et al.*, 1988; Fagotto, 1990; Nordin *et al.*, 1990; Masetti *et al.*, 1998). We speculate that during embryogenesis of the blue crab, proteases and lipases in vitellophages hydrolyze lipovitellin to amino acids and fatty acids, which the cuboidal cells then use to assemble Lpl.

Our evidence suggests that hepatopancreas cells of zoeae, megalopae, and adult blue crabs are involved in the synthesis of Lpl, as indicated by their intense immunoreactivity. Unlike the midgut cells of the developing lobster, *Homarus americanus* (Biesiot and McDowell, 1995), the hepatopancreatic cells of the blue crab do not show light microscopic features of cytologic specialization until after the megalope stage. Thereafter, the site of synthesis may be the F-cells, since they have extensive endoplasmic reticulum and Golgi network (Al-Mohanna and Nott, 1989). After assembly in F-cells, Lpl is assumed to be transported to R- or B-cells, followed by transfer into the hemolymph. These R- or B-cells may effectively concentrate Lpl as suggested by their more intense immunoreactivity.

The hepatopancreas of arthropods is analogous in function to the liver (and pancreas) of vertebrates. In vertebrates, liver parenchymal cells synthesize plasma lipoproteins, with final assembly, addition of lipid, and secretion being coordinated by the Golgi apparatus (Dolphin, 1985; Havel 1987). Future planned work will determine if cuboidal embryo cells and hepatopancreas cells in other stages express apoLpl mRNA. It seems likely that R cells, which have large lipid stores, may be responsible for adding lipid to apoLpl to form Lpl.

Insect and crustacean hemolymph lipoproteins differ in structure, function, and their presence or absence in the eggs. In adult insects and crustaceans, most of the hemolymph lipid is associated with high-density lipoproteins, namely lipophorin in insects and Lpl in crustaceans (Gilbert and Chino, 1974; Van der Horst, 1990; Lee 1991). Lipophorin accounts for more than 50% of the total hemolymph protein in insects (Chino *et al.*, 1981), whereas Lpl accounts for only 3% of the total hemolymph protein in crustaceans (Ruiz-Verdugo *et al.*, 1997).

The site of lipophorin synthesis in insects is the fat body. In females, lipophorin is transported by the hemolymph to the ovaries, where it is taken up by developing oocytes (Kawooya and Law, 1988; Kanost *et al.*, 1990). Although the major constituent of insect yolk is vitellin, a considerable amount of lipophorin is present as well. As much as one molecule of lipophorin for every 3 molecules of vitellin has been found in insect eggs (Telfer and Pan, 1988). It has been suggested that lipophorin provides a major source of lipid, and vitellin serves as a source of protein (Chino *et al.*, 1977).

Our results indicate that the site of Lpl synthesis in adult and larval crabs is the hepatopancreas. There is good evidence that, like lipophorin in insects, Lpl is an important carrier of lipid to the ovary in the adult (Harry *et al.*, 1979; Telfer *et al.*, 1991; Ravid *et al.*, 1999). However, whereas Lpl may transfer its lipid to the ovary and then recirculate, as apoLpl, to the hepatopancreas to pick up more lipid, in insects, the lipophorin, after losing some of its lipid, is transferred into the developing oocytes (Harry *et al.*, 1979; Telfer *et al.*, 1991).

There are other important differences between insect lipophorin and crab Lpl. Lipophorin has a high diacylglycerol content, while phosphatidyl choline is the major Lpl lipid. There are also important differences in the major yolk protein, vitellin, of insects compared with the major yolk protein, lipovitellin (LplI), of crabs. Insect vitellin is 7%–10% lipid, with the lipids being primarily diacylglycerol and phospholipid (Beenakkers *et al.*, 1985; Wheeler and Kawooya, 1990). Crab lipovitellin is 40%–50% lipid, most of which is phospholipid (Lee and Puppione, 1988; Lee and Walker, 1995).

Differences in function may explain the presence of lipophorin in insect embryos and the absence of Lpl in early stages of developing crustaceans. As noted above, both lipophorin and Lpl apparently carry lipid to the ovary. However, Lpl is also involved in the adult crustacean immune system, whereas lipophorin is not known to have such a role in insects. We hypothesize that the importance of Lpl in late crab embryo stages and in larvae is related to its function in the developing immune system. The role of Lpl in lipid transport may not become critical until the juvenile stages.

Acknowledgments

This work was partially supported by the NOAA Coastal Ocean Program through the South Carolina Sea Grant Consortium pursuant to National Oceanic and Atmospheric Administration Award No NA96PO113.

Literature Cited

Al-Mohanna, S. Y., and J. A. Nott. 1989. Functional cytology of the hepatopancreas of *Penaeus semisulcatus* (Crustacea: Decapoda) during the moult cycle. *Mar. Biol.* **101:** 535–544.

Beenakkers, A. M. T., D. J. Van der Horst, and W. J. A. Van Marrewuk. 1985. Insect lipids and lipoproteins, and their role in physiological processes. *Prog. Lipid Res.* **24:** 19–67.

Biesiot, P. M., and J. E. McDowell. 1995. Midgut-gland development during early life-history stages of the American lobster *Homarus americanus*. *J. Crustac. Biol.* **15:** 679–685.

Bradford, M. M. 1976. A rapid method of total lipid extraction and purification. *Can. J. Biochem. Physiol.* **72:** 248–254.

Chino, H., R. G. H. Downer, and K. Takahashi. 1977. The role of diacylglycerol-carrying lipoprotein 1 in lipid transport during insect vitellogenesis. *Biochim. Biophys. Acta* **487:** 508–516.

Chino, H., H. Katase, R. G. H. Downer, and K. Takahashi. 1981. Diacylglycerol-carrying lipoprotein of hemolymph of the American cockroach: purification, characterization, and function. *J. Lipid Res.* **22:** 7–15.

Dolphin, P. J. 1985. Lipoprotein metabolism and the role of apolipoproteins as metabolic programmers. *Can. J. Biochem. Cell Biol.* **63:** 850–869.

Ezquieta, B., and C. G. Vallejo. 1985. The trypsin-like proteinase of *Artemia:* yolk localization and developmental activation. *Comp. Biochem. Physiol.* **82B:** 731–736.

Fagotto, F. 1990. Yolk degradation in tick eggs: II. Evidence that cathepsin L-like proteinase is stored as a latent, acid-activable proenzyme. *Arch. Insect Biochem. Physiol.* **14:** 237–252.

Galfre, G., and C. Milstein. 1981. Preparation of monoclonal antibodies: strategies and procedures. *Methods Enzymol.* **73:** 3–46.

Garesse, R., R. Perona, R. Marco, and C. G. Vallejo. 1980. The unmasking of proteolytic activity during the early development of *Artemia salina*. *Eur. J. Biochem.* **106:** 225–231.

Gilbert, L. I., and H. Chino. 1974. Transport of lipids in insects. *J. Lipid Res.* **15:** 439–456.

Hall, M., M. C. Van Housed, and K. Söderhäll. 1995. Identification of the major lipoproteins in crayfish hemolymph as proteins involved in immune recognition and clotting. *Biochem. Biophys. Res. Commun.* **216:** 939–946.

Harry, P., M. Pines, and S. W. Applebaum. 1979. Changes in the pattern of secretion of locust female diglyceride-carrying lipoprotein and vitellogenin by the fat body *in vitro* during oocyte development. *Comp. Biochem. Physiol.* **63B:** 287–293.

Havel, R. 1987. Lipid transport function of lipoproteins in blood plasma. *Am. J. Physiol.* **253:** E1–E5.

Hornbeck, P., S. E. Winston, and S. A. Fuller. 1992. Enzyme-linked immunosorbent assay (ELISA). Pp. 11-5–11-17 in *Short Protocols in Molecular Biology*, F.L.M. Ausubel, R. Brent, R.E. Kingston, D.D. Moore, J.G. Seidman, J.A. Smith, and K. Struhl, eds. John Wiley & Sons, New York.

Kang, B. K., and E. Spaziani. 1995. Uptake of high-density-lipoprotein by Y-organs of the crab *Cancer antennarius*. I. Characterization *in vitro* and effects of stimulators and inhibitors. *Arch. Insect Biochem. Physiol.* **30:** 61–75.

Kanost, M. R., J. K. Kawooya, J. H. Law, R. O. Ryan, M. C. Van Heuden, and R. Ziegler. 1990. Insect haemolymph proteins. *Adv. Insect Physiol.* **22:** 299–396.

Kawooya, J. K., and J. H. Law. 1988. Role of lipophorin in lipid transport to the insect egg. *J. Biol. Chem.* **263:** 8748–8753.

Khayat, M., O. Shenker, B. Funkenstein, M. Tom, E. Lubzens, and A. Tietz. 1994. Fat transport in the penaeid shrimp *Penaeus semisulcatus* (de Haan). *Israeli J. Aquacul.* **46:** 22–32.

Laemmli, U. K. 1970. Cleavage of structural proteins during the assembly of the head of bacteriophage T4. *Nature* **227:** 680–685.

Lee, R. F. 1991. Lipoproteins from the hemolymph and ovaries of marine invertebrates. *Adv. Comp. Environ. Physiol.* **7:** 187–207.

Lee, R. F., and D. L. Puppione. 1988. Lipoproteins I and II from the hemolymph of the blue crab *Callinectes sapidus:* Lipoprotein II associated with vitellogenesis. *J. Exp. Zool.* **248:** 278–289.

Lee, R. F., and A. Walker. 1995. Lipovitellin and lipid droplet accumulation in oocytes during ovarian maturation in the blue crab, *Callinectes sapidus*. *J. Exp. Zool.* **271:** 401–412.

Lindren, F. T. 1975. Preparative ultracentrifugal laboratory procedures and suggestions for lipoprotein analysis. Pp. 204–224 in *Analysis of Lipids and Lipoproteins*, E.G. Perkins, ed. American Oil Chemists Society, Champaign, IL.

Lovett, D. L., and D. L. Felder. 1990. Ontogenetic changes in enzyme distribution and midgut function in developmental stages of *Penaeus setiferus* (Crustacea, Decapoda, Penaeidae). *Biol. Bull.* **178:** 160–174.

Masetti, M., A. Cecchettini, and F. Giorgi. 1998. Mono- and polyclonal antibodies as probes to study vitellin processing in embryos of the stick insect *Carausius morosus*. *Comp. Biochem. Physiol.* **120B:** 625–631.

McGregor, D. A., and B. G. Loughton. 1974. Yolk-protein degradation during embryogenesis of the African migratory locust. *Can. J. Zool.* **52:** 907–917.

Milne, R. W., P. K. Weech, and Y. L. Marcel. 1992. Immunological methods for studying and quantifying lipoproteins and apolipoproteins. Pp. 61–84 in *Lipoprotein Analysis-A Practical Approach*, C.A. Converse and E.R. Skinner, eds. Oxford University Press, Oxford.

Nordin, J. E., E. L. Beaudoin, and X. Lin. 1990. Proteolytic processing of *Blatella germanica* vitellin during early embryo development. *Arch. Insect Biochem.* **15:** 119–135.

Perona, R., and C. G. Vallejo. 1985. Acid hydrolases during *Artemia* development: a role in yolk degradation. *Comp. Biochem. Physiol.* **81B:** 993–1000.

Purcell, J. P., J. G. Kunkel, and J. H. Nordin. 1988. Yolk hydrolase activities associated with polypeptide and oligosaccharide processing of *Blattella germanica* vitellin. *Arch. Insect Biochem. Physiol.* **8:** 39–58.

Ravid, T., A. Tietz, M. Khayat, E. Boehm, R. Michelis, and E. Lubzens. 1999. Lipid accumulation in the ovaries of a marine shrimp *Penaeus semisulcatus* (De Haan). *J. Exp. Biol.* **202:** 1819–1829.

Ruiz-Verdugo, L. M., M. L. Garcia-Banuelos, R. Vargas-Albores, I. Higuera-Ciapara, and G. M. Yepiz-Placencia. 1997. Amino acids and lipids of the plasma HDL from the white shrimp *Penaeus vannamei* Boone. *Comp. Biochem. Physiol.* **118B:** 91–96.

Spaziani, E. 1988. Serum high-density lipoprotein in the crab, *Cancer antennarius* Stimpson: II. annual cycles. *J. Exp. Zool.* **246:** 315–318.

Spaziani, E., and W. L. Wang. 1991. Serum high-density lipoproteins in the crab, *Cancer antennarius*. III. Density-gradient profiles and lipid composition of subclasses. *Comp. Biochem. Physiol.* **98B:** 555–561.

Stratakis, E., G. Fragkiadakis, and E. Carpeli-Moustaizi. 1992. Isolation and characterization of a non sex-specific lipoprotein from hemolymph of fresh water crab *Potamon potamios*. *Biol. Chem. Hoppe-Seyler* **373:** 665–677.

Telfer, W. H., and M-L. Pan. 1988. Adsorptive endocytosis of vitellogenin, lipophorin, and microvitellogenin during yolk formation in *Hyalophora. Arch. Insect Biochem. Physiol.* **9:** 339–355.

Telfer, W. H., M.-L. Pan, and J. H. Law. 1991. Lipophorin in developing adults of *Hyalophora cecropia:* support of yolk formation and preparation for flight. *Insect Biochem.* **21:** 653–663

Tom, M., O. Shenker, and M. Ovadia. 1993. Partial characterization of three hemolymph proteins of *Penaeus semisulcatus* de Haan (Crustacea, Decapoda, Penaeidae) and their specific antibodies. *Comp. Biochem. Physiol.* **104B:** 811–816.

Van der Horst, D. J. 1990. Lipid transport function of lipoproteins in flying insects. *Biochim. Biophys. Acta* **1047:** 195–211.

Wheeler, D. E., and J. K. Kawooya. 1990. Purification and characterization of honey bee vitellogenin. *Arch. Insect Biochem. Physiol.* **13:** 253–267.

Yepiz-Plascencia, G. M., R. Sotelo-Mundo, L. Vasques-Morena, R. Ziegler, and I. Higurera-Ciapara. 1995. A non-sex specific hemolymph lipoprotein from white shrimp *Penaeus vannamei* Boone. Isolation and partial characterization. *Comp. Biochem. Physiol.* **111B:** 181–187.

Yepiz-Plascencia, G., F. Vargas-Albores, F. Jimenez-Vega, L.M. Ruiz-Verdugo, G. Romo-Figueroa. 1998. Shrimp plasma HDL and β-glucan binding protein (BGBP): comparison of biochemical characteristics. *Comp. Biochem. Physiol.* **121B:** 309–314.

Reference: *Biol. Bull.* **204:** 57–67. (February 2003)

Reproductive Biology of *Hemiramphus brasiliensis* and *H. balao* (Hemiramphidae): Maturation, Spawning Frequency, and Fecundity

RICHARD S. McBRIDE* AND PAUL E. THURMAN

Florida Marine Research Institute, Florida Fish and Wildlife Conservation Commission, 100 8th Avenue SE, St. Petersburg, Florida 33701-5095

Abstract. Analyses of life-history data show that both the size-specific batch fecundities and the age-specific spawning frequencies differ for two halfbeak species, *Hemiramphus brasiliensis*, the ballyhoo, and *H. balao*, the balao. Halfbeak ages were determined from sectioned otoliths; histological data was used to describe oocyte development and estimate spawning frequency; and batch fecundity was measured from counts of whole oocytes in final maturation. *Hemiramphus brasiliensis* lived longer (4 *versus* 2 years) and had a higher survival rate (14.9% *versus* 7.5% annually) than *H. balao* did. Of the two species the larger and longer-lived congener, *H. brasiliensis*, reached sexual maturity at a larger size (fork length 198 *versus* 160 mm). The spawning period of age-0 females was strongly related to season, whereas spawning by older females occurred throughout the year. Reproduction by both species peaked during late spring or early summer, and all mature females were spawning daily during April (*H. brasiliensis*) or June (*H. balao*). This is the first demonstration of iteroparity for the family Hemiramphidae. *H. brasiliensis* had a lower batch fecundity (about 1164 *versus* 3743 hydrated oocytes for a 100-g female) than *H. balao* did. Such low batch fecundities are typical of the order Beloniformes, but quite different from those of other fishes that live in association with coral reef habitats. *H. balao*'s higher batch fecundity is consistent with the life-history theory that predicts higher numbers of eggs for shorter-lived species; this is possible because *H. balao* produces smaller hydrated oocytes than *H. brasiliensis* (modal diameter about 1.6 *versus* 2.4 mm). The high spawning frequency of *Hemiramphus* species compensates for their low batch fecundity. The annual fecundity of both species is similar to that of other reef fish species, after adjusting for body size and spawning frequency. The lifetime fecundity of *H. balao* was very similar to that of *H. brasiliensis*, after accounting for the differences in survival for each species. This suggests a fine tuning of different reproductive traits over the entire life cycle that results in roughly equivalent lifetime fecundity for both species.

Received 21 June 2002; accepted 6 November 2002.

* To whom correspondence should be addressed. E-mail: richard.mcbride@fwc.state.fl.us

Introduction

Two pelagic halfbeak species, *Hemiramphus brasiliensis* and *H. balao*, are conspicuous and abundant elements of the Atlantic Ocean's coral reef fauna (Collette, 1965; Nybakken, 1997, p. 368; McBride *et al.*, 2003). These congeners are similar in size and shape (about 30 cm maximum length; McBride *et al.*, 1996) but differ in both habitat use and diet. Both halfbeak species intermingle above coral reef habitats; otherwise, *H. brasiliensis* is found only inshore of reef habitats and *H. balao* is found only offshore of reefs (McBride *et al.*, 2003). *H. brasiliensis* preys on zooplankton and grazes on seagrasses, whereas *H. balao* is a planktivore (Berkeley and Houde, 1978). Berkeley and Houde (1978) also characterized both species as oviparous summer-spawners with low batch fecundities (*i.e.*, the number of eggs released per spawning event; Hunter *et al.*, 1985), and they reported that *H. brasiliensis* lived longer but had a lower batch fecundity than *H. balao*. These life-history patterns (*i.e.*, age, reproduction, and mortality) are particularly intriguing because such patterns suggest a trade-off between survival and reproductive output.

Comparing life-history traits within species and between morphologically similar species in different habitats is a powerful method for understanding life-history evolution

(Partridge and Harvey, 1988). If the life-history patterns of fishes evolve largely in response to their environment, it is striking that *H. brasiliensis* and *H. balao* have much larger eggs but lower batch fecundities (*i.e.*, egg diameter >1 mm and thousands of eggs per batch; Berkeley and Houde, 1978) than other coral reef fishes (*e.g.*, see Thresher, 1984). These large eggs and low batch-fecundity values may simply reflect the evolutionary history of hemiramphids. Average batch fecundities for other oviparous hemiramphids range from one hundred (Silva and Davies, 1988; Coates and Van Zwieten, 1992) to a few thousand eggs per female (Talwar, 1962, 1967). In contrast, an average female coral reef fish with a body size similar to that of a *Hemiramphus* species produces about 100,000 eggs (Thresher, 1984). Such low fecundities for *Hemiramphus* species imply either high fertilization success, high survival rates, or the production of multiple batches of eggs. Multiple spawning is a common life-history trait among marine fishes and can greatly increase lifetime reproductive output. Although multiple spawning has been suspected to occur in several hemiramphids, it has never been demonstrated conclusively (*e.g.*, Ling, 1958; Talwar, 1967; Coates and Van Zwieten, 1992).

In this study, multiple spawning is demonstrated for both *H. brasiliensis* and *H. balao*, and new measurements are made of other life-history variables, namely age, mortality, size at maturity, egg size, batch fecundity, and spawning frequencies. Such detailed measurements demonstrate the interaction of phenotypic traits that determine fitness in two congeneric hemiramphids. We also compare these traits for *Hemiramphus* species with those of other hemiramphids and other coral reef fish species to evaluate the importance of evolutionary history in constraining allocation of reproductive effort.

Materials and Methods

Fishes were collected in the coastal waters of southeastern Florida (approx. 26.0° N, 80.0° W to 24.5° N, 82.2° W). *Hemiramphus brasiliensis* and *H. balao* were collected together near the surface in association with coral reefs. *H. brasiliensis* alone was collected in other inshore habitats such as bank habitats in nearby Florida Bay, and so it is more numerous in our collections overall. From July 1997 to October 1998, 100 to 200 fish were subsampled, on each of 4 days per months from the catch of commercial fishing operations. Additional specimens were collected independent of the commercial fishery for a target number of 4 additional trips per month and a sample size of 12 fish per trip. Fish were kept on ice and brought to the laboratory for processing. Fish lengths and weights were measured in the laboratory. Fork length (FL) was measured to the nearest millimeter from the tip of the upper jaw to the fork of the tail. Whole body weight was recorded to the nearest 0.1 g.

Ages of halfbeaks were determined by examining annual increments deposited on otoliths. For each trip in the months from July 1997 to June 1998, 12 fish were selected, at random, for aging; their sagittal otoliths were removed and stored dry. A low-speed saw was used to cut multiple 500-μm-thick sections along the transverse plane through the otolith core. Otoliths were cut only from fish larger than 200 mm in FL, because otoliths of smaller fish are known to be age-0 (Berkeley and Houde, 1978). Sectioned otoliths were mounted to coded glass slides and examined, usually at 40 ×, with reflected light under a dissecting microscope. The annuli were counted as a measure of fish age, in years, by two readers. If the two independent counts did not agree, then a third reading was conducted, with both readers working together. Only 5% of the otoliths were so difficult to evaluate by both readers that they were rejected ($n = 61$). The frequency of annulus formation was confirmed as annual by a marginal increment analysis. In such an analysis, the percentage of age-1 ballyhoo with an opaque margin, which was interpreted as a second annulus, was calculated for each month; monthly frequencies were checked for periodicity of annulus formation.

Annual survival estimates ($\hat{S}$) for each species were derived using the estimator from Robson and Chapman (1961):

$$\hat{S} = \sum_{x=0}^{k} x f_x \Big/ \left(\sum_{x=0}^{k} f_x + \sum_{x=0}^{k} x f_x - 1 \right),$$

where x is the coded age class (0 = youngest age [in years] fully vulnerable to fishing), f_x is the number of fish per age-class x, and k is the oldest age class observed. The data for this analysis were only from the period October–May, because age-0 fish are not fully vulnerable to the sampling gear during the summer months (Berkeley and Houde, 1978).

Gonads from 12 randomly selected fish in each collection were removed during the period of July 1997 to October 1998 and prepared for histology. Ovarian tissue was initially fixed in 10% buffered formalin; a section of tissue was then transferred to ethanol, embedded in glycol methacrylate, sectioned along the transverse plane, stained with the periodic acid-Schiff (PAS) reaction, iron-hematoxylin, and counterstained with metanil yellow (Quintero-Hunter *et al.*, 1991). Gonads were assigned a stage based on the most advanced stage of oocyte development, namely perinucleolar, cortical alveolar, vitellogenic, nucleus migration, or nucleus breakdown. Cellular atresia such as postovulatory follicles (POF) and PAS-positive melano-macrophage centers were also noted. Characterization of POFs follows the descriptions of Hunter and Macewicz (1985). Identification of PAS-positive bodies follows the descriptions in Grier and Taylor (1998; pp. 531, 539–540) and McBride *et al.* (2002).

Table 1

Maturity categories for female Hemiramphus *spp.*

Maturity Category	Most Advanced Oocyte Stage	Atresia and POFs[a]
Immature	Perinucleolar stage	Little or no atresia
Maturing	Cortical alveolar (CA)	Little or no atresia
Mature	Vitellogenic or FOM[b] stage	may be POFs; PAS+ bodies[c]
Regressed	Perinucleolar or CA stage	PAS+ bodies[c]

Females were scored according to their most advanced oocyte stage, and past spawning was inferred based on the presence of postovulatory follicles (POFs) and PAS-positive melano-macrophage centers (see text for details). The dashed line separates immature from mature stages, the division used for calculating size at 50% maturity.

[a] Postovulatory follicles (POFs) were observed as newly collapsed structures after dusk. They were readily observed for about 24 h, after which they became more compact and darker.

[b] Final oocyte maturation (FOM) began with migration of the nucleus, continued with breakdown of the nucleus (=hydration), and ended with ovulation of eggs.

[c] PAS-positive (PAS+) melano-macrophage centers appeared as compact, bright purple bodies when our staining technique was used and are similar to yellow or brown bodies when other stains were used.

The presence of vitellogenic oocytes was the primary indication of maturity (Table 1). Vitellogen, a protein secreted by the liver and endocytosed by oocytes, accumulates in yolk globules that appear in the cytoplasm of oocytes during the spawning season (Wallace and Selman, 1978). Mature females with regressed ovaries were distinguished from immature virgin or maturing virgin females by the presence of PAS-positive melano-macrophage centers. Such PAS-positive bodies are involved in focal tissue degradation, and their presence increases during and after gonad regression (Grier and Taylor, 1998). Size at 50% maturity was calculated as the inflection point of a logistic equation modeling the percent frequency of mature females: maturity $= 1/(1 + \exp(-A[\mathrm{FL} - B]))$, where A = the instantaneous rate of increase at the origin and B = the inflection point or the point where 50% of the individuals are mature. Model parameters were estimated by the logistic procedure of SAS software (SAS, 1990).

Spawning frequency was estimated by the "post-ovulatory follicle method" of Hunter and Macewicz (1985). We assumed that POFs became indistinguishable from other atretic bodies after about 24 h, so their presence as collapsed structures with identifiable thecal and granulosa layers indicated that an individual female had spawned during the previous day.

Batch fecundities and oocyte diameters were determined from examination of whole oocytes. Batch fecundities were estimated for 41 specimens of *H. brasiliensis* and 3 of *H. balao* collected in March 1997, May 1997, February–April 1998, and March 1999. About 1 g of tissue was removed from the anterior and posterior sections of the left and right ovaries, blotted dry, and weighed to the nearest 0.001 g. After the tissue was washed, teased apart, and placed in a solution of 33% glycerin:67% water, the number of hydrated oocytes was counted. Batch fecundity was estimated according to the total weight of the ovary, following the methods of Hunter *et al.* (1985). To increase sample size, these data are presented together with data from Berkeley and Houde (1978), who used a similar method for estimating batch fecundity and obtained similar results. Whole oocyte diameters, for at least 300 oocytes per female, were then measured to the nearest micrometer with the aid of a video system and image-analysis software.

Results

Age, growth, and survival

Sectioned otoliths revealed an alternating pattern of opaque and translucent bands (Fig. 1). The darker, translucent areas represented the periods of faster growth during the summer; the whitish, opaque bands reflected the periods of slower growth during the winter. Marginal increment analysis of *Hemiramphus brasiliensis* otoliths showed that a single annulus was formed each year and that annulus formation was complete by June of each year (Fig. 2). Although too few specimens of *H. balao* were available for the marginal increments of this species to be similarly analyzed, we chose June as the biological hatchdate for both species.

Our aging results indicated that *H. brasiliensis* lives longer than *H. balao* (4 *versus* 2 years; Fig. 3). At a given age, individuals of *H. brasiliensis* were also larger on average than those of *H. balao*, and females of each species were larger than male conspecifics. Of the 1022 specimens of *H. brasiliensis* aged, the largest was 294 mm FL, whereas of the 132 *H. balao* specimens aged, the largest was 251 mm FL. Annual survival of *H. brasiliensis* during the study period averaged 14.9% (95% confidence limits: 12.2%–17.6%) and was double that of *H. balao* (7.5% on average; 2.01%–13.0%, 95% c.l.).

Reproduction

Ovaries of both halfbeak species were composed of two cylindrical lobes, roughly equal in size. During initial maturation of the specimens we examined, and again during spring recrudescence, these lobes increased in girth, developed a pinkish color, and extended anteriorly along the coelomic cavity. Each lobe was a hollow sac with oocytes arranged in lamellae that extended into a central lumen (Fig. 4A-C). Virgin females lacked any PAS-positive melano-macrophage centers and had a thin gonad wall (Fig. 4A, C); mature, regressed females had PAS-positive melano-macrophage centers and a thick gonad wall (Fig. 4B). Oocytes

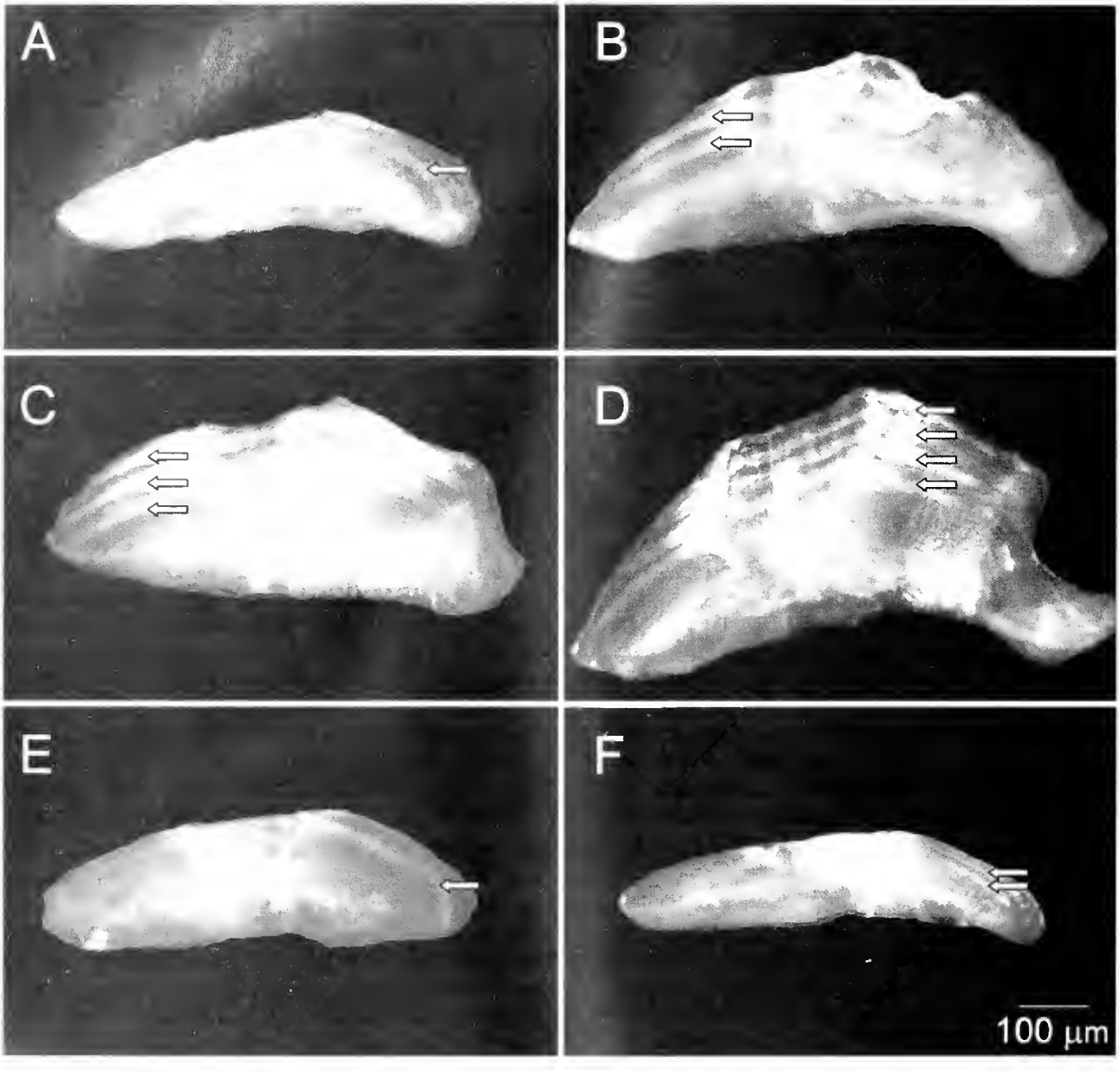

Figure 1. Photomicrographs of sectioned otoliths representing various age classes for *Hemiramphus brasiliensis* (ballyhoo) and *H. balao* (balao). (A) *H. brasiliensis* age-1, (B) *H. brasiliensis* age-2, (C) *H. brasiliensis* age-3, (D) *H. brasiliensis* age-4, (E) *H. balao* age-1, (F) *H. balao* age-2. Arrows indicate annulus locations.

developed in a group-synchronous pattern. Maturing females had oocytes measuring about 200–500 μm in diameter and had cortical alveoli present in the cytoplasm (Fig. 4E). These cortical alveoli appeared as open vacuoles in the cytoplasm, and their color changed from clear (Fig. 4C) to clear with dark specks or purple (Fig. 4D, E) as the oocytes matured. The development of yolk protein, which characterizes a vitellogenic or mature oocyte, was indicated by a red hue in the cytoplasm of oocytes about 400–700 μm in diameter. This yolk protein appeared initially near the nucleus (Fig. 4F, G) but later expanded throughout the cytoplasm and became globular (Fig. 4H). Vitellogenic oocytes with migratory nuclei (*i.e.*, the beginning of final oocyte maturation) always had globular yolk (Fig. 4I, J) and were as small as about 600 μm in diameter. Nucleus migration continued as oocytes enlarged to about 2000 μm in diameter, and the yolk dominated the cytoplasm (Figs. 4K, 5A). Subsequently, the cytoplasm changed from red to pink as the result of hydration, and nucleus breakdown occurred (Figs. 4L, 5B). Ovulating females were collected at dusk,

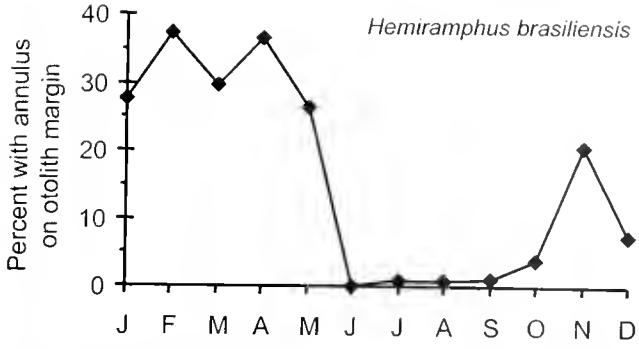

Figure 2. Percent of age-1 *Hemiramphus brasiliensis* (ballyhoo), with a whitish, opaque annulus on the margin of the sectioned otolith, by month. Otoliths were collected from July 1997 to June 1998 (n = 1019).

and fresh postovulatory follicles could be observed (Figs. 4J, M; 5C). Vitellogenic oocytes not in the final stages of oocyte maturation were observed together with oocytes that had migrating nuclei and with hydrated oocytes (Fig. 4N), which suggested a fairly rapid turnover of oocytes. The patterns of oocyte development for the two species did not appear to differ, except that the modal diameter of hydrated oocytes was only about 1.6 mm for *H. balao* compared to about 2.4 mm for *H. brasiliensis* (Fig. 5B, D). In addition, females of *H. balao* matured (size at 50% maturity = 160 mm FL) at a smaller size than females of *H. brasiliensis* (*i.e.*, size at 50% maturity = 198 mm FL; Fig. 6). Both species became mature as age-0 fish (*i.e.*, young-of-the-year).

There were distinct seasonal trends in maturation, and the seasonal patterns of POF occurrence indicated prolonged, albeit slightly staggered, spawning periods for both species (Figs. 7, 8). During autumn, the incidence of immature and maturing individuals increased because age-0 fish were more frequently caught in the sampling gear; and the gonads of older fish were regressing as winter approached. Spawning frequency peaked in April for *H. brasiliensis* and in June for *H. balao*, but spawning by some females was evident year-round based on the continued presence of POFs in older fish. Spawning frequencies were clearly age-specific, even for such short-lived species. All age classes of both species were spawning on a daily, or near-daily, basis, during spring or summer (Fig. 8). In other seasons, age-1 females spawned more frequently than age-0 females did, but age-2 ballyhoo females did not necessarily spawn more frequently than age-1 ballyhoo females. In terms of environmental associations, spawning activity peaked when the photoperiod was longest (*i.e.*, June), and most juveniles were growing when temperatures were highest (*i.e.*, August; Fig. 9).

Batch fecundity was higher for *H. balao* than for *H. brasiliensis* across the range of mature sizes (Fig. 10). Batch fecundity also increased more rapidly with increasing fish size in *H. balao* than in *H. brasiliensis*. The average batch size for a 100-g female of *H. balao* (3743 oocytes) was more than three times that of a 100-g female of *H. brasiliensis* (1164 oocytes). At a common size of 200 g, the batch fecundity of *H. balao* (8346 oocytes) was more than five times that of *H. brasiliensis* (1538 oocytes).

Discussion

We report here, for the first time, the evidence that *Hemiramphus* species are multiple-spawners with group-synchronous oocyte development. Many general life-history patterns are similar for the two species of halfbeak. Both are short-lived, fast-growing, gonochoristic, and oviparous. Still, there were interspecific life-history differences, some of which varied in a manner predicted by life-history theory. The results of this study show the interplay between different phenotype-based life-history traits that are balanced out once lifetime reproductive output is calculated.

Maximum ages for both species in our study were 1 or 2 years older than the ages determined in a previous study, but our results do not alter the conclusions that these are fast-growing and short-lived species (Berkeley and Houde, 1978). Berkeley and Houde (1978) reported that the maximum age of 1100 specimens of *H. brasiliensis* was age-2 and the maximum age of 135 specimens of *H. balao* was age-1. They read annuli on fish scales, and some researchers have noted that this method tends to underestimate ages compared to the use of otoliths (*e.g.*, Lowerre-Barbieri *et al.*, 1994). Our results may also differ by mere chance from

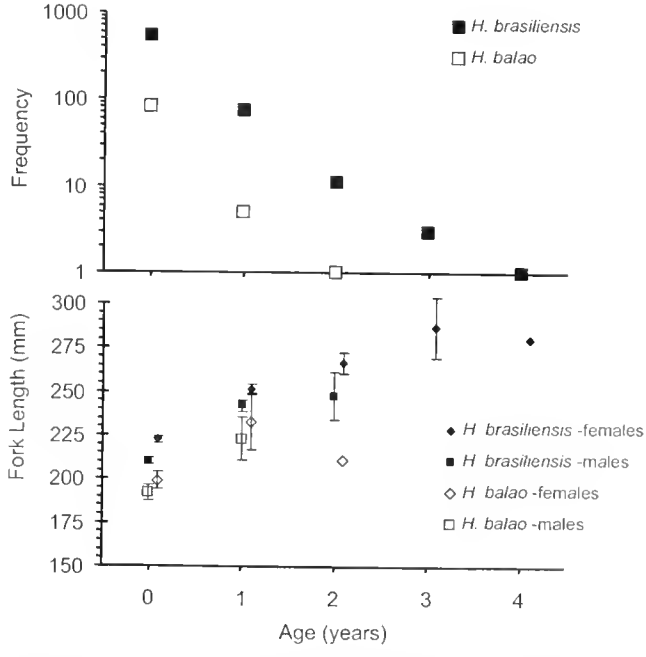

Figure 3. Number of *Hemiramphus brasiliensis* (ballyhoo) and *H. balao* (balao), collected by age class (upper panel) and the sizes of each age class, by species and sex (lower panel; mean ± 95% confidence limits).

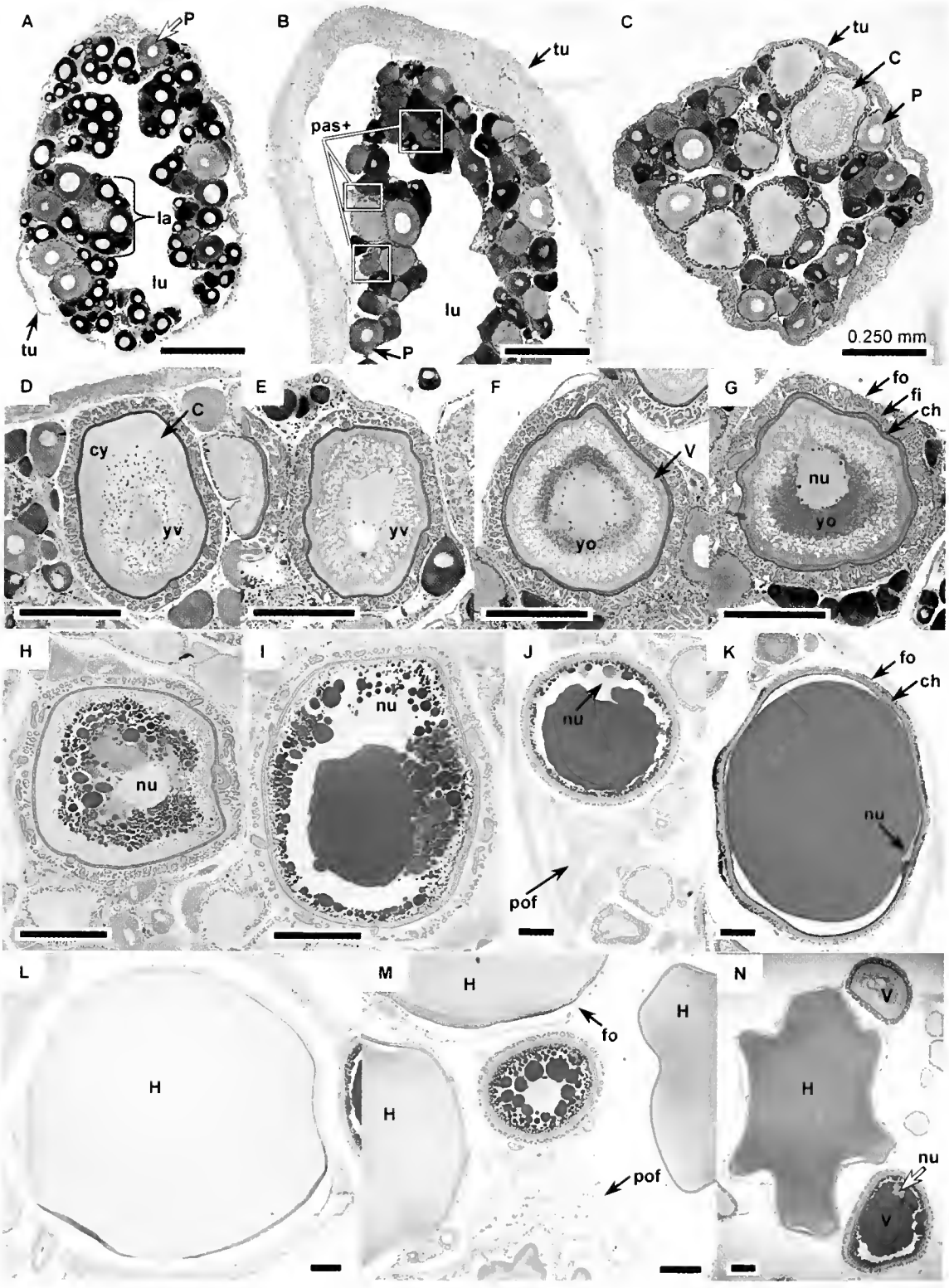

Figure 4. Histological features of ovarian and oocyte development for *Hemiramphus brasiliensis* (ballyhoo). (A) whole cross section from a virgin, immature female; (B) partial cross section from a regressed, mature female; (C) whole cross section from a virgin, maturing female; (D) enlargement of detail of a late-stage "yolk vesicle" oocyte with cortical alveoli; (E) an even later-stage "yolk vesicle" oocyte; (F) a very early-stage "yolked" or vitellogenic oocyte; (G) a slightly more advanced vitellogenic oocyte; (H) a vitellogenic oocyte with yolk globules (probably a cell undergoing nucleus migration); (I) a vitellogenic oocyte with a migrating nucleus,

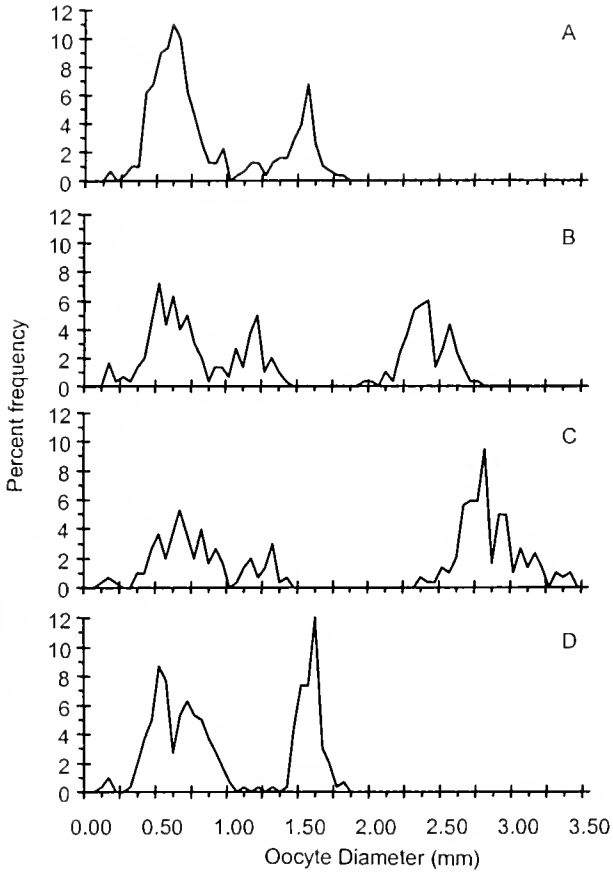

Figure 5. Oocyte diameter frequencies for *Hemiramphus brasiliensis* (ballyhoo) (A-C) and *H. balao* (balao) (D), in the final stages of oocyte maturation. The largest mode in each figure represents a developing batch of oocytes in final oocyte maturation, whereas the smallest mode represents a reservoir of primary growth oocytes and vitellogenic oocytes prior to nucleus migration. A third, middle mode of oocytes represents a batch of oocytes just entering final oocyte maturation. Measurements were made from (A) a mature *H. brasiliensis* whose most advanced oocyte stage was nucleus migration, (B) a hydrated *H. brasiliensis* whose most advanced oocyte stage was nucleus breakdown, (C) a spawning *H. brasiliensis* with ovulated eggs, (D) a hydrated *H. balao* whose most advanced oocyte stage was nucleus breakdown. At least 300 oocytes were measured per female.

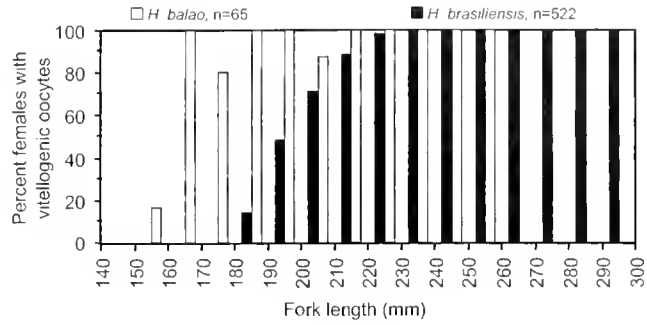

Figure 6. Percent frequency of mature (vitellogenic) female *Hemiramphus brasiliensis* (ballyhoo) and *H. balao* (balao). Values are calculated by fork length intervals of 10 mm from fish collected during the peak spawning season (March-August). *n* = number of fish.

those of Berkeley and Houde; for *H. brasiliensis* we found only three age-3 individuals and one age-4; for *H. balao* we found only a single age-2 individual. Sample sizes in both studies were larger for *H. brasiliensis* because this species is more commonly caught and is found in a wider range of habitats than *H. balao* (McBride *et al.*, 2003). At least one other hemiramphid, *Reporhamphus melanochir*, lives longer and grows larger (7 years, 380-mm FL; Ling, 1958). So even among hemiramphids, *H. brasiliensis* and *H. balao* are short-lived and grow to only modest lengths.

Sizes of age-1 fish (mean = 248-mm FL for *H. brasiliensis* and 226-mm FL for *H. balao*) were significantly different for the two species and were generally larger than previously reported. Berkeley and Houde (1978) reported that size at age-1 can vary between years for *H. brasiliensis* (1974 = 216-mm FL, 1975 = 230-mm FL) and that at age-1, *H. balao* was smaller (209-mm FL) than *H. brasiliensis*. The sizes of both species overlapped (McBride *et al.*, 1996), and the mean sizes may vary from year to year naturally. Efforts to estimate the growth rates by nonlinear models failed because the short life spans of both species made it impossible to reasonably fit a growth model to the data. *H. brasiliensis*, however, spawns about 2 months earlier than *H. balao* (*i.e.*, April *versus* June modes), so their growth rates may be fairly similar on a daily or monthly basis. We also found, as did Berkeley and Houde (1978), that females were longer than males at a common age.

Survival rates differed between the two species. In our study, *H. brasiliensis* had a higher annual survival rate than *H. balao* did: 14.9% and 7.5%, respectively. We found the

indicating the beginning of final oocyte maturation; (J) a vitellogenic oocyte with a migrating nucleus next to a fresh postovulatory follicle (POF); (K) a late-stage vitellogenic oocyte with the nucleus positioned against the chorion; (L) a fully hydrated oocyte after nucleus breakdown; (M) three hydrated oocytes, one without a follicle and adjacent to a fresh POF; and (N) juxtaposition of a vitellogenic oocyte prior to nucleus migration, a vitellogenic oocyte undergoing nucleus migration, and a hydrated oocyte following nucleus breakdown. The major stages of oocyte development are indicated by capitalized letters: Perinucleolar (P), cortical alveolar (C) (=yolk vesicle), vitellogenic (V) (=yolked), hydrated (H). Other features include the chorion (ch), cytoplasm (cy), fibrils (fi), follicle (fo), lamellae (la), lumen (lu), nucleus (nu), periodic acid-Schiff reaction-positive (pas+) melano-macrophage centers, post-ovulatory follicle (pof), tunic (tu) (=gonad wall), yolk formation (yo), and yolk vesicles (yv). All scale bars, 0.250 mm.

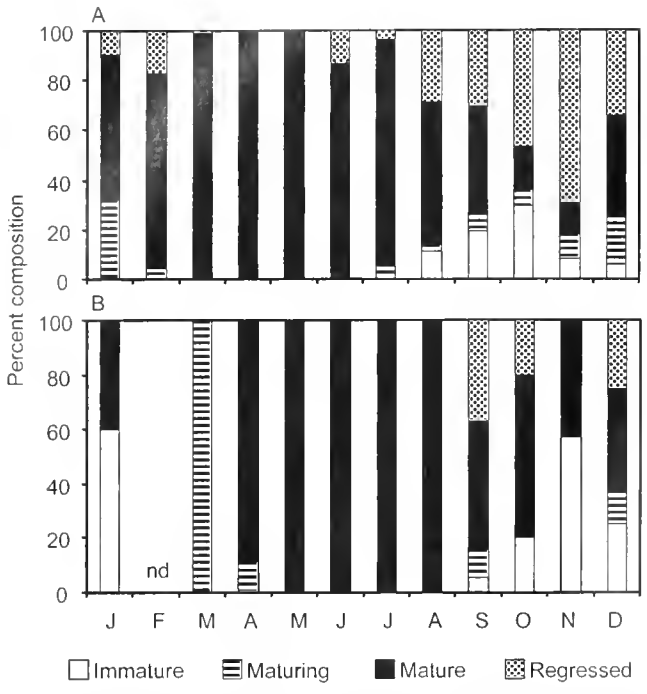

Figure 7. Seasonal reproductive cycles of (A) female *Hemiramphus brasiliensis* (ballyhoo) and (B) female *H. balao*, (balao) based on histological criteria for fish collected from July 1997 to October 1998. Values were calculated from mature fish sizes only (fork length ≥ 198 mm for *H. brasiliensis* and ≥160 mm for *H. balao*). Nd = no data.

same pattern when we calculated survival rates using data from Berkeley and Houde (1978), the only previous study available: estimates of *H. brasiliensis* survival varied between the collection years (1974 = 23.8%, 1975 = 17.3%); these values were higher than that for *H. balao* (1974 = 12.4%). Even if the use of scales by Berkeley and Houde resulted in truncated ages (not identifying fish older than age-2), the number of fish aged was so large that the estimates of survival should not have been biased (Murphy, 1997). The more likely cause of the interannual variation is that survival rates may have declined since the mid-1970s or that violations of steady-state assumptions (variable recruitment of age-0 fish) may have biased the estimates of annual survival as calculated here.

The macroscopic appearance and development of *Hemiramphus* species gonads were similar to those of *Hyporhamphus (Reporhamphus) melanochir* (Ling, 1958). The group-synchronous nature of oocyte development and large egg sizes have been noted for other hemiramphids (Ling, 1958; Talwar, 1967). The pattern of final oocyte maturation follows the diel cycle, and both species spawn at dusk (McBride *et al.*, 2003). At sunset, the modal diameter of ovulated *H. brasiliensis* eggs was 2.8 mm. Berkeley and Houde (1978) illustrated an *H. brasiliensis* embryo that was about 2.5 mm in diameter and a near-hydrated oocyte that was 2.2 mm. The modal size of hydrated *H. balao* oocytes (1.6 mm) was also very close to the size of the *H. balao* egg (1.5 mm) illustrated by Rass (1972). These independent descriptions and illustrations of mature oocytes and eggs confirm that interspecific differences in egg sizes exist for these two congeners.

Sizes at maturity for both species were smaller than sizes attained by the first winter, and we agree with Berkeley and Houde (1978) that both species mature in their first year. In our study, the size at 50% maturity was 63.3% of the maximum body size for *H. brasiliensis* (313 mm FL) and 58.6% for *H. balao* (273 mm FL; McBride *et al.*, 1996). To our knowledge, no study of hemiramphids has determined size at maturity with the precision that we achieved here, but other studies have reported the size of the smallest females with hydrated oocytes. Size at maturity in these other species is 56.8% maximum body length for *Hyporhamphus melanochir* (Ling, 1958), 58.2% for *Hemiramphus limbatus* (Silva and Davies, 1988), and 58.0% for *Zenarchopterus kampeni* (Coates and Van Zwieten, 1992). Size at maturity is very close to 60% maximum body size for a number of hemiramphids, and this percentage value may be useful for predicting the size at maturity of hemiramphid that have not been studied.

Both *H. brasiliensis* and *H. balao* spawn frequently, even daily, for at least a few months of the year. Although a

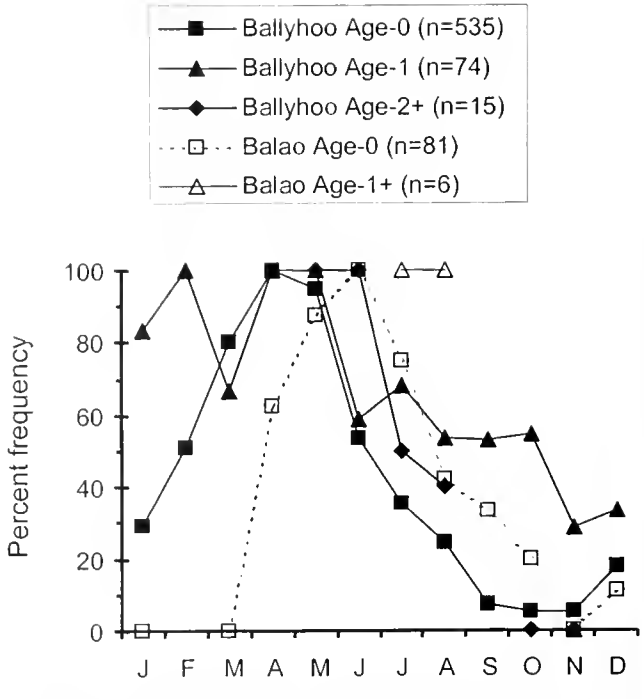

Figure 8. Average spawning frequency for *Hemiramphus brasiliensis* (ballyhoo), and *H. balao* (balao), by age class. Spawning frequency is based on the percent frequency of females with fresh postovulatory follicles (POFs). A value of 100% means that all females in a particular age class were spawning every day of that month. *n* = number of fish.

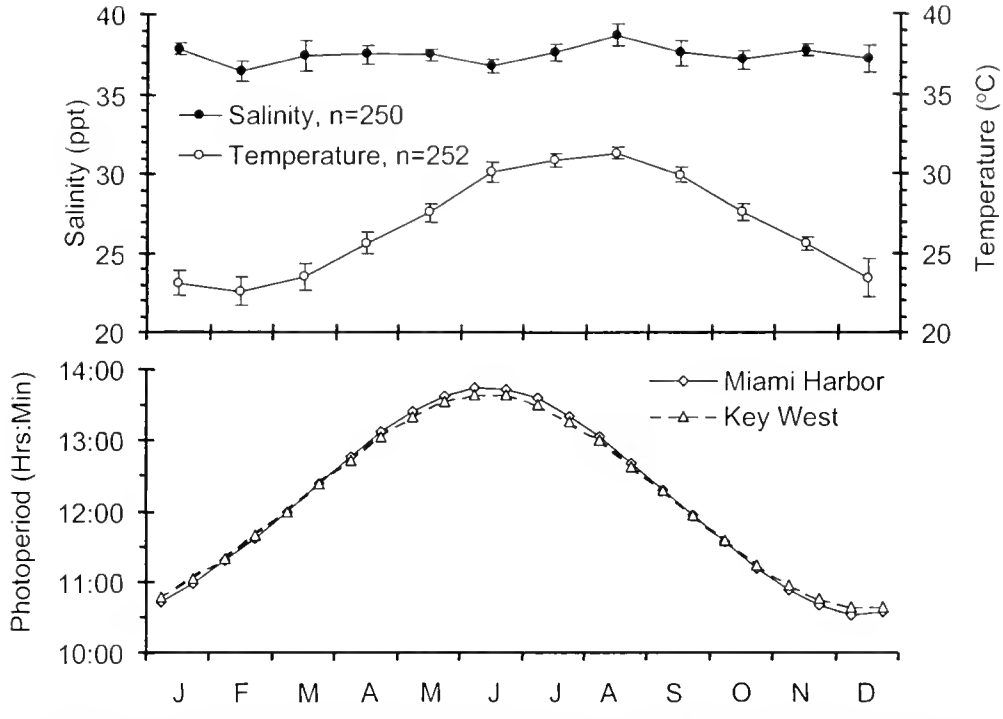

Figure 9. Monthly average salinity and temperature (upper panel) measured at the sea surface at the time of fish collection. Error bars are 95% confidence limits. Seasonal change in photoperiod for Miami Harbor entrance and Key West (lower panel; data source: National Oceanic and Atmospheric Administration Tide Tables).

prolonged reproductive season has been noted for other hemiramphids (Ling, 1958; Coates and Van Zwieten, 1992), this study provides the first conclusive evidence of multiple spawning within a year for any hemiramphid. Moreover, our age-specific analysis demonstrates that older fish spawn more frequently and for longer periods than age-0 fish do. In

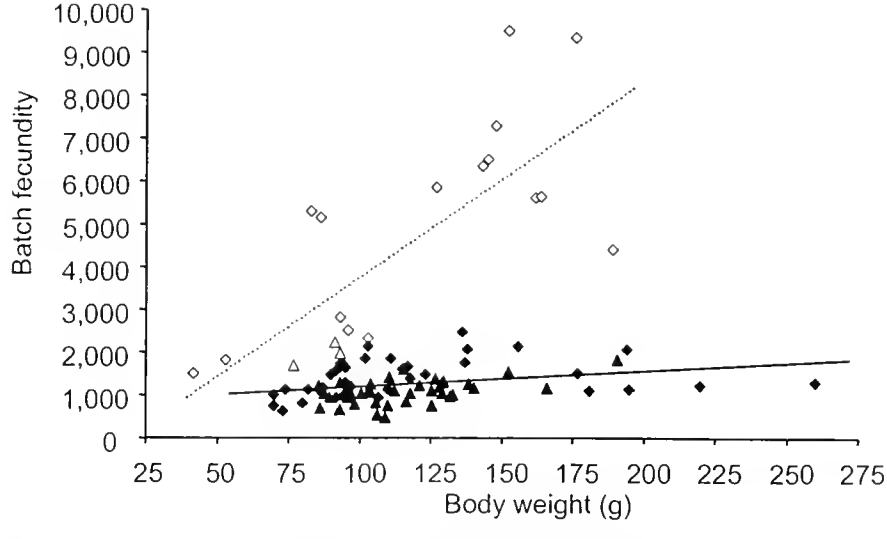

Figure 10. Batch fecundity for female *Hemiramphus brasiliensis* (ballyhoo) (filled symbols) and *H. balao* (balao) (open symbols), as related to fish size. Data from Berkeley and Houde (1978) are included (diamond symbols), together with data from this study (triangles), to show overlap of values and to increase sample size. Batch fecundity for *H. brasiliensis* was not significantly correlated with fish size ($Y = 790.57 + [3.7411^*X]$, $r^2 = 0.11$, $n = 74$), but batch fecundity for *H. balao* was significantly correlated with fish size ($Y = 858.79 + [46.024^*X]$, $r^2 = 0.56$, $n = 20$).

Table 2

A matrix approach to estimate the expected lifetime fecundity of two species of Hemiramphus *as the average number of eggs produced in the next generation by each female in the present generation*

Species	x (years)	l_x	d_x	f_x	w_x	m_x	$l_x m_x$
H. brasiliensis							
	0	1.00000	151	1117.3	87.3	168,719	168,719
	1	0.14870	240	1264.6	126.7	303,507	45,133
	2	0.02211	240	1353.2	150.4	324,757	7,181
	3	0.00329	240	1493.4	187.9	358,419	1,179
	4	0.00049	240	1445.0	174.9	346,809	170
						$\Sigma l_x m_x$ =	222,381
H. balao							
	0	1.00000	129	2124.91	64.8	274,114	274,114
	1	0.07527	240	4226.33	110.5	1,014,319	76,347
	2	0.00567	240	2787.75	79.2	669,060	3,791
						$\Sigma l_x m_x$ =	354,251

Variables are calculated by age classes in years (x). Survival by age class (l_x) was determined by the results of the Robson-Chapman survival estimate (see text for details). The number of days spawning by age class (d_x) was generalized from Figure 8. The batch fecundity by the average size female in each age class (f_x) was estimated from Figure 10, and the average weight of females in each age class (w_x) was calculated from length-weight relationships (McBride, unpubl.). Annual fecundity by age class (m_x) is the product of the spawning frequency (d_x) and batch fecundity (f_x), and the expected reproductive output ($l_x m_x$) is the expected contribution of eggs produced by each age class after accounting for survival.

fact, histological examination shows that some spawning by *H. brasiliensis* occurred year-round.

Altogether, our data demonstrate that *H. balao* is a smaller, shorter-lived fish than *H. brasiliensis*, but it matures at a smaller size and produces more, albeit smaller, eggs per batch. Morphological constraints of body size probably lead to this inverse relationship between size and number of eggs produced per spawning event (Elgar, 1990), and the larger batch size of *H. balao* is consistent with the life-history theory that predicts larger batch size for shorter-lived species (Stearns, 1976). *H. balao* is also more common offshore of the reef tract, where food may be patchier than it is inshore; and various models predict that this would select for more numerous but smaller eggs (Wootton, 1994). Ultimately, the life-history traits that typically represent trade-offs in evolutionary terms (*i.e.*, survival and growth rates, age-specific spawning frequency, size-specific batch fecundity) are balanced so that the lifetime egg production of both *Hemiramphus* species is the same order of magnitude; Table 2).

Certainly the environment is shaping some elements of the reproductive traits of these *Hemiramphus* species, but the influence of their phylogenetic history is clearly evident. Although *Hemiramphus* species are not structure-oriented, they are associated with coral reef habitat and thus are exposed to environmental cues similar to those encountered by coral reef fish. (*e.g.*, warm temperature, high salinity, open coastal hydrodynamics, and tropical weather disturbances). However, compared to most marine teleosts, and particularly other coral reef fishes, *H. brasiliensis* and *H. balao* both have very large eggs, high spawning frequencies, and low batch fecundities (*e.g.*, Thresher, 1984; Gross, 1987). Their reproductive style is typical of the order Beloniformes, with its large eggs, low fecundity, multiple spawning events, and embryos that attach to floating vegetation (Berkeley and Houde, 1978; Collette *et al.*, 1984). In fact, Hemiramphidae is a particularly interesting family to study while exploring trade-offs in reproductive traits because there is remarkable variation in the egg size, fecundity, and reproductive mode of its species. For example, the diameters of hemiramphid eggs range from 1.3 to 3.5 mm, and reproductive modes include producing demersal eggs, buoyant pelagic eggs, or precocious young (Wourms, 1981; Collette *et al.*, 1984; Meisner and Burns, 1997).

Although many of the life-history traits of *H. brasiliensis* and *H. balao* are not shared by other coral reef fishes that have similar habitats, the annual fecundities of these two species might well be in line with those of other coral reef fishes. To illustrate this point, annual individual fecundities of *H. brasiliensis* and *H. balao* range from 169,000 to 1,014,000 eggs per year (Table 2), and these estimates are within the range of annual fecundity for a relatively small lutjanid, *Rhomboplites aurorubens* (140,000–3,000,000 eggs; Cuellar *et al.*, 1996). Although the maximum fecundity of *R. aurorubens* is considerably higher than that estimated for halfbeaks, *R. aurorubens* spawns at larger sizes than the two *Hemiramphus* species do (approx. range: 100–700 g; Cuellar *et al.*, 1996).

We conclude that once adjustments are made for their size, *H. brasiliensis* and *H. balao* do not have low annual or lifetime fecundities, when compared either to other hemiramphids or to other coral reef fishes. This descriptive study of hemiramphid life-history patterns suggests that consideration of atypical but reef-associated species, such as half-

beaks, in future ecological and evolutionary analyses can improve our understanding of adaptation and community dynamics of coastal fishes. Moreover, the special traits in the early life history of *H. brasiliensis* and *H. balao*, such as large eggs that are attached to floating vegetation near the surface, should be considered in the development of larval dispersal models so that the variable responses of fishes to environmental and anthropogenic processes can be more completely understood (*e.g.*, Roberts, 1997; Cowen *et al.*, 2000).

Acknowledgments

We are grateful to the fishers of the south Florida lampara net fishery and others who assisted in this study. D. Snodgrass and J. Styer assisted in collecting supplemental fish. J. Hunt and T. Matthews provided logistical support in Marathon. H. Patterson, F. Stengard, C. Stevens, and the FMRI Histology team assisted in the laboratory. R. E. Matheson and S. Lowerre-Barbieri contributed comments that improved the manuscript, and J. Leiby and J. Quinn provided editorial assistance. This research was funded in part by a grant from the National Oceanic and Atmospheric Administration to the Florida Fish and Wildlife Conservation Commission (Saltonstall-Kennedy Program, NOAA Award No. NA77FD0069). The views expressed herein are those of the authors and do not necessarily reflect the views of NOAA or any of its subagencies.

Literature Cited

Berkeley, S. A., and E. D. Houde. 1978. Biology of two exploited species of halfbeaks, *Hemiramphus brasiliensis* and *H. balao* from southeast Florida. *Bull. Mar. Sci.* **28:** 624–644.

Coates, D., and P.A.M. Van Zwieten. 1992. Biology of the freshwater halfbeak *Zenarchopterus kampeni* (Teleostei: Hemiramphidae) from the Sepik and Ramu River basin, northern Papua New Guinea. *Ichthyol. Explor. Freshw.* **3:** 25–36.

Collette, B. B. 1965. Hemiramphidae (Pisces, Synentognathi) from tropical west Africa. *Atl. Rep.* **8:** 217–235.

Collette, B. B., G. E. McGowen, N. V. Parin, and S. Mito. 1984. Beloniformes: development and relationships. Pp. 335–354 in *Ontogeny and Systematics of Fishes*. American Society of Ichthyologists and Herpetologists, Spec. Publ. No. 1, Allen Press, Lawrence, KS.

Cowen, R. K., L. M. M. Lwiza, S. Sponaugle, C. B. Paris, and D. B. Olson. 2000. Connectivity of marine populations: open or closed? *Science* **287:** 857–859.

Cuellar, N., G. R. Sedberry, and D. M. Wyanski. 1996. Reproductive seasonality, maturation, fecundity, and spawning frequency of the vermilion snapper, *Rhomboplites aurorubens*, off the southeastern United States. *Fish. Bull. (US)* **94:** 635–653.

Elgar, M. A. 1990. Evolutionary compromise between a few large and many small eggs: comparative evidence in teleost fish. *Oikos* **59:** 283–287.

Grier, H. J., and R. G. Taylor. 1998. Testicular maturation and regression in the common snook. *J. Fish Biol.* **53:** 521–542.

Gross, M. R. 1987. Evolution of diadromy in fishes. *Am. Fish. Soc. Symp.* **1:** 14–25.

Hunter, J. R., and B. J. Macewicz. 1985. Measurement of spawning frequency in multiple spawning fishes. Pp. 79–94 in *An Egg Production Method for Estimating Spawning Biomass of Pelagic Fish: Application to the Northern Anchovy*, Engraulis mordax, R. Lasker, ed. NOAA Tech. Rep. NMFS 36. U.S. Dept. Commerce, Washington, DC.

Hunter, J. R., N. C. H. Lo, and R. J. H. Leong. 1985. Batch fecundity in multiple spawning fishes. Pp. 67–78 in *An Egg Production Method for Estimating Spawning Biomass of Pelagic Fish: Application to the Northern Anchovy*, Engraulis mordax, R. Lasker, ed. NOAA Tech. Rep. NMFS 36. U.S. Dept. Commerce, Washington, DC.

Ling, J. K. 1958. The sea garfish, *Reporhamphus melanochir* (Cuvier & Valenciennes) (Hemiramphidae), in South Australia: breeding, age determination, and growth rate. *Aust. J. Mar. Freshw. Res.* **9:** 60–110.

Lowerre-Barbieri, S. K., M. E. Chittenden, Jr., and C. M. Jones. 1994. A comparison of a validated otolith method to age weakfish, *Cynoscion regalis*, with the traditional scale method. *Fish. Bull. (US)* **92:** 555–568.

McBride, R. S., L. Foushee, and B. Mahmoudi. 1996. Florida's halfbeak, *Hemiramphus* spp., bait fishery. *Mar. Fish. Rev.* **58:** 29–38.

McBride, R. S., F. Stengard, and B. Mahmoudi. 2002. Maturation and diel reproductive periodicity of round scad (Carangidae: *Decapterus punctatus*). *Mar. Biol.* **140:** 713–722.

McBride, R. S., J. Styer, and R. Hudson. 2003. Spawning cycles and habitats for ballyhoo and balao (Hemiramphidae: *Hemiramphus*) in South Florida. *Fish. Bull. (US)* **101**(3) (in press).

Meisner, A. D., and J. R. Burns. 1997. Viviparity in the halfbeak genera *Dermogenys* and *Nomorhamphus* (Teleostei: Hemiramphidae). *J. Morphol.* **234:** 295–317.

Murphy, M. D. 1997. Bias in Chapman-Robson and least-squares estimators of mortality rates for steady-state populations. *Fish. Bull. (US)* **95:** 863–868.

Nybakken, J. W. 1997. *Marine Biology: an Ecological Approach*, 4th ed. Addison Wesley Longman, Menlo Park, CA. 481 pp.

Partridge, L., and P. H. Harvey. 1998. The ecological context of life history evolution. *Science* **241:** 1449–1455.

Quintero-Hunter, I., H. Grier, and M. Muscato. 1991. Enhancement of histological detail using metanil yellow as counterstain in periodic acid Schiff's hemotoxylin staining of glycol methacrylate tissue sections. *Biotech. Histochem.* **66:** 169–172.

Rass, T. S. 1972. On the occurrence of ichthyoplankton in Cuban waters: pelagic eggs. *Tr. Inst. Okeanol. Akad. Nauk. SSSR* **93:** 5–41. (In Russian).

Roberts, C. M. 1997. Connectivity and management of Caribbean coral reefs. *Science* **278:** 1454–1457.

Robson, D. S., and D. G. Chapman. 1961. Catch curves and mortality rates. *Trans. Am. Fish. Soc.* **90:** 181–189.

SAS Institute Inc. 1990. *SAS/STAT User's Guide*, Vols. I and II. SAS Institute, Cary, NC. 1686 pp.

Silva, E. I. L., and R. W. Davies. 1988. Notes on the biology of *Hemiramphus limbatus* (Hemiramphidae: Pisces) in Sri Lanka. *Trop. Freshw. Biol.* **1:** 42–49.

Stearns, S. C. 1976. Life-history tactics: a review of the ideas. *Q. Rev. Biol.* **51:** 3–47.

Talwar, P. K. 1962. A contribution to the biology of the halfbeak, *Hyporhamphus georgii* (Cuv. & Val.) (Hemirhamphidae). *Indian J. Fish.* **9:** 168–196.

Talwar, P. K. 1967. Studies on the biology of *Hemirhamphus marginatus* (Forskal) (Hemirhamphidae-Pisces). *J. Mar. Biol. Assoc. India* **9:** 61–69.

Thresher, R. E. 1984. Patterns in the reproduction of reef fishes. Pp. 343–388 in *Reproduction in Reef Fishes*, T.F.H. Publications, Neptune, NJ.

Wallace, R., and K. Selman. 1978. Oogenesis in *Fundulus heteroclitus*. *Dev. Biol.* **62:** 354–369.

Wootton, R. J. 1994. Life histories as sampling devices: optimum egg size in pelagic fishes. *J. Fish Biol.* **45:** 1067–1077.

Wourms, J. P. 1981. Viviparity: the maternal-fetal relationship in fishes. *Am. Zool.* **21:** 473–515.

Reference: *Biol. Bull.* **204:** 68–80. (February 2003)

Collection and Culture Techniques for Gelatinous Zooplankton

KEVIN A. RASKOFF[1,*], FREYA A. SOMMER[2], WILLIAM M. HAMNER[3], AND KATRINA M. CROSS[4]

[1] *Monterey Bay Aquarium Research Institute, Moss Landing, California 95039-9644;* [2] *Hopkins Marine Station, Pacific Grove, California 93950-3094;* [3] *University of California, Los Angeles, California 90095-1606; and* [4] *Monterey Bay Aquarium, Monterey, California 93940-1085*

Abstract. Gelatinous zooplankton are the least understood of all planktonic animal groups. This is partly due to their fragility, which typically precludes the capture of intact specimens with nets or trawls. Specialized tools and techniques have been developed that allow researchers and aquarists to collect intact gelatinous animals at sea and to maintain many of these alive in the laboratory. This paper summarizes the scientific literature on the capture, collection, and culture of gelatinous zooplankton and incorporates many unpublished methods developed at the Monterey Bay Aquarium in the past 15 years.

Introduction

Gelatinous zooplankton is a generic term for transparent and delicate planktonic animals with mesoglea-like internal tissues that aid in regulating buoyancy. These animals include some radiolarians and foraminifera, as well as medusae, siphonophores, ctenophores, chaetognaths, pteropods, heteropods, appendicularians, salps, doliolids, and pyrosomes (*e.g.*, Hamner *et al.*, 1975). These taxonomic groups are widely distributed in large numbers in all the world's oceans, throughout the water column. They are the least understood of all planktonic animal groups. This is partly due to their fragility, which typically precludes the capture of intact specimens with nets or trawls. In fact, many systematic descriptions of hydromedusae and siphonophores during the past 200 years were based only on fragments of animals (*e.g.*, Mayer, 1910; Russell, 1953). Fortunately, during the past 30 years, specialized tools and techniques have been developed that permit researchers and aquarists to collect intact gelatinous animals at sea and to maintain many of these alive in the laboratory. These new methods and technologies have allowed scientists to resolve the life cycles of many organisms whose hydroid and hydromedusa stages were previously thought to be separate species, and to conduct a variety of experimental studies in the laboratory. In addition, aquarists are now able to rear and display many species of medusae and ctenophores for the first time in public aquariums. Paffenhöfer and Harris (1979) and Strathmann (1987) provide good reviews of many gelatinous zooplankton culture studies, as well as a detailed review of culture methods for non-gelatinous organisms. The general lack of information about gelatinous zooplankton is due not only to their extreme fragility, but also to a shift of emphasis in the discipline of biological oceanography that occurred more than 100 years ago. The change led from a qualitative interest in the systematics and developmental biology of all zooplankton, to the present quantitative concern for the fisheries implications of certain components of the zooplankton as they relate to cycles of energy and material in the sea.

This dramatic shift of emphasis was advocated by Victor Hensen (1887). Ernst Haeckel and others used fine-meshed plankton nets towed slowly at the surface from small boats, or they carefully dipped individual animals from the sea surface by hand. In contrast, Hensen (1887) used large, vertically hauled plankton nets from large ships to collect fish eggs and copepods. This procedure produced quantitative information on the distribution and abundance of fish eggs, copepods, and larval forms, but it seriously undersampled and physically damaged the gelatinous fauna. Even though Haeckel believed that Hensen's approach to oceanic

Received 24 April 2002; accepted 6 November 2002.

* To whom correspondence should be addressed. E-mail: kraskoff@mbari.org

biology was flawed. Hensen's attempt to quantify planktonic ecology has prevailed, and the most recent manual on zooplankton methodology (Harris *et al.*, 2000) is still primarily concerned with crustaceans and fish eggs.

Throughout the first half of the 20th century, systematists continued to collect individual gelatinous animals (*e.g.*, Kramp, 1965), but interest in the developmental biology of these animals diminished as Haeckel's ideas about phylogenetic recapitulation through ontogeny lost favor. In the 1950s, neurophysiologists such as Pantin (1952), Bullock (1943), and Mackie (1960) began to investigate the neurology of the so-called lower invertebrates (anemones, medusae, siphonophores, flatworms, and ctenophores), an effort that required that these animals be collected carefully at sea and also maintained alive, if only briefly, in the laboratory.

The first use of scuba to collect or view planktonic animals at sea was in the 1960s by divers who collected siphonophores in the Mediterranean (frontispiece in Totton, 1965) and by Ragulin (1969), who first viewed krill underwater in the Antarctic. Soon thereafter, use of scuba to investigate oceanic gelatinous animals became routine in the epipelagic blue waters of the Gulf Stream (*e.g.*, Gilmer, 1972; Hamner *et al.*, 1975). Research submersibles in midwater extended these *in situ* observations of gelatinous plankton from the upper 30 m of the sea to thousands of meters below the surface (*e.g.*, Larson *et al.*, 1992; Robison *et al.*, 1998; Raskoff, 2001, 2002).

In situ observations of epipelagic and midwater animals stimulated a revival of attention to all aspects of the living biology of gelatinous zooplankton. We know today that gelatinous animals are an important component of marine ecosystems, with particular significance for fisheries management (*e.g.*, Purcell, 1997; Purcell and Arai, 2001), an issue anticipated by Haeckel (1893). We now know that gelatinous organisms are often the dominant macrozooplankton of oceanic ecosystems (*e.g.*, Robison *et al.*, 1998). Recent studies with *in situ* techniques have shown that scyphomedusae, hydromedusae, siphonophores, and ctenophores are abundant, often quite large, and apt to play disproportionately important roles as top predators in their food webs (see Mills, 2001; Purcell *et al.*, 2001). Yet these animals continue to be neglected in many syntheses of biological oceanography.

Our ignorance of gelatinous plankton biology is thus partly due to the history of oceanography, partly to inadequate collection and observational technologies, and partly to the fragility of many gelatinous taxa. Although it is now possible to capture most species of gelatinous animals in good condition, it is still difficult or impossible to keep many of these taxa alive in laboratory aquaria for observation and experimentation. This paper summarizes the scientific literature on the culture of gelatinous zooplankton and incorporates many unpublished culturing and displaying techniques developed at the Monterey Bay Aquarium during the past 15 years.

Methods

Collection

The primary goal of all collection methods for gelatinous zooplankton is to minimize handling and damage.

Surface collection. Many common species can be collected easily from surface waters by using a small boat or while snorkeling. Ocean slicks, glassy patches on the ocean's surface caused by a combination of wind and current (Haeckel's "animal roads"), are excellent sources of epipelagic species (Alldredge and Hamner, 1980; Hamner and Schneider, 1986; Larson, 1991). Smooth-rimmed glass beakers and glass jars (perhaps attached to the end of a pole) are good collecting containers, since most cnidarian tentacles do not adhere to glass as readily as to plastic. Larger specimens can be collected in plastic buckets or in plastic bags. Some hardy species can be collected with dip nets or small plankton nets. The smaller the mesh size the better, as larger meshes can cut into the soft gelatinous tissue. Knotless mesh of broad, flat strands of soft material in the shape of a gusseted bag is the most effective type of hand-held dip net. It is important not only to minimize the stress and disturbance to the animal, but also to avoid introducing air bubbles into the body cavity; air bubbles are exceptionally difficult to remove, and if left within the animal either produce tissue embolisms or cause the animal to rise to the surface, where exposure to air can damage it further.

Subsurface collection. Although many specimens can be collected in good condition at or just under the surface, others may already be damaged, particularly those garnered from surface convergences crowded with flotsam. Furthermore, for the vast array of species not routinely found at the air-water interface, collectors may need to employ other methods. Use of scuba is one possibility. When working in the disorienting, featureless, blue-water environment of the open sea, protocols for diving-safety must be followed (see Hamner, 1975; Heine, 1986). Divers who are even slightly negatively buoyant can easily sink below safe depths. Also, divers who are not connected to one another and to the support boat often come to the surface away from the boat, where they can be difficult to see in a choppy sea. However, blue-water diving techniques, properly executed, provide a safe and effective way to collect specimens and to observe the behavior of undisturbed animals in their natural habitat. Many ethological discoveries in the last 20 years have been made using these techniques (*e.g.*, Madin, 1974; Hamner, 1985; Matsumoto and Harbison, 1993).

For collection of specimens deeper than the limits of safe scuba diving, or when diving conditions are not optimum, various nets have been deployed successfully from the surface. Midwater trawls, bottom trawls, and plankton nets

can all be effective in capturing delicate living specimens (Sameoto *et al.*, 2000) if the nets are pulled slowly (<1.0 km h^{-1}) for a relatively short time, and if the cod end of the net is large and without side windows, which generate turbulence in the collecting well (Baker, 1963; Reeve, 1981; Childress and Thuesen, 1993). Thermally insulated cod ends have also proved very successful in the capture of gelatinous organisms in good physiological condition (Childress *et al.*, 1978; Thuesen and Childress, 1994). The use of research submersibles and remotely operated vehicles (ROVs) has permitted gelatinous species to be collected from meso- and bathypelagic depths when the use of nets is not an option (Youngbluth, 1984; Robison, 1993). These vehicles may be equipped with large collection cylinders open at both ends, permitting the vehicle pilot to slide the collecting container over a gelatinous animal by maneuvering the entire vehicle and then gently closing the ends of the sampler. Some species are so delicate that they have never survived even these samplers: descriptions of several deep-sea species, such as *Kiyohimea usagi* (Matsumoto and Robison, 1992) and *Lampocteis cruentiventer* (Harbison *et al.*, 2001), were based on *in situ* observations and photography.

Transport of specimens

Once collected, specimens can be safely transported to the rearing facility either in their collection containers or in larger jars or tubs. If the animals are transferred to a larger container, it is important to minimize their exposure to air and to avoid pouring them roughly from one container to the other. Each animal must be dipped gently out of the collecting container with a transfer jar, which is then emptied by tipping it below the surface of the water in the transport container. Several devices have been designed for the transfer of individual gelatinous zooplankton (Acuña *et al.*, 1994; Sato *et al.*, 1999). The water in the transport containers should be free of bubbles and have the same temperature and salinity as the water in the collecting vessel; if not, small volumes of water should be exchanged between them slowly, over the course of perhaps an hour, to permit temperature and osmotic adjustment by the animals. Transport vessels can then be put into an insulated box or cooler with cold or hot packs as needed for the duration of the trip. The water can be saturated with oxygen before transport, but this is more crucial for large animals, those being shipped in warm water, or those kept in the shipping container for a long time. All air must be removed from the container before sealing because even small air bubbles can damage gelatinous specimens. With an appropriately low ratio of biomass to volume of water (<1:2), the animals often survive trips of 18 h or more. For small medusae and polyp cultures, air-permeable plastic fish bags are very effective.

Culture

Once organisms have been collected, cultures can be started in a number of ways. The most common method is to facilitate natural spawning by grouping both sexes together in a small controlled space. Spawning can often be induced by crowding (some scyphozoans), by leaving animals in the dark for several hours followed by periods of light (some hydrozoans), or by simply permitting the temperature of the water to slowly rise over several hours (see Mills and Strathmann, 1987). In some cnidarian genera, such as *Aurelia*, females brood their planulae on their oral arms. It is often sufficient to place the brooding female in a small volume of seawater and wait for a few hours for the planulae to be released. Alternatively, larvae may be removed from the edges of the oral arms with a pipette. A more labor intensive spawning technique involves *in vitro* fertilization. For this procedure, gonadal tissue from both males and females are incubated together in a small volume of water for several hours until the eggs are fertilized and larvae begin to develop. The sexing of zooplankton can be difficult, but the eggs can often be seen inside the female reproductive tissue. The most accurate way to determine the sex of the specimens is to remove a small piece of the gonad and examine the tissue under a compound or dissecting microscope to look for sperm and eggs. This will also help determine if the specimen is mature.

After a spawning event, it is necessary to examine the water for larvae or fertilized eggs. Collection and handling techniques for many larval taxa are summarized in Strathmann (1987). Planulae range in length from 100 to 1000 μm in hydrozoans, range from 100 to 400 μm in scyphozoans, and up to 160 μm in cubozoans (Martin and Koss, 2002). Ctenophore larvae range in length from 280 to 1000 μm (Baker and Reeve, 1974; F. Sommer, unpubl. data).

Cnidarian planulae will typically settle and attach to the substrate within a few days, often within hours if a suitable substrate is available. Planulae will settle on many types of substrate (Brewer, 1984). Glass or plastic microscope slides or cover slips are often used due to the ease of post-settlement manipulation. Some species may preferentially settle on substrates that have been "conditioned" by several days' immersion in seawater to accumulate a light microbial film (Brewer, 1984; Schmahl, 1985). Several chemicals (TPA, DAG, Cs^+, Li^+, NH_4^+) have been shown to positively affect larval settlement (Siefker *et al.*, 2000). Larvae typically settle to the bottom of the chamber and often are thigmotactic, tending to settle at the edges (Brewer, 1976; Orlov, 1996). Some species (*Aurelia aurita, Cyanea capillata, Ptychogena lactea*) are also light sensitive and will settle under opaque objects such as small rocks or shell (Custance, 1964; Brewer, 1978, 1984; Raskoff, unpubl. data), while others (*Clava multicornis*) are positively phototactic (Orlov, 1996). There is evidence that some species

settle preferentially in areas with a high density of conspecifics (Keen, 1987). Some larvae may also settle at the air-water interface, attaching upside down onto the surface film (Pagliara *et al.*, 2000). These can be dislodged by gently disturbing the surface tension with a drop of water, whereupon the polyps drop to the bottom and reattach to a benthic substrate. Additionally, planulae will attach to a floating substrate that is gently placed on the water surface. Larvae induced to settle on microscope slides can be raised off the bottom of the culture chamber after they have started to reproduce asexually, and inverted so the polyps hang upside down. This facilitates their feeding and allows their wastes to fall to the bottom of the tank, reducing fouling.

With consistent feeding and a debris-free environment, healthy polyps will generally grow and produce juvenile medusae. However, several treatments can be used to initiate or speed up the process. Scyphozoan polyps typically produce juvenile medusae by the process of strobilation, which can be induced in various ways. These include brief temperature increases of ≈5.0 °C, prolonged (4–6 weeks) reduction of water temperature by ≈5-10 °C followed by a return to normal temperatures over a few days, and changes in the amount of feeding (Abe and Hisada, 1969; Calder, 1974; Cargo, 1975). Other inducers found to have some success are changes in illumination level and pH, increases in salinity, and treatment with various chemicals (iodine, thyroxine, etc.) (Spangenberg, 1971; Olmon and Webb, 1974).

When the polypoid phase begins to release juvenile medusae, it is helpful to remove them from the culture chamber and place them into a rearing tank as soon as possible. Young ephyrae and hydromedusae can be injured or eaten by other members of the polyp colony. The young medusae will often be swept out the outflow of the polyp culture tank (Fig. 1) and into the grow out tank, but transporting them *via* a large-diameter pipette is preferable because it reduces the stress on the juvenile medusae.

The medusae of most species can be placed directly into flow-through or aerated rearing tanks after release (Fig. 1), although some species such as *Pelagia colorata* and *Aequorea victoria* respond better if first placed into small dishes with still, filtered water for several days to weeks. Juvenile medusae may need to be transferred into several grow-out tanks of increasing sizes and decreasing conspecific densities throughout their development, depending on the species and size of the medusae (Spangenberg, 1965).

Once a polyp culture has been started, it is often necessary to propagate the polyps in additional culture containers. Propagated polyps can be used to set up replicate cultures for experimentation, for transfer to other researchers or aquarium facilities, or as backup in case of problems. Both hydrozoan and scyphozoan polyps can be removed from substrates by gently scraping with a small instrument, such as a plastic toothpick or a trimmed, hard-bristled paint

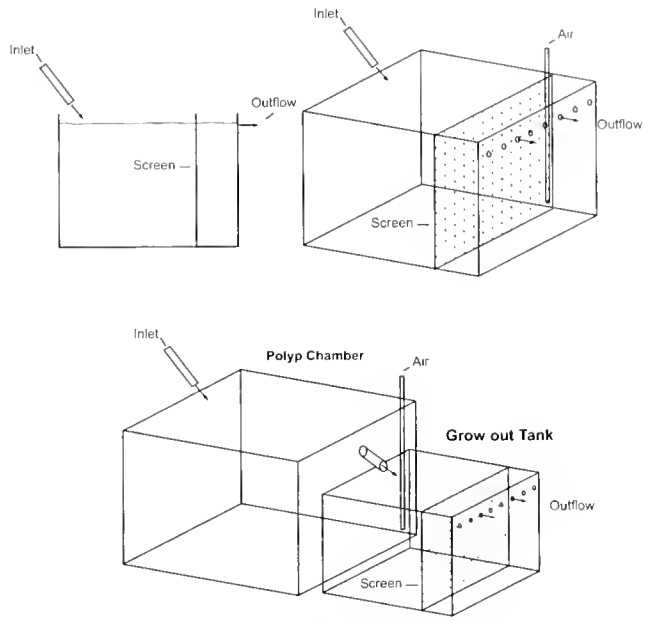

Figure 1. Flow-though culture tanks and grow-out facility. Tank sizes should allow for free, unrestricted feeding and movements of specimens. Mesh sizes should be smaller than the smallest dimension of the organism.

brush. Razor blades or narrow-tipped utility knives are helpful for scraping polyps off smooth, flat surfaces such as glass slides. Once removed, polyps are placed into separate tanks and allowed to resettle. Many species reattach quickly when simply resting on the bottom of a dish; others may take longer. One method for raising these polyps off the bottom to facilitate feeding is to tie a tight loop of small-gauge monofilament line around, or slip a small rubber band over, a glass microscope slide, and then insert the base of the polyp under the line on the flat portion of the microscope slide (Groat *et al.*, 1980; F. Boero, Universita di Lecce, Italy, pers. comm.). The tension of the monofilament line holds the polyp next to the surface of the slide without cutting through the stalk of the polyp. The microscope slides can then be inverted, allowing the polyp's tentacles to hang freely. After several days to weeks, the polyp will attach to the slide, and the monofilament can be cut and removed. Asexual reproductive bodies, such as cysts and frustules, can also be removed from the original tank to seed a replicate culture. Cysts can be removed by scraping, and the damage caused to the capsule of the cyst sometimes stimulates excystment and subsequent growth of the polyp, as can changes in temperature (Brewer and Feingold, 1991). Swimming frustules are produced in some species (hydroid example: *Craspedacusta;* scyphozoan example: certain rhizostomes such as *Cassiopeia* and *Mastigias*), and these can be pipetted into a dish where they will settle and develop into polyps. After settlement, the dish can be transferred to a flow-through tank.

The use of antibiotics to aid in the culture of gelatinous

organisms has not had much study. Strathmann (1987) lists several antibiotics and fungicides that might help fight infections. The antibiotic tetracycline has been used to treat bacterial infections on large scyphomedusae. After being placed in a 20-ppm bath for 2 h a day, 5 days in a row (B. Upton, Monterey Bay Aquatium, pers. comm.), the infected medusae improved markedly. This technique shows great promise for treating the common "bell rot" encountered with many large medusae.

Feeding

Among the types of food that can be used to feed gelatinous zooplankton are *Artemia* nauplii, krill, chopped squid and fish tissue, medusae, wild plankton (copepods, etc.), rotifers, trochophore larvae, agar-based foods, algae, bivalve hepatopancreas, and "grow-lights" for those species of medusae with zooxanthellae. *Artemia* nauplii are the most common food items used in culture of polyps and medusae and provide the backbone of most species' diets in laboratory conditions. Most species can be fed *Artemia* daily, but some very small polyps may have difficulty capturing and ingesting prey of this size (about 400 μm). Tentaculate ctenophores thrive on *Artemia*, but non-tentaculate beroid ctenophores need gelatinous prey. The lack of appropriate food items is a major stumbling block for the culture and study of many gelatinous taxa. For example, the natural food of many pteropods is other species of pteropods, which are difficult to culture in the laboratory; therefore, even if the animals themselves can be successfully maintained in tanks, providing them with adequate nutrition over long periods of time is a challenge (Conover and Lalli, 1972).

Hatching times and water temperatures vary between the different species and strains of *Artemia*, so recommendations provided by the supplier should be consulted. After hatching, the nauplii should be fed for a day or so with a food supplement (Super Selco, Algamac, algae, yeast, etc.). By enriching the content of protein and free amino acids in the nauplii acid (Helland *et al.*, 2000), these supplements contribute to the subsequent growth and health of the animals to which the nauplii are fed. The nauplius must have a mouth (2nd instar stage) before it can ingest the enrichment medium, which must be dispersed (emulsified, aerated, or otherwise kept in the water column) so that the nauplii can eat it. The "shells" of the *Artemia* cysts can be removed to reduce fouling and increase hatching efficiency. Several methods of cyst decapsulation are available on the Internet. Decapsulated cysts can be kept for extended periods, refrigerated in water, until they are needed.

Krill, squid, and other large or fleshy prey can be cut or homogenized to an appropriate size and fed to many polyps, medusae, and heteropods. A disadvantage is that these food items quickly sink to the bottom of the tank and thus are available for capture only briefly. These foods must be removed or they rot and promote growth of fouling organisms. Live *Aurelia* and other medusae are a good and sometimes necessary dietary supplement for many medusivorous jellyfish, including *Pelagia*, *Cyanea*, *Chrysaora*, *Phacellophora*, and *Aequorea*. Smaller stages of these medusivores can be fed *Aurelia* ephyrae, finely diced adult medusae, or small hydromedusae. Small, newly released hydromedusae, such as *Aequorea*, *Eutonina*, and *Bougainvillea*, are especially important in the diet of *Pelagia colorata* ephyrae, which are difficult to raise on *Artemia* alone (Sommer, 1993). Wild-caught plankton also offer an important dietary supplement to gelatinous zooplankton in culture. Live copepods are desirable for tentaculate ctenophores and scyphomedusae. Recent research has pointed out the importance of utilizing natural prey whenever possible. The reason that at least two species of naturally bioluminescent medusae do not produce light when reared in the laboratory is a dietary deficiency of the luciferin coelenterazine (Haddock *et al.*, 2001). Thus, even seemingly healthy cultured animals may not receive all of their nutritional needs from convenient laboratory prey, and alternative or supplemental foods should be tried routinely.

Small and newly metamorphosed animals can be difficult to feed due to their diminutive size. Various live single-celled algae, such as *Tetraselmis* spp., *Isochrysis galbana*, and *Nannochloropsis* spp., can be valuable food sources for small polyps, as well as for filter-feeding salps and doliolids (Paffenhöfer, 1970, 1973; Heron, 1972; Paffenhöfer and Harris, 1979). Rotifers ($\approx$100–200 μm), such as *Brachionus plicatilis*, and oyster trochophores ($\approx$50 μm) are in the right size range for capture and consumption by polyps, which may be unable to consume the much larger *Artemia* nauplii. Rotifers can be fed on the above algae as well. All of the above prey items are commercially available. Rotifers and algae are easily cultured in tanks similar to those used for *Artemia*, and the trochophores can be purchased frozen. Another food that has been used with some success is agar-enriched medium. Homogenized food items mentioned above, as well as amino acids, lipids, and protein sources, can be mixed into heated agar and, when cooled, a gel is formed. This gel can be cut into small pieces and fed by hand to polyps, medusae, and beroid ctenophores. This is labor intensive but useful for some species that are otherwise difficult to feed. Another common feeding technique uses bivalve hepatopancreatic tissue, finely chopped and cleaned in successive changes of seawater. These pieces are then hand-fed to individual polyps. Common intertidal copepods can be cultured in shallow pans as a food source.

Several species of medusae depend on the photosynthetic products of zooxanthellae for nutrition. In addition to a normal diet of prey, these species require a strong light with an appropriate action spectrum for photosynthesis by the zooxanthellae. The type and power of the light can be

variable depending on tank size and depth. For example, at the Monterey Bay Aquarium, the scyphozoans *Mastigias papua* and *Cassiopeia xamachana* have been reared for several months in tanks with metal halide and actinic or daylight fluorescent lamps.

Tanks

Benthic stages. With careful cleaning and frequent water changes, benthic hydroids and polyps can be kept in simple jars and dishes (*e.g.*, Miglietta *et al.*, 2000). However, when dealing with large cultures, or when flowing water is desired for efficient feeding, more complex facilities are needed. Rees and Russell (1937) designed the first successful large-scale culture system for cnidarian polyps. This consisted of rows of glass beakers that held the polyps, and vertical microscope slides attached to a rocker arm driven by an automatic pipette washer. This moved the slides gently forward and back at the top of the beaker, keeping the water stirred and aerated, and the food in suspension. This type of system has also been used to raise a variety of larvae (Strathmann, 1987). The water in the beakers was changed and the beakers were cleaned regularly. A better arrangement for polyp cultivation uses flowing seawater, and the culture tank therefore requires an incoming water line and an exit drain. Rectangular clear plastic boxes of various sizes (pet cages available from most pet stores) make ideal culture and grow-out tanks. Plastic containers can be easily modified and are inexpensive, but any small tank can suffice. Depending on the purpose of the tank, the drainage can flow into another tank to collect newly released medusae, or the drainage can be screened off with mesh (Fig. 1). If the exit drain is to be screened, the screen mesh must be smaller than the smallest medusae that will be released (mesh sizes of 120–500 μm are commonly used). In addition, the surface area of the exit screen must be maximized so that the drain pressure at any one point is low enough to prevent the medusae from being trapped against the screen. Screens are typically put across one entire side of the tank, several centimeters from the drain.

A simple way to set up a "medusa factory" using this technique is to clip a beaker or dish containing polyps to an edge of the culture chamber, suspending it slightly above the water level of the tank. Incoming water runs into the polyp beaker and spills over the side into the tank (Sommer, 1993). In this manner, newly produced medusae are washed out of the polyp beaker into the catch tank, where they will be safe from capture by the polyps (Fig. 1A). Alternatively, the polyps can be kept at the bottom of a tank without a screened-off outflow. As the medusae are produced, they tend to swim up; eventually most will go out the outflow. A second catch tank with a screened-off outflow is placed below to collect the juvenile medusae (Utter, 2001). This catch tank can be of similar design to the tanks described above (Fig. 1B). The addition of an air line close to the screen in any catch or grow-out tank will cause bubbles to rise along the screen, and these will create a gentle upward current that encourages juvenile medusae to stay up in the water column and off the screen.

Pelagic stages. Tanks for pelagic animals offer unique challenges, but the aim is to mimic a natural environment as closely as possible. The vast majority of gelatinous zooplankton are pelagic, and their tanks must minimize contact between the animal and all tank surfaces. That being said, many gelatinous taxa have been maintained or cultured in the laboratory in nothing more than jars or aquaria of still water in temperature-controlled environments. Radiolarians (Sugiyama and Anderson, 1997) and foraminifera (Hemleben and Kitazato, 1995) have been kept for extended periods in small jars and culture dishes. Reeve (1970) and Reeve and Walter (1972) raised chaetognaths in 30-l aquaria with daily water changes. Conover and Lalli (1972) kept the pteropod *Clione limacina* "indefinitely" in small dishes and beakers with filtered water. Baker and Reeve (1974) and Martindale (1987) raised the ctenophore *Mnemiopsis mccradyi* in 30-l aquaria with gentle aeration, but had very low survival. Hirota (1972) used large jars for the culture of the ctenophore *Pleurobrachia bachei*. Heron (1972) raised the salp *Thalia democratica* in small tanks with lids that prevented the salps from encountering the air-water interface. Many researchers continue to raise small hydromedusae, ctenophores, and other gelatinous organisms in dishes, small-volume culture plates, and jars of various sizes (Rees, 1979; Mills *et al.*, 2000).

The standard pelagic tank designs used today are all variations of the planktonkreisel designed originally by Greve (1968, 1970, 1975), which was modified and redesigned for shipboard use by Hamner (1990) and for public display by the Monterey Bay Aquarium (Sommer, 1992, 1993). Paffenhöfer (1970) described a rotating culture apparatus used very successfully for copepods, appendicularians, and doliolids, which has been modified to various degrees (*e.g.*, Sato *et al.*, 2001; Gibson and Paffenhöfer, 2000). Ward (1974) described some simple aquarium systems for maintenance of ctenophores and jellyfish. Dawson (2000) devised a horizontal mesocosm that stratified by various salinity layers and may hold promise for species that require complex water masses for development. The planktonkreisel design, however, has proved to be the most useful, and it has been modified over the years into several designs that offer more complex flow patterns and easier access to the inside of the tank and to the animals (Sommer, 1992, 1993). Despite these alterations, the basic principles of the planktonkreisel remain unchanged.

The main chamber of the tanks is circular, with curved sides and bottom and a flat back and front (Fig. 2). The water inlets and drains are designed to keep organisms from coming in contact with the screen that shields the drain.

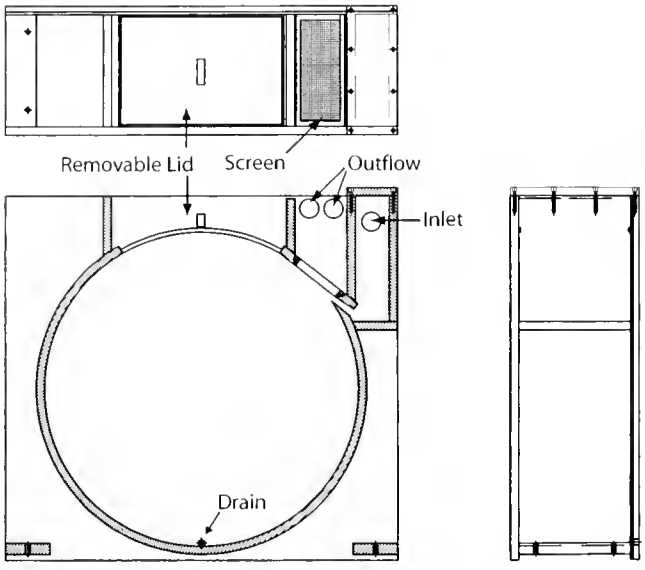

Figure 2. Contemporary planktonkreisel design showing separated inlet/outlet chamber and tank access lid. Detailed plans of this tank are available online at http://www.mbari.org/midwater/tank/tank.htm.

Water flows from the inlet chamber and jets in a laminar flow across the lower side of a fine-mesh screen, which separates the main tank from the drain outflow. In this way any specimen that drifts near the outflow screen will be pushed away by the incoming water. The placement of a few parallel layers of polycarbonate double-wall sheet, commonly used as greenhouse siding, into the space between the inlet chamber and the main tank will force the inlet water to enter with a smooth laminar flow. Modifications to the planktonkreisels made by the Monterey Bay Aquarium include the construction of a separate outflow and lid, which allows animals to be put into or removed from the kreisel without danger of being sucked down the drain. A larger lid allows for easier access into the tank for cleaning and manipulation of the specimens (Sommer, 1993). For scientific purposes, a matte black back plate allows for side lighting of transparent plankton, achieving dark-field illumination (Hamner, 1990). For display aquaria, a matte translucent blue-and-white acrylic back, illuminated from behind with fluorescent lamps, can be used to create the appearance of a lifelike blue-water environment. Spotlights from the sides of the tank are used to illuminate animals for display or photographic purposes. Strong lights do not appear to bother many gelatinous species, which typically have limited visual equipment. Most gelatinous organisms can do well in planktonkreisels (see Tables 1 and 2 for a summary). Plans of a planktonkreisel developed by Kim Reisenbichler at the Monterey Bay Aquarium Research Institute (Fig. 2) are available for download at http://www.mbari.org/midwater/tank/tank.htm.

Another variation on the planktonkreisel design is the stretch kreisel, or Langmuir kreisel (Fig. 3). The tank has two inlet/outlet chambers that are located on each side of a rectangular tank, sending flow upward. The dimensions of the rectangular tank (still with circular ends) must be about twice as wide as tall, permitting the formation of two gyres, one of which rotates clockwise and the other counterclockwise. The top of the tank is open and the flows meet in the middle, where they are joined by water added from a horizontally positioned perforated tube, creating convergent currents that descend down the center of the tank. The two opposing circular flows result in downwelling at the center of the tank and upwelling at either end. This design works well with species that tend to swim actively into a current

Table 1

Selected culture techniques for medusae commonly used for display

Species	Diet	Temperature (°C)	Lifespan	Tanks*
Scyphozoa				
Aurelia aurita	*Artemia*, Krill	10–15	2–4 y+	K, PK, HP
Aurelia labiata	*Artemia*, Krill	10–15	2–4 y+	K, PK, HP
Phacellophora camtschatica	*Artemia*, Juvenile *Aurelia*, Krill	10–15	1 y+	K, PK, SK
Pelagia colorata	*Artemia*, Juvenile *Aurelia*, Krill	10–15	1 y+	K, SK, PK
Chrysaora fuscescens	*Artemia*, Juvenile *Aurelia*, Krill	10–15	2 y+	K, SK, PK
Cassiopeia xamachana	*Artemia*, Lighting	24–27	1 y+	RF
Mastigias papua	*Artemia*, Lighting	27–29	3 mo+	K, PK, HP
Hydrozoa				
Aequorea victoria	*Artemia*, Rotifers (hydroids), Juvenile *Aurelia*, *Eutonina*	10–15	6 mo+	K, PK
Eutonina indicans	*Artemia*, Rotifers	10–15	3 mo+	K, PK
Polyorchis penicillatus	*Artemia*	10–15	3 mo+	PK, K
Craspedacusta sowerbii	Wild freshwater plankton, Frozen *Daphnia*	Freshwater 27	<3 mo	K, RT
Tima formosa	*Artemia*, Rotifers	24–27	6 mo+	PK, K

Data summarized from Sommer (1992, 1993) for the Monterey Bay Aquarium.
* K = Kreisel; PK = Pseudokreisel; SK = Stretch kreisel; RF = Reverse flow; HP = Horizontal pseudokreisel; RT = Rectangular tank.

Table 2

Selected culture techniques of non-cnidarian gelatinous zooplankton

Species	Diet	Temperature (°C)	Lifespan	Tanks*	Reference
Ctenophores					
Pleurobrachia bachei	*Artemia*	10–15	2 mo+	K, PK	Sommer, 1992
	Wild-caught zooplankton	15	nd	Large jars	Hirota, 1972
Pleurobrachia pileus	Wild-caught copepods	15	8 mo+	Modified PK	Greve, 1970
Bolinopsis infundibulum	*Artemia*	10–15	8 mo+	K, PK	Sommer, 1992
	Wild-caught zooplankton	16	7 mo	Modified PK	Greve, 1970
Mnemiopsis mccradyi	Wild-caught zooplankton	21–31	<2 mo	30 l tanks	Baker and Reeve, 1974
Beroe spp.	Ctenophores, gelatin	10–15	<3 mo	K, PK	Sommer, 1992
Beroe gracilis	*Pleurobrachia pileus*	15	6 mo	Modified K	Greve, 1970
Beroe cucumis	*Bolinopsis infundibulum*	15	1 mo+	Modified K	Greve, 1970
Molluses					
Clione limacina	None	10–15	2 mo+	PK, K	This study
	Wild-caught pteropods	12–14	4 mo+	Dishes	Conover and Lalli, 1972
Cliopsis krohni	None	10–15	6 mo+	PK, K	This study
Chaetognaths					
Sagitta hispida	Copepods	17–31	2 mo+	30-l tanks	Reeve, 1970; Reeve and Walter, 1972
	nd	nd	nd	Modified K	Greve, 1968
Pelagic Tunicates					
Oikopleura dioica	Cultivated phytoplankton	13	8–12 days	RJ	Paffenhöfer, 1973
Fritillaria borealis	Cultivated phytoplankton	12	nd	RJ	Paffenhöfer and Harris, 1979
Thalia democratica	Phytoplankton	nd	8–20 days	Large jars	Heron, 1972

nd = no data.
* K = Kreisel; PK = Pseudokreisel; RF = Reverse flow; RJ = Rotating jars.

(such as *Chrysaora fuscescens*), since they will tend to congregate in the center of the tank, away from the walls (Tables 1 and 2).

Any rectangular tank can be modified into a "pseudo-kreisel," but care must be taken to ensure that the height and width of the tank are about equal, or the water in the tank will not be able to rotate in a perfect circle and will create areas within the tank of limited flow where the animals may accumulate and contact the sides. Rectangular tanks are modified by glueing a screen across the upper corner at an angle of about 30°–40° from vertical in front of the overflow (Fig. 4). Water enters the tank through a perforated tube positioned so that the flow sweeps across the screen down towards the bottom of the tank. It is important that the tube is positioned so that the flow is parallel to the screen and covers the entire screen so that specimens are swept away rather than drawn against it. Curved plastic or vinyl inserts are glued with silicone into the bottom corners to round them into a more circular shape. Friction-fitting stiff screens can also be used to round the corners, although this option makes the tank more difficult to clean and maintain than one with solid corners.

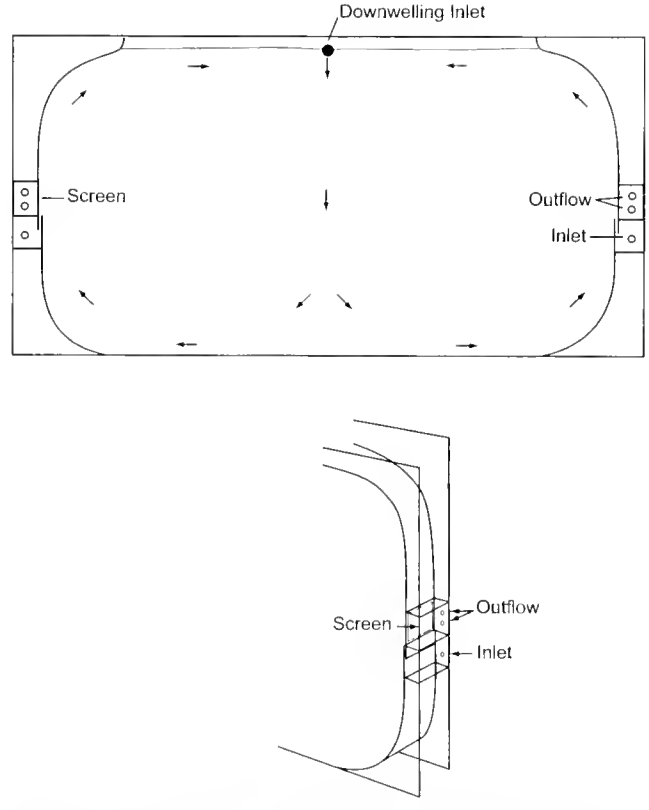

Figure 3. Stretch kreisel design showing the two rotating Langmuir cells set up by the placement of the side and downwelling inlets.

Water

Several water quality issues are important for the successful culture and rearing of gelatinous organisms. Temperature and salinity must be kept within a range appropri-

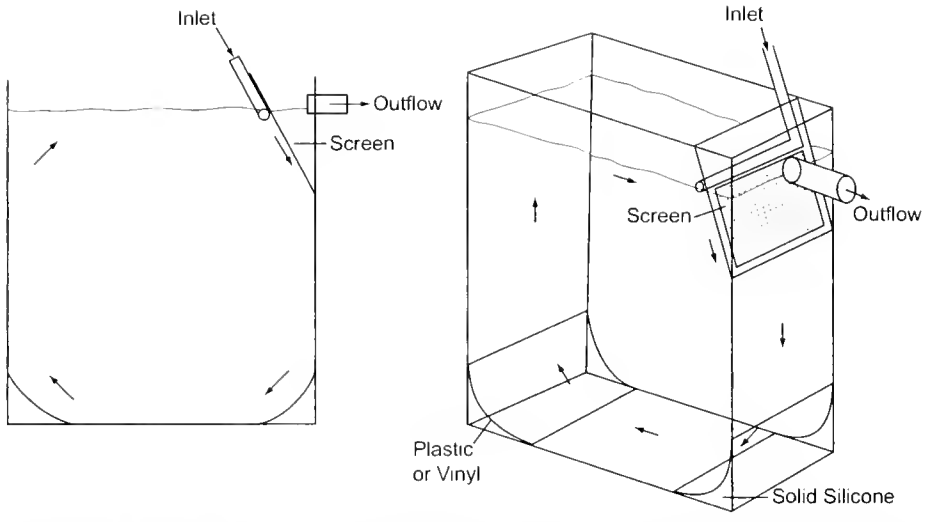

Figure 4. Pseudokreisel design made from a standard tank. Bottom corners are filled in with silicone and solid pieces of plastic or vinyl. Outflow is separated from the tank by the inlet and screen.

ate for the species being reared. The water must be relatively clean and filtered, especially if the animals are to be used for any display purpose. Small particles in the water will quickly clog the outflow screens. Filtering the water with 20-μm pleated cartridge filters is usually sufficient; however, some cultures that are very sensitive to biological fouling (such as many hydroid species) may need additional filtration to the 3 μm level. Although air bubbles can be helpful in the culture of many small gelatinous animals by increasing water circulation, they can be detrimental to larger adult sizes (>3 cm). The bubbles can be ingested and collect in the gut and radial canals of medusae and ctenophores, causing the animals to become positively buoyant, disrupting their normal swimming and feeding behaviors. A more serious problem is that these bubbles will slowly work themselves through the mesoglea, which can lead to infection. A degassing system for the water may be needed if the incoming water tends to be supersaturated. A degassing tower in which the water trickles down through small plastic balls or other material serves to degas the water before it enters the tank. Deep-sea animals may be sensitive to the high oxygen concentrations of surface waters. Reducing the oxygen concentration in tank water by bubbling nitrogen gas has been used in the past with some success, although it does not appear to be critical for most deep-sea species.

Maintenance

Throughout the course of feeding and rearing, tanks accumulate debris that should be removed regularly. The use of pipettes, small brushes, basters, and siphons for removing larger debris, including waste, uneaten *Artemia*, and other food items, will help keep the tanks clean and discourage fouling growth. Pipettes of any size and type can be used to gently lift and collect debris. Kitchen basters work well for removing larger items because of their large reservoir volume and wide bore. Siphons are best constructed from small-bore acrylic tubes with flexible plastic tubing attached, so that the tubing may be pinched to stop flow if an animal gets too close to the suctioning tip. Additionally, siphoning the "waste water" into a temporary container allows for the retrieval of any specimen that might inadvertently be removed. To protect the insides of the tanks from scratches, it is helpful to dip the end of the acrylic tube into liquid plastic, available from most hardware stores; alternatively, a small ring of Nalgene tubing may be placed on the end of the siphon tube. Floating layers of lipid-rich materials can be removed by skimming with small jars or beakers or fine-meshed nets, or by absorbing the material onto paper towels floated on the surface of the water. The sides of the tanks can be cleaned by wiping with brushes (firm paint brushes work well) or non-abrasive pads. For larger tanks (>75 l), painting or scrub pads can be covered with nonabrasive nylon mesh fabric and attached to poles for cleaning hard-to-reach areas of the tanks. The wood or metal handles of these scrubbers can be covered in plastic tubing to reduce the adherence of tentacles. Flow to the tanks can also be temporarily shut off and the animals allowed to collect on the bottom of the tank during cleaning. Also, tanks can be cleaned just after the animals have been fed, when tentacles are typically retracted and less apt to become ensnared (C. Widmer, Monterey Bay Aquarium, per. comm.). Screens in the tanks collect debris quickly and need to be scrubbed and cleaned at regular intervals. When screens become clogged, organisms are more likely to stick to them, possibly with fatal results.

Even with proper cleaning and filtration, biofouling in

culture and rearing tanks can become a serious problem. In some cases of diatom and algae fouling, reducing the light that shines on the tank can help reduce growth, but typically, scrubbing the tanks eventually becomes necessary. When diatom, hydroid, or other fouling organisms cannot be satisfactorily removed by any of the means discussed previously, bleaching is necessary. This can be especially useful on the screens, pumps, and waterlines, which can be very difficult to clean by other means. The entire tank system may need to be bleached every 1–6 months, depending on the size and fouling rate. During bleaching, the occupants of the tank must be removed and transferred to a holding facility. The longer the tanks and lines are allowed to bleach, the more complete the fouling kill will be. Overnight is preferred, but bleaching for even an hour kills most fouling organisms. As a rule of thumb, 1 l of standard 3%–6% sodium hypochlorite (NaOCl) bleach will treat about 200 l of water (≈1 gallon bleach/800 gallons of water), but this amount can be increased or decreased depending on the severity of the fouling and the time available to let the tank bleach. The water level in the tank should be dropped so that there is no overflow when the bleach is added. If the tanks have self-contained pumps, these should be run at a high flow rate to mix the bleach and flush it into the pump housings.

To complete the process, the bleach must be neutralized. This can be accomplished by adding about 60 g of sodium thiosulfate ($Na_2S_2O_3$) per liter of bleach used (≈1 cup/gallon). The sodium thiosulfate crystals may be dissolved in a bucket of water prior to adding to the tank. When the color of the water in the aquarium changes from yellow-green to clear, sufficient thiosulfate has been added for neutralization. Allow the thiosulfate several minutes to run through the entire tank and pumps. The treated water is then drained from the tank and discarded. While draining, thoroughly rinse out the tank with freshwater. Stubborn growth can be removed at this time by scrubbing. After all debris and treated water is removed, begin to refill the tank with seawater, minimizing turbulence and bubbles during the refilling since bubbles will stick to the walls of the tank and will have to be removed before gelatinous animals are returned.

Discussion

The use of the techniques described herein for the capture, culture, and rearing of gelatinous zooplankton has allowed researchers to address many important biological issues. Historically, these contributions were limited primarily to the disciplines of systematics, developmental biology, and evolution. More recently, new advances in our understanding of behavior, physiology, ecology, and oceanographic processes from the sea surface to the abyssal depths have also been possible.

Through the use of culture methodologies, laboratory-based experimentation on salps and larvaceans has begun to address important ecological questions about the role these animals play in the nutrient cycling of the oceans and their impact on the ecosystem. These organisms have some of the fastest generation times and largest nutrient turnovers in the world, and their fecal pellets and associated "marine snow" are important sources of carbon transport into the deep sea (*e.g.*, Alldredge, 1972; Silver *et al.*, 1998).

Recent laboratory studies have shown that some species of medusa have chemically-regulated feeding behaviors (Arai, 1991, 1997; Tamburri *et al.*, 2000), with several different chemical stimuli controlling the feeding and swimming of both hydrozoan and scyphozoan medusae. Tank-based studies on the vertical migration of medusae (Mackie *et al.*, 1981; Mills, 1983) and on their swimming and feeding behaviors (*e.g.*, Costello and Colin, 1995; Suchman and Sullivan, 2000) have provided much information on the physiological and behavioral components of medusa locomotion as it relates to prey selection and capture.

The interactions between gelatinous zooplankton and humans are increasing, whether from envenomation (Burnett, 2001); blooms that clog power plant intakes (Masilamoni *et al.*, 2000); interactions, both positive and negative, with fisheries (Mutlu *et al.*, 1994; Mutlu, 1999; Mills, 2001; Purcell and Arai, 2001); or the general increase in gelatinous zooplankton populations in perturbed or eutrophic environments (Mills, 1995, 2001; Arai, 2001). The opportunities for scientific studies of gelatinous zooplankton are vast and largely untouched. We hope researchers can use some of the techniques presented here to expand the research being done on these important but poorly understood marine organisms.

The public's fascination with and appreciation of gelatinous zooplankton is growing rapidly. What were once considered nasty animals that might sting or otherwise disturb beachgoers are now a major attraction in public aquaria all over the globe. The time and money spent by the aquarium industry to provide compelling exhibits on gelatinous zooplankton is a testament to their appeal. Over 3.4 million people visited the Monterey Bay Aquarium during the temporary "Planet of the Jellies" exhibit in 1992 and 1993 (Powell, 2001; J. Tomulonis, Monterey Bay Aquarium, pers comm.). Jellyfish and ctenophores were given permanent starring roles in the Outer Bay Wing, and in a new temporary exhibit, "Jellies: Living Art." Aquarists in the United States and elsewhere are responsible for many of the techniques discussed in this paper. Aquariums around the world provide the bulk of the layperson's information on gelatinous zooplankton, and we hope that the rising public appreciation of these important and beautiful animals may lead to increased financial and societal support for their continued study.

Acknowledgments

F. Boero, A. Case, M. Coates, J. Connor, J. Costello, R. Hamilton, C. Harrold, G. Matsumoto, S. McDaniel, C. Priewe, K. Reisenbichler, B. Robison, R. Sherlock, J. Tomulonis, B. Upton, B. Utter, G. VanDykhuizen, C. Widmer, and D. Wrobel provided information and support for this review. J. Connor, B. Robison, G. Matsumoto, M. LaBarbera, and two anonymous reviewers provided valuable comments on this manuscript. This work was supported by the David and Lucile Packard Foundation through MBARI/MBA Joint Projects Committee.

Literature Cited

Abe, Y., and M. Hisada. 1969. On a new rearing method of common jellyfish, *Aurelia aurita*. *Bull. Mar. Biol. Stn. Asamushi* **13:** 205–209.

Acuña, J. L., D. Deibel, and S. Sonley. 1994. A simple device to transfer large and delicate planktonic organisms. *Limnol. Oceanogr.* **39:** 2001–2003.

Alldredge, A. L. 1972. Abandoned larvacean houses: a unique food source in the pelagic environment. *Science* **177:** 885–887.

Alldredge, A. L., and W. M. Hamner. 1980. Recurring aggregation of zooplankton by a tidal current. *Estuar. Coast. Mar. Sci.* **10:** 31–37.

Arai, M. N. 1991. Attraction of *Aurelia* and *Aequorea* to prey. *Hydrobiologia* **216–217:** 363–366.

Arai, M. N. 1997. *A Functional Biology of Scyphozoa.* Chapman and Hall, London.

Arai, M. N. 2001. Pelagic coelenterates and eutrophication: a review. *Hydrobiologia* **451:** 69–87.

Baker, A. C. 1963. The problem of keeping planktonic animals alive in the laboratory. *J. Mar. Biol. Assoc. UK* **43:** 291–294.

Baker, L. D., and M. R. Reeve.1974. Laboratory culture of the lobate ctenophore *Mnemiopsis mccradyi* with notes on feeding and fecundity. *Mar. Biol.* **26:** 57–62.

Brewer, R. H. 1976. Larval settling behavior in *Cyanea capillata* (Cnidaria: Scyphozoa). *Biol. Bull.* **150:** 183–199.

Brewer, R. H. 1978. Larval settlement behavior in the jellyfish *Aurelia aurita* (Linnaeus) (Scyphozoa: Semaeostomeae). *Estuaries* **1:** 120–122.

Brewer, R. H. 1984. The influence of the orientation, roughness, and wettability of solid surfaces on the behavior and attachment of planulae of *Cyanea* (Cnidaria: Scyphozoa). *Biol. Bull.* **166:** 11–21.

Brewer, R. H., and J. S. Feingold. 1991. The effect of temperature on the benthic stages of *Cyanea* (Cnidaria: Scyphozoa), and their seasonal distribution in the Niantic River estuary, Connecticut. *J. Exp. Mar. Biol. Ecol.* **152:** 49–60.

Bullock, T. H. 1943. Neuromuscular facilitation in scyphomedusae. *J. Cell. Comp. Physiol.* **22:** 251–272.

Burnett, J. W. 2001. Medical aspects of jellyfish envenomation: pathogenesis, case reporting and therapy. *Hydrobiologia* **451:** 1–9.

Calder, D. R. 1974. Strobilation of the sea nettle, *Chrysaora quinquecirrha,* under field conditions. *Biol. Bull.* **146:** 326–334.

Cargo, D. G. 1975. Comments on the laboratory culture of scyphozoa. Pp. 145–154 in *Culture of Marine Invertebrate Animals; Proceedings,* W. L. Smith and M. H. Chanley, eds. Plenum Press, New York.

Childress, J. J., and E. V. Thuesen. 1993. Effects of hydrostatic pressure on metabolic rates of six species of deep-sea gelatinous zooplankton. *Limnol. Oceanogr.* **38:** 665–670.

Childress, J. J., A. T. Barnes, L. B. Quetin, and B. H. Robison. 1978. Thermally protecting cod ends for the recovery of living deep-sea animals. *Deep-Sea Res.* **25:** 419–422.

Conover, R. J., and C. M. Lalli. 1972. Feeding and growth in *Clione limacina* (Phipps), a pteropod mollusc. *J. Exp. Mar. Biol. Ecol.* **9:** 279–302.

Costello, J. H., and S. P. Colin. 1995. Flow and feeding by swimming scyphomedusae. *Mar. Biol.* **124:** 399–406.

Custance, D. R. N. 1964. Light as an inhibitor of strobilation in *Aurelia aurita*. *Nature* **204:** 1219–1220.

Dawson, M. N. 2000. Variegated mesocosms as alternatives to shore-based planktonkreisels: notes on the husbandry of jellyfish from marine lakes. *J. Plankton Res.* **22:** 1673–1682.

Gibson, D. M., and G. A. Paffenhöfer. 2000. Feeding and growth rates of the doliolid, *Dolioletta gegenbauri* Uljanin (Tunicata, Thaliacea). *J. Plankton Res.* **22:** 1485–1500.

Gilmer, R. W. 1972. Free-floating mucus webs: a novel feeding adaptation for the open ocean. *Science* **176:** 1239–1240.

Greve, W. 1968. The "planktonkreisel", a new device for culturing zooplankton. *Mar. Biol.* **1:** 201–203.

Greve, W. 1970. Cultivation experiments on North Sea ctenophores. *Helgol. Meeresunters.* **20:** 304–317.

Greve, W. 1975. The "Meteor Planktonküvette": a device for the maintenance of macrozooplankton aboard ships. *Aquaculture* **6:** 77–82.

Groat, C. S., C. R. Thomas, and K. Schurr. 1980. Improved culture of *Aurelia aurita* scyphistomae for bioassay and research. *Ohio J. Sci.* **80:** 83–87.

Haddock, S. H. D., T. J. Rivers, and B. H. Robison. 2001. Can coelenterates make coelenterazine? Dietary requirements for luciferin in cnidarian bioluminescence. *Proc. Natl. Acad. Sci. USA* **98:** 11148–11151.

Haeckel, E. 1893. Planktonic studies: a comparative investigation of the importance and constitution of the pelagic fauna and flora (Eng. transl.) Appendix 6. Re. Comm. for 1889-1891. *U.S. Comm. Fish. and Fisheries.*

Hamner, W. M. 1975. Underwater observations of blue-water plankton: logistics, techniques, and safety procedures for divers at sea. *Limnol. Oceanogr.* **13:** 1045–1051.

Hamner, W. M. 1985. The importance of ethology for investigations of marine zooplankton. *Bull. Mar. Sci.* **37:** 414–424.

Hamner, W. M. 1990. Design developments in the planktonkreisel, a plankton aquarium for ships at sea. *J. Plankton Res.* **12:** 397–402.

Hamner, W. M., and D. Schneider. 1986. Regularly spaced rows of medusae in the Bering Sea: Role of Langmuir circulation. *Limnol. Oceanogr.* **31:** 171–177.

Hamner, W. M., L. P. Madin, A. L. Alldredge, R. W. Gilmer, and P. P. Hamner. 1975. Underwater observations of gelatinous zooplankton: sampling problems, feeding biology, and behavior. *Limnol. Oceanogr.* **20:** 907–917.

Harbison, G. R., G. I. Matsumoto, and B. H. Robison. 2001. *Lampocteis cruentiventer* gen. nov., sp. nov.: a new mesopelagic lobate ctenophore, representing the type of a new family (Class Tentaculata, Order Lobata, Family Lampoctenidae, fam. nov.). *Bull. Mar. Sci.* **68:** 299–311.

Harris, R. P., P. H. Wiebe, J. Lenz, H. R. Skjoldal, and M. Huntley, eds. 2000. *ICES Zooplankton Methodology Manual.* Academic Press, San Diego, CA.

Heine, J. ed. 1986. *Blue Water Diving Guidelines.* California Sea Grant College Publ. T-CSGCP-014, La Jolla, CA.

Helland, S., G. V. Triantaphyllidis, H. J. Fyhn, M. S. Evjen, P. Lavens, and P. Sorgeloos. 2000. Modulation of the free amino acid pool and protein content in populations of the brine shrimp *Artemia* spp. *Mar. Biol.* **137:** 1005–1016.

Hemleben, C., and H. Kitazato. 1995. Deep-sea foraminifera under long time observation in the laboratory. *Deep-Sea Res.* **42:** 827–832.

Hensen, V. 1887. Über die Bestimmung des Planktons oder des im Meere treibenden Materials an Pflanzen und Thieren. *Komm. Wiss. Untersuch. Deutsch. Meere* **5:** 1–107.

Heron, A. C. 1972. Population ecology of a colonizing species: the pelagic tunicate *Thalia democratica*. I. Individual growth rate and generation time. *Oecologia* **10:** 269–293.

Hirota, J. 1972. Laboratory culture and metabolism of the planktonic ctenophore, *Pleurobrachia bachei* A. Agassiz. Pp. 465–484 in *Biological Oceanography of the Northern North Pacific Ocean*, A. Y. Takenouti, ed. Idemitsu Shoten, Tokyo.

Keen, S. L. 1987. Recruitment of *Aurelia aurita* (Cnidaria: Scyphozoa) larvae is position-dependent, and independent of conspecific density, within a settling surface. *Mar. Ecol. Prog. Ser.* **38:** 151–160.

Kramp, P. L. 1965. The hydromedusae of the Pacific and Indian Oceans. *Dana-Rep. Carlsberg Found.* **63:** 1–162.

Larson, R. 1991. Why jellyfish stick together—Caribbean thimble jellies travel in the same circles. *Nat. Hist.* 66–71.

Larson, R. J., G. I. Matsumoto, L. P. Madin, and L. M. Lewis. 1992. Deep-sea benthic and benthopelagic medusae: recent observations from submersibles and a remotely operated vehicle. *Bull. Mar. Sci.* **51:** 277–286.

Mackie, G. O. 1960. The structure of the nervous system in *Velella*. *Q. J. Microsc. Sci.* **101:** 119–131.

Mackie, G. O., R. J. Larson, K. S. Larson, and L. M. Passano. 1981. Swimming and vertical migration of *Aurelia aurita* (L) in a deep tank. *Mar. Behav. Physiol.* **7:** 321–329.

Madin, L. P. 1974. Field observations on the feeding behavior of salps (Tunicata: Thaliacea). *Mar. Biol.* **25:** 143–147.

Martin, V. J., and R. Koss. 2002. Phylum Cnidaria. Pp. 51–108 in *Atlas of Marine Invertebrate Larvae*, C. M. Young, ed. Academic Press, San Diego, CA.

Martindale, M. Q. 1987. Larval reproduction in the ctenophore *Mnemiopsis mccradyi* (order Lobata). *Mar. Biol.* **94:** 409–414.

Masilamoni, J. G., K. S. Jesundoss, K. Nandakumar, K. K. Satpathy, K. V. K. Nair, and J. Azariah. 2000. Jellyfish ingress: a threat to the smooth operation of coastal power plants. *Curr. Sci. (Bangalore)* **79:** 567–569.

Matsumoto, G. I., and G. R. Harbison. 1993. *In situ* observations of foraging, feeding, and escape behavior in three orders of oceanic ctenophores: Lobata, Cestida, and Beroida. *Mar. Biol.* **117:** 279–287.

Matsumoto, G. I., and B. H. Robison. 1992. *Kiyohimea usagi*, a new species of lobate ctenophore from the Monterey Submarine Canyon. *Bull. Mar. Sci.* **51:** 19–29.

Mayer, A. G. 1910. *Medusae of the World. Vol. I: The Hydromedusae.* Carnegie Institution of Washington, Washington, DC.

Miglietta, M. P., L. Della Tommasa, F. Denitto, C. Gravili, P. Pagliara, J. Bouillon, and F. Boero. 2000. Approaches to the ethology of hydroids and medusae (Cnidaria, Hydrozoa). *Sci. Mar.* **64:** 63–71.

Mills, C. E. 1983. Vertical migration and diel activity patterns of hydromedusae: studies in a large tank. *J. Plankton Res.* **5:** 619–635.

Mills, C. E. 1995. Medusae, siphonophores, and ctenophores as planktivorous predators in changing global ecosystems. *ICES J. Mar. Sci.* **52:** 575–581.

Mills, C. E. 2001. Jellyfish blooms: Are populations increasing globally in response to changing ocean conditions? *Hydrobiologia* **451:** 55–68.

Mills, C. E., and M. F. Strathmann. 1987. Reproduction and development of marine invertebrates of the northern Pacific coast: data and methods for the study of eggs, embryos, and larvae. Pp. 44–71 in *Reproduction and Development of Marine Invertebrates of the Northern Pacific Coast: Data and Methods for the Study of Eggs, Embryos, and Larvae*, University of Washington Press, Seattle.

Mills, C. E., F. Boero, A. Migotto, and J. M. Gili, eds. 2000. *Trends in Hydrozoan Biology-IV. Sci. Mar.* **64** (Supl. 1).

Mutlu, E. 1999. Distribution and abundance of ctenophores and their zooplankton food in the Black Sea. II. *Mnemiopsis leidyi*. *Mar. Biol.* **135:** 603–613.

Mutlu, E., F. Bingel, A. C. Gucu, V. V. Melnikov, U. Niermann, N. A. Ostr, and V. E. Zaika. 1994. Distribution of the new invader *Mnemiopsis* sp. and the resident *Aurelia aurita* and *Pleurobrachia pileus* populations in the Black Sea in the years 1991-1993. *ICES J. Mar. Sci.* **51:** 407–421.

Olmon, J. E., and K. L. Webb. 1974. Metabolism of ^{131}I in relation to strobilation of *Aurelia aurita* L. (Scyphozoa). *J. Exp. Mar. Biol. Ecol.* **16:** 113–122.

Orlov, D. 1996. Observations on the settling behaviour of planulae of *Clava multicornis* Forskal (Hydroidea, Athecata). *Sci. Mar.* **60:** 121–128.

Paffenhöfer, G.-A. 1970. Cultivation of *Calanus helgolandicus* under controlled conditions. *Helgol. Meeresunters* **20:** 346–359.

Paffenhöfer, G.-A. 1973. The cultivation of an appendicularian through numerous generations. *Mar. Biol.* **22:** 183–185.

Paffenhöfer, G.-A., and R. P. Harris. 1979. Laboratory culture of marine holozooplankton and its contribution to studies of marine planktonic food webs. *Adv. Mar. Biol.* **16:** 211–308.

Pagliara, P., J. Bouillon, and F. Boero. 2000. Photosynthetic planulae and planktonic hydroids: contrasting strategies of propagule survival. *Sci. Mar.* **64:** 173–178.

Pantin, C.F.A. 1952. The elementary nervous system. *Proc. R. Soc. Lond. Ser. B* **140:** 147–168.

Powell, D. C. 2001. *A Fascination for Fish: Adventures of an Underwater Pioneer.* UC Press/Monterey Bay Aquarium, Berkeley.

Purcell, J. E. 1997. Pelagic cnidarians and ctenophores as predators: selective predation, feeding rates, and effects on prey populations. *Ann. Inst. Oceanogr.* **73:** 125–137.

Purcell, J. E., and M. N. Arai. 2001. Interactions of pelagic cnidarians and ctenophores with fish: a review. *Hydrobiologia* **451:** 27–44.

Purcell, J. E., D. L. Breitburg, M. B. Decker, W. M. Graham, M. J. Youngbluth, and K. A. Raskoff. 2001. Pelagic cnidarians and ctenophores in low dissolved oxygen environments. Pp. 77–100 in *Coastal Hypoxia: Consequences for Living Resources and Ecosystems*, N. N. Rabalais and R. E. Turner, eds. American Geophysical Union, Washington, DC.

Ragulin, A. G. 1969. Underwater observations on krill. *Tr. Vses. Nauchno-Issled. Inst. Morsk. Rybn. Khoz. Okeanogr.* **66:** 231–234 (Engl. transl.).

Raskoff, K. A. 2001. The impact of El Niño events on populations of mesopelagic hydromedusae. *Hydrobiologia* **451:** 121–129.

Raskoff, K. A. 2002. Foraging, prey capture, and gut contents of the mesopelagic narcomedusa, *Solmissus* (Cnidaria, Hydrozoa). *Mar. Biol.* **141:** 1088–1107.

Rees, J. T. 1979. Laboratory and field studies on *Eutonina indicans* (Coelenterata: Hydrozoa), a common leptomedusa of Bodega Bay, California. *Wasmann J. Biol.* **36:** 201–209.

Rees, W. J., and F. S. Russell. 1937. On rearing the hydroids of certain medusae, with an account of the methods used. *J. Mar. Biol. Assoc. UK* **22:** 61–82.

Reeve, M. R. 1970. Complete cycle of development of a pelagic chaetognath in culture. *Nature* **227:** 381.

Reeve, M. R. 1981. Large cod-end reservoirs as an aid to the live collection of delicate zooplankton. *Limnol. Oceanogr.* **26:** 577–580.

Reeve, M. R., and M. A. Walter. 1972. Conditions of culture, food-size selection, and the effects of temperature and salinity on growth rate and generation time in *Sagitta hispida* Conant. *J. Exp. Mar. Biol. Ecol.* **9:** 191–200.

Robison, B. H. 1993. Midwater research methods with MBARI's ROV. *Mar. Technol. Soc. J.* **26:** 32–39.

Robison, B. H., K. R. Reisenbichler, R. E. Sherlock, J. M. B. Silguero, and F. P. Chavez. 1998. Seasonal abundance of the siphonophore, *Nanomia bijuga*, in Monterey Bay. *Deep-Sea Res. II* **45:** 1741–1751.

Russell, F. S. 1953. *The Medusae of the British Isles: Anthomedusae,*

Leptomedusae, Limnomedusae, Trachymedusae and Narcomedusae. The University Press, Cambridge.

Sameoto, D., P. H. Wiebe, J. Runge, L. R. Postel, J. Dunn, C. Miller, and S. Coombs, 2000. Collecting zooplankton. Pp. 55–81 in *ICES Zooplankton Methodology Manual,* R. P. Harris, P. H. Wiebe, J. Lenz, H. R. Skjoldal, and M. Huntley, eds. Academic Press, San Diego, CA.

Sato, R., J. Yu, Y. Tanaka, and T. Ishimaru, 1999. New apparatuses for cultivation of appendicularians. *Plank. Biol. Ecol.* **46:** 162–164.

Sato, R., Y. Tanaka, and T. Ishimaru, 2001. House production by *Oikopleura dioica* (Tunicata, Appendicularia) under laboratory conditions. *J. Plankton Res.* **23:** 415–423.

Schmahl, G. 1985. Bacterially induced stolon settlement in the scyphopolyp of *Aurelia aurita* (Cnidaria, Scyphozoa). *Helgol. Meeresuntersuch.* **39:** 33–42.

Siefker, B., M. Kroiher, and S. Berking, 2000. Induction of metamorphosis from the larval to the polyp stage is similar in Hydrozoa and a subgroup of Scyphozoa (Cnidaria, Semaeostomeae). *Helgoland Mar. Res.* **54:** 230–236.

Silver, M. W., S. L. Coale, C. H. Pilskaln, and D. R. Steinberg, 1998. Giant aggregates: importance as microbial centers and agents of material flux in the mesopelagic zone. *Limnol. Oceanogr.* **43:** 498–507.

Sommer, F. A. 1992. Husbandry aspects of a jellyfish exhibit at the Monterey Bay Aquarium. Pp. 362–369 in *American Associations of Zoological Parks and Aquariums Annual Conference Proceedings,* Toronto.

Sommer, F. A. 1993. Jellyfish and beyond, husbandry of gelatinous zooplankton at the Monterey Bay Aquarium. Pp. 249–261 in *Proceedings of the Third International Aquarium Congress,* Boston, MA.

Spangenberg, D. B. 1965. Cultivation of the life stages of *Aurelia aurita* under controlled conditions. *J. Exp. Zool.* **159:** 303–309.

Spangenberg, D. B. 1971. Thyroxine induced metamorphosis in *Aurelia. J. Exp. Zool.* **178:** 183–194.

Strathmann, M. F. 1987. *Reproduction and Development of Marine Invertebrates of the Northern Pacific Coast: Data and Methods for the Study of Eggs, Embryos, and Larvae.* University of Washington Press, Seattle.

Suchman, C. L., and B. K. Sullivan, 2000. Effect of prey size on vulnerability of copepods to predation by the scyphomedusae *Aurelia aurita* and *Cyanea* sp. *J. Plankton Res.* **22:** 2289–2306.

Sugiyama, K., and O. R. Anderson, 1997. Experimental and observational studies of radiolarian physiological ecology, 6. Effects of silicate-supplemented seawater on the longevity and weight gain of spongiose radiolarians, *Spongaster tetras* and *Dictyocoryne truncatum. Mar. Micropalcontol.* **29:** 159–172.

Tamburri, M. N., M. N. Hall, and B. H. Robison, 2000. Chemically regulated feeding by a midwater medusa. *Limnol. Oceanogr.* **45:** 1661–1666.

Thuesen, E. V., and J. J. Childress, 1994. Oxygen consumption rates and metabolic enzyme activities of oceanic California medusae in relation to body size and habitat depth. *Biol. Bull.* **187:** 84–98.

Totton, A. K. 1965. *A Synopsis of the Siphonophora.* Br. Mus. (Nat. Hist.), London.

Utter, B. D. 2001. Culturing the umbrella jelly, *Eutonina indicans* (Romanes, 1876). *Drum and Croaker* **32:** 38–44.

Ward, W. W. 1974. Aquarium systems for the maintenance of ctenophore and jellyfish and for hatching and harvesting of brine shrimp (*Artemia salina*) larvae. *Chesapeake Sci.* **15:** 116–118.

Youngbluth, M. J. 1984. Water column ecology: *in situ* observations of marine zooplankton from a manned submersible. Pp. 45–57 in *Divers, Submersibles and Marine Science,* N. C. Fleming, ed. Memorial University of Newfoundland, Occasional Papers in Biology, Vol. 9.

Reference: *Biol. Bull.* **204**: 81–95. (February 2003)

Branchial Musculature of a Venerid Clam: Pharmacology, Distribution, and Innervation

LOUIS F. GAINEY, JR.[1,*], JAMES C. WALTON[1], AND MICHAEL J. GREENBERG[2]

[1] *Department of Biological Sciences, University of Southern Maine, Portland, Maine 04104; and* [2] *The Whitney Laboratory of the University of Florida, 9505 Ocean Shore Blvd., St. Augustine, Florida 32086*

Abstract. This study was meant to analyze the neural control of the branchial muscles of the clam *Mercenaria mercenaria*. Gills isolated from the animal contract in response to 5-hydroxytryptamine (5HT), dopamine (DA), and acetylcholine (ACh); but the ACh contraction occurred only if the gills had been pretreated with the cholinesterase inhibitor eserine. The 5HT antagonists cyproheptadine and mianserin blocked the contractile effects of all of the agonists. However, gills exposed to the 5HT antagonists and eserine relaxed in response to ACh. The DA antagonist SCH-83566 inhibited the effects of DA, but had no effect on contractions induced by 5HT and ACh. The ACh antagonist hexamethonium inhibited both the excitatory and inhibitory effects of ACh, but had no effect on contractions induced by 5HT and DA. 5HT and DA in gill tissue were visualized by using immunohistochemistry. Within each gill filament are dorsoventral neurons running adjacent to the epithelium and containing immunoreactive 5HT and DA. A complex network of 5HT-positive fibers is associated with the septa, blood vessels, and muscles, whereas DA-positive fibers are restricted to the septa. We propose that 5HT is the excitatory transmitter to the gill muscles, and that DA and ACh exert their excitatory effects by stimulating 5HT motor nerves. ACh may also be an inhibitory transmitter of the muscles.

Introduction

In most clams, the water current that supports respiration and feeding is driven through the gills by the beat of the lateral cilia. But the diameter and shape of the passages through the gill—and thus the flow of water—are controlled by contractions of the branchial musculature. These two fundamental activities of the branchial pump—ciliary and muscular—are regulated and coordinated by transmitters and modulators that are released at synapses by neurons that constitute an extensive network in the gill. The neural control of bivalve gill cilia has been extensively studied; this paper focuses on the musculature.

The gills of the venerid clam *Mercenaria mercenaria* are eulamellibranch and plicate (Kellogg, 1892). That is, the filaments are connected to adjacent filaments *via* tissue junctions, and the descending and ascending lamellae are connected to each other and thrown into a series of folds (the plicae) by interlamellar septa (Fig. 1). The dorsoventral spaces within the gill, defined by adjacent septa and the intervening plicae, are the water tubes. The plicae exist in two conformations (Fig. 1C): either their contours are smooth—the "primary folds" of Kellogg, or the "major plicae" of Eble (2001)—or smaller depressions appear at the apexes of the plicae, giving rise to "secondary folds" (Kellogg), or "minor plicae" (Eble). We have seen the plicae alternate between these two conformations. Dorsoventral blood vessels lie at the apex of each plica, within each septum, and within each filament (Kellogg, 1892; Eble, 2001). The blood channels of the branchial filaments are connected with the dorsoventral and septal blood vessels by a meshwork of horizontal blood vessels that are actually interlamellar abfrontal extensions of the filaments (see fig. 34 of the venerid *Tapes aurens* in Ridewood, 1903; fig. 4.20 in Eble, 2001; fig. 1 in Medler and Silverman, 2001). The horizontal meshwork of vessels (collectively called the "subfilamentar tissue"; see Ridewood, 1903) lines the water tubes (Fig. 1D).

That bivalve gills contain muscle fibers and are capable

Received 8 July 2002; accepted 12 December 2002.

* To whom correspondence should be addressed. Department of Biological Sciences, University of Southern Maine, PO Box 9300, Portland, ME 04104-9300. E-mail: gainey@usm.maine.edu

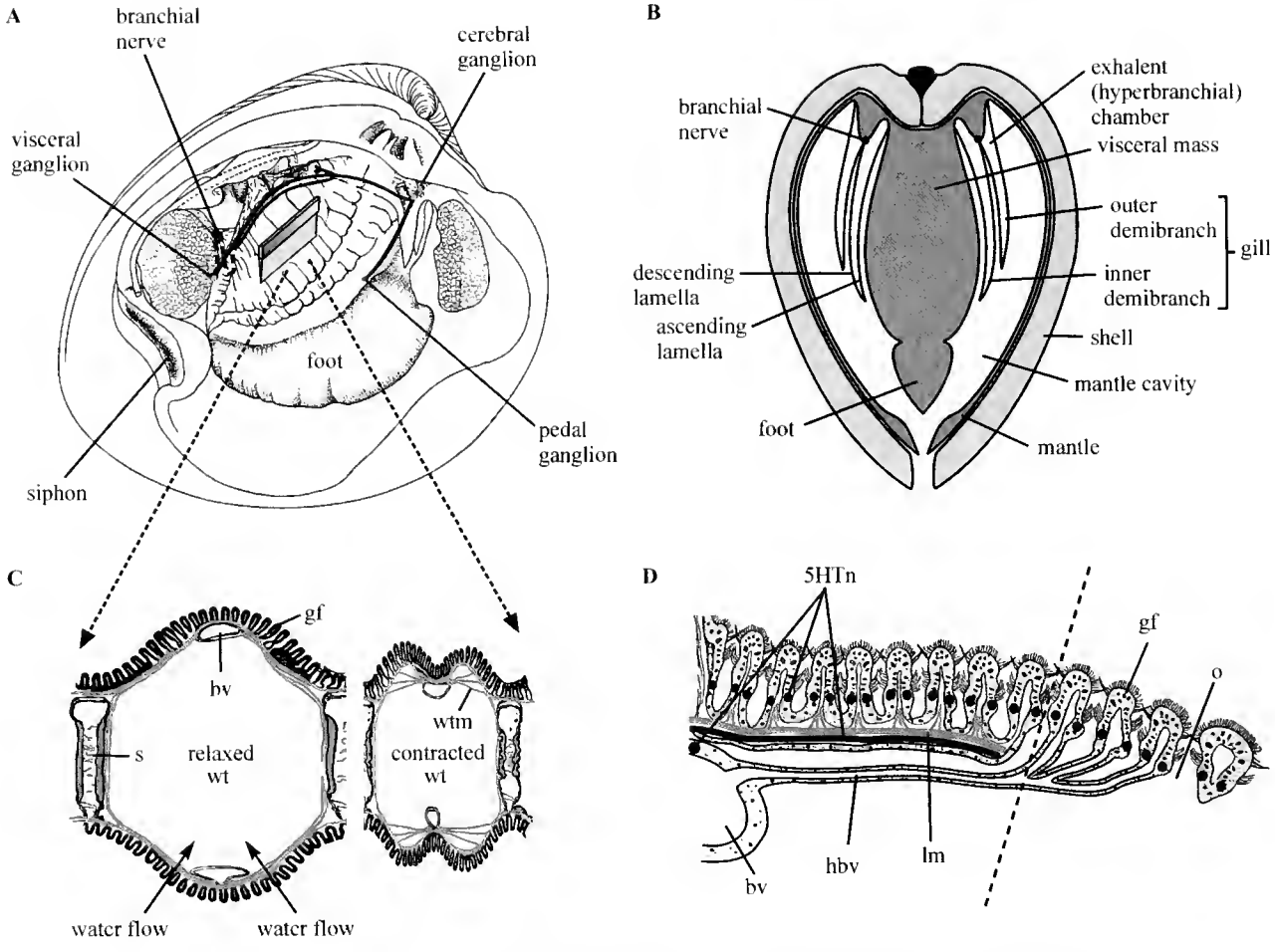

Figure 1. Diagramatic anatomy of *Mercenaria mercenaria:* adapted from various sources on the basis of our own observations. (A) A clam on the half shell. (B) Cross section of a clam. (C) Cross section of a water tube: with the musculature relaxed (left), and contracted (right). The water tube muscles are within the walls of the horizontal blood vessels; the vessels are not shown here. (D) Details of a relaxed demibranch (as in C, left). This cross section is slightly out of the horizontal plane; thus, the filaments to the left of the dashed line are at the level of the interfilamentar tissue junctions that contain the longitudinal muscles; whereas the filaments to the right of the line are at the level of the ostia and horizontal blood vessels. The walls of the horizontal blood vessels contain both the water-tube muscles and a dense network of serotonergic nerves; neither of these is shown. Abbreviations: bv = blood vessel; gf = gill filament; hbv = horizontal blood vessel; lm = longitudinal muscle; o = ostium; s = septum; wt = water tube; wtm = water tube muscle; 5HTn = serotonergic neuron.

of muscular activity has been known for over a hundred years since Kellogg (1892) published his observations on branchial anatomy and movement in a variety of bivalves, including *Mercenaria.* Longitudinal muscle fibers have been described in the interfilament tissue junctions and septa of *Mercenaria* (Kellogg, 1892; Ridewood, 1903; Eble, 2001) and many other bivalve gills. In addition to these longitudinal muscles, called "horizontal muscles" by Atkins (1943) and others, Medler and Silverman (1997) noted the presence of a diffuse network of muscle fibers in the water-tube epithelium of the non-plicate gills of *Dreissena polymorpha.* The plicate gills of *Mercenaria* lack a water-tube epithelium, but they contain a similar network of muscle fibers in the walls of the horizontal blood vessels (Fig. 1).

Neural elements occur within the filaments of both filibranch and eulamellibranch gills (*e.g.,* Setna, 1930; Aiello, 1990), but they also occur in the gills of eulamellibranchs (like *Mercenaria*) in association with the septa, blood vessels, and interfilamentar muscles; structures that, by definition, do not occur in filibranch gills. Indeed, neurons have been reported in association with the longitudinal muscles in a unionid mussel, *Ligumia subrostrata* (Dietz *et al.,* 1985), in *Mercenaria* (Gainey *et al.,* 1999a), and in an oyster, *Crassostrea virginica* (Nelson, 1960). Nerves have

also been observed in the interlamellar septa in *Solen marginatus* and *Ensis siliqua* (Atkins, 1937), *Mercenaria* (Gainey *et al.*, 1999a), and *Crassostrea* (Nelson, 1960, Galtsoff, 1964); and in the water-tube muscles and ostia of *Mercenaria* (Candelario-Martinez *et al.*, 1993).

An extensive literature indicates that the flow of water through bivalve gills varies continuously within wide limits in response to both physical and biological factors (summarized by Dame, 1996; Jorgensen, 1996; Bayne, 1998). But the lateral cilia in both *Mercenaria* and *Mytilus edulis* beat only within a relatively narrow range of frequencies (about 10–25 beats/s) (Aiello, 1960; Catapane, 1983; Gainey *et al.*, 1999a), so the stimulatory and inhibitory motor nerves to the cilia seem to be activating a simple on-off switch. Medler and Silverman (2001) found, in *Mercenaria*, that the geometry of the water tubes changed, and their diameters decreased, in response to 5-hydroxytryptamine (5HT; serotonin). Such changes would tend to modify flow (Grunbaum *et al.*, 1998), so changes in the tone of the branchial musculature might well be participating in the continuously variable regulation of water flow through the gill.

Although the branchial muscles have the potential to modulate water flow through the gills, and neural elements are clearly present, the pharmacology and neural control of these muscles has received relatively little attention. In brief, acetylcholine (ACh) contracts the gill muscles in both *Dreissena polymorpha* and *Corbicula fluminea* (Snow *et al.*, 1995; Medler and Silverman, 1997), whereas 5HT relaxes the gill muscles of *Ligumia subrostrata* (Gardiner *et al.*, 1991) and contracts those of *Mercenaria* (Gainey *et al.*, 1998; Medler and Silverman, 2001). In addition, the peptide FMRFamide contracts the gill muscles of *Dreissena* (Medler and Silverman, 1997). The relationships between the effects of possible neurotransmitters on gill muscles, the distribution of these agents in identifiable neural networks, and the interactions among the elements of the networks are at present unexplored.

We have been using the gill of the quahog *Mercenaria mercenaria* to study the neural control of branchial water flow. In a previous study, we found that 5HT and dopamine (DA), respectively, switch the activity of the lateral cilia on and off, and that YFAFPRQamide, an SCP-like peptide endogenous to *Mercenaria*, modulates the effects of DA (Gainey *et al.*, 1999a). Now we report on the pharmacology of the branchial muscles, focusing especially on the actions of 5HT, DA, ACh, and their antagonists. We have also investigated the distribution of the branchial muscles and their innervation by immunoreactive serotonergic and dopaminergic nerves, expecting the findings to be consistent with our pharmacological observations. Preliminary results of this study have been presented to the Society for Integrative and Comparative Biology (Gainey *et al.*, 1998, 2001).

Materials and Methods

Animals

Quahogs (*Mercenaria mercenaria* L.) that had been dug from various locales along the northeast Atlantic coast were purchased from Harbor Fish, Portland, Maine. The animals were held at 10 °C in natural seawater (30 ppt) on a 12-h light/dark cycle. Individuals were held a minimum of 3 days before use.

Gill preparation and apparatus

Gills were dissected away from the body wall and separated into demibranchs, and the branchial nerves removed (Fig. 1). Muscular contractions were recorded as changes in the length of the anterior-posterior axis of the isolated demibranchs.

Contractions of the branchial muscles were recorded in either of two ways: (1) Isolated demibranchs were suspended in organ baths and attached with thread to isometric force transducers (Grass FT03 and UFI 1030) equipped with springs; the resulting contractions were therefore semi-isotonic. The transducers were interfaced to Biopac DA 100 amplifiers and a Biopac MP100 analog-to-digital converter. (2) Ultratrasonic crystal transceivers (Sonometrics) were tied to the ends of demibranchs with thread. One end of the demibranch was pinned to a piece of rubber band that was glued with rubber cement to the bottom of a plastic petri dish (4.7-cm diameter); the petri dishes were placed on a cooling plate to maintain temperature. Under these conditions, the muscles were unrestrained and contracted against virtually no external load. The isotonic contractions were measured with a digital ultrasonic measurement system (Sonometrics TRX series 8). In both cases, the magnitude of the contractions was measured with AcqKnowledge version 3.5 (Biopac Systems).

All experiments were carried out at 10 °C in aerated artificial seawater (ASW; recipe in Welsh *et al.*, 1968). To retard the oxidation of dopamine (DA), the water was buffered with an ascorbic acid buffer as described by Malanga (1975); this buffered seawater was used in all of the experiments.

Production and analyses of dose-response curves

Our initial experiments were performed with force transducers; but prolonged contraction against the load of the springs used with these devices caused the gill muscles to fatigue. Consequently, we exposed each demibranch only once to a single concentration of agonist, and the dose-response curve was constructed from these individual responses. In later experiments with the Sonometrics digital ultrasound measurement system, no external force was applied to the muscles. No evidence of fatigue was observed,

so a single demibranch could be used to construct an entire dose-response curve. Because the response to serotonin (5HT) and DA has a seasonal component (Gainey, pers. obs.), the dose-response data reported here were collected between November and July.

All contractions and relaxations, measured in millimeters, were expressed as a percentage of the initial length of each demibranch. Regression lines were fitted with a logistic function of the form: response = $\alpha/1 + \exp(\beta_0 + \beta_1 * \log(\text{agonist}))$, where α is the asymptotic value of the maximal contraction, and β_0 and β_1 are intercept and slope parameters. Initially, all three parameters were estimated using nonlinear regression (Systat, v 9); later, α was fixed in the model, reducing the error estimates of the remaining parameters. The concentrations of agonist giving half-maximal responses (EC_{50}) were estimated according to the following formula: $EC_{50} = 10\text{^}(-\beta_0/\beta_1)$.

Effects of antagonists

Each of the four demibranchs from the same clam were suspended in an organ bath and attached to a force transducer. After 15 min of relaxation, each of the demibranchs was exposed to an agonist at a standard concentration: 5HT = 2×10^{-5} *M*; DA and acetylcholine (ACh) = 5×10^{-5} *M*. After the resulting contractions had stabilized, the baths were flushed, and an antagonist at 10^{-4} *M* was added to three of the four demibranchs. After 60 min, the standard dose of agonist was reapplied to all four demibranchs, with the antagonist still present on the three demibranchs. The total number of demibranchs treated with a specific antagonist is given in the data tables.

The effect of the antagonist was expressed as the ratio between the second and first agonist-induced contraction (contraction ratio). Analysis of the contraction ratios of untreated controls with a Kolmogorov-Smirnov one-sample test revealed that these data were not normally distributed ($P < 0.001$, two-tailed, $n = 139$). The contraction ratios were therefore normalized by a logarithmic transformation, and the normality of this transformation was checked as above (Kolmogorov-Smirnov; $P = 0.614$). The ln transformed ratios of the controls were tested against a mean of 0 (since ln 1 = 0) with a one-sample *t* test. This is mathematically equivalent to a paired *t* test because the contractions used to construct the ratios were from the same demibranch.

Since the contraction ratios of the controls for 5HT, DA, and ACh were all significantly greater than 1, the normalized contraction ratios of the antagonists were compared to the normalized contraction ratios of the appropriate agonist control using *post hoc* paired Tukey HSD tests after an initial one-way ANOVA. But some of the antagonist contraction ratios were 0, thus these ratios become undefined by a logarithmic transformation. To overcome this limitation, 0.1 was added to all contraction ratios prior to the logarithmic transformation. Although the statistical tests were performed on the ln-transformed data, tabular data are presented in the Results section untransformed for clarity. The *P* values reported for these tests are one-tailed probabilities; *P* values less than 0.05 were considered significant. In some of the experiments—*e.g.*, ACh after exposure to cyproheptadine or mianserin—the gills relaxed rather than contracted; these data are coded in the tables as negative values.

The concentration of antagonist that produced 50% inhibition (IC_{50}) was calculated using the experimental design described above, except that the demibranchs were exposed to lower concentrations of antagonists. Contraction ratios—*i.e.*, the ratios of the second to the first contractions—were regressed against the log of the concentration of antagonist. Because the contraction ratios were significantly greater than 1 for all of the controls, the IC_{50} was calculated by solving the regression equation for a contraction ratio that was 50% of the mean contraction ratio of the control.

Branchial anatomy

For relaxed specimens, isolated demibranchs were kept overnight, at 5 °C, in isotonic $MgCl_2$ in ASW (7.6% $MgCl_2$ in distilled water added to an equal volume of ASW). For contracted specimens, the isolated demibranchs were placed in 10^{-4} *M* 5HT immediately after dissection. To observe the inner face of the water tubes, we cut dorsoventrally along several septa with fine scissors, separating a section of the demibranch into two layers. One of these was removed, and the remainder of the demibranch was then pinned to the bottom of a small petri dish, which had been coated with Sylgard. Fixation—always carried out at 5 °C—varied with the object to be observed (*e.g.*, muscle, 5HT, DA) and is described below. Because mammalian antibodies were used for the immunohistochemistry, subsequent rinses and solutions were made with mammalian phosphate-buffered saline (PBS).

Crysostat sections were prepared as follows. After fixation and a 15-min rinse in PBS (0.1 *M* sodium phosphate, 140 m*M* NaCl; pH 7.3), the demibranchs were placed in a solution of 30% sucrose/PBS overnight at 5 °C. Pieces of demibranch were then placed in Tissue Tek OCT compound, frozen, and sectioned at 12 μm. Sections were placed on gel-coated slides and stored at −20 °C until used.

Thick sections were prepared as follows. After fixation and three 15-min rinses in PBS, pieces of demibranch were placed in a plastic mold and covered with 12% Type A pigskin gelatin in 0.1 *M* PBS that had been heated to 50 °C. After the gelatin had cooled, the tissue was sectioned at 100 μm with a vibratome. The sections were heated briefly at 50 °C on gel-coated slides to melt the excess gelatin.

We usually processed whole mounts and sections simultaneously and therefore followed a schedule designed for whole mounts. All of the steps in this protocol were carried out at 5 °C.

- After fixation, rinse four times (1 h for each rinse) in PBS (0.1 *M*, pH 7.3); or for DA, in 0.05 *M* PBS with 1% sodium metabisulfite.
- Incubate overnight in blocking solution (0.25% goat serum/1% Triton X-100/1% BSA/PBS); for DA, include 1% sodium metabisulfite.
- Incubate overnight in primary antibody diluted appropriately with PBS.
- Rinse four times in PBS (two 30-min rinses, one overnight rinse, one 30-min rinse).
- Incubate overnight in secondary antibody, phalloidin, or both, the reagents diluted appropriately in PBS.
- Rinse three times in PBS (1 h, overnight, 1 h).
- Mount the specimens under coverslips in 60% glycerol-1% *n*-propyl gallate/PBS.

Muscle. The branchial muscles were visualized with phalloidin conjugated to the fluorescent probe Alexa Fluor 488 (Molecular Probes, Eugene, Oregon), the conjugate used in a concentration of 1 unit/100 μl in 0.1 *M* PBS. For single-stained preparations, whole mounts were fixed for 1 h in 4% formaldehyde with 0.01 *M* PBS (pH 7.3; 530 m*M* NaCl), rinsed twice, and then stained overnight. To double-label immunochemically stained preparations, the phalloidin was added to the tissues at the same time as the secondary antibody.

5HT and YFAFPRQamide. Pieces and sections of demibranch were fixed overnight in 4% paraformaldehyde in 0.01 *M* PBS (pH 7.3; 530 m*M* NaCl); the fixative was prepared as described in Gainey *et al.* (1999a). For 5HT, the primary polyclonal antiserum was raised in rabbit to 5HT conjugated to BSA with paraformaldehdye (Diasorin, Stillwater, Minnesota). For YFAFPRQamide, the primary polyclonal antiserum was raised in rabbit to the peptide conjugated to thyroglobulin (custom synthesis, etc., by SynPep, Dublin, California). In both cases, the secondary antibody was raised in goat to rabbit IgG conjugated to Alexa Fluor 594 (Molecular Probes).

Dopamine. Pieces and sections of demibranch were fixed for 2 h in 5% glutaraldehyde/1% sodium metabisulfite/PBS (0.01 *M;* pH 7.3; 530 m*M* NaCl). The primary polyclonal antiserum was raised in rabbit to DA conjugated to BSA with glutaraldehyde (Diasorin). The secondary antibody was raised in goat to rabbit IgG and conjugated to Alexa Fluor 594 (Molecular Probes). For negative controls, the primary antibodies were omitted from a slide in each series of preparations.

Confocal images of 5HT distribution were made with a Leica LSCM SP2 microscope at the Whitney Laboratory, St. Augustine, Florida. Fluorescent images were made with a Nikon Eclipse TE200 microscope equipped with a Spot RT digital color camera (Diagnostic Instruments). Images were prepared for publication with Adobe Photoshop.

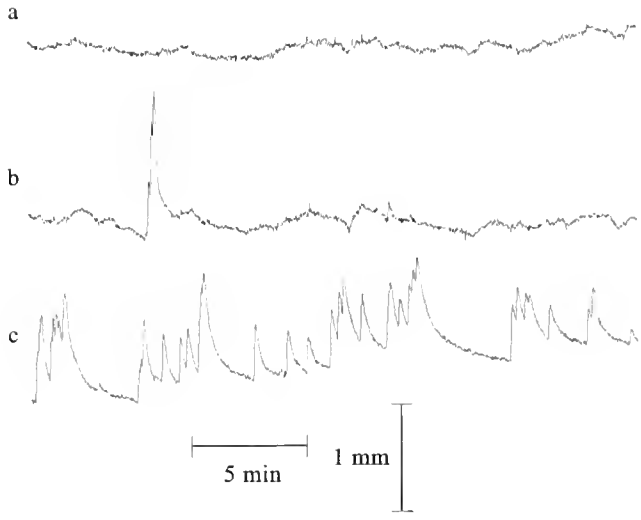

Figure 2. Traces of contractile activity recorded from three untreated demibranchs taken from a single clam. (A) Quiescent. (B) Occasional, spontaneous contraction. (C) Arrhythmic, spontaneous contractions. Contractions were recorded with force transducers.

Drugs

All chemicals were purchased from Sigma-Aldrich, St. Louis, Missouri, or ICN Pharmaceuticals, Costa Mesa, California. The specificities of the antagonists listed in the tables were obtained from the *Cell Signaling & Neuroscience* catalog (2000/2001 ed.) of Sigma/RBI.

Results

Activity of isolated gills

Most of the isolated demibranchs were quiescent in the organ baths (Fig. 2a), but occasionally gills would contract spontaneously and relax (Fig. 2b), and on rare occasions they would beat arrhythmically (Fig. 2c). All three demibranchs in Figure 2 were from the same clam; the fourth, not pictured, was also quiescent. Of the hundreds of preparations we have observed, only a handful showed the spontaneous, arrhythmic contractions seen in Figure 2c.

Pharmacology of branchial muscles

Agonists. 5HT, DA, and ACh contracted the gill muscles in a dose-dependent manner, but the response to ACh was observed only in gills pretreated for 15 min with 10^{-4} *M* eserine (Fig. 3). The responses to all three agonists were

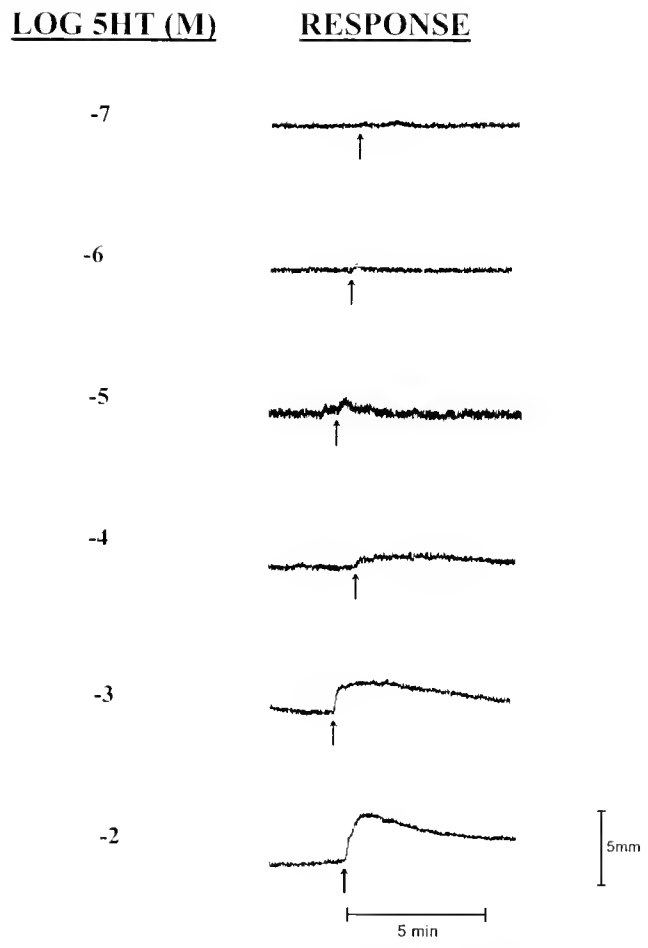

Figure 3. Traces of contractions in response to increasing concentrations of 5HT; successive doses were added at the arrows. Each response is from a separate demibranch; data were recorded with force transducers.

indistinguishable: the gills contracted tonically and, after 30 s to several minutes, reached their maxima.

Dose-response curves for the three agonists were prepared (Fig. 4), and their characteristics are listed in Table 1. The rankings of the EC_{50} values are ACh < 5HT < DA, and since the 95% confidence intervals do not overlap, the values are statistically different. The maximal contractions in response to 5HT and DA are equal, and both are significantly larger than the maximal contractions induced by ACh. The comparative data noted above were independent of the method used to record the contractions. However, if we consider each agonist separately, then its EC_{50} is significantly less, and its induced contractions were larger (except for DA) when the contractions were recorded with the digital ultrasound system rather than with force transducers (Table 1).

The following neurotransmitters, all applied to the tissue at 10^{-4} *M*, neither contracted nor relaxed the gills: ATP, GABA, histamine, and octopamine. Furthermore, the following three peptides—all found in *Mercenaria* and all applied at 10^{-6} *M*—neither contracted nor relaxed the gills: FMRFamide, AMSFYFPRMamide, and YFAFPRQamide.

Previously, we found that YFAFPRQamide modulates the effects of DA on the lateral cilia and those of 5HT on the frontal cilia (Gainey *et al.*, 1999a). Therefore, to determine whether the peptide would modulate the effects of 5HT or

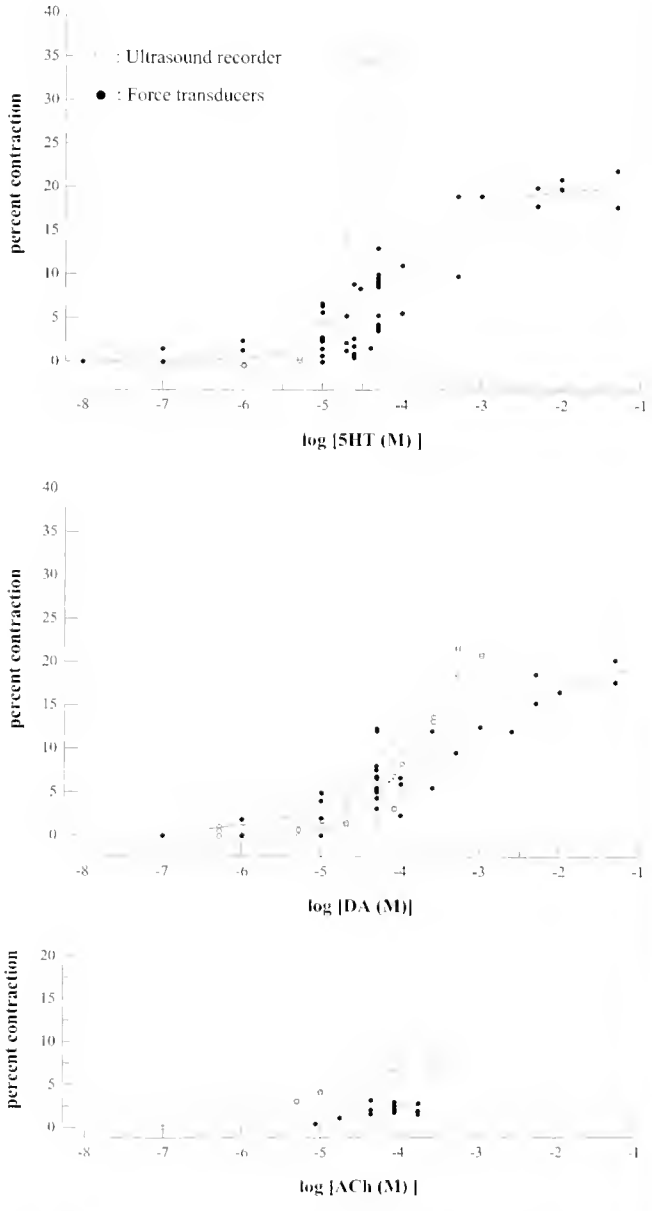

Figure 4. Dose-dependent muscle contractions (as percentages of the resting length) in response to 5HT, DA, and ACh. Solid circles and lines: data recorded with force transducers; each datum is the response of a separate demibranch. Open circles on dashed lines: data recorded with an ultrasound system from either two (5HT, ACh) or five (DA) demibranchs; each preparation was exposed to increasing concentrations of agonist. Demibranchs exposed to ACh were pretreated with 10^{-4} *M* eserine.

Table 1

Summary of dose-response effects for 5HT, DA, and ACh

Agonist	Type*	EC_{50} (M)†	(95% CI)‡	Cmax (%)§	(95% CI)‡
5HT	ft	1.1×10^{-4}	$(0.5–1.8 \times 10^{-4})$	20	(17–23)
	us	2.1×10^{-5}	$(1.9–2.5 \times 10^{-5})$	33	(28–38)
DA	ft	5.9×10^{-4}	$(2.3–9.5 \times 10^{-4})$	21	(14–29)
	us	1.4×10^{-4}	$(1.2–1.7 \times 10^{-4})$	32	(17–48)
ACh	ft	1.5×10^{-5}	$(0.34–3.3 \times 10^{-5})$	2	(1–3)
	us	8.6×10^{-6}	$(0.2–1.3 \times 10^{-5})$	9	(7–11)

* ft = force transducers used to measure contractions; us = ultrasound used to measure contractions.
† Concentration of agonist giving a half maximal response.
‡ 95% confidence intervals associated with the estimates.
§ Maximal predicted contraction.

DA on the muscle, we applied YFAFPRQamide to the demibranchs before exposing them to 2×10^{-5} *M* 5HT or DA. At concentrations ranging from 10^{-9} to 10^{-6} *M* (5HT) or 10^{-8} to 10^{-6} *M* (DA), and exposures ranging from 15 min to 1 h (5HT) or 1 h (DA), the peptide had no effect upon contractions induced by either 5HT or DA.

Antagonists. Because the three effective agonists contract the gill, and since the mechanical responses to 5HT, DA, and ACh are indistinguishable, we asked whether the muscles have receptors for each of the agonists, or whether one or more of the agonists are acting indirectly by stimulating the release of another agonist from motor nerves. To test these possibilities, antagonists were sought for each agonist, and these agents were cross-tested against the other agonists.

- ***Controls.*** In control experiments, each gill received two consecutive, equal doses of the same agonist. For each of these agonists, the second contraction in response to the same concentration was usually larger than the first, and the contraction ratios were significantly greater than 1 (Table 2). Moreover, when

Table 2

The effect of antagonists on the actions of 5HT, DA, and ACh

Antagonist	Type*	Agonist†	Mean contraction ratio ± SD (*n*)‡	*P*§
None (control)	—	5HT	2.20 ± 1.86 (72)	<0.001*p
None (control)	—	DA	2.18 ± 1.74 (46)	<0.001*p
None (control)	—	ACh	3.21 ± 3.65 (18)	0.001*p
Cyproheptadine	$5HT_2$	5HT	0.324 ± 0.495 (11)	<0.001*i
		DA	0.076 ± 0.162 (10)	<0.001*i
		ACh	−1.19 ± 2.10 (9)	*r
Mianserin	$5HT_2$	5HT	0.475 ± 0.193 (8)	0.002*i
		DA	0.494 ± 0.490 (8)	<0.001*i
		ACh	−0.449 ± 0.701 (9)	*r
SKF-83566	DA_1	DA	0.483 ± 0.300 (9)	0.003*i
		5HT	0.869 ± 0.233 (9)	0.32
		ACh	0.881 ± 0.530 (3)	0.22
Hexamethonium	ACh_n	ACh	0.215 ± 0.262 (5)	<0.001*i
		DA	1.05 ± 0.593 (6)	0.49
		5HT	2.14 ± 0.850 (8)	0.50

* The primary type of mammalian receptor blocked by the antagonist.
† Agonist concentrations: 5HT = 2×10^{-5} *M*; DA & ACh = 5×10^{-5} *M*. Antagonist concentrations were 10^{-4} *M*.
‡ Contraction ratio: height of contraction after exposure to the antagonist/height of contraction before exposure to the antagonist.
§ *P* values are one-tailed probabilities: *i = significant inhibition; *p = significant potentiation; *r = relaxation, the second contraction was coded as a negative value.

Table 3

Antagonists that had no significant effect upon the action of 5HT and DA

Antagonist	Type*	Agonist†	Mean contraction ratio ± SD (*n*)‡	*P*§
Ergonovine	DA/5HT	5HT	1.42 ± 1.38 (4)	0.5
NAN-190	$5HT_{1A}$	5HT	1.66 ± 1.52 (6)	0.49
Ketanserin	$5HT_2$	5HT	1.68 ± 1.15 (6)	0.5
Ritanserin	$5HT_2$	5HT	1.47 ± 1.67 (7)	0.49
MDL 72222	$5HT_3$	5HT	3.50 ± 1.73 (6)	0.43
Tropisetron	$5HT_3$	5HT	1.78 ± 0.680 (6)	0.5
Bulbocapnine	DA	DA	3.58 ± 6.29 (6)	0.50
Butaclamol	DA	DA	1.78 ± 1.60 (17)	0.33
Ergonovine	DA/5HT	DA	1.55 ± 1.24 (4)	0.50
Apomorphine	DA_2	DA	4.23 ± 4.93 (7)	0.49
Chlorpromazine	DA_2	DA	3.60 ± 1.06 (5)	0.45
Fluphenazine	DA_2	DA	2.60 ± 1.61 (6)	0.50
Pimozide	DA_2	DA	2.72 ± 1.67 (6)	0.50
Spiperone	DA_2	DA	1.04 ± 0.812 (16)	0.28
Sulpiride	$DA_{2/3}$	DA	0.580 ± 2.23 (8)	0.50

* The primary type of mammalian receptor blocked by the antagonist.

† Agonist concentrations: 5HT = 2×10^{-5} *M*; DA = 5×10^{-5} *M*. Antagonist concentrations were 10^{-4} *M*.

‡ Contraction ratio: height of contraction after exposure to the antagonist/height of contraction before exposure to the antagonist.

§ *P* values are one-tailed probabilities.

ANOVA was performed, none of the contraction ratios were significantly different from each other [$F(2, 132) = 1.315$; $P = 0.272$]. These control responses rendered the usual analytical techniques inapplicable, so the effects of antagonists were examined with the statistical tests described in the Methods section.

- ***5HT.*** The effects of 5HT were inhibited by the $5HT_2$ antagonists cyproheptadine and mianserin. The IC_{50} for cyproheptadine was 1.2×10^{-7} *M*, while that for mianserin was 1.6×10^{-5} *M*. These antagonists also blocked the effects of DA and, unexpectedly, caused ACh to relax the gill muscles (Table 2). The following 5HT antagonists were ineffective at 10^{-4} *M*: ergonovine, NAN-190, ketanserin, ritanserin, MDL 72222, and tropisetron (Table 3).
- ***DA.*** SKF-83566, a DA_1 antagonist, significantly inhibited the effects of DA but had no effect upon the activity of either 5HT or ACh (Table 2). The IC_{50} for SKF-83566 was 3.0×10^{-5} *M*. The following DA antagonists were ineffective at 10^{-4} *M*: bulbocapine, butaclamol, ergonovine, apomorphine, chlorpromazine, fluphenazine, pimozide, spiperone, and sulpiride (Table 3).
- ***ACh.*** Hexamethonium, an ACh_n antagonist, significantly inhibited the relatively small contractions induced by ACh, but hexamethonium had no effect upon the activity of either 5HT or DA (Table 2). The IC_{50} for hexamethonium was 1.0×10^{-5} *M*.

When gills were pretreated, not only with 10^{-4} *M* eserine, but also with 10^{-4} *M* cyproheptadine or mianserin, then ACh would produce a dose-dependent relaxation of the branchial muscles. For gills treated with cyproheptadine, the EC_{50} was 3.3×10^{-5} *M* (95% CI: 2.3×10^{-5} to 4.3×10^{-5} *M*), and the maximal relaxation was 6.2% (95% CI: 3.9% to 8.5%; Fig. 5). For gills treated with mianserin, the EC_{50} was

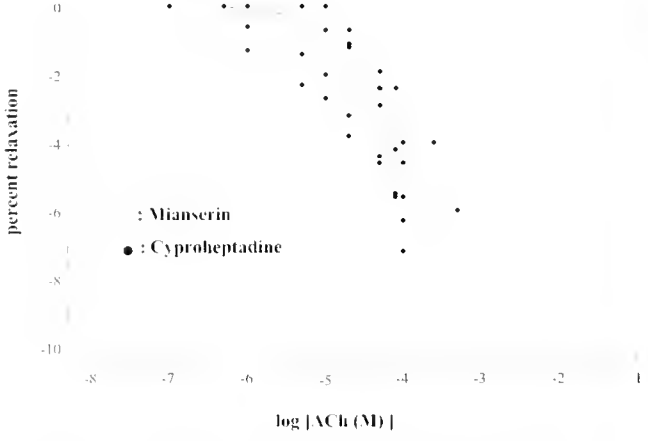

Figure 5. Dose-dependent muscle relaxation in response to ACh. Relaxations were expressed as a percentage of the resting length, and plotted as a negative value. Solid circles: data from five demibranchs pretreated with 10^{-4} *M* cyproheptadine. Open circles: data from four demibranchs pretreated with 10^{-4} *M* mianserin. In addition, all demibranchs were pretreated with 10^{-4} *M* eserine. Data were recorded with an ultrasound system. Ultrasound echoes in the organ baths prevented the measurements of some of the responses.

5.5×10^{-5} *M* (95% CI: 4.0×10^{-5} to 7.0×10^{-5} *M*); and the maximal relaxation was 6.1% (95% CI: 4.3% to 7.8%; Fig. 5). The ranges of the 95% confidence intervals for both the EC_{50} and the maximal relaxation overlap; that is, the parameters are not different.

Branchial anatomy

Distribution of muscles in the gill. The structure and disposition of the branchial musculature in the inner and outer demibranchs are indistinguishable, and three groups of these muscles have been observed: longitudinal muscles, dorsoventral muscles, and water-tube muscles. The well-defined longitudinal muscle bands are about 50 μm wide and about 125 μm apart. They run at right angles to the gill filaments, at their base, and are contained within the interfilament tissue junctions that hold adjacent filaments together. The longitudinal muscle bands run the length of a demibranch, passing through each septum, and between each dorsoventral blood vessel and the filaments lying over it (Fig. 6A, B, C).

The dorsoventral muscles run through the center of each gill filament. Where the gill filaments intersect with the interfilament tissue junctions, these dorsoventral muscles send branches into the underlying longitudinal muscles (Fig. 6B).

The water-tube muscles form a complex, but regular, lattice-like network associated with the horizontal blood vessels of the subfilamentar tissue (Fig. 6A). Because most of these muscles cross the septa—from one side of a water tube to the other—and appear to be continuous with the network of muscle fibers within the blood vessels, they form a mesh of circular muscles within the inner wall of each water tube. In cross section, at least some of these muscles also run diagonally from the abfrontal face of the gill filaments towards the septa and blood vessels (Fig. 6C).

Finally, comparison of relaxed and contracted gills revealed the following: (1) the distance between adjacent septa decreased; (2) the vertical spacing between the longitudinal muscle bands decreased, as well as the vertical spacing between the water-tube muscles; and (3) the interfilament space decreased (Fig. 6D). As a result of muscle contraction, the outer, frontal, faces of the gills take on a zigzag appearance. In addition, in freshly dissected gills in which the water tube had been cut open, we observed that if the blood vessel was gently pinched, contraction of the water-tube muscles brought the blood vessel towards the center of the water tube. This resulted in the formation of secondary folds (plicae) and decreased the cross-sectional area of the water tube (Fig. 1C). The blood vessel also constricted in response to the mechanical stimulation.

Distribution of 5HT in the gill. Two distinct networks of immunoreactive serotonergic varicose nerve fibers are observable in the gill. Each gill filament contains two dorsoventral nerves that run under the epithelium near the lateral cilia and parallel to the dorsoventral muscle fibers (Fig. 6B); we observed no cross connections between the two fibers within a filament.

The second, more complex, network of serotonergic fibers is associated with the gill musculature; the unit of this network is a water tube. First, two large bundles of nerves run dorsoventrally within the septa, and another large bundle runs the length of each of the blood vessels. In addition to these large dorsoventral bundles, four finer ones run parallel to the septa, and two run parallel to the large nerve bundle in the blood vessel (Fig. 6E). These fine dorsoventral nerves are all associated with the subfilamentar tissue. Longitudinally disposed nerves run at right angles to and between the septa and the blood vessels in each water tube; these cross connectives are located within the interfilament tissue junctions adjacent and parallel to the longitudinal muscles (Fig. 6B). We also observed what appear to be fine branches of this longitudinal nerve running into the dorsoventral muscles of the filament (see the filament just above the measurement bar in Fig. 6B). Other longitudinal nerves are associated with the water-tube muscles (Fig. 6E). Finally, we observed connections between the dorsoventral nerves within the gill filaments and those associated with the longitudinal muscles. The primary antibody was omitted from the control sections (not shown), which had minimal background fluorescence comparable to the background in Figure 6E.

Distribution of DA in the gill. Immunoreactive dopamine was found only in the gill filaments and the septa. Within the gill filament epithelium, there are several pairs of dorsoventral cords (Fig. 6F). When viewed from the outer face of the gill, these cords have a granular, rather than a smooth, appearance. The dopaminergic fibers that are confined to the septal epithelium are a pair of bundles connecting the ascending and descending lamellae (Fig. 6F, G). Thus, each septum contains paired cross connectives that are stacked vertically in the gill and spaced at about the same distance as the longitudinal muscles. No dopaminergic fibers are associated with either the longitudinal or water-tube muscles. Moreover, control sections prepared without the primary antibody (not shown) had minimal background fluorescence, comparable to the background in Figure 6F.

Distribution of YFAFPRQamide in the gill. Immunoreactive YFAFPRQmide was concentrated in the outer half of the gill filament epithelium (Fig. 7). Weak fluorescence was found in the subfilamentar tissue (the abfrontal face of the filaments) and the blood vessel epithelium. The level of fluorescence in the musculature was comparable to background fluorescence in negative controls.

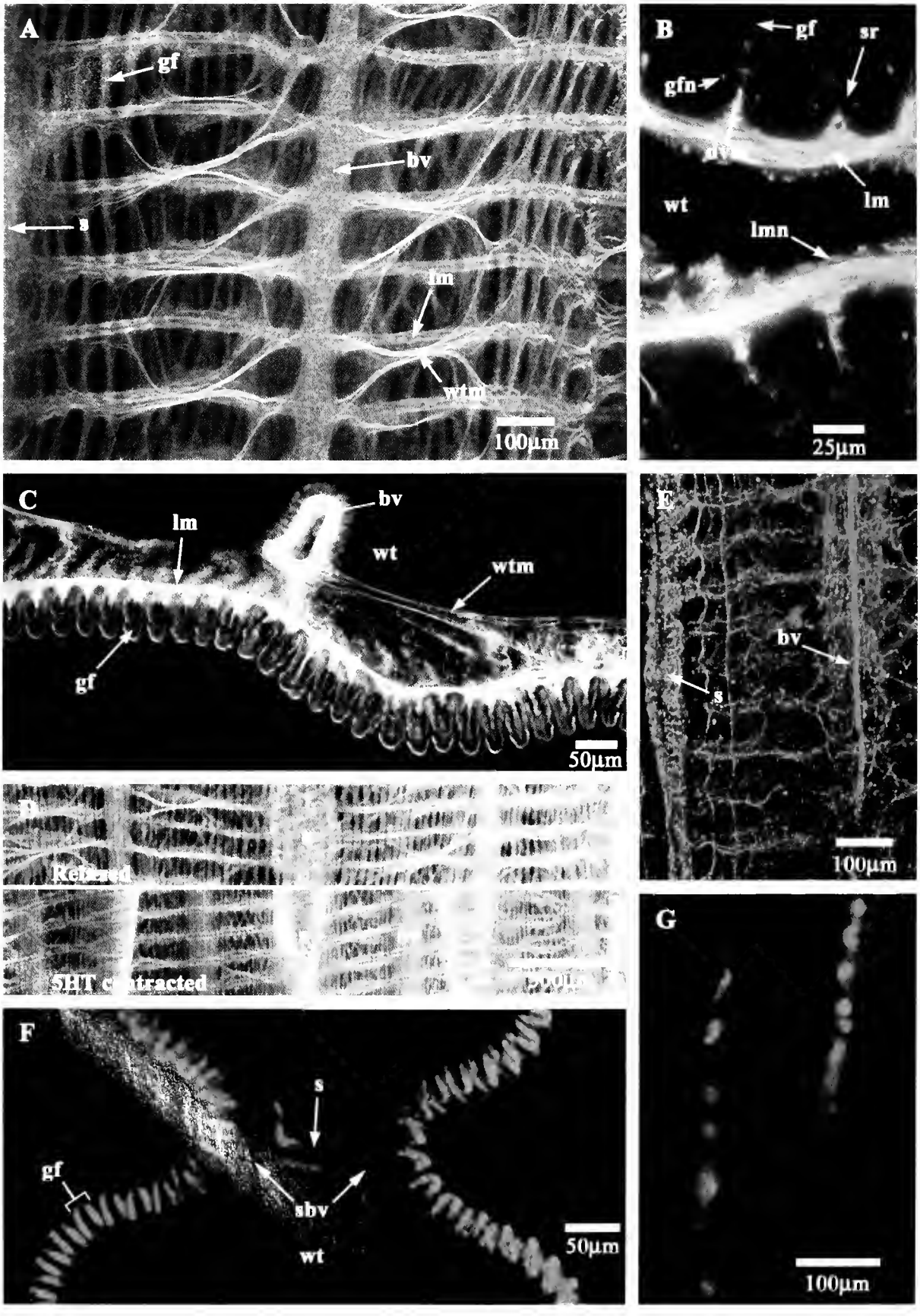
A
gf
bv
s
lm
wtm
100µm
B
gf
sr
gfn
dv
wt
lm
lmn
25µm
C
bv
lm
wt
wtm
gf
50µm
D
Relaxed
5HT contracted
E
bv
s
100µm
F
s
gf
sbv
wt
50µm
G
100µm

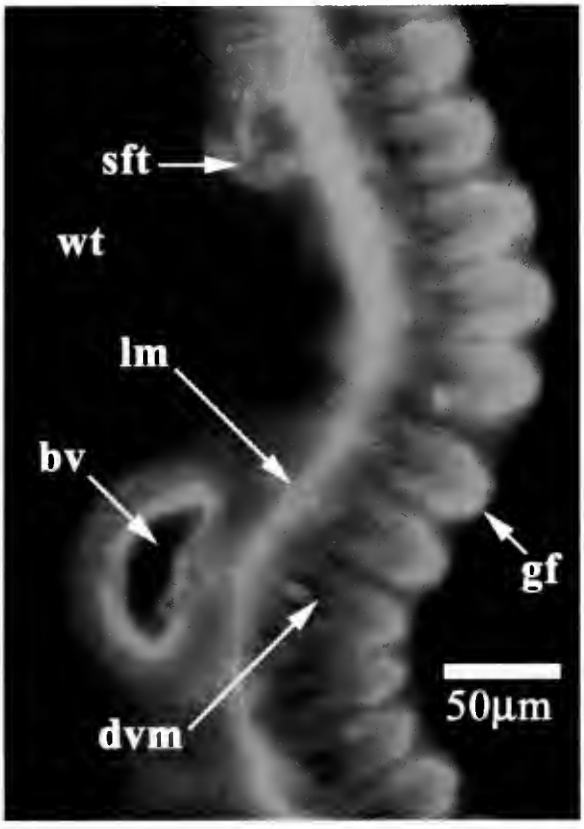

Figure 7. Thick (100 μm) cross section of a demibranch showing the distribution of muscle fibers and the SCP-like peptide YFAFPRQamide. The muscle fibers are stained with phalloidin and fluoresce green. Red fluorescence is associated with YFAFPRQamide and is concentrated in the tips of the filaments, but lesser amounts are also found on the abfrontal face of the filaments in the subfilamentar tissue. Abbreviations: bv = blood vessel; dvm = dorsoventral muscle; gf = gill filament; lm = longitudinal muscle; sft = subfilamentar tissue; wt = water tube.

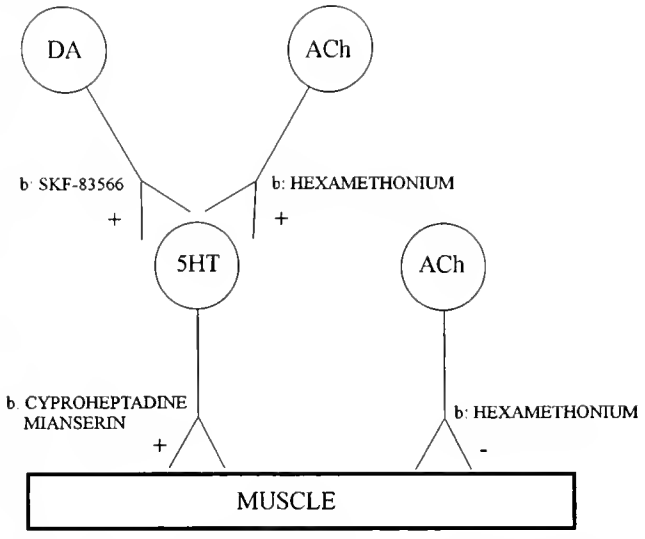

Figure 8. A diagrammatic summary of the most parsimonious model of the control of gill muscle. Abbreviations: b = block by specific antagonists; + = postsynaptic stimulation; − = muscle relaxation. Based upon our immunohistochemical observations, we hypothesize that the synapses between the DA and 5HT neurons are within the gill septa. See text for further details.

Discussion

We have shown that isolated demibranchs of *Mercenaria* contract in response to 5-hydroxytryptamine (5HT), dopamine (DA), and acetylcholine (ACh). Moreover, although two 5HT antagonists block the excitatory effects of all three agonists, the DA and ACh antagonists act specifically, blocking only the effects of their respective agonists. We have also demonstrated that immunoreactive 5HT is localized in varicose fibers associated with the longitudinal and water-tube muscles, whose contractions were recorded in the pharmacological experiments. The DA-containing fibers, in contrast, are not associated with these muscles. We hypothesize, therefore, that 5HT is the excitatory transmitter released at neuromuscular junctions in the gill, whereas DA and ACh act by stimulating serotonergic motor neurons (Fig. 8). Furthermore, because the networks of DA- and 5HT-containing neurons are distinct in their distribution and overlap most extensively in the septa, we suggest that these

Figure 6. Anatomical details of branchial muscles and nerves. The muscle fibers are stained with phalloidin and fluoresce green; the neurons are immunochemically stained for 5HT or DA and fluoresce red. (A) Inner face of a water tube showing the iterated arrangement of muscle fibers. (B) Cross section (12 μm) of a demibranch showing immunoreactive serotonergic neurons associated with branchial muscle. (C) Thick (100 μm) cross section of a demibranch showing muscle fibers associated with the gill filaments and blood vessel. (D) Inner face of two water tubes, top with muscles relaxed, bottom with muscles contracted in response to 10^{-4} *M* 5HT. (E) Inner face of a water tube showing the distribution of the dense serotonergic nerve net. (F) Thick (100 μm) cross section of a demibranch; DA immunoreactivity is restricted to the epithelium of the filaments and the septum. (G) DA immunoreactivity in a dorsoventral section through a septum on the inner face of a water tube (the same orientation as E). Note the faint staining of the filaments, which are well out of the plane of focus. Abbreviations: bv = blood vessel; dvm = dorsoventral muscle; gf = gill filament; gfn = gill filament nerve (serotonergic); lm = longitudinal muscle; lmn = longitudinal muscle nerve; s = septum; sbv = septum blood vessel; sr = skeletal rod; wt = water tube; wtm = water tube muscle.

dorsoventral structures are the sites of the proposed excitatory dopaminergic synapses on the 5HT motor neurons.

The dual effect of acetylcholine

Our pharmacological experiments have also revealed an additional action of ACh. When gills were exposed to one of the 5HT antagonists, as well as to the cholinesterase inhibitor eserine, the muscles would *relax* in response to ACh. Moreover, this effect was blocked by the nicotinic antagonist hexamethonium. These data imply that, in addition to exciting the muscle by releasing 5HT, ACh also inhibits the muscle directly (Fig. 8). This dual effect of ACh explains part of its weak stimulatory action; that is, the maximal contraction produced by ACh was only about 25% of the maximal response to either 5HT or DA. But because ACh stimulates the muscle in the absence of 5HT antagonists, we infer that this stimulatory action of ACh is more potent than its inhibitory effect. However, even accounting for the inhibitory effect of ACh, the excitatory effect is still only about 50% of the maximal effect of either 5HT or DA. We conclude that the weak ACh stimulation of the branchial muscles in *Mercenaria* reflects characteristics of the cholinergic innervation, the postsynaptic receptors, or the signal transduction mechanism in this species. The distribution of cholinergic fibers has, however, not yet been investigated.

Innervation and function of the branchial musculature

Our morphological studies indicate that the serotonergic and dopaminergic innervations of the *Mercenaria* gill are distinct and that the musculature lacks dopaminergic innervation. Furthermore, the motor innervation of the gill muscles and cilia seems to be organized in three divisions: the serotonergic neural network associated with the water-tube muscles; the serotonergic innervation of the longitudinal and dorsoventral muscles; and the innervation of the cilia on the surface of the gill filaments, including serotonergic, dopaminergic, and peptidergic elements. When these findings are considered together with our pharmacological data and behavioral observations, a picture of integrated gill function begins to emerge.

The water-tube muscles and their neural network. The water-tube muscles occur in the walls of the major dorsoventral blood vessels, the subfilamentar horizontal vessels, and in the septa. When relaxed gills are exposed to 5HT, the plicae narrow, and secondary folds appear (see Fig. 1C; also fig. 4 in Medler and Silverman, 2001). We have also observed that if a dorsoventral blood vessel is gently pinched, the adjacent water-tube muscles contract, bringing the vessel inwards towards the center of the water tube, producing the secondary plical fold. This response decreases the cross-sectional area and modifies the shape of the water tubes, thus reducing the flow of water through the gill. In addition, pinching the blood vessel causes it to constrict locally, suggesting that the water-tube muscles also regulate the diameter of the blood vessels and thus the flow of hemolymph through them.

The longitudinal and dorsoventral muscles and their innervation. The longitudinal muscles run along the inside of the interfilament tissue junctions, perpendicular to the gill filaments and to the dorsoventral muscles, which lie within the filaments. However, the two sets of muscles are closely apposed, and more important, the dorsoventrals appear to be composed of branches of the longitudinals (Fig. 6B, C). Thus, we speculate that this orthogonal net of muscle acts as a unit. The longitudinal muscle is accompanied by a serotonergic neural plexus, and we have observed serotonergic varicosities among the longitudinal muscle fibers. Moreover, the dorsoventral muscles appear to be innervated by branches of the neural plexus (Fig. 6B).

In response to 5HT, the overall length of the gill decreases, as does the spacing between individual filaments, and thus the diameter of the ostia; this is the action of the longitudinal muscle. In addition, however, the 5HT-treated gill decreases in height in a dose-dependent manner (Gainey, pers. obs.)—the action of the dorsoventral muscles. When gills are exposed to 10^{-4} *M* 5HT, the dorsoventral contraction of the gill is very strong and produces a zigzag formation of the filaments on the frontal face of the gill. This phenomenon has also been observed in contracted gills of *Corbicula fluminea* (Medler and Silverman, 2001, fig. 2).

Innervation of the branchial filaments. The gill filaments bear the functionally and morphologically distinct tracks of cilia for which the bivalves are well known. Among these effectors, the lateral cilia—which constitute the branchial pump and thus produce the water current—have been studied best. In *Mercenaria*, the beat of these cilia is stimulated by 5HT and inhibited by DA (Aiello, 1970; Gainey *et al.*, 1999a), results that are consistent with our identification of both serotonergic and dopaminergic fibers within the gill filaments. Furthermore, an identical pattern of structure and function has been demonstrated in a filibranch, the blue mussel *Mytilus edulis* (reviewed by Aiello, 1990), so we presume that these fibers, in fact, innervate the lateral cilia in *Mercenaria*. The frontal cilia, which move food particles along the gill, are slowed only weakly by 5HT (Gainey *et al.*, 1999a). But the function of the innervation is not clear, for the frontal cilia continue beating even when the clam is closed (Shirley Baker, University of Florida, pers. comm.).

An endogenous SCP-like peptide, YFAFPRQamide, modulates the effects of DA on the lateral cilia and those of 5HT on the frontal cilia (Gainey *et al.*, 1999a); but this peptide has no effect—direct or indirect—on the branchial musculature. YFAFPRQamide-related immunoreactivity occurs almost exclusively in the region under the epithelium

Table 4

Effects of classic neurotransmitters on the branchial muscles of bivalves

SUBCLASS			Effect‡			
Species	Method*	Habitat†	5HT	DA	ACh	Source
PTERIOMORPHIA						
Mytilus edulis	DVO	M	+			Jorgensen, 1975
	TR		+	+		Gainey, pers. obs
Crassostrea virginica	TR	M			+	Roop & Greenberg, 1967
PALEOHETERODONTA						
Anodonta grandis	Ostia	F	−			Gardiner *et al.*, 1991
Ligumia subrostrata	Ostia	F	−	0	0	Gardiner *et al.*, 1991
HETERODONTA						
Dreissena polymorpha	V/TR	F			+	Snow *et al.*, 1995
	V/Ostia		−		+	Medler & Silverman, 1997
Corbicula fluminea	IFD/Ostia	F			+	Medler & Silverman, 2001
Mercenaria mercenaria	TR	M	+	+	+/−	This study

* DVO, direct visual observation of isolated gills. IFD, interfilament distance, recorded on videotape. Ostia, change in diameter of ostia measured. TR, direct measurement with a transducer of movement or force development. V, measurement of length or area changes recorded on video tape.

† M, marine; F, fresh water. Habitat is defined in terms of salinity. Note that the species listed here as "marine" are all at least moderately euryhaline (5–15‰ to 30–40‰). The criterion for designation of habitat as "fresh water" (F) is the ability of animals to live and reproduce (or survive prolonged immersion) in fresh water.

‡ +, excitation [increased tone (or ostia increased in diameter); or increased rate, regularity, or amplitude of contractions]. −, inhibition [relaxation (or decreased diameter of ostia), or reduced rate, amplitude, or regularity of contractions]. 0, no response observed. The predominant responses of the tissues to each transmitter are listed.

bearing the gill cilia, and in nerves running out to that region (Gainey *et al.*, 1999a). We have certainly not identified all of the transmitters in the innervation of the filaments, but the morphological restriction of YFAFPRQamide to the filaments, and its physiological restriction to effects on cilia, suggests that innervation of the branchial filaments may be exclusively in the service of the cilia, and that the remaining two neural divisions regulate the muscles. These considerations also support our hypothesis that the proposed synapses of dopaminergic and cholinergic neurons onto serotonergic neurons will be found in the septa.

Coordination between the ciliary pump and the branchial muscles. Two video endoscopic observations suggest that the lateral cilia and the gill muscles act in a coordinated fashion. First, when the gills of a unionid, *Pyganodon cataracta*, stop pumping, the water tubes constrict, but re-open when pumping resumes (Tankersley, 1996). Second, when the valves of *Mercenaria* are closed, the lateral cilia are immobile, and the gills are tonically contracted, both longitudinally and dorsoventrally (Baker, pers. comm.).

When the clam is actively pumping, we expect that serotonergic stimulation of the muscles is reduced and the muscles are relaxed. Under these circumstances, the ostia, water tubes, and blood vessels would be open, so the flow of water and hemolymph would be maximized. When the clam closes, the dopaminergic innervation would become active, switching the lateral cilia off and stimulating the serotonergic plexus. The longitudinal and dorsoventral muscles and the water-tube muscles would then constrict, closing the ostia and constricting the water tubes and blood vessels.

Comparative aspects of branchial muscle pharmacology

Although there is an extensive literature on the pharmacology of bivalve muscles, it is largely focused on the anterior byssus retractor muscle of *Mytilus* and isolated ventricles of a variety of bivalves including that of *Mercenaria*. In contrast, the pharmacology of branchial muscles has been studied in relatively few species of bivalves, in part because the branchial musculature is not an advantageous model for the study of muscle cells *per se*. Branchial muscles are small and are embedded in a complex organ; thus they cannot be directly attached to a recording apparatus. Furthermore, their neural supply is complex, and the innervation of specific muscles is not readily accessible. However, the pharmacology of these muscles has been studied by those interested in the physiology of bivalve gills; the available data are summarized in Table 4.

The effect of 5HT on the muscle varies with species. The gills of *Mytilus* and *Mercenaria* are contracted by 5HT, whereas those of *Dreissena polymorpha*, *Anodonta grandis*, and *Ligumia subrostrata* are relaxed. There is no taxonomic order in these data; but 5HT contracted the gills of the two marine species and relaxed those of the three freshwater species. Because the sample size is miniscule, however, the

apparent relationship between 5HT action and habitat may be coincidental.

ACh had a net excitatory effect on five of the six species on which it was tested; one species (*Ligumia subrostrata*) showed no effect, but the gills were not pretreated with eserine. The effect of ACh on the gills of *Mercenaria* was revealed only after pretreating them with eserine; in addition, the inhibitory effect of ACh became evident only when the gills were exposed to a 5HT antagonist and eserine. The relaxing effect of ACh has not been seen in any of the other gills tested, but then the pharmacological analysis reported here was not used in the other studies.

Painter and Greenberg (1982) examined the effects of 5HT and FMRFamide on the ventricles of 50 species of bivalves and remarked that "the responses were strikingly diverse, varying qualitatively with dose as well as species." In their analysis, however, clear taxonomic relationships were discernable. In comparison to ventricles, gills are much more complex and interact directly with the environment. For example, sodium transport in the gills of freshwater mussels appears to be regulated by a serotonergic neural mechanism (data summarized in Dietz *et al.*, 1985).

The odd response of the control gills in experiments with antagonists

When two successive equal doses of any agonist (*i.e.*, 5HT, DA, or ACh) were applied to the control gills, the second contraction was typically larger than the first, and this result was initially inexplicable. Later, however, we discovered that the gills produce nitric oxide (NO) in response to 5HT, and that NO potentiates gill muscle contractions (Gainey *et al.*, 1999b). This mechanism may also explain another experimental observation: that ultrasonic transducers record higher maximal contractions than force transducers, and they produce dose-response curves with lower EC_{50}s. Thus, when force transducers were used, demibranchs could be exposed only to a single dose of agonist, so the individual contractions constituting the dose-response curves were not potentiated by NO. In contrast, when ultrasonic transducers were used, the demibranchs could be exposed to a set of increasing doses of agonist, so NO was produced, the contractions were potentiated, and the resulting dose-response curves were steeper.

Summary

The gills of *Mercenaria* are equipped with an array of muscles and four distinct sets of cilia, and the activity of these effectors—coordinated by a complex neural network—transports water and particles in support of respiration and feeding. This paper and a previous one on the modulation of ciliary activity (Gainey *et al.*, 1999a) lay the groundwork for studies of the integrated control of gill function.

Acknowledgments

We thank David Chicoine, Robert Pirone, and Kelly J. Vining (University of Southern Maine) for their assistance in performing the pharmacology experiments. In addition, David Chicoine helped assemble Figures 6 and 7. The following individuals at the Whitney Lab provided assistance: Dr. Dimitri Budko provided the basic protocol used for whole mounts; Dr. Paul J. Linser provided technical assistance with immunohistochemistry and confocal microscopy and took the picture used for Figure 6E; Leslie Van Ekeris made the cryostat sections and provided technical assistance with the immunohistochemistry; M. Lynn Milstead drew and prepared Figure 1 for publication. Finally, Seth Tyler (University of Maine) advised on the phalloidin staining of muscle. Support was provided to LFG by grants from the Maine Science and Technology Foundation and the Bioscience Research Institute of Southern Maine (at the University of Southern Maine).

Literature Cited

Aiello, E. L. 1960. Factors affecting ciliary activity on the gill of the mussel *Mytilus edulis*. *Physiol. Zool.* **23:** 120–135.

Aiello, E. L. 1970. Nervous and chemical stimulation of gill cilia in bivalve molluscs. *Physiol. Zool.* **43:** 60–70.

Aiello, E. L. 1990. Nervous control of gill ciliary activity in *Mytilus edulis*. Pp. 189–208 in *Neurobiology of* Mytilus edulis, G. B. Stefano, ed. Manchester University Press, Manchester, U.K.

Atkins, D. 1937. On the ciliary mechanisms and interrelationships of lamellibranchs. Part I: New observations on sorting mechanisms. *Q. J. Microsc. Sci.* **79 (New Series):** 181–308.

Atkins, D. 1943. On the ciliary mechanisms and interrelationships of lamellibranchs. Part VIII: Notes on gill musculature in the microciliobranchia. *Q. J. Microsc. Sci.* **84 (New Series):** 187–256.

Bayne, B. L. 1998. The physiology of suspension feeding by bivalve molluscs: an introduction to the Plymouth "TROPHEE" workshop. *J. Exp. Mar. Biol. Ecol.* **219:** 1–19.

Candelario-Martinez, A., D. M. Reed, S. J. Prichard, K. E. Doble, T. D. Lee, W. Lesser, D. A. Price, and M. J. Greenberg. 1993. SCP-related peptides from bivalve mollusks: identification, tissue distribution, and actions. *Biol. Bull.* **185:** 428–439.

Catapane, E. J. 1983. Comparative study of the control of lateral ciliary in marine bivalves. *Comp. Biochem. Physiol.* **75C:** 403–405.

Dame, R. F. 1996. *Ecology of Marine Bivalves: an Ecosystem Approach.* CRC Press, Boca Raton, FL.

Dietz, T. H., W. L. Steffens, W. T. Kays, and H. Silverman. 1985. Serotonin localization in the gills of the freshwater mussel, *Ligumia subrostrata*. *Can. J. Zool.* **63:** 1237–1243.

Eble, A. F. 2001. Anatomy and histology of *Mercenaria mercenaria*. Pp. 117–220 in *Biology of The Hard Clam*, J. N. Kraeuter and M. Castagna, eds. Elsevier Science, Amsterdam.

Gainey, L. F., Jr., K. J. Vining, and M. J. Greenberg. 1998. Pharmacology of gill muscle fibers in *Mercenaria mercenaria*. *Am. Zool.* **38:** 122A.

Gainey, L. F., Jr., K. J. Vining, K. E. Doble, J. M. Waldo, A. Cande-

lario-Martinez, and M. J. Greenberg. 1999a. An endogenous SCP-related peptide modulates ciliary beating in the gills of a venerid clam, *Mercenaria mercenaria*. *Biol. Bull.* **197:** 159–173.

Gainey, L. F., Jr., R. T. Pirone, and M. J. Greenberg. 1999b. Nitric oxide potentiates gill muscle contraction in *Mercenaria mercenaria*. *Am. Zool.* **39:** 71A.

Gainey, L. F., Jr., J. Walton, and M. J. Greenberg. 2001. Neuromuscular anatomy of clam gills. *Am. Zool.* **41:** 448 (Abstract).

Galtsoff, P. 1964. The American oyster. Chapter VII: The gills. *Fish. Bull. US Fish Wildl. Serv.* **64:** 121–151.

Gardiner, D. B., H. Silverman, and T. H. Dietz. 1991. Musculature associated with the water canals in freshwater mussels and response to monoamines *in vitro*. *Biol. Bull.* **180:** 453–465.

Grunbaum, D., D. Eyre, and A. Fogelson. 1998. Functional geometry of ciliated tentacular arrays in active suspension feeders. *J. Exp. Biol.* **201:** 2575–2589.

Jorgensen, C. B. 1975. On gill function in the mussel, *Mytilus edulis* L. *Ophelia* **13:** 187–232.

Jorgensen, C. B. 1996. Bivalve filter feeding revisited. *Mar. Ecol. Prog. Ser.* **142:** 287–302.

Kellogg, J. L. 1892. A contribution to our knowledge of the morphology of lamellibranchiate molluscs. *Bull. U.S. Fish. Comm.* **10:** 389–436.

Malanga, C. J. 1975. Dopaminergic stimulation of frontal ciliary activity in the gill of *Mytilus edulis*. *Comp. Biochem. Physiol.* **51C:** 25–34.

Medler, S., and H. Silverman. 1997. Functional organization of intrinsic gill muscles in zebra mussels, *Dreissena polymorpha* (Mollusca: Bivalvia), and response to transmitters *in vitro*. *Invertebr. Biol.* **116:** 200–212.

Medler, S., and H. Silverman. 2001. Muscular alteration of gill geometry *in vitro*: implications for bivalve pumping processes. *Biol. Bull.* **200:** 77–86.

Nelson, T. C. 1960. The feeding mechanism of the oyster. II. On the gills and palps of *Ostrea edulis*, *Crassostrea virginica* and *C. angulata*. *J. Morphol.* **107:** 163–203.

Painter, S. D., and M. J. Greenberg. 1982. A survey of the responses of bivalve hearts to the molluscan neuropeptide FMRFamide and to 5-hydroxytryptamine. *Biol. Bull.* **162:** 311–332.

Ridewood, W. G. 1903. On the structure of the gills of the Lamellibranchia. *Philos. Trans. R. Soc. Lond.* **195:** 147–284.

Roop, T., and M. J. Greenberg. 1967. Acetylcholinesterase activity in *Crassostrea virginica* and *Mercenaria mercenaria*. *Am. Zool.* **7:** 737–738.

Setna, S. B. 1930. The neuromuscular mechanism of the gill of *Pecten*. *Q. J. Microsc. Sci.* **73:** 365–392.

Snow, V., J. Duncan, and J. L. Ram. 1995. Contractile responses of zebra mussel gills. *Exp. Biol.* **95:** A640. Abstract # 3711.

Tankersley, R. A. 1996. Multipurpose gills: effect of larval brooding on the feeding physiology of freshwater unionid mussels. *Invertebr. Biol.* **115:** 243–255.

Welsh, J. H., R. I. Smith, and A. E. Kammer. 1968. *Laboratory Exercises in Invertebrate Physiology*, 3rd ed. Burgess, Minneapolis, MN.

Reference: *Biol. Bull.* **204:** 96–103. (February 2003)

Salinity Tolerance of Larval *Rapana venosa:* Implications for Dispersal and Establishment of an Invading Predatory Gastropod on the North American Atlantic Coast

ROGER MANN* AND JULIANA M. HARDING

Department of Fisheries Science, Virginia Institute of Marine Science, College of William and Mary, Gloucester Point, Virginia 23062

Abstract. The lack of quantitative data on the environmental tolerances of the early life-history stages of invading species hinders estimation of their dispersal rates and establishment ranges in receptor environments. We present data on salinity tolerance for all stages of the ontogenetic larval development of the invading predatory gastropod *Rapana venosa*, and we propose that salinity tolerance is the dominant response controlling the potential dispersal (=invasion) range of the species into the estuaries of the Atlantic coast of the United States from the current invading epicenter in the southern Chesapeake Bay. All larval stages exhibit 48-h tolerance to salinities as low as 15 ppt with minimal mortality. Below this salinity, survival grades to lower values. Percentage survival of *R. venosa* veligers was significantly less at 7 ppt than at any other salinity. There were no differences in percentage survival at salinities greater than 16 ppt. We predict that the counterclockwise, gyre-like circulation within the Chesapeake Bay will initially distribute larvae northward along the western side of the DelMarVa peninsula, and eventually to the lower sections of all major subestuaries of the western shore of the Bay. Given the observed salinity tolerances and the potential for dispersal of planktonic larvae by coastal currents, establishment of this animal over a period of decades from Cape Cod to Cape Hatteras is a high probability.

Introduction

The Norway/United Nations Conference on Alien Species considers alien invasive species as the second most important threat, after habitat destruction, to indigenous biodiversity (Sandlund *et al.*, 1999). Despite the widespread historical records of both intentional and accidental introductions of fauna and flora to novel environments beyond their natural ranges, the ability to predict establishment and subsequent range expansion in the receptor environment remains poor for both terrestrial and aquatic systems (Williamson, 1996; Sandlund *et al.*, 1999). This should not be surprising given the difficulty of describing the niche (*sensu* Hutchinson, 1979) of the invader in its native range, let alone in a novel, receptor environment. In examining the success of introductions, Vermeij (1996) poses the question "What factors prevent populations from spreading beyond their geographical limits?" He then proffers one possible answer—that physiological tolerances are evolutionarily conservative, resulting in ranges being set by physical circumstances that prevent reproduction or survival. Thus physiological tolerances probably set the maximum spatial limits of the species, again to quote Vermeij (1996), by "the presence of competitors, predators, or disease organisms, or the absence of a critical host, food, or symbiotic species." The gravity of the impact of invasions on current biodiversity dictates the need to move beyond our current, often anecdotal, understanding of range limitation so that we can predict the effects of invasions and develop suitable control measures.

Marine and estuarine molluscs are well represented in the fauna that have been introduced over historical time to new locations where they have become established and, in some instances, dominant factors in shaping the extant communities (Carlton, 1999). The western Pacific Ocean has emerged as a donor region for invading species that have

Received 2 July 2002; accepted 4 November 2002.
* To whom correspondence should be addressed. E-mail: rmann@vims.edu

become established in the eastern Pacific and Atlantic Oceans, the Mediterranean and Black Seas, and parts of Australasia. Invading western Pacific gastropods are mostly small, their dispersal being facilitated as a component of surface fouling communities or within rock ballast. Invasions of large predatory gastropods have, by comparison, been modest. Their generally infaunal habit and large adult size serves them poorly in maintaining attachment to exposed fouling communities, and their late maturation limits recruitment to exposed and disturbed fouling communities in transit. The recent emergence of ballast water as a vector in effecting invasions (Carlton, 1996, 1999) has, however, expanded the potentially invading gastropod fauna to include species characterized by a life history that combines large adult size with planktonic larval dispersal phases. A prime example of this newly facilitated invader is the predatory gastropod *Rapana venosa* Valenciennes 1846. This species was formerly classified in the subclass Prosobranchia, order Neogastropoda, but is currently placed in the subclass Orthogastropoda, family Muricidae, subfamily Rapaninae (=subfamily Thaididae; see Kool, 1993). *Rapana venosa*, commonly termed the rapa whelk, is native to the Sea of Japan, the Yellow Sea, the Bohai Sea, the East China Sea to Taiwan in the south, and Peter the Great Bay off Vladivostok in the north (Golikov, 1967; Lai and Pan, 1980; Tsi *et al.*, 1983). The introduction of *R. venosa* to the Novorossiysky Bay in the Black Sea in the 1940s, probably as a species associated with oysters transported from the Orient, is described by Drapkin (1963). Limited records of occurrence of *R. venosa* have also been made on the Pacific coast of Canada and in Willapa Bay, Washington, in the United States (Hanna, 1966, page 47). These introductions were probably associated with commercial importation of oysters from Japan during the same time frame that rapa whelks were first observed on the Pacific Coast. *R. venosa* has not become established on the Pacific coast of North America. In sharp contrast, the species has become established in the Black Sea with significant damage to native benthos (*e.g.*, bivalves; notably *Ostrea edulis, Pecten ponticus*, and *Mytilus galloprovincialis* [Zolotarev, 1996], and its subsequent invasion of the Aegean, Adriatic, and Mediterranean Seas has been well documented (Drapkin, 1963; Ghisotti, 1971, 1974; Mel, 1976; Terreni, 1980; Cucaz, 1983; Chukchin, 1984; Rinaldi, 1985; Marinov, 1990; Koutsoubas and Voultsiadou-Koukoura, 1990; Bombace *et al.*, 1994; Zolotarev, 1996).

Recent transoceanic invasions by *R. venosa*, probably facilitated by transport of larval stages in ballast water, have resulted in occurrence of the species in the Chesapeake Bay on the Mid-Atlantic coast of the United States (Harding and Mann, 1999; Mann and Harding, 2000), on the Brittany coast of France (Dr. Philippe Goulletquer, IFREMER, pers. comm., 1999), and in the Rio del Plata between Uruguay and Argentina (Pastorino *et al.*, 2000; F. Scarabino, National Museum of Natural History and National Institute of Fisheries, Uruguay, pers. comm. 2000). Furthermore, regions formerly insulated from contact with this predatory species must now be considered susceptible to continued exposure to it in ballast water. The ecological and economic impacts associated with the arrival and possible establishment of *R. venosa* in the southern Chesapeake Bay has stimulated a program to quantitatively describe the niche of the species in this new location. Such a description will be helpful in predicting the potential of the species to become established within the Chesapeake Bay and further afield along the Atlantic coast. This report describes the response of pelagic larval stages of *R. venosa* to variations in salinity. Because salinity tolerance is an evolutionarily conservative feature of the species, we argue that it sets a maximal range on the distribution of the organism in this new location.

Materials and Methods

Individuals of *Rapana venosa* mature at 1–2 years of age, are dioecious as adults, and display mating activity all year in laboratory populations (Harding and Mann, unpubl. data). Eggs are laid in masses characteristic of the genus *Rapana* (see Chung *et al.*, 1993; Morton, 1994; Harding and Mann, 1999). Adult broodstock for the current study were collected as by-catch of commercial crab and clam fisheries in the Hampton Roads region of the Chesapeake Bay (Fig. 1) in the spring of 2000. These animals were maintained at the Gloucester Point laboratory of the Virginia Institute of Marine Science, on the York River, Virginia, until the initiation of the larval studies. They were held in 800-l tanks supplied with flowing seawater from the York River. The water was kept at ambient temperature and salinity (20–26 °C and 18–21 ppt respectively for the experimental period), and the animals were fed *ad libitum* with clams, *Mercenaria mercenaria*, as prey. Egg masses for the current study were laid during the months of June through September.

The egg masses, which typically were attached to the walls of the holding tank, were collected within 24 h of deposition. Individual egg masses were maintained in 1 l of static filtered seawater (18 to 21 ppt) at 20 to 26 °C and 10 h light/14 h dark conditions through hatching. After hatching or release of veliger larvae from egg cases within an egg mass, the larvae were maintained in aerated filtered seawater under the same conditions as the egg masses and at densities of about 500 veligers per liter of seawater. Veligers were fed a mixed diet of *Pseudoisochrysis paradoxa*, *Chaetocerus gracilis*, and *Tetrasalmis* sp. every other day.

Larval cultures designated for experiments on salinity tolerance, except for trials on newly hatched larvae, were maintained at initial experimental salinities for 48 h before an experiment. One hour before the beginning of an experiment, the cultures were sieved through an 80-μm mesh to condense the larvae into a small volume of water. A 1-ml

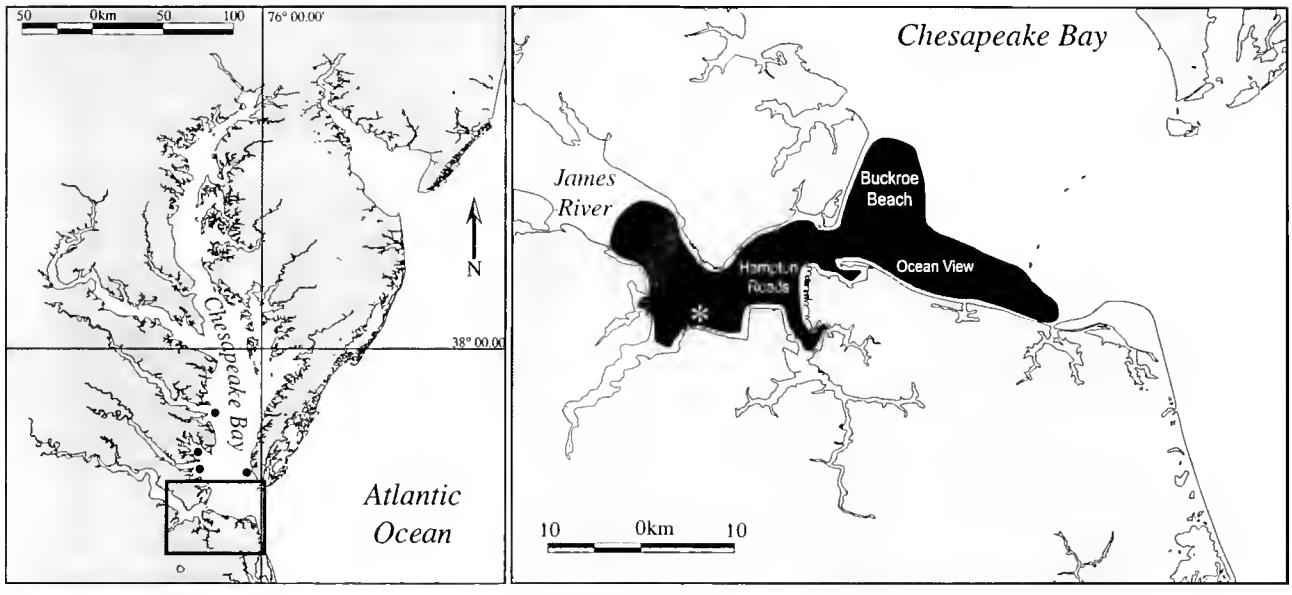

Figure 1. (A) Current distribution of *Rapana venosa* in the Chesapeake Bay, and (B) distribution of *R. venosa* in the lower James River, Hampton Roads, Buckroe Beach, and Ocean View regions of the Chesapeake Bay. Most collections to date are from these areas (after Harding and Mann, 1999). *marks the site of the first collection in 1998.

subsample was removed and examined under a dissecting microscope to determine both the health of the larvae (as indicated by the percentage of veligers with velum extended and filtering) and their concentration (number/ml). This initial subsample was preserved in 10% neutral buffered formalin as an index collection for each experiment.

During the summer of 2000, a series of 48-h salinity-tolerance experiments at salinities from 7 ppt through 32 ppt were completed using veligers ranging in age from immediately post-hatch (day 0) through the onset of settlement (day 27). The salinity range chosen represents conditions in Chesapeake Bay mainstem areas and tributaries that are potentially most vulnerable to tidal advection of *R. venosa* veligers from downstream sites (see Fig. 2). Each salinity-tolerance experiment tested a single age of larvae and incorporated at least three replicates at each of eight salinity levels (*e.g.*, 7, 10, 13, 16, 19, 22, 25, and 32 ppt). Replicates were obtained from larval cultures that originated from different parents. Ages of veligers at the beginning of each experiment are recorded as days post-hatch and include day 0, 2, 4, 6, 9, 11, 13, 15, 17, 19, 21, 23, 25, and 27. By day 27, at least 10% of veliger larvae within experimental cultures were settled, had shed their velum, and were completing metamorphosis to the crawling benthic stage.

Individual boiling tubes were used as experimental chambers and were filled with 20 ml of filtered seawater at 24 to 26 °C. *R. venosa* veligers were added to individual boiling tubes to give densities of at least 1 veliger per milliliter at initial salinities. Salinities within individual tubes were decreased at 5-min intervals by the serial addition of 1 ml of deionized water. Tube 1 (the control tube) received no additions of deionized water and remained at its initial salinity throughout each experiment. During the experiments, larvae were fed 1 ml of *Pseudoisochrysis paradoxa*, 1 ml of *Chaetoceros gracilis*, and 0.3 ml of *Tetrasalmis* sp. per chamber daily. After 44 h, 1 ml of concentrated neutral red in filtered seawater solution was added to each experimental chamber. Neutral red is a nontoxic vital stain that is absorbed by living tissue; veligers that were alive at 44 h absorbed the stain and could then be distinguished from dead veligers by their pink tissue. Experiments were terminated after 48 h by the addition of 5 ml of 10% neutral buffered formalin to each tube. Fixed veliger larvae were examined under a dissecting microscope to determine the percentage survival in each chamber after 48 h exposure to the experimental salinity.

Percentage survival data from all salinity-tolerance experiments satisfied assumptions of homogeneity of variance but failed to meet the assumptions of normality regardless of the transformation (arcsin, square root, $\log_e$, logarithm, reciprocal). A two-factor ANOVA (initial veliger age × salinity) was used to evaluate percentage survival data. Fisher's multiple comparison test was used for *post hoc* comparisons when appropriate. All significance levels were established at $P = 0.05$ *a priori*.

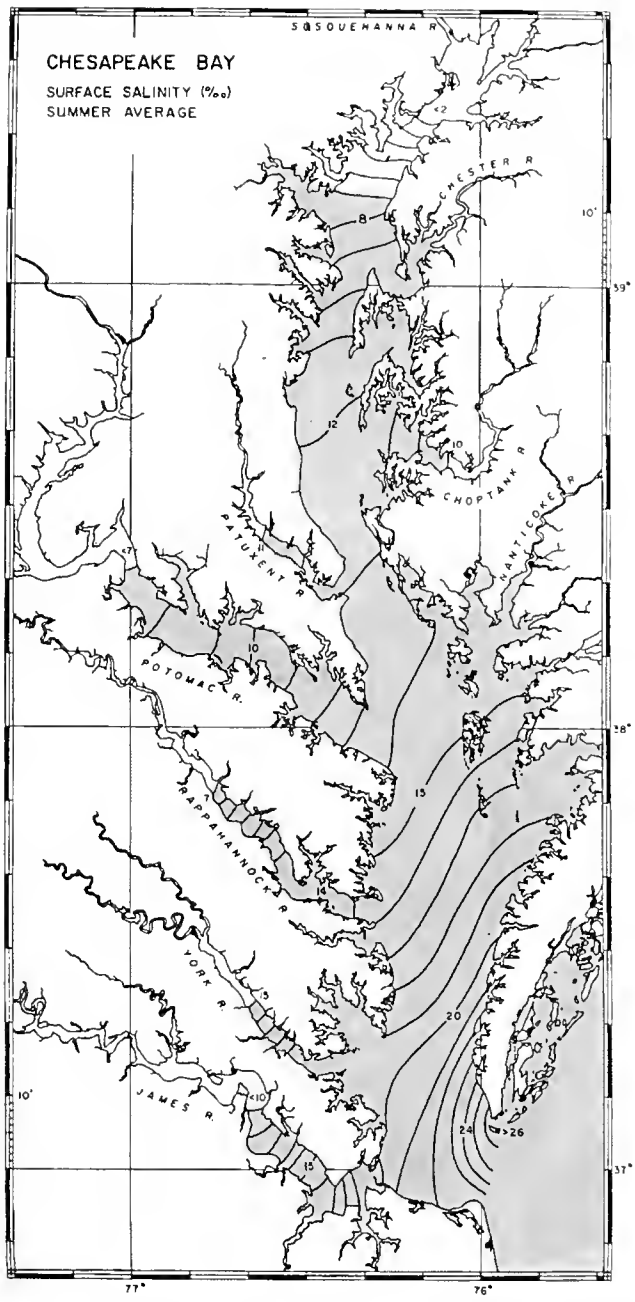

Figure 2. Average summer surface salinity in the Chesapeake Bay (modified from Stroup and Lynn, 1963; data in agreement with Rennie and Neilson, 1994). Shaded regions have salinities suitable for short-term survival of *Rapana venosa* veligers. Bottom type, availability of suitable prey, and residual circulation to effect larval dispersal support possible establishment within this same region.

Results

Mean percentage survival of *Rapana venosa* veligers ranged from 2.3% at 15 d and 7 ppt to 100% at 27 d and 22 ppt (Table 1). Veliger age and salinity significantly affected the percentage survival (ANOVA, $P < 0.001$; Table 2). There was a significant interaction between veliger age and salinity (ANOVA, $P < 0.001$; Table 2). Veligers aged 15 and 17 d were significantly less tolerant of salinity changes than veligers of all other ages (ANOVA, $P < 0.001$; Fisher's test, $P < 0.05$). Veligers older than 25 d post-hatch had a significantly higher percentage survival than all other ages except 11 d and 21 d (ANOVA, $P < 0.001$; Fisher's test, $P < 0.05$). Veligers aged 21 d had a significantly higher percentage survival than all younger veligers as well as those with an age of 23 d (ANOVA, $P < 0.001$; Fisher's test, $P < 0.05$). Eleven-day-old veligers were significantly more tolerant of salinity changes than were those at ages of 6, 9, 13, 19, or 23 d (ANOVA, $P < 0.001$; Fisher's test, $P < 0.05$).

Percentage survival of *R. venosa* veligers was significantly less at 7 ppt than at any other salinity (ANOVA, $P < 0.001$; Fisher's test, $P < 0.05$). There were no differences in percentage survival at salinities greater than 16 ppt (ANOVA, $P < 0.001$; Fisher's test, $P < 0.05$). Percentage survival was significantly lower at 10 ppt than at salinities ranging from 16 to 32 ppt (ANOVA, $P < 0.001$; Fisher's test, $P < 0.05$). Percentage survival at 13 ppt was significantly lower than at salinities from 16 to 25 ppt (ANOVA, $P < 0.001$; Fisher's test, $P < 0.05$).

Discussion

Larvae of *Rapana venosa* exhibit broad tolerance to salinity as an environmental stressor. With the exception of the combinations of 6-day-old and 13- to 17-day-old veligers at low salinity, all age-salinity combinations in the current study demonstrated substantial survival, in many instances exceeding 90%, over the experimental period. The prospect for larval salinity tolerance to be a limiting factor in further upstream invasion of the Chesapeake Bay from the extant adult population thus appears to be poor. For adults of this species, neither salinity tolerance nor distribution in estuarine systems of graded salinity are well described in the literature for native or invading populations. The current adult population in the Chesapeake Bay (see Fig. 1) rarely experiences bottom salinities below 20 ppt. In the Black Sea, where the annual water temperature range is about 7°C to 24°C, *R. venosa* occupies a salinity range of 25 to 32 ppt (Golikov, 1967). In the Sea of Azov, which is ice covered for 2 to 4 months of the year, *R. venosa* was restricted to the southernmost region adjoining the Kerch Strait by low persistent salinity in the remaining water body (mean annual value <12 ppt). However, a range extension did occur in 1975-1979 when riverine discharge into the Sea of Azov was markedly reduced by water diversion projects (Rubinshtein and Hiznjak, 1988). These projects were discontinued in 1990, and the fresher environment again persists. The current distribution of *R. venosa* in the Sea of Azov with respect to prevailing salinity is

Table 1

Average percentage survival (standard error in parentheses) for Rapana venosa *veligers of various ages (0–27 days post-hatch) exposed to 8 different salinities for 48 h; n > 20 veligers per treatment*

Salinity (ppt)	Veliger age (days post-hatch)						
	0	2	4	6	9	11	13
7	76.9 (3.8)	65.5 (5.6)	51.0 (5.4)	20.5 (6.6)	62.3 (6.8)	79 (12.4)	29.4 (8.0)
10	74.8 (5.3)	70.9 (5.5)	76.0 (3.4)	67.1 (4.3)	72.1 (5.0)	92.4 (1.8)	42.6 (2.9)
13	77.9 (2.4)	79.3 (2.8)	59.5 (6.5)	75.9 (9.7)	75.7 (6.5)	90.9 (3.0)	69.2 (2.6)
16	80.7 (2.4)	80.7 (3.1)	90.7 (3.1)	82.2 (3.0)	83.8 (3.9)	89.2 (1.7)	83.5 (2.2)
19	78.9 (3.4)	82.6 (3.4)	97.1 (0.8)	90.9 (2.6)	77.3 (3.7)	86.9 (5.2)	83.1 (3.1)
22	85.7 (3.0)	80.9 (5.4)	97.8 (1.4)	90.4 (2.2)	69.5 (3.2)	88.7 (2.4)	87.8 (1.8)
25	83.5 (6.7)	81.4 (2.4)	94.7 (2.8)	94.9 (0.9)	74.9 (7.3)	93.5 (1.5)	87.6 (1.9)
32	59.5 (3.8)	90.5 (4.1)	89.3 (1.4)	97.3 (1.4)	79.6 (0.9)	85.8 (6.5)	84.3 (4.1)
	15	17	19	21	23	25	27
7	2.3 (2.3)	23.3 (14.4)	58.4 (6.7)	95.8 (2.1)	75.9 (1.7)	97.2 (2.8)	92.5 (3.8)
10	42.5 (12.2)	69.4 (3.9)	82.2 (4.2)	93.3 (3.5)	66.4 (4.5)	97.0 (3.0)	88.7 (8.0)
13	59.9 (8.0)	54.6 (14.4)	83.0 (0.7)	88.9 (5.9)	75.0 (0.9)	89.9 (1.4)	79.5 (8.8)
16	74.3 (3.5)	59.7 (5.9)	87.0 (1.9)	93.9 (6.1)	67.7 (6.4)	97.2 (2.8)	82.6 (11.5)
19	68.8 (12.5)	61.4 (4.2)	84.1 (2.1)	92.0 (5.4)	74.8 (4.1)	97.4 (2.5)	95.2 (4.8)
22	78.8 (4.3)	68.8 (4.9)	78.7 (5.4)	86.1 (4.3)	81.0 (1.9)	87.1 (6.5)	100 (0.0)
25	71.5 (2.6)	73.0 (4.1)	72.7 (3.8)	96.7 (1.7)	80.9 (1.0)	98.0 (2.0)	98.7 (1.3)
32	56.3 (10.3)	67.6 (3.3)	73.7 (4.2)	94.5 (2.8)	69.9 (2.4)	93.7 (3.4)	96.4 (1.8)

unclear. The limited observations from the Kerch Strait region suggest that an upstream limit of 12–13 ppt in the Chesapeake Bay is possible, and that low winter temperatures will not exclude *Rapana* from regions that infrequently experience winter ice. Wu (1988) reports that in its native range, *R. venosa* can exploit estuarine regions that have warm summer temperatures and avoid possible surface freezing in winter by migrating into deeper water in these regions.

Larvae of *R. venosa* exhibit considerable plasticity in the duration of their planktonic development under experimental conditions of temperature and salinity that mimic the summer conditions in the Chesapeake Bay, and they do not require specific metamorphic cues to complete the transition to the crawling, benthic post-larval phase (Harding and Mann, unpubl. data). Laboratory-cultured individuals can exploit a variety of native bivalves as prey, including the hard clam *Mercenaria mercenaria* (Savini *et al.*, 2003), the oyster *Crassostrea virginica*, the soft shell clam *Mya arenaria*, and the mussel *Mytilus edulis* (Harding and Mann, unpubl. data).

Table 2

Summary of two-factor ANOVA (veliger age × salinity) used to describe salinity tolerances of larval Rapana venosa *in laboratory experiments conducted during July 2000*

Source	df	*F*-value	*P*-value
Veliger age (days post-hatch)	13	31.4	<0.001
Salinity (ppt)	7	32.0	<0.001
Veliger age × salinity	91	4.1	<0.001

The salinity tolerance of both the larvae and adults of *R. venosa* is greater than that of adults of the genera *Busycon* and *Busycotypus*. Thus we predict that in the lower Chesapeake Bay, *Rapana* will compete directly for space and for prey (notably infaunal pelecypods) with these native species of large predatory gastropods. Indeed, two recent observations indicate that exploitation of this resource by *Rapana* is increasing.

First, the distinctive boring signature of *Rapana* (chipping or rasping of the shell margin as described by Morton, 1994) has been seen on specimens of *Mercenaria* in the lower Chesapeake Bay (Harding, Mann, Kingsley-Smith, and Savini, unpubl. data). Second, studies of the shell morphology of invading *Rapana* (Green, 2001) point to the same conclusion. Vermeij (1993) examined allometry as a morphological descriptor of shape in gastropods, and noted that high allometric growth rates in gastropods have been correlated with low overall growth rates. Green (2001) demonstrated higher rates of allometric growth in Black Sea populations of *R. venosa* compared to native Korean and Chesapeake Bay populations, which suggests food limitation in the Black Sea location. This finding is consistent with long-term observations of the Black Sea invasion: in its

initial phase of establishment, *Rapana* all but eliminated many endemic prey species, resulting in a subsequent phase of very high densities of invaders in intraspecific competition for limited resources of available prey. The suggestion that the Chesapeake Bay populations are not food limited is particularly troubling given the population demographics (see Harding and Mann, 1999, and Mann and Harding, 2000) and the co-location of the invasion with a native hard clam population that supports a local (to the Hampton Roads region of the Chesapeake Bay) fishery with a dock landing value in excess of $3 million per year (see Harding and Mann, 1999, fig. 7). Allometric inferences may be challenged where the number of observations is limited; however, one of the strengths of Green's (2001) study is the very large number of observations (Korea, $n = 226$; Black Sea, $n = 74$; Chesapeake Bay, $n = 107$) and the range of sizes examined for all geographic populations. Further, the large adult sizes typical of many Chesapeake Bay specimens is unmatched in extant Korean populations, whereas museum collections (U.S. National Museum of Natural History, Smithsonian Institution) of Asian specimens from an era prior to extensive fishing effort match local collections in terms of size. The demographics of the Korean population are indicative of fishing effort on size frequencies that recruit to the fishing gear, whereas that of the Chesapeake Bay population is an ominously threatening indicator of an unexploited stock in the presence of abundant food.

The fact that *R. venosa* combines broad dietary capabilities with broad salinity tolerance suggests that no substantial extant bivalve resources in the lower Chesapeake Bay are in a spatial refuge from predation. The native oyster populations, already depleted by the long-term effects of disease, overfishing, and environmental decline, are included in the susceptible resources. Oyster populations, currently the target of extensive restoration activity (see Luckenbach *et al.*, 1999; Mann, 2000, 2001), are limited to lower salinity sanctuaries from disease in the upper bay and its subestuaries. Although oyster distribution extends into salinities below that tolerated by both larval and adult *Rapana* (compare distribution data in Kennedy *et al.*, 1996, with Figs. 1 and 2 of this study), significant oyster stocks—which may be disproportionately important as broodstock given their higher salinity locations—are within the salinity tolerance of invading *Rapana*. The fact that Bombace *et al.* (1994) observed *Rapana* in the Adriatic Sea on isolated artificial reef structures similar in concept to those being constructed in the Chesapeake Bay as local foci of increased habitat diversity (see Luckenbach *et al.*, 1999), raises concern for the long-term stability of oyster populations in regions of restored habitat within the bay.

The combination of pelagic larval dispersal and broad salinity tolerance in *R. venosa* potentially complicates the ability of the native oyster drill, *Urosalpinx cinerea*, to re-establish its former range within the Chesapeake Bay. *Urosalpinx* populations were once extensive and abundant within the bay, but the freshets associated with Hurricane Agnes in 1972 decimated these populations. Post-Agnes survival was limited to a region near the Bay mouth—essentially all oyster beds in the subestuaries of the Bay were purged of *Urosalpinx* by this single event. Unlike *Rapana*, *Urosalpinx* has no pelagic larval stage. Juveniles of *Urosalpinx* hatch and crawl away from the substrate-attached egg masses. *Urosalpinx* has been recolonizing its former Bay habitat over the past three decades by crawling up the Bay bottom over "islands" of suitable substrate. In the absence of an invader, the temporary displacement of *Urosalpinx* is but a minor perturbation in evolutionary time; however, the introduction of *Rapana* adds a new and opportunistic component to this reestablishment process. There arguably now exists a race to reoccupy this temporarily vacated niche; a race that may favor the invader because of the sequence of events that temporarily displaced the native species.

Vermeij (1996) theorized that physiological tolerances are evolutionarily conservative parameters contributing to the determination of the range of survival. In this context we predict that, as a result of the counterclockwise, gyre-like circulation within the Chesapeake Bay, pelagic larvae of *Rapana venosa* originating from parents in the Hampton Roads region will initially be distributed northward along the western shore of the DelMarVa peninsula, and will eventually reach the lower sections of all the major subestuaries of the western shore of the Bay. This entire region is within the salinity tolerance of the larval forms (compare Table 1 with Fig. 2). The potential for long-distance dispersal within a single generation remains to be determined, although recent collections of small (<75 mm in length) adults on the Virginia Bay shore of the peninsula suggest that a distance of tens of kilometers per generation is possible. Dispersal onto and along the coastal shelf outside of the Bay mouth may be influenced by both northward- and southward-flowing residual current. The effects on dispersal depend on depth, wind conditions, and time within the known egg laying period of the invader in the southern Chesapeake Bay. Establishment over a period of decades by natural dispersal in estuaries and coastal regions from Cape Cod to Cape Hatteras was considered a high probability by Mann and Harding (2000). This prediction still stands and is supported by the essentially continuous distribution of mollusc species suitable as prey in shallow waters throughout this range (for examples, see Theroux and Wigley, 1983). The time frame may, however, be considerably reduced by dispersal of larval forms in ballast water during intra-coastal maritime trade, a suggestion reinforced by the tolerance of the larval form (this study) and the location of both the Norfolk, Virginia, U.S. Naval base and an international

container terminal within the extant adult range of invasion in Hampton Roads. If, as Vermeij (1996) suggests, factors such as "the presence of competitors, predators, or disease organisms, or the absence of a critical host, food, or symbiotic species" prevent a species from extending its range, it is unlikely that *Rapana* will be further restricted within the projected range. Large individuals of *R. venosa* appear admirably equipped to compete with large native gastropods and have few obvious predators in the Middle Atlantic coastal region when they are full grown. We can find no reports of diseases of *R. venosa* in any of its native or introduced ranges. Finally, the only notable parasite of *R. venosa* in both its Black Sea and Chesapeake Bay populations are shell-boring polychaetes of the genus *Polydora* (Gutu and Marinescu, 1979; Mann and Harding, 2000). The actions of *Polydora* appear to have little, if any, detrimental effect on infected individuals in either location; may be limited to some individuals of *R. venosa* that forage epifaunally; and may be terminated by burial of the host whelks as they grow and shift to an infaunal habit. Indeed, observations on rapa whelk biology and physiological tolerances in the Chesapeake Bay strongly suggest that this animal is capable of successful colonization and establishment of viable populations within estuarine habitats up and down the East Coast of the United States.

Acknowledgments

Support for this project was provided by Virginia Sea Grant (R/MG-98-3), the Department of Fisheries Science, Virginia Institute of Marine Science, and partial support to RM by the National Science Foundation (OCE-9810624). Special thanks are extended to local watermen and seafood processors who donated adult *Rapana* to our research collection. We thank D. Bryn Jones, Dario Savini, Melissa Southworth, Rhonda Howlett, Peter Kingsley-Smith, Erica Westcott, Stephanie Haywood, and Catherine Ware for assistance in maintenance of adult brood stock and larval cultures. This manuscript is dedicated to the late Professor Ruth Dixon Turner, whose enthusiasm for the larval ecology of marine molluscs remains as an inspiration to us all. This is Contribution Number 2506 from the Virginia Institute of Marine Science.

Literature Cited

Bombace, G., G. Fabi, L. Fiorentini, and S. Speranza. 1994. Analysis of the efficacy of artificial reefs located in five different areas of the Adriatic Sea. Fifth International Conference on Aquatic Habitat Enhancement. *Bull. Mar. Sci.* **55(2–3):** 559–580.

Carlton, J. 1996. Pattern, process, and prediction in marine invasion ecology. *Biol. Conserv.* 78: 97–106.

Carlton, J. 1999. Molluscan invasions in marine and estuarine communities. *Malacologia* **41:** 439–454.

Chukchin, V. 1984. *Ecology of the Gastropod Molluscs of the Black Sea.* Acad. Sc. USSR, Naukova Dumka, Kiev. 175 pp. (in Russian).

Chung, E.Y, S. Y. Kim, and Y. G. Kim. 1993. Reproductive ecology of the purple shell, *Rapana venosa* (Gastropoda: Muricidae), with special reference to the reproductive cycle, deposition of egg capsules and hatching of larvae. *Korean J. Malacol.* **9(2):** 1–15.

Cucaz, M. 1983. *Rapana venosa* (Valenciennes, 1846) vivente nel Golfo di Trieste. *Boll. Malacol.* **19(9–12):** 261–262.

Drapkin, E. 1963. Effect of *Rapana bezoar* Linne (Mollusca, Muricidae) on the Black Sea fauna. *Dokl. Akad. Nauk. SSSR.* **151:** 700–703.

Ghisotti, F. 1971. *Rapana thomasiana* Crosse, 1861 (Gastropoda, Muricidae) nel Mar Nero. *Conchiglie (Milan)* **7:** 55–58.

Ghisotti, F. 1974. *Rapana venosa* (Valenciennes), nuova ospite Adriatica? *Conchiglie (Milan)* **10:** 125–126.

Golikov, A. N. 1967. Gastropoda: Pp. 79–91 in *Animals and Plants of Peter the Great Bay.* Nauka, Leningrad.

Green, R. 2001. Morphological variation of three populations of the veined rapa whelk, *Rapana venosa,* an invasive predatory gastropod species. Master's thesis, College of William and Mary, Gloucester Point, VA.

Gutu, M., and A. Marinescu. 1979. *Polydora ciliata* Polychaeta perforates the gastropod *Rapana thomasiana* of the Black Sea. *Trav. Mus. Hist. Nat. "Grigore Antipa"* **20:** 35–42.

Hanna, G. D. 1966. The introduced mollusks of Western North America. *Occas. Pap. Calif. Acad. Sci.* Vol. 48. 108 pp.

Harding, J. M., and R. Mann. 1999. Observations on the biology of the veined rapa whelk, *Rapana venosa* (Valenciennes, 1846) in the Chesapeake Bay. *J. Shellfish Res.* **18:** 9–17.

Hutchinson, G. E. 1979. *An Introduction to Population Ecology.* Yale University Press, New Haven, CT.

Kennedy, V. S., R. I. E. Newell, and A. F. Eble, eds. 1996. *The Eastern Oyster,* Crassostrea virginica. University of Maryland Sea Grant Press, College Park, MD. 734 pp.

Kool, S. 1993. Phylogenetic analysis of the Rapaninae (Neogastropoda: Muricidae). *Malacologia* **35:** 155–259.

Koutsoubas, D., and E. Voultsiadou-Koukoura. 1990. The occurrence of *Rapana venosa* (Valenciennes, 1846) (Gastropoda, Thaididae) in the Aegean Sea. *Boll. Malacol.* **26(10–12):** 201–204.

Lai, K. Y., and C. W. Pan. 1980. The *Rapana* shells of Taiwan. *Bull. of Malacology, Republic of China.* **7:** 27–32.

Luckenbach, M., R. Mann, and J. E. Wesson, eds. 1999. *Oyster Reef Habitat Restoration: A Synopsis of Approaches.* Virginia Institute of Marine Science, Gloucester Point, VA. 366 pp.

Mann, R. 2000. Restoring oyster reef communities in the Chesapeake Bay: a commentary. *J. Shellfish Res.* **19:** 335–340.

Mann, R. 2001. Restoration of the oyster resource in the Chesapeake Bay. *Bull. Aquacul. Assoc. Can.* **101:** 38–42.

Mann, R., and J. M. Harding. 2000. Invasion of the North American Atlantic coast by a large predatory Asian mollusc. *Biol. Invasions* **2:** 7–22.

Marinov, T. M. 1990. *The Zoobenthos From the Bulgarian Sector of the Black Sea. Academy of Science Publications Sofia.* 195 pp. [In Bulgarian].

Mel, P. 1976. Sulla presenza di *Rapana venosa* (Valenciennes) e di *Charonia variegata sequenzae* (Ar. & Ben.) nell'Alto Adriatico. *Conchiglie, (Milan)* **12(5–6):** 129–132.

Morton, B. 1994. Prey preference and method of attack by *Rapana bezoar* (Gastropoda: Muricidae) from Hong Kong. Pp. 309–325 in *The Malacofauna of Hong Kong and Southern China III,* B. Morton, ed. Hong Kong University Press, Hong Kong.

Pastorino, G. P., A. Penchaszadeh, L. Schejter, and C. Bremec. 2000. *Rapana venosa* (Valenciennes) (Mollusca: Muricidae): a new gastropod in South Atlantic waters. *J. Shellfish Res.* **19:** 897–900.

Rennie, S., and B. Nielson. 1994. *Chesapeake Bay Atlas.* Virginia Institute of Marine Science, Gloucester Point, VA.

Rinaldi, E., 1985. *Rapana venosa* (Valenciennes) spiaggiata in notevole quantita sufla spiaggia di Rimini (Fo). *Boll. Malacol.* **21:** 318.

Rubinshtein, I. G., and V. I. Hiznjak. 1998. Stocks of *Rapana thomasiana* in the Kerch Strait. *Rybn. Khoz* **1:** 39–41 (in Russian).

Sandlund, O. T., P. J. Schei, and A. Viken. 1999. Introduction: the many aspects of the invasive alien species problem. Pp. 1–7 in *Invasive Species and Biodiversity Management,* O. T. Sandlund, P. J. Schei, and A. Viken, eds. Kluwer Academic Publishers, Dordrecht. 413 pp.

Savini, D., J. M. Harding, and R. Mann. 2003. Rapa whelk *Rapana venosa* (Valenciennes, 1846) predation rates on hard clams *Mercenaria mercenaria* (Linneaus, 1758). *J. Shellfish Res.* **21(2).** (In press).

Stroup, E., and R. Lynn. 1963. *Atlas of Salinity and Temperature Distributions in Chesapeake Bay 1952-61 and Seasonal Averages 1949-61.* Graphical Summary Report 2. *Report 63-1.* The Chesapeake Bay Institute, The Johns Hopkins University.

Terreni, G. 1980. Molluschi poco conosciuti dell'Arcipelago Toscano: 1-Gasteropodi. *Boll. Malacol.* **16:** 9–17.

Theroux, R. B., and R. L. Wigley. 1983. *Distribution and Abundance of East Coast Bivalve Mollusks Based on Specimens in the National Marine Fisheries Service Woods Hole Collections.* NOAA Technical Report NMFS SSRF-768. 172 pp.

Tsi, C. Y., X. T. Ma, Z. K. Lou, and F. S. Zhang. 1983. *Illustrations of the Fauna of China (Mollusca).* Vol. 2, plates I–IV. Science Press, Beijing. 150 pp.

Vermeij, G. J. 1993. *A Natural History of Shells.* Princeton University Press, Princeton, NJ.

Vermeij, G. J. 1996. An agenda for invasion biology. *Biol. Conserv.* **78:** 3–9.

Williamson, M. 1996. *Biological Invasions.* Chapman and Hall, London. 244 pp.

Wu, Y. 1988. Distribution and shell height-weight relation of *Rapana venosa* Valenciennes in the Laizhou Bay. *Marine Science/Haiyang Kexue* **6:** 39–40.

Zolotarev, V. 1996. The Black Sea ecosystem changes related to the introduction of new mollusc species. *Mar. Ecol.* **17:** 227–236.

Reference: *Biol. Bull.* **204:** 104–108. (February 2003)

Short-Distance Spawning Migration of Tropical Freshwater Eels

JUN AOYAMA[1,*], SAM WOUTHUYZEN[2], MICHAEL J. MILLER[1], TADASHI INAGAKI[1], AND KATSUMI TSUKAMOTO[1]

[1] *Ocean Research Institute, The University of Tokyo, 1-15-1 Minamidai, Nakano, Tokyo 164-8639, Japan; and* [2] *Research Center for Oceanography, Indonesian Institute of Sciences, Anchor, Jakarta, Indonesia*

The freshwater eels have fascinated biologists because of their spectacular long-distance migrations between their freshwater habitats and their spawning areas far out in the ocean (1, 2, 3). Recent progress on the molecular phylogeny of freshwater eels suggests that they originated in the tropics (4), and information on the reproductive ecology and recruitment of tropical species will provide new insight into the evolution of the spawning migration of the freshwater eels (5, 6). However, the larvae (leptocephali) of the many sympatric tropical species are morphologically similar (7), so they are impossible to identify, and their spawning areas are thus virtually unknown. Recently, however, we have collected small leptocephali from around Sulawesi, Indonesia, and have used species-specific genetic markers to identify them as larvae of Anguilla celebesensis *and* A. borneensis, *which provides the first definitive information about the general spawning areas of these tropical eels. Moreover, the discovery of a spawning area of* A. celebesensis *in Tomini Bay and the presence of small specimens of two species in the Celebes Sea indicate that, in contrast to the long migrations made by temperate eels, tropical eels make much shorter migrations to spawn in areas near their freshwater habitats. This difference in migratory behavior may reflect an evolutionary cline among freshwater eels that extends from tropical to temperate regions.*

Early in the last century, the Danish oceanographer Johannes Schmidt succeeded in collecting small anguillid leptocephali in the Sargasso Sea thousands of kilometers away from their growth habitats in Europe and North America, which indicated that the two species of Atlantic freshwater eels make remarkably long spawning migrations (1). After this finding, he and his colleagues shifted their efforts to search for the spawning areas of freshwater eels in the Indo-Pacific region where most of the species in the genus are found. They successfully collected more than 1400 leptocephali in the Indo-Pacific region (7) during the Carlsberg Foundation's oceanographic expedition around the world from 1928 to 1930. However, most of these leptocephali were relatively large, and the overlap in their morphological characters made it difficult to identify them exactly (7, 8). Since then, the spawning areas of the Indo-Pacific anguillid species have remained a mystery, except for the Japanese eel, *Anguilla japonica,* which was found to spawn to the west of the Mariana Islands in the western North Pacific (3).

Molecular phylogenetic research on the genus *Anguilla* has recently stimulated interest in the spawning migrations of tropical freshwater eel species by suggesting that the tropical eel, *Anguilla borneensis,* which is endemic to Borneo, is the most basal species, and that the genus radiated out from the tropics to colonize temperate regions (4). Because of these studies, species-specific genetic markers can be used to identify all species of anguillid leptocephali (9). Molecular techniques have, for the first time, allowed studies on the distribution of tropical anguillid leptocephali that can reveal the location of eel spawning areas and the nature of their migrations. In this study, we have collected the smallest tropical eel leptocephali ever reported and used molecular genetic methods to identify species of anguillid leptocephali from the Celebes Sea and Tomini Bay on the east side of Sulawesi. We provide the first definitive information on the spawning areas of tropical freshwater eels.

A cruise of the R/V *Hakuho Maru* (Ocean Research

Received 20 June 2002; accepted 4 December 2002.

* To whom correspondence should be addressed. E-mail: jaoyama@ori.u-tokyo.ac.jp

Institute, University of Tokyo) in the western Pacific, Celebes, and Sulu Seas was conducted from 14 January to 10 March 2000 (Fig. 1). A subsequent cruise of the R/V *Baruna Jaya VII* (Research Center for Oceanography, Indonesian Institute of Sciences), made in the waters around Sulawesi from 8 to 30 May 2001, partly overlapped the sampling area of the *Hakuho Maru* cruise (Fig. 1). Leptocephali were collected during both cruises using identical Isaacs-Kidd midwater trawls with 8.7-m^2 mouth openings and 0.5-mm mesh. The collections usually consisted of 60-min oblique or step tows within the upper 300 m. Aboard ship, the leptocephali were tentatively identified on the basis of morphological characteristics (7, 8), but these characteristics could not always indicate one species. Total length and other measurements were recorded, and the specimens were preserved in 95% ethanol. In the laboratory, the specimens were identified by comparing their mitochondrial 16S rRNA gene sequences with those of morphologically well-identified adult specimens, as has been previously reported (9). Briefly, total genomic DNA was extracted from each leptocephalus according to a standard protocol (9). A portion of the mitochondrial 16S ribosomal RNA gene (about 500 base pairs) was amplified by the polymerase chain reaction (PCR) using two oligonucleotide primers, H2510 and H3058 (9). Amplification parameters were 30 cycles of denaturation at 94 °C for 30 s, annealing at 55 °C for 30 s, and extension at 72 °C for 60 s. The PCR products were sequenced according to the manufacturer's protocol (Applied Biosystems Inc.) on a 373A DNA sequencer (Applied Biosystems Inc.). Sequences were determined from the light strand only. The sequence data obtained from the leptocephali were directly compared, without any alignments, to homologous data for anguillids in the Pacific region (*A. japonica*, *A. australis*, *A. borneensis*, *A. celebesensis*, *A. dieffenbachii*, *A. bicolor*, *A. megastoma*, *A. marmorata*, *A. reinhardtii*, *A. obscura*, and *A. interioris*), deposited in DDBJ/EMBL/GenBank under accession numbers AB021748, AB021751–AB021754, AB021757, AB021758, AB021760–AB021762, AB021764. Within species the sequences were the same or had only one or two site differences, but among species the differences were more than threefold (6–74 sites). All of the sequences determined in the present study will appear in the DDBJ/EMBL/GenBank nucleotide sequence databases with the accession numbers: AB097700–AB097767, in sequence.

During the two research cruises, we collected 67 leptocephali and one glass eel (the transparent early juvenile stage of eels) of the genus *Anguilla* (15 leptocephali from the *Hakuho Maru* cruise and 53 from the *Baruna Jaya VII* cruise, which included the glass eel). Genetic species identification of the leptocephali clearly distinguished 12 *A. marmorata* (34.0–50.7 mm in total length and one glass eel of 47.8 mm), 41 *A. celebesensis* (13.0–47.8 mm), 3 *A. borneensis* (8.5, 13.0, 35.4 mm), 4 *A. bicolor* (42.6–49.2 mm), and 1 *A. interioris* (48.9 mm), all from the waters around Sulawesi (Fig. 1). Also identified were 3 *A. bicolor* (31.3–46.0 mm) from the waters to the north of New Guinea, and 2 *A. marmorata* (28.0, 36.5 mm), 1 *A. obscura* (36.7 mm), and 1 *A. australis* (47.0 mm) from the western South Pacific (their distributions are not shown).

This is the first description of the distribution of anguillid leptocephali identified using genetic markers from Indonesian waters, and these data suggest that as many as five species of the genus *Anguilla* may use the Indonesian waters as an area for spawning and larval development. Jespersen (7) reported on collections of relatively large anguillid leptocephali from many of these same areas, but could not make precise species identifications. Another more recent study used the same molecular genetic techniques used in this study to identify anguillid leptocephali as small as 16.3 mm in the western North and South Pacific, but did not make collections in the Indonesian Seas (9). Of particular interest in our study were the small leptocephali of *A. borneensis* that were 8.5 and 13.0 mm (indicating an age of about 16 and 26 days after hatching [10, 11]), which were collected in the Celebes Sea to the east of Borneo, and the specimen (35.4 mm) that was collected to the south in Makassar Strait, where water from the Celebes Sea is transported (12). The freshwater growth habitat of *A. borneensis* is limited to the east-central part of Borneo (5, 6), which strongly suggests that this species spawns in the Celebes Sea and then migrates back to its growth habitat adjacent to the spawning area (Table 1). Another tropical anguillid species, *Anguilla celebesensis*, has a wider distribution that extends from Luzon of the Philippines to across Sulawesi (5, 6). Interestingly, the small leptocephali of this species collected about 25 days after hatching (10, 11) were found in two different seasons and in two different areas separated by the northern arm of Sulawesi: a 12.3-mm specimen was found at Station 50 in the Celebes Sea in February, and a 13-mm specimen was found at Station 21 in Tomini Bay in May (Fig. 1). Further, the collection of nine *A. celebesensis* leptocephali at Station 21 in Tomini Bay ranged in total length from 13 to 48.9 mm (fully grown larval stage [10, 11]). These facts indicate that individuals of *A. celebesensis* inhabiting the watershed of Tomini Bay spawn over a relatively long period and that their leptocephali are retained in Tomini Bay because it is semi-enclosed and its waters apparently do not mix much with those of other areas (13). Therefore, these eels are probably geographically isolated from those in the Celebes Sea.

The findings reported here indicate that freshwater eels living in tropical areas may have life-history characteristics that differ markedly from those of their temperate relatives, which have a single spawning site for each species, long spawning migrations in both the North Atlantic (1, 2) and North Pacific Ocean (3), and distinct spawning seasons (Table 1). This distinction is supported by recent analyses of

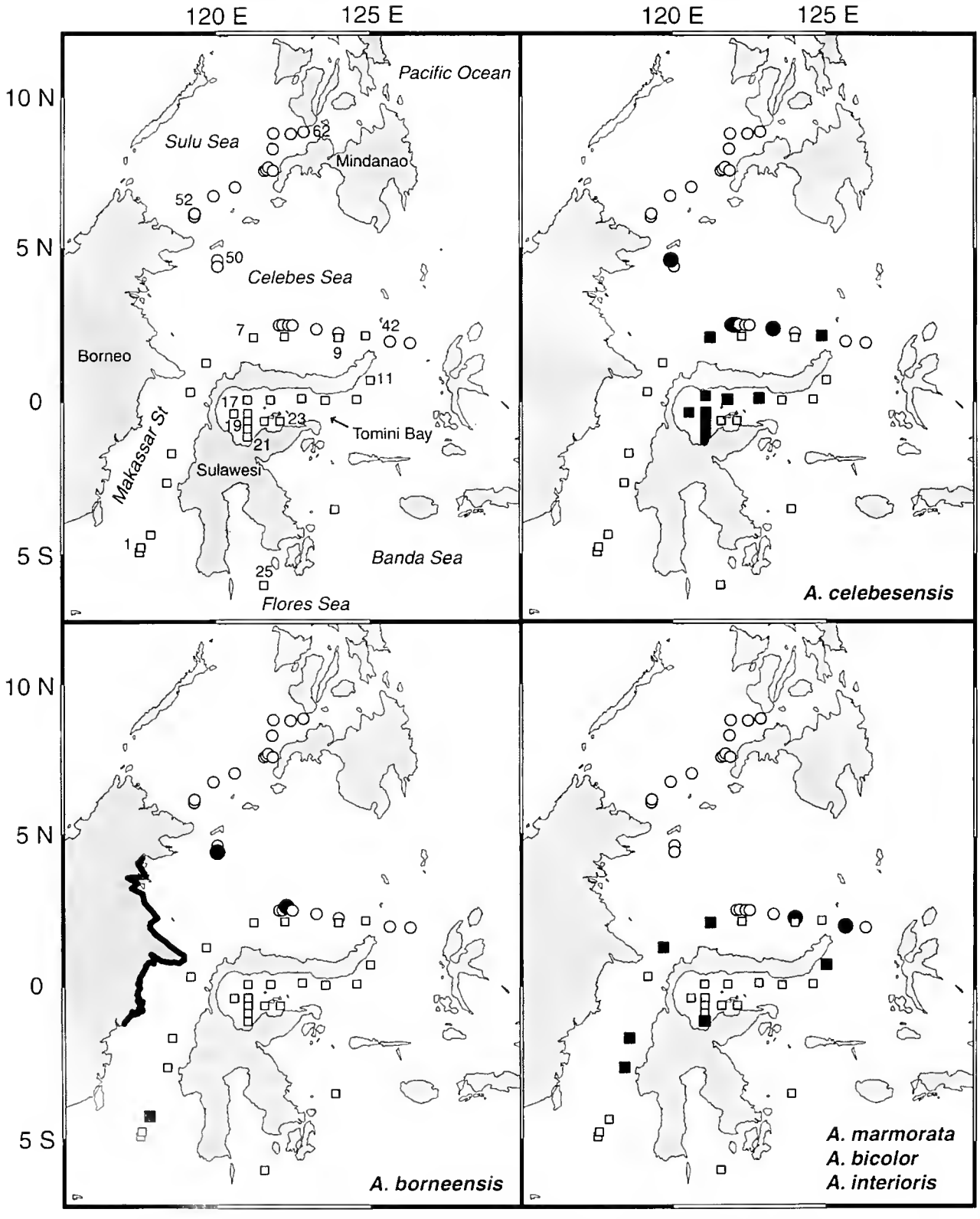

Figure 1. The study area, showing the sampling stations and the locations where the various species of anguillid leptocephali were collected. Upper left: Stations during cruises of the R/V *Hakuho Maru* (circles) in February 2000 and the R/V *Baruna Jaya VII* (squares) in May 2001. Only a few station numbers are shown to indicate the order of sampling or to identify those mentioned in the text. Upper right: Solid symbols indicate sampling stations where *A. celebesensis* leptocephali were collected and open symbols indicate negative stations. Lower left: Collection locations of *A. borneensis*. Lower right: Collection locations of *A. marmorata*, *A. bicolor*, and *A. interioris*. Symbols same as for upper right panel.

Table 1

Comparison of presumed spawning areas, ranges, and distance of migration of temperate and tropical eels. (genus Anguilla*)*

Species	Presumed spawning area	Approximate latitudinal range (5)	Approximate distance to spawning area (6)	
			Nearest	Endmost
European eel *A. anguilla*	Sargasso Sea (2) 25°N, 60°W	28°N–68°N	4000 km Azores, Cape Verde Is.	8000 km Norway, Mediterranean
American eel *A. rostrata*	Sargasso Sea (2) 25°N, 60°W	10°N–62°N	900 km Greater Antilles	5500 km Iceland
Japanese eel *A. japonica*	West of Mariana Is. (3) 15°N, 142°E	18°N–43°N	2000 km Taiwan	3500 km Northern Japan
A. borneensis	Celebes Sea 3°N, 122°E	Equator-7°N	480 km Tawau, Borneo	650 km Mahakam Riv., Borneo
*A. celebesensis**	Tomini Bay 1°S, 121°E	1.4°S–0.5°N	80 km Coastal areas around the bay	300 km

Numbers in parentheses are reference citations; see Literature Cited.
* For a part of a species or population found in the present study.

otolith microstructure which showed that tropical anguillids in the Indonesian region may spawn (14) and recruit to freshwater (15) throughout much of the year. Catadromous freshwater eels have been suggested to have originated in the tropical waters near present-day Indonesia sometime around the late-Cretaceous to Eocene, and the endemic tropical species *A. borneensis* has been found to be the most likely basal catadromous eel species (4). Various characteristics of the migrations of present-day anguillid species clearly show at least a partial geographic cline (Table 1). For example, the most likely basal species, *A. borneensis*, is distributed narrowly over about 7 degrees of latitude (Equator to 7 °N) and spawns nearby in the Celebes Sea at a distance of only 480–650 km; in contrast, the growth habitat of the European eel extends widely over 40 degrees of latitude, and the distance to its spawning area in the Sargasso Sea ranges from about 4000 to 8000 km (Table 1). This and the short spawning migration of *A. celebesensis* in Tomini Bay suggest that freshwater eels of the genus *Anguilla* originally had migrated only short distances to local spawning areas in the warm waters surrounding their freshwater growth habitats in the tropics. But following the passive, long-range dispersion of their leptocephalus stages by currents, freshwater eels may have had to evolve long-distance migrations to return from their temperate growth habitats to their tropical spawning grounds.

The Atlantic species of freshwater eels are often used, even in basic biological textbooks, as a classic example of a species with a spectacular long-distance migration. However, our findings provide the first evidence that this long-distance migration is an adaptation by eels that colonized temperate regions. Therefore, a new era of research on the ecology and behavior of tropical eels has begun, and it promises to unveil the mystery of the origin and evolution of the catadromous migrations of the genus *Anguilla*.

Acknowledgments

We thank all of the scientists who participated in the eel cruises and who worked together discussing the sampling design, operating the nets, and sorting samples. We wrote this paper on behalf of all the scientists aboard, and we also thank all the crew of the *Hakuho Maru* and the *Baruna Jaya VII* for their help during the cruise. This work was supported in part by Grants-in-Aid Numbers 07306022, 07556046, 08041139, 08456094, 10460081, and 11691177 from the Ministry of Education, Science, Sports and Culture, Japan, and by grant Numbers JSPS-RFTF 97L00901 from the "Research for the Future Program" of the Japan Society for the Promotion of Science. KT was supported by the Research Foundation "Touwa Shokuhin Shinkoukai" and the Eel Research Foundation "Noborika."

Literature Cited

1. **Schmidt, J. 1922.** The breeding places of the eel. *J. Philos. Trans. R. Soc. B* **211:** 179–208.
2. **McCleave, J. D., R. C. Kleckner, and M. Castonguay. 1987.** Reproductive sympatry of American and European eels and implications for migration and taxonomy. *Am. Fish. Soc. Symp.* **1:** 286–297.
3. **Tsukamoto, K. 1992.** Discovery of spawning area for the Japanese eel. *Nature* **356:** 789–791.
4. **Aoyama, J., M. Nishida, and K. Tsukamoto. 2001.** Molecular phylogeny and evolution of the freshwater eels, genus *Anguilla*. *Mol. Phylogenet. Evol.* **20:** 450–459.
5. **Ege, V. 1939.** A revision of the genus *Anguilla* Shaw. *Dana-Rep.* **16:** 1–256.

6. **Tesch, F. W. 1977.** *The Eel: Biology and Management of Anguillid Eels.* Chapman and Hall, London.
7. **Jespersen, P. 1942.** Indo-Pacific leptocephalids of the genus *Anguilla. Dana-Rep.* **22:** 1–128.
8. **Castle, P. H. J. 1963.** Anguillid leptocephali in the southwest Pacific. *Zool. Publ. Victoria Univ.* **33:** 1–14.
9. **Aoyama, J., N. Mochioka, T. Otake, S. Ishikawa, Y. Kawakami, P. H. J. Castle, M. Nishida, and K. Tsukamoto. 1999.** Distribution and dispersal of anguillid leptocephali in the western Pacific revealed by molecular analysis. *Mar. Ecol. Prog. Ser.* **188:** 193–200.
10. **Arai, T., J. Aoyama, S. Ishikawa, M. J. Miller, T. Otake, T. Inagaki, and K. Tsukamoto. 2001.** Early life history of tropical *Anguilla* leptocephali in the western Pacific Ocean. *Mar. Biol.* **138:** 887–895.
11. **Ishikawa, S., K. Suzuki, T. Inagaki, S. Watanabe, Y. Kimura, A. Okamura, T. Otake, N. Mochioka, Y. Suzuki, H. Hasumoto, M. Oya, M. J. Miller, T. W. Lee, H. Fricke, and K. Tsukamoto. 2001.** Spawning time and place of the Japanese eel, *Anguilla japonica*, in the North Equatorial Current of the western North Pacific Ocean. *Fish. Sci.* **67:** 1097–1103.
12. **Miyama, T., T. Awaji, K. Akitomo, and N. Imasato. 1995.** Study of seasonal transport variations in the Indonesian Seas. *J. Geophys. Res.* **100:** 20,517–20,541.
13. **Hatayama, T., T. Awaji, and K. Akitomo. 1996.** Tidal currents in the Indonesian Seas and their effect on transport and mixing. *J. Geophys. Res.* **101:** 12,353–12,373.
14. **Arai, T., D. Limbong, T. Otake, and K. Tsukamoto. 2001.** Recruitment mechanisms of tropical eels *Anguilla* spp. and implications for the evolution of oceanic migration in the genus *Anguilla. Mar. Ecol. Prog. Ser.* **216:** 253–264.
15. **Sugeha, H. Y., T. Arai, M. J. Miller, D. Limbong, and K. Tsukamoto. 2001.** Inshore migration of the tropical eels, *Anguilla* spp., recruiting to the Poigar River estuary on Sulawesi Island. *Mar. Ecol. Prog. Ser.* **221,** 233–243.

THE BIOLOGICAL BULLETIN

2003 Subscription Rates
Volumes 204-205

***Paid Subscriptions include both print and electronic subscriptions at:** www.biolbull.org

	Institutional*	Individual*
One year subscription (6 issues - 2 volumes)	$280.00	$105.00
Single volume (3 issues)	$140.00	$52.50
Single Issues	$ 50.00	$20.00

*Surface delivery included in above prices.
For prompt delivery, we encourage subscribers outside the U.S. to request airmail service.

Airmail Delivery Charge

U.S. and Canada:	$ 25.00
Mexico:	$ 60.00
All other locations:	$100.00

Orders Must Be Prepaid in U.S. Dollars, Check Payable to The Marine Biological Laboratory

About *The Biological Bulletin*
ISSN: 0006-3185
Frequency: Bimonthly
Number of issues per year: 6
Months of Publication: February, April, June, August, October, December
Subscriptions entered for calendar year
Volume indexes contained in June and December issues
Annual report of the Marine Biological Laboratory contained in August issue
Most back issues available
Claims handled upon receipt
No agency discounts
Internet:
www.biolbull.org

Please address orders to:
Wendy Child
Subscription Administrator
The Biological Bulletin
Marine Biological Laboratory
7 MBL Street
Woods Hole, MA 02543-1015 U.S.A.
Fax: 508-289-7922 Tel: 508-289-7402 Email: wchild@mbl.edu

Published by the Marine Biological Laboratory
Woods Hole, Massachusetts, 02543 U.S.A.

THE BIOLOGICAL BULLETIN
(www.biolbull.org)
2003 SUBSCRIPTION FORM
(VOLUMES 204-205, 6 ISSUES)

All subscriptions run on the calendar year; price includes both print and online journals.

(please print)

NAME: _____

INSTITUTION: _____

ADDRESS: _____

CITY: _____ STATE: _____

POSTAL CODE: _____ COUNTRY: _____

TELEPHONE: _____ FAX: _____

E-MAIL ADDRESS: _____

❒ **Please send me a 2003 subscription to *The Biological Bulletin* at the rate indicated below:**

❒ Individual: $105.00 (6 ISSUES) ❒ Institutional: $280.00 (6 ISSUES)
❒ Individual: $ 52.50 (3 ISSUES) ❒ Institutional: $140.00 (3 ISSUES)
Check one: ❒ February, April, June or ❒ August, October, December

❒ **Please send me the following back issue(s):** _____

❒ Individual: at $20.00 (PER ISSUE) ❒ Institutional: at $50.00 (PER ISSUE)

Delivery Options

_____ Surface Delivery (Surface delivery is included in the subscription price.)

_____ Air delivery (Please add the correct amount to your payment.)

❒ U.S. and Canada: $25.00 ❒ Mexico: $60.00 ❒ All other locations: $100.00

Payment Options

_____ Enclosed is my check or U.S. money order for $ _____ payable to The Marine Biological Laboratory

_____ Please send me an invoice. (Note: Payment must be received before subscription commences.)

_____ Please charge my ❒ VISA, ❒ MasterCard ❒ Discover Card $_____

Account No.: _____ Exp. Date: _____

Signature: _____ Date: _____

Return this form with your check or credit card information to:

Marine Biological Laboratory
Subscription Office ◆ The Biological Bulletin ◆7 MBL Street ◆ Woods Hole, MA 02543-1015

Marine Resources Center

MARINE BIOLOGICAL LABORATORY • WOODS HOLE, MA 02543 • (508)289-7700
WWW.MBL.EDU/SERVICES/MRC/INDEX.HTML

zebrafish facilities

Animal and Tissue Supply for Education & Research

- 150 aquatic species available for shipment via online catalog: <http://www.mbl.edu/animals/index.html>; phone: (508)289-7375; or e-mail: specimens@mbl.edu
- zebrafish colony containing limited mutant strains
- custom dissection and furnishing of specific organ and tissue samples

MRC Services Available

- basic water quality analysis
- veterinary services (clinical, histopathologic, microbial services, health certificates, etc.)
- aquatic systems design (mechanical, biological, engineering, etc.)
- educational tours and collecting trips aboard the R/V Gemma

Using the MRC for Your Research

- capability for advanced animal husbandry (temperature, light control, etc.)
- availability of year-round, developmental life stages
- adaptability of tank system design for live marine animal experimentation

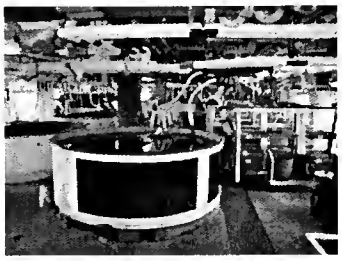

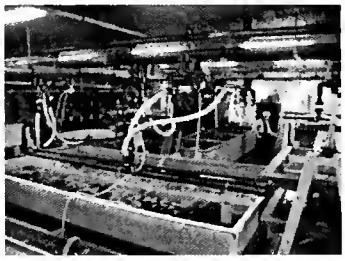

It's Worth A Closer Look.

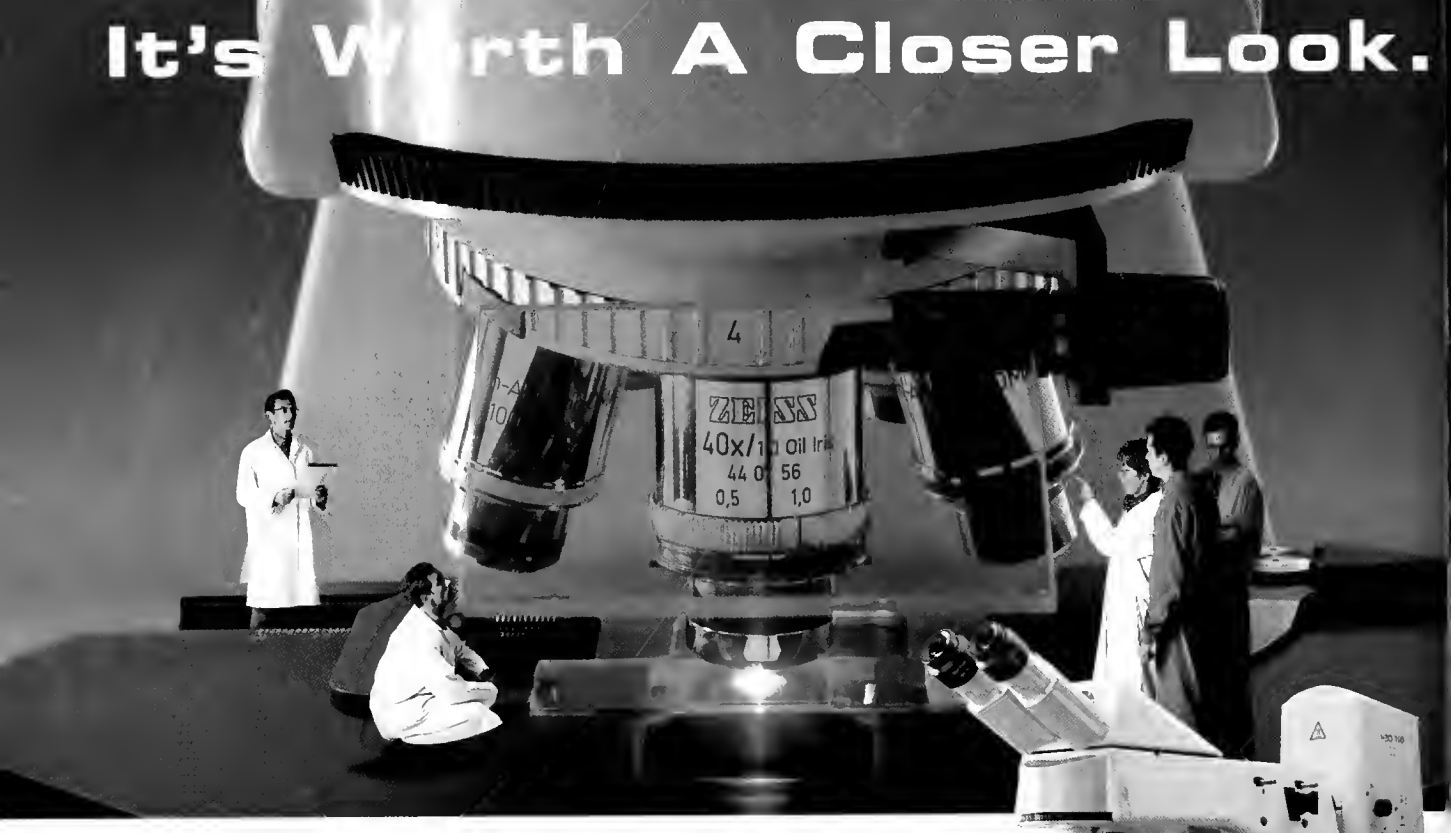

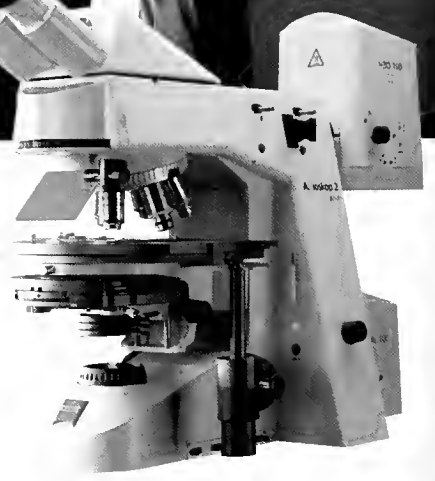

New Axioskop 2 Plus. The Ultimate Microscope For Life Science.

Brilliant and easy.

Supporting all fluorescence techniques, producing brilliant images with outstanding documentation and digital image processing, the **Axioskop 2 Plus** and motorized **Axioskop 2 MOT** offer new levels of comfort and productivity in biomedical research.

Ergonomics made to order.

The Axioskop 2 Plus effortlessly adjusts to your individual viewing posture. Move the eyepiece tubes up or down, or change the angle for optimum comfort. With low-positioned focusing knobs, you can simply rest your elbows on the table for hours of fatigue free observation. An adjustable height stop gets you back to focus fast after a specimen change. Rotating stage with click-stops retrieves your initial stage position quickly.

Fluorescence. Quick and quintuple.

New reflector turret holds up to 5 different filter combinations for fast, easy and vibration free exchange. Pre-adjusted filter sets are mounted in cubes and can be quickl exchanged using new Push & Click mechanism And with the smart condenser, switchin between DIC, BF, DF, or Phase is easy Illumination/condenser settings will adjus automatically. Streamlined beam patl ensures high UV range transmission, maximun brightness, and homogeneous illumination.

For more information call 800.233.2343 or email micro@zeiss.com.

Carl Zeiss MicroImaging, Inc.
Thornwood, NY 10594
800.233.2343

Fax 914.681.7446
micro@zeiss.com
zeiss.com/micro

ZEISS

THE

AI

B

Published by [illegible]

WHEN IT COMES TO SPEED AND HANDLING,

ABOUT THE ONLY THING NOT MOTORIZED IS YOU.

ROCKET SCIENCE.™

800 446 5967 olympusamerica.com/microscopes

Cover

The background image on the cover of this issue shows an area (1–2 m^2) of intertidal microbial mats, 0.5 to 2 cm thick, adjacent to the largest salt works in North America—Exportadora de Sal—located in Guerrero Negro, Baja California Sur, Mexico. Hypersaline ponds belonging to the salt works harbor extensive cyanobacterial mats, which are extraordinarily diverse, complex, and highly organized ecosystems. On p. 160 of this issue, David J. Des Marais reviews his own and others' comprehensive studies of these mats. He asks how such systems respond in a coordinated fashion to cyclical or transient environmental changes and how they influence sedimentation and produce gases.

Microbial mats are laminated, and the component microorganisms in the community are localized to layers at specific depths. Layering is visible in the inset on the cover—a Nomarski image of a section through the upper 2 mm of a mat. The productivity of the mat is dominated by *Microcoleus chthonoplastes*, a filamentous cyanobacterium (the yellow-green region near the top of the section). During the day, photosynthesis by *Microcoleus* and many other cyanobacteria is intense, and the oxygen generated diffuses downward. But the light is strongly absorbed, and the oxygen is rapidly consumed by heterotrophs, so an aphotic, anoxic zone develops, beginning at a depth of only about 1.5 mm (the dark region near the bottom of the section). Meanwhile, anaerobic organisms generate H_2S, which diffuses upward, but is consumed by photosynthetic bacteria (which function in very dim, infrared light) and chemoautotrophs like *Beggiatoa* (the beaded filaments visible adjacent to the dark region). The dark layer thus marks the interface between the diminished concentrations of oxygen and sulfide. At night, photosynthesis ceases, the upper levels of the mat become sulfidic as the oxygen concentration falls, and motile organisms may move upward. Thus, the position of a microorganism in the mat is determined by many factors, including the steep gradients of light, oxygen, and sulfide, physiological adaptations to changes in those gradients, trophic mechanisms, and relationships with other organisms at higher and lower levels in the system.

In a related paper in this issue of *The Biological Bulletin*, John R. Spear and colleagues from the laboratory of Norman R. Pace (p. 168) report on molecular approaches to identifying the components of mat communities in Guerrero Negro and thus quantifying the extent of diversity. They also characterize, partially, a novel, relatively simple, laminated microbial community that occurs in crystalline gypsum; this finding documents further the enormous diversity of microorganisms at this site.

The articles by Des Marais and Spear *et al.* are both part of a workshop entitled *Outcomes of Genome-Genome Interactions* (p. 155). This meeting was meant to establish links among biogeochemical factors, microbial metabolic processes, maintenance of microbial population structures in nature, and microbial symbioses with multicellular hosts. The workshop was held at Woods Hole, Massachusetts (May 1–3, 2002) and was sponsored by the Center for Advanced Studies in the Space Life Sciences at the Marine Biological Laboratory (MBL).

The large, background image of the microbial mats *in situ* was taken by John R. Spear (University of Colorado, Boulder), and the Nomarsky image was taken by Jack D. Farmer (Arizona State University, Tempe). The composite picture on the cover was produced by Beth Liles at the MBL.

THE
BIOLOGICAL BULLETIN
APRIL 2003

Published by
Marine Biological Laboratory
Woods Hole, Massachusetts

http://www.biolbull.org

Cool. Fast. Reliable.

Launch a Microway® Linux cluster and solve your problems in life sciences, structure design, weather, astronomy . . .

Run cool. Microway's **CoolFlow**™ 1U chassis is designed to provide the best cooling in the industry. Low temperatures result in higher CPU and memory reliability, plus longer cluster life.

Take control. Monitor *and* control your cluster remotely via our secure web-based GUI. Microway's **NodeWatch**™ hardware and **MCMS**™ cluster management software report on temperatures, voltages, and chassis fans, and let you set thresholds for notification and/or failsafe shutdown if problems occur.

Today's HPC market is wilder than ever. Microway's expert design team will guide you through the whitewater of hardware, software, and storage solutions. Our clusters are competitively priced and delivered on time—and their proven reliability yields low total lifetime cost. What's more, our tech support is legendary.

Call us to test drive **NodeWatch**™ online, arrange a benchmark, and discuss your next Linux cluster with people who speak your language. Visit our website for *HPC Times* technical news.

CoolRak™ Cabinet
Features Xeon XBlade™
Technology

- 1.056 Teraflops per 44U cabinet running 3.06 GHz Xeons
- NodeWatch™ remote control and monitoring
- CoolFlow™ proprietary 1U and 4U chassis
- Myrinet, GigE, or InfiniBand™ connectivity

Microway

Scientists have been counting on us for over 20 years.℠

intel inside ITANIUM 2 AMD Opteron intel inside

508.746.7341 • www.microway.com

CONTENTS

VOLUME 204, NO. 2: APRIL 2003

THE BIOLOGICAL BULLETIN

THE BIOLOGICAL BULLETIN is published six times a year by the Marine Biological Laboratory, 7 MBL Street, Woods Hole, Massachusetts 02543.

Subscriptions and similar matter should be addressed to Subscription Administrator, THE BIOLOGICAL BULLETIN, Marine Biological Laboratory, 7 MBL Street, Woods Hole, Massachusetts 02543. Subscription includes both print and online journals. Subscription per year (six issues, two volumes): $280 for libraries; $105 for individuals. Subscription per volume (three issues): $140 for libraries; $52.50 for individuals. Back and single issues (subject to availability): $50 for libraries; $20 for individuals.

Communications relative to manuscripts should be sent to Michael J. Greenberg, Editor-in-Chief, or Pamela Clapp Hinkle, Managing Editor, at the Marine Biological Laboratory, 7 MBL Street, Woods Hole, Massachusetts 02543. Telephone: (508) 289-7149, FAX: 508-289-7922, E-mail: pclapp@mbl.edu.

http://www.biolbull.org

THE BIOLOGICAL BULLETIN is indexed in bibliographic services including *Index Medicus* and MEDLINE, *Chemical Abstracts, Current Contents, Elsevier BIOBASE/Current Awareness in Biological Sciences,* and *Geo Abstracts.*

Printed on acid free paper,
effective with Volume 180, Issue 1, 1991.

POSTMASTER: Send address changes to THE BIOLOGICAL BULLETIN, Marine Biological Laboratory, 7 MBL Street, Woods Hole, MA 02543.

Periodicals postage paid at Woods Hole, MA, and additional mailing offices.
ISSN 0006-3185

INSTRUCTIONS TO AUTHORS

The Biological Bulletin accepts outstanding original research reports of general interest to biologists throughout the world. Papers are usually of intermediate length (10–40 manuscript pages). A limited number of solicited review papers may be accepted after formal review. A paper will usually appear within four months after its acceptance.

Very short, especially topical papers (less than 9 manuscript pages including tables, figures, and bibliography) will be published in a separate section entitled "Research Notes." A Research Note in *The Biological Bulletin* follows the format of similar notes in *Nature*. It should open with a summary paragraph of 150 to 200 words comprising the introduction and the conclusions. The rest of the text should continue on without subheadings, and there should be no more than 30 references. References should be referred to in the text by number, and listed in the Literature Cited section in the order that they appear in the text. Unlike references in *Nature*, references in the Research Notes section should conform in punctuation and arrangement to the style of recent issues of *The Biological Bulletin*. Materials and Methods should be incorporated into appropriate figure legends. See the article by Lohmann *et al.* (October 1990, Vol. **179:** 214–218) for sample style. A Research Note will usually appear within two months after its acceptance.

The Editorial Board requests that regular manuscripts conform to the requirements set below; those manuscripts that do not conform will be returned to authors for correction before review.

1. ***Manuscripts.*** Manuscripts, including figures, should be submitted in quadruplicate, with the originals clearly marked. (Xerox copies of photographs are not acceptable for review purposes.) If possible, please include an electronic copy of the text of the manuscript. Label the disk with the name of the first author and the name and version of the wordprocessing software used to create the file. If the file was not created in some version of Microsoft Word, save the text in rich text format (rtf). The submission letter accompanying the manuscript should include a telephone number, a FAX number, and (if possible) an E-mail address for the corresponding author. The original manuscript must be typed in no smaller than 12 pitch or 10 point, using double spacing (*including* figure legends, footnotes, bibliography, etc.) on one side of 16- or 20-lb. bond paper, 8 by 11 inches. Please, no right justification. Manuscripts should be proofread carefully and errors corrected legibly in black ink. Pages should be numbered consecutively. Margins on all sides should be at least 1 inch (2.5 cm). Manuscripts should conform to the *Council of Biology Editors Style Manual*, 5th Edition (Council of Biology Editors, 1983) and to American spelling. Unusual abbreviations should be kept to a minimum and should be spelled out on first reference as well as defined in a footnote on the title page. Manuscripts should be divided into the following components: Title page, Abstract (of no more than 200 words), Introduction, Materials and Methods, Results, Discussion, Acknowledgments, Literature Cited, Tables, and Figure Legends. In addition, authors should supply a list of words and phrases under which the article should be indexed.

2. ***Title page.*** The title page consists of a condensed title or running head of no more than 35 letters and spaces, the manuscript title, authors' names and appropriate addresses, and footnotes listing present addresses, acknowledgments or contribution numbers, and explanation of unusual abbreviations.

3. ***Figures.*** The dimensions of the printed page, 7 by 9 inches, should be kept in mind in preparing figures for publication. We recommend that figures be about 1 times the linear dimensions of the final printing desired, and that the ratio of the largest to the smallest letter or number and of the thickest to the thinnest line not exceed 1:1.5. Explanatory matter generally should be included in legends, although axes should always be identified on the illustration itself. Figures should be prepared for reproduction as either line cuts or halftones. Figures to be reproduced as line cuts should be unmounted glossy photographic reproductions or drawn in black ink on white paper, good-quality tracing cloth or plastic, or blue-lined coordinate paper. Those to be reproduced as halftones should be mounted on board, with both designating numbers or letters and scale bars affixed directly to the figures. All figures should be numbered in consecutive order, with no distinction between text and plate figures and cited, in order, in the text. The author's name and an arrow indicating orientation should appear on the reverse side of all figures.

Digital art: The Biological Bulletin will accept figures submitted in electronic form; however, digital art must conform to the following guidelines. Authors who create digital images are wholly responsible for the quality of their material, including color and halftone accuracy.

Format. Acceptable graphic formats are TIFF and EPS. Color submissions must be in EPS format, saved in CMKY mode.

Software. Preferred software is Adobe Illustrator or Adobe Photoshop for the Mac and Adobe Photoshop for Windows. Specific instructions for artwork created with various software programs are available on the Web at the Digital Art Information Site maintained by Cadmus Professional Communications at http://cpc.cadmus.com/da/

Resolution. The minimum requirements for resolution are 1200 DPI for line art and 300 for halftones.

Size. All digital artwork must be submitted at its actual printed size so that no scaling is necessary.

Multipanel figures. Figures consisting of individual parts (*e.g.*, panels A, B, C) must be assembled into final format and submitted as one file.

Hard copy. Files must be accompanied by hard copy for use in case the electronic version is unusable.

Disk identification. Disks must be clearly labeled with the following information: author name and manuscript number; format (PC or Macintosh); name and version of software used.

Color: The Biological Bulletin will publish color figures and plates, but must bill authors for the actual additional cost of printing in color. The process is expensive, so authors with more than one color image should—consistent with editorial concerns, especially citation of figures in order—combine them into a single plate to reduce the expense. On request, when supplied with a copy of a color illustration, the editorial staff will provide a pre-publication estimate of the printing cost.

4. ***Tables, footnotes, figure legends, etc.*** Authors should follow the style in a recent issue of *The Biological Bulletin* in preparing table headings, figure legends, and the like. Because of the high cost of setting tabular material in type, authors are asked to limit such material as much as possible. Tables, with their headings and footnotes, should be typed on separate sheets, numbered with consecutive Arabic numerals, and placed after the Literature Cited. Figure legends should contain enough information to make the figure intelligible separate from the text. Legends should be typed double spaced, with consecutive Arabic numbers, on a separate sheet at the end of the paper. Footnotes should be limited to authors' current addresses, acknowledgments or contribution numbers, and explanation of unusual abbreviations. All such footnotes should appear on the title page. Footnotes are not normally permitted in the body of the text.

5. ***Literature cited.*** In the text, literature should be cited by the Harvard system, with papers by more than two authors cited as Jones *et al.*, 1980. Personal communications and material in preparation or in press should be cited in the text only, with author's initials and institutions, unless the material has been formally accepted and a volume number can be supplied. The list of references following the text should be headed Literature Cited, and must be typed double spaced on separate pages, conforming in punctuation and arrangement to the style of recent issues of *The Biological Bulletin*. Citations should include complete titles and inclusive pagination. Journal abbreviations should normally follow those of the U. S. A. Standards Institute (USASI), as adopted by BIOLOGICAL ABSTRACTS and CHEMICAL ABSTRACTS, with the minor differences set out below. The most generally useful list of biological journal titles is that published each year by BIOLOGICAL ABSTRACTS (BIOSIS List of Serials; the most recent issue). Foreign authors, and others who are accustomed to using THE WORLD LIST OF SCIENTIFIC PERIODICALS, may find a booklet published by the Biological Council of the U.K. (obtainable from the Institute of Biology, 41 Queen's Gate, London, S.W.7, England, U.K.) useful, since it sets out the WORLD LIST abbreviations for most biological journals with notes of the USASI abbreviations where these differ. CHEMICAL ABSTRACTS publishes quarterly supplements of additional abbreviations. The following points of reference style for THE BIOLOGICAL BULLETIN differ from USASI (or modified WORLD LIST) usage:

A. Journal abbreviations, and book titles, all underlined (for *italics*)

B. All components of abbreviations with initial capitals (not as European usage in WORLD LIST *e.g.*, *J. Cell. Comp. Physiol.* NOT *J. cell. comp. Physiol.*)

C. *All* abbreviated components must be followed by a period, whole word components *must not* (*i.e.*, *J. Cancer Res.*)

D. Space between all components (*e.g.*, *J. Cell. Comp. Physiol.*, not *J.Cell.Comp.Physiol.*)

E. Unusual words in journal titles should be spelled out in full, rather than employing new abbreviations invented by the author. For example, use *Rit Vísindafjélags Islendinga* without abbreviation.

F. All single word journal titles in full (*e.g.*, *Veliger*, *Ecology*, *Brain*).

G. The order of abbreviated components should be the same as the word order of the complete title (*i.e.*, *Proc.* and *Trans.* placed where they appear, not transposed as in some BIOLOGICAL ABSTRACTS listings).

H. A few well-known international journals in their preferred forms rather than WORLD LIST or USASI usage (*e.g.*, *Nature, Science, Evolution* NOT *Nature, Lond., Science, N.Y.; Evolution, Lancaster, Pa.*)

6. ***Reprints, page proofs, and charges.*** Authors may purchase reprints in lots of 100. Forms for placing reprint orders are sent with page proofs. Reprints normally will be delivered about 2 to 3 months after the issue date. Authors will receive page proofs of articles shortly before publication. They will be charged the current cost of printers' time for corrections to these (other than corrections of printers' or editors' errors). Other than these charges for authors' alterations, *The Biological Bulletin* does not have page charges.

Reference: *Biol. Bull.* **204:** 109–113. (April 2003)

Ultraviolet-Light-Absorbing Tunic Cells in Didemnid Ascidians Hosting a Symbiotic Photo-oxygenic Prokaryote, *Prochloron*

TADASHI MARUYAMA[1,*,‡], EUICHI HIROSE[2], AND MASAHARU ISHIKURA[1]

[1] *Marine Biotechnology Institute, Kamaishi Laboratories, Heita 3-75-1, Kamaishi, Iwate 026-0001, Japan; and* [2]*Department of Chemistry, Biology, and Marine Sciences, Faculty of Science, University of the Ryukyus, Nishihara, Okinawa, 903-0213, Japan*

Coral reef invertebrates that host phototrophic symbionts are thought to protect themselves and their symbionts with mycosporine-like amino acids (MAAs)—UV-absorbing substances that act as sunscreens (Dunlap, W. C., and J. M. Shick, 1998. J. Phycol. *34: 418–430). However, the histological distribution of MAAs in the host tissues has not yet been visualized. We have localized the UV-absorbing substances in the tissues of two colonial didemnid ascidians—*Lissoclinum patella *and* Diplosoma *sp.—that contain the symbiotic photo-oxygenic prokaryote* Prochloron *sp. Cross-sections of unfixed tissue from these ascidians were examined by UV-light microscopy at 320 or 330 nm, wavelengths at which UV light is absorbed by MAAs. Within the tunic, the gelatinous integument of the colony, UV light was exclusively absorbed by a particular type of cell, the tunic bladder cell. Tunic bladder cells with strong UV absorption were denser in the upper tunic, which lies over a colony's zooids, than in the basal tunic underlying the zooid. In the upper tunic, those cells with strong UV absorption were most dense near the surface. The tunic bladder cell is highly vacuolated, and the vacuole contains strong acid, which destabilizes MAAs. Furthermore, the UV-absorbing portion of tunic bladder cells seemed to be cup-shaped, indicating that the MAAs are not localized in the vacuole, but in the cytoplasm. These results strongly suggest that didemnid ascidians accumulate MAAs in tunic bladder cells as a protection against UV radiation.*

Received 21 June 2002; accepted 22 January 2002.

* To whom correspondence should be addressed. E-mail: tadashim@jamstec.go.jp

‡ Current address: Marine Ecosystem Research Department, Japan Marine Science and Technology Center (JAMSTEC), Natsushima 2-15, Yokosuka, Kanagawa 237-0061, Japan.

Ultraviolet (UV) radiation poses severe problems for organisms in tropical marine environments, because the path for sunlight through the atmosphere is shorter (1) and the seawater is clearer (2). Since the discovery of UV-absorbing substances in marine organisms in the Great Barrier Reef (3), it has been thought that many coral reef invertebrates hosting symbiotic microalgae or photo-oxygenic prokaryotes protect themselves and their symbionts by using, as sunscreens, mycosporine-like amino acids (MAAs) which absorb UV (for review see 4, 5, 6).

The MAAs (λ_{max} 310–360 nm) have strong absorption in the UVA (320–400 nm) and UVB (280–320 nm) range, and some, porphyra-334 (7) and shinorine (8), have been shown to be photochemically stable to UV irradiation. Under ultraviolet radiation (UVR), they neither fluoresce nor produce radical intermediates (9). The MAAs are transparent to visible light (*i.e.*, photosynthetically active radiation, PAR), which is required by the phototrophic symbionts of many invertebrates whose tissues are also exposed to the UVR.

UVR induces an increase in the MAA content of zooxanthellate corals, microalgae, and seaweeds (for review see 6). Corals and some red macroalgae living in shallow water have greater MAA concentrations than those from deeper or shadowed waters (for review see 4, 6). The photosynthetic ability of symbionts isolated from their host tissues is severely damaged by UVR, whereas that of the symbionts within the host is more resistant (10, 11; for review see 6).

The MAAs are thought to be synthesized by the shikimic acid pathway, which has not been reported in metazoan cells (12, 13; for review see 6). It is thought that the host invertebrates acquire MAAs from their diet or from their symbionts (13; for review see 4). In summary, MAAs, which may be synthesized by the symbiont upon stimulation by UV radiation, function as a sunscreen for the symbionts as well as the host.

In tropical waters, some didemnid ascidians host the symbiotic photo-oxygenic prokaryote *Prochloron* (for review see 14). The symbiont cells are usually sequestered within the host colony under an integument, the ascidian tunic, which is transparent to visible light (PAR), but which absorbs maximally at about 320 nm (10). In a symbiotic didemnid, *Lissoclinum patella*, 93%–98% of UV light (312 nm) was reduced by a slice of its integument tunic, thickness 0.5–1.0 mm, whereas 83%–90% of visible light was passed through the slice (10). The tunic of *L. patella* also contains MAAs, such as shinorine, mycosporine-glycine, and palythine (10, 15, 16). Although the tissue content and chemistry of MAAs have been studied intensively in *L. patella* and a variety of other organisms (5), the detailed distribution of these MAAs in the ascidian tunic—whether they are localized in certain tunic cells or in the tunic matrix—remains to be determined. To approach this problem, we studied the histological distribution of UV-absorbing substances in the tunic of two photo-symbiotic didemnid ascidians hosting *Prochloron;* we used UV-light microscopy at 320 or 330 nm, the wavelengths at which MAAs typically show maximal absorption.

A sheet-like colony of didemnid ascidians usually consists of three layers: a layer of zooids and cloacal cavity (ZC in Fig. 1) sandwiched between two layers of tunic (UT and BT in Fig. 1). Both the upper and basal layers of tunic are transparent to visible light (Fig. 2A; also see fig. 3 in reference 10). In photo-symbiotic didemnid ascidians, the *Prochloron* cells are exclusively distributed within the cloacal cavity, *i.e.,* outside the host tissue (CC in Fig. 1). In one of the host ascidians, *Diplosoma* sp., UV microscopy revealed a strong layer of UV absorbance in the upper tunic and a similar layer with less UV absorption in the basal tunic (Fig. 2B). The strength of the UV absorption seemed to depend upon the density of UV-absorbing objects in the layer. Moreover, the UV absorption of each object seemed to be stronger in the layer of the upper tunic than in the basal tunic (Fig. 2B). Similar UV-absorbing layers were also observed in the other host ascidian studied, *L. patella* (data not shown). These results agree well with a previous report that MAA concentration is higher in the upper tunic than in the basal tunic in *L. patella* (10). *Prochloron* cells occupying the cloacal cavity in the middle layer of *Diplosoma* sp. (ZC layer in Fig. 2) also absorbed UV light. Observation of

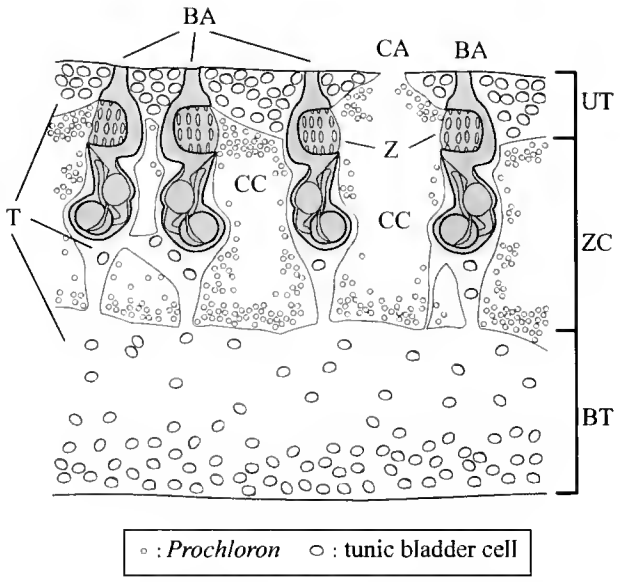

Figure 1. Schematic drawing of a cross-section of a colony of a symbiotic didemnid ascidian. BA, branchial aperture; BT, basal tunic layer; CA, cloacal aperture; CC, cloacal cavity; T, tunic (lightly shaded area); UT, upper tunic layer; Z, zooid (more darkly shaded area); ZC, layer of zooid and cloacal cavity.

the upper tunic at higher magnification revealed that each UV-absorbing object was round or cup-shaped, with a diameter (of the openings of the cup) of 30–43 μm (Fig. 3). When cross-sections of fixed, embedded, and stained ascidian tissues were observed, the tunic was seen to contain many bladder cells, about 50 μm in diameter; moreover, these cells correspond to the UV-absorbing objects (Fig. 4A). This obviously indicates that the MAAs are not localized in the matrix of the tunic, but in the tunic bladder cells. The bladder cell is characterized by a large vacuole occupying most of the cytoplasm (Fig. 4B). Such bladder cells are common in the tunic of many ascidians in the family Didemnidae (17), and their vacuoles usually contain a strongly acidic fluid (18). The cup shape of the UV-absorbing objects (Fig. 3) indicates that the UV-absorbing substance is contained in the cytoplasm of the bladder cell, and that the large vacuole lacks this substance. Because the vacuoles of the bladder cell are known to contain strong acid (17, 18), and because MAAs are unstable in acidic conditions (19), it is reasonable that these MAAs are localized in the cytoplasm.

We have previously reported that the tunic of *L. patella* contains shinorine, one of the most common MAAs, as a major UV-absorbing substance, together with two minor MAAs, mycosporine-glycine and palythine (10); in Australia, however, *L. patella* was reported to contain shinorine and mycosporine-glycine (15), or only mycosporine-glycine (16). In this study, we freeze-dried *Diplosoma* sp., extracted the material with a methanol-tetrahydrofuran (4:1) mixture,

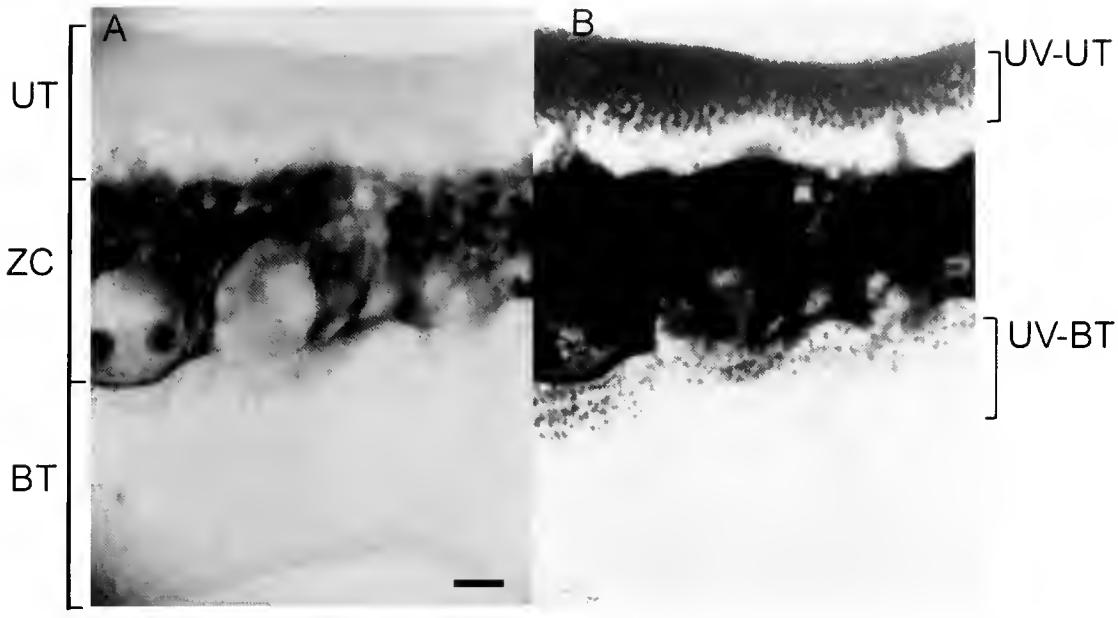

Figure 2. Visible- and ultraviolet-light micrographs of a cross-section of a living colonial ascidian, *Diplosoma* sp. The ascidian sample was collected at Akajima, an island in the Ryukyu Archipelago, Japan. Thin slices of living specimens were cut with a razorblade by hand. They were placed on a quartz slide and immersed in filtered seawater surrounded by glycerol, covered with a quartz coverslip, and observed under a light microscope with Nikon Fluor objectives (10× NA = 0.5, 20× NA = 0.75). The glass eyepiece and condenser lens were removed, because they absorb UV light. An interference filter (bandpass) for 319 ± 11 nm (median ± 50% maximum transparency) or for 331 ± 5 nm (median ± 50% maximum transparency) was inserted between a reflex camera body (Olympus OM-2) mounted on the microscope and the objective lens. The light source was a UV lamp (Vilber-Lourmat T15-N, France; or Toshiba F6T5 UV-B lamp, Japan). Black-and-white film (Fuji Neopan F) was used to record the images. Because the focal plane for the UV light is different from that for visible light, it was determined before the experiment by making test exposures. For visible-light microscopy, the interference UV bandpass filter was removed from the light path, and an UV-opaque filter was inserted between the light source and the specimen. (A) Visible-light micrograph; (B) UV-light micrograph (320 nm). UT, upper tunic layer; BT, basal tunic layer; ZC, zooid and cloacal cavity layer; UV-UT, UV-light-absorbing zone in the upper tunic; UV-BT, UV-light-absorbing zone in the basal tunic. Scale, 200 μm.

and analyzed the extracts for MAAs by reversed-phase liquid chromatography according to Dionosio-Sese *et al.* (10); the MAAs from another ascidian, *Halocynthia roretzi*, were used as references (20). The major MAA (about 94%) was shinorine, and the minor MAA was palythine. Because these substances are soluble in water (21), MAAs probably exist as soluble components in the cytoplasm of the bladder cells. Isolated *Prochloron* cells from *L. patella* contained shinorine, which was also dominant in the host tunic (10). MAAs are thought to be synthesized by the shikimic acid pathway, which has not been reported in metazoans cells (12, 13). In symbiotic didemnid ascidians, the MAAs are probably synthesized in the symbiont algal cells, then transferred to the host tissue, and accumulated in the cytoplasm of the bladder cells mostly in the upper tunic.

Because the UV-absorbing layer in the upper tunic is transparent to PAR but absorbs UVR, the underlying host tissues and the symbionts are protected from the UVR, but they can still receive PAR needed for photosynthesis. The

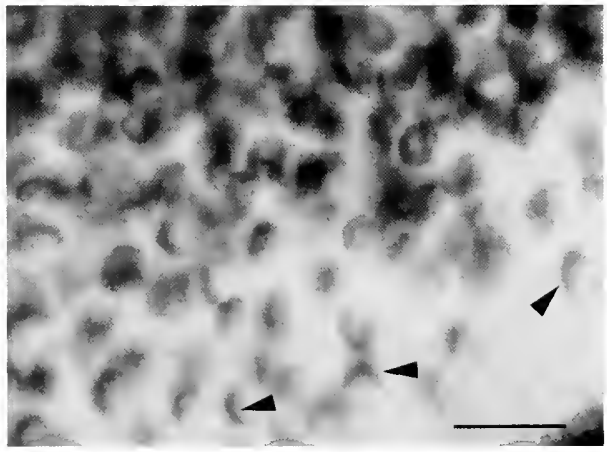

Figure 3. Higher magnification UV micrograph (320 nm): cross-section of a UV-absorbing zone in the upper tunic of a living colony of *Diplosoma* sp. The cytoplasm of tunic bladder cells was observed as dark, round or cup-shaped, UV-absorbing objects (arrowheads). Scale, 100 μm. For UV microscopy, see the legend of Figure 2.

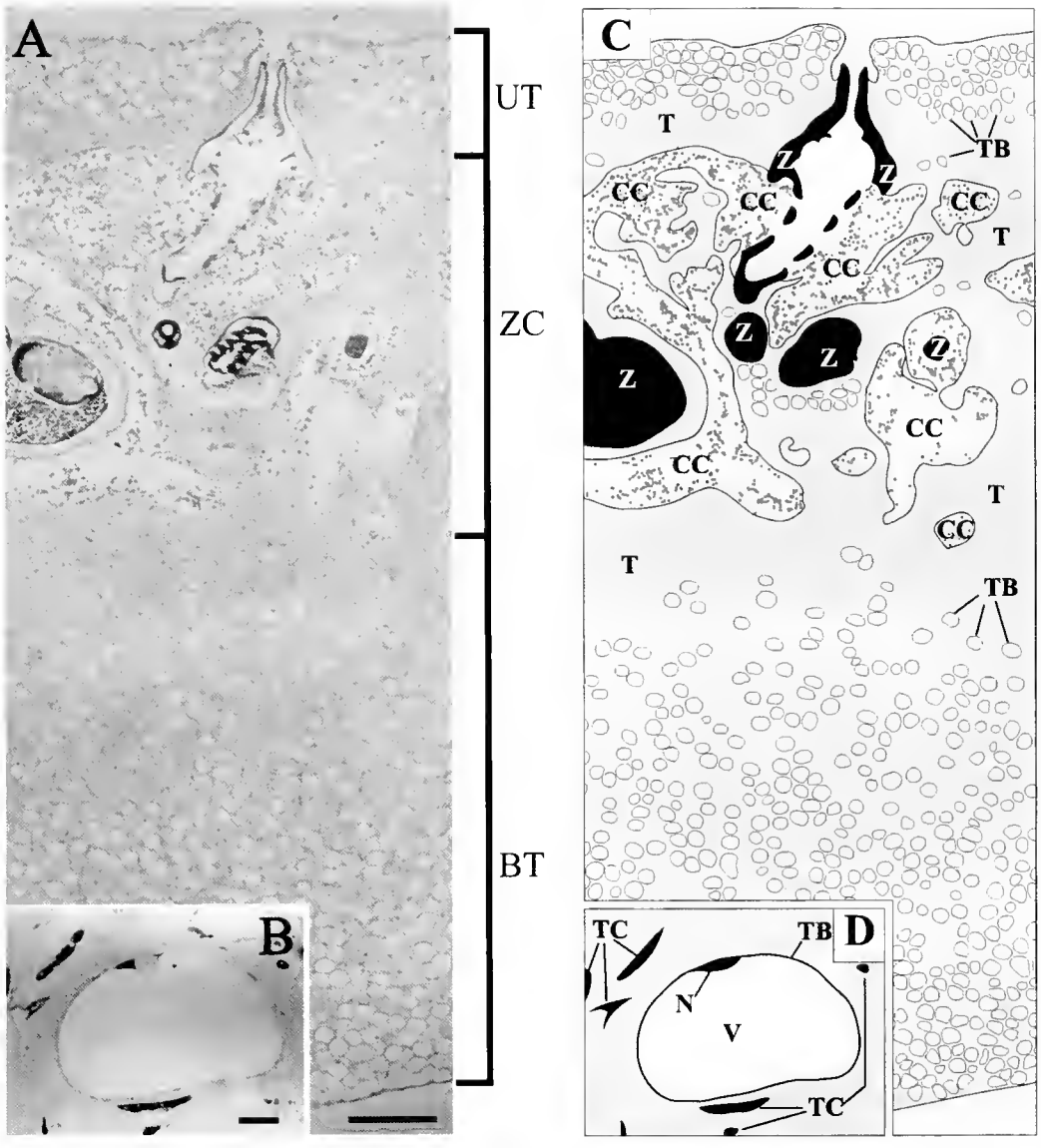

Figure 4. (A) Light micrograph of a cross-section of a colony of *Diplosoma* sp. (10% formalin-seawater fixation; 10-μm-thick paraffin section stained with hematoxylin and eosin). Scale, 200 μm. (B) Higher magnification light micrograph of a tunic bladder cell (2.5% glutaraldehyde prefixation and 1% OsO_4 postfixation; 1-μm-thick resin section stained with toluidine blue). Scale, 10 μm. (C and D) Schematic representations of A and B, respectively. CC, cloacal cavity; N, nucleus of tunic bladder cell; TB, tunic bladder cell; TC, other tunic cells; V, vacuole of tunic bladder cell; Z, zooid; small structures (dots) in CC, cells of *Prochloron* sp.

mechanisms underlying translocation of MAAs and their uptake by the tunic bladder cells remain to be elucidated.

Acknowledgments

We are grateful to Prof. R. A. Lewin for discussion. Staff members at Akajima Marine Science Laboratory are acknowledged for their help during sample collection. This work was performed as a part of The Industrial Science and Technology Project, Technological Development of Biological Resources in Bioconsortia, supported by the New Energy and Industrial Technology Development Organization (NEDO). The present study is partly supported by a JSPS Grant-in-Aid.

Literature Cited

1. **Barker, K. S., R. C. Smith, and A. E. S. Green. 1980.** Middle ultraviolet radiation reaching the ocean surface. *Photochem. Photobiol.* **32:** 367–374.

2. **Fleischmann, E. M. 1989.** The measurement and penetration of ultraviolet radiation into tropical marine water. *Limnol. Oceanogr.* **34:** 1623–1629.
3. **Shibata, K. 1969.** Pigments and a UV-absorbing substance in corals and a blue-green alga living in the Great Barrier Reef. *Plant Cell Physiol.* **10:** 325–335.
4. **Dunlap, W. C., and J. M. Shick. 1998.** Ultraviolet radiation-absorbing mycosporine-like amino acids in coral reef organisms: a biochemical and environmental perspective. *J. Phycol.* **34:** 418–430.
5. **Karentz, D. 2001.** Chemical defenses of marine organisms against solar radiation exposure: UV-absorbing mycosporine-like amino acids and scytonemin. Pp. 481–520 in *Marine Chemical Ecology,* J. B. McClintock and B. J. Baker, eds. CRC Press, Boca Raton, FL.
6. **Shick, J. M., and W. C. Dunlap. 2002.** Mycosporine-like amino acids and related gadusols: biosynthesis, accumulation, and UV-protective functions in aquatic organisms. *Annu. Rev. Physiol.* **64:** 223–262.
7. **Conde, F. R., M. S. Churio, and C. M. Previtali. 2000.** The photoprotector mechanism of mycosporine-like amino acids. Excited-state properties and photostability of porphyra-334 in aqueous solution. *J. Photochem. Photobiol. B Biol.* **56:** 139–144.
8. **Adams, N. L., and J. M. Shick. 1996.** Mycosporine-like amino acids provide protection against ultraviolet radiation in eggs of the green sea urchin *Strongylocentrotus droebachiensis. Photochem. Photobiol.* **64:** 149–158.
9. **Shick, J. M., W. C. Dunlap, and G. R. Buettner. 2000.** Ultraviolet (UV) protection in marine organisms II. Biosynthesis, accumulation, and sunscreening function of mycosporine-like amino acids. Pp. 215–228 in *Free Radicals in Chemistry, Biology and Medicine,* T. Yoshikawa, S. Toyokuni, Y. Yamamoto, and Y. Naito eds. OICA International, London.
10. **Dionisio-Sese, M. L., M. Ishikura, and T. Maruyama. 1997.** UV-absorbing substances in the tunic of a colonial ascidian protect its symbiont, *Prochloron* sp., from damage by UV-B radiation. *Mar. Biol.* **128:** 455–461.
11. **Ishikura, M., C. Kato, and T. Maruyama. 1997.** UV-absorbing substances in zooxanthellate and azooxanthellate clams. *Mar. Biol.* **128:** 649–655.
12. **Favre-Bonvin, J., J. Bernillon, N. Salin, and N. Arpin. 1987.** Biosynthesis of mycosporines: mycosporine glutaminol in *Trichothecium roseum. Phytochemistry* **26:** 2509–2514.
13. **Shick, J. M., S. Romaine-Lioud, C. Ferrier-Pagès, and J.-P. Gattuso. 1999.** Ultraviolet-B radiation stimulates shikimate pathway-dependent accumulation of mycosporine-like amino acids in the coral *Stylophora pistillata* despite decreases in its population of symbiotic dinoflagellates. *Limnol. Oceanogr.* **44:** 1667–1682.
14. **Lewin, R. A., and L. Cheng, eds. 1989.** Prochloron: *A Microbial Enigma.* Chapman and Hall, New York.
15. **Dunlap, W. C., and Y. Yamamoto. 1995.** Small-molecule antioxidants in marine organisms: antioxidant activity of mycosporine-glycine. *Comp. Biochem. Physiol.* **112B:** 105–114.
16. **Lesser, M. P., and W. R. Stochaj. 1990.** Photoadaptation and protection against active forms of oxygen in the symbiotic procaryote *Prochloron* sp. and its ascidian host. *Appl. Environ. Microbiol.* **56:** 1530–1535.
17. **Hirose, E. 2001.** Acid containers and cellular networks in the ascidian tunic with special remarks on the ascidian phylogeny. *Zool. Sci.* **18:** 723–731.
18. **Hirose, E., H. Yamashiro, and Y. Mori. 2001.** Properties of tunic acid in the ascidian *Phallusia nigra* (Ascidiidae, Phlebobranchia). *Zool. Sci.* **18:** 309–314.
19. **Lemoyne, F., J. Bernillon, J. Favre-Bonvin, M. L. Bouillant, and N. Arpin. 1985.** Occurrence and characteristics of amino alcohols and cyclohexenone, components of fungal mycosporines. *Z. Naturforsch.* **40c:** 612–616.
20. **Nakamura, H., J. Kobayashi, and Y. Hirata. 1982.** Separation of mycosporine-like amino acids in marine organisms using reversed-phase high-performance liquid chromatography. *J. Chromatogr.* **250:** 113–118.
21. **Ito, S., and Y. Hirata. 1977.** Isolation and structure of a mycosporine from the zoanthid *Palythoa tuberculosa. Tetrahedron Lett.* **28:** 2429–2430.

Reference: *Biol. Bull.* **204:** 114–125. (April 2003)

Transcription and Translation Inhibitors Permit Metamorphosis up to Radiole Formation in the Serpulid Polychaete *Hydroides elegans* Haswell

EUGENIO CARPIZO-ITUARTE[1,2] AND MICHAEL G. HADFIELD

Kewalo Marine Laboratory and Department of Zoology, University of Hawaii, 41 Ahui St., Honolulu, Hawaii 96813

Abstract. Settlement and metamorphosis in most well-studied marine invertebrates are rapid processes, triggered by external cues. How this initial environmentally mediated response is transduced into morphogenetic events that culminate in the formation of a functional juvenile is still not well understood for any marine invertebrate. The response of larvae of the serpulid polychaete *Hydroides elegans* to inhibitors of mRNA and protein synthesis was examined to determine if metamorphosis requires these molecular processes. Competent larvae of *H. elegans* were induced to metamorphose by exposing them to a bacterial film or a 3-h pulse of 10 m*M* CsCl in the presence of the gene-transcription inhibitor DRB (5,6-dichloro-1-β-D-ribofuranosylbenzimidazole) or the translation inhibitor emetine. When induced to metamorphose in the presence of either inhibitor, larvae of *H. elegans* progressed through metamorphosis to the point at which branchial radioles start to develop. DRB and emetine inhibited the incorporation of radiolabeled uridine into RNA and radiolabeled methionine into peptides, respectively, indicating that they were effective in blocking the appropriate syntheses. Taken together, these results indicate that the induction of metamorphosis in *H. elegans* does not require *de novo* transcription or translation, and that the form of the juvenile worm is achieved in two phases. During the first phase, larvae respond to the inducer by attaching to the substratum, secreting a primary tube, resorbing the prototroch cilia, undergoing caudal elongation, and differentiating the collar; once the collar is formed, they begin secreting the secondary, calcified tube. During the second phase, the small worm develops branchial radioles and begins to grow, requiring new mRNA and protein syntheses.

Received 16 April 2002; accepted 9 December 2002.

[1] Present address: Instituto de Investigaciones Oceanológicas, UABC, Apdo. Postal 453, Ensenada, B.C. México 22800.

[2] To whom correspondence should be addressed. E-mail: ecarpizo@uabc.mx

Abbreviations: DRB, 5,6-dichloro-1-β-D-ribofuranosylbenzimidazole.

Introduction

Complex life histories in which a larval stage undergoes metamorphosis to achieve a juvenile form are common throughout the animal kingdom, including at least 15 phyla of marine invertebrates (Strathmann, 1993). Well-known examples of this postembryonic transformation are amphibians and insects, which have been used as model systems for vertebrates and invertebrates for decades (see: Gilbert *et al.*, 1996; Nijhout, 1999; Rose, 1999). In both groups, the metamorphic process is driven by the action of stage-specific hormones that activate gene expression. In amphibians, thyroid hormones act directly on target tissues by interacting with specific nuclear thyroid-hormone receptors that regulate transcription of target genes containing thyroid-hormone response elements (Evans, 1988; Tata, 1996, 1999). Similarly, metamorphosis in insects is regulated by a complex interaction between a unique group of compounds, the juvenile hormones and ecdysteroids, which also activate transcription factors (see Gilbert *et al.*, 1996).

In contrast, metamorphosis in most well-studied marine invertebrates is set in motion by environmental cues that trigger the developmental events that culminate in the transformation of a larva into a functional juvenile (Hadfield, 2000). This complex set of interactions, from the perception of an inducer signal to the acquisition of the juvenile form, is poorly understood. Some insights into the signal-transduction mechanisms have been gained for different groups,

including coelenterates (Freeman and Ridgway, 1990; Schneider and Leitz, 1994; Leitz, 1997; D. W. McCauley, 1997; Thomas *et al.*, 1997; Berking, 1998), polychaetes (Jensen and Morse, 1990; Pawlik, 1990; Ilan *et al.*, 1993; Holm *et al.*, 1998; Biggers and Laufer, 1999), molluscs (Trapido-Rosenthal and Morse, 1985a, b; Baxter and Morse, 1987; Hadfield, 1998; Hadfield *et al.*, 2000; Pires *et al.*, 2000), and crustaceans (Clare *et al.*, 1995; Clare, 1996; Knight *et al.*, 2000). Recent data on the tropical nudibranch *Phestilla sibogae* show that the apical sensory organ in the veliger larvae bears the receptors for the inducer of settlement and metamorphosis (Hadfield *et al.*, 2000). However, little is yet known about how initial inducer-signal transduction mechanisms are coupled with the morphogenetic changes of metamorphosis or to what extent metamorphosis in marine invertebrates requires *de novo* gene expression.

To date, the molecular mechanisms that shape the morphogenetic changes during metamorphosis have been documented in only two aquatic invertebrate phyla. In coelenterates, pattern formation has been analyzed for *Hydra* spp. (summarized by Steele, 2002), and the molecular events during metamorphosis have been documented for *Hydractinia echinata* (summarized by Berking, 1998; Leitz, 1998). Recently, many new signaling molecules that have morphogenetic activity and genes that participate in head formation have been characterized in *Hydra* spp. (see: Broun *et al.*, 2000; Takahashi *et al.*, 2000; Yan *et al.*, 2000a, b; Leontovich *et al.*, 2000). Intensive efforts to understand the molecular events during metamorphosis in molluscs have been made in the nudibranch *Phestilla sibogae* (B. J. McCauley, 1997; Hadfield, 1998; Del Carmen and Hadfield, 1999) and the red abalone *Haliotis rufescens* (Cariolou and Morse, 1988; Degnan and Morse, 1993, 1995; Fenteany and Morse, 1993; Degnan *et al.*, 1995).

In the serpulid polychaete *Hydroides elegans*, most of the morphogenetic changes of metamorphosis are completed during the first 3.5 h after contact with a metamorphic cue contained in bacterial biofilms (Carpizo-Ituarte and Hadfield, 1998; Unabia and Hadfield, 1999). Within 5 min of being exposed to a biofilmed surface, larvae of *H. elegans* begin to crawl upon it and then quickly tether themselves to the surface by a thin mucous thread secreted from their posterior segments. They next lie prone upon the surface and rapidly secrete a primary membranous tube. Within the primary tube, the prototroch is resorbed, the larval body elongates, and the collar region becomes functional. When processes are complete, the small worm begins to secrete the calcified secondary tube, starting from the aperture of the primary tube. Two to three hours after the initiation of settlement, the lobes that will form the branchial radioles become apparent on the head. At this point metamorphosis is complete (Carpizo-Ituarte and Hadfield, 1998). Before the present investigation, attempts to characterize the molecular mechanisms that regulate metamorphosis had not been reported for a polychaete.

The major questions addressed in this study are, can metamorphosis be triggered in *Hydroides elegans*, and how far can it progress without *de novo* synthesis of mRNA or proteins? *Hydroides elegans* is an excellent model for studies of metamorphosis in marine invertebrates because it has a short generation time (about 21 days), it reproduces year-round in Hawaii, and its metamorphosis may be manipulated by natural and artificial inducers (Hadfield *et al.*, 1994; Carpizo-Ituarte and Hadfield, 1998; Holm *et al.*, 1998; Unabia and Hadfield, 1999). The results of the present study show the extent to which syntheses of RNA and protein are involved in the progression of metamorphosis in *Hydroides elegans*.

Materials and Methods

Collection of adults and culture of larvae

Adults of *Hydroides elegans* were collected from Pearl Harbor, Hawaii. Gametes were collected, and competent larvae were reared by methods described previously (Hadfield *et al.*, 1994; Carpizo-Ituarte and Hadfield, 1998). Competence is defined for this species as the ability of larvae to settle and metamorphose when exposed to a well-developed marine biofilm. Larvae attained metamorphic competence as three-segmented nectochaetes about 4–5 days after fertilization (at 25–26 °C).

Effects of 5,6-dichloro-1-β-D-ribofuranosylbenzimidazole (DRB) and emetine

Assays for metamorphosis, using 5–6-day-old competent larvae, were conducted in 5-ml petri dishes containing natural seawater that had been passed through a 0.22-μm filter (FSW). Four replicates per treatment were used in all experiments.

To examine the effects of inhibitors of transcription (DRB) or translation (emetine) on the ability of larvae to complete metamorphosis, 30–90 competent larvae were added to each dish containing one of the inhibitors. To induce metamorphosis, the larvae were exposed to a marine biofilm or a 3-h pulse of 10 m*M* CsCl in the presence of one of the inhibitors. Two types of experiments were performed. In one, larvae were exposed to the inducer (marine biofilm or CsCl) and the inhibitor (DRB or emetine) simultaneously. In the second type, larvae were preincubated in DRB for 1–12 h or in emetine for 1–2 h before inducing them to metamorphose in the presence of the inhibitor. The number of larvae that had metamorphosed was determined between 4 and 24 h after initial induction by observing them with a dissecting microscope. Larvae were considered to have metamorphosed when they had elongated, resorbed the prototroch, and secreted the primary and secondary (calcar-

eous) tubes. At higher concentrations of inhibitors, the branchial radioles did not differentiate, and the newly metamorphosed worms were transferred from the solution with the inhibitor to fresh FSW and observed for an additional 16–24 h.

In all experiments, either pieces of plastic mesh or petri dishes that had accumulated a marine biofilm while soaking in the laboratory seawater tables for several days were used as a positive control to verify that the larvae were metamorphically competent. A negative control, included to measure spontaneous metamorphosis, consisted of placing larvae in FSW in clean plastic petri dishes during the experimental period.

Stock solutions of emetine (Sigma Chemical Co.) and DRB (Calbiochem) were prepared in 100% ethanol (ETOH) and added to filtered seawater to desired concentrations. Controls were included in each experiment to detect possible effects of ETOH on metamorphosis.

Labeling of RNA and protein synthesis "in vivo"

To confirm that DRB and emetine were effectively inhibiting RNA and protein synthesis, respectively, the synthesis of these macromolecules was measured *in vivo* in the presence and absence of the inhibitors. All of the experiments were conducted in 1.5-ml microcentrifuge tubes (Eppendorf) using artificial seawater (ASW) (Cavanaugh, 1956) containing antibiotics (0.1 mg/l penicillin; 0.1 mg/l streptomycin).

Two experiments were carried out to measure the effects of DRB. In the first, 400–1000 larvae were incubated for 2.25 h with 10, 30, 50, or 70 μM DRB, and then 0.3 μl (0.3 μCi) of [5,6-^{3}H]uridine (Amersham, 38 Ci/mmol) was added for the last 45 min of incubation in the inhibitor. In the second experiment, 400–1000 larvae were exposed to 10 μM DRB for 3, 6, 12, or 24 h, and then 3 μl (0.3 μCi) of [5,6-^{3}H]uridine was added during the last 45 min of incubation in DRB. The labeling was stopped by centrifuging the tubes (15,120 $\times$ *g*, 5 min) at room temperature (RT = 25 °C) and then removing the supernatant fluid and immersing the pelleted larvae, still in the tubes, in liquid nitrogen. The pellets were homogenized on ice and resuspended in 1 ml of SSC buffer (sodium chloride/sodium citrate, pH 7.0) prior to trichloroacetic acid (TCA) precipitation and protein-concentration analysis. TCA precipitation of RNA was carried out according to the protocol described by Fenteany and Morse (1993). Absolute TCA was added to 800 μl of resuspended sample (to a final concentration of 10% TCA). Immediately afterward, the sample was vortexed and allowed to precipitate on ice for 30 min. The precipitate was collected on a microfiber filter (Gelman, Type E), washed three times with 5% TCA and twice with 100% ETOH, and dried for an hour at RT. The filters were introduced to vials with 5 ml of scintillation fluid (ScintiSafe, Econo 2, Fisher Scientific), and radioactivity was measured in a Beckman LS 7000 liquid scintillation system or a Packard liquid scintillation analyzer 1900 TR. The remaining 200 μl from the initial samples was used to measure protein concentrations by the Bradford method (Ausubel *et al.*, 1992).

Four experiments were carried out to measure the effect of emetine on metamorphosis. In each of the experiments, 400–1000 competent larvae were used. In the first experiment, larvae were incubated for 4 h in 0, 250, 500, and 1000 nM emetine, and 1 μl (0.01 mCi) of ^{35}S-methionine (Amersham, 10 mCi/ml) was added during the last 1.5 h of incubation in the inhibitor. In a second experiment, larvae were incubated in 250 nM emetine for 0, 6, and 9 h before adding 1 μl (0.01 mCi) of ^{35}S-methionine (Amersham, 10 mCi/ml) during the last 2 h of incubation. That is, for the treatment of 0 h, emetine was added simultaneously with ^{35}S-methionine and incubated for 2 h. In a third experiment, the effect of different periods of incubation in 1 μM emetine was measured. Larvae were incubated for 1, 2, 4, and 6 h in 250 nM emetine, and 1 μl (0.01 mCi) of ^{35}S-methionine was added to the emetine-FSW solution for an additional 45 min. Larvae in the treatment of 1-h emetine remained a total of 1 h and 45 min in emetine, but were only in the presence of both emetine and ^{35}S-methionine for the last 45 min. During the fourth experiment, the effect of 250 nM emetine was measured when larvae were induced to metamorphose with a 3-h pulse of 10 mM CsCl. During this experiment, larvae were placed for 1 or 2 h in 250 nM emetine before being exposed to a 3-h pulse of CsCl (10 mM) in the emetine-FSW solution. One microliter (0.01 mCi) of ^{35}S-methionine was added during the last 1.5 h of the Cs^+ pulse. After the period of incubation in ^{35}S-methionine, the larvae were centrifuged (15,120 $\times$ *g*, 2 min), and a 50-μl sample of the supernatant fluid was recovered to measure the radioactivity remaining in it. The remaining supernate was removed from the tube, and the larvae were washed once with ASW and resuspended in 500 μl of 50 mM sodium phosphate buffer, pH 7.2. The larval tissue was lysed by sonication for 30 s in a Branson Sonifier (model 450, Branson Ultrasonics Corporation). The sample was removed from the sonicator every 10 s and put on ice for 20 s to prevent overheating of the tissue. TCA precipitation was carried out according to the protocol described by Ausubel *et al.* (1987) to measure incorporation of ^{35}S-methionine into newly synthesized proteins. The sonicated sample was centrifuged (15,120 $\times$ *g*, 2 min) at RT, and the supernatant fluid was transferred to a clean 1.5-ml microtube (Eppendorf). To a 50-μl sample of this supernate was added 0.5 ml of bovine serum albumin (0.1 mg/ml) containing 0.02% NaN_3 followed by 0.5 ml of ice-cold 20% TCA, and the suspension was incubated on ice for 30 min. After incubation, the suspension was filtered under vacuum onto a microfiber filter (Gelman, Type E), washed twice with ice-cold

10% TCA and twice with 100% ETOH, and the filters were allowed to dry for 30–45 min at RT. To quantify the incorporation of ^{35}S-methionine, radioactivity was measured by introducing the fiberglass filters with the TCA precipitate into vials containing 5 ml of scintillation fluid (ScintiSafe, Econo 2; Fisher Scientific). Radioactivity in the vials was measured in a Beckman LS 7000 liquid scintillation system or a Packard liquid scintillation analyzer 1900 TR. Results were expressed as DPM/μg of protein. The protein concentration in the remaining sample (250–450 μl) was measured using the spectrophotometric method described by Whitaker and Granum (1980).

Statistical analysis of metamorphosis

The proportion of larvae that underwent metamorphosis was determined, and these values were arcsine-transformed to estimate statistical differences among treatments using one-way ANOVAs or Kruskal-Wallis ANOVAs of ranks when equal-variance tests failed. Pairwise multiple comparisons were tested using the Student-Newman-Keuls test or Dunnett's method when all treatments were compared to each other, or Bonferroni's method when treatments were compared to a control. All statistical tests were conducted with the aid of SigmaStat software (SPSS Inc.).

Results

Effects of the transcription inhibitor DRB on metamorphosis

When competent larvae of *Hydroides elegans* were induced to metamorphose with a bacterial biofilm or a 3-h pulse of CsCl in the presence of DRB, they completed metamorphosis of the larval body after 3–4 h but did not develop branchial radioles (Fig. 1). The minimum effective concentration of DRB to prevent branchial radiole formation in all the larvae tested with either inducer was 10 μM (Figs. 2, 3; Bonferroni test, $P < 0.05$). Lower concentrations of DRB tested either had no effect (0.1 μM, Figs. 2, 3) or showed only a slight, but significant (Bonferroni test, $P < 0.05$), reduction in the proportion of larvae that completed formation of branchial radioles (1 μM, Fig. 2).

Preincubation of competent larvae of *H. elegans* in 10 μM DRB for up to 9 h before addition of an inducer (biofilm or CsCl) did not inhibit metamorphosis (Figs. 4, 5). In fact, larvae responded significantly faster (Student-Newman-Keuls test, $P < 0.05$) to biofilm in the presence of DRB than in its absence (Fig. 4A), a difference that was reduced after 14 h of incubation when the experiment was stopped (Fig. 4B).

Preincubation in 10 μM DRB for up to 9 h did not stop the larvae from metamorphosing in response to a pulse of CsCl, but a significant reduction in the percentage that metamorphosed was observed (Bonferroni's method, $P < 0.05$, Fig. 5).

Effects of the protein-synthesis inhibitor emetine on metamorphosis

Competent larvae of *H. elegans* metamorphosed when exposed to a biofilm in the presence of 1 μM emetine (Fig. 6), with no significant reduction in the proportion of larvae that metamorphosed after 3 h compared with induction by a biofilm alone. The larvae progressed in metamorphosis to the point at which branchial radioles begin to develop; concentrations of emetine as low as 250 nM were effective in preventing the formation of these structures. Preincubation for 1 h in 1 μM emetine prior to exposure to a biofilm did not curtail metamorphosis (Fig. 7), but the proportion of larvae that had metamorphosed after 3 h was slightly reduced.

Results similar to the ones observed when a biofilm was used as inducer were obtained when larvae were stimulated to metamorphose with a 3-h pulse of 10 mM CsCl in the presence of emetine (Fig. 8). The proportion of larvae that metamorphosed was similar in the presence and absence of 1 μM emetine, and the proportions that metamorphosed in these treatments were similar to those obtained in response to a bacterial biofilm.

Labeling RNA and proteins in vivo

Incorporation of [5,6 ^{3}H]uridine into RNA by competent larvae of *H. elegans* in the presence of DRB varied with concentration and period of exposure. In comparison to incorporation without an RNA-synthesis inhibitor, [5,6 ^{3}H]uridine incorporation was reduced up to 80% after an incubation period of 2.25 h in 70 μM DRB (Fig. 9A). Even with the lowest concentration of DRB tested (10 μM), incorporation of [5,6 ^{3}H]uridine was reduced by 60% (Fig. 9A).

When larvae were exposed to 10 μM DRB for 24 h before addition of [5,6 ^{3}H]uridine, incorporation of [5,6 ^{3}H]uridine was reduced up to 88% in comparison to that in larvae incubated in the absence of DRB (Fig. 9B). A substantial decrease in incorporation of [5,6 ^{3}H]uridine, up to 42%, was evident after the first 3 h of exposure to DRB (Fig. 9B). Spontaneous metamorphosis was 3.2% and 6% in the two experiments in control larvae kept in conditions equivalent to those of larvae incubated in the presence of DRB.

Synthesis of new proteins in larvae of *H. elegans* exposed to emetine was dependent on the concentration and length of exposure to the inhibitor. When larvae were exposed to different concentrations of emetine for 4 h, a decrease in ^{35}S-methionine incorporation was observed. A reduction of 41% in incorporation of ^{35}S-methionine into proteins

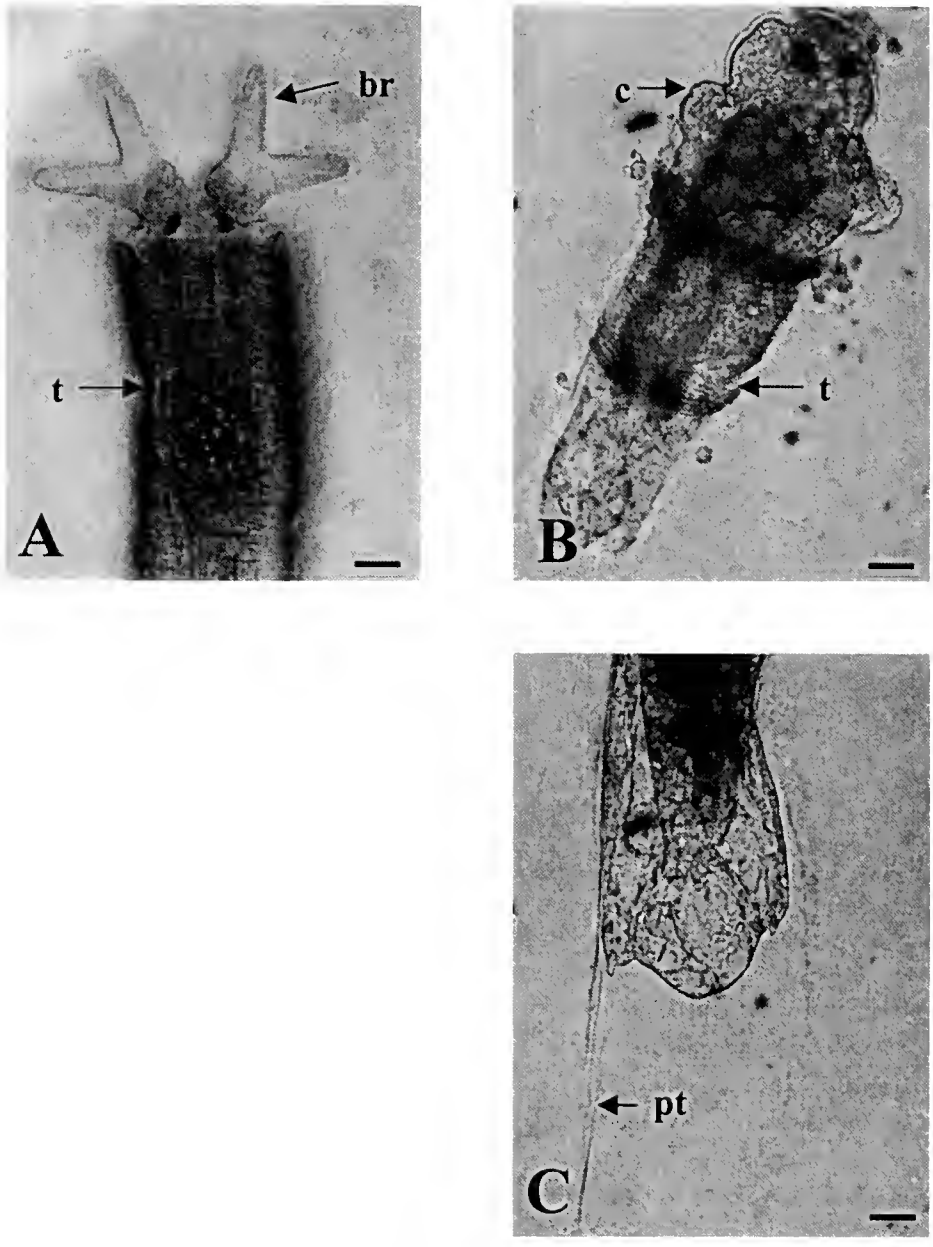

Figure 1. Metamorphosis in *Hydroides elegans* in the absence or presence of an inhibitor of macromolecular synthesis. (A) A worm newly metamorphosed in response to a bacterial biofilm. (B) A worm in which metamorphosis was induced in the presence of the translation inhibitor emetine. (C) The posterior section of the tube of the worm shown in B. Newly metamorphosed worms exposed to induction cues in the presence of the trancription inhibitor DRB have the morphology shown in B. br, branchial radioles; c, collar, pt, primary tube; t, secondary calcareous tube. Scale bar = 20 μm for all micrographs.

occurred with exposure to 250 n*M* emetine, and a reduction of up to 87% occurred in response to 1 μM emetine (Fig. 10A). Exposure of larvae to 1 μM emetine for 1 h was sufficient to reduce incorporation of ^{35}S-methionine into newly synthesized protein by 79%. An increase in the length of exposure to 1 μM emetine did not substantially reduce the incorporation of the radiolabeled amino acid. A maximum reduction of 81% in ^{35}S-methionine incorporation was detected after 6 h of exposure to 1 μM emetine (Fig. 10B).

An increase in the length of exposure of larvae to 250 n*M* emetine resulted in lower levels of incorporation of ^{35}S-methionine. Periods of exposure to the inhibitor of 6 and 9 h reduced ^{35}S-methionine incorporation by 68% and 74% respectively, in comparison to controls where no emetine

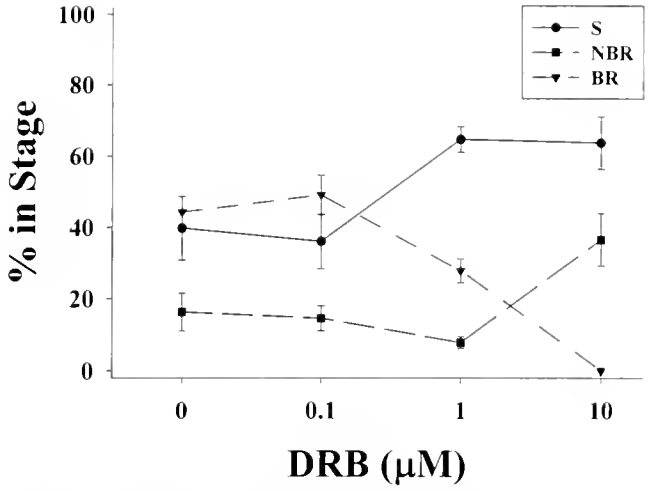

Figure 2. Effects of the transcription inhibitor DRB on metamorphosis and differentiation of branchial radioles in *Hydroides elegans*. Larvae were induced to metamorphose with a marine biofilm in the presence (0.1, 1, and 10 μM) and absence (0) of DRB for 3.5 h. Points indicate mean percentages of larvae ± 1 SE (n = 4 replicates/treatment) that were swimming (S), metamorphosed without branchial radioles (NBR), or metamorphosed with branchial radioles (BR) at the end of the experiment.

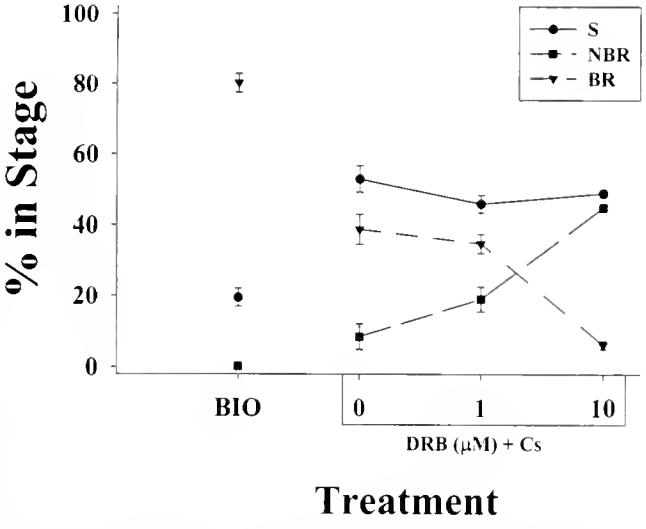

Figure 3. Effects of the transcription inhibitor DRB on metamorphosis and differentiation of branchial radioles in *Hydroides elegans*. Larvae were exposed to a 3-h pulse of 10 mM CsCl in the presence (treatments 1 and 10) and absence (treatments 0 and BIO) of DRB. After the cesium pulse, the solution was replaced with fresh filtered seawater (FSW) containing 1 or 10 μM DRB in the treatments where DRB was included, or only FSW in the treatments where DRB was absent. Points indicate mean percentages of larvae ± 1 SE (n = 4 replicates/treatment) that were swimming (S), metamorphosed without branchial radioles (NBR), or metamorphosed with branchial radioles (BR) 24 h after initiation of the cesium pulse.

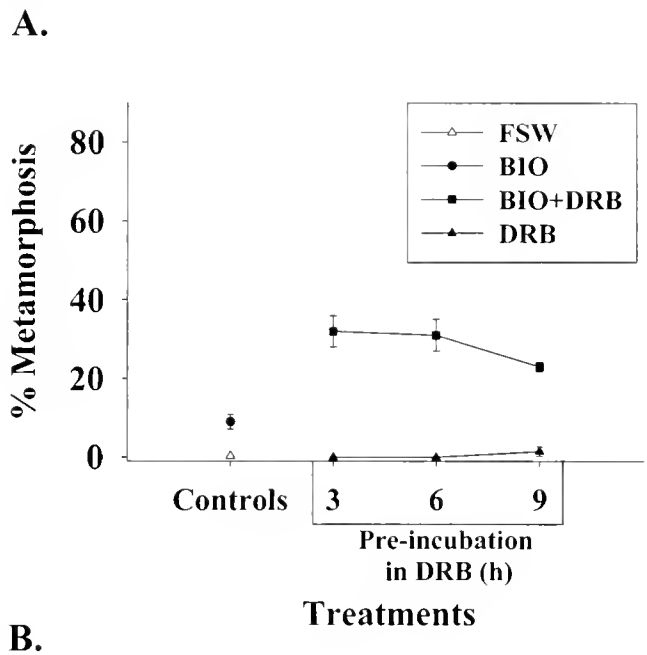

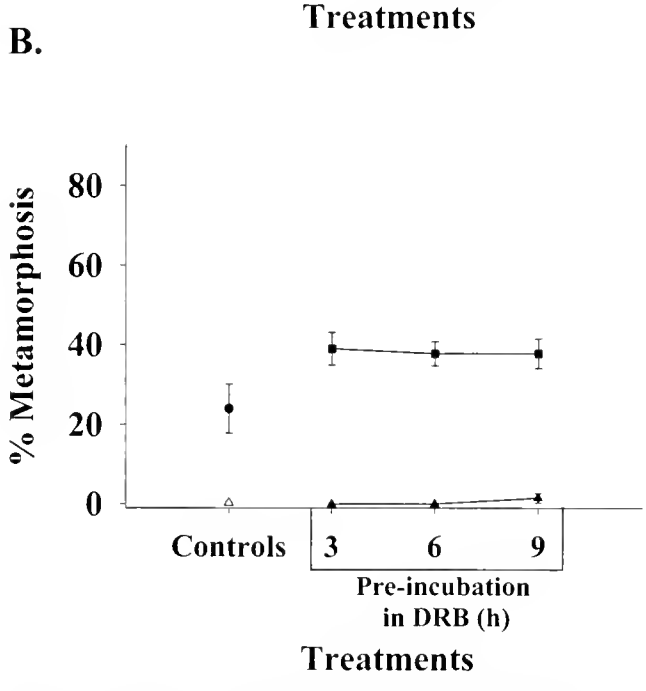

Figure 4. Effects of preincubation in DRB on metamorphosis of *Hydroides elegans*. Larvae were preincubated in 10 μM DRB for 3, 6, or 9 h before transfer to a biofilmed petri dish. In the treatments with DRB, the inhibitor was present throughout the experiment. Points indicate percentages of larvae that metamorphosed ± 1 SE (n = 4 replicates/treatment) after being transferred to the petri dish. (A) 3 h afer tranfer to the inducing biofilm, larvae had metamorphosed to the pre-radiole stage in the treatments where DRB was present. (B) 14 h after transfer to the biofilmed dish, small branchial radioles began to develop in the treatment where DRB was present. BIO, substratum coated with a marine biofilm; FSW, seawater filtered through a 0.22-μm filter; in DRB control, no biofilm was added.

was present (Fig. 11A). In contrast, the lowest level of incorporation of ^{35}S-methionine into newly synthesized protein (97% reduction) was observed when the larvae were induced with CsCl after being incubated for 2 h in 250 nM emetine (Fig. 11B). Interestingly, induction of larvae to metamorphose with CsCl alone showed a reduction in

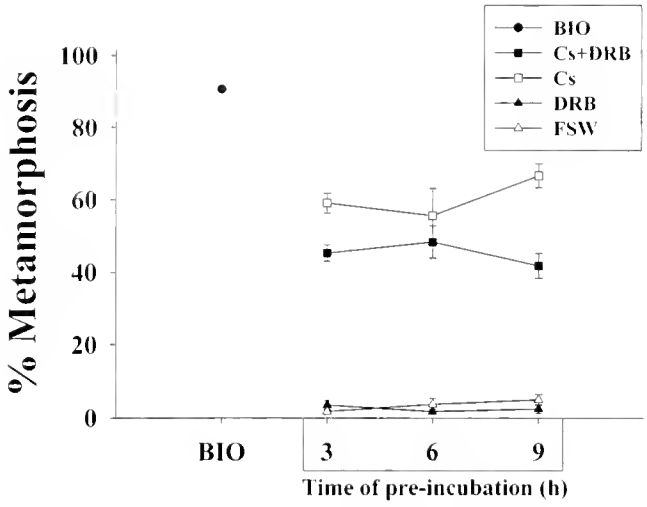

Figure 5. Effects of preincubation in DRB on metamorphosis of *Hydroides elegans*. Larvae were preincubated in 10 μM DRB for 3, 6, or 9 h before being induced to metamorphose with a 3-h pulse of filtered seawater (FSW) containing 10 mM CsCl and 10 μM DRB. After the CsCl pulse, solutions were replaced with FSW, and metamorphosis was allowed to progress for 21 h. Points indicate mean percentages of larvae that metamorphosed ± 1 SE (n = 4 replicates/treatment) 24 h after initial exposure to CsCl. DRB, 10 μM DRB; Cs, 10 mM CsCl/ 3 h; BIO, substratum coated with a marine biofilm; FSW, seawater filtered through a 0.22-μm filter. In the treatment where Cs was present with DRB (DRB + Cs), larvae metamorphosed to the pre-radiole stage.

incorporation of ^{35}S-methionine of 82% compared to a control where no CsCl or emetine were present (Fig. 11B).

Discussion

Results from the present study demonstrate two important elements of metamorphosis in *Hydroides elegans*. First, settlement, attachment, secretion of the primary and secondary tubes, velar loss, collar formation, and caudal elongation proceed in the presence of inhibitors that drastically reduce transcription and translation. Second, in the presence of transcription and translation inhibitors, metamorphosis stops at the point when branchial radioles begin to grow.

When competent larvae of *H. elegans* were induced to metamorphose with a bacterial biofilm or CsCl in the presence of effective concentrations of DRB, they completed metamorphosis to the point at which branchial radioles begin to develop. Development of the radioles can be considered the initiation of early juvenile development in *H. elegans*, after all larval structures have been lost and the juvenile shape has been realized. These changes include loss of the prototroch, differentiation of the collar, caudal elongation, and secretion of primary and secondary tubes. Similar results were reported initially for the tropical nudibranch *Phestilla sibogae* by Hadfield (1978) and later confirmed in the same species by B. J. McCauley (1997) and Del Carmen and Hadfield (1999, 2000). In the presence

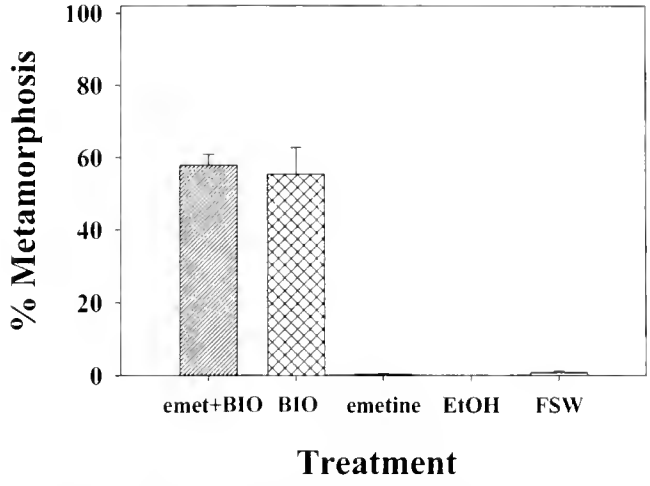

Figure 6. Effects of the translation inhibitor emetine on metamorphosis in *Hydroides elegans*. Larvae were exposed to a marine biofilm in the presence (emet + BIO) or absence (BIO) of 1 μM emetine. Bars indicate percentages of larvae that metamorphosed ± 1 SE (n = 4 replicates/treatment) after 3 h of exposure to the biofilm. BIO, substratum coated with a marine biofilm; emetine, emetine 1 μM control; EtOH, equivalent concentration of ethanol used to dissolve emetine; FSW, seawater filtered through a 0.22-μm filter. In the treatment where the biofilm was present with emetine (emet + BIO), larvae metamorphosed to the pre-radiole stage.

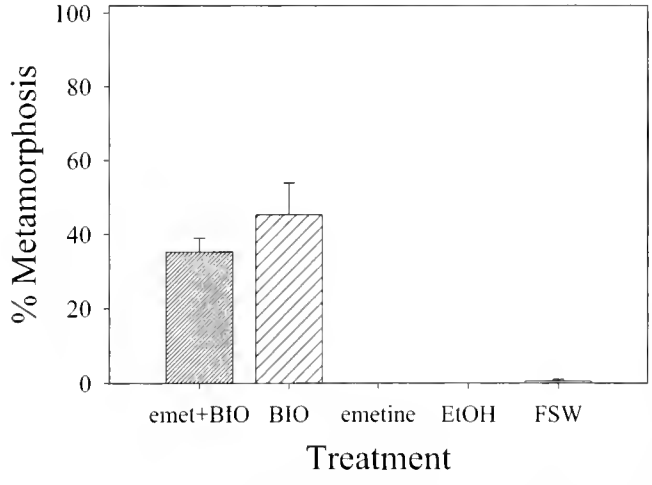

Figure 7. Effects of preincubation in the translation inhibitor emetine on metamorphosis in *Hydroides elegans*. Larvae were incubated for 1 h in 1 μM emetine in a clean petri dish and then transferred to a biofilm-coated petri dish, still in the presence of emetine (emet + BIO). Bars indicate percentages of larvae that metamorphosed ± 1 SE (n = 4 replicates/treatment) after 3 h of exposure to the biofilm. Emetine, emetine 1 μM control; EtOH, equivalent concentration of ethanol used to dissolve emetine; FSW, seawater filtered through a 0.22-μm filter. In the treatment where the biofilm was present with emetine (emet + BIO), larvae metamorphosed to the pre-radiole stage.

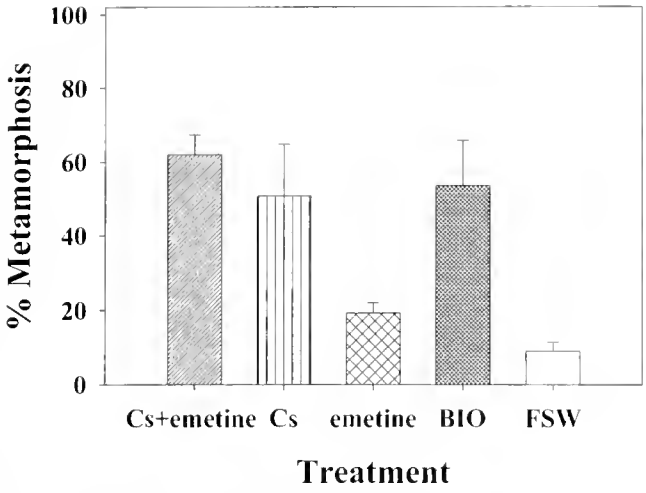

Figure 8. Effects of the translation inhibitor emetine on induction of metamorphosis in *Hydroides elegans*. Larvae were incubated for 3 h in 1 μM emetine in filtered seawater (FSW) that also contained 10 mM CsCl to induce metamorphosis. Solutions were replaced with FSW after 3 h, and the larvae were allowed to complete metamorphosis for another 16 h. Bars indicate percentages of larvae that metamorphosed ± 1 SE (n = 4 replicates/treatment). Cs, 10 mM CsCl/3 h; emetine, 1 μM emetine; BIO, substratum coated with a marine biofilm; FSW, seawater filtered through a 0.22-μM filter.

of DRB, transcription and translation were drastically reduced without inhibiting induction of metamorphosis in competent larvae of *P. sibogae*. Further experiments showed that activation of the receptor for the metamorphic signal is not affected by reduction in transcription, but new transcription appears to be necessary for the final, elongation phase of metamorphosis in *P. sibogae* (Del Carmen and Hadfield, 2000).

The observation that metamorphosis in *H. elegans* progresses in the presence of DRB, together with the demonstration that DRB effectively inhibits RNA synthesis, indicates that the initiation and early phases of metamorphosis in this species are independent of new RNA synthesis. However, the fact that we were never able to completely inhibit RNA synthesis leaves open the possibility that synthesis of some mRNAs was resistant to the action of DRB, and thus that new transcripts may play an essential role during metamorphosis for the first hours after induction. Transcriptional resistance to DRB in HeLa cells was reported by Zandomeni *et al.* (1982).

The observation that development in the presence of DRB stops at the point when branchial radiole development begins indicates that new transcripts are necessary for the growth of the radioles and that these transcripts are among the more than 80% of RNA syntheses inhibited by DRB. Even a 40% reduction in synthesis of RNA, measured by incorporation of [5,6 ^{3}H]uridine, was sufficient to prevent the formation of branchial radioles. It is not surprising that active growth of new structures, such as the branchial radioles, is dependent on transcription, because a broad spectrum of new tissues—including nerves, muscles, and secretory epithelium—must be generated, each requiring many new proteins. Experiments on the hydrozoan *Hydractinia echinata* revealed that morphogenesis of the adult polyp can be influenced by pulse applications of α-amanitin or cordycepin. These compounds, which block mRNA transcription at different levels, inhibit the formation of tentacles and stolons in *H. echinata* when applied during late gastrulation or 3 h after induction of metamorphosis (Eiben, 1982).

When larvae of *Hydroides elegans* were induced to meta-

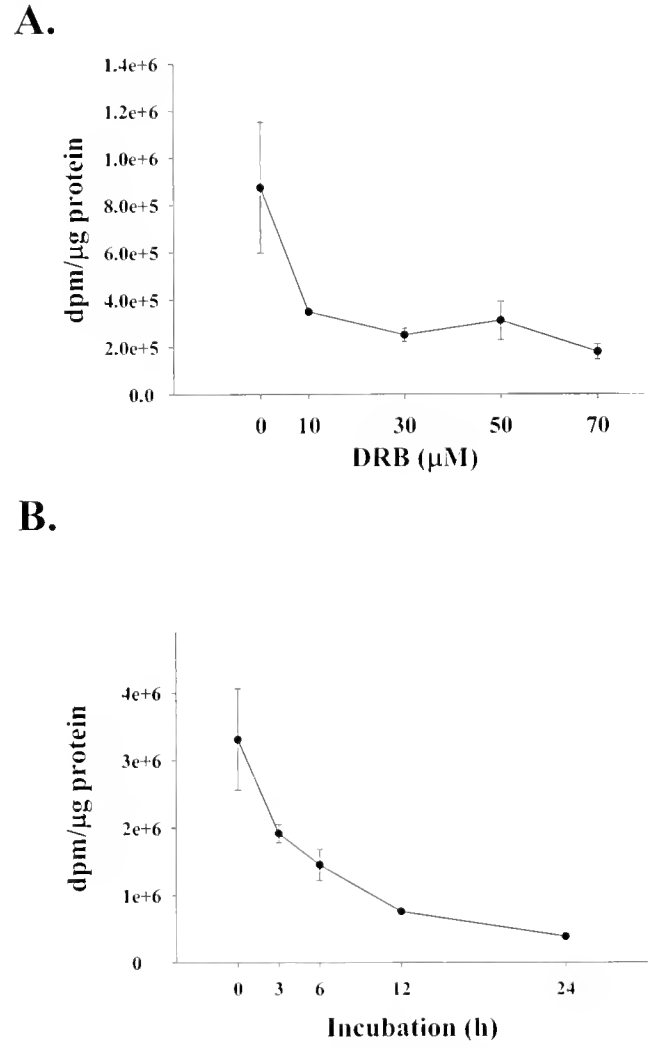

Figure 9. Incorporation of [5–6 ^{3}H]uridine into newly synthesized RNA by larvae of *Hydroides elegans*. In (A), larvae were incubated for 2.15 h in the presence of the different concentrations of DRB indicated on the x axis. In (B), larvae were incubated in 10 μM DRB in FSW for the different periods of exposure indicated on the x axis. In both (A) and (B), larvae were allowed to incorporate [5–6 ^{3}H]uridine during the last 45 min. Points are means of uridine incorporation ± 1 SE (n = 2 replicates/treatment).

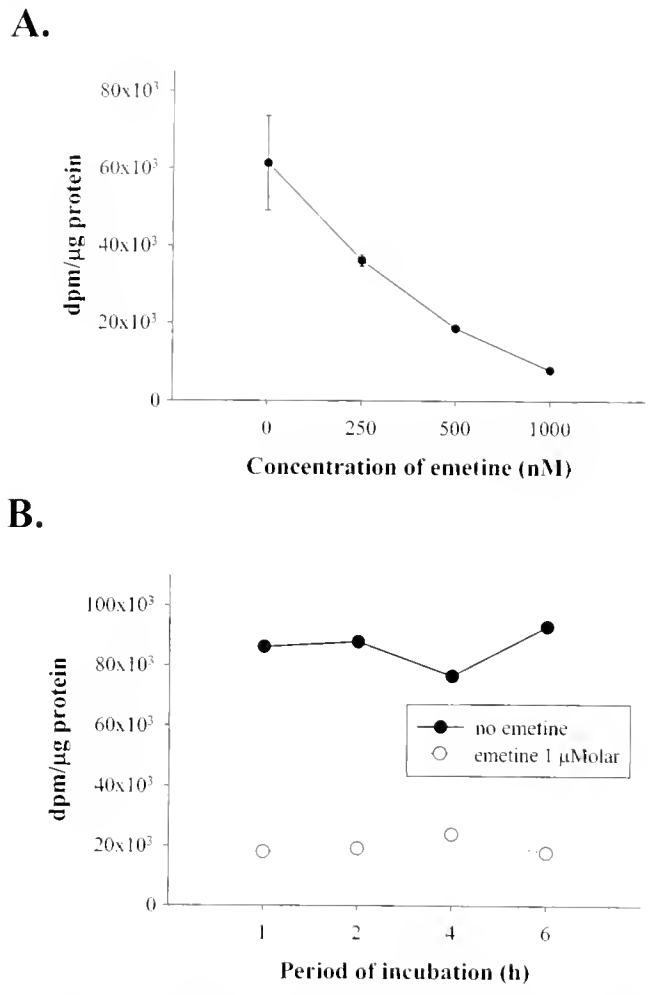

Figure 10. Incorporation of ^{35}S-methionine into newly synthesized proteins by larvae of *Hydroides elegans* in the presence of the translation inhibitor emetine. In (A), larvae were incubated in varying concentrations of emetine, shown on the *x* axis, for 4 h with incorporation of ^{35}S-methionine during the last 1.5 h. Points are means of methionine incorporation ± 1 SE (n = 2 replicates/treatment). In (B), larvae were incubated in 1 μM emetine for the intervals indicated on the *x* axis and allowed to incorporate ^{35}S-methionine for an additional 45 min. Points are mean methionine incorporation ± 1 SE.

morphose with either a bacterial biofilm or a pulse of CsCl in the presence of the translation inhibitor emetine, just as with DRB, they completed metamorphosis and stopped developing before the outgrowth of the branchial radioles. Neither the highest concentration of emetine used (1 μM) nor an extended preincubation period in emetine stopped initiation of metamorphic morphogenesis in response to a bacterial biofilm or cesium as inducers. These results are consistent with the hypothesis that initiation of metamorphosis in *H. elegans* is also highly independent of synthesis of new proteins, a result that is concordant with previous studies of other species, especially certain molluscs (Fenteany and Morse, 1993; Del Carmen and Hadfield, 1999).

Larvae of the archaeogastropod *Haliotis rufescens* (Fenteany and Morse, 1993) and the nudibranch *Phestilla sibogae* (B. J. McCauley, 1997; Del Carmen and Hadfield, 1999) initiate metamorphosis in the presence of translation inhibitors. When competent larvae of *H. rufescens* were induced to metamorphose in the presence of concentrations of emetine or anisomycin sufficient to block protein synthesis, settlement and plantigrade attachment still occurred, indicating that these premetamorphic processes do not require *de novo* protein synthesis (Fenteany and Morse, 1993). The authors suggest that the induction of settlement

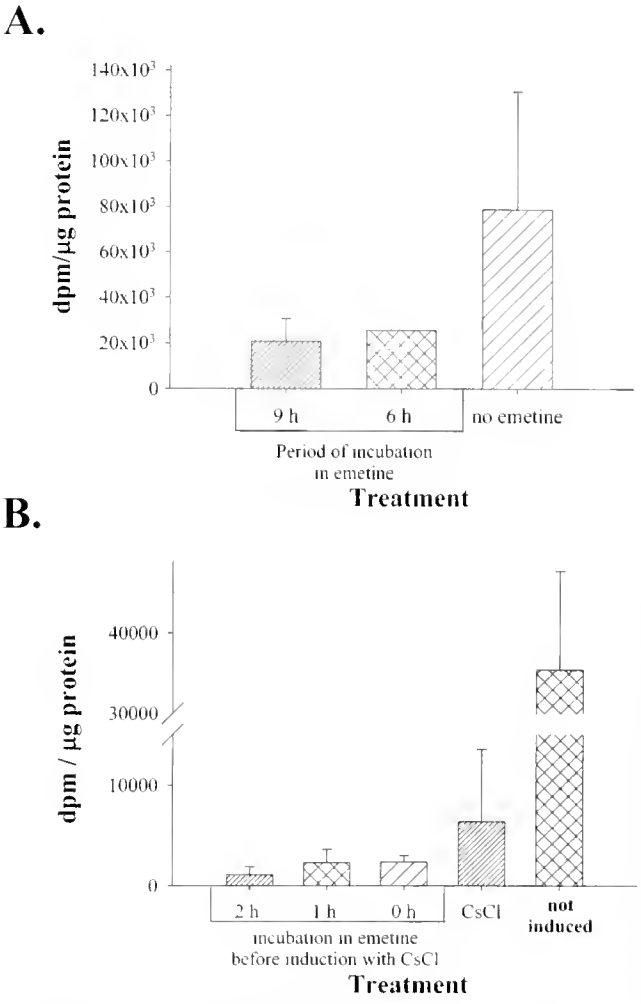

Figure 11. Incorporation of ^{35}S-methionine into newly synthesized proteins by larvae of *Hydroides elegans* after different periods of incubation in 250 nM emetine. In (A), larvae were incubated in emetine at the concentrations indicated on the x axis and allowed to incorporate ^{35}S-methionine during the last 2 h. Points are means of methionine incorporation ± 1 SE (n = 2 replicates/treatment, except for 6 h, which represents 1 sample). In (B), larvae were first incubated in 1 μM emetine in filtered seawater (FSW) before being induced to metamorphose with a 3-h pulse of CsCl (10 mM) and allowing larvae to incorporate methionine for 45 min after the CsCl pulse and in the presence of emetine. Points are mean methionine incorporation ± 1 SE (n = 4 replicates/treatment for 2, 1, and 0 h, and 2 replicates/treatment for CsCl and not induced (no CsCl)).

and plantigrade attachment in the presence of protein-synthesis inhibitors is consistent with the notion that these behavioral responses are controlled by chemosensory mechanisms mediated by the nervous system. Similar results were reported for the larvae of *P. sibogae:* experiments with emetine showed that metamorphosis can be initiated in the presence of the translation inhibitor and that development stops just before final elongation of the body (B. J. McCauley, 1997).

It is particularly interesting that protein synthesis in larvae of *Hydroides elegans* was reduced even further when CsCl was added to induce metamorphosis (Fig. 11B). Kroiher *et al.* (1991) also reported decreased incorporation of amino acids into proteins when larvae of the hydrozoan *Hydractinia echinata* were exposed to CsCl, attributing it to a reduction in the Na^+ concentration of the medium when CsCl is added. Transport of amino acids across the cell membrane is known to be a function of a Na^+-transport in marine invertebrates (Stephens, 1988).

Inhibition of development of the branchial radioles by emetine at concentrations at which protein synthesis was reduced by only 40% is consistent with the data obtained with DRB. Thus, unsurprisingly, both new mRNA transcripts and their translation products are necessary for production of the branchial radioles.

Taken together, the data on RNA and protein synthesis in metamorphosing *Hydroides elegans* strongly support the conclusion that metamorphosis and juvenile development occur in two phases—one independent of new gene transcription and translation, and a second in which these two molecular processes are necessary for development and growth to continue. During the first phase, larvae respond rapidly to the bacterial inducer, change their swimming behavior, attach, secrete primary and secondary tubes, lose the prototroch cilia, differentiate the collar, and elongate the caudal region (Carpizo-Ituarte and Hadfield, 1998). During the second phase, the metamorphosed worm develops branchial radioles, a process that requires new RNA and protein synthesis. Results reported for larvae of other marine invertebrates reinforce the idea that metamorphic competence in many marine invertebrate larvae is a developmental stage primed to metamorphose and in which the activation and near completion of metamorphosis requires neither *de novo* synthesis of mRNA nor proteins (Hadfield, 2000).

Since larvae of *H. elegans* survive through metamorphosis with very reduced synthesis of new mRNAs or proteins, cell proliferation, which requires both processes, probably does not play an essential role during metamorphosis. Previous studies in other invertebrate species are consistent with this hypothesis. In *Phestilla sibogae*, labeling of dividing cells with an antibody against a proliferating cell nuclear antigen (PCNA) decreases when larvae reach competency and is detected again only after the larvae have completed metamorphosis and begun early juvenile development (B. J. McCauley, 1997). In embryos of *Hydractinia echinata,* the index of cell proliferation measured by the BrdU method decreased to 4% by 78 h after fertilization. In larvae of *H. echinata* kept at low temperatures, the cell proliferation index went to zero after 60 to 70 days without affecting the ability of the larvae to undergo metamorphosis (Plickert *et al.*, 1988). Preliminary observations on *Hydroides elegans* using PCNA indicated that cell proliferation decreases sharply when larvae become competent and increases notably in the developing branchial radioles of newly settled juveniles (Carpizo-Ituarte, unpubl. results).

Metamorphosis in most well-studied insects and amphibians is a relatively slow process wherein hormonal transcription factors mediate essential cascades of "*de novo*" transcription and translation to regulate metamorphic morphogenesis (Gilbert *et al.*, 1996; Tata, 1996, 1999; Shimizu-Nishikawa *et al.*, 2002). In contrast, the experimental results obtained with the polychaete *Hydroides elegans* support a generalization noted by Hadfield *et al.* (2001): for most well-studied marine invertebrates, the competent larva carries within it a well-formed juvenile body, which metamorphosis need only liberate from larval structures. In this case, metamorphosis should require little or no *de novo* transcription or translation, processes that will be necessitated when juvenile growth begins. This may be the result of adaptation to undergo rapid metamorphosis and make an extremely vulnerable period—that of a planktonically adapted larva residing on the benthos—as brief as possible (Hadfield, 2000).

The more precisely we define the molecular events of metamorphosis in *Hydroides elegans* and other marine invertebrates, the better we are able to make comparisons with model systems among insects and amphibians. So far, the capacity for metamorphosis to proceed almost independently of new gene expression in many marine invertebrates points toward different mechanisms to initiate postlarval development. To what extent these mechanisms are different from those known in insects and amphibians awaits further investigation. Knowledge of the signal-transduction pathways that are activated during induction of metamorphosis and how the initial triggering event orchestrates the genetic machinery to turn a larva into a juvenile in a wide variety of marine invertebrates will help us to understand how the widespread phenomenon of metamorphosis in marine invertebrates evolved.

Acknowledgments

Contributions of colleagues in the Hadfield lab at the University of Hawaii's Kewalo Marine Laboratory were many, and we are grateful for all of them. This research was supported by ONR grants N00014-95-1015 and N00014-

95-1-0196. EC-I was the recipient of a scholarship for graduate studies from CONACyT, México.

Literature Cited

Ausubel, F. M., R. Brent, R. E. Kingston, D. D. Moore, J. G. Seidmann, J. A. Smith, and K. Struhl. 1987. Section VI. Specialized Applications. Unit 10.18. Biosynthetic Labeling of Proteins. Pp. 10.18.1–10.18.9 In *Current Protocols in Molecular Biology*, Vol II. John Wiley, Boston.

Ausubel, F. M., R. Brent, R. E. Kingston, D. D. Moore, J. G. Seidmann, J. A. Smith, and K. Struhl. 1992. Section 1. Quantitation of Proteins. Unit 10.1. Colorimetric Methods: Bradford Method. Pp. 10.5–10-6 in *Short Protocols in Molecular Biology*, 2nd ed. John Wiley, Boston.

Baxter, G. T., and D. E. Morse. 1987. G protein and diacylglycerol regulate metamorphosis of planktonic molluscan larvae. *Proc. Natl. Acad. Sci. USA* **84:** 1867–1870.

Berking, S. 1998. Hydrozoa metamorphosis and pattern formation. Pp. 81–131 in *Current Topics in Developmental Biology*, R. A. Pedersen and G. P. Schatten, eds. Academic Press, New York.

Biggers, W. J., and H. Laufer. 1999. Settlement and metamorphosis of *Capitella* larvae induced by juvenile hormone-active compounds is mediated by protein kinase C and ion channels. *Biol. Bull.* **196:** 187–198.

Broun, M., S. Sokol, and H. R. Bode. 2000. *Cngsc*, a homologue of goosecoid, participates in the patterning of the head, and is expressed in the organizer region of *Hydra*. *Development* **126:** 5245–5254.

Cariolou, M. A., and D. E. Morse. 1988. Purification and characterization of calcium-binding conchiolin shell peptides from the mollusc, *Haliotis rufescens*, as a function of development. *J. Comp. Physiol. B* **157:** 717–729.

Carpizo-Ituarte, E., and M. G. Hadfield. 1998. Stimulation of metamorphosis in the polychaete *Hydroides elegans* Haswell (Serpulidae). *Biol. Bull.* **194:** 14–24.

Cavanaugh, G. M. 1956. *Formulae and Methods VI*. Marine Biological Laboratory, Woods Hole, MA. Pp. 62–69.

Clare, A. S. 1996. Signal transduction of barnacle settlement: calcium re-visited. *Biofouling* **10:** 141–159.

Clare, A. S., R. F. Thomas, and D. Rittschof. 1995. Evidence for involvement of cyclic AMP in the pheromonal modulation of barnacle settlement. *J. Exp. Biol.* **198:** 655–664.

Degnan, B. M., and D. E. Morse. 1993. Identification of eight homeobox-containing transcripts expressed during larval development and at metamorphosis in the gastropod mollusc *Haliotis rufescens*. *Mol. Mar. Biol. Biotech.* **2:** 1–9.

Degnan, B. M., and D. E. Morse. 1995. Developmental and morphogenetic gene regulation in *Haliotis rufescens* larvae at metamorphosis. *Am. Zool.* 35: 391–398.

Degnan, B. M., J. C. Groppe, and D. E. Morse. 1995. Chymotrypsin mRNA expression in digestive gland amoebocytes: cell specification occurs prior to metamorphosis and gut morphogenesis in the gastropod, *Haliotis rufescens*. *Roux's Arch. Dev. Biol.* **205:** 97–101.

Del Carmen, K. A., and [illegible] Hadfield. 1999. Metamorphosis in a marine gastropod: the role of transcription and translation. *Am. Zool.* **39:** 20A.

Del Carmen, K. A., and M. G. Hadfield. 2000. Metamorphosis in a marine gastropod: the role of transcription. P. 37A in *Larval Biology Meetings Abstract Book*, Santa Cruz, CA.

Eiben, R. 1982. Storage of embryonically transcribed poly(A) RNA and its utilization during metamorphosis of the hydroid *Hydractinia echinata*. *Roux's Arch. Dev. Biol.* **191:** 270–276.

Evans, R. M. 1988. The steroid and thyroid hormone receptor superfamily. *Science* **240:** 889–895.

Fenteany, G., and D. E. Morse. 1993. Specific inhibitors of protein synthesis do not block RNA synthesis or settlement in larvae of a marine gastropod mollusk (*Haliotis rufescens*). *Biol. Bull.* **184:** 6–14.

Freeman, G., and E. B. Ridgway. 1990. Cellular and intracellular pathways mediating the metamorphic stimulus in hydrozoan planulae. *Roux's Arch. Dev. Biol.* **199:** 63–79.

Gilbert, L. I., J. R. Tata, and B. G. Atkinson, eds. 1996. *Metamorphosis: Postembryonic Reprogramming of Gene Expression in Amphibian and Insect Cells*. Academic Press, San Diego, CA.

Hadfield, M. G. 1978. Metamorphosis in marine molluscan larvae: an analysis of stimulus and response. Pp. 165–175 in *Settlement and Metamorphosis of Marine Invertebrate Larvae*, F. S. Chia and M. Rice, eds. Elsevier/North-Holland, New York.

Hadfield, M. G. 1998. Research on settlement and metamorphosis of marine invertebrate larvae: past, present and future. *Biofouling* **12:** 9–29.

Hadfield, M. G. 2000. Why and how marine invertebrate larvae metamorphose so fast. *Semin. Cell Dev. Biol.* **11:** 437–443.

Hadfield, M. G., C. C. Unabia, C. M. Smith, and T. M. Michael. 1994. Settlement preferences of the ubiquitous fouler *Hydroides elegans*. Pp. 65–72 in *Recent Developments in Biofouling Control*, M. F. Thompson, R. Nagabhushanam, R. Sarojini, and M. Fingerman, eds. Oxford and IBH Publishing, New Delhi.

Hadfield, M. G., E. A. Meleshkevitch, and D. Y. Boudko. 2000. The apical sensory organ of a gastropod veliger is a receptor for settlement cues. *Biol. Bull.* **198:** 67–76.

Hadfield, M. G., E. Carpizo-Ituarte, K. Del Carmen, and B. T. Nedved. 2001. Metamorphic competence, a major adaptive convergence in marine invertebrate larvae. *Am. Zool.* **41:** 1123–1131.

Holm, E. R., B. T. Nedved, E. Carpizo-Ituarte, and M. G. Hadfield. 1998. Metamorphic-signal transduction in *Hydroides elegans* (Polychaeta: Serpulidae) is not mediated by a G protein. *Biol. Bull.* **195:** 21–29.

Han, M., R. A. Jensen, and D. E. Morse. 1993. Calcium control of metamorphosis in polychaete larvae. *J. Exp. Zool.* **267:** 423–430.

Jensen, R. A., and D. E. Morse. 1990. Chemically induced metamorphosis of polychaete larvae in both the laboratory and the ocean environment. *J. Chem. Ecol.* **16:** 911–930.

Knight J., A. F. Rowley, M. Yamazaki, and A. S. Clare. 2000. Eicosanoids are modulators of larval settlement in the barnacle, *Balanus amphitrite*. *J. Mar. Biol. Assoc. UK* **80:** 113–117.

Kroiher, M., M. Walther, and S. Berking. 1991. Necessity of protein synthesis for metamorphosis in the marine hydroid *Hydractinia echinata*. *Roux's Arch. Dev. Biol.* **200:** 336–341.

Leitz, T. 1997. Induction of settlement and metamorphosis of cnidarian larvae: signals and signal transduction. *Invertebr. Reprod. Dev.* **31:** 109–122.

Leitz, T. 1998. Induction of metamorphosis of the marine hydrozoan *Hydractinia echinata* Fleming, 1828. *Biofouling* **12:** 173–187.

Leontovich, A. A., J. Zhang, K. Shimokawa, H. Nagase, and M. P. Sarras, Jr. 2000. A novel hydra matrix metalloproteinase (HMMP) functions in extracellular matrix degradation, morphogenesis and the maintenance of differentiated cells in the foot process. *Development* **127:** 907–920.

McCauley, B. J. 1997. Metamorphosis without gene expression or cell proliferation in a marine mollusk. Ph.D. dissertation. University of Hawaii. 54 pp.

McCauley, D. W. 1997. Serotonin plays an early role in the metamorphosis of the hydrozoan *Phialidium gregarium*. *Dev. Biol.* **190:** 229–240.

Nijhout, H. F. 1999. Hormonal control in larval development and evolution—insects. Pp. 217–254 in *The Origin and Evolution of Larval Forms*, B. K. Hall and M. H. Wake, eds. Academic Press, San Diego, CA.

Pawlik, J. R. 1990. Natural and artificial induction of metamorphosis of *Phragmatopoma lapidosa californica* (Polychaeta: Sabellaridae), with a critical look at the effects of bioactive compounds on marine invertebrate larvae. *Bull. Mar. Sci.* **46:** 512–536.

Pires, A., R. P. Croll, and M. G. Hadfield. 2000. Catecholamines modulate metamorphosis in the opisthobranch gastropod *Phestilla sibogae*. *Biol. Bull.* **198:** 319–331.

Plickert, G., M. Kroiher, and A. Munck. 1988. Cell proliferation and early differentiation during embryonic development and metamorphosis of *Hydractinia echinata*. *Development* **103:** 795–803.

Rose, C. S. 1999. Hormonal control in larval development and evolution—amphibians. Pp. 167–216 in *The Origin and Evolution of Larval Forms*, B. K. Hall and M. H. Wake, eds. Academic Press, San Diego, CA.

Schneider, T., and T. Leitz. 1994. Protein kinase C in hydrozoans: involvement in metamorphosis of *Hydractinia* and pattern formation of *Hydra*. *Roux's Arch. Dev. Biol.* **203:** 422–428.

Shimizu-Nishikawa, K., Y. Shibata, A. Takei, M. Kuroda, and A. Nishikawa. 2002. Regulation of specific developmental fates of larval- and adult-type muscles during metamorphosis of the frog *Xenopus*. *Dev. Biol.* **251:** 91–104.

Steele, R. E. 2002. Developmental signaling in *Hydra*: What does it take to build a "simple" animal? *Dev. Biol.* **248:** 199–219.

Stephens, G. C. 1988. Epidermal amino acid transport in marine invertebrates. *Biochim. Biophys. Acta* **947:** 113–138.

Strathmann, R. S. 1993. Hypotheses on the origins of marine larvae. *Annu. Rev. Ecol. Syst.* **24:** 89–117.

Takahashi, T., O. Koizumi, Y. Ariura, A. Romanovitch, T. C. G. Bosch, Y. Kobayakawa, S. Mohri, S. Yum, M. Hatta, and T. Fujisawa. 2000. A novel neuropeptide, Hym-355, positively regulates neuron differentiation in *Hydra*. *Development* **127:** 997–1005.

Tata, J. R. 1996. Hormonal interplay and thyroid hormone receptor expression during amphibian metamorphosis. Pp. 466–503 in *Metamorphosis, Postembryonic Reprogramming of Gene Expression in Amphibian and Insect Cells*, L. I. Gilbert, J. R. Tata, and B. G. Atkinson, eds. Academic Press, New York.

Tata, J. R. 1999. Amphibian metamorphosis as a model for studying the developmental actions of thyroid hormone. *Biochimie* **81:** 359–366.

Thomas, M. B., N. C. Edwards, B. E. Ball, and D. W. McCauley. 1997. Comparison of metamorphic induction in hydroids. *Invertebr. Biol.* **116:** 277–285.

Trapido-Rosenthal, H. G., and D. E. Morse. 1985a. Availability of chemosensory receptors is down regulated by habituation of larvae to a morphometric signal. *Proc. Natl. Acad. Sci. USA* **83:** 7658–7662.

Trapido-Rosenthal, H. G., and D. E. Morse. 1985b. Regulation of receptor-mediated settlement and metamorphosis in larvae of a gastropod mollusc (*Haliotis rufescens*). *Bull. Mar. Sci.* **39:** 383–392.

Whitaker, J. R., and P. E. Granum. 1980. An absolute method for protein determination based on difference in absorbance at 235 and 280 nm. *Anal. Biochem.* 109: 156–159.

Unabia, C. C., and M. G. Hadfield. 1999. Role of bacteria in larval settlement and metamorphosis of the polychaete *Hydroides elegans*. *Mar. Biol.* **133:** 55–64.

Yan, L., K. Fei, J. Zhang, S. Dexter, and M. P. Sarras, Jr. 2000a. Identification and characterization of hydra metalloproteinase 2 (HMP2): a meprin-like astacin metalloproteinase that functions in foot morphogenesis. *Development* **127:** 129–141.

Yan, L., A. Leontovich, K. Fei, and M. P. Sarras, Jr. 2000b. *Hydra* metalloproteinase 1: a secreted astacin metalloproteinase whose apical axis expression is differentially regulated during head regeneration. *Dev. Biol.* **219:** 115–128.

Zandomeni, R., B. Mittleman, D. Bunick, S. Ackerman, and R. Weinmann. 1982. Mechanisms of action of dichloro-β-D-ribofuranosylbenzimidazole: effect on *in vitro* transcription. *Proc. Natl. Acad. Sci. USA* **79:** 3167–3170.

Reference: *Biol. Bull.* **204:** 126–137. (April 2003)

Role of Maxilla 2 and Its Setae During Feeding in the Shrimp *Palaemon adspersus* (Crustacea: Decapoda)

A. GARM[1,*], E. HALLBERG[2], AND J. T. HØEG[1]

[1]*Department of Zoomorphology, Zoological Institute, University of Copenhagen, Universitetsparken 15, 2100 Copenhagen, Denmark; and* [2]*Department of Cell and Organism Biology, University of Lund, Helgolandsvegen 17, Lund, Sweden*

Abstract. The movements of the basis of maxilla 2 in *Palaemon adspersus* were examined using macro-video recordings, and the morphology of its setae was examined using both scanning and transmission electron microscopy. The basis of maxilla 2 performs stereotypical movements in the latero-medial plane and gently touches the food with a frequency of 3–5 Hz. The medial rim of the basis of maxilla 2 carries three types of seta. Type 1 is serrate, type 2 and 3 are serrulate, and type 2 has a prominent terminal pore. Type 2 is innervated by 18–25 sensory cells whose cilia protrude through the terminal pore and are in direct contact with the external environment. The structure of type 2 setae indicates that they are mainly gustatory, although still bimodal due to their innervation by presumed chemosensory and mechanosensory neurons. Distally, the three types of setae have a complex arrangement of the cuticle involving water-filled canals, which may serve to improve flexibility. Type 1 and 3 setae have fewer sensory cells (4–9) but probably also have a bimodal sensory function. The function of type 1 setae is probably to protect type 2 setae, while type 3 setae might serve to groom the ventral side of the basis of maxilla 1.

Introduction

The decapod mouth apparatus comprises six pairs of limbs, which have as many as 40 parts capable of independent movement (Garm and Høeg, 2001). The parts, which are arranged bilaterally in pairs, have different functions such as collecting, holding, moving, tearing, biting, and adjusting the position of food; creating and directing water currents; and grooming (Robberts, 1968; Kunze and Anderson, 1979; Schembri, 1982; Stemhuis *et al.*, 1998; Garm and Høeg, 2001). These functions depend on the position, movement, and gross morphology of the mouthpart in question, and especially on its setation (Stemhuis *et al.*, 1998; Coelho *et al.*, 2000; Garm and Høeg, 2001). The mouthpart functions just listed are all mechanical in nature; however, like most other crustacean setae, those found on the mouthparts are also part of the sensory system (Paffenhöfer and Loyd, 2000), being either mechanosensory, chemosensory, or both (bimodal). The external morphology of the mouthpart setae of decapods is highly diverse (Schembri, 1982; Lavalli and Factor, 1992; Stemhuis *et al.*, 1998; Johnston, 1999; Garm and Høeg, 2000), which indicates that they have a wide range of both mechanical and sensory functions. A rather good correlation between morphology and function has been demonstrated in insect sensilla (Steinbrecht, 1997, 1998; Keil, 1998); but in crustaceans, only the aesthetasc type of seta is understood in detail (Hallberg *et al.*, 1992, 1997; Steullet and Derby, 1997; Derby, 2000; Steullet *et al.*, 2000a, b). Almost nothing is known about the sensory properties of mouthpart setae except for a few studies on copepods (Paffenhöfer and Loyd, 1999, 2000). Many of the mechanical functions of mouthpart setae are understood, but little is known about their sensory functions, such as when they are used during food handling and what they are sensing.

In decapods, maxilla 2 is responsible for ventilating the gills *via* the scaphognathite (gill bailer), and it therefore moves more-or-less constantly and in a stereotypical way (Garm and Høeg, 2001). This must have a limiting effect on the mechanical functions of this mouthpart during food handling, but it might be suitable for chemosensation of food objects held by the other mouthparts. The constant movement would provide the animal with discrete samples of sensory input, which seems to be important for stimulus

Received 30 August 2002; accepted 2 December 2002.

*To whom correspondence should be addressed. E-mail: Algarm@zi.ku.dk

processing by some chemosensory setae (Goldman and Koehl, 2001). In the squat lobsters *Munida sarsi* and *M. tenuimana,* external morphology correlated with behavior suggests that setae on the medial rim of the basis of maxilla 2 have gustatory properties (Garm and Høeg, 2001). When squat lobsters are sorting the sediment in search of edible items, these setae probe sediment particles frequently (3–4 Hz) just before they are rejected; almost no particles are rejected before they reach maxilla 2. These setae therefore seem to play an important role in deciding whether to eat or reject a food object.

Palaemon adspersus is an omnivorous species of caridean shrimp with a reduced maxilla 2 that lacks the coxal endite (Boas, 1880). This morphology indicates a reduced mechanical function of this limb, making the species especially suited for studying the sensory functions. In this paper, we examine the role of maxilla 2 and its setae during feeding in *P. adspersus*.

Materials and Methods

Video recordings

Adult male and female specimens of *Palaemon adspersus* (carapace lengths 14–20 mm) were obtained from Øresund in Denmark and kept in a 200-l aquarium at Danmarks Akvarium in Copenhagen. Behavioral observations of feeding shrimps were made in 25-l aquaria. Both systems had running seawater at 12 °C. The animals were starved for 3–5 d, then fed mussels, fish meat, live and dead artemia, krill, squid, algal tissue, and muddy sediment; they were then videotaped. During recordings, the carapace was attached to a thin iron bar, which could be moved in all three planes ensuring that position and angle of observation could be manipulated. The animals had a steel nut glued to their carapace with cyanoacrylate glue, and the iron bar was screwed into the nut. A SONY DXC 950P color (Y/C) 3CCD camera equipped with a Micronikkor 105-mm macro lens placed outside the aquarium enabled us to resolve structures about 5 μm wide. Recordings were made on PAL super VHS. Light was obtained from a 120-W bulb. Representative images of mouthpart movements were grabbed with a time resolution of 0.02 s (50 fields/s) using the frame grabber card DVRaptor from Canopus, then imported into CorelDraw 10.0, with a resolution of 720 × 564 pixels. We outlined the involved mouthparts and used the outlines for the serial drawings in Figure 2, which therefore accurately reflect the positions and movements of mouthparts in the video sequences.

Light and scanning electron microscopy

Specimens from the behavioral study were dissected and fixed in 2% formalin. For SEM, the mouthparts were cleaned with a sonicator and manually with a beaver-hair brush. A standard dissection microscope with a camera lucida was used for creating the drawing in Figure 1. SEM preparation followed standard procedures, which did not include using osmium tetraoxide. The micrographs were taken on a JEOL 840 scanning electron microscope and stored digitally with a resolution of 1262 × 1616 pixels using the program SEMafore (JEOL).

Transmission electron microscopy

Clean specimens were obtained by maintaining them in clean artificial seawater for 2 d without feeding. The specimens were anesthetized on ice, dissected, and fixed in cold 2.5% glutaraldehyde and 2% paraformaldehyde in 0.2 *M* sodium cacodylate buffer (pH 7.2) for 3 days. The basis of maxilla 2 was dissected from the rest of the limb to shorten the diffusion distance for the fixative. The specimens were postfixed in 1% osmium tetraoxide for 1 h at room temperature, dehydrated in an ethanol series and acetone, and embedded in Epon resin. Ultrathin sections about 50 nm thick were cut on a Leica UCT ultramicrotome, placed on single-slot grids, and stained with uranyl acetate for 20 min at 60 °C and lead citrate for 4 min at 20 °C. The sections were viewed in a JEOL 1230 transmission electron microscope, and digital pictures with a resolution of 1024 × 1024 pixels were taken using a GATAN 791 Multiscan camera.

Results

Movements

As in all other decapods, the mouth apparatus of *Palaemon adspersus* consists of maxillipeds 1–3 (Mxp1–3), maxillae 1–2 (Mx1–2), mandible, paragnath (not visible in Fig. 1), and labrum (La) (Fig. 1). The endopods of Mxp2–3 are elongate 5-segmented appendages with a high degree of freedom of movement, and Mxp1 and Mx1–2 are flattened and arranged in dorso-ventral layers below the mandible. Mx2 is narrowly placed between Mxp1 and Mx1 and can therefore move rather freely in the medio-lateral plane but has restricted movement in the dorso-ventral plane. When handling food, Mx2 performs medio-lateral movements with a frequency of 3–5 Hz, resulting in the medial edge probing the food (Fig. 2). These movements are stereotypical and do not depend on food type. The size of the food object determines the amplitude of the movements. Mx2 can move to some degree in the dorso-ventral plane and thereby touch the food object in different places without moving it. The left and right Mx2 normally alternate in their movements. When the right Mx2 Bas1 touches the food object, the left Mx2 Bas1 is in a lateral position and starts moving medially (Fig. 2B). After the left Mx2 Bas1 has made contact with the food object, the right Mx2 Bas1 starts moving laterally (Fig. 2C). When in lateral position, the left Mx2 Bas1 moves laterally, and the process starts again (Fig.

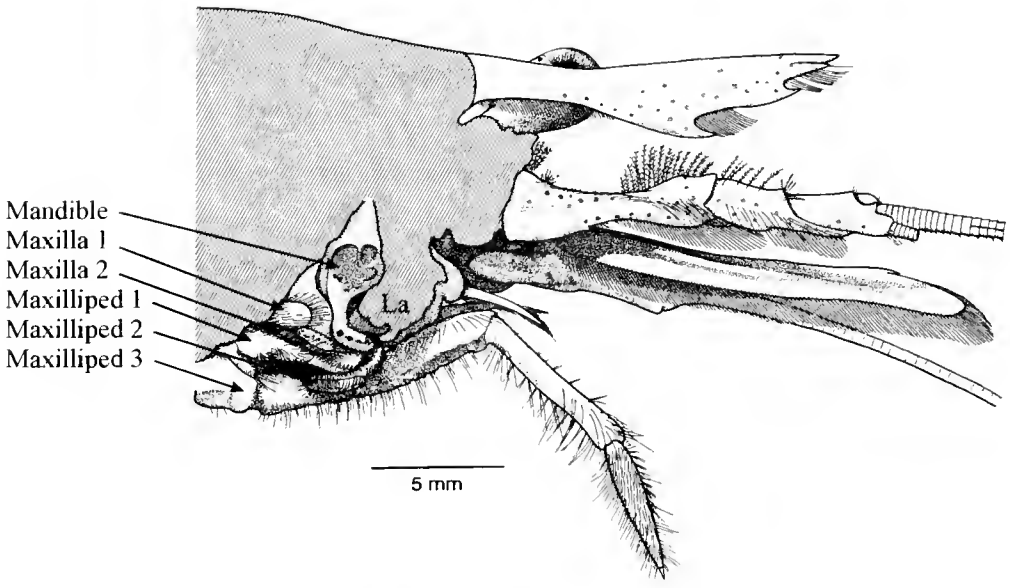

Figure 1. Drawing of the anterior part of *Palaemon adspersus* cut in the medial plane and viewed from the medial side. Striated area indicates cut surface. Position of mouthparts represents the position in an animal not handling any food objects. La = labrum.

2D–F). These movements are made with very few pauses, and Mx2 was never seen to hold the food object. There is a tendency, though, for Mx2 to stop in the lateral position when the mandibles are performing a bite. During the movements, the dorsalmost setae scrape across the ventral side of Mx1 Bas (not shown in Fig. 2 for the sake of simplicity).

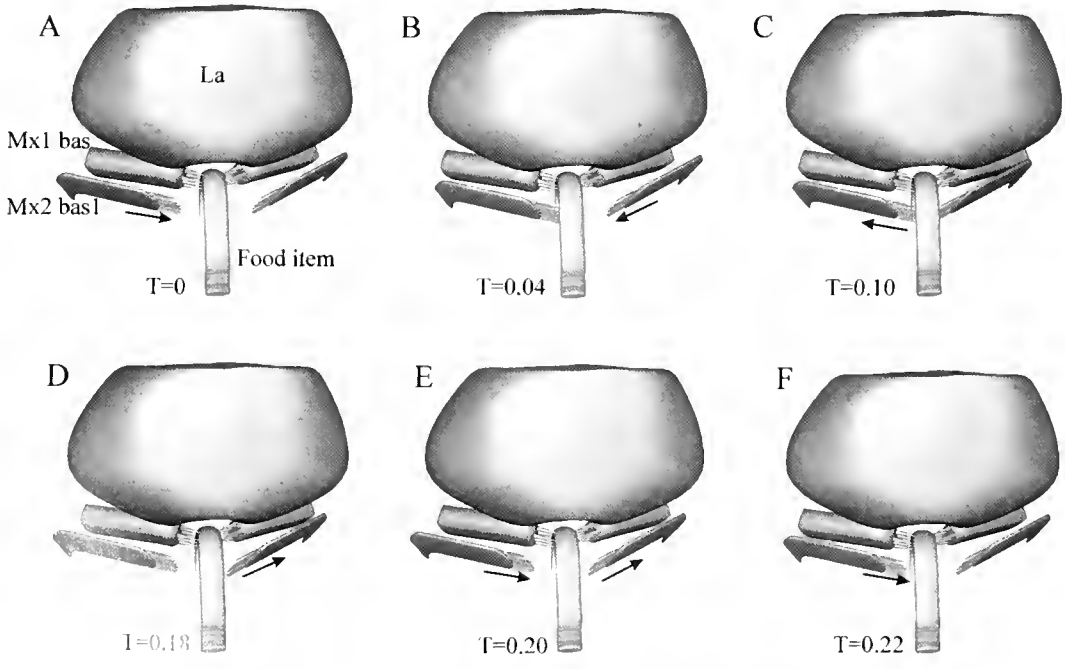

Figure 2. Schematic drawings of latero-medial movements of basis 1 of maxilla 2 during food handling (anterio-ventral view). For simplicity, only the labrum (La), the basis of maxilla 1 (Mx1 Bas), and basis 1 of maxilla 2 (Mx2 Bas1) with type 2 setae are drawn. Arrows indicate direction of movements, and T = time in seconds. (A) Food is held just ventral to La by Mx1 Bas. Mx2 Bas1 are in lateral position, and right Mx2 Bas1 moves medially. (B) Right Mx2 Bas1 in the medial position touches the food, and left Mx2 Bas1 starts moving medially. (C) When left Mx2 Bas1 touches food in medial position, right Mx2 Bas1 moves laterally. (D) When right Mx2 Bas1 is in lateral position, left Mx2 Bas1 moves laterally. (E) Just before left Mx2 Bas1 is in lateral position, right Mx2 Bas1 starts moving medially. (F) A new cycle of movements begins.

External morphology

Mx2 is composed of four parts: the large scaphognathite, a reduced endopod, a very reduced coxa, and a basis (Fig. 3A). The coxa has no endite, but the endite of the basis is well developed and divided into two parts (Fig. 3B, Bas1–2). The medial rim of Bas1, along with the distal part of the medial rim of Bas2, contacts the food objects. This area bears three types of setae arranged in more or less separate rows (Fig. 3C). The terminology in the following descriptions is adapted from the setal classification system proposed by Lavalli and Factor (1992).

Type 1 setae are serrate (setae having denticles in two or more rows) and are the longest (250–350 μm) and most robust of the three types. They form the ventralmost row of 15–18 setae. The seta is slightly curved, tapering distally into a pointed tip, which points dorso-anteriorly (Fig. 4A, B). It lacks terminal and subterminal pores (Fig. 4B). The part of the shaft distal to the annulus carries outgrowths. On one side, they are arranged in two rows angled 120 ° to each other and extend to the tip except for the last 5–10 μm. The rows start as about 10-μm-long setules (articulated with the shaft), gradually changing into 7- to 8-μm-long denticles (not articulated with the shaft) in the distal part of the rows. The denticles get smaller towards the tip. Randomly distributed setules lying flat against the shaft and pointing distally are found opposite the two rows. Proximally, they are 10 to 12-μm long, decreasing to 7–8 μm distally. They terminate 20–30 μm from the tip. The sockets of type 1 setae are reduced and have an intracuticular articulation (Fig. 4A).

Type 2 setae are highly modified, serrulate setae (setae with small elongate or scale-like serrate setules) found in the middle area of Mx2 Bas1+2, but they are not arranged in strict rows (Fig. 3C). They are the most numerous type, with a total of 50–60 on Bas1 + 2. They are slender, a little shorter than type 1 (150–200 μm), and bent slightly into the shape of an S (Fig. 5A). The distal third carries scale-like setules of about 5 μm in length and arranged in three rows. Proximally, the setules lay flat against the shaft, and their tips touch the base of the next setule. More distally on the shaft, the setules are more densely packed so that near the tip they overlap in two to three layers (Fig. 5D). But here they are smaller, reduced to about 1–2 μm in length. The very tip of the seta is a tube, 2 μm long and 1 μm wide, that points dorso-posteriorly and has a prominent terminal pore about 0.5 μm in diameter (Fig. 5B, C). The socket of type 2 setae has an intracuticular articulation and a well-devel-

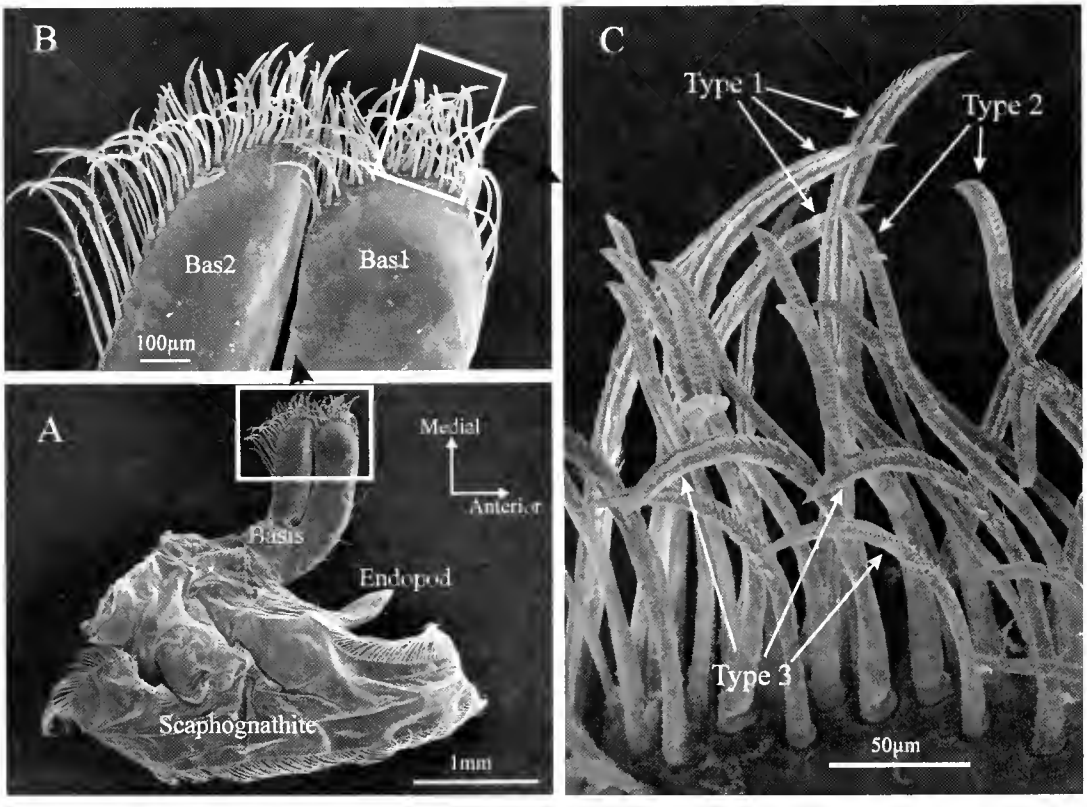

Figure 3. Scanning electron micrographs of maxilla 2 (dorsal view). (A) Whole Mx2 composed of four parts: Scaphognathite (gill bailer), endopod, a divided basis, and coxa (reduced and not visible). (B) Enlargement of framed area in A showing the medial rim of basis 1 and 2 (Bas1, Bas2). Note the change in setation on Bas 2 when moving posteriorly. (C) Enlargement of the framed area in B showing the arrangement of the three types of setae found on the medial rim of Bas1 and Bas2.

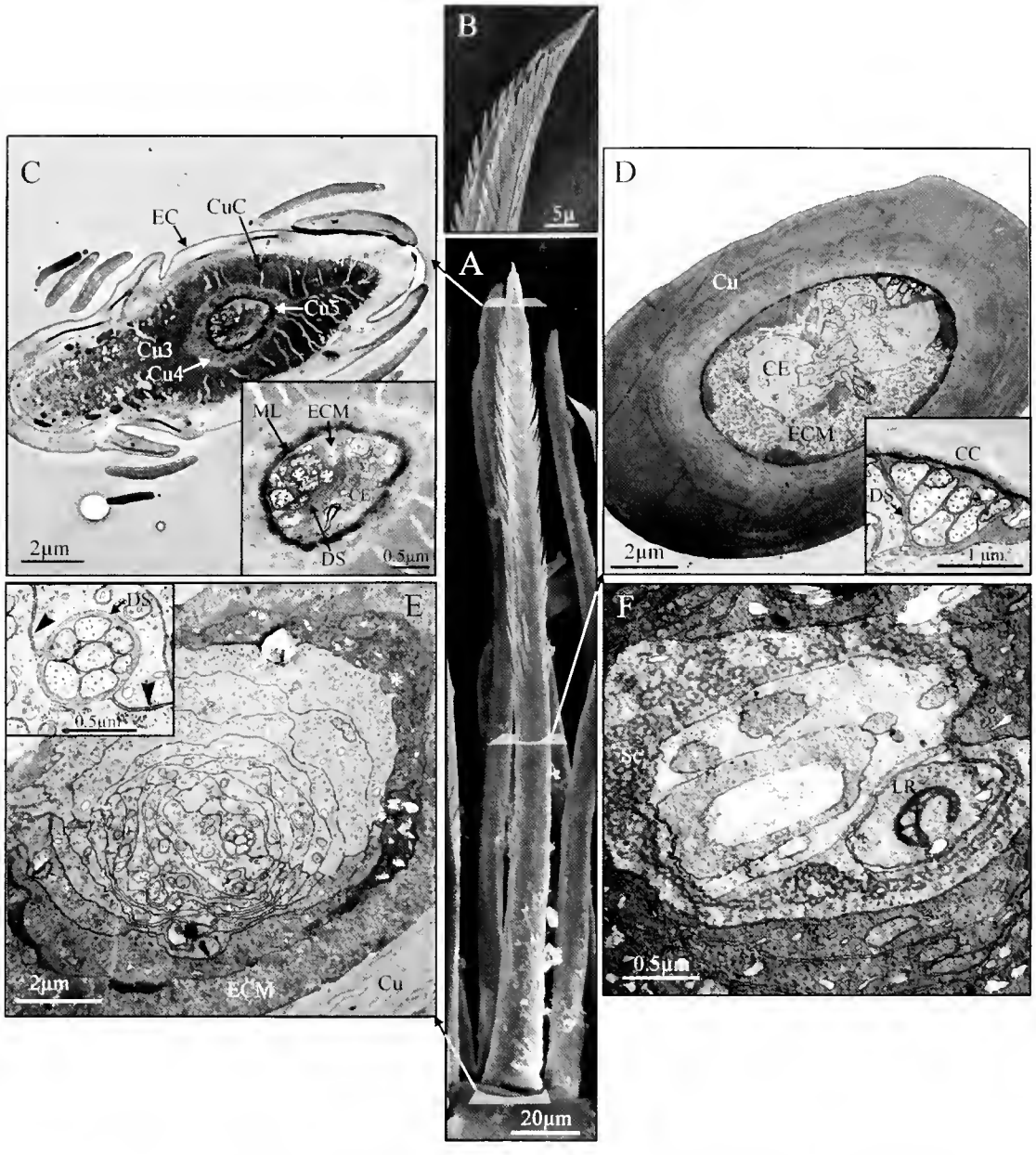

Figure 4. Type 1 seta. (A) Scanning electron micrograph of type 1 seta, which is the longest and most robust seta on Mx2 Bas1. Planes indicate approximate area of transmission electron micrographs. (B) Close-up of pointed tip without pore. (C) Transmission electron micrograph of semi cross-section *ca.* 20 µm from the tip. Cuticle is divided into six distinct layers (EC, Cu2–Cu5, ML). Insert = close-up of lumen containing ciliary compartment (CC, 7 modified cilia) enclosed by a dendritic sheet (DS), one cell extension (CE), and a sparse extracellular matrix (ECM). (D) Cross-section in middle region of seta. Cuticle layers 2 and 3 have fused (Cu). Lumen contains a ciliary compartment with a prominent dendritic sheet (insert), eight cell extensions, and a large amount of extracellular matrix. Insert = close-up of CC. (E) Cross-section just below the base of the seta. Cilia are enclosed by more than 20 sheet cells. Outermost sheet cells are very electron dense and vacuolated (asterisk). Extracellular matrix encircles sheet cell. Insert = close-up of ciliary compartment. Cilia are enclosed by a dendritic sheet, and the sheet cells are connected by septate junctions (arrowheads). (F) Cross-section *ca.* 50 µm below E, showing a large rootlet (LR) in one of the sensory cells. In this area, the innermost sheet cell contains a scolopale (Sc).

oped membranous socket area, which makes the seta rather flexible.

Type 3 setae are serrulate and found in a dorsal row containing about 30 setae (Fig. 3C). It is the shortest of the three types (100–150 µm), is slender, and curves dorsally. The distal half has small setules (5–10 µm) arranged in four

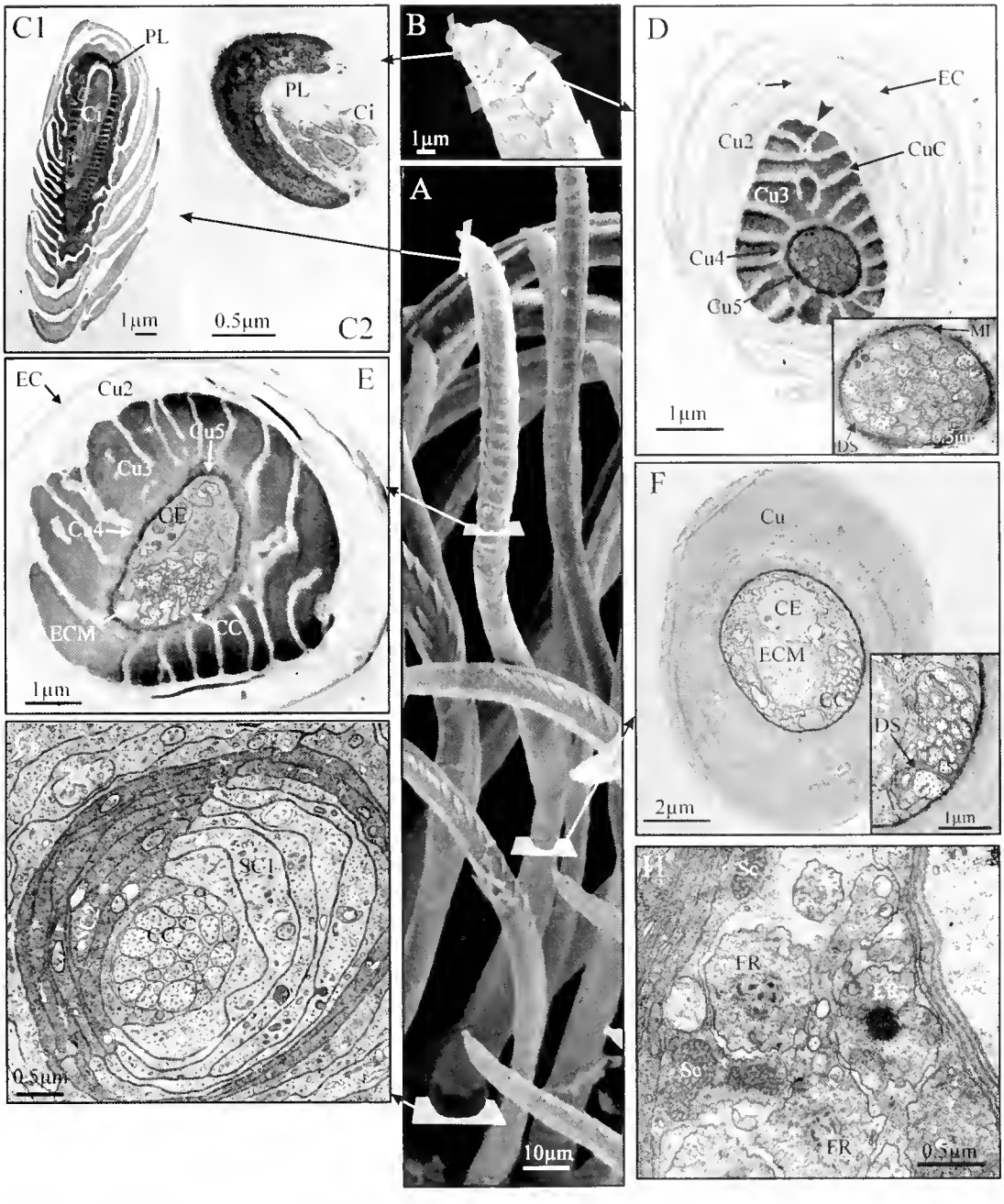

Figure 5. Type 2 seta. (A) Scanning electron micrograph of type 2 seta. Planes indicate approximate area of transmission electron micrographs. (B) Close-up of tip showing prominent terminal pore at the end of a tubular extension. (C1) Longitudinal section of tip showing sensory cilia (Ci) lying in pore lumen (PL). Note that fourth and fifth cuticle layers are missing. (C2) Cross-section of pore showing Ci protruding through pore. (D) Cross-section *ca.* 5 µm from tip. Lumen is completely filled with 30 Ci. Cuticle divided in six layers (EC, Cu2–Cu5, M1). Cu3 with very prominent cuticular canals (CuC). Insert = close-up of lumen. (E) Cross-section in the proximal end of setulate region. Cuticle in five distinct layers and lumen with two cellular extensions (CE), sparse extracellular matrix (ECM), and a ciliary compartment (CC). (F) Cross-section in middle part of nonserrulate area. Cuticular layers are more or less fused. Lumen contains 5 cellular extensions, a large amount of extracellular matrix, and a ciliary compartment enclosed by a dendritic sheet (insert, DS). Insert = close up of CC. (G) Cross-section just below the base of the seta. A ciliary compartment with 24 modified cilia encircled by two types of semicircular sheet cells (SC1, SC2); no dendritic sheet in this area. (H) Approximately 40 µm after G, showing two types of ciliary rootlets and a reduced scolopale. FR = fragmented rootlet, LR = solid rootlet, Sc = scolopale.

rows terminating 5 μm from the setal tip, which lacks pores (Fig. 6A, B). The setules are serrate and decrease in size towards the tip of the seta. The socket forms an intracuticular articulation, and the membranous area is prominent, which adds flexibility to the seta.

Internal morphology

Type 1 setae (Fig. 4) are innervated by five to nine sensory cells (mean = 7.5, n = 10), each of which gives rise to one modified cilium (Fig. 4D). The unbranched cilia continue to the tip of the seta and contain relatively few strands of microtubules (Fig. 4C). Two of the sensory cells contain a large rootlet in their distal end of the cell proper (Fig. 4F, LR), while the other cells have small fragmented rootlets. The numerous sheet cells (>20) tend to lie in semicircles around the bundle of modified cilia (Fig. 4E) and fall into two types. The majority are rather electron-lucent, but two to four of them are electron-dense and contain many vacuoles (Fig. 4E, asterisk). The innermost sheet cell contains a scolopale (Fig. 4F) and forms a dendritic sheet, which encircles the cilia from just below the basal part of the seta to the distalmost 20 μm. In the region of the scolopale, the innermost sheet cell makes a projection that surrounds one of the sensory cells with a large rootlet (Fig. 4F). The extracellular matrix within the lumen of the dendritic sheet is electron-dense. The next five to eight sheet cells send projections into the lumen of the setal shaft (Fig. 4D), and one of these projections continues to within at least 20 μm below the tip (Fig. 4C). We could not identify which sheet cell makes this projection. An extracellular matrix encircles both the ciliary compartment and the cell projections in the setal lumen. The extracellular matrix is most prominent at the base and barely detectable near the tip (Fig. 4C). It contains both electron-dense and electron-lucent areas. The cuticle of the seta is rather thick, and in the distal part it is divided into six distinct layers (Fig. 4C). The outermost thin epicuticle and the *ca.* 1-μm-thick, electron-lucent second layer are the only ones present in the outgrowths of the seta (Fig. 4C). The third layer is electron-dense and contains radially projecting canals that seem to be composed of the same material as the second layer. The cuticle of the convex side of the seta is more granular and without canals. Due to an oblique cross-section of the seta, the third layer varies between 1 and 2 μm in thickness. The fourth layer is about 0.5 μm thick, fibrous, and changes gradually into the fifth layer, which is similarly fibrous but very electron-dense and about 0.1 μm thick. A sixth membranous layer encircles the lumen (Fig. 4C, insert: ML). In the proximal two-thirds of the shaft, the second and third layers have gradually merged to form one homogeneous electron-dense layer 2–4 μm thick (Fig. 4D). The fourth layer has expanded to a thickness of about 1 μm. The fifth layer is not detectable, but the innermost membranous layer remains unchanged.

Type 2 (Fig. 5) is innervated by 18–25 sensory cells, which give rise to 18–25 modified cilia (mean = 23.25, n = 12) (Fig. 5G). Some of these cilia branch, and there are 28–30 ciliary branches in the distal end of the lumen (Fig. 5D, F). The cilia continue all the way to the tip of the seta, where they protrude through the terminal pore, which lies in the extension of the setal lumen (Fig. 5, C1, C2). All the sensory cilia are alike and contain rather few microtubules, in the distal part only 4–10 strands. Two of the sensory cells have a large rootlet; the rest have a small fragmented rootlet. The sensory cells are again surrounded by numerous semicircular sheet cells (>20), which are dimorphic in their

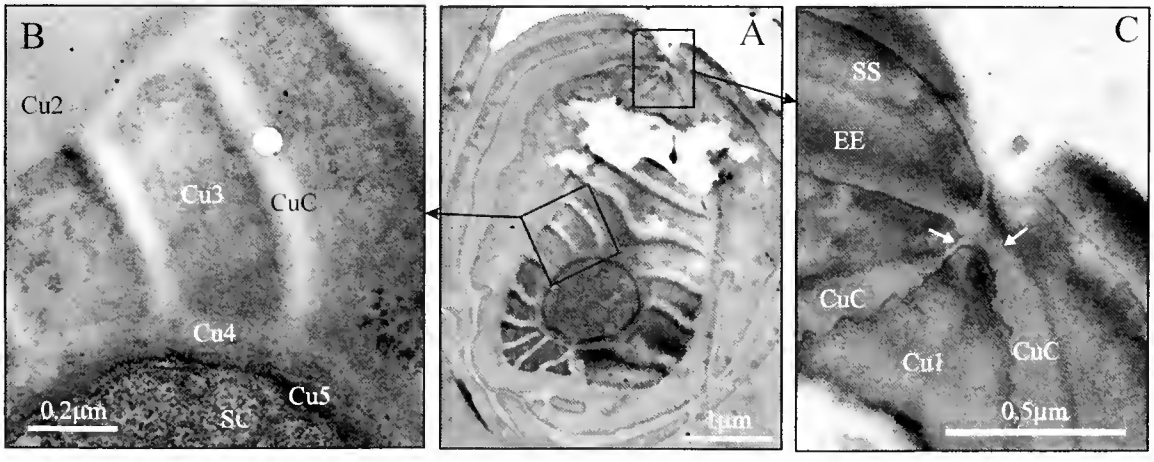

Figure 6. Canal system in the third layer of cuticle of seta type 2. (A) Cross-section of type 2 seta *ca.* 5 μm from the tip. Section is in a rather poor condition because it is the first in a series. (B) Close-up of section in A, showing cuticular canals (CuC) interconnected by circular canal. (C) Close-up of section in A, showing the pores (arrows) where cuticular canals connect with external environment (EE). Cu2–Cu5 = cuticular layers 2–5, SC = sensory cilia, SS = scale-like setule.

electron density and arranged in a variable pattern. About 10 of the sheet cells send projections into the setal lumen. Midway up the setal shaft, the number of cell projections is reduced to three to four, and at the tip only the modified sensory cilia are present within the lumen (Fig. 5D–F). The innermost sheet cell forms the dendritic sheet, which runs from just below the base of the seta all the way to the tip (Fig. 5D, insert) and thus encloses the sensory cilia in a sparse electron-dense extracellular matrix. The innermost sheet cell also contains a rather rudimentary scolopale (Fig. 5H). From the base of the seta, there is also an extracellular matrix in the setal lumen outside the ciliary compartment, which narrows distally and is absent at the tip. The cuticle is of the same thickness and structure as described for type 1 setae, but it is not granular, and the canals in the electron-dense third layer are better developed. The second layer is also thinner in the distal part (Fig. 5D). The tube of the terminal pore appears to be formed from the third layer, but it does not contain any canals (Fig. 5, C1, C2). The canals in type 2 setae are connected to the external environment (Fig. 6). The radial canals are interconnected by a circular canal, which runs on the outside of the third cuticle layer (Fig. 5D, arrowhead; Fig. 6B). This canal in turn is connected to the exterior *via* a pore (Fig. 6C, arrow). These pores are made from infoldings of the epicuticle and second cuticular layer (Fig. 5D, arrow). Unfortunately, the series of sections is not complete, and we are therefore not able to show if the openings are really pores or if they continue and expand further distally.

Type 3 setae (Fig. 7) are innervated by four to nine sensory cells (mean = 6.1, n = 11), each giving rise to one modified cilium (Fig. 7E, F). These cilia continue unbranched to the tip (Fig. 7C). One or two of the sensory cells have a large rootlet; the rest have fragmented rootlets. The type 3 seta has fewer (<20) enveloping cells than the two other types (Fig. 7E). At least six of them send projections into the lumen, and one proceeds to at least 20 μm below the tip (Fig. 7C). The innermost cell forms the dendritic sheet and contains a well-developed scolopale. In the region of the scolopale, the innermost sheet cell encircles one or two of the sensory cells. As in the other types, the dendritic sheet forms the ciliary compartment, which contains the modified cilia and a sparse extracellular matrix. The extracellular matrix in the setal lumen is similar to that found in the two other types. The cuticle is also similar to what is found for type 2, except that the tube is lacking in type 3.

Discussion

We found that maxilla 2 of *Palaemon adspersus* performs stereotypical movements when the animal is handling food items. The medial rims of basis 1 and 2 of maxilla 2 touch the food items gently and were never seen to directly manipulate them. This area of maxilla 2 carries three types of setae, each with different external and internal morphology. Type 1 is serrate, robust, and has 5–9 sensory cells. Type 2 is serrulate, slender, and has 18–25 sensory cells; it also has a terminal pore from which sensory cilia protrude into the external environment. Type 3 is serrulate, short, and possesses four to nine sensory cells. In all three types, the sensory cells fall into two distinct morphological groups. Putative sensory properties of the three types are summarized in Table 1.

Our results on the activity and morphology of maxilla 2 and its setae in *Palaemon adspersus* lead us to conclude that the basis of maxilla 2 collects chemical information from a dense population of gustatory setae before the food item is either eaten or rejected.

The ultrastructure indicates that the three types of setae have distinct and separate functions. Type 1 and type 3 setae are innervated by four to nine sensory cells, one or two of which have a well-developed rootlet in close contact with a scolopale in the innermost sheet cell. A scolopale is an electron-dense structure made of closely packed strands of microtubules bound together with accessory proteins. This indicates that these cells are mechanoreceptors, since it is believed that desmosomal connections between the scolopale and the cilia rootlet are necessary for transduction of the mechanical signal (Schmidt and Gnatzy, 1984; Derby, 1989; Crouau, 2001). The remaining sensory cells have a small fragmented rootlet that is not in contact with the scolopale; they lack dynein arms in the ciliary region, and there are few strands of microtubules in the paraciliary region. This suggests that they are chemoreceptor neurons, but this assumption is based on the absence of mechanoreceptive structures (Schmidt and Gnatzy, 1984; Derby, 1989; Gleeson *et al.*, 1996; Hallberg and Hansson, 1999). We therefore conclude that type 1 and type 3 setae are bimodal sensors capable of detecting both mechanical and chemical stimuli. The existing ultrastructural studies on decapod setae suggest that this is the most common type of sensory innervation (Altner *et al.*, 1983; Schmidt and Gnatzy, 1984; Derby, 1989; Cate and Derby, 2001, 2002). We emphasize that our conclusions are based on behavior and morphology alone, and that no certainty about the sensory properties can be obtained without employing other methods such as electro-physiological recordings from the sensory cells. Although both type 1 and 3 setae are probably bimodal, their size, shape, and arrangement indicate that they have different functions.

The long, robust, and almost straight type 1 setae seem well suited to act as "guard setae," protecting the rather fragile type 2 setae from too much mechanical stress when food objects are being handled. A similar system is found on the first antennae of many decapod crustaceans, including the spiny lobster, *Panulirus argus,* where the aesthetascs (fragile chemosensory setae) are protected by long robust guard setae (Steullet *et al.*, 2000b; Cate and Derby, 2001). In the case of the spiny lobster, the ultrastructure of these setae is still unknown, and the protective function is as-

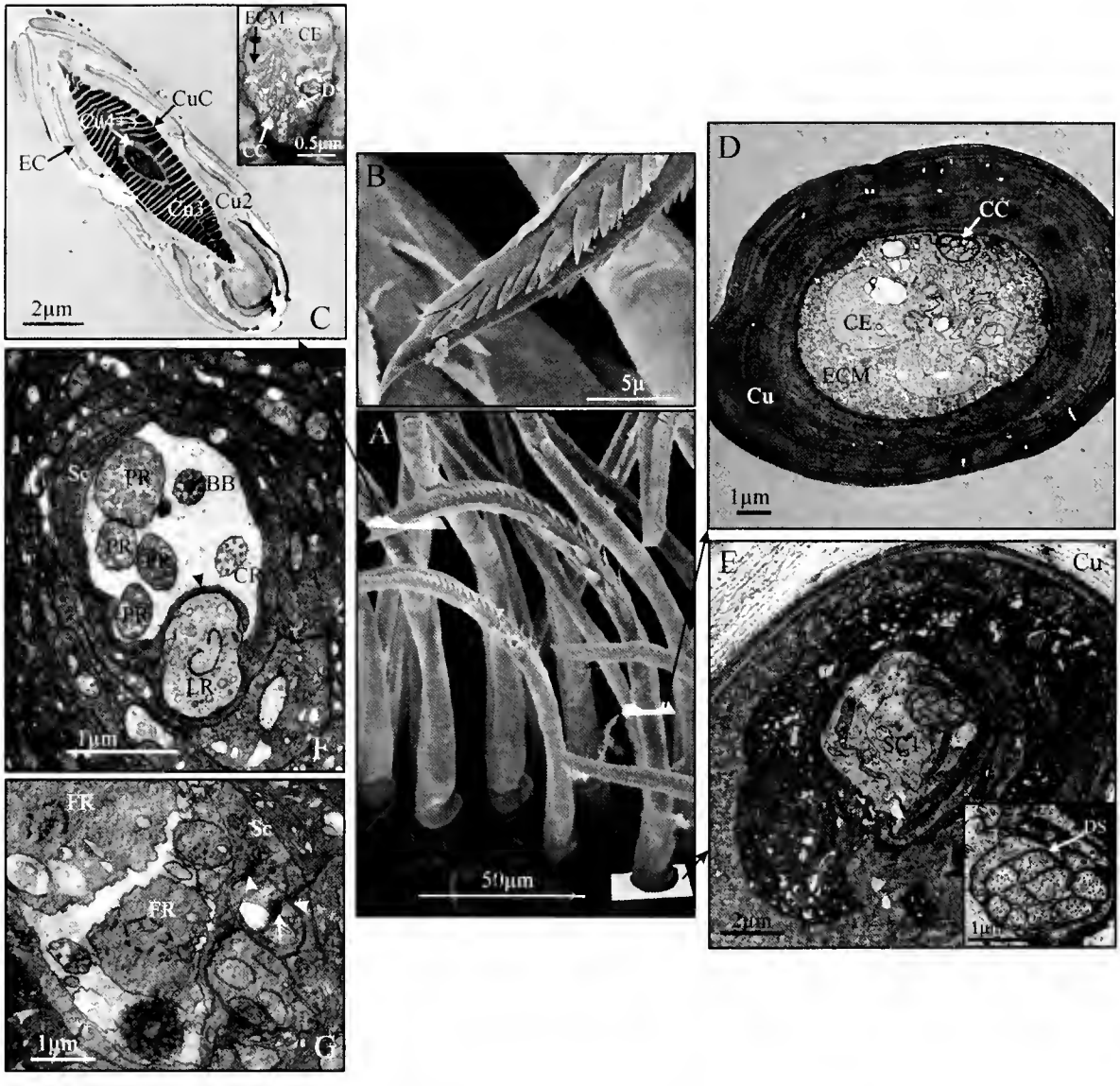

Figure 7. Type 3 seta. (A) Scanning electron micrograph of type 3 seta in dorsal row. Planes indicate approximate area of transmission electron micrographs. (B) Close-up of the tip. (C) Semi cross-section *ca.* 10 μm from tip. The cuticle is divided into six distinct layers (EC, Cu2-Cu5, ML not shown). Cu3 has prominent canals (CuC). Insert = close-up of lumen with ciliary compartment (CC) enclosed by the dendritic sheet (DS), one cell extension (CE), and a sparse extracellular matrix (ECM). (D) Cross-section in nonserrulate part of seta. Cuticle layers 2–5 have fused to form one more or less homogenous layer. Prominent lumen with large amount of extracellular matrix, eight to nine cell extensions, and a ciliary compartment with nine sensory cilia. (E) Cross-section just below the base of the seta. The ciliary compartment is enclosed by a dendritic sheet and 15–20 semicircular sheet cells of two types (SC1, SC2). The sheet cells are surrounded by extracellular matrix. Insert = close-up of ciliary compartment. (F) Cross-section *ca.* 50 μm after E. One cell has a large rootlet (LR); the other cells are sectioned in the region of the basal body (BB) or in the ciliary region (CR) or the paraciliary region (PR). A weak scolopale is seen (Sc). Arrowhead indicates extrusion of sheet cell enclosing sensory cell. (G) Cross section *ca.* 5 μm after F. The putative chemosensory cells contain a fragmented rootlet (FR). The mechanosensory cell is in contact with the scolopale *via* desmosomes (arrowheads). Arrow indicates large ciliary rootlet.

sumed from their arrangement and external morphology. The guard setae on *P. argus* are not serrate but simple (no outgrowths). Most other systems with crustacean mechanosensitive setae studied so far are sensitive to movements of the surrounding water (Wiese, 1976; Heinisch and Wiese, 1987; Derby, 1989); but this does not seem to be the case with the type 1 setae since the socket is reduced, they have no outgrowths suitable to receive water movements, and they are themselves moved all the time. Due to the activity and position of type 1 setae in *Palaemon adspersus*, we

Table 1

Summary of the structures and suggested functions for seta type 1, 2, 3 of Palaemon adspersus

	Type of seta	Length in μm	Pore*	Neurons/cilia	Scolopale*	Modality	Primary function
Type 1	Serrate	250–300	−	4–9	+	Bimodal	Protection
Type 2	Serrulate	200–250	+	18–25	+	Bimodal	Gustation
Type 3	Serrulate	150–200	−	4–9	+	Bimodal	Grooming

* Plus indicates presence; − indicates absence.

believe that they contain mechanoreceptor neurons that function as proprioceptors, providing information on the amount of pressure the animal puts on the food object and thus ensuring that it does not break the setae. The chemosensory function of type 1 setae is not clear but might be gustatory.

Due to their position, curvature, and small size, the serrulate type 3 setae cannot be guard setae. They are more likely used for grooming the ventral side of the basis of maxilla 1, which they scrape every time these mouthparts pass each other. This explanation is consistent with previous studies on decapods in which serrulate setae have been found to be involved in grooming (Martin and Felgenhauer, 1986; Bauer, 1989, 1999; Nickell *et al.*, 1998), and the scale-like setules serve to remove debris.

The type 2 setae are also bimodal sensors, and their primary function is probably gustatory, as indicated by their many chemosensory cells and by the observation that the sensory cilia protrude through the terminal pore. This also indicates that even though type 1 and 3 setae may be chemosensory, the type 2 setae are probably the primary chemosensors of Mx2, and their mechanosensory function may again be proprioceptive.

The type 2 seta is the first decapod seta to be reported in which cilia protrude from a terminal pore. Terminal pores are rather common in decapod setae, but so far they have been studied only with SEM (Altner *et al.*, 1986; Pinn *et al.*, 1999; Garm and Høeg, 2000; Coelho and Rodrigues, 2001). This might fail to reveal protruding cilia, because the treatment during dehydration and critical-point drying may cause shrinkage of the soft tissue, thereby retracting the sensory cilia. Naked sensory cilia of presumed chemosensors of other crustaceans, *Hutchinsoniella macracantha* (Cephalocarida) and *Pachypygus gibber* (Copepoda), have been shown by TEM, and in the former case also by SEM, although the documentation is not of the highest quality (Hipeau-Jacquotte, 1986; Elofsson and Hessler, 1994). In both cases, these setae are suggested to be gustatory, but they differ structurally from what is described here for type 2 setae of *Palaemon adspersus* in that they are small (<30 μm), have a very thin cuticle, and are innervated by only two to three sensory cells. They are also presumed to be unimodal gustatory setae (no mechanosensory function) (Hipeau-Jacquotte, 1986; Elofsson and Hessler, 1994), which has also been suggested for setae of the amphipod *Anonyx lilljeborgi* (Steele and Steele, 1999).

The number and arrangement of the sheet cells resemble earlier reports from decapod setae (Wiese, 1976; Ball and Cowan, 1977; Hallberg *et al.*, 1992). The division into two types of sheet cells might have a functional explanation. In the mysid *Neomysis integer*, the sheet cells are arranged in populations, with each creating a separate part of the cuticle of the setae (Guse, 1980). Our results show a tendency toward an outer population of electron-dense cells and an inner population of electron-lucent cells, the latter sending cell extensions into the lumen of the seta. Although we have no direct proof, we suggest that the electron-dense cells form the basal part of the cuticle of the seta and the electron-lucent cells form the distal part. A projection of the innermost sheet cell that encircles the mechanosensory cells has not been reported before for any crustacean setae. We are not sure of the function of this arrangement, but it could help to anchor the sensory cells and thereby improve the transduction of the mechanosensory signal.

In all three types of setae, the arrangement of the cuticle is extremely complex, with the differentiation throughout the shaft giving the distal part as many as six distinct layers (EC, Cu2–Cu5, ML) and water-filled canals. This could indicate that the distal parts of these setae are experiencing great mechanical stress, which they overcome by having several kinds of cuticle with different mechanical properties. The highly specialized water-filled canals have not been reported before in crustacean setae. One functional explanation could be that some setae involved in handling food objects must be flexible in their distal parts. This means that the cuticle must be able to fold, stretch, or change volume. Having a water-filled canal system gives the tissue the capability of locally changing the volume by moving water. The opening to the exterior also makes it possible to change the volume of the entire canal system; however, the minute size of the opening may limit the speed of this process. As mentioned earlier, cross-sections of the distalmost part of the canal system are missing, and it is possible that the openings expand further distally. Some earlier studies found similar electron-lucent canals in the cuticle (Crouau, 1997; Matsuura and Nishida, 2000; Cate and Derby, 2002) but did not discuss them in detail, and no connection to the exterior was described.

The activity of maxilla 2 in *Palaemon adspersus* is very stereotypic. We never observed the Mx2 to mechanically influence or hold the food; it merely touched it frequently (3–5 Hz). This behavior supports the idea that some of the setae on the medial rims of basis 1 and 2 of maxilla 2 have gustatory properties like those proposed for maxilla 2 of other decapods (Schembri, 1982; Garm and Høeg, 2001). Mechanical functions of maxilla 2 are, however, described for these other decapods. In the anomurans *Munida sarsi* and *M. tenuimana*, the basis of maxilla 2 is additionally used to reorient small food objects (Garm and Høeg, 2001). In the hermit crab *Pagurus rubricatus*, the basis of maxilla 2 assists in filtering sediment before eating (Schembri, 1982). In the case of *Homarus gammarus*, maxilla 2 is described as having mechanical functions, but the observations are not very detailed (Barker and Gibson, 1977). In other decapods for which detailed observations of mouthpart movements have been made, no account is given for the movements of maxilla 2 (Hunt *et al.*, 1992; Stemhuis *et al.*, 1998; Johnston, 1999), but judging from the descriptions of the morphology and feeding behavior in general, the usage is likely to be similar to what we found for *P. adspersus*.

Acknowledgments

The authors gratefully acknowledge the excellent laboratory work done by Rita Wallén, Department of Cell and Organism Biology, University of Lund. We are very grateful to the staff of the Danmarks Akvarium, Copenhagen, who collected and kept the animals for us. Jens T. Høeg acknowledges grants from the Danish National Science Research Council for financial support.

Literature Cited

Altner, H., H. Hall, and I. Altner. 1986. Structural and functional properties of the mechanoreceptors and chemoreceptors in the anterior oesophageal sensilla of the crayfish, *Astacus astacus*. *Cell Tissue Res.* **244:** 537–547.

Altner, I., H. Hatt, and H. Altner. 1983. Structural properties of bimodal chemo- and mechanosensitive setae on the pereiopod chelae of the crayfish, *Austropotamobius torrentium*. *Cell Tissue Res.* **228:** 357–374.

Ball, E. E., and A. N. Cowan. 1977. Ultrastructure of the antennal sensilla of *Acetes* (Crustacea, Decapoda, Natantia, Sergestidea). *Philos. Trans. R. Soc. Lond. B* **227:** 429–457.

Barker, P., and R. Gibson. 1977. Observations on the feeding mechanism, structure of the gut, and digestive physiology of the European lobster *Homarus gammarus* (L.) (Decapoda: Nephropidea). *J. Exp. Mar. Biol. Ecol.* **26:** 297–324.

Bauer, R. T. 1989. Decapod crustacean grooming: functional morphology, adaptive value, and phylogenetic significance. Pp. 49–74 in *Crustacean Issues 6, Functional Morphology of Feeding and Grooming in Crustacea*, B. Felgenhauer, L. Watling, and A. B. Thistle, eds. A. A. Balkema, Rotterdam.

Bauer, R. T. 1999. Gill-cleaning mechanisms of a dendrobranchiate shrimp, *Rimapenaeus similis* (Decapoda, Penaeidae): description and experimental testing of function. *J. Morphol.* **242:** 125–139.

Boas, J. E. V. 1880. *Studier over Decapodernes Slægtsskabsforhold.*, Bianco Lunds Kgl. Hof-Bogtrykkeri, Copenhagen. Pp. 1–210.

Cate, H. S., and C. D. Derby. 2001. Morphology and distribution of setae on the antennules of the Caribbean spiny lobster *Panulirus argus* reveal new types of bimodal chemo-mechanosensilla. *Cell Tissue Res.* **304:** 439–454.

Cate, H. S., and C. D. Derby. 2002. Ultrastructure and physiology of the hooded sensillum, a bimodal chemo-mechanosensillum of lobsters. *J. Comp. Neurol.* **442:** 293–307.

Coelho, V. R., and S. A. Rodrigues. 2001. Trophic behaviour and functional morphology of the feeding appendages of the laomediid shrimp *Axianassa australis* (Crustacea: Decapoda: Thalassinidea). *J. Mar. Biol. Assoc. UK* **81:** 441–454.

Coelho, V. R., A. B. Williams, and S. A. Rodrigues. 2000. Trophic strategies and functional morphology of feeding appendages, with emphasis on setae of *Upogebia omissa* and *Pomatogebia operculata* (Decapoda: Thalassinidea: Upogebiidae). *Zool. J. Linn. Soc.* **130:** 567–602.

Crouau, Y. 1997. Comparison of crustacean and insect mechanoreceptive setae. *Int. J. Insect Morphol. Embryol.* **26:** 181–190.

Crouau, Y. 2001. Cellules méchanosensorielles des soies des Hexapodes, des Crustacés et des Myriapodes: une comparaison d'un point de vue phylogénétique. *Ann. Soc. Entomol. Fr.* **37:** 233–242.

Derby, C. D. 1989. Physiology of sensory neurons in morphologically identified cuticular sensilla of crustaceans. Pp. 27–48 in *Crustacean Issues 6, Functional Morphology of Feeding and Grooming in Crustacea*, B. Felgenhauer, L. Watling, and A. B. Thistle, eds. A. A. Balkema, Rotterdam.

Derby, C. D. 2000. Learning from spiny lobsters about chemosensory coding of mixtures. *Physiol. Behav.* **69:** 203–209.

Elofsson, R., and R. R. Hessler. 1994. Sensory structures associated with the body cuticle of *Hutchinsoniella macracantha* (Cephalocarida). *J. Crustac. Biol.* **14:** 454–462.

Garm, A., and J. T. Høeg. 2000. Functional mouthpart morphology of the squat lobster *Munida sarsi*, with comparison to other anomurans. *Mar. Biol.* **137:** 123–138.

Garm, A., and J. T. Høeg. 2001. Function and functional groupings of the complex mouth apparatus of the squat lobsters *Munida sarsi* Huus and *M. tenuimana* G. O. Sars (Crustacea: Decapoda). *Biol. Bull.* **200:** 281–297.

Gleeson, R. A., L. M. McDowell, and H. C. Aldrich. 1996. Structure of the aesthetasc (olfactory) sensilla of the blue crab, *Callinectes sapidus*: transformations as a function of salinity. *Cell Tissue Res.* **284:** 279–288.

Goldman, J. A., and M. A. R. Koehl. 2001. Fluid dynamic design of lobster olfactory organs: high speed kinematic analysis of antennule flicking by *Panulirus argus*. *Chem. Senses* **6:** 385–398.

Guse, G. W. 1980. Development of antennal sensilla during moulting in *Neomysis integer* (Leach) (Crustacea, Mysidacea). *Protoplasma* **105:** 53–67.

Hallberg, E., and B. S. Hansson. 1999. Arthropod sensilla: morphology and phylogenetic considerations. *Microsc. Res. Tech.* **47:** 428–439.

Hallberg, E., K. U. I. Johansson, and R. Elofson. 1992. The aesthetasc concept: structural variations of putative olfactory receptor cell complexes in Crustacea. *Microsc. Res. Tech.* **22:** 325–335.

Hallberg, E., K. U. I. Johansson, and R. Wallén. 1997. Olfactory sensilla in crustaceans: morphology, sexual dimorphism, and distribution patterns. *Int. J. Insect Morphol. Embryol.* **26:** 173–180.

Heinisch, P., and K. Wiese. 1987. Sensitivity to movement and vibration of water in the North Sea shrimp *Crangon crangon* (L.). *J. Crustac. Biol.* **7:** 401–413.

Hipeau-Jacquotte, R. 1986. A new cephalic type of presumed sense organ with naked dendritic ends in the atypical male of the parasitic copepod *Pachypygus gibber* (Crustacea). *Cell Tissue Res.* **245:** 29–35.

Hunt, M. J., H. Winsor, and C. G. Alexander. 1992. Feeding by the penaeid prawns: the role of the anterior mouthparts. *J. Exp. Mar. Biol. Ecol.* **160:** 33–46.

Johnston, D. J. 1999. Functional morphology of the mouthparts and alimentary tract of the slipper lobster *Thenus orientalis* (Decapoda: Scyllaridae). *Mar. Freshw. Res.* **50:** 213–223.

Keil, T. A. 1998. The structure of integumental mechanoreceptors. Pp. 385–404 in *Microscopic Anatomy of Invertebrates, Insecta,* F. W. Harrison and M. E. Rice, eds. Wiley-Liss, New York.

Kunze, J., and D. Anderson. 1979. Functional morphology of the mouthparts and gastric mill in the hermit crabs *Clibanarius taenitua* (Milne Edwards), *Clibanarius virescens* (Krauss), *Paguristes squamosus* McCulloch and *Dardanus setifer* (Milne-Edwards) (Anomura: Paguridea). *Aust. J. Mar. Freshw. Res.* **30:** 683–722.

Lavalli, K. L., and J. R. Factor. 1992. Functional morphology of the mouthparts of juvenile lobsters, *Homarus americanus* (Decapoda: Nephropidae), and comparison with the larval stages. *J. Crustac. Biol.* **12:** 467–510.

Martin, J. W., and B. W. Felgenhauer. 1986. Grooming behaviour and the morphology of grooming appendages in the endemic South American crab genus *Aegla* (Decapoda, Anomura, Aeglidea). *J. Zool. Lond.* **209:** 213–224.

Matsuura, H., and S. Nishida. 2000. Fine structure of the "button setae" in the deep-sea pelagic copepods of the genus *Euaugaptilus* (Calanoida: Augaptilidae). *Mar. Biol.* **137:** 339–345.

Nickell, L. A., J. A. Atkinson, and E. H. Pinn. 1998. Morphology of thalassinidean (Crustacea: Decapoda) mouthparts and pereiopods in relation to feeding, ecology and grooming. *J. Nat. Hist.* **32:** 733–761.

Paffenhöfer, G. A., and P. A. Loyd. 1999. Ultrastructure of the setae of the maxilliped of the marine planktonic copepod *Temora stylifera*. *Mar. Ecol. Prog. Ser.* **178:** 101–107.

Palfenhöfer, G. A., and P. A. Loyd. 2000. Ultrastructure of cephalic appendages setae of marine planktonic copepods. *Mar. Ecol. Prog. Ser.* **203:** 171–180.

Pinn, E. H., L. A. Nickell, A. Rogerson, and J. A. Atkinson. 1999. Comparison of the mouthpart setal fringes of seven species of mud-shrimps (Crustacea: Decapoda: Thalassinidea). *J. Nat. Hist.* **33:** 1461–1485.

Robberts, M. H. 1968. Functional morphology of the mouth parts of the hermit crab, *Pagurus longicarpus* and *Pagurus pollicaris*. *Chesapeake Sci.* **9:** 9–20.

Schembri, P. J. 1982. Functional morphology of the mouthparts and associated structures of *Pagurus rubricatus* (Crustacea: Decapoda: Anomura) with special reference to feeding and grooming. *Zoomorphology* **101:** 17–38.

Schmidt, M., and W. Gnatzy. 1984. Are the funnel-canal organs the 'campaniform sensilla' of the shore crab *Carcinus maenas* (Decapoda: Crustacea)? II. Ultrastructure. *Cell Tissue Res.* **237:** 81–97.

Steele, V. J., and D. H. Steele. 1999. Cellular organization and fine structure of type II microtrich sensilla in gammaridean amphipods (Crustacea). *Can. J. Zool.* **77:** 88–107.

Steinbrecht, R. A. 1997. Pore structure in insect olfatory sensilla: a review of data and concepts. *Int. J. Insect Morphol. Embryol.* **26:** 229–245.

Steinbrecht, R. A. 1998. Bimodal thermo- and hygrosensitive sensilla. Pp. 405–422 in *Microscopic Anatomy of Invertebrates, Insecta,* F. W. Harrison and M. E. Rice, eds. Wiley-Liss, New York.

Stemhuis, E. J., B. Dauwe, and J. J. Videler. 1998. How to bite the dust: morphology, motion pattern and function of the feeding appendages of the deposit-feeding thalassinid shrimp *Callianassa subterranea*. *Mar. Biol.* **132:** 43–58.

Steullet, P., and C. D. Derby. 1997. Coding of blend ratios of binary mixtures by olfactory neurons in the Florida spiny lobster, *Panulirus argus*. *J. Comp. Physiol. A* **180:** 123–135.

Steullet, P., H. S. Cate, and C. D. Derby. 2000a. A spatiotemporal wave of turnover and functional maturation of olfactory receptor neurons in the spiny lobster *Panulirus argus*. *J. Neurosci.* **20:** 3282–3294.

Steullet, P., H. S. Cate, W. C. Michel, and C. D. Derby. 2000b. Functional units of a compound nose: aesthetasc sensilla house similar populations of olfactory receptor neurons on the crustacean antennule. *J. Comp. Neurol.* **418:** 270–280.

Wiese, K. 1976. Mechanoreceptors for near-field water displacement in crayfish. *J. Neurophysiol.* **39:** 816–833.

Reference: *Biol. Bull.* **204**: 138–145. (April 2003)

Variation in Skeletal Microstructure of the Coral *Galaxea fascicularis:* Effects of an Aquarium Environment and Preparatory Techniques

PETA L. CLODE AND ALAN T. MARSHALL*

Analytical Electron Microscopy Laboratory, Department of Zoology, La Trobe University, Melbourne, Victoria 3086, Australia

Abstract. To compare the crystalline microstructure of exsert septa, polyps of the scleractinian coral *Galaxea fascicularis* were sampled from shallow reef flat colonies, from colonies living at a depth of 9 m, and from colonies kept in a closed-circuit aquarium. Septal crystal structure and orientation was markedly different between corals in the field and in aquaria. In samples collected from deep water, acicular crystals were composed of conglomerates of finer crystals, and skeletal filling was considerably reduced when compared with samples collected from shallow water. Comparisons were also made between septa prepared in sodium hypochlorite (commercial bleach), sodium hydroxide (NaOH), hydrogen peroxide (H_2O_2), and distilled water (dH_2O). Commercial bleach was the most effective solvent for tissue dissolution in investigations of skeletal structure. Samples prepared in NaOH commonly displayed crystalline artefacts, while the use of dH_2O and H_2O_2 was labor intensive and often resulted in unclean preparations. Fusiform crystals were seen only on *G. fascicularis* septa prepared in bleach and on *Acropora formosa* axial corallites prepared in either bleach or dH_2O. We suggest that the mechanical agitation and additional washing necessary for samples prepared in dH_2O, NaOH, or H_2O_2 resulted in the loss of fusiform crystals from these preparations.

Introduction

The use of aquaria to grow and maintain corals for scientific experimentation has become increasingly popular (see Carlson, 1999) and, with the degradation of coral reefs across the globe, it may soon be necessary for experimental corals to be constantly maintained in this way. In the past, keeping scleractinian corals alive under artificial conditions for long periods of time was exceedingly difficult, but advances in filtration, lighting, and water systems have made the propagation of these corals in aquaria much easier. However, little is known about the impact of artificial environments upon scleractinian coral calcification, behavior, growth, and reproduction, with direct comparisons between field and aquarium-maintained corals rare.

Studies of the crystalline and overall skeletal structure of scleractinian corals necessitate the removal of the surrounding epithelia to visualize the $CaCO_3$ skeleton underneath. Many treatments have been used to dissolve the epithelial tissue, including H_2O_2 (Jell, 1974), freshwater (Wainwright, 1963; Johnston, 1979), NaOH (Johnston, 1979; Isa, 1986), and commercial bleach (sodium hypochlorite) (Sorauf, 1972, 1974; Gladfelter, 1982, 1983; Brown *et al.*, 1983; Hidaka, 1988, 1991a, b; LeTissier, 1988, 1990, 1991; Constantz, 1989; Hidaka and Shirasaka, 1992). Unfortunately, the possible effects of these chemicals upon the underlying crystal structure have been ignored. Comparisons between studies are complicated by the variety of methods used to prepare samples and by the broad range of species studied.

In this study, we describe differences in crystal structure, orientation, and patterns of deposition between corals collected from field conditions and closed-circuit aquaria. In addition, we evaluate and compare the suitability of several chemical treatments commonly used to prepare scleractinian coral skeletons for examination with a scanning electron microscope.

Received 6 June 2002; accepted 31 January 2003.

* To whom correspondence should be addressed. E-mail: zooam@zoo.latrobe.edu.au

Materials and Methods

Collection and maintenance of Galaxea fascicularis

Colonies of brown and green color morphs of the scleractinian coral *Galaxea fascicularis* were collected at Heron Reef in the Capricorn Bunker Group of the Great Barrier Reef, Australia. Morphs of both colors were obtained at low tide from the reef flat; brown morphs only were collected by scuba divers from a depth of 9 m.

Specimens to be maintained under field conditions were transported in buckets of seawater to Heron Island Research Station, where they were kept in well-aerated, flow-through aquaria in natural seawater at 24–25 °C. Colonies collected from the reef flat were kept in outdoor, sunlit aquaria, with light levels equivalent to those experienced on the reef flat; colonies collected at depth were kept in shaded aquaria, with light levels similar to those at a depth of 9 m in the field.

Specimens to be maintained in an aquarium environment were sealed into plastic bags with a small amount of seawater, and the bags were put into small insulated boxes for transport to La Trobe University, Melbourne. These colonies were kept in a closed-circuit marine aquarium. The aquarium contained natural, well-aerated seawater at 25 °C and was subjected to an illumination cycle of 14 h of light and 10 h of darkness; the light was provided by metal halogen lamps (photosynthetic photon flux density 150 μmol photons m^{-2} s^{-1}). Conditions in the aquarium were monitored regularly: 25% of the water was changed twice weekly; pH was kept between 8.1 and 8.2 and salinity from 900 to 1200 mosmol kg^{-1}. Corals were fed a mixture of brine shrimp and fish weekly.

Sample preparation

Colonies were allowed to recover for at least 2 days after collection before being used in experiments. Individual polyps of *G. fascicularis* were separated from colonies (see Marshall and Wright, 1991) at 1200 h. Five polyps were placed in either commercial bleach (12% NaOCl) or NaOH (5 N) at 60 °C for 30 min; H_2O_2 (10%) for 3 h at room temperature (RT); or dH_2O at RT for at least 24 h, to remove the overlying soft tissue. The resultant corallites were rinsed well in running water and then several times in dH_2O. Any soft tissue remaining upon the exsert septa was removed by agitation and pipetting of dH_2O onto the sample. The corallites were then dried at 60 °C for 24 h. Aquarium-maintained corals were kept in the closed-circuit aquarium at La Trobe University for 26 weeks before polyps (n = 5) from each of two colonies were sampled at 1200 h and prepared in either bleach, NaOH, or dH_2O.

Electron microscopy

Exsert septa were removed from *G. fascicularis* corallites under a dissecting microscope and mounted flat using carbon tape. Samples (n = 50+) were coated with 5 nm platinum and previewed in a JEOL JSM 840A scanning electron microscope at 10 kV. High-resolution imaging was subsequently conducted on a JEOL 6340-F field emission scanning electron microscope at 2 kV. In addition to being mounted flat, septa from colonies growing in shallow field conditions (n = 5) and the aquarium (n = 9) were secured upright in an appropriate substage, with indium foil placed between the sample and the stage to improve conductivity and provide flexible compression. Samples were coated with platinum, then fractured to provide a cross-sectional area. Following fracturing, the samples were re-coated and viewed by high-resolution field emission scanning electron microscopy (FESEM).

Acropora formosa

White-tipped branches (which possess few symbiotic zooxanthellae) were sampled from *A. formosa* colonies at low tide from Heron Reef at 1200 h and immediately placed into bleach (n = 5) for 30 min or into dH_2O at ambient temperature (n = 5) for 24 h, for investigation of the axial corallite. Branches were washed in running water for 24 h before being rinsed in dH_2O and dried at 60 °C for 24 h. Branch tips were secured upright in hollow stubs, using partially polymerized araldite, so that the axial corallite extended about 3 mm above the upper surface of the stub. Polymerization was completed at 60 °C for a further 30 h. Conductivity of the corallites was improved by overlaying the araldite with conductive silver epoxy (ProSciTech) and coating with 10 nm platinum. Samples were viewed in a JEOL JSM 6340-F field emission scanning electron microscope at 1 kV or 2 kV.

Results

Comparison of field and aquarium samples

Marked differences in crystal orientation and deposition were detected between septa from polyps collected from their natural environment (shallow reef flat) and those sampled from polyps that had been maintained in a closed-circuit aquarium for 26 weeks. When sampled from the natural reef environment, septa possessed acicular crystals that remained highly ordered and extended to the outer edge of the growing septa (Fig. 1A). In contrast, septa sampled from aquaria-maintained polyps had small, unordered crystals deposited with little uniformity (Fig. 1B). This pattern of unordered skeletal deposition extended to a depth of 1 $\pm$ 0.06 μm (n = 25). Little variation in this pattern of deposition was observed within or between colonies.

Structural features typically associated with normal *Galaxea fascicularis* septa, such as acicular and fusiform crystals and well-defined fasciculi (Fig. 2A), were rarely discerned on septa sampled from polyps maintained in the closed-circuit aquarium. Instead, much of the septal surface of aquarium-maintained polyps was covered with small (<100 nm in diameter) spherulitic crystals (Fig. 2B). *G. fascicularis* polyps sampled from the closed-circuit aquarium were also typically paler than corals living on the reef flat, and they appeared to have fewer symbiotic zooxanthellae, although this was not quantified.

In contrast, the crystal structure of septa from deep field-collected *G. fascicularis* colonies was only marginally different from that of septa from shallow field-collected colonies. Acicular crystals of septa sampled from colonies collected from the shallow reef flat appeared as solid, broad crystals tightly packed together (Fig. 3A). However, acicular crystals upon septa collected from deeper water tended to be composed of conglomerates of finer, elongated crystals that were loosely associated (Fig. 3B). This loose assembly gave the appearance of increased porosity, with skeletal filling somewhat reduced. Little structural difference in the other crystal types—nano, lamellar, and fusiform—was noted between septa taken from shallow reef-flat corals and those living in deeper water.

Septum length also varied between polyps from the two field conditions. Septa sampled from polyps growing at depth were considerably longer than those from corallites living on the shallow reef flat (results not shown). We are unsure whether this feature was related to depth or was simply natural morphological variation. No other structural differences were observed between septa sampled from corallites collected from the reef flat and from deeper water.

Chemical treatments

Commercial bleach was the best chemical treatment for digesting soft tissue from corallites of the scleractinian corals *G. fascicularis* and *A. formosa;* dissolution occurred in less than 30 min at 60 °C. Washing samples well in running water, followed by brief rinses in dH_2O, ensured that the septa on the resultant corallites were free of residual tissue (Fig. 4). No intensive cleaning or agitation was necessary. Skeletons prepared in bleach were rapidly cleaned, so the crystalline structure of the septa could be readily observed with SEM. All of the crystal types described by Clode and Marshall (2003) (nano, acicular, lamellar, and fusiform) were clearly observable upon septa prepared in this manner. An example of fusiform crystals is shown in Figure 5.

NaOH was also very effective in removing soft tissue from *G. fascicularis* corallites; tissue was rapidly digested at 60 °C. However, large, crystalline structures regularly observed on septa prepared in NaOH (Fig. 6), were never seen in samples prepared in any other chemical treatment; thus they are probably artefactual. The only way to prevent the appearance of such structures was to ensure that the corallites were washed well after treatment in NaOH, with additional agitation and washing of samples prior to drying. This resulted in septa free from crystalline artefacts. In such cases, nano, acicular, and lamellar crystals were all clearly visible upon the septal surface; however, fusiform crystals were never observed on septa prepared in this manner.

In contrast, the use of dH_2O to remove the overlying soft tissues from *G. fascicularis* septa was difficult, time consuming, and often left corallites unclean. The crystalline surface was masked by overlying material and thus could not be viewed with SEM. Furthermore, polyps immersed into dH_2O secreted excess mucus, which further complicated tissue removal. As a result, many *G. fascicularis* septa prepared in dH_2O were coated in an amorphous material of unknown composition, which completely obscured the crystalline structures underneath (Fig. 7). Clean septa free of tissue remnants and this coating could be obtained by extensive rinsing and pipetting of dH_2O onto the sample. Like septa prepared in NaOH, *G. fascicularis* septa prepared in dH_2O did not possess fusiform crystals.

The perforate nature of *A. formosa* skeletons made treatment with dH_2O much easier and more successful than it was for *G. fascicularis*. Although gentle agitation was necessary to completely remove the soft tissue overlying the axial corallite, the process was considerably less stringent than the rinsing protocol necessary to prepare *G. fascicularis* septa. *A. formosa* axial corallites prepared in dH_2O were clean and free of epithelial remnants following gentle agitation, and fusiform crystals were regularly observed along the primary septa extending into the calyx (Fig. 8).

Tissue dissolution by H_2O_2 was both difficult and highly ineffective (Fig. 9). *G. fascicularis* septa, despite being covered by only a thin layer of soft tissue, took several days to prepare, and the process was exceptionally tedious and labor intensive. Extensive additional agitation and washing was required to produce clean septa, so that the crystalline structure could be seen with SEM. With this treatment, like dH_2O, excessive secretion of mucus added to the difficulty of obtaining suitable preparations. All crystal types, except fusiform crystals, could be readily observed upon septa that had been adequately prepared in H_2O_2 and extensively cleaned with dH_2O.

Discussion

A comparison of the crystalline structure of exsert septa between colonies growing under aquarium conditions and natural, field conditions has revealed that drastic changes to crystal deposition and skeletal formation may occur in

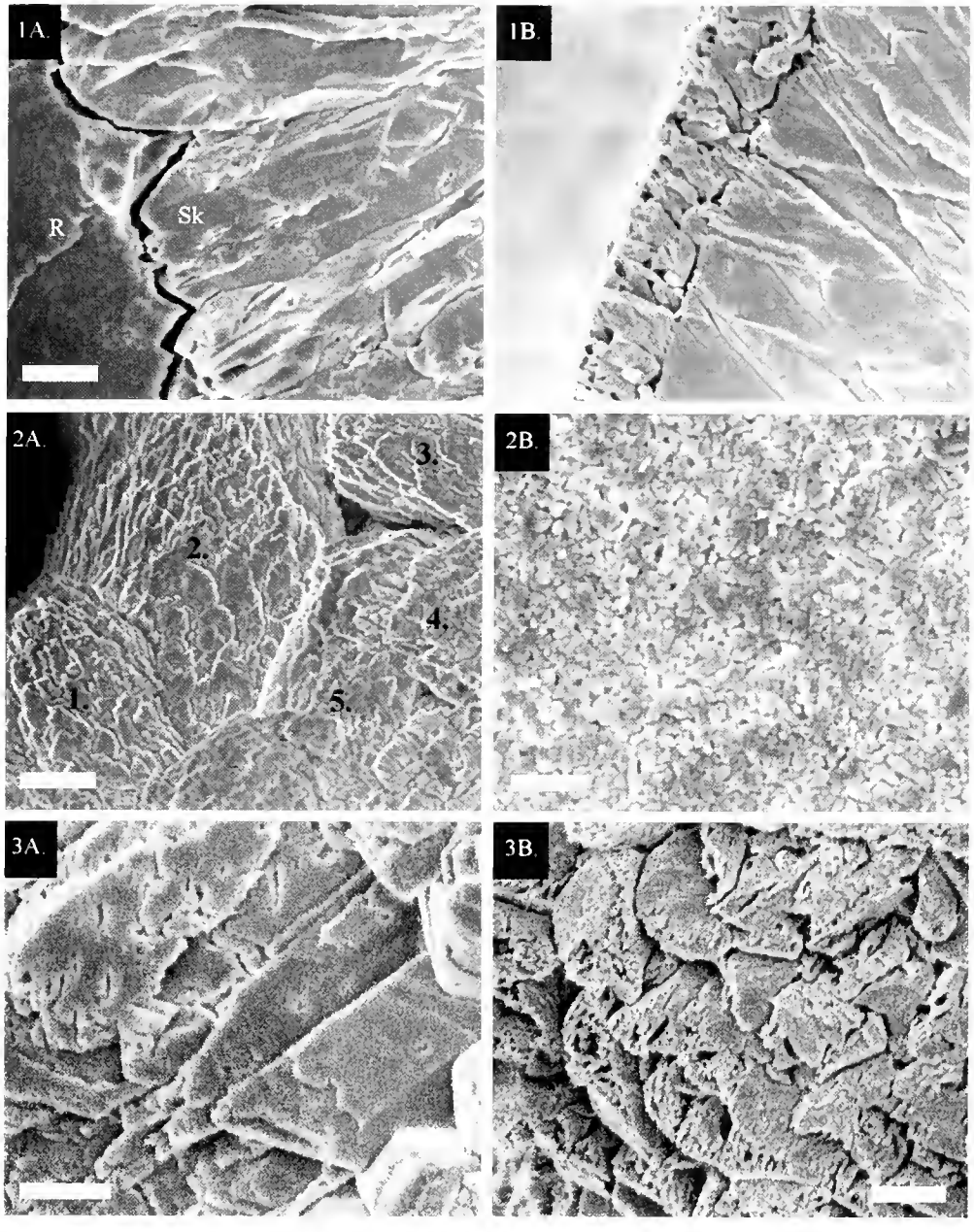

Figure 1. Electron micrographs of cross-fractured exsert septa from *Galaxea fascicularis* corallites sampled (A) directly from the reef flat; and (B) after 26 weeks in a closed-circuit aquarium. Mucus or tissue residue (R) can also be seen in (A) adjacent to the skeleton (Sk). Scale bars: A = 1 μm; B = 500 nm.

Figure 2. Electron micrographs of typical growth surfaces of *Galaxea fascicularis* exsert septa sampled (A) from the reef flat; and (B) after maintenance in a closed-circuit aquarium for 26 weeks. Scale bars: A = 500 nm; B = 300 nm. Distinct clusters of similarly oriented acicular crystals, known as fasciculi, are clearly evident in septa sampled from the reef flat (A; clusters numbered 1–5) but were not observed on septa sampled from the aquarium (B).

Figure 3. Electron micrographs detailing the different nature of acicular crystals at the growing edge of exsert septa of *Galaxea fascicularis* sampled (A) on the reef flat; and (B) at a depth of 9 m. Scale bars: A = 250 nm; B = 400 nm.

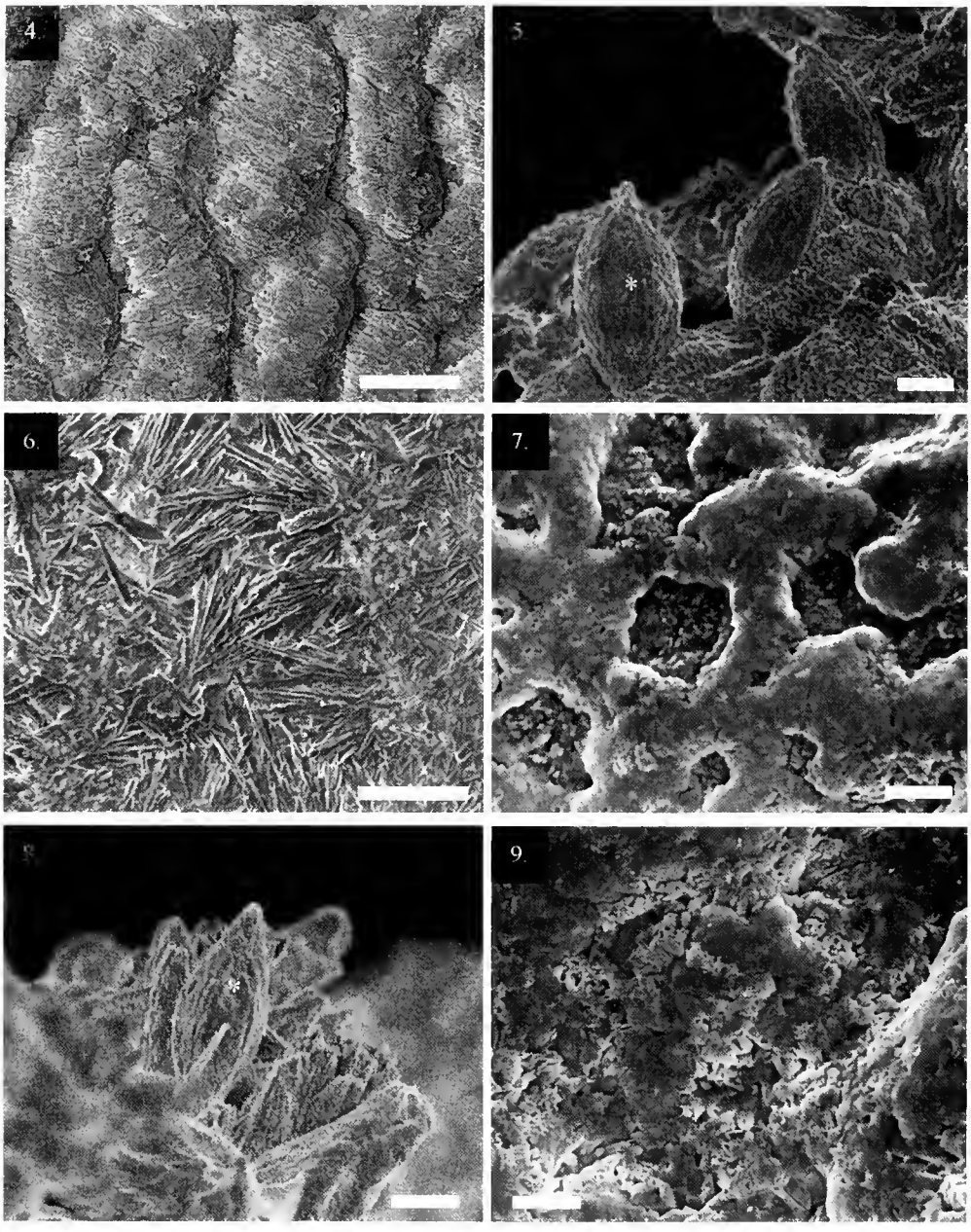

Figure 4. Electron micrograph detailing the crystalline structure of a *Galaxea fascicularis* exsert septum that was readily observed following tissue digestion in commercial bleach. Scale bar = 10 μm.

Figure 5. Electron micrograph of fusiform crystals (*) evident along the lateral edge of a *Galaxea fascicularis* exsert septum prepared in commercial bleach. Scale bar = 1 μm.

Figure 6. Electron micrograph of crystalline artefacts commonly observed on *Galaxea fascicularis* exsert septa prepared in NaOH. Scale bar = 1 μm.

Figure 7. Electron micrograph of amorphous remnants that regularly covered the crystalline surface of *Galaxea fascicularis* exsert septa prepared in distilled water. Scale bar = 5 μm.

Figure 8. Electron micrograph of an *Acropora formosa* axial corallite prepared in distilled water, showing fusiform crystals (*) upon a primary septum. Scale bar = 1 μm.

Figure 9. Electron micrograph of tissue-like remnants that regularly remained attached to *Galaxea fascicularis* exsert septa after preparation in hydrogen peroxide. Scale bar = 5 μm.

corals maintained for long periods in closed-circuit aquaria. In addition, preparing such samples in commercial bleach may result in the complete loss of fusiform crystals from the skeletal surface.

Comparison of field and aquarium samples

It is evident that calcification in scleractinian corals can be severely affected by changes in the surrounding environment. Much recent attention has focused upon how major changes in environmental conditions such as atmospheric CO_2 levels and water temperature affect coral calcification (Done, 1999; Kleypas *et al.*, 1999; Pittock, 1999). Our results indicate that even relatively small modifications to the surrounding environment, particularly those that are artificially generated, may significantly alter the pattern of crystal deposition and the rate of calcification in captive corals. Variability in the growth rate of aquarium-kept corals may be influenced by, and dependent upon, what are often considered minor details, such as water quality and movement, food availability (Mortensen, 2001), and subtle changes in light intensity and wavelength (see Carlson, 1999).

Acicular crystal growth on the exsert septa of *Galaxea fascicularis* is probably continuous, as evidenced by their lack of crystal substructure (Clode and Marshall, 2003). However, septa sampled from aquarium-maintained polyps did not exhibit this pattern of crystal deposition. Instead, small, randomly oriented, spherulitic crystals covered the entire septal surface. As a result of the discontinuous, unordered growth, skeletal porosity was likely to increase. When compared with those growing in their natural environment, a variety of scleractinian corals show a significant reduction in skeletal porosity following containment within an aquarium (see Carlson, 1999).

The fact that the region of disoriented growth in *G. fascicularis* extends to an approximate depth of only 1 μm in septa sampled from corals kept in aquaria for 26 weeks suggests that calcification and growth rates of these corals may be significantly reduced, with drastic changes in calcification patterns also expected. In many branching scleractinian corals, gross colony morphology changes dramatically following maintenance in aquaria (see Carlson, 1999), with colonies developing unnatural morphological traits.

In addition to directly affecting the physical processes of coral calcification, suboptimal conditions may also invoke changes indirectly through stress responses. Colonies maintained under aquarium conditions appeared to lose a large proportion of their symbiotic algae. Loss of zooxanthellae from gastrodermal cells in times of stress is common to many zooxanthellate scleractinian corals (Hoegh-Guldberg and Smith, 1989; Brown *et al.*, 1995), and calcification rates can be greatly reduced through the induced expulsion of these symbionts (Goreau, 1959). Biomineralization anomalies also occur in symbiont-bearing foraminifera exposed to stressful environmental conditions (Toler and Hallock, 1998).

These results raise concerns about the validity of experiments, particularly those investigating calcification rates, *etc.*, with corals kept in closed-circuit aquaria, where artificially modified or unnatural environments may have induced atypical patterns of calcification. Marked differences in skeletal organization between corals sampled from natural and artificial environments highlight the importance of accurately imitating natural conditions in closed-circuit aquaria where experimental corals are to be maintained.

Comparison of the crystal structure of corals living under shallow- and deep-water field conditions revealed only minor differences in septal microstructure. The principal difference in crystal structure between polyps from the two different water depths was that acicular crystals of samples from 9 m were much more finely structured and appeared to have a higher porosity than their counterparts from the reef flat. Skeletal "filling," or secondary thickening (Gladfelter, 1982), was also clearly reduced in septa sampled from corallites collected from the deeper water. A reduced calcification rate because of lower light intensities would account for the differences between septa sampled from the two environments. Further research into the calcification rates of such colonies would help to clarify the cause of the differences, as would an accurate determination of porosity.

Chemical treatments

Despite large variation in skeletal preparatory methods, commercial bleach has been the solvent used most often for digestion of scleractinian coral tissue. Our results confirm that commercial bleach is highly effective in dissolving the soft tissue of the corals *G. fascicularis* and *A. formosa*, particularly when it is heated to 60 °C. Excellent skeletal preparations for SEM can be rapidly obtained with relatively little effort and without discernible deleterious effects upon skeletal microstructure, even if corallites are incubated in bleach for up to 12 h (P. Clode, S. Howe, and A. Marshall, La Trobe University, unpubl. data).

We initially believed that the fusiform crystals we saw on *G. fascicularis* corallites prepared in bleach were artefacts, because they were not present in other preparations. However, the finding that *A. formosa* axial corallites prepared in dH_2O also possessed these crystals ruled out the possibility of a chemically induced origin. We conclude that the additional cleaning of corallites with jets of water and mechanical agitation, which was necessary for corallites prepared in either NaOH, H_2O_2, or dH_2O, removed the fusiform crystals from exposed growing edges.

In *A. formosa* corallites prepared in both bleach and dH_2O, fusiform crystals were observed along the primary septa extending into the calyx, areas protected by the wall of the corallite. Furthermore, the widely spaced skeletal elements and highly perforate nature of the skeleton, which is typical of white-tipped *A. formosa* axial corallites (Oliver, 1984), made the removal of soft tissue easier and the need for extensive cleaning unnecessary. Fusiform crystals observed on axial spines of *Acropora cervicornis* (Gladfelter, 1982) were not seen in *A. formosa*. It is possible that the fusiform crystals on these exposed areas were lost during preparation.

The suitability of NaOH for dissolving soft tissue from *G. fascicularis* corallites is unquestioned, with activity at 60 °C highly effective. However, generation of artefacts and the loss of fusiform crystals from skeletal preparations, which was also noted by Isa (1986) in *Acropora hebes* axial corallites prepared in NaOH, limits the applications of this chemical for coral skeleton preparation.

The use of dH_2O to remove soft tissue was thought to be ideal for maintaining crystal structure, due to the low water solubility of $CaCO_3$ and the unlikelihood of artefact generation. However, we found the method to be time-consuming and difficult, and thus impractical for use with many species of corals. For perforate corals such as *A. formosa*, dH_2O can be effectively applied to remove much of the soft tissue. However, without extensive rinsing, many *G. fascicularis* septa prepared in dH_2O remained coated in a film of unknown material that completely obscured the skeletal structure beneath. The lack of any discernible features in this film suggest that it was not epithelial in nature, but was perhaps either a thin layer of mucus that was subsequently removed in well-washed preparations or a remnant of the mesogloea, as suggested by Hidaka (1991a).

Similarly, the use of H_2O_2 to investigate the skeletal microstructure of *G. fascicularis* exsert septa was inappropriate and labor intensive. As with dH_2O and NaOH, additional cleaning and agitation of samples resulted in the loss of fusiform crystals from the skeletal surface. An additional disadvantage is that H_2O_2 may begin to actively dissolve the $CaCO_3$ skeleton of scleractinian corals (Mitsuguchi *et al.*, 2001).

Our investigations provide an overview of chemical treatments and their suitability for dissolving soft tissue from coral skeleton. We have found that the suitability of these chemicals is species-specific. For example, NaOH is not suitable for use with the azooxanthellate scleractinian corals *Tubastrea faulkneri* and *Dendrophyllia* sp. or the zooxanthellate scleractinian coral *Seriatopora hystrix* (A. Marshall and P. Clode, La Trobe University, unpubl. data). These findings may help to explain why several different techniques have been used in the past and may also account for some of the contradictory results that can be found in the literature on the skeletal and crystal structure of corals.

Acknowledgments

This research was conducted with the assistance of an Australian Research Council grant to ATM. All samples were collected under Great Barrier Reef Marine Park Authority permits to ATM. We wish to thank the staff at Heron Island Research Station for their services and Ms. Collette Bagnato for her assistance with sample collection.

Literature Cited

Brown, B. E., R. Hewit, and M. D. LeTissier. 1983. The nature and construction of skeletal spines in *Pocillopora damicornis* (L.). *Coral Reefs* **2:** 81–89.

Brown, B. E., M. D. A. LeTissier, and J. C. Bythell. 1995. Mechanisms of bleaching deduced from histological studies of reef corals sampled during a natural bleaching event. *Mar. Biol.* **122:** 655–663.

Carlson, B. A. 1999. Organism responses to rapid change: what aquaria can tell us about nature. *Am. Zool.* **39:** 44–55.

Clode, P. L., and A. T. Marshall. 2003. Skeletal microstructure of *Galaxea fascicularis* exsert septa: a high-resolution SEM study. *Biol. Bull.* **204:** 146–154.

Constantz, B. R. 1989. Skeletal organization in Caribbean *Acropora* spp. (Lamarck). Pp. 175–199 in *Origin, Evolution and Modern Aspects of Biomineralization in Plants and Animals*, R. E. Crick, ed. Plenum Press, New York.

Done, T. J. 1999. Coral community adaptability to environmental change at the scales of regions, reefs and reef zones. *Am. Zool.* **39:** 66–79.

Gladfelter, E. H. 1982. Skeletal development in *Acropora cervicornis* I. Patterns of calcium carbonate accretion in the axial corallite. *Coral Reefs* **1:** 45–51.

Gladfelter, E. H. 1983. Skeletal development in *Acropora cervicornis* II: Diel patterns of calcium carbonate accretion. *Coral Reefs* **2:** 91–100.

Goreau, T. F. 1959. The physiology of skeleton formation in corals. I. A method for measuring the rate of calcium deposition by corals under different conditions. *Biol. Bull.* **116:** 59–75.

Hidaka, M. 1988. Surface structure of skeletons of the coral *Galaxea fascicularis* formed under different light conditions. Pp. 95–100 in *Proceedings of the Sixth International Coral Reef Symposium*, Vol. 3, J. H. Choat *et al.*, eds. 6th International Coral Reef Symposium Executive Committee, Townsville, Australia.

Hidaka, M. 1991a. Deposition of fusiform crystals without apparent diurnal rhythm at the growing edge of septa of the coral *Galaxea fascicularis*. *Coral Reefs* **10:** 41–45.

Hidaka, M. 1991b. Fusiform and needle-shaped crystals found on the skeleton of a coral, *Galaxea fascicularis*. Pp. 139–143 in *Mechanisms and Phylogeny of Mineralization in Biological Systems*, S. Suga and H. Nakahara, eds. Springer Verlag, Tokyo.

Hidaka, M., and S. Shirasaka. 1992. Mechanism of phototropism in young corallites of the coral *Galaxea fascicularis*. *J. Exp. Mar. Biol. Ecol.* **157:** 69–77.

Hoegh-Guldberg, O., and G. J. Smith. 1989. The effect of sudden changes in temperature, light and salinity on the pollution density and export of zooxanthellae from the reef corals *Stylophora pistillata* Esper and *Seriatopora hystrix* Dana. *J. Exp. Mar. Biol. Ecol.* **129:** 279–303.

Isa, Y. 1986. An electron microscope study on the mineralization of the skeleton of the staghorn coral *Acropora hebes*. *Mar. Biol.* **93:** 91–101.

Jell, J. S. 1974. The microstructure of some scleractinian corals. Pp. 301–320 in *Proceedings of the Second International Coral Reef Symposium*, A. M. Cameron, ed. Great Barrier Reef Committee, Brisbane, Australia.

Johnston, I. S. 1979. The organization of a structural organic matrix within the skeleton of a reef-building coral. *Scanning Electron Microsc.* **1979 II:** 421–431.

Kleypas, J. A., R. W. Buddemeier, D. Archer, J.-P. Gattuso, C. Langdon, and B. N. Opdyke. 1999. Geochemical consequences of increased atmospheric carbon dioxide on coral reefs. *Science* **284:** 118–119.

LeTissier, M. D. 1988. Diurnal patterns of skeleton formation in *Pocillopora damicornis* (Linnaeus). *Coral Reefs* **7:** 81–88.

LeTissier, M. D'A. A. 1990. The ultrastructure of the skeleton and skeletogenic tissues of the temperate coral *Caryophyllia smithi*. *J. Mar. Biol. Assoc. UK* **70:** 295–310.

LeTissier, M. D'A. A. 1991. The nature of the skeleton and skeletogenic tissues in the Cnidaria. *Hydrobiologia* **216/217:** 397–402.

Marshall, A. T., and A. Wright. 1991. Freeze-substitution of scleractinian coral for confocal scanning laser microscopy and X-ray microanalysis. *J. Microsc.* **162:** 341–354.

Mitsuguchi, T., T. Uchida, E. Matsumoto, P. Isdale, and T. Kawana. 2001. Variations in Mg/Ca, Na/Ca, and Sr/Ca ratios of coral skeletons with chemical treatments: implications for carbonate geochemistry. *Geochim. Cosmochim. Acta* **65:** 2865–2874.

Mortensen, P. B. 2001. Aquarium observations on the deepwater coral *Lophelia pertusa* (L., 1758) (Scleractinia) and selected associated invertebrates. *Ophelia* **54:** 83–104.

Oliver, J. K. 1984. Intra-colony variation in the growth of *Acropora formosa:* extension rates and skeletal structure of white (zooxanthellae-free) and brown-tipped branches. *Coral Reefs* **3:** 139–147.

Pittock, A. B. 1999. Coral reefs and environmental change: adaptation to what? *Am. Zool.* **39:** 10–29.

Sorauf, J. E. 1972. Skeletal microstructure and microarchitecture in Scleractinia (Coelenterata). *Palaeontology* **15:** 11–23.

Sorauf, J. E. 1974. Observations on microstructure and biocrystallization in coelenterates. *Biomineralization* **7:** 37–55.

Toler, S. K., and P. Hallock. 1998. Shell malformation in stressed *Amphistegina* populations: relation to biomineralization and paleoenvironmental potential. *Mar. Micropaleontol.* **34:** 107–115.

Wainwright, S. A. 1963. Skeletal organisation in the coral, *Pocillopora damicornis*. *Q. J. Microsc. Sci.* **104:** 169–183.

Reference: *Biol. Bull.* **204:** 146–154 (April 2003)

Skeletal Microstructure of *Galaxea fascicularis* Exsert Septa: A High-Resolution SEM Study

PETA L. CLODE AND ALAN T. MARSHALL*

Analytical Electron Microscopy Laboratory, Department of Zoology, La Trobe University, Melbourne, Victoria 3086, Australia

Abstract. The deposition of four crystal types at the growth surface of the septa of several color morphs of the coral *Galaxea fascicularis* was investigated over a 24-h period. Results suggest that nanocrystals, on denticles at the apices of exsert septa, may be the surface manifestation of centers of calcification. These crystals were also found on the septa of the axial corallite of *Acropora formosa*. The deposition of nanocrystals appears to be independent of diurnal rhythms. Internally and proximal to the septal apices, distinct clusters of polycrystalline fibers originate from centers of calcification and form fanlike fascicles. Upon these fascicles, acicular crystals grow and extend to form the visible fasciculi at the skeletal surface. Deposition of aragonitic fusiform crystals in both *G. fascicularis* and *A. formosa* occurs without diurnal rhythm. Nucleation of fusiform crystals appears to be independent of centers of calcification and may occur by secondary nucleation. Formation of semi-solid masses by fusiform crystals suggests that the crystals may play a structural role in septal extension. Lamellar crystals, which have not been reported as a component of scleractinian coral skeletons before, possess distinct layers of polyhedral plates, although these layers also do not appear to be associated with daily growth increments. The relationship of lamellar crystals to other components of the scleractinian coral skeleton and their involvement in skeletal growth is unknown.

Introduction

The microstructural components of the $CaCO_3$ skeleton from a wide range of scleractinian corals have been well documented (see Wainwright, 1963; Vahl, 1966; Sorauf, 1970, 1972, 1974, 1980; Wise, 1970, 1972; Chevalier, 1974; Jell, 1974; Constantz, 1986, 1989). However, descriptions of skeletal microstructure are inconsistent, reflecting differences in both interpretation and structural variation. The relationships between the various crystalline microstructures found on the surface and within the interior of the skeleton are not fully understood, although this is fundamental to an understanding of the origin of crystal formation, deposition and growth.

The basic structure of the coral polyp is a tubelike skeleton, or corallum, divided by longitudinal and horizontal partitions. Sitting in the top of this tube is the living polyp. The key elements of the corallum are the longitudinal divisions, the septa, which are joined laterally by the wall (theca) of the corallum. Those septa that extend above the top of the theca are referred to as exsert septa. Exsert septa are one of the primary sites of $CaCO_3$ deposition and skeletal extension in the scleractinian coral *Galaxea fascicularis* (Marshall and Wright, 1998). These elongated septa protrude upward from the wall of the corallite and encircle the oral disc (see Fig. 1). This arrangement allows for individual septa to be easily detached from the corallite, without significant damage, for subsequent investigation of the crystalline microstructure with scanning electron microscopy (SEM).

The internal structure of the coral skeleton has been primarily studied by light microscopy. It was established early (Ogilvie, 1896) that the internal structure of septa is composed of arrays of vertically elongated centers of calcification from which polycrystalline fibers extend radially to form fascicles. These fanlike systems are regarded as the basic building blocks of the skeleton. On the external surface, two major crystal types have been described. These are clusters of acicular crystals that form fasciculi and spindle-shaped crystals referred to as fusiform crystals. The latter have been suggested to be deposited with a diel periodicity and to be the site of nucleation of fasciculi (Gladfelter,

Received 6 June 2002; accepted 31 Jan 2003.
*To whom correspondence should be addressed. E-mail: zooam@zoo.latrobe.edu.au

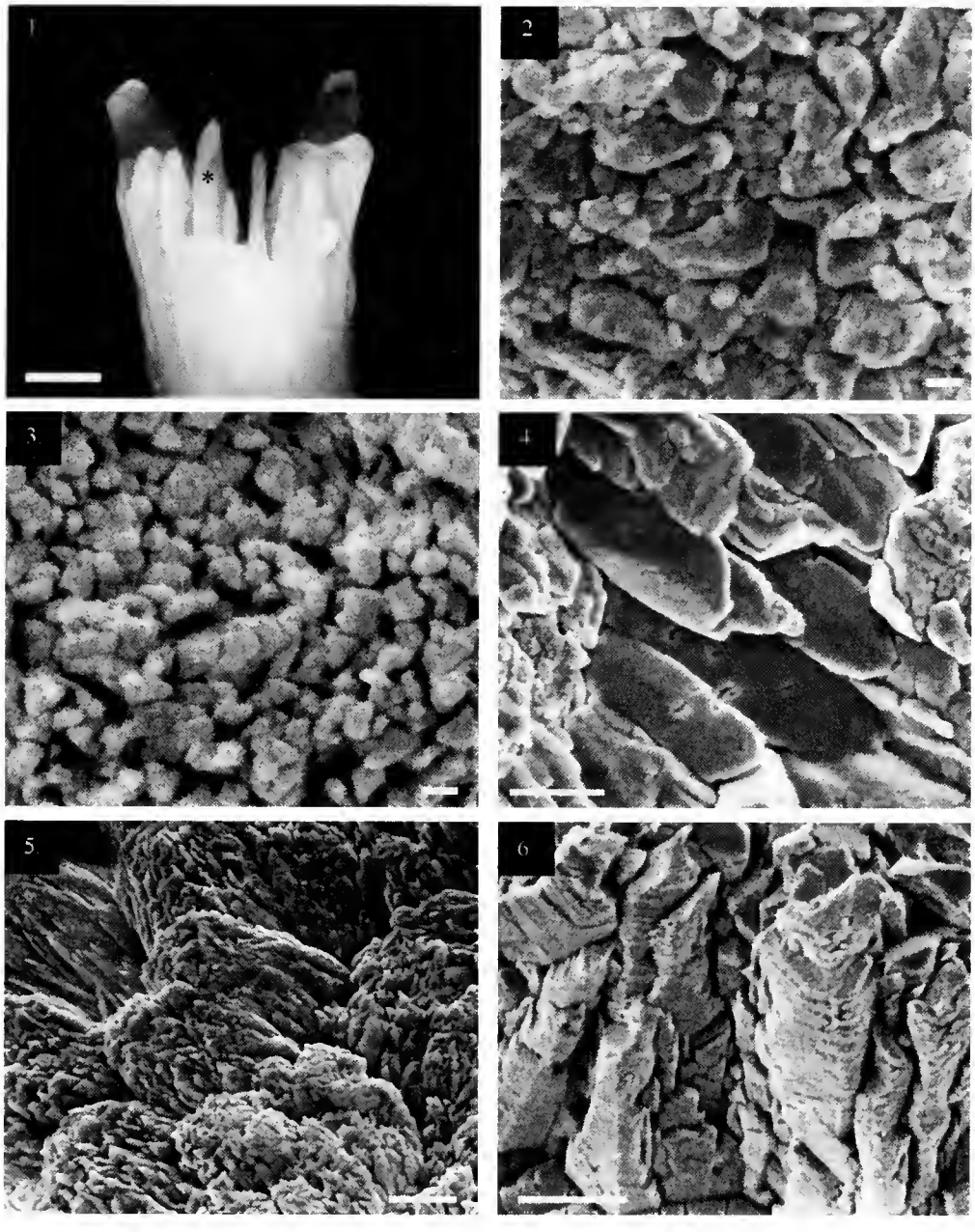

Figure 1. A corallite of *Galaxea fascicularis*, showing exsert septa (*) protruding from the wall of the corallite and encircling the oral disc. Scale bar = 2 mm.

Figure 2. Granular nanocrystals located upon the distal growth edge of a *Galaxea fascicularis* exsert septum. Scale bar = 100 nm.

Figure 3. Granular nanocrystals observed upon a septum of an axial corallite of *Acropora formosa*. Scale bar = 100 nm.

Figure 4. Highly ordered acicular crystals at the distal edge of a *Galaxea fascicularis* exsert septum. Scale bar = 500 nm.

Figure 5. Fasciculi, composed of distinct clusters of similarly oriented acicular crystals, constituting much of the distal surface of a *Galaxea fascicularis* exsert septum. Scale bar = 5 μm.

Figure 6. Lamellae crystals located proximal to the distal growth edge of a *Galaxea fascicularis* exsert septum. Scale bar = 1 μm.

1982, 1983). Fusiform crystals (Gladfelter, 1983) have been suggested to be calcite, in contrast to the bulk of the skeleton, which is formed from aragonite.

In this study we have investigated, over a 24-h period, the crystalline microstructure at the growth surface of exsert septa from the reef coral *G. fascicularis*. Structural charac-

teristics of four crystal types, including one crystal type not previously reported in scleractinian corals, are described at a new level, with magnifications greater than 50,000× achievable by low voltage, high-resolution field emission (FE) scanning electron microscopy. We find no evidence of rhythmic deposition of any crystal types. We also show by X-ray microanalysis that the composition of fusiform crystals does not appear to differ from the remainder of the aragonite skeleton.

Materials and Methods

Coral collection and maintenance

Green, yellow, and brown color morphs of colonies of the reef coral *Galaxea fascicularis* L. (different from the Japanese morphs described by Hidaka and Yamazato (1985)), and white-tipped branches of the reef coral *Acropora formosa* (Dana) were collected at low tide from the reef flat at Heron Reef in the Capricorn Bunker Group of the Great Barrier Reef, Australia. The corals were transported in buckets of seawater to the Heron Island Research Station, where they were maintained in sunlit, well-aerated flow-through aquaria in natural seawater at 24–25 °C. Following collection, the corals were allowed to recover for at least 2 days before being used for experimentation. On occasion, individual *G. fascicularis* polyps and *A. formosa* axial branches were sampled directly from the reef flat and immediately placed into the appropriate chemical treatment. *G. fascicularis* polyps of the green color morph were routinely used for all experiments.

Sample preparation for field emission scanning electron microscopy

Individual *G. fascicularis* polyps were sampled from colonies over a 24-h period (0600, 1200, 1800, and 2400 h; $n = 5$ for each time period). Individual polyps were easily separated from colonies with forceps, as the fragile coenosteum joining individual polyps could be removed without damaging the polyp itself. Axial tips of *A. formosa* branches were sampled at 1200 h ($n = 6$) and 2400 h ($n = 6$). All samples were placed in 12% NaOCl (commercial bleach) at 60 °C for 30 min, and the resultant corallites were rinsed well in running water and then in distilled water (dH_2O) several times. Any tissue remaining on the corallite was removed by gentle agitation and pipetting of dH_2O onto the sample, before being dried at 60 °C for 24 h (Clode and Marshall, 2003b).

G. fascicularis exsert septa (four septa from each polyp) were removed from the corallite with forceps, under a dissecting microscope, and mounted flat using carbon tape. Septa were coated with 5 nm platinum and previewed in a JEOL JSM 840A scanning electron microscope at 10 kV. High-resolution imaging was conducted on a JEOL 6340-F field emission (FE) scanning electron microscope at 2 kV. *A. formosa* branch tips ($n = 12$) were secured upright in hollow stubs with partially polymerized araldite, so that the axial polyp extended about 3 mm above the upper surface of the stub. Polymerization was then completed at 60 °C for a further 30 h. Conductive silver epoxy (ProSciTech) was used to improve the conductivity of the upright corallite, before it was coated with 10 nm platinum. Axial polyps were viewed in a JEOL JSM 6340-F FE scanning electron microscope at 1 kV and 2 kV.

All size measurements were obtained using the computer software package UTHSCSA Image Tool ver. 1.23 (University of Texas). All statistical analyses were performed using the computer software package JMP ver. 3.1.6 (SAS Institute, Inc).

X-ray microanalysis

For comparative elemental analyses of fusiform crystals and typical skeleton, *G. fascicularis* septa were mounted flat as described above, coated with 200 Å Al, and analyzed by X-ray microanalysis in a JEOL JSM 840A SEM fitted with a Link exL X-ray analyzer (Oxford Instruments). The analyzer was equipped with an LZ5 light element detector with a takeoff angle of 40°. Selected area analyses were conducted at 15 kV and a beam current of 2×10^{-10} A, from an area of 1 μm × 1 μm, for 100 s livetime. Element concentrations were calculated against microprobe reference standards (BioRad) using the PhiRhoZ model (Oxford Instruments) (Marshall, 1982; Marshall and Condron, 1987), and element ratios calculated. Because the X-rays from elements of interest could be generated from a depth of up to 2 μm at 15 kV, only large fusiform crystals were analyzed, reducing the likelihood that extraneous X-rays would be derived from skeleton below the crystal itself and affect the element ratios. The areas selected for analysis were horizontal relative to the X-ray detector.

Transverse slices

Small *G. fascicularis* polyps were rapidly frozen in liquid propane (−180 °C) and freeze-substituted in a mixture of 10% acrolein in diethyl ether, according to the protocol outlined by Marshall and Wright (1991). Transverse slices of freeze-substituted material, 400 μm thick, were prepared with a diamond saw (see Marshall and Wright, 1991), attached to glass slides with araldite, and then polished with aluminium oxide. The polished slices were rinsed in dH_2O and air-dried. Samples were viewed unmounted on a Zeiss Axioskop microscope with polarized light.

Results

Crystal types

Using low voltage, high-resolution FESEM, we identified four principal crystal forms on the growth surface of exsert septa sampled from polyps of *Galaxea fascicularis*. These

four crystal forms were nano, acicular, lamellar, and fusiform. All four types were common to septa collected at 0600, 1200, 1800, and 2400 h, and all appeared consistently similar in structure across the four sampling periods. Similarly, no notable differences were observed in the crystal structure of septa sampled from different color morphs, nor were there differences between corallites sampled directly from the reef flat and those allowed to recover in aquaria at Heron Island Research Station for 2 days.

Granular nanocrystals were commonly observed at the actively growing distal tip of *G. fascicularis* exsert septa predominantly on denticles. These crystals appeared as small, clustered groups of rounded crystals that exhibited little order in orientation or pattern of deposition (Fig. 2). Nanocrystals were also observed on septal surfaces of *A. formosa* axial corallites (Fig. 3). Nanocrystals were highly variable in size: the smallest resolvable crystals averaged 19 ± 0.8 nm ($n = 12$) in diameter, and the largest were about 400 nm in diameter.

Acicular crystals were the predominant crystal form on the surface of *G. fascicularis* exsert septa. These crystals were evident over much of the septal surface and extended perpendicular to the plane of the skeletal surface. Acicular crystals were typically large, solid crystals elongated along the *c* axis (Fig. 4), although smaller and more needlelike crystals were also observed. In contrast to nanocrystals, individual acicular crystals were elongated and exhibited a high degree of order and orientation. Groups of acicular crystals growing parallel to each other extended from an unseen origin, which was presumably the underlying fascicles. This arrangement resulted in the appearance of distinct clusters of similarly oriented acicular crystals termed fasciculi, visible at the skeletal surface (Fig. 5). No notable growth increments were evident within individual acicular crystals, suggesting a pattern of continuous growth.

Lamellar structures were typically observed in positions proximal to the extending distal edge of *G. fascicularis* septa. These crystals were similar to acicular crystals in that initially, at low magnification, they appeared to be large, elongate crystals extending perpendicular to the *c* axis. However, at high magnification it became evident that these were not single crystals, but layers of polyhedral plates resembling tabular crystals, which formed lamellar-like stacks (Fig. 6). These crystal stacks were distinctly different from acicular crystals: the apparent continuous nature of acicular crystal growth contrasted with the formation of distinct layers and the obvious discontinuous pattern of crystal deposition in lamellar stacks. Individual crystal layers within these stacks were less than 100 nm in thickness, whereas the crystal stacks themselves were highly variable in both height and diameter.

Fusiform crystals were observed principally along the lateral edges of *G. fascicularis* exsert septa (Fig. 7) and upon *A. formosa* primary septa extending into the calyx of axial corallites (Fig. 8). These crystals were regularly observed on all coral samples, regardless of time of sampling. Fusiform crystals appeared as large, tapered structures that were usually clustered together to form a semisolid, crystalline mass along the lateral edges of the septa (Fig. 7). In *G. fascicularis*, these crystals averaged 4.6 ± 0.2 μm in length and 2.3 ± 0.1 μm in width ($n = 28$). Fusiform crystals observed on *A. formosa* axial corallites were significantly shorter (3.7 ± 0.2 μm; $n = 28$; $P < 0.01$: Student's *t* test) and narrower (1.6 ± 0.1 μm; $n = 28$; $P < 0.0001$: Student's *t* test) than those on *G. fascicularis* septa.

Using high-resolution FESEM, we determined that fusiform crystals were not monocrystalline, but were instead composed of small, polycrystalline aggregates 21 ± 0.8 nm ($n = 20$) in diameter (Fig. 9). These spherical crystals upon the surface of fusiform crystals were not dissimilar to the nanocrystals at the growth edge. Needlelike crystals were never observed upon, or seen to be extending from, the surface of fusiform crystals in either *G. fascicularis* or *A. formosa*.

The ratios of the three major skeletal elements, Ca, Sr, and Mg, present in individual fusiform crystals and typical skeleton of *G. fascicularis* exsert septa, determined by X-ray microanalysis, revealed that fusiform crystals were of a very similar elemental composition to the main skeletal component. Differences ($P > 0.05$; Student's *t* test) observed in the Ca:Mg ratio, the Sr:Mg ratio, and the Ca:Sr ratio between fusiform crystals and skeleton were highly insignificant (Table 1).

No differences were observed, with respect to microstructure or chemical composition, between color morphs of *G. fascicularis* or between corals processed immediately on collection from the reef and corals processed after being kept in aquaria for 2 days after collection.

Freeze-substituted transverse slices

The major structural components of septa were clearly visible in transverse sections of whole freeze-substituted *G. fascicularis* polyps visualized with polarized light (Fig. 10). Centers of calcification, which appeared as distinctly darker (denser) regions, were evident along the midline of each septum. The closeness of the centers to each other and the thickness of the section made it difficult in a single focal plane to resolve the centers as separate structures; this was possible, however, when the plane of focus was changed. The centers possessed a granular substructure, but again, because of the thickness of the section, this was difficult to illustrate photographically. These centers of calcification extended along the central region of each septum, ceasing just short of the lateral edges. From these centers of calcification, highly ordered fascicles with distinct orientations radiated outwards to form fanlike systems (Fig. 10). Bundles of acicular crystals that form fasciculi at the septal surface cannot be visualized.

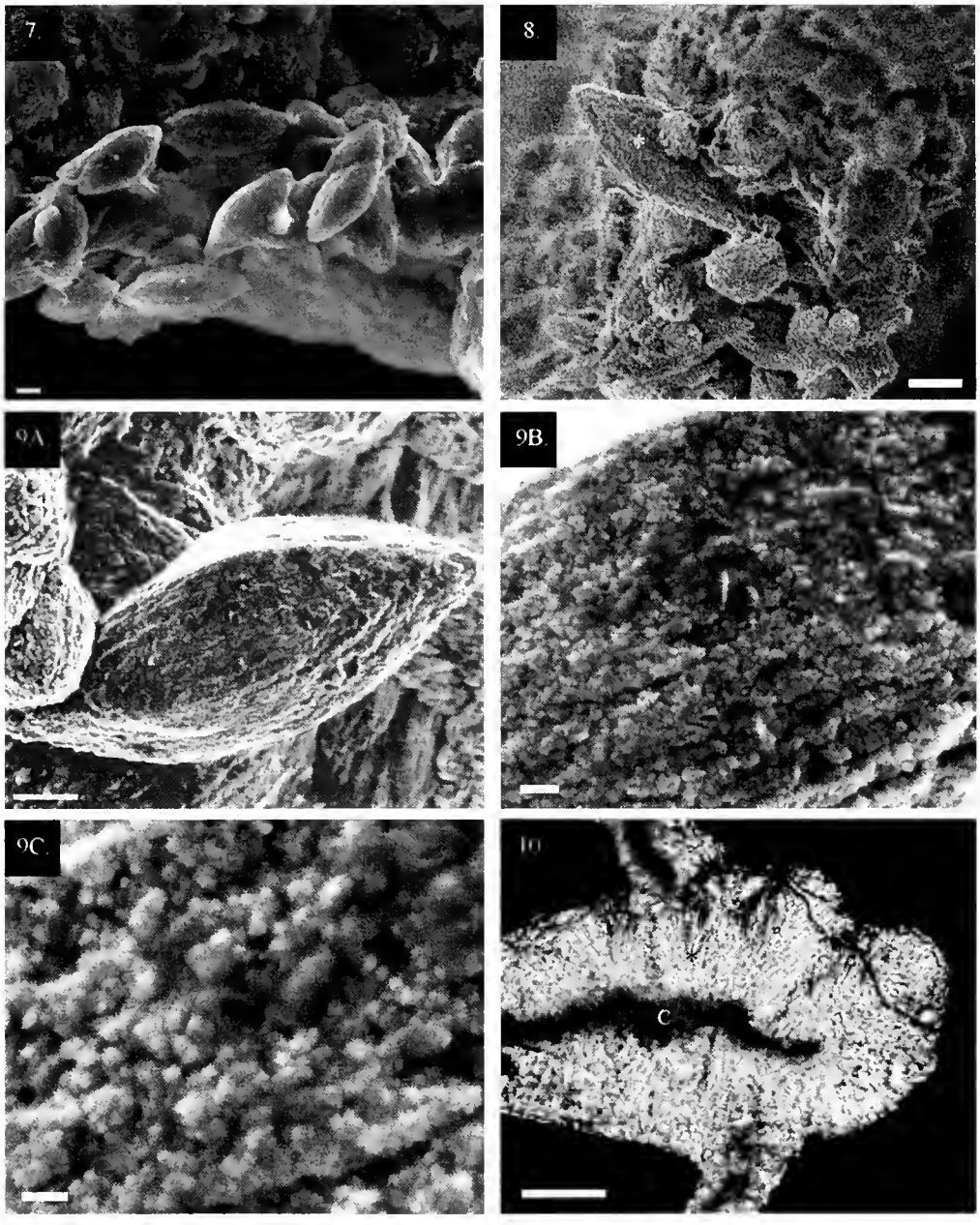

Figure 7. Clusters of fusiform crystals forming a semisolid crystalline mass along the lateral edge of a *Galaxea fascicularis* exsert septum. Scale bar = 1 μm.

Figure 8. Fusiform crystals (*) upon a primary septum extending into the calyx of an *Acropora formosa* axial corallite. Scale bar = 1 μm.

Figure 9. An isolated fusiform crystal from a *Galaxea fascicularis* exsert septum, shown in increasing magnifications. At high magnification, the surface of the tapered polycrystallite is seen to be covered in small, spherulitic crystals. Scale bars: A = 1 μm; B = 200 nm; C = 100 nm.

Figure 10. Transverse section through a freeze-substituted *Galaxea fascicularis* septum, viewed with polarized light, showing granular centers of calcification (C) and centrically arranged fascicles (*) radiating from these centers of calcification to form fanlike trabeculae. An array of trabeculae forms the entire septum. Scale bar = 100 μm.

Discussion

The most significant finding of this investigation is the presence of nanocrystals at the major growth points—the denticles—on the skeletal septa of *Galaxea fascicularis*. These nanocrystals may represent nucleation sites for the deposition of acicular crystals that ultimately form fanlike systems, or fascicles, of polycrystalline fibers, which are the major building blocks of the skeleton. Also found on septa were clusters of acicular crystals forming fasciculi, fusiform

Table 1

Comparison of the ratios of the primary skeletal elements present in individual fusiform crystals and typical skeleton from Galaxea fascicularis *exsert septa, as determined by X-ray microanalysis*

	n	Ca:Mg	Sr:Mg	Ca:Sr
Skeleton	6	143:1	2:1	76:1
Fusiform crystals	7	134:1	1.9:1	76:1
P Value*		0.77	0.82	0.99

* Student's *t* test; *n* = number of analyses.

crystals, and a novel lamellar type of crystal. None of these crystals appeared to be deposited in a diurnal rhythm. The structure of the exsert septum and the structure and location of the various crystal types is summarized in Figure 11. No differences were observed between different color morphs or between corals processed immediately on collection and corals maintained in aquaria for 2 days before processing.

Crystal types

Granular nanocrystals as small as 19 nm in diameter were observed by FESEM on the apical denticles of *G. fascicularis* septa. These nanocrystals have not been previously described. They may be the basic elements of centers of calcification, since denticles are the terminations of trabecular axes, which are extended centers of calcification in the septa (Ogilvie, 1896). Nanocrystals were also observed on the septa of the axial corallites of *A. formosa*. The nanocrystals appear to have some similarity to the crystals forming the nuclear packets described by Constantz (1989) and to the granulated crystallites upon the surface of "spherular crystals" noted by Isa (1986). Constantz suggested that

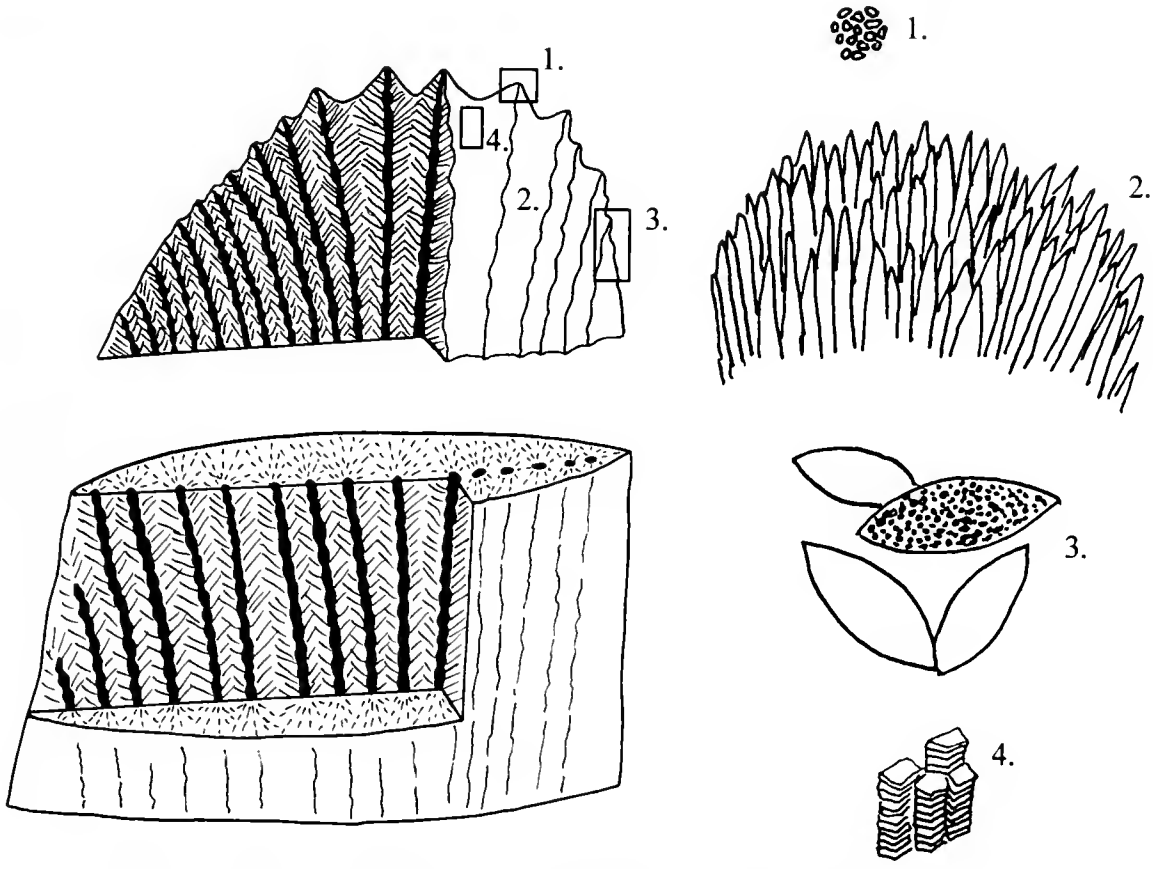

Figure 11. Diagrammatic representation of an exsert septum of *Galaxea fascicularis* showing the internal structure and distribution of crystal types. The internal structure is based partially on Ogilvie (1896). The diagram represents the upper part of the exsert septum with a transverse slice removed. The exsert septum is orientated so that the interior of the corallum would be to the left. Centers of calcification are depicted in black and terminate at denticles. Fibers form systems of trabecullae around the centers of calcification. New centers of calcification appear as the exsert septum extends. The different crystal types are drawn approximately to scale relative to each other, and their typical locations are indicated. Granular nanocrystals (1) are located at the growth edge (see Fig. 2). Acicular crystals (2) are widely distributed on the septal surface (see Figs. 4 and 5). Fusiform crystals (3) are found at the lateral edge (see Fig. 7), and lamellar crystals (4) are located close to the distal growth edge of the exsert septum (see Fig. 6).

nuclear packets were centers of calcification, describing them as small clusters of tiny crystals less than 100 nm in size that existed in high frequency near rapidly growing regions.

The mechanisms involved in the formation and deposition of the nanocrystals, so that they may act as nucleating centers for future crystal growth, remains unknown. There is evidence, however, that small nascent crystals of $CaCO_3$ may develop upon a fibrillar organic matrix, which is evident within small pockets formed between calicoblastic ectodermal cells and the pre-existing skeleton (Clode and Marshall, 2003a).

Clusters of acicular crystals form the distinctive fasciculi, which are visible on the surface of septa in *G. fascicularis*. The surface of coral skeleton is frequently characterized by groups of nearly parallel acicular crystals termed fasciculi (Wise, 1972). Depending upon the orientation of the crystals within the fasciculi, the skeletal surface may appear to be granular or relatively smooth. The acicular crystals presumably nucleate and extend from the apical edges of fascicles. Fascicles are fanlike systems of polycrystalline fibers radiating from centers of calcification (Ogilvie, 1896). The relationship between the smaller fasciculi and the larger underlying fascicles is not clear, since individual fasciculi cannot be readily recognized below the skeletal surface (Jell, 1974). Presumably, fasciculi give rise to the underlying fascicles; however, fascicles are also present in corals that do not have fasciculate skeletal surfaces (Wise, 1972).

Fusiform crystals were predominantly observed along the lateral edges of the septa. The term "fusiform" was first coined by Gladfelter (1982, 1983) to describe large, tapered crystals found on the growing surface of *Acropora cervicornis* axial corallites. Hidaka (1988) also employed the term to describe similar crystals observed on *G. fascicularis* exsert septa. Our observations on the size and shape of fusiform crystals from the septa of both *A. formosa* and *G. fascicularis* are consistent with these studies. The significant size differences evident between the fusiform crystals of *G. fascicularis* and *A. formosa* are likely to reflect differences in polyp size, with *G. fascicularis* polyps considerably larger than those of *A. formosa*. Earlier studies have also reported similar crystals, but these were described as "equant" crystals (see Constantz, 1989), while Isa (1986) preferred to use the term "spindle-shaped crystals." Le-Tissier (1988) also reported fusiform crystals upon the surface of *Pocillopora damicornis* corallites, but these lacked the characteristic tapered ends and may be a different crystal type.

Fusiform crystals on *G. fascicularis* septa were typically observed at the lateral edges where centers of calcification do not persist (Cuif and Dauphin, 1998). This is consistent with the suggestion of Constantz (1989) that centers of calcification were not required for nucleation and growth of fusiform crystals. Fusiform crystal formation may result from secondary nucleation, which can occur due to the presence of already existent crystal structures (Simkiss, 1986).

Upon the surface of fusiform crystals it was possible to resolve small spherical nanocrystals that were, on average, 21 nm in diameter. Isa (1986) reported that the surface structure of spindle-shaped (fusiform) crystals was composed of clusters of small, rounded crystals less than 50 nm in size, indicating that fusiform crystals were polycrystalline in nature. Isa (1986) also found that the fusiform crystals were hollow; however, the preparations had been treated with osmium tetroxide, which will react with $CaCO_3$ to cause dissolution and recrystallization.

We observed no evidence of acicular crystal growth upon individual fusiform crystals, contrary to the proposal of Gladfelter (1982, 1983) that clusters of needlelike crystals extended from fusiform crystals to ultimately form fasciculi. Instead, large clusters of fusiform crystals were typically cemented together to form a semisolid crystalline mass, a feature also noted by Hidaka (1991b), which bore little resemblance to the distinctive fasciculi. In addition, fasciculi, which were common to the entire septal surface, may be spatially isolated from fusiform crystals, which were typically confined to the distal (Hidaka, 1991a) or lateral edges. Hidaka (1991b) also recognised this paradox and suggested that fasciculi may form in several different ways.

Variability in the reported distribution of fusiform crystals on septa (Gladfelter, 1982, 1983; Hidaka, 1991a,b; Hidaka and Shirasaka, 1992) has made interpretation and understanding of crystal deposition and skeletal extension in corals difficult. Reasons for these reported differences are unknown, but preparatory techniques and environmental conditions may have significant effects upon skeletal microstructure (Carlson, 1999; Clode and Marshall, 2003b).

To our knowledge, lamellar crystals have not been reported as a component of any recent scleractinian coral skeleton. There is some suggestion that lamellar structures are existent in hydrozoans and tabulate and rugose anthozoans (see Wendt, 1990), although these appear to refer more to the orientation of fibrillar-type crystals than to true crystalline stacks of polyhedral plates. Lamellar stacks composed of polyhedral plates are very common in molluscs (Watabe and Dunkelberger, 1979), particularly in *Nautilus* shell nacre (Gregoiré, 1987). While molluscan lamellar structures may be either aragonite or calcite, lamellar crystals on mature *G. fascicularis* skeletons are likely to be aragonitic, as calcite persists only in the developing skeletal elements of coral larvae. The function of these lamellar structures in scleractinian corals is unknown, as is their relationship to other crystal types and their involvement in the overall extension and growth of skeletal elements.

Compositional analysis of fusiform crystals

X-ray microanalysis of individual fusiform crystals suggests that fusiform crystals are identical to skeleton in

element composition; therefore, they are aragonitic and not calcitic in nature. Constantz (1989) also suggested that fusiform crystals were likely to be composed of aragonite, although he provided no supporting evidence. Gladfelter (1982), using X-ray microanalysis of large areas of the skeleton of *Acropora cervicornis*, found that Mg concentrations were higher in areas where fusiform crystals were common than in other regions of the skeleton. Since calcite has a higher proportion of Mg than aragonite, it was suggested that fusiform crystals were composed of calcite. However, under these circumstances, it would be impossible to determine exactly what was analyzed, with the presence of fusiform crystals in each region of analysis not confirmed.

Diurnal rhythms

All four crystal types found on the exsert septa of *G. fascicularis* were present and remained similar in structure and disposition, regardless of time of sampling over a 24-h period. Apparent diurnal rhythms of crystal deposition have been reported in *Plesiastrea versipora* (Howe and Marshall, 2002), *Acropora cervicornis* (Gladfelter, 1983), *Pocillopora damicornis* (LeTissier, 1988), and *Manicina areolata* (Barnes, 1972). Hidaka (1988) initially reported a diurnal pattern of fusiform crystal deposition in the exsert septa of *G. fascicularis* corallites, but he later retracted this interpretation in favor of crystal deposition being without rhythm (Hidaka, 1991a). Similarly, we report that *A. formosa* axial corallites, whether sampled at 1200 or 2400 h, possessed fusiform crystals along the primary septa extending into the calyx. This finding is not in accordance with that of Gladfelter (1983), who only observed fusiform crystals upon axial corallites of *A. cervicornis* branches sampled in darkness.

Gladfelter (1982, 1983) hypothesized that fusiform crystals form a loose scaffolding on the surface of exsert septa at night and that acicular crystals nucleate on the fusiform crystals during the day, ultimately giving rise to fasciculi. This diel cycle of deposition of fusiform crystals was proposed to account for skeletal extension in zooxanthellate corals at night. However, diel deposition of fusiform crystals is apparently not a universal phenomenon (*e.g.*, Hidaka, 1991a), and such crystals are not present in all corals (*e.g.*, Howe and Marshall, 2002).

The universal presence of acicular crystals as a predominant component of scleractinian coral skeletons during both day and night, in combination with their lack of discernible substructure, suggests that the growth of these crystals is continuous. Whether the rate of crystal extension and growth varies throughout the day is unknown, but diurnal variations in skeletal extension have been reported (Barnes and Crossland, 1980). In contrast, the presence of distinct layers within lamellar stacks suggests an intermittent, highly regulated process of crystal deposition. Each layer is likely to represent growth increments; however, as no intermediate stages of deposition were observed over the 24-h sampling period, these layers do not appear to be associated with a daily pattern of crystal deposition and growth.

Acknowledgments

This research was conducted with the assistance of an Australian Research Council grant to ATM. All samples were collected under Great Barrier Reef Marine Park Authority permits to ATM. We wish to thank the staff at Heron Island Research Station for their services, Ms Collette Bagnato for her assistance with sample collection and preparation and Mr Alan Jacka for polishing sliced material.

Literature Cited

Barnes, D. J. 1972. The structure and formation of growth ridges in scleractinian coral skeletons. *Proc. R. Soc. Lond. B* **182:** 331–350.

Barnes, D. J., and C. J. Crossland. 1980. Diurnal and seasonal variations in the growth of a staghorn coral measured by time lapse photography. *Limnol. Oceanogr.* **25:** 1113–1117.

Carlson, B. A. 1999. Organism responses to rapid change: what aquaria can tell us about nature. *Am. Zool.* **39:** 44–55.

Chalker, B. E. 1976. Calcium transport during skeletogenesis in hermatypic corals. *Comp. Biochem. Physiol.* **54A:** 455–459.

Chevalier, J. P. 1974. On some aspects of the microstructure of recent scleractinia. Pp 345–351 in *Proceedings of the Second International Coral Reef Symposium,* A. M. Cameron, ed. Great Barrier Reef Committee, Brisbane, Australia.

Clode, P. L., and A. T. Marshall. 2003a. Calcium associated with a fibrillar organic matrix in the scleractinian coral *Galaxea fascicularis. Protoplasma* 220:153–161.

Clode, P. L., and A. T. Marshall. 2003b. Variation in skeletal microstructure of the coral *Galaxea fascicularis:* effects of an aquarium environment and preparatory techniques. *Biol. Bull.* **204:** 138–145.

Constantz, B. R. 1986. Coral skeleton construction: a physiochemically dominated process. *Palios* **1:** 152–157.

Constantz, B. R. 1989. Skeletal organization in Caribbean *Acropora* spp. (Lamarck). Pp. 175–199 in *Origin, Evolution and Modern Aspects of Biomineralization in Plants and Animals,* R. E. Crick, ed. Plenum Press, New York.

Cuif, J. P., and Y. Dauphin. 1998. Microstructural and physico-chemical characterization of 'centers of calcification' in septae of some recent scleractinian corals. *Palaeontol. Z.* **72:** 257–270.

Gladfelter, E. H. 1982. Skeletal development in *Acropora cervicornis* I. Patterns of calcium carbonate accretion in the axial corallite. *Coral Reefs* **1:** 45–51.

Gladfelter, E. H. 1983. Skeletal development in *Acropora cervicornis* II. Diel patterns of calcium carbonate accretion. *Coral Reefs* **2:** 91–100.

Grégoire, C. 1987. Ultrastructure of the *Nautilus* shell. Pp. 463–486 in *Nautilus: The Biology and Paleobiology of a Living Fossil,* W. B. Saunders and N. H. Landman, eds. Plenum Press, New York.

Hidaka, M. 1988. Surface structure of skeletons of the coral *Galaxea fascicularis* formed under different light conditions. Pp. 95–100 in *Proceedings of the Sixth International Coral Reef Symposium,* Vol. 3, J. H. Choat *et al.*, eds. 6th International Coral Reef Symposium Executive Committee, Townsville, Australia.

Hidaka, M. 1991a. Deposition of fusiform crystals without apparent diurnal rhythm at the growing edge of septa of the coral *Galaxea fascicularis. Coral Reefs* **10:** 41–45.

Hidaka, M. 1991b. Fusiform and needle-shaped crystals found on the skeleton of a coral, *Galaxea fascicularis,* Pp. 139–143 in *Mechanisms*

and Phylogeny of Mineralization in Biological Systems, S. Suga and H. Nakahara, eds. Springer Verlag, Tokyo.

Hidaka, M., and S. Shirasaka. 1992. Mechanism of phototropism in young corallites of the coral *Galaxea fascicularis*. *J. Exp. Mar. Biol. Ecol.* **157:** 69–77.

Hidaka, M., and K. Yamazato. 1985. Color morphs of *Galaxea fascicularis* found in the reef around the Sesoko Marine Science Center. *Galaxea* **4:** 33–35.

Howe, S. A., and A. T. Marshall. 2002. Temperature effects on calcification rate and skeletal deposition in the temperate coral, *Plesiastrea versipora* (Lamarck). *J. Exp. Mar. Biol. Ecol.* **275:** 63–81.

Isa, Y. 1986. An electron microscope study on the mineralization of the skeleton of the staghorn coral *Acropora hebes*. *Mar. Biol.* **93:** 91–101.

Jell, J. S. 1974. The microstructure of some scleractinian corals. Pp. 301–320 in *Proceedings of the Second International Coral Reef Symposium*, A.M. Cameron, ed. Great Barrier Reef Committee, Brisbane, Australia.

LeTissier, M. D. 1988. Diurnal patterns of skeleton formation in *Pocillopora damicornis* (Linnaeus). *Coral Reefs* **7:** 81–88.

Marshall, A. T. 1982. Application of ϕ (pz) curves and a windowless detector to the quantitative X-ray microanalysis of frozen-hydrated bulk specimens. *Scanning Electron Microsc.* **1982 I:** 243–260.

Marshall, A. T., and R. J. Condron. 1987. A simple method of using ϕ (pz) curves for the X-ray microanalysis of frozen-hydrated biological bulk samples. *Micron Microsc. Acta* **18:** 23–26.

Marshall, A. T., and A. Wright. 1998. Coral calcification: autoradiography of a scleractinian coral *Galaxea fascicularis* after incubation in ^{45}Ca and ^{14}C. *Coral Reefs* **17:** 37–47.

Marshall, A. T., and O. P. Wright. 1991. Freeze-substitution of scleractinian coral for confocal scanning laser microscopy and X-ray microanalysis. *J. Microsc.* **162:** 341–354.

Ogilvie, M. M. 1896. Microscopic and systematic study of madreporarian types of corals. *Phil. Trans.* **187:** 85–345.

Simkiss, K. 1986. The processes of biomineralization in lower plants and animals—an overview. Pp. 19–37 in *Biomineralization in Lower Plants and Animals*, B. S. C. Leadbeater and R. Riding, eds. Published for Systematics Association by Clarendon Press, Oxford.

Sorauf, J. E. 1970. Microstructure and formation of dissepiments in the skeleton of the recent Scleractinia (hexacorals). *Biomineralization* **2:** 1–22.

Sorauf, J. E. 1972. Skeletal microstructure and microarchitecture in Scleractinia (Coelenterata). *Palaeontology* **15:** 11–23.

Sorauf, J. E. 1974. Observations on microstructure and biocrystallization in coelenterates. *Biomineralization* **7:** 37–55.

Sorauf, J. E. 1980. Biomineralization, structure and diagenesis of the coelenterate skeleton. *Acta Palaeontol. Pol.* **25:** 327–343.

Vahl, J. 1966. Sublichtmikroskopische Untersuchungen der Kristallinen Grundbauelemente und der Matrixbeziehung zwischen Weichkörper und Skelett an *Caryophyllia* Lamarck 1801. *Z. Morphol. Ökol. Tiere* **56:** 21–38.

Wainwright, S. A. 1963. Skeletal organisation in the coral, *Pocillopora damicornis*. *Q. J. Microsc. Sci.* **104:** 169–183.

Watabe, N., and D. G. Dunkelberger. 1979. Ultrastructural studies on calcification in various organisms. *Scanning Electron Microsc.* **1979 II:** 403–415.

Wendt, J. 1990. Corals and coralline sponges. Pp. 45–66 in *Skeletal Biomineralization: Patterns, Processes and Evolutionary Trends*, J. G. Carter, ed. Van Nostrand Reinhold, New York.

Wise, S. W. 1970. Scleractinian coral skeletons: surface microarchitecture and attachment scar patterns. *Science* **169:** 978–980.

Wise, S. W. 1972. Observations of fasciculi on developmental surfaces of scleractinian exoskeletons. *Biomineralization* **6:** 160–175.

Outcomes of Genome-Genome Interactions

Proceedings
of a workshop
sponsored by
THE CENTER FOR ADVANCED STUDIES
IN THE SPACE LIFE SCIENCES
AT THE MBL

1 to 3 May 2002

J. Erik Jonsson Center
for the National Academy of Sciences,
Woods Hole, Massachusetts

Funded by THE NATIONAL AERONAUTICS AND SPACE ADMINISTRATION under Cooperative Agreement NCC 2-1266. Reprints of this symposium can be obtained from the Center for Advanced Studies in the Space Life Sciences, 7 MBL Street, Woods Hole, MA 02543.

CONTENTS

Outcomes of Genome–Genome Interactions

Reference: *Biol. Bull.* **204:** 159. (April 2003)

Introduction

MITCHELL SOGIN[1] AND DIANA E. JENNINGS[2]

[1]*The Josephine Bay Paul Center for Comparative Molecular Biology and Evolution and* [2]*The Center for Advanced Studies in the Space Life Sciences, Marine Biological Laboratory, Woods Hole, Massachusetts*

For more than 3.5 billion years, microbes of untold diversity have dominated every corner of our biosphere. For example, the cyanobacteria *Synechococcus* and *Prochlorococcus*, with a global biomass of approximately 1 billion metric tons, are responsible for 10% to 50% of the ocean's primary productivity. Microorganisms are also responsible for key processes in geochemical cycling, biodegradation, and the protection of entire ecosystems from environmental insult. Thus, they control global utilization of nitrogen through nitrogen fixation, nitrification, and nitrate reduction; and they drive the bulk of carbon, sulfur, iron, and manganese biogeochemical cycles. At higher trophic levels, rarely studied bacterial mutualists provide essential nutrients and other compounds to diverse plant and animal hosts, and thus have a pervasive impact on the distribution, productivity, and diversification of multicellular organisms. Therefore, although Earth's early history teaches us that microbial life can thrive in diverse environments devoid of multicellular organisms, the continued survival of later evolving multicellular plants and animals is completely dependent upon interactions with microorganisms.

Although microorganisms have a central role in shaping planetary environments, little is known about how they function in consortia, *i.e.*, extraordinarily diverse, complex, and highly organized communities. And even less is known about the responses of these microbial communities to cyclic and transient environmental shifts. Clearly, the activities of the varied microbes constituting a consortium must be coordinated, and these structured populations must also be able to detect and respond to their ever-changing environments; but we lack comprehensive descriptions of the biochemical and genetic mechanisms underlying these obligatory relationships. The control of microbial growth and biogeochemical activity in all ecosystems must include the coordinated expression of multiple genomes from different organisms. Moreover, such genome-genome interactions should scale from thousands of species of microbes that function within consortia to maintain or shape the environment, to relatively simple binary interactions between species (*i.e.*, a symbiont or a pathogen and its host). In recent years, advances in molecular biology have revolutionized the life sciences. In the near future, microbial ecologists and evolutionary biologists will decipher the molecular language that coordinates the expression and evolution of microbial genomes and entire ecosystems.

This workshop—entitled *Outcomes of Genome-Genome Interactions*—derives from previous discussions between Mitchell Sogin and John Hobbie of the Marine Biological Laboratory (MBL), Andreas Teske of the Woods Hole Oceanographic Institution, and David Stahl of the University of Washington. The discussions were about how to link biogeochemical measurements with metabolic processes and microbial population structures existing in natural settings. This meeting is meant to start a continuing conversation among a variety of investigators—microbiologists, biogeochemists, ecosystem experts, molecular phylogeneticists, and molecular ecologists—who are united by their interest in complex microbial processes on Earth. The ultimate objective is to foster novel interdisciplinary studies in ecosystems biology and evolution that are relevant to the interests of the National Aeronautics and Space Administration (NASA) in fundamental space biology and the exploration of life beyond planet earth.

This workshop was sponsored by the Center for Advanced Studies in the Space Life Sciences (CASSLS) and the Josephine Bay Paul Center for Comparative Molecular Biology and Evolution—both at the MBL. CASSLS was established in 1995 through a cooperative agreement between the MBL and the Life Sciences Division of NASA. The Center acts as an interface between NASA and the basic science community, promoting interactions and discussion in areas of mutual interest. The Josephine Bay Paul Center sponsors research that integrates the powerful tools of genome science, molecular phylogenetics, and molecular ecology. The aims are to advance our understanding of the relationships among living organisms, to quantify and assess biodiversity, and to identify molecular mechanisms of biomedical importance.

Reference: *Biol. Bull.* **204:** 160–167. (April 2003)

Biogeochemistry of Hypersaline Microbial Mats Illustrates the Dynamics of Modern Microbial Ecosystems and the Early Evolution of the Biosphere

DAVID J. DES MARAIS

Ames Research Center, Moffett Field, California 94035

Photosynthetic microbial mats are remarkably complete self-sustaining ecosystems at the millimeter scale, yet they have substantially affected environmental processes on a planetary scale. These mats may be direct descendents of the most ancient biological communities in which even oxygenic photosynthesis might have developed. Photosynthetic mats are excellent natural laboratories to help us to learn how microbial populations associate to control dynamic biogeochemical gradients.

Light sustains both oxygenic and anoxygenic photosynthesis; in turn, photosynthesis provides energy, organic substrates, and oxygen to the community (Fig. 1). Although photosynthetic bacteria might dominate the biomass and productivity of the mat, many aspects of the emergent properties of this ecosystem ultimately reflect the activities of the associated nonphotosynthetic microbes, including the anaerobic populations. These nonphotosynthetic processes constitute the ultimate biological filter on chemical biomarkers (*e.g.*, porphyrins, hopanes, isoprenoids, and other biogenic hydrocarbons), and also on isotopic and geologic biosignatures that subsequently enter the fossil record. Also, the transformation of photosynthetic productivity by the microbial community can contribute diagnostic "biosignature" gases that might represent examples of search targets for remote detection of astronomical life (*e.g.*, Des Marais *et al.*, 2002a). To understand the overall structure and function of mat communities, it is thus critical to determine the nature and extent of interaction between photosynthetic and nonphotosynthetic, including anaerobic, microbiota.

Both the diversity of biota and the functional complexity within the mats, coupled with the highly proximal and ordered spatial arrangement of microorganisms, offer the potential for a staggering number of interactions. The products of each group can affect the responses of other groups in both positive and negative ways. For example, cyanobacteria generate organic matter (a potential growth and energy substrate for other organisms) but also oxygen (a toxin for many anaerobic processes). Anaerobic activity recycles nutrients to the phototrophic community, but it also generates potentially toxic sulfide (Van Gemerden, 1993). Accordingly, microorganisms have developed strategies to cope with the daily oscillation between extremes of eutrophy and toxicity.

A study of subtidal cyanobacterial mats growing in the hypersaline seawater evaporation ponds of the salt producer Exportadora de Sal, S.A. (ESSA) is ongoing at Guerrero Negro, in Baja California, Mexico. This study is furnishing examples of the steep environmental gradients experienced by mat microorganisms, and providing preliminary evidence for intimate interactions between these populations. These observations indicate that future studies of genome-genome interactions will contribute substantially to our understanding of the origins, environmental impacts, and biosignatures of photosynthetic microbial mats.

The Microenvironment Within Photosynthetic Microbial Mats

To understand the function of a microbial mat community, the physical and chemical microenvironment in which the microbes live must be known well and in detail. At Guerrero Negro, the environment within the mat differs substantially from that in the overlying water column. The

E-mail: David.J.DesMarais@nasa.gov

The paper was originally presented at a workshop titled *Outcomes of Genome-Genome Interactions*. The workshop, which was held at the J. Erik Jonsson Center of the National Academy of Sciences, Woods Hole, Massachusetts, from 1–3 May 2002, was sponsored by the Center for Advanced Studies in the Space Life Sciences at the Marine Biological Laboratory, and funded by the National Aeronautics and Space Administration under Cooperative Agreement NCC 2-1266

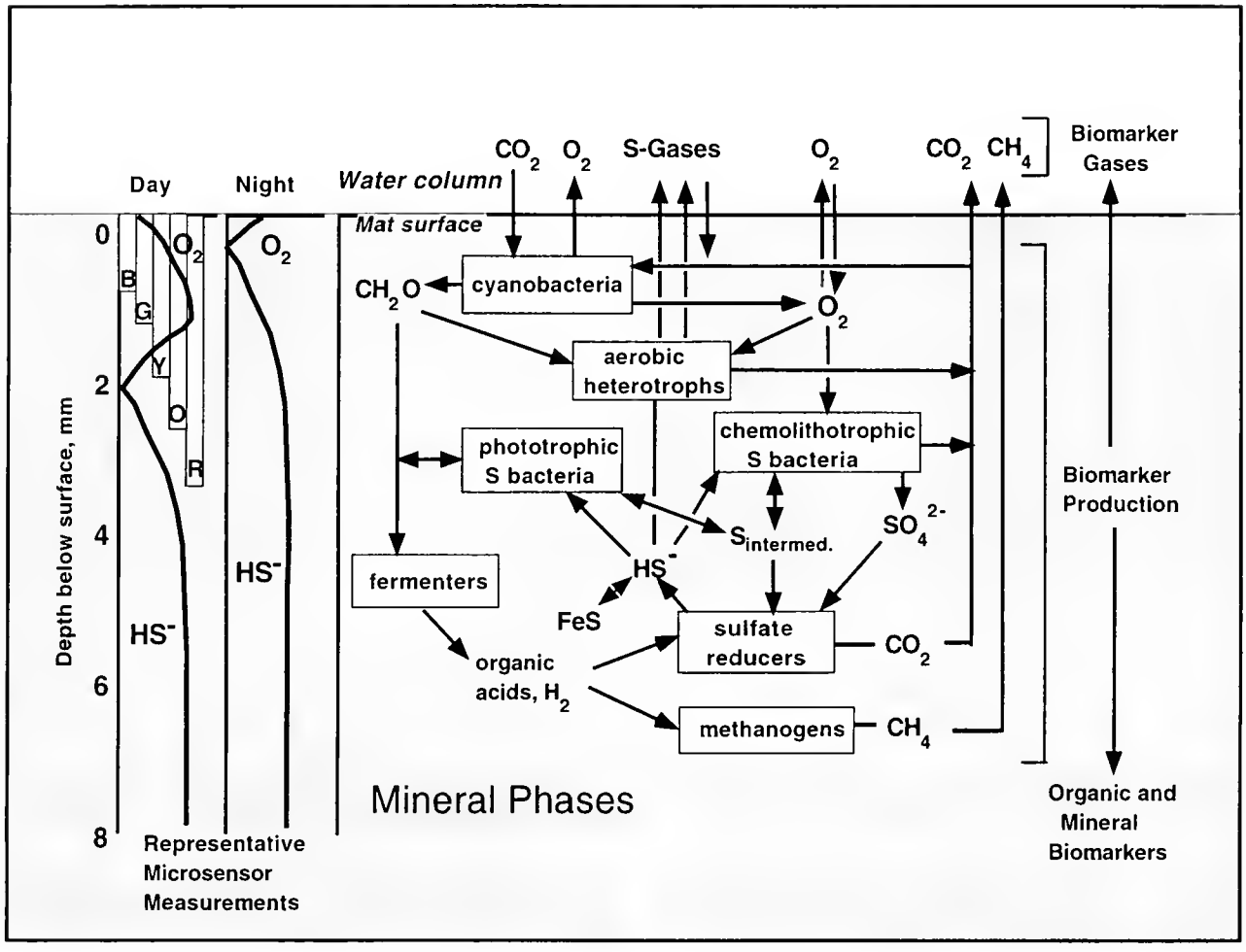

Figure 1. Schematic of a cyanobacterial microbial mat with associated depth-related light and chemical gradients. Flow diagram at center is modeled after Fenchel and Finlay (1995). Boxes denote functional groups of microorganisms, and arrows denote flows of chemical species into or out of microorganisms. $S_{intermed}$ indicates sulfur in intermediate oxidation states. Schematic at left depicts vertical gradients of O_2 and sulfide during the day and at night. Oxygen concentrations are shown decreasing to zero at a depth of 2 mm during the day, and just below the mat surface at night. The vertical bars at upper left represent the relative depths of penetration of blue (B), green (G), yellow (Y), orange (O), and red (R) light. Such chemical gradients and light penetration profiles of both filamentous and unicellular mats are qualitatively similar, although the depth scale (mm) of such profiles tends to be greater for unicellular mats.

community just beneath the mat surface typically experiences steep vertical gradients of light intensity and redox conditions that change markedly during the diel cycle.

The intensity and spectral composition of the light that penetrates the mat is changed by absorption and scattering. Motile photosynthetic organisms optimize their position with respect to the resultant light gradient; some biota harvest light in the infrared spectral range (Jørgensen *et al.*, 1987; Jørgensen and Des Marais, 1988). When oxygenic photosynthesis ceases at night, the upper layers of the mat become highly reduced and sulfidic (Jørgensen *et al.*, 1979; Jørgensen, 1994). Counteracting gradients of oxygen and sulfide shape the chemical environment and provide daily-contrasting microenvironments that are separated on a scale of a few millimeters (Fig. 1; Revsbech *et al.*, 1983). Radiation hazards (UV, *etc.*, Garcia-Pichel, 2000) as well as oxygen and sulfide toxicity elicit motility and other physiological responses. This combination of benefits and hazards of light, oxygen, and sulfide promotes the allocation of the various essential mat processes to the periods of light and dark periods (Fründ and Cohen, 1992; Bebout *et al.*, 1994) and to various depths in the mat.

Light microenvironment

The light flux penetrating the mat can be measured both as downward irradiance (the total down-welling light that passes through a horizontal plane) and as scalar irradiance (the sum of all light that converges upon a given point within the mat). Due to the high density of photosynthetic

organisms, bacterial mucilage, and mineral particles in mats, light absorption is dominated by the light-harvesting pigments of the phototrophic bacteria, and light is strongly scattered. Because absorption and scattering of light are quite substantial within the mat, scalar irradiance can differ substantially from downward irradiance (Jørgensen and Des Marais, 1988). Because scalar irradiance measures the total light actually available at a given location, it constitutes the most meaningful description of the environment of a microorganism.

Measurements of scalar irradiance were obtained both for a microbial mat that was dominated by a filamentous cyanobacterium, *Microcoleus chthonoplastes*, and for a mat that grew at higher salinity and was dominated by unicellular cyanobacteria (Jørgensen and Des Marais, 1988). A strong decline in intensity and a marked change in spectral composition of the light are both typically observed with depth in the dark olive mat, dominated by *Microcoleus* cyanobacteria. Minima in the spectra correspond to the absorption maxima of the photosynthetic pigments of cyanobacteria. Chlorophyll *a* (Chl *a*) absorbs at wavelengths of about 430 and 670 nm, phycocyanin at about 620 nm, and various carotenoids in the range of 450 to 500 nm. In contrast, the mat that was dominated by unicellular cyanobacteria had a lower density of cells, a more gelatinous texture, and a light orange-tan color. Light penetrated more deeply into the unicellular cyanobacterial mat, although blue light was strongly attenuated. Carotenoids achieved most of the light absorption in this mat. In both the *Microcoleus* and unicellular mats, longer-wavelength light, particularly longer than 900 nm, penetrated farthest into the mat (Fig. 1).

Such studies illustrate how the mat matrix affects the penetration of light and the physiology of the biota. For example, mat cyanobacteria that use light that has been filtered by overlying diatoms exhibit greatest photosynthetic activity at wavelengths between 550 and 650 nm (Jørgensen *et al.*, 1987), a region that lies between the absorption maxima of Chl *a*. In contrast, planktonic cyanobacteria exposed to a broader spectrum of light in their natural environment show significant activity at wavelengths corresponding to the absorption maxima of Chl *a* (Jørgensen and Des Marais, 1988).

Chemical gradients

The high rates of oxygenic photosynthesis that occur in the narrow photic zone of the mat create steep and variable gradients (Revsbech *et al.*, 1983) in pH and in concentrations of dissolved inorganic carbon (DIC) and O_2 (DO). The oxic zone reflects a dynamic balance between photosynthetic O_2 production and O_2 consumption by a host of sulfide-oxidizing and heterotrophic bacteria.

Using microelectrodes, the depth distribution of [DO], sulfide concentrations, and pH was determined in a mat dominated by *M. chthonoplastes* (Jørgensen and Des Marais, 1986). These depth profiles are typical for these mats (*e.g.*, Canfield and Des Marais, 1993). Extremely high rates of oxygenic photosynthesis create DO levels that are nearly five times the value of air-saturated brine, yet this O_2 has a residence time of only 2 min. Oxygen production can become negligible at a depth of only 0.5 mm, due to light limitation (Fig. 2a). However, O_2 diffuses farther down to a point at which it overlaps with sulfide diffusing up from below. This interval is typically inhabited by abundant green nonsulfur phototrophic bacteria (*e.g.*, *Chloroflexus*) and by *Beggiatoa* (Fig. 3b). As sunset approaches, the oxic zone collapses quickly, and the oxic-anoxic boundary approaches the mat surface (Canfield and Des Marais, 1993). Accordingly, conditions alternate between O_2 supersaturation and millimolar concentrations of sulfide. Remarkably, diverse microbiota have apparently become well adapted to these conditions.

The relative abundances of photoautotrophic bacteria (*e.g.*, purple sulfur bacteria and green nonsulfur bacteria) and chemolithotrophic sulfide-oxidizing bacteria can be affected by the amount of light that reaches the chemocline (Jørgensen and Des Marais, 1986). Light levels as low as 1% of the incident near-infrared radiation (800 to 900 nm) are sufficient for *Chromatium*, a phototrophic purple sulfur bacterium, to dominate the chemocline (Fig. 2b). Thus the balance between the penetration of O_2 and the penetration of light into the sulfide-rich zone determines the balance in the populations of sulfur bacteria.

Biogeochemical Cycling of Key Elements and Their Compounds

The waters that host well-developed microbial mats are typically depleted in the basic nutrient elements (Javor, 1983), yet microbial mats are highly productive aquatic ecosystems. This remarkable productivity reflects the efficient recycling of key nutrients within the mat ecosystem. The cycling of carbon, oxygen, sulfur, and nutrients has been studied in mats dominated by *M. chthonoplastes* (*e.g.*, Canfield and Des Marais, 1993; Bebout *et al.*, 1994).

The potential for substantial coupling among populations arises through cyanobacterial production of hydrogen and small organic acids (Fig. 1; Stal *et al.*, 1989; Van Der Oost *et al.*, 1989; Stal, 1991). Such substances can serve as substrates for energy and growth for a broad array of microorganisms. Bacterial production of low-molecular-weight nitrogen and sulfur compounds is also important. These compounds lie at the center of energy and electron flow in anaerobic ecosystems and thus are potential basis for microbial interactions. For example, interspecies transfer of hydrogen facilitates many well-studied anaerobic consortia (*e.g.*, Ferry and Wolfe, 1976; McInerney *et al.*, 1979). Hydrogen can represent not only an agent of electron transfer but also an important thermodynamic control with the potential for significantly altering the metabolic function of

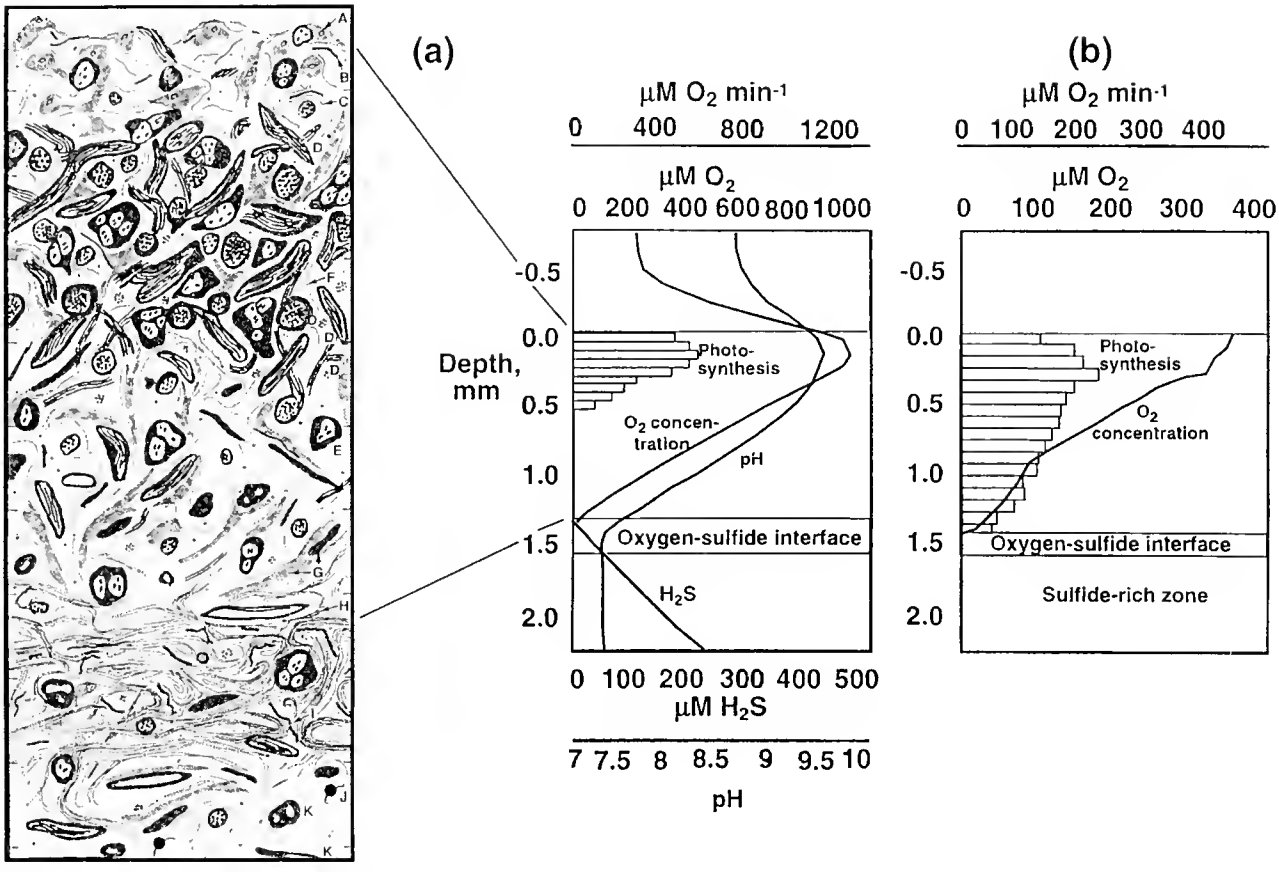

Figure 2. Depth gradients in O_2, oxygenic photosynthesis, sulfide, pH, and microbiota. (a) At left is a schematic vertical section of the topmost 2 mm of subtidal mat dominated by *Microcoleus chthonoplastes* cyanobacteria. Letters along the right margin indicate the following: A: diatoms; B: *Spirulina* spp. cyanobacteria; C: *Oscillatoria* spp. cyanobacteria; D: *Microcoleus chthonoplastes* cyanobacteria; E: nonphotosynthetic bacteria; F: unicellular cyanobacteria; G: fragments of bacterial mucilage; H: green nonsulfur bacteria; I: *Beggiatoa* spp.; J: metazoans (*e.g.*, nematodes); K: abandoned cyanobacterial sheaths. Also shown are depth profiles for key chemical constituents in the Pond 5 mat, as follows: photosynthetic O_2 production rates (horizontal bars), and concentrations of O_2 and sulfide, and pH (data from Jørgensen and Des Marais, 1986).

each partner. Virtually every member of the anaerobic community is subject to such effects (Schink, 1988; Zinder, 1993); therefore, the participation of cyanobacteria in the cycling of hydrogen and organic acids could substantially affect biogeochemical function and community composition (Hoehler *et al.*, 2001). Similarly, anaerobes consume these thermodynamically sensitive end products and thus can provide an important feedback on fermentation and nitrogen fixation by cyanobacteria at the levels of both enzyme and gene regulation.

Carbon, oxygen, and sulfur budgets

Several general observations can be made about the cycling of carbon, oxygen, and sulfur (Canfield and Des Marais, 1993; Des Marais *et al.*, 2002b). During the day, most of the O_2 produced is recycled within the mat by O_2 respiration and some sulfide oxidation. At night, O_2 is consumed principally by sulfide oxidation near the mat-water interface. Microbial sulfate reduction is the principal source of DIC at night. Although abundant *Chloroflexus*-type (anoxic phototroph) filaments are visible microscopically at the O_2-sulfide interface, anoxygenic photosynthesis accounts for less than 10% of the total carbon fixation rate.

A careful comparison of the relative O_2 and DIC fluxes across the mat-water interface reveals that, during the day, more DIC diffuses into the mat than O_2 diffuses out (Canfield and Des Marais, 1993; Des Marais *et al.*, 2002b). At night, more DIC diffuses out of the mat than O_2 diffuses in. However, both the net O_2 and the net DIC fluxes are balanced over the full 24-h cycle. This budget indicates that, during the day, carbon having an oxidation state greater than zero is incorporated into the mat, and carbon having a similarly high oxidation state is liberated at night. The chemical nature of this carbon is unknown.

Although all of the key processes are strongly influenced by temperature, their rates scale with temperature by

roughly the same amount (Canfield and Des Marais, 1993; Des Marais *et al.*, 2003). Over a 24-h period, the overall impact of these very high metabolic rates is that the net accumulation of carbon is low. Apparently this mat is a closely coupled system in which high rates of photosynthetic carbon fixation fuel high rates of carbon oxidation. This efficient oxidation of organic components regenerates nutrients that, in turn, maintain high rates of primary production.

Gas production

The high productivity associated with photosynthetic microbial mats, coupled with their proximity to the atmosphere and prominent role in ancient coastal environments, indicates that such mats probably influenced the early atmosphere substantially. Cyanobacteria and diatoms provide large quantities of photosynthate to anaerobes in the mat. In the *Microcoleus* mats at night, O_2 is consumed by sulfide oxidation at the mat surface and lowermost water column (Canfield and Des Marais, 1993), thus the entire mat becomes anoxic (Fig. 1). Accordingly, mat cyanobacteria must ferment to obtain energy at night, and they probably produce an array of reduced low-molecular-weight compounds. At Guerrero Negro, Hoehler *et al.* (2001) observed that subtidal *Microcoleus* mats generated CO, CH_4, and significant quantities of H_2. Rates of emission of CO correlated with rates of photosynthesis, implicating cyanobacteria, diatoms, or both as sources. Emission rates of H_2 were greatest at night, consistent with fermentation under anoxic conditions. Methane emission rates were unchanged during the diel cycle, indicating a source beneath the zone in the mat that becomes oxygenated during the day. Abundant organic photosynthates apparently interact also with sulfides in mat pore waters to produce dimethyl sulfide and other organosulfur gases, some of which escape the mat (Visscher *et al.*, 2003).

These fluxes of reduced gases are significant for at least three reasons. First, microorganisms that inhabit cyanobacterial mats benefit from abundant products of photosynthesis. Therefore, the advent of oxygenic photosynthesis billions of years ago perhaps triggered a profound evolutionary transformation and diversification within the anaerobic microbial world. Second, the proximity of photosynthetic mats to the atmosphere allows a substantial fraction of reduced gases to escape biological recycling and to enter and profoundly alter atmospheric composition (Hoehler *et al.*, 2001). Early in Earth history, atmospheric reduced biogenic gases such as methane and organosulfides might have been important both as greenhouse gases and as substrates for energy and growth of other biota, including those that were geographically distant from the sources of these gases. Third, if analogous microbial ecosystems indeed exist on habitable planets orbiting other stars, they should influence the compositions of their atmospheres. The closest of these planets might soon be observable by astronomers (*e.g.*, Des Marais *et al.*, 2002a).

Specific Microbe-Microbe Interactions

The mat ecosystem depends upon intimate interactions between key groups of bacteria. Oxygenic photosynthesis by cyanobacteria and diatoms maintains a "food chain"—that is, a flow of both photosynthetic products and their derivatives that nourishes a vast consortium of mat microorganisms (*e.g.*, Fig. 3). The specific details of this flow of reduced species are so important that they might account for several key unanticipated observations; two such examples are described below.

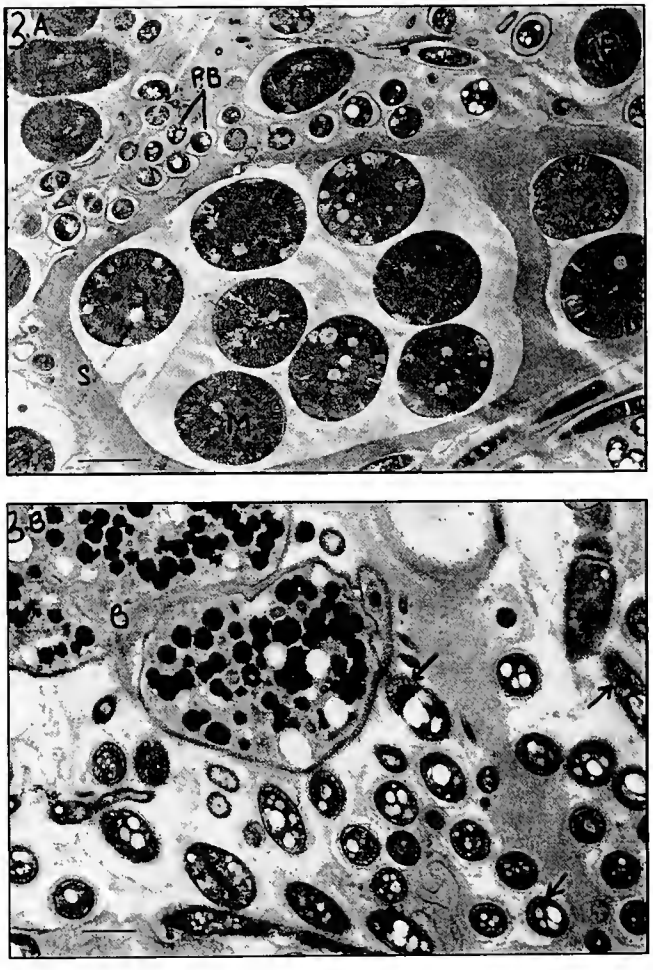

Figure 3. Transmission electron micrographs of biota in the subtidal *Microcoleus* mat (Elisa D'Antoni D'Amelio, Ames Research Center, unpubl.). (3A) Community at about 0.2 mm depth, showing several *Microcoleus* (M) trichomes situated within a common exopolymer sheath (S). Nearby are *Phormidium* cyanobacteria (P) and anoxygenic phototropic bacteria (PB), possibly green nonsulfur bacteria. Scale bar at lower left equals 1 μm. (3B) Community at about 1.4 mm depth, just below the O_2 sulfide chemocline. Large *Beggiatoa* filaments (B) are accompanied by photosynthetic green nonsulfur bacteria exhibiting their characteristic intracellular photosynthetic bodies, chlorosomes (arrows). Scale bar at lower left equals 1 μm.

Association between cyanobacteria and anoxygenic phototrophic bacteria

An unidentified filamentous phototrophic bacterium has been described which actually lives inside the sheaths of viable *Microcoleus* cyanobacteria (D'Amelio *et al.*, 1987). Its occurrence inside cyanobacterial sheaths is interesting because O_2 inhibits anoxygenic photosynthesis. D'Amelio *et al.* (1987) proposed that, because light levels and DO vary during the day, this bacterium alternates between photoheterotrophic growth (at high light levels; using organic matter excreted by the cyanobacteria) and sulfide co-metabolism with cyanobacteria (at relatively low light levels, where O_2 production is minimal). This anoxygenic phototroph might even assist cyanobacteria by consuming sulfide after sunrise and thus relieving sulfide inhibition of oxygenic photosynthesis.

Aerobic sulfate reduction

Sulfate-reducing bacteria are quantitatively important consumers of dissolved organic matter. Furthermore, the sulfide they produce sustains a wide variety of phototrophic and chemotrophic bacteria. The highest rates of sulfate reduction occur in the shallowest part of the subtidal *Microcoleus* mat, close to the photosynthetic source of fresh organic matter (Canfield and Des Marais, 1993). Although O_2 is typically an effective inhibitor of bacterial sulfate reduction, the highest reduction rates actually occur within the mat's aerobic zone during the daytime (Canfield and Des Marais, 1991). A thorough search was made for anaerobic microenvironments within the aerobic zone that might serve as refugia for the sulfate-reducing bacteria, yet none were found. The specific factors that attenuate this O_2 inhibition of sulfate reduction are not known. However, fermentation products are probably abundant in the vicinity of the cyanobacteria, and their roles as chemical reductants might offset the toxic effects of oxidants such as O_2.

Future Research

The studies described above have been performed principally on subtidal marine hypersaline cyanobacterial mats. Although intertidal and supratidal cyanobacterial mats also have received some attention, the level of effort summarized in this review must continue to be applied to other mat types. Examples of such mats include those dominated by unicellular cyanobacteria, eukaryotic algae, and nonphotosynthetic bacteria such as sulfide-oxidizing bacteria in deep-sea communities (*e.g.*, Ward *et al.*, 1992; Stal and Caumette, 1994). Mats growing in low-sulfate environments such as lakes, streams, and thermal springs also merit more attention.

Studies of biogeochemical cycling in mats should be broadened to include additional populations of mat microorganisms (*e.g.*, heterotrophs, methanogens, and novel bacteria) that probably contribute substantially to the community. We must better understand how key nutrients such as nitrogen and phosphorus are regenerated and retained by the various types of mats. Mats that coexist with active mineral precipitation (*e.g.*, with calcium carbonate: Fouke *et al.*, 1999; Reid *et al.*, 2000) merit study to help us understand the roles of the microbes in the precipitation of minerals and the impact of mineral formation upon mat biogeochemistry.

Perhaps most promising is the use of gene sequences and gene expression studies to understand the ecology of microbial mat communities. Methods for the identification and interpretation of 16s RNA and other macromolecules are improving rapidly and hold great promise. These phylogenic investigations should be combined with studies of biogeochemistry and gene expression to elucidate the key linkages between microbial populations, processes, and the emergent products and environmental impacts of microbial mats.

Acknowledgments

The preparation of this manuscript was supported by a grant from NASA's Astrobiology Institute. I thank Exportadora de Sal, S. A., for continuing field support at Guerrero Negro, Baja California Sur, Mexico.

Literature Cited

Bebout, B. M., H. W. Paerl, J. E. Bauer, D. E. Canfield, and D. J. Des Marais. 1994. Nitrogen cycling in microbial mat communities: the quantitative importance of N-fixation and other sources of N for primary productivity. Pp. 265–272 in *Microbial Mats*, L.J. Stal and P. Caumette, eds. NATO ASI Series, Vol. G 35. Springer-Verlag, Berlin.

Canfield, D. E., and D. J. Des Marais. 1991. Aerobic sulfate reduction in microbial mats. *Science* **251:** 1471–1473.

Canfield, D. E., and D. J. Des Marais. 1993. Biogeochemical cycles of carbon, sulfur, and free oxygen in a microbial mat. *Geochim. Cosmochim. Acta* **57:** 3971–3984.

D'Amelio, E. D., Y. Cohen, and D. J. Des Marais. 1987. Association of a new type of gliding, filamentous, purple phototrophic bacterium inside bundles of *Microcoleus chthonoplastes* in hypersaline cyanobacterial mats. *Arch. Microbiol.* **147:** 213–220.

Des Marais, D. J., M. Harwit, K. Jucks, J. F. Kasting, J. I. Lunine, D. Lin, S. Seager, J. Schneider, W. Traub, and N. Woolf. 2002a. Remote sensing of planetary properties and biosignatures on extrasolar terrestrial planets. *Astrobiology* **2:** 153–181.

Des Marais, D. J., D. Albert, B. Bebout, M. Discipulo, T. Hoehler, and K. Turk. 2002b. Biogeochemical contrasts between subtidal and intertidal-to-supratidal hypersaline microbial mats (abstract). *Astrobiology Science Conference 2002:* 188. NASA Ames Research Center, Moffett Field; CA.

Des Marais, D. J., B. M. Bebout, S. Carpenter, M. Discipulo, and K. Turk. 2003. Carbon and oxygen budgets of hypersaline cyanobacterial mats: effects of diel cycle and temperature (abstract). *American Society of Limnology and Oceanography, 2003 Annual Meeting*, Salt Lake City.

Fenchel, T., and B. J. Finlay. 1995. *Ecology and Evolution in Anoxic Worlds.* Oxford University Press, Oxford.

Ferry J. G., and R. S. Wolfe. 1976. Anaerobic degradation of benzoate to methane by a microbial consortium. *Arch. Microbiol.* **107:** 33–40.

Fouke, B. W., J. D. Farmer, D. J. Des Marais, L. Pratt, N. C. Sturchio, P. C. Burns, and M. K. Discipulo. 1999. Depositional facies and aqueous-solid geochemistry of travertine-depositing hot springs (Angel Terrace, Mammoth Hot Springs, Yellowstone National Park, USA). *J. Sediment. Res.* **70:** 565–585.

Fründ, C., and Y. Cohen. 1992. Diurnal cycles of sulfate reduction under oxic conditions in cyanobacterial mats. *Appl. Environ. Microbiol.* **58:** 70–77.

Garcia-Pichel, F. 2000. Cyanobacteria. Pp. 907–929 in *Encyclopedia of Microbiology*, 2nd ed., Vol. 1. J. Lederberg, ed. Academic Press, San Diego, CA.

Hoehler, T. M., B. M. Bebout, and D. J. Des Marais. 2001. The role of microbial mats in the production of reduced gases on the early Earth. *Nature* **412:** 324–327.

Javor, B. 1983. Nutrients and ecology of the Western Salt and Exportadora de Sal Saltern brines. Pp. 195–205 in *Sixth International Symposium on Salt*, B. C. Schreiber and H. L. Harner, eds. Salt Institute, Alexandria, VA.

Jørgensen, B. B. 1994. Sulfate reduction and thiosulfate transformations in a cyanobacterial mat during a diel oxygen cycle. *FEMS Microbiol. Ecol.* **13:** 303–312.

Jørgensen, B. B., and D. J. Des Marais. 1986. Competition for sulfide among colorless and purple sulfur bacteria in cyanobacterial mats. *FEMS Microbiol. Ecol.* **38:** 179–186.

Jorgensen, B. B., and D. J. Des Marais. 1988. Optical properties of benthic photosynthetic communities: fiber optic studies of cyanobacterial mats. *Limnol. Oceanogr.* **33:** 99–113.

Jørgensen, B. B., N. P. Revsbech, T. H. Blackburn, and Y. Cohen. 1979. Diurnal cycle of oxygen and sulfide microgradients and microbial photosynthesis in a cyanobacterial mat. *Appl. Environ. Microbiol.* **38:** 46–58.

Jørgensen, B. B., Y. Cohen, and D. J. Des Marais. 1987. Photosynthetic action spectra and adaptation to spectral light distribution in a benthic cyanobacterial mat. *Appl. Environ. Microbiol.* **53:** 879–886.

McInerney, M. J., M. P. Bryant, and N. Pfennig. 1979. Anaerobic bacterium that degrades fatty acids in syntrophic association with methanogens. *Arch. Microbiol.* **122:** 129–135.

Reid, R. P., P. T. Visscher, A. W. Decho, J. Stolz, B. M. Bebout, I. G. MacIntyre, H. W. Paerl, J. L. Pinckney, L. Prufert-Bebout, T. F. Steppe, and D. J. Des Marais. 2000. The role of microbes in accretion, lamination and early lithification of modern marine stromatolites. *Nature* **406:** 989–992.

Revsbech, N. P., B. B. Jørgensen, and T. H. Blackburn. 1983. Microelectrode studies of the photosynthesis and O_2, H_2S, and pH profiles of a microbial mat. *Limnol. Oceanogr.* **28:** 1062–1074.

Schink B. 1988. Principles and limits of anaerobic degradation. Pp. 771–846 in *Biology of Anaerobic Microorganisms*, A. J. B. Zehnder, ed. John Wiley, New York.

Stal, L. J. 1991. The metabolic versatility of the mat-building cyanobacteria *Microcoleus chthonoplastes* and *Oscillatoria limosa* and its ecological significance. *Algol. Stud.* **64:** 453–467.

Stal, L. J., and P. Caumette. 1994. *Microbial Mats; Structure, Development and Environmental Significance.* Series G: Ecological Sciences, Springer-Verlag, Berlin.

Stal, L. J., H. Heyer, S. Bekker, M. Villbrandt, and W. E. Krumbein. 1989. Aerobic-anaerobic metabolism in the cyanobacterium *Oscillatoria limnosa*. Pp. 255–276 in *Microbial Mats. Physiological Ecology of Benthic Microbial Communities*, Y. Cohen and E. Rosenberg, eds. American Society for Microbiology, Washington, DC.

Van Der Oost, J., B. A. Bulhuis, S. Feitz, K. Krab, and R. Kraayenhof. 1989. Fermentation metabolism of the unicellular cyanobacterium *Cyanothece* PCC 7822. *Arch. Microbiol.* **152:** 415–419.

Van Gemerden, H. 1993. Microbial mats: a joint venture. *Mar. Geology* **113:** 3–25.

Visscher, P. T., L. K. Baumgartner, D. H. Buckley, D. R. Rogers, M. Hogan, C. Raleigh, K. Turk, and D. J. Des Marais. 2003. Dimethyl sulfide and methanethiol as biogenic signatures in laminated microbial ecosystems. *Appl. Environ. Microbiol.* (In press).

Ward, D. M., J. Bauld, R. W. Castenholz, and B. K. Pierson. 1992. Modern phototrophic microbial mats: anoxygenic, intermittently oxygenic/anoxygenic, thermal, eukaryotic and terrestrial. Pp. 309–324 in *The Proterozoic Biosphere: A Multidisciplinary Study*, J. W. Schopf and C. Klein, eds. Cambridge University Press, New York.

Zinder S. H. 1993. Physiological ecology of methanogens. Pp. 128–206 in *Methanogenesis: Ecology, Physiology, Biochemistry and Genetics.* J. G. Ferry, ed. Chapman and Hall, New York.

Discussion

QUESTION: As you mentioned, Dave, cylindrical sheaths made of exopolymeric material have within them two populations of organisms that you have proposed might maintain a relationship responsive to diurnal phenomena. Do you think that the mat structure is very heterogeneous, containing clusters of organisms that would, based upon our current understanding, not be expected to co-exist? For example, do some associations between populations protect organisms from harmful products?

DES MARAIS: Yes, I included these examples of associations between populations of organisms to illustrate this point. I think also that this is one of the reasons why Mitch Sogin had me talk early in this meeting; that is, to show that there is, potentially, a long menu of important ecological phenomena that could be addressed by genomic studies. Again, in the example I showed, sulfide is removed in the morning by the anoxygenic phototrophic bacteria, which benefits the cyanobacteria. This example also includes the cross feeding by the cyanobacteria that benefits the anoxygenic phototrophs. Evidence for cross feeding has actually been documented in Yellowstone Park by David Ward. Using isotopic labeling, he observed that photosynthate does flow from cyanobacteria to green non-sulfur bacteria. I think we have demonstrated that sulfide inhibits at least some types of oxygenic photosynthesis in these mats. Also, anoxygenic phototrophs can reduce sulfide levels in natural environments. Another example is that the surface-dwelling microbial populations screen the deeper ones from UV and shorter wavelengths that would be injurious to their photosynthetic apparatus. Dick Castenholz, Ferran Garcia-Pichel and others have documented this extensively.

QUESTION: I am wondering whether other organisms are sequestered in a way that enhances certain processes. You presented

measurements of very high rates of sulfate reduction. Are the high rates possible because sulfate-reducing bacteria are protected by other organisms that you are just not observing directly?

DES MARAIS: I will defer to Dave Stahl to discuss current studies of bacterial sulfate reduction that occurs in the presence of molecular oxygen. But, some ten years ago, Don Canfield and I probed extensively, with electrodes, for anoxic micro-environments within the oxygenated photic zone of cyanobacterial mats. In these mat porewaters, oxygen diffuses some 50 to 100 microns in just a few seconds, and so we spaced our electrode sampling profiles about one mm apart. But we just couldn't find anoxic microenvironments. However, even though oxygen is a strong oxidant, the rate at which it oxidizes other substances is not as fast as the rates of some other oxidants, such as radicals, etc. Perhaps the deleterious oxidation reactions involving oxygen are mitigated by faster reactions carried out by reductants such as hydrogen. Relatively fast-acting reducing compounds in the mats might confer the advantage that the sulfate-reducing bacteria need to maintain these very high rates in the presence of oxygen. So, the relative rates of reactions, as well as mechanisms of physical protection, might play key roles in these mat communities.

QUESTION: What about migration? There is another dynamic with biota moving in response to chemical gradients.

DES MARAIS: What I find interesting is that some populations migrate, whereas others don't even under circumstances where migration would seem to benefit both of these populations. For example, microorganisms can migrate vertically within cyanobacterial mats in response to changes in the depth of oxygen and light penetration, which can vary diurnally by a few mm. *Beggiatoa* are nonphotosynthetic bacteria that oxidize sulfide with oxygen, and so it is advantageous for them to occupy zones where both sulfide and oxygen coexist. But, there are different diameters of *Beggiatoa*, and I recollect that the ones having smaller diameters tend to be much more mobile than the big ones. Also, some photosynthetic populations, particularly purple sulfur bacteria, have been observed to migrate. How does the community select between populations that migrate as conditions change, *versus* the more stationary populations?

There are examples of two environmental cues for migration that appear be in conflict with each other. What causes *Beggiatoa* to migrate downward after sunrise? Is it the light or is it the oxygen and sulfide chemical gradients? It can't be just an avoidance response to high oxygen concentrations. When *Beggiatoa* is still at the surface in the morning, bathed in sunlight, oxygen production is starting beneath it. At some point, *Beggiatoa* must dive down through an oxygen rich zone to get down to the darker sulfide-oxygen interface that is most suitable during the daytime. So the question "What are all of the cues that drive these organisms to migrate?" is both an important question and one that is still in search of definitive answers.

Reference: *Biol. Bull.* **204:** 168–173. (April 2003)

Complexity in Natural Microbial Ecosystems: The Guerrero Negro Experience

JOHN R. SPEAR, RUTH E. LEY, ALICIA B. BERGER, AND NORMAN R. PACE*

Department of Molecular, Cellular and Developmental Biology, University of Colorado, Boulder, 347 UCB, Boulder, Colorado 80309

The goal of this project is to describe and understand the organismal composition, structure, and physiology of microbial ecosystems from hypersaline environments. One collection of such ecosystems occurs at North America's largest saltworks, the Exportadora de Sal, in Guerrero Negro, Baja California Sur. There, seawater flows through a series of evaporative basins with an increase in salinity until saturation is reached and halite crystallization begins. Several of these ponds are lined with thick (10 cm) microbial mats that have received some biological study. To determine the nature and extent of diversity of the microbial organisms that constitute these ecosystems, we are conducting a phylogenetic analysis using molecular approaches, based on cloning and sequencing of small subunit (SSU) rRNA genes (16S for Bacteria and Archaea, 18S for Eukarya). In addition, we report preliminary results on the microbial composition of a laminated community that occurs in a crystallized gypsum-halite matrix in near-saturated salt water. Exposure of the interior of these large (kilogram) wet, endoevaporite crystals reveals a multitude of colors: layers of yellow, green, pink, and purple microbiota. To date, analyses of these two environments indicate the ubiquitous dominance of uncultured organisms of phylogenetic kinds not generally thought to be associated with hypersaline environments.

*To whom correspondence should be addressed. E-mail: nrpace@colorado.edu

The paper was originally presented at a workshop titled *Outcomes of Genome-Genome Interactions.* The workshop, which was held at the J. Erik Jonsson Center of the National Academy of Sciences, Woods Hole, Massachusetts, from 1-3 May 2002, was sponsored by the Center for Advanced Studies in the Space Life Sciences at the Marine Biological Laboratory, and funded by the National Aeronautics and Space Administration under Cooperative Agreement NCC 2-1266

The Endoevaporite Study

The goals for this portion of the study were to examine the nature of life in the "extreme" environment of an endoevaporite (endo-life within, evaporite-sedimentary rock of precipitating salt deposits), add to what is known about life and where it exists on Earth, and test the application of molecular phylogenetic methods in hypersaline communities. Evaporative salt deposits (evaporites) that contain halite (NaCl), gypsum ($CaSO_4 \cdot 2H_2O$), or anhydrite ($CaSO_4$) are widespread, and are well known in the rock record. These hypersaline conditions are considered by humans to be a "harsh" environment for life (Stolz, 1990; Rothschild *et al.*, 1994; Litchfield, 1998).

Evaporites develop by crystallization from brine of at least 30 g/l NaCl. They are formed by platy deposition of one or more of these minerals in the saturated zone. Expansive pressure from crystal growth within the deposits can break up the plate, producing irregular plates that break the air-water interface and give rise to fins, or teepees (Warren, 1988, 1999). These teepees can extend tens of centimeters above the brine. Teepees of gypsum are porous, and that porosity determines the nature of the endoevaporite, since air, water (brine), and light all have potential for zonation relevant for microbial life. Depending on the crystals present (*e.g.*, halite or gypsum), incoming solar irradiation is heavily attenuated by the translucent crystal lattice. This creates different zones of filtered sunlight where distinct microbial communities can reside (Oren *et al.*, 1995; Vreeland and Powers, 1999). Gypsum needles and clear halite crystals can both act as "light pipes" to diffuse light farther into the evaporative crystal than surface-sun exposure alone. The incoming sunlight is filtered by the crystal matrix to longer wavelengths at greater depth into an endoevaporite. The light may be less accessible to the surface as permeability in the structure changes, porosity decreases,

and permeability changes during early diagenesis (Warren, 1988, 1999).

The endoevaporites used in this study were obtained from the gypsum flats on the south end of the Pond 9 crystallization basin at the Exportadora de Sal, in Guerrero Negro, Baja California Sur. Hectares of teepee-like structures rise out of this saturated gypsum crust and are clearly visible. When pieces of teepees are broken off and viewed in cross section, laminated colors are apparent. The surface exposed to the sun has a white or brown salt crystal color; a bright yellow, 1-cm-thick layer is next; followed by a 1-cm-thick green layer; then a 1-cm-thick pink-to-purple layer; and finally a black core in the interior of the crystals. Light microscopy of these layers shows that most of the cells are either in the pore spaces between salt crystals or enveloping the crystals, possibly as complex biofilms. Little is known about how the microbial colonization of the evaporite occurs. Potential mechanisms presumably are cellular transport by incoming seawater *via* pond flow; groundwater infiltration; air transport and deposition, and animal transport and deposition. X-ray diffraction studies of these particular crystals have revealed that the outer layers of the evaporite—the yellow and green layers—, are primarily composed of gypsum, with a trace of halite. The pink layer and the inner core are primarily halite.

This stratification indicates that different microbes are responsible for the colors. This study then asks several questions: Are there few or many different kinds of microbes present? Is this the province of Archaea—thought to be the more "extreme" of the three domains of life? What kinds of life can thrive in this "extreme" environment? Does photosynthesis provide primary productivity for the entire community? Does the microbiota contribute to crystal formation?

The basic methods employed in this study involved the determination of ribosomal RNA sequences present in the ecosystems. Samples were acquired in the field and transported to the laboratory, where community genomic DNAs were isolated. Amplification by PCR with various universal and domain-specific primers for the 16S or 18S rRNA gene was followed by cloning of the product to separate individual rRNA genes. This process provided a library of signatures, the rRNA sequences or "phylotypes," for the organisms that compose the communities (for methods see Reysenbach *et al.*, 1994; Pace, 1997, 2001; Hugenholtz *et al.*, 1998a, b). Although this molecular approach to the identification of the makeup of natural ecosystems is complex and fraught with complications, it has afforded the first glimpse of environmental diversity without culturing the organisms.

Results to date have revealed that the endoevaporite environment harbors high biological diversity. Table 1 describes the bacterial phylotypes revealed by analysis of several hundred rRNA gene clones from the three pigmented strata of the evaporite crystals. The uppermost yellow layer contains about 25% cyanobacteria, dominated by a *Euhalothece* sp. Sequences were compared with the Basic Local Alignment Search Tool (BLAST)(Altschul *et al.*, 1990). None of the sequences are identical to any others in the rRNA sequence databases. However, in accordance with

Table 1

Bacteria from endoevaporite

Closest Relative by BLAST	% Identity	Layer		
		Yellow	Green	Pink
CFB group; Rhodothermus group; Salinibacter	92–97	46	25	37
Firmicutes; Bacillus/Clostridium group	85–90			15
Proteobacteria; alpha subdivision; Rhodobacter	90–95	15	14	7
Proteobacteria; delta subdivision; Desulfobacter	90–97		8	19
Proteobacteria; gamma subdivision; Chromatiaceae	85–90		19	7
Proteobacteria; epsilon subdivision	90–93			4
Bacteria; Green sulfur bacteria	95–97			4
Cyanobacteria; Chroococcales; Halothece cluster	97–100	23	22	4
Bacteria; Planctomycetales	90–95	8	3	
Other; Environmental Sample or Clone	80–88	8	9	3
Unique = RFLP Patterns sequenced		13	37	27
Screened = # of clones		48	144	96

Numbers under the three layers reflect % of sequences that match the closest relative as determined with the Basic Local Alignment Search Tool (BLAST)(Altschul *et al.*, 1990). Percent identity reflects the range of identity that sequences from the endoevaporite correspond to known sequences by pairwise BLAST comparison. Unique numbers reflect the number of unique patterns sequenced as determined by restriction fragment length polymorphism analysis (RFLP). Screened numbers reflect number of clones considered per library. The universal bacterial primers 8F(5′-AGAGTTTGATCCTGGCTCAG-3′) and 1492R (5′-GGTTACCTTGTTACGACTT-3′) were used to develop the libraries.

Stackebrandt and Goebel (1994), we consider an rRNA sequence identity of 97% or above to represent organisms of the same species. The predominant species in this and the deeper layers are representatives of the Cytophaga/Flexibacter/Bacterioides (CFB) group of Bacteria, with a dominant *Salinibacter ruber*-like organism. Other bacterial divisions identified here by sequence type include uncultivated *Planctomyces* spp. and *Rhodobacter* spp., the latter representatives of the α-Proteobacteria.

The green layer also contains about 25% cyanobacteria, mainly *Euhalothece* sp. and *Cyanothece* sp. Along with a large percentage of CFB phylotypes, α-Proteobacteria occur, as do a diverse set of δ-Proteobacteria, several of which are closely related to anaerobic sulfate-reducing organisms. Presence of these organisms, along with the occurrence of diverse γ-Proteobacteria, dominantly represented by *Alcalilimnicola halodurans*, an extremely halotolerant anaerobe, indicate that anaerobic metabolisms may occur in conjunction with cyanobacterial oxygenic photosynthesis. With further light attenuation, the underlying pink layer contains very few cyanobacteria, a large percentage of CFB (30% by sequence), and a large number of uncultivated δ-Proteobacteria phylotypes. A general anaerobic theme of metabolism appears to dominate the innermost layers of the endoevaporite with the addition of both γ-and ε-Proteobacteria, along with *Clostridium* spp., representatives of the Low G + C gram-positive bacterial division.

We used an Archaea-specific PCR primer set (333Fa, 5′-TCCAGGCCCTACGGG-3′ and 1391R, 5′-GACGGGCGGTGWGTRCA-3′) (Lane, 1991) with the DNA extracts from the endoevaporitive layers and found surprisingly less diversity of Archaea in terms of numbers and kinds of sequences than we found with bacterial primers. All three layers examined in the endoevaporite contained a large number of archaeal phylotypes that are closely related to *Halobacterium* sp. (50% to 75% of sequences, depending on layer). Additionally, a few methanogens were encountered in all three layers. Interestingly, of about 400 clones screened, not one representative of Crenarchaeota was encountered; all were representatives of Euryarchaeota. As often seen (Spear, unpubl.), the archaeal primer set also provided some phylotypes representative of the bacterial domain, including members of the CFB group, *Bacillus* spp., α-Proteobacteria, and the spirochete phylogenetic division. Some of this bacterial diversity was not captured with the bacterial primers.

Conclusions of Endoevaporite Study

From the DNA sequences obtained in this study, we find that the microbial diversity is high within these evaporative salt crystals. This is indicated by the numbers and kinds of sequences revealed by the application of both bacterial and archaeal PCR primers. Of note is the fact that the archaeal primers yielded several bacterial sequences, but not *vice versa*. This indicates the importance, in any molecular microbial ecological study of any environment, of using different sets of PCR priming pairs. Considering the broad diversity of life seen in this environment, it is likely that multiple mechanisms, from oxygenic photosynthesis to heterotrophic metabolisms, allow for life in saturated salt. In addition, it is likely that there is widespread use of some mechanism—a major osmotica such as intracellular potassium chloride, magnesium chloride, or glycine betaine—to tolerate the saturated salt conditions. Indeed, as indicated by the diverse organisms seen herein, the ability to either live in or adapt to hypersaline environments is probably more widespread in both the bacterial and archaeal domains than previously thought. The protection afforded these organisms by their localization within the endoevaporite environment expands the habitable zone of life on this planet and potentially elsewhere in the solar system.

The Microbial Mat Study

The primary goal of this study was to identify organisms in the "extreme" environment of hypersaline microbial mats by using the phylogenetic method. A second goal was to determine the biochemical basis of this extremely complex ecosystem by correlating discovered phylotypes with the known or measured physical and chemical properties of the mats. Correlations of biological and chemical information are currently restricted because there has been no comprehensive survey of the kinds of organisms that compose these hypersaline mats. Such mats occur globally and have been studied, especially chemically, as model systems for early life (Jørgensen *et al.*, 1983; Cohen, 1984; D'Amelio D'Antoni *et al.*, 1989; Jørgensen, 1989; Des Marais, 1995; Hoehler *et al.*, 2001).

Certainly some of the most remarkable examples of hypersaline microbial mats on Earth occur in the evaporative basins of the Exportadora de Sal, long studied by Des Marais and co-workers (Holser *et al.*, 1981; Canfield and Des Marais, 1993; Des Marais, 1995). Several teams of the Ecogenomics Focus Group of the National Aeronautics and Space Administration (NASA) Astrobiology program are working together to understand this hypersaline ecosystem more completely. A description of the microbiota of this environment, obtained through analysis of their molecular phylotypes, will provide us with some understanding of the microbial complexity and with a biological context through which to understand the chemical processes of the ecosystems. We are conducting such a survey of organisms present both in *in situ* and in *ex situ* settings (mats collected from these environments are being maintained in a greenhouse at the NASA-Ames Research Center, Moffett Field, California). The particular natural setting is Pond 4 near Pond 5, in the Guerrero Negro saltworks (see also Des Marais, 2003).

For this molecular study, we obtained samples as cores, pooled locations within different cores, froze samples in the field on liquid nitrogen, and then subjected the samples to molecular analyses in the laboratory as outlined above.

We began the study with *ex situ* mats maintained in the NASA-Ames greenhouse environment. Table 2 tabulates the diversity observed with the application of several different PCR primer pairs to genomic DNA extracted from the top 2 mm and the 2–4-mm section of the mat. Four clone libraries were examined with four different primer pairs—three bacterial and one archaeal. We encountered a tremendous amount of diversity in the mat, and found that, surprisingly, rRNA sequences representative of cyanobacteria are outnumbered 3:1 by, among others, the green nonsulphur (GNS) bacteria. This result was seen with three different bacterial PCR primer pairs. With the archaeal primer pair we found several diverse methanogens, halophytic Euryarchaeota and, unlike in the case of the endoevaporite, several sequences representative of Crenarchaeota. Different phylotypes, but overlapping phylogenetic groups, occurred in the 2–4-mm section and the very bottom of the mat (not shown). Profiles of oxygen *versus* depth show that anoxic conditions occur immediately below the surface of the mat, and we find that rRNA sequences characteristic of anaerobic bacteria are abundant there, including δ-Proteobacteria, clostridia, spirochetes, GNS representatives, and others. Additionally, we encountered a number of rRNA phylotypes with less than 85% identity to known sequences using BLAST analysis (Altschul *et al.*, 1990).

Table 2

Phylogenetic distribution of rRNA gene sequences from an ex situ *(greenhouse maintained) Guerrero Negro hypersaline microbial mat*

Bacterial Division	Top 2 mm	2–4 mm
Green Nonsulfur	29.8	25.0
Proteobacteria; alpha subdivision	20.0	17.5
Proteobacteria; delta subdivision	1.3	17.5
Proteobacteria; gamma subdivision	7.5	7.5
CFB group; Flavobacteria	11.3	8.7
Cyanobacteria; Oscillatoriales	7.2	4.0
Thermus/Deinococcus group	11.3	9.0
Verrucomicrobia	3.8	3.0
Candidate Division OP11	1.3	1.3
Spirochaetales	1.3	1.3
Planctomycetales	1.3	1.3
Candidate division KSA2	1.3	1.3
Candidate Division OP 10 or OP 12	1.3	1.3
Unknown	1.3	1.3
	$n = 80$	$n = 80$

As described in the text, PCR with bacteria-specific primers was used to develop clone libraries from extracted environmental DNA obtained from mat layers indicated. Sequence analysis of cloned rRNA genes provided identities of the sequences, which correspond to representatives of the phylogenetic groups tabulated. Numbers reflect percent of sequences; n is number of clones screened.

We also surveyed for eukaryotes by amplification with eukaryote-specific PCR primers (515F, 5′-GTGCCAGC-MGCCGCGGTAA-3′ and 1195RE, 5′-GGGCATCACA-GACCTG-3′) (Lane, 1991; Dawson and Pace, 2002) on environmental DNA from the bottom 2 mm of the greenhouse mat. The kinds of organisms detected from analysis of about 200 clones screened included Stramenopiles, 28%; Nematoda, 20%; Arthopoda, 20%; Alveolates, 12%; Acantharea, 12%; and Crenarchaeota, 8%. As found in both marine and freshwater sediments (Dawson and Pace, 2002), the extent of novel eukaryal diversity in the greenhouse hypersaline microbial mat appears to be enormous.

Molecular phylogenetic studies are currently underway to examine the microbial diversity in the naturally occurring mats. Preliminary findings are similar to those seen with the greenhouse mat, again, with a 3:1 proportion of green nonsulfur bacteria to cyanobacteria. In addition, comparison of the uppermost portion of the mat between day and night indicates that a number of bacterial phylotypes appear to migrate within the mat. For instance, δ-Proteobacteria (*e.g.*, relatives of anaerobic sulfate-reducing bacteria) are present in the upper layer during the day but are absent at night. The converse is found for both α-and γ-Proteobacteria. These results are from an early analysis of about 150 sequences; a more complete study of 2000 sequences from all layers within the mat is in progress. In general there are few differences between the *in situ* mats and those maintained in the greenhouse. We find it remarkable that a complex community such as this can be maintained away from the native environment (Bebout *et al.*, 2002).

Conclusions of Microbial Mat Study

The results presented here are clearly preliminary. Work is ongoing in our laboratory to describe in much greater detail the diversity of life of all three phylogenetic domains, throughout the depth of the Guerrero Negro mats. Early results (for example, the large proportion of GNS phylotypes) await confirmation. Work has shown that there is little difference between the kinds of organisms in *in situ* and greenhouse-maintained mats. Additionally, the variability in numbers of different kinds of organisms at different times and different depths in the mats is extensive, indicating an enormous level of complexity within the mats and individual strata. In the more "simple" ecosystem of the endoevaporative crystals, the same holds true. To resolve even some of this complexity will require the analysis and sequencing of thousands of clones, until some level of repetition is observed. Collectively, the results indicate that the diversity of microbial life is rich, even in these seemingly inhospitable hypersaline environments.

Acknowledgments

Funding for this work has been provided by the NASA Astrobiology Program, an NSF Microbiology Postdoctoral Fellowship (J.S.), a NASA Astrobiology Postdoctoral Fellowship (R.L.), and funds for A.B. from the University of Colorado's UROP program and the Boettcher Foundation. We thank members of the Pace Lab for thoughts and critiques of this manuscript. We also thank the two anonymous reviewers for their insightful and helpful comments. We gratefully acknowledge all the members of the Ecogenomics Focus Group of the NASA Astrobiology Institute for assistance in the field.

Literature Cited

Altschul, S. F., W. Gish, W. Miller, E. W. Myers, and D. J. Lipman. 1990. Basic local alignment search tool. *J. Mol. Biol.* **215:** 403–410.

Bebout, B. M., S. P. Carpenter, D. J. Des Marais, M. Discipulo, T. Embaye, F. Garcia-Pichel, T. M. Hoehler, M. Hogan, L. L. Jahnke, R. M. Keller, S. R. Miller, L. E. Prufert-Bebout, C. Raleigh, M. Rothrock, and K. Turk. 2002. Long-term manipulations of intact microbial mat communities in a greenhouse collaboratory: simulating Earth's present and past field environments. *Astrobiology.* **2:** 383–402.

Canfield, D. E., and D. J. Des Marais. 1993. Biogeochemical cycles of carbon, sulfur, and free oxygen in a microbial mat. *Geochim. Cosmochim. Acta* **57:** 3971–3984.

Cohen, Y. 1984. The Solar Lake cyanobacterial mats: strategies of photosynthetic life under sulfide. Pp. 133–148 in *Microbial Mats: Stromatolites,* Y. Cohen, R.W. Castenholz, and H.O. Halvorson, eds. Alan R. Liss, New York.

D'Amelio D'Antoni, E., Y. Cohen, and D. J. Des Marais. 1989. Comparative functional ultrastructure of two hypersaline submerged cyanobacterial mats: Guerrero Negro, Baja California Sur, Mexico, and Solar Lake, Sinai, Egypt. Pp. 97–113 in *Microbial Mats: Physiological Ecology of Benthic Microbial Communities,* Y. Cohen and E. Rosenberg, eds. American Society for Microbiology, Washington DC.

Dawson, S. C., and N. R. Pace. 2002. Novel kingdom-level eukaryotic diversity in anoxic sediments. *Proc. Natl. Acad. Sci. USA* **99:** 8324–8329.

Des Marais, D. J. 1995. The biogeochemistry of hypersaline microbial mats. *Adv. Microbiol. Ecol.* **14:** 251–274.

Des Marais, D. J. 2003. Biogeochemistry of hypersaline microbial mats illustrates the dynamics of modern microbial ecosystems and the early evolution of the biosphere. *Biol. Bull.* **204:** 160–167.

Hoehler, T. M., B. M. Bebout, and D. J. Des Marais. 2001. The role of microbial mats in the production of reduced gases on the early Earth. *Nature* **412:** 324–327.

Holser, W. T., B. Javor, and C. Pierre. 1981. Geochemistry and ecology of salt pans at Guerrero Negro, Baja California. Field Trip #1, Geological Society of America, Cordilleran Section, 1981 Annual Meeting. Geological Society of America, Boulder, Colorado.

Hugenholtz, P., C. Pitulle, K. L. Hershberger, and N. R. Pace. 1998a. Novel division level bacterial diversity in a Yellowstone hot spring. *J. Bacteriol.* **180:** 366–376.

Hugenholtz, P., B. M. Goebel, and N. R. Pace. 1998b. Impact of culture-independent studies on the emerging view of bacterial diversity. *J. Bacteriol.* **180:** 4765–4774.

Jorgensen, B. B. 1989. Light penetration, absorption, and action spectra in cyanobacterial mats. Pp. 123–137 in *Microbial Mats: Physiological Ecology of Benthic Microbial Communities,* Y. Cohen and E. Rosenberg, eds. American Society for Microbiology, Washington DC.

Jorgensen, B. B., N. P. Revsbech, and Y. Cohen. 1983. Photosynthesis and structure of benthic microbial mats: microelectrode and SEM studies of four cyanobacterial communities. *Limnol. Oceanogr.* **28:** 1075–1093.

Lane, D. J. 1991. 16S, 23S rRNA sequencing. Pp. 115–175 in *Nucleic Acid Techniques in Bacterial Systematics,* E. Stackebrandt and M. Goodfellow, eds. John Wiley and Sons, New York.

Litchfield, C. D. 1998. Survival strategies for microorganisms in hypersaline environments and their relevance to life on early Mars. *Meteorit. Planet. Sci.* **33:** 813–819.

Oren, A., M. Kuhl, and U. Karsten. 1995. An endoevaporitic microbial mat within a gypsum crust: zonation of phototrophs, photopigments, and light penetration. *Mar. Ecol.* **128:** 151–159.

Pace, Norman R. 1997. A molecular view of microbial diversity and the biosphere. *Science* **276:** 734–740.

Pace, Norman R. 2001. The universal nature of biochemistry: *Proc. Natl. Acad. Sci. USA* **98:** 805–808.

Reysenbach, A.-L., G. S. Wickham, and N. R. Pace. 1994. Phylogenetic analysis of the hyperthermophilic pink filament community in Octopus Spring, Yellowstone National Park. *Appl. Environ. Microbiol.* **60:** 2113–2119.

Rothschild, L. J., L. J. Giver, M. R. White, and R. L. Mancinelli. 1994. Metabolic activity of microorganisms in evaporites. *J. Phycol.* **30:** 431–438.

Stackebrandt, E., and B. M. Goebel. 1994. Taxonomic note: A place for DNA-DNA reassociation and 16S rRNA sequence analysis in the present species definition in bacteriology. *Int. J. Syst. Bacteriol.* **44:** 846–849.

Stolz, J. F. 1990. Distribution of phototrophic microbes in the flat laminated microbial mat at Laguna Figueroa, Baja California, Mexico. *Biosystems* **23:** 345–358.

Vreeland, R. H., and D. W. Powers. 1999. Considerations for microbiological sampling of crystals from ancient salt formations. Pp. 53–73 in *Microbiology and Biogeochemistry of Hypersaline Environments,* A. Oren, ed. CRC Press, Boca Raton, FL.

Warren, J. K. 1988. *Evaporite Sedimentology.* Prentice-Hall, Englewood Cliffs, NJ.

Warren, J. K. 1999. *Evaporites: Their Evolution and Economics.* Blackwell Science, Malden, MA.

Discussion

SPEAR: Dr. Linda Amaral Zettler asked whether the eukaryotic signal extends down to the bottom of the mat, whether the oxygen concentration varies with depth, and whether that concentration is affected by nematodes boring in the mat. First, the eukaryotic signal extends to all levels of the mat, and Berger is leading the ongoing characterization of the diversity and vertical range of

eukaryotes living within the mat. Second, the work of others in the Ecogenomics Focus Group (Miller, Bebout, DesMarais, and Hoehler) indicates that the oxygen profile, as measured with microelectrodes, stays relatively constant during the day: *i.e.*, oxic on the surface, declining to anoxia by 2–3 mm into the mat, and with very little oxygen present in the mat at night. Finally, the number and diversity of nematode sequences that we have obtained to date is sufficiently large that the effect of these animals on the functioning of the microbial mat must be considered. Nematode boring must surely have some deleterious effect on the mat, particularly at the microscopic scale of resolution. However, the mats have the look and feel of human tissue, like a liver; and as a human liver can regenerate when injured, the microbial mats can also recover relatively quickly from microscopic disturbances.

Reference: *Biol. Bull.* **204:** 174–179. (April 2003)

Modeling Microbial Consortiums as Distributed Metabolic Networks

JOSEPH J. VALLINO

Ecosystems Center, Marine Biological Laboratory, Woods Hole, Massachusetts 02543

Biogeochemistry is the study of how living systems in combination with abiotic reactions process and cycle mass and energy on local, regional, and global scales (Schlesinger, 1997). Understanding how these biogeochemical cycles function and respond to perturbations has become increasingly important, as anthropogenic impacts have significantly altered many of these cycles (Galloway and Cowling, 2002; Houghton et al., *2002). Biogeochemistry is strongly governed by microbial processes, and it appears to closely follow thermodynamic constraints in that electron acceptor (O_2, NO_3^-, SO_4^{2-},* etc.*) utilization closely follows* a priori *expectations based on energetics (Vallino* et al., *1996; Hoehler* et al., *1998; Jakobsen and Postma, 1999; Amend and Shock, 2001). Consortiums of microorganisms seem to have evolved to exploit chemical potentials wherever they exist in the environment, as manifested by the recent discovery of anaerobic methane oxidation by sulfate (Boetius* et al., *2000) or sulfide oxidation by nitrate (Schulz* et al., *1999). Three and a half billion years of natural selection have produced living systems capable of degrading most chemical potentials. We may therefore ask: If all ecosystem niche space is filled, is the biogeochemistry we observe in the environment dependent on the organisms that occupy that environment, or is the biogeochemistry determined by fundamental forces, with the evolution of living systems being the implementation of those forces? Recent developments in nonequilibrium thermodynamics (NET) are beginning to support the latter alternative, and advances in genomics are allowing us to explore microbial consortiums in detail. Taking advantage of ideas being suggested by NET, we have developed a modeling framework that views microbial consortiums as an inter-species distributed metabolic network. When combined with experimental observations, the model should help us test hypotheses that govern how living systems function.*

E-mail: jvallino@mbl.edu

The paper was originally presented at a workshop titled *Outcomes of Genome-Genome Interactions*. The workshop, which was held at the J. Erik Jonsson Center of the National Academy of Sciences, Woods Hole, Massachusetts, from 1-3 May 2002, was sponsored by the Center for Advanced Studies in the Space Life Sciences at the Marine Biological Laboratory, and funded by the National Aeronautics and Space Administration under Cooperative Agreement NCC 2-1266

The main challenge to understanding microbial biogeochemistry is understanding the complex, but mostly cooperative, metabolism that develops among organisms that orchestrate biogeochemical cycles. Consider, for example, the metabolism found in the rumen of ruminant organisms such as cows (Madigan *et al.*, 2000). The ecosystem of the rumen develops dozens of functional groups consisting of hundreds of species that degrade cellulose and starch to many intermediate organic acids and alcohols, as well as to CO_2, methane, and hydrogen. Many of these organisms cannot survive without the presence of others. For instance, ethanol fermentation to acetate and H_2 is unfavorable due to the accumulation of H_2, which is also toxic to many organisms. However, if the fermenting organisms are coupled with methanogens (*i.e.*, syntrophy), the overall reactions can proceed, and are very efficient (Jackson and McInerney, 2002). Furthermore, these systems are controllable, hence predictable, as the host organism is able to utilize a food source that it is not capable of digesting without the organisms in its rumen. What governs the development of this biochemistry? Interestingly, no one organism conducts all these biochemical transformations. Instead, the overall metabolism of the system is distributed across hundreds of different microbial species. Yet the system is well coordinated due to multiple levels of organization and multiple levels of proliferation, not by Darwinian selection (Caldwell *et al.*, 1997). Can this enigmatic coordination be explained by nonequilibrium thermodynamics?

Nonequilibrium Thermodynamics

The application of thermodynamics to living systems dates back to Schrödinger (1944) and his examination of the creation of order from disorder. Although at first it appears that living systems violate the second law of thermodynamics in that they synthesize order from disorder, Schrödinger solved this problem by turning to nonequilibrium thermodynamics (NET). In an open system, energy flux from outside the system can reduce the system's internal entropy, which is offset by an equal or greater increase in entropy outside the system. Since Schrödinger, many investigators have extended the application of NET to living systems (Prigogine, 1955; Margalef, 1968; Morowitz, 1968) with many recent advances (Allen, 1985; Johnson, 1988; Schneider, 1988; Wiley, 1988; Choi *et al.*, 1999; Jorgensen *et al.*, 2000; Toussaint and Schneider, 1988). Schneider and Kay (1994) succinctly describe the current restatement of the Second Law:

> Thermodynamic systems exhibiting temperature, pressure and chemical equilibrium resist movement away from their equilibrium states. When moved away from a local equilibrium state a system will behave in a way which opposes the applied gradients and moves it back to its local equilibrium attractor. The stronger the applied gradient, the greater the effect of the equilibrium attractor on the system. The more a system is moved from equilibrium, the more sophisticated its mechanisms for resisting being moved from equilibrium. If dynamic and/or kinetic conditions permit, self-organization processes are to be expected. This behaviour is not sensible from a classical second law perspective, but is what is expected given the restated second law. No longer is the emergence of coherent self-organizing structures a surprise, but rather it is an expected response of a system as it attempts to resist and dissipate externally applied gradients which would move the system away from equilibrium.

Dissipative systems need not always operate at an optimum (Ulanowicz, 1997), because perturbations can reduce system organization, which will result in slower gradient degradation. For example, a perturbation of significant magnitude can destabilize the rumen microbial system and kill the host organism. If the feed changes abruptly from cellulose (grasses) to starch (grains), the organization of the microbial system can collapse due to a rapid increase in the bacteria that produce lactic acid, thus causing acidosis. Interestingly, if the feed is gradually changed, destabilization does not occur. Such phenomena are the essence of self-organization, which occurs in many autocatalytic systems (Ulanowicz, 1997).

Simple examples of the restated second law abound. For example, a chamber of gas isolated from any energy gradients soon reaches equilibrium in which the gas molecules are uniformly distributed (*i.e.*, its highest entropy state). If the chamber is placed within a thermal gradient, the molecular gas distribution is no longer uniform, but shows increased order since a higher density of molecules will reside near the cold end of the chamber. Hence, the thermal gradient has lowered the internal entropy of the chamber. Once more, if the thermal gradient is sufficiently strong, a density-driven circulation will develop, further increasing system order, while reducing system entropy. This self-organization can also be seen in hurricanes, which are the organized structures that develop to facilitate degradation of the thermal gradient that has built up between the atmosphere and ocean over the summer. In an analogous manner, living systems are the organized structures that develop to degrade incoming solar radiation and chemical potential. Indeed, by examining emitted thermal radiation, Schneider and Kay (1994) have found that mature forests degrade incoming solar radiation more effectively than early successional forests or arid land.

The observation that ecosystem function may be governed by laws that transcend Darwinian selection is not new. Many theories related to, or derived from, NET have been developed to describe objective functions living systems tend to follow; however, the choice of an appropriate objective function still remains controversial. This is understandable, since current theories of NET apply only to linear approximations in the neighborhood of an equilibrium (Onsager, 1931; Prigogine, 1978). Theories for systems far from equilibrium are still under development. As a result, objective functions that ecosystems might track are numerous, and include optimizations of exergy (Jørgensen, 1994; Nielsen, 1995, Jorgensen *et al.*, 2000) emergy (Odum, 1983), ascendancy (Ulanowicz, 1986), power (Odum and Pinkerton, 1955; Odum, 1971), biomass to maintenance (Margalef, 1968), thermodynamic efficiency (Nielsen and Ulanowicz, 2000), or entropy (Prigogine and Nicolis, 1971). As NET theories develop, perhaps many of these observations and theories will be collapsed or falsified.

Our objective is to develop a modeling framework that can be used to test these various objective hypotheses, but we must first have a basis for the model. Johnson (1988) argues that the rotational pattern of the earth converts the rectilinear energy output of the sun into a pulsed energy input to the earth, which induces cyclical energy flows, resonance, and time delays. This allows the energy of the system to be pumped up before it decays back towards ground state. Metabolically, this is what we see. Autotrophs use incoming solar radiation to create chemical potential in the form of redox gradients. Material at equilibrium, H_2O and CO_2, is pumped into a high-energy state by its conversion to O_2 (oxidizing) and glucose (reducing). Heterotrophs return this redox gradient to ground state in a cyclical manner. Real ecosystem biogeochemistry is more complex when we include abiotic reactions, anaerobic environments, alternate electron acceptors and donors, nutrient constraints, and transport limitations. Nevertheless, it is the buildup and

Table 1

Reactions used to model planktonic microbial community.

Reaction	Stoichiometry
C-fixation	$6\ CO_2 + 24\ H^+ + 24\ e^- \Leftrightarrow C_6H_{12}O_6 + 6\ H_2O$
NH_4^+ uptake	$NH_4^+ + 0.58\ C_6H_{12}O_6 + 0.034\ SO_4^{2-} + 0.9\ e^- \Leftrightarrow AA + 1.9\ H_2O$
NO_3^- uptake	$NO_3^- + 10\ H^+ + 0.58\ C_6H_{12}O_6 + 0.034\ SO_4^{2-} + 8.9\ e^- \rightarrow AA + 4.9\ H_2O$
Nitrification	$NH_4^+ + 3\ H_2O \rightarrow NO_3^- + 10\ H^+ + 8\ e^-$
N_2 fixation	$\frac{1}{2}\ N_2 + 4\ H^+ + 0.58\ C_6H_{12}O_6 + 0.034\ SO_4^{2-} + 3.9\ e^- \rightarrow AA + 1.9\ H_2O$
Photosynthesis	$2\ H_2O \rightarrow O_2 + 4\ H^+ + 4\ e^-$
Respiration	$O_2 + 4\ H^+ + 4\ e^- \rightarrow 2\ H_2O$
Protein	$AA + (Protein)_n \Leftrightarrow (Protein)_{n+1} + H_2O$
Chlorophyll	$4\ AA + 6.8\ C_6H_{12}O_6 + Mg^{2+} + 46.2\ H^+ + 48.6\ e^- \Leftrightarrow Chl + 42.3\ H_2O + 0.14\ SO_4^{2-}$
Lipids	$8\ C_6H_{12}O_6 + PO_4^{3-} + 92\ H^+ + 89\ e^- \Leftrightarrow C_{48}H_{96}O_6P + 46\ H_2O$
Glycogen	$C_6H_{12}O_6 + (C_6H_{10}O_5)_n \Leftrightarrow (C_6H_{10}O_5)_{n+1} + H_2O$
DNA/RNA	$4\ AA + 2\ PO_4^{3-} \Leftrightarrow DNA + 0.73\ C_6H_{12}O_6 + 0.14\ SO_4^{2-} + 1.9\ H_2O + 1.9\ H^+ + 7.5\ e^-$

Abbreviations: AA, amino acids ($C_{3.5}H_{7.1}O_{1.7}NS_{0.034}^{0.03+}$); Chl, chlorophyll ($C_{55}H_{72}O_5N_4Mg$); Protein ($C_{3.5}H_{5.1}O_{0.7}NS_{0.034}^{0.03+}$); DNA ($C_{9.6}H_{14}O_8N_4P_2$). Reactions are either reversible (⇔) or irreversible (→).

decay of redox potential *via* a distributed metabolism that forms the cornerstone of our approach. We focus on microbial systems because these systems exhibit the greatest degree of metabolic capacity, are responsible for the majority of biogeochemistry on earth, display fast dynamics that allows for practical experiments, and are less susceptible to loss of diversity.

Thermodynamically Constrained Metabolic Biogeochemical Model

A traditional reductionist biogeochemical model would include differential equations for growth of each microbial functional group, equations for Monod-type growth kinetics, and numerous conditional statements to direct the use of

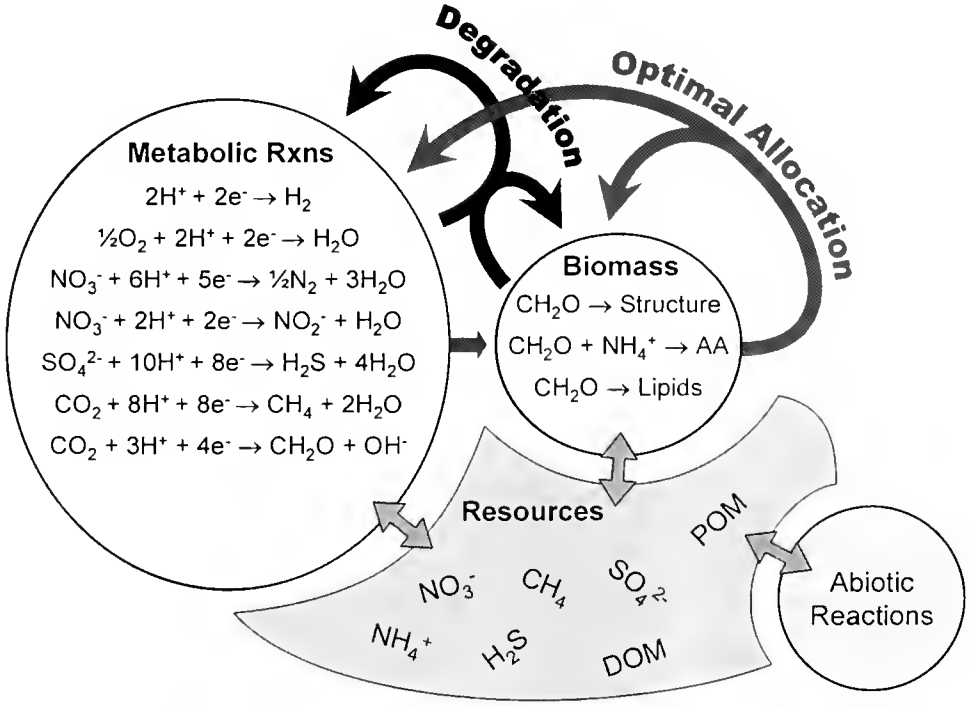

Figure 1. Conceptualization of the metabolic biogeochemistry model. Half reactions lead to production of protein (and other building-block constituents), which is then allocated to reactions governed by an optimization function. Abiotic reactions are incorporated with standard kinetics.

Table 2

Governing equations for the thermodynamically constrained biogeochemistry model

Constraint	Equation
Free energy	$\Sigma_i r_i \Delta G_i$
Redox	$\Sigma_i r_i e_i^- = 0$
Biomass composition	$C{:}N^{Lower} \leq \frac{\Sigma R^C(r_i)}{\Sigma R^N(r_i)} \leq C{:}N^{Upper}$
Reaction kinetics	$r_i \leq E_i f_i(S) \quad \forall i$
Enzyme allocation	$\Sigma_i E_i = E_T$ and $\left.\frac{dE_i}{dt}\right\|_{Min} \leq \frac{dE_i}{dt} \leq \left.\frac{dE_i}{dt}\right\|_{Max}$
Photosynthesis	$r_P \leq \frac{PAR(t)}{h} \frac{1}{\Delta G_{rP}} \frac{[Chl]}{[Chl] + k_{sat}}$
LP Problem	$\underset{r_i E_i}{\text{Maximize}} \Sigma_{i,j} R^C(r_i, E_j) + R^N(r_i, E_j)$

Definitions: r_i are reaction rates (Table 1); e_i are electron-pair transfers associated with reaction i; E_i is concentration of enzyme allocated to reaction i, and E_T is the total protein concentration: R^C and R^N are the subset of reactions (r_i) that lead to C and N accumulation in living biomass, respectively; $f_i(S)$ are functions that describe uptake kinetics of substrate S, such as Michaelis-Menten; PAR(t) is the photosynthetic active radiation; h is water column depth; and r_p is the rate of photosynthesis (Table 1). Solution of the linear programming (LP) problem gives r_i and E_i at time t, which are used in standard C and N conservation equations to obtain solution of state variables over time. See Vallino *et al.* (1996) for a more thorough development.

the various electron donor and acceptor resources that exist within the environment (Koelmans *et al.*, 2001). While this approach has been useful for well-defined laboratory experiments with a few species growing on a limited number of well-defined substrates, it is not practical for extension to more diverse microbial ecosystems with numerous or ill-defined substrates. Reductionist-based biological models fail to incorporate the governing laws that define living systems (Lawton, 1999); the models are based solely on empirical observations. Consequently, these models are brittle and often fail as the system's state changes significantly over time and space (Vallino, 2000).

To develop a robust model that can predict microbially governed biogeochemistry in spatially and temporally diverse environments, a more holistic, systems-based perspective must be taken. Our governing philosophy is that living systems synthesize and allocate metabolic capability in such a way as to optimally utilize available resources in the environment as governed by NET. What we seek to determine is the nature of the objective function that living systems tend to follow, and what causes living systems to diverge from this function.

This optimization-based approach was first developed in a thermodynamically constrained metabolic framework to examine bacterial utilization of dissolved organic matter (Vallino *et al.*, 1996). However, this model still uses an

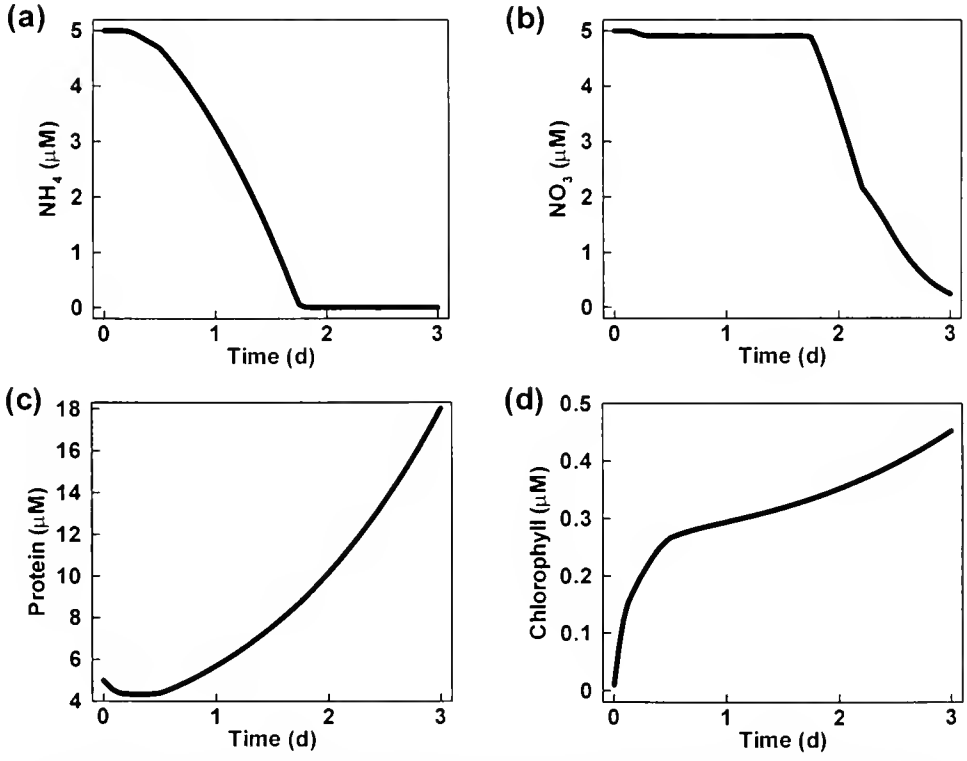

Figure 2. Metabolic model. Changes in resource concentrations of (a) ammonium and (b) nitrate, and accumulation of biological structure (c) protein and (d) chlorophyll over the course of the simulation.

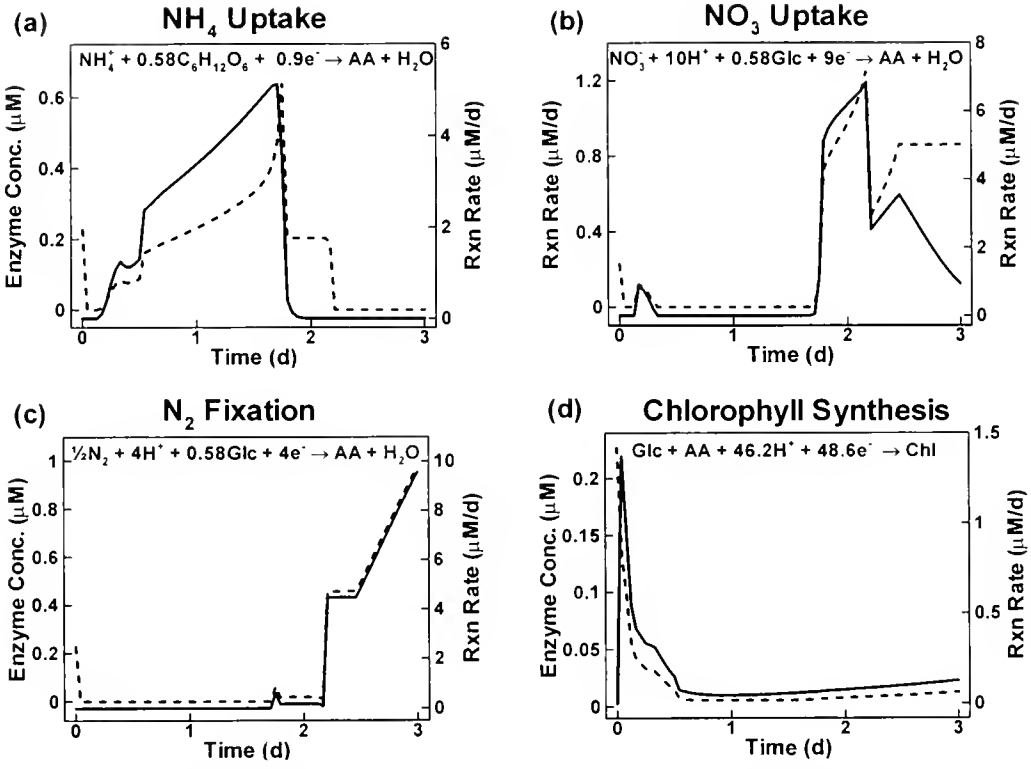

Figure 3. Reaction rates (solid line) and allocation of protein (enzyme concentration, dashed line) for reactions involving (a) ammonium uptake, (b) nitrate uptake, (c) N_2 fixation, and (d) chlorophyll synthesis during the course of the simulation. Abbreviations: Glc, glucose; AA, amino acids, Chl, chlorophyll.

organismal approach, in that the model tracks bacterial biomass. We increase the applicability of our modeling approach by removing emphasis on synthesizing bacterial biomass and placing it instead on synthesis of metabolic capability exhibited by the whole ecosystem. The model consists of a set of metabolic half-reactions that represents the major metabolic capability of a planktonic ecosystem (Table 1). But instead of synthesizing bacteria, reactions produce protein, chlorophyll, storage compounds, and other fundamental building materials observed in living systems (Fig. 1). These building materials represent those summed over all organisms in the ecosystem, not any one particular organism. Indeed, organisms are not directly modeled. Newly synthesized protein is then allocated to those metabolic reactions that optimize the specified objective criteria, while enzymes no longer in use can be degraded back into constituent amino acids (Fig. 1). A linear programming (LP) problem is used to determine the reaction rates (r_i) and enzyme concentrations (E_i) that maximize a given objective function, subject to fundamental constraints, such as energy, redox, composition, kinetics, and light-capturing capabilities (Table 2). Although the model does not distinguish species in a classic sense, it does from a functional perspective. As environmental conditions change, so do allocations of resources to metabolic reactions. Real systems accomplish this same objective *via* relative changes in species abundances and magnitude of gene expression.

As an example of the model, we simulate a marine phytoplankton bloom, where metabolic reactions associated with ammonium (NH_4^+) and nitrate (NO_3^-) uptake, N_2-fixation, carbon dioxide (CO_2) fixation, and biomass synthesis (protein and chlorophyll) are included in the model (Table 1). The optimization goal chosen was maximizing the rate of biomass synthesis, though others could be formulated. Resources made available were 5 μM NH_4^+, 5 μM NO_3^-, atmospheric N_2, and light. The model simulation proceeds by preferentially consuming NH_4^+ over NO_3^- (Fig. 2a,b), which is evident by the allocation of protein (in the form of enzyme) to NH_4^+ uptake (Fig. 3a), but not to NO_3^- uptake nor N_2 fixation (Fig. 3b,c). There is also a strong initial allocation of protein to chlorophyll synthesis (Figs. 2d, 3d), but this protein is rapidly reallocated after 0.5 d due to diminished returns on the investment in light harvesting capacity (*i.e.*, chlorophyll), which saturates at high chlorophyll concentration (Fig. 3d). As NH_4^+ becomes exhausted (Fig. 2a), protein is reallocated from NH_4^+ to NO_3^- uptake (Fig. 3a, b). Subsequently, as NO_3^- becomes depleted (Fig 2b), protein is allocated to N_2 fixation (Fig. 3c).

Conclusions

If nonequilibrium thermodynamics governs biogeochemistry, our metabolic modeling approach represents a more direct means of capturing ecosystem dynamics than classic, organismal-based approaches. The approach also predicts how whole-system genomic transcription and translation should proceed, which can be compared to actual systems using techniques currently being advanced in molecular biology. Because the metabolic ecosystem model is based on fundamental governing equations, it should prove more robust and have a greater operating range than organismal-based models.

Acknowledgments

This research has been supported by NSF grants OCE-9726921 and DEB-9815598 and the Mellon Foundation.

Literature Cited

Allen, P. M. 1985. Ecology, thermodynamics, and self-organization: towards a new understanding of complexity. *Can. Bull. Fish. Aquat. Sci.* 213: 3–26.

Amend, J. P., and E. L. Shock. 2001. Energetics of overall metabolic reactions of thermophilic and hyperthermophilic Archaea and Bacteria. *FEMS Microbiol. Rev.* **25:** 175–243.

Boetius, A., K. Ravenschlag, C. J. Schuber, D. Rickert, F. Widdel, A. Gieseke, R. Amann, B. B. Jorgensen, U. Witte, and O. Pfannkuche. 2000. A marine microbial consortium apparently mediating anaerobic oxidation of methane. *Nature* **407:** 623–626.

Caldwell, D. E., G. M. Wolfaardt, D. R. Korber, and J. R. Lawrence. 1997. Do bacterial communities transcend Darwinism? *Adv. Microb. Ecol.* **15:** 105–191.

Choi, J. S., A. Mazumder, and R. I. C. Hansell. 1999. Measuring perturbation in a complicated, thermodynamic world. *Ecol. Model.* **117:** 143–158.

Galloway, J. N., and E. B. Cowling. 2002. Reactive nitrogen and the world: two hundred years of change. *Ambio* **31:** 64–71.

Hoehler, T. M., M. J. Alperin, D. B. Albert, and C. S. Martens. 1998. Thermodynamic control on hydrogen concentrations in anoxic sediments. *Geochim. Cosmochim. Acta* **62:** 1745– 1756.

Houghton, J. T., Y. Ding, D. J. Griggs, M. Noguer, P. J. van der Linden, and D. Xiaosu. 2002. *Climate Change 2001: The Scientific Basis: Contribution of Working Group I to the Third Assessment Report of the Intergovernmental Panel on Climate Change (IPCC).* Cambridge University Press, Cambridge, UK. Pp. 1–944.

Jackson, B. E., and M. J. McInerney. 2002. Anaerobic microbial metabolism can proceed close to thermodynamic limits. *Nature* **415:** 454–456.

Jakobsen, R., and D. Postma. 1999. Redox zoning, rates of sulfate reduction and interactions with Fe-reduction and methanogenesis in a shallow sandy aquifer, Romo, Denmark. *Geochim. Cosmochim. Acta* **63:** 137–151.

Johnson, L. 1988. The thermodynamic origin of ecosystems: a tale of broken symmetry. Pp. 75–105 in *Entropy, Information, and Evolution: New Perspectives on Physical and Biological Evolution,* B. H. Weber, D. J. Depew, and J. D. Smith, eds. MIT Press, Cambridge, MA.

Jorgensen, S. E. 1994. Review and comparison of goal function in system ecology. *Vie Milieu* **44:** 11–20.

Jorgensen, S. E., B. C. Patten, and M. Straskraba. 2000. Ecosystems emerging: 4. growth. *Ecol. Model.* **126:** 249–284.

Koelmans, A. A., A. Van Der Heijde, L. M. Knijff, and R. H. Aalderin. 2001. Integrated modelling of eutrophication and organic contaminant fate and effects in aquatic ecosystems. A review. *Water Res.* **35:** 3517–3536.

Lawton, J. H. 1999. Are there general laws in ecology? *Oikos* **84:** 177–192.

Madigan, M. T., J. M. Martinko, and J. Parker. 2000. *Brock Biology of Microorganisms,* 9th ed. Prentice Hall, Upper Saddle River, NJ.

Margalef, R. 1968. *Perspectives in Ecological Theory,* University of Chicago Press, Chicago.

Morowitz, H. J. 1968. *Energy Flow in Biology: Biological Organization As a Problem in Thermal Physics.* Academic Press, New York.

Nielsen, S. N. 1995. Optimization of exergy in a structural dynamic model. *Ecol. Model.* **77:** 111–122.

Nielsen, S. N., and R. E. Ulanowicz. 2000. On the consistency between thermodynamical and network approaches to ecosystems. *Ecol. Model.* **132:** 23–31.

Odum, H. T. 1971. *Environment, Power and Society.* John Wiley, New York.

Odum, H. T. 1983. *Systems Ecology.* John Wiley, Toronto.

Odum, H. T., and R. C. Pinkerton. 1955. Time's speed regulator: the optimum efficiency for maximum power output in physical and biological systems. *Am. Sci.* **43:** 321–343.

Onsager, L. 1931. Reciprocal relations in irreversible processes. *Phys. Rev.* **37:** 405–426.

Prigogine, I. 1955. *Introduction to Thermodynamics of Irreversible Processes,* John Wiley, New York.

Prigogine, I. 1978. Time, structure, and fluctuations. *Science* **201:** 777–785.

Prigogine, I., and G. Nicolis. 1971. Biological order, structure and instabilities. *Q. Rev. Biophys.* **4:** 107–148.

Schlesinger, W. H. 1997. *Biogeochemistry: An Analysis of Global Change,* 2nd ed. Academic Press, San Diego, CA.

Schneider, E. D. 1988. Thermodynamics, ecological succession, and natural selection: a common thread. Pp. 107–138 in *Entropy, Information, and Evolution: New Perspectives on Physical and Biological Evolution,* B. H. Weber, D. J. Depew, and J. D. Smith, eds. MIT Press, Cambridge, MA.

Schneider, E. D., and J. J. Kay. 1994. Complexity and thermodynamics: towards a new ecology. *Futures* **26:** 626–647.

Schrödinger, E. 1944. *What Is Life?* Cambridge University Press, Cambridge, UK.

Schulz, H. N., T. Brinkhoff, T. G. H. M. M. Ferdelman, A. Teske, and B. B. Jorgensen. 1999. Dense populations of a giant sulfur bacterium in Namibian shelf sediments. *Science* **284:** 493–495.

Toussaint, O., and E. D. Schneider. 1998. The thermodynamics and evolution of complexity in biological systems. *Comp. Biochem. Physiol. A* **120:** 3–9.

Ulanowicz, R. E. 1986. *Growth and Development: Ecosystems Phenomenology.* Springer-Verlag, New York.

Ulanowicz, R. E. 1997. *Ecology, the Ascendent Perspective.* Columbia University Press, New York.

Vallino, J. J. 2000. Improving marine ecosystem models: use of data assimilation and mesocosm experiments. *J. Mar. Res.* **58:** 117–164.

Vallino, J. J., C. S. Hopkinson, and J. E. Hobbie. 1996. Modeling bacterial utilization of dissolved organic matter: optimization replaces Monod growth kinetics. *Limnol. Oceanogr.* **41:** 1591–1609.

Wiley, E. O. 1988. Entropy and evolution. Pp. 173–188 in *Entropy, Information, and Evolution: New Perspectives on Physical and Biological Evolution,* B. H. Weber, D. J. Depew, and J. D. Smith, eds. MIT Press, Cambridge, MA.

Reference: *Biol. Bull.* **204:** 180–185. (April 2003)

Geomicrobiology of the Ocean Crust: A Role for Chemoautotrophic Fe-Bacteria

KATRINA J. EDWARDS*, WOLFGANG BACH, AND DANIEL R. ROGERS

Geomicrobiology Group, Department of Marine Chemistry and Geochemistry, McLean Lab, MS#8, Woods Hole Oceanographic Institution, Woods Hole, Massachusetts 02536

The delicate balance of the major global biogeochemical cycles greatly depends on the transformation of Earth materials at or near its surface. The formation and degradation of rocks, minerals, and organic matter are pivotal for the balance, maintenance, and future of many of these cycles. Microorganisms also play a crucial role, determining the transformation rates, pathways, and end products of these processes. While most of Earth's crust is oceanic rather than terrestrial, few studies have been conducted on ocean crust transformations, particularly those mediated by endolithic (rock-hosted) microbial communities. The biology and geochemistry of deep-sea and sub-seafloor environments are generally more complicated to study than in terrestrial or near-coastal regimes. As a result, fewer, and more targeted, studies usually homing in on specific sites, are most common. We are studying the role of endolithic microorganisms in weathering seafloor crustal materials, including basaltic glass and sulfide minerals, both in the vicinity of seafloor hydrothermal vents and off-axis at unsedimented (young) ridge flanks. We are using molecular phylogenetic surveys and laboratory culture studies to define the size, diversity, physiology, and distribution of microorganisms in the shallow ocean crust. Our data show that an unexpected diversity of microorganisms directly participate in rock weathering at the seafloor, and imply that endolithic microbial communities contribute to rock, mineral, and carbon transformations.

*To whom correspondence should be addressed. E-mail: kedwards@whoi.edu

The paper was originally presented at a workshop titled *Outcomes of Genome-Genome Interactions*. The workshop, which was held at the J Erik Jonsson Center of the National Academy of Sciences, Woods Hole, Massachusetts, from 1–3 May 2002, was sponsored by the Center for Advanced Studies in the Space Life Sciences at the Marine Biological Laboratory, and funded by the National Aeronautics and Space Administration under Cooperative Agreement NCC 2-1266

Weathering reactions in Earth's near-surface environments play pivotal roles in balancing chemical exchange between the lithosphere, hydrosphere, and atmosphere. Microorganisms at and beneath the surface affect the transformation rates, mechanisms, and pathways of exchange for many elements. Over 70% of the Earth's exposed crust is oceanic, and most of this material occurs well below the euphotic upper ocean regime. The oceanic crust is composed largely of basalt (~50 wt % SiO_2; 4–15 wt % each of MgO, FeO, CaO, Al_2O_3), although metal sulfide minerals (*e.g.*, pyrite, FeS_2) are prominent at seafloor hydrothermal ridge axes. After their formation at seafloor spreading centers, ocean crust rocks undergo weathering, either by reaction with seawater while exposed at the ocean floor or from fluid-rock interaction below the seafloor.

While the effects of crustal weathering and fluid-rock interaction are well documented (Alt, 1995), the role of microorganisms in these processes is poorly understood. To date, investigations of sub-seafloor endolithic (rock-hosted) microbial communities have been largely limited to examination of textural features, such as channels and pits, which appear in petrographic thin sections and other microscopic preparations, and are thought to indicate microbial activity (*e.g.*, Fisk *et al.*, 1998). However, the physiological functions of members of sub-seafloor ecosystems have not been elucidated, precluding our ability to place these hypothesized communities into proper global biogeochemical context. Here, we first briefly review the physical and chemical weathering regime of the ocean crust, and then discuss our recent findings regarding the physiological activities and phylogenetic relationships among prokaryotes that actively participate in crustal alteration at the ocean floor.

The uppermost 200–500 m of basaltic ocean crust is characterized by high permeabilities (10^{-12}–10^{-15} m^2) that facilitate the circulation of large quantities of seawater (Fisher,

1998; Fisher and Becker, 2000). Chemical reactions between seawater and seafloor rocks change the compositions of both the oceans and the aging ocean crust (Hart and Staudigel, 1986; Mottl and Wheat, 1994; Alt *et al.*, 1996; Staudigel *et al.*, 1996; Elderfield *et al.*, 1999; de Villiers and Nelson, 1999; Wheat and Mottl, 2000). Basaltic rocks react with oxygenated deep-sea water to form secondary hydrous alteration minerals, including a variety of Fe-oxyhydroxides and micas, and clay minerals such as celadonite ($K(Mg,Fe)(Fe,Al)Si_4O_{10}(OH)_2$) and smectite (*e.g.*, montmorillinite, $(1/2Ca,Na)(Al,Mg,Fe)_4(Si,Al)_8O_{20}(OH)_4{*}nH_2O$)(Honnorez, 1981; Alt, 1995). These minerals replace glass and primary minerals such as olivine ($(Mg, Fe)_2SiO_4$), sulfides (*e.g.*, pyrite), and to lesser extents plagioclase ($NaAlSi_3O_8$) and clinopyroxene ($(Ca,Mg,Fe,Al)_2(Si,Al)_2O_6$), and they fill fractures and void space in the crust. The extent of oxidation associated with low-temperature alteration is extremely variable at different spatial scales. Age dating of celadonite suggests that the products of oxidative alteration persist in crust of significant age (10–40 million years; Peterson *et al.*, 1986; Hart and Staudigel, 1986; Gallahan and Duncan, 1994); these products can be detected and analyzed and the data used to interpret past fluid-rock interactions in ocean crust.

The chemical reactions that occur from fluid-rock interaction in the sub-seafloor not only change the mineralogy of the ocean crust, but also remove many important seawater constituents, such as magnesium and sulfate, while other constituents, such as calcium, are added. These reactions are thus generally responsible for maintaining the chemical composition of the oceans over geological time frames, and they participate in controlling the balance of the greenhouse gases such as CO_2. Because the entire volume of the ocean is circulated through the ocean crust roughly once every million years, we must have a fundamental understanding of the rates, mechanisms, and pathways of ocean crust water-rock reactions so that we may better predict feedbacks such as those between climate change and seawater-crust exchange.

Many of the low-temperature water-rock reactions we have mentioned release energy, yet are kinetically sluggish; consequently, where conditions are otherwise suitable (appropriate temperature, availability of nutrients, etc.), this chemical energy could be used by microorganisms for metabolic growth. Textural observations (Fisk *et al.*, 1998; Torsvik *et al.*, 1998; Furnes and Staudigel, 1999) and highly variable carbon isotope measurements (Furnes *et al.*, 2001) have indeed suggested that microbial activity is present in the ocean crust. These textural criteria—which include recognition and interpretation of "pit-textures," "sponge-textures," and "zoned palagonite"—can be easily and rapidly applied to a large number of samples for qualitative initial screenings and surveys, but they cannot provide definitive evidence of specific microbial activity in the crust. Furthermore, studies of crust-hosted microbial communities have not yet elucidated how they might function physiologically. Hence, the ocean crust is an understudied, yet potentially vast, microbial habitat. Because sample access, contamination, preservation, low biomass, and activity are problematic in the deep sea, many of the usual methods of detecting microbial communities and measuring their activities are not practical. Consequently, the actual fraction of ocean crust that is microbially altered is difficult to estimate. Textural signatures in the alteration products of certain rocks suggest that up to 75% of the uppermost crust is microbially altered (Furnes and Staudigel, 1999), whereas such features in other samples suggest that most alteration is probably abiogenic (Alt and Mata, 2000). Studies of microbial crust alteration have been infrequent, so we cannot conclusively assess the extent and importance of microbial activity within the ocean crust. Hence, the physical, chemical, and energetic regimes of young upper ocean crust must be considered with special care, so that specific predictions may be made and tested for use in focused environmental studies.

To address the inferences made from previous geochemical studies, we have explored microbial weathering reactions that may occur in the upper ocean crust during early-stage (crust $<$10 million years old) oxidative alteration of basaltic glass and sulfide minerals. In July of 2000, *in situ* weathering and colonization experiments were initiated at the Juan de Fuca Ridge axis off the northwestern coast of America (Edwards *et al.*, 2003a). A variety of naturally occurring sulfide minerals were reacted for 2 months at the seafloor at low-temperature ($\sim$3°C), ambient seafloor conditions. Upon collection, the sulfide surfaces were heavily colonized by bacteria and densely encrusted with weathering products that were largely composed of Fe oxides (Fig. 1). The mineralogical and fluorescent hybridization data (FISH; Fig. 1) suggest that these Fe oxide minerals owe their presence to the activity of neutrophilic Fe-oxidizing bacteria within surface pits (Edwards *et al.*, 2003a). Surface pits are ideal colonization sites for aerobic Fe-oxidizing bacteria because, once biofilms have formed and Fe oxide crusts have been produced, the bacteria are partially protected from free advective (initially) and diffusive exchange with well-oxygenated deep-sea water. This allows pit-colonizing, Fe-oxidizing bacteria to more readily compete with very rapid abiotic oxidation kinetics of ferrous iron so that they may harness this oxidation energy for growth.

Both culture-independent (molecular phylogenetic) and culture-dependent studies have been used to further explore the occurrence and diversity of mineral-oxidizing microorganisms. For both types of studies, we examined prokaryotic populations associated with weathering habitats in the deep sea (Fig. 2). These habitats include the surfaces of brecciated sulfide rubble material that derives from collapsed chimney, flange, or other structures common in hydrothermal vent environments. We also examined metalliferous

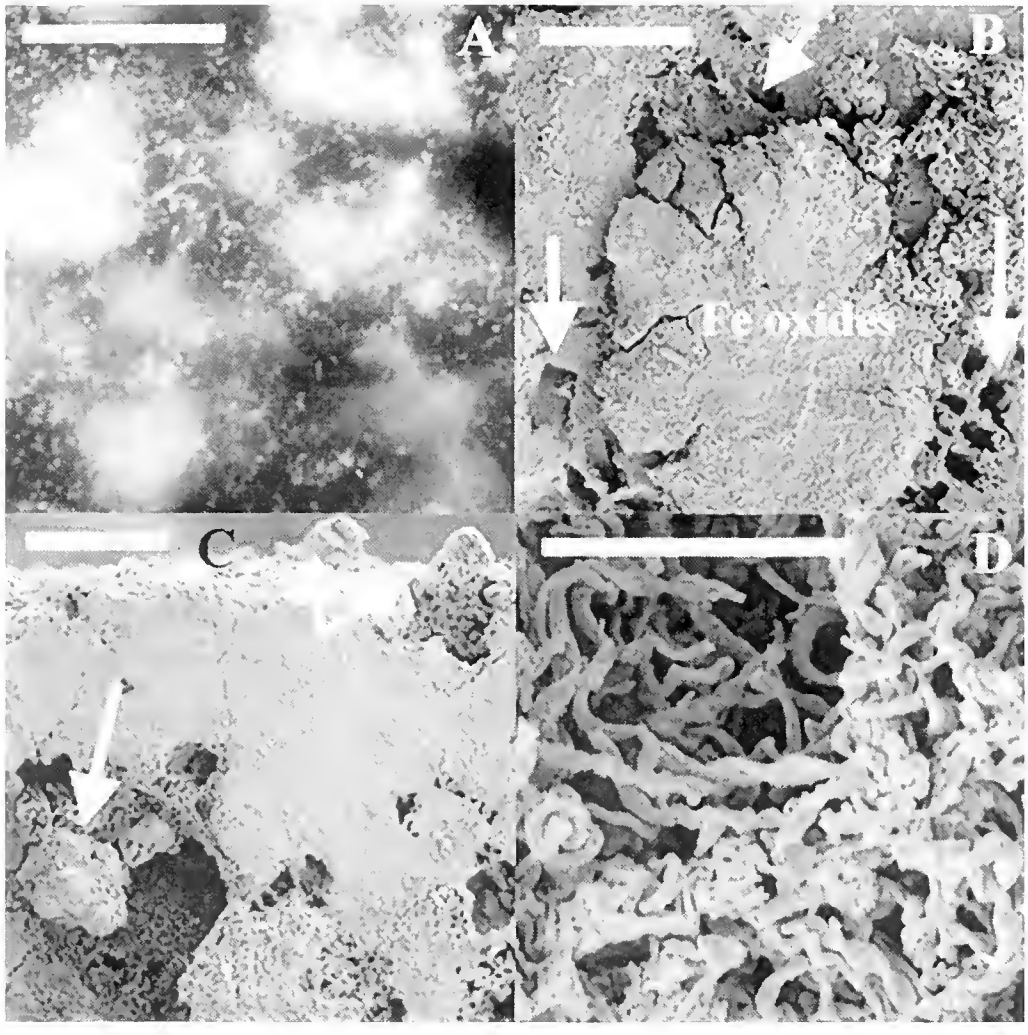

Figure 1. Patterns of cell and oxide accumulation on the surface of a seafloor reacted sulfide mineral. (A) DAPI-stained image of surface that was heavily colonized by Bacteria (determined by fluorescent *in situ* hybridizations; FISH); scale = 50 μm. Cells are bright white dots and patches, predominately colonizing pores and pits on sample, the outlines of which are dark and coincide with the edges of the cell masses. (B,C) scanning electron micrographs of the same surface, showing thick Fe oxide accumulations over top of (B) or within (C) pits and pores on surface; scale = 100 μm. (D) Fe oxides in C at higher magnification; scale = 10 μm. In B, Fe oxides form an effective cap over the pits (arrows). In C, the oxides (arrows) are less well formed and are growing inside pits. We hypothesize that the more unformed Fe oxides in C are the precursors to the massive forms seen in B.

sediments that accumulate in the vicinity of seafloor hydrothermal sites as the result of plume events or the collapse of sulfide-anhydrite structures.

Our culture-independent studies are based on comparative analysis of 16S rDNA sequences from uncultured organisms present in environmental samples, and restriction fragment length polymorphism (RFLP; Hugenholtz *et al.*, 1998). RFLP analyses indicate that all of the weathering habitats examined are characterized by very low microbial diversity. In most cases, the microbial community is dominated by only one to three operational taxonomic units (OTUs; Moyer *et al.*, 1994) or phylogenetically coherent taxonomic groupings as defined by RFLP analysis (D.R. Rogers, C.M. Santelli, and K.J. Edwards, unpubl. data). Comparative analyses of 16S rDNA sequences obtained from these uncultured organisms indicate that sulfur(S)-oxidizing bacteria that are to varying degrees related to the genus *Thiomicrospira* represent one dominant microbial group in these samples (Rogers and Edwards, unpubl. data). These observations are consistent with findings from other studies (both culture-dependent and culture-independent) that have been conducted at seafloor hydrothermal vent sites (*e.g.*, Wirsen *et al.*, 1993), and they support previous inferences that minerals play an important role in supporting the

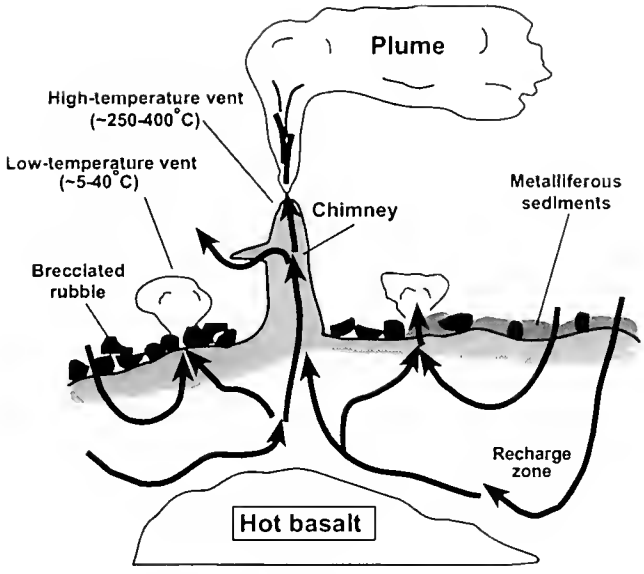

Figure 2. Schematic cross-section of a submarine hydrothermal vent system, emphasizing sulfide weathering habitats. Mineral surfaces exposed to oxygenated water are favorable environments for aerobic lithoautotrophs that can oxidize the minerals to obtain metabolic energy. Such environments include the surfaces of hydrothermal chimneys, brecciated rubble resulting from the collapse of extinct chimneys, and metalliferous sediments formed by particulates settling out of the vent plume. In some instances, mounds of sediments and brecciated rubble are infiltrated by low-temperature hydrothermal fluids formed by mixing of high-temperature fluids and seawater, providing aerobic environments at moderate temperatures (~25–40°C). Figure modified after McCollom (2000) with permission from Elsevier.

growth of S-oxidizing prokaryotes over geological time scales, long after hydrothermal activity dissipates (Eberhard *et al.*, 1995).

In contrast to our FISH studies and microscopic observations (Fig. 1), our culture-independent phylogenetic approaches failed to support our findings that suggest that Fe-oxidizing microorganisms are present in low-temperature weathering deposits. We did not identify any 16S rDNA sequences bearing similarity with gene sequences from any known Fe-oxidizing prokaryotes. This lack of sequence-based support for the presence of Fe-oxidizing microorganisms within environmental samples is not unusual in studies of microbial weathering in the deep sea. For example, Thorseth *et al.* (2001) used both scanning electron microscopy and 16S rDNA sequence analysis on seafloor basalt glass to study microbial weathering at the seafloor. Although their SEM studies reveal Fe oxide particles remarkably similar to those observed in environmental and culture studies of neutrophilic Fe-oxidizing bacteria, their culture-independent, phylogenetic analyses failed to produce any 16S rDNA sequences related to known Fe-oxidizing species.

In contrast to our culture-independent studies, our culture-dependent studies have revealed a wide diversity of novel, autotrophic, Fe-oxidizing bacterial strains that previously had no known Fe-oxidizing or autotrophic relatives represented in pure culture (Edwards *et al.*, 2003b). Our culture techniques are based on the FeS gradient-tube method originally devised by Kucera and Wolfe (1957) and modified by Emerson and Moyer (1997). Using the same samples as were used for our culture-independent studies (above) for inoculum, we first initiated enrichment cultures on an organic carbon-free artificial seawater (ASW: modified after Jannasch *et al.*, 1985; Edwards *et al.*, 2003b) medium, using sulfide minerals such as pyrite as the sole energy source. Following initial enrichment, pure cultures of Fe-oxidizing bacteria were obtained by successive serial dilutions of enrichments to extinction in FeS gradient-tubes (Kucera and Wolfe, 1957). Putative isolates of Fe-oxidizing bacteria were determined to be clonally pure using RFLP analysis (Edwards *et al.*, unpubl. data). Physiological analyses have revealed that all of these isolates are obligate lithotrophs, capable of growth with Fe^{2+}, but not with any alternate electron donors tested so far (sulfide, thiosulfate, Mn^{2+}). Autotrophy has been confirmed by determining ^{14}C fixation in FeS, FeS_2, and basalt (~10 wt. % FeO)-based gradient tubes (Edwards *et al.*, 2003b).

Table 1 shows the phylogenetic affiliations among some of our Fe-oxidizing isolates. Most of our strains fall within the alpha- or gamma-subdivisions of the Proteobacteria and have moderately close relatives within broad groups of known heterotrophic bacteria, the Hypomicrobia and Mari-

Table 1

Phylogenetic affiliations among axenic Fe-oxidizing strains

Strain number	Bacterial division	BLAST database match (% related)	Metabolism inferred from closest relative
FO1	α-Proteobacteria	*Hyphomonas jannaschiana* (81%)	Heterotrophy
FO3	α-Proteobacteria	Uncultured Marine bacterium SCRIPPS_94 (95%)	Heterotrophy
FO4	γ-Proteobacteria	Uncultured Marinobacter sp. PCOB-2 (94%)	Heterotrophy
FO6	γ-Proteobacteria	Uncultured Marinobacter sp. PCOB-2 (95%)	Heterotrophy
FO8	γ-Proteobacteria	Uncultured Marinobacter sp. ME108 (99%)	Heterotrophy
FO10	γ-Proteobacteria	Uncultured DCM-ATT-12 (90%)	Unknown

nobacter, respectively. If these sequences had not been derived from pure cultures of Fe-oxidizing lithoautotrophs, they (and thus their *in situ* physiological activity) would probably have been classified as heterotrophic on the basis of their phylogenetic relationships with known physiological groups.

Our findings indicate that Fe-oxidizing autotrophs may be overlooked in culture-independent studies in the deep sea (if not other habitats as well) due to their close phylogenetic affiliations with physiologically distinct (heterotrophic) species. Our studies and others (*e.g.*, Emerson *et al.*, 1999; Emerson and Moyer, 1997, 2002) clearly indicate that neutrophilic Fe-oxidizing bacteria harbor unexpected diversity, which is just now becoming appreciated. This has important implications for how we study deep-sea microbial communities within the context of their ecological and geochemical functions, and suggests critical shortcomings in the most commonly applied approaches based on 16S rDNA, comparative gene sequence analysis.

The occurrence of Fe-oxidizing capacity among an ever-broadening range of bacteria may have important ecological and evolutionary ramifications. For example, in relatively isolated environments, such as the oligotrophic, low-carbon, bare-rock oceanic crustal habitat, diverse groups of microorganisms may converge on functions that are well suited to the particular environment. Alternatively, the capacity for Fe-oxidation may have been lost by some species after they occupied more carbon-rich habitats. Such occurrences among marine lithoautotrophs may be supported by an alpha-Proteobacterium that possesses genes for both the large and small subunits of ribulose-1,5-bisphosphate carboxylase/oxygenase (RubisCO), yet the heterotrophic strain has not been shown to fix carbon (Francis *et al.*, 2001). Indeed, although heterotrophic Fe- and Mn-oxidizing bacteria have long been recognized in the environment, the physiological purpose of this oxidation is often unknown (Ghiorse, 1984, and references therein). Rather than serving some explicit biological role, this oxidation in some species may be an evolutionary holdover that no longer has physiological relevance. As one final explanation, Fe-oxidation among groups that we would typically classify as heterotrophic may be an example of a multifunctional metabolism that allows them to adapt to a rapidly changing environment.

Further studies, both laboratory and field-based, are needed to explore the implications of microbial activity within the ocean crust. Studies on Fe-oxidizing bacteria should provide critical information about sub-seafloor communities and biogeochemical processes. Useful laboratory investigations of Fe-oxidizing bacteria would include the following. (1) Studies to determine the mechanism of Fe-oxidation among known strains of Fe-oxidizing bacteria: knowledge of the pathway and key genes and enzymes for Fe-oxidation could be used to develop molecular diagnostics for this activity, and these could be applied in environmental settings. (2) Isotopic studies both to define the carbon fixation pathways and associated stable carbon isotope fractionations and to determine any stable Fe isotope fractionation that occurs during oxidation in pure cultures: these studies are key to developing geochemical diagnostics that can be applied to rocks long after activity diminishes.

Acknowledgments

Funding for this work was provided by NSF grants OCE-0096992 and EAR-0073998 to KJE. Special thanks to present and past members of the Edwards lab for various contributions to this work, and to two anonymous reviewers for their helpful comments and insights. WHOI contribution number 10876.

Literature Cited

Alt, J. C. 1995. Sub seafloor processes in mid-ocean ridge hydrothermal systems. Pp. 85–114 in *Seafloor Hydrothermal Systems,* S.E. Humphris, R.A. Zierenberg, L.S. Mullineaux, and R.E. Thomson, eds. American Geophysical Union, Washington, DC.

Alt, J. C., and P. Mata. 2000. On the role of microbes in the alteration of submarine basaltic glass: A TEM study. *Earth Planet. Sci. Lett.* **181:** 301–313.

Alt, J. C., D. A. Teagle, C. Laverne, D. A. Vanko, W. Bach *et al.* 1996. Ridge flank alteration of upper oceanic crust in the eastern Pacific: A synthesis of results for volcanic rock of Holes 504B and 896A. Pp. 435–450 in *Proceedings of the Ocean Drilling Program Scientific Results 148,* J. C. Alt, H. Kinoshita, L. B. Stokking, and P. J. Michael, eds. Ocean Drilling Program, Texas A & M University, College Station, TX.

de Villiers, S., and B. K. Nelson. 1999. Detection of low-temperature hydrothermal fluxes by seawater Mg and Ca anomalies. *Science* **285:** 721–723.

Eberhard, C., C. O. Wirsen, and H. W. Jannasch. 1995. Oxidation of polymetal sulfides by chemolithoautotrophic bacteria from deep-sea hydrothermal vents. *Geomicrobiol. J.* **13:** 145–164.

Edwards, K. J., T. M. McCollom, H. Konishi, and P. R. Buseck. 2003a. Seafloor bio-alteration of sulfide minerals: results from *in situ* incubation studies. *Geochim. Cosmochim. Acta.* (In press).

Edwards, K. J., D. R. Rogers, C. O. Wirsen, and T. M. McCollom. 2003b. Isolation and characterization of novel psychrophilic, neutrophilic, Fe-oxidizing chemolithoautotrophic alpha- and gamma-Proteobacteria from the deep-sea. *Appl. Environ. Microbiol.* (In press).

Elderfield, H., C. G. Wheat, M. J. Mottl, C. Monnin, and B. Spiro. 1999. Fluid and geochemical transport through oceanic crust: A transect across the eastern flank of Juan de Fuca Ridge. *Earth Planet. Sci. Lett.* **172:** 151–165.

Emerson, D., and C. L. Moyer. 1997. Isolation and characterization of novel iron-oxidizing bacteria that grow at circumneutral pH. *Appl. Environ. Microbiol.* **63:** 4784–4792.

Emerson, D., and C. L. Moyer. 2002. Neutrophilic Fe-oxidizing bacteria are abundant at the Loihi seamount hydrothermal vents and play a major role in Fe oxide deposition. *Appl. Environ. Microbiol.* **68:** 3085–3093.

Emerson, D., J. V. Weiss, and J. P. Megonigal. 1999. Iron-oxidizing bacteria are associated with ferric hydroxide precipitates (Fe-plaque) on the roots of wetland plants. *Appl. Environ. Microbiol.* **65:** 2758–2761.

Fisher, A. T. 1998. Permeability within basaltic ocean crust. *Rev. Geophys.* **36:** 143–182.

Fisher, A. T., and K. Becker. 2000. Channelized fluid flow in oceanic crust reconciles heat-flow and permeability data. *Nature* **403:** 71–74.

Fisk, M. R., S. J. Giovannoni, and I. H. Thorseth. 1998. Alteration of oceanic volcanic glass: textural evidence of microbial activity. *Science* **281:** 978–980.

Francis, C. A., E. M. Co, and B. M. Tebo. 2001. Enzymatic manganese (II) oxidation by a marine alpha-proteobacterium. *Appl. Environ. Microbiol.* **67:** 4024–4029.

Furnes, H., and H. Staudigel. 1999. Biological mediation in ocean crust alteration: how deep is the deep biosphere? *Earth Planet. Sci. Lett.* **166:** 97–103.

Furnes, H., K. Muehlenhachs, T. Torsvik, I. H. Thorseth, and O. Tumyr. 2001. Microbial fractionation of carbon isotopes in altered basaltic glass from the Atlantic Ocean, Lau Basin, and Costa Rica Rift. *Chem. Geol.* **173:** 313–330.

Gallahan, W. E., and R. A. Duncan. 1994. Spatial and temporal variability in crystallization of celadonites within the Troodos ophiolite, Cyprus: implications for low temperature alteration of the oceanic crust. *J. Geophys. Res.* **99:** 3147–3161.

Ghiorse, W. C. 1984. Biology of iron-and manganese-depositing bacteria. *Annu. Rev. Microbiol.* **38:** 515–550.

Hart, S. R., and H. Staudigel. 1986. Ocean crust vein mineral deposition: Rb/Sr ages, U-Th-Pb geochemistry, and duration of circulation of DSDP sites 261, 462, and 516. *Geochim. Cosmochim. Acta* **50:** 2751–2761.

Honnorez, J. 1981. The aging of the oceanic crust at low temperature. Pp 525–587 in *The Sea*, C. Emiliani, ed. Wiley, New York.

Hugenholtz, P., C. Pitulle, K. L. Hershberger, and N. R. Pace. 1998. Novel division level bacterial diversity in a Yellowstone hot spring. *J. Bacteriol.* **180:** 366–376.

Jannasch, H. W., C. O. Wirsen, D. C. Nelson, and L. A. Roberson. 1985. *Thiomicrospira crunogena* sp. nov., a colorless, sulfur-oxidizing bacterium from a deep-sea hydrothermal vent. *Int. J. Syst. Bacteriol.* **35:** 422–424.

Kucera, S., and R. S. Wolfe. 1957. A selective enrichment method for *Gallionella ferruginea*. *J. Bacteriol.* **74:** 344–349.

McCollom, T. M. 2000. Geochemical constraints on primary productivity in submarine hydrothermal vent plumes. *Deep-Sea Res. I* **47:** 85–101.

Mottl, M. J., and C. G. Wheat. 1994. Hydrothermal circulation through mid-ocean ridge flanks: fluxes of heat and magnesium. *Geochim. Cosmochim. Acta* **58:** 2225–2237.

Moyer, C. L., F. C. Dobbs, and D. M. Karl. 1994. Estimation of diversity and community structure through restriction fragment length polymorphism distribution analysis of bacterial 16S rRNA genes from a microbial mat at an active, hydrothermal vent system, Loihi Seamount, Hawaii. *Appl. Environ. Microbiol.* **60:** 871–879.

Peterson, C., R. Duncan, and K. F. Scheidegger. 1986. Sequence longevity of basalt alteration at Deep Sea Drilling Project Site 597. Pp. 505–515 in *Initial Reports DSDP 92M*. D. K. Leinen and E. A. Rea, eds. U.S. Government Printing Office, Washington, DC.

Staudigel, H., T. Plank, B. While, and H.-U. Schmincke. 1996. Geochemical fluxes during seafloor alteration of the basaltic upper oceanic crust: DSDP Sites 417 and 418. Pp 19–38 in *Subduction Top to Bottom*, G.E. Bebout, S.W. Scholl, S.H. Kirby, and J.P. Platt, eds. American Geophysical Union, Washington, DC.

Thorseth, I. H., T. Torsvik, V. Torsvik, F. L. Daae, R. B. Pedersen, Keldysh-98 Scientific Party. 2001. Diversity of life in ocean floor basalt. *Earth Planet. Sci. Lett.* **194:** 31–37.

Torsvik, T., H. Furnes, K. Muehlenbachs, I. H. Thorseth, and O. Tumyr. 1998. Evidence for microbial activity at the glass-alteration interface in oceanic basalts. *Earth Planet. Sci. Lett.* **162:** 165–176.

Wheat, C. G., and M. J. Mottl. 2000. Composition of pore and spring waters from Baby Bare: global implications of geochemical fluxes from a ridge flank hydrothermal system. *Geochim. Cosmochim. Acta* **64:** 629–642.

Wirsen, C. O., H. W. Jannasch, and S. J. Molyneaux. 1993. Chemosynthetic microbial activity at Mid-Atlantic Ridge hydrothermal vent sites. *J. Geophys. Res.* **98:** 9693–9703.

Reference: *Biol. Bull.* **204:** 186–191. (April 2003)

Genomic Markers of Ancient Anaerobic Microbial Pathways: Sulfate Reduction, Methanogenesis, and Methane Oxidation

ANDREAS TESKE[1,*,‡], ASHITA DHILLON[2], AND MITCHELL L. SOGIN[2]

[1]*Biology Department, Woods Hole Oceanographic Institution, Woods Hole, Massachusetts 02543; and*
[2]*Josephine Bay Paul Center for Comparative Molecular Biology and Evolution, Marine Biological Laboratory, Woods Hole, Massachusetts 02543*

Genomic markers for anaerobic microbial processes in marine sediments—sulfate reduction, methanogenesis, and anaerobic methane oxidation—reveal the structure of sulfate-reducing, methanogenic, and methane-oxidizing microbial communities (including uncultured members); they allow inferences about the evolution of these ancient microbial pathways; and they open genomic windows into extreme microbial habitats, such as deep subsurface sediments and hydrothermal vents, that are analogs for the early Earth and for extraterrestrial microbiota.

Sulfate reduction and methanogenesis are two terminal anaerobic bioremineralization pathways that convert low-molecular-weight products of other bacterial processes (degradation of polymers, fermentation) to CO_2 and methane. Sulfate-reducing bacteria are physiologically and phylogenetically highly diverse (Castro *et al.*, 2000; Widdel and Bak, 1992); they oxidize a wide variety of low-molecular-weight compounds (short-chain fatty acids, alcohols, alkanes, aromatic compounds, acetate) to CO_2. In marine sediments, the range of sulfate-reducing bacteria is limited by sulfate availability. When sulfate is depleted, methanogenic archaea become the dominant anaerobic microbial population. Autotrophic methanogens utilize hydrogen as energy source for the reduction of CO_2 to methane; specialized genera of methanogens are also capable of inter- and intramolecular disproportionation of C_1 and C_2 carbon compounds (methanol, methylamines, acetate) to methane and CO_2 (Boone *et al.*, 1993). Where methane and sulfate coexist (for example, at the interface of sulfate-reducing and methanogenic sediment layers, or at marine methane seeps and vents), sulfate-dependent anaerobic methane oxidation takes place; methane of biogenic origin is oxidized to CO_2 with sulfate as the terminal electron acceptor (Valentine and Reeburgh, 2000). As proposed originally on the basis of biogeochemical field data and thermodynamic considerations (Hoehler *et al.*, 1994), anaerobic methane oxidation is carried out by syntrophic consortia of methanotrophic archaea and sulfate-reducing bacteria, in which the sulfate-reducing partner catalyzes the electron transfer from methane to sulfate and assimilates a portion of the methane oxidation products (Boetius *et al.*, 2000; Orphan *et al.*, 2001b). Methanotrophic archaea of different phylogenetic affiliation can form dense, highly ordered clusters with sulfate-reducing syntrophs, or may occur in less tight associations (Orphan *et al.*, 2002).

The sulfate-reducing, methanogenic, and methane-oxidizing microbial populations that are found in anaerobic marine microbial ecosystems today are the modern descendants of ancient microbiota whose isotopic imprints are pervasive in the carbon- and sulfur-isotopic record, from the present back to the Archaean-Proterozoic transition (Knoll and Canfield, 1998). The only oxidants that these pathways require are CO_2 or carbonate, and sulfate, which existed before the photosynthetic oxygenation of the Earth's bio-

‡ Current Address: Department of Marine Sciences, CB # 3300, Venable Hall 12-1, University of North Carolina at Chapel Hill, Chapel Hill, NC 27599.

*To whom correspondence should be addressed. E-mail: teske@email.unc.edu

The paper was originally presented at a workshop titled *Outcomes of Genome-Genome Interactions*. The workshop, which was held at the J. Erik Jonsson Center of the National Academy of Sciences, Woods Hole, Massachusetts, from 1–3 May 2002, was sponsored by the Center for Advanced Studies in the Space Life Sciences at the Marine Biological Laboratory, and funded by the National Aeronautics and Space Administration under Cooperative Agreement NCC 2-1266.

sphere and the appearance of free oxygen in the atmosphere and the marine water column. Isotopic evidence for widely expressed microbial sulfate reduction, in the form of ^{34}S-depleted sedimentary sulfides, goes back to the middle and early Proterozoic, 2.2 to 2.3 billion years ago (Canfield *et al.*, 2000). The mineralization of organic matter by methanogenesis, followed by methane oxidation, may even predate the onset of sulfate reduction. The carbon isotopic imprint of this process, in the form of highly ^{13}C-depleted kerogen ($\delta^{13}C \geq -60‰$), is found in late Archaean and early Proterozoic kerogens, 2.8 billion years old (Strauss and Moore, 1992). This isotopic record was originally interpreted as evidence for widespread aerobic methane oxidation (Hayes, 1994). Anaerobic methane oxidation is more likely, since evidence for the stepwise and pervasive oxygenation of the proterozoic biosphere begins to appear only at a later time, about 2.2 billion years ago (Des Marais *et al.*, 1992).

Key Genes for Sulfate Reduction and Anaerobic Methane Cycling

The antiquity and evolutionary significance of these microbial pathways is shown in the high degree of phylogenetic conservation of their key genes and key enzymes. In sulfate-reducing prokaryotes, the *aps* gene codes for the key enzyme adenosine-5′-phosphosulfate reductase, which catalyzes the activation and subsequent reduction of sulfate to sulfite (Friedrich, 2002). A second key gene of dissimilatory sulfate reduction, *dsrAB*, codes for the alpha and beta subunits of the enzyme dissimilatory sulfite reductase, which catalyzes the reduction of sulfite to sulfide (Wagner *et al.*, 1998). The *dsrAB* and *aps* genes are phylogenetically conserved in several deeply branching phyla of bacterial and archaeal sulfate reducers. When specific gene transfer events are taken into account, the *dsrAB* and *aps* genes allow a simultaneous phylogenetic and metabolic identification of sulfate-reducing prokaryotes (Klein *et al.*, 2001; Friedrich, 2002).

Coenzyme M methyl reductase is the key enzyme of methanogenesis; it catalyzes the terminal and highly exergonic step of the methanogenesis pathway, the reduction and release of the coenzyme-M-bound methyl group as free methane. The Coenzyme M methyl reductase gene (*mrcA*) is found in methanogenic archaea; it is sufficiently conserved and consistent with 16S rRNA phylogenies to allow the identification of methanogenic archaeal lineages in environmental samples (Springer *et al.*, 1995; Lueders *et al.*, 2001; Ramakrishnan *et al.*, 2001). At present it is not known whether anaerobic methane-oxidizing archaea are using a version of this enzyme for the activation and reoxidation of methane. If anaerobic methane oxidation by archaea could proceed through a reversal of classical methanogenesis pathways, the Coenzyme M methyl reductase reaction would be the most difficult and energy-demanding step to reverse (Hoehler and Alperin, 1996). Current full-genome sequencing efforts using purified ANME-1 and ANME-2 archaea from environmental samples are testing whether the genomes of these methanotrophic archaea carry coenzyme M methyl reductase genes (Orphan *et al.*, 2002).

The Guaymas Basin Hydrothermal Vent Sites as Model System

To search for deeply branching and (possibly) ancestral representatives of sulfate-reducing, methanogenic, and methane-oxidizing microorganisms and their key genes in modern environments, we focus on hydrothermal vent habitats. Hydrothermal vents represent some of the earliest and best protected microbial habitats that may have survived repeated environmental disturbances in the surface biosphere; vents can in principle occur on every planet with oceans and active plate tectonics or volcanism. On Earth, hydrothermal vents sustain complex microbial ecosystems that utilize inorganic energy sources (such as sulfide, hydrogen, and reduced metals) and geothermal sources of carbon (such as methane, CO_2, and geothermally synthesized low-molecular-weight organic compounds) (Kelley *et al.*, 2002). The hydrothermally active sediments of the Guaymas Basin (Gulf of California, Mexico) provide a relatively well-studied model system for the complexity of the microbial communities that are involved in sulfate reduction, methanogenesis, and methane oxidation. Cultivations, lipid biomarker analyses, 16S rRNA, and functional gene sequencing are beginning to reveal unusually complex microbial communities that include sulfate-reducing prokaryotes, methanogenic archaea, and anaerobic methanotrophic archaea and their sulfate-reducing syntrophs (Fig. 1). Specifically, results of the Guaymas Basin survey (Teske *et al.*, 2002; Dhillon *et al.*, unpubl.) will also help to identify novel sulfate-reducing, methanogenic, and methane-oxidizing microorganisms in deep subsurface sediments, where these processes are predominant (D'Hondt *et al.*, 2002). These anoxic environments represent analogs to subsurface life under extraterrestrial conditions in which an inhospitable surface environment might have driven microbial life underground or never allowed its evolution within a phototrophic, oxygenated biosphere.

Guaymas Basin Microbial Communities

Sulfate-reducing bacteria and archaea are dominant terminal oxidizers of organic matter in the Guaymas Basin, as shown by high rates of sulfate reduction measured over wide temperature ranges up to about 100°C (Jorgensen *et al.*, 1990, 1992; Elsgaard *et al.*, 1994; Weber and Jorgensen, 2002). Hyperthermophilic, autotrophic, or mixotrophic archaea of the genus *Archaeoglobus* were found by cultivation (Burggraf *et al.*, 1990) and 16S rRNA sequencing

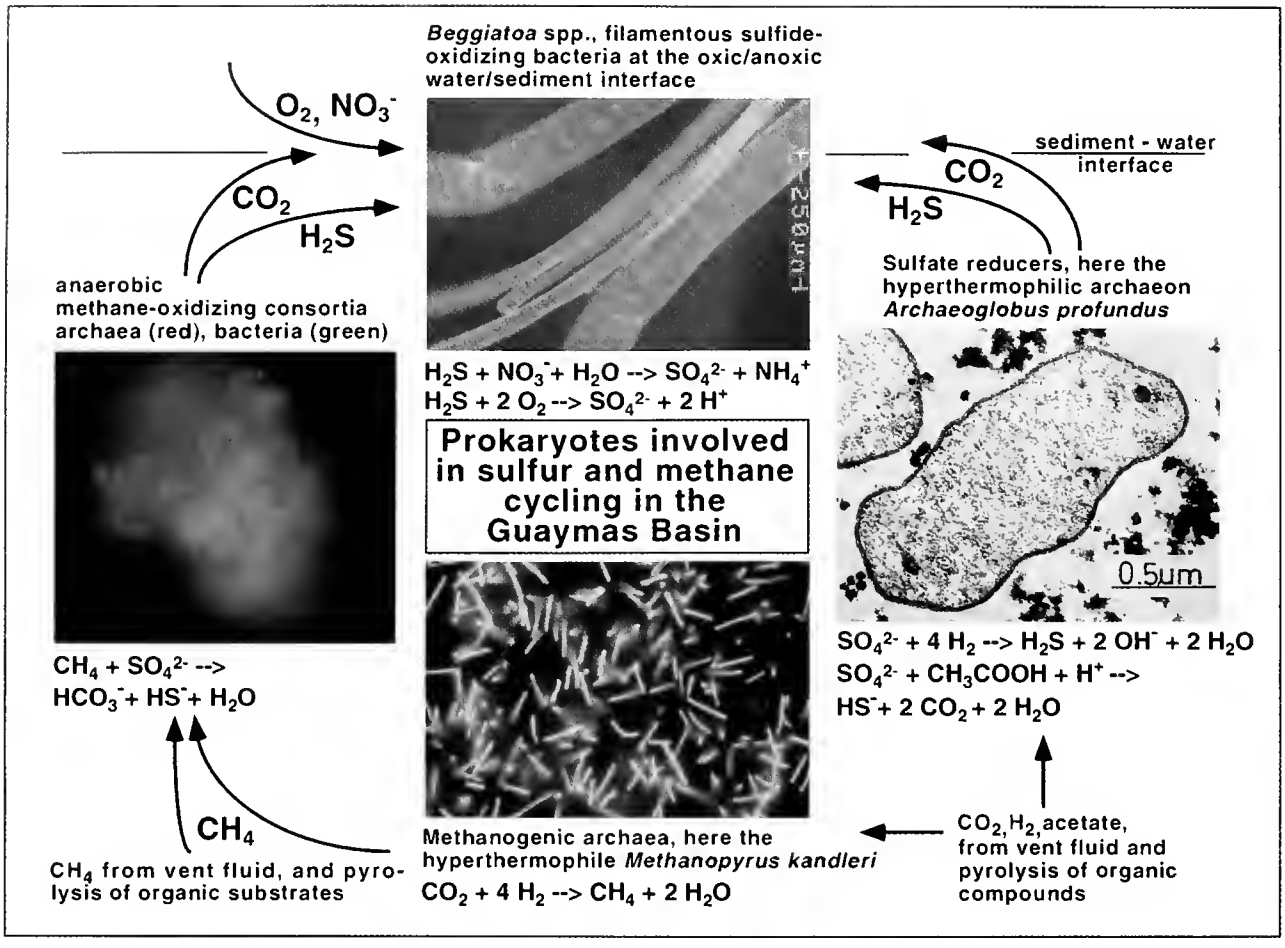

Figure 1. Simplified scheme of microorganisms and their reactions (sulfate reduction, methanogenesis, methane oxidation, sulfide oxidation) in the methane and sulfur cycles in the Guaymas Basin hydrothermal vents. Clockwise, sulfate-reducing bacteria and archaea (*Archaeoglobus profundus*), methanogenic archaea (*Methanopyrus kandleri*), methane-oxidizing consortia, and sulfide-oxidizing bacteria (*Beggiatoa* spp.). Fluorescence *in situ* hybridization image of anaerobic methane-oxidizing consortium, courtesy K. Knittel and A. Boetius (Max Planck Institute for Marine Microbiology, Bremen, Germany). The bacterial and archaeal species shown here are representatives of metabolically and phylogenetically diversified functional classes of prokaryotes. It has to be noted that sulfate reduction and sulfate-dependent methane oxidation are almost certainly uncoupled in the Guaymas sediments. The highly diversified sulfate-reducing prokaryotic community can oxidize a wide range of substrates (H_2 and acetate are just the simplest examples), whereas methane-oxidizing syntrophs are most likely restricted to methane oxidation intermediates provided by their archaeal partners.

(Teske *et al.*, 2002). Moderately thermophilic or mesophilic fatty acid oxidizing sulfate reducers have been cultured from Guaymas (Rueter *et al.*, 1994). Surveys with 16S rRNA detected predominantly members of the propionate-oxidizing, acetate-producing family Desulfobulbaceae (Teske *et al.*, 2002) and members of the acetate-oxidizing family Desulfobacteriaceae (Dhillon *et al.*, 2002). A molecular survey based on *dsrAB* genes revealed the existence of novel sulfate reducers in the Guaymas Basin that are not related to any cultured group of sulfate-reducing prokaryotes (Dhillon *et al.*, 2003).

Methanogenic archaea in the Guaymas Basin include hyperthermophilic, autotrophic methanogens of the genera *Methanococcus* (Jones *et al.*, 1989; Canganella and Jones, 1994) and *Methanopyrus* (Kurr *et al.*, 1991), and members of the formate-utilizing, mesophilic or moderately thermophilic family Methanomicrobiales (Teske *et al.*, 2002). Methane produced by these diverse methanogenic communities combines with the methane pool originating from pyrolysis of organic matter buried in the Guaymas sediments; the resulting methane concentrations in the Guaymas vent fluids are orders of magnitude higher than at non-sedimented, bare lava vent sites (Welhan, 1988).

Anaerobic methanotrophic communities in the Guaymas Basin include ANME-1 and ANME-2 archaea, as shown by 16S rRNA gene sequence analysis and ^{13}C-isotopic analysis

of diagnostic archaeal lipids (Teske *et al.*, 2002). The sulfate-reducing syntrophs in the Guaymas Basin sediments could not be identified unambiguously by 16S rRNA sequencing; their ^{13}C-depleted membrane lipids (mono- and dialkylglycerol ethers) indicate deeply branching bacteria or sulfate-reducing bacteria of the family Desulfosarcinales (Teske *et al.*, 2002). In classical ANME-2 consortia at Hydrate Ridge and Eel River Basin, the archaeal core was surrounded by an outer layer of sulfate-reducing bacteria of the family Desulfosarcinales (Boetius *et al.*, 2000; Orphan *et al.*, 2001a, b). In Guaymas Basin samples that yielded ANME-2 sequences, fluorescence *in situ* hybridization revealed a different structure; archaeal cells were intertwined with irregular lobes of syntrophic bacteria that did not hybridize with the probe for members of the Desulfosarcinales (Knittel *et al.*, 2002). A similar structure of ANME-2 archaea intertwined with unidentified bacteria has been observed in anaerobic methane-oxidizing consortia from Eel River Basin (Orphan *et al.*, 2002), and in the Haakon-Mosby Mud Volcano in the Norwegian Arctic Ocean (Knittel *et al.*, 2002).

Autotrophic sulfide-oxidizing bacteria of the genus *Beggiatoa* (Nelson *et al.*, 1989) that grow in dense mats on the sediment surface assimilate CO_2 from seawater and sediments; the latter CO_2 pool includes contributions from sulfate reduction and methane oxidation. The assimilation of methane oxidation products by sulfur-oxidizing bacteria appears to be highly variable. The ^{13}C isotopic signals of *Beggiatoa* biomass from hydrocarbon and methane seeps range from typical values of about $-20‰$ to $-30‰$ (Sassen *et al.*, 1993) to strong ^{13}C depletion indicative of assimilation of methane oxidation products (Paull *et al.*, 1992). The oxidation of sulfide and other sulfur intermediates (produced by sulfate-reducing bacteria) by *Beggiatoa* spp. depends on the availability of oxygen or nitrate as the terminal electron acceptor (McHatton *et al.*, 1996). Therefore, *Beggiatoa* spp. and other free-living and symbiotic sulfide-oxidizing bacteria that represent the basis of the food chain at hydrothermal vents could not survive in a strictly anoxic microbial habitat that does not receive molecular oxygen from the photosynthetic biosphere. In this way, the Guaymas Basin shows the caveats and limits of early-earth or astrobiological analogs. Also, sulfate reduction and methanogenesis in the Guaymas sediments are ultimately fuelled by high sedimentation of terrestrial organic matter and upper water column primary production; in other words, they depend on products of the oxygenated, photosynthetic biosphere.

Potential of Conserved Functional Genes for Genomics

Screening a microbial community for highly conserved key genes of sulfate reduction, methanogenesis, and methane oxidation results in a diversity census, with emphasis on taxonomy or microbial ecology. At the same time, it reveals the evolutionary divergence that has accumulated in these genes since the early Proterozoic or the Archaean, and the phylogenetic depth of these metabolisms in the bacterial and archaeal tree of life. With a growing database, homologous and ancestral traits of these genes, including secondary structure motifs and conserved sites, can be found that significantly increase our understanding of environmental and functional constraints that have shaped the evolution of these ancient microbial pathways and enzymes.

However, in spite of continuing primer development (Klein *et al.*, 2001), it is not certain whether PCR-based approaches can reliably detect all environmental genes of interest, in particular the most ancestral and deeply branching lineages or key genes with nonconserved primer sites. Primer site conservation can never be taken for granted. For example, 16S rRNA sequence motifs that were regarded as universally conserved show substantial variation between different bacterial lineages (Daims *et al.*, 1999), and can render 16S rRNA gene amplification with standard primers impossible (Huber *et al.*, 2002). To circumvent primer limitations, surveys of PCR-accessible genes (such as *dsrAB*, *apsA*, and *mrcA*) could be extended by shotgun cloning and fosmid library construction followed by sequence analysis. This approach also addresses the problem of phylogenetic congruence of different marker genes with partially discordant phylogenies. Proving the affiliation of different marker genes to each other and to their host organism requires an extensive database of pure cultures and strains, as shown for the 16S rRNA, *dsrAB* and *apsA* genes in sulfate-reducing prokaryotes, and their partially discordant gene trees (Friedrich, 2002). A genomic solution has to be found if marker genes belong to uncultured lineages in which this ground-truthing approach is not possible. Inferences based on co-occurrence at particular sampling locations with specific geochemical regimes cannot prove that novel phylotypes (for example 16S rRNA and *dsrAB*) belong to the same source organism (Thomson *et al.*, 2001). Tying together such phylotypes in the absence of cultures may require an extensive database of long genomic fragments, in which multiple key genes serve as "phylogenetic anchors" that identify the source organism of a larger genomic fragment and its phylogenetic position in addition to its function (Beja *et al.*, 2000).

Acknowledgments

This study was supported by NASA Astrobiology Institute "Environmental Genomes." Sampling at the Guaymas hydrothermal vents was supported by NSF (LExEN program, Grant OCR 9714195).

Literature Cited

Beja, O., M. T. Suzuki, E. V. Koonin, L. Aravind, A. Hadd, L. P. Nguyen, R. Villacorta, M. Amjadi, C. Garrigues, S. B. Jovanovich,

R. A. Feldman, and E. F. DeLong. 2000. Construction and analysis of bacterial artificial chromosome libraries from a marine microbial assemblage. *Environ. Microbiol.* **2:** 516–529.

Boetius, A., K. Ravenschlag, C. Schubert, D. Rickert, F. Widdel, A. Gieseke, R. Amann, B. B. Jørgensen, U. Witte, and O. Pfannkuche. 2000. A marine microbial consortium apparently mediating anaerobic oxidation of methane. *Nature* **407:** 623–626.

Boone, D. R., W. B. Whitman, and P. Rouvière. 1993. Diversity and taxonomy of methanogens. Pp. 35–80 in *Methanogenesis*, J. G. Ferry, ed. Chapman and Hall, New York.

Burggraf, S., H. W. Jannasch, B. Nicolaus, and K. O. Stetter. 1990. *Archaeoglobus profundus* sp. nov. represents a new species within the sulfate-reducing archaebacteria. *Syst. Appl. Microbiol.* **13:** 24–28.

Canfield, D. E., K. Habicht, and B. Thamdrup. 2000. The archaean sulfur cycle and the early history of atmospheric oxygen. *Science* **288:** 658–661.

Canganella, F., and W. J. Jones. 1994. Microbial characterization of thermophilic archaea isolated from the Guaymas Basin hydrothermal vent. *Curr. Microbiol.* **28:** 299–306.

Castro, H. F., N. H. Williams, and A. Ogram. 2000. Phylogeny of sulfate-reducing bacteria. *FEMS Microbiol. Ecol.* **31:** 1–9.

Daims, H., A. Brühl, R. Amann, K.-H. Schleifer, and M. Wagner. 1999. The domain-specific probe EUB338 is insufficient for the detection of all bacteria: development and evaluation of a more comprehensive probe set. *Syst. Appl. Microbiol.* **22:** 434–444.

Des Marais, D. J., H. Strauss, R. E. Summons, and J. M. Hayes. 1992. Carbon isotopic evidence for the stepwise oxidation of the Proterozoic environment. *Nature* **359:** 605–609.

Dhillon, A., A. Teske, J. Dillon, D. A. Stahl, and M. L. Sogin. 2003. Molecular characterization of sulfate-reducing bacteria in the Guaymas Basin. *Appl. Environ. Microbiol.* **69** (in press).

D'Hondt, S., S. Rutherford, and A. Spivack. 2002. Metabolic activity of subsurface life in deep-sea sediments. *Science* **295:** 2067–2070.

Elsgaard, L., M. F. Isaksen, B. B. Jørgensen, A.-M. Alayse, and H. W. Jannasch. 1994. Microbial sulfate reduction in deep-sea sediments at the Guaymas basin hydrothermal vent area: influence of temperature and substrates. *Geochim. Cosmochim. Acta* **58:** 3335–3343.

Friedrich, M. 2002. Phylogenetic analysis reveals multiple lateral transfers of adenosine-5′-phosphosulfate reductase genes among sulfate-reducing microorganisms. *J. Bacteriol.* **184:** 278–289.

Hayes, J. M. 1994. Global methanotrophy at the archaean-proterozoic transition. Pp. 220–239 in *Early Life on Earth*, S. Bengtson, J. Bergstrom, V. Gonzalo, and A. Knoll, eds. Nobel Symposium, Columbia University Press, New York.

Hoehler, T. M., and M. J. Alperin. 1996. Anaerobic methane oxidation by a methanogen-sulfate reducer consortium: geochemical evidence and biochemical considerations. Pp. 326–333 in *Microbial Growth on C1-Compounds*, M. E. Lidstrom and F. R. Tabita, eds. Kluwer, Dordrecht.

Hoehler, T. M., M.J. Alperin, D.B. Albert, and C. S. Martens. 1994. Field and laboratory studies of methane oxidation in an anoxic marine sediment: evidence for a methanogen-sulfate reducer consortium. *Global Biogeochem. Cycles* 8: 451–463.

Huber, H., M. Hohn, R. Rachel, T. Fuchs, V. Wimmer, and K. Stetter. 2002. A new phylum of Archaea represented by a nanosized hyperthermophilic symbiont. *Nature* **417:** 63–67.

Jones, W. J., C. E. Stugard, and H. W. Jannasch. 1989. Comparison of thermophilic methanogens from submarine vent sites. *Arch. Microbiol.* **151:** 314–318.

Jorgensen, B. B., L. X. Zawacki, and H. W. Jannasch. 1990. Thermophilic bacterial sulfate reduction in deep-sea sediments at the Guaymas Basin hydrothermal vents (Gulf of California). *Deep-Sea Res. Part I* **37:** 695–710.

Jørgensen, B. B., M. F. Isaksen, and H. W. Jannasch. 1992. Bacterial sulfate reduction above 100°C in deep-sea hydrothermal vent systems. *Science* **258:** 1756–1757.

Kelley S., J. A. Baross, and J. R. Delaney. 2002. Volcanoes, fluids and life at Mid-Ocean Ridge spreading centers. *Annu. Rev. Earth Planet. Sci.* **30:** 385–491.

Klein, M., M. Friedrich, A. J. Roger, P. Hugenholtz, S. Fishbain, H. Abicht, L. L. Blackall, D. A. Stahl, and M. Wagner. 2001. Multiple lateral transfers of dissimilatory sulfite reductase genes between major lineages of sulfate-reducing prokaryotes. *J. Bacteriol.* **183:** 6028–6035.

Knittel, K., T. Losekann, A. Boetius, T. Nadalig, and R. Amann. 2002. Diversity of microorganisms mediating anaerobic oxidation of methane. *Geochim. Cosmochim. Acta* **66:** A407 (Abstract).

Knoll, A. H., and D. E. Canfield. 1998. Isotopic inferences on early ecosystems. Pp. 212–243 in *Isotope Paleobiology and Paleoecology*, The Palaeontological Society Papers, Vol. 4. R. D. Norris and R. M. Corfield, eds. Publication of the Palaeontological Society, Pittsburgh, PA.

Kurr, M., R. Huber, H. König, H. W. Jannasch, H. Fricke, A. Trincone, J. K. Kristjans-son, and K. O. Stetter. 1991. *Methanopyrus kandleri*, gen. and sp. nov. represents a novel group of hyperthermophilic methanogens, growing at 110°C. *Arch. Microbiol.* **156:** 239–247.

Lueders, T., K.-J. Chin, R. Conrad, and M. Friedrich. 2001. Molecular analyses of methyl-coenzyme M reductase α-subunit (*mcrA*) genes in rice field soil and enrichment cultures reveal the methanogenic phenotype of a novel archaeal lineage. *Environ. Microbiol.* **3:** 194–204.

McHatton, S. C., J. P. Barry, H. W. Jannasch, and D. C. Nelson. 1996. High nitrate concentrations in vacuolate, autotrophic marine *Beggiatoa*. *Appl. Environ. Microbiol.* **62:** 954–958.

Nelson, D. C., C. O. Wirsen, and H. W. Jannasch. 1989. Characterization of large autotrophic *Beggiatoa* abundant at hydrothermal vents of the Guaymas Basin. *Appl. Environ. Microbiol.* **55:** 2909–2917.

Orphan, V. J., K.-U. Hinrichs, C. K. Paull, L. T. Taylor, S. Sylva, and E. F. DeLong. 2001a. Comparative analysis of methane-oxidizing archaea and sulfate-reducing bacteria in anoxic marine sediments. *Appl. Environ. Microbiol.* **67:** 1922–1934.

Orphan, V. J., C. H. Howes, K.-U. Hinrichs, K. D. McKeegan, and E. F. DeLong. 2001b. Methane-consuming archaea revealed by directly coupled isotopic and phylogenetic analysis. *Science* **293:** 484–487.

Orphan, V. J., C. H. House, K.-U. Hinrichs, K. D. McKeegan, and E. F. DeLong. 2002. Multiple groups mediate methane oxidation in anoxic cold seep sediments. *Proc. Natl. Acad. Sci. USA* **99:** 7663–7668.

Paull, C. K., J. P. Chanton, A. C. Neumann, J. A. Coston, and C. S. Martens. 1992. Indicators of methane-derived carbonates and chemosynthetic organic carbon deposits: examples from the Florida Escarpment. *Palaios* **7:** 361–375.

Ramakrishnan, B., T. Lueders, P. F. Dunfield, R. Conrad, and M. W. Friedrich. 2001. Archaeal community structures in rice field soils from different geographical regions before and after initiation of methane production. *FEMS Microbiol. Ecol.* **37:** 175–186.

Rueter, P., R. Rabus, H. Wilkes, F. Aeckersberg, F. A. Rainey, H. W. Jannasch, and F. Widdel. 1994. Anaerobic oxidation of hydrocarbons in crude oil by new types of sulphate-reducing bacteria. *Nature* **372:** 455–458.

Sassen, R., H. H. Roberts, P. Aharon, J. Larkin, E. W. Chinn, and R. Carney. 1993. Chemosynthetic bacterial mats at cold hydrocarbon seeps, Gulf of Mexico continental slope. *Org. Geochem.* **20:** 77–89.

Springer, E., M. S. Sachs, C. R. Woese, and D. R. Boone. 1995. Partial gene sequences for the alpha-subunit of methy-coenzyme M reductase

(MCR1) as a phylogenetic tool for the family *Methanosarcinaceae*. *Int. J. Syst. Bacteriol.* **45:** 554–559.

Strauss, H., and T. Moore. 1992. Abundances and isotopic compositions of carbon and sulfur species in whole rock and kerogen samples. Pp. 709–789 in *The Proterozoic Biosphere*, J. W. Schopf and C. Klein, eds. Cambridge University Press, Cambridge.

Teske, A., K.-U. Hinrichs, V. Edgcomb, A. d. V. Gomez, D. Kysela, S. P. Sylva, M. L. Sogin, and H. W. Jannasch. 2002. Microbial diversity of hydrothermal sediments in the Guaymas Basin: evidence for anaerobic methanotrophic communities. *Appl. Environ. Microbiol.* **68:** 1994–2007.

Thomsen, T. R., K. Finster, and N. B. Ramsing. 2001. Biogeochemical and molecular signatures of anaerobic methane oxidation in a marine sediment. *Appl. Environ. Microbiol.* **67:** 1646–1656.

Valentine, D. L., and W. S. Reeburgh. 2000. New perspectives on anaerobic methane oxidation. *Environ. Microbiol.* **2:** 477–484.

Wagner, M., A. J. Roger, J. L. Flax, G. A. Brusseau, and D. A. Stahl. 1998. Phylogeny of dissimilatory sulfite reductases supports an early origin of sulfate respiration. *J. Bacteriol.* **180:** 2975–2982.

Weber, A., and B. B. Jørgensen. 2002. Bacterial sulfate reduction in hydrothermal sediments of the Guaymas Basin, Gulf of California, Mexico. *Deep-Sea Res. Part I* **49:** 827–841.

Welhan, J. A. 1988. Origins of methane in hydrothermal systems. *Chem. Geol.* **71:** 183–198.

Widdel, F., and F. Bak. 1992. Gram-negative mesophilic sulfate-reducing bacteria. Pp. 3352–3378 in *The Prokaryotes*, 2nd ed. A. Balows, H. G. Trüper, M. Dworkin, W. Harder, and K.-H. Schleifer, eds. Springer, New York.

Reference: *Biol. Bull.* **204:** 192–195. (April 2003)

Viral Influence on Aquatic Bacterial Communities

J. A. FUHRMAN* AND M. SCHWALBACH

University of Southern California, Los Angeles, California 90089-0371

Bacterial viruses, or bacteriophages, have numerous roles in marine systems. Although they are now considered important agents of mortality of bacteria, a second possible role of regulating bacterial community composition is less well known. The effect on community composition derives from the presumed species-specificity and density-dependence of infection. Although models have described the "kill the winner" hypothesis of such control, there are few observational or experimental demonstrations of this effect in complex natural communities. We report here on some experiments that demonstrate that viruses can influence community composition in natural marine communities. Although the effect is subtle over the time frame suitable for field experiments (days), the cumulative effect over months or years would be substantial. Other virus roles, such as in genetic exchange or microbial evolution, have the potential to be extremely important, but we know very little about them.

For many years, viruses were not included in our conceptual models of how natural aquatic ecosystems function. This was primarily because they simply were not observed. However, it was learned about 10 years ago that viruses are highly abundant in such systems, roughly 10^{10} per liter, or about 10–20 times the bacterial abundance (Bergh *et al.*, 1989; Proctor and Fuhrman, 1990). Because viruses require a host to reproduce, this high abundance raised the obvious question of what organisms these viruses were infecting. Field studies showed that viral counts are much better correlated to bacterial counts than to chlorophyll. Therefore, although viruses infecting eukaryotes certainly occur and can be important components of food webs, the majority of native marine viruses are thought to infect bacteria or archaea (Fuhrman, 1999; see also Wilhelm and Suttle, 1999; Wommack and Colwell, 2000).

Abundance alone does not tell how active the viruses may be in infecting hosts. Viral activities in natural communities have been estimated by a few approaches, all yielding the conclusion that viral infection is an important component of bacterial mortality. The first approach is to observe and count infected host cells by transmission electron microscopy (Proctor and Fuhrman, 1990). Although only a small percentage of bacteria are visibly infected, that translates into 10% to 50% of the mortality (less for cyanobacteria). Viral activity has also been estimated *via* virus decay rates. Viral decay is caused by sunlight, enzymes, and other factors. These rates are typically a few percent per hour, and when one considers that the viruses are replaced by replication in infected host cells, these rates also translate into 10% to 50% of total bacterial mortality (reviewed by Fuhrman, 1999). Virus production rates have also been estimated directly, by three independent methods: (a) tritiated thymidine incorporation into viral DNA (Steward *et al.*, 1992), (b) dilution of fluorescently labeled viruses added to trace production and loss (Noble and Fuhrman, 2000), and (c) virus increase in samples filtered to reduce viral abundance (Wilhelm *et al.*, 2002). The results of such studies show that virus production is typically a few percent per hour, matching decay. This again translates into between 10% and 50% of bacterial mortality. (Note that the mortality estimates are not additive, but rather they represent estimates of the same process determined by a variety of approaches.) Mortality from viruses has been compared directly to that from protists, as estimated by loss of tritiated DNA over several generations, and the results are the same (Fuhrman and Noble, 1995). Overall, the evidence is strong that viruses can have a significant impact on mortality of bacteria and phytoplankton.

* To whom correspondence should be addressed. E-mail: fuhrman@usc.edu

The paper was originally presented at a workshop titled *Outcomes of Genome-Genome Interactions.* The workshop, which was held at the J. Erik Jonsson Center of the National Academy of Sciences, Woods Hole, Massachusetts, from 1–3 May 2002, was sponsored by the Center for Advanced Studies in the Space Life Sciences at the Marine Biological Laboratory, and funded by the National Aeronautics and Space Administration under Cooperative Agreement NCC 2-1266

Viruses impact nutrient cycling because viral activity leads to fragmentation of host organisms. Lysis products are dissolved substances and small particles that can be assimilated by heterotrophic bacteria. The result is a loop in the food web that has the net effect of oxidizing organic matter and regenerating inorganic nutrients. It also helps keep nutrients in the ocean top layer, where they can fuel production, instead of sinking out and being effectively lost from the euphotic zone (reviewed by Fuhrman, 1999).

One of the most interesting aspects of viruses in marine systems is their potential effect on community composition. This is expected because (1) viruses are generally specific to certain hosts, thought to be species or genus in most cases (Ackermann and DuBow, 1987), although some viruses have a broad range of hosts (Riemann and Middelboe, 2002); and (2) infection is density-dependent—that is, infection is more likely at high host densities due to increased contact rates. The presumed narrow host range and density dependence together suggest that viruses should preferentially infect the most common hosts: high abundance makes one more susceptible; rarity makes one less susceptible. This has the opposite effect compared to competitive dominance, and is called the "kill the winner" hypothesis (Thingstad and Lignell, 1997).

Thus, viruses might help to control monospecific blooms and increase diversity of host organisms in general. An important question is whether the effect is only replacement of sensitive strains with closely related virus-resistant strains, or whether completely different species can replace the infected ones. Probably both occur, but this process is not well studied. Although laboratory experiments suggest that development of resistance can help avoid infection, it is not so simple in natural systems where there are many species and complex interactions. Resistance is thought to have a cost in most instances and may allow other species to compete, as discussed in Fuhrman (1999) and Riemann and Middelboe (2002).

There have been some recent theoretical analyses of the interactions between virus infection and community composition. One set of models (Thingstad and Lignell, 1997) indicates that viruses can control host species composition even when they are responsible for a very small portion of the mortality. This is because, over several generations, even a small selective effect can have a major long-term influence. Even prior to the development of this theory, there were some relevant field studies. Waterbury and Valois (1993) examined cultivable marine *Synechococcus* and their viruses from near Woods Hole, Massachusetts. Despite a low reported viral impact on mortality, the *Synechococcus* strains dominant at any given time tended to be resistant to co-occurring viruses. Thus, viruses seemed to influence the strain composition, but the same genus persisted throughout the study period.

We have asked if the Waterbury and Valois (1993) result from cultivable *Synechococcus* can be generalized to other bacteria—that is, will variety of closely related strains persist over long periods? Perhaps the *Synechococcus* story is not applicable to other groups, because this genus may occupy a unique photosynthetic niche that another marine genus cannot fill in that environment.

Our own experiments on viral effects have included a few kinds of experiments. One type is growth of mixed bacterial communities in the presence and absence of viruses. The protocol for growing such communities was developed several years ago (Wilcox and Fuhrman, 1994). The inoculum we used was seawater from Santa Monica Bay, California, filtered through a 0.6-μm polycarbonate Nuclepore filter (twice) to remove protists. The growth medium was cell-free filtered seawater made two different ways: virus-free seawater was made by filtering through a 0.02-μm pore size Anodisc filter, and seawater containing natural viruses was made by filtering through a 0.2-μm Nuclepore filter. The cultures grew within 1–2 days and were observed for 5 days. Bacterial community composition was monitored by a genetic fingerprinting method called terminal restriction fragment length polymorphism (TRFLP), which provides a list of operational taxonomic units based upon variations in 16S rRNA sequences (Avaniss-Aghajani *et al.*, 1994). The bacterial primers and *Hha* 1 restriction enzyme we used were from Gonzalez *et al.* (2000), who also discuss the interpretation of this sort of TRFLP.

The data in Figure 1 demonstrate that the presence of viruses apparently reduced the dominance of a few taxa, particularly the most abundant one that was presumptively identified as marine α Proteobacteria related to *Roseobacter*. The TRFLP peak representing this group dropped significantly, although even without viruses it was the peak with the most amplified DNA. Several taxa, as indicated by other TRFLP peaks, were detectable in only one or the other treatment, grown with or without the presence of viruses. Therefore, the viruses appeared to have an impact on bacterial community composition, helping some groups and hurting others. Although most of the same common taxa were present in both treatments, it should be noted that the experiment lasted only a few generations. Therefore, the relatively subtle effects we observed on a time scale of days would be amplified considerably over weeks or months. Therefore, the data are consistent with the "kill the winner" hypothesis.

Virus-mediated genetic exchange occurs by a process known as transduction. It has been shown to occur in natural environments—for example, freshwater (Ripp *et al.*, 1994) and marine habitats (Jiang and Paul, 1998)—as detected by transfer of selectable markers. Preliminary calculations show that, considering high bacterial abundance, it can be a frequent event: Jiang and Paul (1998) estimated 10^{14} transduction events per year in Tampa Bay alone. Despite this high potential, genes transferred this way in natural envi-

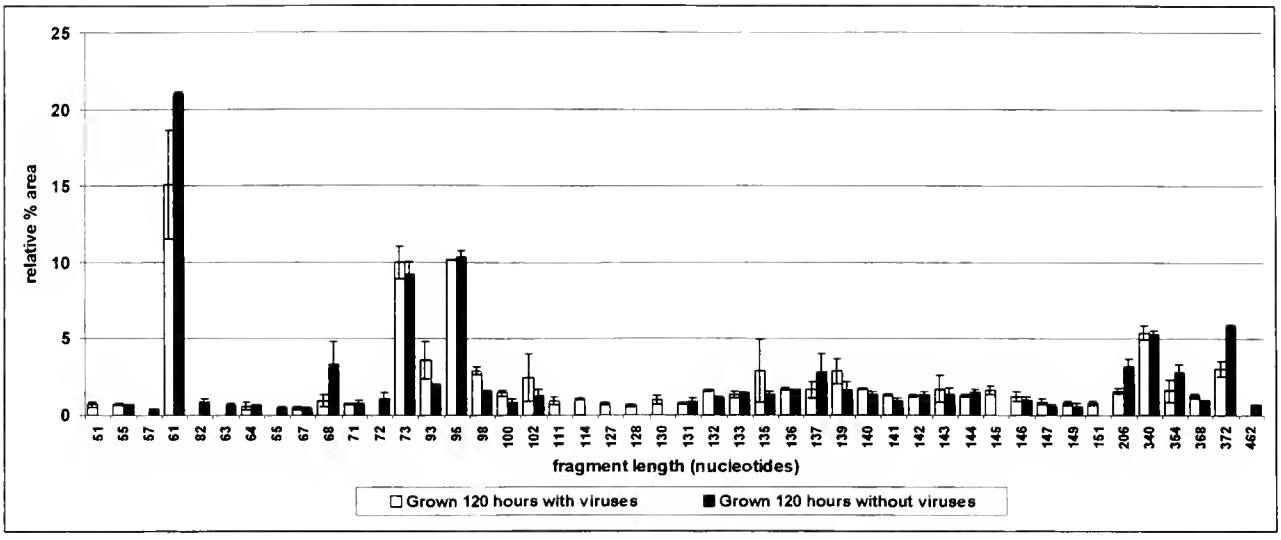

Figure 1. Analysis, by terminal restriction fragment length polymorphism, of bacterial community composition in seawater inocula (filtered to remove protists) grown in seawater that had been filtered to remove all cellular organisms and viruses ("without viruses") or cellular organisms only ("with viruses"). Each bar represents an operational taxonomic unit, and its height is proportional to the amount of amplified DNA in that particular fragment. Error bars are ± one standard error of the mean.

ronments are not characterized, and we know very little about the overall process.

Virus effects on bacterial evolution can stem from both negative and positive interactions. Negative interactions include infection-mediated mortality that can provide selective pressure. Resistance of hosts and viral adaptation to resistance is probably an ongoing process—it can be viewed as a "war," with measures and counter-measures and constant adaptation of both partners. It would seem that viruses are unlikely to lead to extinctions, because as the host population size got smaller, the viruses would have more and more difficulty in "finding" a host by diffusion. Nevertheless, a local reduction in population size might cause an evolutionary bottleneck. Positive interactions include viral conversion whereby viral genetic material codes for new host capabilities. Also, bacteria may use viruses as a nutrition source, maybe even using "decoy" receptors to lure "unsuspecting" viruses to attempt infection (Fuhrman, 1999). There are obviously additional evolutionary effects of genetic exchange mediated by viruses. On evolutionary time scales, this process helps to homogenize genomes, especially within close relatives, which may help to keep a bacterial "species" together.

Acknowledgments

This work was supported by NSF grants OCE9906989 and DEB0072770. We also thank Lita Proctor, Rachel Noble, Robin Wilcox, and Ian Hewson for helpful conversations and assistance with experiments.

Literature Cited

Ackermann, H.-W., and M. S. DuBow. 1987. *Viruses of Prokaryotes. Vol. 1. General Properties of Bacteriophages.* CRC Press, Boca Raton, FL.

Avaniss-Aghajani, E., K. Jones, D. Chapman, and C. Brunk. 1994. A molecular technique for identification of bacteria using small subunit ribosomal RNA sequences. *Biotechniques* **17:** 144–149.

Bergh, O., K. Y. Børsheim, G. Bratbak, and M. Heldal. 1989. High abundance of viruses found in aquatic environments. *Nature* **340:** 467–468.

Fuhrman, J. A. 1999. Marine viruses: biogeochemical and ecological effects. *Nature* **399:** 541–548.

Fuhrman, J. A., and R. T. Noble. 1995. Viruses and protists cause similar bacterial mortality in coastal seawater. *Limnol. Oceanogr.* **40:** 1236–1242.

Gonzalez, J. M., R. Simo, R. Massana, J. S. Covert, E. O. Casamayor, C. Pedros-Alio, and M. A. Moran. 2000. Bacterial community structure associated with a dimethylsulfoniopropionate-producing North Atlantic algal bloom. *Appl. Environ. Microbiol.* **66:** 4237–4246.

Jiang, S. C., and J. H. Paul. 1998. Gene transfer by transduction in the marine environment. *Appl. Environ. Microbiol.* **64:** 2780–2787.

Noble, R. T., and J. A. Fuhrman. 2000. Rapid virus production and removal as measured with fluorescently labeled viruses as tracers. *Appl. Environ. Microbiol.* **66:** 3790–3797.

Proctor, L. M., and J. A. Fuhrman. 1990. Viral mortality of marine bacteria and cyanobacteria. *Nature* **343:** 60–62.

Riemann, L., and M. Middelboe. 2002. Viral lysis of marine bacterioplankton: implications for organic matter cycling and bacterial clonal composition. *Ophelia* **56:** 57–68.

Ripp, S., O. A. Ogunseitan, and R. V. Miller. 1994. Transduction of a freshwater microbial community by a new *Pseudomonas aeruginosa* generalized transducing phage, Ut1. *Mol. Ecol.* **3:** 121–126.

Steward, G. F., J. Wikner, D. C. Smith, W. P. Cochlan, and F. Azam. 1992. Estimation of virus production in the sea: I. Method development. *Mar. Microb. Food Webs* **6:** 57–78.

Thingstad, T. F., and R. Lignell. 1997. Theoretical models for the control of bacterial growth rate, abundance, diversity and carbon demand. *Aquat. Microb. Ecol.* **13:** 19–27.

Waterbury, J. B., and F. W. Valois. 1993. Resistance to co-occurring phages enables marine *Synechococcus* communities to coexist with cyanophages abundant in seawater. *Appl. Environ. Microbiol.* **59:** 3393–3399.

Wilcox, R. M., and J. A. Fuhrman. 1994. Bacterial viruses in coastal seawater: lytic rather than lysogenic production. *Mar. Ecol. Prog. Ser.* **114:** 35–45.

Wilhelm, S. W., and C. A. Suttle. 1999. Viruses and nutrient cycles in the sea—viruses play critical roles in the structure and function of aquatic food webs. *Bioscience* **49:** 781–788.

Wilhelm, S. W., S. M. Brigden, and C. A. Suttle. 2002. A dilution technique for the direct measurement of viral production: a comparison in stratified and tidally mixed coastal waters. *Microb. Ecol.* **43:** 168–173.

Wommack, K. E., and R. R. Colwell. 2000. Virioplankton: viruses in aquatic ecosystems. *Microbiol. Mol. Biol. Rev.* **64:** 69–114.

Reference: *Biol. Bull.* **204:** 196–199. (April 2003)

A(r)Ray of Hope in Analysis of the Function and Diversity of Microbial Communities

MARTIN F. POLZ*, STEFAN BERTILSSON†, SILVIA G. ACINAS, AND DANA HUNT

Department of Civil and Environmental Engineering, Massachusetts Institute of Technology, Cambridge, Massachusetts 02139

The vast majority of microorganisms in the environment remain uncultured, and their existence is known only from sequences retrieved by PCR. As a consequence, our understanding of the ecological function of dominant microbial populations in the environment is limited. We will review microbial diversity studies and show that these may have moved from an extreme underestimation to a potentially severe overestimation of diversity. The latter results from a simple PCR-generated artifact: the cloning of heteroduplex molecules followed by Escherichia coli *mismatch repair, which may generate an exponential increase in observed sequence diversity. However, simple modifications to current PCR amplification protocols minimize such artifactual sequences and may bring within our reach estimation of bacterial diversity in environmental samples. Such estimates may spur new culture-independent approaches based on genomic and microarray technology, allowing correlation of phylogenetic identity with the ecological function of unculturable organisms. In particular, we are developing a DNA microarray that enables identification of individual populations active in utilization of specific organic substrates. The array consists of 16S and 23S rDNA-targeted oligonucleotides and is hybridized to RNA extracted from samples incubated with ^{14}C-labeled organic substrates. Populations that metabolize the substrate can be identified by the radiolabel incorporated in their rRNA after only one to two cell doublings, ensuring realistic preservation of community structure. Thus, the microarray approach may provide a powerful means to link microbial community structure with* in situ *function of individual populations.*

The last two decades have seen a radical shift in our understanding of microbial diversity. Previously the number of bacterial and archaeal species had been estimated to be in the thousands. It is now generally accepted that the number may actually be as high as several million (Torsvik *et al.*, 2002). This change was brought about by a gradual replacement of diversity estimates based on pure-culture isolation of strains with a determination of diversity based on co-occurring gene sequences, largely ribosomal RNA (rRNA) genes (Head *et al.*, 1998). Although early attempts were made to screen diversity by shotgun cloning of environmental DNA, with subsequent detection and sequencing of rRNA gene inserts (Schmidt *et al.*, 1991), large-scale application of the molecular approach was dependent on PCR protocols that allow the enrichment of rRNA genes from genome mixtures using universal primers (Head *et al.*, 1998). Today, the assessment of the entire diversity of rRNA sequences (ribotypes) coexisting within specific microbial communities has become a realistic possibility due to the ease of PCR implementation and the increased availability of high-throughput sequencing facilities.

Although the exact magnitude of microbial diversity still remains an open question, the PCR-based approach has led to the retrieval of large numbers of sequences from almost any environment examined (Hugenholtz *et al.*, 1998). Thus extensive comparative databases are now available from which patterns of microbial community structure are beginning to emerge. For example, studies of bacterioplankton diversity in the ocean, which represents one of the best-studied environments, have shown that, surprisingly, the major phylogenetic groups in the open ocean and the coastal ocean are similar, despite marked differences in trophic

* To whom correspondence should be addressed. E-mail: mpolz@mit.edu

†Present address: Department of Evolutionary Biology, Limnology, Uppsala University, Norbyvägen 20, SE-75236, Uppsala, Sweden.

The paper was originally presented at a workshop titled *Outcomes of Genome-Genome Interactions*. The workshop, which was held at the J. Erik Jonsson Center of the National Academy of Sciences, Woods Hole, Massachusetts, from 1–3 May 2002, was sponsored by the Center for Advanced Studies in the Space Life Sciences at the Marine Biological Laboratory, and funded by the National Aeronautics and Space Administration under Cooperative Agreement NCC 2-1266.

state and habitat quality between these environments (Giovannoni and Rappé, 2000). Such observations have provided important insights; yet they also highlight the major problem of the molecular diversity approach: because very few of the retrieved sequences have closely related cultured representatives available, the ecological role of an organism in question cannot even be guessed (Hugenholtz *et al.*, 1998). Furthermore, even when closely related cultured organisms exist, they can display quite significant genomic, physiological, or metabolic differences (Gray and Head, 2001). New alternatives for diversity studies, such as analysis of large genome fragments retrieved from the environment (Béja *et al.*, 2000) or gene cassette PCR for recovery of complete open reading frames from environmental DNA (Stockes *et al.*, 2001), can enhance our understanding of uncultured organisms. Nonetheless, elucidation of structure-function relationships or niche differentiation of populations within microbial communities remains one of the big challenges in microbial ecology.

During the last few years, molecular diversity studies have been augmented with tracer techniques that allow assignment of biogeochemical function to uncultured microbial populations [recently reviewed by Gray and Head (2001)]. Most notably, combined microautoradiography and *in situ* hybridization (STAR- or MICROFISH) (Lee *et al.*, 1999; Ouverney and Fuhrman, 1999; Cottrell and Kirchman, 2000) or stable isotope probing (Boschker *et al.*, 1998; Radajewski *et al.*, 2000) allow identification of microbial populations responsible for the metabolism of specific organic compounds. In both cases, environmental samples are incubated with isotopically labeled substrates. In STAR- or MICROFISH, microautoradiography and *in situ* hybridization are carried out on the same microscope slide with the goal of matching uptake of radiochemicals with phylogenetic identification on the single-cell level. In stable isotope probing, either lipid biomarkers (Boschker *et al.*, 1998) or DNA (Radajewski *et al.*, 2000) are extracted from communities incubated with ^{13}C-labeled compounds. If cells grow on the added compounds, their pool of macromolecules will be isotopically heavy compared to those of metabolically inactive organisms. This makes it possible to identify the organism in one of two ways: (1) by mass spectrometry of labeled "signature" lipids (Boschker *et al.*, 1998); or (2) by separation by ultracentrifugation of community DNA according to mass differences, followed by identification of rRNA genes in the isotopically heavy DNA pool by PCR, cloning, and sequencing (Radajewski *et al.*, 2000).

The above approaches have already produced interesting insights into the ecological roles of uncultured Bacteria and Archaea. For example, using MICROFISH, it was demonstrated that low-temperature Archaea, which represent a dominant group in deep ocean water but are currently known only from rRNA gene clone libraries, readily take up amino acids at low ambient concentrations (Ouverney and Fuhrman, 1999). In another study, incubation of anaerobic sediments with ^{13}C-acetate yielded signature lipids of gram-positive bacteria rather than those of the more readily isolated delta Proteobacteria sulfate-reducing bacteria (Boschker *et al.*, 1998). However, each of the techniques has distinct drawbacks. Stable isotope probing requires very high substrate concentrations and long incubation times, so that the procedure actually resembles enrichment cultures (Radajewski *et al.*, 2000); MICROFISH involves labor-intensive hybridization and microautoradiography, which limits the number of populations whose metabolism can be explored.

We are currently developing a combination of DNA microarrays and radiotracer incubations, the "functional diversity array," as a high-throughput complement to the above methods (Bertilsson and Polz, 2001). DNA microarrays can carry hundreds to thousands of specific nucleic acid probes, which are arrayed in discrete spots. During the hybridization process, these probes capture their specific target from mixtures of templates. If these are either radioactively or fluorescently labeled, the presence or, to a certain extent, the quantity of all specific templates for which probes have been spotted can be ascertained. The application of DNA microarrays for screening and monitoring microbial community structure by arraying rRNA-specific oligonucleotide probes is being explored by a number of laboratories (Cho and Tiedje, 2001; Small *et al.*, 2001; Koizumi *et al.*, 2002). In the functional diversity array, diversity screening is combined with detection of populations responsible for specific transformations in the community (Fig. 1). Samples are spiked with ^{14}C-labeled compounds, leading to incorporation of radionuclides into rRNA of populations that actively metabolize the compound of interest (Bertilsson and Polz, 2001). RNA is subsequently extracted, fluorescently labeled, and hybridized to the microarray, which contains oligonucleotide probes specific for each "ribotype" in the community. Radioactivity in each spot due to hybridization can be determined by either microautoradiography or phosphor-imaging, so that in combination with the fluorescent signal, a specific activity can be estimated for each population (Fig. 1).

For the functional diversity array to be generally applicable, differentiation of populations by the arrayed probes is not, by itself, sufficient. In addition, several critical questions must be evaluated. First, what is the detection limit for ^{14}C-labeled rRNA hybridized to the array? Second, can realistic substrate concentrations be used, and what are the kinetics of rRNA synthesis after uptake of label under environmental conditions? Third, to what extent can an entire microbial community be represented on the array? Below, we evaluate these questions, with special emphasis on approaches for studying rRNA gene diversity in microbial communities as a necessary precondition for determining biogeochemical activity of previously unidentified populations.

Quantification of the radioactive signal on arrays shows

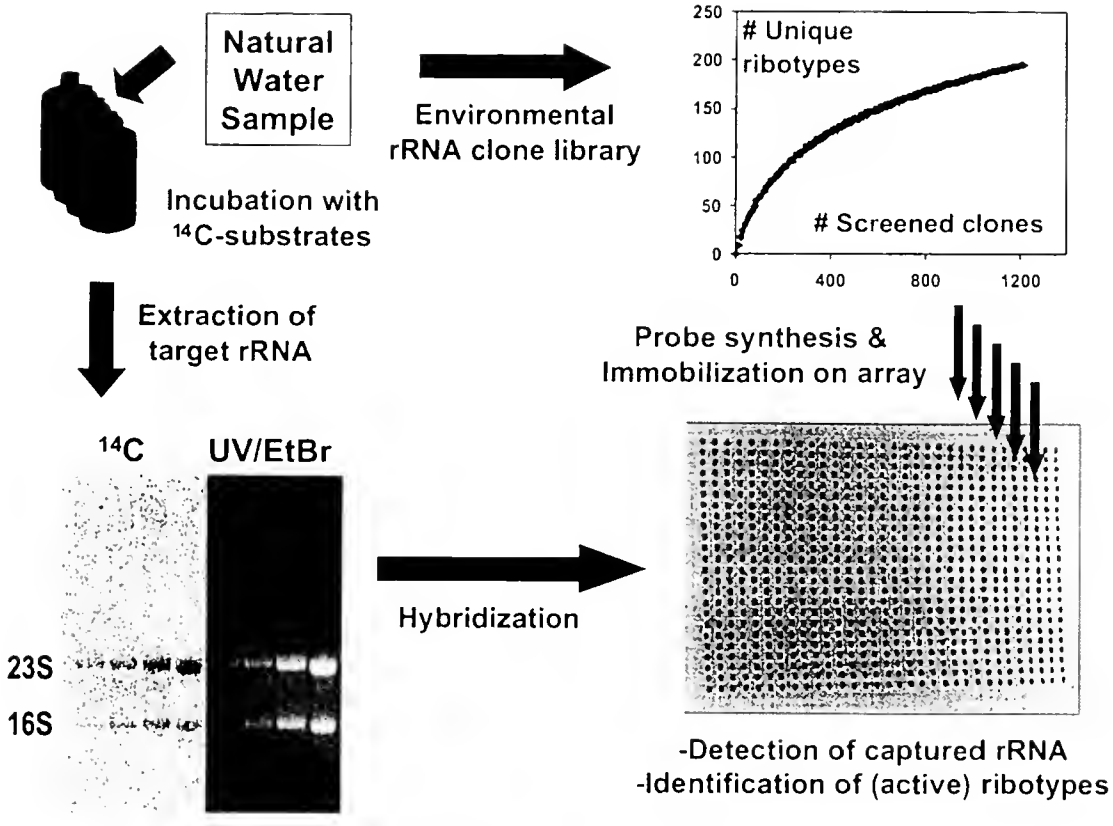

Figure 1. Outline of the experimental approach used for the functional diversity array.

that the approach is sensitive enough to detect populations at naturally occurring levels. The use of phosphor-imaging screens, to which the entire array is exposed, allows ^{14}C bound to each spot to be quantified. We have experimentally determined the detection limit for ^{14}C on these screens to be 0.1 DPM for a spot 150 μm in diameter, which consists of about 10^8 oligonucleotide probes. Assuming that the rRNA molecules fragment to about 300 bp and that only 1% of the oligonucleotide probes will be bound to templates after hybridization, the detection limit is between 10^2 and 10^3 cells. This estimate is based on a cellular rRNA content between 1,000 and 10,000 molecules, which is in the range of slow- and fast-growing cells, respectively. Using this procedure, we have been able to specifically detect and differentiate rRNA from sulfate-reducing strains grown on ^{14}C-labeled lactate (Klepac and Polz, unpubl. data).

For the array to represent the actual microbial populations responsible for metabolism of a specific compound, realistic substrate concentrations must be used in the incubations to avoid introducing a major bias in community structure due to selective growth of specific populations. In coastal waters, which we are using as a model ecosystem, we found that even low additions of ^{14}C-labeled organic substrates (representing <3% of the total organic carbon) produced highly radiolabeled rRNA after 7 h incubation at *in situ* conditions. This incubation time is similar to the average generation time for the entire bacterial community (9 h), and both the uptake rate and the growth yield on the labeled substrates were linear during the incubation, suggesting that there were no major shifts in the microbial community. These tests also showed that the proportion of labeled C allocated to rRNA was strongly dependent on the quality of the substrate (*e.g.*, 12%–19% for adenine, 1.1%–1.3% for acetate). In addition, tests with exponentially growing bacteria in pure culture showed that a constant fraction of the total cellular ^{14}C (average 8% for *Vibrio cholera* and 17% for *E. coli*) could be recovered in rRNA after about one cell doubling. Thus, the major advantages of rRNA detection are the linearity of the labeling process and the possible limitation to few cell doublings, which ensure that community structure will be only minimally biased.

The third question, whether rRNA diversity can be ascertained with realistic effort, requires a reexamination of the PCR-based approach. We have recently presented the hypothesis that a simple, PCR-induced artifact may lead to severe overestimation of diversity of rRNA genes (Thompson *et al.*, 2002). During the co-amplification of homologous templates with universal primers, a significant fraction (up to 50%) of products may be present as heteroduplices. These were increasingly prevalent as template diversity increased or primer availability became limiting (Thompson *et al.*, 2002). After cloning, heteroduplex molecules may

become subject to mismatch repair by the *E. coli* MutHLS system. This can theoretically lead to independent repair of each mismatched position since the repair system, *in vivo*, is directed by hemimethylation (Modrich, 1987), which is absent in PCR products. A model exploring the effects of heteroduplex repair demonstrated that the undirected repair process might be responsible for large overestimation of rRNA diversity (Thompson *et al.*, 2002). For example, a simple system of 2 sequences with 3 shared mismatched positions can result in 8 sequence permutations; for 4 sequences with 10 shared mismatched positions, the number increases to 6136 (Thompson *et al.*, 2002). Although this is a dramatic example, the potential contribution of heteroduplex repair to sequence diversity can easily be avoided by "reconditioning PCR," a low-cycle-number reamplification of a 10-fold diluted, mixed-template PCR product.

Although the exact contribution of heteroduplex repair to diversity estimates is still being analyzed in our laboratory, we have used the modified amplification protocol (reconditioning PCR) to estimate bacterial diversity in a coastal bacterial community. We generated a clone library from amplified 23S rRNA genes, then assessed sequence diversity in the library by a combination of rarefaction analysis and Chao-1 estimators, which are based on capture-recapture statistics (Hughes *et al.*, 2001). The results demonstrated that diversity was relatively moderate, with the number of coexisting sequence types remaining in the low 100s (Acinas, Hunt, Bertilsson, and Polz, unpubl. data). This ongoing analysis is currently complemented with rarefaction of a 16S rRNA gene library derived from the same sample, demonstrating that it may indeed be possible to represent entire communities with reasonable effort on DNA microarrays.

Acknowledgments

This work was supported by grants from NSF and Sea Grant. We are also grateful to Mitch Sogin for providing access to the MBL sequencing facility, and to Byron Crump and John Hobbie for help during sampling.

Literature Cited

Béja, O., M. T. Suzuki, E. V. Koonin, L. Aravind, A. Hadd, L. P. Nguyen, R. Villacorta, M. Amjadi, C. Garrigues, S. B. Jovanovich, R. A. Feldman, and E. F. DeLong. 2000. Construction and analysis of bacterial artificial chromosome libraries from a marine microbial assemblage. *Environ. Microbiol.* **2:** 516–529.

Bertilsson, S. A., and M. F. Polz. 2001. Application of a diversity array to study specific substrate utilization in individual populations of heterotrophic bacteria. P. 503 in *Abstracts*, American Society for Microbiology, 101st General Meeting, Orlando, FL.

Boschker, H. T. S., S. C. Nold, P. Wellsbury, D. Bos, W. de Graaf, R. Pel, R. J. Parkes, and T. E. Cappenberg. 1998. Direct linking of microbial populations to specific biogeochemical processes by ^{13}C-labeling of biomarkers. *Nature* **392:** 801–805.

Cho, J.-C., and J. M. Tiedje. 2001. Bacterial species determination from DNA-DNA hybridization by using genome fragments and DNA microarrays. *Appl. Environ. Microbiol.* **67:** 3677–3682.

Cottrell, M. T., and D. L. Kirchman. 2000. Natural assemblages of marine proteobacteria and members of the *Cytophaga-Flavobacter* cluster consuming low- and high-molecular-weight dissolved organic matter. *Appl. Environ. Microbiol.* **66:** 1692–1697.

Giovannoni, S., and M. Rappé. 2000. Evolution, diversity, and molecular ecology of marine prokaryotes. Pp. 47–84 in *Microbial Ecology of the Oceans*, D. L. Kirchman, ed. Wiley-Liss, New York.

Gray, N. D., and I. M. Head. 2001. Linking genetic identity and function in communities of uncultured bacteria. *Environ. Microbiol.* **3:** 481–492.

Head, I. M., J. R. Saunders, and R. W. Pickup. 1998. Microbial evolution, diversity, and ecology: a decade of ribosomal RNA analysis of uncultivated microorganisms. *Microb. Ecol.* **35:** 1–21.

Hugenholtz, P., B. M. Goebel, and N. R. Pace. 1998. Impact of culture-independent studies on the emerging phylogenetic view of bacterial diversity. *J. Bacteriol.* **180:** 4765–4774.

Hughes, J. B., J. J. Hellmann, T. H. Ricketts, and B. J. M. Bohannan. 2001. Counting the uncountable: statistical approaches to estimating microbial diversity. *Appl. Environ. Microbiol.* **67:** 4399–4406.

Koizumi, Y., J. J. Kelly, T. Nakagawa, H. Urakawa, S. El-Fantroussi, S. Al-Muzaini, M. Fukui, Y. Urushigawa, and D. A. Stahl. 2002. Parallel characterization of anaerobic toluene- and ethylbenzene-degrading microbial consortia by PCR-denaturing gradient gel electrophoresis, RNA-DNA membrane hybridization, and DNA microarray technology. *Appl. Environ. Microbiol.* **68:** 3215–3225.

Lee, N., P. H. Nielsen, K. H. Andreasen, S. Juretschko, J. L. Nielsen, K.-H. Schleifer, and M. Wagner. 1999. Combination of fluorescent in situ hybridization and microautoradiography—a new tool for structure-function analyses in microbial ecology. *Appl. Environ. Microbiol.* **65:** 1289–1297.

Modrich, P. 1987. DNA mismatch correction. *Annu. Rev. Biochem.* **56:** 435–466.

Ouverney, C. C., and J. A. Fuhrman. 1999. Combined microautoradiography–16S rRNA probe technique for determination of radioisotope uptake by specific microbial cell types in situ. *Appl. Environ. Microbiol.* **65:** 1746–1752.

Radajewski, S., P. Ineson, N. R. Parekh, and J. C. Murrell. 2000. Stable-isotope probing as a tool in microbial ecology. *Nature* **403:** 646–649.

Schmidt, T. M., E. F. DeLong, and N. R. Pace. 1991. Analysis of marine picoplankton community by 16S rRNA gene cloning and sequencing. *J. Bacteriol.* **173:** 4371–4378.

Small, J., D. R. Call, F. J. Brockman, T. M. Straub, and D. P. Chandler. 2001. Direct detection of 16S rRNA in soil extracts by using oligonucleotide microarrays. *Appl. Environ. Microbiol.* **67:** 4708–4716.

Stokes, H. W., A. J. Holmes, B. S. Nield, M. P. Holley, K. M. H. Nevalainen, B. C. Mabbutt, and M. R. Gillings. 2001. Gene cassette PCR: sequence-independent recovery of entire genes from environmental DNA. *Appl. Environ. Microbiol.* **67:** 5240–5246.

Thompson, J. R., L. A. Marcelino, and M. F. Polz. 2002. Heteroduplexes in mixed-template amplifications: formation, consequences and elimination by 'reconditioning PCR.' *Nucleic Acids Res.* **30:** 2083–2088.

Torsvik, V., L. Ovreas, and T. F. Thingstad. 2002. Prokaryotic diversity: magnitude, dynamics, and controlling factors. *Science* **296:** 1064–1066.

Reference: *Biol. Bull.* **204:** 200–204. (April 2003)

Human Oral Cavity as a Model for the Study of Genome-Genome Interactions

JAMIE S. FOSTER, ROBERT J. PALMER, JR., AND PAUL E. KOLENBRANDER*

Oral Infection and Immunity Branch, National Institute of Dental and Craniofacial Research, National Institutes of Health, Building 30, Room 310, 30 Convent Drive MSC 4350, Bethesda, Maryland 20892-4350

The enormous diversity of culturable bacteria within the oral microbial community coupled with experimental accessibility renders the human oral cavity a valuable model to investigate genome-genome interactions. The complex interactions of oral bacteria result in the formation of biofilms on the surfaces of the oral cavity. One mechanism thought to be important in biofilm formation is the coaggregation of bacterial partners. In this paper, we examine the role of coaggregation in oral biofilms and develop protocols to elucidate the spatial organization of bacterial species retained within oral biofilms. To explore these issues, we have employed two experimental systems: the saliva-coated flowcell and the retrievable enamel chip. From flowcell studies, we have determined that coaggregation can greatly influence the ability of an oral bacterial species to grow and be retained within the developing biofilm. To examine the spatial architecture of oral biofilms, fluorescent in situ *hybridization protocols were developed that successfully target specific members of the oral microbial community. Together, these approaches provide insight into the development of oral biofilms and expand our understanding of genome-genome interactions.*

The human oral cavity contains more than 500 species of bacteria that interact among themselves and with their host tissues (Kroes *et al.*, 1999; Paster *et al.*, 2001). These complex interspecies associations result in the formation of microbial biofilms on the hard and soft tissues of the oral cavity (Gibbons and Hay, 1988; Hallberg *et al.*, 1998). Within these oral biofilms, numerous molecular and biochemical exchanges result in communication between distinct genomes (here called genome-genome interactions). To explore the nature of genome-genome interactions in the oral cavity, it is necessary to understand the composition of the microbial community, the mechanisms by which oral bacteria associate, and the spatial arrangement of the community. Until recently, description of plaque community composition relied on culture-dependent techniques (Moore and Moore, 1994; Socransky and Haffajee, 1994). Culture-independent methods have identified previously unknown and uncultured community members. These uncultured oral bacteria constitute a low percentage of the total bacterial numbers compared to the high percentage of uncultured bacteria in other natural environments (Kroes *et al.*, 1999; Paster *et al.*, 2001). Although these studies provide information on species composition, they do not address the spatial organization of the oral community. The juxtaposition of different bacteria in three-dimensional oral biofilms such as dental plaque probably contributes to and may direct metabolic cross-feeding symbioses and transcriptional signal exchange between organisms. Examining the precise architecture of oral biofilms may provide a clearer understanding of the role each organism plays in the overall community structure and in genome-genome interactions.

One mechanism through which oral bacteria may communicate and facilitate genome-genome interactions is coaggregation. In coaggregation, oral bacterial cells bind to specific bacterial partners (Cisar *et al.*, 1979). To date, all oral bacteria tested coaggregate with at least one other bacterial species (Whittaker *et al.*, 1996; Andersen *et al.*, 1998; Kolenbrander *et al.*, 2002). Coaggregation occurs

* To whom correspondence should be addressed. E-mail: pkolenbrander@dir.nidcr.nih.gov

The paper was originally presented at a workshop titled *Outcomes of Genome-Genome Interactions.* The workshop, which was held at the J. Erik Jonsson Center of the National Academy of Sciences, Woods Hole, Massachusetts, from 1–3 May 2002, was sponsored by the Center for Advanced Studies in the Space Life Sciences at the Marine Biological Laboratory, and funded by the National Aeronautics and Space Administration under Cooperative Agreement NCC 2-1266

between genetically distinct bacteria and is mediated by protein adhesins on one cell type that recognize complementary carbohydrate receptors on the partner cell type. This phenomenon has been hypothesized to be essential to the formation of oral biofilms (Kolenbrander *et al.*, 2002), although little direct work has been performed on the consequences of coaggregation interactions. Several outcomes of these pairwise interactions are conceivable: (a) only one organism benefits, (b) one organism is detrimentally influenced, (c) both organisms benefit, (d) both organisms suffer, and (e) neither organism is influenced by the presence of the other. Although these scenarios are an oversimplification of what can occur in multispecies environments such as the oral cavity, they serve as starting points for assessing the consequences of coaggregation *in vivo*. Furthermore, it is becoming clear that coaggregation interactions exist outside the oral cavity in freshwater biofilms (Rickard *et al.*, 2000, 2002). Therefore, the significance of contact-based cell-cell interactions in the bacterial world has probably been underestimated, and the outcomes of these genome-genome interactions are likely to be a universal driving force in biofilm development.

Several experimental designs have been developed to examine the formation of oral biofilms (Wilson, 1999; Wimpenny, 2000). These model systems often rely on the flow of nutrients over a surface on which bacteria are able to attach and grow. In our laboratory we use two experimental models, a saliva-coated flowcell (Kolenbrander *et al.*, 1999) and a retrievable enamel chip (Palmer *et al.*, 2001a). Each method has its own advantages for the examination of oral microbial communities. The flowcell enables biofilms to form under defined conditions of species and nutrients. The basic design of a flowcell is a microscope slide and coverslip separated by a two-channel molded silicone gasket (Kolenbrander *et al.*, 1999). Inlet and outlet ports enable saliva, the sole nutrient source, to coat the glass surfaces with a salivary conditioning film of host proteins. After the salivary conditioning film is established, bacterial strains are injected into the flowcell chamber. As the biofilm forms within the flowcell, colonization and growth can be examined noninvasively by confocal laser microscopy (CLM). In comparison, the enamel chip facilitates the understanding of natural biofilms that form within the human oral cavity. Enamel chips cut from human third molars are placed into two acrylic appliances worn intraorally by volunteers. The chips are then recovered and examined using microscopy (Palmer *et al.*, 2001a).

Initial studies on the outcomes of coaggregation interactions have been conducted in the flowcell model with three primary colonizers of the tooth surface: *Streptococcus gordonii* DL1, *Actinomyces naeslundii* T14V, and *Streptococcus oralis* 34 (Palmer *et al.*, 2001b). Each bacterium can coaggregate with the other two. The behavior of the strains as monocultures was assessed by examining their abilities to grow planktonically (as liquid cultures) in saliva, and to grow as biofilms in saliva. In planktonic culture, *S. gordonii* reproducibly reached a cell density of 10^7 cells per milliliter of saliva and was transferable (*i.e.*, growth was maintained over three transfers). *A. naeslundii* numbers consistently tapered off within 18 h after the initial transfer to saliva. *S. oralis* behaved inconsistently: growth occurred, but the maximum cell density varied between 10^5 and 10^6 cells per milliliter of saliva, and cultures were not always transferable. These behaviors were duplicated in the flowcell system: monoculture biofilms of *S. gordonii* grew reproducibly, those of *A. naeslundii* never grew, and those of *S. oralis* grew only once in six experiments.

Once behavior as monocultures was assessed, the outcome of pairwise interactions between the strains in biofilms was investigated (Palmer *et al.*, 2001b). The first strain was inoculated into the flowcell and allowed to adhere for 20 min; nonadherent cells were then washed out and the second strain was introduced and allowed to adhere for 20 min. After the subsequent washout of nonadherent cells, the coculture biofilm was examined immediately (time 0), after 4 h, and after overnight growth with flowing saliva. When the initial strain was *S. gordonii*, combination with either of the other two strains produced identical results: *S. gordonii* grew as it did in monoculture, and the partner strain (*A. naeslundii* or *S. oralis*) failed to grow (Fig. 1A). Cells of the partner strain were retained within the *S. gordonii* biofilm, but biomass of either partner strain was clearly reduced over the course of the experiment. Thus, the growth of *S. gordonii* was apparently unaffected by the presence of *A. naeslundii* or *S. oralis*. In marked contrast to these interactions, when *S. oralis* and *A. naeslundii* were combined in a biofilm, both bacteria grew luxuriantly (Fig. 1B). Growth as a coculture biofilm of these two organisms (neither of which could grow reproducibly as a monoculture biofilm) was much greater than that of *S. gordonii*, which grew independently under identical culture conditions. This is a clear example of a mutualism in which both organisms benefit from the interaction. Such interactions may be important in establishment of regional heterogeneity in oral biofilms *in vivo*, and we are currently using the retrievable enamel chip system to relate the results of our *in vitro* investigations to the situation *in vivo*.

The study of bacterial symbiotic interactions described above was conducted by using antibodies to identify the organisms and give spatial information on the oral community. To complement these studies, we have begun to employ fluorescence *in situ* hybridization (FISH) coupled with the flowcell and enamel chip models. The advantages of using FISH are that uncultured bacteria can be detected and that development of the probes is more rapid than production and characterization of antibodies. Fluorescently labeled oligonucleotide probes designed to the 16S rRNA sequence of different oral bacteria were hybridized *in situ*

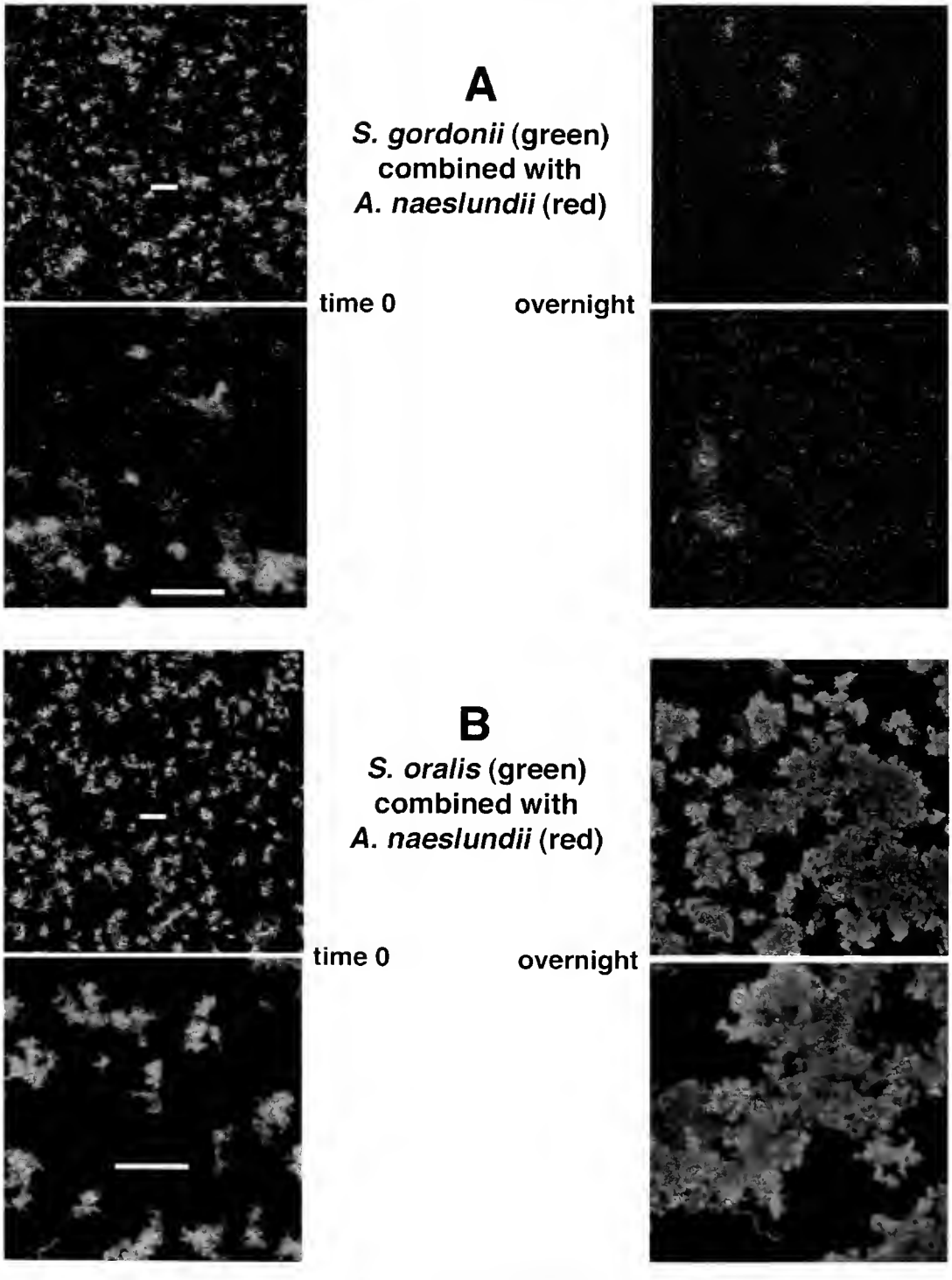

Figure 1. Coculture biofilms showing multiple outcomes of coaggregation. (A) *Streptococcus gordonii* interaction with *Actinomyces naeslundii*. *S. gordonii* was introduced first, followed by *A. naeslundii*. Biofilms were examined with confocal microscopy at time 0 (immediately after washout of nonadherent cells, left panels) and after overnight growth on saliva (right panels). Lower panels of each vertical pair are 3× zooms of the center of the corresponding upper panels. *S. gordonii* (green) was detected by constitutive green fluorescent protein fluorescence; *A. naeslundii* (red) was detected by secondary immunofluorescence. (B) *Streptococcus oralis* interaction with *A. naeslundii*. Details as above, except that *S. oralis* (green) was detected by primary immunofluorescence. All scales, 25 μm.

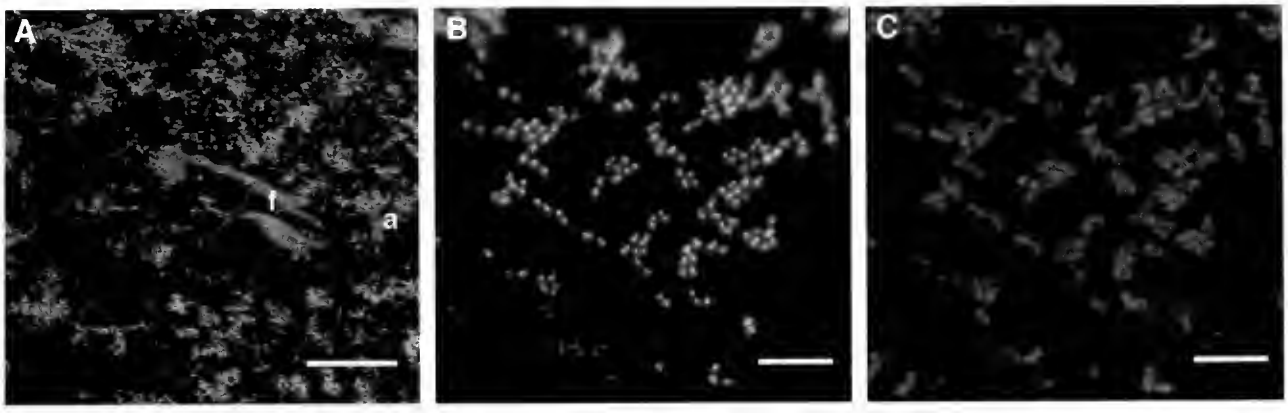

Figure 2. Confocal micrographs of oral biofilms examined with fluorescence *in situ* hybridization. (A) Mixed-species biofilm containing *Streptococcus gordonii* DL1, *Actinomyces naeslundii* PK19(a), and *Fusobacterium nucleatum* PK1594(f) grown on saliva in a flowcell for 4 h. The biofilm was stained with an FITC-labeled oligonucleotide probe (green) targeted to *S. gordonii* and counterstained with the nucleic acid stain Syto 59 (red). Colocalized stains are yellow. Scale, 25 μm. (B, C) Monospecies biofilms inoculated with *S. gordonii* DL1 and grown on enamel chips for 4 h. Biofilms were stained with an oligonucleotide probe specific for *S. gordonii* and the nucleic acid stain DAPI. Scale, 10 μm. (B) High-magnification image of enamel chip showing total number of cells visualized by DAPI stain. (C) Same location on enamel chip as in B, but only detecting cells labeled with oligonucleotide probe.

with the growing biofilm, thus enabling bacterial species to be located without biofilm disruption (Fig. 2). Flowcells were consecutively inoculated with cultures of *S. gordonii* DL1, *A. naeslundii* PK19 (each an early colonizer), and *Fusobacterium nucleatum* PK1594 (late colonizer). After 4 h of saliva flow, biofilms were probed with a fluorescently labeled oligonucleotide designed to target streptococci (5′-GCTGCCTCCCGTAGGAGT-3′; JF20) as well as with a general nucleic acid stain to detect all cells (Fig. 2A). Based on distinctive morphologies of *S. gordonii* (coccus shaped), *A. naeslundii* (rod shaped), and *F. nucleatum* (slender rods with tapered ends), all cell types could be visualized within the biofilm by staining with the nucleic acid marker Syto 59 (Molecular Probes, Eugene, OR). However, labeling by the fluorescent oligonucleotide probe was visible only in *S. gordonii* cells; the other two organisms did not bind the streptococcal probe (JF20) (Fig. 2A). RNA levels *in situ* are frequently very low, and therefore detection can be problematic. To test the detection efficiency of FISH probes compared with general nucleic acid stains, monospecies biofilms containing *S. gordonii* were grown in saliva *in vitro* on enamel chip surfaces and exposed to a streptococcal-specific probe (Fig. 2B, C). The biofilms were also stained with the nucleic acid stain diamidino-2-phenylindole dihydrochloride (DAPI) to fluorescently mark all cells within the biofilm. All of the *S. gordonii* cells could be stained with the oligonucleotide probe without high background fluorescence (Fig. 2C). Taken together, these results suggest that our FISH protocols can be employed in conjunction with the flowcell and enamel chip systems.

This work represents just a few of the approaches used to study oral bacterial interactions. Despite the complexity and diversity of organisms present within the human oral cavity, experimental model systems such as these can be used to explore the consequences of the interactions between distinct genomes and to elucidate common underlying mechanisms of communication within microbial biofilms.

Acknowledgments

The authors thank Paul Egland and David Blehert for their useful comments on this manuscript.

Literature Cited

Andersen, R. N., N. Ganeshkumar, and P. E. Kolenbrander. 1998. *Helicobacter pylori* adheres selectively to *Fusobacterium* spp. *Oral Microbiol. Immunol.* **13:** 51–54.

Cisar, J. O., P. E. Kolenbrander, and F. C. McIntire. 1979. Specificity of coaggregation reactions between human oral streptococci and strains of *Actinomyces viscosus* or *Actinomyces naeslundii*. *Infect. Immun.* **24:** 742–752.

Gibbons, R. J., and D. I. Hay. 1988. Absorbed salivary proline-rich proteins as bacterial receptors on apatitic surfaces. Pp. 143–163 in *Molecular Mechanisms of Microbial Adhesion*, L. Switalski, M. Hook, and E. Beachey, eds. Springer-Verlag, New York.

Hallberg, K., K. J. Hammarstrom, E. Falsen, G. Dahlen, R. J. Gibbons, D. I. Hay, and N. Strömberg. 1998. *Actinomyces naeslundii* genospecies 1 and 2 express different binding specificities to N-acetyl-beta-D-galactosamine, whereas *Actinomyces odontolyticus* expresses a different binding specificity in colonizing the human mouth. *Oral Microbial. Immunol.* **13:** 327–336.

Kolenbrander, P. E., R. N. Andersen, K. Kazmerzak, R. Wu, and R. J. Palmer, Jr. 1999. Spatial organization of oral bacteria in biofilms. *Methods Enzymol.* **310:** 322–332.

Kolenbrander, P. E., R. N. Andersen, D. S. Blehert, P. G. Egland, J. S. Foster, and R. J. Palmer, Jr. 2002. Communication among oral bacteria. *Microbiol. Mol. Biol. Rev.* **66:** 486–505.

Kroes, I., P. W. Lepp, and D. A. Relman. 1999. Bacterial diversity

within the human subgingival crevice. *Proc. Natl. Acad. Sci. USA* **96:** 14,547–14,552.

Moore, W. E. C., and L. V. H. Moore. 1994. The bacteria of periodontal diseases. *Periodontol. 2000* **5:** 66–77.

Palmer, R. J., Jr., R. Wu, S. Gordon, C. G. Bloomquist, W. F. Liljemark, M. Kilian, and P. E. Kolenbrander. 2001a. Retrieval of biofilms from the oral cavity. *Methods Enzymol.* **337:** 393–403.

Palmer, R. J., Jr., K. Kazmerzak, M. C. Hansen, and P. E. Kolenbrander. 2001b. Mutualism versus independence: strategies of mixed-species oral biofilms *in vitro* using saliva as the sole nutrient source. *Infect. Immun.* **69:** 5794–5804.

Paster, B. J., S. K. Boches, R. E. Galvin, R. E. Ericson, C. N. Lau, V. A. Levanos, A. Sahasrahudhe, and F. E. Dewhirst. 2001. Bacterial diversity in human subgingival plaque. *J. Bacteriol.* **183:** 3770–3783.

Rickard, A. H., S. A. Leach, C. M. Buswell, N. J. High, and P. S. Handley. 2000. Coaggregation between aquatic bacteria is mediated by specific-growth-phase-dependent lectin-saccharide interactions. *Appl. Environ. Microbiol.* **66:** 431–434.

Rickard, A. H., S. A. Leach, L. S. Hall, C. M. Buswell, N. J. High, and P. S. Handley. 2002. Phylogenetic relationships and coaggregation ability of freshwater biofilm bacteria. *Appl. Environ. Microbiol.* **68:** 3644–3650.

Socransky, S. S., and A. D. Haffajee. 1994. Evidence of bacterial etiology: a historical perspective. *Periodontol. 2000* **5:** 7–25.

Whittaker, C. J., C. M. Klier, and P. E. Kolenbrander. 1996. Mechanisms of adhesion by oral bacteria. *Annu. Rev. Microbiol.* **50:** 513–552.

Wilson, M. 1999. Use of constant depth film fermentor in studies of biofilms of oral bacteria. *Methods Enzymol.* **310:** 264–279.

Wimpenny, J. 2000. An overview of biofilms as functional communities. Pp. 1–24 in *Community Structure and Co-operation in Biofilms*, D. G. Allison, P. Gilbert, H. M. Lappin-Scott, and M. Wilson, eds. Cambridge University Press, Cambridge.

Reference: *Biol. Bull.* **204:** 205–209. (April 2003)

From Genes to Genomes: Beyond Biodiversity in Spain's Rio Tinto

LINDA A. AMARAL ZETTLER[1], MARK A. MESSERLI[1,2], ABBY D. LAATSCH[1], PETER J. S. SMITH[2], AND MITCHELL L. SOGIN[1,*]

[1] *The Josephine Bay Paul Center for Comparative Molecular Biology and Evolution, Marine Biological Laboratory, 7 MBL Street, Woods Hole, Massachusetts; and* [2] *The BioCurrents Center, Marine Biological Laboratory, 7 MBL Street, Woods Hole, Massachusetts*

Spain's Rio Tinto, or Red River, an example of an extremely acidic (pH 1.7–2.5) environment with a high metal content, teems with prokaryotic and eukaryotic microbial life. Our recent studies based on small-subunit rRNA genes reveal an unexpectedly high eukaryotic phylogenetic diversity in the river when compared to the relatively low prokaryotic diversity. Protists can therefore thrive in and dominate extremely acidic, heavy-metal-laden environments. Further, because we have discovered protistan acidophiles closely related to neutrophiles, we can hypothesize that the transition from neutral to acidic environments occurs rapidly over geological time scales. How have these organisms adapted to such environments? We are currently exploring the alterations in physiological mechanisms that might allow for growth of eukaryotic microbes at acid extremes. To this end, we are isolating phylogenetically diverse protists in order to characterize and compare ion-transporting ATPases from cultured acidophiles with those from neutrophilic counterparts. We predict that special properties of these ion transporters allow protists to survive in the Rio Tinto.

Earth harbors many extreme environments. Previous investigations of the microbial diversity in these environments have been constrained by preconceived notions about the range of habitability for both eukaryotic and prokaryotic microorganisms. We have been exploring the genetic and physiological diversity of organisms living at pH extremes, both acidic (pH < 3) and alkaline (pH > 10). Our research ranges from environments like the warm (45 °C), acidic (pH 2.7) Nymph Creek in Yellowstone National Park to temperate alkaline lakes in the Sandhills region of western Nebraska. The focus of this report is the acidic, heavy-metal-rich Rio Tinto in southwestern Spain.

The Rio Tinto flows 100 km through the world's largest pyritic (FeS_2) belt. The river gets its red color from the high levels of iron dissolved in its acidic waters (pH ~2.0). Ferric hydroxide ($Fe^{3+}/Fe(OH)_3$, pKa 2.5) and SO_4^{2-}/HSO_4^- (pKa 2.0) act as buffers to maintain the pH of the river at about 2. The concentration of iron can be as high as 20 g/l, and the river also contains other heavy metals at concentrations orders of magnitude higher than those in typical freshwater environments.

Much of the past research on the Rio Tinto has focused on the prokaryotes that play an important role in shaping the acidic environment of the Rio Tinto through their metabolism of iron-rich pyrite and chalcopyrite. Recent paleontological research shows that iron-oxidizing bacteria existed in the Rio Tinto river basin 300,000 years ago, long before its 5000-year mining history (Leblanc *et al.*, 2000). Other chemolithotrophs such as sulfur-oxidizing bacteria and archaea also contribute to the river's probably ancient ecosystem structure (Gónzalez-Toril *et al.*, 2001).

Some of these prokaryotes, along with fungi, contribute to the formation of biofilms on the surface of rocks. These biofilms, in turn, are the site of metal and mineral precipitation that ultimately forms stromatolites. Biofilms provide a substrate for communities to develop within the river. However, in many parts of this river basin, eukaryotic

* To whom correspondence should be addressed. E-mail: sogin@evol5.mbl.edu

The paper was originally presented at a workshop titled *Outcomes of Genome-Genome Interactions.* The workshop, which was held at the J. Erik Jonsson Center of the National Academy of Sciences, Woods Hole, Massachusetts, from 1–3 May 2002, was sponsored by the Center for Advanced Studies in the Space Life Sciences at the Marine Biological Laboratory, and funded by the National Aeronautics and Space Administration under Cooperative Agreement NCC 2-1266

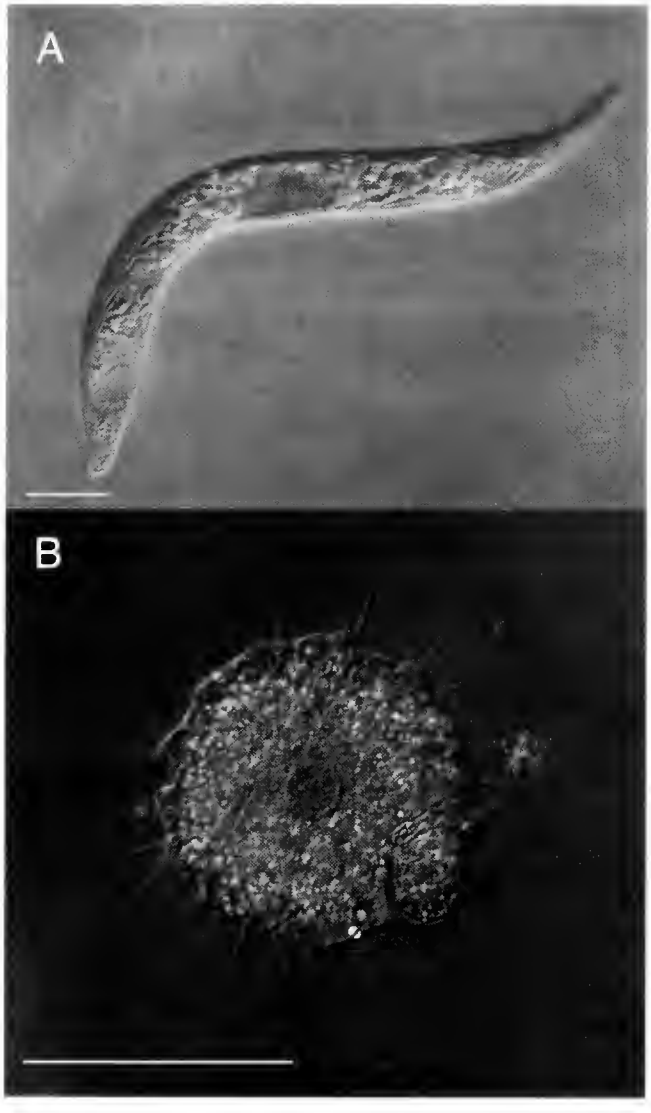

Figure 1. Some representative eukaryotes found in the Rio Tinto. (A) *Euglena* cf. *mutabilis;* scale bar = 10 μm. Photomicrograph by Linda Amaral Zettler and David Patterson. (B) A heliozoan, most likely belonging to the genus *Actinophrys;* scale bar = 100 μm. Photomicrograph by Linda Amaral Zettler and Erik Zettler.

microbes (Fig. 1) are the major contributors of biomass (López-Archilla *et al.*, 2001). Eukaryotes not only form the foundations of some of these biofilm communities, but they are also conspicuous inhabitants of them (López-Archilla *et al.*, 1993, 1994, 1995; López-Archilla and Amils, 1999). This makes the Rio Tinto system unique among acidic environments described to date.

Figure 2 shows a phylogenetic tree depicting the breadth of eukaryotic diversity in the river. In our rRNA gene diversity survey of biofilm samples, we obtained sequences representing most of the major eukaryotic lineages, including the fungi, animals, green algae, land plants, stramenopiles, and alveolates (Amaral Zettler, 2002). Many of the sequences from the Rio Tinto represent photosynthetic lineages that were previously identified employing light microscopy (López-Archilla *et al.*, 2001). These included members of the Euglenozoa (euglenids), Chlorophyta (chlamydomonad and chlorella-like relatives), Viridiplantae (*Zygnema*-relatives), and Bacillariophyta (diatoms). However, our molecular data also unveiled a significant nonphotosynthetic component to the Rio Tinto. Phagotrophic lineages such as the ciliates, cercomonads, and vahlkampfiid amoebae, as well as heterotrophic fungi and possibly myxotrophic lineages—as known to occur in members of the stramenopiles such as *Ochromonas* (Porter *et al.*, 1985)—also populate the Rio Tinto.

We discovered a diversity of fungi that escaped detection using traditional identification methods. None of our fungal clones showed high similarity to those species already described from the Rio Tinto. Fungi undoubtedly play an important role in community structure in the Tinto since most of them are metal resistant and can sequester specific metals (Durán *et al.*, 1999). Such sequestration of potentially toxic metals could allow less tolerant species to exist where they might not have otherwise, possibly enhancing biodiversity in these areas. Similar studies on metal sequestration have not been conducted on protists living in the Tinto. We hope to apply new tools in genome science to address these questions surrounding the rich microbial diversity of the Rio Tinto.

Our studies also revealed a diversity that we were not able to readily characterize using molecular techniques. Clones such as RT5iin16 and RT5iin14 are most likely examples of novel eukaryotic lineages that at best branch at the base of the animal-fungal-nucleariid radiation. Other clones (RT5iin21 and RT5iin44) branched with the recently sequenced filose amoeba *Filamoeba nolandi,* whose own taxonomic placement is equivocal. Because our study was

Figure 2. A minimum evolution phylogeny for small subunit rRNA genes using a likelihood model. Bold letters indicate environmental clones. "RT" indicates the sequence is from the Rio Tinto, and "cul" indicates cultured species. Underlined taxa represent genera that have been identified in the river based on microscopic observation. Sampling sites were as follows: RT1, La Palma; RT3, Berrocal Upper; RT5i, the Origin, black filamentous biofilm; RT5ii, the Origin, green filamentous biofilm; RT7i, Anabel's Garden green biofilm; RT7ii, Anabel's Garden yellow biofilm. Bootstrap support values are shown, and the scale bar represents the number of substitutions per site. GenBank accession numbers AY082969-AY083001.

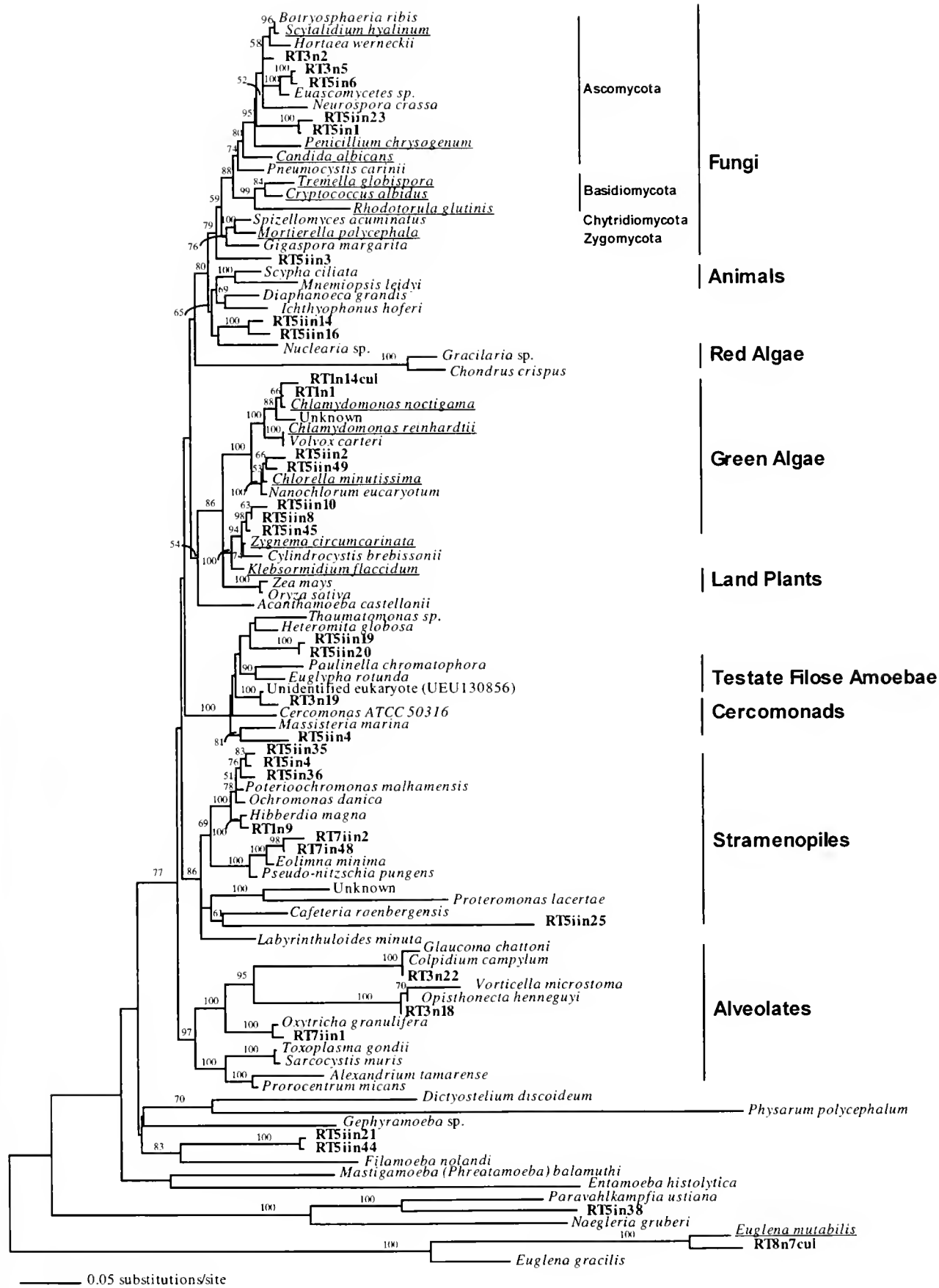
Botryosphaeria ribis
Scytalidium hyalinum
Hortaea werneckii
RT3n2
RT3n5
RT5in6
Euascomycetes sp.
Neurospora crassa
RT5iin23
RT5in1
Penicillium chrysogenum
Candida albicans
Pneumocystis carinii
Tremella globispora
Cryptococcus albidus
Rhodotorula glutinis
Spizellomyces acuminatus
Mortierella polycephala
Gigaspora margarita
RT5iin3
Scypha ciliata
Mnemiopsis leidyi
Diaphanoeca grandis
Ichthyophonus hoferi
RT5iin14
RT5iin16
Nucleariа sp.
Gracilaria sp.
Chondrus crispus
RT1n14cul
RT1n1
Chlamydomonas noctigama
Unknown
Chlamydomonas reinhardtii
Volvox carteri
RT5iin2
RT5iin49
Chlorella minutissima
Nanochlorum eucaryotum
RT5iin10
RT5iin8
RT5in45
Zygnema circumcarinata
Cylindrocystis brebissanii
Klebsormidium flaccidum
Zea mays
Oryza sativa
Acanthamoeba castellanii
Thaumatomonas sp.
Heteromita globosa
RT5iin19
RT5iin20
Paulinella chromatophora
Euglypha rotunda
Unidentified eukaryote (UEU130856)
RT3n19
Cercomonas ATCC 50316
Massisteria marina
RT5iin4
RT5iin35
RT5in4
RT5in36
Poterioochromonas malhamensis
Ochromonas danica
Hibberdia magna
RT1n9
RT7iin2
RT7in48
Eolimna minima
Pseudo-nitzschia pungens
Unknown
Proteromonas lacertae
Cafeteria roenbergensis
RT5iin25
Labyrinthuloides minuta
Glaucoma chattoni
Colpidium campylum
RT3n22
Vorticella microstoma
Opisthonecta henneguyi
RT3n18
Oxytricha granulifera
RT7iin1
Toxoplasma gondii
Sarcocystis muris
Alexandrium tamarense
Prorocentrum micans
Dictyostelium discoideum
Physarum polycephalum
Gephyramoeba sp.
RT5iin21
RT5iin44
Filamoeba nolandi
Mastigamoeba (Phreatamoeba) balamuthi
Entamoeba histolytica
Paravahlkampfia ustiana
RT5in38
Naegleria gruberi
Euglena mutabilis
RT8n7cul
Euglena gracilis
Ascomycota
Basidiomycota
Chytridiomycota
Zygomycota
Fungi
Animals
Red Algae
Green Algae
Land Plants
Testate Filose Amoebae
Cercomonads
Stramenopiles
Alveolates
0.05 substitutions/site

not exhaustive, we surmise that there are still more undiscovered novel lineages in the river.

Despite our growing knowledge of the Tinto's eukaryotic diversity, we know little about the role eukaryotes play in shaping the varied ecosystems that occur along the river. For example, we do not know if these biofilm communities have microenvironments that enhance survival of their members. Could fungal metal sequestration protect nontolerant species? Furthermore, we know little about how these organisms have evolved adaptations to extreme concentrations of acid and metals.

To explore these questions, we have been isolating organisms from the river for *ex situ* physiological experiments. We have established monocultures of *Chlamydomonas* sp., *Euglena* cf. *mutabilis*, *Chlorella* sp., and *Vannella* sp. isolated from enrichments of river water and are currently exploring the physiology of these protists from extreme environments.

We have initiated our physiological studies on an acidophilic species of a chlamydomonad alga isolated from the river—*Chlamydomonas* sp. Our first question about the physiology of the Tinto acidophiles was the nature of the cytosolic pH (pH_i). There are published reports of acidophiles from all domains of life with internal pH values that deviate from neutral—these include the archaebacterium *Picrophilus oshimae*, $pH_i = 4.6$ (van de Vossenberg *et al.*, 1998); the eubacterium *Bacillus acidocaldarius*, $pH_i = 5.6–5.8$ (Thomas *et al.*, 1976); and the eukaryotic alga *Euglena mutabilis*, $pH_i = 5.0–6.4$ (Lane and Burris, 1981). Using the fluorescent H^+ indicator BCECF, we determined that our acidophilic chlamydomonad isolate maintains an average internal pH of 6.6 at an external pH of 2 (M. A. Messerli, L. A. Amaral Zettler, S.-K. Jung, P. J. S. Smith, and M. L. Sogin, unpubl.). Our other isolates await similar measurements.

Given that there is a 40,000-fold difference in hydrogen ion activity between the inside and the outside of these cells, we propose the existence of active transport mechanisms that help these organisms regulate their internal pH. We hypothesize that novel diversity in H^+-ATPases may explain the ability of different protist species to thrive in the low pH, high-metal Rio Tinto environment. There are two major families of H^+-ATPases: the V/F/A-ATPases and the P-type-ATPases. The V-type ATPases can occur in the plasma membrane of eukaryotes (but are more commonly associated with vacuolar membranes) and consist of at least 11 subunits and a molecular mass approaching 10^6 Da. In contrast, eukaryotic P-type ATPases consist of either monosubunits (as with H^+-ATPases) or a hetero-subunit (alpha and beta, as found in the Na^+/K^+-ATPases and H^+/K^+-ATPases); have a molecular weight of about 100 kDa; and form a phosphorylated intermediate during the course of ATP hydrolysis. Indirect evidence of novel ATPases comes from studies of the protozoan parasite *Leishmania donovani*, which has the ability to switch between living in a neutral environment, pH 7.5, as a promastigote (flagellated stage) and in an acidic environment, pH 5.0, as an amastigote (nonflagellated stage) (Meade *et al.*, 1989). The plasma membrane of this organism contains a P-type ATPase that has two isoforms with slightly different sequences. Isoform 1a is expressed in both promastigotes and amastigotes, whereas isoform 1b is expressed more abundantly in the amastigotes (Meade *et al.*, 1989). This difference suggests the use of a sequence change to accommodate the acidic condition. Modifications to ion regulatory machinery might be reflected by convergent amino acid substitution patterns or by accelerated rates of change in acidophilic protist lineages, as revealed in phylogenetic analyses. For example, portions of membrane-bound V- and P-type ATPases that are exposed to the acidic external environment may display different amino acid substitution patterns than do domains that face the cytoplasm.

We are currently using degenerate primers designed against two conserved regions, the phosphorylation site and the ATP-binding site, to amplify members of the P-type superfamily of ion transporters. Thus far, all of our clones fall into the heavy-metal P-type class but may represent different metal transporters. We have found more diverse sequences in the acidophilic *Chlamydomonas* than in the neutrophilic *C. reinhardtii*. We are screening additional clones for H^+-transporting ATPases.

Once we obtain ion-transporter sequence information from these acidophiles, we will focus on correlating the expression of these transporters in space and time to biogeochemical characteristics in the river. This will bring us beyond the study of biodiversity in the river to questions at the heart of potential genomic interactions between members of the microbial consortia. With this kind of approach, we may also be able to determine whether symbiotic interactions are occurring in this environment.

Acknowledgments

This work was supported by the National Science Foundation's Lexen Program DEB-0085486, the NASA Astrobiology Program NCC2-1054, and an NIH:NCRR 01395. The authors wish to acknowledge the support of the Amils lab at the Autonomous University of Madrid and the technical assistance of Brendan Keenan and Erik Zettler.

Literature Cited

Amaral Zettler, L. A., F. Gómez, E. R. Zettler, B. G. Keenan, R. Amils, and M. L. Sogin. 2002. Eukaryotic diversity in Spain's River of Fire. *Nature* **417:** 137.

Durán, C., I. Marín, and R. Amils. 1999. Specific metal sequestering acidophilic fungi. Pp. 521–530 in *Biohydrometallurgy and the Environment Towards the Mining of the 21st Century*, Proceedings of the International Biohydrometallurgy Symposium, tBS '99, R. Amils and A. Ballester, eds. Elsevier, Amsterdam.

Gónzalez-Toril, E., F. Gómez, N. Rodríguez, D. Fernández-Remolar, J. Zuluaga, I. Marín, and R. Amils. 2001. Geomicrobiology of the Tinto River, a model of interest for biohydrometallurgy. Pp. 639–650 in *Biohydrometallurgy: Fundamentals, Technology, and Sustainable Development*, V. S. T. Ciminelli and O. García, eds. Elsevier, Amsterdam.

Lane, A. E., and J. E. Burris. 1981. Effects of environmental pH on the internal pH of *Chlorella pyrenoidosa*, *Scenedesmus quadricauda*, and *Euglena mutabilis*. *Plant Physiol.* **68:** 439–442.

Lehlanc, M., J. A. Morales, J. Borrego, and F. Elbaz-Poulichet. 2000. 4,500 year-old mining pollution in southwestern Spain: long-term implications for modern mining pollution. *Econ. Geol.* **95:** 655–662.

López-Archilla, A. I., and R. Amils. 1999. A comparative ecological study of two acidic rivers in southwestern Spain. *Microb. Ecol.* **38:** 146–156.

López-Archilla, A. I., I. Marín, and R. Amils. 1993. Bioleaching and interrelated acidophilic microorganisms from Rio Tinto, Spain. *Geomicrobiol. J.* **11:** 223–233.

López-Archilla, A. I., D. Moreira, I. Marín, and R. Amils. 1994. El río Tinto, un curso de agua vivo pero con mala fama. *Quercas* (September): 19–22.

López-Archilla, A. I., I. Marín, and R. Amils. 1995. Microbial ecology of an acidic river: biotechnological applications. Pp. 63–73 in *Biohydrometallurgical Processing*, C. A. Jerez, T. Vargas, H. Toledo, and J. W. Wiertz, eds. University of Chile, Santiago.

López-Archilla, A. I., I. Marín, and R. Amils. 2001. Microbial community composition and ecology of an acidic aquatic environment: the Tinto River, Spain. *Microb. Ecol.* **41:** 20–35.

Meade, J. C., K. M. Hudson, S. L. Stringer, and J. R. Stringer. 1989. A tandem pair of *Leishmania donovani* cation transporting ATPase genes encode isoforms that are differentially expressed. *Mol. Biochem. Parasitol.* **33:** 81–91.

Porter, K. G., E. B. Sherr, B. F. Sherr, M. Pace, and R. W. Sanders. 1985. Protozoa in planktonic food webs. *J. Protozool.* **32:** 409–415.

Thomas, J. A., R. E. Cole, and T. A. Langworthy. 1976. Intracellular pH measurements with a spectroscopic probe generated *in situ*. *Fed. Proc.* **35:** 1455.

van de Vossenberg, J. L., A. J. M. Drissen, W. Zillig, and W. N. Konings. 1998. Bioenergetics and cytoplasmic membrane stability of the extremely acidophilic, thermophilic Archaeon *Picrophilus oshimae*. *Extremophiles* **2:** 67–74.

Reference: *Biol. Bull.* **204:** 210–214. (April 2003)

Isolation of Symbiotically Expressed Genes From the Dinoflagellate Symbiont of the Solitary Radiolarian *Thalassicolla nucleata*

REBECCA J. GAST[1,*], DAVID J. BEAUDOIN[2], AND DAVID A. CARON[3]

[1]*Woods Hole Oceanographic Institution, Woods Hole, Massachusetts 02543;* [2]*Marine Biological Laboratory, Woods Hole, Massachusetts 02543; and* [3]*University of Southern California, Los Angeles, California 90089-0371*

Symbiotic associations are fundamental to the survival of many organisms on Earth. The ability of the symbiont to perform key biochemical functions often allows the host to occupy environments that it would otherwise find inhospitable. This can have profound impacts upon the diversification and distribution of the host. Cellular organelles (chloroplasts and mitochondria) represent the final stages of integration of endosymbionts. These organelles were of critical importance to the evolution and success of eukaryotic lineages on our planet because they allowed the host cells to harness light energy and to thrive in the presence of oxygen. The marine photosymbiotic associations that we study represent an earlier stage in the process of symbiont integration—one in which the photobiont can still be removed from the host and exist on its own. These systems are of interest to us for two reasons. First, they are ecologically important in the marine environment where they occur. These organisms form zones of photosynthetic production in oceanic regions typically low in nutrients. Second, investigation of these interactions may shed light on the molecular and evolutionary mechanisms involved in the integration of cells and their genomes.

Associations between microbial symbionts and their hosts are fundamental trophic relationships that occur in both terrestrial and aquatic environments and depend upon regulated genomic communication between the interacting organisms. We are particularly interested in the photosymbiotic relationships that involve microscopic (protistan) algae in association with a variety of "invertebrate" hosts (protistan and metazoan); these relationships are fairly common in the marine environment and contribute significantly to nutrient flow in the nutrient-poor regions of the ocean where they occur. The symbiosis is essential to the survival of the host organisms, although the algal symbiont can exist in the free-living state.

Besides the conspicuous invertebrate photosymbioses that most people are familiar with (anemones and corals), a variety of protistan species also harbor cytoplasmic algal symbionts. Most notably, protozoa within the subphylum Sarcomastigophora (the foraminifera, radiolaria, and acantharia; collectively referred to as "sarcodine protozoa") exist in symbioses with a wide array of algae (Anderson, 1983; Lee and McEnery, 1983; Caron and Swanberg, 1990; Michaels, 1991). These sarcodine protozoa are often large for single-celled organisms. Solitary cells often attain sizes more than 1 mm in diameter (some benthic foraminifera form discs more than 1 cm in diameter), and the presence of complex pseudopodial networks can increase the effective size of these organisms up to a few centimeters (Fig. 1). Some colonial species of radiolaria even form gelatinous pseudopodial matrices several centimeters in diameter and more than 1 m in length. These organisms are important contributors to the biological assemblages in all tropical and subtropical oceans of the world. Sarcodines form conspicuous zooplankton assemblages in oligotrophic surface waters, where they contribute significantly to primary productivity (by virtue of their intracellular symbionts), predation,

* To whom correspondence should be addressed. E-mail: rgast@whoi.edu

The paper was originally presented at a workshop titled *Outcomes of Genome-Genome Interactions.* The workshop, which was held at the J. Erik Jonsson Center of the National Academy of Sciences, Woods Hole, Massachusetts, from 1–3 May 2002, was sponsored by the Center for Advanced Studies in the Space Life Sciences at the Marine Biological Laboratory, and funded by the National Aeronautics and Space Administration under Cooperative Agreement NCC 2-1266.

Figure 1. Solitary planktonic radiolarian *Thalassicolla nucleata*. The central capsule of the organism is the dark circle in the center; it is surrounded by the rhizopodia containing the symbionts (small dots around the central capsule). The entire organism is about a millimeter in diameter.

and the vertical flux of organic material and crystal minerals, such as calcium carbonate and strontium sulfate (Caron and Swanberg, 1990; Swanberg and Caron, 1991; Caron *et al.*, 1995; Michaels *et al.*, 1995).

Our interest in the regulation of photosymbiotic relationships arose while working on the identification of the symbionts in planktonic foraminifera and radiolaria to determine whether co-evolution of host and symbiotic alga occurred (Gast and Caron, 1996; Gast *et al.*, 2000). We molecularly identified several taxonomically different algae that form symbioses in the planktonic sarcodines. Dinoflagellates are the most common of these, but we also found prymnesiophyte and prasinophyte algae. Furthermore, it appears that most algal symbionts are actually genetically more similar to *non*-symbiotic algae than they are to other symbiotic algal lineages. This led us to wonder about what made very different algae suitable as symbionts, sometimes in the same host (Gast and Caron, 2001), and to hypothesize that symbiotic algae have something in common, which can be identified genetically, that makes them acceptable as symbionts. We have undertaken comparative studies of gene expression in a symbiotic alga to investigate the mechanisms of symbiotic communication.

We are studying the symbiont-host relationship between the dinoflagellate alga *Scrippsiella nutricula* and the solitary planktonic radiolarian *Thalassicolla nucleata*. The radiolarian system allows us to compare the genes expressed in the symbiotic state of the algal symbiont with those expressed in the free-living state of the alga in culture. The information that we obtain from this system can be used to identify the genes necessary for maintaining the interaction, determine the timing of gene expression, examine the genomic characteristics associated with symbiotic-competence (why one alga is a good symbiont and another is not), and examine the mechanisms of secondary and higher level endosymbiotic events.

We chose to begin our work of isolating algal genes expressed in the symbiotic state by studying the dinoflagellate symbiont (*Scrippsiella nutricula*) of the solitary radiolarian *T. nucleata* (Fig. 1). To identify genes being expressed in the symbiosis, we required RNA from both the free-living and symbiotic states of the alga. We currently have the different algal symbionts as free-living laboratory cultures, but the intact association must be collected from the environment. *T. nucleata* generally harbors thousands of symbiotic algae, it can be collected from the environment fairly easily, and, most importantly, the host and symbiont can be separated from each other with minimal host RNA contamination of the sample. The host nucleus, organelles, and ribosomes are separated from the symbionts by the central capsule (pp. 90–94, Anderson, 1983). We believe that very little host mRNA will be present in the extracapsular material, and we are careful not to destroy the central capsule when stripping away the desired extracapsular matrix.

Thalassicolla nucleata was collected by plankton net tows in the Sargasso Sea and the San Pedro Channel. Individuals were transferred to sterile seawater in multiwell culture dishes and placed in lighted incubators or on workbenches at ambient temperatures. This allowed the hosts to clear themselves of prey items prior to recovery of the symbiont. All hosts were examined for prey before the extracapsular material was stripped away from the central capsule. Studies involving host incorporation of ^{14}C through the uptake of symbiont-produced photosynthate indicated that the interaction continued to function normally when the host was held in the laboratory (Anderson, 1978; Gast, unpubl. results). We believe that the symbiotic pattern of gene expression is also maintained. Stripped extracapsular material was immediately placed in RNALater (Ambion) until processed for RNA extraction (RNAqueous, Ambion). At least 200 individual hosts were collected and processed for each subtraction analysis.

Due to the relatively small amount of symbiotic-state RNA available for our project, we used a subtraction method that would permit the analysis of very small amounts of starting material. Through the use of two PCR enrichment amplifications, suppression subtractive hybridization (SSH; Diatchenko *et al.*, 1996) allows as little as 25 ng of mRNA (or 50 ng of total RNA) to be analyzed. We used the Clontech PCR-Select cDNA Subtraction Kit to analyze both total RNA and mRNA from the dinoflagellate symbionts (Fig. 2). To date, we have completed five subtractions—one from total RNA that failed, three from total RNA that were successful but yielded mostly host and bacterial ribosomal genes, and one from mRNA that was successful. We switched to analyzing mRNA because we recovered as many ribosomal clones as symbiosis clones when we analyzed total RNA. Contaminating ribosomal fragments were not unexpected since they would not be

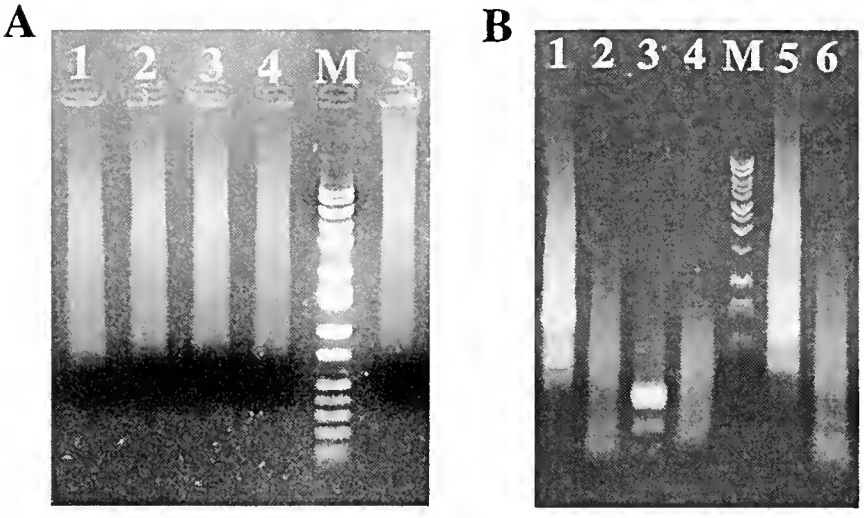

Figure 2. Results from suppression subtractive hybridization. (A) cDNA synthesis from symbiotic (lanes 1 & 2), free-living (lanes 3 & 4), and control (lane 5) RNA. M = 1-kb ladder. (B) Final PCR products from subtracted samples. Lane 1—symbiotic, subtracted; lane 2—symbiotic unsubtracted; lane 3—free-living subtracted; lane 4—free-living unsubtracted; lane 5—control subtracted; lane 6—control unsubtracted. M = 1-kb ladder. cDNAs were generated and subtracted by using the PCR-Select cDNA Subtraction kit from Clontech. Total RNA was isolated from the algae in the symbiotic state and the free-living state using either the Ambion RNAEasy kit or the Epicentre MasterPure RNA Purification kit, and mRNA was recovered using the Qiagen Oligotex mRNA kit. In both instances, the RNA from each state was separately reverse transcribed using MMLV-reverse transcriptase (Superscript II) to generate double-stranded cDNAs. Both sets of cDNAs were restriction digested with *Rsa*I to generate fragments with blunt ends, and the digested cDNAs from the symbiotic state were divided into two aliquots. Each aliquot was ligated to one of two different adaptors supplied in the kit. The strategy of the forward subtraction is to identify cDNAs up-regulated or unique to the symbiotic state of the alga. In this process, an excess of cDNAs from the free-living state (without ligated adapters) was mixed in two separate reactions with the adaptor-ligated cDNAs from the symbiotic state. The two tubes were separately heated to 95°C to denature the cDNAs, and then each was allowed to hybridize at 68°C for 8 h. This step promotes hybridization between the cDNAs expressed in common in the symbiotic and free-living states. To further enhance the subtraction of common cDNAs, the contents of the two tubes were then mixed together without a second denaturation step, combined with an additional excess of heat-denatured cDNAs from the free-living state, and hybridized overnight at 68°C. PCR primers specific to the two adapters (Clontech) were used to amplify cDNAs created during the subtraction that possessed one DNA strand ligated to adapter 1 and the other DNA strand ligated to adapter 2R. Only cDNAs from the symbiotic state of the alga should be able to amplify in this step, so we are enriching for the differentially regulated transcripts. The subtracted and amplified cDNAs were cloned into pGEM-T (Promega) and used to transform JM109 competent cells (Promega). A reverse subtraction was also performed in which the adaptor-free cDNA was from the symbiotic state and the adaptor-ligated cDNAs had been isolated from the free-living state. These subtracted cDNAs are therefore enriched in genes specific to the free-living state.

removed by subtraction with cultured dinoflagellate RNA. We identified 23 clones as being potentially up-regulated in the symbiotic state of the alga.

Nucleotide Blast searches (Altschul *et al.*, 1997) were conducted for sequences from each of the putatively up-regulated clones that were isolated. Of the 23 selected clones, 8 turned out to be ribosomal genes from the host, bacteria, or fungi. Twelve of the remaining clones (C4 group) were very similar to each other, varying primarily by small differences in length. These clones had no significant sequence match in the database (Table 1). Of the remaining three clones, only F7 showed significant homology to database sequences. The homology between F7 and Cyplasin S is the result of three 30-base repeats in the clone sequence that are also present in the gene. This 30-base repeat seems to occur in other proteins as well, and may represent a shared structural region. There are generally very few algal or protist cDNA sequences in GenBank, so the overall lack of homology to sequences in the database is disappointing but not unexpected. We are continuing to screen clones from the final PCR products of our mRNA subtraction to obtain more genes unique to the symbiotic state of the alga.

Because of the small amount of RNA available from our symbiotic state, it was not possible to confirm differential gene expression using northern blot. Instead, we used cDNA generated from the free-living and symbiotic state RNAs in a dot blot format (Fig. 3). Clone F9 was included as a control for positive hybridization to the free-living

Table I

List of clones recovered and analyzed with suppression subtractive hybridization

Clone group	BLASTn results	E value	Number of clones	Size of fragment (bp)
C4	Human DNA clone RP11-100A16	0.049	12	278
F7	*Aplysia punctata* mRNA for Cyplasin S	1e-60	1	161
E7	*Klebsiella pneumoniae* SL032 plasmid	0.003	1	635
B8	Human chromosome 16 clone RP11-407623	0.095	1	367

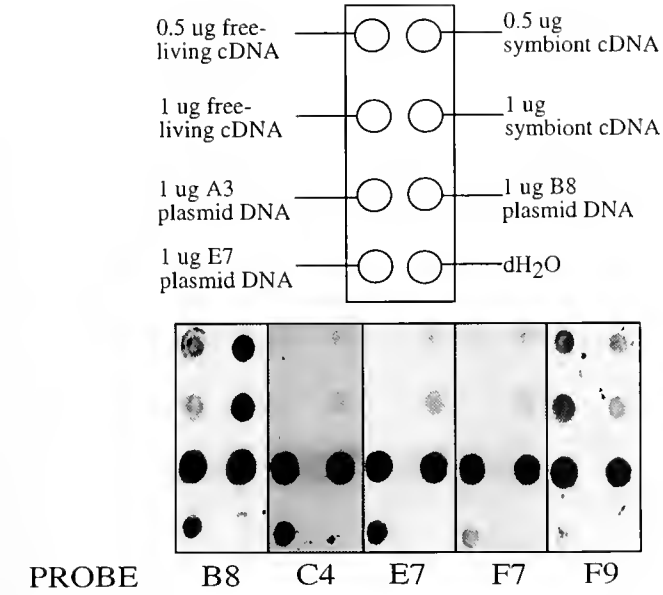

Figure 3. Confirmation of clone expression in symbiotic cDNA. To determine if the subtracted library contained clones up-regulated in the symbiotic state, 96 colonies were randomly chosen, and the cDNA insert from each was PCR amplified with the adapter-specific primers. Amplified products were denatured by addition of an equal volume of 0.6 *N* NaOH and then spotted onto Hybond NX nylon membranes and baked at 80°C for 1 h. The membrane was then hybridized to either a forward-subtracted or reverse-subtracted cDNA probe. Probes were generated by incorporating biotin-labeled nucleotides into either the secondary PCR products or the original cDNAs. Membranes were prehybridized for 1 h at 65 or 72°C in hybridization buffer (5XSSC, 0.1% N-lauroylsarcosine, 0.02% SDS, 1% blocking powder). The denatured probe was added to the prehybridization and allowed to hybridize overnight at 65 or 72°C. Membranes were washed twice, for 5 min each, in 2XSSC, 1.0% SDS at room temperature. The next two washes, 15 min each, were in 2XSSC, 0.1% SDS at the hybridization temperature. Hybridization was detected using the CDP-Star Southern Star chemiluminescent method. Only those inserts that showed hybridization to the forward-subtracted probe but not to the reverse-subtracted probe were examined further. To confirm that these clones were differentially regulated, inserts from these positive clones were PCR amplified and digested with *Rsa*I, *Sma*I, and *Eag*I to remove adaptors. Samples (0.5 and 1 mg) of the unsubtracted cDNAs from the symbiotic and free-living states, along with the plasmid clones A3, E7 and B8, were denatured, spotted onto membranes, and probed with the labeled inserts. The results for the symbiotically up-regulated clones (B8, C4, E7, and F7) are shown, along with one clone that is down-regulated in the symbiotic state (F9).

cDNA. This and other clones represent potentially down-regulated genes in the symbiotic state of the alga. We have not begun to analyze these clone sequences, but we recognize that these are potentially informative as well. The dot blots allowed us to confirm that our differentially expressed clones were not expressed, or were expressed at a reduced level, in the free-living cDNA populations.

Suppression subtractive hybridization analysis generates fairly small cDNA fragments, so rapid amplification of cDNA ends (RACE) analyses must be used to obtain the full cDNA sequence. We began our RACE analysis with the B8 clone because we knew that we had the 3′ end of the transcript. Currently we have about 800 basepairs of sequence for this clone. It has two open reading frames that are interrupted by a single stop codon in each. Neither of these reading frames has a start codon, and because the few dinoflagellate cDNAs that have been examined indicate the presence of fairly long 3′ untranslated regions (300–500 basepairs), we may still not have reached the 5′ end of the transcript. New primers are being designed to try and recover more of the 5′ end. Our other clones are less defined as to whether they are at the 5′ or 3′ end of the cDNA, and we are currently extending from both ends.

In this decidedly ambitious project, we have been successful in recovering several genes that appear to be up-regulated in the symbiotic state of the dinoflagellate symbiont *S. nutricula*. We know of only one other study using SSH in a non-mammalian context. That study, on the sexual stages of diatoms (Armbrust, 1999), confirmed only 10 up-regulated clones, so our low number of recovered clones may not be unusual, especially since our RNA quantities were so limiting. We plan to acquire the full-length cDNA sequences for the clones we have; to pursue the construction of a cDNA library for the dinoflagellate symbiotic-state RNA; and to develop microarrays to aid in screening for differentially expressed genes.

Acknowledgments

We thank the anonymous reviewers of this manuscript for their helpful comments. This work was supported by the NASA Astrobiology Program through grant number NCC 2-1054 to the MBL Astrobiology Center. WHOI contribution number 10815.

Literature Cited

Altschul, S. F., T. L. Madden, A. A. Schäffer, J. Zhang, Z. Zhang, W. Miller, and D. J. Lipman. 1997. Gapped BLAST and PSI-BLAST: a new generation of protein database search programs. *Nucleic Acids Res.* **25:** 3389–3402.

Anderson, O. R. 1978. Fine structure of a symbiont-bearing colonial radiolarian, *Collosphaera globularis* and 14C isotopic evidence for assimilation of organic substances from its zooxanthellae. *J. Ultrastruct. Res.* **62:** 181–189.

Anderson, O. R. 1983. *Radiolaria.* Springer-Verlag, New York.

Armbrust, E. V. 1999. Identification of a new gene family expressed during the onset of sexual reproduction in the centric diatom *Thalassiosira weissflogii*. *Appl. Environ. Microbiol.* **65:** 3121–3128.

Caron, D. A., and N. R. Swanberg. 1990. The ecology of planktonic sarcodines. *Rev. Aquat. Sci.* **3:** 147–180.

Caron, D. A., A. F. Michaels, N. R. Swanberg, and F. A. Howse. 1995. Primary productivity by symbiont-bearing planktonic sarcodines (Acantharia, Radiolaria, Foraminifera) in surface waters near Bermuda. *J. Plankton Res.* **17:** 103–129.

Diatchenko, L., C. Y.-F. Lau, A. P. Campbell, A. Chenchik, F. Moqadam, B. Huang, S. Lukyanov, K. Lukyanov, N. Gurskaya, E. D. Sverdlov, and P. D. Siebert. 1996. Suppression subtractive hybridization: A method for generating differentially regulated or tissue-specific cDNA probes and libraries. *Proc. Natl. Acad. Sci.* **93:** 6025–6030.

Gast, R. J., and D. A. Caron. 1996. Molecular phylogeny of symbiotic dinoflagellates from Foraminifera and Radiolaria. *Mol. Biol. Evol.* **13:** 1192–1197.

Gast, R. J., and D. A. Caron. 2001. Photosymbiotic associations in planktonic foraminifera and radiolaria. *Hydrobiologia* **461:** 1–7.

Gast, R. J., T. A. McDonnell, and D. A. Caron. 2000. srDNA-based taxonomic affinities of algal symbionts from a planktonic foraminifer and a solitary radiolarian. *J. Phycol.* **36:** 172–177.

Lee, J. J., and M. E. McEnery. 1983. Symbiosis in foraminifera. Pp. 37–68 in *Algal Symbiosis*, E. L. Goff, ed. Cambridge University Press, Cambridge.

Michaels, A. F. 1991. Acantharian abundance and symbiont productivity at the VERTEX seasonal station. *J. Plankton Res.* **13:** 399–418.

Michaels, A. F., D. A. Caron, N. R. Swanberg, F. A. Howse, and C. M. Michaels. 1995. Planktonic sarcodines (Acantharia, Radiolaria, Foraminifera) in surface waters near Bermuda: abundance, biomass and vertical flux. *J. Plankton Res.* **17:** 131–163.

Swanberg, N. R., and D. A. Caron. 1991. Patterns of sarcodine feeding in epipelagic oceanic plankton. *J. Plankton Res.* **13:** 287–312.

Reference: *Biol. Bull.* **204:** 215–220. (April 2003)

Plants, Mycorrhizal Fungi and Endobacteria: a Dialog Among Cells and Genomes

P. BONFANTE

Dipartimento di Biologia Vegetale dell' Università di Torino and Istituto di Protezione delle Piante, Sezione di Torino, Viale Mattioli 25, 10125 Torino, Italy

This review focuses on mycorrhizas, which are associations between fungi and the roots of 90% of terrestrial plants. These are the most common symbioses in the world; they involve about 6000 species of fungi distributed through all the fungal phyla and about 240,000 species of plants, including forest and crop plants. Thanks to mycorrhizal symbiosis and nutrient exchanges, regulated by complex molecular signals, the plant improves its vegetative growth, while the fungus accomplishes its life cycle. Molecular and cellular analyses demonstrate that during colonization the cellular organization of the two eukaryotes is completely remodeled. For example, in cortical cells, structural modifications involve both the host and the microbiont. Recent studies revealed that in arbuscular mycorrhizas (AM), system complexity is increased by the presence of a third symbiont: a bacterium living inside the fungus. The presence of this resident genome makes the investigation of the molecular dialogues among the symbiotic partners even more complex. Molecular analysis showed that the bacterium has genes involved in the acquisition of mineral nutrients. The experimental data support the current view that mycorrhizal symbioses are often tripartite associations.

Endosymbioses are excellent systems with which to investigate the dialog among genomes and cells. The aim of this short report is to demonstrate that mycorrhizas are of particular interest in an evolutionary context, because they offer a fine example of interactions between plants, fungi, and bacteria in the rhizosphere (Fig. 1).

E-mail: paola.bonfante@unito.it, p.bonfante@ipp.cnr.it

The paper was originally presented at a workshop titled *Outcomes of Genome-Genome Interactions.* The workshop, which was held at the J. Erik Jonsson Center of the National Academy of Sciences, Woods Hole, Massachusetts, from 1–3 May 2002, was sponsored by the Center for Advanced Studies in the Space Life Sciences at the Marine Biological Laboratory, and funded by the National Aeronautics and Space Administration under Cooperative Agreement NCC 2-1266.

Defining Mycorrhizas

Mycorrhizas are complex interactions comprising fungi belonging to different taxonomic groups and about 90% of land plants (Smith and Read, 1997). Mycorrhizas are successful in colonizing diverse environments, and their ecological success reflects a high degree of diversity in the genetic and physiological abilities of the fungal endophytes. About 6000 species in the Zygo-, Asco-, and Basidiomycotina have been recorded as mycorrhizal, but the advent of molecular techniques is increasing the number, since new mycorrhizal species as well as new associations are described on the basis of their DNA fingerprinting (Bidartondo *et al.*, 2002). The taxonomic position of plant and fungal partners defines the types of mycorrhiza, the main distinction of which is between endomycorrhiza and ectomycorrhiza. Generally speaking, the fungal hyphae in endomycorrhiza penetrate the root cells to establish an intracellular symbiosis, whereas in ectomycorrhiza the hyphae remain extracellular. However, various patterns of colonization are adopted by mycorrhizal fungi during their interactions with the host, mostly among endomycorrhizal fungi. In addition to arbuscular mycorrhizal (AM) fungi, which will be discussed in greater detail, ericoid mycorrhizal fungi colonize the root cells of their host, producing an infection unit that involves a single host cell without spreading to the neighboring root cells. In orchid mycorrhizas, intracellular coils in cortical cells are usually produced by Basidiomycetes during both the protocorm and root colonization; in this case, the infection unit comprises a larger number of host cells. Ectomycorrhizal fungi have a more recent evolutionary history; they do not penetrate the host cell wall, and they complete their colonization through two major

events: the production of a tissue-like structure (the mantle) covering the root surface, and the development of a labyrinthine, extracellular hyphal network within the root tissues, termed the Hartig net (Bonfante, 2001).

This report focuses on arbuscular mycorrhizal (AM) fungi, which have been recently classified in a new taxon, the *Glomeromycota* (Schüssler *et al.*, 2001).

Fossil and molecular data suggest that roots and AM fungi have shared a cooperative life since Devonian times (Simon *et al.*, 1993). The success of mycorrhizas in evolution is mainly due to the central role that AM fungi play in the capture of nutrients from the soil in almost all ecosystems (Smith and Read, 1997), and in phosphate uptake in particular (Smith and Barker, 2002, for a review). As a consequence, they are crucial determinants of plant biodiversity, ecosystem variability, and plant community productivity (van der Heijden *et al.*, 1998). AM fungi are not only an essential feature of the biology and ecology of most terrestrial plants, they also interact with different classes of bacteria during their life cycles. In fact, AM fungi establish interactions both with bacteria living in the rhizosphere (Fig. 1) during their extraradical phase and with endosymbiotic bacteria that live in the cytoplasm of some fungal isolates (Perotto and Bonfante, 1997; Bonfante *et al.*, 2001).

To understand these multiple interactions and to apply them in low-chemical-input agricultural systems is one of the most exciting challenges of current research in the field of molecular microbe-plant interactions.

Plant-Fungal Interactions: Cells, Genes, and Signals

The impressive diversity of the plant and fungal taxa involved in mycorrhizal symbiosis has resulted in their anatomical description in many hosts since the early twentieth century (Smith and Smith, 1997, for a review). The characterization of mycorrhizal phenotypes has led to a well-defined picture of the colonization by AM fungi, the main aspects of which are summarized on the web site ⟨http://www.bioveg.unito.it/lotus.htm⟩.

The availability of plant mutants with impaired symbiotic capabilities has demonstrated that colonization is a multistep, genetically regulated process that is under the control of specific loci (Bonfante *et al.*, 2000; Novero *et al.*, 2002). As a consequence of this process, the cellular organization of the two eukaryotes is completely remodeled. A detailed analysis of cell-to-cell interactions between host and mycobiont identifies the cell walls, membranes, and cytoskeleton of both partners as the structures where crucial changes occur (Bonfante, 2001).

However, analyzing the molecular bases of the dialogue

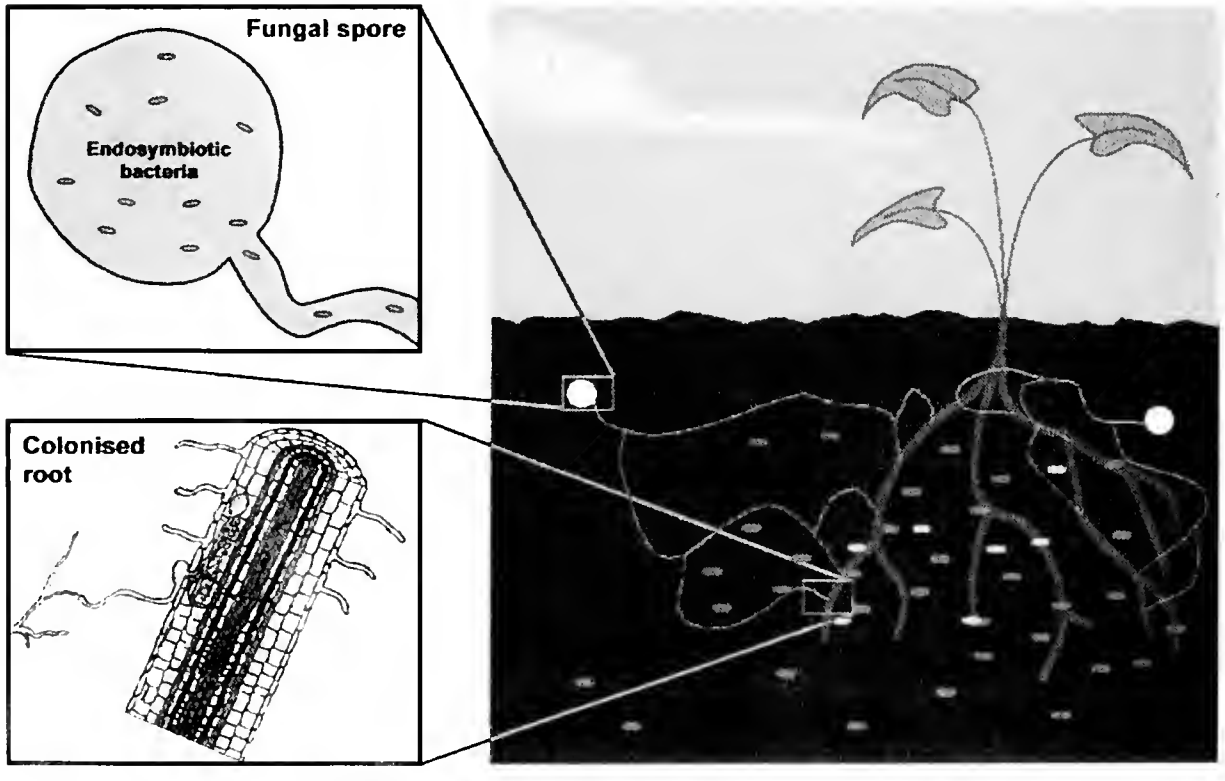

Figure 1. The scheme illustrates the multiple cellular interactions established among AM fungi, root cells, and bacteria in the rhizosphere. The magnification of the spore (insert at top left) shows the endobacteria living in the cytoplasm.

between the two partners is not an easy task. Other symbiotic systems are more advanced; for example, the interaction between *Rhizobium* and legumes is finely regulated by signal molecules, which are perceived by receptors that activate a signal transduction cascade, eventually leading to the activation of target genes and to the production of a nodule (Long, 1996). In AMs, knowledge of these steps is in its infancy; potential signal molecules have been found but not characterized (Buee *et al.*, 2000). Attention is therefore mostly focused on the genes that code for proteins responsible for the functional traits in AM fungi; for example, the phosphate transporter (Harrison and van Buuren, 1995) or a metallothionein gene (Lanfranco *et al.*, 2002). Further challenges are posed by other, obscure aspects of AM: their obligate biotrophic status, their multinuclear condition, and an unexpected level of genetic variability (Hijri *et al.*, 1999; Lanfranco *et al.*, 1999; Kuhn *et al.*, 2001). The genome of AM fungi is in fact huge, ranging from 0.3 pg to 1.12 pg/DNA for the nucleus, depending on the species (Gianinazzi-Pearson *et al.*, 2001). For all these reasons, genomic projects have not been attempted.

On the plant side, other problems are encountered. *Arabidopsis thaliana*, the first plant genome to be sequenced, does not establish any symbiotic interactions (the *Arabidopsis* Genome Initiative, 2000). However, rice does establish mycorrhizal associations, and genomic data accrued for rice will provide significant information (Goodman *et al.*, 2002; Sasaki *et al.*, 2002). Other plants are also being investigated. Breakthroughs from recent research on genomics, involving plants such as *Medicago truncatula* and *Lotus japonicus*, have led to the availability of about 100,000 expressed sequence tags (ESTs). Moreover, the availability of mutants that are impaired in their symbiotic properties has recently led to the discovery of plant genes that code for proteins that are essential to the dialogue between plants and both symbiotic microbes—AM fungi and rhizobia (Stracke *et al.*, 2002; Endre *et al.*, 2002). The genes NORK and SYMRK belong to a large class of plant and animal genes that code for receptor complexes (Kistner and Parniske, 2002). Both SYMRK and NORK present a repeated leucine-rich motif (RLM) in their extracellular domain and an intracellular receptor like-kinase domain (RLK). The discovery of these genes—which encode plant receptor kinases required for fungal and bacterial symbioses—opens the way for detailed analysis of signal perception and downstream signaling pathways that are associated with microbial recognition (Spaink, 2002; Kistner and Parniske, 2002).

Plant-Fungal-Bacterial Interactions

In addition to the well-known interactions between plants and fungi, mycorrhizal roots offer excellent ecological niches for other microbes; some rhizosphere bacteria adhere tightly to fungal hyphae, whereas others are directly associated with the root surfaces (Bianciotto *et al.*, 2001; Bianciotto and Bonfante, 2002). In addition, mycorrhizal fungi may host bacteria that complete their life cycles within fungal cells. As opposed to many other eukaryotic cells, which show some level of integration with bacteria and are increasingly appreciated by ecologists and evolutionary biologists for their huge diversity (Moran and Wernergreen, 2000), fungi offer only a limited number of examples. One of the best known is *Geosiphon pyriforme*, a zygomycete closely related to Glomales. It can host cyanobacteria inside characteristic bladders in the apical hyphal region (Schüssler and Kluge, 2001).

AM fungi are unique in hosting bacteria in their cytoplasm. Intracellular structures very similar to bacteria and bacteria-like organisms (BLOs) were first described in the 1970s (Scannerini and Bonfante, 1991 for a review). Ultrastructural observations clearly revealed their presence in many field-collected fungal isolates. Further investigation of these BLOs, including the demonstration of their prokaryotic nature, was long hampered because they could not be cultured. Only a combination of morphological observations (electron and confocal microscopy) and molecular analyses allowed us to identify BLOs as true bacteria and to start unraveling their symbiotic relationship with AM fungi (Bianciotto *et al.*, 1996).

Isolate BEG 34 of the fungus *Gigaspora margarita* contains a large number of BLOs that can be easily detected by staining with fluorescent dyes that are specific for bacteria and can distinguish between live and dead ones. On the basis of the 16S rDNA sequences, the bacterial endosymbionts living in *G. margarita* (BEG 34) were first identified as belonging to the genus *Burkholderia* (Bianciotto *et al.*, 1996). As a further step, on the basis of the 16S rDNA amplified from isolates of *Scutellospora persica*, *S. castanea*, and *G. margarita*, a strongly supported clade was obtained, which contained all endosymbiotic bacteria so far sequenced in Gigasporaceae. It was located close to the genus *Burkholderia*, as well as to the genera *Ralstonia* and *Pandorea*. A new bacterial taxon was therefore proposed: *Candidatus* Glomeribacter gigasporarum (Bianciotto *et al.*, 2003). The results demonstrate that endobacteria are widespread in Gigasporaceae, and suggest that they represent a stable cytoplasmic component. Preliminary results showing that bacteria move along with the fungi from one generation to the next, following a vertical transmission mechanism (V. Bianciotto and G. Bécard, unpubl.), provide a first experimental confirmation of the statement. A number of morphological observations showing bacteria living inside *Glomus* spores and hyphae (Scannerini and Bonfante, 1991) might suggest that endobacteria are not limited to the Gigasporaceae. However, attempts to obtain ribosomal sequences and to identify these endophytes on the basis of their DNA sequences have been so far unsuccessful, suggesting that

these bacteria are limited in number or, if present, belong to a mixed population.

The functional significance of AM fungal endobacteria is not clear; many attempts to cultivate them have been unsuccessful. The finding that a genomic library developed from *G. margarita* spores also has bacterial sequences (van Buuren *et al.*, 1999) helped us to identify some genes belonging to *Candidatus* Glomeribacter gigasporarum. Among the bacterial genes so far identified, the most interesting are those involved in nutrient uptake (*i.e.* a putative phosphate transporter operon, *pst*); in colonization events by bacterial cells (*vac*); and in chemotaxis (Ruiz-Lozano and Bonfante, 1999, 2000; Minerdi *et al.*, 2002). A DNA region containing putative nitrogenase coding genes (*nif* operon) was also found (Minerdi *et al.*, 2001), but these genes have not yet been demonstrated to belong to the *Candidatus* Glomeribacter genome.

Conclusions

In conclusion, the analysis of the multiple interactions established by AM fungi with plant and bacterial cells offers new keys for understanding the complexity of AM symbiosis. In addition to the still-open question about the signal molecules produced by AM fungi and recognized by potential receptors, the widespread presence of bacteria inside or specifically associated with AM fungi suggests that many AM symbioses are tripartite associations. This possibility will lead to the definition of new parameters in the design of mixed inocula, while the identification of fungal strains that contain endosymbiotic bacteria with important genetic traits opens up new strategies for the practical use of AM fungi.

Acknowledgments

P.B. thanks Dr. Diana Jennings for her support during the meeting and for her careful revision of the text. Many thanks are due to the AM symbiosis group (L. Lanfranco, A. Genre, A. Faccio, M. Novero, I. Martini, M. T. Della Beffa), and to the *Glomeribacter* group (V. Bianciotto, D. Minerdi, E. Lumini, S. Abbà). The research illustrated in this review has been funded by the EU GENOMYCA project, QLK5-CT-2000-01319, and by the Italian National Council of Research.

Literature Cited

***Arabidopsis* Genome Initiative. 2000.** Analysis of the genome sequence of the flowering plant *Arabidopsis thaliana*. *Nature* **408:** 796–815.

Bianciotto, V., and P. Bonfante. 2002. Arbuscular mycorrhizal fungi: a specialized niche for rhizospheric and endocellular bacteria. *Antonie Leeuwenhoek* **81:** 365–375.

Bianciotto, V., C. Bandi, D. Minerdi, M. Sironi, H. V. Tichy, and P. Bonfante. 1996. An obligately endosymbiotic fungus itself harbors obligately intracellular bacteria. *Appl. Environ. Microbiol.* **62:** 3005–3010.

Bianciotto, V., S. Andreotti, R. Balestrini, P. Bonfante, and S. Perotto. 2001. Mucoid mutants of the biocontrol strain *Pseudomonas fluorescens* CHA0 show increased ability in biofilm formation on mycorrhizal and nonmycorrhizal carrot roots. *Mol. Plant-Microbe Interact.* **14:** 255–260.

Bianciotto, V., E. Lumini, P. Bonfante, and P. Vandamme. 2003. '*Candidatus* Glomeribacter gigasporarum', an endosymbiont of arbuscular mycorrhizal fungi. *Int. J. Syst. Evol. Microbiol.* **53:** 121–126.

Bidartondo, M. I., D. Redecker, I. Hijri, A. Wiemken, T. D. Bruns, L. Dominguez, A. Sersic, J. R. Leake, and D. J. Read. 2002. Epiparasitic plants specialized on arbuscular fungi. *Nature* **419:** 389–392.

Bonfante, P. 2001. At the interface between mycorrhizal fungi and plants: the structural organization of cell wall, plasma membrane and cytoskeleton. Pp. 45–91 in *Mycota, IX: Fungal Associations*, B. Hock, ed. Springer Verlag, Berlin.

Bonfante, P., A. Genre, A. Faccio, I. Martini, L. Schauser, J. Stougaard, J. Webb, and M. Parniske. 2000. The *Lotus japonicus* LjSym4 gene is required for the successful symbiotic infection of root epidermal cells. *Mol. Plant-Microbe Interact.* **13:** 1109–1120.

Bonfante, P., V. Bianciotto, J. M. Ruiz-Lozano, D. Minerdi, E. Lumini, and S. Perotto. 2001. Arbuscular mycorrhizal fungi and their endobacteria. Pp. 323–337 in *Symbiosis*, J. Seckbach, ed. Kluwer, Dordrecht.

Buee, M., M. Rossignol, A. Jauneau, R. Ranjeva, and G. Becard. 2000. The presymbiotic growth of arbuscular mycorrhizal fungi is induced by a branching factor partially purified from plant root exudates. *Mol. Plant-Microbe Interact.* **13:** 693–698.

Endre, G., A. Kereszt, Z. Kevei, S. Mihacea, P. Kaló, and G. B. Kiss. 2002. A receptor kinase gene regulating symbiotic nodule development. *Nature* **417:** 962–966.

Gianinazzi-Pearson, V., D. van Tuinen, E. Dumas-Gaudot, and H. Dulieu. 2001. Exploring the genome of Glomalean fungi. Pp 3–17 in *Mycota, IX: Fungal Associations*, B. Hock, ed. Springer Verlag, Berlin.

Goodman R. M., R. Naylor, H. Tefera, R. Nelson, and W. Falcon. 2002. The rice genome and the minor grains. *Science* **296:** 1801–1804.

Harrison, M. J., and M. L. van Buuren. 1995. A phosphate transporter from the mycorrhizal fungus *Glomus versiforme*. *Nature* **378:** 626–629.

Hijri, M., M. Hosny, D. van Tuinen, and H. Dulieu. 1999. Intraspecific ITS polymorphism in *Scutellospora castanea* (Glomales, Zygomycota) is structured within multinucleate spores. *Fungal Genet. Biol.* **26:** 141–151.

Kistner, C., and M. Parniske. 2002. Evolution of signal transduction in intracellular symbiosis. *Trends Plant Sci.* **7:** 511–518.

Kuhn, G., M. Hijri, and I. R. Sanders. 2001. Evidence for the evolution of multiple genomes in arbuscular mycorrhizal fungi. *Nature* **414:** 745–748.

Lanfranco, L., M. Delpero, and P. Bonfante. 1999. Intrasporal variability of ribosomal sequences in the endomycorrhizal fungus *Gigaspora margarita*. *Mol. Ecol.* **8:** 37–45.

Lanfranco, L., A. Bolchi, E. Cesale Ros, S. Ottonello, and P. Bonfante. 2002. Differential expression of a metallothionein gene during the presymbiotic versus the symbiotic phase of an arbuscular mycorrhizal fungus. *Plant Physiol.* **130:** 58–67.

Long, S. R. 1996. *Rhizobium* symbiosis: nod factors in perspective. *Plant Cell* **8:** 1885–1898.

Minerdi, D., R. Fani, R. Gallo, A. Boarino, and P. Bonfante. 2001. Nitrogen fixation genes in an endosymbiotic *Burkholderia* strain. *Appl. Environ. Microbiol.* **67:** 725–732.

Minerdi, D., R. Fani, and P. Bonfante. 2002. Identification and evolutionary analysis of putative cytoplasmic *Mcp*A-like protein in a bacterial strain living in symbiosis with a mycorrhizal fungus. *J. Mol. Evol.* **54:** 815–824

Moran, N. A., and J. J. Wernegreen. 2000. Lifestyle evolution in symbiotic bacteria: insights from genomics. *Tree* **15:** 321–326.

Novero, M., A. Faccio, A. Genre, J. Stougaard, K. J. Webb, L. Mulder, M. Parniske, and P. Bonfante. 2002. Dual requirement of the *LiSym4* gene for mycorrhizal development in epidermal and cortical cells of *Lotus japonicus* roots. *New Phytol.* **154:** 741–750.

Perotto, S., and P. Bonfante. 1997. Bacterial associations with mycorrhizal fungi: close and distant friends in the rhizosphere. *Trends Microbiol.* **5:** 496–503.

Ruiz-Lozano, J. M., and P. Bonfante. 1999. Identification of a putative P-transporter operon in the genome of a *Burkholderia* strain living inside the arbuscular mycorrhizal fungus *Gigaspora margarita*. *J. Bacteriol.* **181:** 4106–4109.

Ruiz-Lozano, J. M., and P. Bonfante. 2000. Intracellular *Burkholderia* of the arbuscular mycorrhizal fungus *Gigaspora margarita* possesses the *vacB* gene, which is involved in host cell colonization by bacteria. *Microb. Ecol.* **39:** 137–144.

Sasaki, T., T. Matsumoto, K. Yamamoto, K. Sakata, *et al.*, 2002. The genome sequence and structure of rice chromosome 1. *Nature* **420:** 312–316.

Scannerini, S., and P. Bonfante. 1991. Bacteria and bacteria like objects in endomycorrhizal fungi (Glomaceae). Pp. 273–287 in *Symbiosis as Source of Evolutionary Innovation: Speciation and Morphogenesis,* L. Margulis and R. Fester, eds. The MIT Press, Cambridge, MA.

Schüssler, A., and M. Kluge. 2001. *Geosiphon pyriforme*, an endocytosymbiosis between fungus and cyanobacteria, and its meaning as a model system for arbuscular mycorrhizal research. Pp. 151–161 in *Mycota, IX: Fungal Associations,* B. Hock, ed. Springer Verlag, Berlin.

Schüssler, A., H. Gehrig, D. Schwarzott, and C. Walker. 2001. Analysis of partial Glomales SSU rRNA genes: implications for primer design and phylogeny. *Mycol. Res.* **105:** 5–15.

Simon, L., J. Bousquet, R. C. Lévesque, and M. Lalonde. 1993. Origin and diversification of endomycorrhizal fungi and coincidence with vascular land plants. *Nature* **363:** 67–69.

Smith, F. A., and S. E. Smith. 1997. Tansley Review No. 96. Structural diversity in (vesicular)-arbuscular mycorrhizal symbioses. *New Phytol.* **137:** 373–388.

Smith, S. E., and S. J. Barker. 2002. Plant phosphate transporter genes help harness the nutritional benefits of arbuscular mycorrhizal symbiosis. *Trends Plant Sci.* **7:** 189–190.

Smith, S. E., and D. J. Read. 1997. *Mycorrhizal Symbiosis.* Academic Press, London.

Spaink, H. P. 2002. A receptor in symbiotic dialogue. *Nature* **417:** 910–911.

Stracke, S., C. Kistner, S. Yoshida, L. Mulder, S. Sato, T. Kaneko, S. Tabata, N. Sandal, J. Stougaard, K. Szczyglowski, and M. Parniske. 2002. A plant receptor-like kinase required for both bacterial and fungal symbiosis. *Nature* **417:** 959–962.

van Buuren, M., L., Lanfranco, S. Longato, D. Minerdi, M. J. Harrison, and P. Bonfante. 1999. Construction and characterization of genomic libraries of two endomycorrhizal fungi: *Glomus versiforme* and *Gigaspora margarita*. *Mycol. Res.* **103:** 955–960.

van der Heijden, M. G. A., J. N. Klironomos, M. Ursic, P. Moutoglis, R. Streitwolf-Engel, T. Boller, A. Wiemken, and I. R. Sanders. 1998. Mycorrhizal fungal diversity determines plant biodiversity, ecosystem variability and productivity. *Nature* **396:** 69–72.

Discussion

QUESTION: Can you cure the fungal symbiont of the bacterial symbiont and then look at the differential effect of the fungus with and without the bacterial symbiont or the plant?

BONFANTE: This is a crucial question. We are facing the problem together with Dr. G. Becard from Toulouse. Dr. Becard's group has demonstrated that the bacteria are not sensitive to many antibiotic treatments. In fact, some antibiotics seemed to increase bacterial growth.

QUESTION: Can you grow the fungus in nitrogen-free medium?

BONFANTE: Yes, arbuscular mycorrhizas fungal spores usually germinate in water. It is well known that the first growth steps (non-symbiotic phases) proceed without other nutrients.

COMMENT (JOHN HOBBIE): In Europe, scientists seem to appreciate—much more than in the U.S.—the importance of the mycorrhizal fungi in incorporating nutrients into shrubs and trees. A recent book points out that, in forests, most of the nitrogen and phosphorus enters the trees by way of the mycorrhizal fungi. It is also well known that most of the forests of the world are nitrogen limited. Most research until now has involved the uptake of phosphorus by mycorrhizae. Plants grown with mycorrhizae clearly grow much better than those grown without, but in many cases nitrogen could have had an effect as well. What the fungi can do, of course, is to get at the organically bound nitrogen, which is most of the nitrogen in the soil. This organically bound nitrogen is not available to the plant without the microbial "mineralization" to ammonium and nitrate, or without an enzymatic breakdown to amino acids, uptake, and transport to the roots by the mycorrhizal fungi. The fungi obtain sugars from the tree roots and provide nitrogen, phosphorus, and even water to the tree or shrub. Up to 30% of the carbohydrates fixed in photosynthesis can be transported under ground and respired by the fungi.

The importance of the symbiosis between plant roots and mycorrhizal fungi is just beginning to be investigated. Ecologists want to know about the regulation of the fungal breakdown of proteins and other nitrogen compounds, and how much of the total pool of organic nitrogen in soil is available.

BONFANTE: While the role of AM fungi in phosphate uptake is largely acknowledged, their role in nitrogen uptake is a recent discovery. Fitter's laboratory recently published an interesting article in *Nature*, which shows that AM fungi use an organic N source[1]. The role of ectomycorrhizal fungi in nutrient cycles is

[1] Hodge, A., C. D. Campbell, and A. H. Fitter. 2001. An arbuscular mycorrhizal fungus accelerates decomposition and acquires nitrogen directly from organic material. *Nature* 413: 297–299.

well demonstrated, and molecular mechanisms are being explored. The most recent views on these topics can be found in the book by van der Heijden and Sanders[2].

QUESTION: Is there any evidence yet that, in a forced succession, there might be a concomitant succession of fungi in the soil?

BONFANTE: Under natural conditions, a fungal succession is known to accompany that in the roots. This has been well described in ectomycorrhizae: early colonizers and later colonizers have been identified in many plant communities. The development of molecular probes is now providing new views and opened new questions on the identification of spatial and temporal factors underlying community structures[3]. The new approaches of molecular ecology will allow us to directly monitor the fungal succession under microcosmal conditions.

[2] van der Heijden, M. G. A., and I. R. Sanders, eds. 2002. *Mycorrhizal Ecology*, Ecological Studies, Vol. 157. Springer, New York.

[3] Dahlberg, A. 2001. Community ecology of ectomycorrhizal fungi: an advancing interdisciplinary field. *New Phytol.* 150: 555.

Reference: *Biol. Bull.* **204:** 221–231. (April 2003)

Genome Evolution in an Insect Cell: Distinct Features of an Ant-Bacterial Partnership

JENNIFER J. WERNEGREEN,* PATRICK H. DEGNAN, ADAM B. LAZARUS, CARMEN PALACIOS, AND SETH R. BORDENSTEIN

Josephine Bay Paul Center for Comparative Molecular Biology and Evolution, Marine Biological Laboratory, 7 MBL Street, Woods Hole, Massachusetts 02543

Bacteria that live exclusively within eukaryotic host cells include not only well-known pathogens, but also obligate mutualists, many of which occur in diverse insect groups such as aphids, psyllids, tsetse flies, and the ant genus Camponotus *(Buchner, 1965; Douglas, 1998; Moran and Telang, 1998; Baumann* et al., *2000; Moran and Baumann, 2000). In contrast to intracellular pathogens, these primary (P) endosymbionts of insects are required for the survival and reproduction of the host, exist within specialized host cells called bacteriocytes, and undergo stable maternal transmission through host lineages (Buchner, 1965; McLean and Houk, 1973). Due to their long-term host associations and close phylogenetic relationship with well-characterized enterobacteria (Fig. 1), P-endosymbionts of insects are ideal model systems to examine changes in genome content and architecture that occur in the context of beneficial, intracellular associations. Since these bacteria have not been cultured outside of the host cell, they are difficult to study with traditional genetic or physiological approaches. However, in recent years, molecular and computational approaches have provided important insights into their genetic diversity and ecological significance. This review describes some recent insights into the evolutionary genetics of obligate insect-bacteria symbioses, with a particular focus on an intriguing association between the bacterial endosymbiont* Blochmannia *and its ant hosts.*

* To whom correspondence should be addressed. E-mail: jwernegreen@mbl.edu

The paper was originally presented at a workshop titled *Outcomes of Genome-Genome Interactions.* The workshop, which was held at the J. Erik Jonsson Center of the National Academy of Sciences, Woods Hole, Massachusetts, from 1–3 May 2002, was sponsored by the Center for Advanced Studies in the Space Life Sciences at the Marine Biological Laboratory, and funded by the National Aeronautics and Space Administration under Cooperative Agreement NCC 2-1266

The specific functions of most insect P-endosymbionts remain unknown. However, the typically unbalanced diets of their hosts suggest these bacteria play a nutritional role. In fact, nutritional functions are well documented in certain P-endosymbionts such as *Buchnera aphidicola,* which provides essential amino acids that are lacking in the plant sap diet of its aphid host (Sandstrom *et al.,* 2000), and *Wigglesworthia glossinidia,* which provisions its tsetse fly host with B-complex vitamins lacking in vertebrate blood (Nogge, 1981; Aksoy, 2000). The bacterium SOPE (*Sitophilus oryzae* primary endosymbiont) oxidizes excess methionine consumed by the weevil (Gasnier-Fauchet and Nardon, 1986) and increases mitochondrial enzymatic activity of the host by providing vitamins such as panthothenic acid and riboflavin (Wicker and Nardon, 1982; Heddi *et al.,* 1991, 1999). *Blattobacterium,* a symbiont that lives within fat bodies of cockroaches, may be involved in tyrosine biosynthesis (Goldberg and Pierre, 1969) and apparently recycles uric acid of the host, as evidenced by elevated uric acid levels in hosts from which the bacteria have been eliminated (Cochoran, 1985). The biosynthetic abilities of these bacteria allow hosts to exploit food sources and habitats that would otherwise be inadequate; therefore, symbiont acquisition can be viewed as a key innovation in the evolution of these insect lineages (Moran and Telang, 1998). Indeed, sister genera lacking P-endosymbionts typically utilize a different, more nutrient-rich dietary resource (Nardon and Grenier, 1991). These insect-bacteria relationships are reciprocally beneficial, as the highly specialized bacteria rely on the host cellular environment for their survival.

We are studying the evolutionary outcome of an obligate association between ants and a bacterial endosymbiont recently designated *Candidatus* Blochmannia gen. nov. (*Blochmannia*) (Sauer *et al.,* 2000). This bacterium lives

within host cells that are typically adjacent to or within the midgut epithelium, and forms an obligate association with at least three closely related genera in the ant subfamily Formicinae: *Polyrhachis*, *Colobopsis*, and *Camponotus* (Dasch *et al.*, 1984; Schroder *et al.*, 1996; Sameshima *et al.*, 1999). *Camponotus* is the second largest ant genus; it includes 931 species and is found in almost every biogeographic region (Bolton, 1995). Although *Blochmannia* is the best characterized ant endosymbiont, we know little about its gene content and nothing about its functional role. Building upon relatively rich molecular datasets currently available for *Buchnera* and *Wigglesworthia*, we are using comparative approaches to explore the impact of endosymbiosis on sequence and genome evolution in *Blochmannia*, including rates and patterns of DNA and protein sequence evolution and changes in genome size and content. In future work, genomic comparisons and experimental approaches promise to shed light on the physiological and ecological roles of this bacterium.

Forces Shaping Sequence Evolution in Endosymbionts

Phylogenetic analysis of insect mutualists

Analyses of 16S rDNA genes show that many insect endosymbionts group with the γ-3 subdivision of Proteobacteria, along with *Escherichia coli* and related enterobacteria (Fig. 1) (Munson *et al.*, 1991; Schroder *et al.*, 1996; Sameshima *et al.*, 1999). Furthermore, many previous studies suggest that *Buchnera*, *Wigglesworthia*, and *Blochmannia* share a very close phylogenetic relationship and may be monophyletic (*e.g.*, Schroder *et al.*, 1996; Spaulding and von Dohlen, 1998; Sauer *et al.*, 2000). However, these phylogenies were often estimated using maximum parsimony or distance approaches, which may be highly biased by the fast evolutionary rates and strong AT bias of endosymbiont sequences. In contrast, maximum likelihood analysis (Fig. 1) strongly suggests that *Buchnera* is phylogenetically distinct from *Wigglesworthia* and *Blochmannia*, but that the last two are closely related to each other. This aspect of the phylogeny agrees with that proposed by Charles *et al.* (2001). Multiple, independent origins of endosymbiotic lifestyles are not entirely surprising, since endosymbiotic bacteria have arisen in many classes of bacteria, including α-Proteobacteria, β-Proteobacteria, and flavobacteria (Douglas, 1989; Moran and Telang, 1998). Indeed, multiple origins of endosymbiosis within the γ-Proteobacteria makes this group an ideal model to explore (i) phylogenetically independent transitions to an endosymbiotic lifestyle (*e.g.*, *Buchnera versus Wigglesworthia* and *Blochmannia*), and (ii) adaptation of closely related bacterial species to quite different host associations (*Wigglesworthia versus Blochmannia*).

The phylogenies of P-endosymbionts within a single host system are generally congruent with their hosts' species, indicating that the symbiont origin traces back to a single, often ancient, infection event within each host group. This pattern of host-symbiont cospeciation has been demonstrated for the aphid-*Buchnera* symbiosis (Munson *et al.*, 1991; Clark *et al.*, 2000; Funk *et al.*, 2000), the tsetse fly-*Wigglesworthia* symbiosis (Chen *et al.*, 1999), and the psyllid-*Carsonella* symbiosis (Thao *et al.*, 2000). Thus, in contrast to facultative symbionts or pathogens that can transfer horizontally to new hosts, P-endosymbionts have been vertically inherited over long evolutionary timescales. These ancient insect-bacterial associations date back as far as 150-200 MYA for the aphid-*Buchnera* association (Munson *et al.*, 1991) and about 50-100 MYA for tsetse fly-*Wigglesworthia* (Moran and Wernegreen, 2000). Phylogenetic congruence between *Camponotus* and *Blochmannia* also holds true across a large number of host species (Sameshima *et al.*, 1999; Sauer *et al.*, 2000; P. H. Degnan *et al.*, unpubl. data) as well as within a single *Camponotus* species (A. B. Lazarus *et al.*, unpubl. data), indicating the ant-bacterial association is evolutionarily stable and at least as old as the genus *Camponotus* (>20 MY; Wilson, 1985) if not even older.

Population bottlenecks and genetic drift

Maternal transmission of P-endosymbionts is thought to impose a population bottleneck that reduces the number of bacteria passed on from mother to offspring (Mira and Moran, 2002). Successive bottlenecks throughout the evolution of these ancient associations are expected to reduce the effective population size (N_e) of the bacterial partner. Consequently, endosymbiont population sizes may be determined by insect host population sizes, which are orders of magnitude smaller than the extremely large populations of free-living bacteria ($N_e \sim 10^9$ for species of enterobacteria; Selander *et al.*, 1987). Models of nearly neutral evolution predict that reduced N_e will lower the efficacy of natural selection and will elevate rates of fixation of deleterious mutations through random genetic drift (Ohta, 1973). Over time, the accumulation of deleterious mutations may negatively affect the fitness of the symbiont and host (Rispe and Moran, 2000; Wernegreen and Moran, 2000). Exacerbating the effect of genetic drift in P-endosymbionts is their apparent lack of recombination among genetically distinct lineages (Funk *et al.*, 2000; Wernegreen and Moran, 2001). This strict asexuality contrasts with recombination in free-living bacterial strains, and may produce an effect known as Muller's ratchet (Muller, 1964, Moran, 1996) in which genetic drift in small populations is increased because wild-type genotypes cannot be introduced through recombination.

Several studies show that the repair of slightly deleterious mutations is important in shaping sequence evolution of P-endosymbionts. Evidence for drift includes fast rates of

sequence evolution, changes that destabilize the 16S rRNA secondary structure, elevated rates of amino acid substitutions, and higher ratio of nonsynonymous to synonymous substitutions (dN/dS) compared to free-living bacteria (Moran, 1996; Brynnel *et al.*, 1998; Lambert and Moran, 1998; Wernegreen and Moran, 1999; Clark *et al.*, 1999). Similarly, protein-coding genes of *Blochmannia* show accelerated rates of evolution and elevated dN/dS, suggesting this ant symbiont may also experience strong genetic drift (unpubl. data). Pervasive acceleration of protein evolution across the genome is not easily explained by relaxed or positive selection, which is expected to act at individual genes. Nor can elevated mutation alone explain the observed rate increase, since mutation would affect dN and dS equally, with no expected change in dN/dS. Finally, population genetic analyses of *Buchnera* associated with two aphid species show low levels of sequence polymorphism consistent with population bottlenecks, and an excess of rare alleles and nonsynonymous polymorphisms that suggest strong effects of genetic drift (Funk *et al.*, 2001; Abbot and Moran, 2002). In total, the pervasive rate elevation across genes, elevated dN/dS, and intraspecific polymorphism data are most consistent with reduced efficacy of selection across the genome due to genetic drift in small populations. Intracellular pathogens also show elevated rates of protein evolution that suggest genome degradation through genetic drift (Andersson and Andersson, 1999).

On a related note, a recent study attributed accelerated protein evolution in *Buchnera* to mutational bias alone (Itoh *et al.*, 2002). The authors argued against any role of genetic drift, on the basis that *Buchnera* presumably did not show an increase in dN/dS. However, the dN and dS values used to calculate this ratio were derived from different studies of different *Buchnera* loci. Thus, the apparent lack of elevated dN/dS must be weighed against the results of several studies that show a significant elevation of this ratio when dN and dS are calculated from the same dataset (Moran, 1996; Brynnel *et al.*, 1998; Wernegreen and Moran, 1999; Clark *et al.*, 1999). Itoh *et al.* (2002) also raise the intriguing suggestion that if slightly deleterious mutations are fixed in populations over time, these mutations will eventually render all genes functionless. However, mutations that severely impair or eliminate functions of necessary genes are not slightly deleterious; rather, these mutations would have high selective coefficients and would be eliminated even from small endosymbiont populations. For example, in the AT-rich *Buchnera* genome, high-expression genes (*e.g.*, chaperonins and ribosomal proteins) have distinct amino acid usage patterns compared to genes with putatively low expression levels (Palacios and Wernegreen, 2002). High-expression genes tend to use amino acids that are less aromatic and are encoded by relatively GC-rich codons, suggesting strong selection against aromatic amino acids and against amino acids with AT-rich codons. Thus, while AT mutational bias and genetic drift influence amino acid usage in *Buchnera*, selection at high-expression genes is sufficiently strong to attenuate the effects of mutational bias on amino acid content. We could generalize that, despite strong effects of genetic drift, selection still constrains deleterious amino acid changes in *Buchnera*, especially at high-expression loci.

Mutational bias in endosymbionts: random or adaptive?

Along with genetic drift, intracellular mutualists and pathogens also experience strong mutational pressure that, over time, can severely alter the base composition of their genomes. In contrast to the moderate base compositions of the enterics, sequences of intracellular bacteria are characterized by extremely low percentage content of GC (Fig. 2). A 37-kb fragment of the *Carsonella ruddii* genome was recently found to be just 19.9% GC, making this psyllid symbiont the most AT-rich bacterial genome yet characterized (Clark *et al.*, 2001). Analysis of six kilobases of *Blochmannia* sequences (unpubl. data) corroborates earlier evidence of low GC content for this bacterial genome (~30% GC; Dasch, 1975). This AT bias has a strong impact on the amino acid composition of *Buchnera*, *Carsonella*, and *Wigglesworthia* proteins, which are highly biased toward amino acids encoded by AT-rich codons (Clark *et al.*, 1999, 2001; Akman *et al.*, 2002; Palacios and Wernegreen, 2002).

Two main hypotheses have been proposed to explain base compositional biases observed in most obligately intracellular mutualists and pathogens. First, AT richness may reflect strong mutational bias resulting from the loss of DNA repair genes by random genetic drift (Eisen and Hanawalt, 1999; Moran and Wernegreen, 2000). According to this hypothesis, an underlying AT mutational bias is repaired less efficiently in small intracellular genomes that lack certain repair functions. Second, AT bias may be an adaptive feature of an intracellular lifestyle, explained by the high energetic cost and lower accessibility of GTP and CTP compared to ATP and UTP (Rocha and Danchin, 2002). ATP, for example, plays a significant role in cellular metabolism and is the most abundant nucleotide. Under this hypothesis, a nucleotide pool biased toward UTP and ATP and a corresponding AT mutational bias would be more efficient and thus would allow intracellular bacteria to exploit the host cell more effectively. Selection on each GC→AT mutation would be miniscule, but selection might favor larger changes (such as gene loss) that contribute to an overall mutation bias. Consistent with this adaptive hypothesis, the AT contents of other intracellular elements (*e.g.*, plasmids, phage, and insertion sequences) are also generally higher than those of their hosts, and base composition of phage corresponds to infection type, as virulent phages are more AT-rich than temperate ones (Rocha and Danchin, 2002).

Figure 1. Phylogenetic relationships among insect endosymbionts (boldface) and related γ-Proteobacteria, estimated from the 16S rDNA gene. Both maximum likelihood (ML) and Bayesian analyses give the tree topology presented. Values above nodes (in boldface) are bootstrap values for maximum likelihood analysis, and values below nodes are posterior probability values generated by the Bayesian analysis. Branch lengths reflect genetic distance under the maximum likelihood model used. This phylogeny strongly supports the following hypotheses: (i) a single origin of endosymbionts in the ancestor of the ant genera *Camponotus, Colobopsis,* and *Polyrhachis,* (ii) independent origins of symbiosis in the ants *Formica* and *Plagiolepis,* and (iii), that *Buchnera* is a phylogenetically distinct lineage from *Wigglesworthia* and *Blochmannia,* which are closely related.

16S rDNA sequence data: Most 16S rDNA sequences were obtained from GenBank (with the exception new *Blochmannia,* obtained as described below). Nucleotide sequence accession numbers for other 16S rDNA sequences used in phylogenetic analysis are as follows: *Antonina crawii* S-endosymbiont AB030020; *Buchnera-Acyrthosiphon pisum* (P-endosymbiont) NC002528; *Arsenophonus-Triatoma infestans* (S-endosymbiont) U91786; *Colobopsis nipponicus* endosymbiont AB018676; *Dysmicoccus neobrevipes* S-endosymbiont AF476104; *Enterobacter asburiae* AB004744; *Escherichia coli* NC000913; *Erwinia herbicola* AB004757; *Formica fusca* endosymbiont AB018684; *Wigglesworthia-Glossina austeni* (P-endosymbiont) AF022879; *Wigglesworthia-Glossinia brevipalpis* (P-endosymbiont) L37341; *Glossinia pallidipes* S-endosymbiont M99060; *Haemophilus influenzae* NC000907; *Klebsiella pneumoniae* AB004753; *Arsenophonus-Nasonia vitripennis* (S-endosymbiont) M90801; *Plagiolepis pigmaea* endosymbiont AB018683; *Pseudomonas aeruginosa* NC002516; *Polyrhachis lamellidens* P-endosymbiont AB018680; *Proteus vulgaris* J01874; *Buchnera -Schizaphis graminum* (P endosymbiont) L18927; *Sitophilus oryzae* P-endosymbiont AF005235; *Salmonella typhimurium* NC003197; *Uroleucon astronomus* S-endosymbiont (U type) AF293623; *Yersinia pestis* NC003143; *Yamatocallis tokyoensis* S-endosymbiont AB064515.

Obtaining Blochmannia 16S rDNA data: Genomic DNA was extracted from individual *Camponotus festinatus* and *C. pennsylvanicus* workers using the DNeasy tissue kit (Qiagen) according to the manufacturer's instructions. This DNA was used as template for PCR reaction using SL and SR universal eubacterial 16S rDNA primers (Schroder *et al.,* 1996). The single 1.6-kb band PCR product was then cleaned up using a column purification kit (Qiagen) and sequenced on an ABI 3700 automated sequencer. SL, SR, and two internal primers were used to sequence the PCR product. The resulting sequences were assembled and edited using PHRED,

Notable exceptions to the link between an intracellular lifestyle and AT bias include the relatively GC-rich genomes of the pathogen *Mycobacterium leprae* (57.8% GC; Cole *et al.*, 2001); the weevil endosymbiont, SOPE (54% GC; Heddi *et al.*, 1998); and the β-Proteobacterial subdivision endosymbiont of mealybugs, *Tremblaya* (57.1% GC across a 35-kb region; Baumann *et al.*, 2002). Interestingly, both SOPE and *M. leprae* also differ from most other obligately intracellular bacteria in having relatively large genome sizes (~3 Mb and 3.27 Mb, respectively) (Fig. 2). The genome size of *Tremblaya* is unknown, but its close relative *Burkholderia pseudomallei* has a very large genome (7.25 Mb; unpubl. data of the *B. pseudomallei* Sequencing Group at the Sanger Institute; http://www.sanger.ac.uk/Projects/B_pseudomallei/). These larger genomes may retain DNA repair functions that are missing from small, AT-rich genomes of most intracellular bacteria. Understanding the physiology of *M. leprae*, in particular, may help to distinguish whether the AT mutational bias of most intracellular bacteria is due to a loss of DNA repair functions by genetic drift or to selection for energetic efficiency. This pathogen experiences elevated mutation rates that drive genome deterioration, yet is relatively GC-rich. The hypothesis of adaptive mutational bias would predict that *M. leprae* has access to more energetic resources and competes less severely with its host for nutrients.

Genome Evolution in Endosymbionts: Size Matters

Full genome sequences of endosymbionts have provided new insights into the mechanisms and consequences of genome reduction. Recently published endosymbiont genomes include those of *Buchnera aphidicola* associated with the pea aphid *Acyrthosiphon pisum* (Ap) (Shigenobu *et al.*, 2000), the greenbug *Schizaphis graminum* (Sg) (Tamas *et al.*, 2002), and the gall-forming aphid *Baizongia pistacea* (van Ham *et al.*, 2003); and *Wigglesworthia glossinidia* of the tsetse fly *Glossina brevipalpis* (Akman *et al.*, 2002). Additional endosymbiont genomes, including that of *Blochmannia*, are being sequenced.

Comparative genome analyses illustrate striking parallels between P-endosymbionts of insects and intracellular pathogens. As described previously, pathogens and insect mutualists are characterized by reductive genome evolution, a syndrome that includes severely reduced genome size compared to free-living bacterial relatives, elevated rates of sequence evolution, and low genomic GC contents (Andersson and Kurland, 1998) (Fig. 1). The small chromosome sizes of *Buchnera* (450-650 kb; Charles and Ishikawa, 1999; Wernegreen *et al.*, 2000; Gil *et al.*, 2002) and *Wigglesworthia* (698 kb; Akman *et al.*, 2002) imply substantial gene loss since their divergence from the enteric bacteria (4.5-5.5 Mb genome size range for *E. coli;* Bergthorsson and Ochman, 1995). Because most bacterial genomes contain primarily coding DNA, genome reduction in endosymbionts

---

PHRAP, and CONSED. These 16S rDNA genes of *Blochmannia-C. pennsylvanicus* and *Blochmannia-C festinatus* are assigned GenBank accession numbers AY196850 and AY196851, respectively.

Phylogenetic analysis methods: Alignments were created using the Ribosomal Database Project II sequence aligner (Maidak *et al.*, 2001), then manually edited in MacClade v. 4.05 (Maddison and Maddison, 2002). Maximum likelihood parameters were identified according to the Akaike information criterion (AIC) of Modeltest v. 3.06 (Posada and Crandall, 1998). The most likely model was a general time reversible (GTR) model in which invariant sites and the gamma distribution were estimated from the data. The optimized parameters (Rmat = [0.8676 4.6744 2.0447 1.0516 7.4521], shape of gamma distribution = 0.5500, and proportion of invariant sites = 0.5115) were used for all ML searches. The tree topology presented is the consensus of 100 separate heuristic ML searches, each starting from random trees, using PAUP v. 4.0b10; (Swofford, 2002). ML bootstrap values were determined from 100 bootstrap replicates, with each replicate starting from 10 random trees. Replicates were performed in parallel on a Beowulf cluster using the clusterpaup program (A.G. McArthur, http://jhpc.mbl.edu/mcarthur). Bayesian analysis was performed on the same data matrix (MrBayes ver. 2.01; Huelsenbeck and Ronquist, 2001) by running four simultaneous chains for 300,000 generations, sampling every 100 generations. Stationarity in likelihood scores was determined by plotting the -lnL against the generation. All trees below the observed stationarity level were discarded, resulting in a "burnin" of 5000 generations. The 50% majority-rule consensus tree was determined to calculate the posterior probabilities for each node. The selected model for Bayesian analysis was the GTR, using empirical base frequencies, and estimating the shape of the gamma distribution and proportion of invariant sites from the data. The Bayesian tree with the best likelihood score was identical to the ML tree presented, and the parameter values across this tree were virtually identical to those obtained in the ML analysis.

Limited sequence data (<570 bp of 16S rDNA gene) were available for four taxa included in the phylogeny (*Formica fusca, Plagiolepis pigmaea, Polyrhachis lamellidens* and *Colobopsis nipponicus*), compared to >1202 bp available for the rest of the taxa. Removal of these four taxa from ML or Bayesian analysis did not affect the overall tree topology; however, their removal greatly increased the statistical confidence in the node marked with the open circle. Comparisons of these analyses indicate that including *Plagiolepis pigmaea* drives down the confidence in that node, and suggest ambiguity in its position on the tree. However, given the incomplete sequence for that endosymbiont, this topology is the best estimate of its phylogenetic placement.

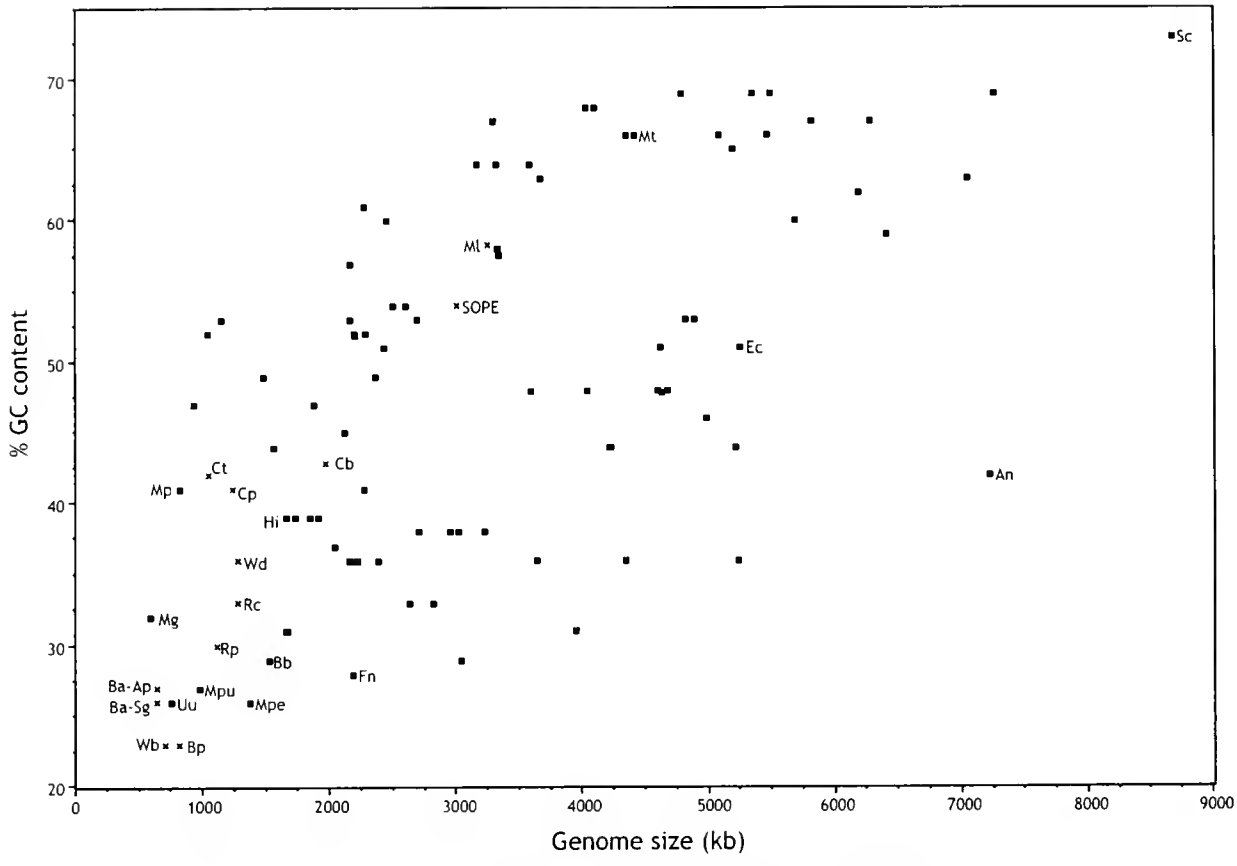

Figure 2. Comparison of genome sizes and %GC contents of select eubacterial genomes. Obligately intracellular bacteria, including pathogens and P-endosymbionts of insects, are marked with x, while facultatively intracellular or extracellular bacteria are marked with ■. Pathogens classified as obligately intracellular in this figure are classified as such on the IslandPath website (http://www.pathogenomics.sfu.ca/islandpath/current/islandpath.html). In certain cases, a close phylogenetic relationship of particular species may contribute to the observed positive relationship between genome size and genomic %GC content. However, since selected species span diverse subdivisions of Proteobacteria, the observed trend cannot be explained by shared phylogenetic history alone. Abbreviations for bacterial species of particular interest for this article are noted as follows: An *Anabaena* spp.; Ba-Sg *Buchnera aphidicola-S. graminum;* Ba-Ap *Buchnera aphidicola-A.pisum;* Bb *Borrelia burgdorferi;* Bp *Blochmannia-C. pennsylvanicus;* Ca *Clostridium acetobutylicum;* Cb *Coxiella burnetii;* Cp *Chlamydia pneumoniae;* Ct *Chlamydia trachomatis;* Ec *Escherichia coli;* Hi *Haemophilus influenzae;* Hp *Helicobacter pylori;* Mg *Mycoplasma genitalium;* Ml *Mycobacterium leprae;* Mp *Mycoplasma pneumoniae;* Mpe *Mycoplasma penetrans;* Mpu *Mycoplasma pulmonis;* Mt *Mycobacterium tuberculosis;* Rc *Rickettsia conorii;* Rp *Rickettsia prowazekii;* SOPE *Sitophylis oryzae* Primary Endosymbiont; Sc *Streptomyces coelicolor;* Uu *Ureaplasma urealyticum;* Wb *Wigglesworthia brevipalpis;* Wd *Wolbachia drosophila.* With the exception of SOPE and *Blochmannia,* all genome sizes and base composition data were obtained from full genome sequence data, summarized in the "DNA Structural Analysis of Sequenced Microbial Genomes" webpage (http://www.cbs.dtu.dk/services/GenomeAtlas/ created by Dr. David Ussery, Center for Biological Sequence Analysis, Technical University of Denmark). Genome size and base composition of SOPE were obtained from a previous study (Charles *et al.,* 1997). The genome size of *Blochmannia* has been estimated at ~809 kb by pulsed-field gel electrophoresis (Wernegreen *et al.,* 2002) and a GC content of 29.7%–31.6% was estimated by buoyant density and melting temperature (Dasch, 1975).

must involve the loss of metabolic functions and may have important, irreversible phenotypic implications (Moran and Wernegreen, 2000; Ochman and Moran, 2001). Strong genetic drift may contribute to this observed genome reduction by increasing the selective coefficient required to maintain a given gene in the genome (Lawrence and Roth, 1999).

Full genome sequences have taught us that obligate pathogens and mutualists retain a disproportionate number of essential genes (*e.g.,* those for cellular processes, translation, and protein fate and transcription), and have lost many genes for metabolic diversity that may be redundant in a nutrient-rich, relatively constant intracellular environment. As described above, the loss of DNA repair functions in these small genomes may contribute to elevated mutation

rates and AT mutational biases in pathogens and mutualists alike (Andersson and Andersson, 1999). The depletion of metabolic capabilities accounts for the inability to culture P-endosymbionts and obligate pathogens apart from a eukaryotic cell, and may constrain the ability of these bacteria to switch among lifestyles (Tamas *et al.*, 2002). For example, a lack of gene acquisition in *Buchnera* implies that this small genome cannot regain critical metabolic functions required for extracellular existence, nor can it acquire virulence loci or novel biosynthetic functions that could mediate new host associations.

In contrast to intracellular pathogens, the fitness of obligate mutualists depends not just upon their own replication and transmission but also on the success of their host. Not surprisingly, despite severe gene loss in most functional categories, endosymbiont genomes show conspicuous signatures of host-level selection and retain specific functions that are important for survival and reproduction of the insect (Zientz *et al.*, 2001). For example, *Wigglesworthia* retains genes encoding the biosynthesis of cofactors, prosthetic groups, and carriers, which is consistent with its known nutritional function for the host (Akman *et al.*, 2002). Likewise, *Buchnera* retains the genetic potential to synthesize practically all essential amino acids (Shigenobu *et al.*, 2000; Tamas *et al.*, 2002; van Ham *et al.*, 2003), as expected from its primary role to supplement the plant sap diet of the host (Sandstrom *et al.*, 2000). Nutrient exchange between *Buchnera* and its aphid host is complementary and mutually dependent (Shigenobu *et al.*, 2000): because it lacks the genes to synthesize them, the symbiont must import nonessential amino acids from the cytoplasm of its host. Another example of genome interdependence is that *Buchnera* can perform the pantothenate-to-pyruvate reaction, but only the host can convert pyruvate to CoA. Thus, while genomes of P-endosymbionts and pathogens show striking parallels, mutualists show reciprocally beneficial integration with host metabolism that is lacking in chronic pathogens.

Bacterial Associates of Ants: Distribution and Possible Functions

Independent origins of symbiosis in the Formicinae

Ants have evolved a wide range of interactions with other species, including plants, fungi, other insects, and as discovered more recently, associations with diverse bacteria (*e.g.*, Dasch *et al.*, 1984; Boursaux-Eude and Gross, 2000; Currie, 2001). These bacterial associates include intracellular endosymbionts, like *Blochmannia*, that live exclusively within ant cells. In contrast to the bacteriocytes of aphids and many other insects, ant cells that house beneficial bacteria are typically located beside or within the midgut epithelium (Dasch *et al.*, 1984). For example, *in situ* analysis shows that *Blochmannia* of *Camponotus* occurs exclusively in ant ovaries, consistent with its maternal transmission, and within bacteriocytes that are intercalated among enterocytes of the ant midgut (Sauer *et al.*, 2002). Phylogenetic analysis (Fig. 1) and a previous study (Sameshima *et al.*, 1999) suggest a single infection of *Blochmannia* prior to the divergence of *Camponotus*, *Colobopsis*, and *Polyrhachis*.

Bacteria related to *Blochmannia* infect the formicid genera *Formica*, in which the presence of symbionts varies among species, and *Plagiolepis*, which is poorly studied to date (reviewed in Dasch *et al.*, 1984). These bacteria can vary in their location within the ant host. In contrast to the endosymbionts of *Blochmannia*, those of *Formica* and *Plagiolepis* are not intercalated among midgut cells, but form symmetrical unicellular layers of bacteriocytes on either side of the midgut epithelium. Unlike the straight rods (1 μM by 5-15 μM) of *Blochmannia*, the *Formica* and *Plagiolepis* endosymbionts are shorter (3-4 μM) and crescent-shaped (Dasch *et al.*, 1984). Consistent with observed differences in bacterial morphologies and location in the host, the *Formica* and *Plagiolepis* endosymbionts are probably the results of independent infections (Fig. 1). The actual abundance, diversity, and origins of endosymbionts in ants remain unknown, since most ant taxa have not been tested for bacterial associates.

Possible functions of endosymbionts in ants: food and pheromones?

The function of even the best-studied ant endosymbiont, *Blochmannia*, remains a mystery. In a thorough study of the distribution of *Blochmannia* within host tissues, *Camponotus* workers were cured of their endosymbionts with no obvious harmful effects to laboratory reared animals (Sauer *et al.*, 2002). The ants' apparent ability to exist without *Blochmannia* raises the question of whether these endosymbionts are required for survival, or whether the presence of the bacteria is a relict from a past mutualism. However, the presence of *Blochmannia* in all *Camponotus* species sampled thus far and the long-term maintenance of this symbiosis suggest an important benefit to the host.

Whether *Blochmannia* plays a dietary role in ants is difficult to answer. It is clear that selection has favored mutualistic endosymbionts in specialized feeders, but *Camponotus* spp. are usually considered omnivorous and are thought to consume a wide assortment of arthropods and plant matter, in addition to homopteran secretions (Dasch *et al.*, 1984; Hölldobler and Wilson, 1990). Certain *Camponotus* species clearly have an unbalanced diet, particularly those species that live in the canopy of tropical rain forests and feed primarily on extrafloral nectar and insect exudates. Stable isotope technologies have determined the nitrogen (N) sources for several ant species in field populations (Davidson, 1997, 1998). Isotope profiles of many arboreal ants, including certain species of *Camponotus* and *Polyrhachis*, resemble those of herbivores (*i.e.*, low delta N) and

may even resemble those of sap-feeding insects (with still lower delta N values) (Davidson, 1997, 1998). The ancestral host of *Blochmannia* might have fed on a similarly restricted diet. However, given the current habitat diversity of its hosts (including live and dead trees and soil, across temperate, desert, and tropical regions), it seems unlikely that diets of all extant *Camponotus, Polyrhachis,* and *Colobopsis* are lacking any single nutrient that *Blochmannia* could provide.

Ant endosymbionts might also play a secondary nutritional role by augmenting an existing metabolic process in the host. For example, SOPE (the aforementioned weevil symbiont and a close relative of *Blochmannia*) has a positive effect on weevil mitochondrial enzymatic activity that results in increased female fertility, decreased larval development time, and longer flight distances (Heddi *et al.,* 1999). If *Blochmannia* had similar effects in ants, these traits would be especially advantageous to young ant queens starting new colonies. Any symbiont-induced increase in energetic efficiency would provide an important selective advantage during colony founding (Dasch, 1975). This stage of the colony life cycle imposes severe intra- and interspecific competition, when the queen must find an appropriate nesting site, raise a small worker force entirely from her own energy reserves, and then rely on this first generation of daughters to establish a viable colony (Hölldobler and Wilson, 1990). The gradual loss of bacteria from older queens (Sauer *et al.,* 2002) suggests that the significance of *Blochmannia* may lie in colony founding and growth rather than in adult maintenance. The fact that *Blochmannia* has been found only in formicine genera with relatively large body sizes (Dasch *et al.,* 1984; Sameshima *et al.,* 1999) deserves further investigation. The larger body size of these genera might reflect a longstanding relationship with a bacterium that increases metabolic efficiency.

In addition, pheromones and hydrocarbons mediate important behaviors ranging from kin recognition to suppression of non-queen egg-laying (Hölldobler and Wilson, 1990). It is possible that *Blochmannia* manufactures a component of these complex organic molecules. Unlike other P-endosymbionts that are sequestered within discrete bacteriocytes in the host body cavity, *Blochmannia* might be able to mediate precursors that it requires directly from the lumen of the gut. The proximity of *Blochmannia* to raw materials could augment pheromone production to any number of the ant's excretory glands. For example, it has been suggested that *Blochmannia* may play some role in producing the pheromones that *Camponotus* uses for food recruitment (Sauer, 2000).

In addition, a potential role of *Blochmannia* in ant reproduction is intriguing, and may involve genetic conflicts in the colony. Research on other maternally transmitted bacteria of insects (*e.g., Wolbachia*) has also illustrated that some endosymbionts can dramatically affect host reproduction, through feminization, male-killing, parthenogenesis, and cytoplasmic incompatibility (O'Neill *et al.,* 1998). All these effects impart a fitness advantage to the bacteria by increasing the number of transmitting hosts (*e.g.,* females) in a population. If *Blochmannia* is similarly involved in manipulating ant reproduction and sex ratios toward females, it would in part share this "preference" with colony workers, who are also favored to manipulate sex ratios owing to relatedness asymmetries under haplodiploid genetics. In a haplodiploid genetic system (diploid females produced from fertilized eggs and haploid males produced from unfertilized eggs), workers are more closely related to their sisters (3/4) than to either their brothers (1/4) or mothers (1/2) (Hölldobler and Wilson, 1990). Workers can therefore increase their inclusive fitness by preferentially caring for sisters or killing male larvae, resulting in an increase in the number of females produced (Sundstrom *et al.,* 1996; Chapuisat *et al.,* 1997; Passera *et al.,* 2001; Hammond *et al.,* 2002). With similar interests in increased female production, *Blochmannia* and workers could be considered allies in their respective genetic conflicts. However, this is speculative, and further research is needed to explore potential links among *Blochmannia,* pheromone production, and sex ratios of the host.

Genome evolution in Blochmannia

To further explore the effects of symbiosis on bacterial genome size and architecture, the genome size of *Blochmannia* was estimated using pulsed-field gel electrophoresis (Wernegreen *et al.,* 2002). Like other P-endosymbionts, *Blochmannia* has a very small genome (~809 kb) that contrasts with the much larger genomes of related enterobacteria. Clearly, *Blochmannia* has deleted most of the genetic machinery of free-living and commensal bacterial species, and consequently depends entirely upon its eukaryotic host. Since *Blochmannia* and other obligate endosymbionts experience restricted gene exchange, this severe gene loss may reflect irreversible specialization to the host cellular environment.

It is difficult to predict the gene content of *Blochmannia* when its functional role in the ant symbiosis is so unclear. However, the gene complements of fully sequenced insect mutualists such as *Wigglesworthia* might provide some hints (Akman *et al.,* 2002). Like *Wigglesworthia, Blochmannia* is probably a relatively young symbiont (~30–40 MY old), has a slightly larger genome size than *Buchnera,* and lives directly within cytoplasm rather than host-derived membranes (Sauer *et al.,* 2000). Therefore, *Blochmannia* may retain certain characteristics of free-living bacteria that have been found in *Wigglesworthia,* such as a robust cell membrane and perhaps a flagellar apparatus (Akman *et al.,* 2002). The strong AT bias of this symbiont might reflect the depletion of DNA repair pathways (Andersson and Anders-

son, 1999). If the *Blochmannia* genome parallels those of other "resident genomes," then one might expect the loss of many genes involved in central cellular pathways such as transcription and protein synthesis, but a more severe depletion of genes for metabolic diversity (Andersson and Kurland, 1998). One key to unraveling the functional role of this bacterium will be to identify host-selected functions. Good candidates for those functions include genes that are preserved in *Blochmannia* but are typically lost in other small bacterial genomes.

Conclusions and Prospects

Among obligate endosymbionts of insects, independent transitions to an intracellular lifestyle have been coupled with elevated rates of evolution, strong AT base compositional bias, and extreme genome reduction. This syndrome of reductive genome evolution parallels the patterns observed in chronic bacterial pathogens, and suggests that similar evolutionary forces operate across intracellular bacteria generally. Full genome sequences of *Buchnera* and *Wigglesworthia* have provided important insights into the evolutionary forces shaping mutualist genomes, including strong effects of mutational bias and genetic drift, but also host-level selection for beneficial traits. Determining the gene inventories of additional endosymbionts will allow comparisons among the diverse strategies by which mutualists specialize to their hosts, and the extent to which mutational pressure and genetic drift may limit their evolutionary potential.

Blochmannia, an obligate bacterial symbiont of ants, shows striking parallels with P-endosymbionts characterized to date, including close specialization with its insect host, reduced genome size compared to free-living relatives, and evidence for mutational bias and genetic drift. However, *Blochmannia* also shows important differences, including its distinct location among midgut-associated cells, and its slightly larger genome size compared to many other P-endosymbionts. The proximity of *Blochmannia* to the ant midgut suggests that the bacteria may provide the host with essential nutrients. However, the relatively complex and diverse diet of *Camponotus* hosts (Hölldobler and Wilson, 1990) contrasts with the strict, unbalanced diets of other insects with bacteriocyte-associated symbionts (*e.g.*, the phloem diet of aphids and other sap-sucking insects, the blood diet of tsetse flies, the grain diet of certain weevils) and suggests that this bacteria has an alternative role. Future genomic studies of *Blochmannia* may inform our understanding of its physiological and ecological significance for the host, which is currently unknown. Genes that are specifically retained in *Blochmannia* will provide promising candidates for host-specific, functionally important loci in this bacterial-ant association and will be the subject of further study.

Acknowledgments

The authors thank Nancy Moran, Jennifer Wilcox, Serap Aksoy, Rita Rio, and Claude Rispe for helpful discussions about endosymbiont evolution and genomics. We are grateful to Diana Davidson, Dan Hahn, and Stefan Cover for sharing their expertise in the nutritional physiology and ecology of ants. We also thank the OGGI Workshop organizers Mitchell Sogin and Diana Jennings, and two anonymous reviewers for their helpful comments on the manuscript. This work was made possible by support to J.J.W. from the NIH (R01 GM62626-01), NSF (DEB 0089455), the Josephine Bay Paul and C. Michael Paul Foundation. C.P. received support from the NASA Astrobiology Institute (NCC2-1054). S.R.B. was supported by a National Research Council Associateship Award.

Literature Cited

Abbot, P., and N. A. Moran. 2002. Extremely low levels of genetic polymorphism in endosymbionts (*Buchnera*) of aphids (*Pemphigus*). *Mol. Ecol.* **11:** 2649–2660.

Akman, L., A. Yamashita, H. Watanabe, K. Oshima, T. Shiba, M. Hattori, and S. Aksoy. 2002. Genome sequence of the endocellular obligate symbiont of tsetse flies, *Wigglesworthia glossinidia*. *Nat. Genet.* **32:** 402–407.

Aksoy, S. 2000. Tsetse—A haven for microorganisms. *Parasitol. Today* **16:** 114–118.

Andersson, J. O., and S. G. Andersson. 1999. Insights into the evolutionary process of genome degradation. *Curr. Opin. Genet. Dev.* **9:** 664–671.

Andersson, S. G., and C. G. Kurland. 1998. Reductive evolution of resident genomes. *Trends Microbiol.* **6:** 263–268.

Baumann, L., M. L. Thao, J. M. Hess, M. W. Johnson, and P. Baumann. 2002. The genetic properties of the primary endosymbionts of mealybugs differ from those of other endosymbionts of plant sap-sucking insects. *Appl. Environ. Microbiol.* **68:** 3198–3205.

Baumann, P., N. A. Moran, and L. Baumann. 2000. Bacteriocyte-associated endosymbionts of insects. In *The Prokaryotes: An Evolving Electronic Resource for the Microbiological Community*, 3rd edition, release 3.1, January 20, 2000. M. Dworkin *et al.*, eds. [www.prokaryotes.com] Springer-Verlag, New York.

Bergthorsson, U., and H. Ochman. 1995. Heterogeneity of genome sizes among natural isolates of *Escherichia coli*. *J. Bacteriol.* **177:** 5784–5789.

Bolton, B. 1995. *Identification Guide to the Ant Genera of the World.* Harvard University Press, Cambridge, MA.

Boursaux-Eude, C., and R. Gross. 2000. New insights into symbiotic associations between ants and bacteria. *Res. Microbiol.* **151:** 513–519.

Brynnel, E. U., C. G. Kurland, N. A. Moran, and S. G. Andersson. 1998. Evolutionary rates for *tuf* genes in endosymbionts of aphids. *Mol. Biol. Evol.* **15:** 574–582.

Buchner, P. 1965. *Endosymbiosis of Animals With Plant Microorganisms.* Interscience Publishers, Inc, New York.

Chapuisat, M., L. Sundstrom, and L. Keller. 1997. Sex-ratio regulation: the economics of fratricide in ants. *Proc. Soc. Lond. B Biol. Sci.* **264:** 1255–1260.

Charles, H., and H. Ishikawa. 1999. Physical and genetic map of the genome of *Buchnera*, the primary endosymbiont of the pea aphid *Acyrthosiphon pisum*. *J. Mol. Evol.* **48:** 142–150.

Charles, H., G. Condemine, C. Nardon, and P. Nardon. 1997. Genome size characterization of the endocellular symbiotic bacteria of the

weevil *Sitophilus oryzae*, using pulse field gel electrophoresis. *Insect Biochem. Mol. Biol.* **27:** 345–350.

Charles, H., A. Heddi, and Y. Rahbe. 2001. A putative insect intracellular endosymbiont stem clade, within the Enterobacteriaceae, inferred from phylogenetic analysis based on a heterogeneous model of DNA evolution. *C.R. Acad. Sci. Ser. III* **324:** 489–494.

Chen, X., S. Li, and S. Aksoy. 1999. Concordant evolution of a symbiont with its host insect species: molecular phylogeny of genus *Glossina* and its bacteriome-associated endosymbiont, *Wigglesworthia glossinidia*. *J. Mol. Evol.* **48:** 49–58.

Clark, M. A., N. A. Moran, and P. Baumann. 1999. Sequence evolution in bacterial endosymbionts having extreme base compositions. *Mol. Biol. Evol.* **16:** 1586–1598.

Clark, M. A., N. A. Moran, P. Baumann, and J. J. Wernegreen. 2000. Cospeciation between bacterial endosymbionts (*Buchnera*) and a recent radiation of aphids (*Uroleucon*) and pitfalls of testing for phylogenetic congruence. *Evolution* **54:** 517–525.

Clark, M. A., L. Baumann, M. L. Thao, N. A. Moran, and P. Baumann. 2001. Degenerative minimalism in the genome of a psyllid endosymbiont. *J. Bacteriol.* **183:** 1853–1861.

Cochoran, D. 1985. Nitrogen excretion in cockroaches. *Annu. Rev. Entomol.* **30:** 29–49.

Cole, S. T., K. Eiglmeier, J. Parkhill, K. D. James, N. R. Thomson, P. R. Wheeler, N. Honore, T. Garnier, C. Churcher, D. Harris, K. Mungall, D. Basham, D. Brown, T. Chillingworth, R. Connor, R.M. Davies, K. Devlin, S. Duthoy, T. Feltwell, A. Fraser, N. Hamlin, S. Holroyd, T. Hornsby, K. Jagels, C. Lacroix, J. Maclean, S. Moule, L. Murphy, K. Oliver, M. A. Quail, M. A. Rajandream, K. M. Rutherford, S. Rutter, K. Seeger, S. Simon, M. Simmonds, J. Skelton, R. Squares, S. Squares, K. Stevens, K. Taylor, S. Whitehead, J. R. Woodward, and B. G. Barrell. 2001. Massive gene decay in the leprosy bacillus. *Nature* **409:** 1007–1011.

Currie, C. R. 2001. A community of ants, fungi, and bacteria: a multilateral approach to studying symbiosis. *Annu. Rev. Microbiol.* **55:** 357–380.

Dasch, G., E. Weiss, and K. Chang. 1984. Endosymbionts of insects. Pp 811–833 in *Bergy's Manual of Systematic Bacteriology*, Vol. 1, J. Holt, and N. Krieg, eds. Williams & Williams, Baltimore.

Dasch, G. A. 1975. Morphological and molecular studies on intracellular bacterial symbiotes of insects. Ph.D. thesis, Yale University, New Haven, CT. 329 pp.

Davidson, D. 1997. The role of resource imbalances in the evolutionary ecology of tropical arboreal ants. *Biol. J. Linn. Soc.* **61:** 153–181.

Davidson, D. 1998. Resource discovery versus resource domination in ants: a functional mechanism for breaking the trade-off. *Ecol. Entomol.* **23:** 484–490.

Douglas, A. 1998. Nutritional interactions in insect-microbial symbioses: aphids and their symbiotic bacteria *Buchnera*. *Annu. Rev. Entomol.* **43:** 17–37.

Douglas, A. E. 1989. Mycetocyte symbiosis in insects. *Biol. Rev. Camb. Philos. Soc.* **64:** 409–434.

Eisen, J. A., and P. C. Hanawalt. 1999. A phylogenomic study of DNA repair genes, proteins, and processes. *Mutat. Res.* **435:** 171–213.

Funk, D. J., L. Helbling, J. J. Wernegreen, and N. A. Moran. 2000. Intraspecific phylogenetic congruence among multiple symbiont genomes. *Proc. R. Soc. Lond. B* **267:** 2517–2521.

Funk, D. J., J. J. Wernegreen, and N. A. Moran. 2001. Intraspecific variation in symbiont genomes: bottlenecks and the aphid-*Buchnera* association. *Genetics* **157:** 477–489.

Gasnier-Fauchet, F., and P. Nardon. 1986. Comparison of methionine metabolism in symbiotic and aposymbiotic larvae of *Sitophilus oryzae* L. (Coleoptera, Curculionidae) II. Involvement of the symbiotic bacteria in the oxidation of methionine. *Comp. Biochem. Physiol.* **85B:** 251–254.

Gil, R., B. Sabater-Munoz, A. Latorre, F. J. Silva, and A. Moya. 2002. Extreme genome reduction in *Buchnera* spp.: toward the minimal genome needed for symbiotic life. *Proc. Natl. Acad. Sci. USA* **99:** 4454–4458.

Goldberg, C., and L. L. Pierre. 1969. Tyrosinase activity of the symbionts and fat bodies of the cockroach, *Leucophaea maderae*. *Can. J. Microbiol.* **15:** 253–255.

Hammond, R. L., M. W. Bruford, and A. F. Bourke. 2002. Ant workers selfishly bias sex ratios by manipulating female development. *Proc. R. Soc. Lond. B Biol. Sci.* **269:** 173–178.

Heddi, A., F. Lefebvre, and P. Nardon. 1991. The influence of symbiosis on the respiratory control ratio (RCR) and the ADP/O ratio in the adult weevil—*Sitophilus oryzae* (Coleoptera, Curculionidae). *Endocytobiosis Cell. Res.* **8:** 61–73.

Heddi, A., H. Charles, C. Khatchadourian, G. Bonnot, and P. Nardon. 1998. Molecular characterization of the principal symbiotic bacteria of the weevil *Sitophilus oryzae:* a peculiar G + C content of an endocytobiotic DNA. *J. Mol. Evol.* **47:** 52–61.

Heddi, A., A. M. Grenier, C. Khatchadourian, H. Charles, and P. Nardon. 1999. Four intracellular genomes direct weevil biology: nuclear, mitochondrial, principal endosymbiont, and *Wolbachia*. *Proc. Natl. Acad. Sci. USA* **96:** 6814-6819.

Hölldobler, B., and E. O. Wilson. 1990. *The Ants.* Belknap Press of Harvard University Press, Cambridge, MA.

Huelsenbeck, J. P., and F. Ronquist. 2001. MRBAYES: Bayesian inference of phylogenetic trees. *Bioinformatics* **17:** 754–755.

Itoh, T., W. Martin, and M. Nei. 2002. Acceleration of genomic evolution caused by enhanced mutation rate in endocellular symbionts. *Proc. Natl. Acad. Sci. USA* **99:** 12944–12948.

Lambert, J. D., and N. A. Moran. 1998. Deleterious mutations destabilize ribosomal RNA in endosymbiotic bacteria. *Proc. Natl. Acad. Sci. USA* **95:** 4458–4462.

Lawrence, J., and J. Roth. 1999. Genomic flux: genome evolution by gene loss and acquisition. Pp. 263–289 in *Organization of the Prokaryotic Genome*, R. Charlesbois, ed. ASM Press, Washington, DC.

Maddison, D. R., and W. P. Maddison. 2002. *MacClade* 4: *Analysis of Phylogeny and Character Evolution.* Sinauer Associates, Sunderland, MA.

Maidak, B. L., J. R. Cole, T. G. Lilburn, C. T. Parker, Jr., P. R. Saxman, R. J. Farris, G. M. Garrity, G. J. Olsen, T. M. Schmidt, and J. M. Tiedje. 2001. The RDP-II (Ribosomal Database Project). *Nucleic Acids Res.* **29:** 173–174.

McLean, D., and E. Houk. 1973. Phase contrast and electron microscopy of the mycetocytes and symbionts of the pea aphid *Acyrthosiphon pisum*. *J. Insect Physiol.* **19:** 625–633.

Mira, A., and N. A. Moran. 2002. Estimating population size and transmission bottlenecks in maternally transmitted endosymbiotic bacteria. *Microb. Ecol.* **44:** 137–143.

Moran, N., and A. Telang. 1998. Bacteriocyte-associated symbionts of insects. *Bioscience* **48:** 295–304.

Moran, N. A. 1996. Accelerated evolution and Muller's ratchet in endosymbiotic bacteria. *Proc. Natl. Acad. Sci. USA* **93:** 2873–2878.

Moran, N. A., and P. Baumann. 2000. Bacterial endosymbionts in animals. *Curr. Opin. Microbiol.* **3:** 270–275.

Moran, N. A., and J. J. Wernegreen. 2000. Lifestyle evolution in symbiotic bacteria: insights from genomics. *Trends Ecol. Evol.* **15:** 321-326.

Muller, J. 1964. The relation of recombination to mutational advance. *Mutat. Res.* **1:** 2–9.

Munson, M. A., P. Baumann, M. A. Clark, L. Baumann, N. A. Moran, D. J. Voegtlin, and B. C. Campbell. 1991. Evidence for the establishment of aphid-eubacterium endosymbiosis in an ancestor of four aphid families. *J. Bacteriol.* **173:** 6321–6324.

Nardon, P., and A. Grenier. 1991. Serial endosymbiosis theory and

weevil evolution: the role of symbiosis. Pp. 154–169 in *Symbiosis as a Source of Evolutionary Innovation*, L. Margulis, and R. Fester, eds. MIT Press, Cambridge, MA.

Nogge, G. 1981. Significance of symbionts for the maintenance of an optimal nutritional state for successful reproduction in hematophagous arthropods. *Parasitology* **82:** 299–304.

O'Neill, S., A. Hoffman, and J. Werren. 1998. *Influential Passengers: Inherited Microorganisms and Arthropod Reproduction*. Oxford University Press, Oxford.

Ochman, H., and N. A. Moran. 2001. Genes lost and genes found: evolution of bacterial pathogenesis and symbiosis. *Science* **292:** 1096–1099.

Ohta, T. 1973. Slightly deleterious mutant substitutions in evolution. *Nature* **246:** 96–98.

Palacios, C., and J. J. Wernegreen. 2002. A strong effect of AT mutational bias on amino acid usage in *Buchnera* is mitigated at high expression genes. *Mol. Biol. Evol.* **19:** 1575–1584.

Passera, L., S. Aron, E. L. Vargo, and L. Keller. 2001. Queen control of sex ratio in fire ants. *Science* **293:** 1308–1310.

Posada, D., and K. A. Crandall. 1998. MODELTEST: testing the model of DNA substitution. *Bioinformatics* **14:** 817-818.

Rispe, C., and N. A. Moran. 2000. Accumulation of deleterious mutations in endosymbionts: Muller's ratchet with two levels of selection. *Am. Nat.* **156:** 424–441.

Rocha, E. P., and A. Danchin. 2002. Base composition bias might result from competition for metabolic resources. *Trends Genet.* **18:** 291–294.

Sameshima, S., E. Hasegawa, O. Kitade, N. Minaka, and T. Matsumoto. 1999. Phylogenetic comparison of endosymbionts with their host ants based on molecular evidence. *Zool. Sci.* **16:** 993–1000.

Sandstrom, J., A. Telang, and N. A. Moran. 2000. Nutritional enhancement of host plants by aphids—a comparison of three aphid species on grasses. *J. Insect Physiol.* **46:** 33–40.

Sauer, C. 2000. Charakterisierung intrazellulärer, bakterieller Endosymbionten im Mitteldarm von Ameisen der Gattung *Camponatus*. Ph. D. thesis, Universität Würzburg, Würzburg, Germany. 112 pp.

Sauer, C., E. Stackebrandt, J. Gadau, B. Hölldobler, and R. Gross. 2000. Systematic relationships and cospeciation of bacterial endosymbionts and their carpenter ant host species: proposal of the new taxon *Candidatus* Blochmannia gen. nov. *Int. J. Syst. Evol. Microbiol.* **50 Pt 5:** 1877–1886.

Sauer, C., D. Dudaczek, B. Hölldobler, and R. Gross. 2002. Tissue localization of the endosymbiotic bacterium "*Candidatus* Blochmannia floridanus" in adults and larvae of the carpenter ant *Camponatus floridanus*. *Appl. Environ. Microbiol.* **68:** 4187–4193.

Schroder, D., H. Deppisch, M. Obermayer, G. Krohne, E. Stackebrandt, B. Hölldobler, W. Goebel, and R. Gross. 1996. Intracellular endosymbiotic bacteria of *Camponotus* species (carpenter ants): systematics, evolution and ultrastructural characterization. *Mol. Microbiol.* **21:** 479–489.

Selander, R. K., D. A. Caugant, and T. S. Whittam. 1987. Genetic structure and variation in natural populations of *Escherichia coli*. Pp. 1625–1648 in Escherichia coli *and* Salmonella typhimurium: *Cellular and Molecular Biology*, F. Neidhardt, ed. American Society for Microbiology, Washington, DC.

Shigenobu, S., H. Watanabe, M. Hattori, Y. Sakaki, and H. Ishikawa. 2000. Genome sequence of the endocellular bacterial symbiont of aphids *Buchnera* sp. APS. *Nature* **407:** 81–86.

Spaulding, A., and C. D. von Dohlen. 1998. Phylogenetic characterization and molecular evolution of bacterial endosymbionts in psyllids (Hemiptera:Sternorrhyncha). *Mol. Biol. Evol.* **15:** 1506–1513.

Sundstrom, L., M. Chapuisat, and L. Keller. 1996. Conditional manipulation of sex ratios by ant workers: a test of kin selection theory. *Science* **274:** 993–995.

Swofford, D. L. 2002. *PAUP* Phylogenetic Analysis Using Parsimony (*and Other Methods)*. Version 4. Sinauer Associates, Sunderland, MA.

Tamas, I., L. Klasson, B. Canback, A. K. Naslund, A. S. Eriksson, J. J. Wernegreen, J. P. Sandstrom, N. A. Moran, and S. G. Andersson. 2002. 50 million years of genomic stasis in endosymbiotic bacteria. *Science* **296:** 2376-2379.

Thao, M. L., N. A. Moran, P. Abbot, E. B. Brennan, D. H. Burckhardt, and P. Baumann. 2000. Cospeciation of psyllids and their primary prokaryotic endosymbionts. *Appl. Environ. Microbiol.* **66:** 2898–2905.

van Ham, R. C., J. Kamerbeek, C. Palacios, C. Rausell, F. Abascal, U. Bastolla, J. M. Fernandez, L. Jimenez, M. Postigo, F. J. Silva, J. Tamames, E. Viguera, A. Latorre, A. Valencia, F. Moran, and A. Moya. 2003. Reductive genome evolution in *Buchnera aphidicola*. *Proc. Natl. Acad. Sci. USA* **100:** 581–586.

Wernegreen, J. J., and N. A. Moran. 1999. Evidence for genetic drift in endosymbionts (*Buchnera*): analyses of protein-coding genes. *Mol. Biol. Evol.* **16:** 83–97.

Wernegreen, J. J., and N. A. Moran. 2000. Decay of mutualistic potential in aphid endosymbionts through silencing of biosynthetic loci: *Buchnera* of *Diuraphis*. *Proc. R. Soc. Lond. B Biol. Sci.* **267:** 1423–1431.

Wernegreen, J. J., and N. A. Moran. 2001. Vertical transmission of biosynthetic plasmids in aphid endosymbionts (*Buchnera*). *J. Bacteriol.* **183:** 785–790.

Wernegreen, J. J., H. Ochman, I. B. Jones, and N. A. Moran. 2000. Decoupling of genome size and sequence divergence in a symbiotic bacterium. *J. Bacteriol.* **182:** 3867–3869.

Wernegreen, J. J., A. B. Lazarus, and P. H. Degnan. 2002. Small genome of *Candidatus* Blochmannia, the bacterial endosymbiont of *Camponotus*, implies irreversible specialization to an intracellular lifestyle. *Microbiology* **148:** 2551–2556.

Wicker, C., and P. Nardon. 1982. Development responses of symbiotic and aposymbiotic weevils *Sitophilus oryzae* L. (Coleoptera, Curculionidae) to a diet supplemented with aromatic amino acids. *J. Insect Physiol.* **28:** 1021–1024.

Wilson, E. O. 1985. Invasion and extinction in the west Indian ant fauna: evidence from the Dominican Amber. *Science* **229:** 265–267.

Zientz, E., F. J. Silva, and R. Gross. 2001. Genome interdependence in insect-bacterium symbioses. *Genome Biol.* **2:** Reviews 1032.

Reference: *Biol. Bull.* **204:** 232–235. (April 2003)

Participants

Amaral Zettler, Linda
Bay Paul Center for Comparative Molecular Biology and Evolution
Marine Biological Laboratory
7 MBL Street, L-313
Woods Hole, MA 02543
tel: 508/289/7393
fax: 508/457/2169
e-mail: amaral@evol5.mbl.edu

Beaudoin, David
Bay Paul Center for Comparative Molecular Biology and Evolution
Marine Biological Laboratory
7 MBL Street, L-332a
Woods Hole, MA 02543
tel: 508/289/7291
fax: 508/457/2169
e-mail: beaudoin@evol5.mbl.edu

Bebout, Brad
NASA/Ames Research Center
Mailstop 239-4
Moffett Field, CA 94035-1000
tel: 650/604/3227
fax: 650/604/1088
e-mail: bbebout@mail.arc.nasa.gov

Bonfante, Paola
Plant Biology Department
dell'Universita Centro di Studio sulla Micologia del Terreno del CNR
Viale Mattioli 25
10125 Torini, Italy
tel: +39 011 650 2927
fax: +39 011 670 7459
e-mail: p.bonfante@csmt.to.cnr.it

Crookes, Wendy
Pacific Biomedical Research Center
University of Hawaii—Manoa
41 Ahui Street
Honolulu, HI 96813
tel: 808/539/7321
fax: 808/59/4817

Crump, Byron
The Ecosystems Center
Marine Biological Laboratory
7 MBL Street, SB-319
Woods Hole, MA 02543
tel: 508/289/7695
e-mail: bcrump@mbl.edu

Degnan, Patrick
Bay Paul Center for Comparative Molecular Biology and Evolution
Marine Biological Laboratory
7 MBL Street, L-311
Woods Hole, MA 02543
tel: 508/289/3705
fax: 508/457/4727
e-mail: pdegnan@mbl.edu

Des Marais, David J.
NASA/Ames Research Center
Mail Stop 239-4
Moffett Field, CA 94035-1000
tel: 650/604/3220
fax: 650/604/1088
e-mail: ddesmarais@mail.arc.nasa.gov

Dhillon, Ashita
Bay Paul Center for Comparative Molecular Biology and Evolution
Marine Biological Laboratory
7 MBL Street, L-311
Woods Hole, MA 02543
tel: 508/289/6654
fax: 508/457/4727
e-mail: ashita@evol5.mbl.edu

Dillon, Jesse
Depts of Microbiology/Civil and Environmental Engineering
University of Washington
Box 352700, 168 Wilcox
Seattle, WA 98195
tel: 206/685/3493
fax: 206/685/3836
e-mail: jdillon@u.washington.edu

EDGCOMB, VIRGINIA P.
Biology Department
Woods Hole Oceanographic Institution
MS #33, Redfield 2
Woods Hole, MA 02543
tel: 508/289/3734
e-mail: vedgcomb@whoi.edu

EDWARDS, KATRINA
Department of Marine Chemistry and Geochemistry
Woods Hole Oceanographic Institution
McLean Lab 203
MS #8
Woods Hole, MA 02543
tel: 508/289/3620
fax: 508/457/2183
e-mail: kedwards@whoi.edu

FUHRMAN, JED A.
Department of Biological Sciences
University of Southern California
MC 0371
Los Angeles, CA 90089-0371
tel: 213/740/5757
fax: 213/740/8123
e-mail: fuhrman@usc.edu

GAST, REBECCA J.
Woods Hole Oceanographic Institution
Biology Department
Redfield Building
MS #32
Woods Hole, MA 02543
tel: 508/289/3209
fax: 508/457/2169
e-mail: rgast@whoi.edu

GONZALEZ-ACINAS, SILVIA
Massachusetts Institute of Technology
77 Massachusetts Avenue, Room 48-421
Cambridge, MA 02139
tel: 617/253/7128
fax: 617/258/8850
e-mail: sacinas@mit.edu

HOBBIE, JOHN E.
The Ecosystems Center
Marine Biological Laboratory
7 MBL Street, SB-223
Woods Hole, MA 02543
tel: 508/289/7470
e-mail: jhobbie@mbl.edu

HOPKINSON, CHARLES
The Ecosystems Center
Marine Biological Laboratory
7 MBL Street, SB-337
Woods Hole, MA 02543
tel: 508/289/7688
e-mail: chopkins@mbl.edu

JENNINGS, DIANA
Marine Biological Laboratory—CASSLS
7 MBL Street
Woods Hole, MA 02543
tel: 508/289/7535
fax: 508/289/7951
e-mail: djennings@mbl.ed

KOLENBRANDER, PAUL E.
National Institutes of Health/NIDCR
Building 30, Room 310
30 Convent Drive MSC 4350
Bethesda, MD 20892-4350
tel: 301/496/1497
fax: 301/402/0396
e-mail: pkolenbrander@dir.nidcr.nih.gov

LAATSCH, ABBY
Bay Paul Center for Comparative Molecular Biology and Evolution
Marine Biological Laboratory
7 MBL Street
Woods Hole, MA 02543
tel: 508/289/7259
fax: 508/457/4727
e-mail: laatsch@evol5.mbl.edu

LEY, RUTH E.
Department of Molecular, Cellular and Developmental Biology
University of Colorado—Boulder
334 UCB
Boulder, CO 80309-0334
tel: 303/492/2557
fax: 303/492/7744
e-mail: ruth.ley@colorado.edu

MACELROY, ROBERT D.
NASA Ames Research Center
MS 19-20
Moffett Field, CA 94035
tel: 650/604/5573
e-mail: rmacelroy@mail.arc.nasa.gov

McFall-Ngai, Margaret
Pacific Biomedical Research Center
University of Hawaii—Manoa
41 Ahui Street
Honolulu, HI 96813
tel: 808/539/7310
fax: 808/59/4817
e-mail: mcfallng@hawaii.edu

Mills, Aaron L.
NASA affiliation—John F. Kennedy Space Center
Department of Biological Research
Department of Environmental Sciences
University of Virginia
P.O. Box 400123
Charlottesville, VA 22904-4123
tel: 434/924/0564
fax: 434/982/2137
e-mail: amills@virginia.edu

Moran, Nancy A.
Department of Ecology and Evolutionary Biology
University of Arizona
BSW 310
Tucson, AZ 85721
tel: 520/621/3581
fax: 520/621/9190
e-mail: nmoran@u.arizona.edu

Palacios, Carmen
Bay Paul Center for Comparative Molecular Biology and Evolution
Marine Biological Laboratory
7 MBL Street, L-311
Woods Hole, MA 02543
tel: 508/289/7339
fax: 508/457/4727
e-mail: palacios@mbl.edu

Palmer, Robert J., Jr.
National Institutes of Health/NIDCR
Building 30, Room 308
30 Convent Drive MSC 4350
Bethesda, MD 20892-4350
tel: 301/496/2088
fax: 301/402/0396
e-mail: rp169u@nih.gov

Polz, Martin
Massachusetts Institute of Technology
Room 48-421
77 Massachusetts Avenue
Cambridge, MA 02139
tel: 617/253/7128
fax: 617/258/8850
e-mail: mpolz@mit.edu

Rogers, Daniel
Woods Hole Oceanographic Institution
Marine Chemistry and Geochemistry Department
McLean Lab 203
MS #8
Woods Hole, MA 02543
tel: 508/289/3620
fax: 508/457/2183
e-mail: drogers@whoi.edu

Schmidt, Thomas M.
Department of Microbiology and Molecular Genetics
Michigan State University
202 Giltner Hall
East Lansing, MI 48824-1101
tel: 517/353/1796
fax: 517/353/8957
e-mail: tschmidt@msu.edu

Schwalbach, Michael
Department of Marine Environmental Biology
University of Southern California
MC 0371
Los Angeles, CA 90089-0371
tel: 213/740/5759
fax: 213/740/8123
e-mail: schwalba@usc.edu

Sogin, Mitchell L.
Bay Paul Center for Comparative Molecular Biology and Evolution
Marine Biological Laboratory
7 MBL Street, L-301
Woods Hole, MA 02543
tel: 508/289/7393
fax: 508/289/4727
e-mail: sogin@evol5.mbl.edu

Spear, John R.
Department of Biology—MCD Instruction
University of Colorado at Boulder
347 UCB
Boulder, CO 80309-0347
tel: 303/735/1808
fax: 303/492/7744
e-mail: spearj@colorado.edu

Stahl, David A.
Department of Civil and Environmental Engineering
University of Washington
302 More Hall, Box 352700
Seattle, WA 98195-2700
tel: 206/685/3464
fax: 206/685/9185
e-mail: dastahl@u.washington.edu

Stevenson, Bradley
Department of Microbiology and Molecular Genetics
Michigan State University
203 Giltner Hall
East Lansing, MI 48824-1101
tel: 517/432/1140
fax: 517/353/8957
e-mail: steven77@msu.edu

Teske, Andreas
Biology Department
Woods Hole Oceanographic Institution
Redfield Lab 2-40
MS #33
Woods Hole, MA 02543
tel: 508/289/2305
fax: 508/457/2134
e-mail: ateske@whoi.edu

Vallino, Joseph
The Ecosystems Center
Marine Biological Laboratory
7 MBL Street, SB-330
Woods Hole, MA 02543
tel: 508/289/7648
e-mail: jvallino@mbl.edu

Welch, David Mark
Bay Paul Center for Comparative Molecular Biology and Evolution
Marine Biological Laboratory
7 MBL Street, L-313
Woods Hole, MA 02543
tel: 508/289/6657
e-mail: dmarkwelch@evol5.mbl.edu

Wernegreen, Jennifer
Bay Paul Center for Comparative Molecular Biology and Evolution
Marine Biological Laboratory
7 MBL Street, L-304
Woods Hole, MA 02543
tel: 508/289/7750
fax: 457/4727
e-mail: jwernegreen@mbl.edu

Wilcox, Jennifer L.
Department of Ecology and Evolutionary Biology
University of Arizona
P.O. Box 210088
BSW 310
Tucson, AZ 85721
tel: 520/621/1588
fax: 520/621/9190
e-mail: wilcoxjl@e-mail.arizona.edu

THE BIOLOGICAL BULLETIN

2003 Subscription Rates
Volumes 204-205

***Paid Subscriptions include both print and electronic subscriptions at:** www.biolbull.org

	Institutional*	Individual*
One year subscription (6 issues - 2 volumes)	$280.00	$105.00
Single volume (3 issues)	$140.00	$52.50
Single Issues	$ 50.00	$20.00

*Surface delivery included in above prices.
For prompt delivery, we encourage subscribers outside the U.S. to request airmail service.

Airmail Delivery Charge

U.S. and Canada:	$ 25.00
Mexico:	$ 60.00
All other locations:	$100.00

Orders Must Be Prepaid in U.S. Dollars, Check Payable to The Marine Biological Laboratory

About *The Biological Bulletin*
ISSN: 0006-3185
Frequency: Bimonthly
Number of issues per year: 6
Months of Publication: February, April, June, August, October, December
Subscriptions entered for calendar year
Volume indexes contained in June and December issues
Annual report of the Marine Biological Laboratory contained in August issue
Most back issues available
Claims handled upon receipt
No agency discounts
Internet:
www.biolbull.org

Please address orders to:
Wendy Child
Subscription Administrator
The Biological Bulletin
Marine Biological Laboratory
7 MBL Street
Woods Hole, MA 02543-1015 U.S.A.
Fax: 508-289-7922 Tel: 508-289-7402 Email: wchild@mbl.edu

Published by the Marine Biological Laboratory
Woods Hole, Massachusetts, 02543 U.S.A.

THE BIOLOGICAL BULLETIN
(www.biolbull.org)
2003 SUBSCRIPTION FORM
(VOLUMES 204-205, 6 ISSUES)

All subscriptions run on the calendar year; price includes both print and online journals.

(please print)

NAME: _____

INSTITUTION: _____

ADDRESS: _____

CITY: _____ STATE: _____

POSTAL CODE: _____ COUNTRY: _____

TELEPHONE: _____ FAX: _____

E-MAIL ADDRESS: _____

❒ **Please send me a 2003 subscription to *The Biological Bulletin* at the rate indicated below:**

❒ Individual: $105.00 (6 ISSUES) ❒ Institutional: $280.00 (6 ISSUES)
❒ Individual: $ 52.50 (3 ISSUES) ❒ Institutional: $140.00 (3 ISSUES)
Check one: ❒ February, April, June or ❒ August, October, December

❒ **Please send me the following back issue(s):** _____

❒ Individual: at $20.00 (PER ISSUE) ❒ Institutional: at $50.00 (PER ISSUE)

Delivery Options

_____ Surface Delivery (Surface delivery is included in the subscription price.)

_____ Air delivery (Please add the correct amount to your payment.)

❒ U.S. and Canada: $25.00 ❒ Mexico: $60.00 ❒ All other locations: $100.00

Payment Options

_____ Enclosed is my check or U.S. money order for $ _____ payable to The Marine Biological Laboratory

_____ Please send me an invoice. (Note: Payment must be received before subscription commences.)

_____ Please charge my ❒ VISA, ❒ MasterCard ❒ Discover Card $_____

Account No.: _____ Exp. Date: _____

Signature: _____ Date: _____

Return this form with your check or credit card information to:

Marine Biological Laboratory
Subscription Office ◆ The Biological Bulletin ◆7 MBL Street ◆ Woods Hole, MA 02543-1015

Marine Resources Center

MARINE BIOLOGICAL LABORATORY • WOODS HOLE, MA 02543 • (508)289-7700
WWW.MBL.EDU/SERVICES/MRC/INDEX.HTML

zebrafish facilities

Animal and Tissue Supply for Education & Research

- 150 aquatic species available for shipment via online catalog: <http://www.mbl.edu/animals/index.html>; phone: (508)289-7375; or e-mail: specimens@mbl.edu
- zebrafish colony containing limited mutant strains
- custom dissection and furnishing of specific organ and tissue samples

MRC Services Available

- basic water quality analysis
- veterinary services (clinical, histopathologic, microbial services, health certificates, etc.)
- aquatic systems design (mechanical, biological, engineering, etc.)
- educational tours and collecting trips aboard the R/V Gemma

Using the MRC for Your Research

- capability for advanced animal husbandry (temperature, light control, etc.)
- availability of year-round, developmental life stages
- adaptability of tank system design for live marine animal experimentation

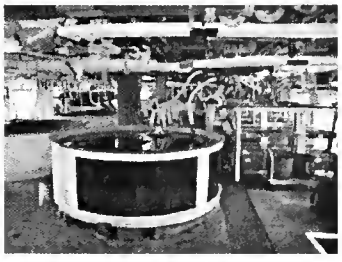

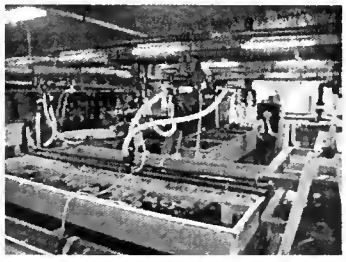

June 2003 Volume 204 • Number 3

THE BIOLOGICAL BULLETIN

Published by the Marine Biological Laboratory

www.biolbull.org

Cover

Sea star larvae in field collections of plankton from tropical and subtropical areas of the Atlantic Ocean are often observed to reproduce asexually. In this process, called larval cloning, a sequestered region of larval tissue (*e.g.*, part of the pre-oral lobe, an arm, or a bud) dedifferentiates, then redifferentiates, and the clone—either a secondary embryo or a larva—is released.[1]

The cover depicts a right lateral view of a bipinnaria larva of *Luidia* sp. (~2.75 mm in length), which was collected from surface waters (~30 m depth) in the Gulf Stream, offshore from Fort Pierce on the east coast of Florida. The larva bears, on its lower right side, a spherical white object—an attached clone developing from a modified posteriolateral larval arm. Though only one is seen here, this type of larva can produce clones from both posteriolateral arms. Each clone will eventually detach from the "parent," becoming an independent larva. The remaining "sickle-shaped," non-cloning larval arms function in feeding and locomotion. The two arms at the upper left extend from the pre-oral lobe, and the mouth is visible toward the right side of the image between the two non-cloning arms. The yellow esophagus (from whence the common name, "golden-throat larva") connects the mouth to the red stomach and tubular intestine. The bright yellow tissue surrounding the digestive system is part of the developing juvenile sea star.

Larval cloning introduces further complexity into the already diverse array of reproductive modes observed in sea stars. Increasing the number of larvae and juveniles produced by a single adult and the duration of an individual's planktonic life may be among the adaptive roles of cloning, thus increasing dispersal capacity and facilitating genetic communication between distant populations and, possibly, transoceanic transport. Sea star larvae are morphologically similar, so field-collected individuals are often difficult to classify on the basis of structure—even to family. This difficulty has been a barrier to further study of larval cloning. But in this issue of *The Biological Bulletin* (p. 246), K. Emily Knott and her colleagues describe experiments done in the laboratory of Gregory A. Wray that lower the barrier. In brief, by comparing gene sequences from individual field-collected larvae with complementary reference sequences from adults of many different species, cloning larvae can now be identified to genus.

The cloning larva displayed on the cover was collected and photographed by Elizabeth J. Balser, and she and William B. Jaeckle drafted the legend. The cover was designed by Beth Liles (Marine Biological Laboratory).

[1] **Jaeckle, W. B. 1994.** Multiple modes of asexual reproduction by tropical and subtropical sea star larvae: an unusual adaptation for genet dispersal and survival. *Biol. Bull.* **186:** 62–71.

THE
BIOLOGICAL BULLETIN
JUNE 2003

Published by
Marine Biological Laboratory
Woods Hole, Massachusetts

http://www.biolbull.org

Cool. Fast. Reliable.

Launch a Microway® Linux cluster and solve your problems in life sciences, structure design, weather, astronomy . . .

Run cool. Microway's **CoolFlow**™ 1U chassis is designed to provide the best cooling in the industry. Low temperatures result in higher CPU and memory reliability, plus longer cluster life.

Take control. Monitor *and* control your cluster remotely via our secure web-based GUI. Microway's **NodeWatch**™ hardware and **MCMS**™ cluster management software report on temperatures, voltages, and chassis fans, and let you set thresholds for notification and/or failsafe shutdown if problems occur.

Today's HPC market is wilder than ever. Microway's expert design team will guide you through the whitewater of hardware, software, and storage solutions. Our clusters are competitively priced and delivered on time—and their proven reliability yields low total lifetime cost. What's more, our tech support is legendary.

Call us to test drive **NodeWatch**™ online, arrange a benchmark, and discuss your next Linux cluster with people who speak your language. Visit our website for *HPC Times* technical news.

CoolRak™ Cabinet
Features Xeon XBlade™
Technology

- 1.056 Teraflops per 44U cabinet running 3.06 GHz Xeons
- NodeWatch™ remote control and monitoring
- CoolFlow™ proprietary 1U and 4U chassis
- Myrinet, GigE, or InfiniBand™ connectivity

GSA# GS-35F-0431N

Microway

Scientists have been counting on us for over 20 years.℠

508.746.7341 • www.microway.com

CONTENTS

VOLUME 204, NO. 3: JUNE 2003

THE BIOLOGICAL BULLETIN

THE BIOLOGICAL BULLETIN is published six times a year by the Marine Biological Laboratory, 7 MBL Street, Woods Hole, Massachusetts 02543.

Subscriptions and similar matter should be addressed to Subscription Administrator, THE BIOLOGICAL BULLETIN, Marine Biological Laboratory, 7 MBL Street, Woods Hole, Massachusetts 02543. Subscription includes both print and online journals. Subscription per year (six issues, two volumes): $280 for libraries; $105 for individuals. Subscription per volume (three issues): $140 for libraries; $52.50 for individuals. Back and single issues (subject to availability): $50 for libraries; $20 for individuals.

Communications relative to manuscripts should be sent to Michael J. Greenberg, Editor-in-Chief, or Pamela Clapp Hinkle, Managing Editor, at the Marine Biological Laboratory, 7 MBL Street, Woods Hole, Massachusetts 02543. Telephone: (508) 289-7149. FAX: 508-289-7922. E-mail: pclapp@mbl.edu.

http://www.biolbull.org

THE BIOLOGICAL BULLETIN is indexed in bibliographic services including *Index Medicus* and MEDLINE, *Chemical Abstracts, Current Contents, Elsevier BIOBASE/Current Awareness in Biological Sciences,* and Geo *Abstracts.*

Printed on acid free paper,
effective with Volume 180, Issue 1, 1991.

POSTMASTER: Send address changes to THE BIOLOGICAL BULLETIN, Marine Biological Laboratory, 7 MBL Street, Woods Hole, MA 02543.

Periodicals postage paid at Woods Hole, MA, and additional mailing offices.
ISSN 0006-3185

INSTRUCTIONS TO AUTHORS

The Biological Bulletin accepts outstanding original research reports of general interest to biologists throughout the world. Papers are usually of intermediate length (10–40 manuscript pages). A limited number of solicited review papers may be accepted after formal review. A paper will usually appear within four months after its acceptance.

Very short, especially topical papers (less than 9 manuscript pages including tables, figures, and bibliography) will be published in a separate section entitled "Research Notes." A Research Note in *The Biological Bulletin* follows the format of similar notes in *Nature.* It should open with a summary paragraph of 150 to 200 words comprising the introduction and the conclusions. The rest of the text should continue on without subheadings, and there should be no more than 30 references. References should be referred to in the text by number, and listed in the Literature Cited section in the order that they appear in the text. Unlike references in *Nature,* references in the Research Notes section should conform in punctuation and arrangement to the style of recent issues of *The Biological Bulletin.* Materials and Methods should be incorporated into appropriate figure legends. See the article by Lohmann *et al.* (October 1990, Vol. **179:** 214–218) for sample style. A Research Note will usually appear within two months after its acceptance.

The Editorial Board requests that regular manuscripts conform to the requirements set below; those manuscripts that do not conform will be returned to authors for correction before review.

1. ***Manuscripts.*** Manuscripts, including figures, should be submitted in quadruplicate, with the originals clearly marked. (Xerox copies of photographs are not acceptable for review purposes.) If possible, please include an electronic copy of the text of the manuscript. Label the disk with the name of the first author and the name and version of the wordprocessing software used to create the file. If the file was not created in some version of Microsoft Word, save the text in rich text format (rtf). The submission letter accompanying the manuscript should include a telephone number, a FAX number, and (if possible) an E-mail address for the corresponding author. The original manuscript must be typed in no smaller than 12 pitch or 10 point, using double spacing (*including* figure legends, footnotes, bibliography, etc.) on one side of 16- or 20-lb. bond paper, 8 by 11 inches. Please, no right justification. Manuscripts should be proofread carefully and errors corrected legibly in black ink. Pages should be numbered consecutively. Margins on all sides should be at least 1 inch (2.5 cm). Manuscripts should conform to the *Council of Biology Editors Style Manual,* 5th Edition (Council of Biology Editors, 1983) and to American spelling. Unusual abbreviations should be kept to a minimum and should be spelled out on first reference as well as defined in a footnote on the title page. Manuscripts should be divided into the following components: Title page, Abstract (of no more than 200 words), Introduction, Materials and Methods, Results, Discussion, Acknowledgments, Literature Cited, Tables, and Figure Legends. In addition, authors should supply a list of words and phrases under which the article should be indexed.

2. ***Title page.*** The title page consists of a condensed title or running head of no more than 35 letters and spaces, the manuscript title, authors' names and appropriate addresses, and footnotes listing present addresses, acknowledgments or contribution numbers, and explanation of unusual abbreviations.

3. ***Figures.*** The dimensions of the printed page, 7 by 9 inches, should be kept in mind in preparing figures for publication. We recommend that figures be about 1 times the linear dimensions of the final printing desired, and that the ratio of the largest to the smallest letter or number and of the thickest to the thinnest line not exceed 1:1.5. Explanatory matter generally should be included in legends, although axes should always be identified on the illustration itself. Figures should be prepared for reproduction as either line cuts or halftones. Figures to be reproduced as line cuts should be unmounted glossy photographic reproductions or drawn in black ink on white paper, good-quality tracing cloth or plastic, or blue-lined coordinate paper. Those to be reproduced as halftones should be mounted on board, with both designating numbers or letters and scale bars affixed directly to the figures. All figures should be numbered in consecutive order, with no distinction between text and plate figures and cited, in order, in the text. The author's name and an arrow indicating orientation should appear on the reverse side of all figures.

Digital art: The Biological Bulletin will accept figures submitted in electronic form; however, digital art must conform to the following guidelines. Authors who create digital images are wholly responsible for the quality of their material, including color and halftone accuracy.

Format. Acceptable graphic formats are TIFF and EPS. Color submissions must be in EPS format, saved in CMKY mode.

Software. Preferred software is Adobe Illustrator or Adobe Photoshop for the Mac and Adobe Photoshop for Windows. Specific instructions for artwork created with various software programs are available on the Web at the Digital Art Information Site maintained by Cadmus Professional Communications at http://cpc.cadmus.com/da/

Resolution. The minimum requirements for resolution are 1200 DPI for line art and 300 for halftones.

Size. All digital artwork must be submitted at its actual printed size so that no scaling is necessary.

Multipanel figures. Figures consisting of individual parts (*e.g.*, panels A, B, C) must be assembled into final format and submitted as one file.

Hard copy. Files must be accompanied by hard copy for use in case the electronic version is unusable.

Disk identification. Disks must be clearly labeled with the following information: author name and manuscript number; format (PC or Macintosh); name and version of software used.

Color: The Biological Bulletin will publish color figures and plates, but must bill authors for the actual additional cost of printing in color. The process is expensive, so authors with more than one color image should—consistent with editorial concerns, especially citation of figures in order—combine them into a single plate to reduce the expense. On request, when supplied with a copy of a color illustration, the editorial staff will provide a pre-publication estimate of the printing cost.

4. ***Tables, footnotes, figure legends, etc.*** Authors should follow the style in a recent issue of *The Biological Bulletin* in preparing table headings, figure legends, and the like. Because of the high cost of setting tabular material in type, authors are asked to limit such material as much as possible. Tables, with their headings and footnotes, should be typed on separate sheets, numbered with consecutive Arabic numerals, and placed after the Literature Cited. Figure legends should contain enough information to make the figure intelligible separate from the text. Legends should be typed double spaced, with consecutive Arabic numbers, on a separate sheet at the end of the paper. Footnotes should be limited to authors' current addresses, acknowledgments or contribution numbers, and explanation of unusual abbreviations. All such footnotes should appear on the title page. Footnotes are not normally permitted in the body of the text.

5. ***Literature cited.*** In the text, literature should be cited by the Harvard system, with papers by more than two authors cited as Jones *et al.*, 1980. Personal communications and material in preparation or in press should be cited in the text only, with author's initials and institutions, unless the material has been formally accepted and a volume number can be supplied. The list of references following the text should be headed Literature Cited, and must be typed double spaced on separate pages, conforming in punctuation and arrangement to the style of recent issues of *The Biological Bulletin*. Citations should include complete titles and inclusive pagination. Journal abbreviations should normally follow those of the U. S. A. Standards Institute (USASI), as adopted by BIOLOGICAL ABSTRACTS and CHEMICAL ABSTRACTS, with the minor differences set out below. The most generally useful list of biological journal titles is that published each year by BIOLOGICAL ABSTRACTS (BIOSIS List of Serials; the most recent issue). Foreign authors, and others who are accustomed to using THE WORLD LIST OF SCIENTIFIC PERIODICALS, may find a booklet published by the Biological Council of the U.K. (obtainable from the Institute of Biology, 41 Queen's Gate, London, S.W.7, England, U.K.) useful, since it sets out the WORLD LIST abbreviations for most biological journals with notes of the USASI abbreviations where these differ. CHEMICAL ABSTRACTS publishes quarterly supplements of additional abbreviations. The following points of reference style for THE BIOLOGICAL BULLETIN differ from USASI (or modified WORLD LIST) usage:

A. Journal abbreviations, and book titles, all underlined (for *italics*)

B. All components of abbreviations with initial capitals (not as European usage in WORLD LIST *e.g., J. Cell. Comp. Physiol.* NOT *J. cell. comp. Physiol.*)

C. *All* abbreviated components must be followed by a period, whole word components *must not* (*i.e., J. Cancer Res.*)

D. Space between all components (*e.g., J. Cell. Comp. Physiol.*, not *J.Cell.Comp.Physiol.*)

E. Unusual words in journal titles should be spelled out in full, rather than employing new abbreviations invented by the author. For example, use *Rit Vísindafjélags Islendinga* without abbreviation.

F. All single word journal titles in full (*e.g., Veliger, Ecology, Brain*).

G. The order of abbreviated components should be the same as the word order of the complete title (*i.e.*, *Proc.* and *Trans.* placed where they appear, not transposed as in some BIOLOGICAL ABSTRACTS listings).

H. A few well-known international journals in their preferred forms rather than WORLD LIST or USASI usage (*e.g.*, *Nature, Science, Evolution* NOT *Nature, Lond., Science, N.Y.; Evolution, Lancaster, Pa.*)

6. ***Sequences.*** By the time a paper is sent to the press, all nucleotide or amino acid sequences and associated alignments should have been deposited in a generally accessible database (*e.g.*, GenBank, EMBL, SwissProt), and the sequence accession number should be provided.

7. ***Reprints, page proofs, and charges.*** Authors may purchase reprints in lots of 100. Forms for placing reprint orders are sent with page proofs. Reprints normally will be delivered about 2 to 3 months after the issue date. Authors will receive page proofs of articles shortly before publication. They will be charged the current cost of printers' time for corrections to these (other than corrections of printers' or editors' errors). Other than these charges for authors' alterations, *The Biological Bulletin* does not have page charges.

CONTENTS
for Volume 204

No. 1: February 2003

No. 2: April 2003

No. 3: June 2003

Reference: *Biol. Bull.* **204:** 237–240. (June 2003)

Horizontal Transfer of Functional Nuclear Genes Between Multicellular Organisms

SIDNEY K. PIERCE*, STEVEN E. MASSEY, JEFFREY J. HANTEN, AND NICHOLAS E. CURTIS

Department of Biology, University of South Florida, SCA 110, 4202 E. Fowler Ave., Tampa, Florida 33620

The horizontal transfer of functional genes between organisms is the theoretical foundation of the endosymbiotic origin of cellular organelles, as well as the basis of genetic therapies and the technology of genetic modification. Without doubt, transfer of functional genes is routine between prokaryotes (1), has occurred between both mitochondria (2) and chloroplasts (3), and the cell nucleus. In addition, DNA has been transferred from endosymbiotic bacteria into insect host cell nuclei (4). However, no direct evidence exists for the natural transfer of nuclear genes between multicellular organisms. We have recently presented circumstantial and pharmacological evidence that nuclear genes encoding for chloroplast proteins are transferred from an alga to an ascoglossan sea slug (5, 6). We now demonstrate, using molecular techniques, that such a gene is present in the genomic DNA of the slug.

Elysia (= Tridachia) crispata is one of a few species of elysiid sea slugs that has an intracellular symbiosis of several months' duration with chloroplasts acquired from specific, siphonaceous algal food. The slug slits open the algal filament with its radula and sucks the contents into its digestive system. As digestion proceeds, certain cells lining the digestive diverticula phagocytize the plastids into intracellular vacuoles. In some species, the chloroplasts reside in their vacuole for as long as 8–9 months (5, 6, 7), 3–4 months in *E. crispata* (8, 9). In several elysiid slugs, including *E. crispata*, the plastids remain photosynthetically active, and photosynthetic carbon fixation contributes to a variety of molecules that participate in the slug's energy metabolism and mucus production (9, 10, 11).

Maintenance of a chloroplast's photosynthetic functions requires that a variety of proteins associated with the photosystems turn over, but chloroplast genomes only code for a small fraction of the proteins needed for plastid function (*e.g.*, 11, 12). For example, in chromophytic algae—the food source of some species of elysiids—the chloroplast genome encodes only 13% of the plastid proteins (13). In higher plants, the genes for as many as 90% of plastid proteins, including many of the photosystem components, are located in the cell nucleus (3). Therefore, the persistence of photosynthesis in the endosymbiotic plastids indicates that protein turnover must be occurring, and that support from the nuclear genome of the slug must be necessary.

The algal species providing the plastids in *E. crispata* (and many other species of elysiid slugs) is unknown and controversial. Some reports indicate that *E. crispata* eats, primarily, species of *Caulerpa*, especially *C. verticellata* (14). Others (9) report that *E. crispata* does not consume *Caulerpa* spp. at all, but rather eats other genera, such as *Batophora, Bryopsis, Halimeda,* and *Penicillus.* These conflicting results suggest that *E. crispata* eats a variety of ulvophytic, coenocytic algae; but whether it retains chloroplasts from multiple algal species is unknown and is a matter that we are currently investigating. Regardless of their origin, the endosymbiotic chloroplasts in *E. crispata* are unexceptional in that they require substantial protein synthesis support from the nucleus. When slugs are incubated in ^{35}S-methionine (methods in 6, 15), radioactivity is incorporated into many plastid proteins (Fig. 1). In *E. crispata*, some of this protein synthesis is inhibited by chloramphenicol, a well-studied blocker of organelle-encoded protein synthesis on organellar ribosomes. The synthesis of the remaining chloroplast proteins is blocked by cycloheximide, an inhibitor of nuclear-encoded protein synthesis on cytosolic ribosomes (Fig. 1). These results, to-

Received 10 February 2003; accepted 22 April 2003.

*To whom correspondence should be addressed. E-mail: pierce@chuma1.cas.usf.edu

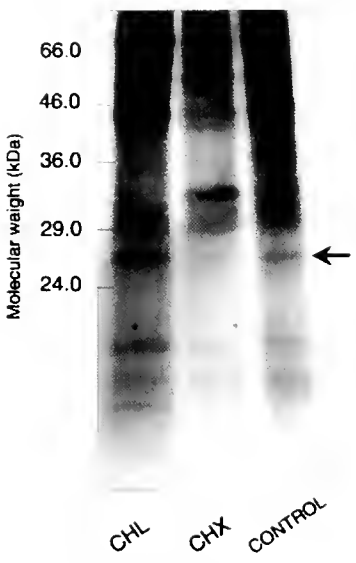

Figure 1. Fluor-enhanced autoradiogram of a 12.5% SDS-polyacrylamide gel electrophoresis (PAGE), showing the differential effects of chloramphenicol (CHL) and cycloheximide (CHX) on the synthesis of *E. crispata* chloroplast proteins. After dose-response curves determined effective concentrations, slugs were preincubated, for 2 h under intense artificial light, in one of the inhibitors (chloramphenicol, 2.5 mg ml^{-1}; cycloheximide, 2.0 mg ml^{-1}) or (as a control) in DMSO carrier (0.024 %). The solutions were made in artificial seawater. After this pre-incubation, ^{35}S-methionine (40 μCi/ml) was added, and the slugs were incubated for an additional 6 h. A chloroplast fraction was then prepared, and the proteins were extracted (6) and electrophoresed. The gels were stained with Coomassie Brilliant Blue, dried, and exposed to X-ray film. The arrow indicates the position of a protein, which we have identified as FCP (see text); note that its synthesis is inhibited by CHX.

gether with similar findings we have reported from a closely related species, *Elysia chlorotica* (6), indicate that a variety of chloroplast proteins are being synthesized while the plastids reside in the cytoplasm of the slug's digestive cells. More important, the cycloheximide inhibition clearly demonstrates that several of the proteins are being translated on cytoplasmic ribosomes, indicating, in turn, that the genes encoding those proteins are located in the animal cell nucleus.

We used antibodies on Western blots and immunoprecipitations to identify the proteins in *E. crispata* whose synthesis was blocked by cycloheximide. Antibody screening, based on both molecular weights and available antibodies, was done on Western blots of protein extracts from radiolabeled isolated chloroplasts. A polyclonal antibody raised against fucoxanthin-chlorophyll binding protein (FCP) from *Pavlova gyrans* was kindly made available to us by Dr. Marvin Fawley at North Dakota State University. This antibody binds to a Western blot (Fig. 2) at a position corresponding to the molecular weight of a prominent, cycloheximide-inhibited band (Fig. 1)—a result similar to those with *E. chlorotica* (6, 7). The FCP antibody also precipitates radioactivity from ^{35}S-labeled chloroplast proteins (using standard protein A Sepharose procedures), and the amount of radioactive immunoprecipitate is reduced by 71% in the presence of cycloheximide. These immunoprecipitation results clearly indicate that synthesis of FCP is blocked by cycloheximide.

To ensure that the immunolabeled protein in the Western blot was indeed FCP, we purified it from *E. chlorotica* chloroplasts and determined the N-terminal amino acid sequence and three internal sequences. BLAST searching indicated that the N-terminal 30 amino acids had a 66% identity to those of the FCP protein of the chromophyte, *Cylindrotheca fusiformis* (AAN08832); and one of the internal sequences (11 amino acids) had an 81% identity with the FCP protein (Q40300) of *Macrocystis pyrifera*, another chromophyte. The remaining two internal sequences showed no significant similarity to known FCP sequences, but few algal FCP sequences are available in the databases, and sequence variation is high in some regions of the protein. Together, therefore, the immunological results and amino acid sequence similarities show that a chloroplast protein in *E. crispata*, whose synthesis is blocked by cycloheximide, is FCP.

Degenerate primers, based on the N-terminal and internal amino acid sequences of the native FCP, were used in PCR to amplify the gene encoding FCP from *Vaucheria litorea*, an alga eaten by *E. chlorotica* (5) and, according to our feeding experiments, by juveniles of *E. crispata*. A 350 bp PCR product was generated and sequenced. BLAST searching of the translated sequence confirmed that the PCR

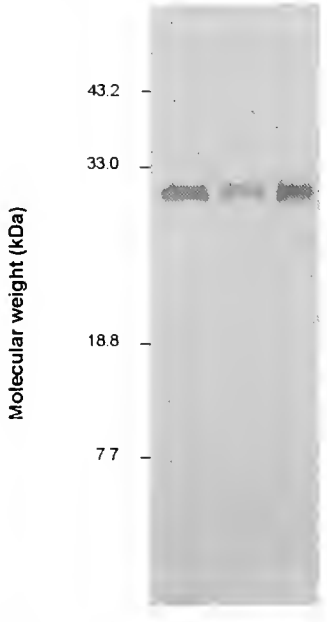

Figure 2. Western blot of a PAGE of chloroplast proteins extracted from *E. crispata* exposed to chloramphenicol (left lane), cycloheximide (center lane), or DMSO carrier (right lane), as described in Figure 1. The blot was exposed to a primary antibody (anti-FCP, see text), and then labeled with secondary antibody (HRP-conjugated, anti-rabbit IgG).

product is the gene encoding FCP, with a 51% amino acid sequence identity with *Laminaria saccharina* FCP (*lhcf7*) (AF226863). Moreover, the two unidentified internal amino acid sequences mentioned above were identical with portions of the translated gene sequence.

The most conserved region of our native FCP amino acid sequence was used to design a 100 bp probe for Southern blotting of *E. crispata* genomic DNA, which had been prepared by differential centrifugation on cesium chloride gradients (16). A prominent *fcp* homolog was revealed on blots of *E. crispata* DNA (Fig. 3), but not on the negative control—genomic DNA from *Aplysia brasiliana*, another herbivorous opisthobranch sea slug, which does not retain chloroplasts. The *fcp* probe also labeled Southern blots of genomic DNA from *Vaucheria litorea* (not shown), not surprising since FCP's are always encoded by the algal nuclear genome (17).

Together, the pharmacological, immunological, and molecular results establish that a gene for an algal chloroplast protein is present in the genomic DNA of *E. crispata*, where it waits for the acquisition of new plastids in each generation of slugs. Similar pharmacological and immunological results suggested that genes for another group of chloroplast proteins, light harvesting complex (LHC), have been transferred from the nuclear genome of *V. litorea* to that of *E. chlorotica* (6).

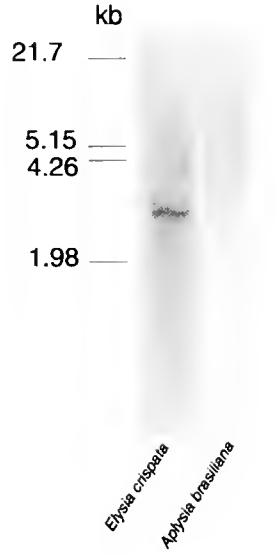

Figure 3. Autoradiogram of a Southern blot of genomic DNA from *E. crispata* and *A. brasiliana* labeled with a ^{32}P-labeled 100 bp nucleotide sequence constructed from the native FCP amino acid sequence. Genomic DNA was purified from the two species using cesium chloride density centrifugation (16). *Hind*III-digested genomic DNA from each species (5 μg) was electrophoresed on a 0.8% agarose gel. The DNA was transferred and UV crosslinked to a Pall Biodyne Plus nylon membrane. The membrane was hybridized with the radiolabeled probe in buffer (6× SSPE, 0.5% SDS, and 50 μg ml^{-1} heparin) (16) overnight at 42°C. The blot was washed at 50°C with 0.1 × SSC, 0.1% SDS and exposed overnight to X-ray film (16).

Always lurking in the background, casting doubt on these conclusions, is the concern that, somehow, algal nuclear DNA, either from nuclei remaining in the gut lumen, or taken up with the chloroplasts, has contaminated the slug genomic DNA. This is most improbable for several reasons. First, the slugs were starved for at least 7 days before any of the experiments were done. Thus, the guts were empty, and contamination from that source was therefore unlikely. Second, we used primers designed from conserved regions of the 18S rRNA gene to generate a PCR product from *E. crispata* DNA. This product (accession number AY292202) was 98% identical to the 18S rRNA gene sequence of the elysiid slug *Thuridilla bayeri*, and 96% similar to that of *Limapontia nigra*, also an ascoglossan species. Therefore, the DNA we used in the Southern blots and PCR experiments was molluscan, not algal. Third, neither other molecular probing (18, 19) nor extensive electron microscopy (5, 20) has ever revealed any evidence of algal nuclear material in the slugs. Finally, it seems extremely unlikely that that algal nuclei could be taken up by all the chloroplast-containing cells in every animal.

If the gene-encoding FCP is located in the slug DNA, a horizontal gene transfer between algal and slug nuclei must have occurred. The means by which such a transfer of genes between multicellular organisms might occur is presently unknown. However, every specimen of *E. chlorotica* that we have examined for it over the last decade has contained an endogenous virus with several characteristics of the Retroviridae. The virus is present in hemocytes, digestive cells, and plastids and is expressed just before the annual synchronous death of the population (5). A comparable virus has not yet been demonstrated in *E. crispata*, nor have other transferred genes been reported in other species of chloroplast-retaining elysiids. However, a retroviral mechanism of gene transfer offers an interesting explanation of our results, and may be an important, even common, mechanism of evolution.

Acknowledgments

This work was supported by National Science Foundation grant #IBN-0090118. We thank Mike Greenberg for his usual unusually thorough editorial assistance.

Literature Cited

1. **Jain, R., M. C. Rivera, J. E. Moore, and J. A. Lake. 2002.** Horizontal gene transfer in microbial genome evolution. *Theor. Popul. Biol.* **61:** 489–495.
2. **Palmer, J. D., K. L. Adams, Y. Cho, C. L. Parkinson, Y-L. Qiu, and K. Song. 2000.** Dynamic evolution of plant mitochondrial genomes: mobile genes and introns and highly variable mutation rates. *Proc. Natl. Acad. Sci. USA* **97:** 6960–6966.
3. **Martin, W., T. Rujan, E. Richly, A. Hansen, S. Cornelsen, T. Lins,**

D. Leister, B. Stoebe, M. Hasegawa, and D. Penny. 2002. Evolutionary analysis of *Arabidopsis*, cyanobacterial, and chloroplast genomes reveals plastid phylogeny and thousands of cyanobacterial genes in the nucleus. *Proc. Natl. Acad. Sci. USA* **99:** 12,246–12,251.

4. **Kondo, N., N. Nikoh, N. Ijichi, M. Shimada, and T. Fukatsu. 2002.** Genome fragment of *Wolbachia* endosymbiont transferred to X chromosome of host insect. *Proc. Natl. Acad. Sci. USA* **99:** 14,280–14,285.
5. **Pierce, S. K., T. K. Maugel, M. E. Rumpho, J. J. Hanten, and W. L. Mondy. 1999.** Annual viral expression in a sea slug population: life cycle control and symbiotic chloroplast maintenance. *Biol. Bull.* **197:** 1–6.
6. **Hanten, J. J., and S. K. Pierce. 2001.** Synthesis of several light-harvesting complex 1 polypeptides is blocked by cycloheximide in symbiotic chloroplasts in the sea slug, *Elysia chlorotica* (Gould): A case for horizontal gene transfer between alga and animal? *Biol. Bull.* **201:** 34–44.
7. **Green, B. J., W -Y. Li, J. R. Manhart, T. C. Fox, E. L. Summer, R. A. Kennedy, S. K. Pierce, and M. E. Rumpho. 2000.** Mollusc-algal chloroplast endosymbiosis. Photosynthesis, thylakoid protein maintenance, and chloroplast gene expression continue for many months in the absence of the algal nucleus. *Plant Physiol.* **124:** 331–342.
8. **Trench, R. K., and S. Olhorst. 1976.** The stability of chloroplasts from siphonaceous algae in symbiosis with sacoglossan molluscs. *New Phytol.* **76:** 99–109.
9. **Clark, K. B., and M. Busacca. 1978.** Feeding specificity and chloroplast retention in four tropical Ascoglossa, with a discussion of the extent of chloroplast symbiosis and the evolution of the order. *J. Molluscan Stud.* **44:** 272–282.
10. **Greene, R. W. 1970.** Symbiosis in sacoglossan opisthobranchs: functional capacity of symbiotic chloroplasts. *Mar. Biol.* **7:** 138–142.
11. **Rumpho, M. E., E. J. Summer, and J. R. Manhart. 2000.** Solar-powered sea slugs: mollusc/algal chloroplast symbiosis. *Plant Physiol.* **123:** 29–38.
12. **Reith, M. 1995.** Molecular biology of rhodophyte and chromophyte plastids *Annu. Rev. Plant Physiol. Plant Mol. Biol.* **46:** 549–575.
13. **Martin, W., and R. G. Herrmann. 1998.** Gene transfer from organelles to the nucleus: how much, what happens and why? *Plant Physiol.* **118:** 9–17.
14. **Jensen, K., and K. B. Clark. 1983.** Annotated checklist of Florida ascoglossan Opisthobranchia. *Nautilus* **97:** 1–13.
15. **Pierce, S. K., R. W. Biron, and M. E. Rumpho. 1996.** Endosymbiotic chloroplasts in molluscan cells contain proteins synthesized after plastid capture. *J. Exp. Biol.* **199:** 2323–2330.
16. **Sambrook, J., E. F. Fritsch, and T. Maniatis. 1989.** *Molecular Cloning, A Laboratory Manual.* 2nd ed. Cold Spring Harbor Laboratory Press, Cold Spring Harbor, NY.
17. **Durnford, D. G., J. A. Deane, S. Tan, G. I. McFadden, E. Gantt, and B. R. Green. 1999.** A phylogenetic assessment of the eukaryotic light-harvesting antenna proteins, with implications for plastid evolution. *J. Mol. Evol.* **48:** 59–68.
18. **Mujer, C. V., D. L. Andrews, J. R. Manhart, S. K. Pierce, and M. E. Rumpho. 1996.** Chloroplast genes are expressed during intracellular symbiotic association of *Vaucheria litorea* plastids with the sea slug *Elysia chlorotica*. *Proc. Natl. Acad. Sci. USA* **93:** 1233–1238.
19. **Green, B. J., W-Y. Lei, J. R. Manhart, T. C. Fox, E. J. Summer, R. A. Kennedy, S. K. Pierce, and M. J. Rumpho. 2000.** Mollusc-algal chloroplast endosymbiosis. Photosynthesis, thylakoid protein maintenance and chloroplast gene expression continue for many months in the absence of the algal nucleus. *Plant Physiol.* **124:** 331–342.
20. **Mondy, W. L., and S. K. Pierce. 2003.** Apoptotic-like morphology is associated with the annual synchronized death of a population of kleptoplastic sea slugs (*Elysia chlorotica*). *Invertebr. Biol.* (In press).

Reference: *Biol. Bull.* **204:** 241–245. (June 2003)

Settlement Cues in the Locally Dispersing Temperate Cup Coral *Balanophyllia elegans*

ANDREW H. ALTIERI*

Department of Biology, University of California, Santa Cruz, California 95064

Most studies of settlement cues in sessile marine invertebrates have focused on species with the potential to disperse over great distances. This persistent focus has perpetuated the idea that long-distance dispersing species may rely on cues to settle in specific habitats, whereas short-distance dispersers are delivered directly into a favorable habitat. I tested the effects of water movement and substrate on the settlement of the temperate solitary cup coral Balanophyllia elegans, *a species whose crawl-away larvae disperse just centimeters before settling. Ninety percent of larvae settled within 3 days of release in the presence of both natural rock substrate and moving water, but fewer than 11% settled in the same period when either or both factors were absent. An additional experiment revealed that when natural rock substrate was available, water velocities of less than 25 cm · s^{-1} triggered a 5-fold increase in settlement rate relative to standing water. When settling, the larvae of* B. elegans *respond strongly to the interactive effects of water flow and substrate. Thus, settlement cues may play a significant role in generating the patchy distribution of* B. elegans, *a pattern previously attributed to short-distance dispersal.*

Larval settlement is a critical stage in the life history of sessile marine invertebrates. This transition from a mobile larval stage to a sessile juvenile stage represents a commitment to a particular location, and determines the subsequent conditions that an individual will encounter, including predation pressure (1), severity of physical stress (2), competition for space (2), competition for food (3), and fertilization success (4). Numerous studies have revealed that two factors influence the spatial pattern of settling larvae: a variable supply of larvae, which can lead to a correlated variable settlement pattern (5, 6); and selective larval settlement in response to patchy environmental cues, which can refine settlement patterns set by larval supply (7, 8). Variable larval supply can lead to heterogeneous settlement patterns in both long-distance (scale of kilometers) (6) and short-distance (scale of cm or m) (9, 10) dispersing species. Settlement cues, on the other hand, have been observed primarily in long-distance dispersers (but see 10, 11), and reviews on the topic typically ignore settlement cues in species whose larvae disperse and settle within the area immediately surrounding parent individuals, particularly those with crawl-away larvae (7, 8). The patchy distribution of short-distance dispersers remains largely attributed to patterns of larval supply (12–16); however, few studies have investigated the alternative hypothesis that larval settlement of species with limited dispersal is influenced by environmental cues.

The stony (scleractinian) aclonal cup coral *Balanophyllia elegans* is an ideal species with which to test the widely accepted hypothesis that species with limited dispersal do not show strong settlement response to environmental conditions. Unlike the planktonic larvae characteristic of most marine invertebrate species, which can disperse kilometers, the wormlike planula larvae of *B. elegans* disperse locally by crawling along the substrate (13). Adults of *B. elegans* are patchily distributed at a scale of meters—a pattern largely attributed to an average dispersal distance of just 39 cm, though larvae are capable of traveling more than 1.3 m before settling (13, 17, 18). Thus, larvae generally settle closer to parent individuals than their dispersal potential would predict, indicating that environmental factors may influence the settlement behavior of larvae and contribute to the patchy distribution of adults. Settlement cues have been largely overlooked as a potential cause of the patchy settlement distribution of *B. elegans* and many other species with short-distance dispersal, perhaps because short-distance dis-

Received 30 September 2002; accepted 14 April 2003.

*Current Address: Department of Ecology and Evolutionary Biology, Box G-W, Brown University, Providence, RI 02912. E-mail: Andrew_Altieri@Brown.edu

persal is perceived as delivering larvae directly to habitats that have already proven suitable for reproductive adults (19–22). The alternative hypothesis that the settlement behavior of *B. elegans* is influenced by environmental conditions has not been tested, even though cues often cause species to aggregate where environmental variables are favorable to the fitness of the adults (23, 24), and *B. elegans* belongs to a taxon (scleractinian corals) for which larval settlement cues are common in species with long-distance dispersal (25, 26). The purpose of this study was to establish whether environmental cues influence the settlement behavior of the solitary cup coral *Balanophyllia elegans*.

I tested the effect of water movement and substrate on the settlement rate of *B. elegans* larvae, since both factors influence the settlement behavior of other scleractinian corals (25, 27). In the first of two experiments, single larvae were placed in polycarbonate cups (75 × 75 mm diameter × height) within 24 h of release, and exposed to one of three substrate treatments and one of two water-movement treatments. The substrate treatments were live rock (rock collected from *B. elegans* habitat), sterilized rock (live rock that had been boiled for 2 h in de-ionized water), and polycarbonate (no additional substrate added to cup). The water-movement treatments were moving water (stream of seawater entering cup at 17 ml · s^{-1}) or standing water (no stream of water). Larvae were monitored daily for settlement, indicated by irreversible metamorphosis from worm-like crawling larvae (3–5 mm long) to radially symmetrical sessile polyps (~1.2 mm diameter) (28). Larvae in all treatments were observed to crawl until settlement or end of the experiment at a rate consistent with Gerrodette's observation of 0.03–0.04 cm · min^{-1} (13). In laboratory conditions, Gerrodette (13) found that larvae of *B. elegans* settled an average of 3 days after release, and remained competent to settle for more than 14 days. To determine if the experimental treatments of my study shifted the timing of settlement relative to that average, larvae were recorded as either settling or not settling in the first 2 days of the experiment (due to a 1-day lag between larval release and placement in experimental treatments). Differences between treatments in the proportions of larvae settled during the first 2 days were evaluated by chi-square analysis. Results showed that the proportion of larvae settling during this period was 9 times higher in treatments with both natural substrate (live or sterilized rock) and moving water than in treatments with either or both conditions absent (Fig. 1A). This dramatic difference ($\chi^2 = 90.30$, $P < 0.001$, df = 1) demonstrates that the settlement rate of *B. elegans* larvae is strongly affected by both environmental factors.

A second experiment was conducted to estimate the water velocity necessary to trigger settlement of *B. elegans*, and to verify that the high settlement rate exhibited by larvae in the first experiment was due to water movement rather than to some artifact such as varying concentration of solutes in the inflowing seawater or depletion of oxygen in the standing water treatment. Single larvae were placed in polystyrene petri dishes within 24 h of release, and exposed to one of two substrate treatments—sterilized rock (live rock that had been boiled for 2 h in deionized water) or polystyrene (no additional substrate added to petri dish)—and to one of two water-movement treatments—moving water (shaker table at 80 rpm) or standing water (stationary table). Water movement was generated by an orbital shaker table, rather than a stream of seawater, to eliminate potential variability of inflowing seawater. Shallow polystyrene petri dishes (60 × 15 mm) were used instead of polycarbonate cups to ensure ample surface area for diffusion of oxygen into the water. Settlement was scored and analyzed similarly to the first experiment. As observed in the first experiment, settlement rates were significantly higher in the presence of both moving water and rock substrate than when either or both conditions were absent ($\chi^2 = 19.7$, $P < 0.001$, df = 1). Based on the petri dish dimensions, it was determined that water velocities of less than 25 cm · s^{-1} were sufficient to trigger a 5-fold higher settlement rate relative to standing water (Fig. 1B), a range of water flow commonly encountered by *B. elegans* within its geographic range (29).

To validate the *a priori* 2-day settlement criterion used for analysis, and to examine settlement patterns of *B. elegans* on a finer temporal scale, the shaker table experiment (Fig. 1B) was allowed to run for 8 days, and the cumulative proportion of larvae settled was recorded daily. The plot of larval settlement over time illustrates that the sterilized rock-moving water treatment diverged sharply from the other three treatments within the first day, a difference that persisted for the remainder of the 8-day experiment (Fig. 2). Settlement did not occur in the polystyrene-standing water treatment until the 8th day, suggesting that in poor conditions settlement can be delayed, taking up to 4 times longer than in favorable conditions. In many marine species with selective larvae, settlement is similarly delayed to lengthen the search time for suitable habitat (7).

The significantly higher settlement rate of *B. elegans* larvae exposed to water movement and rocky substrate is probably due to both the reliability of the cues as indicators of suitable settlement areas (30) and the potential costs of not using those cues (31). Water movement is critical for delivery of food, nutrients, and dissolved gasses to scleractinian corals, and has been correlated with their distribution on the scale of meters (32). The results of this study suggest that correlation could be due in part to selective larval settlement. It is generally presumed that the mechanical characteristics of water movement influence the settlement behavior of larvae (33–35), and this study did not test the alternative hypothesis that the flux of solutes correlated with water movement could have induced settlement. Nevertheless, water movement proved to be an excellent predictor of settlement behavior in *B. elegans*. Settlement rates were

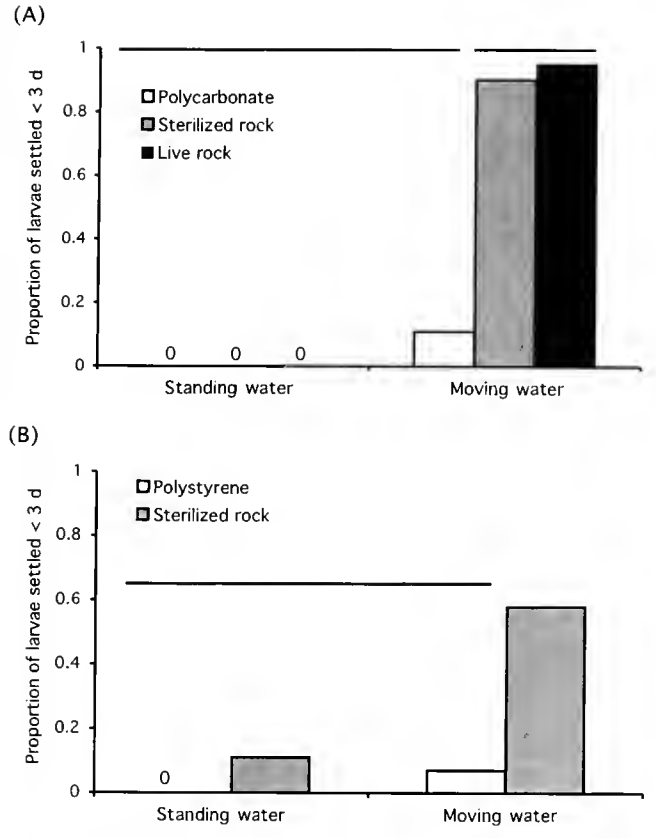

Figure 1. (A) A significantly higher proportion of *Balanophyllia elegans* larvae settled during the first 2 days of the experiments in treatments with both natural substrate (live or sterilized rock) and moving water than in treatments with either or both conditions absent ($\chi^2 = 90.30$, $P < 0.001$, df = 1). The two treatments of sterilized rock and live rock in moving water treatments were similar ($\chi^2 = 0.367$, $P > 0.54$, df = 1), and all other treatments were similar to one another ($\chi^2 = 5.66$, $P > 0.1$, df = 3). All experiments were conducted in January–March 1998 at the Long Marine Laboratory of the University of California at Santa Cruz in water temperatures of 14.0–16.5°C. Larvae used in the experiments were spontaneously released in the laboratory by a group of individuals collected from a depth of 4–8 m below MLLW at the Breakwater in Monterey, California (36°37′N, 121°53′W) in December 1997. Live rocks (15 × 15 × 10 to 25 × 20 × 15 mm) were collected from the same area, and were encrusted primarily by coralline algae. Sterilized rocks were collected as live rocks and prepared by boiling for 2 h in deionized water, a preparation which largely inactivates the polysaccharide and peptide in the crustose coralline algaes that respectively induce settlement of other corals and molluscs (39, 40). Thus the similarly high rate of larval settlement in both the live and sterilized rock treatments (in presence of moving water) was probably due to the texture of the substrate, and not to inductive compounds in the coralline algae.

(B) A second experiment was conducted to estimate the rate of water movement necessary to trigger settlement of *Balanophyllia elegans*, and to ensure that the strong settlement response exhibited by the larvae in the first experiment was due to water movement and not to some characteristic of inflowing water such as changes in concentration of solutes. Results were qualitatively similar to the first experiment: natural substrate and water movement acted together to induce a significantly higher rate of settlement relative to the other treatments in which either or both factors were absent ($\chi^2 = 19.7$, $P < 0.001$, df = 1). Results of the latter set of treatments were statistically similar ($\chi^2 = 4.12$, $P > 0.1$, df = 2). For the moving water treatments, petri dishes were placed on a shaker table with circular motion after larvae had been allowed to adhere to tested substrate for 1 h. Rocks remained relatively motionless in moving water treatments, and larvae remained adhered to substrate in all treatments for the duration of the experiment (when collecting larvae from brood stock, several vigorous blasts from a transfer pipette were commonly required to dislodge larvae from substrate, due in part to a mucous trail). By multiplying the circumference of the petri dish (18.84 cm) by the orbital rate of the shaker table (80 rpm), the wave generated by the shaker table was estimated to reach a velocity of 25 cm · s^{-1} at the edge of the dish and to diminish toward the opposite side. Since the water itself would have traveled more slowly than the wave due to encounter with the sides and bottom of the dish, 25 cm · s^{-1} is a conservative estimate of the velocity required to trigger preferential settlement.

For both experiments, differences between treatments in proportions of larvae settled during the first 2 days were assessed by chi-square analysis. Contingency tables with expected values of less than 5 in greater than 20% of the cells were analyzed by log-likelihood ratio goodness of fit test to avoid bias in the chi-squared statistic. When contingency table analysis showed significant results, the tables were partitioned to determine the treatment or combination of treatments responsible for the experiment-wide statistically significant result. Sample size was 14–20 for all treatments. Histogram bars under shared horizontal lines do not differ significantly at $P < 0.05$.

also strongly affected by substrate. Though larvae were capable of settling on the artificial (polycarbonate and polystyrene) surfaces tested, settlement rates were dramatically lower than on natural substrates (live and sterilized rock). The lack of biogenic structures may indicate an inhospitable habitat. Conversely, the relatively smooth surface of polycarbonate may mimic the smooth surfaces of encrusting organisms, such as ascidians and algae, that can overgrow *B. elegans*. Potential interactions with spatial competitors are known to affect the settlement choices of marine larvae (36), and competition for space is a significant factor in establishing the post-settlement distribution of *B. elegans* in the rocky subtidal (18, 37, 38). The comparison between substrates of natural rock and polycarbonate limits our ability to predict substrate preference under natural conditions; however, the results are valuable in demonstrating one extreme in the timing of settlement (Fig. 2).

Water movement and substrate appear to be of such importance to the coral *B. elegans* that the larvae have developed a sensitivity to those factors when settling. For the species to have evolved such settlement preferences, water movement and substrate must vary at a spatial scale smaller than the potential larval dispersal distance of only 1.3 m. Gradients of topography and water movement similar to those tested in this study exist over a range of scales from millimeters to kilometers in the rocky subtidal where *B. elegans* occurs (29), and the lower end of that range is well within the larval dispersal distance.

The selective behavior of *B. elegans* larvae probably translates into an effect on dispersal patterns and adult spatial distributions. Gerrodette (13) found that the larvae of *B. elegans* moved randomly away from parent individuals

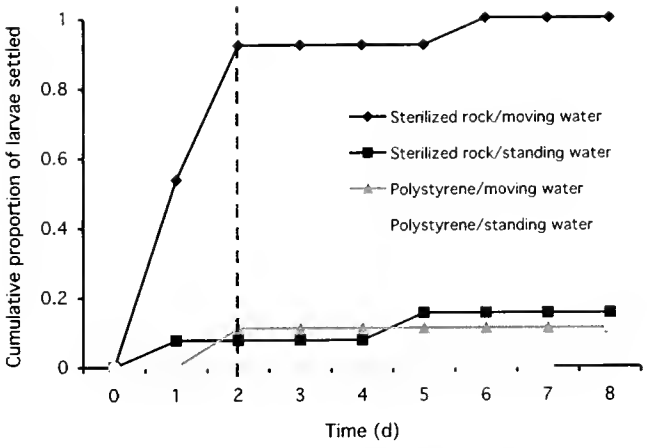

Figure 2 As detected by the chi-square analysis, cumulative larval settlement in the sterilized rock-moving water treatment shows a marked departure from the other three treatments by day two of the experiment. This relationship persisted for the remainder of the 8-day experiment, though larvae continued to settle through the end of the experiment. Values at the 2-day mark used for statistical analysis (indicated by the vertical dashed line) were thus an accurate descriptor of longer-term behavioral trends.

in a pattern analogous to diffusion at a rate of $\sim 10\ \text{cm} \cdot \text{d}^{-1}$. The results of this study indicate that as larvae move randomly about an area that is heterogeneous with respect to substrate and water movement, they are more likely to settle and accumulate in areas where specific conditions are present. Thus, the patchy distribution of *B. elegans* that has been quantified in several studies may be due to preferential settlement in areas of higher water movement and rugose substrate. Such selectivity for water movement and topography leads to patchy distribution in other sessile marine invertebrates, including barnacles (33), ascidians (34), bryozoans, hydroids, and polychaetes (35).

The crawl-away larvae of *Balanophyllia elegans* are extremely sensitive to environmental conditions, and they base their settlement behavior on factors including water movement and substrate. This suggests that the environment is variable enough at the scale of dispersal (centimeters) to have generated an adaptive advantage for selective larvae, just as in more widely dispersing species. Though the relative importance of water movement and substrate as settlement cues remains to be tested in the field for *B. elegans*, these two factors are likely to be significant in establishing the settlement patterns of this species with short-distance dispersal.

Acknowledgments

I thank A. Boxshall, M. Carr, D. Lohse, and P. Raimondi for insightful discussion. They, along with M. J. Greenberg, B. Silliman, R. Wahle, J. Witman, and two anonymous reviewers, improved earlier versions of this manuscript with their comments. J. Pearse, P. Raimondi, and B. Steele made lab space and expertise available for this study. Divers A. Boullard, A. Boxshall, D. Huang, S. Lonhart, and M. Readdie assisted in field collections, and D. Canestro supported field operations. D. Huang provided a place for me to stay during portions of this study. Funding was provided by a University of California President's Undergraduate Fellowship, a Friends of Long Marine Lab Student Research Award, and a UCSC Department of Biology Independent Study Research Support Award.

Literature Cited

1. **Keough, M. J., and B. J. Downes. 1982.** Recruitment of marine invertebrates: the role of active larval choices and early mortality. *Oecologia* **54:** 348–352.
2. **Connell, J. H. 1961.** The influence of interspecific competition and other factors on the distribution of the barnacle *Chthamalus stellatus*. *Ecology* **42:** 710–723.
3. **Buss, L. W., and J. B. C. Jackson. 1981.** Planktonic food availability and suspension-feeder abundance: evidence of *in situ* depletion. *J. Exp. Mar. Biol. Ecol.* **49:** 151–161.
4. **Levitan, D. R., M. A. Sewell, and F.-S. Chia. 1992.** How distribution and abundance influence fertilization success in the sea urchin *Strongylocentrotus franciscanus*. *Ecology* **73:** 248–254.
5. **Connell, J. H. 1985.** The consequences of variation in initial settlement vs. post-settlement mortality in rocky intertidal communities. *J. Exp. Mar. Biol. Ecol.* **93:** 11–45.
6. **Gaines, S. D., and J. Roughgarden. 1985.** Larval settlement rate: a leading determinant of structure in an ecological community of the marine intertidal zone. *Proc. Natl. Acad. Sci. USA* **82:** 3707–3711.
7. **Crisp, D. J. 1974.** Factors influencing the settlement of marine invertebrate larvae. Pp. 177–265 in *Chemoreception in Marine Organisms*, P.T. Grant and A.M. Mackie, eds. Academic Press, London.
8. **Pawlick, J. R. 1992.** Chemical ecology of the settlement of benthic marine invertebrates. *Oceanogr. Mar. Biol.* **30:** 273–335.
9. **Stoner, D. S. 1992.** Vertical distribution of a colonial ascidian on a coral reef: the roles of larval dispersal and life-history variation. *Am. Nat.* **139:** 802–824.
10. **Carlon, D. B., and R. R. Olson. 1993.** Larval dispersal distance as an explanation for adult spatial pattern in two Caribbean reef corals. *J. Exp. Mar. Biol. Ecol.* **173:** 247–263.
11. **Sebens, K. P. 1983.** Settlement and metamorphosis of a temperate soft-coral larva (*Alcyonium siderium* Verrill): induction by crustose algae. *Biol. Bull.* **165:** 286–304.
12. **Ostarello, G. L. 1976.** Larval dispersal in the subtidal hydrocoral *Allopora californica* Verrill (1866). Pp. 331–337 in *Coelenterate Ecology and Behavior*, G.O. Mackie, ed. Plenum Press, New York.
13. **Gerrodette, T. 1981.** Dispersal of the solitary coral *Balanophyllia elegans* by demersal planular larvae. *Ecology* **62:** 611–619.
14. **Olson, R. R. 1985.** The consequences of short-distance larval dispersal in a sessile marine invertebrate. *Ecology* **66:** 30–39.
15. **Keough, M. J., and H. Chernoff. 1987.** Dispersal and population variation in the bryozoan *Bugula neritina*. *Ecology* **68:** 199–210.
16. **Davis, A. R., and A. J. Butler. 1989.** Direct observations of larval dispersal in the colonial ascidian *Podoclavella moluccensis* Sluiter: evidence for closed populations. *J. Exp. Mar. Biol. Ecol.* **127:** 189–203.
17. **Fadlallah, Y. H. 1983.** Population dynamics and life history of a solitary coral, *Balanophyllia elegans*, from Central California. *Oecologia* **58:** 200–207.
18. **Coyer, J. A., R. F. Ambrose, J. M. Engle, and J. C. Carroll. 1993.**

Interactions between corals and algae on a temperate zone rocky reef: mediation by sea urchins. *J. Exp. Mar. Biol. Ecol.* **167:** 21–37.

19. **Mileikovsky, S. A. 1971.** Types of larval development in marine bottom invertebrates, their distribution and ecology significance: a re-evaluation. *Mar. Biol.* **10:** 193–213.
20. **Vance, R. R. 1973.** On reproduction strategies in marine benthic invertebrates. *Am. Nat.* **107:** 339–352.
21. **Obrebski, S. 1979.** Larval colonizing strategies in marine benthic invertebrates. *Mar. Ecol. Prog. Ser.* **1:** 293–300.
22. **Strathmann, R. R. 1985.** Feeding and nonfeeding larval development and life-history evolution in marine invertebrates. *Annu. Rev. Ecol. Syst.* **16:** 339–361.
23. **Young, C. M., and F.-S. Chia. 1984.** Microhabitat associated variability in survival and growth of subtidal solitary ascidians during the first 21 days after settlement. *Mar. Biol.* **81:** 61–68.
24. **Raimondi, P. T. 1991.** Settlement behavior of *Chthamalus anisopoma* larvae largely determines the adult distribution. *Oecologia* **85:** 349–360.
25. **Harrison, P. L., and C. C. Wallace. 1990.** Reproduction, dispersal and recruitment of scleractinian corals. Pp. 133–207 in *Ecosystems of the World 25: Coral Reefs,* Z. Dubinsky, ed. Elsevier, Amsterdam.
26. **Morse, A. N. C., K. Iwao, M. Baba, K. Shimoike, T. Hayashibara, and M. Omori. 1996.** An ancient chemosensory mechanism brings new life to coral reefs. *Biol. Bull.* **191:** 149–154.
27. **Abelson, A., D. Weihs, and Y. Loya. 1994.** Hydrodynamic impediments to settlement of marine propagules, and adhesive filament solutions. *Limnol. Oceanogr.* **39:** 164–169.
28. **Fadlallah, Y. H., and J. S. Pearse. 1982.** Sexual reproduction in solitary corals: overlapping oogenic and brooding cycles, and benthic planulas in *Balanphyllia elegans. Mar. Biol.* **71:** 223–231.
29. **Denny, M. 1995.** Predicting physical disturbance: mechanistic approaches to the study of survivorship on wave-swept shores. *Ecol. Monogr.* **65:** 371–418.
30. **Strathmann, R. R., and E. S. Branscomb. 1979.** Adequacy of cues to favorable sites used by settling larvae of two intertidal barnacles. Pp. 7–89 in *Reproductive Ecology of Marine Invertebrates,* S.E. Stranger, ed. University of South Carolina Press, Columbia, SC.
31. **Raimondi, P. T. 1988.** Settlement cues and determination of the vertical limit of an intertidal barnacle. *Ecology* **69:** 400–407.
32. **Sebens, K. P., and A. S. Johnson. 1991.** Effects of water movement on prey capture and distribution of reef corals. *Hydrobiologia* **226:** 91–101.
33. **Crisp, D. J. 1955.** The behaviour of barnacle cyprids in relation to water movement over a surface. *J. Exp. Biol.* **32:** 569–590.
34. **Havenhand, J. N., and I. Svane. 1991.** Roles of hydrodynamics and larval behavior in determining spatial aggregation in the tunicate *Ciona intestinalis. Mar. Ecol. Prog. Ser.* **68:** 271–276.
35. **Mullineaux, L. S., and E. D. Garland. 1993.** Larval recruitment in response to manipulated field flows. *Mar. Biol.* **116:** 667–683.
36. **Grosberg, R. K. 1981.** Competitive ability influences habitat choice in marine invertebrates. *Nature* **290:** 700–702.
37. **Chadwick, N. E. 1991.** Spatial distribution and the effects of competition on some temperate scleractinia and corallimorpharia. *Mar. Ecol. Prog. Ser.* **70:** 39–48.
38. **Bruno, J. F., and J. D. Witman. 1996.** Defense mechanisms of scleractinian cup corals against overgrowth by colonial invertebrates. *J. Exp. Mar. Biol. Ecol.* **207:** 229–241.
39. **Morse, D. E., N. Hooker, A. N. C. Morse, and R. A. Jensen. 1988.** Control of larval metamorphosis and recruitment in sympatric agariciid corals. *J. Exp. Mar. Biol. Ecol.* **116:** 193–217.
40. **Morse, D. E., H. Duncan, N. Hooker, A. Balsun, and G. Young. 1980.** Gaba induces behavioral and developmental metamorphosis in planktonic molluscan larvae. *Fed. Proc.* **39:** 3237–3241.

Reference: *Biol. Bull.* **204:** 246–255. (June 2003)

Identification of Asteroid Genera With Species Capable of Larval Cloning

K. EMILY KNOTT[1,*], ELIZABETH J. BALSER[2], WILLIAM B. JAECKLE[2], AND GREGORY A. WRAY[1,†]

[1] *Department of Ecology and Evolution, State University of New York, Stony Brook, New York 11794-5245; and* [2] *Department of Biology, Illinois Wesleyan University, Bloomington, Illinois 61702-2900*

Abstract. Asexual reproduction in larvae, larval cloning, is a recently recognized component of the complex life histories of asteroids. We compare DNA sequences of mitochondrial tRNA genes (Ala, Leu, Asn, Pro, and Gln) from larvae in the process of cloning collected in the field with sequences from adults of known species in order to identify asteroid taxa capable of cloning. Neighbor-joining analysis identified four distinct groups of larvae, each having no, or very little, sequence divergence (p distances ranging from 0.00000 to 0.02589); thus, we conclude that each larval group most likely represents a single species. These field-collected larvae cannot be identified to species with certainty, but the close assemblage of known taxa with the four larval groups indicates generic or familial identity. We can assign two of the larval groups discerned here to the genera *Luidia* and *Orcaster* and another two to the family Ophidiasteridae. This study is the first to identify field-collected cloning asteroid larvae, and provides evidence that larval cloning is phylogenetically widespread within the Asteroidea. Additionally, we note that cloning occurs regularly and in multiple ways within species that are capable of cloning, emphasizing the need for further investigation of the role of larval cloning in the ecology and evolution of asteroids.

Introduction

With the discovery of larval cloning (Bosch, 1988, 1992; Bosch *et al.*, 1989; Rao *et al.*, 1993; Jaeckle, 1994), new complexity has been recognized in the diverse developmental modes exhibited by asteroid echinoderms (sea stars). Nearly all asteroids reproduce sexually and have complex life cycles in which larval stages, having very different morphologies and habits from the adults, alternate with adult stages (Mortensen, 1921; Hyman, 1955; Chia and Walker, 1991). Asexual reproduction by adults is prevalent in some asteroid groups (*e.g.*, *Linckia*, *Coscinasterias*) and supplements the product of sexual reproduction by increasing the number of individuals derived from a given lineage. Asexual reproduction by larvae, larval cloning, is poorly understood, including which species are capable of it and what role it might play in the ecology and evolution of asteroids.

Three distinct modes of larval cloning have been observed in planktotrophic asteroid larvae collected from the field and reared in the laboratory (Bosch, 1988; Bosch *et al.*, 1989; Rao *et al.*, 1993; Jaeckle, 1994; Vickery and McClintock, 2000; Kitazawa and Komatsu, 2001). These modes—paratomy of the posterolateral arms, autotomization of the preoral lobe, and budding from the larval body and arm tips—share in common a period of dedifferentiation of larval tissues that are then redifferentiated in the clone (see Jaeckle, 1994, for details). Larval cloning in benthic, brooded, and pelagic lecithotrophic larvae has not been observed but may occur through some as yet unrecognized process. Clones are able to develop to and through metamorphosis and may themselves exhibit larval cloning (EJB and WBJ, pers. obs.; Vickery and McClintock, 2000; Kitazawa and Komatsu, 2001). However, it is not known whether juveniles derived from cloned larvae will develop to sexual maturity, or if larval cloning has fitness consequences for either the primary or cloned larvae. Larval

Received 18 October 2002; accepted 13 March 2003.

* To whom correspondence should be addressed. Present address: Department of Biological and Environmental Sciences, University of Jyväskylä, 40014 Jyväskylä, Finland. Email: kknott@cc.jyu.fi

† Current address: Department of Biology, Duke University, Durham, NC 27708-0338.

cloning could possibly have a significant impact on asteroid life history by altering such parameters as dispersal, number of individuals, or fitness, thus emphasizing the need to identify those asteroid species capable of larval cloning.

Asteroid larvae in the process of cloning have been collected from portions of the tropical and subtropical western Atlantic Ocean (Jaeckle, 1994), including the Sargasso Sea (Bosch, 1988; Bosch *et al.*, 1989), and from the Bay of Bengal (Rao *et al.*, 1993). These larvae can be very common in collections, constituting from 10% to 90% of the asteroid larvae present (Bosch, 1988; Bosch *et al.*, 1989; Jaeckle, 1994; EJB and WBJ, pers. obs.). However, field-collected cloning larvae have not been identified specifically. Initially, cloning larvae were thought to be restricted to species in the genus *Luidia*, which have bipinnaria larvae that lack a brachiolar complex and are, in some *Luidia* species, quite large (Wilson, 1978; Domanski, 1984; Bosch *et al.*, 1989). But Bosch (1992) and Jaeckle (1994) showed that larval cloning is not taxonomically restricted when they reported larval cloning in brachiolaria larvae, which are common to all asteroid orders except the Paxillosida (to which *Luidia* belongs).

Cloning larvae have been observed in laboratory cultures as well. Previous laboratory studies have noted larval cloning in members of the Paxillosida and Forcipulatida (EJB and WBJ, pers. obs.; Vickery and McClintock, 2000; Kitazawa and Komatsu, 2001). These occurrences, in species found in the north Pacific, indicate that larval cloning may be more widely distributed geographically than previously recognized. However, field-collected cloning larvae have not been reported in these areas, and whether larval cloning occurs naturally in these species (*i.e.*, outside the laboratory) is not known.

Our goal is to identify asteroid larvae capable of cloning by comparing the DNA sequences of unknown, field-collected cloning larvae and known adult species. Because most asteroid larvae are morphologically similar, field-collected larvae can rarely be identified to family level, much less to genus or species, by visual inspection of morphological characteristics. Indirect identification of asteroid larvae based on correlations with geographical distributions of adults is unlikely because larvae may have great dispersal potential and do not necessarily remain close to their parental population (Thorson, 1961; Strathmann, 1974; Scheltema, 1986). Morphological identification of juveniles after metamorphosis is possible, but not always practical or dependable. Asteroid larvae are sensitive to laboratory culturing conditions (Strathmann, 1987), can take weeks to develop (*e.g.*, Komatsu *et al.*, 1991), and can delay metamorphosis for several months if a suitable settlement cue is not found (Pechenik, 1990). Often, laboratory cultures die before the larvae reach metamorphosis or before juveniles are large enough to be identified. As an alternative to culturing methods, we have used DNA sequence similarity to identify field-collected cloning asteroid larvae. DNA sequencing techniques are universally known and easily implemented in the laboratory for a quick assessment of potential larval identity. Identity then can be verified with more time-consuming laboratory culturing techniques.

Materials and Methods

We investigated the identity of field-collected cloning asteroid larvae by comparing the DNA sequences of five mitochondrial tRNA genes (Ala, Leu, Asn, Pro, and Gln) from the larvae to complementary sequences from adults of known species. The suitability of this gene region for species identification was initially assessed by comparing sequences obtained from a single known larva of *Luidia clathrata* to sequences from related, known adult asteroids. Comparison of sequences from the *L. clathrata* larva, a *L. clathrata* adult from a different locality, other *Luidia* species, and species from the closely related genera *Astropecten* and *Ctenodiscus* are shown in Table 1. The sequences obtained for the *L. clathrata* larva and adult are identical. However, significant nucleotide changes are observed between *L. clathrata* (larva and adult) and other *Luidia* species, as well as between *L. clathrata* (larva and adult) and species in other genera, which are reflected in genetic distances among species (Table 2).

Larvae used in our comparisons were collected from the tropical and subtropical western Atlantic Ocean, specifically from off the western shore of Barbados (31° 2″ N, 59° 4″ W) and from the Gulf Stream off the eastern shore of Florida (27.3° N, 79.6° W), by EJB and WBJ. Cloning larvae have been collected consistently and in large numbers at the Gulf Stream site (EJB and WBJ, pers. obs.). Individual larvae were scored for the presence and type of cloning exhibited. Most of the larvae were cloning by paratomy, but one was cloning by autotomy of the preoral lobe. Those that were not cloning (14 of 65) were similar to cloning larvae found in the same or in other collections, and so were assumed to have the ability to clone (Fig. 1). All larvae were preserved in 95% EtOH and shipped to SUNY Stony Brook for processing.

The five mitochondrial tRNA genes of interest (Ala, Leu, Asn, Pro, and Gln) were amplified from individual larvae using the polymerase chain reaction (PCR) and published echinoderm-specific primers (Smith *et al.*, 1993; Hart *et al.*, 1997). A typical total genomic DNA extraction was avoided because these extraction techniques often require a large amount of starting material. Instead, the entire larval body (first air-dried to remove traces of EtOH) was used in PCR as the DNA template (Medeiros-Bergen *et al.*, 1995). The thermocycling conditions of PCR are severe enough to disrupt the larval cells, releasing their DNA. Amplifications

Table 1

Alignment of tRNA sequences (Ala, Leu, Asn, Pro, and Gln) showing complete sequence identity between Luidia clathrata *adult and larva; sequence differences between* Luidia clathrata *and other* Luidia *species (*), other closely related genera (+), or both (^) are marked*

```
                Ala
Luidia clathrata      -GTGAATTTAGTTTAAAA-GAA--AAAACCTTTGATTTGCATTCAAAAA----------A-TTTAGGT--TTAAGACCTAAAATTTACA---
L. clathrata larva    -GTGAATTTAGTTTAAAA-GAA--AAAACCTTTGATTTGCATTCAAAAA----------A-TTTAGGT--TTAAGACCTAAAATTTACA---
L. magellanica        -GTGAATTTAGTTTAACA-GAA--AAAACATTTGATTTGCACTCAAACA----------A-TTTAGGT--TTAAACCCTAAAGTTTACA---
L. foliolata          -GTGAATTTAATTTAAAA-GAA--AAAATATTTGATTTGCATTCAAACA----------A-TTTAGGT--TTAAAGCCTAAAGTTCACA---
L. alternata          -GTGAATTCAGTTTAAGA-GAA--AAAACTTTTGACTTGCATTCAAAAA----------A-TTTAGGT--TTAACTCCTAAAATTTACA---
Astropecten           -GTGAATTTAGTTTAAAA-GAC--AAAACATTTGATTTGCATTTAAAAA----------A-TCCAGGT--TTAATTCCTGGAATTCACA---
Ctenodiscus           -GTGAATTTAGTTTAAAA-GAT--AAAACATTTAATTTGCATTTAAAAA----------C-TTCAAGT--TTAACCCCTGAAATCCACA---
                             * *     *    +      *^   + *     * +   *                  +  ++          ^^    ++ * +^
                Leu
Luidia clathrata      -GCTAAAATAGCAAAGTG-GTA--AATGCTGTAGATTTAGGTTCTATTA----------T-CAAAGGTTCAAATCCTTTTTTTAGTT---
L. clathrata larva    -GCTAAAATAGCAAAGTG-GTA--AATGCTGTAGATTTAGGTTCTATTA----------T-CAAAGGTTCAAATCCTTTTTTTAGTT---
L. magellanica        -GCTAGAATAGCAAAGGG-GTA--AATGCAATAGATTTAGGATTTATTA----------T-CAAAGGTTCAATTCC-TTTTTTAGTT---
L. foliolata          -GCTAAAATAGCAAAGTG-GTA--AATGCAATAGATTTAGGATTTATTA----------C-CAAAGGTTCAATTCCTTTTTTTAGTT---
L. alternata          -ACTTAGGTAGCAAAGCG-GTA--AATGCGGTAGATTTAGCATCTATTA----------T-CAGGGGTTCGATTCTCTTCCTTAGTT---
Astropecten           -GTTAGAATAGCAAAGGG-GAA--AATGCAATAGATTTAGGATCTGTCA----------T-CAAGAGTTCGAGTCTCTTTTCTAGTT---
Ctenodiscus           -ACTGAGGTAGCAAAGTG-GTG--AATGCGGCAGATTTAGGATTTGTTA----------T-CAAGGGTTCTAATCCCTTTCTTAGTT---
                       ^+ ^^^^       ^   ++      ^^+        ^ ^ + +               *   *^+    ^ ^  ^^  *^+
                Asn
Luidia clathrata      -TGGGTTGTAGCCTAGT--GGA--AAGGCAACTGGCCGTTAACCAGGAG----------ATAACAAGATCAATACTTGTCAACTCAG---
L. clathrata larva    -TGGGTTGTAGCCTAGT--GGA--AAGGCAACTGGCCGTTAACCAGGAG----------ATAACAAGATCAATACTTGTCAACTCAG---
L. magellanica        -TGGGTTGTAGCCTAGC--GGA--AAGGCAACTGGCCGTTAACCAGGAG----------ATAACAAGATCAATACTTGTCAACTCAG---
L. foliolata          -TGGGTTGTAGCCTAGT--GGA--AAGGCAACTGGCCGTTAACCAGGAG----------ATAACAAGATCAATACTTGTCAACTCAG---
L. alternata          -TGGGTTGTAGCCTAGT--GGA--AAGGCAACTGGCCGTTAACCAGGAG----------ATAACAAGATCAATACTTGTCAACTCAG---
Astropecten           -TGGGTTGTAGCCTAAT--GGA--AAGGCAATTGGCCGTTAACCAGGAG----------ATAGTAAGATCAATACTTACCAACTCAG---
Ctenodiscus           -TGGGTTGTAGCCTAGT--GGA--AAGGCAATTGGCCGTTAACCAGGAG----------ATAACAAGATCAATACTTGTCAACTCAG---
                              +*             +                                    ++            ++
                Pro
Luidia clathrata      -CAGAGAATAGTTTAATT-TAG--AGAATTGTAACTTTGGGAGTTATTG----------G-TACAAATATA-GAGTTTTGTTTCTCTGA---
L. clathrata larva    -CAGAGAATAGTTTAATT-TAG--AGAATTGTAACTTTGGGAGTTATTG----------G-TACAAATATA-GAGTTTTGTTTCTCTGA---
L. magellanica        -CA?AGAATAGTTTAATT-TAAA-AGAATTGTAACTTTGGGAGTTATTG----------G-TGCAAATGTA-AAGTTTTGTTTCTCTGA---
L. foliolata          -CAGAGAATAGTTTAACA-TAAA-AGAATTATAACTTTGGGAGTTATAG----------G-TGCAAATGTA-GAGTTTTGTCTCTCTGA---
L. alternata          -CAGAGAATAGTTTAGTT-T----AGAATAATAACTTTGGGAGTTATTG----------G-TGCAAATATA-GAGTTTTGTTTCTCTGA---
Astropecten           -CAGAAAATAGTTTAATT------AGAATAATAACTTTGGGAGTTATTG----------G-TGTAAATATA-GAGTTTTATTTTTCTGA---
Ctenodiscus           -CAGGAAATAGTTTAATA------AGAATGATAGCTTTGGGAGTTGTTA----------G-TGTAAATATG-GAATTTTACTTTTCTGA---
                          ++          *^  +^^*       ^^   +                        ^+    * + * +    ++* +
                Gln
Luidia clathrata      -TAGAAAGTAGTATAAT--GGA--ATTACAAAGATCTTTGACTTCTTAA----------A-TATAAGTTCAATCCTTATCTTTCTAA---
L. clathrata larva    -TAGAAAGTAGTATAAT--GGA--ATTACAAAGATCTTTGACTTCTTAA----------A-TATAAGTTCAATCCTTATCTTTCTAA---
L. magellanica        -TAGAAAGTAGTATAAA--GGT--ATTACAAAGATCTTTGACTTCTTAA----------A-CATAAGTTCAATTCTTATCTTTCTAA---
L. foliolata          -TAGAAAGTAGTATAAA--GGC--ATTACAAAGATCTTTGACTTCTTAA----------A-CATAAGTTCAATTCTTATCTTTCTAA---
L. alternata          -TAGAAAGTAGTATAGGC-GGA--ATTACAAAGACCTTTGACCTCTTAA----------A-CATAAGTTCAACTCTTGTCTTTCTAA---
Astropecten           -TAGAAAGTAGTATAAT--GGT--AAAACAAAGAACTTTGACTTCTTTA----------A-TATAAGTTCAATTCTTATCTTTCTAA---
Ctenodiscus           -TAGAAAGTAGTATAAC--GGC--AATACATAGAACTTTGATTTCTTAA----------C-TACAAGTTCAATTCTTGTCTTTCTAA---
                             *^*   ^   ++   +   ^       +*     +                  + * +       *^   ^
```

Table 2

Genetic distances calculated using methods for uncorrected (p) *distance between tRNA genes from a known* Luidia clathrata *larva, other* Luidia *species and species from closely related genera*

	1	2	3	4	5	6	7
1. *Luidia clathrata*	----						
2. *Luidia clathrata* larva	0.00000	----					
3. *Luidia magellanica*	0.06422	0.06422	----				
4. *Luidia foliolata*	0.06948	0.06948	0.04450	----			
5. *Luidia alternata*	0.09243	0.09243	0.10482	0.11230	----		
6. *Astropecten*	0.12597	0.12597	0.12657	0.13699	0.14601	----	
7. *Ctenodiscus*	0.14561	0.14561	0.16100	0.15135	0.14592	0.14566	----

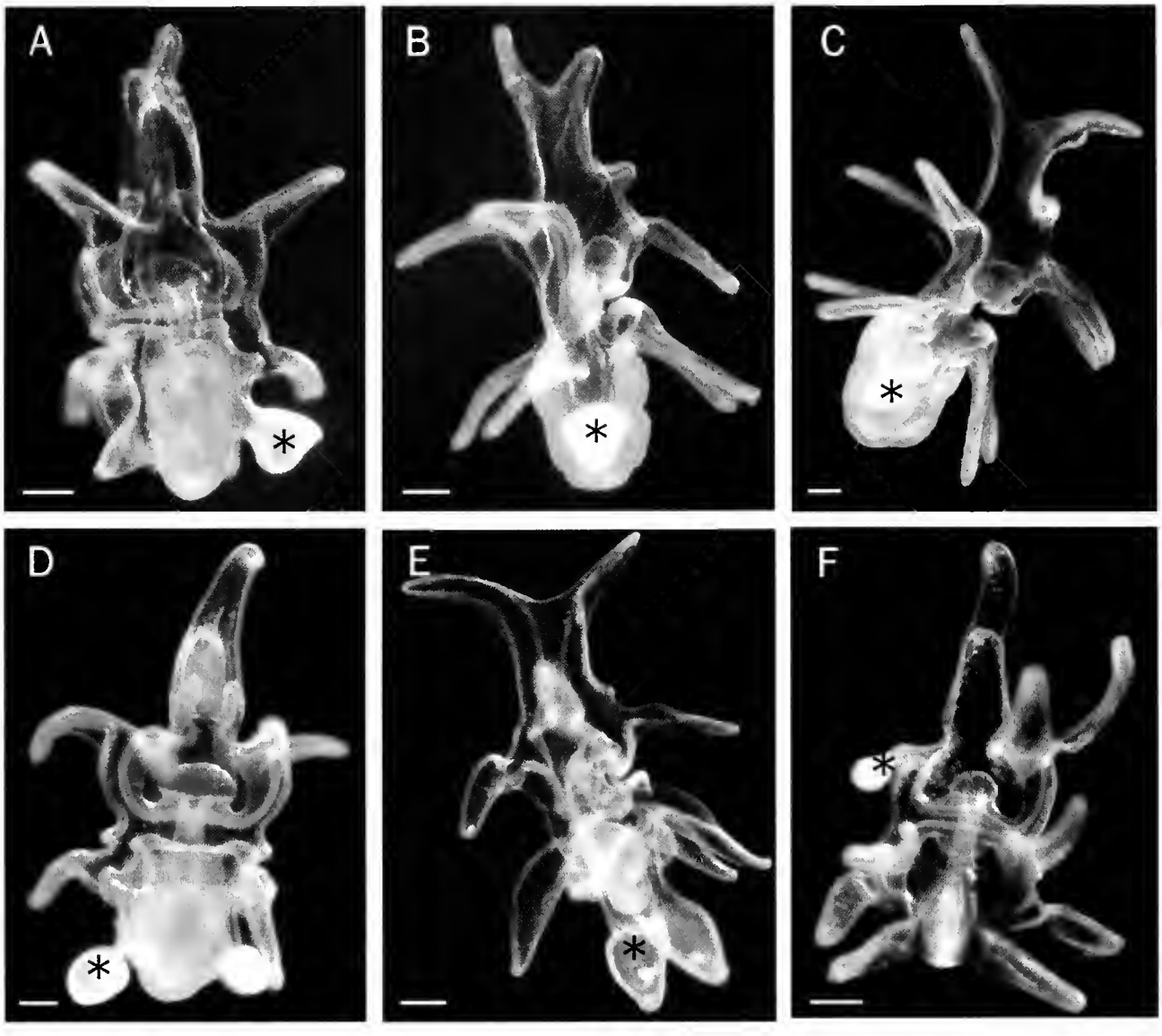

Figure 1. Representative asteroid larvae with clones collected from plankton samples taken off the eastern coast of Florida. Obvious morphological characters such as color and arm length appear to be labile and are unreliable as taxonomic characters. Definitive morphotypic characters distinguishing species have not yet been identified. (A-D) Brachiolariae included in larval group 1. (E) Bipinnaria of larval group 2, which includes at least one *Luidia* species. (F) Bipinnaria from larval group 3/4. Asterisks indicate larval clones. Scale bars = 150 μm.

were successful for 44 out of 65 (68%) larvae collected. Amplification reactions were carried out in 25-μl volumes of a standard reaction mix with Taq DNA polymerase (GIBCO Life Technologies) using a MJ Research PTC-200 thermocycler. All samples were purified in 2% NuSieve agarose (FMC BioProducts) and gel extracted (QIAGEN or GIBCO Life Technologies kits). Purified samples were chemically transformed (Brown, 1991) into XLI Blue (Stratagene) competent cells using pGEM-T vector (Promega). Cloned samples were purified with Wizard *Plus* Miniprep purification kit (Promega), sequenced in forward and reverse directions using vector sequence primers [M13 (−20) M13 (rev)] and dye-terminator sequencing reaction mix, and analyzed with an ABI 373 automated sequencer (PE Applied Biosystems). Sequence data from both strands were combined and edited with Sequencher 3.0 (Gene Codes Corporation, 1995) and aligned by eye in accordance with established tRNA alignment of other taxa based on the molecular structure of tRNAs (Sprinzl *et al.*, 1998). Larval sequences were then aligned to similarly aligned sequences

of the same genes from known adult asteroid species (Himeno *et al.*, 1987; Hart *et al.*, 1997; Knott and Wray, 2000; KEK, unpubl. data). Regions between the tRNA genes were also sequenced. These sequences were variable among the asteroid taxa and could not be aligned. Since an assessment of homology of the inter-gene sequences could not be made, they were eliminated from the data set.

The combined aligned data set was analyzed with multiple distance criteria using PAUP* ver. 4.0b4a (Swofford, 1998) to assess the degree of sequence similarity. Sequence differences were calculated first as uncorrected (*p*) distance, a measure of the number of aligned sequence positions containing non-identical nucleotides divided by the total number of positions compared. Genetic distance was then calculated using modified methods that account for superimposed mutational events according to the Jukes-Cantor and Kimura 2-parameter models of evolutionary change (described in Swofford *et al.*, 1996). Genetic distances obtained from all methods were then used in neighbor-joining analysis. Differences in trees obtained using different genetic distance calculations were assessed with the Kishino and Hasegawa (1989) and Templeton (1983) nonparametric tests in PAUP*. Stability of clades in the resulting trees was assessed by bootstrap analyses (1000 replicates; Felsenstein, 1985).

Results and Discussion

Neighbor-joining analysis using three methods of calculating genetic distances resulted in only slightly different tree topologies. Analysis of uncorrected (*p*) distances and Jukes-Cantor distances yielded identical tree topologies. Analysis of Kimura 2-parameter distances yielded a longer tree topology that was statistically different when tested with the Kishino and Hasegawa test ($P = 0.013$) and Templeton nonparametric test ($P = 0.013$). However, because none of the relationships in clades including cloning larvae were affected by the genetic distance calculation used, only the tree generated using uncorrected (*p*) distances is shown and discussed (Fig. 2).

Analysis of sequence similarity identified four distinct groups of cloning larvae. Within these groups there was very little sequence divergence (*p* distances ranging from 0.00000 to 0.02589), indicating that each group most likely represents a single species (Table 3). However, neighbor-joining analysis of the tRNA sequences did not place any of the 44 known adult asteroid species analyzed here within the larval groups (Fig. 2). The field-collected larvae thus cannot be identified to species with the limited number of sequences from known asteroid species available for comparison. However, the close assemblage of adults of known taxa with the four larval groups identifies those genera or families with species capable of larval cloning and indicates species likely to be capable of larval cloning. Representative larvae from the identified larval groups are shown in Figure 1. This is the first study to identify field-collected cloning larvae.

The largest group of cloning larvae (group 1: 24 individuals) has sequences with high similarity to those from two *Oreaster* species, which group basally to the larvae. Both larval group 1 and the *Oreaster* clade are well supported (bootstrap percentages: 100 and 73 respectively), as is the grouping of larval group 1 with the *Oreaster* clade (100% bootstrap support). *Oreaster reticulatus* is common in the tropical western Atlantic where the cloning larvae were collected, whereas *O. occidentalis* is found in the eastern Pacific. The only other species of *Oreaster* in the Atlantic Ocean is *O. clavatus*, found in the eastern Atlantic from Cape Verde to the Gulf of Guinea (Clark and Downey, 1992). *O. clavatus* was not included in this analysis, and may be a good candidate species for the identity of larval group 1. The genetic distance observed between the *Oreaster* species and larval group 1 is not large (range: 0.06745 to 0.10026; average: 0.08262) and is comparable to other intra-genus distances (Table 3). However, some very closely related genera (within the same family) have genetic distances as low as that seen between larval group 1 and the *Oreaster* clade. Thus, it is also possible that the larvae could belong to a species in a genus closely related to *Oreaster*. If so, the species identity of larval group 1 must lie with a very close relative of *Oreaster*, perhaps within its taxonomic family, the Oreasteridae, or within another closely related family, the Asteropseidae (Blake, 1987).

Generic identification is more certain for a smaller group of cloning larvae (group 2; 5 individuals) and a single cloning larva, both of which fall within a clade of *Luidia* species (96% bootstrap support). There are seven *Luidia* species in the tropical and subtropical western Atlantic Ocean (Clark and Downey, 1992). Our analysis includes two of these, as well as other *Luidia* species from the Pacific Ocean. The western Atlantic species not represented here are good candidates for the species identity of larval group 2 and the single cloning larva contained in this clade. Relationship of the five individuals in larval group 2 is well supported, in 100% of bootstrap replicates. The single cloning larva does not group with larval group 2, and instead is unresolved in a polytomy with the Pacific *Luidia* species. The grouping of this individual with the Pacific species is only moderately supported with bootstrap analyses (68%), so its affinities to other *Luidia* species are unclear. However, genetic distance between this individual and larval group 2 is high (averaging 0.08958). Since genetic distances within larval group 2 are over 30 times lower (average: 0.00278), it is unlikely that the single cloning larva is also member of this group. Likewise, genetic distances between known *Luidia* species and larval group 2 are also high (range: 0.07524

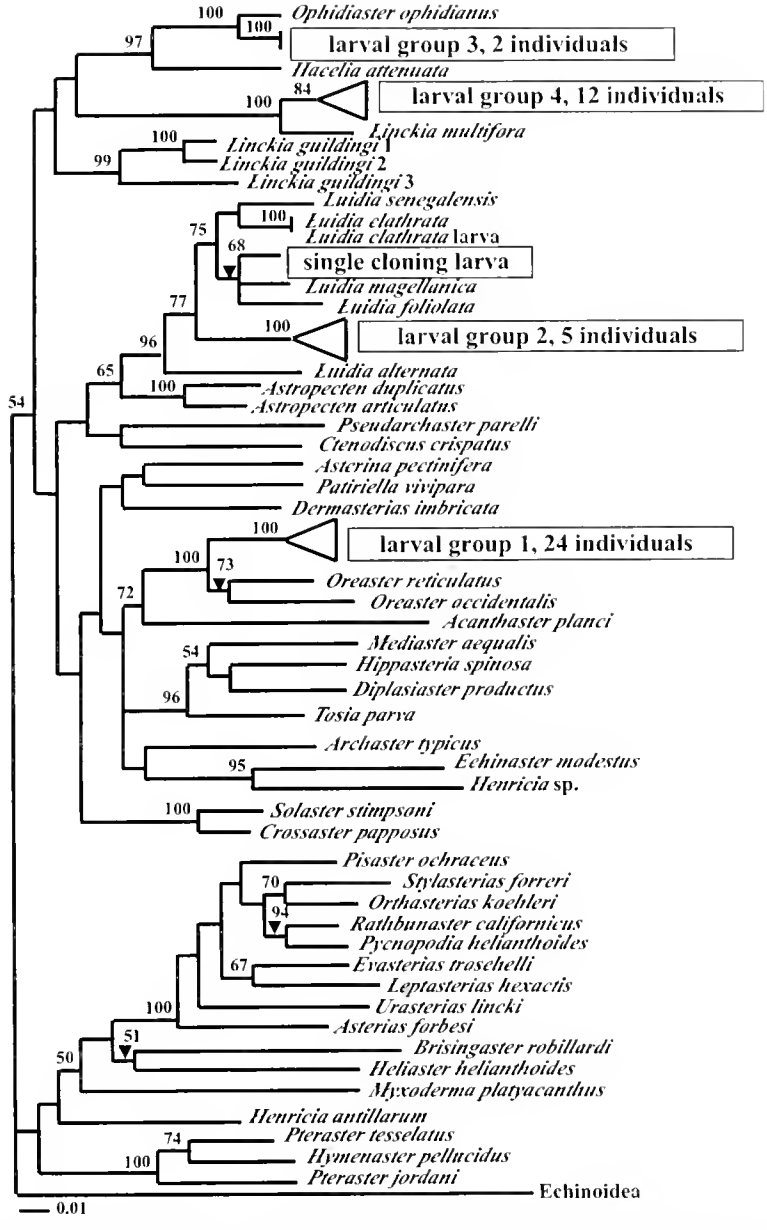

Figure 2. Phylogenetic tree resulting from neighbor-joining analysis of uncorrected (*p*) distances between mitochondrial tRNA sequences of known asteroid species and field-collected cloning larvae. Field-collected cloning larvae fall into four distinct groups and one single cloning larva (boxed), which are phylogenetically widespread. Numbers of larvae in each larval group are indicated. Numbers at nodes within the tree are bootstrap percentages from 1000 replicates. Larval tRNA sequences are accessioned in GenBank under numbers AY249946–AY249978. GenBank accession numbers for known asteroid taxa include some published previously (Himeno *et al.*, 1987; Hart *et al.*, 1997; Knott and Wray, 2000) and AY245490–AY245506.

to 0.11438), similar to those seen between species of the same genus (Table 3). The sequence differences between larval group 2, the single cloning larva, and other *Luidia* species suggests that multiple species within *Luidia* are capable of larval cloning. The alternative, that there may be genetic variation within species complicating our similarity analyses, is not likely given that intra-species genetic distances determined in this and other studies are very low (Table 3). Sequences from a known larva of *L. clathrata* and an adult representative of this species from a different locality are identical and group together in neighbor-joining analysis with 100% bootstrap support (Tables 2 and 3).

The remaining two groups of cloning larvae (group 3 with 2 individuals and group 4 with 12 individuals) show

Table 3

Genetic distances observed between asteroid taxa at different taxonomic levels; genetic distance reported is calculated from tRNA genes (*) or the COI gene (°)

Taxonomic Level	Species	Distance	Reference
Intra-species	Larval group 1	0.00000*	This paper
	Larval group 2	0.00278*	This paper
	Larval group 3	0.00557*	This paper
	Larval group 4	0.00000*	This paper
	Luidia clathrata	0.00000*	This paper
	Linckia guildingi	0.00000°	Williams 2000
	Patiriella brevispina	0.00843*	Hart *et al.* 1997
Intra-genus	Larval group 1 and *Orcaster* species	0.08262*	This paper
	Larval group 2 and single cloning larva	0.08958*	This paper
	Larval group 3 and *Ophidiaster* species	0.03354*	This paper
	Luidia clathrata and *Luidia altemata*	0.09243*	This paper
	Linckia guildingi and *Linckia laevigata*	0.15940°	Williams 2000
	Orcaster reticulatus and *Orcaster occidentalis*	0.07812*	Hart *et al.* 1997
	Asterina gibbosa and *Asterina miniata*	0.10050*	Hart *et al.* 1997
Inter-genus	*Luidia clathrata* and *Astropecten articulatus*	0.11293*	This paper
	Linckia guildingi and *Fromia indica*	0.21626°	Williams 2000
	Asterina gibbosa and *Patiriella brevispina*	0.10687*	Hart *et al.* 1997
	Orcaster reticulatus and *Asterinia miniata*	0.14916*	Hart *et al.* 1997

affinities to the asteroid family Ophidiasteridae. The two cloning larvae in larval group 3 have very low genetic distance (0.00557), and their relationship is well supported with bootstrap analyses (100% of replicates). These larvae are most closely related to *Ophidiaster ophidianus*, a species that ranges in the eastern Atlantic from the Azores to the Gulf of Guinea (Clark and Downey, 1992). Most likely, *O. ophidianus* larvae would not be collected in the western Atlantic Ocean, so the larvae in group 3 probably belong to some other *Ophidiaster* species. Genetic distances between *O. ophidianus* and the cloning larvae of group 3 (0.02796 and 0.03354) are higher than intra-species genetic distances for other asteroids (Table 3), giving more evidence that their species identity is probably not *O. ophidianus*, but some other close relative. The other "ophidiasterid" group of cloning larvae (group 4; 12 individuals) is strongly supported with bootstrap analyses (84% of replicates). Together, the larvae group with the species *Linckia multifora* (100% bootstrap support). *L. multifora* does not exist in the Atlantic Ocean (Clark and Downey, 1992), so the larvae examined here are not expected to be members of this species. *Linckia guildingi* specimens collected from three localities also included in this study do not group with *L. multifora* and larval group 4 directly, as would be expected for species in the same genus. Instead, these species group basally to all the ophidiasterid taxa, a grouping that is not supported by bootstrap analyses. Genetic distances among the 12 individuals in larval group 4, and between these larvae and other ophidiasterid species, are shown in Table 4. Certainly, additional species should be sequenced to test these relationships, particularly other *Linckia* species not sampled in this study.

One of the larval groups identified here (group 1; 24 individuals), has members that display different modes of larval cloning (paratomy and autotomy). Although different modes of cloning were not exhibited by individuals simultaneously, the species represented by larval group 1, identified here, has the capability to reproduce asexually in multiple ways. The fact that a single species is capable of multiple modes of larval cloning has been reported for laboratory-cultured species (Vickery and McClintock, 2000; Kitazawa and Komatsu, 2001) but not for field-collected individuals.

Our results also indicate that larval cloning occurs regularly within asteroid species. The three larval groups containing more than two individuals (groups 1, 2, and 4) are composed of larvae that were collected at different localities (Barbados and Florida). In addition, cloning larvae with morphological types identical to those studied here have been collected at these sites over multiple years. Regular occurrence of larval cloning is implied in a recent experimental study of larval cloning in the laboratory. Vickery and McClintock (2000) show that cloning occurs in laboratory-cultured *Pisaster ochraceus* only at temperatures and food regimes similar to those the larvae would encounter in the field, rather than of extremes of temperature and food abundance or composition. We expect that the regular occurrence of larval cloning is more common than sporadic cloning in response to environmental variation. The effects

Table 4

Genetic distances between the 12 individuals in larval group 4 and closely related taxa in the Ophidiasteridae, calculated using methods for uncorrected (p) *distance*

TAXA	1.	2.	3.	4.	5.	6.	7.	8.	9.	10.	11.	12.	13.	14.	15.	16.
1. larva 1	----															
2. larva 2	0.0028	----														
3. larva 3	0.0028	0.0057	----													
4. larva 4	0.0000	0.0029	0.0028	----												
5. larva 5	0.0000	0.0029	0.0028	0.0000	----											
6. larva 6	0.0028	0.0057	0.0057	0.0028	0.0028	----										
7. larva 7	0.0028	0.0057	0.0057	0.0028	0.0028	0.0057	----									
8. larva 8	0.0000	0.0028	0.0028	0.0000	0.0000	0.0028	0.0028	----								
9. larva 9	0.0057	0.0085	0.0085	0.0057	0.0057	0.0085	0.0085	0.0057	----							
10. larva 10	0.0028	0.0029	0.0058	0.0028	0.0028	0.0057	0.0057	0.0028	0.0087	----						
11. larva 11	0.0057	0.0085	0.0085	0.0057	0.0057	0.0085	0.0085	0.0057	0.0113	0.0086	----					
12. larva 12	0.0172	0.0201	0.0201	0.0172	0.0172	0.0201	0.0201	0.0172	0.0230	0.0203	0.0230	----				
13. *Linckia multifora*	0.0398	0.0427	0.0427	0.0398	0.0398	0.0426	0.0426	0.0398	0.0456	0.0432	0.0455	0.0549	----			
14. *L. guildingi* 1	0.2170	0.2199	0.2198	0.2170	0.2170	0.2169	0.2199	0.2170	0.2227	0.2228	0.2228	0.2170	0.2287	----		
15. *Hacelia attenuata*	0.2027	0.2056	0.2054	0.2027	0.2027	0.2026	0.2055	0.2027	0.2084	0.2053	0.2083	0.2083	0.2226	0.1552	----	
16. *Ophidiaster ophidianus*	0.1998	0.2026	0.2026	0.1998	0.1998	0.1997	0.2027	0.1998	0.2054	0.2024	0.2056	0.2026	0.2195	0.1581	0.1032	----

of regular cloning on asteroid life history and population dynamics are unknown.

Conclusions

Identification of asteroid species capable of larval cloning is an important first step for continued study of this unusual reproductive strategy, and we have shown that field-collected cloning larvae can be identified using molecular techniques. Beyond a broad understanding of the morphological changes involved in larval cloning, very little is known about the processes of cloning or its role, if any, in the ecology and evolution of asteroids (Jaeckle, 1994). Once field-collected cloning larvae are identified, experiments for determining the role of larval cloning in asteroid life history, population dynamics, and developmental evolution can be pursued.

Our results indicate that there are four (possibly five) species capable of larval cloning in the tropical/subtropical western Atlantic Ocean. Species cannot be definitively identified at this time, but we can tentatively assign two of the larval groups discerned here to the genera *Luidia* and *Oreaster* and another two to the family Ophidiasteridae. Our identification of a *Luidia* species that is capable of larval cloning is not surprising. The initial description of paratomy in a field-collected larva was diagnosed to the asteroid genus *Luidia* on the basis of unique larval anatomical features (see Introduction). Our results, with a tentative identification to *Oreaster* and with larval groups falling outside the Paxillosida, support Bosch's (1992) and Jaeckle's (1994) observations that larval cloning is not restricted to *Luidia* and the Paxillosida. Within the asteroid family Ophidiasteridae, many species are capable of asexual reproduction as adults, particularly *Linckia*. The presence of larval cloning in species that also alternate between sexual and asexual reproduction as adults would be a complex twist to more typical asteroid life-history strategies.

Although Lacalli (2000) has claimed that larval cloning in asteroids is not common, our results indicate the opposite. This phenomenon has most likely been overlooked by echinoderm biologists, and as yet we cannot be sure how common it is. For example, clones in laboratory cultures may appear to be malformed embryos resulting from irregular development or unusual laboratory conditions and thus disregarded. Similarly, field-collected cloning larvae or developing clones may be misinterpreted as individuals that were damaged during collection (Bosch *et al.*, 1989). We feel certain that increased awareness by echinoderm biologists will produce more reports of larval cloning in asteroids, and perhaps in other echinoderms. Cloning has already been observed in the Ophiuroidea, sister group to the Asteroidea (Balser, 1998). Species identifications are necessary for studying larval cloning in a phylogenetic context. Results presented here are the beginning of an ongoing evolutionary analysis of the possibly ancient origin of larval cloning, with losses in some asteroid groups; or alternatively, multiple origins of larval cloning within the Asteroidea. Certainly, evidence of parallel evolution of derived larval forms is common among marine invertebrates (Strathmann, 1978;

Wray, 1996; Hart, 2000). Despite being only recently confirmed in asteroids (Bosch *et al.*, 1989; Jaeckle 1994), larval cloning may have an ancient evolutionary origin.

The larval groups, or species, discerned here consist of multiple cloning larvae collected from different localities. Widespread occurrence of cloning larvae may not be surprising, since planktonic larvae of asteroids can disperse great distances. In addition, the adults of many asteroid species have broad geographic ranges that in some cases extend beyond the area sampled here. The identification of different modes of larval cloning within one species (larval group 1) is a bit more surprising, despite observations of multiple modes of cloning in laboratory-cultured species (Vickery and McClintock, 2000; Kitazawa and Komatsu, 2001). The modes of larval cloning observed here, paratomy and autotomy, are morphologically very distinct. They affect different regions of the larval body, and they lead to different developmental regimes for the resulting clones (Jaeckle, 1994). Our results imply that the different modes of larval cloning may be less distinct than previously thought and call for further investigation of the developmental mechanisms involved in larval cloning.

Acknowledgments

Many thanks go to Bill Allison, Richard Emlet, Igor Gorchakov, Dan Janies, Sue Lisin, Christopher Lowe, Chris Mah, Peter Wirtz, and Craig Young for providing the adult samples used in this study. This work was supported in part by a National Geographic Society grant 6267-98 to E. J. Balser and W. B. Jaeckle. We also thank the Smithsonian Marine Station in Ft. Pierce, Florida, for laboratory space and assistance collecting specimens. Collection of larvae in Barbados was facilitated by the Bellairs Research Institute and IWU students, Tyrone Summers, Kristopher Mitchell, and Andrew Boyden. Contribution 1100 from the Department of Ecology and Evolution at the State University of New York, Stony Brook.

Literature Cited

Balser, E. J. 1998. Cloning by ophiuroid echinoderm larvae. *Biol. Bull.* **194:** 187–193.

Blake, D. B. 1987. A classification and phylogeny of post-Paleozoic sea stars (Asteroidea: Echinodermata). *J. Nat. Hist.* **21:** 481–528.

Bosch, I. 1988. Replication by budding in natural populations of bipinnaria larvae from the sea star genus *Luidia*. P. 728 in *Echinoderm Biology*, R D. Burke, P.V. Mladenov, P. Lambert, and R.L. Parsley, eds. A.A. Balkema, Rotterdam.

Bosch, I. 1992. Symbiosis between bacteria and oceanic cloning sea star larvae in the western North Atlantic Ocean. *Mar. Biol.* **114:** 495–502.

Bosch, I., R. B. Rivkin, and S. P. Alexander. 1989. Asexual reproduction by oceanic planktotrophic echinoderm larvae. *Nature* **337:** 169–170.

Brown T. A. 1991. *Essential Molecular Biology: A Practical Approach.* Oxford University Press, New York

Chia, F. S., and C. W. Walker. 1991. Echinodermata: Asteroidea. Pp. 301–353 in *Reproduction of Marine Invertebrates, Vol VI: Echinoderms and Lophophorates*, A. C. Giese, J. S. Pearse, and V. B. Pearse, eds. Boxwood Press, Pacific Grove, CA.

Clark, A. M., and M. E. Downey. 1992. *Starfishes of the Atlantic.* Chapman and Hall, London.

Domanski, P. A. 1984. Giant larvae: prolonged planktonic larval phase in the asteroid *Luidia sarsi*. *Mar. Biol.* **80:** 189–195.

Felsenstein, J. 1985. Confidence limits on phylogenies: an approach using the bootstrap. *Evolution* **39:** 783–791.

Gene Codes Corporation. 1995. *Sequencher 3.0.* Gene Codes Corporation, Ann Arbor, MI.

Hart, M. W. 2000. Phylogenetic analyses of mode of larval development. *Semin. Cell Dev. Biol.* **11:** 411–418.

Hart, M. W., M. Byrne, and M. J. Smith. 1997. Molecular phylogenetic analysis of life-history evolution in asterinid starfish. *Evolution* **51:** 1848–1861.

Himeno, H., H. Masaki, T. Kawai, T. Ohta, I. Kumagai, K. Miura, and K. Watanabe. 1987. Useful genetic codes and a novel gene structure for tRNA (AGY Ser) in starfish mitochondrial DNA. *Gene* **56:** 219–230.

Hyman, L. H. 1955. *The Invertebrates: Echinodermata*, Vol. 4. McGraw-Hill, New York.

Jaeckle, W. B. 1994. Multiple modes of asexual reproduction by tropical and subtropical sea star larvae: an unusual adaptation for genet dispersal and survival. *Biol. Bull.* **186:** 62–71.

Kishino, H., and M. Hasegawa. 1989. Evaluation of the maximum likelihood estimate of the evolutionary tree topologies from DNA-sequence data and the branching order in Hominoidea. *J. Mol. Evol.* **29:** 170–179.

Kitazawa, C., and M. Komatsu. 2001. Larval development and asexual development of the sea star, *Distolasterias nipon* (Doderlein). P. 177 in *Echinoderms 2000*, M. F. Barker, ed. Swets and Zeitlinger, Lisse, The Netherlands.

Knott, K. E., and G. A. Wray. 2000. Controversy and consensus in asteroid systematics: new insights to ordinal and familial relationships. *Am. Zool.* **40:** 382–392.

Komatsu, M., C. Oguro, and J. M. Lawrence. 1991. A comparison of development in three species of the genus *Luidia* from Florida. Pp. 489–498 in *Biology of Echinodermata*, T. Yanagisawa, I. Yasumasu, C. Oguro, N. Suzuki, and T. Motokawa, eds. A. A. Balkema, Rotterdam.

Lacalli, T. C. 2000. Larval budding, metamorphosis, and the evolution of life-history patterns in echinoderms. *Invertebr. Biol.* **119:** 234–241.

Medeiros-Bergen, D. E., R. R. Olson, J. A. Conroy, and T. D. Kocher, 1995. Distribution of holothurian larvae determined with species-specific probes. *Limnol. Oceanogr.* **40:** 1225–1235.

Mortensen, T. 1921. *Studies on the Development and Larval Forms of Echinoderms.* Gottlieb Ernst Clausen Gad Publishers, Copenhagen.

Pechenik, J. A. 1990. Delayed metamorphosis by larvae of benthic marine invertebrates: Does it occur? Is there a price to pay? *Ophelia* **32:** 63–94.

Rao, P. S., K. H. Rao, and K. Shyamasundari. 1993. A rare condition of budding in bipinnaria larva (Asteroidea). *Curr. Sci.* **65:** 792–793.

Scheltema, R. S. 1986. Long distance dispersal by planktonic larvae of shallow water benthic invertebrates among Pacific islands. *Bull. Mar. Sci.* **39:** 241–256.

Smith, M. J., A. Arndt, S. Gorski, and E. Fajber. 1993. The phylogeny of echinoderm classes based on mitochondrial gene arrangements. *J. Mol. Evol.* **36:** 545–554.

Sprinzl, M., C. Horn, M. Brown, A. Ioudovitch, and S. Steinberg. 1998. Compilation of tRNA sequences and sequences of tRNA genes. *Nucleic Acids Res.* **26:** 148–158.

Strathmann, M. F. 1987. *Reproduction and Development of Marine Invertebrates of the Northern Pacific Coast.* University of Washington Press, Seattle, WA.

Strathmann, R. R. 1974. The spread of sibling larvae of sedentary marine invertebrates. *Am. Nat.* **108:** 29–44.

Strathmann, R. R. 1978. The evolution and loss of larval feeding stages of marine invertebrates. *Evolution* **32:** 894–906.

Swofford, D. L. 1998. *PAUP*: Phylogenetic Analysis Using Parsimony (and Other Methods),* Version 4.0. Sinauer Associates, Sunderland, MA.

Swofford, D. L., G. J. Olsen, P. J. Waddell, and D. M. Hillis. 1996. Phylogenetic inference. Pp. 407–514 in *Molecular Systematics,* 2nd ed. D. M. Hillis, C. Moritz, and B. K. Mable, eds. Sinauer Associates, Sunderland, MA.

Templeton, A. R. 1983. Phylogenetic inference from restriction endonuclease cleavage site maps with particular reference to the humans and apes. *Evolution* **37:** 221–244.

Thorson, G. 1961. Length of pelagic larval life in marine bottom invertebrates as related to larval transport by ocean currents. Pp. 455–474 in *Oceanography,* pub. 67, American Association for the Advancement of Science, Washington, D.C.

Vickery, M. S., and J. B. McClintock. 2000. Effects of food concentration and availability on the incidence of cloning in planktotrophic larvae of the sea star *Pisaster ochraceus. Biol. Bull.* **199:** 298–304.

Williams, S. T. 2000. Species boundaries in the starfish *Linckia. Mar. Biol.* **136:** 137–148.

Wilson, D. P. 1978. Some observations on bipinnariae of the starfish genus *Luidia. J. Mar. Biol. Assoc. UK* **58:** 467–478.

Wray, G. A. 1996. Parallel evolution of nonfeeding larvae in echinoids. *Syst. Biol.* **45:** 308–322.

Reference: *Biol. Bull.* **204:** 256–269. (June 2003)

Larval Behavioral, Morphological Changes, and Nematocyte Dynamics During Settlement of Actinulae of *Tubularia mesembryanthemum*, Allman 1871 (Hydrozoa: Tubulariidae)

KEIJI YAMASHITA[1], SATORU KAWAII[2], MITSUYO NAKAI, AND NOBUHIRO FUSETANI[3]

Fusetani Biofouling Project, ERATO, JST (formerly Research & Development Corporation of Japan), Isogo-ku, Yokohama 235-0017, Japan

Abstract. The marine colonial hydroid *Tubularia mesembryanthemum* produces a morphologically unique dispersive stage, the actinula larva. Detailed observations were made on the behaviors and nematocyte dynamics of actinula larvae during attachment and morphogenesis by employing microscopic and time lapse video techniques. These observations produced four primary results. (1) Actinula larvae demonstrated two forms of attachment: temporary attachment by *atrichous isorhiza* (AI)—nematocysts discharged from the aboral tentacle (AT) tips—and permanent settlement by cement secretion from the columnar gland cells of the basal protrusion. (2) During larval settlement, numerous AIs were discharged from the AT tips with sinuous movement and rubbing of the tentacles onto the substrata, leading to "nematocyte-printing" around the settlement site. (3) Simultaneous with the discharge of the AIs, migration of *stenoteles*, *desmonemes*, and *microbasic mastigophores* occurred, resulting in a dramatic change of nematocyte composition in the ATs after larval settlement. This was in parallel with changes in larval behavior and the tentacle function. (4) Nematocyte-printing behavior during settlement could be recognized as metamorphic behavior responsible for irreversible changes in AT function, from attachment to feeding and defense.

Received 20 June 2002; accepted 30 January 2003.

[1] To whom correspondence should be addressed. Present address: Biofouling Group, Himeji EcoTech Co., Ltd., 841-49 Koh, Shirahama-cho, Himeji-shi, Hyogo 672-8023, Japan. E-mail: keiji-y@cb3.so-net.ne.jp

[2] Present address: Faculty of Biotechnology, College of Science and Engineering, Tokyo Denki University, Ishizaka, Hatoyama, Hiki-gun, Saitama 350-0311, Japan

[3] Present address: Laboratory of Aquatic Natural Products Chemistry, Graduate School of Agricultural and Life Sciences, The University of Tokyo, 1-1-1 Yayoi, Bunkyo-ku, Tokyo 113-8657, Japan.

Abbreviations: AI, atrichous isorhiza; AT, aboral tentacle; D, desmosome; MM, microbasic mastigophore; S, stenotele.

Introduction

Many marine sessile invertebrates produce planktonic or benthic larvae as a dispersive phase. These larvae develop to competent stages, attach to suitable substrata, and metamorphose into juveniles in response to certain environmental (physical, biological, and chemical) cues (Crisp, 1974, 1984; Chia and Bickell, 1978; Pawlik, 1992). Many marine colonial hydroids (Cnidaria) produce free-swimming planula larvae for dispersal. Attachment and metamorphosis of some hydroid planulae are induced by certain bacteria, various pharmacologically active compounds, or neurotransmitter peptides (Müller, 1985; Leitz and Müller, 1987; Berking, 1988; Leitz and Klingman, 1990; Leitz *et al.*, 1994). The biochemical and physiological mechanisms involved in attachment and metamorphosis of *Hydractinia* have been described (Chia and Bickell, 1978; Berking, 1991; Leitz, 1993, 1997).

Marine hydrozoans in the genus *Tubularia* are widely distributed in shallow waters throughout the world (Petersen, 1990). Their relatively large polyps have been excellent subjects for biological studies in areas such as regeneration (Barth, 1940; Tardent and Eymann, 1958), early development of the gonophores (Brauer, 1891; Berrill, 1952; Nagao, 1965), growth in culture (Mackie, 1966), field ecology (Hughes, 1983; Östman *et al.*, 1995), physiology (Josephson and Mackie, 1965; Neufeld *et al.*, 1978; Michel and Case, 1986), and taxonomy (Tardent, 1980; Petersen, 1990).

In contrast to the many studies using the adult polyps, only a few studies have been devoted to the larval stage. Instead of a planula larva, *Tubularia* hydroids produce the uniquely shaped actinula larva as the dispersive stage in their life cycle. Only preliminary studies have been carried out on the behavior and settlement process of the actinula larva (Pyefinch and Downing, 1949; Berrill, 1952; Hawes, 1958; Orlov and Marfenin, 1994), and a few ecological studies on larval recruitment have been performed (Lemire and Bourget, 1996; Nellis and Bourget, 1996; Walters and Wethey, 1996). Berrill (1952) and Hawes (1958) suggested that the temporary attachment of the actinula was achieved by nematocyst discharge from the aboral tentacle tips. However, the correlation between larval behavior, development, and nematocyte dynamics was not accurately described. They concluded that actinula development is direct (or nearly direct) development without any marked changes in larval behaviors, structures, and habits.

In this study, to understand actinular settlement, we extensively examined larval behavior, morphological transformation, and nematocyte dynamics in the actinula larvae of *Tubularia mesembryanthemum*. Along the Japanese coasts, dense colonies of this species can be observed throughout the year on artificial substrata used in aquaculture or in the cooling water systems of power plants. With the aid of microscopic and time-lapse video recording techniques, we observed that radical behavioral, morphological, and tentacular functional changes occurred during settlement of the actinula larvae. Nematocytes were important in larval attachment and metamorphosis, and their composition in the tentacles changed radically during this stage. These results contribute to an understanding of the development of actinula larvae and of nematocyte dynamics in the settlement of cnidarian larvae.

Materials and Methods

General observations on seasonal variation of colonies in the field

Colonies of *Tubularia mesembryanthemum* were collected from fishing nets, ropes, and floats near Nagai harbor in Sagami Bay (eastern Japan, 35°10′ N, 139°35′ E) and from near Sakurajima in Kagoshima Bay (southern Japan, 31°35′ N, 130°35′ E). At the former site, colonies of *Tubularia mesembryanthemum* were observed and surface water temperatures were measured once to four times a month between December 1993 and August 1996.

Colony maintenance and liberation of actinulae

Adult colonies were washed several times by shaking them in natural seawater immediately after collection, then transferred to our laboratory in cooled seawater (1 to 3 colonies per liter) in insulated containers. At the laboratory, the colonies were repeatedly washed in filtered seawater (FSW), and predatory nudibranchs and the muddy tubes of amphipods were removed. The colonies were placed in 50- or 200-l tanks, either by hanging them with plastic-coated wires or by putting them in plastic baskets. Tanks were filled with coarsely filtered running seawater to which a water jet was applied from the side (water temperature, 16 ± 3 °C). About 10 female colonies were maintained with 1 or 2 males in a tank. Six times a week, the colonies were fed on newly hatched *Artemia* nauplii or on the nauplii reared on a diet of *Isochrysis galbana* (Haptophycea). Actinula larvae were obtained by placing female branches or polyps in small plastic baskets in 2- or 3-l beakers filled with fresh FSW (about 10 polyps/l).

Larvae were collected from the bottom of the beakers by callus pipettes, which have a large bore, and rinsed three times in fresh FSW. Larval age was defined as the period following liberation from the maternal gonophores. During microscopic observations of behavior, larvae were kept at a temperature of 19 ± 1 °C.

Observations on larval behavior and morphogenesis during settlement

After the actinula larvae were released from the maternal gonophores, their behavior and morphogenesis were observed on either clean or microbial-filmed glass petri dishes under a stereoscopic microscope. Microbial films were grown on deep (Ø 6 cm × h 6 cm) glass petri dishes by exposing the dishes to coarsely filtered running seawater for 1 day to 3 weeks. For larval settlement assays, 15 ± 3 larvae (< 8 h old) were placed in either clean or microbial-filmed glass petri dishes containing 40 ml of 0.22-μm-membrane-filtered seawater (0.22-μm FSW).

In addition, larvae were placed in a glass cell that was dipped in running seawater (0.5 ml/s) and the detailed process of morphogenesis was continuously recorded under an inverted microscope coupled to a time-lapse video disk recorder (Sony LVR-3000 A/N). Larval and post-larval dimensions were measured until stolon elongation occurred in all 30 individuals.

Scanning electron microscopy and histological observation

Larvae were sampled at three stages: at ages 2–4 h, at ages 24–28 h, and at settling. They were fixed in 4% neutralized formaldehyde in artificial seawater (ASW) and dehydrated in a graded series of ethanol. For scanning electron microscopy, the specimens were steeped three times in 100% *t*-butanol for 30 min, frozen at −20 °C overnight, freeze-dried in a Hitachi ES-2300 vacuum freeze dryer, coated with palladium-platinum in a Hitachi E-102 ion spatter-coater, and examined under a Hitachi S-2400 scanning electron microscope.

For histological observation under an optical microscope, the fixed and dehydrated specimens were embedded in Technobit 7100 resin (Heraeus Kulzer GmbH, Germany), sectioned at a thickness of 6 μm, and stained with hematoxylin-eosin.

Nematocyte composition and migration in the tentacles

The composition of nematocytes in the aboral tentacles or their rudiments was examined in star-shaped embryos, preactinulae before liberation, 2–4-h-old larvae, 24–28-h-old larvae, settling larvae, settled individuals, and juvenile polyps 2 days after settlement. After the gonotheca was cut open with a thin needle, the star-shaped embryos and preactinulae were picked up with the needle from the dissociated gonophores. Each specimen was placed on a glass slide to which a drop of approximately 200 m*M* Mg^{2+} ASW was added to prevent shrinkage of the aboral tentacles and discharge of the nematocysts. After 30 min, the specimen was covered with a cover slip. The number of nematocytes in the aboral tentacles (or the rudiments) of each of 10 specimens was counted under a Nomarski interference microscope.

To examine nematocyte migration, a 2–4-h-old larva was placed in a petri dish filled with FSW, and the basal protrusion and the aboral tentacle were held by gentle suction with micropipettes. Nematocyte migration through the aboral tentacle was recorded under an inverted microscope coupled with a time-lapse video disk recorder (Sony LVR-3000 A/N).

Statistical analysis

One-way analysis of variance (ANOVA) with Scheffé's test as a *post hoc* test was used to examine the significance of the changes in nematocyte composition and the effect of the microbial films on larval settlement. A significance level of $P < 0.05$ was used in all statistical analyses, which were performed using StatView version 5.0 (SAS Institute, Inc., USA).

Results

Seasonal variation of colonies in the field

Figure 1 shows the general succession of colonies of *Tubularia mesembryanthemum* on artificial substrata (vinylon nets, ropes, and plastic buoys) hanging from the set nets for fisheries near Nagai harbor during the period from December 1993 to August 1996. No colonies were seen inside the harbor, but colonies were often observed on the shadowed surfaces of fishing nets and ropes (around the depths of 3–10 m) and on the lower surfaces of buoys outside the harbor. They were also seen on the shell surface of the barnacles *Megabalanus rosa* and *M. volcano* and the mussel *Mytilus galloprovincialis* that settled on the artificial substrata. Colonies of *T. mesembryanthemum* were found throughout the year; colony growth and degeneration was repeated in a cycle of 1 to 2 months, with new colonies appearing at new settlement sites. Large numbers of colonies were observed from November to July (surface water temperature, 12–26 °C), and fully matured colonies were dominant in a wide range of water temperature: February-March (12–14 °C), June-July (20–26 °C), and October-November (24–20 °C). Mature colonies reached maximum density in June and July (19–26 °C), covering almost all surfaces of the fishery's nets and ropes. These mature colonies degenerated rapidly, and colonies with only perisarcs were observed in August or September (surface water temperature, 26–30 °C).

Colony maintenance and actinula liberation

The colonies were basically dioecious, although bisexual polyps were occasionally observed; the form of the gonophores was very variable under laboratory culture conditions. Fertilized eggs developed to star-shaped embryos, preactinulae, and then to actinula larvae that were released from the maternal gonophore (Fig. 2A-D).

Maintenance and culture were dependent on the physiological state of the colonies collected; colonies without degeneration of the hydrocaulus stayed mature for 1–2 months in running seawater and released actinula larvae repeatedly, every 1–2 weeks. The number of gonophores gradually decreased during the 2 months after collection.

A polyp released from 20 to 300 actinula larvae, depending on the degree of maturation. Fully matured female polyps released most of their larvae within the first 3 days from the beginning of release. Larvae released later were smaller and sometimes deformed. Larvae released early in the period were used for experiments, because some later-released larvae degenerated before stolon elongation.

Changes in larval behavior and morphology

Newly released actinulae had 4–12 (mainly 8 or 6) aboral tentacles and 4–7 oral tentacle rudiments (Fig. 2D). When larvae were placed in a 2-l beaker filled with FSW so that their tentacles did not touch the surface of vessels, they showed a specific floating behavior with the oral pole turned downward and the tentacles held rigid and stretched backward (resembling the seed of a dandelion). However, as soon as a tentacle tip touched the substrata surface, the larvae moved some of their aboral tentacles up and some down (Fig. 2D). Larvae aged 2–8 h showed the following characteristics: aboral tentacle length, 600–1000 μm (mean ± SD, 792.7 ± 92.2); oral tentacle (rudiment) length, 13–53 μm (33.4 ± 10.6); body length, 233–367 μm (305.1 ± 33.2); body width, 200–310 μm (236.3 ± 29.3). About 12 h after liberation, the larvae began a repeated contraction and expansion of their bodies (Fig. 3A); the

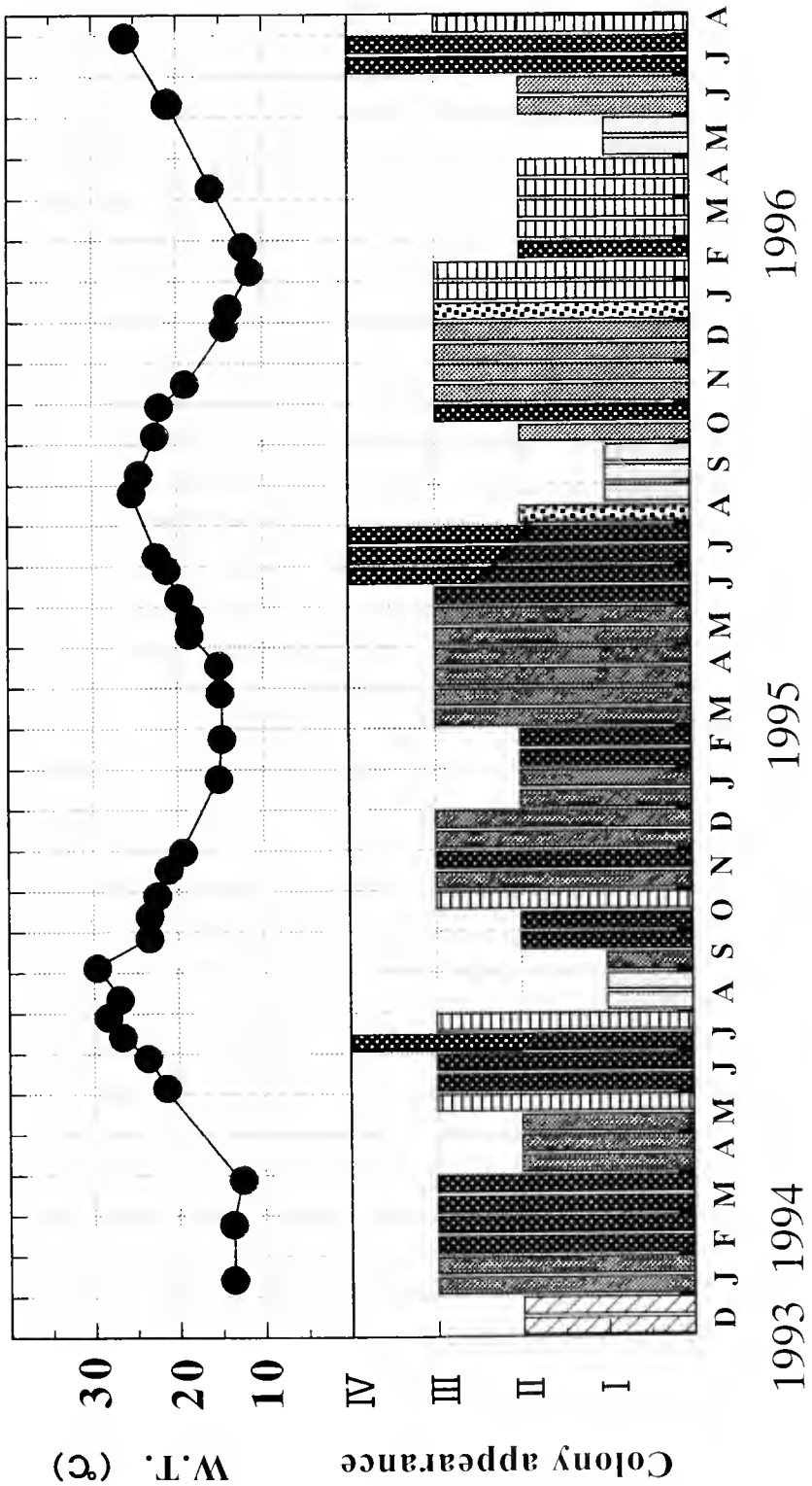

Figure 1. Seasonal variation of the colonies of *Tubularia mesembryanthemum* growing attached to the artificial substrata used in set nets for fisheries at Nagai harbor, from December 1993 to August 1996. Ranks of colony appearance shows the approximate number of observed colonies as I, <10; II, <50; III, ≥50; IV, colonies covered all surfaces (underwater) of most fisheries nets, ropes, and buoys.

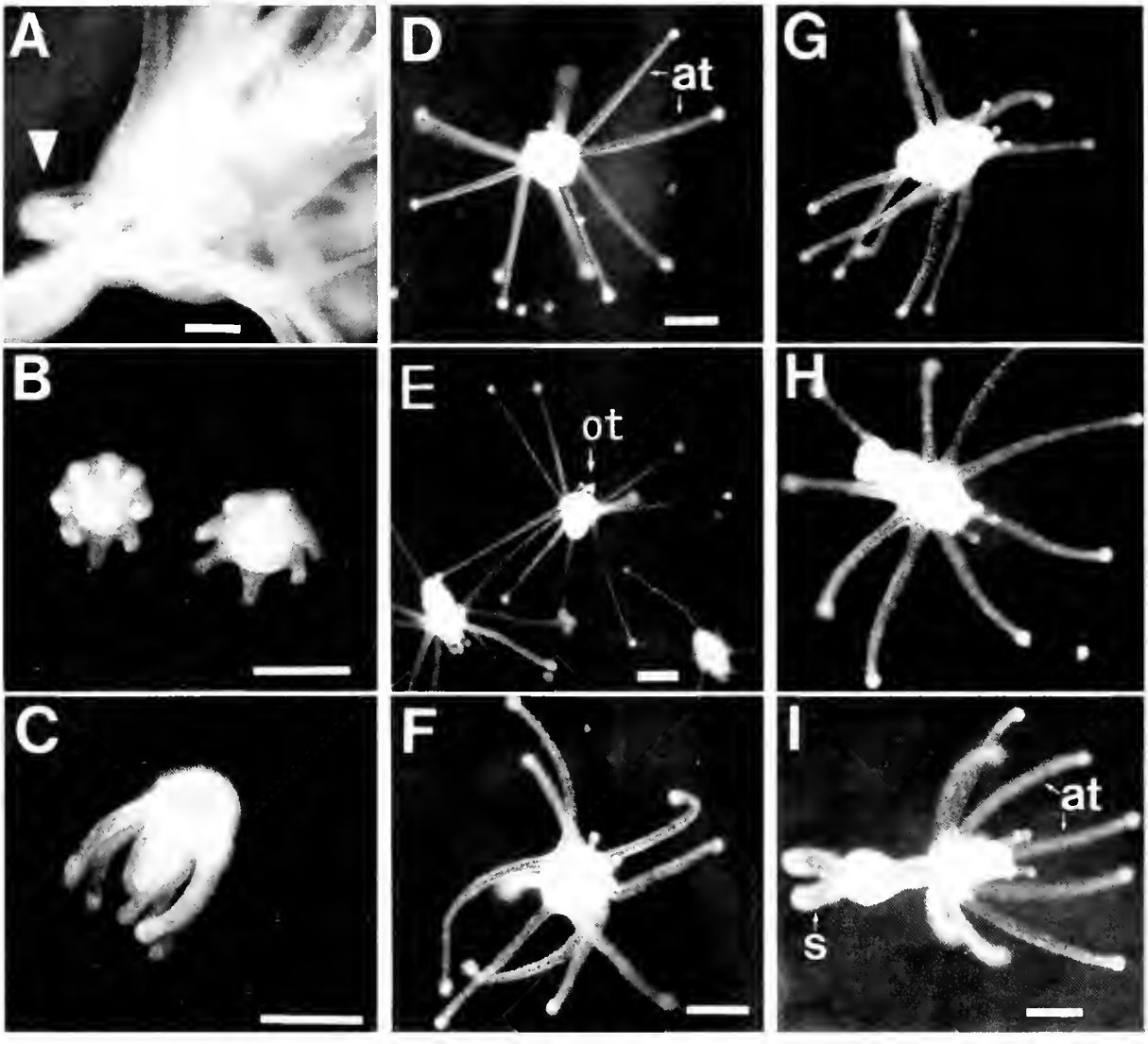

Figure 2. Development and behavior in an actinula larva of *Tubularia mesembryanthemum*. (A) Female polyp bearing actinulae (arrowhead); (B) star-shaped embryos; (C) preactinula (before liberation); (D) actinula larva newly released from maternal gonophore; (E) 1-day-old larva; (F and G) 1-day-old larva during settling behavior; (H) individual settled by the aboral pole (= basal protrusion); (I) stolon-elongated juvenile polyp 1 day after settlement. at = aboral tentacle(s), ot = oral tentacle(s), s = stolon. F–H are same magnification. Bars = 300 μm.

aboral tentacles, particularly the tips, became so sticky that they could not be pipetted away from the substrata, and they eventually formed a temporary attachment after coming in contact with a surface. Later the larvae often bent their tentacles onto the bottom surface and used them to move slowly on the bottom of the beakers.

One day after liberation, the aboral and oral tentacles elongated [aboral tentacles, 700–1050 μm (910.7 $\pm$ 102.4); oral tentacles, 53–120 μm (81.7 $\pm$ 16.9)], body length increased [280–500 μm (345 $\pm$ 52.1)], and the aboral pole (= basal protrusion which later became the location of permanent attachment) gradually began to extend downwards (Fig. 2E). Larvae then positioned themselves by pressing the basal protrusion, composed of long columnar gland cells filled with secretory granules that stained strongly with eosin (Fig. 4A, B), onto the substrata. This action was followed by active sinuous movement and rubbing of the aboral tentacles (around the settlement site), accompanied by swaying of the body on the substrata surface, that was only observed during larval settlement (Fig. 2F, G; Fig. 3B).

Settlement was followed by release of the cement substance. Newly settled individuals temporarily raised their aboral tentacles upward, but if the vessel was shaken, they immediately moved some tentacles downward and touched the substrata surfaces. Then, the larvae irreversibly opened

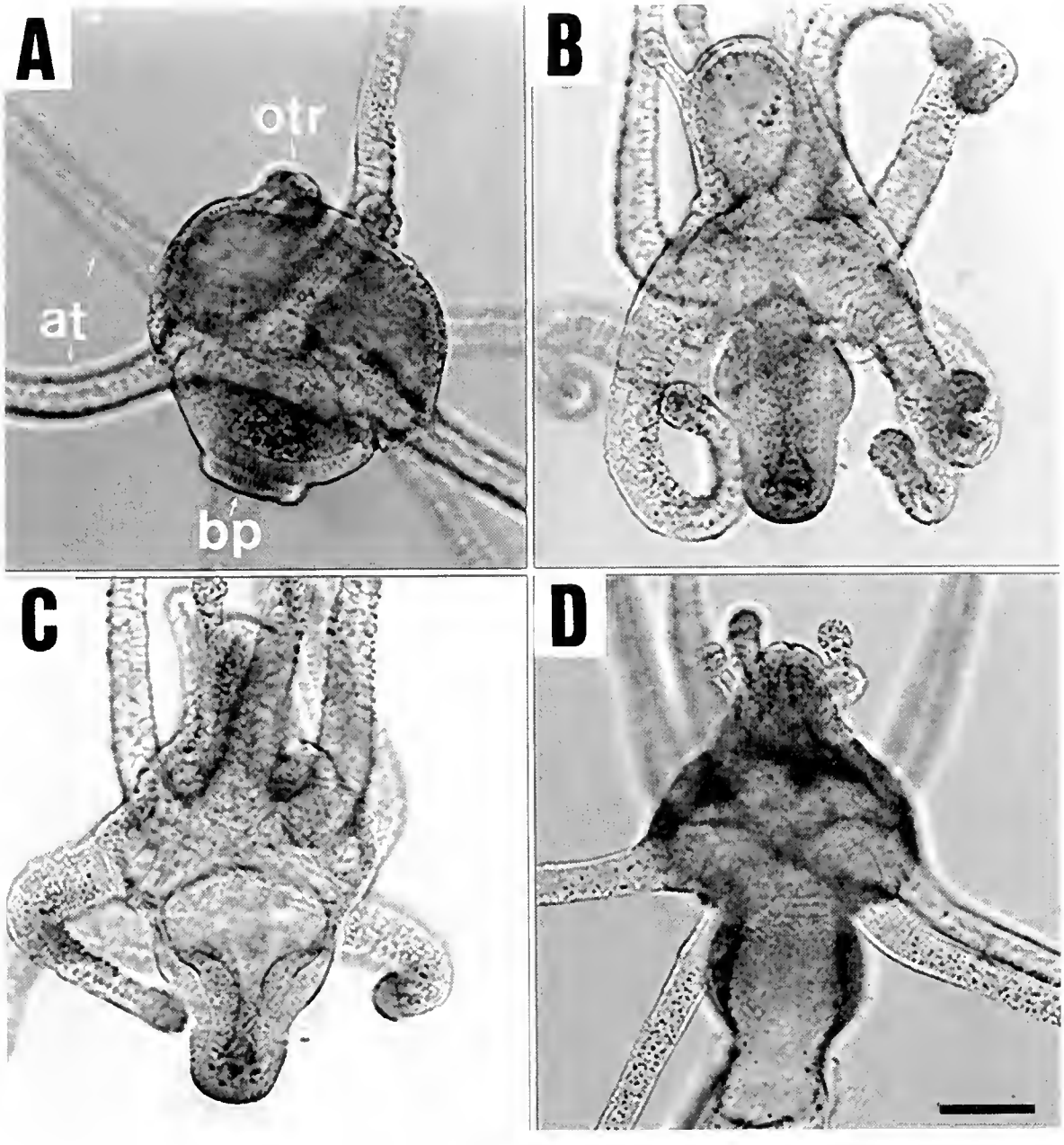

Figure 3. Morphological changes in the body of an actinula larva during settlement (time-lapse video images). (A) Larva undergoing repeated contraction and expansion of the body. (B) Larva beginning settling behavior with sinuous movement and rubbing of the tentacles to surface substrate; this phase was reversible to the temporary attachment phase. (C) Larva that has irreversibly opened the coelenteron in its aboral half to permanent settlement by the basal protrusion. (D) Stolon-elongated juvenile polyp. at = aboral tentacle(s), bp = basal protrusion, otr = oral tentacle rudiment(s). A–D are same magnification. Bar = 100 μm.

the coelenteron in the aboral half of the bodies and achieved permanent attachment at the basal protrusion (Fig. 3C). Subsequently, the stem and stolon differentiated and all tentacles extended upward (Fig. 2H, I; Fig. 3D). In these juvenile polyps, the cushion-like tissue disappeared into the endoderm of the aboral half, and many digestive gland cells developed in the endoderm of the oral half of the hydranth (Fig. 4C, D). The resulting structure contrasts with the well-developed cushion-like tissue in the endoderm of the aboral half of an actinula larva and the absence of digestive gland cells in the endoderm of the oral half of the larval body (Fig. 4A, B). Thus, morphological transformation to the juvenile polyps was completed.

When larvae (< 8 h old) were given clean glass surfaces

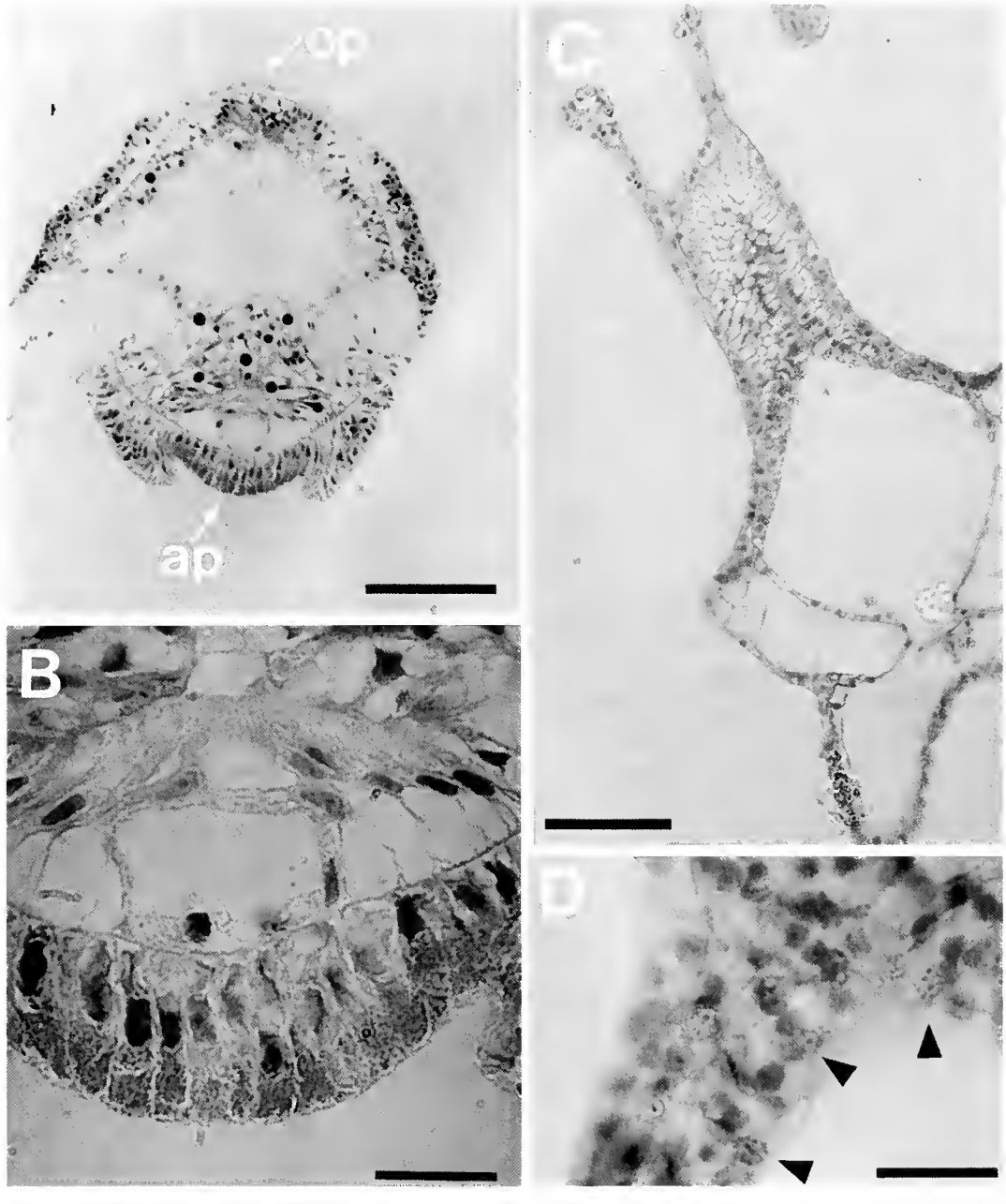

Figure 4. Longitudinal section of actinula larva (2–4 h old) and hydranth of juvenile polyp (1 day after settlement) stained with hematoxylin-eosin. (A and B) Actinula larva; (C and D) juvenile polyp. Long columnar gland cells filled with strongly eosinophilic granules were arranged in the ectoderm of the aboral pole (= basal protrusion) of the actinula larva, and the many digestive gland cells (arrowheads) were observed in the oral endoderm of the hydranth of the juvenile polyp. Bar = 100 μm (A, C) and 20 μm (B, D).

in still water (0.22-μm FSW), almost none of them initiated settling behavior within 16 h (about 24 h from the larval liberation); after 16 h, settled and stolon-elongated individuals represented only 1.5% $\pm$ 4.6% (mean $\pm$ standard deviation) of the total (n = 26). In most cases, settling behavior did not begin for 24 h, then the larvae usually started and stopped the behavior repeatedly and erratically; some larvae did not settle for more than 2 weeks.

In contrast, when they were exposed to surfaces that had acquired microbial films by being kept in running natural seawater for 2 to 3 weeks, < 8 h-old larvae began the settling behavior immediately after their tentacle tips touched the substrata. They then settled quickly, with stolon elongation; percent settled and stolon-elongated individuals after 16 h were 67.4% $\pm$ 25.8% (n = 15) when exposed to 2-week-old films, and 74.5% $\pm$ 15.8% (n = 13) in the case

of 3-week-old films. Thus, microbial films significantly ($P < 0.0001$) promoted actinular settlement. These larval responses did not occur without direct contact of the aboral tentacles to the microbial-filmed surface.

Three days after liberation, juvenile polyps showed the following characteristics: aboral tentacle length, 600–1300 μm (mean ± standard deviation = 800.8 ± 187.2); oral tentacle length, 73–120 μm (89.0 ± 17.3); body length, 433–968 μm (660.9 ± 186.6); body width, 130–200 μm (170.9 ± 23.4).

Discharge and printing of the tentacular nematocytes during larval settlement

Large numbers of *atrichous isorhizas* (AIs) were observed at the tips of the aboral tentacles in the pre-attachment stage (Fig. 5A, C). With time following larval liberation, the knobs of the aboral tentacle tips gradually became indistinct, and so sticky that repeated pipetting could not tear the tips from the substrata. These changes were accompanied by the transformation of the knob surfaces (the number of cnidocils decreased and the number of discharged tubes increased, Fig. 5B). Temporary attachment was achieved by anchoring with the tubes of the discharged AIs to the substrata surface.

Observations with the inverted and scanning electron microscopes showed that the settling larvae discharged many AI nematocytes from the aboral tentacle tips in concert with their sinuous movement, active rubbing of the tentacles, and body-swaying on the glass surfaces during settlement. As a result, the discharged nematocytes were stuck around the settlement site (Figs. 6, 7). In contrast, temporary attachment was achieved by one or two tubes of the discharged AIs from a rigid tentacle; the sinuous tentacular behavior and the AI discharge and sticking (more than 50 from a tentacle) were peculiar to larval settlement (Figs. 6, 7) and thus were termed "nematocyte-printing behavior."

Dynamic changes in nematocyte composition during larval settlement

Figure 8 shows the changes in nematocyte composition of the aboral tentacles during larval development and behavior. No nematocytes were observed in the aboral tentacle rudiments of the star-shaped embryos. The preactinula had only small numbers of atrichous isorhizas (AIs) (20.5 ±

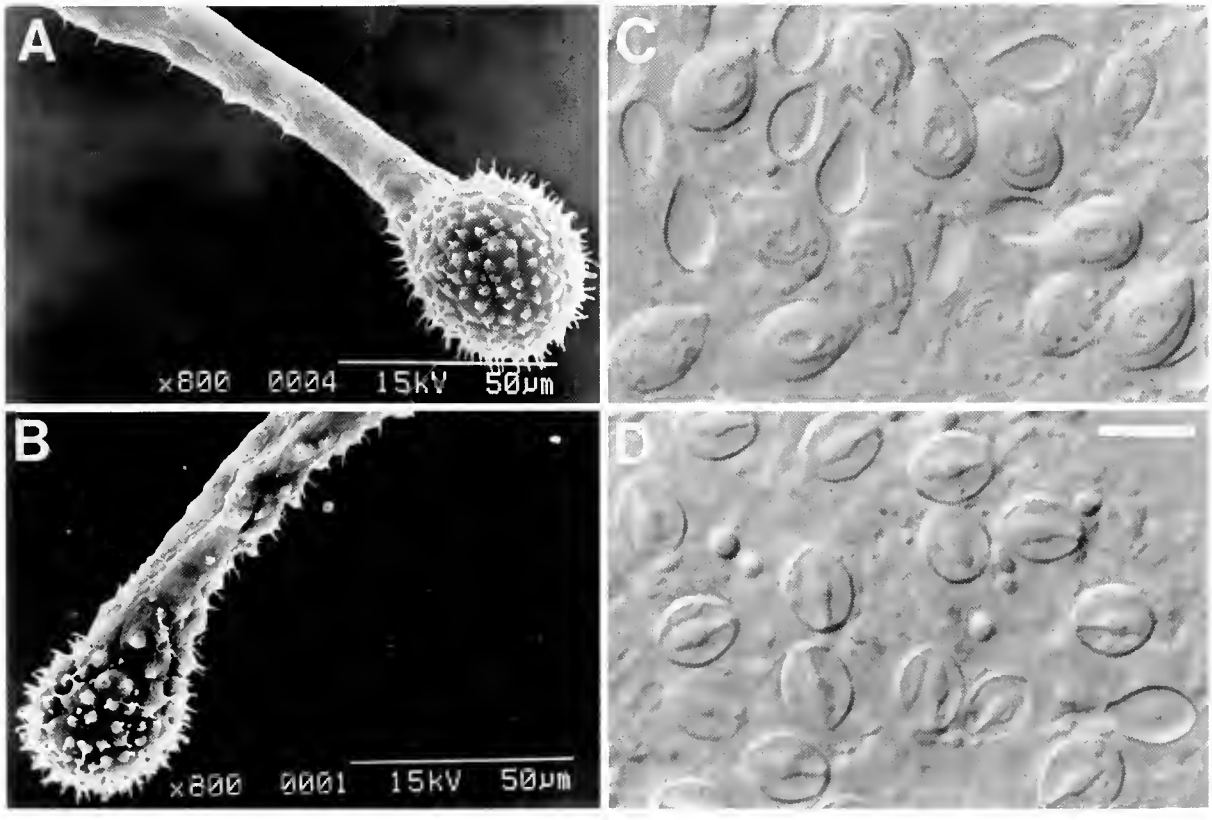

Figure 5. Scanning electron micrographs of aboral tentacle tips of actinula larvae, and Nomarski interference micrographs of nematocysts in the tentacle tip and body wall. (A) 2–4-h-old larva; (B) 1-day-old larva; (C) atrichous isorhiza nematocysts in the tentacle tip; (D) small stenotele nematocysts in the body wall (2–4-h-old larva). C and D are same magnification. Bar = 5 μm.

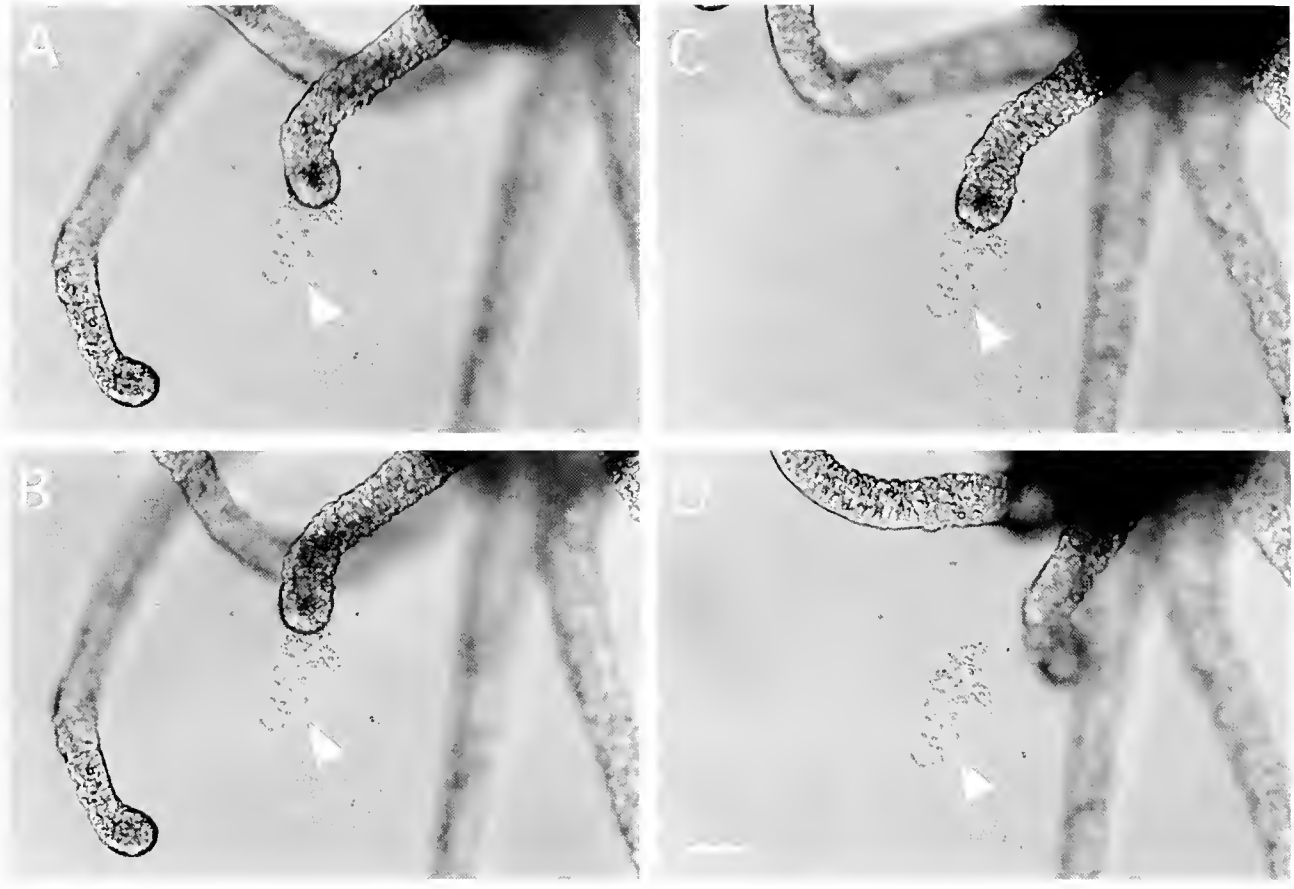

Figure 6. Rubbing of the aboral tentacle tip with sinuous movement, followed by discharge and sticking of atrichous isorhiza nematocytes (arrowheads) on the glass surface during the settlement of an actinula larva. The elapsed time from A to D was about 5 min. A–D are same magnification. Bar = 50 μm.

1.9), which were not deployed in the tentacle tips. In the tentacles of 2–4-h-old larvae four types of nematocytes, namely atrichous isorhiza (AI), stenotele (S), desmoneme (D), and microbasic mastigophore (MM), were observed. About 170 AIs were deployed at a tentacle tip at this stage, while small numbers of S, D, and MM were observed along an aboral tentacle (AI, 168.6 ± 41.3; S, 34.5 ± 13.0; D, 51.8 ± 23.9; MM, 11.8 ± 6.5; the total, 266.7 ± 64.2). In contrast, no AIs but numerous small Ss were present in the body walls of these larvae (Fig. 5). In 24–28-h-old larvae, the number of AIs in the tentacles gradually decreased, while other types of nematocytes (S, D, and MM) increased in number (AI, 82.9 ± 26.3; S, 101.3 ± 20.8; D, 95.3 ± 18.8; MM, 22.3 ± 8.5; the total, 301.8 ± 45.9). During pre-settlement and post-settlement stages, S and D nematocytes actively migrated in the ectoderm from the body wall to the tentacle tips at an speed of 6.0–15.4 μm/min (9.1 ± 5.4) (Fig. 9), which led to dynamic change in the tentacular nematocyte composition. Newly settled individuals that did not develop to hydrocaulus and hydrorhiza elongation retained small numbers of AIs in the aboral tentacle tips (AI, 16.1 ± 13.1; S, 199.3 ± 60.9; D, 168.6 ± 54.7; MM, 35.9 ± 16.5; the total, 419.8 ± 71.8). In polyps of 2 days after settlement, in which all aboral tentacles extended upward completely and the hydrocaulus was so long that the aboral tentacles could not touch the substrata, AI nematocytes disappeared and the aboral tentacles contained many nematocytes of three types (S, D, MM) (AI, 1.6 ± 3.3; S, 269.2 ± 53.8; D, 212.6 ± 42; MM, 32.3 ± 7.8; the total, 515.6 ± 81.8).

From 2–4-h-old larvae to juvenile polyps, the number of AIs decreased significantly (Table 1); however, the number of AIs in an aboral tentacle of the newly settled individuals varied very much (from 0 to 40). The increase in the number of Ss, Ds, and MMs was statistically significant (Table 1). The aboral tentacles of adult polyps had many holotrichous isorhiza-like nematocytes with S, D, and MM nematocytes.

When larvae were placed in clean glass petri dishes at a low density (1 ind./40 ml 0.22-μm-FSW), some actinula larvae remained floating or repeated temporary attachment for more than 2 weeks. These larvae retained many AIs in the aboral tentacle tips. When the aboral tentacle tips of the newly released actinula larvae were cut off, the tips were regenerated and AIs were deployed within 2 to 3 days; this

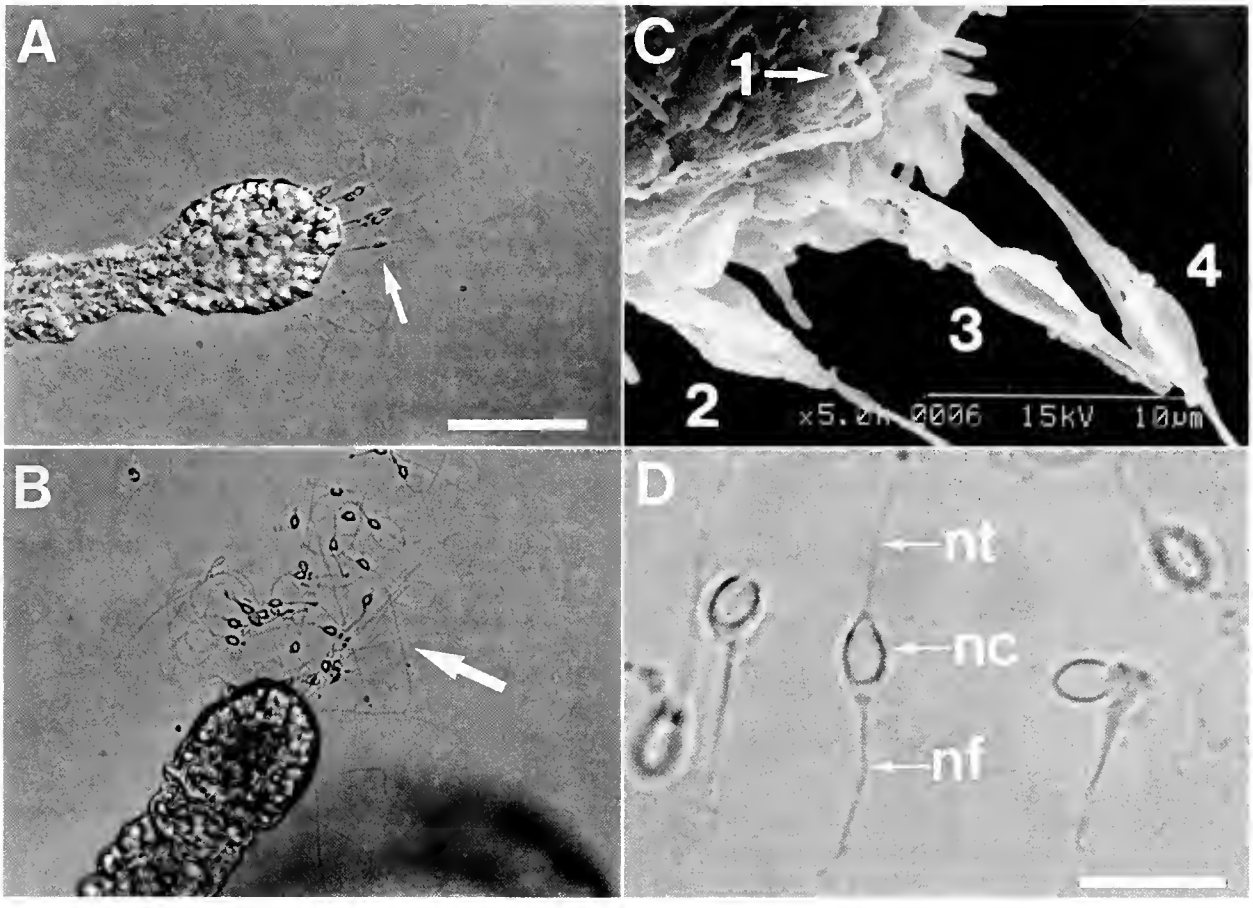

Figure 7. Atrichous isorhiza (At) nematocytes discharged from the aboral tentacle tips during nematocyte-printing behavior. (A and B) Nomarski micrographs: many AIs (arrows) were discharged from the tentacle tip, resulting in "printing" around the settlement site. (C) Scanning electron micrograph: different phases from At nematocyst discharge (1) to nematocyte exclusion (4) from the epithelial tissues of the tentacle tip (at about same phase as in A). (D) At nematocytes printed on glass surface. nc = nematocyst capsule, nf = nematocyte filament, nt = nematocyst tubule. A and B are same magnification. Bar = 50 μm (A, B) and 10 μm (D).

was followed by temporary attachment and larval settlement. In contrast, when the tentacle tips of the juvenile polyps were cut off, regeneration and deployment of Ss occurred in the aboral tentacles.

Discussion

Seasonal variation of colonies and liberation of actinulae

Field observations showed that both asexual and sexual reproduction of *Tubularia mesembryanthemum* continue in a wide range of water temperatures (surface water temperatures ranged from 12 to 26 °C) from October to July in the vicinity of Nagai coast. Supplies of larvae seemed to be most abundant in the range from 18 to 22 °C. Mature colonies were most dense from June to July, and appeared to degenerate within 1 or 2 months on certain substrata. Colonies appeared from late September to October, possibly regenerating from the once-degenerated stolons. Frequent appearance of colonies on the shadowed surfaces of artificial substrata outside the harbor suggests the importance of certain kinds of microbial films and of water currents in actinular settlement followed by colony growth. Defining the reproductive cycle of *T. mesembryanthemum*, which is beyond the scope of this paper, would require tracking the progression of individual colonies, as Hughes (1983) did for *T. indivisa*.

Changes in larval behavior and morphology during settlement

Several researchers preliminarily reported on the settlement behavior of actinula larvae of *Tubularia* spp. (Pyefinch and Downing, 1949; Berrill, 1952; Hawes, 1958; Lemire and Bourget, 1996), concluding that, because of their direct development, these larvae should be considered merely hydranths with rudimentary stalks, or only juvenile

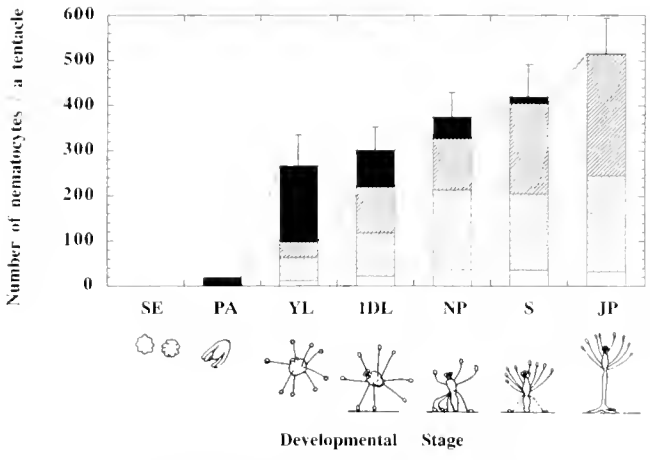

Figure 8. Changes in nematocyte composition of the aboral tentacles during larval development: ■ atrichous isorhizas, ▨ stenoteles, □ desmonemes, □ microbasic mastigophores. SE, star-shaped embryos; PA, preactinulae; YL, young (2–4-h-old) larvae; 1DL, 1-day (24–28 h)-old larvae; NP, nematocyte-printing larvae; S, newly settled individuals; JP, juvenile polyps 2 days after settlement. Vertical bars = standard deviation of total numbers of nematocysts in a tentacle.

polyps. In contrast, our observations revealed that the liberated actinula larvae underwent marked behavioral changes that could be divided into the following phases: floating (or sinking), temporary attachment, nematocyte-printing, and settlement followed by stolon elongation. In parallel with these behavioral changes, we observed functional changes in the aboral tentacles (from floating or temporary attachment to feeding or defense) and physiological changes in the body (disappearance of the cushion-like tissues of the aboral endoderm and development of digestive gland cells of the oral endoderm). In addition to these settlement processes, larvae whose settlement was delayed retained many atrichous isorhizas (AIs), and larvae whose tentacle tips had been cut off showed no settling behavior until the tips and the AI nematocytes regenerated. These results show that the settlement of actinulae occurs through coordination of the aboral tentacles and the basal protrusion, and that nematocyte-printing behavior is both peculiar to and indispensable for settlement and morphogenesis of the actinula larvae of *T. mesembryanthemum*. The settlement process of the actinula larvae thus proved to involve radical

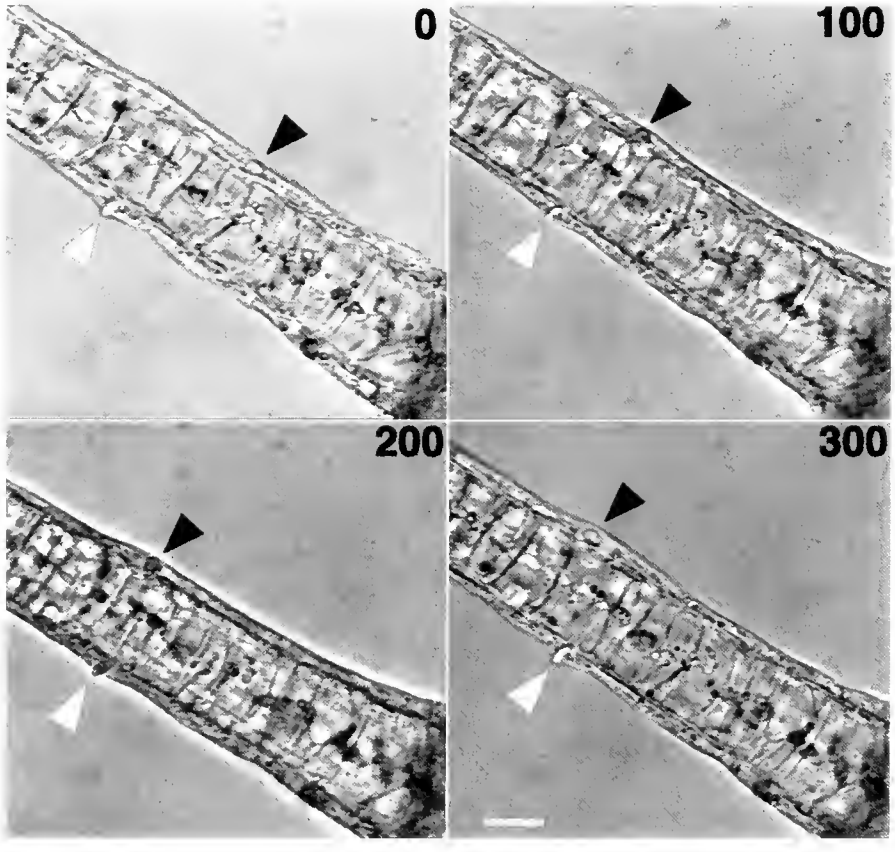

Figure 9. Migrating nematocyte along the epithelium of the aboral tentacle from base to tip of the tentacle before larval settlement. The nematocyte migrated at a speed of 6-15.4 μm/min (average speed of approximately 9 μm/min) toward the tentacle tip. Black arrowhead indicates the migrating nematocyte (probably stenotele), and white arrowhead indicates the deployed nematocyte (probably microbasic mastigophore). Numbers at upper right of each image show the elapsed time (seconds). Every image is the same magnification. Bar = 20 μm.

Table 1

Results of ANOVA (Scheffé's test, significance level $P < 0.05$) to access the change in nematocyte composition of aboral tentacles from 2–4-h-old larvae to juvenile polyps

Stages	Type of nematocyte				
	Atrichous isorhizas	Stenoteles	Desmonemes	Microbasic mastigophores	Total number of nematocysts
2–4h-old larvae, 1-day-old larvae	<0.0001*	0.0048*	0.0891	0.2101	0.7726
2–4h-old larvae, Nematocyst-printing	<0.0001*	0.0015*	<0.0001*	<0.0001*	0.0092*
2–4h-old larvae, Just-settled	<0.0001*	<0.0001*	<0.0001*	<0.0001*	<0.0001*
2–4h-old larvae, Juvenile polyps	<0.0001*	<0.0001*	<0.0001*	<0.0001*	<0.0001*
1-day-old larvae, Nematocyst-printing	0.0939	0.9855	0.0016*	0.1380	0.2792
1-day-old larvae, Just-settled	<0.0001*	<0.0001*	0.0003*	0.0498*	0.0012*
1-day-old larvae, Juvenile polyps	<0.0001*	<0.0001*	<0.0001*	0.2927	<0.0001*
Nematocyst-printing, Just-settled	0.0548	0.0004*	0.9933	0.9999	0.6469
Nematocyst-printing, Juvenile polyps	0.0019*	<0.0001*	0.3347	0.9479	0.0005*
Just-settled, Juvenile polyps	0.5643	0.0003*	0.0289*	0.9219	0.0029*

Numbers show *P* values. Asterisks (*) indicate significant differences.

morphogenetic reorganization. This complex series of behavioral and morphological changes during actinular settlement has not been reported previously.

Furthermore, the coordination of nematocyst discharge from the tentacle tips and cement secretion from the basal protrusion suggests that a physiologically complex set of internal signals controls actinular attachment and morphogenesis.

Nematocyte-printing behavior as active metamorphic event

The role of nematocytes in the temporary attachment of cnidarian larvae has been partially described by others (Hawes, 1958; Teitelbaum, 1966; Donaldson, 1974; Mariscal, 1974; Chia and Crawford, 1977; Chia and Bickell, 1978; Namikawa *et al.*, 1993); however, the correlation between larval settlement, morphogenesis, and nematocyte dynamics has not been accurately defined.

We found that actinula larvae attached temporarily to the substrata by AI discharge, and that the function of the larval tentacles changed irreversibly—from temporary attachment to feeding (and defense)—after larval settlement. Composition of the nematocytes in larval tentacles changed dramatically—from AI dominance to S/D dominance—after nematocyte-printing behavior and in parallel with the functional changes in the larval tentacles. AIs were used for temporary attachment of the actinula larvae, whereas Ss, Ds, and MMs were apparently used by the polyps for feeding or defense, as has been suggested for other species (Ewer, 1947; Mariscal, 1974; Chia and Bickell, 1978; Purcell and Mills, 1988; Tardent, 1995; Östman *et al.*, 1995). Moreover, actinula larvae whose tentacle tips had been cut off regenerated the AIs and then exhibited nematocyte-printing behavior followed by larval settlement.

Thus, AI nematocyte-printing behavior may be recognized as metamorphic behavior responsible for irreversible changes in aboral tentacle function from temporary attachment to feeding and defense. Whereas Berrill (1952) and Hawes (1958) concluded that actinulae of *Tubularia* are merely juvenile polyps and not really "true" larvae, the present study clearly shows that the actinula larvae of *T. mesembryanthemum* are not merely juvenile polyps but "true" larvae specialized for dispersal and attachment as part of the process of indirect development.

In addition, we demonstrated that actinula settlement was promoted by direct contact with microbial films formed on the substrata surface, and that settlement-delayed larvae retained many AIs in their aboral tentacles. These results suggest that actinular settlement is determined by close correlation between larval aging and nematocyte migration (as endogenous environment) and substrata surface environment (as exogenous environment). Further investigation is required to clarify the mechanisms of actinular settlement, though our previous biophysical studies revealed the importance of external and internal Ca^{2+} in larval settlement (Yamashita *et al.*, 1996, 1997; Kawaii *et al.*, 1997, 1999).

This report, which reveals that nematocyte-printing behavior is an active metamorphic event and that nematocyte dynamics is synchronously involved in the attachment and morphogenesis of actinula larvae, provides new insights into the attachment and morphogenesis of cnidarian larvae.

Acknowledgments

We thank Dr. Y. Kakinuma, Kagoshima University, for her helpful discussion, and Dr. S. Kubota, Kyoto University, for identification of our *Tubularia* samples. Also

thanks are due to Mrs. Y. Kayama, T. Funatsuki, Nagai Fishermen's Association; S. Yamamoto, Sagami Bay Marine Laboratory; M. Tabata, Kagoshima City Aquarium; R. Kawagoe, Sakurajima Fishermen's Association for their help in the collection of *Tubularia* colonies; to Dr. K. Matsumura for critically reading our manuscript; and to Dr. G. O. Mackie and the late Dr. P. Tardent for kindly providing useful literature and for fruitful discussion. K.Y. is grateful to the staff of Himeji Kisho Co., Ltd., for the opportunity to participate in this research project and to Ms. Y. Yamashita for her support.

Literature Cited

Barth, L. G. 1940. The process of regeneration in hydroids. *Biol. Rev.* **15:** 405–420.

Berking, S. 1988. Ammonia, tetraethylammonium, barium and amiloride induce metamorphosis in the murine hydroid *Hydractinia*. *Roux's Arch. Dev. Biol.* **197:** 1–9.

Berking, S. 1991. Control of metamorphosis and pattern formation in *Hydractinia* (Hydrozoa, Cnidaria). *BioEssays* **13:** 323–329.

Berrill, N. J. 1952. Growth and form in gymnoblastic hydroids. V. Growth cycle in *Tubularia*. *J. Morphol.* **90:** 583–601.

Brauer, A. 1891. Über die Entstehung der Geschlechtsprodukte und die Entwicklung von *Tubularia mesembryanthemum* Allm. *Z. Wiss. Zool.* **52:** 551–579.

Chia, F. S., and L. Bickell. 1978. Mechanisms of larval settlement and the induction of settlement and metamorphosis: a review. Pp.1–12 in *Settlement and Metamorphosis of Marine Invertebrate Larvae: Proceedings of the Symposium on Settlement and Metamorphosis of Marine Invertebrate Larvae*, American Zoological Society Meeting, December 27–28, 1977. F.-S. Chia and M. E. Rice, eds. Elsevier, New York.

Chia, F. S., and B. Crawford. 1977. Comparative fine structural studies of planulae and primary polyps of identical age of the sea pen, *Ptilosarcus gurneyi*. *J. Morphol.* **151:** 131–158.

Crisp, D. J. 1974. Factors influencing the settlement of marine invertebrate larvae. Pp. 177–265 in *Chemoreception in Marine Organisms*, P. T. Grant and A. M. Mackie, eds. Academic Press, New York.

Crisp, D. J. 1984. Overview of research on marine invertebrate larvae, 1940–1980. Pp. 103–126 in *Marine Biodeterioration: an Interdisciplinary Study*. Naval Inst. Press, Annapolis.

Donaldson, S. 1974. Larval settlement of a symbiotic hydroid: specificity and nematocyst responses in planulae of *Proboscidactyla flavicurrata*. *Biol. Bull.* **147:** 573–585.

Ewer, R. F. 1947. On the functions and mode of action of the nematocysts of *Hydra*. *Proc. Zool. Soc. Lond.* **117:** 365–376.

Hawes, F. B. 1958. Preliminary observations on the settlement of actinula larvae of *Tubularia larynx* (Ellis and Solander). *Annu. Mag. Nat. Hist.* **13:** 147–155.

Hughes, R. G. 1983. The life history of *Tubularia indivisa*, (Hydrozoa: Tubulariidae) with observations on the status of *T. ceratogyne*. *J. Mar. Biol. Assoc. UK* **63:** 467–479.

Josephson, R. K., and G. O. Mackie. 1965. Multiple pacemakers and the behavior of the hydroid *Tubularia*. *J. Exp. Biol.* **43:** 293–332.

Kawaii, S., K. Yamashita, M. Nakai, and N. Fusetani. 1997. Intracellular calcium transients during nematocyst discharge in actinulae of the hydroid, *Tubularia mesembryanthemum*. *J. Exp. Zool.* **278:** 299–307.

Kawaii, S., K. Yamashita, M. Nakai, M. Takahashi, and N. Fusetani. 1999. Calcium dependence of settlement and nematocyst discharge in actinulae of the hydroid *Tubularia mesembryanthemum*. *Biol. Bull.* **196:** 45–51.

Leitz, T. 1993. Biochemical and cytological bases of metamorphosis in *Hydractinia echinata*. *Mar. Biol.* **116:** 559–564.

Leitz, T. 1997. Induction of settlement and metamorphosis of cnidarian larvae: signal and signal transduction. *Invertebr. Reprod. Dev.* **31:** 109–122.

Leitz, T., and G. Klingmann. 1990. Metamorphosis in *Hydractinia*: studies with activators and inhibitors aiming at protein kinase C and potassium channels. *Roux's Arch. Dev. Biol.* **199:** 107–113.

Leitz, T., and W. A. Müller. 1987. Evidence for the involvement of PI-signaling and diacylglycerol second messengers in the initiation of metamorphosis in the hydroid *Hydractinia echinata* Fleming. *Dev. Biol.* **121:** 82–89.

Leitz, T., K. Morald, and M. Mann. 1994. Metamorphosin A, a novel peptide controlling development of the lower metazoan *Hydractinia echinata*. *Dev. Biol.* **200:** 249–255.

Lemire, M., and E. Bourget. 1996. Substratum heterogeneity and complexity influence micro-habitat selection of *Balanus* sp. and *Tubularia crocea* larvae. *Mar. Ecol. Prog. Ser.* **135:** 77–87.

Mackie, G. O. 1966. Growth of the hydroid *Tubularia* in culture. *Symp. Zool. Soc. Lond.* **16:** 397–412.

Mariscal, R. N. 1974. Nematocysts. Pp. 129–178 in *Coelenterate Biology: Reviews and New Perspectives*, L. Muscatine and H. M. Lenhoff, eds. Academic Press, London.

Michel, W. C., and J. F. Case. 1986. Effects of a water-soluble petroleum fraction on the neuroid electrical activity of the hydroid coelenterate *Tubularia crocea*. *Mar. Environ. Res.* **19:** 295–319.

Müller, W. A. 1985. Tumor-promoting phorbol esters induce metamorphosis and multiple head formation in the hydroid *Hydractinia*. *Differentiation* **29:** 216–222.

Nagao, Z. 1965. Studies on the development of *Tubularia radiata* and *Tubularia venusta* (Hydrozoa). *Publ. Akkeshi Mar. Biol. Sta.* **15:** 9–35.

Namikawa, H., S. F. Mawatari, and D. R. Calder. 1993. Reproduction, planula development, and substratum selection in three species of *Stylactaria* (Cnidaria: Hydrozoa) from Hokkaido, Japan. *J. Nat. Hist.* **27:** 521–533.

Nellis, P., and E. Bourget. 1996. Influence of physical and chemical factors on settlement and recruitment of the hydroid *Tubularia larynx*: field and laboratory experiments. *Mar. Ecol. Prog. Ser.* **140:** 123–139.

Neufeld, D. A., S. K. Westly, and B. J. Clarke. 1978. The electrical potential gradient of regenerating *Tubularia*: spatial and temporal characteristics. *Growth* **42:** 347–356.

Orlov, D. V., and N. N. Marfenin. 1994. Behaviour and settling of actinulae of *Tubularia larynx* (Leptolida, Tubulariidae). *Zool. Zh.* **73:** 5–11.

Östman, C., M. Myrdal, P. Nyvall, J. Lindstrom, M. Bjorklund, and A. Aguirre. 1995. Nematocysts in *Tubularia larynx* (Cnidaria, Hydrozoa) from Scandinavia and the northern coast of Spain. *Sci. Mar.* **59:** 165–179.

Pawlik, J. R. 1992. Chemical ecology of the settlement of benthic marine invertebrates. *Oceanogr. Mar. Biol. Annu. Rev.* **30:** 273–335.

Petersen, K. W. 1990. Evolution and taxonomy in capitate hydroids and medusae (Cnidaria, Hydrozoa). *Zool. J. Linn. Soc.* **101:** 101–231.

Purcell, J. E., and C. E. Mills. 1988. The correlation between nematocyst types and diets in pelagic hydrozoa. Pp. 463–485 in *The Biology of Nematocysts*, D. A. Hessinger and H. M. Lenhoff, eds. Academic Press, San Diego.

Pyefinch, K. A., and F. S. Downing. 1949. Notes on the general biology of *Tubularia larynx* Ellis & Solander. *J. Mar. Biol. Assoc. UK.* **28:** 21–43.

Tardent, P. 1980. A giant *Tubularia* (Cnidaria, Hydrozoa) from the waters of the San Juan Islands, Washington. *Syesis* **13:** 17–25.

Tardent, P. 1995. The cnidarian cnidocyte, a high-tech cellular weaponry. *BioEssays* **17:** 351–362.

Tardent, P., and H. Eymann. 1958. Some chemical and physical properties of the regeneration-inhibitor of *Tubularia*. *Acta Embryol. Morphol. Exp.* **1:** 280–287.

Teitelbaum, M. 1966. Behavior and settling mechanism of planulae of *Hydractinia echinata*. *Biol. Bull.* **131:** 410–411 (Abstract).

Walters, L. J., and D. S. Wethey. 1996. Settlement and post-settlement survival of sessile marine invertebrates on topographically complex surfaces: the importance of refuge dimensions and adult morphology. *Mar. Ecol. Prog. Ser.* **137:** 161–171.

Yamashita, K., S. Kawaii, M. Nakai, M. Takahashi, and N. Fusetani. 1996. Exogenous and endogenous factors affecting the behaviour and settlement of actinula larvae of *Tubularia mesembryanthemum* Allman, 1871 (Hydrozoa). [Abstr.] *Proceedings of the Int. Symp. on Settlement and Metamorphosis of Marine Invertebrate Larvae*. Univ. of Plymouth, England. 15–18 July 1996.

Yamashita, K., S. Kawaii, M. Nakai, and N. Fusetani. 1997. Behavior and settlement of actinula larvae of *Tubularia mesembryanthemum*. Pp. 512–516 in *Proceedings of the 6th International Conference on Coelenterate Biology*, J. C. den Hartog, ed. National Museum of Natural History, Leiden, The Netherlands.

Reference: *Biol. Bull.* **204:** 270–277. (June 2003)

Energy Metabolism During Larval Development of Green and White Abalone, *Haliotis fulgens* and *H. sorenseni*

AMY L. MORAN* AND DONAL T. MANAHAN

Department of Biological Sciences and Wrigley Institute for Environmental Studies, University of Southern California, Los Angeles, California 90089-0371

Abstract. An understanding of the biochemical and physiological energetics of lecithotrophic development is useful for interpreting patterns of larval development, dispersal potential, and life-history evolution. This study investigated the metabolic rates and use of biochemical reserves in two species of abalone, *Haliotis fulgens* (the green abalone) and *H. sorenseni* (the white abalone). Larvae of *H. fulgens* utilized triacylglycerol as a primary source of endogenous energy reserves for development (~50% depletion from egg to metamorphic competence). Amounts of phospholipid remained constant, and protein dropped by about 30%. After embryogenesis, larvae of *H. fulgens* had oxygen consumption rates of 81.7 ± 5.9 (SE) pmol larva^{-1} h^{-1} at 15 °C through subsequent development. The loss of biochemical reserves fully met the needs of metabolism, as measured by oxygen consumption. Larvae of *H. sorenseni* were examined during later larval development and were metabolically and biochemically similar to *H. fulgens* larvae at a comparable stage. Metabolic rates of both species were very similar to previous data for a congener, *H. rufescens*, suggesting that larval metabolism and energy utilization may be conserved among closely related species that also share similar developmental morphology and feeding modes.

Introduction

Most marine invertebrates have a distinct larval phase in their early life histories and can be divided into species whose larvae feed in the plankton (planktotrophic) and species whose larvae can develop and metamorphose without feeding (lecithotrophic) (Thorson, 1950; Strathmann, 1985). Understanding the evolution of these developmental modes within and among closely related taxa has been a major research focus in larval biology (Strathmann, 1985; Havenhand, 1995; Wray, 1995). A number of studies have used mathematical models to explore the ecological and evolutionary forces that select for planktotrophy or lecithotrophy (Vance, 1973; Christiansen and Fenchel, 1979; Caswell, 1981; Pechenik, 1987). Lecithotrophic development is believed to have repeatedly evolved from planktotrophic larval forms in echinoderms and many other phyla (*e.g.*, Strathmann, 1985; Emlet, 1990, 1995). Many changes associated with developmental mode have been reported for egg size (Emlet *et al.*, 1987), biochemical composition (Hoegh-Guldberg and Emlet, 1997; Byrne and Cerra, 2000), patterns of embryogenesis (Raff, 1987; Emlet, 1995; Martindale and Henry, 1995), and larval morphology (Olson *et al.*, 1993; Emlet, 1995).

While there are many suites of morphological and ecological characters associated with planktotrophy and lecithotrophy, less is known about the biochemistry and physiology of larval stages. A number of studies have examined the energetics of development of planktotrophic and lecithotrophic species (*e.g.*, Crisp *et al.*, 1985; Gallager *et al.*, 1986; Dawirs, 1987; Anger *et al.*, 1989; Nates and McKenney, 2000; Marsh *et al.*, 2001), and some have compared the physiological energetics of development of congeneric planktotrophic and lecithotrophic species (*e.g.*, Hoegh-Guldberg and Emlet, 1997; Moreno and Hoegh-Guldberg, 1999) as a means of exploring the evolutionary changes that are associated with the switch from feeding to nonfeeding development.

Further studies of larval energetics within closely related

Received 13 August 2002, accepted 8 April 2003.

* To whom correspondence should be addressed. Current address: Department of Marine Sciences, 12-7 Venable Hall, CB#3300, University of North Carolina, Chapel Hill, NC 27599. E-mail: amoran@unc.edu, manahan@usc.edu

lecithotrophs will be helpful in understanding this developmental mode. The genus *Haliotis* (Gastropoda: Haliotidae), or abalone, provides an excellent model system for examining the energetics of lecithotrophic development. Large adult females produce tens of millions of eggs, providing sufficient material for biochemical and metabolic analyses of larvae throughout development. The energetics of the larvae of the red abalone (*Haliotis rufescens* Swainson) have been studied previously (*e.g.*, Jaeckle and Manahan, 1989a, b; Shilling *et al.*, 1996; Vavra and Manahan, 1999), providing a basis for comparisons of the energetics of larval development within the genus. On the basis of morphological characters, the larval development of abalone appears to be highly conserved within the genus; larvae of different species are visually very similar, and those that have been studied in detail undergo similar developmental sequences (Crofts, 1937; Ino, 1952; Seki and Kanno, 1981; Leighton, 2000). As with other archaeogastropods (Hadfield *et al.*, 1997), abalone larvae are nonfeeding. Nonfeeding larvae have been considered to depend on endogenous egg reserves to supply energy for development (Vance, 1973; Strathmann, 1985). Nonfeeding larvae can also augment energy reserves through the uptake of dissolved organic material from seawater (Jaeckle and Manahan, 1989a, b).

The two abalone species examined in this study are the green abalone, *Haliotis fulgens* Philippi, and the white abalone, *H. sorenseni* Bartsch. Both species range from central California to southern Baja California (Abbott and Haderlie, 1980) and have a history of commercial and recreational harvest. The heavy commercial harvesting of *H. sorenseni* has probably contributed to the near extinction of this species and its recent (summer 2001) listing under the Federal Endangered Species Act in the United States. Leighton (2000) has described general features of the larval development of both *H. fulgens* and *H. sorenseni*. Developmental rate is highly dependent on temperature (Leighton, 2000), and the total planktonic developmental time for both species ranges from 3 days at the upper end of their thermal tolerance to 15 days or more at colder temperatures. Here we present the developmental energetics of the larvae of *H. fulgens* and *H. sorenseni*, and compare these results to those for a third congener, *H. rufescens*, the red abalone.

Materials and Methods

Culture

Embryos and larvae were maintained in stirred cultures at 15 ± 2 °C (for *H. fulgens*) or 13 °C (for *H. sorenseni*) in UV-irradiated seawater filtered to 0.2 μm that was changed every 2 days. Larvae were reared at approximately 5 ml^{-1} in either 20- or 200-l vessels, depending on the numbers of larvae in culture. Under these conditions, by day 7 the larvae of *H. fulgens* reached the swimming and crawling stages and had branched cephalic tentacles, a character that indicates metamorphic competence in abalone larvae (Seki and Kanno, 1981). This rate of development is consistent with other studies of this species (Leighton, 2000). Biochemical samples were taken until day 8 and respiration was measured through day 9; thus our results cover the entire course of larval development. Due to limited availability of larvae of the rare white abalone *H. sorenseni*, measurements were made only on 7- to 10-day-old larvae.

Respiration

Respiration rates of embryos and larvae from two cultures of *H. fulgens*, started from gametes obtained from different parents, were measured throughout development to day 9. For larvae of *H. sorenseni*, respiration was measured daily from days 7 to 10. Larval respiration was measured with high replication (n = 10 to 16) using the end-point determination methods of Marsh and Manahan (1999). In brief, larvae were removed from cultures and suspended in fresh-filtered seawater (0.2 μm) in small respiration chambers of known volume (~500 μl, where each respiration chamber was individually calibrated). Different numbers of individuals were added to each chamber to test for concentration-dependent effects on respiration (none were observed over the range of animals used to calculate respiration rates: Fig. 1). Replicates of 10–16 chambers containing larvae were used for each set of stage-specific measurements. Larvae were incubated in the respiration chambers for 2–4 h, after which 300-μl subsamples were taken from each chamber with a temperature-equilibrated gas-tight syringe. Oxygen tension was measured in each sample with a polarographic oxygen sensor (Model 1302, Strathkelvin). Larvae in each chamber were then counted, and oxygen consumption per animal was calculated as the

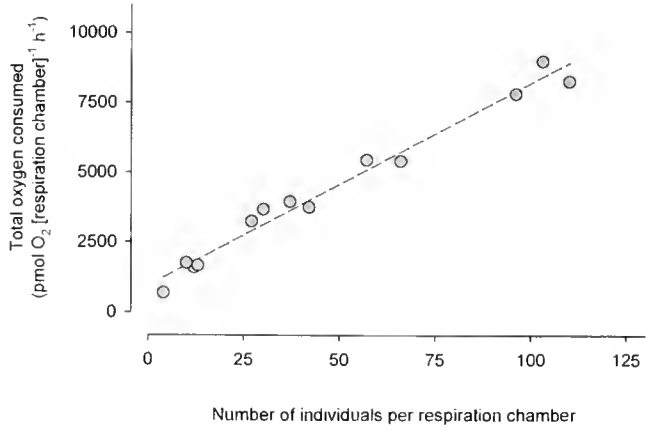

Figure 1. Oxygen consumed by 7-day-old larvae of *Haliotis fulgens* as a function of numbers of larvae used to estimate the respiration rate per individual from the slope (y = 76.3 x + 842; r^2 = 0.98; standard error of slope = 3.4). Each data point represents the oxygen consumed by larvae in a single respiration chamber (500 μl) over 4 h.

slope of the regression line of oxygen consumed per hour against number of larvae in each chamber. The error of each estimate was calculated as the standard error around the slope of the regression line.

Biochemical analysis

The conversion and interpretation of mass-to-energy equivalents in marine invertebrates has long been studied, and remains difficult (*e.g.*, Paine, 1971; Gnaiger and Bitterlich, 1984; Jaeckle and Manahan, 1989a; Moreno *et al.*, 2001). Previously in our laboratory, ash-free dry weight was used successfully as an index of total organic content in larvae of the red abalone, *H. rufescens* (Jaeckle and Manahan, 1989a; Shilling *et al.*, 1996); techniques and instrumentation were identical to those used in the present study. For both species of abalone studied here, we attempted to measure ash-free dry weight but found that the samples never reached a stable dry weight, even after 3 months of drying at 60 °C. As a result, we used direct measurements of carbohydrate, lipid, and protein to determine the general patterns of energy utilization throughout development.

Carbohydrates. Known numbers of animals (500–1000, depending on developmental stage) were aliquoted into 1.7-ml microcentrifuge tubes and centrifuged; seawater was aspirated, and the samples were frozen at −80 °C for later analysis. Total carbohydrates were quantified using the methods of Holland and Gabbott (1971). In brief, samples of eggs (day 0) and metamorphically competent larvae (day 8) were extracted with cold 5% trichloroacetic acid. The supernatant was hydrolyzed for 2 h at 95 °C in 1*M* HCl, then carbohydrates were spectrophotometrically quantified with a ferricyanate reduction reaction using glucose as a standard.

Protein. Samples of known numbers of eggs or larvae were processed as above, and protein was analyzed with the methods of Bradford (1976) as modified by Jaeckle and Manahan (1989a). Protein content was calculated by dividing the total protein in a sample by the total number of animals in that sample. The rate of protein loss during development was estimated as the slope of the regression of total protein per individual over time. Total protein loss during development was calculated as the amount available initially in the egg minus the amount present in an 8-day-old larva.

Lipids. Samples of known numbers of eggs or larvae were collected and processed as above for carbohydrate and protein. For analysis, samples were sonicated, and lipids were extracted using the methanol:chloroform:water extraction of Bligh and Dyer (1959) as modified by Holland and Gabbott (1971) and Holland and Spencer (1973), with additional modifications listed here. Lipids were extracted for 2 h in 2:2:1 (v/v/v) water:methanol:chloroform to which stearyl alcohol had been added as an internal standard. Stearyl alcohol had been previously determined not to interfere with native lipid peaks in abalone larvae (Fig. 2). Phases were separated by the addition of water and chloroform to a final ratio of 4:2:3 water:methanol:chloroform, followed by a centrifugation at 8,000 × *g*. The lower phase was isolated and dried down under nitrogen, and samples were redissolved in a known volume of chloroform. To quantify lipid classes, four replicates were taken at each sampling interval during development. For each replicate, the following procedure was repeated four times. A 1-μl sample of the redissolved lipid in chloroform was taken with a 1.5-μl gas-tight syringe (Precision Sampling Corp.) and applied to a thin-layer chromatography (TLC) "Chromarod" of 1-mm diameter (Iatron Laboratories, Inc). Chromarods were developed in a solvent system of 60:6:0.1 hexane:diethyl ether:formic acid to separate major lipid classes, dried, and immediately analyzed with an Iatroscan MK-5 flame ionization detector (FID). Calibrations were performed for each compound class, using L-α-phosphatidylcholine (phospholipid), cholesterol, tripalmitin (triacylglycerol), lauric acid myristyl ester (wax ester), and stearyl alcohol (fatty alcohol internal standard). Peaks were quantified using E-Lab (OMS Tech, Inc.) chromatography software on a personal computer. The amount of lipid per individual was calculated for each class as the mean of each of the four replicates divided by the number of individuals per sample. Total lipids were calculated as the sum of major lipid classes.

Standards for neutral lipid quantification. Methods for the quantification of specific biochemical components, as above, use an appropriate standard of known composition to quantify the contents of organisms that have unknown or mixed biochemical compositions. For lipid analysis of marine organisms known to have fatty acids with different degrees of carbon-bond saturation, the percent of unsaturation might confound interpretations of lipid content when

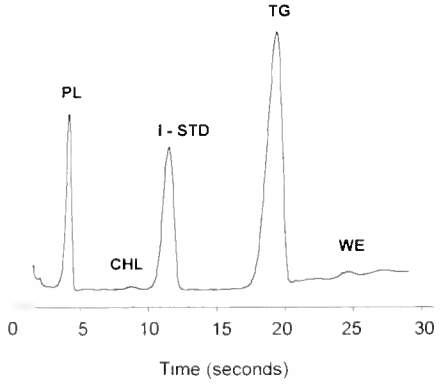

Figure 2. Chromatograph of lipids extracted from eggs of *Haliotis fulgens*. The ordinate is measured in arbitrary units (volts) of peak height. Lipid profile shows large peaks of triacylglycerol (TG) and phospholipid (PL), small peaks of cholesterol (CHL) and wax ester (WE), and the fatty alcohol internal standard stearyl alcohol (I - STD).

using standards that contain a different degree of unsaturation relative to the unknown sample. We addressed this issue of lipid standards and calibration of the FID response in this study of the role of lipids in larval energy metabolism. The peak areas of known standards were compared after chromatographic separation by TLC and quantification by FID of identical quantities of fatty acids containing different numbers of double bonds (unsaturation). Quantification by FID is dependent upon the degree of saturation of each fatty acid. Thus a different FID response per unit mass of lipid containing different numbers of double bonds would be predicted. In an analysis of lipid calibration standards conducted in our laboratory (M. Moore and D.T. Manahan, unpubl. data), 1 μg of each fatty acid was loaded onto a TLC "Chromarod" and quantified by FID for (1) palmitic acid, a fully saturated lipid with no double bonds; (2) oleic acid, with 1 double bond; (3) linoleic acid, with 2 double bonds; and (3) arachidonic acid that contains 4 double bonds. The amount of lipid was quantified by FID using palmitic acid as the 100% calibration standard for each set of samples (n = 3–6). Each sample contained the same quantity of fatty acid but had different numbers of double bonds (levels of saturation). The following values were measured for each fatty acid (values are mean ± SD): palmitic acid, no double bonds = 1.0 μg ± 0.13; oleic acid, 1 double bond = 0.9 μg ± 0.12; linoleic acid, 2 double bonds = 0.8 μg ± 0.08; arachidonic acid, 4 double bonds = 0.6 μg ± 0.12. These data show a trend of decreasing FID response with increasing number of double bonds. Within analytical error, however, there was no significant difference in the FID response for fatty acids with 0, 1, or 2 double bonds (VR = 2.99^{ns} for 2, 12 df). This full analysis was repeated with an additional set of standards, giving a similar result that showed no significant effect of 0, 1, or 2 double bonds on the quantification of fatty acids (VR = 2.89^{ns} for 2, 9 df). For both sets of replicate samples, there was a significant difference for an ANOVA that included arachidonic acid (4 double bonds) in the analysis of FID response to 0, 1, 2, and 4 double bonds. The calibration study was also expanded beyond an analysis of monomers: a comparison of standards based on tripalmitin and triolein also showed no significance difference at 1.00 μg ± 0.04 and 0.97 μg ± 0.04, respectively.

Larvae of *H. fulgens* have 42% of their fatty acids in a fully saturated form, with palmitic acid being the dominant fatty acid at 30% (Nelson *et al.*, 2002). An additional 42% of the fatty acids are monounsaturated—a chemical difference that is not statistically distinguishable from saturated fatty acids by FID in our analysis (as above). Only 13% of the total fatty acids present in larvae of *H. fulgens* tissues are polyunsaturated, and this percent is not likely to cause significant error if tripalmitin is used as a standard for neutral lipid analysis (as in our study). Given the statistical analysis above of the comparison of different fatty acids as standards, we conclude that the use of tripalmitin as a standard for larvae of *H. fulgens* will result in an insignificant error for the quantification of total neutral lipid content.

Results

The respiration rates of larvae of *Haliotis fulgens* were similar for the two cultures spawned from different sets of parents. Larvae in Culture 1 reached the veliger stage by day 2, and their respiration rates through subsequent larval development remained fairly constant, with a mean rate of 83.4 ± 2.6 (SE) pmol O_2 $larva^{-1}$ h^{-1} (Fig. 3). For Culture 2, the mean respiration rate was 80.0 ± 5.3 pmol O_2 $larva^{-1}$ h^{-1} (Fig. 3). Within a specific culture, the respiration rates of pre-veliger stages (< 2-day-old) were lower than in later veliger stages. For *H. sorenseni*, the mean respiration rate of larvae was 58.9 ± 4.7 pmol O_2 $larva^{-1}$ h^{-1} (Fig. 3).

The amount of protein in the eggs from the two spawns of *H. fulgens* was similar (Fig. 4, Day 0). The rate of decrease in total protein during development was not significantly different between the two cultures: by analysis of variance of compared regressions, the variance ratios between the two slopes and the two y-axis intercepts were 0.25 and 0.73, respectively (not significant for 1, 13 df). The data for both cultures were combined into a single regression to calculate a rate of protein loss of 13 ng $individual^{-1}$ day^{-1}, resulting in a total loss of about 30% from the initial content in the egg to 8-day-old larvae (Fig. 4).

Lipid-class analysis of *H. fulgens* showed that triacylglycerol was the dominant class, followed by phospholipid (Fig. 2). Cholesterol and wax ester contents were very low (below quantifiable detection limit: Fig. 2) relative to tri-

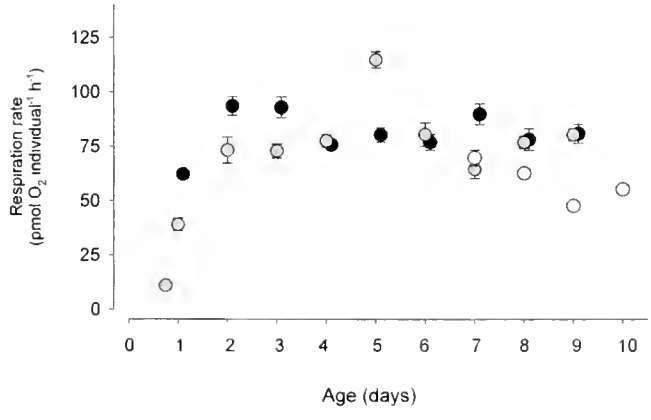

Figure 3. Rates of oxygen consumption over development of larvae from Culture 1 (black symbols) and Culture 2 (grey symbols) of *Haliotis fulgens*, and from day 7 to day 10 of development for larvae of *H. sorenseni* (white symbols). Respiration rates were measured at the rearing temperatures of both species: 15°C for *H. fulgens* and 13°C for *H. sorenseni*. Error bars are the standard error of the slope used to estimate respiration rates of individual larvae (see Fig. 1).

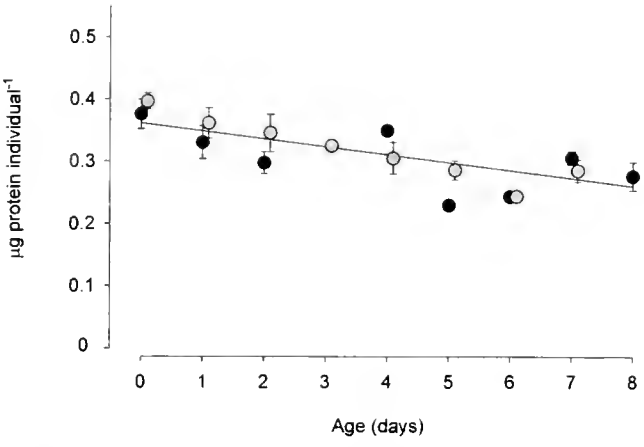

Figure 4. Total protein content during development of *Haliotis fulgens*. Data are from two cultures: Culture 1 (black symbols) and Culture 2 (grey symbols). Each data point represents the mean of 4 independent samples (day 0 = eggs). The rate of protein decline was not different between the two cultures (see text), and all data were combined to calculate the rate of protein loss over development: μg protein individual^{-1} = $-0.013x + 0.361$, where x represents age in days (error bars are ± 1 SE).

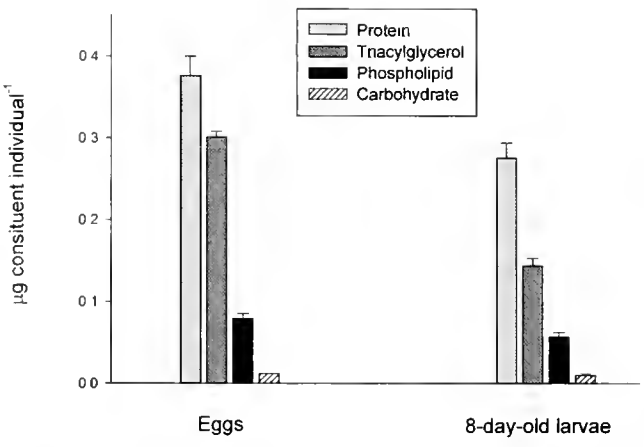

Figure 6. Protein, triacylglycerol, phospholipid, and carbohydrate content of *Haliotis fulgens* measured at day 0 (eggs) and day 8 (late-stage larvae, Culture 1). Error bars are the standard error.

acylglycerol and phospholipid, and are not included in presentation of the developmental changes in lipid content (Fig. 5). In larvae from both cultures of *H. fulgens*, phospholipid content remained constant throughout development, while triacylglycerol decreased by about 50% (Fig. 5). Larvae of *H. sorenseni* had 0.40 ± 0.02 µg protein, 0.36 ± 0.03 µg triacylglycerol, and 0.13 ± 0.01 µg phospholipid per larva (7-day-old).

Carbohydrate content was low. *H. fulgens* contained 1.2 ± 0.05 ng carbohydrate egg^{-1} and 1.0 ± 0.23 ng larva^{-1}. These amounts corresponded to only 1.6% and 2.1% of the total protein and lipid content of eggs and larvae, respectively (Fig. 6).

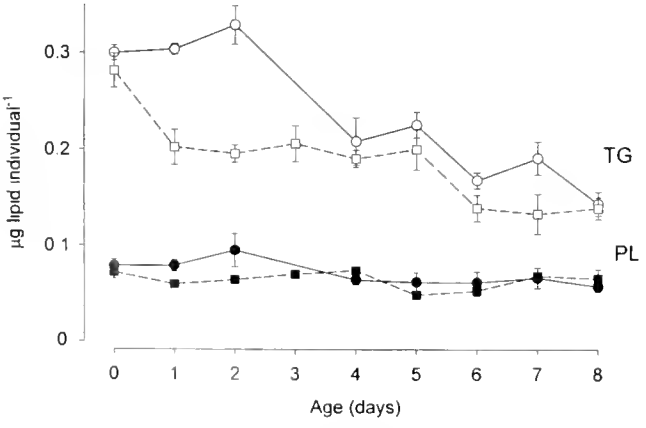

Figure 5. Lipid content of *Haliotis fulgens* larvae over development for Culture 1 (circles) and Culture 2 (squares). White symbols represent triacylglycerol; black symbols represent phospholipid (error bars are ± 1 SE).

Discussion

Energy metabolism and rates of utilization of endogenous reserves in marine invertebrates with planktotrophic larval forms have received considerable attention (*e.g.*, Crisp, 1974; Holland, 1978; Gallager *et al.*, 1986; Anger *et al.*, 1989; Shilling and Manahan, 1994; Marsh *et al.*, 2001). However, fewer species with lecithotrophic modes of development have been studied in similar detail (*e.g.*, echinoderms: Hoegh-Guldberg and Emlet, 1997; crustaceans: Anger, 1996; bryozoans: Wendt, 2000). This has made it difficult to make comparisons and generalizations about the energetics of nonfeeding development, or to understand the role of larval energetics in the evolution of the life-history strategies of marine invertebrates. The genus *Haliotis* offers several advantages as a taxon for studying the comparative energetics of lecithotrophic development among closely related species. All larval forms studied to date within this genus are lecithotrophic, and the findings presented here show that patterns of energy utilization are similar among several species in this genus. Specifically, the biochemical compositions of larvae of the green (*H. fulgens*; this study), white (*H. sorenseni*; this study), and red (*H. rufescens*; Jaeckle and Manahan, 1989a) abalone are similar, with protein and lipid being the dominant macromolecules. Likewise, the metabolic rates of these three species of abalone larvae are similar, even given the 2 °C difference in temperature between the green and white abalone larvae (Fig. 3 this study; *cf.* red abalone larvae at 17 °C = 84 pmol O_2 larva^{-1} h^{-1}: Jaeckle and Manahan, 1989a).

Of the endogenous components used to fuel development in marine invertebrate larvae, lipids are generally considered to be more important than protein and carbohydrates (Holland, 1978). Our results are consistent with

this conclusion for carbohydrates. In eggs and metamorphically competent larvae of *H. fulgens* (Fig. 6), carbohydrates are not a major energy source, making up about 2% of the total content of lipid and protein. In contrast, and in agreement with other biochemical analyses of lecithotrophic larval development, our results also show that lipid is a major source of energy. During larval development from egg to a stage competent to metamorphose (Fig. 5), tricylglycerol decreased while phospholipids remained constant. This pattern is consistent with ontogenetic changes in lipid composition during nonfeeding development of some other marine organisms, in which triacylglycerol decreased while the polar lipid fraction changes little over development (*e.g.*, Takii *et al.*, 1997; Whertmann and Graeve, 1998; Nates and McKenney, 2000). A major portion of the metabolic costs of abalone larval development can be explained by catabolism of triacylglycerol (see below). From Figure 5, taking the amount of triacylglycerol in the egg (Culture 1: 0.30 μg) and subtracting the triacylglycerol content of 8-day-old larvae (0.14 μg), a total of 0.16 μg of lipid was depleted over development. When converted to energy equivalents (39.5 kJ g^{-1}; Gnaiger, 1983), lipid catabolism could provide 6.3 mJ of energy per larva. A similar set of calculations resulted in 5.5 mJ of energy for a larva from Culture 2 (energy equivalents from Gnaiger, 1983). The energetic cost of larval development from Figure 3, based on cumulative oxygen consumption to day 8 (for comparison with lipid depletion to day 8), was 15.6 μmol O_2 $larva^{-1}$ (Culture 1) and 14.4 μmol O_2 $larva^{-1}$ (Culture 2). Based on the oxyenthalpic equivalent of lipid catabolism [441 kJ (mol O_2^{-1})] (Gnaiger, 1983), these oxygen consumption values are equivalent to 6.9 mJ and 6.3 mJ per larva for Culture 1 and Culture 2, respectively. Hence, the energy made available from the depletion of lipid could account for 91% and 87% of metabolism for larvae in Cultures 1 and 2. These calculations support the conclusion that measured depletion of lipid reserves could fuel most of the larval development of *H. fulgens*. This is consistent with the larval energetics of other marine molluscs, in which lipids are a major source of endogenous energy (Millar and Scott, 1967; Holland and Spencer, 1973; His and Maurer, 1988).

In addition to lipid, total protein content also decreased in larvae of *H. fulgens* over development from egg to competent larva (Fig. 4: day 8). Subtracting the protein content of 8-day-old larvae (0.28 μg) from the protein content of the egg (0.38 μg) indicated that larvae in Culture 1 lost a total of 0.1 μg protein $individual^{-1}$. Larvae in Culture 2 also utilized 0.1 μg protein; in both cultures, when this protein loss was converted to energy equivalents of complete oxidation (24.0 kJ g^{-1}), it was equivalent to 2.4 mJ $individual^{-1}$ over 8 days. Clearly, the total energy available to a larva from the depletion of lipid and protein combined (Culture 1 = 8.7 mJ; Culture 2 = 7.9 mJ) could theoretically exceed the metabolic demand as measured by oxygen consumption for larvae of *H. fulgens*. In addition, biochemical fractions not measured as total protein, lipid, and carbohydrate (Holland and Gabbott, 1971; Gnaiger and Bitterlich, 1984) could also contribute to metabolism. The *actual* contribution, however, of any metabolic substrate to metabolism depends on the extent to which that substrate is fully oxidized to release energy. Also, the extent to which the proportional loss of different substrates can be assigned the correct oxyenthalpic equivalent for energy-yield calculations depends on the extent of full oxidation [*e.g.*, protein = 527 kJ (mol O_2^{-1}) *cf.* lipid = 441 kJ (mol O_2^{-1})]. Assumptions about the identity of metabolic substrates and their degree of oxidation are commonly used to calculate energy budgets for marine invertebrate larvae. If, however, not all materials depleted during development are fully oxidized, these assumptions will not be entirely accurate. To fully describe the energetics of larval development, future studies should not only consider oxygen consumption and depletion of specific macromolecules, but also include measurements of the actual rates of oxidation of these biochemical constituents. To our knowledge, this suite of measurements has never been simultaneously taken in larvae of any marine invertebrate species.

For larvae of *H. fulgens*, the energy available from the presumed 100% catabolism of energy reserves was more than adequate to support metabolic demand. This is in contrast to previous studies with other species of abalone larvae (*H. rufescens:* Jaeckle and Manahan, 1989a), in which metabolic demand exceeded energy available from depletion of protein and lipid over development. The chemistry of the seawater used to culture larvae is likely to be important in lecithotrophic larval energetics. The larvae of many soft-bodied marine invertebrates can take dissolved organic material (DOM) up directly from seawater (Manahan, 1990). Both in laboratory and field situations, low concentrations of DOM may force larvae to catabolize endogenous reserves to fuel development, while larvae in DOM-rich seawater may be able to utilize those exogenous sources of energy, thereby sparing endogenous reserves (Jaeckle and Manahan, 1992). Differences in patterns of utilization of endogenous energy reserves among different studies of larvae—for example, the lack of a decrease in lipid during larval development of *H. rufescens* (Jaeckle and Manahan, 1989a)—are most likely attributable to environmental issues, such as the organic "quality" of the seawater used to rear the larvae. Variations in the seawater "quality" used to culture larvae and differences in maternal inputs to egg "quality" (Buchal *et al.*, 1998) may overwhelm small species-specific differences in biochemical composition and larval energy metabolism among closely related organisms with similar life histories.

Acknowledgments

Our thanks to Tom McCormick of Proteus SeaFarms for supplying larvae. We are most grateful to Michael Moore of USC for his insights and excellent analysis of lipid standards. ALM was supported by a postdoctoral fellowship from the Wrigley Institute at USC. This work was supported by USDA grants to DTM. This is contribution number 227 from USC's Wrigley Marine Science Center on Santa Catalina Island.

Literature Cited

Abbott, D. P., and E. C. Haderlie. 1980. Prosobranchia: marine snails. Pp. 231–307 in *Intertidal Invertebrates of California*, R.H. Morris, D.P. Abbott, and E.C. Haderlie, eds. Stanford University Press, Stanford, CA. 690 pp.

Anger, K. 1996. Physiological and biochemical changes during lecithotrophic larval development and early juvenile growth in the northern stone crab, *Lithodes maja* (Decapoda: Anomura). *Mar. Biol.* **126:** 283–296.

Anger, K., J. Harms, C. Puschel, and B. Seeger. 1989. Physiological and biochemical changes during the larval development of a brachyuran crab reared under constant conditions in the laboratory. *Helgol. Meeresunters* **43:** 224–244.

Bligh, E. G., and W. F. Dyer. 1959. A rapid method of total lipid extraction and purification. *Can. J. Biochem. Physiol.* **37:** 911–917.

Bradford, M. 1976. A rapid and sensitive method for the quantitation of microgram quantities of protein utilizing the principle of protein-dye binding. *Anal. Biochem.* **72:** 248–254.

Buchal M., J. E. Levin, and C. Langdon. 1998. *Palmaria mollis* as a settlement substrate and food for the red abalone *Haliotis rufescens*. *Aquaculture* **165:** 243–260.

Byrne, M., and A. Cerra. 2000. Lipid dynamics in the embryos of *Patiriella* species (Asteroidea) with divergent modes of development. *Dev. Growth Differ.* **42:** 79–86.

Caswell, H. 1981. The evolution of "mixed" life-histories in marine invertebrates and elsewhere. *Am. Nat.* **117:** 529–536.

Christiansen, F. B., and T. M. Fenchel. 1979. Evolution of marine invertebrate reproductive patterns. *Theor. Popul. Biol.* **16:** 267–282.

Crisp, D. J. 1974. Energy relations of marine invertebrate larvae. *Thalassia Jugosl.* **10:** 103–120.

Crisp, D. J., A. B. Yule, and K. N. White. 1985. Feeding by oyster larvae—the functional response, energy budget, and a comparison with mussel larvae. *J. Mar. Biol. Assoc. UK* **65:** 759–784.

Crofts, D. R. 1937. The development of *Haliotis tuberculata* with special reference to the organogenesis during torsion. *Philos. Trans. R. Soc. Lond. B* **228:** 219–268.

Dawirs, R. R. 1987. Influence of limited food supply on growth and elemental composition (C,N,H) of *Carcinus maenas* (Decapoda) larvae reared in the laboratory. *Mar. Ecol. Prog. Ser.* **31:** 301–308.

Emlet, R. B. 1990. World patterns of developmental mode in echinoid echinoderms. Pp. 329–335 in *Advances in Invertebrate Reproduction, Vol. 5, Proceedings of the 5th International Congress of Invertebrate Reproduction*, M. Hoshi and O. Yamishita, eds. Elsevier, Amsterdam.

Emlet, R. B. 1995. Larval spicules, cilia, and symmetry as remnants of indirect development in the direct developing sea urchin *Heliocidaris erythrogramma*. *Dev. Biol.* **167:** 405–415.

Emlet, R. B., L. R. McEdward, and R. R. Strathmann. 1987. Echinoderm larval ecology viewed from the egg. Pp. 55–136 in *Echinoderm Studies*, Vol. 2. M. Jangoux and J.M. Lawrence, eds. Balkema, Rotterdam.

Gallager, S. M., R. Mann, and G. C. Sasaki. 1986. Lipid as an index of growth and viability in three species of bivalve larvae. *Aquaculture* **56:** 81–103.

Gnaiger, E. 1983. Calculation of energetic and biochemical equivalents of respiratory oxygen consumption. Pp. 337–345 in *Polarographic Oxygen Sensors: Aquatic and Physiological Applications*, E. Gnaiger and H. Forstner, eds. Springer-Verlag, New York.

Gnaiger, E., and G. Bitterlich. 1984. Proximate biochemical composition and caloric content calculated from elemental CHN analysis: a stoichiometric concept. *Oecologia* **62:** 289–298.

Hadfield, M. G., M. F. Strathmann, and R. R. Strathmann. 1997. Ciliary currents of non-feeding veligers in putative basal clades of gastropods. *Invertebr. Biol.* **116:** 313–321.

Havenhand, J. N. 1995. Evolutionary ecology of larval types. Pp. 79–122 in *Ecology of Marine Invertebrate Larvae*, L. McEdward, ed. CRC Press, Boca Raton, FL.

His, E., and D. Maurer. 1988. Shell growth and gross biochemical composition of *Crassostrea gigas* larvae in the natural environment. *Aquaculture* **69:** 185–194

Hoegh-Guldberg, O., and R. B. Emlet. 1997. Energy use during the development of a lecithotrophic and a planktotrophic echinoid. *Biol. Bull.* **192:** 27–40.

Holland, D. L. 1978. Lipid reserves and energy metabolism in the larvae of benthic marine invertebrates. Pp. 85–123 in *Biochemical and Biophysical Perspectives in Marine Biology*, D.C. Sargent and J.R. Malins, eds. Academic Press, London.

Holland, D. L., and P. A. Gabbott. 1971. A micro-analytical scheme for the determination of protein, carbohydrate, lipid and RNA levels in marine invertebrate larvae. *J. Mar. Biol. Assoc. UK* **51:** 659–668.

Holland, D. L., and B. E. Spencer. 1973. Biochemical changes in fed and starved oysters, *Ostrea edulis* L., during larval development, metamorphosis and early spat growth. *J. Mar. Biol. Assoc. UK* **53:** 287–298.

Ino, T. 1952. Biological studies on the propagation of Japanese abalone (genus *Haliotis*). *Bull. Tokai Reg. Fish. Res. Lab.* **5:** 1–102.

Jaeckle, W. B., and D. T. Manahan. 1989a. Growth and energy imbalance during the development of a lecithotrophic molluscan larva (*Haliotis rufescens*). *Biol. Bull.* **177:** 237–246.

Jaeckle, W. B., and D. T. Manahan. 1989b. Feeding by a "nonfeeding" larva: uptake of dissolved amino acids from seawater by lecithotrophic larvae of the gastropod *Haliotis rufescens*. *Mar. Biol.* **103:** 87–94.

Jaeckle, W. B., and D. T. Manahan. 1992. Experimental manipulations of the organic chemistry of seawater: implications for studies of energy budgets in marine invertebrate larvae. *J. Exp. Mar. Biol. Ecol.* **156:** 273–284.

Leighton, D. L. 2000. *The Biology and Culture of the California Abalones*. Dorrance Publishing, Pittsburg, PA. 216 p.

Manahan, D. T. 1990. Adaptations by invertebrate larvae for nutrient acquisition from seawater. *Am. Zool.* **30:** 147–160.

Marsh, A. G., and D. T. Manahan. 1999. A method for accurate measurements of the respiration rates of marine invertebrate embryos and larvae. *Mar. Ecol. Prog. Ser.* **184:** 1–10.

Marsh, A. G., L. Mullineaux, C. Young, and D. Manahan. 2001. Larval dispersal potential of the tubeworm *Riftia pachyptila* at deep-sea hydrothermal vents. *Nature* **411:** 77–80.

Martindale, M. Q., and J. Q. Henry. 1995. Modifications of cell fate specification in equa-cleaving nemertean embryos: alternate patterns of spiralian development. *Development* **121:** 3175–3185.

Millar, R. H., and J. M. Scott. 1967. The larva of the oyster *Ostrea edulis* during starvation. *J. Mar. Biol. Assoc. UK* **47:** 475–484.

Moreno, G., and O. Hoegh-Guldberg. 1999. The energetics of development of three congeneric seastars (*Patiriella* Verrill, 1913) with different types of development. *J. Exp. Mar. Biol. Ecol.* **235:** 1–20.

Moreno, G., P. Selvakumaraswamy, M. Byrne, and O. Hoegh-Guldberg. 2001. A test of the ash-free dry weight technique on the

developmental stages of *Patiriella* spp. (Echinodermata: Asteroidea). *Limnol. Oceanogr.* **46:** 1214–1220.

Nates, S. F., and C. L. McKenney. 2000. Ontogenetic changes in biochemical composition during larval and early postlarval development of *Lepidophthalmus louisianensis*, a ghost shrimp with abbreviated development. *Comp. Biochem. Physiol. B* **127:** 459–468.

Nelson, M. M., D. L. Leighton, C. F. Phleger, and P. D. Nichols. 2002. Comparison of growth and lipid composition in the green abalone, *Haliotis fulgens*, provided specific macroalgal diets. *Comp. Biochem. Physiol. B* **131:** 695–712.

Olson, R. R., J. L. Cameron, and C. M. Young. 1993. Larval development (with observations on spawning) of the pencil urchin *Phyllacanthus imperialis*: a new intermediate larval form? *Biol. Bull.* **185: 77–85.**

Paine, R. T. 1971. The measurement and application of the calorie to ecological problems. *Annu. Rev. Ecol. Syst.* **2:** 145–164.

Pechenik, J. A. 1987. Environmental influences on larval survival and development. Pp. 551–608 in *Reproduction and Development of Marine Invertebrates*, Vol. 9, A.C. Giese, J. S. Pearse, and V. B. Pearse, eds. Blackwell Scientific Publications and the Boxwood Press, Palo Alto and Pacific Grove, CA.

Raff, R. A. 1987. Constraint, flexibility, and phylogenetic history in the evolution of direct development in sea urchins. *Dev. Biol.* **119:** 6–19.

Seki, T., and H. Kanno. 1981. Observations on the settlement and metamorphosis of the veliger of the Japanese abalone *Haliotis discus hannai* Haliotidae Gastropoda. *Bull. Tokai Reg. Fish. Res. Lab.* **42:** 31–40.

Shilling, F. M., and D. T. Manahan. 1994. Energy metabolism and amino acid transport during early development of Antarctic and temperate echinoderms. *Biol. Bull.* **187:** 398–407.

Shilling, F. M., O. Hoegh-Guldberg, and D. T. Manahan. 1996. Sources of energy for increased metabolic demand during metamorphosis of the abalone *Haliotis rufescens* (Mollusca). *Biol. Bull.* **191:** 402–412.

Strathmann, R. R. 1985. Feeding and non-feeding larval development and life-history evolution in marine invertebrates. *Annu. Rev. Ecol. Syst.* **16:** 339–361.

Takii, K., S. Miyashita, M. Seoka, Y. Tanaka, Y. Kubo, and H. Kumai. 1997. Changes in chemical contents and enzyme activities during embryonic development of bluefin tuna. *Fish. Sci.* **63:**1014–1018.

Thorson, G. 1950. Reproductive and larval ecology of marine bottom invertebrates. *Biol. Rev.* **25:** 1–45.

Vance, R. R. 1973. On reproductive strategies in marine benthic invertebrates. *Am. Nat.* **107:** 339–352.

Vavra, J., and D. T. Manahan. 1999. Protein metabolism in lecithotrophic larvae (Gastropoda: *Haliotis rufescens*). *Biol. Bull.* **196:** 177–186.

Wendt, D. E. 2000. Energetics of larval swimming and metamorphosis in four species of *Bugula* (Bryozoa). *Biol. Bull.* **198:** 346–356.

Whertmann, I. S., and M. Graeve. 1998. Lipid composition and utilization in developing eggs of two tropical marine caridean shrimps (Decapoda: Caridea: Alpheidae, Palaemonidae). *Comp. Biochem. Physiol. B* **121:** 457–463.

Wray, G. A. 1995. Evolution of larvae and developmental modes. Pp. 413–447 in *Ecology of Marine Invertebrate Larvae*, L. McEdward, ed. CRC Press, Boca Raton, FL.

Reference: *Biol. Bull.* **204:** 278–289. (June 2003)

Localization and Quantification of Carbonic Anhydrase Activity in the Symbiotic Scyphozoan *Cassiopea xamachana*

ANNE M. ESTES*, STEPHEN C. KEMPF, AND RAYMOND P. HENRY†

Department of Biological Sciences, 101 Rouse Life Science Building, Auburn University, Auburn, Alabama 36849

Abstract. The relationship between density and location of zooxanthellae and levels of carbonic anhydrase (CA) activity was examined in *Cassiopea xamachana.* In freshly collected symbiotic animals, high densities of zooxanthellae corresponded with high levels of CA activity in host bell and oral arm tissues. Bleaching resulted in a significant loss of zooxanthellae and CA activity. Recolonization resulted in full restoration of zooxanthellar densities but only partial restoration of CA activity. High levels of CA activity were also seen in structures with inherently higher zooxanthellar densities, such as oral arm tissues. Similarly, the oral epidermal layer of bell tissue had significantly higher zooxanthellar densities and levels of CA activity than did aboral bell tissues. Fluorescent labeling, using 5-dimethylaminonapthalene-1-sulfonamide (DNSA) also reflected this tight-knit relationship between the presence and density of zooxanthellae, as DNSA-CA fluorescence intensity was greatest in host oral epithelial cells directly overlying zooxanthellae. However, the presence and density of zooxanthellae did not always correspond with enzyme activity levels. A transect of bell tissue from the margin to the manubrium revealed a gradient of CA activity, with the highest values at the bell margin and the lowest at the manubrium, despite an even distribution of zooxanthellae. Thus, abiotic factors may also influence the distribution of CA and the levels of CA activity.

Received 17 May 2002; accepted 8 April 2003.

* Current Address: Department of Ecology and Evolutionary Biology, University of Arizona, 310 BioScience West, Tucson, AZ 85721.

† To whom correspondence should be addressed. E-mail: henryrp@auburn.edu

Abbreviations: AZ, acetazolamide; CA, carbonic anhydrase; C_i, inorganic carbon; DMF, dimethyl formamide; DNSA, 5-dimethylaminonapthalene-1-sulfonamide; E_o, total concentration of free enzyme; EZ, ethoxyzolamide; i, fractional inhibition of enzyme activity at I_o; I_o, zero concentration of inhibitor; K_i, inhibition constant.

Introduction

The reciprocal translocation of carbon between cnidarian hosts and their endosymbiotic dinoflagellates (zooxanthellae) is essential for maintaining this keystone obligate mutualism. Zooxanthellae require inorganic carbon (C_i), in the form of molecular CO_2, as the substrate for Rubisco-catalyzed C3 photosynthesis, while the host benefits from organic carbon synthesized and secreted by the symbionts (Streamer *et al.*, 1993). However, neither CO_2 produced by host respiration nor molecular CO_2 dissolved in seawater can support maximal rates of photosynthesis (Al-Moghrabi *et al.*, 1996; Gattuso *et al.*, 1999). Instead, the zooxanthellae must somehow gain access to the carbon present as HCO_3^-, the most abundant form of inorganic carbon in seawater (Allemand *et al.*, 1998; Benazet-Tambutte *et al.*, 1996). Accessing the seawater HCO_3^- pool, however, is a problem, since HCO_3^- does not readily diffuse across biological membranes and the uncatalyzed conversion of HCO_3^- to CO_2 is too slow to support maximal photosynthetic rates (Gutknecht *et al.*, 1977; Muscatine *et al.*, 1989; Gattuso *et al.*, 1999). These obstacles to sufficient carbon transport can be overcome by carbonic anhydrase (CA), an enzyme that catalyzes the reversible dehydration of HCO_3^- to CO_2, the freely diffusible form of C_i. A growing body of evidence suggests that CA plays an important role in supplying inorganic carbon to the symbiont by providing zooxanthellar photosynthesis with a virtually unlimited supply of CO_2 through the catalyzed dehydration of seawater HCO_3^- (Weis, 1993; Benazet-Tambutte *et al.*, 1996; Süllemeyer *et al.*, 1998; Furla *et al.*, 2000).

CA activity has been found in 28 species of marine algae and phytoplankton (Graham and Smillie, 1976) and in more

than 40 species of symbiotic marine invertebrates, including 22 cnidarian species (Weis *et al.*, 1989). Furthermore, CA activity is highest in host tissues and apparently depends upon the animal's symbiotic state, as tissues of symbiotic organisms have been shown to have levels of CA activity 29 times greater than tissues of aposymbiotic animals (Weis *et al.*, 1989). In anthozoans such as *Aiptasia,* the presence of algae induces CA activity. Light intensity, water flow, and the photosynthetic rate of the zooxanthellae were also proposed as other factors potentially affecting CA induction (Weis, 1991; Weis *et al.*, 1989). Polyclonal antibodies made against mammalian CA II have been used to localize CA to regions on or near the membrane surrounding the zooxanthellae. Such labeling is consistent with the role of CA in supplying the symbiont with CO_2 for photosynthesis (Weis, 1993). However, because of differences in isozyme structure between organisms, especially across broad phylogenic lines, antibodies are not ideal for localizing CA (Suzuki *et al.*, 1994).

Despite significant advances, two central questions concerning the role of CA in C_i transport remain: (1) is the enzyme localized in the host tissues where it would potentially facilitate CO_2 transport from the surrounding seawater, and (2) what are the factors that control the levels of CA activity in symbiotic animals? This investigation examines these questions in *Cassiopea xamachana,* the upside-down jellyfish, which is an ideal organism for studying physiological mechanisms of CA-mediated carbon cycling in symbiotic cnidarians. Members of the species are densely populated with the zooxanthella, *Symbiodinium* sp., and they have a large bell that allows repeated sampling of individuals over time. Their soft body makes it easy to separate ectodermal epithelium from associated mesoglea to further localize enzyme activity to specific tissues. They also exhibit a unique behavioral adaptation in which the oral portion of the bell is oriented upward and thus receives direct sunlight while the aboral portion of the bell is positioned against the substratum. Furthermore, the tissue of the bell margin receives the highest light intensity and water flow, whereas bell tissue closer to the manubrium is sheltered. Thus, *C. xamachana* provides a unique opportunity to examine the relationship between algal density and CA activity by exploring the microenvironment of its different tissue layers and structures. Localization of CA activity to body region and epithelial surface, under various states of symbiosis, was examined by DNSA (dansylamide, or 5-dimethylaminonaphthalene-1-sulfonamide)-CA fluorescence and by direct enzyme assay.

Materials and Methods

Animal collection and maintenance

Specimens of *Cassiopea xamachana* ranging in bell diameter from 10 to 14 cm were collected from Marathon Key, Florida (mile marker 57) and transported to Auburn University, Auburn, Alabama, in buckets or coolers. The medusae were held in shallow 20-gallon aquaria containing 32 ppt artificial seawater (Reef Crystals, Aquarium Systems, Mentor, OH) with trickle filter systems, undergravel filtration, and protein skimmers. Animals residing on the crushed coral substrate of the aquaria were illuminated with 80 μE m^{-2} s^{-1} actinic light on a 12:12 light:dark photoperiod at ~25–30 °C. Animals were fed newly hatched *Artemia* nauplii three times a week.

Terminology and experimental protocol

Experiments involved animals in three different symbiotic states: (1) field-condition—animals recently collected from the field and in the natural symbiotic state; (2) bleached—the same animals after they had been cold-shocked and incubated in the dark, causing them to lose significant numbers of zooxanthellae; and (3) repopulated—the same cold-shocked and bleached animals that had been placed under actinic light in the laboratory and allowed to undergo repopulation by their remaining symbionts.

Baseline samples of bell margin tissue were taken from eight freshly field-collected symbiotic jellyfish (acclimated in the field to a light intensity of about 1000 μE) and were fixed or frozen as described below for determination of zooxanthella density and CA activity and localization. These eight symbiotic individuals were then cold-shocked for 1 h at 4 °C and incubated in the dark for 1–3 weeks to bleach. Cold-shocked animals expelled 67%–70% of their zooxanthellae and were considered to be bleached. After 3 weeks, bleached animals were exposed to the actinic light (80 μE) of the aquarium for 1–5 weeks to allow zooxanthellae remaining in their tissues to mitotically divide and repopulate bell tissue to algal densities similar to those found in field-collected animals. During bleaching and recolonization, bell margin tissue samples of about 0.5 g were taken every 7 days and treated as described below.

Anatomy and tissue sampling protocol

Several regions of *C. xamachana* tissue, determined by the animal's unique morphology and orientation in its environment, were assayed for carbonic anhydrase (CA) activity and algal density (Fig. 1): (1) bell margin tissue—a concentric ring about 1 cm in width, running around the perimeter of the bell; (2) oral arm tissue—the outpocketings of the gastrovascular cavity and overlying tissue layers that extend up into the water column; (3) the epithelial layer from the oral (subumbrellar) and aboral (exumbrellar) regions of the bell; (4) isolated mesogleal tissue; and (5) samples of intact bell tissue along a radial transect extending from the bell margin to the manubrium (the gastrovascular cavity located at the center of the bell).

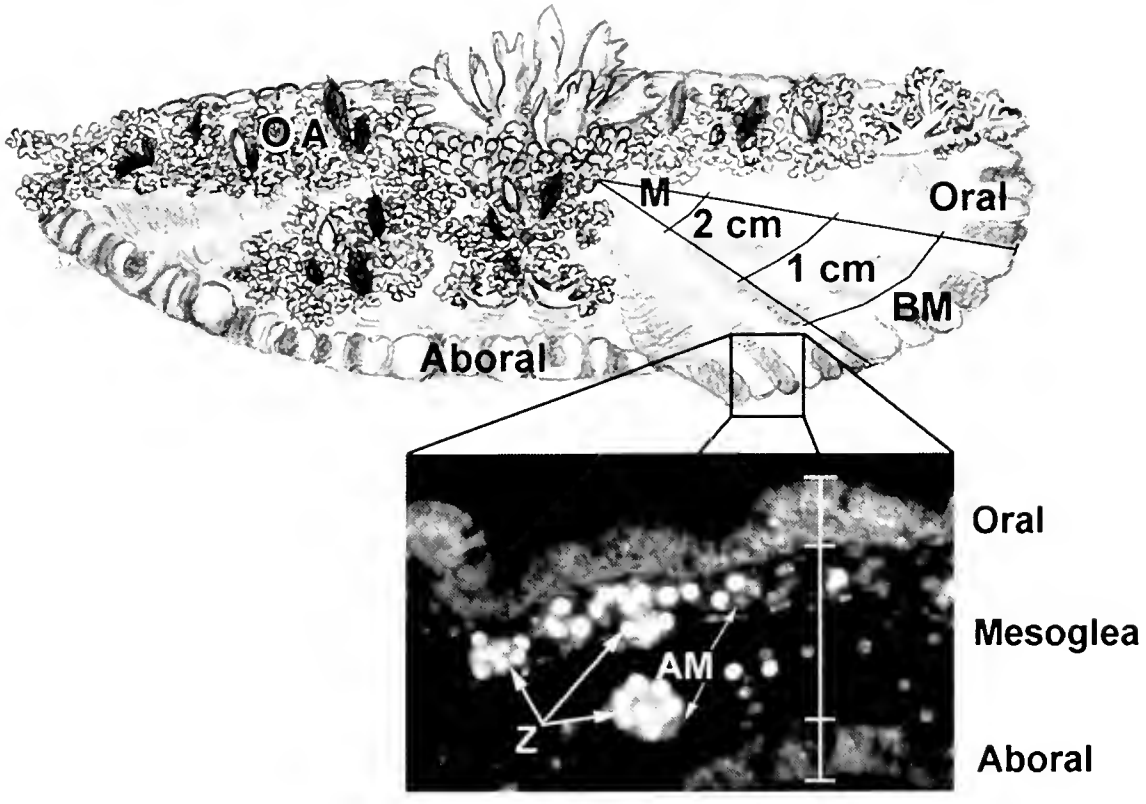

Figure 1. Drawing of *Cassiopea xamachana* showing oral arms (OA) and bell tissues. The left half of the animal is shown in the midst of beating the bell margin, so that the markings of the aboral epithelial layer are evident. The right half of the animal is drawn prostrate, and a transect of the bell is shown illustrating the regions that were used in the various assays described in the methods section. BM—tissue collected at the bell margin, 1 cm—tissue collected 1 cm in from the bell margin, 2 cm—tissue collected 2 cm in from the bell margin, M-manubrium—bell tissue collected from adjacent to the manubrium. The inset is an epi-fluorescent micrograph of a cross section taken through the bell margin. Diffuse fluorescence in the oral and aboral epithelial layers is due to DNSA-CA labeling. The cell membranes of amoebocytes in the mesoglea also exhibit DNSA-CA fluorescence. The bright circles within the amoebocytes are autofluorescing zooxanthellae (Z). In a color micrograph, the DNSA-CA fluorescence would be blue and the algal fluorescence red. Am: amoebocyte.

Tissue samples (~0.5 g) were excised for algal cell counts and determination of CA activity for individuals in different symbiotic states. Samples of intact oral arm tissue from field-condition and bleached animals were also excised from the animal and analyzed for CA activity and algal density. The primary oral arms branch into smaller secondary arms, and these are further subdivided into smaller tertiary arms. Since most zooxanthellae are found in the mouths of the secondary and tertiary oral arms, the large, primary oral arms were removed to eliminate large amounts of mesoglea, which lacks significant numbers of zooxanthellae. Unlike many typical cnidarian-algal symbioses in which the algal symbionts are located in the gastrodermis, in *C. xamachana*, the algal symbionts are present in amoebocytes, mobile cells that migrate through the animal's mesoglea (Fitt and Trench, 1983; see Fig. 1). These amoebocytes also cluster close to the epithelial layer of the oral surface of the jellyfish. All excised *C. xamachana* tissues used for the CA assays were frozen in liquid nitrogen and stored at −95 °C until analyzed.

Tissue fixation for fluorescence localization of carbonic anhydrase

In tandem with tissue collection for measurement of CA activity, portions of *C. xamachana* bell margin tissue were excised and fixed for CA localization with 5-dimethylamino-napthalene-1-sulfonamide (DNSA, dansylamide) (Husic and Hsieh, 1993). About 1 cm^2 of intact bell tissue was fixed in a 2% paraformaldehyde solution with 0.07 *M* NaCl and 0.3 *M* Millonig's phosphate buffer (pH 7.4) for 4 h at room temperature. Mouths from oral arm branches were also fixed as described above. Fixed tissue was initially stored in a solution consisting of 50% Tissue Freeze Media (TFM) (Electron Microscopy Science, Fort Washington, PA.) at 4 °C for up to 1 month. If fixed tissue was stored for

longer than 3 months, subsequent attempts to label it with DNSA showed little or no fluorescence.

Before being sectioned, tissue samples were infiltrated overnight in 100% TFM and subsequently oriented for sectioning such that both oral and aboral epithelial layers would be seen when frozen sections (14 μm) were cut using a Reichert-Jung Fridgocut 2800N cooled to −30 °C. Sections were transferred to slides coated with poly-L-lysine to thaw and were immediately labeled with DNSA. These sections allowed for easy comparison of fluorescence in the epithelial layers. Orientation of the oral epithelial was confirmed by placing the oral side of the tissue on Whatman filter paper and then embedding and sectioning filter paper and tissue together.

K_i values of sulfonamide inhibitors of Cassiopea *carbonic anhydrase*

Inhibition constant (K_i) values for DNSA were determined to help ascertain the minimum useful concentration for the fluorescent labeling studies described in the next sections (*e.g.*, Husic and Hsieh, 1993). DNSA (10 m*M*), dissolved in dimethyl formamide (DMF), as well as DMF alone, and two other inhibitors—acetazolamide (AZ) and ethoxyzolamide (EZ)—were titrated against about 200 μmol $CO_2 \cdot min^{-1} \cdot g^{-1}$ of supernatant *C. xamachana* CA activity, which was approximately a 29-fold increase in the uncatalyzed rate. Inhibition constants were determined using double reciprocal inhibition plots (Easson and Stedman, 1937), according to the following equation:

$$I_o/i = K_i/(1 - i) + E_o$$

where E_o is the total concentration of the free enzyme and i is the fractional inhibition of enzyme activity at an inhibitor concentration of I_o.

AZ and EZ had K_i values of 1.04 and 0.86 n*M*, respectively, and these values were typical for these strong inhibitors. However, DNSA was a much weaker inhibitor, with a K_i of 6.5 μ*M* (Fig. 2). Based on the K_i value for DNSA and the relative intensity of tissue fluorescence observed in incubations at different concentrations of DNSA (see below), 50 μ*M* DNSA (about 10 times the K_i) was used for the subsequent experiments involving the visualization and localization of CA in jellyfish tissue. Furthermore, K_i values for AZ and EZ were used to determine the concentrations of these inhibitors for use in the negative controls.

DNSA labeling of carbonic anhydrase

Final concentrations of all sulfonamide inhibitors of CA activity were diluted in 0.2 *M* potassium phosphate buffer (pH 7.5) from 10 m*M* stock solutions dissolved in 100% DMF (Dermietzel *et al.*, 1985; Husic and Hsieh, 1993).

CA was localized in frozen tissue sections of *C. xamachana* by incubating thawed tissue sections in a graded concentration series of DNSA (1–100 μ*M*). Sections were incubated for 30 min to allow DNSA-CA binding to occur. A comparison of bound DNSA fluorescence to background indicated that 50 μ*M* DNSA provided optimum contrast for subsequent comparisons (Fig. 3). Negative control sections were incubated in either 0.2 *M* potassium phosphate buffer + 200 ml 100% DMF or in 2 m*M* AZ or 100 μ*M* EZ, for 30 min followed by a second 30-min incubation in 50 μ*M* DNSA with 2 m*M* AZ or 100 μ*M* EZ, respectively. Microspheres of 1% intensity (In-Speck Blue calibration kit I-7221, Molecular Probes, Eugene, OR) were added to each slide as an internal standard for fluorescence. Because unbound DNSA does not fluoresce, it was not necessary to rinse the sections after incubation. Incubated sections were placed under coverslips, sealed with fingernail polish, and viewed immediately as described below.

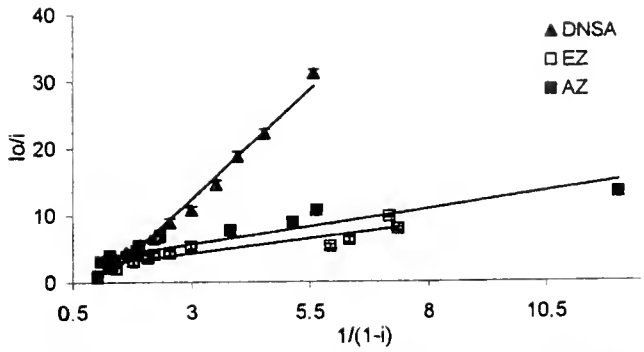

Figure 2. Easson-Stedman plots for dansylamide (DNSA), acetazolamide (AZ), and ethoxyzolamide (EZ) titrated against carbonic anhydrase activity from homogenates of oral arm tissue of field-condition *Cassiopea xamachana*. Mean ± SEM (n = 4). Regression equations and correlation coefficients for each inhibitor are as follows:
DNSA in μ*M*: $y = 6.52x - 7.09$, $R^2 = 0.98$
AZ in n*M*: $y = 1.04x + 2.6$, $R^2 = 0.81$
EZ in n*M*: $y = 0.87x + 1.75$, $R^2 = 0.81$

Carbonic anhydrase localization using DNSA-CA fluorescence

DNSA was chosen, rather than polyclonal antibodies to vertebrate CA II (Kingsley and Watabe, 1987; Weis, 1993), because (1) it binds 1:1 with all isoforms of CA and thus it lends itself to direct quantification of CA; (2) once bound to CA, its resultant fluorescence is extremely stable, unlike that of fluorescent markers conjugated to antibodies; (3) it fluoresces only in a bound state with CA, so there is no background fluorescence; (4) the relative fluorescent intensity of DNSA-CA is easily quantified by comparing DNSA-CA fluorescence to that of standard 1% intensity fluorescent microspheres; and (5) DNSA-CA fluorescence can be quenched by the nonfluorescent sulfonamide inhibitors acetazolamide and ethoxyzolamide.

Sections were viewed and photographed using a Zeiss

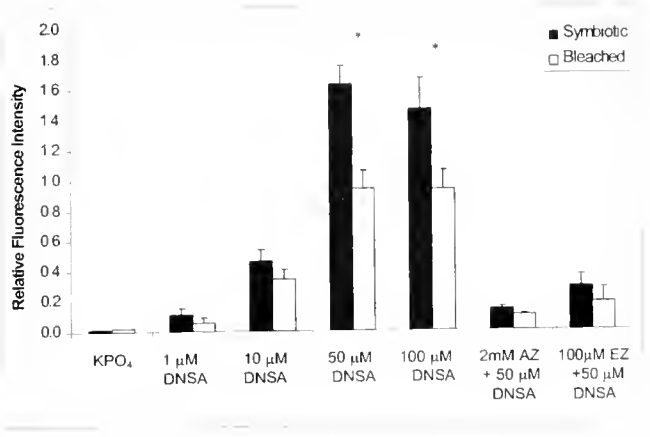

Figure 3. Relative fluorescent intensity values of the DNSA-CA complex in bell margin tissue sections from field-condition and bleached animals. Mean ± SEM ($n = 5$). An asterisk indicates a significant difference ($P < 0.0001$) in the fluorescence value obtained with 50 μM DNSA between field-condition and bleached animals.

ICM 405 inverted microscope illuminated by a mercury arc lamp and equipped with Zeiss Neofluar quartz objectives. An Omega excitation filter of 360 ± 20 nm and emission filter of 460 ± 25 nm provided proper fluorescent excitation of the DNSA-CA complex while preventing interference from algal autofluoresence. For each data point, images of both oral and aboral epithelial layers of five sections were captured with an 8-bit CCD Sony XC-75 video camera and accumulated using a frame accumulation program written by Dr. Thomas Pitta (Department of Biological Sciences, Auburn University) using the Lab-View program (National Instruments; Austin, TX). Only 2–5 frames were necessary to accumulate DNSA-labeled sections; however, to compensate for the low fluorescence of the negative controls, 10–50 frames of those sections were accumulated. Concurrent with each image of DNSA-labeled animal tissue sections, two frames of 1% fluorescence intensity microspheres were accumulated. The intensity of microsphere fluorescence was used to determine the relative fluorescence intensity of labeled cnidarian tissue.

Fluorescent intensity values of sections of *C. xamachana* bell tissue were determined with Sigma Scan 2.0 (Jandel Scientific; San Rafael, CA) using the following procedure. For each section of bell tissue examined, the oral and aboral epithelial layers were each meticulously outlined, and the intensity of each region's area was calculated by Sigma Scan to produce an overall fluorescence intensity score for each epithelial layer examined. The number of frames accumulated for each region varied between DNSA-labeled tissue and negative controls, due to differences in their fluorescence intensity. Therefore, the overall score for each epithelial layer was divided by the number of frames accumulated to yield a final standardized fluorescence intensity score. Likewise, microsphere fluorescence was also calculated by dividing the raw intensity score by the number of frames accumulated. Standardized fluorescent intensity scores of cnidarian tissue were then divided by the In-Speck microsphere's fluorescence intensity to produce a relative fluorescent intensity for each epithelial layer.

The Sigma Scan program was also used to determine the percentage of each labeled section that was epithelial tissue or mesogleal tissue.

Delta pH electrometric assay of carbonic anhydrase activity

Chemicals for the following procedures were purchased from Fisher Scientific (Norcross, GA) or Sigma (St. Louis, MO) unless otherwise noted. Frozen tissue samples were thawed and homogenized in 1 ml of ice-cold reaction buffer (10 mM Tris, 225 mM mannitol, and 75 mM sucrose adjusted to pH 7.4 with phosphoric acid) (Henry, 1991), using 40 complete passes of a 15-ml Wheaton ground glass mortar and Teflon-coated pestle on a Fisher Sted Fast Stirrer Model SL300. Homogenized samples were centrifuged in an Eppendorf 5804R tabletop microfuge at 10,000 × g, 2 min, 4 °C to separate cytosolic host CA from animal tissue debris and algae.

CA activity in the supernatant was analyzed using the electrometric delta pH assay (Henry, 1991). Microscopic analysis of the pellet, performed to determine algal densities (see below), revealed that the algal symbionts were not lysed by the homogenization procedure. This suggests that the supernatant CA activity was primarily, if not exclusively, of animal host origin. Briefly, 50 μl of supernatant was added to 6 ml of buffer in a water-jacketed reaction vessel cooled to 4 °C. The reaction was started by the addition of 100 μl of CO_2-saturated water, and the catalyzed hydration reaction was measured by following the drop in pH of approximately 0.15 units as a result of the production of H^+. CA activity was expressed as μmol $CO_2 \cdot min^{-1} \cdot g$ wet weight of tissue^{-1}.

Algal density determinations

Zooxanthellar population densities were immediately ascertained for each 1-ml sample of homogenized tissue by using a Fisher Scientific Neubauer ruled, Ultraplane hemocytometer. Algal densities were determined as the mean of five aliquots of homogenized samples from five animals. Algal concentrations were standardized per gram of tissue wet weight.

Statistical analysis of data

CA activity and zooxanthellar density were either square root or log transformed as necessary to satisfy the F test for homogeneity. A repeated-measures ANOVA was run to compare changes in CA activity and algal number between field-condition, bleached, and repopulated states in individ-

uals over an 8-week period. Paired Student's t tests were used to compare algal density and CA activity in field-condition, week-3 bleached, and week-5 repopulated samples. A one-way ANOVA was run for algal number and CA activity in the following comparisons: of bell margin *versus* arm tissue; between and among oral, aboral, and mesogleal tissue; and of tissue samples across a transect from bell margin to manubrium. Scheffé PLSD post hoc tests were run on all ANOVAs (Sokal and Rohlf, 1995). All statistical analyses were performed using Stat-View (SAS Institute, Cary, NC).

Results

Localization of carbonic anhydrase via *DNSA-CA fluorescence*

Frozen sections of *Cassiopea xamachana* bell margin incubated with 50 μM DNSA showed intense labeling of oral and aboral epithelial layers. By comparison, there was no significant DNSA-CA fluorescence in the mesogleal tissues (Figs. 1 and 4A). A distinct banding pattern, which was always associated with a cluster of amoebocytes containing zooxanthellae, was also occasionally seen in the oral epithelial layer (Fig. 4B). In field-condition and bleached animals, the oral epithelial layers had, respectively, about 27% and 32% greater DNSA-CA fluorescence than aboral bell margin epithelial layers (field-condition: $P = 0.02$; bleached: $P = 0.03$) (*e.g.*, Figs. 4A, 5A, and 5B). The sum of oral and aboral epithelial labeling of field-condition jellyfish sections had 44% greater DNSA-CA fluorescence than the sum of oral and aboral layers from sections of bleached animals ($P < 0.0001$).

Sectioned tissues of field-condition and bleached animals incubated in 50 μM DNSA alone had respectively 13 and 8 times more DNSA-CA fluorescence than when these tissues were incubated in 2 mM AZ + 50 μM DNSA ($P < 0.0001$

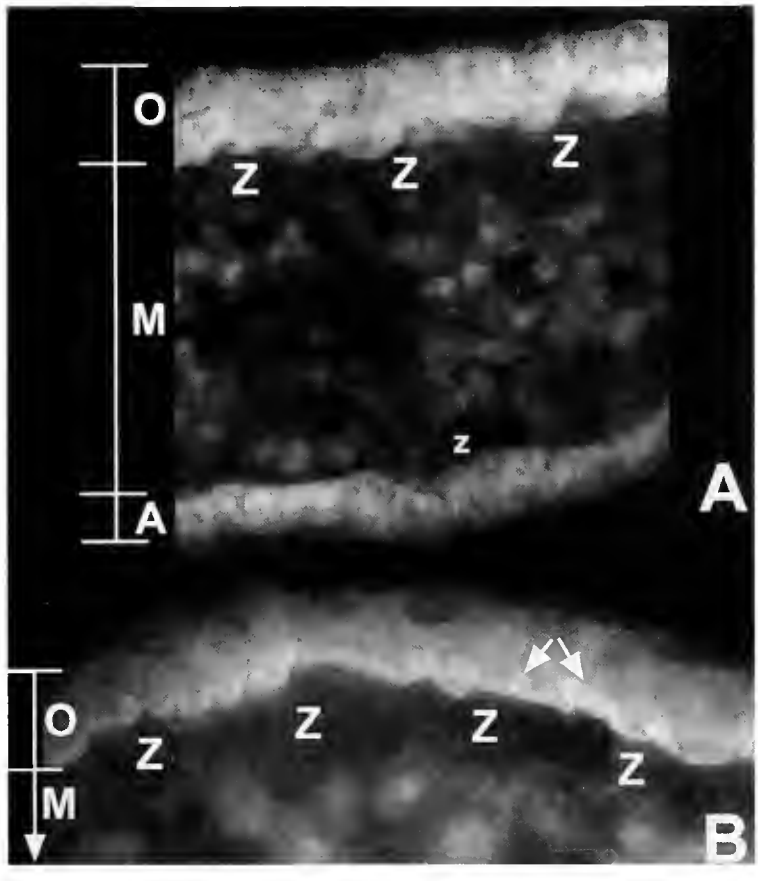

Figure 4. DNSA-CA fluorescence in sectioned tissue of *Cassiopea xamachana* bell margin. Abbreviations: O, oral surface; A, aboral surface; M, mesoglea; Z, zooxanthellae. (A) Image of bell margin tissue incubated in 50 μM DNSA, showing the localization of CA to the oral and aboral epithelial tissue layers. The majority of the zooxanthellae are adjacent to the oral epithelial layer. Comparatively few zooxanthellae are found adjacent to the aboral epithelial layer. (B) In some instances, a distinct band of DNSA-CA fluorescence (arrow) occurred in the oral epithelial layer directly adjacent to underlying aggregations of zooxanthellae (not visible) within amoebocytes (not visible).

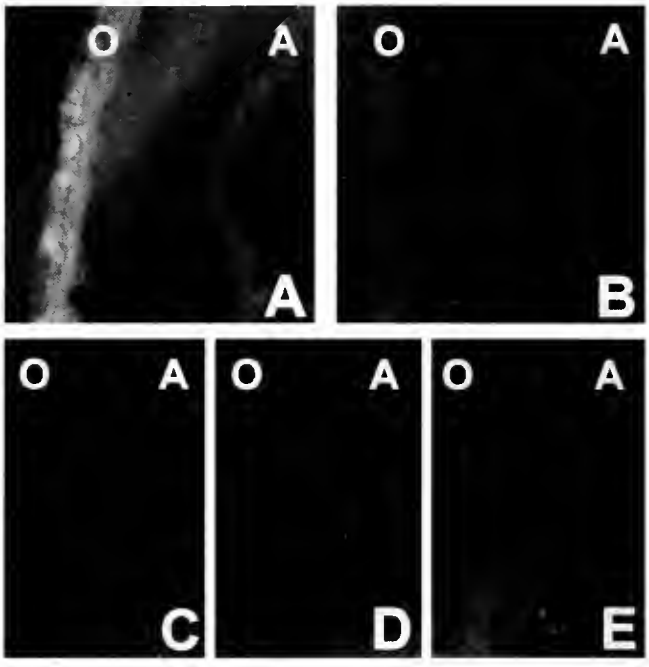

Figure 5. DNSA-CA fluorescence in sectioned tissue of *Cassiopea xamachana* bell margin: O indicates the oral surface and A the aboral surface of the bell. Bell margin tissue from recent field-collected symbiotic jellyfish (A) had higher intensity fluorescence than that from bleached jellyfish (B) when incubated in 50 μM DNSA. Negative controls incubated in potassium phosphate buffer + dimethylformamide (C), 2 mM acetazolamide (AZ) followed by 50 μM DNSA +2 mM AZ (D), and 100 μM ethylzolamide (EZ) followed by 100 μM EZ + 50 μM DNSA (E) had little or no fluorescence.

in both field-condition and bleached comparisions). Also, field-condition and bleached tissues incubated in 50 μM DNSA alone had 5 times brighter DNSA-CA fluorescence than when 100 μM EZ was added to the incubation medium ($P < 0.0001$ in both field-condition and bleached comparisions) (Figs. 3 and 5). Similarly, tissues of field-condition and bleached animals incubated in 50 μM DNSA exhibited fluorescence values that were, respectively, 124 and 37 times greater than those for tissues incubated in KPO_4 + 200 μl DMF ($P < 0.0001$ in both field-condition and bleached comparisions) (Figs. 3 and 5). The differences in the quantitative DNSA-CA fluorescence values between tissues of jellyfish in the field-condition *versus* bleached states were similar to those differences in CA activity found using the electrometric delta pH assay (see below).

Carbonic anhydrase activity and algal densities in field-condition, bleached, and repopulated jellyfish

CA activity was directly related to the presence of zooxanthellae in *C. xamachana*. Field-condition symbiotic jellyfish initially housed algal densities of approximately 2×10^6 cells $\cdot$ g^{-1} wet weight of host tissue and had CA activities of 250 μmoles $CO_2 \cdot$ min$^{-1} \cdot$ g^{-1} (Fig. 6). These symbiotic animals were bleached by cold shock and dark incubation and subsequently lost about 71% of their initial algal densities and 66% of their initial CA activities after one week of treatment. Bleached animals had a translucent beige or blue hue depending on the concentration of the pigment Cassio blue in host tissues and were easily distinguished from the dark brown color typical of field-condition and repopulated jellyfish. Throughout the 3 weeks that jellyfish were in the bleached condition, zooxanthellar density did not decrease after the initial decline, remaining at approximately 6.7×10^5 cells $\cdot$ g^{-1} wet weight of host tissue, a value that was significantly lower than that for algal densities in field-condition symbiotic *C. xamachana* ($P < 0.0001$) (Fig. 6A). However, CA activities in bleached animals did continue to decrease during this 3-week period. Bleached animals lost an additional 16% of CA activity between weeks 2 and 3 resulting in an overall decrease of 83% compared to initial CA activity from field-condition symbiotic animals ($P < 0.0001$) (Fig. 6B)

Exposure to actinic light for 7 days resulted in the repopulation of host tissue by zooxanthellae. Within the first week of light incubation, algal densities in repopulated individuals more than doubled compared to values for animals bleached 3 weeks (Fig. 6A). Algal densities at this point were not different from those in field-condition jellyfish ($P = 1.0$). As animals made the transition from the bleached to the repopulated condition, increased CA activities directly corresponded to increased zooxanthellar densities. CA activity in animals repopulated for one week increased by about 80%, from 43 to 77 μmoles $CO_2 \cdot$ min$^{-1} \cdot$ g^{-1} (Fig 6B). Despite this increase, CA activity in

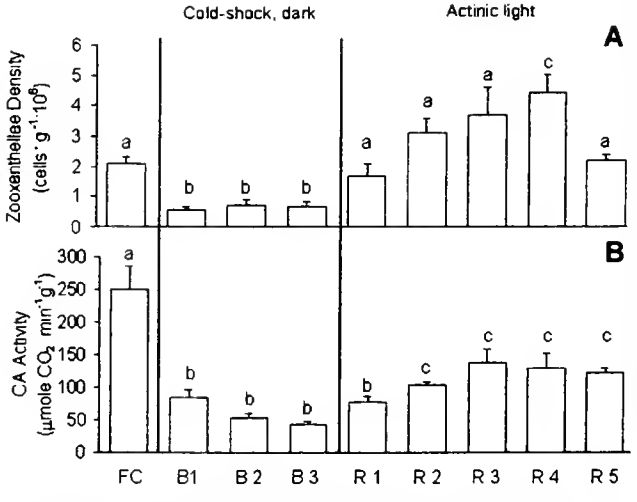

Figure 6. Fluctuation of zooxanthellar density (A) and carbonic anhydrase activity (B) monitored over 8 weeks in the same group of *Cassiopea xamachana* in three symbiotic states: field-condition (S); bleached (cold-shocked and dark-treated; B1–B3); and repopulated (incubated in actinic light; R1–R5). Mean $\pm$ SEM ($n = 8$). Differing lowercase letters above bars indicate conditions that were significantly different at $P \leq 0.01$.

animals repopulated for one week remained at only 30% of the CA activity in field-condition animals, even though algal densities had fully recovered to values found in field-condition animals (Fig. 6). In animals repopulated for 4 weeks, zooxanthellar densities increased to twice those found in field-condition animals. However, at week 5, densities of zooxanthellae decreased to 2.2×10^6 cells $\cdot$ g^{-1}, which was approximately equivalent to the algal densities in field-condition animals ($P = 0.6$). During weeks 3 through 5 of the repopulation state, *C. xamachana* CA activity remained constant at about 129 μmoles $CO_2 \cdot min^{-1} \cdot g^{-1}$, only half the activity found in field-condition jellyfish ($P < 0.003$) (Fig. 6B). Therefore, during the initial repopulation period, CA activities directly corresponded to increased algal densities of repopulated animals. However, enzyme activities stabilized within 3 weeks, whereas zooxanthellar density continued to fluctuate. CA activities of repopulated animals never returned to the values found in field-condition animals, although algal densities from animals repopulated for 5 weeks and field-condition animals were approximately equal (Fig. 6A, B).

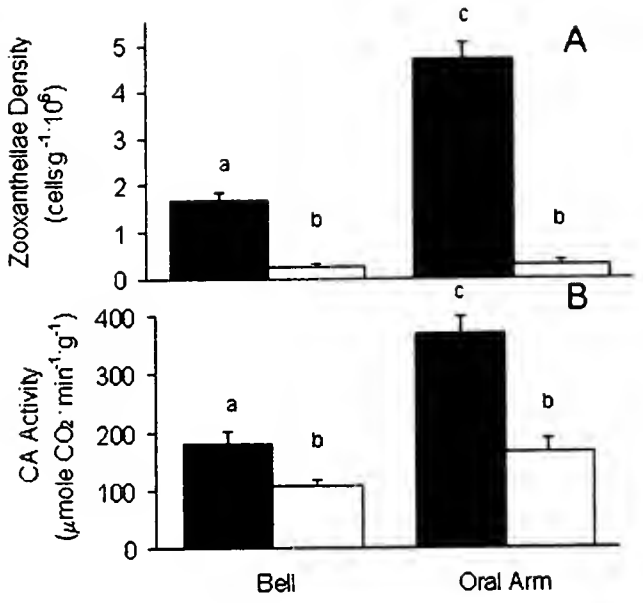

Figure 7. Distribution of zooxanthellar density (A) and CA activity (B) in bell margin and oral arm tissue of field-condition and bleached individuals of *Cassiopea xamachana*. Field-condition animals are represented by black bars; bleached animals are represented by white bars. Mean ± SEM ($n = 21$). Differing lowercase letters above bars indicate conditions that were significantly different at $P < 0.0001$.

Comparison of zooxanthellar densities and carbonic anhydrase activity in bell margin and oral arm tissue in field-condition and bleached animals

Bell margin tissue from bleached animals had zooxanthellar densities that were only 16% of those found in bell margin tissue of field-condition animals ($P < 0.0001$). Similarly, zooxanthellar densities in oral arm tissue from bleached animals were only 6% of those found in corresponding tissue from field-condition animals ($P < 0.0001$) (Fig. 7A). CA activity reflected these trends in zooxanthellar densities. CA activity in bell margin tissue of bleached animals was 61% of that measured in bell margin tissue of field-condition animals ($P = 0.0003$), and activity in oral arm tissue of bleached animals was 45% of activity in oral arm tissue of field-condition animals ($P < 0.0001$) (Fig. 7B).

Comparison of bell margin and oral arm zooxanthellar density and CA activity within groups of field-condition or bleached animals also supported this trend. Oral arm tissues of field-condition animals had 2.8 times greater algal density ($P < 0.0001$) and 2 times greater levels of CA activity ($P < 0.0001$) when compared to bell margin tissues from the same individual. However, bell margin and oral arm tissue from bleached animals were not significantly different in either algal density ($P = 0.17$) or CA activity ($P = 0.06$) (Fig. 7A, B).

Distribution of zooxanthellar density and carbonic anhydrase activity across the bell radius

Algal counts revealed no significant difference in zooxanthellar ($P = 0.74$) density across the bell radius within field-condition ($P = 0.14$) or bleached groups of animals (Fig. 8A). However, CA activity varied along the bell radius, with the outer bell margin of field-condition animals containing significantly higher levels of CA activity than any of the samples from the inner sections of the bell ($P < 0.0001$) (Fig. 8B). CA activity decreased progressively in the tissue samples collected at 1 cm and 2 cm in from the margin, but it was not significantly different between the 2-cm sample and that from the innermost sample, the manubrium ($P > 0.05$, Fig. 8B). There was no significant difference in CA activity in any of the samples from the bleached jellyfish, except for the sample from the manubrium.

Discussion

The regulation of induction and deinduction of CA activity in various structures and tissues of cnidarian hosts has been proposed to be related to changes in zooxanthellar density (Weis, 1991; Weis and Reynolds, 1999). Our analysis of CA activity in *Cassiopea xamachana*, as it relates to zooxanthellar density, anatomical location of the algae, and light or dark treatment of animals, supports this hypothesis. Previous work with the anemones *Aiptasia pulchella* and

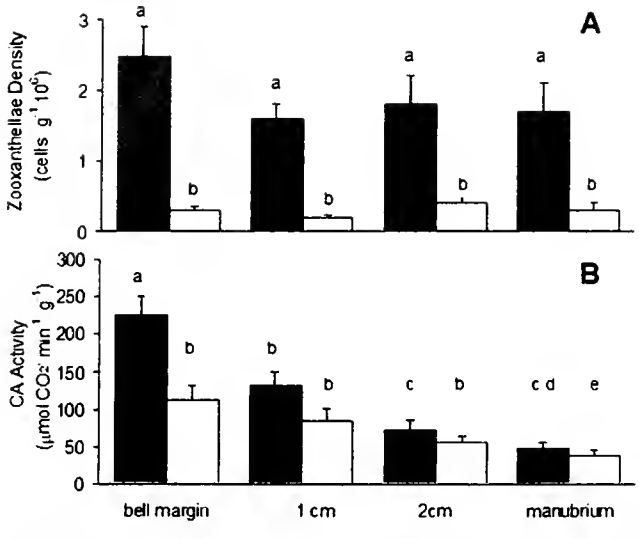

Figure 8. Distribution of zooxanthellar density (A) and CA activity (B) across the bell radius in field-condition and bleached individuals of *Cassiopea xamachana*. See Figure 1 for an explanation of where each tissue sample was taken from across the diameter of the bell. Field-condition animals are represented by black bars; bleached animals are represented by white bars. Mean ± SEM ($n = 13$ for field-condition and 9 for bleached animals). Differing lowercase letters above bars indicate conditions that were significantly different at $P \leq 0.03$.

Anthopleura elegantissima confirmed that the symbiotic state of the host influences the levels of CA activity in the host tissues (Weis, 1991; Weis and Reynolds, 1999). Likewise, the presence and levels of CA activity reported here correspond to algal densities in the bell margin tissue of individual *C. xamachana* under different symbiotic states. Animals, whether freshly collected or repopulated, housed greater numbers of symbionts and had correspondingly higher CA activity within their bell margin tissues than when these same animals were bleached.

The correlation between algal density and CA activity extends to other tissues in *C. xamachana* as well. Oral arm tissue has been shown to contain 3-fold higher densities of zooxanthellae than whole bell tissue (Blanquet, 1979). This corresponds to our results that show oral arm tissues possess 2-fold higher CA activity. A similar relationship between algal density and CA activity has also been found in symbiotic anemones and giant clams (Weis *et al.*, 1989; Verde and McCloskey, 1998; Baillie and Yellowlees, 1998).

The underlying reasons for tissue-specific differences in zooxanthellar density are not known, but they may be related to differences in the microenvironments of different tissue types. Higher algal densities found in oral arms may be the result of increased colonization area provided for endosymbionts in the sinuous folding of the oral arm tertiary branches (as compared to the uniform plane of the bell) and higher amounts of incident light (see below). Zooxanthellae are also randomly dispersed throughout the thinner mesoglea of the arms (Blanquet and Phelan, 1987) instead of being concentrated at the epidermal-mesogleal interface as is the case with the thicker mesoglea of the bell tissue. Thus, differences in the distribution of zooxanthellae, and therefore, corresponding differences in CA activity, could be due to the structure of these tissues that compose the surrounding microenvironment of the algal symbiont.

Nowhere are these tissue-specific differences more obvious than in the oral *versus* aboral epithelial layers of the bell margin. *C. xamachana* exhibits an unusual behavior of residing "upside-down," with its concave exumbrellar portion of the bell on the substratum and its oral arms suspended in the water column to capture planktonic prey (Bigelow, 1900). Higher densities of zooxanthellae have been observed associated with the subumbrellar (oral) epithelial tissue of the bell than with the exumbrellar (aboral) bell tissue (Blanquet and Riordan, 1981; Blanquet and Phelan, 1987). This asymmetry in endosymbiont density may be due to a disparity in the endosymbiotic microenvironment that results from the animal's upside-down posture. The subumbrellar zooxanthellae have more direct access to light and possibly easier access to inorganic carbon in the form of dissolved bicarbonate in the water column. Concurrent with this asymmetric zooxanthellar distribution is a heterogenous oral-aboral distribution of CA activity. Furthermore, within the subumbrellar region itself, areas of intense banding of DNSA-CA fluorescence were occasionally observed directly above amoebocytes that contained zooxanthellae. These may also be examples of differences in CA distribution due to a disparity in the microenvironment. *Symbiodinium microadriaticum*, the symbiont isolated from *C. xamachana*, is positively phototactic in culture (McLaughlin and Zahl, 1966), and the amoebocytes containing the zooxanthellae have been proposed to move about the animal (Fitt and Trench, 1983; Colley and Trench, 1983; Muscatine *et al.*, 1986; Fitt and Cook, 2001). Although a phototactic response has never been demonstrated *in situ*, some evidence indicates that the amoebocytes are more concentrated in tissue areas that receive more direct light (Blanquet and Riordan, 1981). If that proves to be the case, some sort of communication between symbiont and amoebocyte might exist in order for the amoebocytes to be directed to regions of high light intensity. This possibility deserves more systematic investigation, as such a trophism could be mediated not just by light intensity alone, but also by metabolic factors, such as oxygen production or inorganic carbon translocation on the part of the symbiont, that are sensed or recognized by the amoebocyte or perhaps even the host. Thus, just as specific structures appear to exhibit differential levels of CA activity due to differences in the density of zooxanthellae, tissues within a structure may exhibit a disparity in algal density that leads to asymmetric enzyme distributions within that structure.

The relationship between CA activity in the oral epithelial tissue, the presence of amoebocytes clustered below the

oral surface, and the high densities of algae within those amoebocytes raises another interesting possibility in the regulation of CA activity. Given our finding that CA activity is regulated in cells (the oral epithelium) remote from those that contain the symbionts (amoebocytes), a signaling pathway may exist between host and symbiont that is involved in the regulation of CA induction.

One apparent discrepancy between algal density and CA activity may point to the involvement of other factors in the regulation of CA. Algal density is approximately equal along the radius of the bell, from the outer margin to the inner manubrium, whereas CA activity is high in the margin, but decreases in tissue samples taken from areas across the bell approaching the manubrium. This suggests that factors other than the simple presence or density of zooxanthellae influence CA activity.

One such factor could be light intensity, a variable that controls the photosynthetic rate of the zooxanthellae (Weis *et al.*, 1989; Gattuso *et al.*, 1993; Verde and McCloskey, 1998). In *C. xamachana*, light intensity varies seasonally and with water depth, and it could also potentially vary across the bell surface as a function of shading by the oral arms. Variations in light intensity could result in different physiological adaptations of the endosymbionts in different regions of the animal (Patterson *et al.*, 1991; Kühl *et al.*, 1995). In this study, differences in light intensity may help to explain why repopulated animals had significantly lower CA activity than field-condition individuals despite having the same algal densities. Field-condition animals were adapted to 1200–1500 μE m^{-2} s^{-1}, a light intensity that is in the range needed for maximum photosynthetic activity (1497.2 μE m^{-2} s^{-1}; Verde and McCloskey, 1998). The actinic light source of the aquarium, under which the animals were allowed to repopulate with zooxanthellae, was 80 μE m^{-2} s^{-1}, well below the intensity needed for maximal photosynthesis, even taking into account possible photoacclimation (Chang *et al.*, 1983; Muller-Parker, 1984; Prézelin, 1987; Fitt and Cook, 2001). Therefore, although algal density was high, the photosynthetic rate of the zooxanthellae may have been quite low, resulting in lower CA activities. In contrast, symbiotic and repopulated anemones (*Aiptasia pulchella*) had equivalent levels of CA activity (Weis, 1991). This may, however, have been more closely related to the laboratory conditions under which the experiment was conducted. These animals had been maintained under low light intensities (40 μE m^{-2} s^{-1}) for an extended time before being used in the experiments. As a result, they were acclimated to photosynthesizing under constant, low light intensities. Thus, zooxanthellae from these symbiotic and repopulated anemones most likely had similar photosynthetic rates.

Although the intensity of incident light on specific tissues was not measured, the possibility that it may affect CA activity in different tissues of *C. xamachana* is worth considering. The zooxanthellae of *C. xamachana* are adapted for the high light environments their hosts inhabit (Verde and McCloskey, 1998) and may preferentially associate with tissues receiving higher light intensities. The higher zooxanthellar densities found in oral arm *versus* bell tissue reported here and elsewhere (Blanquet, 1979; Verde and McCloskey, 1998) may be due to the increased illumination of oral arm tissue, as the mouths on the tertiary branches of the oral arms are the structures of *C. xamachana* that are most directly exposed to the incident light. Differences in incident light may also explain the higher algal density and CA activity found in the oral *versus* aboral epithelial layers of the bell margin. The oral epithelial layer of the bell margin tissue receives direct sunlight, unlike the aboral portion of the bell, which is shaded by the overlying oral arms; the oral epithelial layer of the bell; and associated mucilage, amoebocytes, and mesoglea. A similar pattern of symbiont distribution in response to light intensity has been reported in species of the coral *Montastrea* (Rowan *et al.*, 1997).

Water motion over the surface of symbiotic cnidarians is another abiotic factor that could potentially affect endosymbiont photosynthesis, and thus host CA activity. Although water flow over the bell was not directly measured, other reports have presented evidence supporting the idea that changes in the rate of water flow could alter the delivery of nutrients (*e.g.*, inorganic carbon) and thus alter the metabolic rates of host and symbiont (Patterson, 1992; Shashar *et al.*, 1993), especially in areas of low water flow (Dennison and Barnes, 1988; Weis *et al.*, 1989; Lesser *et al.*, 1994; Gardella and Edmunds, 2001). Furthermore, evidence suggests that CA activity could be affected by water flow (Lesser *et al.*, 1994; Weis *et al.*, 1989).

In summary, CA activity in host tissue appears to be influenced by a number of factors. The presence and density of the algal symbiont influences the presence and level of CA activity, but that alone cannot explain all of the tissue-specific differences in CA. Abiotic factors, such as light intensity and water flow, which influence the photosynthetic rate of the symbiont, may also play a role in regulating host CA activity. The interaction between algal density and abiotic factors represents a potentially viable avenue for future research.

Acknowledgments

We thank Dr. William K. Fitt and the Key Largo Marine Research Laboratory for providing facilities for collection of animals; S. Cashion, T. Wakefield, W. Bailey, and M. Shawkey for assistance in field collection of animals; Dr. Mary Mendonça for assistance with statistics; and two anonymous reviewers for their constructive comments. Support for this research was provided by an Auburn University graduate school grant to AME; Alabama Agricultural Ex-

periment Station funding to SCK and RPH; and NSF grants (IBN 97-27835 and IBN 02-30005) to RPH.

Literature Cited

Allemand, D., P. Furla, and S. Bénazet-Tambutté. 1998. Mechanism of carbon acquisition for endosymbiont photosynthesis in Anthozoa. *Can. J. Bot.* **76:** 925–941.

Al-Moghrabi, S., C. Goiran, D. Allemand, N. Speziale, and J. Jaubert. 1996. Inorganic carbon uptake for photosynthesis by the symbiotic coral-dinoflagellate association. II. Mechanisms for bicarbonate uptake. *J. Exp. Mar. Biol. Ecol.* **199:** 227–248.

Baillie, B. K., and D. Yellowlees. 1998. Characterization and function of carbonic anhydrases in the zooxanthellae-giant clam symbiosis. *Proc. R. Soc. Lond. B* **265:** 465–473.

Benazet-Tambutte, S., D. Allemand, and J. Jaubert. 1996. Inorganic carbon supply to symbiont photosynthesis of the sea anemone, *Anemonia viridis:* role of the oral epithelial layers. *Symbiosis* **20:** 199–217.

Bigelow, R. P. 1900. The anatomy and development of *Cassiopea xamachana. Mem. Bost. Soc. Nat. Hist.* **5:** 190–244.

Blanquet, R. S. 1979. Zooxanthellae contribution to respiration in the mangrove jellyfish *Cassiopeia. Nat. Geogr. Soc. Res. Rep.* **20:** 17–26.

Blanquet, R. S., and M. A. Phelan. 1987. An unusual blue mesogleal protein from the mangrove jellyfish *Cassiopea xamachana. Mar. Biol.* **94:** 423–430.

Blanquet, R. S., and G. P. Riordan. 1981. An ultrastructural study of the subumbrellar musculature and desmosomal complexes of *Cassiopea xamachana* (Cnidaria: Scyphozoa). *Trans. Am. Microsc. Soc.* **100:** 109–119.

Chang, S., B. B. Prézelin, and R. K. Trench. 1983. Mechanisms of photoadaption in three strains of the symbiotic dinoflagellate *Symbiodinium microadriaticum. Mar. Biol.* **76:** 219–229.

Colley, N. J., and R. K. Trench. 1983. Selectivity in phagocytosis and persistence of symbiotic algae by the scyphistoma stage of the jellyfish *Cassiopeia xamachana. Proc. R. Soc. Lond. B* **219:** 61–82.

Dennison, W. C., and D. J. Barnes. 1988. Effect of water motion on coral photosynthesis and calcification. *J. Exp. Mar. Biol. Ecol.* **115:** 67–77.

Dermietzel, R., A. Leibstein, W. Siffert, N. Zamboglou, and G. Gros. 1985. A fast screening method for histochemical localization of carbonic anhydrase. *J. Histochem. Cytochem.* **33:** 93–98.

Easson, L. H., and E. Stedman. 1937. The absolute activity of choline esterase. *Proc. R. Soc. Lond. B* **121:** 142–164.

Fitt, W. K., and C. B. Cook. 2001. Photoacclimation and the effect of the symbiotic environment on the photosynthetic response of symbiotic dinoflagellates in the tropical marine hydroid *Myrionema amboinense. J. Exp. Mar. Bio. Ecol.* **256:** 15–31.

Fitt, W. K., and R. K. Trench. 1983. Endocytosis of the symbiotic dinoflagellate *Symbiodinium microadriaticum* Freudenthal by endodermal cells of the scyphistomae of *Cassiopeia xamachana* and resistance of the algae to host digestion. *J. Cell. Sci.* **64:** 195–212.

Furla, P., D. Allemand, and M-N. Orsenigo. 2000. Involvement of H^+-ATPase and carbonic anhydrase in inorganic carbon uptake for endosymbiont photosynthesis. *Am. J. Physiol. Regul. Integr. Comp. Physiol.* **278:** R870–R881.

Gardella, D. J., and P. J. Edmunds. 2001. The effect of flow and morphology on boundary layers in the scleractinians *Dichocoenia stokesii* (Milne-Edwards and Haime) and *Stephanocoenia michilini* (Milne-Edwards and Haime). *J. Exp. Mar. Biol. Ecol.* **256:** 279–289.

Gattuso, J. P., D. Yellowlees, and M. Lesser. 1993. Depth- and light-dependent variation of carbon partitioning and utilization in the zooxanthellate scleractinian coral *Stylophora pistillata. Mar. Ecol. Prog. Ser.* **92:** 267–276.

Gattuso, J-P., D. Allemand, and M. Frankignoulle. 1999. Photosynthesis and calcification at cellular, organismal and community levels in coral reefs: a review on interactions and control by carbonate chemistry. *Am. Zool.* **39:** 160–183.

Graham, D., and R. M. Smillie. 1976. Carbonate dehydratase in marine organisms of the Great Barrier Reef. *Aust. J. Plant Physiol.* **3:** 113–119.

Gutknecht, J., M. A. Bisson, and F. C. Tosteson. 1977. Diffusion of carbon dioxide through lipid bilayer membranes. *J. Gen. Physiol.* **69:** 779–794.

Henry, R. P. 1991. Techniques for measuring carbonic anhydrase activity *in vitro:* the electrometric delta pH and pH stat methods. Pp. 119–125 in *The Carbonic Anhydrases,* S. J. Dodgson, R.E. Tashian, G. Gros, and N. D. Carter, eds. Plenum Publishing, New York.

Husic, H. D., and S. Hsieh. 1993. Characterization of the fluorescent dansylamide complex with *Chlamydomonas reinhardtii* carbonic anhydrase. *Phytochemistry* **32:** 805–810.

Kingsley, R. J., and N. Watabe. 1987. Role of carbonic anhydrase in calcification in the gorgonian *Leptogorgia virgulata. J. Exp. Zool.* **241:** 171–180.

Kühl, M., Y. Cohen, T. Dalsgaard, B. B. Jorgensen, and N. P. Revsbech. 1995. Microenvironment and photosynthesis of zooxanthellae in scleractinian corals studied with microsensors for O_2, pH, and light. *Mar. Ecol. Prog. Ser.* **117:** 159–172.

Lesser, M. P., V. M. Weis, M. R. Patterson, and P. L. Jokiel. 1994. Effects of morphology and water motion on delivery and productivity in the reef coral *Pocillopora damicornis* (Linnaeus): diffusion barriers, inorganic carbon limitation, and biochemical plasticity. *J. Exp. Mar. Biol. Ecol.* **178:** 153–179.

McLaughlin, J. J. A., and P. A. Zahl. 1966. Endozoic algae. Pp. 257–297 in *Symbiosis,* M. Henry, ed. Academic Press, New York.

Muller-Parker, G. 1984. Photosynthesis-irradiance responses and photosynthetic periodicity in the sea anemone *Aiptasia pulchella* and its zooxanthellae. *Mar. Biol.* **82:** 225–232.

Muscatine, L. F., P. Wilkerson, and L. R. McCloskey. 1986. Regulation of population density of symbiotic algae in a tropical marine jellyfish (*Mastigias* sp.). *Mar. Ecol. Prog. Ser.* **32:** 279–290.

Muscatine, L., J. W. Porter, and I. R. Kaplan. 1989. Resource partitioning by reef corals as determined from stable isotope composition. *Mar. Biol.* **100:** 185–193.

Patterson, M. R. 1992. A chemical engineering view of cnidarian symbioses. *Am. Zool.* **32:** 566–582.

Patterson, M. R., K. P. Sebens, and R. R. Olson. 1991. *In situ* measurements of flow effects on primary production and dark respiration in reef corals. *Limnol. Oceanogr.* **36:** 936–948.

Prézelin, B. B. 1987. Photosynthetic physiology of dinoflagellates. Pp. 174–223 in *The Biology of Dinoflagellates,* F.J.R. Taylor, ed. Blackwell Scientific, Oxford, UK.

Rowan, R., N. Knowlton, A. Baker, and J. Jara. 1997. Landscape ecology of algal symbionts creates variation in episodes of coral bleaching. *Nature* **388:** 265–269.

Shashar, N., Y. Cohen, and Y. Loya. 1993. Extreme diel fluctuations of oxygen in diffusive boundary layers surrounding stony corals. *Biol. Bull.* **185:** 455–461.

Sokal, R. R., and F. J. Rohlf. 1995. *Biometry: The Principles and Practice of Statistics in Biological Research.* W.H. Freeman, New York.

Streamer, M., Y. R. McNeil, and D. Yellowlees. 1993. Photosynthetic carbon dioxide fixation in zooxanthellae. *Mar. Biol.* **115:** 195–198.

Sültemeyer, D., B. Klughammer, M. R. Badger, and G. D. Prince. 1998. Protein phosphorylation and its possible involvement in the induction of the high-affinity CO_2 concentration mechanism in cyanobacteria. *Can. J. Bot.* **76:** 954–961.

Suzuki, E., Y. Shiraiwa, and S. Miyachi. 1994. The cellular and mo-

lecular aspects of carbonic anhydrase in photosynthetic microorganisms. Pp. 1–54 in *Progress in Phycological Research*, Vol. 10. F.E. Round and D.J. Chapman, eds. Biopress, Bristol, UK.

Verde, E. A., and L. R. McCloskey. 1998. Production, respiration, and photophysiology of the mangrove jellyfish *Cassiopea xamachana* symbiotic with zooxanthellae: effect of jellyfish size and season. *Mar. Ecol. Prog. Ser.* **168:** 147–162.

Weis, V. M. 1991. The induction of carbonic anhydrase in the symbiotic sea anemone *Aiptasia pulchella*. *Biol. Bull.* **180:** 496–504.

Weis, V. M. 1993. Effect of dissolved inorganic carbon concentration on the photosynthesis of the symbiotic sea anemone *Aiptasia pulchella* Carlgren: role of carbonic anhydrase. *J. Exp. Mar. Biol. Ecol.* **174:** 209–225.

Weis, V. M., and W. Reynolds. 1999. Carbonic anhydrase expression and synthesis in the sea anemone *Anthopleura elegantissima* are enhanced by the presence of dinoflagellate symbionts. *Physiol. Biochem. Zool.* **72:** 307–316.

Weis, V. M., G. J. Smith, and L. Muscatine. 1989. A "CO_2 supply" mechanism in zooxanthellate cnidarians: role of carbonic anhydrase. *Mar. Biol.* **100:** 195–202.

Reference: *Biol. Bull.* **204:** 290–304. (June 2003)

Reproductive Behavior in the Squid *Sepioteuthis australis* From South Australia: Ethogram of Reproductive Body Patterns

TROY M. JANTZEN* AND JON N. HAVENHAND†

School of Biological Sciences, Flinders University, GPO Box 2100, Adelaide, South Australia, 5001

Abstract. Squids use a diverse range of body patterns for communication. Each pattern consists of a series of chromatic, postural, and locomotor components that are under neural control and can change within fractions of a second. Here we describe an ethogram of 48 body pattern components from *in situ* observations of reproductively active *Sepioteuthis australis*. In addition, we identify the total time and average duration that each component is shown, to a resolution of 1 s. Our results suggest that only a few components (*e.g.*, "Golden epaulettes," "Stitchwork fins," and "Rigid arms") are temporally common, that is, shown for more than 80% of the time. In contrast to the component classification reported for other species of squid, for this species we suggest a classification system consisting of "short acute" (lasting for < 10 s); some of these same components were also classified as "medium acute" (11–60 s) or "chronic" (> 60 s). Several body patterning components were previously unreported, as were some of the combinations observed. The significance of these patterning components is discussed within the context of the associated behaviors of the squid on the spawning grounds.

Introduction

Cephalopod behavior involves elaborate displays characterized by many visually apparent body patterns (Moynihan and Rodaniche, 1982; Hanlon, 1988; Hanlon *et al.*, 1994, 1999; Hanlon and Messenger, 1996). In squid, each body pattern is a combination of postural, locomotor, or chromatic components that together constitute the total appearance of the animal (Packard and Sanders, 1969, 1971; Packard and Hochberg, 1977; Hanlon, 1982; Roper and Hochberg, 1988; Hanlon *et al.*, 1994, 1999; Hanlon and Messenger, 1996). Of the three types, the most conspicuous and diverse to the human observer are the chromatic components. Chromatic changes result from neuromuscular expansion or retraction of pigmented chromatophore organs in the dermis of the skin (Boycott, 1953; Hanlon, 1982; Packard, 1982, Messenger, 2001). Dark chromatic components arise from the expansion of chromatophores, whereas light chromatic components are the result of retraction of chromatophores to reveal the translucent skin or iridescent reflecting cells (Hanlon, 1982; Hanlon and Messenger, 1996; Messenger, 2001). Postural components denote the postures of arms, tentacles, head, eyes, mantle, and fins; and locomotor components describe movement of the whole animal (Hanlon and Messenger, 1996). Squid display multiple combinations of each component type that may last for several seconds ("acute patterns" *sensu* Packard and Hochberg, 1977; Hanlon and Messenger, 1996), or minutes to hours ("chronic patterns" *sensu* Hanlon and Messenger, 1996). Unfortunately, the classification of squid body patterns is not a simple task. Each chromatic component may be displayed alone, or combined with other components (simultaneously or in sequence) to generate the overall skin pattern of an individual (Hanlon *et al.*, 1994, 1999; Mather and Mather, 1994). Thus, to analyze the nature of squid behavior, body components must first be cataloged, then each combination of components analyzed with respect to the circumstances in which each occurs (Mather and Mather 1994).

Body patterning and reproductive behavior are important tools in quantitative behavioral analysis, in the development of taxonomic identification keys, and for phylogenetic analyses of chromatic expression (Hanlon, 1988). Cephalopod

Received 15 February 2002; accepted 31 January 2003.

* To whom correspondence should be addressed. E-mail: Troy.Jantzen@bms.com

†Current address: Tjarnö Marine Biological Laboratory, Göteborg University, 452 96 Strömstad, Sweden.

body patterns have been studied for many decades, and the suite of body pattern components (ethogram) found in squids has been described for species such as *Sepioteuthis sepioidea* (Moynihan and Rodaniche, 1982), *Loligo vulgaris reynaudii* (Hanlon *et al.*, 1994), *Loligo pealeii* (Hanlon *et al.*, 1999), and several others (table 3.2 in Hanlon and Messenger, 1996).

The commercially important squid *Sepioteuthis australis* spawns throughout the year (Pecl, 2000, 2001), with numbers of spawning adults in shallow coastal areas known to increase during warmer months. Current behavioral research on this species is limited to two preliminary observations of spawning activity, neither of which describes the repertoire of body patterns (Larcombe and Russell, 1971; Jantzen and Havenhand, 2003). In this study, we document and identify 48 components characteristic of *S. australis* reproductive behavior and describe the behaviors associated with each component. In addition, we analyze the occurrence, duration, and frequency of each component.

Materials and Methods

Mating behavior of *Sepioteuthis australis* in the field was observed by scuba and directly from the surface. The presence of divers close to focal animals (< 30 cm) caused no apparent alteration in squid behavior (compared with individuals observed from afar). Observations were therefore routinely made at a distance of less than 2 m.

Reproductively active individuals of *S. australis* were observed by scuba diving and snorkeling during daylight hours on spawning grounds between Marino and Hallet Cove, South Australia (138°29′ E, 38°02′ S; see Jantzen and Havenhand, 2003, for a description of the site) over three consecutive spawning seasons (September to March) between September 1999 and February 2002. Digital video data were obtained from 50 dives over an 18-week period from November 2000 to March 2001.

Ethogram of reproductive body patterns

Reproductive behavior was recorded with a Sony TV120 digital video camera (Sony Corporation, New York) in an Amphibico (Amphibico, Quebec, Canada) housing. Sampling protocols followed those described by Martin and Bateson (1993), which included small amounts of *ad libitum* sampling of specific behaviors. However, the primary sampling method was focal-animal sampling, which involved recording all interactions and behaviors of haphazardly chosen paired individuals for up to 1.5 h. Because males and females are close together when paired, analysis of the focal sampling of one individual provided information on the corresponding behavior of its mate.

Images of behavior were analyzed frame by frame (25 frames $\cdot s^{-1}$) on a high-resolution large-screen color monitor. Each video was analyzed three times to identify postural, locomotor, or chromatic components. All components were assigned a name based either on established component nomenclature for other cephalopod species (Corner and Moore, 1980; Hanlon, 1982, 1988; Moynihan and Rodaniche, 1982; Moynihan, 1985; Yang *et al.*, 1986; Porteiro *et al.*, 1990; Hanlon *et al.*, 1994, 1999; Jantzen and Havenhand, 2003); or, where a new chromatic component was identified, on guidelines proposed by Hanlon and Messenger (1996) in which transverse components are called "bands" or "bars," and lines running longitudinal to the body axis called "stripes" or "streaks." In accordance with convention, only the first letter of each component name was capitalized (Hanlon and Wolterding, 1989).

Still images of selected chromatic and postural components were obtained from digital video using iMovie2 software (Apple Computer, Cupertino, CA). Each chromatic component was then illustrated using CorelDraw 3.0 (Corel Corporation, Ontario, Canada) from a lateral perspective (observations were mostly lateral to the focal animal).

Total component duration

Each chromatic, postural, and locomotor component was scored individually (present, absent, data missing) for each squid at a 1-s-interval scale for the duration of the video, so that the proportion of time each component was displayed could be assessed. Missing values were classed as any points when the body of the squid (or part thereof) was not in the field of view (with the exception of "Oviposition," during which females were obscured by seagrass). All missing data (zeros) were eliminated from the analysis. Because video analysis frequently took several hours, the first two squid pairs analyzed were re-analyzed at the end of the analysis session and compared with the original analysis to ensure consistency in interpretation and data recording. Because significant experimental error in the perception of components may occur between observers in behavioral investigations (Drummond, 1981), all analyses were conducted by the same person (TMJ).

The behavior of 22 focal animals (11 female, 11 male) was recorded for a continuous duration of up to 61 min per pair. The total occurrence of each component (in seconds) was determined with respect to the total number of valid data points (missing values excluded) for each animal. Mean total duration of each component as a proportion of total time observed was calculated from data for individuals that showed the component being analyzed (data for animals not showing a component were omitted). Means generated from fewer than three replicate animals were not included in further analysis. Means and 95% confidence intervals were generated for each component.

Pairwise Student's *t* tests were conducted on the duration of each component shown by males and females within replicate pairs. This procedure tested the hypothesis that

there was no significant difference in mean component duration between sexes. Because this involved multiple unplanned tests with consequent information of Type 1 errors, a sequential Bonferroni test was conducted on the results from the t test to determine significance against the table-wide α-level (Rice, 1989).

Average component duration

The average duration of each component was calculated from the "uninterrupted" data (*i.e.*, excluding all component observations that began or ended due to the beginning or end of video recording, or were interrupted by missing values). Average component duration was calculated for each replicate individual, and a mean value was generated for all females or males. Not all components were shown by each individual; therefore, means from fewer than three replicates were, as before, discarded from the analysis.

As with the data for total component duration, pairwise t tests were conducted on the average duration of each component shown by males *versus* females within pairs.

Results

Several hundred reproductively active individuals of *Sepioteuthis australis* were observed in more than 75 h underwater. About 10 h of focal-sampling video observations of behavior were recorded. The number of reproductively active individuals ranged from 2 (a single spawning pair) to more than 45 per dive. From these data we identified 48 separate body components: 17 chromatic (Table 1, Fig. 1), 16 postural (Table 1, Fig. 2), and 15 locomotor (Table 1). Mating, egg deposition, and agonistic contests were all seen on the spawning grounds in the same manner as described previously by Jantzen and Havenhand (2003).

Ethogram of reproductive body patterns

Components that were previously undescribed or differ from those in the literature (Corner and Moore, 1980; Hanlon, 1982, 1988; Moynihan and Rodaniche, 1982; Moynihan, 1985; Yang *et al.*, 1986; Porteiro *et al.*, 1990; Hanlon *et al.*, 1994, 1997, 1999; Jantzen and Havenhand, 2003) are described below. Where components do not differ from existing definitions, the relevant literature has been cited. Unless stated otherwise, components were observed in both sexes, lateral to the focal animal.

Results for individual components are described below, summarized in Table 1, and illustrated in Figures 1 and 2. Combinations of components for typical behaviors are presented in Figure 3. Photographs of common combinations of chromatic and postural components are shown in Figure 4.

1. Light chromatic components

Clear (Hanlon, 1988; Yang *et al.*, 1986; Porteiro *et al.*, 1990; Hanlon *et al.*, 1994, 1999; Cornwell *et al.*, 1997) was rarely observed (three observations from focal sampling; Table 1) and on each occasion was shown alone as a body pattern. **White dorsal stripe** was a lightened stripe in the center of the dorsal mantle and varied in intensity; it either extended along the entire longitudinal length of the dorsal surface or was restricted to the posterior region. This component often began at the posterior region and extended to cover the entire longitudinal dorsal mantle. Without exception, females showed "White dorsal stripe" in combination with "Male-upturned mating" (see below and Fig. 3). **Golden epaulettes** was a lightened band at the most anterior point of the dorsal mantle that occurred as a result of the contraction of chromatophores (referred to as "Dorsal mantle collar iridophores" by Hanlon, 1988; Hanlon *et al.*, 1994, 1999). This was the most prevalent chromatic component (Table 1) and was shown seemingly indiscriminately with almost all other components. **Iridescent sclera** occurred when the iris of the eye became iridescent, it was observed only in agonistic contests between fighting males (Fig. 3), usually in conjunction with "All dark" (see below). **Golden ocular epaulettes** (described above the eye only as "Light eyebrows" or "Glittering brows" in *S. sepioidea*; Moynihan and Rodaniche, 1982; Moynihan 1985) were observed as a lightened region above and/or below the eye. This component was observed only in females (Table 1) and differs from "Iridescent sclera" in that the area adjacent to the eye becomes iridescent.

2. Dark chromatic components

We describe the manner in which dark chromatic components influence overall appearance without reference to the individual contributions of yellow, orange, red, brown, or black chromatophores (Hanlon and Messenger, 1996), which we were not able to analyze.

Plain was shown as a medium brown coloration over the entire body (referred to as "Basic" by Moynihan and Rodaniche, 1982; Moynihan, 1985). This component was more common in females (Table 1) and was especially seen in females that were "Egg passing" (see below). It was also shown by unpaired males attempting to "Male 'sneak' mate" (see below), and by courting pairs. **All Dark** (Hanlon, 1988; Hanlon *et al.*, 1994, 1999; Cornwell *et al.*, 1997) was shown by fighting males that were "Fin beating" (see below and Fig. 3). A variation of the "All dark" component was **Dark mantle,** in which only the mantle was darkened while the head and arms remained "Plain." This component was rare (Table 1), and the behavior associated with it remains unclear.

Although also shown independently, the following four components were all shown together by paired males in the

Table 1

Component duration (minimum and maximum) and frequency of observations of the ethogram of body pattern components for reproductively active males and females of Sepioteuthis australis

	Component duration(s)				Number of observations			
	Female		Male					
Component	Min.	Max.	Min.	Max.	Female	Male	Total	Uninterrupted
Chromatic components								
Light:								
1 Clear	1	1	10	10	2	1	3	2
2 White dorsal stripe	1	58	1	29	233	89	322	242
3 Golden epaulettes	1	171	1	338	422	259	681	102
4 Iridescent sclera (♂)	-	-	1	11	-	35	35	25
5 Golden ocular epaulettes (♀)	2	16	-	-	12	-	12	12
Dark:								
1 Plain	1	58	1	16	150	10	160	106
2 All dark	3	5	1	17	3	30	33	25
3 Dark mantle	2	4	5	5	2	1	3	3
4 Mantle margin stripe	1	31	1	25	12	96	208	143
5 Fin stripe	1	18	1	51	32	113	145	95
6 Dark arm stripes (♂)	-	-	1	17	-	73	73	52
7 Stitchwork fins	1	103	1	247	202	232	434	88
8 Dark dorsal stripe	2	10	5	10	4	2	6	6
9 Mottled dorsal mantle	1	30	1	120	91	233	324	135
10 Dark posterior ventral mantle	1	27	1	27	74	19	93	68
11 Shaded eye	1	103	1	156	354	182	536	277
12 Bands	1	151	2	89	153	15	168	75
Postural Components								
1 Drooping arms	1	17	1	81	202	271	473	437
2 Rigid arms	1	507	1	393	731	470	1201	880
3 Upward pointing	1	54	1	42	294	12	306	297
4 Downward pointing	1	12	2	5	142	5	147	143
5 Upward curl	1	17	1	2	23	6	29	29
6 Downward curl	1	6	1	12	60	8	68	68
7 Tentacle curl upward	1	18	3	4	251	3	254	254
8 Tentacle curl downward	1	4	2	4	26	3	29	29
9 Downward splayed arms (♂)	-	-	1	10	-	11	11	9
10 Lateral splayed arms (♂)	-	-	1	15	-	23	23	21
11 Raised arms	1	32	1	561	138	399	537	416
12 Curled tentacle club (♀)	1	29	-	-	84	-	84	76
13 Peristaltic arm flare	1	1	1	1	260	14	274	274
14 Arms in mantle (♂)	-	-	4	4	-	1	1	1
15 Forward jetting arms (♀)	1	2	-	-	3	-	3	3
16 Egg passing (♀)	21	33	-	-	22	-	22	22
Locomotor Components								
1 Forward swimming	1	42	1	38	694	679	1373	1259
2 Backward swimming	1	61	1	76	746	675	1421	1301
3 Hovering	1	152	1	479	778	756	1534	1442
4 Jetting	1	12	1	2	79	7	86	81
5 Turning	1	9	1	16	201	248	449	441
6 Parallel Positioning†	1	175	-	-	417	-	417	399
7 Mate guarding (♂)	-	-	1	13	-	108	108	105
8 Parrying (♂)	-	-	1	217	-	334	334	260
9 Fin beating (♂)	-	-	1	13	-	32	32	30
10 Charging (♂)	-	-	1	3	-	7	7	7
11 Oviposition (♀)	1	13	-	-	226	-	226	225
12 Male-upturned mating††	-	-	2	4	-	20	20	19
13 Head-to-head mating††	-	-	3	3	-	1	1	1
14 Male-parallel mating††	-	-	4	4	-	1	1	1
15 Male "sneak" mating	-	-	1	2	-	7	7	7

(♀) = components observed only in females, (♂) = components observed only in males, † = counts made from observations of female individuals only, †† = counts made from observations of male individuals only, - = component not observed. See text for explanation of "uninterrupted" data.

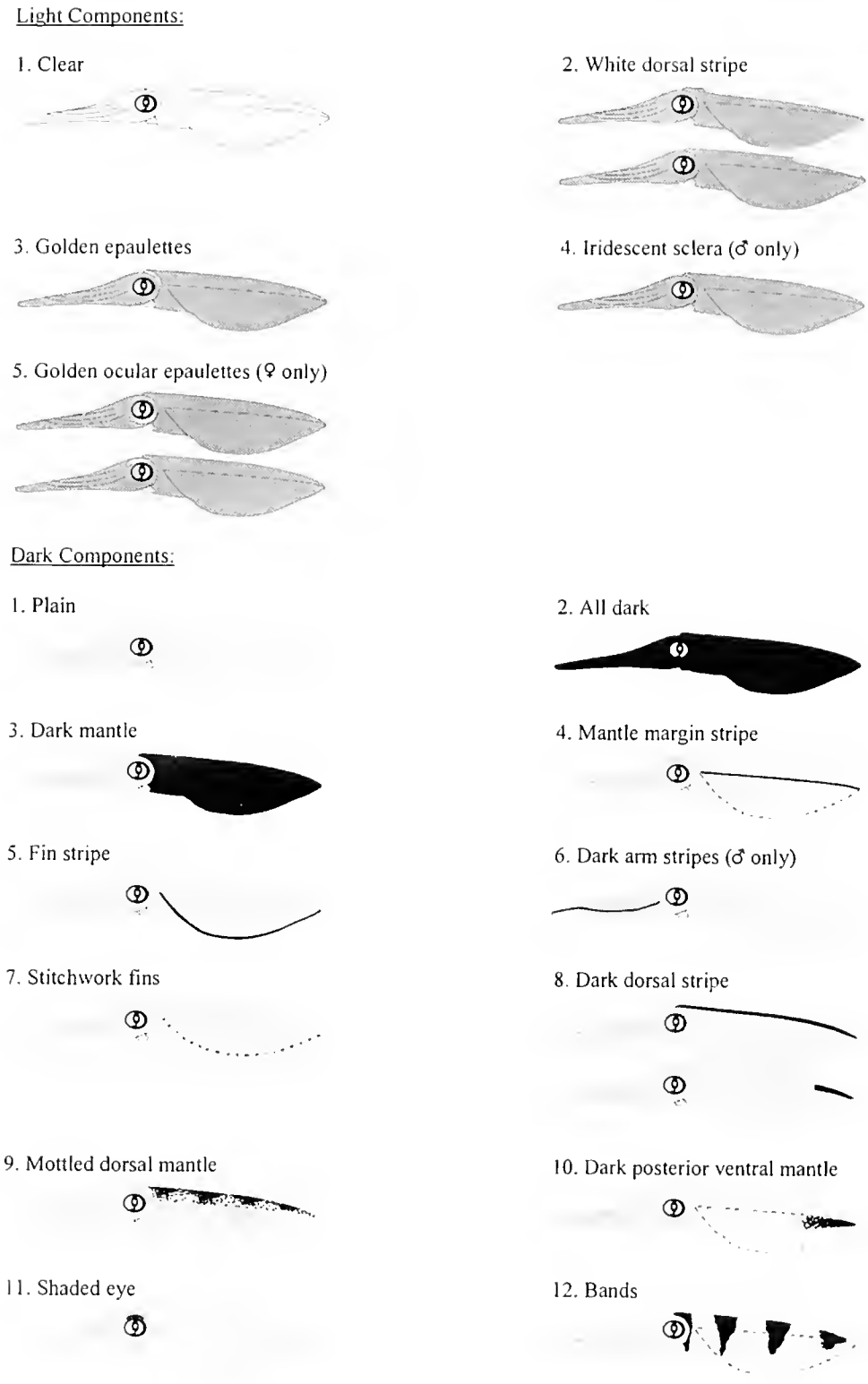

Figure 1. Diagrammatic representation of chromatic components of body patterning in the squid *Sepioteuthis australis*.

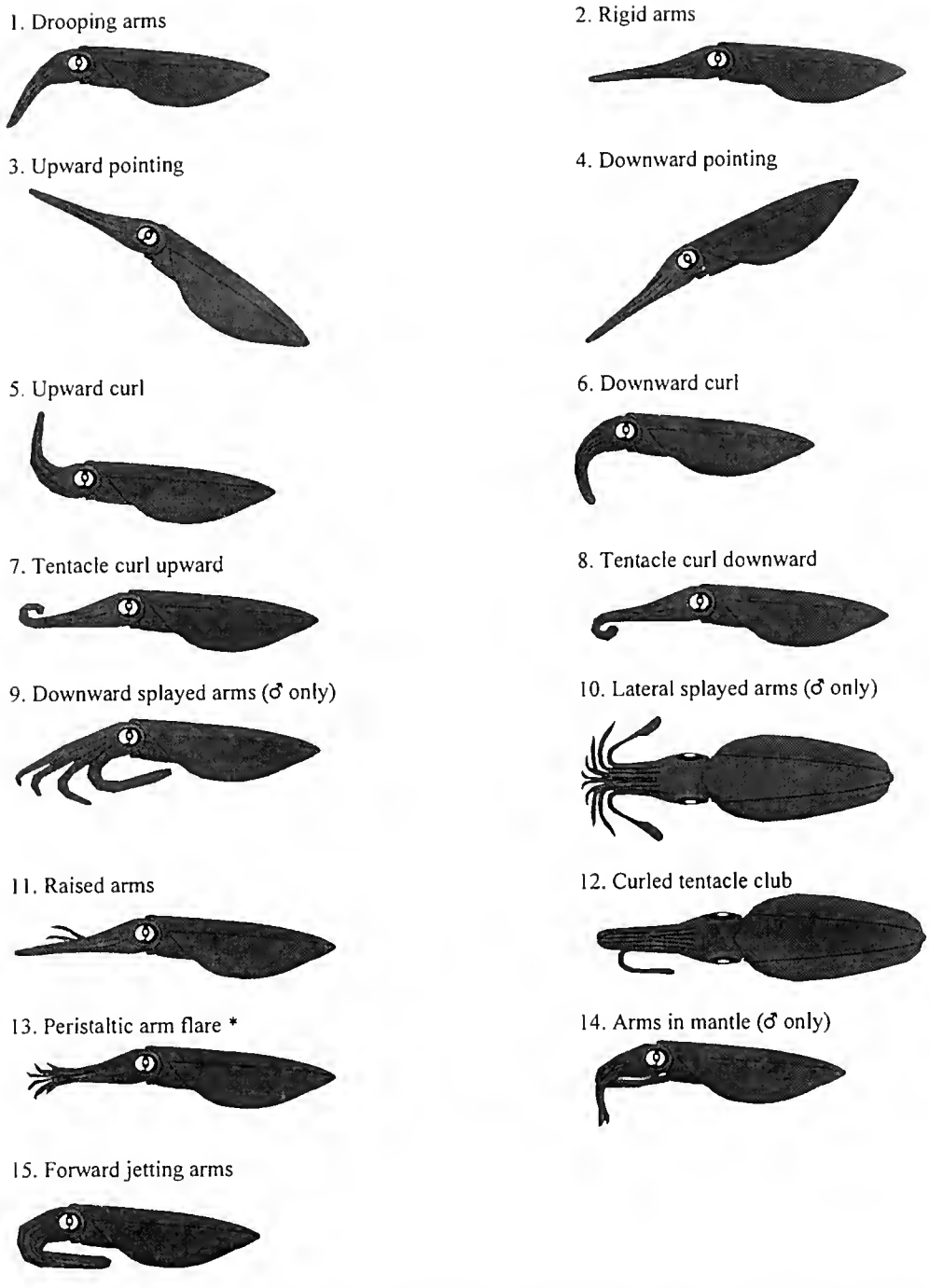

Figure 2. Diagrammatic representation of postural components of body patterning in the squid *Sepioteuthis australis*. Note: "Egg passing" has not been illustrated because it is distinguished by the peristaltic movement of the funnel held flat against the underside of the head. * = component is a transient posture consisting of the radial peristaltic flaring of the arms. Only the final stages of this component are represented by the illustration.

seconds immediately prior to "Male-upturned mating" (see below and Fig. 3). **Mantle margin stripe** (referred to as "Fin stripe" by Moynihan and Rodaniche; 1982, but here we follow the nomenclature of Hanlon *et al.*, 1999) was a darkened stripe running along the fin insertion the entire length of the mantle. **Fin stripe** (Hanlon *et al.*, 1994, 1999) occurred as a darkening of the edge of the fin. **Dark arm stripes** (referred to as "Dark third arms" by Porteiro *et al.*, 1990, and "Arm stripe (first or third)" by Hanlon *et al.*, 1994, but here we follow the nomenclature of Hanlon *et al.*,

Agonistic contests			**Male-upturned mating**		
Cl	4	Iridescent sclera (♂)	Cl	2	White dorsal stripe (♀)
Cd	2	All dark (♂)	P	10	Rigid arms (♀)
Cd	9	Mottled dorsal mantle (♂)	Cd	4	Mantle margin stripe (♂)
P	11	Raised arms (♂)	Cd	5	Fin stripe (♂)
P	10	Lateral splayed arms (♂)	Cd	6	Dark arm stripes (♂)
L	8	Parrying (♂)	Cd	11	Shaded eye (♂)
L	9	Fin beating (♂)	P	2	Lateral splayed arms (♂)
L	10	Charging (♂)	L	12	Male-upturned mating
Egg preparation			**Head-to-head mating**		
Cd	1	Plain (♀)	Cd	1	Plain
P	16	Egg passing (♀)	L	13	Head-to-head mating
L	3	Hovering (♀)			
Egg deposition			**Male-parallel mating**		
Cd	9	Mottled dorsal mantle (♂)	Cd	1	Plain
P	4	Downward pointing (♀)	L	13	Head-to-head mating
P	7	Tentacle curl upward (♀)	**Extra-pair Copulations**		
P	13	Peristaltic arm flare (♀)	Cl	2	White dorsal stripe (♂)
L	7	Mate guarding (♂)	Cd	1	Plain (♂)
L	11	Oviposition (♀)	Cd	2	All dark (♂)
			L	15	Male "sneak" mating

Figure 3. Components consistently identified in agonistic encounters, egg preparation, egg deposition, paired mating, and extra-pair copulations in *Sepioteuthis australis*. Numbers correspond to component numbers in Table 1; letters correspond to component types from Table 1; Cl = Light chromatic, Cd = Dark chromatic, P = Postural, L = Locomotor, (♀) = component shown by females; (♂) = component shown by males.

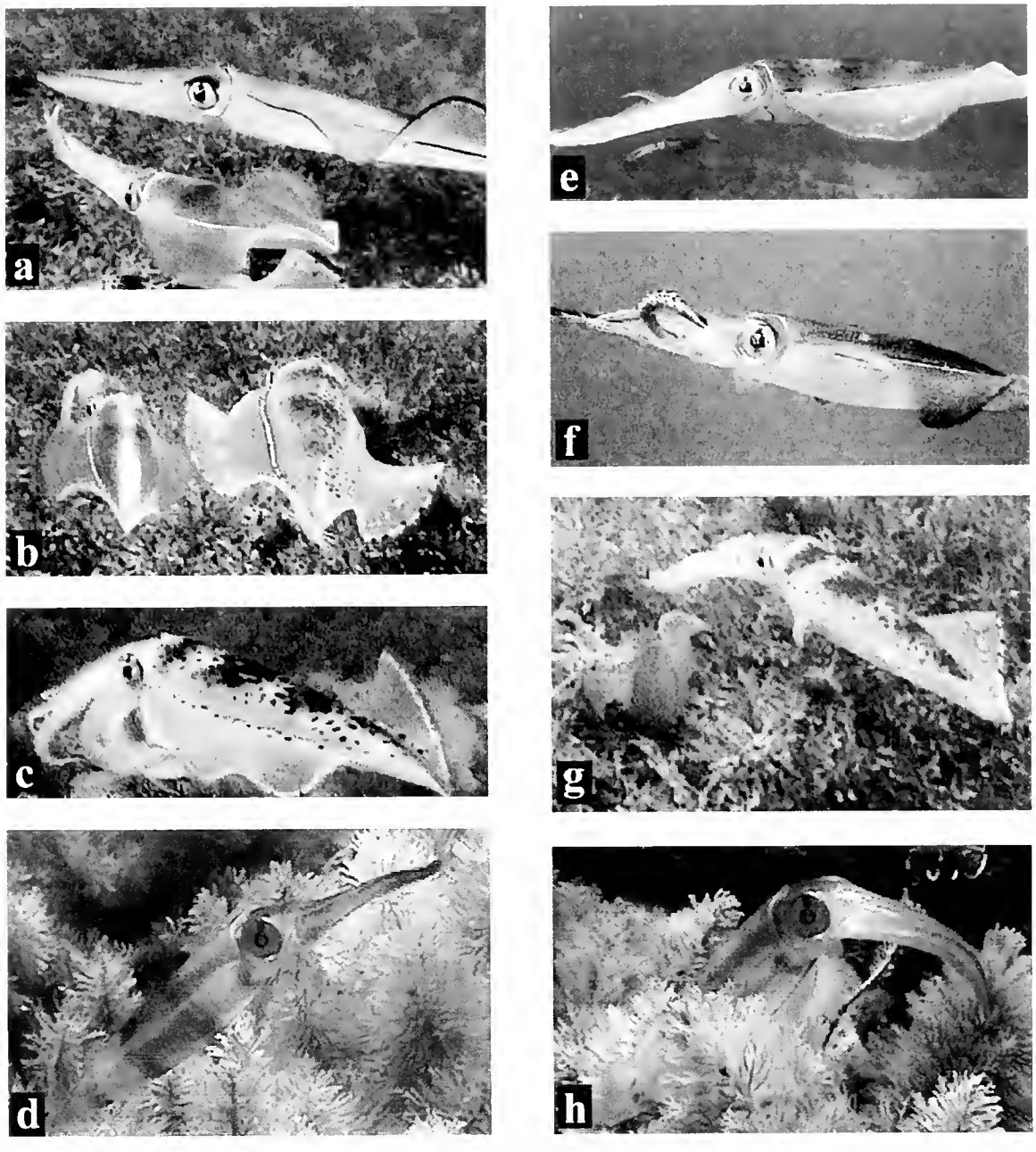

Figure 4. Selected typical body pattern components of *Sepioteuthis australis* taken from digital underwater video images. (a) Male (top) showing "Shaded eye," "Mantle margin stripe," "Fin stripe," "Dark arm stripes," and "Golden epaulettes." Female (Below) showing "Golden epaulettes". Male and female are "Parallel positioning". (b) Female (left) showing "White dorsal stripe" and "Golden epaulettes." Male (right) is showing "Mottled dorsal mantle," "Stitchwork fins," and "Golden epaulettes." Male and female are "Parallel positioning." (c) "Downward arm splay" of a male showing "Mottled dorsal mantle" and "Golden epaulettes." (d) Female showing "Bands" and "Golden epaulettes" while "Upward pointing." (e) Male showing "Raised arms" postural component with "Golden epaulettes," "Mottled dorsal mantle," and "Stitchwork fins" chromatic components. (f) "Curled tentacle club" with "Golden epaulettes." (g) Paired male (right) "Mate guarding" showing "Mottled dorsal mantle," "Golden epaulettes," and "Drooping arms." Only the posterior mantle of the female can be seen as she is "Downward pointing" in the process of "Oviposition" with her head amongst the seagrass substrate. (h) Female showing "Bands," "Downward curl," and "Upward pointing."

1999) involved the darkening of the most lateral arms and was shown exclusively by males (Table 1). **Shaded eye** was expressed as a transverse pigmented "bar" spanning the two eyes (as described in other squid species by Hanlon, 1988; Hanlon *et al.*, 1994, 1999) or as a shading immediately over the eye only. This component was common to both sexes (Table 1).

Stitchwork fins (Hanlon, 1982) comprised alternating black and white dashes that traversed the fins 2–3 cm from the edge. This component was one of the most common chromatic components shown by paired individuals (Table 1). **Dark dorsal stripe** was a darkened stripe along the center of the dorsal mantle. This component varied in length, either extending along the entire dorsal surface of the mantle or being shown only in the posterior region. We have few observations of this component (Table 1) and the behavior associated with it remains unclear. **Mottled dorsal mantle** was an irregular pattern of darkened spots on the dorsal mantle surface grouped together to form a mottle, occasionally extending to include the fins. Paired males showed this component in nonphysical agonistic encounters such as "Parrying" (see below). This component may be cryptic, as the irregularity of the pattern may disrupt the body shape when viewed from above (by predators). **Dark posterior ventral mantle** was an irregular darkening of the posterior ventral mantle (underneath the fins) up to a third of the length of the mantle in both sexes. This was more frequently seen in females (Table 1), but we remain uncertain of its behavioral significance.

Bands is also referred to as "Bars" by Moynihan and Rodaniche (1982) and Moynihan (1985) and as "Ring" by Hanlon (1982), but we follow the nomenclature of Hanlon *et al.* (1994, 1999) and Cornwell *et al.* (1997). This component was observed on all occasions as four transverse bands around the dorsal and ventral mantle. A single longitudinal stripe on the ventral mantle, similar to "Ventral mantle stripe" in *S. sepioidea* (Moynihan and Rodaniche, 1982), was also seen in conjunction with this pattern: because it was never observed independently, it is considered to be an integral part of the "Bands" component in *S. australis*. As in other loliginid squid, this component possibly aids in crypsis and was common in females of lone spawning pairs.

3. Postural components

Drooping arms occurred when the tentacles and arms of the individual were not in a "defined" posture and appeared limp. This component was reported by Hanlon *et al.* (1999) to occur in *Loligo pealei* individuals that were swimming, but we observed this behavior primarily in "Hovering" (see below) individuals of *S. australis* as well as in swimming ones. **Rigid arms** occurred when all arms and tentacles were held together immediately in front of the animal and was the most common arm position of paired animals (Table 1). For consistency in the analysis, the transition from "Rigid arms" to "Drooping arms" was defined as the moment when the average angle of the arms and tentacles exceeded 45° downward from horizontal. **Upward pointing** and **Downward pointing** were scored when the orientation of the whole body exceeded 45° from horizontal in the respective direction. Both of these components were far more prevalent in females (Table 1). "Upward pointing" was more often seen in individuals close to the substrate while "Hovering," but "Downward pointing" was frequently observed in females that were "Forward swimming" (see below) prior to deposition of an egg capsule (Fig. 3). **Upward curl** and **Downward curl** were identical in posture to the descriptions given by Moynihan and Rodaniche (1982) for *S. sepioidea*. **Tentacle curl upward** was the simultaneous rolling back of the tip of the tentacles dorsally along the arms to form a tight circle with the suckers on the club facing out. This component always occurred in the seconds prior to "Oviposition" by the female (Fig. 3) and was a reliable predictor of egg deposition behavior. **Tentacle curl downward** was the rolling back of the tentacle tips downward, along the ventral surface of the arms with the suckers facing inward. This component was rare (Table 1), and the association with specific behaviors remains unclear.

Downward splayed arms (Fig. 4C) was observed only in males (Table 1). The arms and tentacles curled around posteroventrally from the "Rigid arms" posture so that each tentacle was offset from the next. The significance of this component remains unknown. **Lateral splayed arms** (as "Splayed arms" in Hanlon *et al.*, 1999) was recorded in the latter stages of a fight between males, usually coinciding with "Fin beating" (see below and Fig. 3). A series of these components in rapid succession (< 1 s each) was also shown by several paired males poised above the female immediately prior to rotating to the upside-down position for "Male-upturned mating" (see below and Fig. 3). It is as yet unclear whether the duration of this component is significant in these different behaviors. **Raised arms** differed from the observations of this component in *L. pealeii* (Hanlon *et al.*, 1999) in that only the tips of the fourth pair of arms were raised, rather than the entire first pair of arms. This component was shown primarily by paired males (Table 1). As in *L. vulgaris reynaudii* (Hanlon *et al.*, 1994), this is thought to be an intraspecific agonistic signal because we consistently saw it in males that were "Parrying" (see below and Fig. 3).

Curled tentacle club was observed only in a single female; however, Jantzen and Havenhand (2003) previously identified this component in males of *S. australis* (as "Club display"). **Peristaltic arm flare** was a rapid component lasting for ≤ 1 s (Table 1) and involved the peristaltic flaring of the tentacles and arms from the base to the tips as the animal simultaneously pulsed a jet of water across the

arms (referred to as "Puffing" by Corner and Moore, 1980, and as "Cleaning maneuver" by Packard and Sanders, 1971). It appeared to be associated with the removal of excess matter from amongst the arms, and was most prevalent in females after "Oviposition" (Fig. 3). **Arms in mantle** occurred when all of the arms were positioned inside the ventral mantle while the tentacles adopted the "Drooping arms" posture. **Forward jetting arms** occurred when the arms and tentacles were directed posterioventrally coinciding with the rapid forward motion of the animal as it "Jetted" (see below) forward. **Egg passing** identifies a behavior in which females transferred eggs from the oviduct through the funnel into the arms. "Egg passing" was synonymous with the funnel being positioned flat against the underside of the head, with the funnel aperture opening into the bases of the arms. During this behavior, the ventral region of the arm bases enlarged as the eggs and egg capsule material were passed into the arms.

4. Locomotor components

Forward swimming, Backward swimming, Hovering, Jetting (Moynihan and Rodaniche, 1982; Hanlon *et al.*, 1994, 1999), and **Turning** are self-explanatory. For consistency of analysis, **Parallel positioning** was defined here as paired squid aligned laterally and facing in the same direction, where any part of the bodies were closer than the paired male's body length. The high frequency of this component (Table 1) is indicative of the relative closeness of reproductively active pairs. **Mate guarding** is common in loliginid squids (Hanlon and Messenger, 1996) and was defined here as being a consort male within one body length of the female that was in the process of "Oviposition" (Fig. 3). Paired males frequently showed "Mottled dorsal mantle" while "Mate guarding."

The following three components are varying levels of agonistic encounters between males (Fig. 3). **Parrying** was the active positioning of the paired male between the female and an intruder male, within one body length of the intruder. No physical contact occurred between the intruder and paired male at this time. **Fin beating** (Hanlon *et al.*, 1994, 1999; Jantzen and Havenhand, 2003) was the escalation of an agonistic contest into physical contact. The two males collided, beating their mantle and fins together. "Fin beating" consistently occurred with "Dark mantle" and "Iridescent sclera." **Charging** was defined as a rapid movement of a paired male toward a rival male, striking the intruder with the tentacles and radially flaring the arms. This is an intense agonistic encounter by a paired male and appeared similar to that described for *L. pealeii* (King *et al.*, 1999) and *Loligo forbesi* (Porteiro *et al.*, 1990).

Oviposition (Hanlon *et al.*, 1999; Jantzen and Havenhand, 2003) denotes the process of egg deposition by a female (Fig. 3). **Male-upturned mating** (Jantzen and Havenhand, 2003) occurred when the male rotated laterally to an upside-down position above the female to mate. **Head-to-head mating** (Hanlon *et al.*, 1999) occurred when the mating pair approached head-on and intertwined arms to mate. **Male-parallel mating** (Hanlon *et al.*, 1994, 1999) occurred when the paired male approached the female from below and attempted to mate facing the same direction. "Plain" was the only chromatic component shown consistently throughout these prior two mating types (Fig. 3). **Male "sneak" mating** (Hanlon, 1994; Jantzen and Havenhand, 2003) was defined as any mating attempt by an unpaired male with a paired female. Sneaker males also commonly showed the "Plain" chromatic components, or (infrequently) "Dark mantle" and "White dorsal stripe" (Fig. 3).

Total component duration

The most prevalent chromatic component for both sexes was "Golden epaulettes" ("Chromatic Light 3" in Fig. 5), shown for more than 90% of the time. "Stitchwork fins" was also common in males (85% of the time; "Chromatic Dark 7" in Fig. 5), but was less prevalent in females. Other components prevalent in males were "Mottled dorsal mantle" (30%; "Chromatic Dark 9" in Fig. 5), and "Shaded eye" (20%; "Chromatic Dark 11" in Fig. 5). In females, "Shaded eye" (42%) and "Stitchwork fins" (22%) were also prevalent ("Chromatic Dark 11 and Chromatic Dark 7" in Fig. 5).

"Rigid arms" was the only postural component commonly shown by both sexes and was observed about 90% of the time ("Postural 2" in Fig. 5). "Raised arms" was also common in males (42%; "Postural 11" in Fig. 5).

The prevalences of the locomotor components "Forward swimming," "Backward swimming," and "Hovering" were much the same for both sexes ("Locomotor 1, 2, and 3" in Fig. 5). "Parallel positioning" occured ~ 50% of the time (both sexes; "Locomotor 6" in Fig. 5), and males spent 34% of the time "Parrying rival" males ("Locomotor 8" in Fig. 5).

Pairwise t tests of the differences in total component durations between males and females showed that only the durations of "Stitchwork fins" were significantly different (sequential Bonferroni test, table-wide $\alpha = 0.05$). Males showed this pattern for considerably longer periods (Fig. 5, Table 1).

Average component duration

Components that were shown by both males and females had a similar average duration. Only "Stitchwork fins," "Shaded eye," and "Raised arms" showed a large difference in average duration between the sexes ("Chromatic Dark 7," "Chromatic Dark 11," and "Postural 11" respectively; Fig. 6). However, variance was generally high, and pairwise t tests of the differences in average component durations

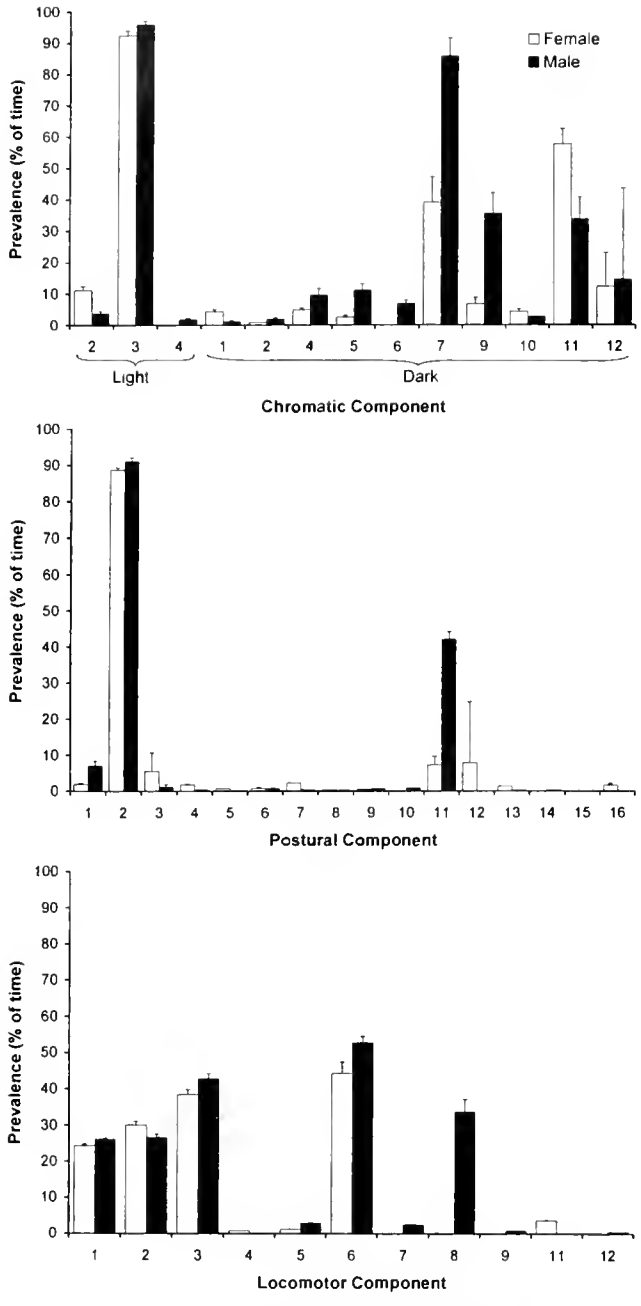

Figure 5. Prevalence (percent of total time observing each animal) of each chromatic, postural, and locomotor component identified in males and females of *Sepioteuthis australis*. Refer to Table 1 for component identification numbers. Error bars represent 95% confidence intervals ($3 \leq n \leq 11$).

between males and females showed that only "Forward swimming" differed significantly (sequential Bonferroni test, table-wide $\alpha = 0.05$).

Most (80%) of the components had an average duration less than 10 s (Fig. 7), 86% had durations less than 20 s, 95% were less than 30 s, and all were less than 60 s. Consequently, all of the components identified in this study can be considered acute (lasting for seconds or minutes; *sensu* Box 3.1, Hanlon and Messenger, 1996). Several of these same components may also be considered chronic (lasting minutes to hours; *sensu* Hanlon and Messenger, 1996) when the maximum duration of each component is also considered (Table 1).

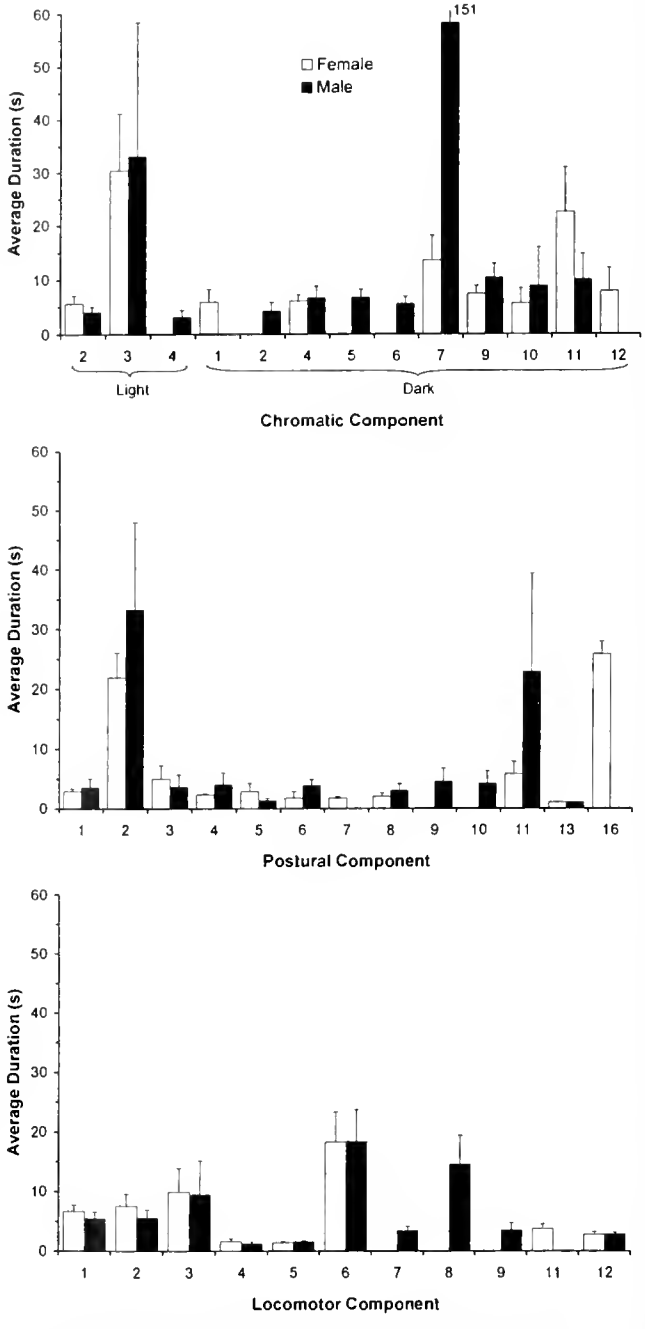

Figure 6. Average duration of each chromatic, postural, and locomotor component identified in females and males of *Sepioteuthis australis* (uninterrupted data only; see text for definitions). Refer to Table 1 for component identification numbers. Error bars represent 95% confidence intervals ($3 \leq n \leq 11$).

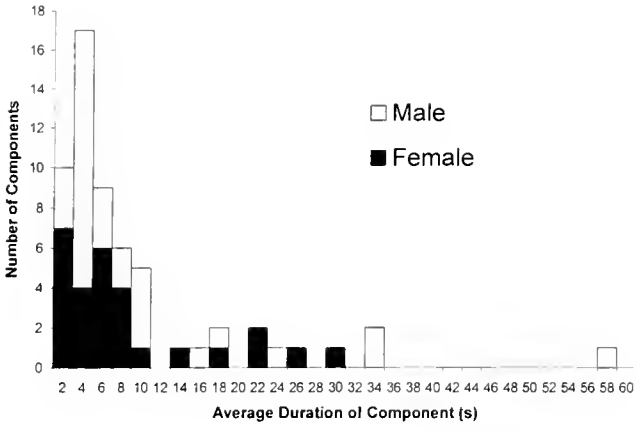

Figure 7. Stacked-column time: frequency distribution of average component duration in males and females of *Sepioteuthis australis*.

Discussion

All of the components we identified in *Sepioteuthis australis* had a mean duration less than 60 s (Figs. 5 and 6) and should therefore be classified as "acute" (*i.e.*, lasting for seconds or minutes, *sensu* Box 3.1, Hanlon and Messenger, 1996). However, because 80% of the components had a duration ≤ 10 s (Fig. 7), the classification may need to be refined to take account of varying levels of "acute" response. We propose a three-tier system consisting of short acute (≤ 10 s), medium acute (11–60 s), and chronic (> 60 s) component durations. Using this system, and treating the components shown by each sex separately, we classify 32% (25/77) of the components in *S. australis* as short acute, 43% (33/77) as both short acute and medium acute, and 25% (19/77) as short acute, medium acute, and chronic (Table 1). This system also permits identification of patterning differences that may be biologically meaningful. For example, components such as "Mottled dorsal mantle," "Drooping arms," and "Raised arms" all had acute durations (short and medium) in females of the species (Table 1), but these same components had chronic as well as acute (short and medium) durations in males. A thorough interpretation of these differences is beyond the scope of the present work; however, we believe that this additional distinction within "acute" will prove useful for interpreting the utilization of cephalopod component signals.

The ethogram of reproductive body components presented in this study has both similarities to and differences from those described for other species (Hanlon, 1988; Yang *et al.*, 1986; Porteiro *et al.*, 1990; Hanlon *et al.*, 1994, 1999). For example, similarities are seen in the "Clear" chromatic component, which was previously identified as an acute component by Hanlon (1988), Yang *et al.* (1986), Porteiro *et al.* (1990), and Hanlon *et al.* (1994, 1999) and also found here to be a short acute component in *S. australis*. Likewise, "Mate guarding" has been identified as an acute component in *Loligo pealeii* (Hanlon *et al.*, 1999) and was also defined as an acute (short and medium) component here for *S. australis*. In contrast, "Dark dorsal stripe" (Hanlon *et al.*, 1994) has previously been identified only as a chronic component, but was identified in our study as a short acute component (Table 1, and see above).

The high number of short acute component durations we identified (Table 1, Fig. 6) indicates intense communication between reproductively active individuals and is probably important in competition for mates and in predator detection. Guilford and Dawkins (1991) have argued that short, intense animal signals (lasting only a few seconds) are more information-rich than longer, weaker signals. The corollary of the observed intensity of short acute component durations is that reproductively active individuals of *S. australis* showed few long (medium acute, or chronic) duration components (Fig. 6). It is possible that signals are communicated by relatively brief absences of these longer duration components (rather than by their chronic presence); however, their significance has yet to be determined.

"Golden epaulettes," "Stitchwork fins" (male only), and "Rigid arms" were all shown for over 80% of the total observation time (see Fig. 5), and these three same components also had the longest average durations (see Fig. 6). Because long component durations were more strongly affected than short durations by our procedure of counting only uninterrupted recordings, more than 80% of the data for "Golden epaulettes" and "Stitchwork fins" was omitted due to interruptions. Consequently, average durations in Figure 6 are probably a marked underestimate of the true durations for these components.

If the catalog of behaviors observed for a species is representative of the entire behavioral repertoire, then a plot of the cumulative rank-order percentage-time frequencies of the behaviors should show a marked asymptote (Lehner, 1979). Relevant plots for our data show an asymptote for both females and males after 30 components (Fig. 8). We identified 38 components for females and 44 for males (Table 1). These numbers exceed the point at which an asymptote is reached in each data set and therefore suggest that the data reported here are indeed a representative catalog of the component repertoire for the reproductive behavior of this species (Lehner, 1979).

The number of chromatic components we identified (n = 17) is less than that described for *S. lessoniana* (23; Moynihan and Rodaniche, 1982; Moynihan, 1985; Hanlon and Messenger, 1996) and *S. sepioidea* (23; Moynihan and Rodaniche, 1982; Hanlon and Messenger, 1996). However, our data for *S. australis* (17 chromatic components, Table 1) relate only to reproductive behavior. Of the 23 chromatic components reported by Moynihan and Rodaniche (1982) for *S. sepioidea*, 17 were observed in reproductively active individuals (*i.e.*, 75% of the total repertoire). In total, 23 chromatic components were also identified in *S. lessoniana*

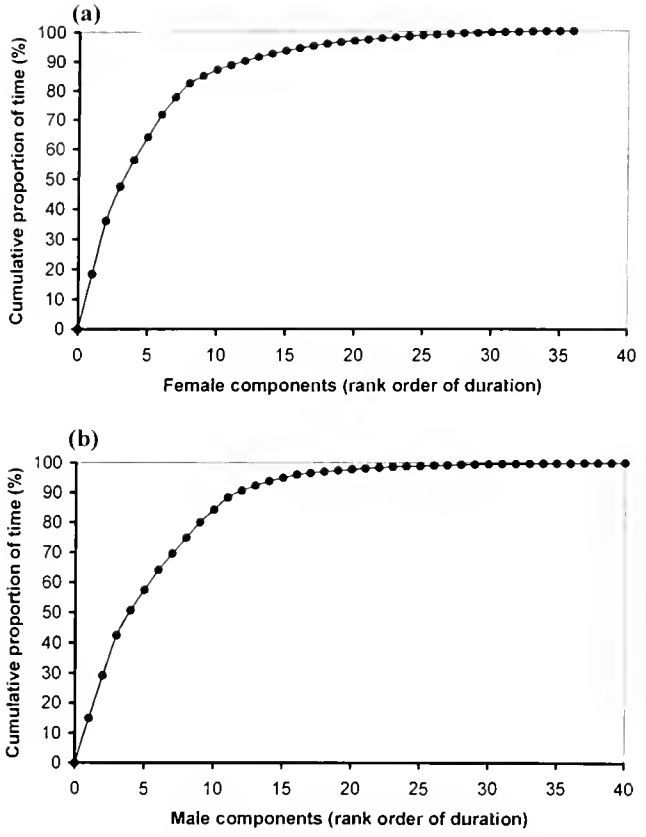

Figure 8. Plot of cumulative rank-order percentage-time frequencies plot of body pattern components identified in (a) females and (b) males of *Sepioteuthis australis*. Numbers on *x* axis refer to the ranked order of component numbers, not the assigned component numbers in Table 1.

(Hanlon and Messenger, 1996), although the number of these components specific to reproductive behavior is not known. We were unable to identify body pattern components associated with nonreproductive behavior, and therefore we do not know the full component complement for *S. australis*. Nonetheless, the full repertoire of chromatic components in cephalopods is thought to be correlated with habitat complexity (table 3.9 in Hanlon and Messenger, 1996). Given that *S. australis* lives in a structurally less complex habitat than *S. sepioidea* (seagrass *versus* coral reefs), it seems likely that the ethogram of reproductive components identified here is a large proportion of the entire ethogram for this species.

As in this current study, the body patterning behavior of *L. pealeii* (Hanlon *et al.*, 1999), and *L. vulgaris reynaudii* (Hanlon *et al.*, 1994) was described primarily from individuals on spawning grounds. It is therefore useful to compare the ethograms of these two *Loligo* species with that of *S. australis*. For *L. pealeii*, 30 chromatic, 5 postural, and 12 locomotor components (plus a further 4 polarized components) were identified (Hanlon *et al.*, 1994); for *L. vulgaris reynaudii*, the numbers were 23 chromatic, 4 postural, and 9 locomotor components (Hanlon *et al.*, 1994). It seems that these two *Loligo* species have a larger repertoire of chromatic components than *S. australis* has, but the repertoire of postural and locomotor components appears considerably larger for *S. australis*. Differences in chromatic component numbers can probably be attributed to differences in habitat structural complexity (table 3.9 in Hanlon and Messenger, 1996), but the significance of differences in postural and locomotor component numbers between species is unclear.

When comparing the ethograms of *L. pealeii* (Hanlon *et al.*, 1999), *L. vulgaris reynaudii* (Hanlon *et al.*, 1994), and *S. australis*, many of the component patterns appear similar, but the comparative frequency that each component is shown varies markedly. The prevalence of some components is quite different between all three species. For example, "All dark" was the most prevalent dark chromatic component shown by *L. pealeii* (Hanlon *et al.*, 1999), it was shown moderately by *L. vulgaris reynaudii* (Hanlon *et al.*, 1994), and it was one of the least common dark chromatic components shown by *S. australis* (Table 1). Alternatively, the display frequency of some components shows signs of differentiation between the two genera. For example, "Clear" was frequently shown by both *L. pealeii* (Hanlon *et al.*, 1999) and *L. vulgaris reynaudii* (Hanlon *et al.*, 1994), but was the least shown light chromatic component for *S. australis*. Body pattern components of behavior are thought to be useful in taxonomic distinction between squid species (Hanlon, 1988; Roper and Hochberg, 1988), and discussions such as the above demonstrate some of the comparisons that can be made.

As well as comparisons of ethograms between species, comparisons between members of a species that are and are not reproductively active could provide an important insight into the visual vocabulary associated with spawning. Anecdotal observations of non-reproductively active (feeding) squids showed that the most common postural component ($> 50\%$) was "Downward pointing" (perhaps as an aid to prey acquisition). We observed the "Downward pointing" posture in reproductively active individuals only in females and only for 2% of the total time (Fig. 5); it generally occurred when the female was seeking out the egg cluster on the substratum prior to egg deposition. Consequently, while our analysis suggests that the ethogram of reproductive components presented here adequately describes the reproductive body patterns of *S. australis*, it seems equally clear that this ethogram does not describe the suite of body patterns exhibited by non-reproductively active individuals.

In a previous study, we reported that "Curled tentacle club" (as "Club display"; Jantzen and Havenhand, 2003) was shown by a male to the female as a signal of intention to mate. It is now clear that this was incorrect. Firstly, all 84 incidences of "Curled tentacle club" in this study were in females (Table 1); secondly, the frequency of this component was not related to copulation frequency.

Each of the four mating types reported here for *S. australis* ("Male-upturned mating," "Head-to-head mating," "Male-parallel mating," and "Male "sneak" mating") had a maximum duration of 4 s (Table 1). It cannot be ruled out that "Male-upturned mating" and "Head-to-head mating" are derivatives of the same mating type, as it is likely that the site of spermatophore deposition is in the arms for both these mating types. However, because the deposition site for "Head-to-head mating" in *S. australis* could not be identified here, we believe these two mating types should be considered as separate behaviors. Interestingly, "Male-upturned mating" was the most common mating type observed here (20 out of 29 matings; Table 1). This mating type has been observed in only one other species of squid (*S. lessoniana*) and only in the laboratory (Boal and Gonzalez, 1998). Those authors report a mating duration similar to that reported here (3 s; Table 1, Fig. 6). Durations of other mating types seen here were also comparable to those observed in other squids (see Segawa *et al.*, 1993; table 6.2 in Hanlon and Messenger, 1996). This suggests that the durations of these behaviors in different species may have evolved in response to similar selective pressures.

Identifying the selective benefits of a given patterning component or behavior is difficult. For example, immediately prior to mating, paired males of *S. australis* always showed "Mantle margin stripe," "Fin stripe," "Dark arm stripes," and "Shaded eye" chromatic components. This proved to be a reliable predictor of a "Male-upturned mating" attempt (Fig. 3). However in *Loligo vulgaris reynaudii*, "Fin stripe," Mantle margin stripe," and "Arm stripes" are all intraspecific signals in agonistic contests between males (Hanlon *et al.*, 1994). Boal (1997) suggested that the mating displays of male cuttlefish function as agonistic signals to other males rather than courting signals to females. Whether these components portray different messages in these two species, or are used agonistically towards other males during mating in *S. australis* is unclear.

"Lateral splayed arms" was shown by males of *S. australis* in association with "Male-upturned mating" as well as in agonistic encounters with rival males. This signal has been identified as exclusively agonistic in *L. vulgaris reynaudii* (Hanlon *et al.*, 1994), *L. plei* (DiMarco and Hanlon, 1997), and *L. pealeii* (Hanlon *et al.*, 1999), although in *S. sepioidea* it is reportedly both agonistic (Moynihan, 1985; Hanlon and Messenger, 1996) and associated with mating (Moynihan and Rodaniche, 1982). Again, it is possible that this component portrays different messages in different species; however, it is also possible that the duration of this component differs subtly between mating and agonistic behaviors. We could not distinguish any consistent differences from our analyses, so this possibility remains to be tested.

In contrast to reports in the literature, we found that mating types were not used consistently within males. Indeed, some males copulated with the same female in all three paired mating positions ("Male-upturned mating," "Head-to-head mating," and "Male-parallel mating"). Previously, no more than three mating positions had been reported within a single squid species (table 6.2 in Hanlon and Messenger, 1996). Whether paired males of *S. australis* show (or have shown) "Sneaker mating" at other times is not known; however, this evidence suggests that *S. australis* may exhibit a greater diversity in mating positions (three, plus "Sneaker mating") than other squids.

We identified three types of agonistic encounters between rival males: "Parrying," "Fin beating," and "Charging" (Fig. 3). While "Parrying" represented a nonphysical intraspecific encounter, "Fin beating" and "Charging" involved physical contact between rival males. "Parrying" (34% of time, Fig. 5; 334 observations, Table 1) was far more prevalent than "Fin beating" (1% of time, Fig. 5; 32 observations, Table 1) and "Charging" (7 observations, Table 1). In addition, "Parrying" had a longer average duration (15 s, Fig. 6) than "Fin beating" (4 s, Fig. 6). This behavior is similar to the fighting tactics of *L. plei* in which physical agonistic contests between rival males are shorter than nonphysical contests (DiMarco and Hanlon, 1997).

In a wider context, chromatic components of behavior are useful in taxonomic distinction of squid species (Hanlon, 1988; Roper and Hochberg, 1988). Comparative allozyme analysis of *S. australis* has identified a discrete genetic divergence between the New Zealand and Australian populations (Triantafillos and Adams, 2001). It is possible that these populations have also evolved a different repertoire of reproductive components. The only report of the reproductive behavior of *S. australis* from New Zealand (Larcombe and Russell, 1971) describes body components generally consistent with "Clear," "Hovering," "Parallel positioning," "Rigid arms," "Oviposition," "Mate guarding," "Downward pointing," "Plain," "Peristaltic arm flare," "Charging," and "Parrying"; unfortunately, their descriptions lack sufficient detail to be directly compared with our observations. Further comparative research on the repertoire, frequency, and duration of reproductive components between these two populations would be valuable. Not only would this aid our understanding of the evolution of behavioral mechanisms or reproductive isolation in cephalopods, but it would also cast considerable light on the behavioral differences between populations of the species observed here.

Acknowledgments

We are grateful to J. Doube, M. Gerner, A. Hirst, D. Keuskamp, L. Kupriyanova, B. Lock, A. Mack, G. Mack, M. Naud, and V. Weisbecker for helping with underwater activities, to C. Turner for assistance with data recording and entry, and especially to R. Hanlon for assistance with the nomenclature of components and important comments

on this manuscript. We also thank P. Fairweather, L. van Camp, and an anonymous reviewer for valuable comments and suggestions on this manuscript. Video equipment was obtained from Sea Optics Australia Pty. Ltd. This work was supported by an Australian Postgraduate Award Scholarship (to TMJ), and a grant from the Australian Research Council (to JNH).

Literature Cited

Boal, J. G. 1997. Female choice of males in cuttlefish (Mollusca: Cephalopoda). *Behaviour* **134:** 975–988.

Boal, J. G., and S. A. Gonzalez. 1998. Social behaviour of individual oval squids (Cephalopoda, Teuthoidea, Loliginidae, *Sepioteuthis lessoniana*) within a captive school. *Ethology* **104:** 161–178.

Boycott, B. B. 1953. The chromatophore system of cephalopods. *Proc. Linn. Soc. Lond.* **164:** 235–240.

Corner, B. D., and H. T. Moore. 1980. Field observations on the reproductive behavior of *Sepia latimanus*. *Micronesia* **16:** 235–260.

Cornwell, C. J., J. B. Messenger, and R. T. Hanlon. 1997. Chromatophores and body patterning in the squid *Alloteuthis subulata*. *J. Mar. Biol. Assoc. UK* **77:** 1243–1246.

DiMarco, F. P., and R. T. Hanlon. 1997. Agonistic behavior in the squid *Loligo plei* (Loliginidae, Teuthoidea): fighting tactics and the effects of size and resource value. *Ethology* **103:** 89–108.

Drummond, H. 1981. The nature and description of behavior patterns. Pp. 1–33 in *Perspectives in Ethology, Volume 4, Advantages of Diversity*, P. P. G. Bateson and P. H. Klopfer, eds. Plenum Press, New York.

Guilford, T., and M. S. Dawkins. 1991. Receiver psychology and the evolution of animal signals. *Anim. Behav.* **42:** 1–14.

Hanlon, R. T. 1982. The functional organization of chromatophores and iridescent cells in the body patterning of *Loligo plei* (Cephalopoda: Myopsida). *Malacologia* **23:** 89–119.

Hanlon, R. T. 1988. Behavioral and body patterning characters useful in taxonomy and field identification of cephalopods. *Malacologia* **29:** 247–264.

Hanlon, R. T., and J. B. Messenger. 1996. *Cephalopod Behaviour*. Cambridge University Press, Cambridge.

Hanlon, R. T., and M. R. Wolterding. 1989. Behavior, body patterning, growth and life history of *Octopus briareus* cultured in the laboratory. *Am. Malacol. Bull.* **7:** 21–45.

Hanlon, R. T., M. J. Smale, and W. H. H. Sauer. 1994. An ethogram of body patterning behavior in the squid *Loligo vulgaris reynaudii* on spawning grounds in South Africa. *Biol. Bull.* **187:** 363–372.

Hanlon, R. T., M. R. Maxwell, and N. Shashar. 1997. Behavioral dynamics that would lead to multiple paternity within egg capsules of the squid *Loligo pealei*. *Biol. Bull.* **193:** 212–214.

Hanlon, R. T., M. R. Maxwell, N. Shashar, E. R. Loew, and K.-L. Boyle. 1999. An ethogram of body patterning behavior in the biomedically and commercially valuable squid *Loligo pealei* off Cape Cod, Massachusetts. *Biol. Bull.* **197:** 49–62.

Jantzen, T. M., and J. N. Havenhand. 2003. Preliminary field observations of mating and spawning in the squid *Sepioteuthis australis*. *Bull. Mar. Sci.* **71:** 1073–1080.

King, A. J., S. A. Adamo, and R. T. Hanlon. 1999. Contact with squid egg capsules increases agonistic behavior in male squid (*Loligo pealei*). *Biol. Bull.* **197:** 256.

Larcombe, M. F., and B. C. Russell. 1971. Egg laying behavior of the broad squid, *Sepioteuthis bilineata*. *N.Z.J. Mar. Freshwat. Res.* **5:** 3–11.

Lehner, P. N. 1979. *Handbook of Ethological Methods*. Garland STPM Press, New York.

Martin, P., and P. Bateson. 1993. *Measuring Behavior: An Introductory Guide*, 2nd ed. Cambridge University Press, Cambridge.

Mather, J. A., and D. L. Mather. 1994. Skin colours and patterns of juvenile *Octopus vulgaris* (Mollusca, Cephalopoda) in Bermuda. *Vie Milieu* **44:** 267–272.

Messenger, J. B. 2001. Cephalopod chromatophores: neurobiology and natural history. *Biol. Rev.* **76:** 473–528.

Moynihan, M. 1985. *Communication and Noncommunication by Cephalopods*. Indiana University Press, Bloomington.

Moynihan, M., and A. F. Rodaniche. 1982. The behavior and natural history of the Caribbean reef squid *Sepioteuthis sepioidea*. With a consideration of social, signal, and defensive patterns for difficult and dangerous environments. *Adv. Ethol.* **25:** 1–151.

Packard, A. 1982. Morphogenesis of chromatophore patterns in cephalopods: are morphological and physiological 'units' the same? *Malacologia* **23:** 193–201.

Packard, A., and F. G. Hochberg. 1977. Skin patterning in *Octopus* and other genera. *Symp. Zool. Soc. Lond.* **38:** 191–231.

Packard, A., and G. D. Sanders. 1969. What the octopus shows to the world. *Endeavour* **28:** 92–99.

Packard, A., and G. D. Sanders. 1971. Body patterns of *Octopus vulgaris* and maturation of the response to disturbance. *Anim. Behav.* **19:** 780–790.

Pecl, G. 2000. Comparative life history of tropical and temperate *Sepioteuthis* squids in Australian waters. Ph.D. thesis, James Cook University, Australia.

Pecl, G. 2001. Flexible reproductive strategies in the tropical and temperate *Sepioteuthis* squids. *Mar. Biol.* **138:** 93–101.

Porteiro, F. M., H. R. Martins, and R. T. Hanlon. 1990. Some observations on the behaviour of adult squids, *Loligo forbesii*, in captivity. *J. Mar. Biol. Assoc. UK* **70:** 459–472.

Rice, W. R. 1989. Analyzing tables of statistical tests. *Evolution* **43:** 223–225.

Roper, C. F. E., and F. G. Hochberg. 1988. Behavior and systematics of cephalopods from Lizard Island, Australia, based on color and body patterns. *Malacologia* **29:** 153–193.

Segawa, S., T. Izuaka, T. Tamashiro, and T. Okutani. 1993. A note on mating and egg deposition by *Sepioteuthis lessoniana* in Ishigaki Island, Okinawa, Southwestern Japan. *Venus Jap. J. Malacol.* **52:** 101–108.

Triantafillos, L., and M. Adams. 2001. Allozyme analysis reveals a complex population structure in the southern calamary, *Sepioteuthis australis*, from Australia and New Zealand. *Mar. Ecol. Prog. Ser.* **212:** 193–209.

Yang, W. T., R. F. Hixon, P. E. Turk, M. E. Krejci, W. H. Hulet, and R. T. Hanlon. 1986. Growth, behavior, and sexual maturation of the market squid, *Loligo opalescens*, cultured through the life cycle. *Fish. Bull.* **84:** 771–798.

Reference: *Biol. Bull.* **204:** 305–317. (June 2003)

Reproductive Behavior in the Squid *Sepioteuthis australis* From South Australia: Interactions on the Spawning Grounds

TROY M. JANTZEN* AND JON N. HAVENHAND†

School of Biological Sciences, Flinders University, GPO Box 2100, Adelaide, South Australia, 5001

Abstract. Squid behavior is synonymous with distinctive body patterns, postures, and movements that constitute a complex visual communication system. These communications are particularly obvious during reproduction. They are important for sexual selection and have been identified as a potential means of species differentiation. Here we present a detailed account of copulation, mating, and egg deposition behaviors from *in situ* observations of the squid *Sepioteuthis australis* from South Australia. We identified four mating types from 85 separate mating attempts: "Male-upturned mating" (64% of mating attempts); "Sneaker mating" (33%); "Male-parallel" (2%); and "Head-to-head" (1%). Intervals between successive egg deposition behaviors were clearly bimodal, with modes at 2.5 s and 70.0 s. Ninety-three percent of egg capsules contained 3 or 4 eggs (mean = 3.54), and each egg cluster contained between 218 and 1922 egg capsules (mean = 893.9). The reproductive behavior of *S. australis* from South Australia was different from that described for other cephalopod species. More importantly, comparison between these results and those for other populations of *S. australis* suggests that behavior may differ from one population to another.

Introduction

Mate choice arises from behavioral interactions that generate selection for gender-specific traits (secondary sexual characteristics) (Ryan, 1997). Differences in reproductive success of individuals are, in turn, typically held to be caused by competition for mates (Andersson, 1994; Ryan, 1997). In systems where female choice is prevalent; sexual selection should favor conspicuous male traits that allow males to out-compete (directly or indirectly) other males (Andersson, 1994). These traits can be morphological, physical, or behavioral (Parker, 1984; Andersson, 1994; Birkhead and Parker, 1997; Ryan 1997).

In cephalopods, secondary sexual characteristics primarily consist of differences in body size, body patterns, sucker size, gonad shape or color, and sometimes photophores (Hanlon and Messenger, 1996). In squid, behavior comprises rapid body pattern changes that result from alterations in chromatic, postural, or locomotor components of behavior (Mather and Mather, 1994; Hanlon and Messenger, 1996). These behavioral patterns form a complex visual communication system. Interpreting this communication system is fundamental to understanding the processes of sexual selection in these species.

Analysis of reproductive behavior can be important when discriminating closely related species (Hanlon, 1988). Although camouflage patterns are likely to be highly conserved due to responses to common predators, reproductive communication is likely to have species-specific signals. Roper and Voss (1983) documented the range of morphological characters for species descriptions of cephalopods, and Hanlon (1988) proposed additional behavioral characters for identification. Some of the characters that Hanlon (1988) cites as being important are intraspecific agonistic behavior, mating behavior, spawning and egg care behavior, and chromatic components of body patterns. In line with these criteria, cephalopod taxa such as the squid *Sepioteuthis lessoniana* from Japan are now being reviewed and reclassified (Segawa *et al.*, 1993a).

Although still regarded as a single species, geographically different populations of *S. lessoniana* are thought to be taxonomically different (Segawa *et al.*, 1993a, b; Izuka *et*

Received 29 October 2002; accepted 31 January 2003.

* To whom correspondence should be addressed. E-mail: Troy.Jantzen@bms.com

† Current address: Tjärnö Marine Biological Laboratory, Goteborg University, 452 96 Strömstad, Sweden.

al., 1994, 1996a, b). Differences between these populations occur both at a genetic level (Izuka *et al.*, 1994) and at a population level in differences between reproductive behavioral characteristics such as egg deposition (Segawa *et al.*, 1993a, b; Izuka *et al.*, 1994).

Similar uncertainty about genetic differences between geographically isolated populations of *S. australis* has arisen recently. Allozyme analysis of Australian and New Zealand populations of this species indicates that they are genetically distinct (Triantafillos and Adams, 2001). However, owing to the lack of comparative data on the behavior of this species in New Zealand and Australia, it is not known whether the genetic differences are expressed as behavioral differences.

The aim of this study was to identify and describe the reproductive behavior of *Sepioteuthis australis* from South Australia. We recently cataloged (as an ethogram) the suite of reproductive body pattern components for this species from South Australia. (Jantzen and Havenhand, 2003a). Here, we report results of underwater digital video imaging, photographs, and field notes that document the reproductive behavior of *S. australis* on spawning grounds over three consecutive spawning seasons. Our descriptions include previously unreported reproductive behaviors. These results are compared with previous descriptions for this, and other, squid species to identify aspects of reproductive behavior that might provide insights into secondary sexual selection in squids and the evolutionary significance of these reproductive strategies.

Materials and Methods

Mating behavior was observed during daylight hours on spawning grounds between Marino and Hallett Cove, South Australia (138° 29′ E, 38° 02′ S) between December 1999 and March 2002. All data were collected during the main spawning season each year (September to March). The substrate on the spawning grounds consists of patches of bare sand and rock interspersed with seagrass (*Amphibolis antarctica*) and brown macroalgae (*Sargassum* spp.) Reproductive activity of squid on spawning grounds was identified by visual observation from the surface at known locations, and by the activity of recreational and professional fishermen. Reproductive activity was observed by scuba diving and directly from the surface in less than 4.5 m of water. The presence of divers close (< 30 cm) to reproductively active individuals caused no apparent alteration in squid behavior (when compared with behavior of individuals observed from afar). Observations were therefore routinely made at a distance of less than 2 m. Still photographs of mating and spawning behavior were taken with a Nikonos V camera (Nikon Corporation, Melville, NY), and video images were recorded with a Sony TV120 digital video camera (Sony Corporation, New York) in an Amphibico housing (Amphibico, Quebec, Canada). Video sampling followed the protocol of Martin and Bateson (1993) for focal-animal sampling, with additional *ad libitum* video sampling of specific behaviors. Detailed notes of reproductive activity were recorded for every observation period and compared with video and still images of behavior for the same period.

We previously identified the reproductive body patterns of *Sepioteuthis australis* (Jantzen and Havenhand, 2003a). The nomenclature of these patterns follows the convention of capitalizing the first letter of formally defined patterns of behaviors (Hanlon and Wolterding, 1989). Terminology applied to the physical characteristics of squid follows that described by Hanlon and Messenger (1996, fig. 2.1, p. 13). Frame-by-frame sequences of selected behaviors were obtained and analyzed using Final Cut Pro software (Apple Computer, Cupertino, CA) at a frame rate of 25 frames per second.

Durations between the completion of "Egg passing" and egg deposition, between egg deposition and "Peristaltic arm flare," and between successive observations of "Peristaltic arm flare" were analyzed using a one-way ANOVA to investigate differences between females. To meet the assumption of homogeneity of variance, data for durations between "Egg passing" and egg deposition were square-root transformed prior to analysis. These analyses were conducted to determine if these behaviors were consistent between females.

Results

Over a period of three consecutive spawning seasons, we observed more than 550 reproductively active individuals of *Sepioteuthis australis* in over 75 hours underwater. Observation sessions lasted as long as 120 min at a time, and the number of reproductively active squid present at any one time ranged from 2 (a single spawning pair) to more than 45 per dive. The length of time that each sex remained on the spawning grounds could not be quantified, because the size of the spawning grounds exceeded the visible range underwater. However, on all but two occasions, focal females remained in a localized area on the spawning ground throughout the observation period. In the two other instances, females swam out of view while being observed, and we do not know whether they remained on the spawning grounds. Furthermore, all observations were conducted during daylight, so we do not know if reproductive activity continued at night. Direct counts of sex ratio on each dive (and subsequent checking of these counts from the video images) showed a male-biased sex ratio between 1:1 (a single pair) and 3:1 (>4 individuals). Females were typically paired with a male, while several unpaired males swam amongst the paired individuals.

Mating

Four mating types were observed during 85 mating attempts. Mating types were classified as paired "Male-upturned mating" (PU), paired "Male-parallel mating" (PM), paired "Head-to-head mating" (PH), and "Sneaker mating" (SM). Paired mating types occurred only between paired individuals, whereas "Sneaker mating" comprised all attempts by unpaired males to mate with paired females. Of the four mating types, PU and SM were most frequently observed (64% and 33%, respectively, Fig. 1), with PM and PH seen on only 2% and 1% of matings respectively (Fig. 1).

Paired Male-upturned mating (PU). Paired Male-upturned mating occurred most frequently (54/85 matings, Fig. 1), with a mean inter-mating interval of 7.09 min (SEM = 3.27 min, $n = 11$). In all cases, males swam into a position over the female prior to PU while showing "Mantle margin stripe," "Dark arm stripes," "Fin stripe," "Shaded eye," and "Rigid arms" body pattern components (Figs. 2A, 3). On six occasions, a male was seen to show up to five rapid "Lateral splayed arms" components in quick succession while above the female. This "Lateral splayed arms" behavior did not appear to evoke a response by the female.

Once above the female, males rotated 180° around the longitudinal axis (Fig. 2B). Simultaneous with this rotation, the hectocotylized arm (left 4th arm) began moving back toward the funnel, and the right 4th arm moved toward the buccal region of the female (Fig. 2B). Once the animal was completely upside-down, spermatophores were ejected through the funnel (Fig. 2C) and gathered with a sweeping action of the hectocotylized arm across the funnel. This arm was then extended beside the right 4th arm (positioned with the tip in the female buccal region; Fig. 2D), and spermatophores were delivered into the buccal region of the female (Fig. 2E). The male then rotated back to the normal swimming position (Fig. 2F). From initial rotation of the male to completion of mating took less than 3 s.

Throughout PU, females showed "White dorsal stripe," "Golden epaulettes," and "Rigid arms" body pattern components (Figs. 2A, 3). Occasionally the posterior mantle of the female was seen to move downward 30°–40° from horizontal as the male began to rotate around to the upside-down position. PU did not occur before every deposition of an egg capsule (Fig. 3); however, this component was always observed after "Egg passing" (see below) and before egg deposition. Throughout PU, females were usually within 1 m of an egg cluster and within one body length of the substrate.

Boal and Gonzalez (1998) describe four classes of PU mating for *S. lessoniana:* "Pre-mating behavior" (mutual swimming of spawning pairs in a back-and-forth motion),

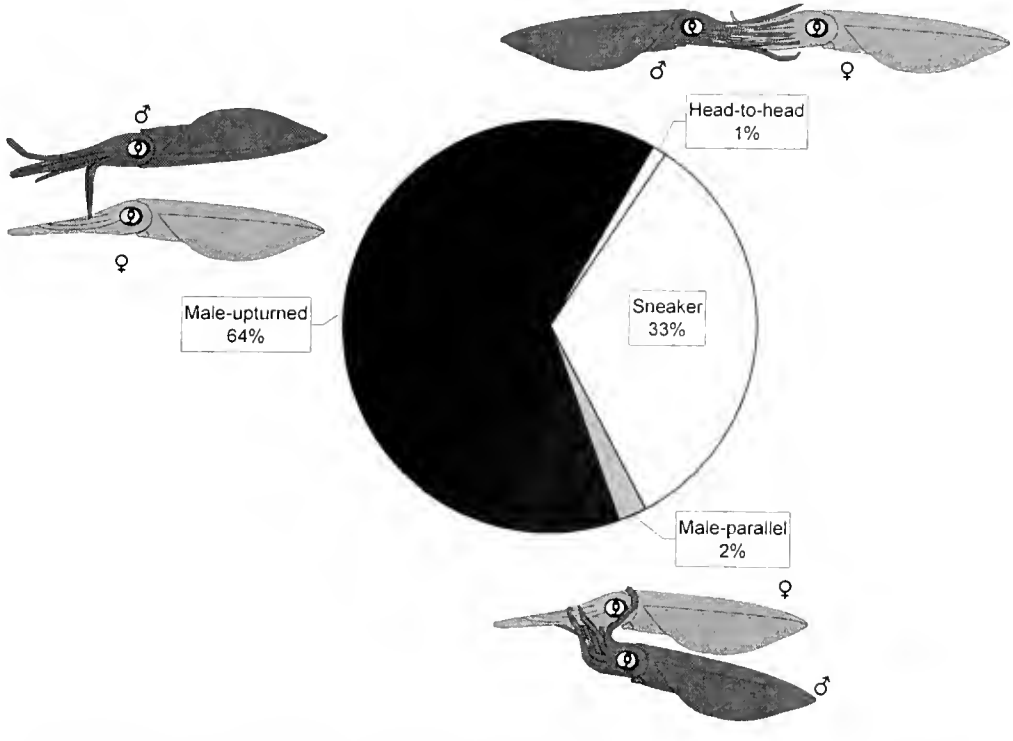

Figure 1. Percentage (of all matings) of each of the four mating types identified in *Sepioteuthis australis*, with illustrations of the three mating types between paired individuals.

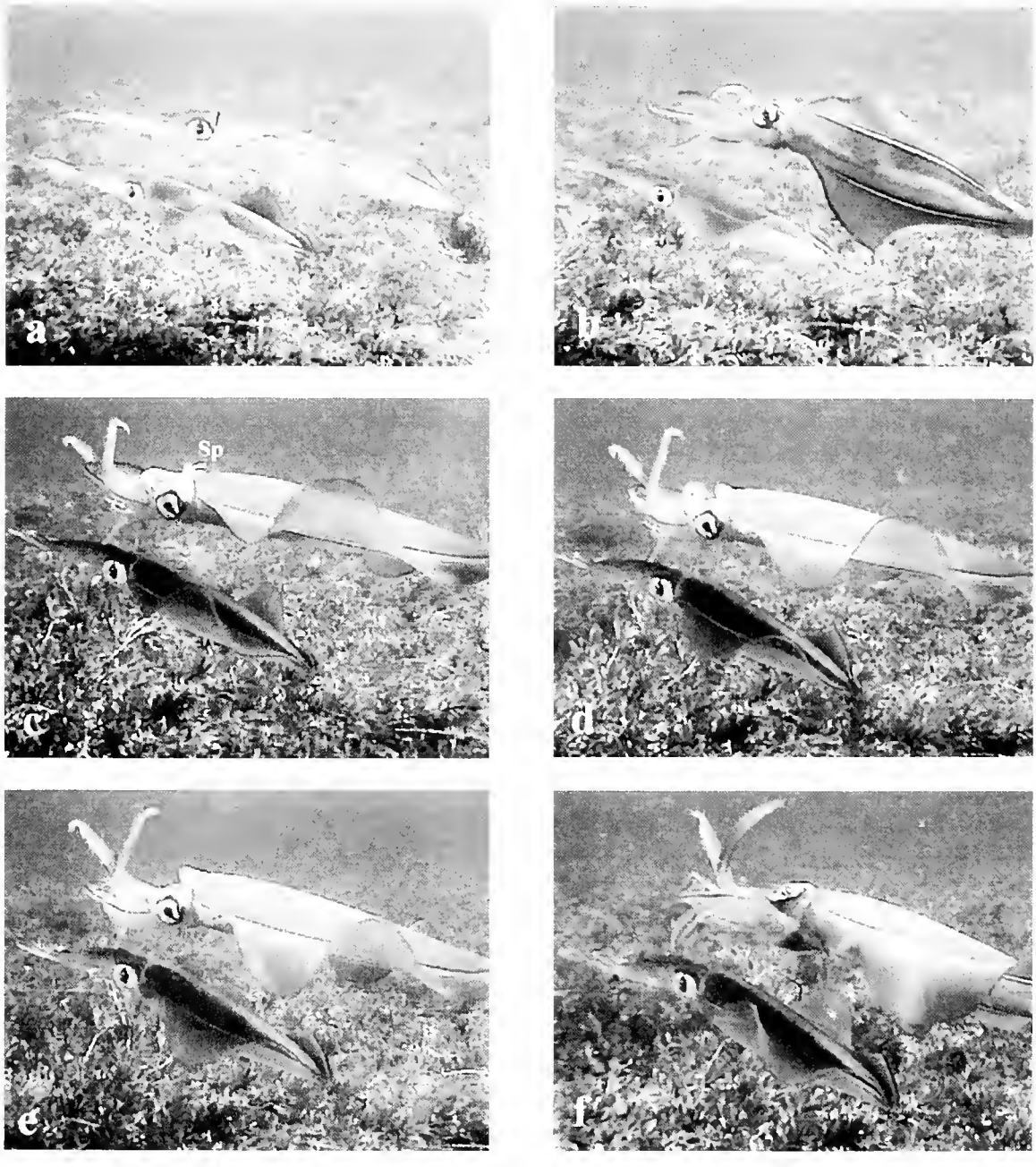

Figure 2. Six-frame sequence of "Male-upturned mating" behavior in *Sepioteuthis australis*. The male (top) swims into a position over the female (bottom: a). The male then rotates to the upside-down position (b) and gathers spermatophores (Sp) from the funnel with the left 4th (hectocotylized) arm (c). The hectocotylized arm then moves down the right 4th arm that is positioned in the buccal area of the female (d) and deposits spermatophores in this area (e). Copulation is complete, and the male rotates back to the normal swimming position (f). Total time elapsed = 3 s.

"Flip" (whereby the male rotated around into an upside-down position), "Contact" (when the male physically contacted the female), and "Attempt" (when no contact was made with the female by the male while in the upside-down position). Only "Pre-mating behavior," "Flip," and "Contact" classes of PU had been previously described in *S. australis* (Jantzen and Havenhand, 2003b). We also observed the "Attempt" class of PU mating, in which mating was clearly unsuccessful (*i.e.*, no physical contact was made with the female).

A few spermatophores (about 3–5) were seen being transferred to the female during PU. Direct counts of the number of spermatophores transferred were impossible due to the speed of PU mating (<3 s). Consequently, these numbers

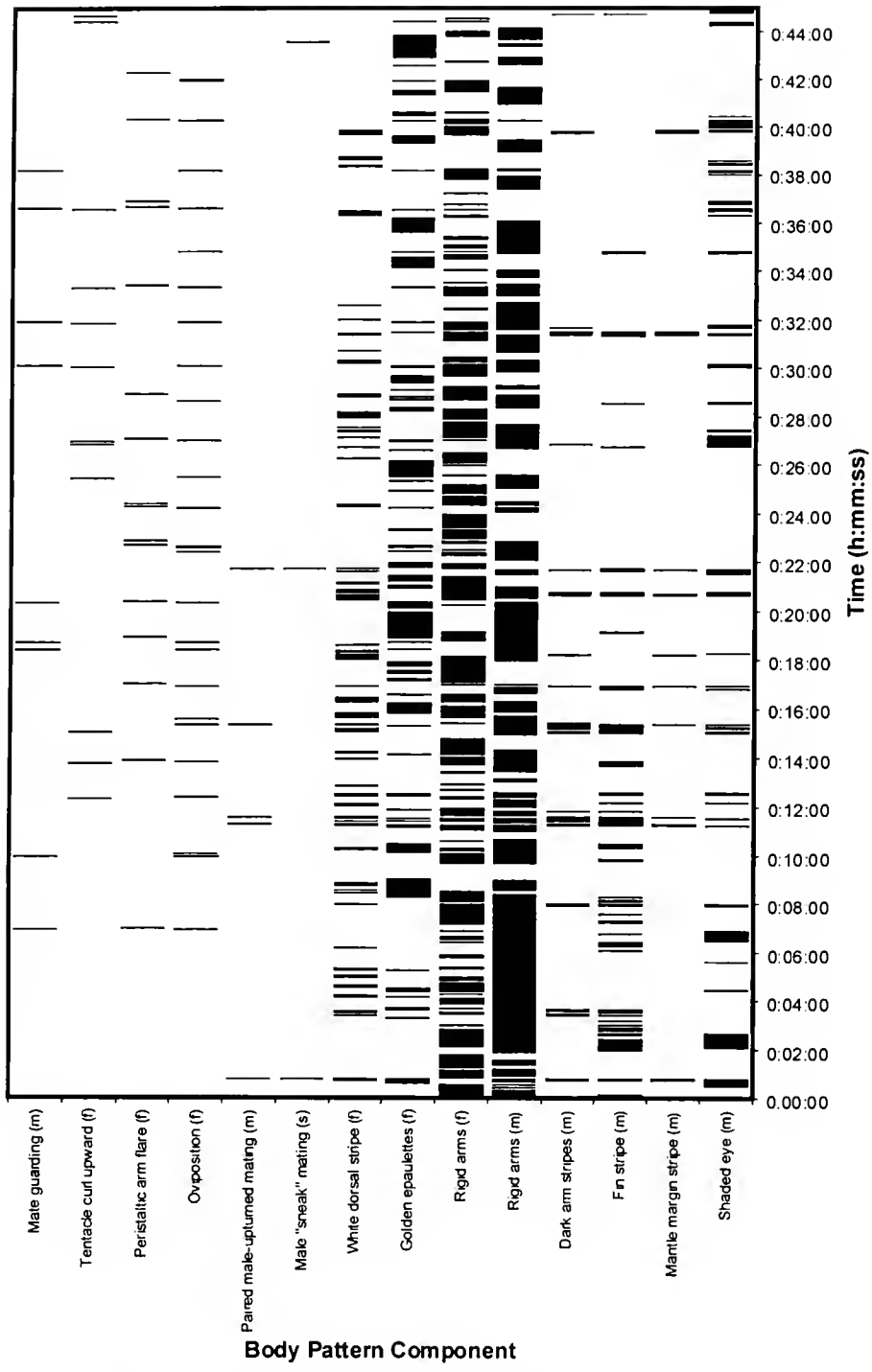

Figure 3. Signal periodicity and duration of selected components associated with egg deposition and mating from a single spawning pair of *Sepioteuthis australis*. Activity was recorded for a continuous focal sampling period of 45 min. Each horizontal bar represents the activity of a single body component from a single animal at any given time. Letters in parentheses indicate sex of the focal animal from which each body pattern component is recorded (m = paired male, f = paired female, s = sneaker male).

were estimated from analysis of digital images of two successful mating attempts and two unsuccessful mating attempts. In the two successful mating attempts, three and five spermatophores were counted. The unsuccessful mating attempts resulted in spermatophores being released into the water column, where they could be counted readily. In these

unsuccessful attempts. spermatophoric reaction (the process by which sperm are ejected from the spermatophore; Mann *et al.*, 1966) had occurred. Both times. three coagulated strands of sperm were identified.

Paired Male-parallel mating (PM). Two PM attempts were observed (2.4% of all mating attempts). On both occasions, both sexes showed the "Plain" chromatic component prior to, and throughout, PM. Our observations of PM were very similar to reports of Male-parallel mating in other squid species (*e.g.*, Drew, 1911; McGowan, 1954; Arnold, 1962). The transfer of spermatophores to the female was not seen, and therefore we could not ascertain whether (or where) spermatophores were deposited on or in the female.

Paired Head-to-head mating (PH). This behavior was seen on only one occasion. The male swam rapidly toward the female head-on and grasped her arms and tentacles. The male remained in this position for less than 1 s before the pair separated. "Plain" was the only chromatic component seen in both sexes, and the transfer of spermatophores was not seen.

Sneaker mating (SM). On 28 occasions, an unpaired male attempted to mate with a paired female. These events were classed as SM, and occurred mostly while a paired female was attempting to deposit an egg capsule at an egg cluster, or simultaneously with the mating attempt of a paired male (Fig. 3). Four types of SM were observed: "Sneaker males" darted amongst the vegetative substrate and made contact with a female while she was at an egg cluster. Sneaker males mated in an upside-down position (consistent with the behavior of the paired male in PU mating, described above) at the egg cluster, but in the "Male-parallel" position if the paired male was "Parrying" a second unpaired male. (Note that in all cases, "Plain" was the only chromatic body pattern consistently shown by the sneaker males in these three SM types.) The fourth SM type involved sneaker males appearing to mimic a paired female. This was seen twice, and no agonistic response was shown by the paired male as the sneaker male approached the paired female. Following these mating attempts, a second unpaired male was seen attempting to mate with the sneaker males. The prominent chromatic body patterns shown by the sneaker males were "Dark mantle," followed by "Dorsal white stripe" as well as "Golden epaulettes" and "Rigid arms." These latter three body pattern components are typical of paired females throughout PU (see above).

General mating behavior. Spermatophores were generally found deposited in the buccal cavity of females; however, several females were observed with spermatophore capsules affixed to the head, arms, or dorsal mantle. The copulation attempts that led to the placement of these spermatophores were not seen; however, in one instance, a sneaker male attempted to make contact with a female on the head. The placement of spermatephores was not identified in this instance. Given that in all paired matings (and paired mating attempts), spermatophores were never seen to be placed outside the buccal cavity, it seems likely that these extra-buccal spermatophores were the result of Sneaker mating.

It was not uncommon for PU and SM to occur simultaneously (Fig. 3); on most of these occasions, females rapidly jetted away from the simultaneous mating attempts.

Egg deposition

When a female approached an egg cluster, her tentacles folded back laterally (Fig. 4a-e) as she descended toward the substrate and deposited a new egg capsule with her arms. In all cases (n = 226), attachment of egg capsules was completed in less than 2 s. Paired males regularly remained a few centimeters above the female as she attached egg capsules to a cluster ("Mate guarding"). New egg capsules appeared translucent immediately upon deposition (Fig. 4f), and the number of eggs within each newly deposited capsule was clearly visible. No more than three females were seen contributing egg capsules to each cluster. The chromatic components of females depositing egg capsules in a cluster were rarely seen, because the female was routinely obscured from view by the substrate.

The interval between deposition of successive egg capsules showed a bimodal distribution (Fig. 5). Modes in interval frequency occurred at 2.5 s and 70.0 s. This pattern was evident for each female recorded (n = 11 females). Short durations always occurred singly (*i.e.*, were followed by at least one long duration; Fig. 3).

Egg capsules contained 5 eggs or less with 93% of egg capsules containing 3 or 4 eggs (Fig. 6). The average number of eggs per capsule was 3.54 (SEM = 0.040, n = 300 capsules). The average number of capsules per egg cluster was 893.9 (min = 218, max = 1922, n = 9).

Following egg deposition, females were often seen radially flaring their arms and tentacles from the base to the tips while simultaneously pulsing a jet of water across the arms and tentacles ("Peristaltic arm flare"; Jantzen and Havenhand, 2003a). Often, small white particles were seen rapidly expelled from the arms of the females as a result of this behavior. This "Peristaltic arm flare" occurred multiple times (commonly twice and occasionally as many as 4 times) within females. The first such event typically occurred within 20 s after the completion of egg deposition (84% of observations, Fig. 7). No significant differences in the duration of the interval between the completion of egg deposition and the first observed "Peristaltic arm flare" were found among separate females (one-way ANOVA, $F_{9,247}$ = 1.630, $P > 0.05$). This supports our observations that duration of the interval between completion of egg deposition and the first observed "Peristaltic arm flare" was consistent between females. Successive "Peristaltic arm flare" compo-

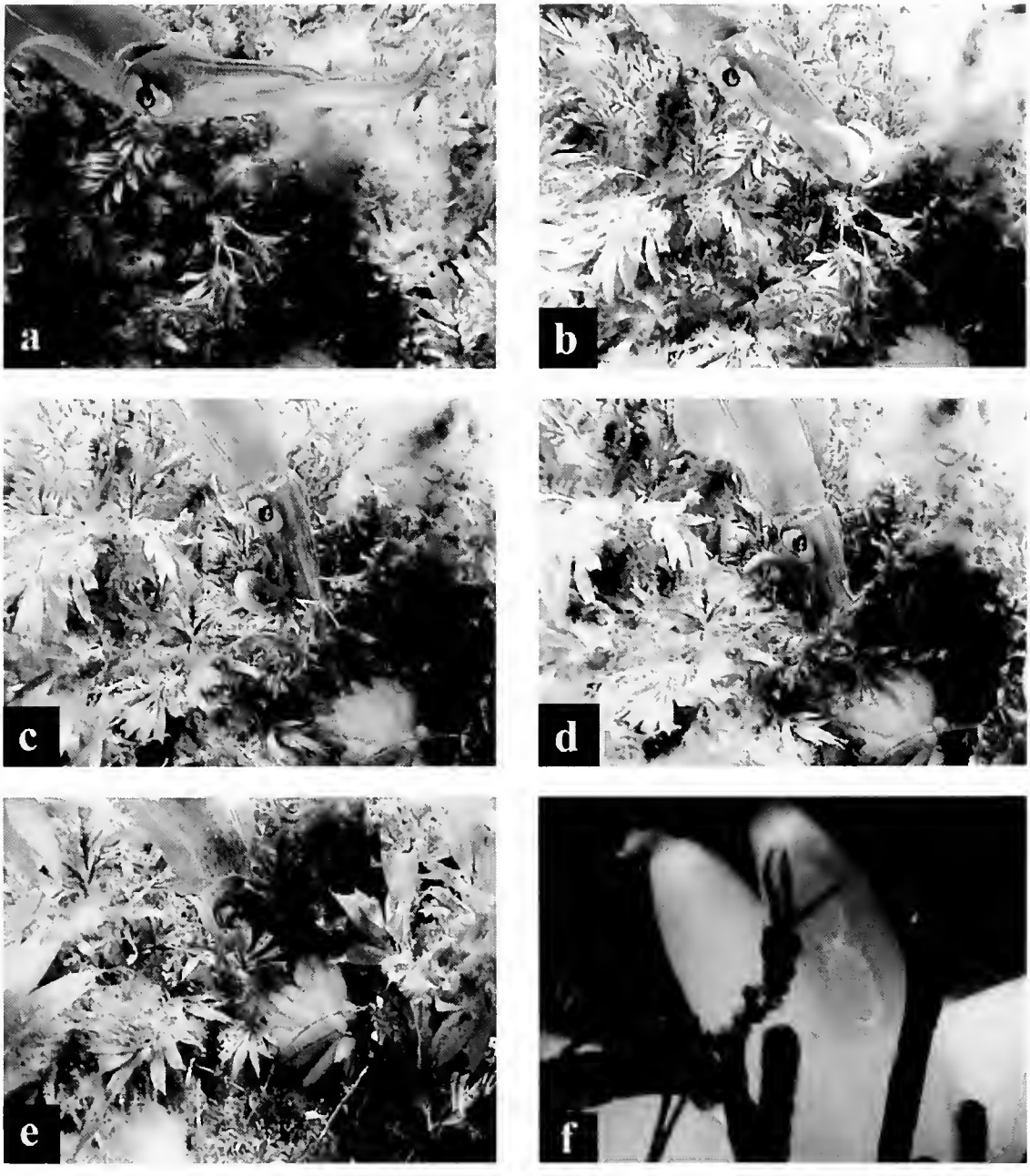

Figure 4. Sequence of "Egg deposition" behavior in *Sepioteuthis australis*. (a) After moving into a position over the egg cluster, the female moves forward towards the egg cluster and curls both tentacles back dorsally, with the suckers on the club facing out (b). Upon nearing the cluster, both tentacles then fold back laterally (c) so that the club of each tentacle is adjacent to each eye (d). The female then attaches a new egg capsule to the existing egg cluster (e). Total time elapsed = 3 s. Following deposition, egg capsules are translucent for a short time, and individual eggs (~ 10 mm long) are clearly visible until the capsule becomes opaque (f).

nents were rapid (27% within 2 s and 58% within 10 s, Fig. 8). Again, no significant difference in the duration of this interval was found among 10 females (one-way ANOVA, $F_{9,91} = 0.496$, $P > 0.05$), suggesting that the interval between successive "Peristaltic arm flare" components is similar between females.

Egg passing

"Egg passing" denotes the process by which female squid pass eggs and associated egg capsule material from within the mantle cavity into the arms in readiness for deposition. The beginning of "Egg passing" was defined when the

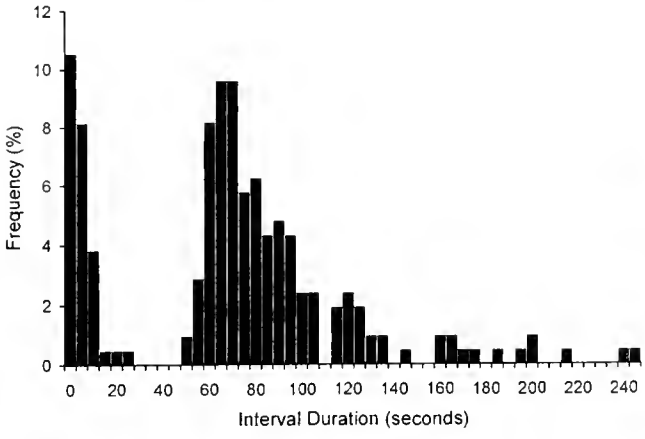

Figure 5. Frequency (%) of interval between the deposition of successive egg capsules in female *Sepioteuthis australis* (n = 209 durations).

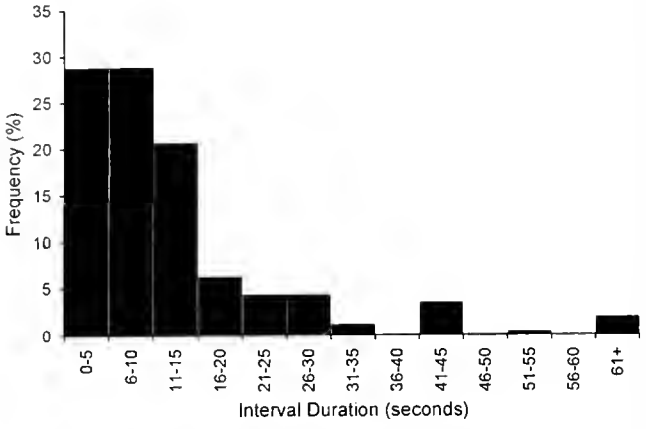

Figure 7. Frequency of observations of interval duration between conclusion of egg deposition and "Peristaltic arm flare" behavior in females of *Sepioteuthis australis* (n = 257 intervals).

funnel was directed upward toward the center of the ventral arm bases. A series of peristaltic movements passed through the funnel from the mantle toward the arms for, on average, 25.8 s (n = 22, SEM = 0.6 s). Throughout "Egg passing," the ventral arm bases extended to about double their normal size (Fig. 9). Within 5 s of the completion of "Egg passing," the ventral arm bases returned to the size observed prior to "Egg passing" behavior. Neither eggs nor egg capsule material was seen throughout "Egg passing," but following this behavior the arms of the female remained in a "Rigid arms" position until the egg capsule was deposited in the cluster.

The mean interval between the completion of "Egg passing" (the moment when the funnel resumed the "normal" position) and the beginning of egg deposition was 30.2 s (SEM = 4.5 n = 30 observations from 8 females). This duration did not differ significantly between females (one-way ANOVA, $F_{7,22} = 1.876$, $P > 0.05$), which agreed with our observations that this behavioral interval was consistent between females.

Male agonistic contests

The behavior of males throughout agonistic contests was consistent with the observations of Jantzen and Havenhand (2003b). Paired males spend considerable time positioning themselves between unpaired males (these attempting to displace paired males from their mate) and the paired female ("Parrying"). "Parrying" is considered to be the very early stages of agonistic contests between rival males and was not associated with any specific chromatic body pattern components. As these contests intensified, rival males began "Fin beating" (described as "swimming fight" in Jantzen and Havenhand, 2003b). "Fin beating" occurred when both males extended their arms and tentacles and collided while swimming backwards. At this time both males showed "Dark mantle" and "Iridescent sclera" chromatic body pattern components. "Fin beating" was quite forceful between males, and the collision of mantles and fins was intense. In

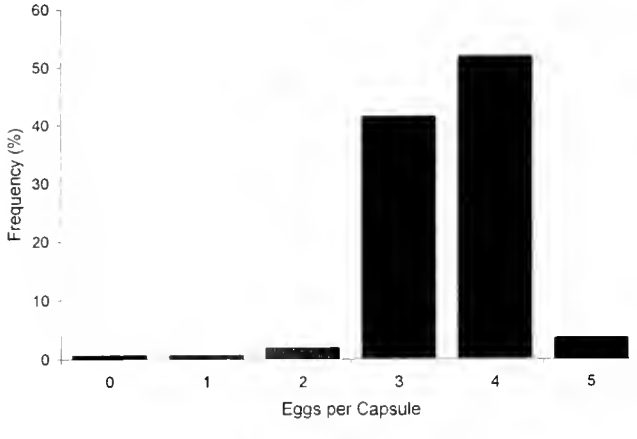

Figure 6. Frequency distribution (as a percentage) of egg number per capsule for *Sepioteuthis australis* (n = 300 capsules).

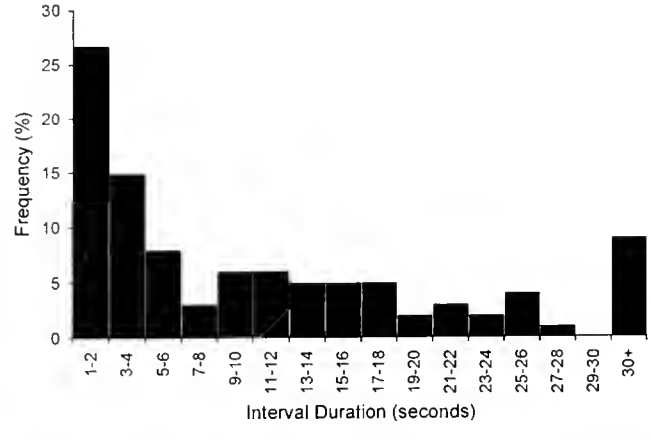

Figure 8. Frequency of observations of interval duration between successive "Peristaltic arm flare" behaviors occurring between successive egg depositions in females of *Sepioteuthis australis* (n = 101 intervals).

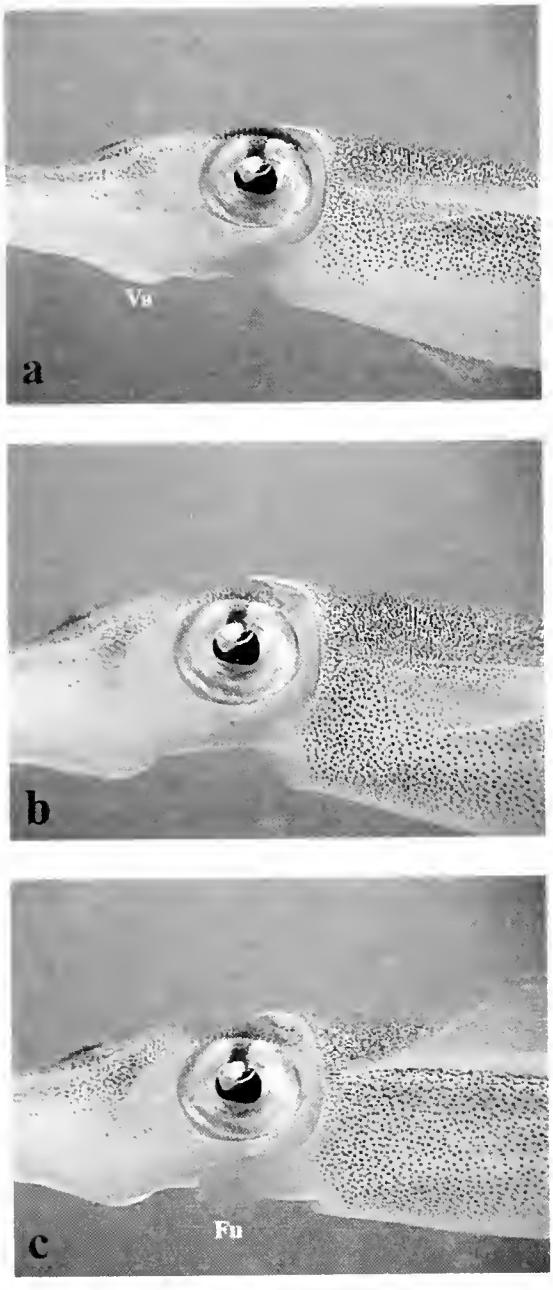

Figure 9. Three-frame sequence of "Egg passing" behavior in females of *Sepioteuthis australis*. Throughout "Egg passing," the ventral arm region (Va) becomes extended, and the funnel (Fu) is positioned flat against the underside of the head (immediately below the eyes; a). "Egg passing" is completed when the ventral arm region becomes substantially engorged (b), and the funnel moves back to the "normal" swimming position (c). Total time elapsed = 3 s.

all fights observed ($n = 67$), the paired male was "victorious" such that it remained paired with the female at the completion of the fight. The unpaired was always the "loser," eventually swimming away from the pair.

Paired males also "Charged" rival males that had approached the paired female. In all observations of "Charging" ($n = 7$), the paired male swam rapidly at the unpaired male, striking it with the tentacles while radially flaring all arms. This is an intense agonistic encounter by a paired male and appeared similar to that described for *L. pealeii* (King *et al.*, 1999) and *Loligo forbesi* (Porteiro *et al.*, 1990). Unpaired males always retreated following this contact.

Discussion

Mating behavior and sexual selection

About 67% of all observed mating attempts were made by paired males (Fig. 1). This indicates that paired males are able to out compete unpaired sneaker males for access to females and that paired mating has probably evolved as a more successful male mating tactic. Within paired males, three mating types were observed ("Male-upturned mating," "Head-to-head mating," and "Male-parallel mating"), with some males mating with a female in all three paired mating positions. Previously, no more than two mating positions had been reported by paired males within a single squid species (table 6.2 in Hanlon and Messenger, 1996). By far the most common paired mating type was "Male-upturned mating" (95.5% of paired mating attempts; 64% of total mating attempts), with "Head-to-head mating" (1.5% of paired, 1% of total), and "Male-parallel mating" (3% of paired, 2% of total) constituting considerably fewer mating attempts. This behavior contrasts with that of other species of squid such as *Loligo plei*, in which "Head-to-head mating" occurs before adults reach the spawning ground and "Male-parallel mating" occurs only when individuals have arrived at the spawning ground (Hanlon and Messenger, 1996). In *Sepioteuthis australis*, all three mating types were seen on the spawning ground (no data are available for possible mating behaviors prior to reaching the spawning grounds). This indicates that individual paired males of this species show considerable flexibility in mating positions. Importantly, there also appears to be flexibility in the placement of spermatophores by males. Spermatophores were most commonly deposited in the female buccal region, but they were occasionally found in the female's mantle or on her head, arms, or dorsal mantle; they may even have been placed directly onto egg capsules as they were deposited.

In addition to outcompeting smaller males, paired males may also increase their copulation frequency as a result of mating flexibility. Different mating strategies are possibly a response that allows an individual to select the most appropriate mating strategy for the surrounding environment (Patridge and Halliday, 1984). The environmental variables influencing the mating frequency of paired male squid are likely to include not only female receptivity but also sex ratio on the spawning ground, density of reproductively active individuals, number of "sneaker" males, and susceptibility to predation while mating (although only the latter of these factors has been quantified; Smale *et al.*, 2001). It is

reasonable to assume that mating positions have evolved to provide maximum chance of successful copulation while minimizing risk to the mating pair. We have no data relating to predation risk during copulation or the potential selective benefits of different mating types; however, it is noteworthy that "Male-upturned mating" was prevalent at low and high densities (2−45+ individuals in the spawning aggregation), as well as in the presence and absence of sneaker matings.

Thirty-three percent of mating attempts were by sneaker males. Like paired males, sneaker males also showed a degree of mating flexibility in that they attempted to mate in different locations (mostly at the egg cluster but occasionally away from it), in different mating positions ("Male-upturned" and "Male-parallel"), and showing different body patterns (*i.e.*, possible female mimicry). Sneaking behavior of unpaired males is widespread among cephalopods (Hanlon *et al.*, 1994, 1997, 1999b; Hanlon, 1996; Hall and Hanlon, 2002; Jantzen and Havenhand, 2003b); however, despite camouflage and mimicry behaviors being used by cephalopods (Hanlon and Messenger, 1996; Hanlon *et al.*, 1999a; Norman *et al.*, 1999, 2001), female mimicry by sneaker males has not been reported in squid and is known only in the giant cuttlefish *Sepia apama* (Norman *et al.*, 1999). Instances when sneaker males were observed to possibly mimic female behavior involved the chromatic signals "Dark mantle" followed by "Dorsal white stripe," "Golden epaulettes," and "Rigid arms" (these latter three components are characteristic signals of females copulating with paired males). The success of this apparent mimicry was evident from the observations ($n = 2$) that other males attempted to mate these males, and spermatophores were clearly seen being delivered to the recipient male. Given the low success rate of unpaired males in agonistic encounters with paired males (see below), it seems likely that this possible mimicry behavior has evolved so smaller males can approach paired females without instigating potentially harmful or costly agonistic contests with competing males.

It is central to sexual selection theory that differences in the reproductive success of individuals are caused by competition for mates (Andersson, 1982, 1994; Ryan, 1997). It must be remembered, however, that mating success in *S. australis* merely places spermatophores within the buccal region of the female—it does not necessarily result in successful fertilization. Females may mate with many males, and spermatophore longevity can be considerable (>2 weeks; Jantzen and Havenhand, unpubl. data). Consequently, female choice may play a vital role in dictating the fertilization success of sperm from different males.

The only behavior akin to direct female choice of spermatophores observed here was that in which females rejected a mating attempt by rapidly retreating ("Jetting" away). This behavior was seen only in simultaneous mating attempts of paired and sneaker males and not in (undisturbed) paired mating attempts. Consequently it seems likely that "Jetting" away was a female response to an attempted "Sneaker mating" (SM) by an unpaired male, rather than the specific rejection of a paired mating attempt. This female response to SM suggests that females are actively selecting paired males as preferred mates, which is a form of intrasexual selection (Wiley and Poston, 1996). This will add to the intense competition between males to form pair bonds with females. In systems where female choice is prevalent, sexual selection favors (among other factors) conspicuous behavioral male traits that allow males to out-compete other males (Andersson, 1982, 1994; Parker, 1984; Birkhead and Parker, 1997; Ryan 1997). It is therefore unsurprising to find intense agonistic contests between males to form pairs with females. Unlike female choice, these behavioral competitions between males for mates are a form of intersexual selection (Wiley and Poston, 1996).

In the squid *S. sepioidea*, a female actively accepts or rejects spermatophores placed on her arms or head (Moynihan and Rodaniche, 1982). Although we also saw spermatophore capsules on the head, arm, and dorsal mantle of females, all spermatophores seen transferred during paired matings were deposited into the buccal region. Therefore, it is likely that those spermatophores placed on the head, arms, and dorsal mantle of females resulted from mating attempts by sneaker males.

The relationship between spermatophore placement and fertilization success is very poorly understood for cephalopods in general. In *S. australis*, most SM attempts occurred while females deposited egg capsules in clusters, and any spermatophores deposited were placed on the female or directly onto the egg capsules. Paired mating attempts usually occurred prior to this egg deposition, and spermatophores were deposited primarily in the female buccal region. In squid, sperm must penetrate several millimeters of egg capsule matrix to fertilize eggs, and fertilization is thought to take place only after the egg capsule has been deposited (Arnold, 1971). Therefore, it is expected that the egg capsules from females that had been mated by two different males would routinely contain sperm from both matings, and these sperm would compete to fertilize the eggs (*sensu* Parker, 1970; Birkhead and Parker, 1997). Because sperm from paired matings contact egg capsules earlier (*i.e.*, when in the arms of the female) than those from sneaker matings (*i.e.*, during egg deposition), they have a longer exposure time to the egg capsule. Sperm contact time with eggs has been widely shown to increase fertilization success in sea urchins (*e.g.*, Vogel *et al.*, 1982; Levitan *et al.*, 1991); however, comparable effects have not been tested in cephalopods. It seems likely that, as a result of longer sperm egg contact times, fertilization success of paired matings will be higher than that of sneaker matings, but the extent to which sneaker mating results in successful fertilization in *S. australis* has not been established.

Analytical protocols to detect the paternity of *S. australis*

embryos have recently been developed, and preliminary analysis indicates that egg clusters contain eggs sired by more than one male (L. van Camp, Flinders University; unpubl. data). Similar analyses have yet to be conducted on individual egg capsules. Multiple paternity of eggs within capsules is common in the squid *Loligo pealeii* and *Loligo forbesi* (Shaw and Boyle, 1997; Buresch *et al.*, 2001), but details of the provenance of the males that sired the eggs (sneaker or paired) were not known. Comparable paternity investigation coupled with behavioral analysis similar to that conducted here should provide valuable information about the relative fertilization success of sneaker and paired males. *Sepioteuthis australis* could become a model species for this type of analysis because (1) the multiple mating strategies of males result in females regularly being copulated by more than one male throughout each spawning period; (2) scuba divers can stay close to reproductively active squid without altering their behavior; (3) the regular, short frequency of egg deposition (approximately every 70 s, Fig. 5) ensures that a large amount of data can be collected in a limited time; (4) the translucence of newly deposited egg capsules (Fig. 4f) means that each new capsule can be individually identified; and (5) the low number of eggs in each capsule (~4–5 compared to 100–300 for *Loligo;* Buresch *et al.*, 2001) simplifies the analysis.

Egg deposition and population discrimination

The egg deposition frequencies of *S. australis* from South Australia differed from those reported for other populations of the species and for related species. Deposition of successive egg capsules in a South Australian population of *S. australis* occurred with clear modes at 2.5 s and at 70 s (Fig. 5), whereas a New Zealand population was reported to deposit egg capsules at roughly 5-min intervals (Larcombe and Russell, 1971). Similar, longer intervals between deposition of successive egg capsules have been reported for *S. sepioidea* (2–3 min; Moynihan and Rodaniche, 1982). The very short modal intervals seen here (2.5 s, Fig. 5) are insufficient for "Egg passing" to occur between capsule depositions (requiring ~ 25 s; table 1 in Jantzen and Havenhand, 2003a). Due to the nature of our data (observational) and the egg deposition habitat (seagrass bed), we do not know whether females actually deposited two egg capsules in quick succession or whether, for some reason, they failed to deposit a capsule on the first attempt but did so soon afterwards on a second attempt. Certainly, "Egg passing" behavior did not appear to vary with egg deposition frequency. The causes of variability and plasticity in capsule deposition frequency are not fully understood (but see below); however, it is evident that even at the slower modal frequency seen here (70 s, Fig. 5), *S. australis* females would be capable of depositing well in excess of 50 egg capsules (~ 175 eggs) per hour.

Female body patterns during egg deposition also appeared to differ among different populations of *S. australis.* During egg deposition, females in South Australia folded only the tentacles back (all other arms remained in a "Rigid arms" position; Fig. 4), but females in New Zealand also folded the four lower arms down and back as they approached egg clusters (Larcombe and Russell, 1971). Larcombe and Russell (1971) also saw females pulsing a jet of water towards an egg cluster after egg deposition and interpreted this behavior as aiding in the hardening of the newly deposited capsule. "Peristaltic arm flare" was the only behavior akin to this that we observed. This behavior occurred within a few seconds of egg deposition (Fig. 6), but water was not specifically directed toward the egg clusters. Behaviors similar to "Peristaltic arm flare" have been reported in the cuttlefish *Sepia latimanus* (as "Puffing," Corner and Moore, 1980) to remove excess "latex-like" substance (= capsule matrix) from among the arms after egg deposition (Corner and Moore, 1980). It is highly likely that "Peristaltic arm flare" in *S. australis* has the same function; the behavior was observed shortly after egg deposition, and white matter was usually expelled from the arms at this time. However, it is also possible that "Peristaltic arm flare" removes spermatophores from the buccal area after fertilization of an egg capsule and before the next mating (providing another avenue for female sexual selection). The material expelled by the female in these "Peristaltic arm flare" behaviors was not analyzed, so we do not know whether it contained sperm/spermatophores or egg capsule matrix.

Investigation of the interval between successive "Peristaltic arm flare" behaviors, between egg deposition and "Peristaltic arm flare," and between "Egg passing" and egg deposition showed no significant differences among females (ANOVA, $P > 0.05$ in all cases, see Results). The consistency of these behaviors is surprising given the potential for variability, and it indicates that these behaviors may have evolved in response to strong selection pressures.

This study has focused on the interactions of *S. australis* on spawning grounds from South Australia and the implications of the observed behaviors for sexual selection. There is no comparable information on mating behaviors in *S. australis* populations from other regions. We have demonstrated differences in egg deposition characteristics between our data and those from geographically distinct populations in Tasmania and New Zealand. Recently, genetic and behavioral differences between populations of *S. lessoniana* from Japan have caused the classification of this species to be revised (Segawa *et al.*, 1993a, b; Izuka *et al.*, 1994, 1996a, b). Allozyme analysis of *S. australis* has already identified genetic divergence between geographically distinct populations (Triantafillos and Adams, 2001) but stopped short of suggesting that these are subspecies. Further genetic characterization, coupled with detailed behav-

ioral investigations such as those reported here should provide valuable insights, not only into the variability of reproductive behaviors and the potential for differences in sexual selection between populations, but also into the importance of those differences as mechanisms of speciation.

Acknowledgments

We are grateful to J. Doube, M. Gerner, A. Hirst, D. Keuskamp, L. Kupriyanova, B. Lock, A. Mack, G. Mack, M. Naud, and V. Weisbecker for helping with underwater activities, and to C. Turner for assistance with data recording and entry. We also thank P. Fairweather and L. van Camp for valuable comments and suggestions on this manuscript. Video equipment was obtained from Sea Optics Australia Pty. Ltd. This work was supported by an Australian Postgraduate Award Scholarship (to TMJ) and a grant from the Australian Research Council (to JNH).

Literature Cited

Andersson, M. B. 1982. Sexual selection, natural selection and quality advertisement. *Biol. J. Linn. Soc.* **17:** 375–393.

Andersson, M. B. 1994. *Sexual Selection.* Princeton University Press, Princeton, NJ.

Arnold, J. M. 1962. Mating behavior and social structure in *Loligo pealii*. *Biol. Bull.* **123:** 53–57.

Arnold, J. M. 1971. Cephalopods. Pp. 265–311 in *Experimental Embryology of Marine and Fresh-water Invertebrates*, G. Reverberi, ed. North-Holland Publishing, Amsterdam.

Birkhead, T. R., and G. A. Parker. 1997. Sperm competition and mating systems. Pp. 121–145 in *Behavioral Ecology: An Evolutionary Approach*, 4th ed. J. R. Krebs and N. B. Davies, eds. Blackwell Science, Oxford.

Boal, J. G., and S. A. Gonzalez. 1998. Social behaviour of individual oval squids (Cephalopoda, Teuthoidea, Loliginidae, *Sepioteuthis lessoniana*) within a captive school. *Ethology* **104:** 161–178.

Buresch, K. M., R. T. Hanlon, M. R. Maxwell, and S. Ring. 2001. Microsatellite DNA markers indicate a high frequency of multiple paternity within individual field-collected egg capsules of the squid *Loligo pealeii*. *Mar. Ecol. Prog. Ser.* **210:** 161–165.

Corner, B. D., and H. T. Moore. 1980. Field observations on the reproductive behavior of *Sepia latimanus*. *Micronesia* **16:** 235–260.

Drew, G. I. 1911. Sexual activities in the squid *Loligo pealii* (Les.). I. Copulation, egg laying, and fertilization. *J. Morphol.* **22:** 327–360.

Hall, K. C., and R. T. Hanlon. 2002. Principal features of the mating system of a large spawning aggregation of the giant Australian cuttlefish *Sepia apama* (Mollusca: Cephalopoda). *Mar. Biol.* **140:** 533–545.

Hanlon, R. T. 1988. Behavioral and body patterning characters useful in taxonomy and field identification of cephalopods. *Malacologia* **29:** 247–264.

Hanlon, R. T. 1996. Evolutionary games that squids play: fighting, courting, sneaking, and mating behaviors used for sexual selection in *Loligo pealei*. *Biol. Bull.* **191:** 309–310.

Hanlon, R. T., and J. B. Messenger. 1996. *Cephalopod Behaviour.* Cambridge University Press, Cambridge.

Hanlon, R. T., and M. R. Wolterding. 1989. Behavior, body patterning, growth and life history of *Octopus briareus* cultured in the laboratory. *Am. Malacol. Bull.* **7:** 21–45.

Hanlon, R. T., M. J. Smale, and W. H. H. Sauer. 1994. An ethogram of body patterning behavior in the squid *Loligo vulgaris reynaudii* on spawning grounds in South Africa. *Biol. Bull.* **187:** 363–372.

Hanlon, R. T., M. R. Maxwell, and N. Shashar. 1997. Behavioural dynamics that would lead to multiple paternity within egg capsules of the squid *Loligo pealei*. *Biol. Bull.* **193:** 212–214.

Hanlon, R. T., J. W. Forsythe, and D. E. Joneschild. 1999a. Crypsis, conspicuousness, mimicry and polyphenism as antipredator defences of foraging octopuses on Indo-Pacific coral reefs, with a method of quantifying crypsis from video tapes. *Biol. J. Linn. Soc.* **66:** 1–22.

Hanlon, R. T., M. R. Maxwell, N. Shashar, E. R. Loew, and K. L. Boyle. 1999b. An ethogram of body patterning behavior in the biomedically and commercially valuable squid *Loligo pealei* off Cape Cod, Massachusetts. *Biol. Bull.* **197:** 49–62.

Izuka, T., S. Segawa, T. Okutani, and K. Numachi. 1994. Evidence on the existence of three species in the oval squid *Sepioteuthis lessoniana* complex in Ishigaki Island, Okinawa, southwestern Japan, by isozyme analyses. *Venus Jpn. J. Malacol.* **53:** 217–228.

Izuka, T., S. Segawa, and T. Okutani. 1996a. Biochemical study of the population heterogeneity and distribution of the oval squid *Sepioteuthis lessoniana* complex in southwestern Japan. *Am. Malacol. Bull.* **12:** 129–135.

Izuka, T., S. Segawa, and T. Okutani. 1996b. Identification of three species in oval squid, *Sepioteuthis lessoniana* complex by chromatophore arrangements on the funnel. *Venus Jpn. J. Malacol.* **55:** 139–142.

Jantzen, T. M., and J. N. Havenhand. 2003a. Reproductive behavior in the squid *Sepioteuthis australis* from South Australia: ethogram of reproductive body patterns. *Biol. Bull.* **204:** 290–304.

Jantzen, T. M., and J. N. Havenhand. 2003b. Preliminary field observations of mating and spawning in the squid *Sepioteuthis australis*. *Bull. Mar. Sci.* **71:** 1073–1080.

King, A. J., S. A. Adamo, and R. T. Hanlon. 1999. Contact with squid egg capsules increases agonistic behavior in male squid (*Loligo pealei*). *Biol. Bull.* **197:** 256.

Larcombe, M. F., and B. C. Russell. 1971. Egg laying behaviour of the broad squid, *Sepioteuthis bilineata*. *N. Z. J. Mar. Freshwat. Res.* **5:** 3–11.

Levitan, D. R., M. A. Sewell, and F.-S. Chia. 1991. Kinetics of fertilization in the sea urchin *Strongylocentrotus franciscanus*: interaction of gamete dilution, age, and contact time. *Biol. Bull.* **181:** 371–378.

Mann, T., A. W. Martin, and J. B. Thiersch. 1966. Spermatophores and spermatophoric reaction of the giant octopus of the north Pacific, *Octopus dolfeini martini*. *Nature* **211:** 1279–1282.

Martin, P., and P. Bateson. 1993. *Measuring Behaviour: An Introductory Guide*, 2nd ed. Cambridge University Press, Cambridge.

Mather, J. A., and D. L. Mather. 1994. Skin colours and patterns of juvenile *Octopus vulgaris* (Mollusca, Cephalopoda) in Bermuda. *Vie Milieu* **44:** 267–272.

McGowan, J. A. 1954. Observations on the sexual behavior and spawning of the squid, *Loligo opalescens*, at La Jolla, California. *Calif. Fish Game* **40:** 47–54.

Moynihan, M., and A. F. Rodaniche. 1982. The behavior and natural history of the Caribbean reef squid *Sepioteuthis sepioidea*. With a consideration of social, signal, and defensive patterns for difficult and dangerous environments. *Adv. Ethol.* **25:** 1–151.

Norman, M. D., J. Finn, and T. Tregenza. 1999. Female impersonation as an alternative reproductive strategy in giant cuttlefish. *Proc. R. Soc. Lond. B* **266:** 1347–1349.

Norman, M. D., J. Finn, and T. Tregenza. 2001. Dynamic mimicry in an Indo-Malayan octopus. *Proc. R. Soc. Lond. B* **268:** 1755–1758.

Parker, G. A. 1970. Sperm competition and its evolutionary consequences in the insects. *Biol. Rev.* **45:** 535–567.

Parker, G. A. 1984. Sperm competition and the evolution of animal

mating strategies. Pp. 1–60 in *Sperm Competition and the Evolution of Animal Mating Systems*. R. L. Smith. ed. Academic Press, Orlando, FL.

Partridge, L., and T. Halliday. 1984. Mating patterns and mate choice. Pp. 222–250 in *Behavioural Ecology: an Evolutionary Approach*, 2nd ed. J. R. Krebs and N. B Davies, eds. Blackwell Scientific Publications, Oxford.

Porteiro, F. M., H. R. Martins, and R. T. Hanlon. 1990. Some observations on the behaviour of adult squids, *Loligo forbesi*, in captivity. *J. Mar. Biol. Assoc. UK* **70:** 459–472.

Roper, C. F. E., and G. L. Voss. 1983. Guidelines for taxonomic descriptions of cephalopod species. *Mem. Natl. Mus. Vic.* **44:** 48–63.

Ryan, M. J. 1997. Sexual selection and mate choice. Pp. 179–202 in *Behavioral Ecology: an Evolutionary Approach*, 4th ed. J. R. Krebs and N. B. Davies, eds. Blackwell Science, Oxford.

Segawa, S., S. Hirayama, and T. Okutani. 1993a. Is *Sepioteuthis lessoniana* in Okinawa a single species? Pp. 513–521 in *Recent Advances in Cephalopod Fisheries Biology*, T. Okutani, R. K. O'Dor, and T. Kubodera, eds. Tokai University Press, Tokyo.

Segawa, S., T. Izuka, T. Tamashiro, and T. Okutani. 1993b. A note on mating and egg deposition by *Sepioteuthis lessoniana* in Ishigaki Island, Okinawa, Southwestern Japan. *Venus Jap. J. Malacol.* **52:** 101–108.

Shaw, P. W., and P. R. Boyle. 1997. Multiple paternity within the brood of single females of *Loligo forbesi* (Cephalopoda: Loliginidae), demonstrated with microsatellite DNA markers. *Mar. Ecol. Prog. Ser.* **160:** 279–282.

Smale, M. J., W. H. H. Sauer, and M. J. Roberts. 2001. Behavioural interactions of predators and spawning chokka squid off South Africa: towards quantification. *Mar. Biol.* **139:** 1095–1105.

Triantafillos, L., and M. Adams. 2001. Allozyme analysis reveals a complex population structure in the southern calamary, *Sepioteuthis australis*, from Australia and New Zealand. *Mar. Ecol. Prog. Ser.* **212:** 193–209.

Vogel, H., G. Czihak, P. Chang, and W. Wolf. 1982. Fertilization kinetics of sea urchin eggs. *Math. Biosci.* **58:** 189–216.

Wiley, R. H., and J. Poston. 1996. Indirect mate choice, competition for mates, and coevolution of the sexes. *Evolution* **50:** 1371–1381.

Reference: *Biol. Bull.* **204:** 318–326. (June 2003)

Genetic Differences Within and Between Species of Deep-Sea Crabs (*Chaceon*) From the North Atlantic Ocean

JAMES R. WEINBERG[1,*], THOMAS G. DAHLGREN[2], NAN TROWBRIDGE[3], AND KENNETH M. HALANYCH[3,†]

[1]*National Marine Fisheries Service, 166 Water Street, Woods Hole, Massachusetts 02543;* [2]*Tjärnö Marine Biological Laboratory, 452 96 Strömstad, Sweden; and* [3]*Woods Hole Oceanographic Institution, Biology Department, Woods Hole, Massachusetts 02543*

Abstract. The deep-sea red crab *Chaceon quinquedens* is a commercially important crustacean on the Atlantic continental shelf and slope of North America. To assess genetic subdivision in *C. quinquedens*, we examined the nucleotide sequence of the mitochondrial 16S rDNA gene and the internal transcribed spacers (ITS) of the nuclear ribosomal repeat in samples from southern New England and the Gulf of Mexico. We compared those data to sequences from two congeners, a sympatric species from the Florida coast, *C. fenneri*, and an allopatric eastern Atlantic species, *C. affinis*. The 16S rDNA data consisted of 379 aligned nucleotides obtained from 37 individuals. The greatest genetic difference among geographical groups or nominal species was between *C. quinquedens* from southern New England and *C. quinquedens* from the Gulf of Mexico. Haplotypes from these two groups had a minimum of 10 differences. All 11 *C. fenneri* samples matched the most common haplotype found in *C. quinquedens* from the Gulf of Mexico, and this haplotype was not detected in *C. quinquedens* from southern New England. The three haplotypes of *C. affinis* were unique to that recognized species, but those haplotypes differed only slightly from those of *C. fenneri* and *C. quinquedens* from the Gulf of Mexico. Based on 16S rDNA and ITS data, genetic differences between *C. quinquedens* from southern New England and the Gulf of Mexico are large enough to conclude that these are different fishery stocks. Our results also indicate that the designation of morphological species within the commercially important genus *Chaceon* is not congruent with evolutionary history. The genetic similarity of *C. affinis* from the eastern Atlantic and *C. quinquedens* from the Gulf of Mexico suggests these trans-Atlantic taxa share a more recent common history than the two populations of "*C. quinquedens*" that we examined.

Received 8 October 2002; accepted 23 March 2003.

* To whom correspondence should be addressed. E-mail: James.Weinberg@noaa.gov

† Current address: Auburn University, Biological Sciences, Auburn, AL 36830.

Introduction

Many genetic studies of marine populations have been carried out along the Atlantic coast of North America to examine geographical divergence within and between species. Range limits of marine species often coincide with major landforms such as Cape Hatteras (Abbott, 1974; Briggs, 1974; Grosslein and Azarovitz, 1982; Theroux and Wigley, 1983) and the Florida Peninsula (Bert, 1986; Avise, 1992, 2000; Seyoum *et al.*, 2000). Ocean temperatures in the Cape Hatteras region can be stressful to subtropical and boreal species, and there are distinct current systems north and south of this location. In the area that is now Florida, episodes of glaciation during the Pleistocene produced major changes in temperature and sea level, which may have separated populations in the Atlantic Ocean from those in the Gulf of Mexico. Most of the marine biogeographic and genetic studies have focused on species from the intertidal zone and inner continental shelf, where terrestrial and atmospheric effects have a relatively large impact on the marine environment. In the deep sea, however, other environmental factors are likely to control species distributions (Haedrich *et al.*, 1980; Blake and Grassle, 1994; Rhoads and Hecker, 1994; Grassle, 1995).

Geryonids are a commercially important, cosmopolitan family of marine crabs typically found in mud, sand, and gravel habitats at depths of 200–1200 m (Hastie, 1995). In this study we have examined the population genetic structure of the deep-sea red crab *Chaceon quinquedens* Smith 1879 (Geryonidae). This species occurs on the outer continental shelf and slope of the western Atlantic Ocean, from the Scotian Shelf off Canada, to the Gulf of Mexico (Haefner and Musick, 1974; Williams and Wigley, 1977; Serchuk and Wigley, 1982; Erdman, 1990). *C. quinquedens* is harvested in Canada (Lawton and Duggan, 1998), in New England (Steimle *et al.*, 2001), and in the southeastern United States (Waller *et al.*, 1995).

Little information about population genetic structure in *C. quinquedens* is available to guide fishery management (Diehl and Biesiot, 1994; Waller *et al.*, 1995). To assess genetic subdivision in *C. quinquedens*, we examined the nucleotide sequence of the mitochondrial 16S rDNA gene and the internal transcribed spacers (ITS) of the nuclear ribosomal repeat. Both 16S rDNA (*e.g.*, Ó Foighil and Jozefowicz, 1999; Schubart *et al.*, 2000; Dahlgren *et al.*, 2001) and ITS (*e.g.*, Fritz *et al.*, 1994; Conole *et al.*, 2001) have been used to differentiate between closely related species and to evaluate intraspecific variation.

To provide a broad phylogeographic perspective, we compared sequence data from *C. quinquedens* with data from two congeners: *C. fenneri* Manning and Holthuis 1984, and an eastern Atlantic species, *C. affinis* Milne-Edwards and Bouvier 1894. *C. fenneri*, the golden crab, is distributed from Cape Hatteras to the Gulf of Mexico (Manning and Holthuis, 1984; Erdman, 1990). *C. quinquedens* and *C. fenneri* are the only two *Chaceon* species described from the Atlantic coast of North America. Their ranges overlap in the southeastern United States (Erdman, 1990; Diehl and Biesiot, 1994), and in the Gulf of Mexico they are segregated by depth, with *C. fenneri* occurring at depths of 300–500 m and *C. quinquedens* at 680 m or greater (Erdman, 1990). *C. affinis*, which occurs at 500–1200 m from the Cape Verde archipelago to Iceland, is allopatric with *C. quinquedens* and *C. fenneri* (Manning and Holthuis, 1981; Hastie, 1995; Pinho *et al.*, 2001; López Abellán *et al.*, 2002).

Study Organism

Manning and Holthuis (1989) revised the taxonomy of geryonid crabs and moved most of the species in the genus *Geryon*, including *G. quinquedens*, into a new genus, *Chaceon*. *C. quinquedens* was first described from specimens collected in the Gulf of Maine (Smith, 1879). *C. quinquedens* reaches a maximum size of about 115–130 mm in carapace width (CW), males grow larger than females, and size at maturity for females is about 70 to 80 mm CW (Wigley *et al.*, 1975; Haefner, 1977; Elner *et al.*, 1987). On the basis of molting frequency (Lux *et al.*, 1982), adult females probably do not mate every year. After mating, females carry fertilized eggs on their pleopods for up to 9 months until the larvae are released (Haefner, 1977, 1978). Brood sizes range from 160,000 to 270,000 eggs, and fecundity increases with female body size (Hines, 1988). Depending on water temperature, *C. quinquedens* larvae may remain planktonic for up to 4 months before settlement (Perkins, 1972; Sulkin and Van Heukelem, 1980; Kelly *et al.*, 1982).

Geryonid growth rates are lower than those of families of shallow-water crabs (Hastie, 1995). Complete growth curves are not available for *C. quinquedens*, although tagging studies (Lux *et al.*, 1982) indicate that the intermolt period of adults can last as long as 7 years. After studying the growth of juvenile crabs in the laboratory, Van Heukelem *et al.* (1983) projected that *C. quinquedens* could attain a carapace width of 114 mm by age 6 years.

Female and male geryonids tend to segregate by depth (Wigley *et al.*, 1975; Haefner and Musick, 1974; Haefner, 1978; Melville-Smith, 1987), but migration patterns during mating have not been described. Wigley *et al.* (1975) hypothesized that *C. quinquedens* larvae settle to the bottom in deep water and then migrate up the continental slope, where they may obtain more food and grow more rapidly. Tagging studies by Lux *et al.* (1982) and Melville-Smith (1987) showed that adult geryonids travel along and across bathymetric lines. Returns of tagged adult *C. quinquedens* over a 7-year period indicate that most recaptures occurred within 20 km of the release location. Principal movements were along the slope; shorter movements of about 6 km were observed up and down the slope, with depth changes of as much as 500 m (Lux *et al.*, 1982).

Materials and Methods

The *Chaceon quinquedens* and *C. fenneri* specimens used in the 16S genetic study were collected from the Atlantic Ocean with traps or otter trawls (Table 1). The 13 *C. quinquedens* that were analyzed from southern New England were collected during a National Marine Fisheries Service survey in May 2001 and were obtained from eight tows made in the vicinity of Veatch and Atlantis Canyons, at depths of 465–931 m. The 10 specimens of *C. quinquedens* that were analyzed from the Gulf of Mexico were collected in August 1995 from 951 m. The 11 specimens of the golden crab (*C. fenneri*) that were analyzed from the Atlantic coast of Florida were collected in January 2002 from 335 m. The 16S rDNA data sets from all three sets of samples included both males and females. Three sequences of *C. affinis*, from the eastern Atlantic (Madeira Islands and Canary Islands), were also available in GenBank from analyses by J. Bautista and Y. Alvarez. Thus, a total of 37 individuals were represented in the 16S data (see Appendix

Table 1

Chaceon quinquedens, C. affinis, *and* C. fenneri: *distribution of 16S rDNA haplotypes*

	Sample Locations by Species					
Haplotype	Southern New England *C. quinquedens*	Gulf of Mexico *C. quinquedens*	Atlantic Florida *C. fenneri*	Eastern Atlantic *C. affinis*	Total	GenBank Accession #
AFI				1	1	AF100914
AFII				1	1	AF100915
AFIII				1	1	AF100916
A		1			1	AY122641
B		1			1	AY122642
C		1			1	AY122643
D		7	11		18	AY122644
E	9				9	AY122645
F	4				4	AY122646
Sample Size	13	10	11	3	37	

For each haplotype, the number of individuals analyzed is given by locality. The name Eastern Atlantic refers to the Madeira and Canary Islands.

for additional collection details). For all samples, tissue was either frozen immediately or placed in 80% ethanol. Total genomic DNA was extracted using the Qiagen DNA easy tissue kit (Valencia, CA) following manufacturer's protocols.

A fragment of the mitochondrial 16S rDNA gene was amplified using standard PCR protocols. Originally, the Palumbi (1996) 16S rDNA primers (16Sar and 16Sbr) were used. Due to variability in PCR and sequencing results, a new 3′ primer was designed (16Sbr.crab: 5′-TAA TTC AAC ATC GAG GTC GC-3′). One of two sets of cycling parameters was used: an initial denaturation at 94 °C for 2 min, 30× (94 °C for 30 s, 55 °C for 30 s, 72 °C for 45 s), and a final extension at 72 °C for 7 min; alternatively, the amplification phase was 35× (94 °C for 20 s, 55 °C for 20 s, 72 °C for 30 s). PCR products were cleaned with the Qiagen PCR cleanup kit (Valencia, CA). The same primers were used in sequencing, following procedures in the Big Dye cycle sequencing kit (ABI, Foster City, CA), except that reactions were 50% Big Dye concentration in 50% volume. After the excess Dye terminators were removed with Sephadex, the reactions were run on an ABI Prism 377 automated sequencer, with samples sequenced in both directions.

Standard laboratory protocols (*e.g.*, sterile technique and negative controls) were employed to avoid contamination between samples. Because the samples of *C. quinquedens* from the Gulf of Mexico were genetically similar to those of *C. fenneri*, *C. fenneri* DNA was re-extracted and amplified from representatives to verify the results. In all cases, the re-extracted sequences matched the originals.

We also explored the internal transcribed spacer (ITS) regions of the nuclear ribosomal genes. The ITS regions of *C. quinquedens* were screened in 5 crabs from southern New England and in 10 crabs from the Gulf of Mexico. A 1376 base pair (bp) fragment was amplified using universal primers in the flanking 18S and 28S regions (ITS4 and ITS5; White *et al.*, 1990). For sequencing, we used an additional pair of primers located in the 5.8S region (5.8Sc and 5:8Sd; Hillis and Dixon, 1991). PCR and sequencing protocols were as described above, except the PCR annealing temperature was between 55 and 57 °C. We report clean single-read sequences from the two *C. quinquedens* populations (total 15 crabs) for the ITS2 region. When ITS primers were used on *C. fenneri*, we recovered multiple products, which would typically require cloning PCR products, sequencing multiple products per individual, and performing analyses that can handle multiple alleles from one individual. For these reasons, we focused our efforts on the 16S data, which were easier to collect and analyze. However, we still report the ITS data because they are relevant.

The sequence data were aligned with Clustal X (Thompson *et al.*, 1997) and proofread by eye. Two computer programs, PAUP 4.0b10 (Swofford, 2002) and MacClade version 4.0 (Maddison and Maddison, 2000), were used in the analyses. Because the results were unambiguous and involved a limited number of nucleotide substitutions, we present results only from a parsimony network analysis (*sensu* Avise *et al.*, 1979). Other analyses, including an exhaustive parsimony phylogenetic analysis, a neighbor-joining analysis using a general-time-reversible model, and maximum-likelihood analysis using a general-time-reversible model all yielded the same topology, and were entirely consistent with the parsimony network. Indels were counted as characters (not missing data) in the parsimony analyses.

Results

The 16S rDNA data consisted of 379 aligned nucleotides. Variation was observed at 17 sites, and 12 of these were

parsimony informative (Table 2). Each unique combination of nucleotides was considered a distinct haplotype. Only three indels were observed, of which two were associated with extra bases in the *Chaceon affinis* sequences. Table 1 shows the distribution, occurrence, and GenBank accession number of each 16S haplotype observed in this study. The aligned data set was deposited in TreeBASE (http://www.treebase.org/treebase/ accession number-SN1246).

Two 16S haplotypes were detected in the southern New England samples of *C. quinquedens*, four in the Gulf of Mexico samples of *C. quinquedens*, and only one in the *C. fenneri* samples from the Atlantic coast of Florida. The *C. affinis* data consisted of three haplotypes (Table 1). The parsimony network (Fig. 1) illustrates the phylogenetic relationships among the nine known haplotypes of *Chaceon*. Position 321 is homoplastic, occurring twice on the network. The largest genetic break observed among geographical groups or nominal species was between *C. quinquedens* from southern New England and *C. quinquedens* from the Gulf of Mexico. Haplotypes from these two groups had a minimum of 10 differences. All 11 *C. fenneri* samples matched the most common haplotype found in the *C. quinquedens* samples from the Gulf of Mexico (haplotype D). However, haplotype D was not detected in *C. quinquedens* samples from southern New England. The three haplotypes of *C. affinis* were unique to that species, although these were very similar to haplotype D, with a maximum of three differences.

The ITS data also show a genetic difference between the two *C. quinquedens* populations. Two ITS2 genotypes were identified (Fig. 2), distinguished by an indel in a microsatellite region close to the 3′ end. The $(AAGG)_4$ allele was shared by all five southern New England specimens, whereas the $(AAGG)_5$ allele was found among all 10 Gulf of Mexico specimens. In addition to the repeat, a single nucleotide difference (A-T at position 1239) further distinguishes the two populations. ITS data can be found under GenBank accession numbers AY123199-AY123200.

Discussion

We detected genetic subdivision between *Chaceon quinquedens* from the New England region of the Atlantic Ocean and *C. quinquedens* from the Gulf of Mexico by using sequence data from two genetic loci (16S and ITS). In addition, we found little or no genetic difference (16S data) between *C. quinquedens* from the Gulf of Mexico, *C. fenneri* from Eastern Florida, and *C. affinis* from the Eastern Atlantic. These results suggest that the designation of morphological species within the commercially important genus *Chaceon* is not congruent with evolutionary history. Furthermore, the genetic similarity of *C. affinis* and Gulf of Mexico *C. quinquedens* suggests these trans-Atlantic taxa share a more recent common history than the two populations of "*C. quinquedens*" that we examined. This is the first examination of large-scale genetic subdivision in *C. quinquedens*, and one of the few to genetically characterize a deep-sea organism (*e.g.*, Doyle, 1972; France and Kocher, 1996; Quattro *et al.*, 2001) not at hydrothermal vents. As such, it provides an interesting comparison to intertidal organisms upon which most of our understanding of marine phylogeography is based.

Management of the *Chaceon quinquedens* fishery began recently in the United States (Steimle *et al.*, 2001), and Cape Hatteras was designated as the dividing point between a northern and southern stock. Our genetic results lend support for managing this fishery as separate stocks. However, additional research will be required to more accurately determine stock boundaries. The genetic differences we detected probably reflect genetic drift during long periods of isolation. Minimal gene flow between these locations could have been caused by low rates of dispersal of adults between regions and by retention of larvae within regions. For intertidal organisms, at least three faunal breakpoints are known along the east coast of North America: Cape Cod, Cape Hatteras, and near Cape Canaveral. These coastal features serve as both species-range boundaries and genetic

Table 2

List of 17 variable positions in 9 haplotypes from samples of Chaceon

	10	30	89	98	104	123	196	219	220	222	275	292	302	321	323	324	379
AFI	G	C	T	G	C	G	C	G	C	T	G	C	—	T	G	C	C
AFII	.	.	.	—	.	.	.	.	.	.	.	.	—	.	.	T	.
AFIII	.	.	.	—	.	.	.	.	.	.	.	.	G	.	.	T	.
A	.	.	.	—	.	.	T	.	.	.	.	.	—	—	.	T	.
B	.	.	.	—	.	A	T	.	T	.	.	.	—	.	.	T	.
C	.	.	C	—	.	.	T	.	.	.	.	.	—	.	.	T	.
D	.	.	.	—	.	.	T	.	.	.	.	.	—	.	.	T	.
E	A	T	.	—	T	.	T	A	T	A	A	T	—	.	A	T	T
F	A	T	.	—	T	.	T	A	T	A	A	T	—	—	A	T	T

Numbers refer to positions along the 379 base pair 16S rDNA alignment. "." refers to an identical base, and "—" refers to an indel.

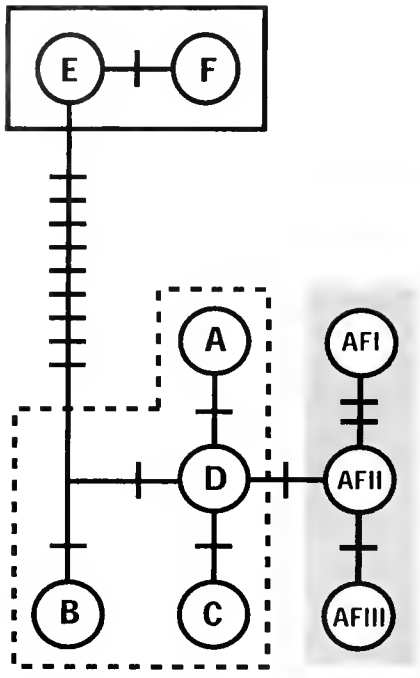

Figure 1. Parsimony network of 16S haplotypes for *Chaceon quinquedens*, *C. fenneri*, and *C. affinis*. Lines crossing branches represent inferred nucleotide substitutions, and thus, the minimum observed number of nucleotide differences between haplotypes. The solid line, dashed line, and shaded area around certain haplotypes indicate three geographical regions: southern New England, Atlantic coast of Florida-Gulf of Mexico, and eastern Atlantic specimens, respectively. Note, 16S position 321 is homoplastic and is represented on the network twice (between A and D, and E and F).

barriers to gene flow (Franz and Merrill, 1980a, b; Avise, 1992, 2000; Bert, 1986; Collin 2001; but see McMillen-Jackson *et al.*, 1994). A recent study by Collin (2001) is the only molecular investigation to date with adequate sampling across all three breakpoints (but see Avise, 1992, 2000). Her results are similar to ours: she found that two traditionally recognized species of the gastropod *Crepidula* show significant genetic subdivision between New England and the Gulf of Mexico. Because our sampling was limited, we cannot distinguish how the three known breakpoints contributed to the large genetic difference we observed. Alternatively, the observed divergence could represent variation at the two ends of a cline. We are currently trying to obtain samples along the North American east coast to address these issues.

Observing at least 10 nucleotide substitutions between New England and the Gulf of Mexico in a gene as conserved as the 16S was surprising. Although no lineage-specific calibration for substitution rates has been determined for geryonid crab 16S data, grapsid crabs have been shown to have a rate of 0.65% per MY (Schubart *et al.*, 1998). Differences in mtDNA sequences between geminate marine invertebrate taxa on the two sides of the Isthmus of Panama suggest that sequence divergence is in the range of 1%–4% per MY (Bermingham and Lessios, 1993; Knowlton *et al.*, 1993). If one assumes that the *Chaceon* rate is between 0.5% and 2% per MY, then the New England and Gulf of Mexico populations have been separated for 0.7–2.9 MY (rate homogeneity test not significantly rejected), placing their separation during the Pleistocene or Pliocene. Their genetic isolation may have arisen in association with fluctuating sea level due to glaciation events. However, without additional sampling to understand where genetic breaks occur, determining the exact mechanism or mechanisms of genetic isolation is not possible.

Based on the finding of only a single substitution separating *C. affinis* from *Chaceon* in the Gulf of Mexico, we conclude that there has been very recent gene exchange with the Old World at subtropical/tropical latitudes. Although adult *C. quinquedens* do not migrate extensively (Lux *et al.*, 1982), the larvae have the potential to disperse great distances because they can spend up to 4 months in the plankton (Perkins, 1972; Sulkin and Van Heukelem, 1980; Kelly *et al.*, 1982). Our sample of *C. affinis* was admittedly limited, and given the cryptic morphology of *Chaceon*, we do not assume that three individuals from the Canary Islands are a representative sample of *C. affinis* throughout its extensive range, reported to extend as far north as Iceland (Manning and Holthuis, 1981; Hastie, 1995; Pinho *et al.*, 2001; López Abellán *et al.*, 2002). Nonetheless, our data provide evidence that this species from the continental shelf

C. quinquedens ITS 2

```
Southern New England: CAAAACGAAGGAAGGAAGGAAGG----GACCGAGACTAAAC

Gulf of Mexico:       CAAAACGAAGGAAGGAAGGAAGGAAGGGACCGAGACTAAAC
```

Figure 2. A partial alignment of ITS2 (positions 1263-1303) in *Chaceon quinquedens*, showing the fixed variation in a microsatellite repeat (AAGG) distinguishing between five southern New England samples and 10 Gulf of Mexico samples. The exact position of the indel could be at any of the five (AAGG) sites.

and slope has experienced transatlantic interchange at lower latitudes, suggesting that North Atlantic biogeography may be more complicated than previously assumed (also see Dahlgren *et al.*, 2000). This finding is in contrast to the widely studied situation of genetic interchange of North Atlantic boreal intertidal organisms at high latitudes (reviewed in Cunningham and Collins, 1998).

Two recognized *Chaceon* species around Florida showed no genetic differentiation even though previous studies have reported various ecological differences between *C. quinquedens* and *C. fenneri*. In the Gulf of Mexico, these two species are segregated by depth, and *C. fenneri* oviposits 3 months later in the year (Erdman, 1990). *C. quinquedens* in southern New England produces larger eggs than *C. fenneri* does in the Gulf of Mexico (Hines, 1988). Given these interspecific differences, we did not expect to find more genetic differences between the two *C. quinquedens* populations than between *C. quinquedens* from the Gulf of Mexico, *C. fenneri*, and *C. affinis*. Several explanations of the genetic similarity between these recognized species are possible, including incomplete lineage sorting, ongoing gene flow, or recent hybridization followed by a mitochondrial sweep (Skibinski *et al.*, 1999). If these lineages diverged recently (which would be consistent with morphology; see below), then the shared haplotype ("D" in *C. fenneri* and Gulf of Mexico *C. quinquedens*) might reflect incomplete sorting of mitochondrial lineages (Hoelzer *et al.*, 1999). Alternatively, the slight differences observed in these three lineages may simply represent within-population variation or environmentally induced variation. For example, *C. fenneri* and *C. quinquedens* from the Gulf of Mexico are geographically sympatric but inhabit different depth zones, which may expose them to different environmental factors. To assess the level of ongoing gene flow between these nominal species, it would be necessary to examine more rapidly evolving molecular markers, such as microsatellites. Lastly, the similarity in the 16S gene of these taxa could be due to hybridization followed by a mitochondrial gene sweep (Skibinski *et al.*, 1999). Studies of hybridization between *Chaceon* species have not been conducted, but hybridization occurs in xanthid crabs in the Gulf of Mexico-Florida region (Bert, 1986; Bert and Harrison, 1988).

Chaceon morphology is consistent with a hypothesis of recent speciation. Due to their similar phenotypes, *C. quinquedens*, *C. fenneri*, *C. affinis*, and even a commercial South African species, *C. maritae* Manning and Holthuis 1981, have been confused in the literature. For example, *C. maritae* was called *C. quinquedens* until 1981 (Manning and Holthuis, 1981; Melville-Smith, 1989). *C. fenneri* was identified as *C. quinquedens* by Rathbun (1937), and later as *C. affinis* by Chace (1940). Manning and Holthuis (1984) eventually described *C. fenneri* as a new species. *C. quinquedens* was reported from the coasts of South America (Rathbun, 1937) and South Africa, but subsequent taxonomic work determined that those crabs were undescribed *Chaceon* species (Manning and Holthuis, 1988; Manning *et al.*, 1989). As in some other crab genera (Schubart *et al.*, 2001a), phenotypic characters used to distinguish among *Chaceon* species are somewhat ambiguous. These characters, which include carapace shape and color, sizes of spines, and shape of the dactyli of the walking legs (Manning and Holthuis, 1984, 1989) are mostly morphometric. Definitive apomorphies are lacking.

Given their phenotypic similarity, it is not surprising that *C. quinquedens*, *C. fenneri*, and *C. affinis* have similar genotypes. The present taxonomic classification of these species, based on phenotypic characters, is not consistent with our genetic results, because we found greater differences between populations of one species than between recognized species. Even though the common names of these species are based on carapace color (*e.g.*, red crab, golden crab), carapace color is not a reliable character for identifying species of *Chaceon*. For example, one of the specimens we genotyped from southern New England had a rare yellowish-tan carapace, which made us think that it might be a golden crab (*C. fenneri*); the *Chaceon* from southern New England are typically deep red to orange in color. The unusual yellowish-tan crab had haplotype F, which is a common haplotype in the southern New England red crab (*C. quinquedens*) population. We should note that the type locality of *C. quinquedens* is from the Gulf of Maine, indicating that if changes are to be made, the Gulf of Mexico individuals should be renamed. Before this can be done, we need a more complete understanding of the morphological and genetic variation along the North American coast.

Similar discrepancies between morphological and molecular genetic data have been noted in other crab species (Schubart *et al.*, 2001a, 2001b). In a study of *Callinectes* spp. in Venezuela, Schubart *et al.* (2001a) found that *C. bocourti* Milne Edwards 1879 and *C. maracaiboensis* Taissoun 1969 had no diagnostic molecular characters to distinguish their 16S mtDNA sequences. After considering the genetic and morphological data on those species, Schubart *et al.* (2001a) concluded that one of the species should be reclassified as a junior synonym of the other, rather than considering them as different species. Another study found a lack of genetic variation between two *Brachynotus* species (Schubart *et al.*, 2001b), and concluded that additional work on reproductive isolation, genetic sequences, and morphology is needed to assess whether these are distinct species. Such examples emphasize the need for more information about the morphological and genetic variations that delimit the boundaries between many marine taxa, including *Chaceon*.

Acknowledgments

We are very grateful to P. Biesiot, H. Perry, P. Brown-Eyo, R. Nielson, D. Harper, C. Keith, and Captain H. Franco and the crew of the *F/V Mary K* for their valuable assistance in collecting new samples or for sharing their older collections. We appreciate contributions from A. Govindarajan and F. Serchuk related to manuscript preparation or data collection. The 16S sequences of *Chaceon affinis* were deposited in GenBank by J. Bautista and Y. Alvarez. This research was supported in part by funds from C. Tryggers Stiftelse to TGD, and from NSF and the Ocean Life Institute at WHOI to KMH. This work is WHOI contribution number 10865.

Literature Cited

Abbott, R. T. 1974. *American Seashells.* Van Nostrand Reinhold, New York.

Avise, J. C. 1992. Molecular population structure and the biogeographic history of a regional fauna: a case history with lessons for conservation biology. *Oikos* **63:** 62–76.

Avise, J. C. 2000. *Phylogeography, the History and Formation of Species,* Harvard Univ. Press, Cambridge, MA.

Avise, J. C., R. A. Lansman, and R. O. Shade. 1979. The use of restriction endonucleases to measure mitochondrial DNA sequence relatedness in natural populations. I. Population structure and evolution in the genus *Peromyscus. Genetics* **92:** 279–295.

Bermingham, E., and H. Lessios. 1993. Rate variation of protein and mtDNA evolution as revealed by sea urchins separated by the Isthmus of Panama. *Proc. Natl. Acad. Sci. USA* **90:** 2734–2738.

Bert, T. M. 1986. Speciation in western Atlantic stone crabs (genus *Menippe*): the role of geological processes and climatic events in the formation and distribution of species. *Mar. Biol.* **93:** 157–170.

Bert, T. M., and R. G. Harrison. 1988. Hybridization in western Atlantic stone crabs (genus *Menippe*): evolutionary history and ecological context influence species interactions. *Evolution* **42:** 528–544.

Blake, J. A., and J. F. Grassle. 1994. Benthic community structure on the U.S. Atlantic slope off the Carolinas: spatial heterogeneity in a current dominated system. *Deep-Sea Res.* **41:** 835–874.

Briggs, J. C. 1974. *Marine Zoogeography.* McGraw Hill, New York.

Chace, F. A., Jr. 1940. The brachyuran crabs. Reports on the scientific results of the *Atlantis* expeditions to the West Indies, under the joint auspices of the University of Havana and Harvard University. *Torreia* **4:** 1–67.

Collin, R., 2001. The effects of mode of development on phylogeography and population structure of North Atlantic *Crepidula* (Gastropoda: Calyptraeidae). *Mol. Ecol.* **10:** 2249–2262.

Conole, J., N. B. Chilton, T. Jarvis, and R. B. Gasser. 2001. Mutation scanning analysis of microsatellite variability in the second internal transcribed spacer (precursor ribosomal RNA) for three species of *Metastrongylus* (Strongylida: Metastrongyloidea). *Parasitology* **122:** 195–206.

Cunningham, C. W., and T. M. Collins. 1998. Beyond area relationships: extinction and recolonization in molecular marine biogeography. Pp. 297–321 in *Molecular Approaches to Ecology and Evolution,* R. DeSalle and B. Schierwater, eds. Birkhäuser Verlag, Basel.

Dahlgren, T. G., J. R. Weinberg, and K. M. Halanych. 2000. Phylogeography of the ocean quahog (*Arctica islandica*): influences of paleoclimate on genetic diversity and species range. *Mar. Biol.* **137:** 487–495.

Dahlgren, T. G., B. Åkesson, C. Schander, K. M. Halanych, and P. Sundberg. 2001. Molecular phylogeny of the model annelid *Ophryotrocha. Biol. Bull.* **201:** 193–203.

Diehl, W. J., and P. M. Biesiot. 1994. Relationships between multilocus heterozygosity and morphometric indices in a population of the deep-sea red crab *Chaceon quinquedens* (Smith). *J. Exp. Mar. Biol. Ecol.* **182:** 237–250.

Doyle, R. W. 1972. Genetic variation in *Ophiomusium lymani* (Echinodermata) populations in the deep sea. *Deep-Sea Res.* **19:** 661–664.

Elner, R. W., S. Koshio, and G. V. Hurley. 1987. Mating behavior of the deep-sea red crab, *Geryon quinquedens* Smith (Decapoda, Brachyura, Geryonidae). *Crustaceana* **52:** 194–201.

Erdman, R. B. 1990. Reproductive ecology and distribution of deep-sea crabs (Family Geryonidae) from southeast Florida and the eastern Gulf of Mexico. Ph.D. dissertation. University of South Florida. 147 pp.

France, S. C., and T. D. Kocher. 1996. Geographic and bathymetric patterns of mitochondrial 16S rRNA sequence divergence among deep-sea amphipods, *Eurythenes gryllus. Mar. Biol.* **126:** 633–645.

Franz, D. R., and A. S. Merrill. 1980a. Molluscan distribution patterns on the continental shelf of the Middle Atlantic Bight (Northwest Atlantic). *Malacologia* **19:** 209–225.

Franz, D. R., and A. S. Merrill. 1980b. The origins and determinants of distribution of molluscan faunal groups on the shallow continental shelf of the northwest Atlantic. *Malacologia* **19:** 227–248.

Fritz, G. N., J. Conn, A. Cockburn, and J. Seawright. 1994. Sequence analysis of the ribosomal DNA internal transcribed spacer 2 from populations of *Anopheles nuneztovari* (Diptera: Culicidae). *Mol. Biol. Evol.* **11:** 406–416.

Grassle, J. F. 1995. Deep-sea biodiversity. *Bull. Mar. Sci.* **57:** 281–285.

Grosslein, M. D., and T. R. Azarovitz. 1982. *Fish Distribution.* MESA New York Bight Atlas Monograph 15. Marine Ecosystems Analysis [MESA] Program. New York Sea Grant Institute, Albany, NY.

Haedrich, R. L., G. T. Rowe, and P. T. Polloni. 1980. The megabenthic fauna in the deep-sea south of New England. *Mar. Biol.* **57:** 165–179.

Haefner, P. A., Jr. 1977. Reproductive biology of the female deep-sea red crab, *Geryon quinquedens,* from Chesapeake Bight. *Fish. Bull.* **75:** 91–102.

Haefner, P. A., Jr. 1978. Seasonal aspects of the biology, distribution and relative abundance of the deep-sea red crab *Geryon quinquedens* Smith, in the vicinity of the Norfolk Canyon, western North Atlantic. *Proc. Natl. Shellfish. Assoc.* **68:** 49–62.

Haefner, P. A., and J. A. Musick. 1974. Observations on the distribution and abundance of red crabs in Norfolk Canyon and the adjacent continental slope. *Mar. Fish. Rev.* **36:** 31–34.

Hastie, L. C. 1995. Deep-water geryonid crabs: a continental slope resource. *Oceanogr. Mar. Biol. Annu. Rev.* **33:** 561–584.

Hillis, D. M., and M. T. Dixon. 1991. Ribosomal DNA: molecular evolution and phylogenetic inference. *Q. Rev. Biol.* **66:** 411–453.

Hines, A. H. 1988. Fecundity and reproductive output in two species of deep-sea crabs, *Geryon fenneri* and *G. quinquedens* (Decapoda: Brachyura). *J. Crustac. Biol.* **8:** 557–562.

Hoelzer, G. A., J. Wallman, and D. J. Melnick. 1999. The effects of social structure, geographical structure, and population size on the evolution of mitochondrial DNA: II. Molecular clocks and the lineage sorting period. *J. Mol. Evol.* **47:** 21–31.

Kelly, P., S. D. Sutkin, and W. F. Van Heukelem. 1982. A dispersal model for larvae of the deep sea red crab *Geryon quinquedens* based on behavioral regulation of vertical migration in the hatching stage. *Mar. Biol.* **72:** 35–43.

Knowlton, N., L. A. Weight, L. A. Solórzano, D. K. Mills, and E. Bermingham. 1993. Divergence of proteins, mitochondrial DNA, and reproductive compatibility across the Isthmus of Panama. *Science* **260:** 1629–1632.

Lawton, P., and D. Duggan. 1998. *Scotian Shelf Red Crab. DFO*

Science Stock Status Report C3-11. Dept. of Fisheries and Oceans, Dartmouth, Nova Scotia, Canada.

López Abellán, L. J., E. Balguerias, and V. Fernandez-Vergaz. 2002. Life history characteristics of the deep-sea crab *Chaceon affinis* population off Tenerife (Canary Islands). *Fish. Res.* **58:** 231–239.

Lux, F. E., A. R. Ganz, and W. F. Rathjen. 1982. Marking studies on the red crab *Geryon quinquedens* Smith off southern New England. *J. Shellfish Res.* **2:** 71–80.

Maddison, W. P., and D. R. Maddison. 2000. *MacClade: Analysis of Phylogeny and Character Evolution version 4.0.* Sinauer Associates, Sunderland, MA.

Manning, R. B., and L. B. Holthuis. 1981. West African brachyuran crabs (Crustacea: Decapoda). *Smithson. Contrib. Zool.* **306:** 379.

Manning, R. B., and L. B. Holthuis. 1984. Two new genera and nine new species of geryonid crabs (Crustacea, Decapoda, Geryonidae). *Proc. Biol. Soc. Wash.* **97:** 666–673.

Manning, R. B., and L. B. Holthuis. 1988. South African species of the genus *Geryon* (Crustacea, Decapoda, Geryonidae). *Ann. S. Afr. Mus.* **98:** 77–92.

Manning, R. B., and L. B. Holthuis. 1989. *Geryon fenneri,* a new deep-water crab from Florida (Crustacea: Decapoda: Geryonidae). *Proc. Biol. Soc. Wash.* **102:** 50–77.

Manning, R. B., M. S. Tavares, and E. F. Albuquerque. 1989. *Chaceon ramosae,* a new deep-water crab from Brazil (Crustacea: Decapoda: Geryonidae). *Proc. Biol. Soc. Wash.* **102:** 646–650.

McMillen-Jackson, A. L., T. M. Bert, and P. Steele. 1994. Population genetics of the blue crab *Callinectes sapidus*: modest population structuring in a background of high gene flow. *Mar. Biol.* **118:** 53–65.

Melville-Smith, R. 1987. Movements of deep-sea red crab (*Geryon maritae*) off South West Africa/Namibia. *S. Afr. J. Zool.* **22:** 143–152.

Melville-Smith, R. 1989. A growth model for the deep-sea red crab (*Geryon maritae*) off South West Africa/Namibia (Decapoda, Brachyura). *Crustaceana* **56:** 279–292.

Ó Foighil, D., and C. J. Jozefowicz, 1999. Amphi-Atlantic phylogeography of direct-developing lineages of *Lasea,* a genus of brooding bivalves. *Mar. Biol.* **135:** 115–122.

Palumbi, S. R. 1996. Nucleic acids II: the polymerase chain reaction. Pp. 205–248 in *Molecular Systematics,* D. M. Hillis, C. Mortiz, and B. K. Mable, eds. Sinauer Associates, Sunderland, MA.

Perkins, H. C. 1972. The larval stages of the deep sea red crab, *Geryon quinquedens* Smith, reared under laboratory conditions (Decapoda: Brachyrhyncha). *Fish. Bull.* **71:** 69–82.

Pinho, M. R., J. M. Goncalves, H. R. Martins, and G. M Menezes. 2001. Some aspects of the biology of the deep-water crab, *Chaceon affinis* (Milne-Edwards and Bouvier, 1894) off the Azores. *Fish. Res.* **51:** 283–295.

Quattro, J. M., M. R. Chase, M. A. Rex, T. W. Greig, and R. J. Etter. 2001. Extreme mitochondrial DNA divergence within populations of the deep-sea gastropod *Frigidalvania brychia. Mar. Biol.* **139:** 1107–1113.

Rathbun, M. J. 1937. The oxystomatous and allied crabs of America. *U. S. Natl. Mus. Bull.* **166:** 1–278.

Rhoads, D. C., and B. Hecker. 1994. Processes on the continental slope off North Carolina with special reference to the Cape Hatteras region. *Deep-Sea Res.* **41:** 965–980.

Schubart, C. D., R. Diesel, and S. B. Hedges. 1998. Rapid evolution to terrestrial life in Jamaican crabs. *Nature* **393:** 363–365.

Schubart, C. D., J. E. Neigel, and D. L. Felder. 2000. Use of mitochondrial 16S rRNA gene for phylogenetic and population studies of Crustacea. *Crustac. Issues* **12:** 817–830.

Schubart, C. D, J. E. Conde, C. Carmona-Suárez, R. Robles, and D. L. Felder. 2001a. Lack of divergence between 16S mtDNA sequences of the swimming crabs *Callinectes bocourti* and *C. maracaiboensis* (Brachyura: Portunidae) from Venezuela. *Fish. Bull.* **99:** 475–481.

Schubart, C. D., J. A. Cuesta, and A. Rodriguez. 2001b. Molecular phylogeny of the crab genus *Brachynotus* (Brachyura: Varunidae) based on the 16S rRNA gene. *Hydrobiologia* **449:** 41–46.

Serchuk, F. M., and R. L. Wigley. 1982. Deep-sea red crab, *Geryon quinquedens.* Pp. 125–129 in *Fish Distribution,* M. D. Grosslein and T. R. Azarovitz, eds. MESA New York Bight Atlas Monograph 15. N. Y. Sea Grant Institute, Albany, NY.

Seyoum, S., M. D. Tringali, T. M. Bert, D. McElroy, and R. Stokes. 2000. An analysis of population genetic structure in red drum, *Sciaenops ocellatus,* based on mtDNA control region sequences. *Fish. Bull.* **98:** 127–138.

Skibinski, D. O. F., C. Gallagher, and H. Quesada. 1999. On the roles of selection, mutation and drift in the evolution of mitochondrial DNA diversity in British *Mytilus edulis* (Mytilidae; Mollusca) populations. *Biol. J. Linn. Soc.* **68:** 195–213.

Smith, S. I. 1879. The stalk-eyed crustaceans of the Atlantic coast of North America north of Cape Cod. *Trans. Connecticut Acad. Arts Sci.* **5:** 27–138.

Steimle, F. W., C. A. Zetlin, and S. Chang. 2001. Red deepsea crab, *Chaceon* (*Geryon*) *quinquedens,* life history and habitat characteristics. *NOAA Tech. Memo. NMFS-NE-163.* U.S. Dept. of Commerce, NOAA, NMFS, Woods Hole, MA.

Sulkin, S. D., and W. F. Van Heukelem. 1980. Ecological and evolutionary significance of nutritional flexibility in planktotrophic larvae of the deep sea red crab *Geryon quinquedens* and the stone crab *Menippe mercenaria. Mar. Ecol. Prog. Ser.* **2:** 91–95.

Swolford, D. L. 2002. *PAUP* 4.0 Phylogenetic Analysis Using Parsimony.* Sinauer, Sunderland, MA.

Theroux, R. B., and R. L. Wigley. 1983. Distribution and abundance of east coast bivalve mollusks based on specimens in the National Marine Fisheries Service Woods Hole Collection. *NOAA Tech. Rept. NMFS SSRF-768.* U.S. Dept. of Commerce, NOAA, NMFS, Seattle, WA.

Thompson, J., T. Gibson, F. Plewniak, F. Jeanmougin, and D. Higgins. 1997. The CLUSTAL_X windows interface: flexible strategies for multiple sequence alignment aided by quality analysis tools. *Nucleic Acids Res.* **22:** 4876–4882.

Van Heukelem, W., M. C. Christman, C. E. Epifanio, and S. D. Sulkin. 1983. Growth of *Geryon quinquedens* (Brachyura: Geryonidae) juveniles in the laboratory. *Fish. Bull.* **81:** 903–905.

Waller, R., H. Perry, C. Trigg, J. McBee, R. Erdman, and N. Blake. 1995. Estimates of harvest potential and distribution of the deep sea red crab, *Chaceon quinquedens,* in the north central Gulf of Mexico. *Gulf Res. Rep.* **9:** 75–84.

White, T. J., T. Burns, S. Lee, and J. Taylor. 1990. Amplification and direct sequencing of fungal ribosomal RNA genes for phylogenetics. Pp. 315–322 in *PCR Protocols: A Guide to Methods and Applications,* M. A. Innis, D. H. Gelfand, J. J. Sninsky, and T. J. White, eds. Academic Press, New York.

Wigley, R. L., R. B. Theroux, and H. E. Murray. 1975. The deep-sea red crab. *Mar. Fish. Rev.* **37:** 1–21.

Williams, A. B., and R. L. Wigley. 1977. Distribution of decapod crustacea off northeastern United States based on specimens at the Northeast Fisheries Science Center, Woods Hole, Massachusetts. *NOAA Tech. Report NMFS Circular* 407. NOAA, Woods Hole, MA.

Appendix

Summary of collection data for specimens of *Chaceon* (deep-sea red crab) used in the 16S genetic study

Southern New England, *Chaceon quinquedens*, leg muscle: collected by J. Weinberg

Sample	Sample ID#	Haplotype	Coordinates Lat/Long	Date	Depth (m)	Carapace Size (mm) Width	Length
Female 17	SNE 179 (#17)	E	Station 179 N39° 53.42′ W69° 42.18′	5/16/01	465	102	
Male 05	SNE 180 (#5)	E	Station 180		502	112	
Female 10	SNE 180 (#10)	F	N39° 52.75′ W69° 45.29′			84	
Female 03	SNE 181 (#3)	E	Station 181	5/17/01	646	90	
Male 16	SNE 181 (#16)	E	N39° 51.81′ W69° 43.66′			113	
Female 07	SNE 182 (#7)	E	Station 182		694	84	
Male 11	SNE 182 (#11)	E	N39° 51.96′ W69° 44.68′			114	
Female 01	SNE 183 (#1)	F	Station 183		731	112	
Male 02	SNE 183 (#2)	E	N39° 51.17′			72	
Female 03	SNE 183 (#3)	E	W69° 51.73′			68	
Male 01	SNE 184 (#1)	E	Station 184 N39° 49.20′ W70° 33.19′	5/18/01	914	114	
Female 02	SNE 185 (#2)	F	Station 185 N39° 49.20′ W70° 33.19′		931	102	
Female 06	SNE 186 (#6)	F	Station 186 N39° 53.32′ W70° 36.51′		557	74	

Gulf of Mexico, *Chaceon quinquedens*, gonad: collected by P. Biesiot & H. Perry

Sample	Sample ID#	Haplotype	Coordinates Lat/Long	Date	Depth	Carapace Size Width	Length
Male 1	GoM-M1	D	N27° 49′ W85° 24′	8/23/95	951	146.9	118.8
Male 2	GoM-M2	D				134.2	108.1
Male 3	GoM-M3	D				131.7	104.2
Male 4	GoM-M4	D				135.4	105.8
Male 5	GoM-M5	D				122.5	97.2
Female 51	GoM-F51	A				118.5	94.1
Female 52	GoM-F52	B				110.9	90.3
Female 53	GoM-F53	C				133.0	104.2
Female 54	GoM-F54	D				110.1	89.4
Female 55	GoM-F55	D				115.9	93.7

Atlantic Side of Florida, *Chaceon affinis*, leg muscle: collected by P. Brown-Eyo, R. Nielson, & D. Harper

Sample	Sample ID#	Haplotype	Coordinates	Date	Depth	Carapace Size Width	Length
01 Male	GC-1M	D	So. FL, Lat 25° Long 79°	1/11/02	335	146	
02 Male	GC-2M	D				172	
03 Male	GC-3M	D				137	
04 Male	GC-4M	D				171	
05 Male	GC-5M	D				125	
01 Female	GC-1F	D				137	
02 Female	GC-2F	D				111	
03 Female	GC-3F	D				117	
04 Female	GC-4F	D				120	
05 Female	GC-5F	D				137	
06 Female	GC-6F	D				121	

Reference: *Biol. Bull.* **204:** 327–338. (June 2003)

Genetic Linkage Map of the Eastern Oyster *Crassostrea virginica* Gmelin

ZINIU YU[1,2] AND XIMING GUO[1,*]

[1]*Haskin Shellfish Research Laboratory, Institute of Marine and Coastal Sciences, Rutgers University, Port Norris, New Jersey 08349; and* [2]*Mariculture Research Laboratory, College of Fisheries, Ocean University of Qingdao, Qingdao 266003, People's Republic of China*

Abstract. Amplified fragment length polymorphisms (AFLPs), along with some microsatellite and Type I markers, were used for linkage analysis in *Crassostrea virginica* Gmelin, the eastern oyster. Seventeen AFLP primer combinations were selected for linkage analysis with two parents and their 81 progeny. The 17 primer combinations produced 396 polymorphic markers, and 282 of them were segregating in the two parents. Chi-square analysis indicated that 259 (91.8%) markers segregated in Mendelian ratio, while the other 23 (8.2%) showed significant ($P < 0.05$) segregation distortion, primarily for homozygote deficiency and probably due to deleterious recessive genes. Moderately dense linkage maps were constructed using 158 and 133 segregating markers (including a few microsatellite and Type I markers) from male and female parents, respectively. The male framework map consisted of 114 markers in 12 linkage groups, covering 647 cM. The female map had 84 markers in 12 linkage groups with a length of 904 cM. The estimated genome length was 858 cM for the male map and 1296 cM for the female map. The observed genome coverage was 84% for the male and female map when all linked markers were considered. Genetic maps observed in this study are longer than the cytogenetic map, possibly because of low marker density.

Introduction

The past decade has brought tremendous advances in genomics. Complete genome sequences are now available for many organisms including several eukaryotes such as *Caenorhabditis elegans*, *Drosophila melanogaster*, and *Homo sapiens*. The list of completed genomes is rapidly growing, and representative organisms of most taxa are now subjects of intensive genomic analysis. Mollusca, the second largest phylum of invertebrates, has received little attention. The number of available markers remains small and inadequate for genomic-wide mapping analysis, and no genetic linkage map has been published for any species. Understanding the genome of molluscs is important for comparative and evolutionary genomics, as well as for genetic improvement of cultured species.

Crassostrea virginica Gmelin, the eastern oyster, is one of the best-understood molluscs. It is a marine bivalve that occurs naturally along the Atlantic coast of North America (Galtsoff, 1964); it is easily cultured and widely available. It has a haploid number of 10 chromosomes (Longwell and Stiles, 1967), one of the lowest among molluscs, making it an ideal model mollusc for genetic and genomic analysis. The eastern oyster is also a species of economic significance, supporting major fishery and aquaculture industries in North America, so studies of its genome would be important for genetic improvement of this species. The development of genetic linkage maps is particularly useful for the mapping of quantitative trait loci (QTLs) and for marker-assisted selection (MAS) (Lander and Botstein, 1989; Cho *et al.*, 1994). Genetic linkage maps have been developed for almost all major aquaculturally important species, including tilapia, rainbow trout, catfish, oysters, and shrimps (Kocher *et al.*, 1998; Young *et al.*, 1998; Sakamoto *et al.*, 2000; Waldbieser *et al.*, 2001; Hubert *et al.*, 2002; Li and Guo, 2002; Moore *et al.*, 1999; Wilson *et al.*, 2002).

Two preliminary linkage maps were recently constructed for the Pacific oyster (*Crassostrea gigas*): one with microsatellites (Hubert *et al.*, 2002) and one with RAPD and AFLP markers (Li and Guo, 2002). However, details of the two maps have not been published. As for the eastern

* To whom correspondence should be addressed: E-mail: xguo@hsrl.rutgers.edu

oyster, only a few microsatellites are available (Brown *et al.*, 2000), but more are being developed for population analysis and mapping (Reece *et al.*, 2002). Two linkage groups have been identified involving seven allozyme markers (Foltz, 1986).

While microsatellites are the most popular markers for genomic mapping, their development and application are slow and expensive. In oysters, many microsatellites suffer from surprisingly high levels of null-alleles, segregation distortion, and influence of repetitive elements (Launey and Hedgecock, 2001; Reece *et al.*, 2002; Gaffney, 2002). Amplified fragment length polymorphisms (AFLPs) are also popular markers for genome mapping, especially in "orphan" species where genetic resources are limited. AFLP markers are specific to restriction sites and thus reliable, and large numbers of polymorphisms can be developed quickly without prior knowledge of DNA sequence (Vos *et al.*, 1995). AFLPs have been developed and used for genome mapping in many aquatic animals, including catfish (Liu *et al.*, 1998, 1999a), rainbow trout (Young *et al.*, 1998;), tilapia (Kocher *et al.*, 1998; Agresti *et al.*, 2000), medaka (Naruse *et al.*, 2000), Pacific oyster (Li and Guo, 2002), and shrimps (Moore *et al.*, 1999; Wilson *et al.*, 2002). We report here the construction of the first linkage maps for the eastern oyster with AFLP and a few microsatellite and Type I markers.

Materials and Methods

Oysters and DNA extraction

Eastern oysters used in this study were from a reference family (NEI-1) produced from the Rutgers NEH strain. The NEH strain was developed from Long Island Sound populations by long-term selective breeding since the early 1960s for resistance against MSX (a parasitic disease caused by *Haplosporidium nelsoni*) (Ford and Haskin, 1987) and recently for resistance against Dermo (a parasitic disease caused by *Perkinsus marinus*). The reference family was produced in 1998 by single-pair mating and was sampled in 1999 when the progeny were about one year old. Oyster tissues were kept in a −80 °C freezer before use. DNA was extracted from adductor muscle or mantle tissue from each animal using the CTAB phenol/chloroform protocol as described in Grewe *et al.* (1993). Two parents and four progeny were used for marker screening, and linkage analysis was based on 81 progeny.

AFLP markers

AFLP analysis was conducted primarily according to Perkin-Elmer's (PE) AFLP plant mapping protocol, with some modifications. Adaptors, preselective primers, selective primers, and PCR reagents were purchased from PE. Restriction enzymes and T4 DNA ligase were purchased from New England Biolabs (NEB). Genomic DNA (~0.5 μg) was digested by restriction enzymes *Eco*RI and *Mse*I, and ligated with relevant adaptors overnight at room temperature. Each reaction (11 μl) contained 5.5 μl DNA, 1.0 μl of 10× T4 DNA ligase buffer with EDTA, 1.0 μl of 0.5 *M* NaCl, 0.5 μl of 1.0 mg/ml BSA, 1.0 μl each of *Mse*I and *Eco*RI adaptors, and 1.0 μl enzyme mix (0.1 μl of 10× T4 DNA ligase buffer with EDTA, 0.1 μl of 0.5 *M* NaCl, 0.05 μl of 1.0 mg/ml BSA, 1.0 U *Mse*I, 5.0 U *Eco*RI, 1.0 Weiss U T4 DNA ligase and proper amount of water).

Preselective primers complementary to each adaptor sequence only were used to amplify the restriction fragments created in the digestion-ligation step. Every 4 μl of diluted (20-fold) digestion-ligation product was amplified in a 20-μl reaction mixture containing 0.5 μl of each *Eco*RI and *Mse*I preselective primers, and 15 μl PCR Core Mix. Preselective PCR was run at a temperature profile of one cycle of 72 °C for 2 min, 25 cycles of 94 °C for 25 s, 56 °C for 30 s, and 72 °C for 2 min, and one cycle of 60 °C for 30 min. Products from preselective PCR were diluted 20-fold with Tris-EDTA buffer and used as templates for selective amplification. Pairs of selective primers, each containing two or three selective nucleotides at their 3′ end, were used for selective PCR, with the *Eco*RI selective primer being fluorescein-labeled. The *Eco*RI and *Mse*I selective primers were coded with letters and numbers, respectively (see Table 1). AFLP markers were named by adding the letter "f" (fragment) and three digits representing fragment size in base pairs to the end of the primer combination names. For example, marker F1f128 refers to a 128-bp fragment amplified from the primer combination of E-ACT [F] and M-CAA [1]. Amplifications were carried out in a 20-μl reaction that was composed of 3.0 μl diluted preselective product, 1.0 μl *Mse*I selective primer at 5.0 μ*M*, 1.0 μl *Eco*RI selective primer at 1 μ*M*, and 15 μl PCR Core Mix. Selective PCR was run with a touch-down profile: 10 cycles of 94 °C for 20 s, 66 °C for 30 s, and 72 °C for 2 min, with a 1 °C decrease in annealing temperature each cycle, followed by 20 cycles of amplification at 94 °C for 20 s, 56 °C for 30 s, and 72 °C for 2 min.

Electrophoresis and data collection were carried out on an ABI 310 genetic analyzer (PE). After selective amplification, 1.0 μl of PCR product was added to a 0.5-ml sample tube containing 12.0 μl deionized formamide and 0.5 μl GeneScan-500 size standard (PE). Samples were denatured at 95 °C for 5 min, and then immediately cooled on ice for 5 min before being loaded onto the ABI 310 genetic analyzer. Electrophoresis parameters were set at injection for 10 s at 15 kv, running for 30 min at 13 kv and 60 °C, with POP4 polymer. Data were collected using the GS STR POP4 A module in the Data Collection Software (ver. 1.0.2), and then analyzed with GeneScan Analysis software (ver. 3.1). Genotyper software was used to analyze and

score genotypes, and electrophoretic histograms were manually examined for genotyping errors.

Microsatellite markers

Ten microsatellite primer pairs were screened for polymorphism in parents. Seven of them were developed by Brown *et al.* (2000): *Cvi6*, *Cvi7*, *Cvi8*, *Cvi9*, *Cvi11*, *Cvi12*, and *Cvi13* (GenBank accession No. AF276247-AF276254). Three were developed in our lab, with one (*RU001*) polymorphic in the female parent. *RU001* is a $(TA)_{28}$ repeat with primer sequences of 5′-GGCTGCCAAATGAATAAATC-3′/5′-GAGTTTGGTCTCACACTTGAAATC-3′, an annealing temperature of 54 °C, and an expected product size of 180. PCR reactions were performed in a 15-μl volume containing 1× PCR buffer, 2.5 m*M* of $MgCl_2$, 0.2 m*M* of each dNTP, 0.5 μ*M* of each primer, 50 ng of genomic DNA, and 0.5 U of *Taq* polymerase (Promega, Madison, WI) using the following temperature profile: 94 °C for 2 min, then 30 cycles of 94 °C for 30 s, 54 °C for 30 s, and 72 °C for 15 s. Amplification products were resolved by electrophoresis on 10% acrylamide gel and stained with ethidium bromide.

Type 1 (EST) markers

cDNA sequences were obtained from suppression subtractive hybridization (SSH) libraries constructed with control and *Perkinsus marinus*-challenged eastern oysters (A. Tanguy *et al.*, Rutgers University, unpubl. data). Ten sequences were selected and screened for single-strand conformation polymorphisms (SSCPs). Two of them (*Rho* and *Vb65*) were polymorphic in at least one of the parents. The primer sequences are 5′-GGAATGGTGCTCTGTTTA CACT-3′/5′-CCTATAATCCTGGTAGGCAACA-3′ for *Rho*, 5′-ACATACAGCACCAAGAAAAAGC-3′/5′-AGAGAT CACTATTTCCCTGCAC-3′ for *Vb65*, and both with an annealing temperature of 52 °C. The amplified fragments were 391 bp for *Rho* and 380 bp for *Vb65*. PCR reactions were performed in 20 μl containing 1× PCR buffer, 2.0 m*M* of $MgCl_2$, 0.2 m*M* of each dNTP, 0.25 μ*M* of each primer, 50 ng of genomic DNA, and 0.5 U of *Taq* polymerase (Promega, Madison, WI) using the following profile: 94 °C for 2 min, then 32 cycles of 94 °C for 45 s, 52 °C for 45 s, and 72 °C for 1 min. PCR fragments were denatured at 95 °C for 5 min and immediately chilled on ice. SSCP was separated on 8% acrylamide gel with 5% glycerol and visualized with silver-staining (Black and Duteau, 1997).

Data analysis and map construction

For AFLPs, primer combinations were evaluated based on the total number of total peaks produced, the number of polymorphic (among two parents) peaks, and peak quality. Each peak was considered as a locus and scored as peak presence (*A/A*, *A/a*), or absence (*a/a*). Loci at which one parent was *A/a* and the other was *a/a* were selected for mapping analysis. Genotypes were coded as H for *A/a* and A for *a/a* in a backcross model. For microsatellite and Type 1 markers where more than two alleles were involved, one of the segregating alleles was selected and coded in the same way as AFLPs in a backcross model: H for present and A for absent. All segregating loci scored were checked with the chi-square test for goodness of fit to the 1:1 Mendelian ratio. Distorted markers were included in mapping analysis for possible identification of regions of distortion. Distorted markers with homozygote deficiency or homozygote excess were designated by adding a "−" or "+" to the end of the marker label. Linkage analysis was performed with MAPMAKER 3.0 (Lander *et al.*, 1987). Markers were grouped at a logarithm of odds (LOD) score of 3.0 and maximum distance of 38 cM first. Small groups (≤ 8 markers) were ordered with multipoint exhaustive analysis using the "compare" command. Large groups were processed with the three-point analysis and "order" command. Additional markers were added by lowering the LOD score to ≥ 2.0 to obtain a framework map. Map order was verified with the "ripple" command. Some markers were clearly linked to specific groups but could not be placed on the maps, because they had more than one possible position (or were in different order) on the map. Typing errors were detected with the "error detection on" option, and map distances were computed in Kosambi function (Ott, 1999). Linkage groups were drawn with MAPCHART (Voorrips, 2001).

Marker distribution and genome coverage

Marker distribution was analyzed by calculating the Pearson correlation coefficient between the number of markers in the linkage groups and the size of the linkage groups (SPSS ver. 8.0). Three methods were used to calculate the estimated genome length. First, we calculated the average marker spacing/interval (s) by dividing the total map length by the number of intervals (number of markers minus number of linkage groups). The estimated genome length (G_{e1}) was determined by adding $2s$ to the length of each linkage group to account for chromosome ends (Fishman *et al.*, 2001). Secondly, an estimated genome length (G_{e2}) was calculated by multiplying the length of each linkage group by $(m + 1)/(m - 1)$, where m is the number of framework markers in each group (Chakravarti *et al.*, 1991). Finally, we estimated genome length with a subset of well-spaced markers by $G_{e3} = N(N - 1)X/K$, where N is the number of markers, X is the maximum interval between two adjacent markers, and K is the number of marker pairs at an LOD score of 3.0 (Hulbert *et al.*, 1988; Chakravarti *et al.*,

1991). The average of the three estimates was used as the estimated genome length (G_e) for the eastern oyster. Two observed genome lengths were calculated, one as the length of the framework map (G_{of}), and the other as the total length considering all markers (G_{oa}) (Cervera *et al.*, 2001). The observed genome coverages, C_{of} and C_{oa}, were determined by G_{of}/G_e and G_{oa}/G_e, respectively.

Results

AFLP markers

Fifty-six selective primer combinations were screened. AFLP profile or peaks generated by the AFLP protocol used were highly specific and reproducible when the selective amplification was successful (Fig. 1A). The majority of the

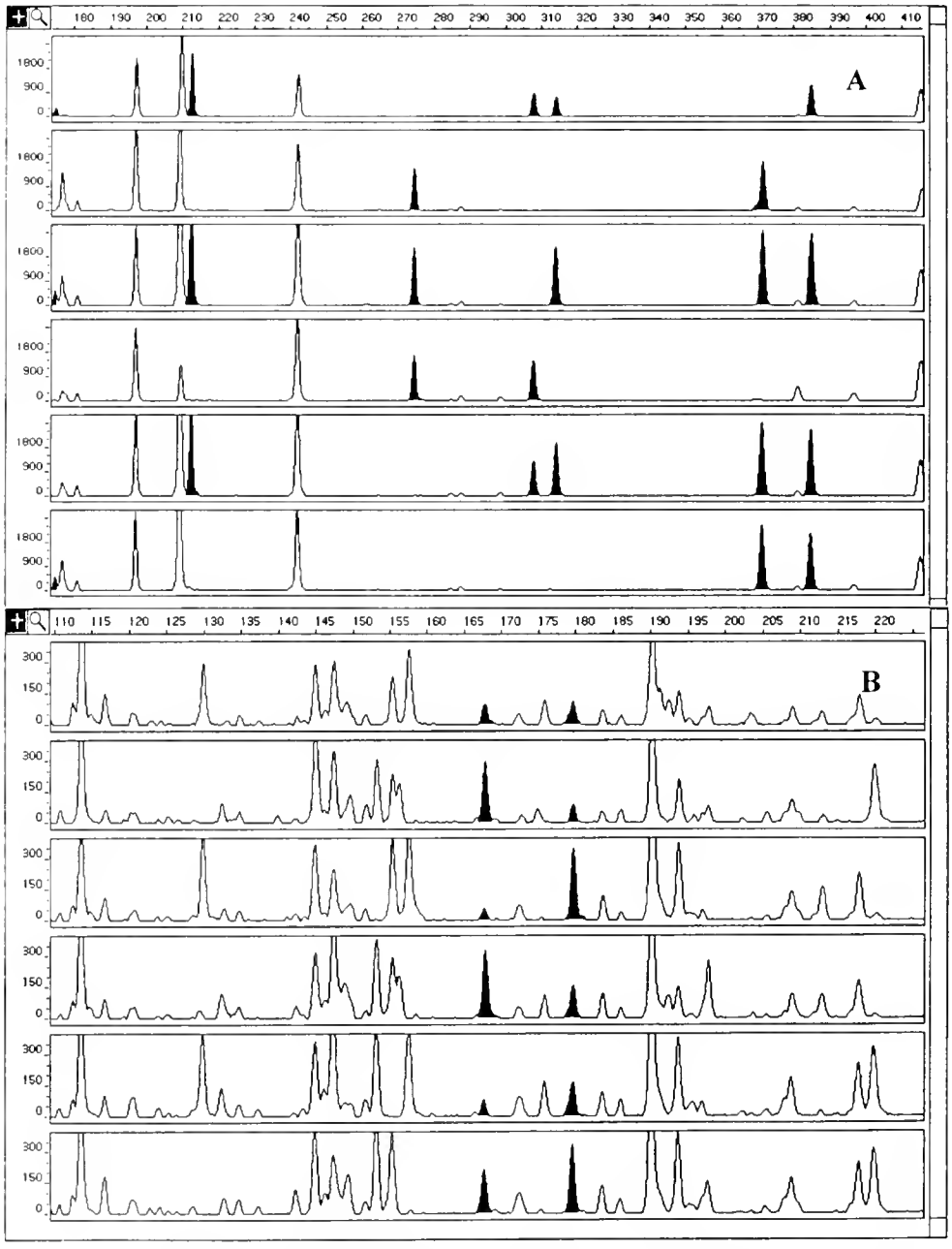

Figure 1. Representative AFLP histograms for two parents (top two panels) and four progeny (bottom four) of *Crassostrea virginica*. (**A**) Segregating peaks (highlighted) from primer combination E-ACT/M-CAG [F3]; peak presence and absence were scored as *Aa* and *aa*, respectively. (**B**) Co-dominant peaks (highlighted) from E-TG/M-CAG [03]; from top to bottom, genotypes were recorded as *Aa*, *AA*, *Aa*, *AA*, *Aa*, and *AA* for the highlighted peak on the left, and *Aa*, *Aa*, *AA*, *Aa*, *Aa*, and *AA* for the highlighted peak on the right.

peaks or fragments were between 60 and 450 bp. Fragments smaller than 60 bp were generally too crowded to score, and fragments bigger than 450 bp had low peak height or intensity. Most AFLPs are dominant markers, although co-dominance was apparent for some peaks (about seven loci), where *A/A* and *A/a* genotypes were distinguishable by dosage or peak height (Fig. 1B). Dosage difference was clear for some peaks, but less certain for others. To be conservative, we did not include these co-dominant markers for mapping.

The number of polymorphic and all peaks produced by each of the 56 primer pairs are presented in Table 1. Except for one primer pair [O1], all primer pairs produced identifiable peaks, ranging from 17 to 106 peaks per pair; 2746 peaks were obtained from 55 primer pairs, averaging 50 peaks per pair. The average number of polymorphic peaks (among the two parents) was 747, or 13 per primer pair, which corresponds to an overall polymorphism of 27.2%.

The number of peaks produced among primer combinations varied considerably. Overall, the difference among the *Mse*I primers was small, but among the *Eco*RI primers it was significant. For example, E-TA [M] produced 647 peaks in combination with eight *Mse*I primers, while E-ACG [E] produced only 162 peaks (Table 1). The level of polymorphism produced by different primer combinations also varied considerably, ranging from 5.0% in E1 to 55.8% in F8. Overall, E-ACT [F] produced the highest level of polymorphism, 172 markers in combination with eight *Mse*I primers or 38.5%.

On the basis of the number of peaks produced, the level of polymorphism, and peak quality, 31 primer combinations were considered as good, 11 as fair, and 14 as poor. The good primer combinations produced large numbers of well-separated peaks with little background. Primer combinations that produced few or poorly defined peaks or high background were considered poor. Seventeen good primer combinations were selected for further evaluation and mapping analysis (printed in bold in Table 1). The 17 selected primer pairs produced 1056 peaks, and 396 of them (37.5%) were polymorphic in the reference family. Among the polymorphic markers, 298 were segregating in either the male or the female parent. Seven co-dominant markers (scored according to dosage difference) were not used for possible genotyping errors, and the remaining markers were scored qualitatively as peak present or absent. Nine markers were discarded because some progeny had unreliable or ambiguous genotypes. For the 282 polymorphic markers used, 153 (54.3%) were segregating through the male parent, and 129 (45.7%) through the female parent. Chi-square analysis indicated that 259 (91.8%) segregated according to the Mendelian ratio (1:1), and 23 (8.24%; 17 in male and 6 in female) showed significant segregation distortion ($P < 0.05$). Among the 23 distorted loci, four (17.4%) were deficient in heterozygotes (*A/a*), and 19 (82.6%) were deficient in homozygotes (*a/a*).

Microsatellite and Type I markers

Five of the ten microsatellites screened were polymorphic and segregating in at least one of the parents: *Cvi9*, *Cvi11*, *Cvi12*, *Cvi13*, and *RU001*. Among these five, *Cvi11* and *RU001* segregated in the female parent; *Cvi9* and *Cvi12* segregated in the male parent; and *Cvi13* segregated in both parents. Two of the 10 Type I markers (*Rho* and *Vb65*) were polymorphic when screened for SSCP. *Rho* was segregating in the male. *Rho* is a family of GTPases that regulate diverse cellular events including transcription, cell growth, development, and endocytosis and exocytosis (Leung *et al.*, 1999). *Vb65* is an unknown gene segregating in both parents. Chi-square analysis indicated that all microsatellite and Type I markers were in agreement with Mendelian ratios.

Table 1

Number of polymorphic and all peaks (before and after slashes, respectively) produced from 56 AFLP primer combinations in a family of Crassostrea virginica *with polymorphic percentages in parenthesis*

Primer	E-AAG [B]	E-ACA [C]	E-ACG [E]	E-ACT [F]	E-AGG [H]	E-TA [M]	E-TG [O]	Mean	Total
M-CAA [1]	4/42 (9.5)	11/51 (23.5)	1/20 (5.0)	**28/71 (39.4)**	**22/59 (37.3)**	7/69 (10.1)	Nodata	12/52 (20.8)	73/312
M-CAC [2]	2/26 (7.7)	9/35 (25.7)	3/19 (15.8)	**21/53 (39.6)**	5/37 (13.5)	10/73 (13.7)	12/49 (24.5)	9/42 (20.1)	62/292
M-CAG [3]	**20/49 (40.8)**	8/26 (30.7)	3/17 (17.6)	**26/57 (45.6)**	**21/53 (39.6)**	19/97 (19.6)	**13/54 (24.1)**	16/50 (31.2)	110/353
M-CAT [4]	11/50 (22.0)	9/42 (21.4)	8/25 (32.0)	**19/81 (23.5)**	7/32 (21.8)	21/106 (19.8)	9/42 (21.4)	12/54 (23.1)	84/378
M-CTA [5]	**21/66 (31.8)**	**33/85 (38.8)**	5/22 (22.7)	**18/46 (39.1)**	8/35 (22.8)	20/79 (25.3)	12/37 (32.4)	17/53 (30.5)	117/370
M-CTC [6]	12/37 (32.4)	**34/73 (46.6)**	4/17 (23.5)	**12/45 (26.7)**	9/55 (16.4)	13/62 (21.0)	8/32 (25.0)	13/46 (27.4)	92/321
M-CTG [7]	8/43 (18.6)	**36/72 (50.0)**	5/21 (23.8)	**19/50 (38.0)**	18/59 (30.5)	**24/90 (26.7)**	2/25 (8.0)	16/51 (28.0)	112/360
M-CTT [8]	15/57 (26.3)	31/96 (32.3)	7/21 (33.3)	**29/52 (55.8)**	4/30 (13.3)	7/71 (9.9)	4/33 (12.1)	14/51 (26.1)	97/360
Mean	12/46 (23.6)	21/60 (33.6)	5/20 (21.7)	22/57 (38.5)	12/45 (24.4)	15/81 (18.3)	9/39 (21.1)	13/50 (25.9)	
Total	93/370	171/480	36/162	172/455	94/360	121/647	60/272		747/2746

*Eco*RI primers (E-) are coded by [letters], and *Mse*I primers (M-) are coded by [numbers]. Numbers in bolds are primer combinations used for linkage mapping in this study.

Linkage maps and marker distribution

Two linkage maps were constructed: one for the male parent, using 158 markers; the other for the female parent, using 133 markers. The male framework map consisted of 114 markers in 12 linkage groups (Fig. 2). Twenty-one markers were not linked to the framework map, including 3 triplets, 5 doublets, and 2 unlinked markers (Table 2). Additionally, 23 unplaced markers were linked to the framework map but not placed, because they had uncertain or conflicting positions on the map. The male map covered 647.4 cM in length, with a maximum interval of 39.1 cM and an average interval of 6.3 cM (Table 3). The length of the linkage groups ranged from 17.4 to 127.3 cM, and the number of markers varied from 4 to 18 per group. Microsatellite markers *Cvi9*, *Cvi12*, and *Cvi13* were mapped to Groups 1, 5, and 9, respectively. Type I marker *Rho* was placed on the distal region of Group 4, and *Vb65* was unlinked to any group. The 17 distorted AFLPs (suffixed with "− or +" in marker names for homozygote or hetero-

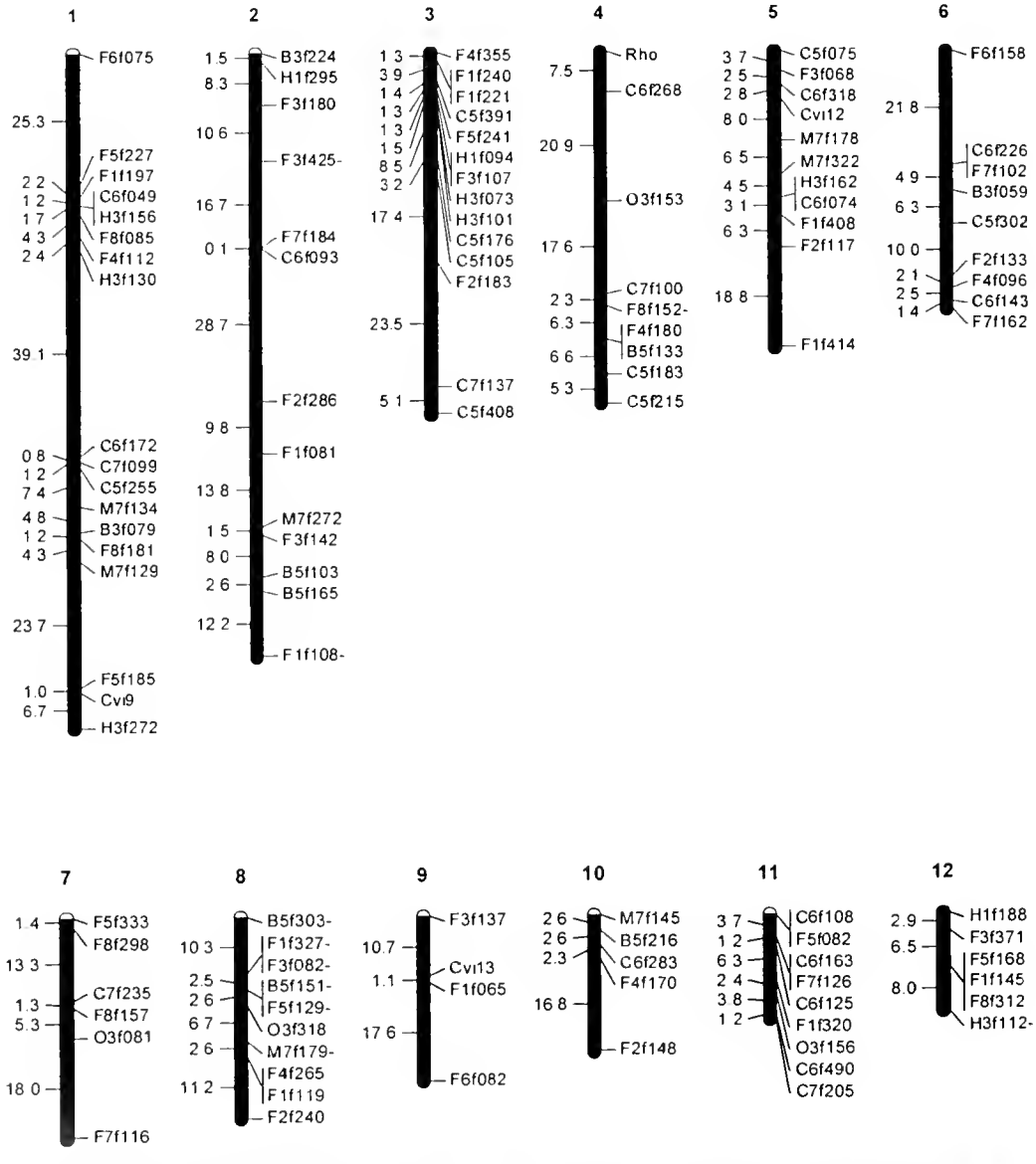

Figure 2. Genetic linkage maps of the male eastern oyster, *Crassostrea virginica*, with 114 markers and 647 cM. AFLP markers are labeled with two characters for the primer combination, followed by the letter "f" (for fragment) and a 3-digit fragment size in base pairs. Markers are indicated on the right; distances between markers (in Kosambi cM) are on the left. The suffix "-" designates distorted markers that are homozygote-deficient. Markers covered by thin vertical lines have no detectable distances among them. The 12 linkage groups were arranged according to map length.

Table 2

Number of markers used, mapped, unplaced, and unlinked in male and female Crassostrea virginica

Features	Male	Female
AFLP markers	153	129
Microsatellites	3	3
Type I markers	2	1
Total markers used	158	133
Mapped framework markers	114	84
Unplaced markers	23	12
Unlinked triplets	3	7
Unlinked doublets	5	4
Unlinked singles	2	8
Distorted AFLPs (%)	16 (10.5)	6 (4.7)

zygote deficiency, respectively) were distributed over five linkage groups, 1 triplet, 1 doublet, and 5 unplaced markers. Surprisingly, 6 of the 17 markers were located within a 22-cM region of Group 8, and all 6 markers were deficient for homozygotes. The six markers (*B5f303*, *F1f327*, *F3f082*, *B5f151*, *F5f129*, and *M7f179*) were not produced from a single primer combination, so the segregation distortion could not arise from anomalous amplification of these markers.

The female framework map consisted 84 markers in 12 linkage groups (Fig. 3). Not included in the framework map were 37 unlinked markers, including 7 triplets, 4 doublets, and 8 singles, and 12 linked but unplaced markers (Table 2). The length of the female map was 904.3 cM, the maximum interval was 35.2 cM, and the average interval was 12.6 cM. The length of the linkage groups ranged from 17.5 to 167.3 cM, and the number of markers varied from 4 to 15 per group (Table 3). Microsatellite markers *Cvi11*, *Cvi13*, and *RU001* were assigned to Groups 7, 2, and 6, respectively; Type I marker *Vb65* was linked to two markers outside the framework map. Four of the six distorted markers were placed on the framework map with each in a different linkage group. The microsatellite marker *Cvi13*, which was the only marker segregating in both male and female, was mapped to Group 9 of the male map and Group 2 of the female map, indicating that the two groups are the same chromosome.

Overall, AFLP markers were randomly distributed in the linkage maps, as indicated by the significant ($P < 0.01$) correlation between the number of markers in the linkage groups and the size (length) of the linkage groups for both female and male maps. Some small clusters and gaps were noticeable in both maps. Clustering was more apparent in the male map than in the female map.

Genome length and genome coverage

Genome length, which was estimated by three methods, was similar, ranging from 799.8 to 958.5 cM for the male, and from 1205.5 to 1489.3 cM for the female (Table 4). The average of the three estimates was used as the expected genome length for *C. virginica*: 858.0 cM for the male, and 1295.9 cM for the female. On the basis of the expected genome length, genome coverage for the male and female framework maps was 75.5% and 69.8%, respectively. When all linked markers (framework plus doublets and triplets) were considered, the observed genome length became 718.4 cM for male and 1091.6 cM for female maps, corresponding to 83.7% and 84.2% coverage over the respective genomes. Clearly, the female map was longer than the male map.

Discussion

Marker evaluation, distribution, and segregation distortion

This study demonstrates that, in *Crassostrea virginica*, the eastern oyster, as in other organisms (Liu *et al.*, 1998; Kocher *et al.*, 1998; Agresti *et al.*, 2000; Wilson *et al.*, 2002), AFLPs are well suited for linkage mapping. AFLPs are highly specific, reproducible, and relatively simple to

Table 3

Length number of markers, average spacing, and largest intervals of linkage groups in female and male map of Crassostrea virginica

Linkage group		Length (cM)	Number of markers	Average interval (cM)	Largest interval (cM)
Male	1	127.3	18	7.5	39.1
	2	113.8	13	9.5	28.7
	3	68.4	14	5.3	23.5
	4	66.5	9	8.3	20.9
	5	56.2	11	5.6	18.8
	6	49.0	9	6.1	21.8
	7	39.3	6	7.9	18.0
	8	35.9	10	4.0	11.2
	9	30.7	4	10.2	17.7
	10	24.3	5	6.1	16.8
	11	18.6	9	2.3	6.3
	12	17.4	6	3.5	6.5
	Total	647.4	114	6.3[a]	
Female	1	167.3	15	12.0	35.2
	2	116.6	9	14.6	34.7
	3	114.9	8	16.4	24.8
	4	111.1	10	12.3	33.1
	5	92.6	7	15.4	24.5
	6	72.8	6	14.6	25.7
	7	68.3	5	17.1	34.5
	8	62.5	6	12.5	28.8
	9	30.6	4	10.2	16.8
	10	26.9	4	9.0	25.3
	11	23.2	5	5.8	11.4
	12	17.5	5	4.4	7.6
	Total	904.3	84	12.6[a]	

[a] Average of all linked markers. Map distance (cM) is in Kosambi units.

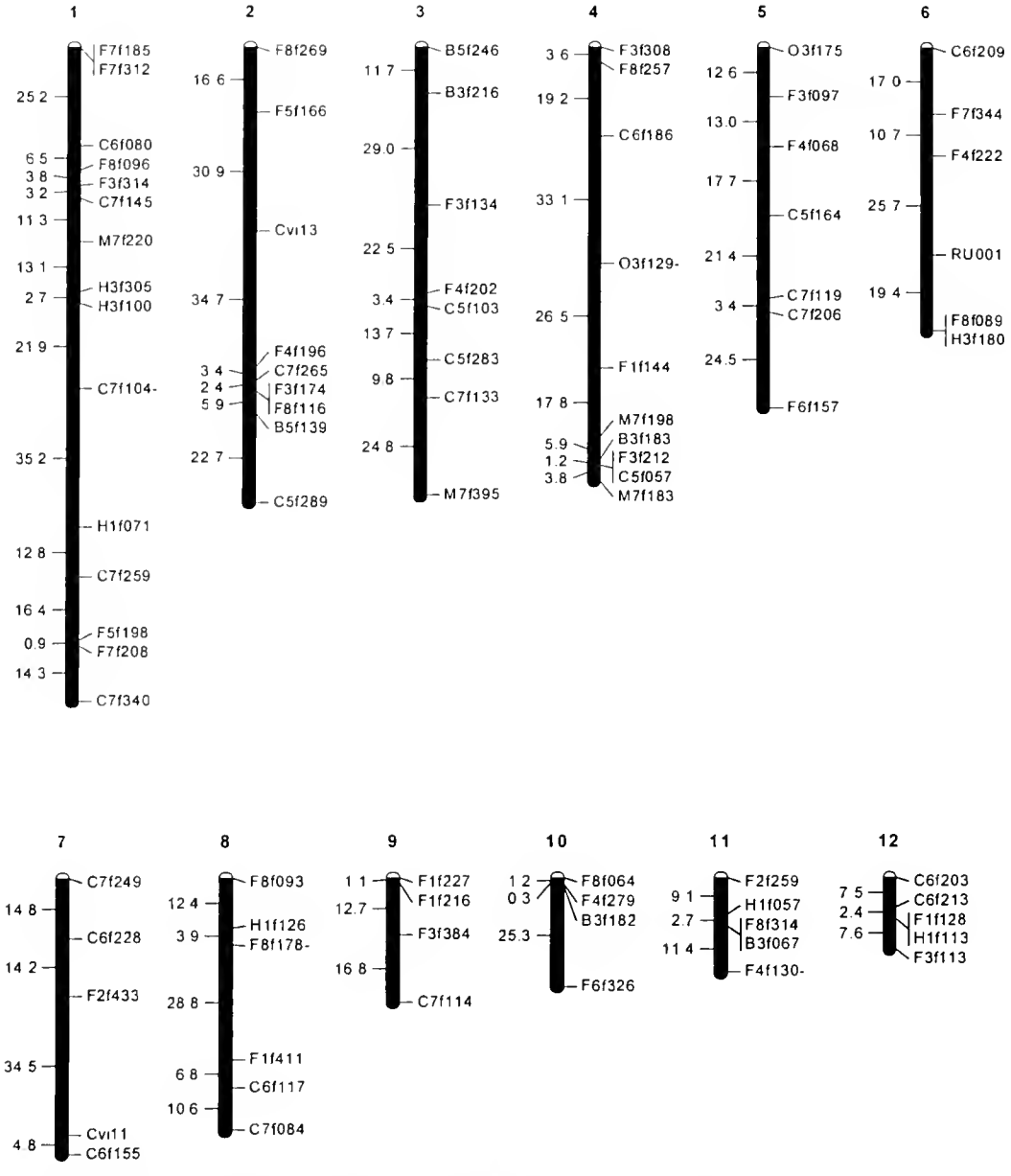

Figure 3. Genetic linkage maps of the female eastern oyster, *Crassostrea virginica*, with 84 markers and 904 cM. AFLP markers are labeled with two characters for the primer combination, followed by the letter "f" (for fragment) and a 3-digit fragment size in base pairs. Markers are indicated on the right; distances between markers (in Kosambi cM) are on the left. The suffix "-" designates distorted markers that are homozygote-deficient. Markers covered by thin vertical lines have no detectable distances among them. The 12 linkage groups were arranged according to map length.

develop. The overall level of polymorphism—27.2% in a reference family with two parents originating from the same population—is reasonably high and adequate for mapping analysis. By selecting the best selective primer combinations, the number of polymorphic markers can be further increased to about 37.5%, or 23 per primer pair for the 17 selected primer pairs in this study. The proportion of polymorphic loci observed in this study is similar to the 42% observed from 12 selected primer combinations in tilapia (Kocher *et al.*, 1998), the 39.1% for 64 primer combinations in catfish (Liu *et al.*, 1998), and the 40% for 35 primer pairs in silkworm (Tan *et al.*, 2001). The use of inter-strain crosses in the eastern oyster may further increase the polymorphism of AFLP markers and mapping efficiency. This study should encourage the use of AFLP markers in other molluscs, where genome mapping has so far been prevented primarily by the lack of molecular markers.

As expected, the majority of AFLP markers followed

Table 4

Map length and genome coverage for Crassostrea virginica

Map length (cM)	Male	Female
Observed length		
G_{of}	647.4	904.3
G_{oa}	718.4	1091.6
Estimated length		
G_{e1}	799.8	1205.5
G_{e2}	815.6	1192.8
G_{e3}	958.5	1489.3
Average G_e	858.0	1295.9
Genome coverage (%)		
C_{of}	75.5	69.8
C_{oa}	83.7	84.2

Mendelian segregation ratios. The level of segregation distortion (8.2% of loci) observed in this study is low and within the range observed in most other species, from none in a shrimp (Moore *et al.*, 1999) and catfish (Liu *et al.*, 1998), to 8% in tilapia (Kocher *et al.*, 1998) and 13.3% in rainbow trout (Young *et al.*, 1998). The silkworm, where 54% of the loci showed segregation distortion in a backcross (Tan *et al.*, 2001) is an apparent exception. Segregation distortion has been reported in the eastern oyster with other types of genetic markers, including in 7% of anonymous single-copy nuclear DNA polymorphism loci (Hu and Foltz, 1996) and in 11.5% of microsatellite loci (Reece *et al.*, 2002). In another study with allozyme markers, segregation distortion was found in 48.3% of cases tested (Foltz, 1986), although there were problems with cross contamination. In the Pacific oyster, segregation distortion has been observed in 31% of allozyme loci (McGoldrick and Hedgecock, 1997), 20.9% of microsatellites (Launey and Hedgecock, 2001), and 27% of AFLP markers (Li and Guo, 2002). Segregation distortion seems to be less frequent in the eastern oyster than in the Pacific oyster, *Crassostrea gigas* which may reflect true differences between the two genomes. Besides oysters, segregation distortion has been also reported in several other bivalves (Beaumont *et al.*, 1983; Gaffney and Scott, 1984; also see review in Wilkins, 1976).

In the Pacific oyster, the high level of segregation distortion is primarily due to a deficiency in identical-by-descent homozygotes caused by high genetic load (Launey and Hedgecock, 2001). Homozygote-deficiency accounted for 76% of all segregation distortions in this study, which also suggests selection against deleterious recessive mutations. Different levels of segregation distortion may reflect differences in the lineage or genetic load of the populations or crosses studied. Families used in the present study and that of Hu and Foltz (1996), where the lowest segregation distortion (7% and 8.2%) was found, came from Rutgers stocks that have been subjected to long-term selection (mass selection over 10 generations for disease resistance). This long-term selective breeding may have eliminated some deleterious recessive genes. The mapping of distorted markers may help us understand the distribution of deleterious recessive genes in the genome. In the male map, 6 of the 17 distorted loci are closely linked, and all 6 loci are homozygote-deficient, indicating that they are linked to an unknown gene with a recessive deleterious allele. We named this gene *Dru01* (deleterious recessive unknown), and on the basis of the level of distortion and distance among the six markers involved, tentatively placed it in a distal region of Group 8 between markers *B5f303* and *F1f327*. It would be interesting to determine when *Dru01* is expressed (before or after metamorphosis) and how prevalent the deleterious allele is.

AFLP markers may distribute randomly in some species (Castiglioni *et al.*, 1999; Remington *et al.*, 1999; Cervera *et al.*, 2001), but form clusters in others (Young *et al.*, 1998; Waldbieser *et al.*, 2001; Sakamoto *et al.*, 2000). The distribution of AFLP markers in the eastern oyster is mostly random, and the level of clustering observed is considerably lower than that in rainbow trout (Young *et al.*, 1998). Clustering in rainbow trout and some plants (Nandi *et al.*, 1997; Castiglioni *et al.*, 1998) occurred in centromere regions. Oyster chromosomes are mostly metacentric, and our maps show that large intervals are often located in the central regions of most large linkage groups in both female and male maps (Figs. 2 and 3); these regions may correspond to recombinant hot regions near centromeres. It has been suggested that crossover hot regions exist in the marine bivalve *Mulinia lateralis* and occur near the centromere region (Guo and Allen, 1996). Because *Eco*RI and *Mse*I restriction sites are relatively AT-rich, clustering may be a reflection of variation in GC content among chromosomal regions. In maize, Castiglioni *et al.* (1999) reported that AFLP markers generated by *Pst*I/*Mse*I primer combinations were more evenly distributed than those by *Eco*RI/*Mse*I primers, because the restriction site of *Pst*I is relatively GC-rich.

Linkage map, map length, and genome coverage

This study provides the first estimated genetic map length in the eastern oyster: 858.0 cM for the male map and 1295.9 cM for the female map. Sex differences in crossover frequencies and map length are commonly observed, with the male map often shorter than the female map in vertebrates (Dib *et al.*, 1996; Dietrich *et al.*, 1996; Sakamoto *et al.*, 2000; Singer *et al.*, 2002). Similar differences in map distances between males and females have been noted in the Pacific oyster (D. Hedgecock, Bodega Marine Laboratory, UC Davis, pers. comm.; Li and Guo, 2002). The estimated length for both male and female maps, however, is considerably longer than the expected length based on chiasma data. Cytogenetic observation of chromosome pairing suggests that there is about 1.1–1.3 chiasmata per chromosome

in eggs and 1.0–1.1 chiasmata per chromosome in primary spermatocytes of the eastern oyster (Guo *et al.*, unpubl. data), which corresponds to a theoretical length of 550–650 cM for the female map, and 500–550 cM for the male map. The estimated genome length based on our linkage data is about 43% and 147% longer than that of the cytogenetic map for the male and female, respectively.

The discrepancy between the cytogenetic and genetic map length may be caused by several factors. First, the number of chiasmata observed at metaphase may be an underestimate of crossover events. It has been suggested that closely formed crossover events can lead to chiasma reduction (Nilsson *et al.*, 1993; Nilsson, 1994). But chiasma reduction has not been accepted as a prevailing meiotic event, and cytogenetic length is close to genetic length in most well-studied model species (Morton, 1991). Chiasma frequency may underestimate cytogenetic map length to some extent; however, it is unlikely to account for the 145% difference in length between the cytogenetic and linkage maps. Secondly, map length may be inflated by the linkage mapping program MAPMAKER (Sybenga, 1996). In yellow monkeyflower, MAPMAKER overestimated map length by 20% (Fishman *et al.*, 2001), which may have happened to our maps; however, it is inconceivable that MAPMAKER could cause 147% inflation. Thirdly, typing errors are known to inflate map length. We constructed maps without error detection first, but the final maps presented here were constructed with the "error detection on" option in MAPMAKER. Error detection resulted in a 20% reduction in length for the male map and a 9% reduction for the female map. Error detection has led to different levels of length reduction in other organisms: 4.3% in the silkworm (Tan *et al.*, 2001), 14% in tilapia (Kocher *et al.*, 1998), and 40.3% in barley (Castiglioni *et al.*, 1998). Finally, the genetic map may be inflated by low marker density. Genetic maps usually shorten with increased marker density. In medaka, for example, 170 markers produced a 2480-cM map in 29 linkage groups (Wada *et al.*, 1995), whereas 663 markers produced a high-density map of just 1354.5 cM in 24 linkage groups (Naruse *et al.*, 2000). Similarly, in the silkworm, 356 AFLP-markers produced a map of 6512 cM (Tan *et al.*, 2001), while 1018 RAPD markers produced a map of only 2000 cM (Yasukochi, 1998). In rice, a map constructed with 762 markers measured 4026.3 cM (Causse *et al.*, 1994), while the map built with 2275 markers measured only 1521.6 cM (Harushima *et al.*, 1998). Low marker density is likely the primary cause for the longer than expected genetic length observed in this study, although other factors may have contributed to the overall increase in map length. We expect that, as marker density increases, the genetic maps will decrease in length and become comparable to the cytogenetic map.

The linkage maps presented here are the first genetic maps for the eastern oyster. They are similar in marker density to a 98-marker, 880-cM microsatellite map (Hubert *et al.*, 2002), and a 104-marker, 1051-cM AFLP map (Li and Guo, 2002) of the Pacific oyster. The eastern oyster maps are obviously incomplete, as indicated by genome coverage and the presence of large gaps. The eastern oyster has a haploid number of 10 chromosomes (Longwell and Stiles, 1967), and the male and female linkage maps both had 12 linkage groups. The small linkage groups, as well as some triplets and doublets, may join other groups as marker density increases and gaps are filled. Despite the presence of gaps, the maps provide reasonably good coverage of the eastern oyster's genome: 83.7% for the male map and 84.2% for the female map when all linked markers are considered. With an average interval of 6.3–12.6 cM, these maps provide a basic framework for gene and QTL mapping in the eastern oyster, though marker density should be increased and more microsatellite and Type 1 markers should be added.

One concern with the AFLP markers is the transferability among populations and laboratories. AFLPs are rather consistent among families and crosses (Moore *et al.*, 1999; Wilson *et al.*, 2002; Roupe van der Voort *et al.*, 1997). Transferability among laboratories may depend on the scoring systems used. Fortunately, poor transferability can be compensated for by the ease of developing a large set of AFLP markers in any population of interest, thus limiting the need for transfer. In some cases, the interest is in a particular stock, and AFLP markers can be developed specifically for mapping and selection in that stock. There is no question that microsatellites, because of their high levels of polymorphism and co-dominance, are better markers for linkage mapping than are AFLPs. They are also more expensive to develop and to use. The best strategy could be to use AFLPs in combination with microsatellites (Kocher *et al.*, 1998; Young *et al.*, 1998; Agresti *et al.*, 2000). Microsatellites can provide a backbone for the linkage map and afford some transferability, while AFLPs would saturate the map and fill gaps with a large number of markers. A large number of oyster ESTs is becoming available (Jenny *et al.*, 2002) and can be added to maps. A high-density AFLP/microsatellite map can facilitate rapid mapping of EST/Type 1 markers and eventually comparative mapping.

Acknowledgments

This work is partly supported by grants from the New Jersey Commission on Science and Technology (No. 00-2042-007-20) and Sea Grant Oyster Disease Research Program (R/OD-9915 and ODRP-29) to XG. The first author is partly supported by a grant from Ministry of Education of China (39600113). We would like to thank Greg A. DeBrosse for caring of oysters and Li Li for help with sampling. This is Publication IMCS-2003-8 and NJSG-03-517.

Literature Cited

Agresti, J. J., S. Seki, A. Cnaani, S. Poompuang, E. M. Hallerman, N. Umiel, G. Hulata, G. A. E. Gall, and B. May. 2000. Breeding new strains of tilapia: development of an artificial center of origin and linkage map based on AFLP and microsatellite loci. *Aquaculture* **185:** 43–56.

Beaumont, A. R., C. M. Beveridge, and M. D. Budd. 1983. Selection and heterozygosity within single families of the mussel *Mytilus edulis* (L.). *Mar. Biol. Lett.* **4:** 151–161.

Black, W. C., and N. M. Duteau. 1997. RAPD-PCR and SSCP analysis for insect population genetic studies. Pp. 361–373 in *The Molecular Biology of Insect Disease Vectors: A Methods Manual*. J. M. Crampton, C. B. Beard, and C. Louis, eds. Chapman & Hall, New York.

Brown, B. L., D. E. Franklin, P. M. Gaffney, M. Hong, D. Dendanto, and I. Kornfield. 2000. Characterization of microsatellite loci in the eastern oyster, *Crassostrea virginica*. *Mol. Ecol.* **9:** 2117–2119.

Castiglioni, P., C. Pozzi, M. Heun, V. Terzi, K. J. Müller, W. Rohde, and F. Salamini. 1998. An AFLP-based procedure for the efficient mapping of mutations and DNA probes in barley. *Genetics* **149:** 2039–2056.

Castiglioni, P., P. Ajmone-Marsan, R. van Wijk, and M. Motto. 1999. AFLP markers in a molecular linkage map of maize: codominant scoring and linkage group distribution. *Theor. Appl. Genet.* **99:** 425–431.

Causse, M. A., T. M. Fulton, G. Cho, S. N. Ahn, and J. Chunwongse. 1994. Saturated molecular map of the rice genome based on an interspecific backcross population. *Genetics* **138:** 1251–1274.

Cervera, M. T., V. Storme, B. Ivens, J. Gusmão, B. H. Liu, V. Hostyn, J. V. Salyeken, M. V. Montagu, and W. Boerjan. 2001. Dense genetic linkage maps of three *Populus* species (*Populus deltoides, P. nigra* and *P. trichocarpa*) based on AFLP and microsatellite markers. *Genetics* **158:** 787–809.

Chakravarti, A., L. K. Lasher, and J. E. Reefer. 1991. A maximum likelihood method for estimating genome length using genetic linkage data. *Genetics* **128:** 175–182.

Cho, Y. G., M. Y. Eun, S. R. McCouch, and Y. A. Chae. 1994. The semi-dwarf gene, *sd-1*, of rice. II. Molecular mapping and marker-assisted selection. *Theor. Appl. Genet.* **89:** 54–59.

Dib, C., S. Faure, C. Fizames, D. Samson, N. Drouot, *et al.* 1996. A comprehensive genetic map of the human genome based on 5264 microsatellites. *Nature* **380:** 152–154.

Dietrich, W. F., J. Miller, R. Steen, M. A. Merchant, D. Damron-Boles, *et al.* 1996. A comprehensive genetic map of the mouse genome. *Nature* **380:** 149–152.

Fishman, L., A. J. Kelly, E. Morgan, and J. H. Willis. 2001. A genetic map in the *Mimulus guttatus* species complex reveals transmission ratio distortion due to heterospecific interactions. *Genetics* **159:** 1701–1716.

Foltz, D. W. 1986. Segregation and linkage studies of allozyme loci in pair crosses of the oyster *Crassostrea virginica*. *Biochem. Genet.* **24:** 941–56.

Ford, S. E., and H. H. Haskin. 1987. Infection and mortality patterns in strains of oysters *Crassostrea virginica* selected for resistance to the parasite *Haplosporidium nelsoni* (MSX). *J. Parasitol.* **73:** 268–376.

Gaffney, P. M. 2002. Associations between microsatellites and repetitive elements in bivalve genomes [Abstract]. Plant, Animal and Microbe Genome X: The International Conference on the Status of Plant, Animal and Microbe Genome Research, January 12–16, 2002, San Diego, CA. (Online). Available: http://www.intl-pag.org/pag/10/abstracts/PAGX-W19.html (accessed 22 April 2003).

Gaffney, P. M., and T. M. Scott. 1984. Genetic heterozygosity and production traits in natural and hatchery populations of bivalves. *Aquaculture* **42:** 289–302.

Galtsoff, P. S. 1964. *The Eastern Oyster*, Crassostrea virginica *Gmelin*. U.S. Department of the Interior, Washington, DC.

Grewe, P. M., C. C. Krueger, C. F. Aquadro, E. Bermingham, H. L. Kincaid, and B. May. 1993. Mitochondrial DNA variation among lake trout (*Salvelinus namaycush*) strains stocked into Lake Ontario. *Can. J. Fish. Aquat. Sci.* **50:** 2397–2403.

Guo, X., and S. K. Allen, Jr. 1996. Complete interference and nonrandom distribution of meiotic crossover in a mollusc, *Mulinia lateralis* (Say) *Biol. Bull.* **191:** 145–148.

Harushima, Y., M. Yano, A. Shomura, M. Sato, and T. Shimano. 1998. A high-density rice genetic linkage map with 2275 markers using a single F2 population. *Genetics* **148:** 479–494.

Hu, Y. P., and D. W. Foltz. 1996. Genetics of senDNA polymorphisms in juvenile oysters (*Crassostrea virginica*). Part 1: characterizing the inheritance of polymorphisms in controlled crosses. *Mol. Mar. Biol. Biotechnol.* **5:** 123–129.

Hubert, S., G. Li, and D. Hedgecock, 2002. Development of a genetic linkage map, using microsatellite markers in the Pacific oyster *Crassostrea gigas* [Abstract]. Plant, Animal and Microbe Genome X: The International Conference on the Status of Plant, Animal and Microbe Genome Research, January 12–16, 2002, San Diego CA. (Online). Available: http://www.intl-pag.org/pag/10/abstracts/PAGX_W16.html (accessed 22 April 2003).

Hulbert, S. H., T. W. Ilott, E. J. Legg, S. E. Lincoln, E. S. Lander, and R. W. Michelmore. 1988. Genetic analysis of the fungus, *Bremia lactucae*, using restriction fragment length polymorphisms. *Genetics* **120:** 947–958.

Jenny, M. J., A. H. Ringwood, E. R. Lacy, A. J. Lewitus, J. W. Kempton, P. S. Gross, G. W. Warr, and R. W. Chapman. 2002. Potential indicators of stress response identified by expressed sequence tag analysis of hemocytes and embryos from the eastern oyster, *Crassostrea virginica*. *Mar. Biotechnol.* **4:** 81–93.

Kocher, T. D., W. Lee, H. Sobolewska, D. Penmanand, and B. McAndrew. 1998. A genetic linkage map of a cichlid fish, the tilapia (*Oreochromis niloticus*). *Genetics* **148:** 1225–1232.

Lander, E. S., and Botstein D. 1989. Mapping Mendelian factors underlying quantitative traits using RFLP linkage maps. *Genetics* **121:** 185–199.

Lander, E. S., P. Green, J. Abrahamson, A. Barlow, M. J. Daly, S. E. Lincoln, and L. Newburg. 1987. MAPMAKER, an interactive computer package for constructing primary genetic linkage maps of experimental and natural populations. *Genomics* **1:** 174–180.

Launey, S., and D. Hedgecock. 2001. High genetic load in the Pacific oyster *Crassostrea gigas*. *Genetics* **159:** 255–265.

Leung, S. M., R. Rojas, C. Maples, C. Flynn, W. G. Ruiz, T. S. Jou, and G. Apodaca. 1999. The small GTPase RhoA alters postendocytic traffic in polarized MDCK cells. *Mol. Biol. Cell.* **10:** 4369–4384.

Li, L., and X. Guo. 2002. A preliminary linkage map for the Pacific oyster *Crassostrea gigas*, constructed with AFLP and RAPD markers. *J. Shellfish Res.* **21:** 433 (Abstract).

Liu, Z., A. Nichols, P. Li, and R. A. Dunham. 1998. Inheritance and usefulness of AFLP markers in channel catfish (*Ictalurus punctatus*), blue catfish (*I. furcatus*) and their F1, F2 and backcross hybrids. *Mol. Gen. Genet.* **258:** 260–268.

Liu, Z., P. Li, H. Kucuktas, A. Nichols, G. Tan, X. Zheng, B. J. Argue, and R. A. Dunham. 1999a. Development of amplified fragment length polymorphism (AFLP) markers suitable for genetic linkage mapping of catfish. *Trans. Am. Fish. Soc.* **128:** 317–327.

Longwell, A. C., and S. S. Stiles. 1967. Chromosome complement of the eastern oyster *Crassostrea virginica*, as seen in meiotic and cleaving eggs. *Can. J. Genet. Cytol.* **9:** 845–858.

McGoldrick, D. J., and D. Hedgecock. 1997. Fixation, segregation and linkage of allozyme loci in inbred families of the Pacific oyster *Crassostrea gigas* (Thunberg): implications for the causes of inbreeding depression. *Genetics* **146:** 321–34.

Moore, S. S., V. Whan, G. P. Davis, K. Byrne, D. J. S. Hetzel, and N.

Preston, 1999. The development and application of genetic markers for the Kuruma prawn *Penaeus japonicus*. *Aquaculture* **173:** 19–32.

Morton, N. E. 1991. Parameters of the human genome. *Proc. Natl. Acad. Sci. USA* **88:** 7474–7476.

Nandi, S., P. K. Subudhi, D. Senadhira, N. L. Manigbas, S. Sen-Mandi, and N. Huang. 1997. Mapping QTLs for submergence tolerance in rice by AFLP analysis and selective genotyping. *Mol. Gen. Genet.* **255:** 1–8.

Naruse, K., S. Fukamachi, H. Mitani, M. Kondo, T. Matsuoka, S. Kondo, N. Hanamura *et al.* 2000. A detailed linkage map of medaka, *Oryzias latipes:* comparative genomics and genome evolution. *Genetics* **154:** 1773–1784.

Nilsson, N. O. 1994. Recombination frequencies, chiasma counts and the process of crossing-over. Ph.D. dissertation, University of Lund, Sweden.

Nilsson, N. O., T. Sall, and B. O. Bengtson. 1993. Chiasma and recombination data in plants: are they compatible? *Trends Genet.* **9:** 344–348.

Ott, J. 1999. *Analysis of Human Genetic Linkage.* Johns Hopkins University Press, Baltimore.

Reece, K. S., C. Morrison, W. L. Ribeiro, P. M. Gaffney, and S. K. Allen. 2002. Microsatellite markers for the eastern oyster *Crassostrea virginica:* linkage mapping and genetic monitoring of restoration projects [Abstract]. Plant, Animal and Microbe Genome X: The International Conference on the Status of Plant, Animal and Microbe Genome Research, January 12–16, 2002, San Diego CA. (Online). Available: http://www.intl-pag.org/pag/10/abstracts/PAGX_W18.html (accessed 22 April 2003).

Remington, D. L., R. W. Whetten, B.-H. Liu, and D. M. O'Malley. 1999. Construction of an AFLP genetic map with nearly complete genome coverage in *Pinus taeda*. *Theor. Appl. Genet.* **98:** 1279–1292.

Roupe van der Voort, J. N. A. M., P. van Zandvoort, H. J. van Eck, R. T. Folkertsma, R. C. B. Huttenm, J. Draaistra, F. J. Gommers, E. Jacobsen, J. Helder, and J. Bakker. 1997. Use of allele specificity of comigrating AFLP markers to align genetic maps from different potato genotypes. *Mol. Gen. Genet.* **255:** 438–447.

Sakamoto T., R. G. Danzmann, K. Gharbi, P. Howard, A. Ozaki, S. K. Khoo, R. A. Woram, N. Okamoto, M. M. Ferguson, L.-E. Holm, R. Guyomard, and B. Hoyheim. 2000. A microsatellite linkage map of rainbow trout (*Oncorhynchus mykiss*) characterized by large sex-specific differences in recombination rates. *Genetics* **155:** 1331–1345.

Singer, A., H. Perlman, Y. Yan, C. Walker, G. Corley-Smith, B. Brandhorst, and J. Postlethwait. 2002. Sex-specific recombination rates in zebrafish (*Danio rerio*). *Genetics* **160:** 649–657.

Sybenga, J. 1996. Recombination and chiasmata: a few intriguing discrepancies. *Genome* **39:** 473–484.

Tan, Y. D., C. Wan, Y. Zhu, C. Lu, Z. Xiang, and H. W. Deng. 2001. An amplified fragment length polymorphism map of the silkworm. *Genetics* **157:** 1277–1284.

Voorrips, R. E. 2001. *MapChart Version 2.0: Windows Software for the Graphical Presentation of Linkage Maps and QTLs.* Plant Research International, Wageningen, The Netherlands.

Vos, P., R. Hogers, M. Bleeker, M. Reijans, T. van de Lee, M. Hornes, A. Frijters, J. Pot, J. Peleman, M. Kuiper, and M. Zabeau. 1995. AFLP: a new technique for DNA fingerprinting. *Nucleic Acids Res.* **23:** 4407–4414.

Wada, H., K. Naruse, A. Shimada, and A. Shima. 1995. Genetic linkage map of a fish, the Japanese medaka *Oryziao latipes*. *Mol. Mar. Biol. Biotech.* **4:** 269–274.

Waldbieser, G. C., B. G. Bosworth, D. J. Nonneman, and W. R. Wolters. 2001. A microsatallite-based genetic linkage map for channel catfish, *Ictalurus punctatus*. *Genetics* **158:** 727–734.

Wilkins, N. P. 1976. Genetic variability in marine Bivalvia: implications and applications in molluscan mariculture. Pp. 549–563 in *Proceedings of the Tenth European Symposium on Marine Biology, Vol. 1 Mariculture,* G. Persoore and F. Jaspers, eds. Universal Press, Wetteren, Belgium.

Wilson K., Y. Li, V. Whan, S. Lehnert, K. Byrne, S. Moore, S. Pongsomhoon, E. Ballment, Z. Fayazi, J. Swan, M. Kenway, and J. Benzie. 2002. Genetic mapping of the black tiger shrimp *Penaeus monodon* with amplified fragment length polymorphism. *Aquaculture* **204:** 297–309.

Yasukochi, Y. 1998. A dense genetic map of the silkworm, *Bombyx mori*, covering all chromosomes based on 1018 molecular markers. *Genetics* **150:** 1513–1525.

Young, W. P., P. A. Wheeler, V. H. Coryell, P. Keimand, and G. H. Thorgaard. 1998. A detailed linkage map of rainbow trout produced using doubled haploids. *Genetics* **148:** 1–13.

Reference: *Biol. Bull.* **204:** 339–349. (April 2003)

Use of Multivariate Analysis to Assess the Nutritional Condition of Fish Larvae From Nucleic Acids and Protein Content

ISABEL CUNHA[1,*], FRAN SABORIDO-REY[2], AND MIQUEL PLANAS[2]

[1]*Centre of Marine and Environmental Research (CIIMAR), R. dos Bragas 177, 4050-123 Porto, Portugal; and* [2]*Institute of Marine Research, CSIC, Eduardo Cabello 6, 36208 Vigo, Spain*

Abstract. The nutritional condition of turbot larvae (*Scophthalmus maximus*) was assessed by a multivariate analysis with DNA, RNA, and protein content as input variables. Special attention was given to the time that feeding began and to the timing and duration of starvation. The combination of the principal components analysis and the stepwise discriminant analysis, both techniques of multivariate analysis, made it possible to allocate the larvae into groups that were defined and identified based on similarities in developmental stage and nutritional condition. The developmental stage was mostly determined by the input variables DNA and protein content, while nutritional condition was determined by the RNA content. In the period studied, the more developed larvae were less resistant to starvation. Furthermore, when initial feeding was delayed as little as 6 h, the variables analyzed were markedly changed, and the effect on the deprived larvae was found to be equivalent to a 3-day delay in development—when compared with the larvae fed immediately after mouth opening. Through this technique, new samples of larvae with unknown history might be classified into groups, using their DNA, RNA, and protein content as input values in the defined classification functions. Results were compared to those obtained using RNA/DNA and RNA/dry weight indices, and the multivariate method was considered to be more sensitive and to provide extra information about larval nutritional history and development.

Introduction

Some events in the early life of fishes are critical to the fluctuations of fish populations in marine environments (Trippel and Chambers, 1995). Among those, larval mortality is widely acknowledged to be one of the most important (Cushing, 1975). Starvation and inadequate food supply are significant causes of mortality (Hjort, 1914; Cushing, 1974, 1975; Lasker, 1975). Feeding studies require that accurate and quantitative criteria be used to characterize the nutritional condition of fish larvae. This approach can also be applied in aquaculture (Quantz, 1989; Planas *et al.*, 1991) to interpret the adequacy of different diets for fulfilling the nutritional requirements of the cultured species and to establish the limits for starting exogenous feeding.

A variety of methods have been used to diagnose the nutritional condition and recent growth rate of fish larvae at different organizational levels: organism, tissue, and cellular. Methods based on biochemical criteria have been considered more effective and sensitive, because changes due to a feeding regime are first reflected at subcellular and cellular levels, and only thereafter in the whole organism (Robinson and Ware, 1988). RNA, DNA, and protein contents of the larvae have been used frequently as biochemical criteria (Bulow, 1970; Buckley, 1979 a,b, 1982, 1984; McGurk, 1984; Clemmesen, 1987, 1994; Buckley *et al.*, 1990, 1991; Bergeron *et al.*, 1991; Cunha, 1991, 1996; Richard *et al.*, 1991; Mathers *et al.*, 1992, 1993; Canino, 1994; Takii *et al.*, 1994; Clemmesen *et al.*, 1997; Gronkjaer *et al.*, 1997; Chícharo *et al.*, 1998; Bergeron, 2000). However, none of these variables alone can indicate a larva's nutritional condition, growth potential, or ability to recover from starvation. Instead, ratios that combine these variables in pairs are generally used (*e.g.*, Clemmensen *et al.*, 1997; Chícharo *et al.*, 1998).

However, the use of ratios is still a univariate technique that may provide only a quantitative description of the variation of such ratios among individuals. (If a single observation or measurement is made for each individual, the

Received 21 June 2002; accepted 14 February 2003.

* To whom correspondence should be addressed: E-mail: isabel.cunha@cimar.org

data are said to be univariate; more than one observation or measurement for each individual produces multivariate data (Krzanowski and Marriott, 1994).) Organisms are integrated units whose variables are intercorrelated to varying degrees. By not taking the interdependency of variables into account, many univariate analyses will overestimate the dimensionality of divergence (Atchley and Bryant, 1975). Hence, these variables should not be analyzed separately; instead the correct approach must be multivariate. Multivariate analysis is the only meaningful technique that examines the relationships among several variables, which helps to determine affinities between individuals and considers the variation in such variables as a whole—that is, allows exploration of variation in a multidimensional scale (Morrison, 1967). In our opinion, nutritional condition, which is the result of the interaction of more than two variables, is better studied through multivariate techniques.

Multivariate analysis has been used extensively in ecological studies (see: Digby and Kempton, 1987; Saila and Martin, 1987; Rodriguez and Magnan, 1995), primarily to analyze morphometric characters of both adult (Reyment *et al.*, 1984; Saborido-Rey, 1994) and larval fish (Theilacker, 1978, 1981, 1986; Powell and Chester, 1985; Polo, 1991; Reichow *et al.*, 1991). It has seldom, and only superficially, been applied to data on the biochemical composition of fish larvae (McGurk and Kusser, 1992; Navarro *et al.*, 1995; Chícharo, 1996).

An interesting feature of multivariate analysis, when used in studies of nutrition, growth, and development, is that it opens the possibility of assessing wild larvae, where the background of nutrition and development is unknown. However, as a first step, a set of experiments with cultured larvae is required to test the statistical methods and establish the models that will classify wild larvae.

In this study, the nutritional condition of cultured turbot larvae was assessed through a multivariate approach using the DNA, RNA, and protein content of larval tissues as variables. Turbot was the preferred species because of its importance in aquaculture and the depth of knowledge available about its biology, especially in relation to its feeding activities (Cunha and Planas, 1995; Cunha, 1996).

Material and Methods

Experimental conditions and sampling

Turbot larvae were obtained from a commercial hatchery where eggs were incubated at 14 °C. At 50% hatching, larvae were transported to the laboratory and stocked in two 250-l tanks (A and B). The temperature was slowly raised over the following 2 days from 14°C to 20–21°C. This temperature was maintained from larval mouth opening (day 3; $t = 0$), when sampling started, until the end of the experimental period.

Treatment A. Larvae in the tank were not fed. After mouth opening, groups of 1500 larvae were transferred after 6, 12, 30, and 54 h of starvation from the tank to 16-l buckets, where food was supplied, and reared according to Cunha and Planas (1995). Food density in the buckets was maintained at 5 items per milliliter, which guarantees an *ad libitum* supply of food. Samples were taken every 24 h until no more larvae were left, *i.e.* about 6.5 d later. Samples from the tank, where the larvae were always starved, were also taken at regular intervals and considered as the control for the starved larvae. The dry weight and protein, DNA, and RNA contents of these samples were determined. Treatment A in the Appendix summarizes the sampling regime and initial conditions for these larvae.

Treatment B. Larvae in this tank were fed *ad libitum* using the same standard technique. After first feeding (day 3), groups of 1500 larvae were transferred after 6, 30, 50, 96, and 150 h from the tank to 15-l buckets, where no food was supplied. These larvae were sampled at 6, 12, 24, 48, and 72 h after the onset of the starvation period, until 50% mortality was reached, *i.e.* about 3 days of food deprivation. Samples from the tank, where the larvae were always fed, were also taken at regular intervals and considered as the control for the fed larvae. The dry weight and protein, DNA, and RNA contents of these samples was determined as in Treatment A. Treatment B in the Appendix summarizes the sampling regime and the initial conditions for these larvae.

Biochemical analyses

Protein content was analyzed according to Lowry *et al.* (1951). Nucleic acids (DNA and RNA) were extracted and separated according to the technique developed by Schmidt and Thannhauser (1945) and modified by Fleck and Munro (1962), Fleck and Begg (1965), and Munro and Fleck (1966, 1969). The larvae for each sample were pooled to ensure that the analyzed biomass would be larger than 800 μg (Buckley, 1979a). Each pooled sample was referred to as a case; 61 cases were analyzed (Appendix).

Data analyses

Content of protein, DNA, and RNA was used to assess larval nutritional condition by a multivariate approach, combining principal components analysis and stepwise discriminant analysis. Before multivariate analysis can be done, it is important to screen the data for outliers and check the normality. However, multivariate analysis is considered robust enough to be insensitive to minor deviations in normality and homoscedasticity (Kirk, 1982; Harris, 1985). Outliers were detected by box plots; the normality of each variable was checked with the Shapiro-Wilks' test.

Principal components analysis (PCA) was performed on both sets of data taken together (Treatments A and B) and assumes no structure for the data. PCA studies the intercorrelations of a number of variables by clustering them into common factors, such that the variables within each factor are highly correlated, but the factors are uncorrelated.

Therefore, each of the factors explains a different part of the total variance in the data. The factors should be treated as new variables; and, therefore, each case has a value on the derived factors. These values are called factor scores. The PCA provides factor scores for each case, which can be plotted and investigated for the existence of any structure in the data, defining groups of cases with similar characteristics.

These groups were defined based not only on their factorial scores but also on the common and differential attributes of each case, that is, their nutritional condition and larval development. Thus, the groups were delimited using a biological definition. Nutritional condition was evaluated by considering the relative time that larvae were fed, or starved. Larval development was assessed by the size and age of the larvae; the age was expressed in *day degrees*. Age in days is not necessarily coupled with development, because larval development is very dependent on temperature. A day degree is a unit that combines temperature and time, and is useful for monitoring and comparing growth when temperatures fluctuate.

Although PCA assumes no structure in the data and the main goal is to sort cases (the so-called ordination technique), stepwise discriminant analysis (SDA) requires the existence of groups and tells us how different these groups are (discrimination or classification technique) by means of a *discriminant function*. The discriminant function is a linear combination of the original variables that best separate groups; therefore, a coefficient for each variable and a constant is calculated. SDA results in k-1 discriminant functions, k being the number of groups analyzed. The importance of each discriminant function in the analysis is given by its canonical correlation and the total variance explained by each function. Wilks' λ was used to assess the discriminatory effectiveness of the analysis (Wilks, 1932). This is a multivariate analysis of variance statistic that tests the equality of group means for the variables in the discriminant function. The smaller the λ, which ranges from 0 to 1, the greater the difference between groups.

On the other hand, SDA also results in *classification functions*, which are computed for each group and can be used directly to classify cases. A case will be classified into the group for which it has the highest classification score. It results in a classification matrix where the efficiency of the analysis can be also evaluated. Further description of multivariate techniques can be found in Hair *et al.* (1998).

The ratios RNA/DNA and DNA/dry weight were determined for each case, and mean values were calculated for each of the groups established by the multivariate analysis. The mean values of the groups were compared through ANOVA. The *post hoc* Tukey's honest significant difference (HSD) test for unequal n was used, since the groups obtained were rather unequal in size.

Statistica for Windows 5.0 (StatSoft Inc., 1995) was used to perform all the statistical analyses.

Results

The original data of protein, RNA, and DNA concentrations included in the statistical analysis for Treatments A and B are given in the Appendix. Dry weight and age (in day degrees) of the larvae are also shown in the table, as well as RNA/DNA and DNA/dry weight indices.

The principal components analysis extracted two factors, PC_1 and PC_2, that explained 99.7% of data variation, 50% each (Table 1). The most determinant variables for PC_1 were larval protein and DNA content, whereas for PC_2 the most determinant variable was RNA content. The graphical representation of the factor scores for each case, computed from loading rotated factors of PC_1 and PC_2, is presented in Figure 1. Based on examination of this plot, cases can be grouped according to the relative positions of their factor scores. At least four groups can be initially defined. To define these groups we also examined two criteria for each case: nutritional background and larval development. Nutritional condition was evaluated considering the relative time that larvae were fed or starved, and larval development was assessed by the size and age of the larvae. This examination revealed that the groups resulting from the PCA are well delimited in relation to these two criteria; thus a clear link is established between the biochemical analysis and the nutritional condition and developmental stage of the larvae. We named these groups G_1, G_2, G_3, and G_4. PC_1 allows the separation of G_2-G_3 from G_1-G_4, while PC_2 splits G_1-G_2 from G_3-G_4 (Fig. 1). Thus the combination of both factors, PC_1 and PC_2, allows the identification of the four groups.

Nevertheless, a continuous gradient was observed in the distribution of the cases on the factorial plot (Fig. 1). This sounds logical, taking into account that larvae used in the analysis not only were those in extreme conditions but also were sampled regularly throughout the experimental period. Thus an intermediate group was also found, distributed among groups G_1, G_2, and G_4, as shown in Figure 1, encircled by a dashed curve. To ascertain the distribution of these intermediate samples among the initial four groups, three different stepwise discriminant analyses were performed: (1) using only the four most distant groups; (2) incorporating the intermediate set of cases as a fifth group; and (3) with a new group definition, using all 61 cases.

Table 1

Standard coefficients of principal components (PC_1 and PC_2) obtained through principal components analysis

Variable	PC_1	PC_2
Protein	0.715	0.695
RNA	0.541	0.840
DNA	0.842	0.538
Variance explained (%)	50.5	49.2

Values show the relative importance of each variable in each principal component. Each PC explains approximately 50% of the total variance.

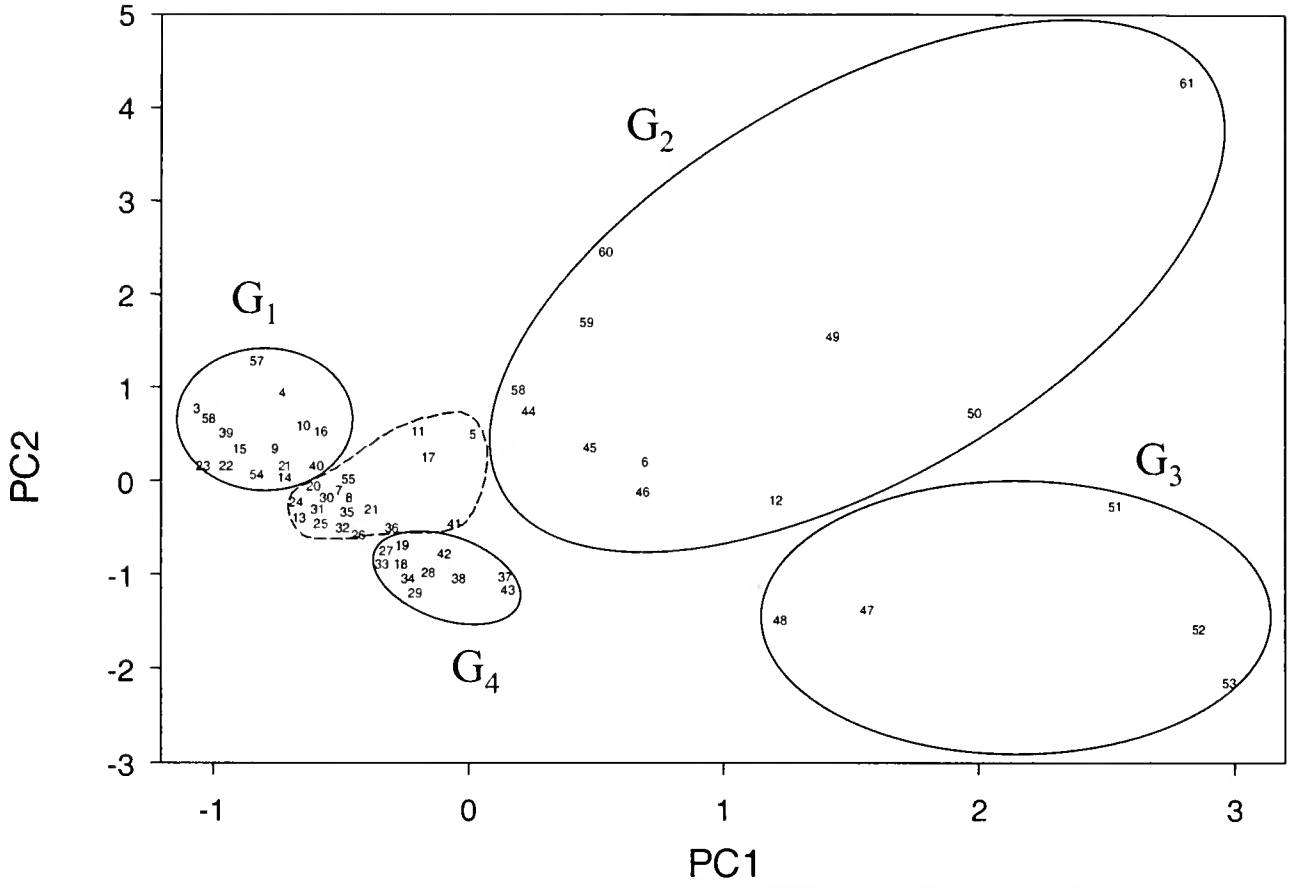

Figure 1. Plot of factor scores of the cases after principal components analysis with respect to first (PC_1) and second (PC_2) principal components. The distribution of the cases was compared with the larval development and the nutritional condition of each case to allow the definition of groups within the plot. Thus four initial groups (continuous line) and an intermediate group (dashed line) were defined.

The results of the first SDA evidenced good discrimination between the four groups. Wilks' λ was very low (0.038), and the final correct classification was high (97.67%). All the cases of groups G_1, G_3, and G_4 were correctly classified within their own groups (*i.e.*, 100% correct classification); and only one case of G_2 was misclassified as belonging to G_4 (90.91% correct classification). Thus, only 1 of 43 cases was misclassified. Therefore, the groups were considered to be distinct and the initial group definition was deemed appropriate.

In the next step, the intermediate group was incorporated into another SDA analysis. The results of this analysis showed a high degree of overlapping between G_1 and the intermediate group. Thus, 22.2% (4 of 18) of the intermediate group cases were classified as G_1; on the other hand, 12.5% (2 of 16) of G_1 cases were classified in the intermediate group. Of the intermediate group cases, 72.2% were correctly classified, as belonging to that group, indicating some degree of independence for this group. However, only one case in the intermediate group was classified as G_4. It was our opinion that G_1 and the intermediate group were highly interrelated, so the intermediate group was included in G_1, except for case 41, which was moved to G_4. The new group delimitation is shown in Figure 2.

A final SDA was then performed on the four newly defined groups. This analysis was done in three steps, including the three original variables in decreasing order of discrimination. In the first step, DNA was entered into the model; the value of Wilks' λ decreased to 0.311, which already indicated very good discrimination. The addition of the RNA in the second step and protein content in the third considerably increased the discriminant capacity of the final function, producing values of λ of 0.076 and 0.064, respectively.

Standardized coefficient values and the constant of each discriminant function are presented in Table 2. The first two functions explained as much as 99.6% of the total variance. Values of the canonical correlation coefficient were 0.9 and 0.8 for the first two canonical variables (Table 3), and 0.16 for the third.

The classification matrix obtained from the discriminant analysis (Table 3) was used to evaluate the accuracy of its discrimination. At the end of the analysis, 98.6% of the cases were correctly assigned into the groups. Only one case

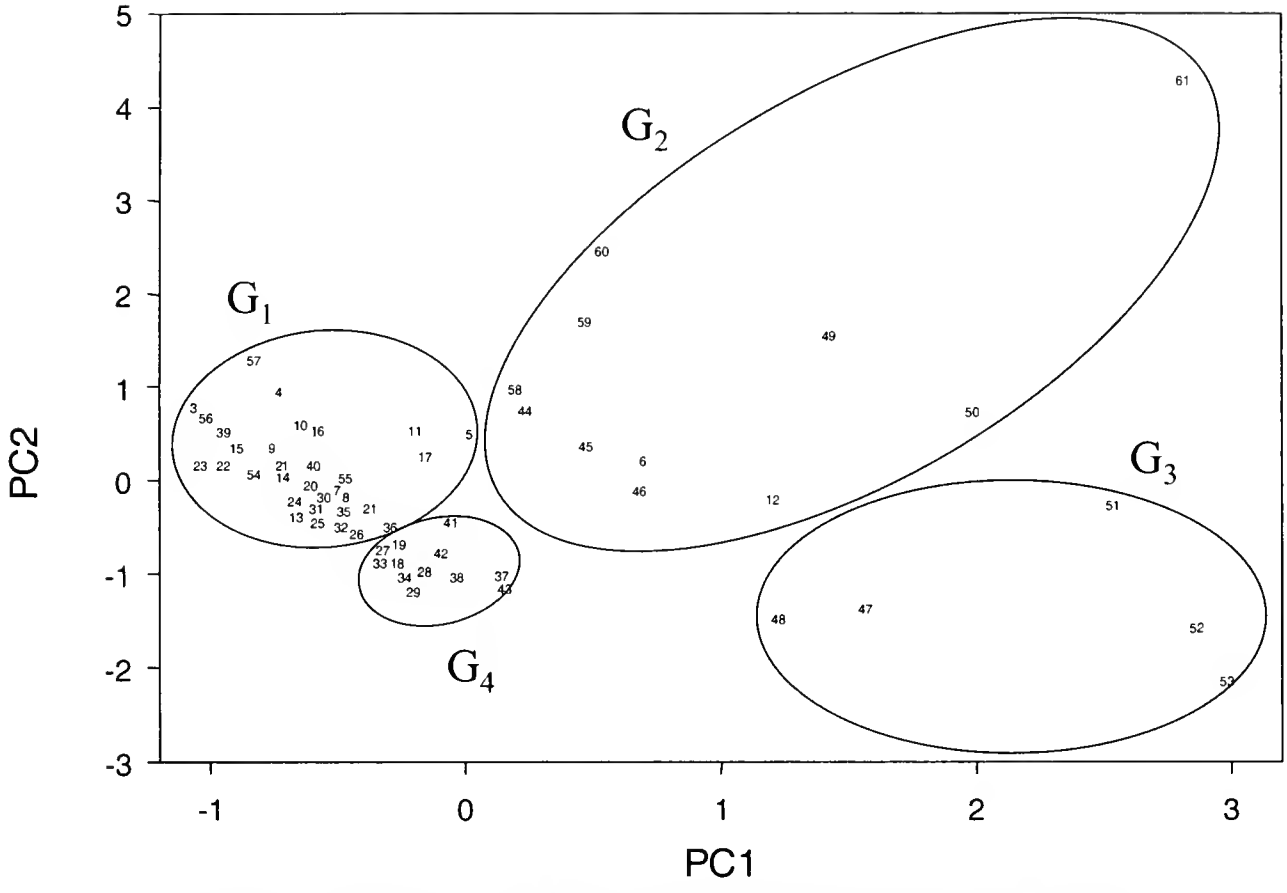

Figure 2. Plot of factor scores of the cases after principal components analysis with respect to first (PC_1) and second (PC_2) principal components, and the delimitation of the four final groups (G_1, G_2, G_3, and G_4). Delimitation of the final groups was obtained after three consecutive stepwise discrimination analyses.

from G_2 was misclassified in G_3. The coefficients and constants of the classification functions resulting from the SDA are presented in Table 4.

Thus, the groups were defined taking into consideration the results of the PCA and SDA, and also the nutritional background and the larval development of each case. The assignment of each case to each group is shown in the Appendix. The group definitions are explained in Table 5 and and illustrated in Figure 3.

More developed larvae were less resistant to starvation: after being starved, they needed a longer feeding period to recover their normal biochemical levels, and thus to be reclassified in the upper groups of the diagram in Figure 3.

All larvae that were never fed after mouth opening died 6.5 d after hatching.

Table 6 shows the mean values of RNA/DNA and DNA/dry weight for the four groups obtained through the previ-

Table 2

Standardized coefficients of each discriminant function of the final stepwise discriminant analysis (SDA) performed on the four groups obtained through principal component analysis and two previous SDAs

Variable	DF1	DF2	DF3
DNA	23.600	−3.848	18.962
RNA	−2.935	−3.911	2.996
Protein	−0.060	0.274	−0.537
Constant	−6.850	2.127	−2.723
Variance explained (%)	74.8	24.7	0.5
Canonical correlation	0.910	0.784	0.179

Table 3

Classification matrix of the final stepwise discriminant analysis (SDA) performed on the four groups obtained through principal components analysis and two previous SDAs

Group	% of correct classification*	G_1	G_2	G_3	G_4
G_1	100.0	33	0	0	0
G_2	90.9	0	10	0	1
G_3	100.0	0	0	5	0
G_4	100.0	0	0	0	12
Total	98.4	33	10	5	13

* A high value indicates that the groups are different and distinct.

Table 4

Classification functions resulting from the final stepwise discriminant analysis (SDA) performed on the four groups obtained through principal components analysis and two previous SDAs

Variable	G_1	G_2	G_3	G_4
DNA	183.9	274.6	345.6	224.6
RNA	0.3	0.3	−27.5	−8.1
Protein	−2.3	−3.2	−2.2	−2.3
Constant	−20.5	−52.8	−84.8	−30.7

The functions permit new cases to be classified into one of the four groups.

ous analysis and the results of the comparative ANOVA. RNA/DNA values are significantly different between G_1-G_3, G_1-G_4, G_2-G_3, and G_2-G_4. Therefore, this index is not useful for distinguishing between G_1-G_2, and G_3-G_4, since only two groups can be identified. DNA/dry weight is significantly different only between G_4 and the other three groups, and does not permit us to distinguish-between G_1, G_2, and G_3.

Discussion

RNA, DNA, and protein content have been used frequently as biochemical criteria to diagnose the nutritional condition in marine fish larvae (Bulow, 1970; Buckley, 1979b, 1984; Clemmesen, 1987, 1994; Cunha, 1991, 1996; Richard *et al.*, 1991; Takii *et al.*, 1994; Chícharo *et al.*, 1998). These variables alone or, more often, the indices RNA/DNA and DNA/dry weight have been used. However, we found the multivariate approach to be a more useful tool when using such biochemical data to assess nutritional condition in turbot larvae. The method was found to be more sensible than the two biochemical indices commonly used (RNA/DNA and DNA/dry weight), since it allowed the discrimination of larvae according to their real nutritional condition, and also provided additional information about the period when larvae were deprived of food. Larvae that never were fed or were deprived of food at an early stage (standard length < 4 mm or 5 d) could be distinguished from those fed and then deprived of food in a later stage of development. When the RNA/DNA index was used, similar values were obtained for larvae with different nutritional backgrounds and developmental stages. The DNA/dry weight index detected only larvae of group G4 as being in poor nutritional condition, appraising the larvae of the other three groups as being in similar good nutritional condition. We know that this is false because some of the larvae belonging to group G3 had been deprived of food for 72 h. Moreover, the appraisal of nutritional condition did not depend on a single variable, and so a multivariate analysis seems more appropriate from a theoretical point of view than a univariate approach. When the groups are unknown *a priori*, an ordination technique is preferable; the usual objective of ordination is to help generate hypotheses about the relationship between possible group composition and the underlying factors. Principal component analysis is one of the most commonly used ordination techniques. Once the

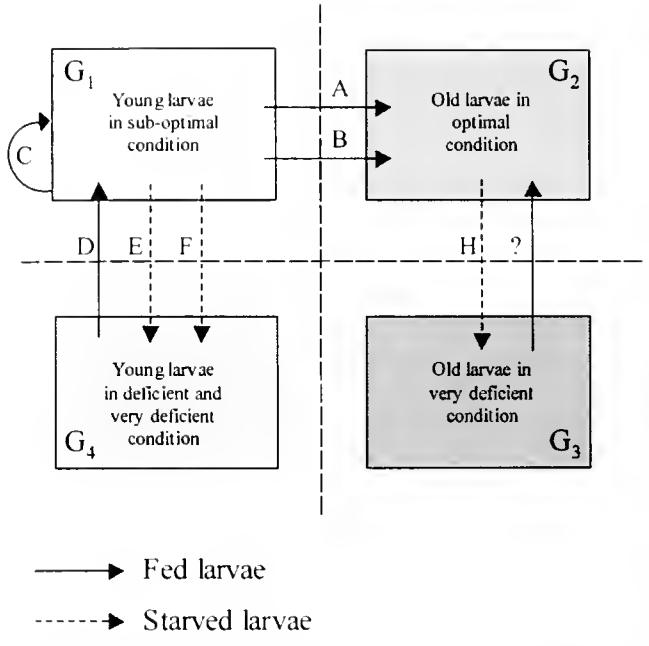

Figure 3. Theoretical scenario describing the evolution of larvae in relation to their developmental stage and nutritional condition, considering the four groups obtained from the principal components analysis (G_1, G_2, G_3, and G_4). (A) Larvae fed since mouth opening; (B) larvae whose first feeding was delayed for less than 12 h; (C) larvae whose first feeding was delayed for 30 h; (D) larvae whose first feeding was delayed for 54 h; (E) larvae in permanent starvation since mouth opening; (F) starved larvae that were previously fed for a period between 0 and 50 h; (H) starved larvae that were previously fed for more than 96 h.

Table 5

Characteristics of larvae classified into the four groups obtained through principal components analysis according to their development and nutritional condition

Group	Age or length of larvae	Nutritional condition
G_1	Until day 5 or 4 mm	Sub-optimal • First days of development when fed adequately • First feeding delayed from 0 to 2 days • Starved less than one day
G_2	After day 5 or 4 mm	Optimal • Well fed • Starved less than one day
G_3	After day 5 or 4 mm	Very deficient • Starved more than one day
G_4	Until day 5 or 4 mm	Deficient and very deficient • First feeding delayed more than 2 days • Starved longer than one day

Table 6

Mean values of RNA/DNA and DNA/dry weight indices of the four groups obtained through multivariate analysis

Group	Mean	SD	Max	Min	Tukey's HSD*			
RNA/DNA								
G1	3.10	0.55	4.36	2.09		G1	G2	G3
G2	3.69	0.58	4.57	2.90	G2	0.0516		
G3	2.02	0.54	2.92	1.59	G3	**0.0089**	**0.0002**	
G4	1.70	0.33	2.46	1.26	G4	**0.0002**	**0.0002**	0.7717
DNA/dry weight								
G1	12.53	1.88	16.28	8.96		G1	G2	G3
G2	10.48	1.10	12.67	8.55	G2	0.0571		
G3	12.78	1.65	14.26	10.94	G3	0.9964	0.2136	
G4	16.41	2.31	19.12	11.37	G4	**0.0002**	**0.0002**	**0.0156**

SD, standard deviation; Max, maximum value; min, Minimum value.

* Results of the Tukey unequal *n* honest significant difference test. Values shown are the *post hoc* probabilities (P). Statistically significant differences occur when $P < 0.001$ (bold values).

data have been classified into groups, the difference between those groups can be determined and a classification function can be estimated to ascertain the group to which a new sampled element belongs. Stepwise discriminant analysis may be, for many purposes, the most widely used classification technique, but it is seldom applied to biochemical data (Navarro *et al.*, 1995).

The multivariate analysis of the biochemical data shows a certain organization of the cases into groups. By examining the larval developmental stage and nutritional condition of each case and relating these two criteria with the biochemical analysis (RNA, DNA, and protein content), four groups were defined. This grouping aids in designing a scenario describing the evolution of the larvae in relation to their nutritional experience and development (Fig. 3). The first criterion, larval development, determines the horizontal position of the larvae in the chart. This determination is based mainly on DNA and protein content, as these two variables were the most important in the PC_1. Larvae in sub-optimal and optimal feeding conditions were classified in groups G_1 and G_2--the younger larvae in the former group and the older larvae in the latter.

The second criterion, nutritional condition, determines the vertical position of the larvae in the chart. This determination is based mainly on their RNA content, because this variable got the highest value in PC_2. Larvae in a deficient or very deficient nutritional condition—that is, those subjected to a long period of starvation and those whose first feeding was delayed for a long period of time (3 d)—had lower RNA content, leading to the discrimination of the inferior groups, G_3 and G_4. The lower RNA content of the larvae included in these groups determines their lower capacity for protein synthesis (Suteliffe, 1965; Bulow, 1970; Millward, 1989). The protein content was also lower in these groups, but not the DNA content, demonstrating that starvation reduced the volume of the cells, not the number. In our opinion, the relationship between these two parameters, protein and DNA, sets the lower limit for starvation and determines larval death: the protein level cannot be lower than that required to maintain basic functions and minimal structures.

Larvae that were formerly classified in the upper groups were classified in the lower ones later, after starvation (Fig. 3). The opposite also occurred: those larvae in a deficient nutritional condition, belonging to group G_4, recovered their RNA levels after feeding and were later classified in group G_1—even those whose first feeding was delayed for 3 d. Owing to the insufficient number of larvae left after sampling, no further conclusions could be made about the point of irreversible starvation. But to the extent that we could sample, all larvae that were never fed after mouth opening died 6.5 d after hatching. This result is in accordance with Jones (1972), who observed 50% mortality in larvae 7 d after hatching; but his study was performed at 17.5 °C, whereas we were working at 20–21 °C. Therefore, the point of irreversible starvation for larvae that are never fed after mouth opening must be between days 3 and 6.5.

The analysis also indicates that, within each group, the most developed larvae are less resistant to starvation. In fact, early larvae that had been starved perform better after being fed for 6 h than those that were previously fed for 1.5 or 2.5 d. The probable explanation is that earlier larvae have larger yolk sac reserves, with a more positive energy balance. Moreover, the lower resistance of the more developed larvae might reflect higher metabolic activity rates and thus faster consumption of energy stores (Cunha, 1996).

The results presented in this paper demonstrate a new approach to determining the nutritional condition of reared fish larvae. They should however, be regarded with caution because larvae from different batches and geographic locations have different nucleic acid levels (Canino *et al.*, 1991). These levels are affected by temperature (Buckley, 1982, 1984; Buckley *et al.*, 1990, 1991; Canino, 1994) and may even show diel variations (Chícharo *et al.*, 1998). Moreover,

the experiments were restricted to the initial development of the larvae, including larvae younger than 12–13 d and smaller than 200 μg in dry weight. In spite of all these constraints, the type of analysis presented here seems promising. If the variables are controlled as discussed above, this classification technique seems very accurate. Current, biochemical analyses of nucleic acids are very precise, with the use of individual larvae, instead of pooled ones, recommended to increase precision. Thus this method can still be useful even if the experimental conditions are less drastic than those presented here, because of the wide range of nutritional conditions analyzed in this paper. However, since laboratory conditions do not always simulate natural conditions, the extrapolation of laboratory-derived values to the wild has often been questioned (Mackenzie *et al.*, 1990; Folkvord and Moksness, 1995). Nevertheless, the technique is straightforward, requiring only three input variables to characterize new samples of larvae, or individual larvae, with unknown nutritional and developmental backgrounds. RNA, DNA, and protein content of the new samples are input in the four classification functions, producing four different classification scores. The sample or individual is classified in the group whose function resulted in the highest score.

Acknowledgments

This study was financially supported by the Comisión Interministerial de Ciencia y Tecnología (CICYT, Spain) under Project AGF 185/92. I. Cunha was supported by a postgraduate scholarship (BD/3489/94) from FCT (Portugal).

Literature Cited

Atchley, W. R., and E. H. Bryant. 1975. *Multivariate Statistical Methods.* Benchmark papers in Systematic and Evolutionary Biology 1. Dowden, Hutchinson and Ross, Stroudsberg, PA.

Bergeron, J. 2000. Effect of strong winds on the nutritional condition of anchovy (*Engraulis encrasicolus* L.) larvae in the Bay of Biscay, Northwest Atlantic, as inferred from an early field application of the DNA/C index. *ICES J. Mar. Sci.* **57:** 249–255.

Bergeron, J., M. Boulhic, and R. Galois. 1991. Effect de la privation de nourriture sur la teneur de ADN de la larve de sole (*Solea solea* L.). *ICES J. Mar. Sci.* **48:** 127–134.

Buckley, L. J. 1979a. Relationships between RNA-DNA ratio, prey density, and growth rate in Atlantic cod (*Gadus morhua*) larvae. *J. Fish. Res. Board Can.* **36:** 1497–1502.

Buckley, L. J. 1979b. Changes in ribonucleic acid, deoxyribonucleic acid and protein content during ontogenesis in the winter flounder *Pseudopleuronectes americanus*, and effect of starvation. *Fish. Bull.* **77:** 703–708.

Buckley, L. J. 1982. Effects of temperature on growth and biochemical composition of larval winter flounder *Pseudopleuronectes americanus*. *Mar. Ecol. Prog. Ser.* **8:** 181–186.

Buckley, L. J. 1984. RNA-DNA ratio: an index of larval fish growth in the sea. *Mar. Biol.* **80:** 291–298.

Buckley, L. J., A. S. Smigielski, T. A. Halavic, and G. C. Laurence. 1990. Effects of water temperature on the biochemical composition of the winter flounder *Pseudopleuronectes americanus* at hatching and feeding initiation. *Fish. Bull.* **88:** 419–428.

Buckley, L. J., A. S. Smigielski, T. A. Halavik, E. M. Caldarone, B. R. Burns, and G. C. Laurence. 1991. Winter flounder *Pseudopleuronectes americanus* reproductive success. I. Among-location variability in size and survival of larvae reared in laboratory. *Mar. Ecol. Prog. Ser.* **74:** 117–124.

Bulow, F. J. 1970. RNA-DNA ratios as indicators of recent growth rates of a fish. *J. Fish. Res. Board Can.* **27:** 2343–2349.

Canino, M. F. 1994. Effect of temperature and food availability on growth and RNA/DNA ratios of walleye pollock *Theragra chalcogramma* (Pallas) eggs and larvae. *J. Exp Mar. Biol. Ecol.* **175:** 1–16.

Canino, M. F., K. M. Bailey, and L. S. Incze. 1991. Temporal and geographic differences in feeding and nutritional condition of walleye pollock larvae *Theragra chalcogramma* in Shelikof Strait, Gulf of Alaska. *Mar. Ecol. Prog. Ser.* **79:** 27–35.

Chícharo, M. A. 1996. Methods for the evaluation of the nutritional state of *Sardina pilchardus* larvae applied on the study of survival conditions in nature. Ph.D. thesis, University of Algarve, Faro, Portugal.

Chícharo, M. A., L. Chícharo, L. Valdez, E. Lopez-Jamar, and P. Ré. 1998. Estimation of starvation and diel variation of the RNA/DNA ratios in field-caught *Sardina pilchardus* larvae off the north of Spain. *Mar. Ecol. Prog. Ser.* **164:** 273–283.

Clemmesen, C. 1987. Laboratory studies on RNA-DNA ratios of starved and fed herring *Clupea harengus* and turbot *Scophthalmus maximus* larvae. *J. Cons. Cons. Int. Explor. Mer* **43:** 122–128.

Clemmesen, C. 1994. The effect of food availability, age or size on the RNA/DNA ratio of individually measured herring larvae: laboratory calibration. *Mar. Biol.* **118:** 377–382.

Clemmesen, C., R. Sanchez, and C. Wongtschowski. 1997. A regional comparison of the nutritional condition of SW Atlantic anchovy larvae, *Engraulis anchoita*, based on RNA/DNA contents. *Arch. Fish. Mar. Res.* **45:** 17–43.

Cunha, I. 1991. Some correlates of growth and nutritional condition in herring, *Clupea harengus*, larvae. M.Sc. thesis, University of Aberdeen, Aberdeen, Scotland.

Cunha, I. 1996. Trophic behaviour and energetic physiology of turbot (*Scophthalmus maximus* L.) larvae in rearing conditions. Ph.D. thesis, University of Santiago de Compostela, Santiago de Compostela, Spain. (in Spanish).

Cunha, I., and M. Planas. 1995. Ingestion rates of turbot larvae (*Scophthalmus maximus*) using different sized live prey. *ICES Mar. Sci. Symp.* **201:** 16–20.

Cushing, D. H. 1974. The possible density dependence of larval mortality and adult mortality in fishes. Pp. 103–111 in *The Early Life History of Fish*, J.H.S. Blaxter, ed. Springer-Verlag, Berlin.

Cushing, D. H. 1975. *Marine Ecology and Fisheries.* Cambridge University Press, Cambridge.

Digby, P. G. N., and R. A. Kempton. 1987. *Multivariate Analysis of Ecological Communities.* Chapman and Hall, London.

Fleck, A., and D. Begg. 1965. The estimation of ribonucleic acid using ultraviolet absorption measurements. *Biochem. Biophys. Acta* **108:** 222–339.

Fleck, A., and H. N. Munro. 1962. The precision of the ultraviolet absorption measurements in the Schmidt-Thannhauser procedure for nucleic acid estimation. *Biochem. Biophys. Acta* **55:** 571–583.

Folkvord, A., and E. Moksness. 1995. RNA/DNA ratios and growth of herring larvae. *Mar. Ecol. Prog. Ser.* **121:** 311–312.

Gronkjaer, P. C., C. Clemmesen, and M. St. John. 1997. Nutritional condition and vertical distribution of the Baltic cod larvae. *J. Fish Biol.* **51A:** 352–369.

Hair, J. F., R. E. Anderson, R. L. Tatham, and W. C. Black. 1998. *Multivariate Data Analysis.* Prentice-Hall, Upper Saddle River, NJ.

Harris, R. J. 1985. *A Primer of Multivariate Statistics.* Academic Press, Orlando, FL.

Hjort, J. 1914. Variations in the great fishery of northern Europe viewed

in the light of biological research. *Rapp. P-V. Réun. Cons. Int. Explor. Mer* **20:** 1–228.

Jones, A. 1972. Studies on egg development and larval rearing of turbot, *Scophthalmus maximus* L., and brill, *Scophthalmus rhombus* L., in laboratory. *J. Mar. Biol. Assoc. UK* **52:** 965–986.

Kirk, R. E. 1982. *Experimental Design: Procedures for the Behavioural Sciences.* Brook/Cole Publications, Belmont, CA.

Krzanowski, W. J., and F. H. C. Marriot. 1994. *Multivariate Analysis.* Arnold, London.

Lasker, R. 1975. Field criteria for the survival of anchovy larvae: relation between chlorophyll maximum layers and successful first feeding. *Fish. Bull.* **73:** 453–462.

Lowry, O. H., N. J. Rosenbrough, A. L. Farr, and R. J. Randall. 1951. Protein measurement with the folin fenol reagent. *J. Biol. Chem.* **193:** 265–275.

Mackenzie, B. R., W. C. Leggett, and R. H. Peters. 1990. Estimating larval fish ingestion rates: can laboratory derived values be reliably extrapolated to the wild? *Mar. Ecol. Prog. Ser.* **67:** 209–225.

Mathers, E. M., D. F. Houlihan, and M. J. Cunningham. 1992. Nucleic acid concentration and enzyme activities as correlates of growth rate of the saithe *Pollachius virens:* growth rates estimates in open sea fish. *Mar. Biol.* **112:** 363–369.

Mathers, E. M., D. F. Houlihan, I. D. McCarthy, and L. J. Burren. 1993. Rates of growth and protein synthesis correlated with nucleic acid content in fry of rainbow trout, *Oncorhynchus mykiss:* effects of age and temperature. *J. Fish Biol.* **43:** 245–263.

McGurk, M. D. 1984. Effects of delayed feeding and temperature on the age of irreversible starvation and on the rates of growth and mortality of Pacific herring larvae. *Mar. Biol.* **84:** 13–26.

McGurk, M. D., and C. W. Kusser. 1992. Comparison of three methods of measuring RNA and DNA concentrations of individual pacific herring, *Clupea harengus pallasi,* larvae. *Can. J. Fish. Aquat. Sci.* **49:** 967–974.

Millward, D. J. 1989. The nutritional regulation of muscle growth and protein turnover. *Aquaculture* **79:** 1–28.

Morrison, D. F. 1967. *Multivariate Statistical Methods.* McGraw-Hill, New York.

Munro, H. N., and A. Fleck. 1966. The determination of nucleic acids. Pp. 113–176 in *Methods of Biochemical Analysis,* Vol. 11, D. Glick, ed. Interscience, New York.

Munro, H. N., and A. Fleck. 1969. Analysis of tissues and body fluids for nitrogenous constituents. Pp 423–525 in *Mammalian Protein Metabolism,* Vol. 3, H. N. Munro and J. B. Allison, eds. Academic Press, New York.

Navarro, J. C., L. A. McEvoy, F. Amat, and J. R. Sargent. 1995. Effects of diet on fatty acid composition of body zones in larvae of the sea bass *Dicentrarchus labrax:* A chemometric study. *Mar. Biol.* **124:** 177–183.

Planas, M., A. Estevez, and J. L. Garrido. 1991. Energy metabolism during early ontogenesis of turbot (*Scophthalmus maximus*) and the effect of starvation. Pp. 210–211 in *Larvi'91—Fish and Crustacean Larviculture Symposium,* Vol. 15, P. Lavens, P. Sorgeloos, E. Jasper, and F. Ollevier, eds. European Aquaculture Society Special Publication, Gent, Belgium.

Polo, A. 1991. Growth and feeding during larval development of reared seabream *Sparus aurata* L. Ph.D. thesis, University of Cadiz, Cadiz, Spain. (in Spanish).

Powell, A. B., and A. J. Chester. 1985. Morphometric indices of nutritional condition and sensitivity to starvation of spot larvae. *Trans. Am. Fish. Soc.* **114:** 338–347.

Quantz, G. 1989. Larvae feeding. Pp. 37–55 in *Cuadernos da Area de Ciencias do Mar,* Seminario de Estudos Galegos, Vol. 3, P. Aguirre, *et al.,* eds. Edicións do Castro, Coruña, Spain.

Reichow, D., C. Largiadèr, C. Klingenberg, C. Clemensen, R. Froese, and B. Ueberschär. 1991. The use of multivariate morphometrics to determine the nutritional condition of marine fish larvae. ICES Council Meeting Papers, ICES, Copenhagen, Denmark.

Reyment, R. A., R. E. Blackith, and N. A. Campbell. 1984. *Multivariate Morphometrics.* Academic Press, New York.

Richard, P., J.-P. Bergeron, M. Boulhic, R. Galios, and J. Person-Le Ruyet. 1991. Effect of starvation on RNA, DNA and protein content of laboratory reared larvae and juveniles of *Solea solea. Mar. Ecol. Prog. Ser.* **72:** 69–77.

Robinson, S. M. C., and D. M. Ware. 1988. Ontogenetic development of growth rates in larval Pacific herring, *Clupea harengus pallasi,* measured with RNA-DNA ratios in the Strait of Georgia, British Columbia. *Can. J. Fish. Aquat. Sci.* **45:** 1422–1429.

Rodriguez, M. A., and P. Magnan. 1995. Application of multivariate analysis in studies of the organization and structure of fish and invertebrate communities. *Can. J. Fish. Aquat. Sci.* **57:** 199–216.

Sahorido-Rey, J. F. 1994. The genus *Sebastes* Cuvier, 1829 (Pisces, Scorpaenidae) in the North Atlantic: species and population identification using morphometric techniques; growth and reproduction of the Flemish Cap populations. Ph.D. thesis, Autonomous University of Madrid, Madrid, Spain. (in Spanish).

Saila, S. B., and B. K. Martin. 1987. A brief review and guide to some multivariate methods for stock identification. Pp. 149–173 in *Proceedings of the Stock Identification Workshop,* November 5–7, 1985, Panama City Beach, FL. H. E. Kumpf, ed. NCAA Tech. Memo.

Schmidt, G., and S. J. Thannhauser. 1945. A method for the determination of deoxyribonucleic acid, ribonucleic acid and phosphoproteins in animal tissue. *J. Biol. Chem.* **161:** 83–89.

StatSoft, Inc. 1995. *STATISTICA for Windows* [Computer program manual]. Tulsa, Oklahoma.

Sutcliffe, W. H. Jr. 1965. Growth estimates from ribonucleic acid content in some small organisms. *Limnol. Oceonogr.* **10:** 253–258.

Takii, K., M. Seoka, O. Takaoka, S. Furuta, M. Nakamura, and H. Kumai. 1994. Chemical composition, RNA and DNA contents, and alkaline phosphatase activity and growth of striped jack larvae through juveniles. *Fish. Sci.* **60:** 73–76.

Theilacker, G. H. 1978. Effect of starvation on the histological and morphological characteristics of jack mackerel, *Trachurus symmetricus,* larvae. *Fish. Bull.* **76:** 403–414.

Theilacker, G. H. 1981. Effect of feeding history and egg size on the morphology of jack mackerel, *Trachurus symmetricus,* larvae. *Rapp. P-V. Reun. Cons. Int. Explor. Mer* **178:** 432–440.

Theilacker, G. H. 1986. Starvation-induced mortality of young sea-caught jack mackerel, *Trachurus symmetricus,* determined with histological and morphological methods. *Fish Bull.* **84:** 1–17.

Trippel, E., and C. Chambers. 1995. The early life history of fishes and its role in recruitment processess. Pp. 31–62 in *Early Life History and Recruitment in Fish Populations,* R. C. Chambers and E. A. Trippel, eds. Chapman & Hall, London.

Wilks, S. S. 1932. Certain generalisations in the analysis of variance. *Biometrika* **24:** 471–494.

Appendix

Initial conditions for turbot larvae in two experimental feeding treatments: nutritional background (time of starvation and feeding periods), age in day degrees, biochemical variables (dry weight, protein, RNA and DNA content) indices of these variables (RNA/DNA and DNA/dry weight). The group column indicates the group assignment in the analyses (see Results section). The case number refers to the number of each case in Figures 1 and 2.

Treatment A. Control (never fed) and experimental (initially starved and later provided with food) larvae

Starvation period (hours)	Feeding period after starvation (hours)	Day degrees	Dry weight (μg)	Protein (μg)	RNA (μg)	DNA (μg)	RNA/DNA	DNA/dry weight (×1000)	Group	Case number
	24	30.0	34.47	18.770	1.381	0.434	3.182	12.59	1	1
	48	50.0	37.67	20.030	1.325	0.419	3.162	11.12	1	2
	72	68.0	41.33	23.125	1.626	0.417	3.899	10.09	1	3
	96	87.0	52.67	26.645	2.171	0.537	4.043	10.20	1	4
	120	107.0	58.50	29.175	2.239	0.639	3.504	10.92	1	5
6	144	130.0	70.13	32.400	2.415	0.748	3.229	10.67	2	6
	24	30.0	32.60	17.140	1.223	0.439	2.786	13.47	1	7
	48	50.0	33.93	16.930	1.168	0.434	2.691	12.79	1	8
	72	68.0	36.47	19.690	1.553	0.453	3.428	12.42	1	9
	96	87.0	47.40	25.780	1.786	0.488	3.660	10.30	1	10
	120	107.0	53.43	28.940	2.062	0.583	3.537	10.91	1	11
12	144	130.0	63.53	32.855	2.363	0.805	2.935	12.67	2	12
	48	50.0	27.67	16.195	0.972	0.389	2.499	14.06	1	13
	72	68.0	33.27	19.050	1.193	0.402	2.968	12.08	1	14
	96	87.0	37.07	18.870	1.437	0.418	3.438	11.28	1	15
	120	107.0	44.87	22.400	1.861	0.512	3.635	11.41	1	16
30	144	130.0	53.88	25.845	1.841	0.562	3.276	10.43	1	17
	72	68.0	23.47	12.265	0.674	0.392	1.719	16.70	4	18
	96	87.0	26.27	13.960	0.819	0.411	1.993	15.65	4	19
	120	107.0	32.80	15.825	1.172	0.422	2.777	12.87	1	20
54	144	130.0	35.60	16.565	1.159	0.448	2.587	12.58	1	21

Control—starved larvae

	Starved during (hours)	Day degrees	Dry weight (μg)	Protein	RNA	DNA	RNA/DNA	DNA/dry weight (×1000)	Group	Case number
Newly hatched	0	0.0	32.13	15.43	1.250	0.391	3.197	12.17	1	22
	6	4.8	31.65	14.21	1.210	0.375	3.227	11.85	1	23
	8	9.6	30.67	14.55	1.189	0.428	2.778	13.96	1	24
	16	19.1	27.00	13.57	1.060	0.414	2.560	15.33	1	25
	30	25.0	25.40	13.79	0.831	0.397	2.093	15.63	1	26
	32	38.4	25.53	12.24	0.752	0.401	1.875	15.71	4	27
	54	45.0	22.33	12.21	0.611	0.401	1.524	17.96	4	28
	82	68.0	19.67	10.39	0.472	0.376	1.255	19.12	4	29

Treatment B. Control (continuously fed) and experimental (initially fed and later starved) larvae

Feeding period (hours)	Starvation period after feeding (hours)	Day degrees	Dry weight (μg)	Protein (μg)	RNA (μg)	DNA (μg)	RNA/DNA	DNA/dry weight (×1000)	Group	Case number
	6	9.6	30.00	14.42	1.209	0.431	2.805	14.37	1	30
	12	14.3	28.47	13.65	1.099	0.419	2.623	14.72	1	31
	24	24.0	26.73	12.81	0.930	0.409	2.274	15.30	1	32
	48	42.9	22.40	11.00	0.660	0.389	1.697	17.37	4	33
6	72	62.4	20.87	10.15	0.512	0.380	1.347	18.21	4	34
	6	28.8	30.80	15.23	1.146	0.435	2.634	14.12	1	35
	12	33.6	26.60	14.73	0.966	0.433	2.231	16.28	1	36
	24	42.9	26.00	13.77	0.807	0.468	1.724	18.00	4	37
30	48	62.4	23.27	12.53	0.632	0.419	1.508	18.01	4	38
	6	47.7	39.40	20.62	1.561	0.426	3.664	10.81	1	39
	12	54.4	38.87	20.16	1.426	0.456	3.127	11.73	1	40
	24	62.4	38.53	18.76	1.212	0.493	2.458	12.80	4	41
	48	81.9	38.00	15.97	0.815	0.432	1.887	11.37	4	42
50	72	103.5	27.40	13.84	0.625	0.440	1.420	16.06	4	43
	6	86.8	64.73	33.82	2.630	0.718	3.663	11.09	2	44
	12	91.6	62.33	33.24	2.369	0.710	3.337	11.39	2	45
	24	103.5	60.00	31.93	1.963	0.676	2.904	11.27	2	46
	48	125.7	50.20	25.63	1.384	0.716	1.933	14.26	3	47
96	72	147.5	44.20	21.97	0.984	0.617	1.595	13.96	3	48
	6	130.7	110.60	56.26	4.180	1.063	3.932	9.61	2	49
	12	135.8	104.20	54.67	3.688	1.063	3.469	10.20	2	50
	24	147.5	96.07	49.47	3.073	1.051	2.924	10.94	3	51
	48	170.0	83.87	41.27	1.876	0.925	2.028	11.03	3	52
150	72	191.0	64.40	35.64	1.420	0.883	1.608	13.71	3	53

Control—fed larvae

Fed during (hours)	Day degrees	Dry weight (μg)	Protein	RNA	DNA	RNA/DNA	DNA/dry weight (×1000)	Group	Case number
6	4.8	31.00	14.36	1.289	0.415	3.106	13.39	1	54
30	24.0	30.53	15.98	1.280	0.452	2.832	14.81	1	55
50	42.9	42.07	20.50	1.699	0.439	3.870	10.43	1	56
80	67.3	61.73	30.24	2.412	0.553	4.362	8.96	1	57
96	81.9	73.27	34.64	2.875	0.749	3.838	10.22	2	58
130	109.0	90.67	46.21	3.758	0.896	4 194	9.88	2	59
150	125.7	117.13	55.90	4.527	1.002	4.518	8.55	2	60
210	175.5	173.87	102.77	7.724	1.690	4 570	9.72	2	61

INDEX

E

F

G

H

I

J

K

L

M

N

O

P

R

S

T

U

V

W

Y

Z

THE BIOLOGICAL BULLETIN
(www.biolbull.org)
2003 SUBSCRIPTION FORM
(VOLUMES 204-205, 6 ISSUES)

All subscriptions run on the calendar year; price includes both print and online journals.

(please print)

NAME: _____

INSTITUTION: _____

ADDRESS: _____

CITY: _____ STATE: _____

POSTAL CODE: _____ COUNTRY: _____

TELEPHONE: _____ FAX: _____

E-MAIL ADDRESS: _____

❒ **Please send me a 2003 subscription to *The Biological Bulletin* at the rate indicated below:**

❒ Individual: $105.00 (6 ISSUES) ❒ Institutional: $280.00 (6 ISSUES)
❒ Individual: $ 52.50 (3 ISSUES) ❒ Institutional: $140.00 (3 ISSUES)
Check one: ❒ February, April, June or ❒ August, October, December

❒ **Please send me the following back issue(s):** _____

❒ Individual: at $20.00 (PER ISSUE) ❒ Institutional: at $50.00 (PER ISSUE)

Delivery Options

_____ Surface Delivery (Surface delivery is included in the subscription price.)

_____ Air delivery (Please add the correct amount to your payment.)

❒ U.S. and Canada: $25.00 ❒ Mexico: $60.00 ❒ All other locations: $100.00

Payment Options

_____ Enclosed is my check or U.S. money order for $ _____ payable to The Marine Biological Laboratory

_____ Please send me an invoice. (Note: Payment must be received before subscription commences.)

_____ Please charge my ❒ VISA, ❒ MasterCard ❒ Discover Card $_____

Account No.: _____ Exp. Date: _____

Signature: _____ Date: _____

Return this form with your check or credit card information to:

Marine Biological Laboratory
Subscription Office ◆ The Biological Bulletin ◆7 MBL Street ◆ Woods Hole, MA 02543-1015